(2)

MINUTES OF THE TWENTY-THIRD EXPLOSIVES SAFETY SEMINAR

Volume II

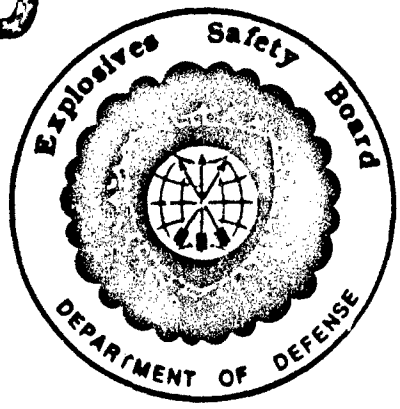

HYATT REGENCY HOTEL
ATLANTA, GA
9-11 AUGUST 1988

Sponsored By
Department of Defense Explosives Safety Board
Alexandria, VA

DISCLAIMER NOTICE

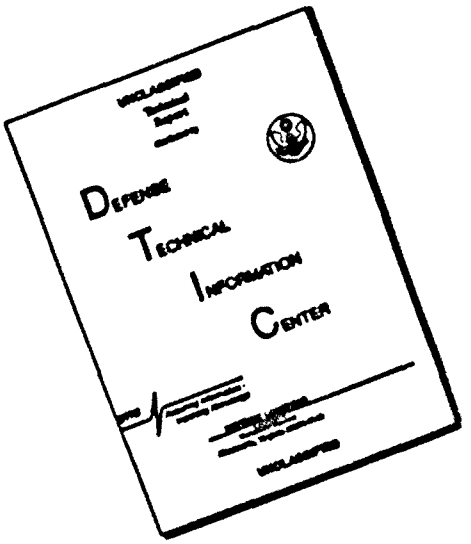

THIS DOCUMENT IS BEST QUALITY AVAILABLE. THE COPY FURNISHED TO DTIC CONTAINED A SIGNIFICANT NUMBER OF PAGES WHICH DO NOT REPRODUCE LEGIBLY.

MINUTES OF THE

TWENTY-THIRD EXPLOSIVES SAFETY SEMINAR

Volume II

Hyatt-Regency Hotel

Atlanta, Georgia

9 - 11 August 1988

Sponsored by

Department of Defense Explosives Safety Board

Alexandria, Virginia 22331-0600

Approved for public release; distribution unlimited

TABLE OF CONTENTS

VOLUME II

HAZARDS AND RISKS OF THE DISPOSAL OF CHEMICAL MUNITIONS USING A CRYOGENIC PROCESS

by
Robert M. Cutler
The MITRE Corporation
McLean, Virginia
and
Gregory St. Pierre
Office of the Program Executive Officer
Program Manager for Chemical Demilitarization
United States Army
Aberdeen Proving Ground, Maryland
for
Department of Defense
Twenty-third Explosives Safety Seminar
Atlanta, Georgia
9-11 August 1988

ABSTRACT

The potential for accidents releasing chemical blister and nerve agents during the process of demilitarizing chemical munitions, and the associated effects of public fatalities in the vicinity of Tooele Army Depot (TEAD), Utah, are evaluated. Concurrent casualties involving plant workers are also addressed. The accidents investigated pertain to the processes of cooling in liquid nitrogen, fracturing in a press, and incinerating the variety of munitions and agents to be demilitarized. Estimates of accident frequency and consequence are developed. Risk is portrayed by using risk curves showing risk to an individual and to the public in the vicinity, together with other risk descriptors such as potential fatalities (both workers and the public), and the distance from the site of an accident of a lethal agent plume.

1.0 INTRODUCTION

The U.S. Army's stockpile of chemical munitions is stored at eight sites throughout the continental United States. The Army's Office of the Program Executive Officer - Program Manager for Chemical Demilitarization has the responsibility for disposing of the existing stockpile. This is a large scale effort that, by Congressional mandate, must be completed by September of 1994.

Two disposal technologies are under consideration for use in the Chemical Stockpile Disposal Program (CSDP): the baseline technology based on the mechanical disassembly of the munitions followed by incineration of the separate components and agent; and the cryofracture technology based on embrittlement and crushing followed by incineration of the unsegregated, fractured components. The baseline technology is represented by the

chemical munition/agent disposal facility currently under construction at Johnston Island. This is the technology on which the recently-completed risk analysis for the CSDP (U.S. Army Toxic and Hazardous Materials Agency, 1986) was based. The cryofracture technology is still under development by the Army, which plans to demonstrate the process at a full-scale facility at the Tooele Army Depot (TEAD). This study describes the risk to public safety of the proposed Cryofracture Chemical Demilitarization Plant (CCDP) as documented in the 60 percent process design submittal, but without the benefit of any facility design submittal.

The Army employs a sophisticated set of procedures and standards to minimize the risks of handling chemical munitions. Nevertheless, the possibility exists that some unexpected or unavoidable accident could occur that would expose a nearby civilian population to lethal chemicals. Such an event could occur even while the Army continues to store the chemical weapons stockpile. Now that the Army proposes to demonstrate a technological alternative for disposal of the stockpile, we need to examine the risk due to a new set of possible accidents: the risk associated with the physical destruction of munitions in the stockpile at TEAD, the site of the proposed CCDP.

1.1 Risk Elements

Risk is a measure of the potential for exposure to unwanted events or consequences (e.g., injuries or fatalities). Any danger to the public or plant workers associated with the proposed CCDP may be described in terms of risk. For purposes of this study, risk is considered to be that due only to accidental release of, and potential human exposure to, chemical agent. Only accidents that could result in a lethal release of agent to the public are included. In this study, members of the public are considered to be at their places of residence, which are outside the boundaries of the military reservation.

To understand the ways in which the CCDP might present risk to the public, one needs first to identify the major features of the CCDP, including:

- the characteristics of the munition types to be destroyed;
- the chemical agents contained in the munitions;
- the activities involved in the CCDP; and
- the accident scenarios that could lead to agent release.

Each of these features is discussed below.

1.1.1 Munitions

The CCDP will entail the destruction of the full range of munition types in the chemical stockpile. These munitions, the code letters used to represent them in this paper, and the CCDP processing rates in munitions per hour are listed in TABLE 1-1. Major munition characteristics taken into account in the risk analysis include: munition size and agent inventory; susceptibility to agent release by puncture, impact, crush, or fire; packing density; and presence of energetic materials (bursters, fuzes, and propellants). Non-energetic items, also called non-bursters items or simply bulk items, include all types of bombs (which are stored without bursters), spray tanks, and ton containers. For convenience of terminology, all items are called munitions in this paper, although strictly speaking spray tanks and ton containers are not munitions.

1.1.2 Agents

As indicated in Table 1-1, munitions containing the agents GB (non-persistent nerve agent), VX (persistent nerve agent), and mustard (blister agent of types H, HD, and HT) are to be destroyed in this program. The risk associated with each of the agent type is different, since their physical and toxicological properties differ. Vapor pressure, which determines the rate at which spilled agent might evaporate, is the most important physical property when estimating risk as a function of agent type. This and other physical properties, as well as toxicological characteristics, are encoded into the Army's D2PC computer model for chemical hazard prediction (C.G. Whitacre *et al.*, 1987), which provides estimates of the downwind distance the chemical hazard might extend in a particular accident. Use of this model in this risk analysis is described in various papers and reports that deal with the CSDP risk analysis. In this paper, the code letters G, H, and V are used to designate the three respective types of agent.

1.1.3 Activities

Handling, on-site transportation, and plant operations are activities involved in the CCDP. Handling and on-site transportation are similar to those activities for the baseline technology and have been dealt with in another report (W.E. Fraize *et al.*, 1987). Since the focus of the present analysis is on the ways the cryofracture technology would affect risk, only activities associated with plant operations are considered in this report.

FIGURE 1-1 is a schematic diagram of the cryofracture process as described in the Sixty Percent Process Design submittal (GA Technologies Inc., 1987a). Cartridges, land mines, mortar rounds, projectiles, and rockets are processed in the same way. Pallets of munitions are received at the munitions demilitarization building. The pallets are placed on a conveyor which transports them to an elevator that will bring them to the

TABLE 1-1
MUNITIONS TYPES AND AGENTS
TO BE DESTROYED IN THE CCDF

Munition Type	Code	Agents Contained	Rate/Hr.
105-mm cartridges	C	GB	95
4.2-inch mortar rounds	D	Mustard	97
Ton containers	K	GB, VX, or mustard	0.89, 0.54, or 0.93
Mines	M	VX	30
155-mm projectiles	P	GB, VX, or mustard	118, 104, or 106
8-inch projectiles	Q	GB or VX	58 or 49
Rockets	R	GB or VX	43 or 34
Spray tanks	S	VX	0.63
500-lb bombs	U	GB	4
750-lb bombs	V	GB	4
Wet-eye bombs	W	GB	1.6
105-mm projectiles	Z	GB	240

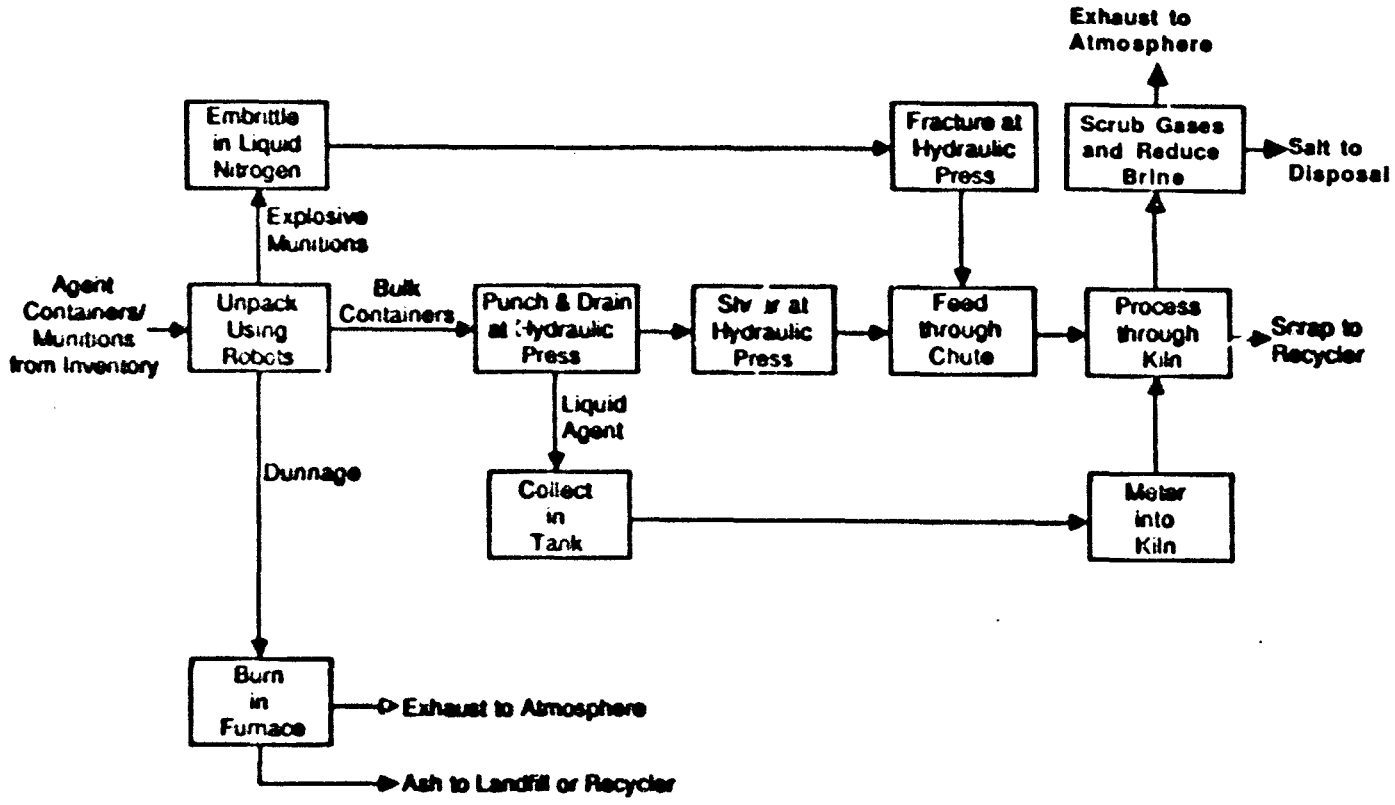

FIGURE 1-1
SIMPLIFIED FLOW DIAGRAM OF THE CRYOFRACTURE PROCESS

upper level of the building for unpacking and processing. On the upper level, the pallets of munitions move from the elevator onto an unpack conveyor. An unpack robot removes the dunnage and places it into a dunnage chute. The robot then picks up the munitions and carries them to a cryobath staging area, where they will be picked up by a pretreat robot which places the munitions (except bulk, non-explosive items) in one of the liquid nitrogen-filled cryobaths. After the munitions have cooled for the minimum required time and have thus been embrittled, the pretreatment robot removes a group from the bath and places it in one of the airlocks. The material transfer robot removes a munition package or unit from the airlock and places it in the hydraulic press. The press tooling for bulk containers is designed to sequentially punch (for draining to a bulk holding tank), crush, and shear the containers. The press tooling for rockets is designed to cut the rockets into pieces with a single stroke of the press. For all other items, the tooling is designed to fracture the munitions. The fragments fall from the press through double isolation valves into a rotary kiln furnace. In the kiln, the metal parts are heated and decontaminated, then discharged onto a scrap conveyor for ultimate disposal. Bulk liquid agent is metered from the holding tank into the kiln. Explosives, agent, and dunnage are burned in the kiln. The off-gases from the kiln are routed via a blast attenuation duct through a cyclone for removal of large particles and through an afterburner where residual combustibles are destroyed. The combustion products then pass through a pollution abatement system where acid gases and other pollutants are removed. The cleaned gases are discharged through a stack to the atmosphere. The scrubber solution from the pollutant abatement system is processed in a brine reduction system, which evaporates the water and produces salt for disposal.

1.1.4 Accident Scenarios

Potential chemical accidents are defined in specific accident scenarios, which are sequences of possible events leading to a release of agent. Accident scenarios have been identified for major classes of accident causes, including events that are internally-initiated (e.g., by equipment failures and human error) and externally-initiated (e.g., by earthquakes).

2.0 METHODOLOGY

The methods used in performing this risk assessment are described in the following sections. Accident scenarios were developed; accident frequencies, agent release amounts, and worker fatalities were estimated with technical assistance from Science Applications International Corporation (SAIC).

2.1 Development of Accident Scenarios

The first step in developing accident scenarios was to characterize the system. This included reviewing the process, based on information

contained in the 60 percent process design documents (GA Technologies 1987a). Relevant properties and characteristics of the munitions and the toxic agents were studied. From this study a list of internally-initiated accident scenarios was developed. To this list was added externally-initiated accidents based on the hazards analysis of the baseline technology (GA Technologies 1987b).

The accident scenarios were restricted to those that would not result in a lethal plume reaching the limits of TEAD (3.3 kilometers from the CCDP), under "worst-case" meteorological conditions. This was done by using the U.S. Army's D2PC dispersion model (Whitacre *et al*, 1987) with inputs of stability class E (moderately stable) and a 1 meter per second wind speed, assumed to occur 10 percent of the time. (For the remaining 90 percent of the time, "most-likely" conditions of stability class D (neutral) and a 3 meter per second wind speed were assumed to prevail.) The release quantities required to send a lethal plume to the nearest boundary 3.3 kilometers away are 14 pounds of GB from a detonation, 28 pounds of GB otherwise released, 300 pounds of HD, or 11 pounds of VX. Accidents were also evaluated to eliminate those whose mean frequency was estimated to be less than 10^{-8} per year (one occurrence every 100 million years). As a result, all externally-caused accidents were eliminated except for earthquakes. The twelve accident scenarios that have been analyzed, and corresponding subjective estimates of agent-related worker casualties (of the total of about 33 employees per shift [Kline 1986]), are listed in TABLE 2-1.

The cryofracture process accident scenarios can be divided into the following groups: those initiated by internal events, those initiated by external events, and those not yet analyzed (because of a lack of sufficient information), which of course may be initiated either internally or externally. The frequencies and agent releases of the accident scenarios that have been analyzed are described below. For each accident scenario that is specific to the CCDP (i.e., not taken from the CSDP risk analysis), the development of the frequency is illustrated by an event tree. For all accidents analyzed, the basis of the quantification of agent release, in terms of numbers of munitions involved, is shown as TABLE 2-2.

2.1.1 Internally-Initiated Events

Eight internally-initiated accident scenarios specific to the cryofracture demilitarization process have been identified and described. They are summarized in the following paragraphs. Their probabilities and range factors (ratios of the 95-percentile or upper bound estimates of probabilities to their median or best estimates) are summarized in TABLE 2-3. Note that MITRE's intent was to develop order-of-magnitude probability estimates; as a result, the probabilities are expressed as integral exponents of ten, and factors of less than one-half order (about three are neglected). Range factors, and other data incorporated into the analysis, probably have no greater true precision than integral exponents of ten, but

TABLE 2-1
ACCIDENT SCENARIOS

Scenario Number	Accident Description	Estimated Worker Casualties (Agent-related)
PC 025	Earthquake breaches UPA and results in fire (suppressed) and munition puncture.	8
PC 026	Earthquake breaches either UPA or cryobath area and results in fire (not suppressed) and munition puncture.	15
PC 029	Earthquake breaches UPA, cryobath area, or bulk agent tank and results in fire (not suppressed); no munition is punctured.	15
PC 033	Earthquake results in fire (not suppressed) involving bulk agent tank or cryobath area; no building is breached.	8
PC 401	Press fails to fracture munition and airlock does not close; munition detonates during extraction and sympathetic detonation occurs in airlock.	3
PC 402	Single munition detonates in cryobath due to impact.	1
PC 405	Munition detonates in dunnage chute.	2
PC 412	Detonation due to impact in cryobath causes second (sympathetic) detonation.	1
PC 415	Munition in chute passes detector and shredder; detonates in dunnage incinerator.	1
PC 417	Intact munition enters kiln, survives incineration, and detonates in scrap bin.	1
PC 427	Intact munition enters kiln, survives incineration and scrap bin, detonating off-site.	0
PC 435	Munition in chute passes detector and shredder, survives dunnage furnace, detonating off-site.	0

TABLE 2-2
NUMBERS OF MUNITIONS RELEASING THEIR AGENT CONTENTS
BY CRYOFRACTURE PLANT ACCIDENT SCENARIO (PC) NUMBER

Munition Code	PC 25		PC 26,29,33		PC 401		PC 402		PC 405, 415 417, 427, 435		PC 412	
	Det.	Spill	Det.	Spill	Det.	Spill	Det.	Spill	Det.	Spill	Det.	Spill
A	--	--	0	500 gal	--	--	--	--	--	--	--	--
C	--	--	119	356	2	2	--	--	1	1	--	--
D	--	--	121	364	2	2	--	--	1	1	--	--
K	0	1	0	6	--	--	--	--	--	--	--	--
M	--	--	75	225	6	18	--	--	3	0	--	--
PG	--	--	74	221	2	6	1	8	1	0	2	12
PH	--	--	66	199	2	6	1	8	1	0	2	12
PV	--	--	65	195	2	6	1	8	1	0	2	12
QG	--	--	36	109	2	4	1	8	1	0	2	12
QV	--	--	31	92	2	4	1	8	1	0	2	12
RG	--	--	32	97	2	3	--	--	--	--	--	--
RV	--	--	26	76	2	3	--	--	--	--	--	--
S	0	1	0	6	--	--	--	--	--	--	--	--
U	0	1	0	12	--	--	--	--	--	--	--	--
V	0	1	0	12	--	--	--	--	--	--	--	--
W	0	1	0	6	--	--	--	--	--	--	--	--
Z	--	--	48	142	2	6	1	8	1	0	2	12

Note: Detonation release denoted by "Det."

TABLE 2-3
ACCIDENT PROBABILITIES AND RANGE FACTORS
FOR INTERNALLY-INITIATED EVENTS

Scenario Number	Probability (events/munition)	Range Factor
PC401	10^{-10}	101
PC402	10^{-9}	141
PC405	10^{-10}	100
PC412	10^{-10}	173
PC415	10^{-8}	17
PC417	10^{-8}	14
PC427	10^{-11}	17
PC435	10^{-11}	17

are incorporated as calculated, since precision of results will be determined by uncertainty calculations (not "significant figures").

PC 401. This scenario involves a sympathetic detonation in the press area. Since the press area is currently specified to contain only single-item detonations (e.g., a detonation of one drum of mines, or one 8-inch projectile, or one rocket), multiple detonations of such munitions may be expected to release sufficient energy to fail the containment afforded by the structure.

The event tree depicting the development of this scenario is shown as FIGURE 2-1. The scenario is initiated by a failure of the press to properly crush a munition. This could result from inadequate press force and stroke, or from structural failure of the punch or tooling (which is more likely if the munition has not been properly embrittled by cooling in the cryobath). The probability of such a press failure has been estimated by the CCDP's designers as 10^{-4} per cycle (Spritzer, 1988). The press force and stroke sensors are assumed to signal the problem and stop the process with a conditional probability of nearly unity. (Otherwise an intact munition may enter the kiln (see PC 417).

Although the next step probably should to be a precautionary closure of the door of the airlock from which the press is fed, no decision has yet been made to automate the closure, which might lead to unnecessary airlock door cycling and perhaps a mechanical hazard to maintenance workers. Therefore, based on the non-routine situation of a failure to fracture, and the fact that the failure to close the airlock door is an act of omission rather than commission, its conditional probability has been assumed to be close to unity.

Next, when the press is raised in an attempt to check, recycle or remove the munition, the conditional probability that the munition will detonate is assumed to be 10^{-4}, because of the possibility that the failure to fracture will have sensitized the munition. (Otherwise, a 10^{-6} conditional probability of detonation would have been assumed - see below.) Finally, the conditional probability of a sympathetic detonation (such as might be caused by a fragment from the initial detonation in the press) in the open airlock is assumed to be 10^{-2}, based primarily on the relatively high effectiveness of fragments from a non-embrittled munition (recall the possible reasons for press failure cited above) at detonating an embrittled munition. Note that this sequence involves common cause (lack of embrittlement causing both failure to fracture, and success at sympathetic detonation). The probability of the accident is 10^{-10} per cycle.

The munitions that could be involved in this accident scenario and result in a lethal release to the environment are the burstered items that have sufficient explosive and propellant quantities to fail the containment structure, and sufficient agent quantities to cause public fatalities. The items include land mines, 8-inch projectiles and rockets.

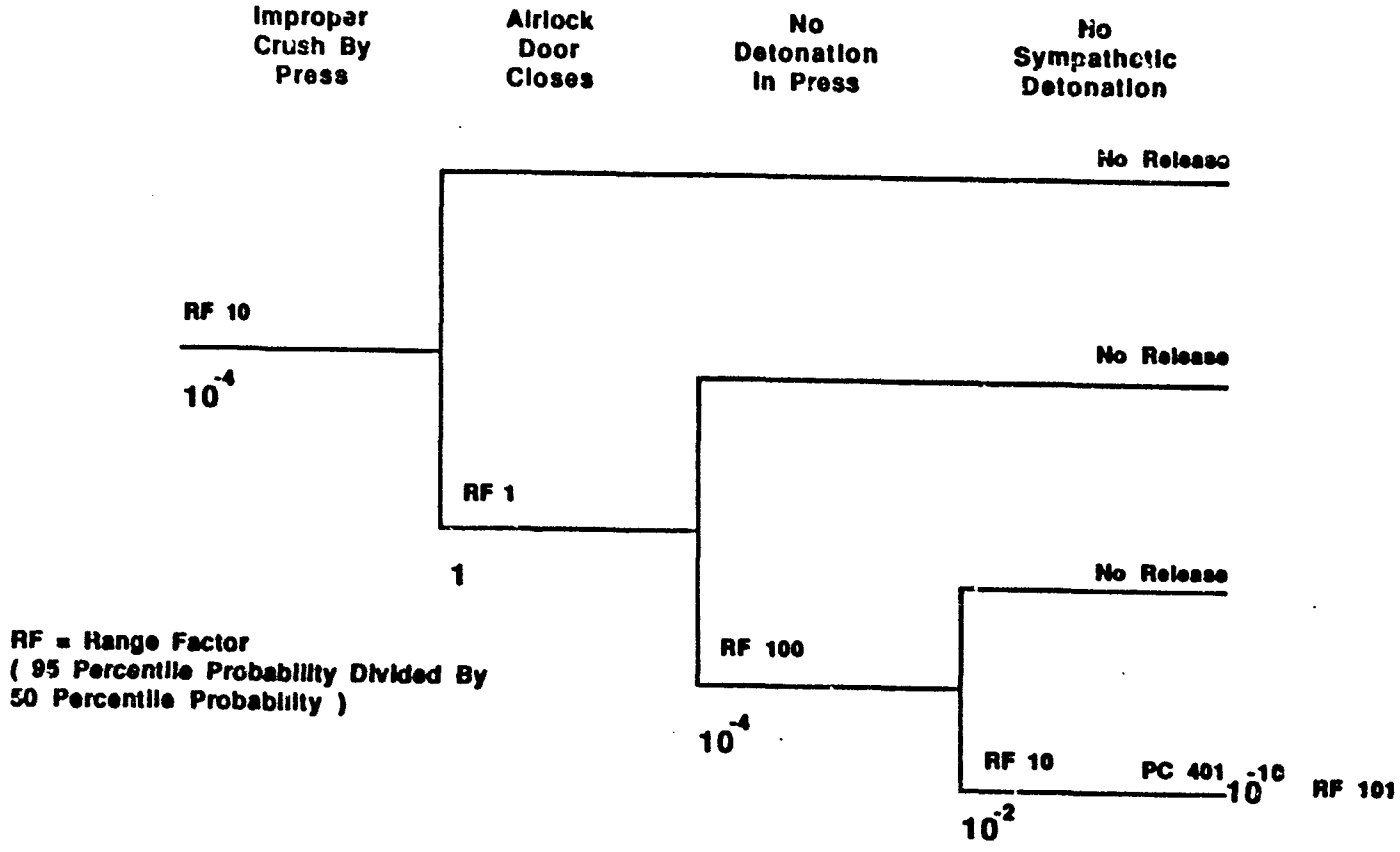

FIGURE 2-1
EVENT TREE FOR SCENARIO PC 401

PC 402. This scenario involves a single detonation due to a minor impact in the cryobath. Since the cryopretreatment area is not currently specified to contain explosions, and the cryobath contains a significant inventory of embrittled munitions subject to breakage in the event of a nearby explosion, this scenario was considered to be of interest as a contributor to public risk.

The event tree for this scenario is shown as FIGURE 2-2. The accident is initiated by a minor mechanical impact that would not be ordinarily expected to result in the detonation of a munition. The impact could result from a munition being dropped or misplaced in the bath, or by an object such as a robot arm end effector or other part falling on or otherwise striking a munition that is already in the bath. Included is the possibility that a munition being placed in or taken out of the bath drops on or otherwise strikes another munition in the bath. At this early point in the design, specification and testing program, the probability of such a minor mechanical impact was assumed to be 10^{-3} per item cryocooled, based on the fact that each item is at risk of being struck several times (during its placement and removal, and during the placement and removal of other items).

In order to be consistent with the CSDP risk analysis (GA Technologies, 1987b), the conditional probability that the minor mechanical impact will result in a detonation was assumed to be 10^{-6} per impact. Thus, the accident probability is 10^{-9} per item cryocooled. Note that the possibility of detonation in the cryobath was not considered to be credible for cases involving boxed, drummed or otherwise packaged munitions (105mm cartridges, 4.2-inch mortar rounds, land mines and rockets) because the minor mechanical impact would be almost entirely absorbed by the packaging materials.

If a single item detonates in the cryobath, it was assumed based on cryogenic test data that only the adjacent items in view of the detonated item would be fractured. Again from the CSDP risk analysis, the items being fractured were assumed to number eight, based on a square arrangement with the fractured items being in 0, 45, 90, 135, 180, 225, 270 and 315 degree directions from the detonated item. The entire amount of agent contained in one-fourth, or two, of the fractured items was assumed to be released immediately to the outdoor atmosphere (probably through the roof of the plant), along with all of the agent in the detonated item. During the subsequent six hours, it was assumed that essentially all of the remaining spilled agent (the contents of six items) would evaporate into the atmosphere if the agent were the relatively volatile GB, but that only an insignificant fraction of the spilled HD or VX would evaporate.

The munitions that could be involved in this accident scenario and result in lethal releases to the environment include the projectiles that contain sufficient quantities of agent to cause public fatalities. The

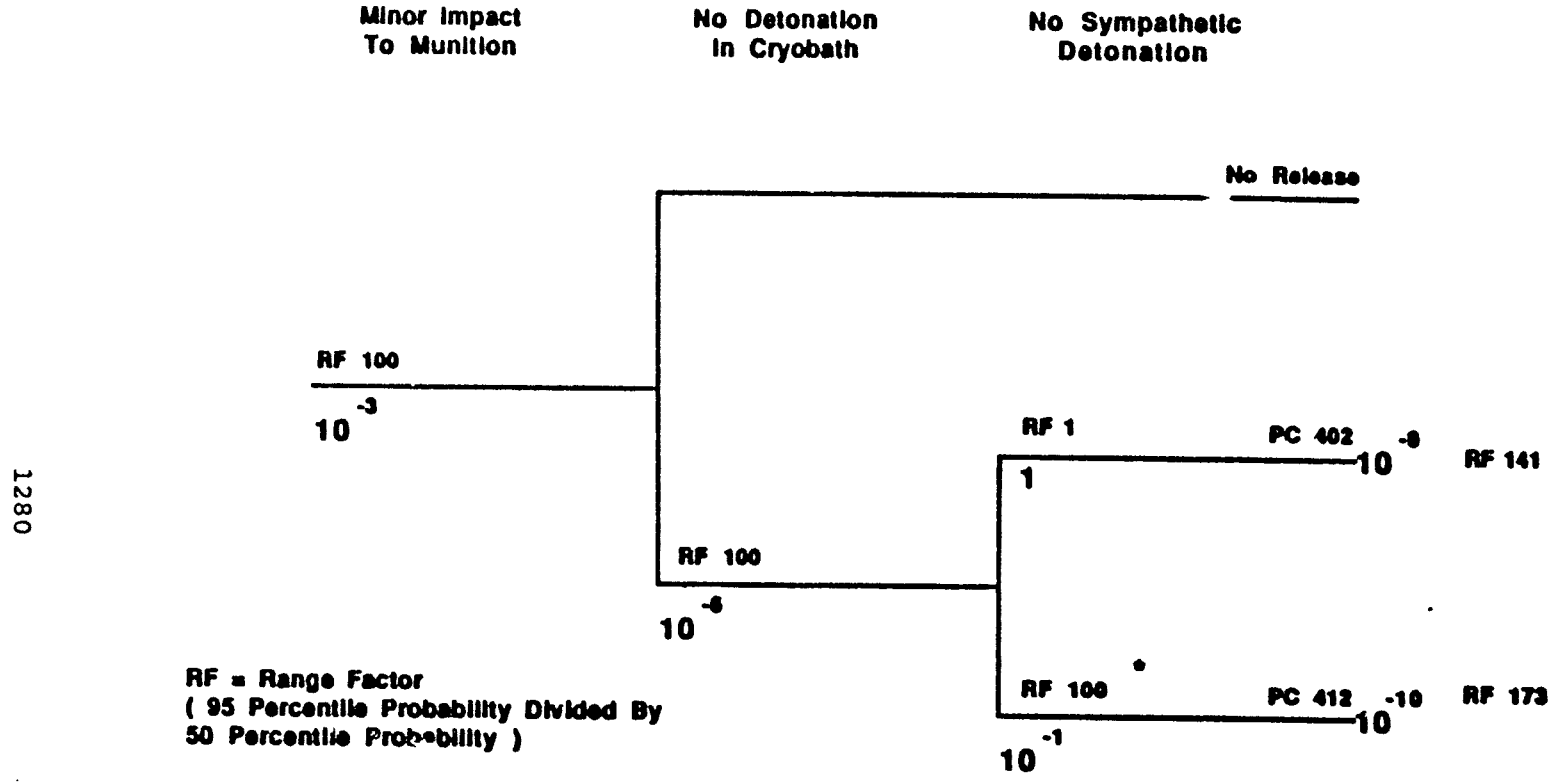

FIGURE 2-2
EVENT TREE FOR SCENARIOS PC 402 AND PC 412

items include are 155mm projectiles with GB or VX, and 8-inch projectiles with GB or VX.

PC 405. This scenario involves the detonation of an item that inadvertently has entered the dunnage chute. This possibility was considered to be of interest because the dunnage system is not currently specified to provide explosion containment.

The event tree for this scenario is shown as FIGURE 2-3. The accident is initiated by the inadvertent entry of an explosively configured item into the dunnage chute. This event was assumed to have a probability of 10^{-4} per item (except in the case of rockets, which were assumed to be too long to enter the chute). It could occur as a result of a failure to lift and deliver, or a miscount, during robotic unpacking. The metal detector in the dunnage chute was assumed to detect the item, alert the operator and result in a shut-down of the system with a conditional probability of close to unity. However, the subsequent attempt to remove the item was assumed to result in a detonation with a conditional probability of 10^{-6}.

An alternative possibility is that the item eludes detection, or otherwise progresses to the two-stage shredder, with a conditional probability of 10^{-2}. After possible impairment and sensitization by the shredder, and the attempted extraction of the item with a conditional probability near unity, the conditional probability of detonation can be assumed to have increased from 10^{-6} to 10^{-4}.

In either case, the probability of the accident is 10^{-10} per item. (The factor of two for the two alternative paths is insignificant, and thus neglected.) The munitions that could be involved in this scenario and result in a lethal release of agent to the environment include the burstered items with sufficient quantities of agent to cause public fatalities. the items include are 8-inch VX projectiles and drums of land mines.

PC 412. This scenario is similar to PC 402, except that more munitions become involved. Specifically, the initial detonation in the cryobath was assumed to result in the secondary or sympathetic detonation of one of the eight adjacent munitions.

The event tree for this scenario is shown as Figure 2-2. The conditional probability of the sympathetic detonation was assumed to be 10^{-1}, based primarily on the possibility that the primary detonation may involve a non-embrittled item whose fragments can be expected to penetrate the bursters of adjacent munitions. (Refer to the above description of PC 401, but consider that the munitions in the press and airlock are separated by a greater distance, hence the 10^{-2} used for the conditional probability of the PC 401 sympathetic detonation.) Thus, the accident probability is 10^{-10} per item cryocooled.

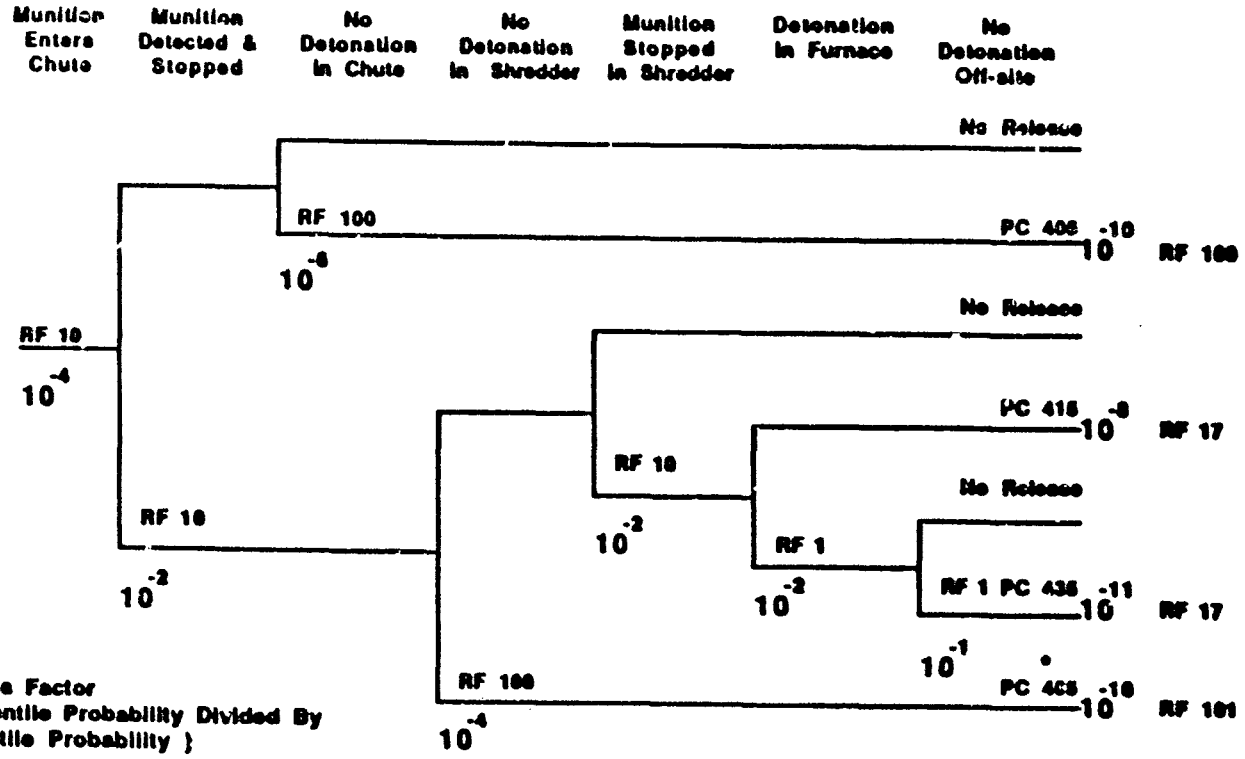

FIGURE 2-3
EVENT TREE FOR SCENARIOS PC 405, PC 415, AND PC 435

Since the initial detonation was assumed to result in the sympathetic detonation of one of the eight adjacent items, the remaining seven were assumed to be fractured. Then, the sympathetically detonated item was assumed to be incompletely surrounded by intact items, so that only five more would be fractured, resulting in a total of 12 fractured items. Therefore, the entire amount of agent contained in the two detonated items, plus one-fourth, or three, of the fractured items, was assumed to be released immediately to the environment. During the following six hours, the amount of agent equivalent to the remaining nine items was assumed to evaporate, in the case of agent GB. The evaporation of spilled HD or VX was assumed to be insignificant. The munitions involved are the same as those involved in PC 402.

PC 415. This scenario is similar to PC 405, except that the munition reaches the dunnage furnace and explodes. Since the dunnage furnace is not currently specified so as to provide explosion containment, the agent is released into the environment.

The event tree for this scenario is shown as Figure 2-3. The conditional probability of the munition eluding the metal detector or failing to be stopped by the operator was assumed to be 10^{-2}. The conditional probability of an agent-containing munition passing through the shredder in an explodable condition was assumed to be 10^{-2} for the following reasons: (1) the current version of the two-stage shredder specification says nothing about minimum clearances between blades or rotors or their housings, (2) the specified size of shredded material is not specified as an absolute maximum, (3) the existing test data show that 2-inch by 4-inch feed was not always reduced to the specified 1-inch by 2-inch size and in some cases was not reduced at all, and (4) the possibilities of bending, breaking, deterioration, or even faulty specification, design, purchasing or installation, cannot be discounted at this stage of the development of the shredder system. Although this 10^{-2} conditional probability may seem too high, the reader should consider that a defective or deteriorated shredder could operate without failing for an extended period during which only dunnage is processed, and then fail when it is first challenged by a projectile, which is much stronger than dunnage. (Note also that the shredder teeth are not specified at this time so as to preclude their engagement of a munition, e.g., at its lifting ring.) However, land mines were assumed to be too weak (because of their thin walls) to escape shredding.

Therefore, based on a conditional probability of nearly unity for the munition exploding in the dunnage furnace or soon after leaving the furnace (which might occur as a result of the time required for heat to penetrate to the munition's burster tube), the probability of the accident is 10^{-8} per item. The only munition that can reach the dunnage furnace and explode there with a lethal release of agent is the 8-inch VX projectile.

PC 417. This scenario involves the passage of an item in explodable condition into and through the kiln, and the item's subsequent detonation in an area of the plant that (unlike the kiln) does not provide explosion containment.

The event tree for this scenario is shown as FIGURE 2-4. The initiating event is the entry of an explodable, agent-containing item into the kiln, at an estimated probability of 10^{-6} per item. The event could occur if: (1) the item drops from or rolls off the press prior to impact, and if the low press load does not lead to the item's retrieval; or (2) insufficient press load and travel do not lead to its retrieval (see PC 401); or (3) a process control interruption or fault of another type results in the omission of the press cycle; or (4) the tooling fails or is not installed; or (5) the press is bypassed because of a human error; or (6) the kiln is being fed through the dunnage chute and shredder (see PC 415). Based on a conditional probability of 10^{-2} that the item will survive its passage through the kiln, and a conditional probability of nearly unity that the item will subsequently explode or rupture in the hot metal scrap bin, the probability of the accident is 10^{-8} per item.

The selection of a 10^{-2} conditional probability for survival in the kiln is based on the possibility of operation at a residence time of somewhat less than the 53.3 to 58.8 minutes presently contemplated (but not specified in the current design package). This residence time range corresponds to a kiln rotational velocity of one-third of a revolution per minute (plus or minus 0.05 rpm as specified). The maximum kiln velocity is specified as 1.00 ± 0.05 rpm, which corresponds to a minimum residence time in the range of 17.8 to 19.6 minutes. Whether by intent (e.g., after tests showing that design to date has been conservative for the purpose of decontamination fractured items) or by error, it is possible that the residence time will be significantly lower than currently planned. The survival times of items in the kiln have been estimated by MITRE at 13 to 23 minutes, depending on munition, as shown in TABLE 2-4, and are approximated by the results of tests in which rocket warheads (but not propellant) were engulfed in fire (see Darling 1974). The results ranged from 14 to 31 minutes to detonation or rupture. Furthermore, these estimates are considered to include significant uncertainties, and may be in error by a factor of approximately two. For these reasons, MITRE has allowed for the possibility of munition survival at a 10^{-2} conditional probability.

The munitions for which this scenario can lead to a lethal release are land mines (in drums of three) and 8-inch projectiles.

PC 427. This scenario is similar to PC 417, except that the munition is assumed to survive the hot metal scrap bin. The event tree for this scenario is shown as Figure 2-4. The conditional probability of survival in the scrap bin was estimated to be 10^{-3}, based primarily on the possibility that the munition drops into a nearly empty bin whose filling is soon discontinued at the end of the weekly shift. Thus, the munition

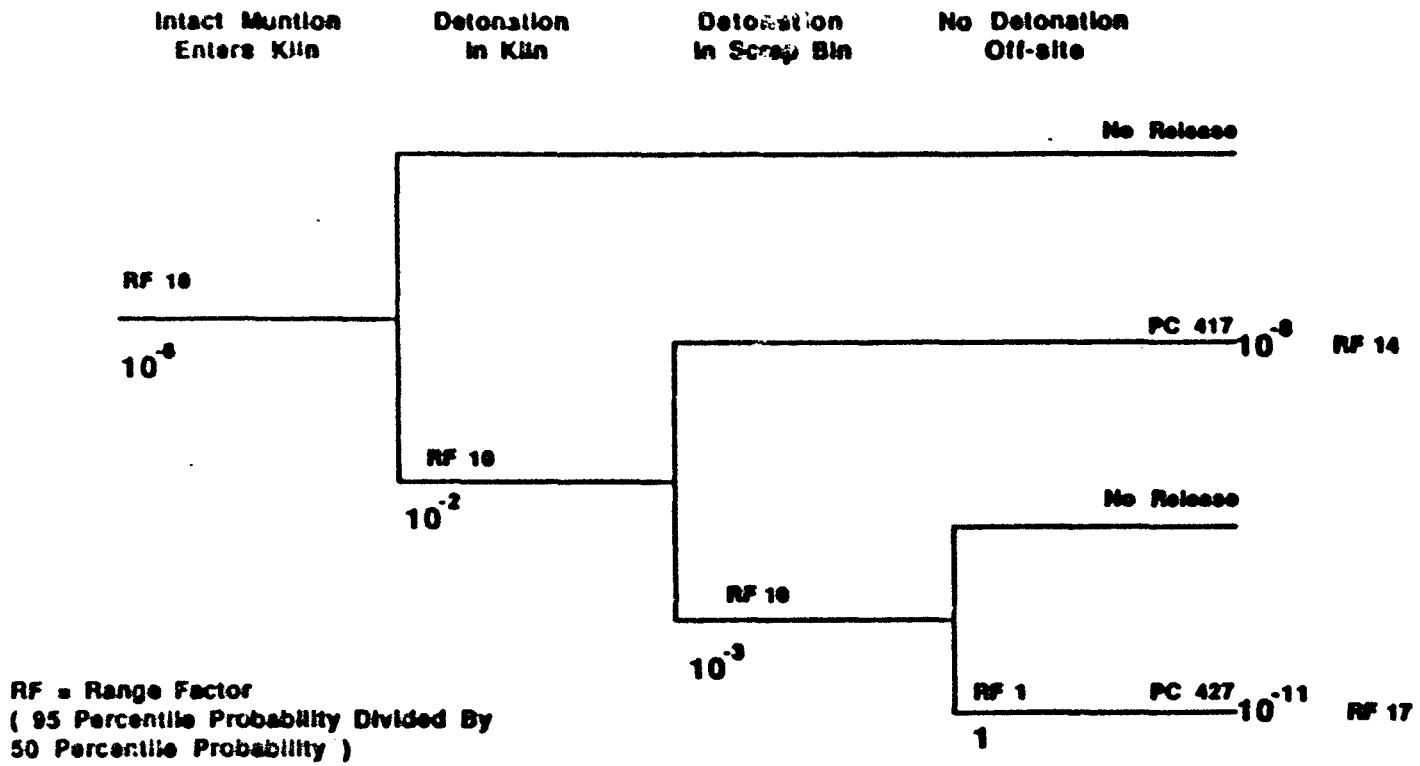

FIGURE 2-4
EVENT TREE FOR SCENARIOS PC 417 AND PC 427

TABLE 2-4
ESTIMATION OF TIMES TO DETONATION
FOR MUNITIONS IN KILN[a]

Munition Code	Metal (#)	Organic (#)	Surface (ft^2)	Time (minutes)
C	30	3[b]	1.4	13
D	19	6[b]	0.9	20
M (3+drum)	50	34	4.4[c]	17
PG&PV	90	9	2.8	20
PH	90	12	2.8	21
Q	183	22	5.1	23
Z	30	3	1.4	13

Notes:

[a]The time to increase from -300F metal and -200F organic to a uniform 400F in 1000F environment is from [Metal # × 0.11 Btu/#F × 700F + Organic # × (30 Btu/# + 0.4 Btu/#F × 600F)]/[(0.8 emissivity × 0.17 × 10^{-8} Btu/hrft^2 R^4 × 1460^4R^4 + 4 Btu/hrft^2 × 1000F) (Area ft^2/60 min/hr)].

[b]Not including the wooden box, which is assumed to be destroyed quickly.

[c]Including only the exposed surfaces on the sides of the three stacked mines.

could be afforded an opportunity to cool before being buried in hot metal scrap. The conditional probability of 10^{-3} was selected based on the relationship of typical munition dimensions and weights to those of the 32 scrap bins to be filled weekly. Each of the 20-ton bins will be about 4-8 feet deep, 8 feet wide and 16 to 26 feet long, and will be respotted along its length at least once during filling to improve the distribution of scrap in the bin.

The surviving item is assumed to detonate away from TEAD, but probably somewhere in the area of Salt Lake City, with a conditional probability of nearly unity. This would be likely to occur in a steel mill as the scrap is remelted in a furnace with a higher temperature and a greater residence time than the kiln at TEAD. The probability of the accident is 10^{-11} per item. The scenario is pertinent for any burstered item except a rocket, which is too long to enter the kiln intact and is too susceptible to propellant ignition to survive passage through the kiln.

PC 435. This scenario is similar to PC 415, except that the munition survives passage through the dunnage furnace with a conditional probability of 10^{-3} (see above). The dunnage furnace is currently estimated to require a residence time in the range of 35 to 45 minutes (which is not currently specified), and must achieve the same level of decontamination of scrap (e.g., metal bands) as the kiln. Thus, the same conditional probability of munition survival was used for both furnaces.

The fault tree for this scenario is shown in Figure 2-3. Since the ash leaving the dunnage furnace is a poor thermal conductor with low bulk density and heat capacity, and is stored in small (1-2 cubic yard) containers filled intermittently, the munition is assumed to survive until it shipment away from TEAD, probably to a landfill but possibly to a recycling facility of undetermined type, with a conditional probability of nearly unity. The item may remain buried for an extended period. It may ultimately detonate or it may deteriorate, safely or otherwise. In order to allow for the possible consequences to public health and safety, the item was assumed to detonate with a conditional probability of 10^{-1}, and otherwise to deteriorate without causing any public fatalities.

The accident has a probability of 10^{-11} per item. It is pertinent for any burstered munition except a land mine (which cannot pass through the dunnage shredder intact) and a rocket (which is too long, too weak-walled and too susceptible to propellant ignition to pass through the dunnage system intact).

2.1.2 Externally-Initiated Events

The only externally-initiated accident scenarios found in the CSDP risk analysis (GA Technologies, 1987b) whose frequencies are of possible significance and whose releases could result in public fatalities are those initiated by earthquakes. The frequencies and range factors of these

scenarios are summarized in TABLE 2-5. For detailed descriptions of the derivation of the frequencies and consequences of these accident scenarios, the reader is referred to the CSDP risk analysis (Fraize *et al.* 1987). The agent release quantities listed there were modified by MITRE in accordance with the CCDP munition inventories (by munition-agent code letters, the numbers of munitions in the plant are 420 CH, 475 CG, 485 DH, 300 MV, 295 PG, 265 PH, 260 PV, 145 QG, 123 QV, 129 RG, 102 RV, or 190 ZG) or to the six pallets of bulk (non-burstered) items assumed in the CSDP risk analysis to be present in the unpack area (UPA). The resulting release quantities correspond to the numbers of munitions listed in Table 2-2.

PC 025. This accident scenario corresponds to CSDP risk analysis scenario PO 025. The accident results from an earthquake that breaches the plant containment structure in the unpack area (UPA), causes a bulk agent container to fall onto a probe and be punctured, and culminates in a fire that involves the entire contents of the container before the fire can be suppressed. For the CCDP, the only bulk agent containers whose releases could result in lethal exposures to the public are ton containers of GB and VX, and spray tanks.

PC 026. This accident scenario corresponds to CSDP risk analysis scenario PO 026. The accident is similar to PC 025, except that the fire is not suppressed, but rather involves the entire inventory of the UPA or the cryofracture processing area, whichever is greater. The munitions and containers that could be punctured and involved in a fire leading to a lethal release include rockets, ton containers, spray tanks, and all types of bombs.

PC 029. This accident scenario, which corresponds to CSDP risk analysis scenario PO 029, results from an earthquake that breaches the containment structure (UPA, cryofracture processing area, or bulk agent collection-incineration area) and subsequently involves the area's entire agent inventory. All 18 munition-agent combinations, as well as bulk agent tanks containing GB or VX, could be expected to result in lethal releases.

PC 033. This accident scenario, which corresponds to CSDP risk analysis scenario PO 033, is similar to PC 029 except that the earthquake does not breach the containment structure. However, the subsequent fire leads to a failure of the structure, and thus to a lethal release of agent. The scenario applies to all burstered munitions as well as to bulk agent tanks containing GB or VX. (The bulk agent tank design and specification is not sufficiently advanced at this time to determine whether its burning would actually fail the containment structure.)

TABLE 2-5
ACCIDENT FREQUENCIES AND RANGE FACTORS
FOR EXTERNALLY-INITIATED EVENTS

Scenario Number	Munition Type	Frequency (events/year)	Range Factor
PC 025	Ton container	1.6×10^{-6}	7
PC 025	Spray tank	8.4×10^{-6}	7
PC 025	Wet-eye bomb	1.9×10^{-7}	7
PC 026	Ton container	4.9×10^{-8}	13
PC 026	Rocket	1.0×10^{-8}	14
PC 026	Spray tank	2.7×10^{-7}	13
PC 026	Bomb	6.1×10^{-9}	13
PC 029	All	2.2×10^{-5}	10
PC 033	All	4.8×10^{-5}	20

2.2 Unidentified and Unquantified Events

No list of accident scenarios can be expected to include all possible event sequences. For the present risk analysis, the goal was to include scenarios that would represent fairly but conservatively the risks inherent in the cryofracture process as described in the 60 percent process design submittal--risks such as those inherent in robotic unpacking, cryocooling, cryofracturing, and incineration of munitions and dunnage. As the process design continues toward completion, as the facility design develops, and as additional test data become available, additional accident scenarios should be identified and analyzed.

Already, numerous types of hazards have been identified that will require consideration as additional information becomes available. The hazards that appear to be of greatest concern in this regard are the following:

- The possibility of the accumulation of liquid oxygen in the cryo-baths or elsewhere.
- The possibility of the accumulation of excess explosive material at the press.
- The possibility of the accumulation of flammable or explosive mixtures in the feed chute.
- The possibilities for accidents (including but not limited to earthquake-related spills) involving the bulk agent collection, metering and feeding system.
- The possibility of the loss of kiln or afterburner function for a period of sufficient length to release a lethal quantity of agent. For example, this could occur if excess liquid nitrogen were to be fed to the kiln.
- The possibility of the inadvertent release from TEAD of agent-contaminated solids or liquids.
- The possibility of an internally-initiated fire that involves the agent inventory and fails the structural containment (possibly by penetrating the HVAC system). However, the consequences of facility-wide fires are already represented by the earthquake-initiated accident scenarios, whose conservatively-high estimated frequencies appear to be adequate to represent those of all such fires, regardless of their modes of initiation.

3.0 RESULTS AND CONCLUSIONS

The results of this risk analysis have been described in terms of risk measures whose definitions and significance are presented in several other papers and reports that describe CSDP risk analyses. (As in these other studies, in order to obtain accident frequency estimates [in units of events per year], the accident probability estimates [in units of events per munition] were multiplied by CCDP processing rates [in units of munitions per hour], multiplied by a 6,000 hour per year processing period, and divided by the 18 munition-agent combinations assumed to share equally in each year's processing time.) The single measure that combines consequence and frequency is the fatality expectation value or "expected fatality value," which is the product of fatality count and frequency (or the sum of several such products). Several major conclusions can be drawn from this risk analysis:

- The accident scenarios described in this paper were of necessity analyzed on a subjective basis. This was necessary because of the limited detail of the Sixty Percent Process Design submittal, the absence of a facility design when the work was undertaken, the lack of data from tests that have been scheduled but not yet performed, and the limited time that was available for the completion of this study. The principal quantitative results representing risk to the public are summarized in TABLE 3-1.

- Based on the accident scenarios analyzed in this paper, which include only accidents that would be expected to result in public fatalities, the minor mechanical impact-initiated detonations of projectiles containing nerve agents in the cryobaths (scenario numbers PC 402 and PC 412) occurs with the greatest frequency (0.00044 per year, with a 95 percentile value of 0.065 per year).

- The greatest lethal downwind distances (up to 33 kilometers from the CCDP) are associated with large-scale fires involving the CCDP inventory (scenario numbers PC 026, PC 029 and PC 033). These fires could be initiated by external events such as earthquakes, or by internal events such as electrical faults or combustible fluid leaks. These scenarios are also associated with the maximum public fatality counts in the TEAD area (up to about 1,000), which are shown as the horizontal intercept of the TEAD area risk curve, FIGURE 3-1.

- Cartridges, mortar rounds, land mines and projectiles that enter and pass through the furnaces intact, leave the TEAD area buried in ash or scrap containers, and subsequently detonate in a more densely populated area such as Salt Lake City (scenario numbers PC 427 and PC 435) result in the greatest contribution to the fatality expectation value (0.0024 "expected fatalities" per year, with a 95 percentile value of 0.041 per year). These scenarios are also

TABLE 3-1

RISK CONTKIBUTIONS BY CRYOFRACTURE PLANT ACCIDENT SCENARIO

Scenario	Expected Fatalities No.	Pct.	Frequency Per Yr. Rate	Pct.	Max. Lethal Distance (km)	Max. Fatalities	Est. Worker Casualties
PC025	Negligible	0	Negligible	0	6	1	8
PC026	Negligible	0	Negligible	0	21	1072	15
PC029	0.0001	3	0.00002	3	33	1072	15
PC033	0.0005	14	0.00008	13	33	1072	8
PC401	Negligible	0	0.00001	2	11	2	3
PC402	0.0003	10	0.00033	58	11	2	1
PC405	Negligible	0	Negligible	0	5	1	2
PC412	0.0001	3	0.00010	18	14	2	1
PC415	Negligible	0	0.00001	1	4	1	1
PC417	Negligible	0	0.00001	2	5	1	1
PC427	0.0012	35	0.00001	2	5	2272	0
PC435	0.0012	33	0.00001	2	4	894	0

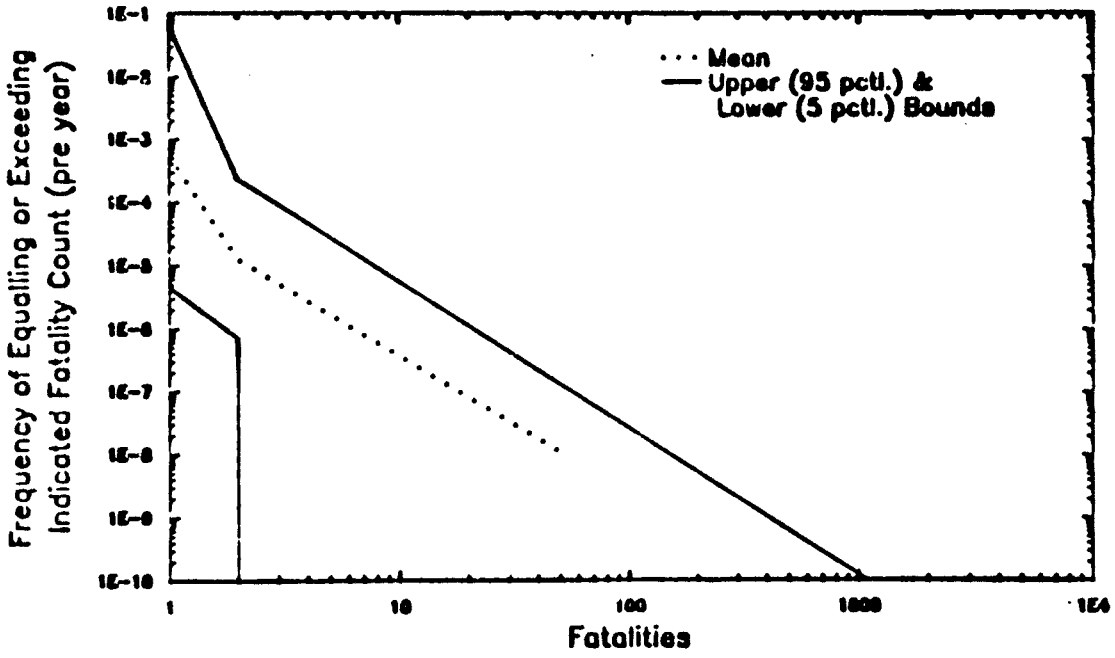

FIGURE 3-1
COMMUNITY RISK FOR THE CCDP: TEAD AREA

associated with the maximum public fatality counts (up to about 2,000, which corresponds to a lethal downwind distance of 5 kilometers). The maximum public fatality counts are shown as the horizontal intercept of the Salt Lake City area risk curve, FIGURE 3-2.

- The remaining scenarios whose contributions to the total public risk have been analyzed involve small-scale fires (scenario PC 025), detonations initiated at the press and propagated to the airlock (scenario PC 401), detonations of munitions entering the dunnage chute (scenario PC 405), detonations of munitions reaching the dunnage furnace (scenario PC 415), and detonations of munitions reaching the scrap bins (scenario PC 417). The contributions of these scenarios to risk are probably relatively small, but this conclusion is not definite because of the uncertainties associated with the analysis.

- The total frequency of all accidents analyzed that would be expected to result in public fatalities is 0.00058 per year, with a 95 percentile value of 0.068 per year. This result is shown as the vertical intercept of the risk curve for the TEAD area, Figure 3-1.

- The total expected fatality value pertaining to the general public for all accidents analyzed is 0.0035 per year, with a 95 percentile value of 0.12 per year. This is equivalent to the area under the risk curve (if it was redrawn using rectilinear rather than logarithmic scales) for the TEAD-Salt Lake City region, FIGURE 3-3.

- The maximum risk (in terms of fatality frequency) to an individual assumed to be located at the TEAD boundary, 3.3 kilometers from the CCDP, is 3.5×10^{-6} per year, with a 95 percentile value of 0.00049 per year. This result is shown on the individual risk curve for the TEAD area in FIGURE 3-4

- The maximum risk to an individual assumed to be located 0.1 kilometers from an agent release at an indeterminate location away from TEAD is 3.9×10^{-7} per year, with a 95 percentile value of 6.6×10^{-6} per year. (See Figure 3-4.)

- Agent-related worker casualty estimates have been tabulated only for accidents resulting in public fatalities. The frequency of such worker casualties is 0.00056 per year, with a 95 percentile value of 0.068 per year. The maximum number of worker casualties is estimated to be 15 (out of the average number of personnel per shift, 33). The expected value of worker casualties is 0.0013 per year, with a 95 percentile value of 0.072 per year. These expected fatality values are approximately equal to those for the general public in the area of TEAD. The average risk to any one of the 99 workers directly involved in plant operation, maintenance and

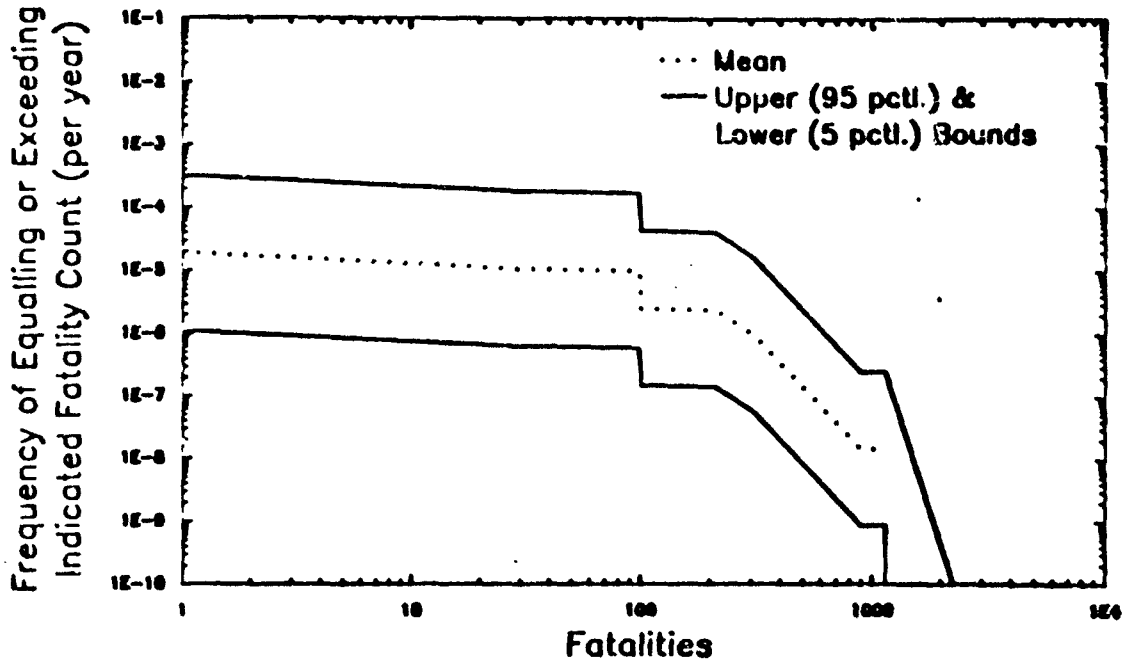

FIGURE 3-2
COMMUNITY RISK FOR THE CCDP: SLC AREA

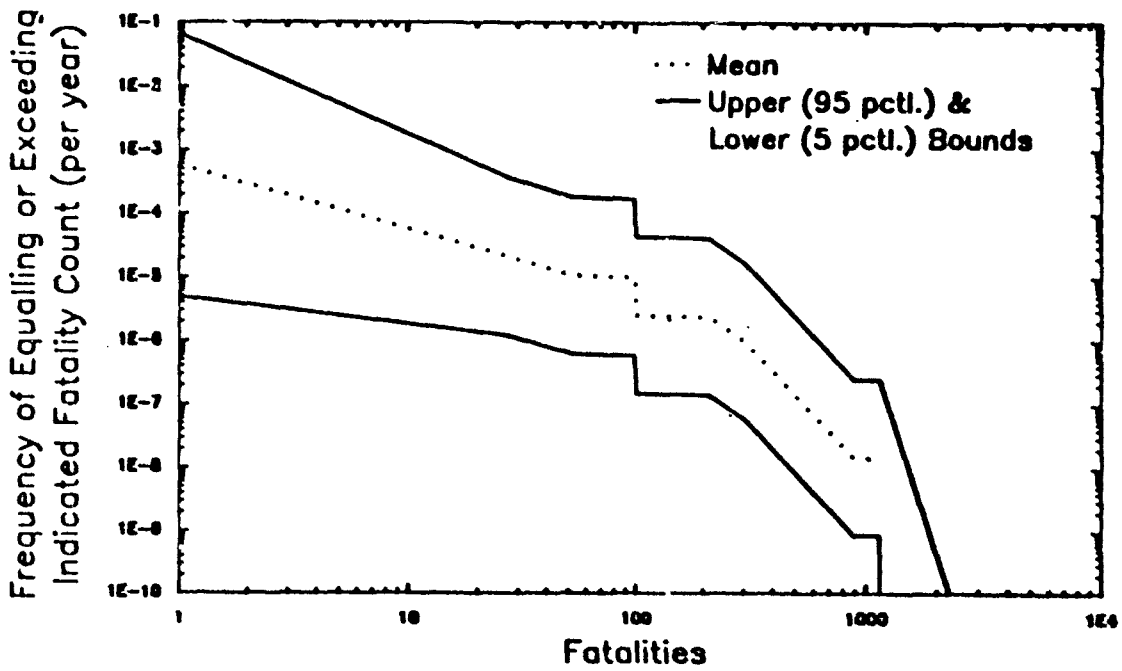

FIGURE 3-3
REGIONAL RISK FOR THE CCDP

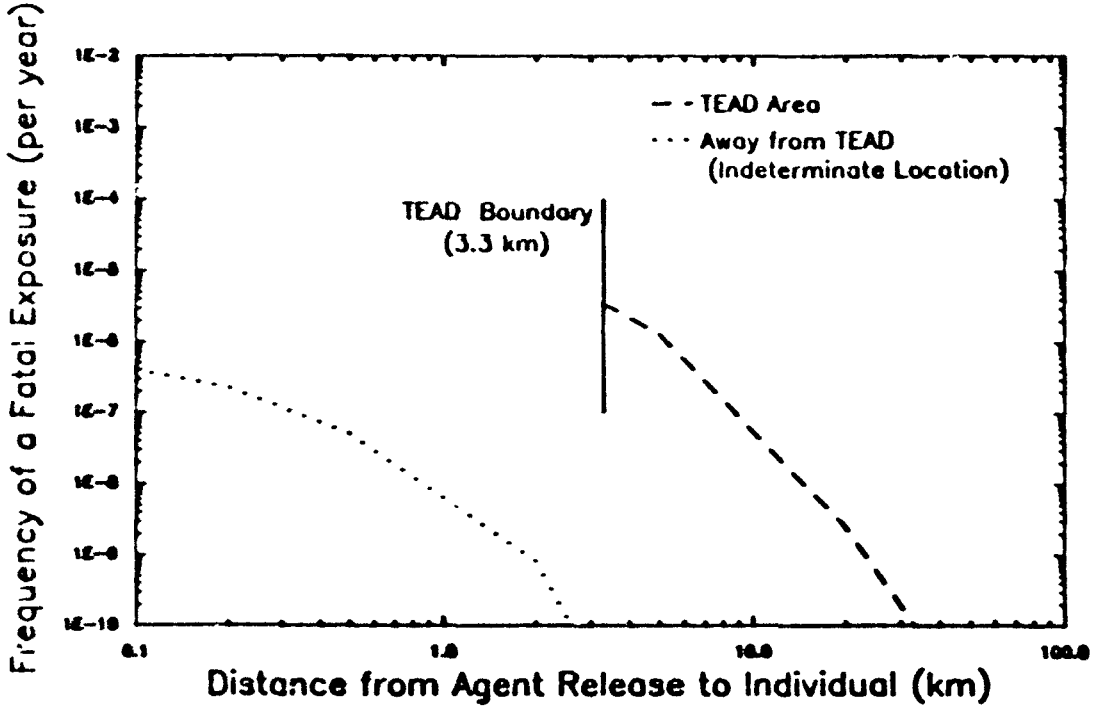

FIGURE 3-4
INDIVIDUAL RISK FOR THE CCDP

monitoring is 1.3×10^{-5} per year, with a 95 percentile value of 0.00073 per year.

- The risks associated with numerous hazards have not been analyzed yet. Many of these hazards are listed in this report, and others have not yet been identified. The identified but incompletely analyzed hazards that appear to be of greatest concern involve accumulations in various locations of liquid oxygen, excess explosive material, or flammable or explosive mixtures; faults in the design or operation of the bulk agent collection, metering and feeding system; the loss of the thermal agent destruction function, such as might occur if excess liquid nitrogen were fed to the kiln; and the inadvertent release of agent-contaminated solids or liquids from TEAD.

- The results presented in this report are not final. Estimates of risk will increase insofar as additional hazards are identified and analyzed. However, estimates of risk will decrease as design and testing proceed, and as hazards are mitigated. Ultimately, through the application of established risk management principles and practices, the estimated risk of the cryofracture process should be determined to be acceptable to the Army and to the public.

4.0 RECOMMENDATIONS

The cryofracture risk analysis reported here has lead us to submit the following recommendations.

- The initial, subjective estimates of probabilities, frequencies, uncertainties and release characteristics should be improved as additional design detail and test data become available.

- Additional hazard identification should be performed, and both the newly identified hazards and the hazards already identified but not yet analyzed should be incorporated into the risk analysis. Of greatest concern at this time are hazards involving accumulations of liquid oxygen, excess explosive material, or flammable or explosive mixtures; faults in the bulk agent system; loss of thermal destruction (including the feeding of excess liquid nitrogen); and inadvertent release of agent-contaminated wastes from TEAD.

- These improvements and extensions to the risk analysis should be undertaken on a schedule coordinated with the availability of major design submittals, such as the 35 percent, 60 percent, 95 percent and 100 percent facility designs, as well as the 95 percent and 100 percent process designs. If significant test data become available after design is complete, the risk analysis should be updated again, as well as in conjunction with any additions or changes that

occur during purchasing, construction, installation, inspection, start-up, etc.

- Additional testing should be considered where necessary to better define hazards and risks. Examples of areas of current concern include oxygen condensation and accumulation on cryocooled surfaces, press clearing between cycles, feed chute and bulk feed system atmospheres, and the effect of liquid nitrogen carryover into the Thermal Destruct System. Such testing would require the careful development and execution of test plans at a suitably configured and operated facility.

- Mitigation should be implemented wherever unacceptable risks are thought to be present in the process, until re-analysis demonstrates that the risks are acceptable. Wherever possible, reductions of both probabilities and consequences should be considered. Where possible, hardware changes should be made instead of software changes, and either type should be preferred to administrative controls. In order to maximize the effectiveness of risk management, these measures should be performed as early in the program as possible, and should be continued at all stages in order to maximize the safety of cryofracture plant operations.

REFERENCES

Darling, B.W. (April 1974). 115mm Rocket Sensitivity Tests, AEO Project T-222, Chemical Demilitarization Project No. 200. U.S. Army Ammunition Equipment Office, Tooele Army Depot, UT.

Fraize, W.E. *et al.* (December 17, 1987). Risk Analysis Supporting the Chemical Stockpile Disposal Program (CSDP), MTR-87W00230, McLean, VA: The MITRE Corporation, prepared for the U.S. Army Office of the Program Executive Officer - Program Manager for Chemical Demilitarization, Aberdeen Proving Ground, MD.

GA Technologies Inc. (February, 1987a). Sixty Percent Process Design for the Cryofracture Chemical Demilitarization Plant (CCDP) at Tooele Army Depot, Tooele, Utah, Document 907531. Prepared for the U.S. Army, Office of the Program Executive Officer - Program Manager for Chemical Demilitarization, Aberdeen Proving Ground, MD.

GA Technologies Inc. (August, 1987b). Risk Analysis of the Onsite Disposal of Chemical Munitions, GA-C18562. Prepared for the U.S. Army, Office of the Program Executive Officer - Program Manager for Chemical Demilitarization, Aberdeen Proving Ground, MD.

Kline, J. (September 15, 1986). U.S. Army Toxic and Hazardous Materials Agency, Aberdeen Proving Ground, MD. Personal communication to The MITRE Corporation, McLean, VA.

Perry, R.H. and C.H. Chilton, editors (1973). Chemical Engineer's Handbook, 2nd edition, McGraw-Hill. New York, NY.

Spritzer, M. (1988). GA Technologies Inc., San Diego, CA. Personal communication with R.M. Cutler, The MITRE Corporation, McLean, VA.

U.S. Army Toxic and Hazardous Materials Agency (March 15, 1986). Chemical Stockpile Disposal Concept Plan, AMXTH-CD-FR-85047. Aberdeen Proving Ground, MD.

Whitacre, C.G. *et al.* (1987). Personal Computer Program for Chemical Hazard Prediction, CRDEC-TR 87021. Aberdeen Proving Ground, MD: Chemical Research, Development and Engineering Center.

Wilson, W. *et al.* (January 1988). Hazards Associated with the Cryofracture Chemical Demilitarization Plant at Tooele, Utah, Science Applications International Corporation, San Diego, CA.

SPECIAL EQUIPMENT FOR DEMILITARIZATION OF LETHAL CHEMICAL AGENT FILLED MUNITIONS

Franklin D. Seat and Mark M. Zaugg
Ammunition Equipment Directorate
Tooele Army Depot, Tooele, Utah

From the beginning of the programs to demilitarize lethal chemical agent filled munitions, the Ammunition Equipment Directorate, (AED), has been involved in the design, development, testing, fabrication, and building of specialized chemical munitions demil equipment.

Over the years, the demil programs at Rocky Mountain Arsenal, and at the Chemical Agent Munitions Disposal System (CAMDS), Tooele Army Depot, AED has provided most of the equipment used in disassembly, draining, shearing, sawing, or otherwise preparing the munitions for destruction by incineration. Operations featuring this equipment have been featured in previous DoD Explosive Safety Seminars. This report provides a brief description of the latest generation of specialized equipment to be used in the Johnston Atoll Chemical Agent Disposal System (JACADS), on Johnston Atoll, and which may also be used in the Stockpile Disposal Plants currently scheduled to be constructed at each chemical munitions storage site.

That which follows is a general description of the five major machines involved with the disposal of the entire variety of munitions in the lethal chemical stockpile.

Multi-Purpose Demil Machine

Multi-Purpose Demil Machine (MDM), Figure 1 is designed to remove the burster well and drain the agent from a variety of chemical agent filled projectiles. The empty projectile with the burster well is then fed into a deactivation furnace for thermal deactivation.

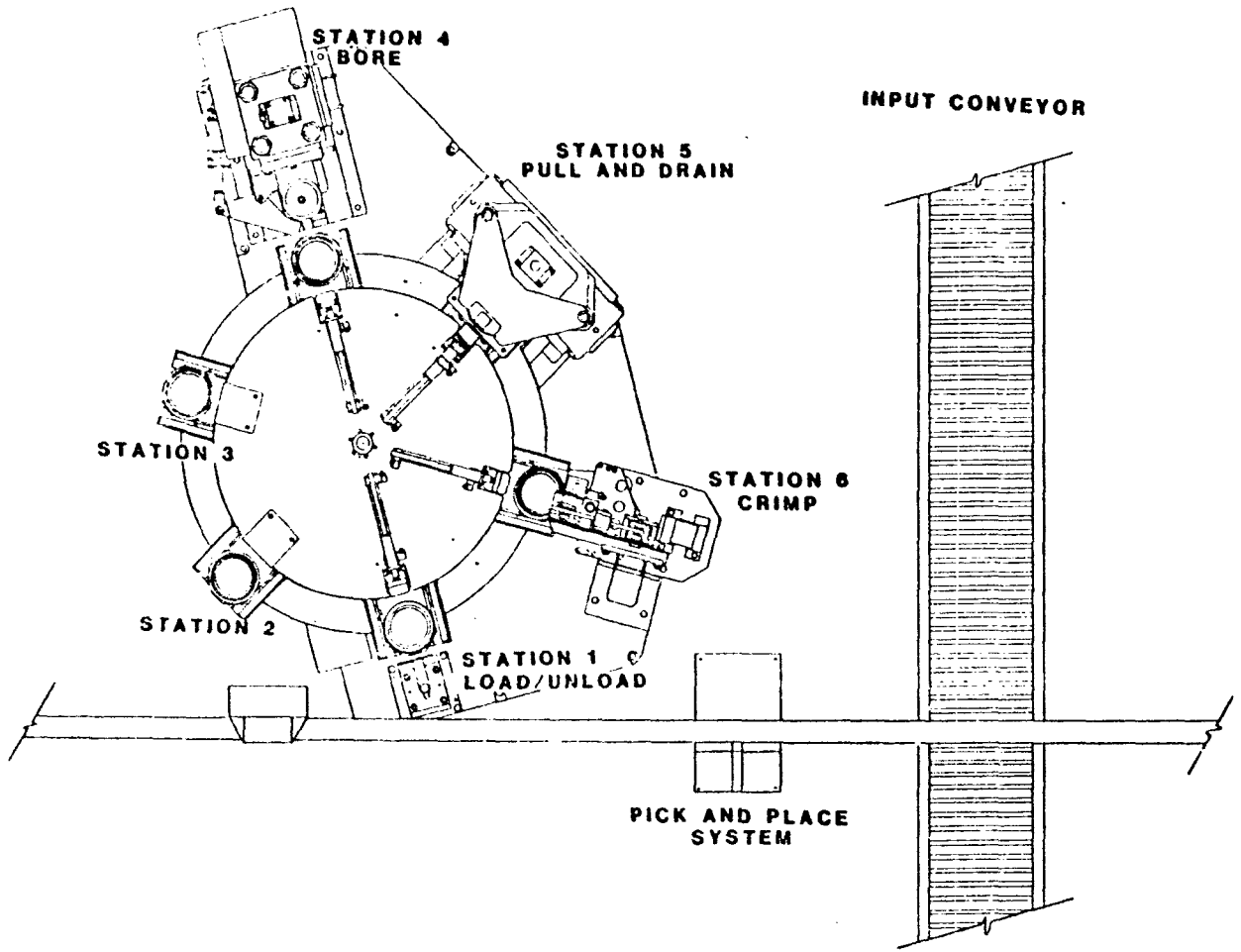

FIGURE 1. MULTI-PURPOSE DEMIL MACHINE.

The MDM is capable of removing the burster well and draining the agent from the following projectiles:

Projectile, 8 inch, M426
Projectile, 155mm, M110, M121, and M121A1
Projectile, 105mm M60, and M360
Mortar, 4.2 inch, M2, and M2A1

The MDM consists of the following stations or assemblies:

Indexing Conveyor Assembly
Pick and Place System (PPS)
Load/Unload Station
Bore Station
Pull and Drain Station
Burster Well Crimp Station
Controls and Instruments for Machine Operation

The MDM is operated automatically by a Programmed Logic Controller, (PLC). A Local Maintenance Panel is also provided for operating the machine locally while performing machine maintenance. The production capability of the MDM is from 55 to 75 projectiles per hour depending on projectile size.

Projectile Mortar Disassembly Machine

The Projectile Mortar Disassembly (PMD) Machine, Figure 2, is a multipurpose machine that is designed to remove the explosive components from a variety of chemical agent filled munitions. The explosive components are then fed into a Deactivation Furnace for thermal destruction, and the chemical filled munitions, now minus the explosives, are sent to the MDM described earlier.

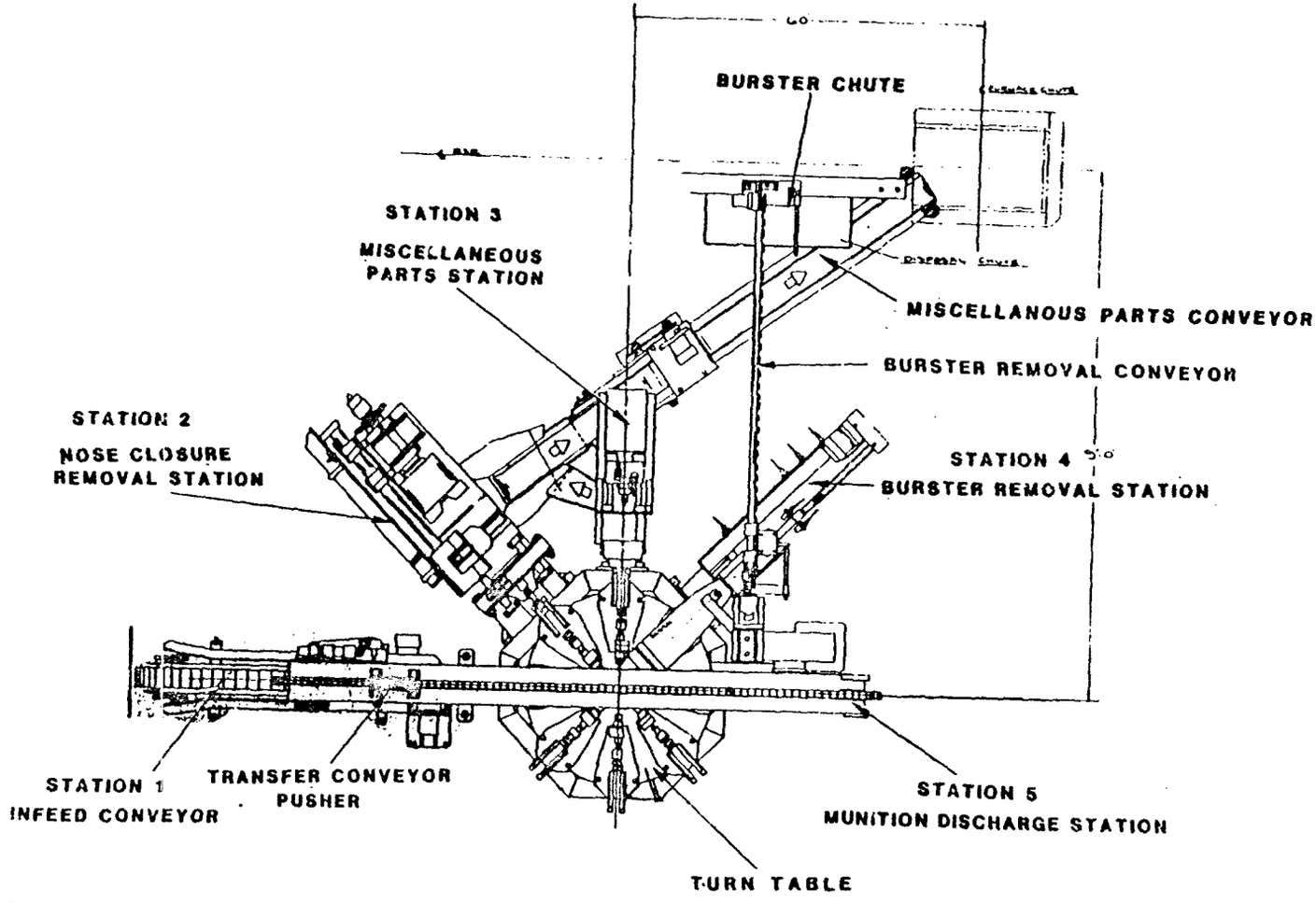

FIGURE 2. PROJECTILE MORTAR DISASSEMBLY MACHINE (PMD).

The PMD Machine is capable of removing the nose closures, fuzes, supplementary charges and support cups, and bursters from the following chemical munitions;

105mm, (M60)
105mm, (M360)
155mm, (M110)
155mm, (M121 and M121A1)
8 inch, (M426)
4.2" mortar, (M2 and M2A1)

The PMD machine is capable of removing the PD M557 Fuze from 105mm, (M60 and M360) projectiles and then punching the booster cup to allow it to burn without detonation. It can also remove the M8 fuze from a 4.2" mortar (M2 and M2A1) and separate the burster from the fuze for processing through the Deactivation Furnace.

The PMD consists of five stations: A munition Infeed/Transfer Station, a Nose Closure Removal Station (NCRS) where fuzes or lifting plugs are removed, a Miscellaneous Parts Removal Station (MPRS) where supplementary charges or fuze well cups are removed, a Burster Removal Station (BRS), and a Munitions Discharge Station. The machine also has a Miscellaneous Parts Conveyor and a large Index Table to accommodate a maximum of eight munitions. A Local Maintenance Control Panel (LMCP) is also provided for operating the machine locally while performing machine maintenance.

The production capabilities vary, depending on the operations to be completed; however, the approximate production rates are listed in Table 1.

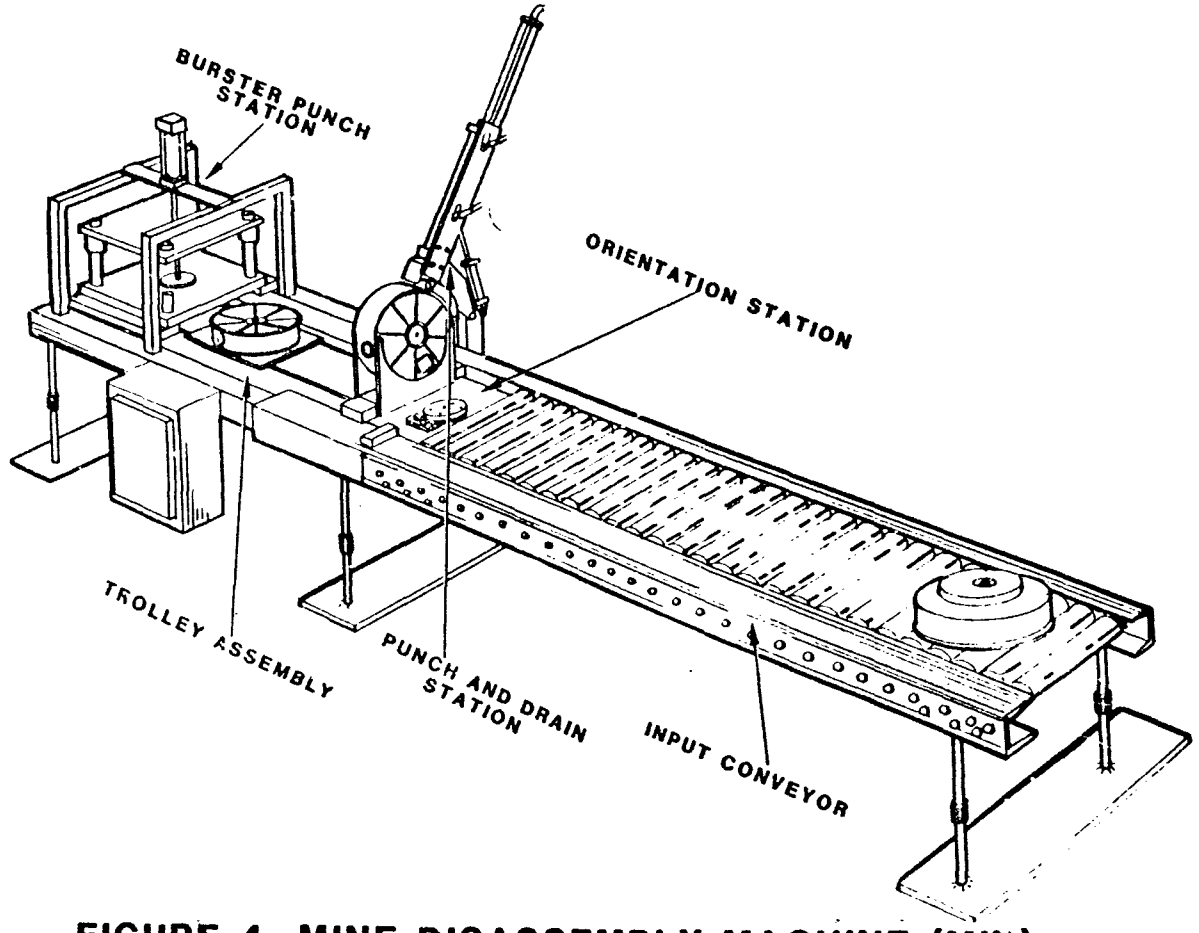

FIGURE 4. MINE DISASSEMBLY MACHINE (MIN).

TALBE 1. PMD PRODUCTION RATES (PROJECTILES PER HOUR).

MUNITIONS	MODEL	PEAK
4.2 mortar	M2 & M2A1	137
105mm	M60	143.8
105mm	M360	143.8
155mm	M110	138
155mm	M121 and M121A1	138
8 Inch	M426	45.4

The time period between start and stop operations, at each particular sequence of operation is controlled by a series of proximity sensors and hydraulic valves.

Munitions enter the machine base end first to allow them to be positioned onto the index table ready for disassembly operations.

The PMD Machine is provided with special kits for each munition to be processed.

Rocket Shear Machine

The Rocket Shear Machine (RSM), Figure 3, consists of a Rotate and Drain Station, a Rocket Transport Assembly, a Shear Station, a Fuze Segregator, and Controls and Instruments for operating the machine. A Local Maintenance Control Panel is also provided for operating the machine locally while performing machine maintenance.

The RSM is designed to punch and drain the agent from M55 rockets and then shear them into five sections for burning in the deactivation furnace. The production capability of the RSM is one rocket per minute or

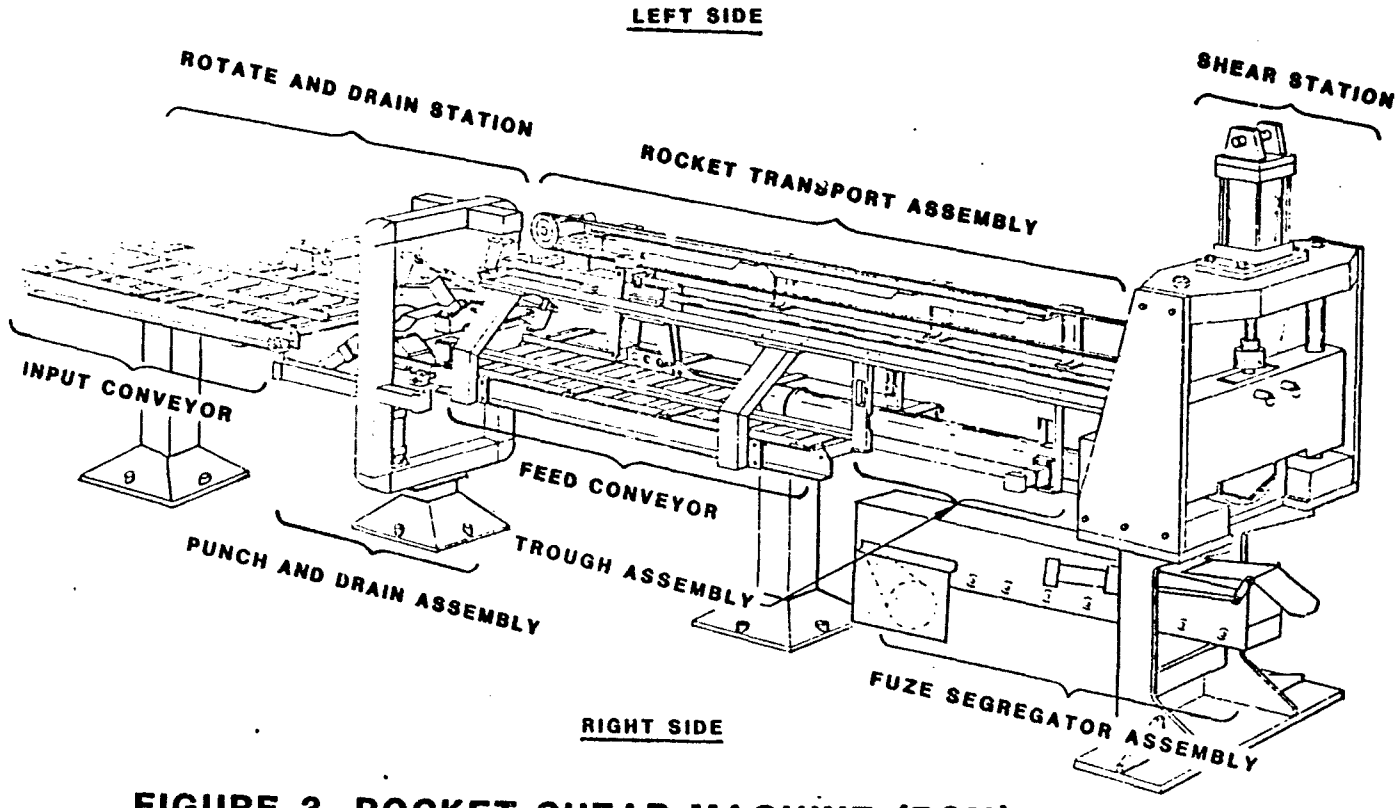

FIGURE 3. ROCKET SHEAR MACHINE (RSM).

60 per hour. During operation the machine will process two rockets simultaneously. While one rocket is being sheared, another is being drained. The rockets must be placed in the machine fuze end forward to insure the warhead is punched and drained. With the application of a special kit, the RSM can be converted to accomplish shearing of explosive filled bursters.

Mine Disassembly Machine

The Mine Disassembly Machine (MIN), Figure 4, consists of an Orientation Station, a Punch and Drain Station, a Trolley Pickup Assembly, a Burster Punch Station, and controls and Instruments for operating the machine. A Local Maintenance Control Panel is also provided for operating the machine locally while performing machine maintenance.

The Mine machine is designed to punch and drain the agent from M23 mines and then punch through the burster and push out the booster pellet for burning in the deactivation furnace. The production capability is 82 mines per hour. During operation the machine will process two mines simultaneously. While the burster is being punched on one mine, another will be in the punch and drain station.

After the agent has drained, the punch and drain clamp releases the mine. The rotary actuator rotates the mine from the vertical to the horizontal position (180° from input position). In this position the mine is placed on the trolley.

The trolley moves the mine into the Burster Punch Station. The burster punch cylinder is actuated and a hole is punched through the burster and the booster assembly is pushed out of the mine. The booster falls into a chute leading to the deactivation furnace for thermal deactivation.

Next the trolley reverses while the mine is retained by the burster punch and remains at the punch station. The burster punch cylinder retracts allowing the mine to sit on the punch station frame. The trolley returns and pushes the mine into the deactivation furnace feed chute.

Bulk Drain Station

The Bulk Drain Station (BDS), Figure 5, consists of a Main Frame Assembly, an Item Transfer Conveyor, a Punch Station and a Drain Station. A set of load cells mounted on hydraulic cylinders as part of the conveyor are provided to determine the weight of agent removed from each of the items that are punched and drained.

The BDS is designed to punch and drain the agent from 500 pound MK-94 bombs, 750 pound MC-1 bombs, one-ton containers, and TMU 28/B spray tanks. Prior to draining and after draining, the component load cells obtain the full and empty weights of the items being drained.

After draining, the items are transferred from the BDS onto a connecting conveyor for subsequent transfer and processing in the Metal Parts Furnace. The production capability of the BDS is: MK94 bombs, 13.0 units per hour, MC1 bombs, 9.8 units per hour; one-ton containers, 2.9 units per hour; and, TMU28/B spray tanks, 2.9 units per hour.

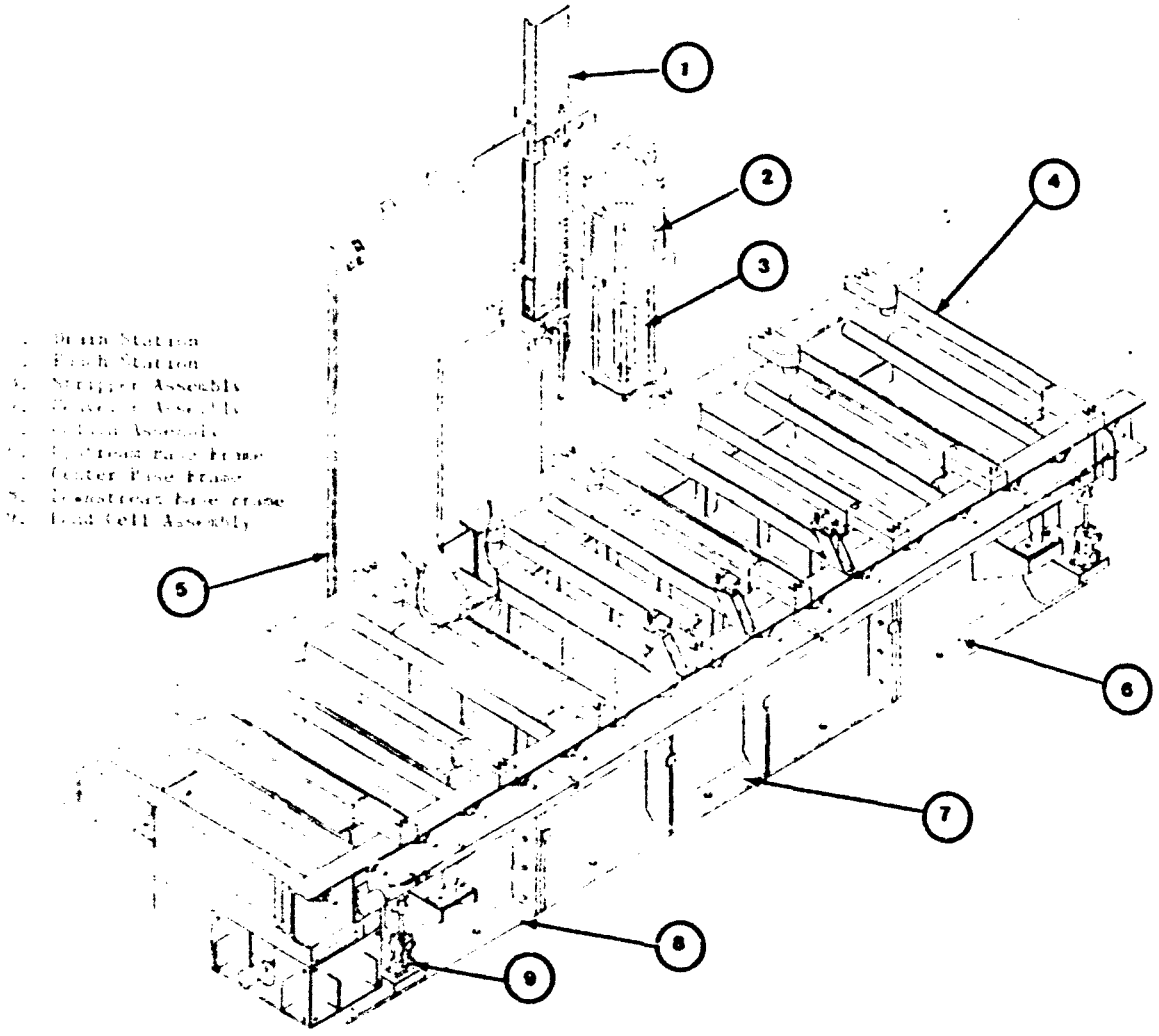

FIGURE 5. BULK DRAIN STATION (BDS).

EXPLOSIVE CONTAINMENT ROOM (ECR) REPAIR
JOHNSTON ATOLL CHEMICAL AGENT DISPOSAL SYSTEM (JACADS)

BY:
BOYCE L. ROSS, P.E.[1]

ABSTRACT

The first incineration disposal facility for destruction of chemical weapons has been constructed on Johnston Island in the Central Pacific. This facility, the Johnston Atoll Chemical Agent Disposal Facility (JACADS), will be used as the prototype facility for construction of eight similar facilities within the Continental United States. The heart of the disposal process takes place within the Munitions Demilitarization Building (MDB) in Explosive Containment Rooms (ECRs). During construction of the ECRs, a labor dispute led to concrete placement problems and subsequently deficient containment walls. This presentation will discuss the steps taken to evaluate, repair and approve these highly critical containment rooms.

PROGRAM BACKGROUND

Project management of the JACADS facilities is assigned to the Program Executive Officer - Program Manager for Chemical Demilitarization (PEO-Chem Dml) located in Edgewood, Maryland. The U.S. Army Engineer Division Huntsville (USAEDH) acted as facility design manager and as the contracting authority for the JACADS facility and process designs. The JACADS facilities were designed by Stearns Roger Inc., Denver Colorado. The JACADS process design was done by the Ralph M. Parsons Company, Pasadena California. The JACADS facility design was completed in late 1984; construction began in early 1986 under the supervision of the U.S. Army Engineer Pacific Ocean Division (USAEPOD) and was completed in November of 1987. Equipment installation is currently underway with a scheduled completion date of 1 April 1989. Disposal operations are scheduled to begin in mid-August 1989.

FUNCTIONAL DESCRIPTION

All hazardous disassembly and disposal operations within the JACADS disposal process are performed within the Munitions Demilitarization Building (MDB). The MDB is a two story building having a total area of 87000 s.f. The MDB is equipped with a cascading negative pressure ventilation system designed to contain toxic nerve gas and by-products resulting from the disposal process by providing increasing levels of negative pressures from non-hazardous areas towards hazardous areas. Figures 1 and 2 show the first and second floor plans of the MDB, respectively.

Lethal chemical agents are configured in a variety of munitions and containers as can be seen in Table 1. Munitions which are configured with ex-

1. U.S. Army Engineer Division Huntsville

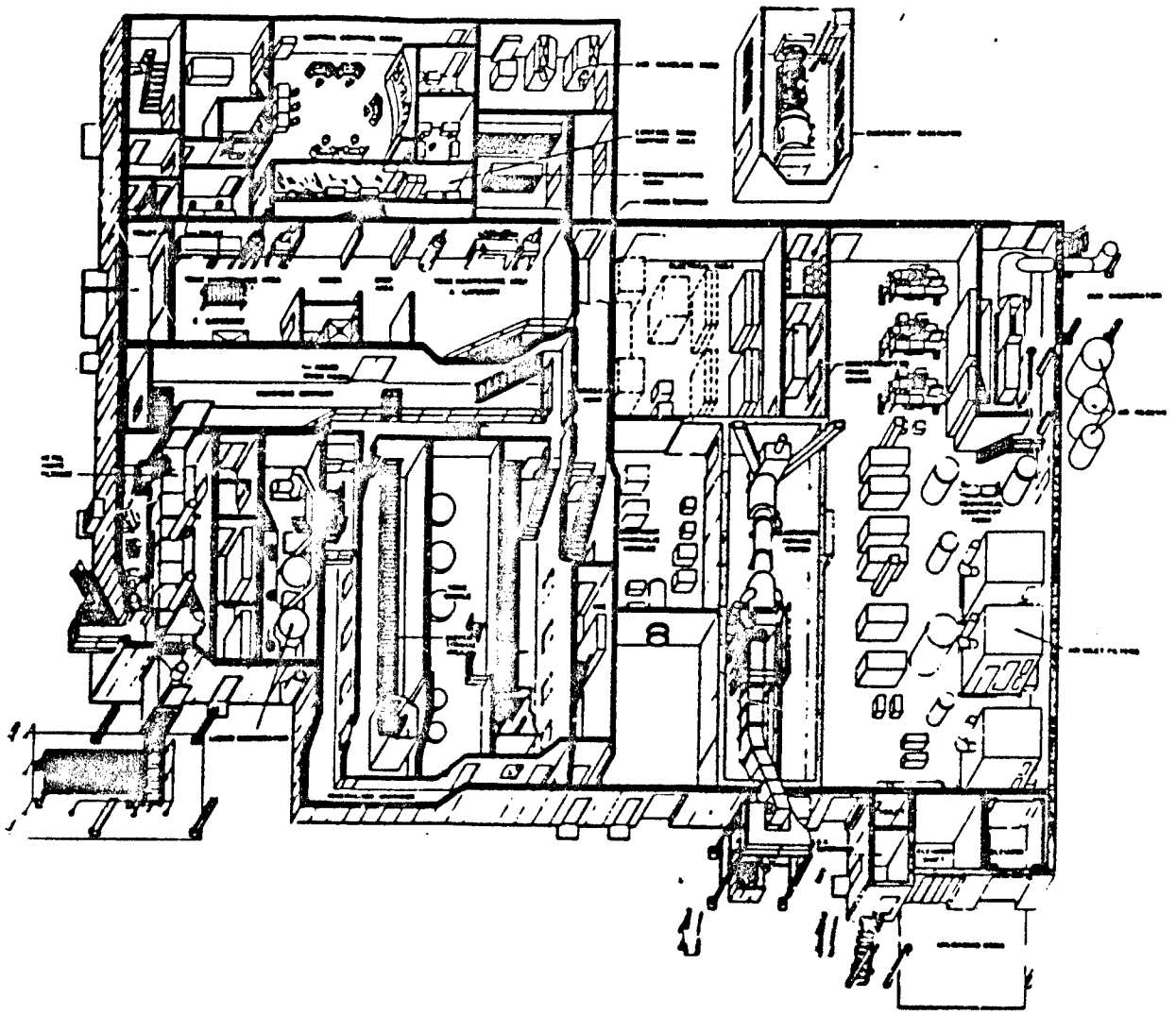

FIGURE 1 - MUNITIONS DEMILITARIZATION BUILDING (MDB) FIRST FLOOR

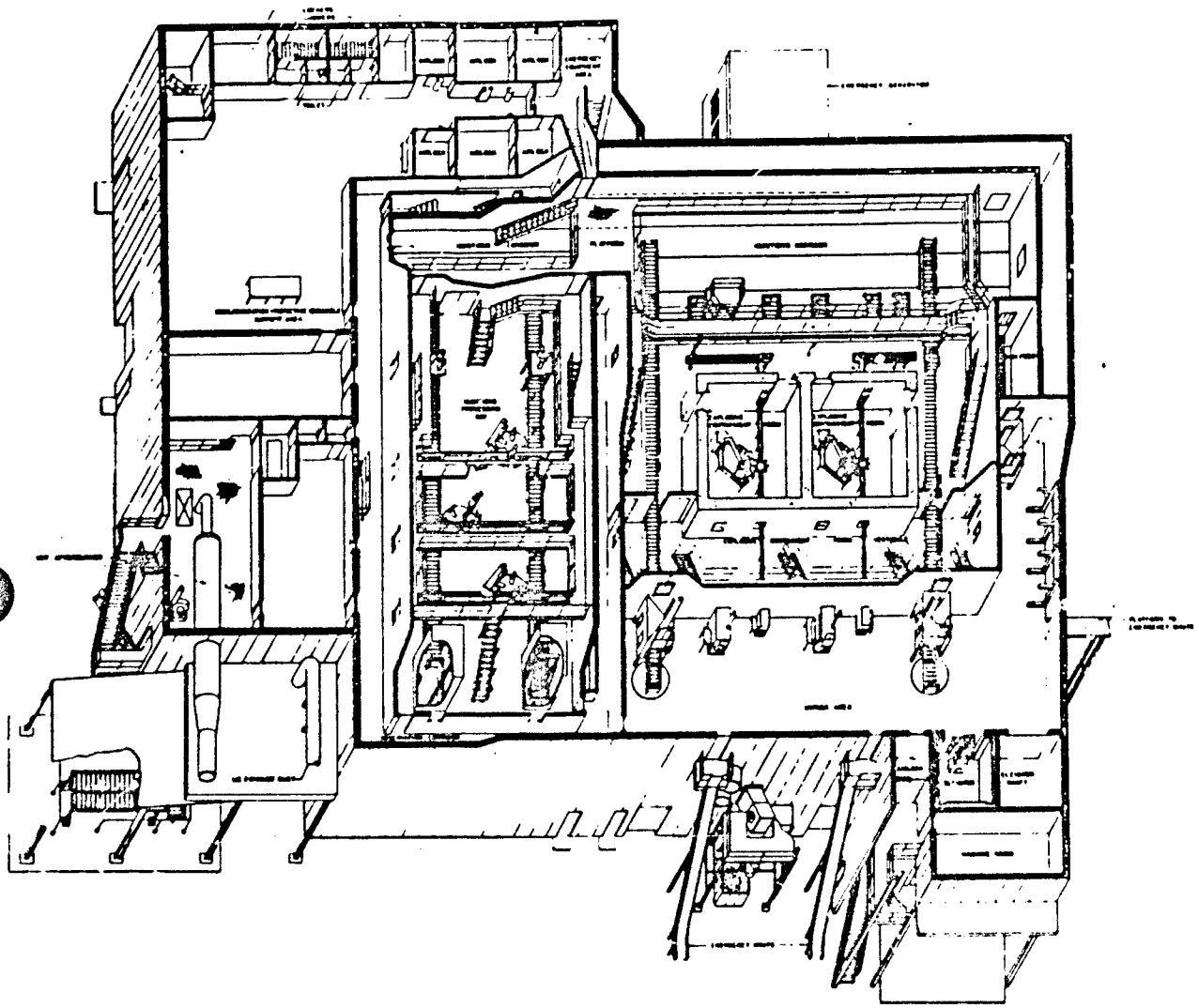

FIGURE 2 - MUNITIONS DEMILITARIZATION BUILDING (MDB) SECOND FLOOR

CHEMICAL STOCKPILE

ITEM	CONFIGURATION	AGENT
ROCKETS	M 55	GB, VX
PROJECTILES	105 MM 4.2 IN 155 MM 8 IN	GB, VX, HD
LANDMINES	M 23	VX
BOMBS	MC-1, MK 94, M 43, M 130	GB BZ
GENERATOR	M 44, M 16	BZ
BULK	TON CONTAINERS	GB, VX, HD, BZ

TABLE 1

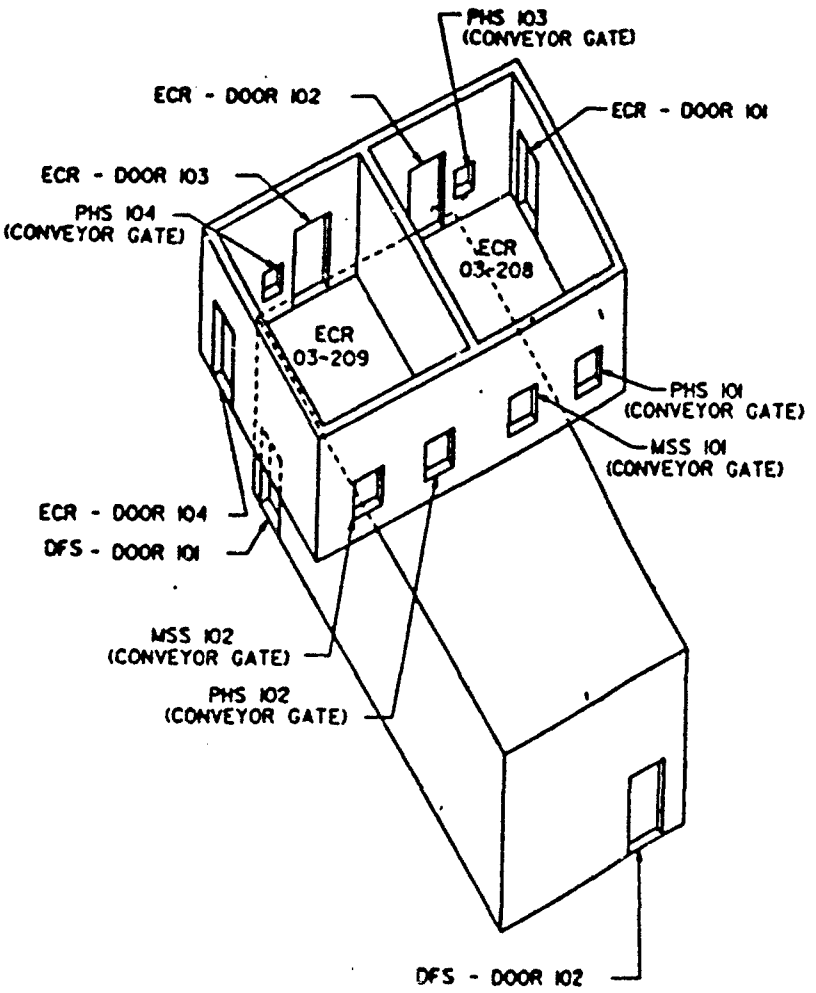

FIGURE 3 - ECR/DFS ISOMETRIC

plosives are remotely disassembled in functionally identical Explosive Containment Rooms (ECRs) on the second floor of the MDB. The hazardous operations performed in the ECRs consist of punching and draining munition bodies, draining of propellant and shearing of bursters and rockets. After the disassembly process, contaminated munition parts and explosives are dropped through a feed chute in the ECR floor into the Deactivation Furnace Room (DFS) where they are incinerated. Drained nerve agent is piped from the ECRs to a toxic cubicle where it is stored prior to incineration in the Liquid Incinerator. Whole munition bodies are conveyed from the ECRs via material handling systems to a Metal Parts Furnace. An isometric view of the ECR/DFS structure is shown in Figure 3.

EXPLOSIVE CONTAINMENT ROOM CRITERIA

As has been previously explained and formally documented in Reference 1, disassembly of explosively configured munitions occurs remotely in the ECRs. The highly toxic nature of the chemical agents in the munitions dictates that the ECRs provide a high degree of containment of the post-accident gas products. This near total containment of high temperature contaminated gas must be contained until the heat resulting from an accidental detonation is conducted away by the ECR structure. An explosive event of 18.75 lb. TNT EQ. was determined to be the Maximum Credible Event (MCE) which could occur within the ECRs. This event, in addition to the contribution of agent combustion, results in a pressure-time loading as shown in Figure 4. The ECRs were designed as concrete structures in accordance with TM5-1300 to provide Category I protection in accordance with AMCR 385-100 and DOD STD. 6055.9. Not only were the ECRs designed to contain the effects of blast pressures, but fragmentation effects also. All mechanical, electrical and instrumentation penetrations are protected with 2-1/2 inch thick fragmentation plates. Material handling blast gates and personnel access doors are made of 2-1/2 inch thick steel. In addition to containing blast and fragmentation effects the ECRs were required to be reusable after an explosive event. Structural design criteria used in the ECR design is shown in Table 2.

ECR CONSTRUCTION PROBLEMS

In early April of 1987 the JACADS construction contractor began preparations for the final concrete placement of the ECR containment walls. The limits of this final placement are depicted by the hatched area in Figure 5. Concrete with a compressive strength of 4000 psi. was batched at an on island batch plant and transported to the site via trucks. At the construction site a superplastizer was added to the concrete to increase the workability of the mix. The concrete was then placed using buckets and cranes. During the final placement, a labor dispute led to the regular concrete workers walking off the job. The Contractor attempted to complete the final placement using unskilled concrete laborers. The workers used in the attempt to complete the placement were unfamiliar with proper placement techniques and consequently were slower in placing the concrete. As a result the concrete mix became very stiff and workability of the concrete became difficult. Forms were removed from the placement 14 days later and numerous deficiencies were visible. These deficiencies consisted of areas of poor consolidation, cold joints, surface honeycomb, and voids. Figures 6 through 8 show approximate locations of defects and their extent. As a result of the numerous surface deficiencies the capability of the ECRs to perform their containment function became uncer-

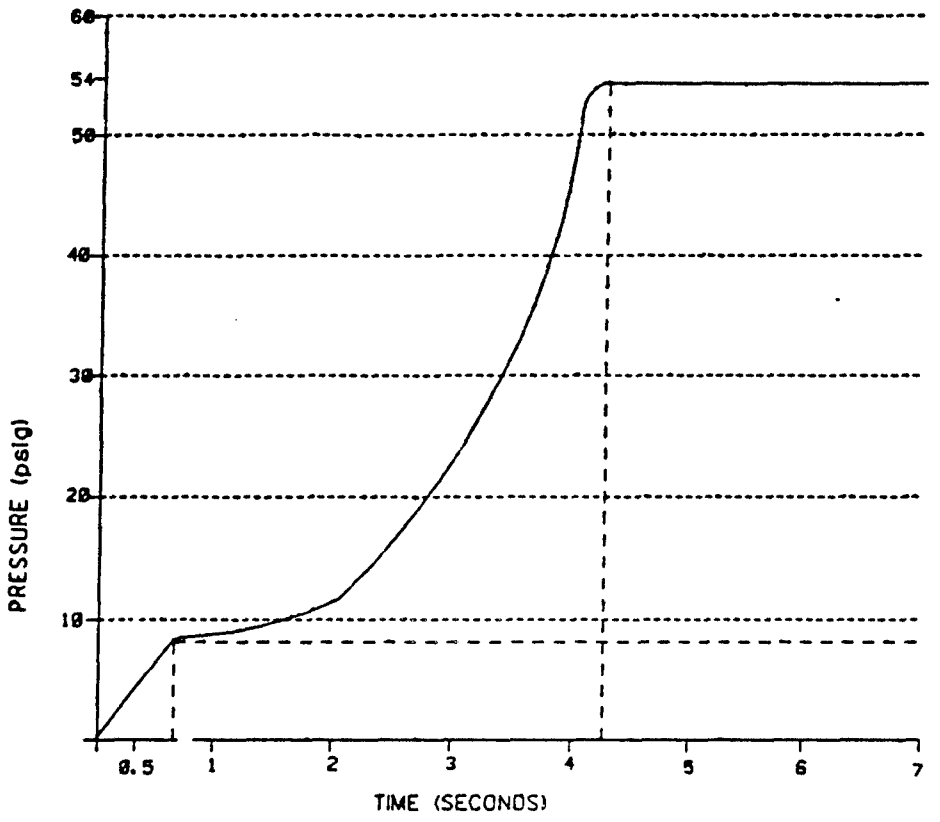

FIGURE 4 -PRESSURE TIME HISTORY FOR 8-INCH PROJECTILE AT JACADS

DURING SHOCK PHASE, $T \leq T_M$

JOINT ROTATION $\leq$ 1 DEGREE OR $\mu \leq 3$
MATERIAL DYNAMIC INCREASE FACTORS USABLE

DURING QUASI-STATIC PRESSURE PHASE, $T \geq T_M$

MATERIAL STRESSES NOT ALLOWED TO EXCEED ELASTIC LIMITS
DYNAMIC INCREASES NOT USEABLE

OTHER

NO SPALLING OF EXTERIOR SURFACES
REUSABLE AFTER THE MCE INCIDENT

TABLE 2-STRUCTURAL DESIGN CRITERIA

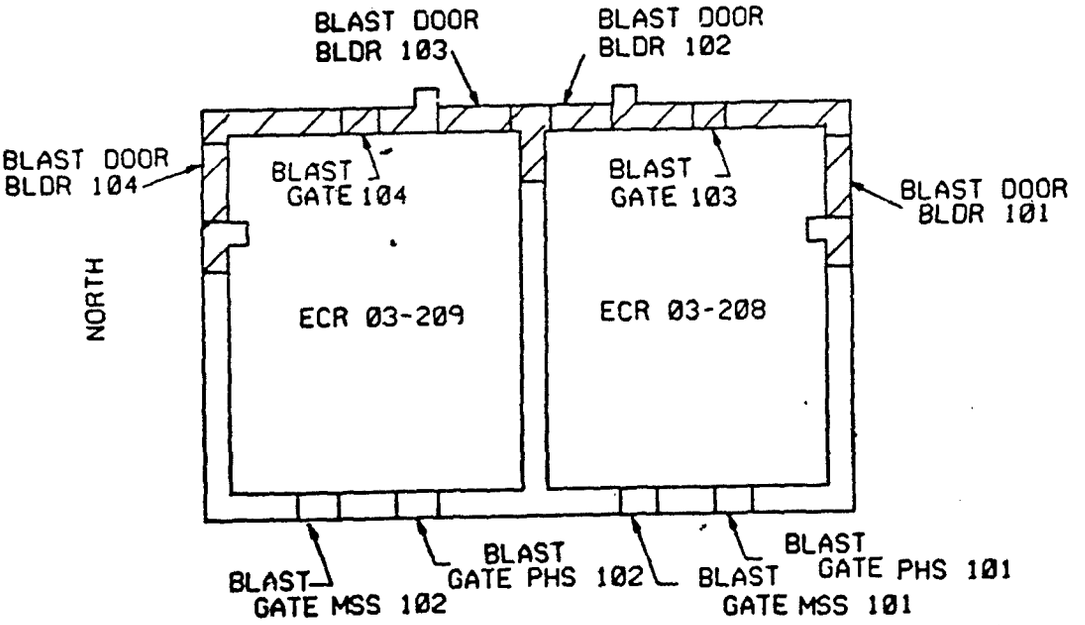

--DEFECTIVE SECOND PLACEMENT

FIGURE 5 - PLACEMENT PLAN

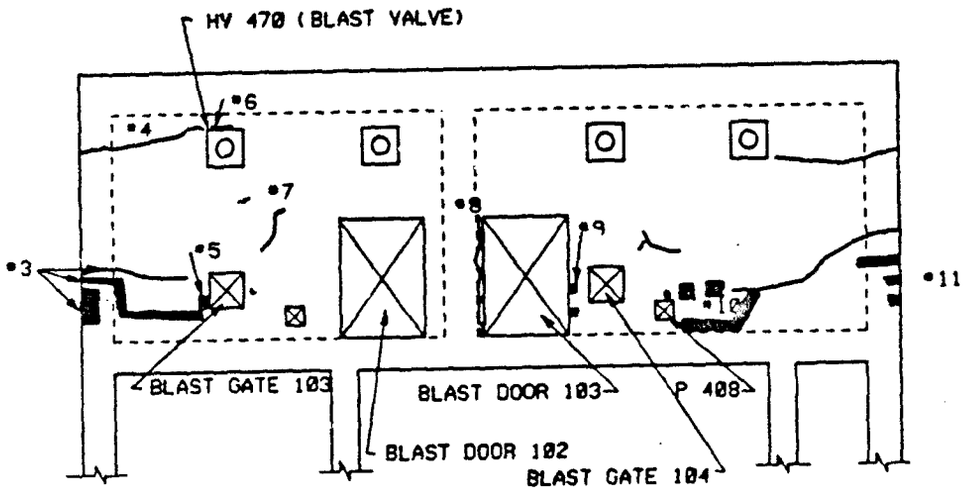

OR DEFECTIVE AREA

FIGURE 6 ECR EAST ELEVATION

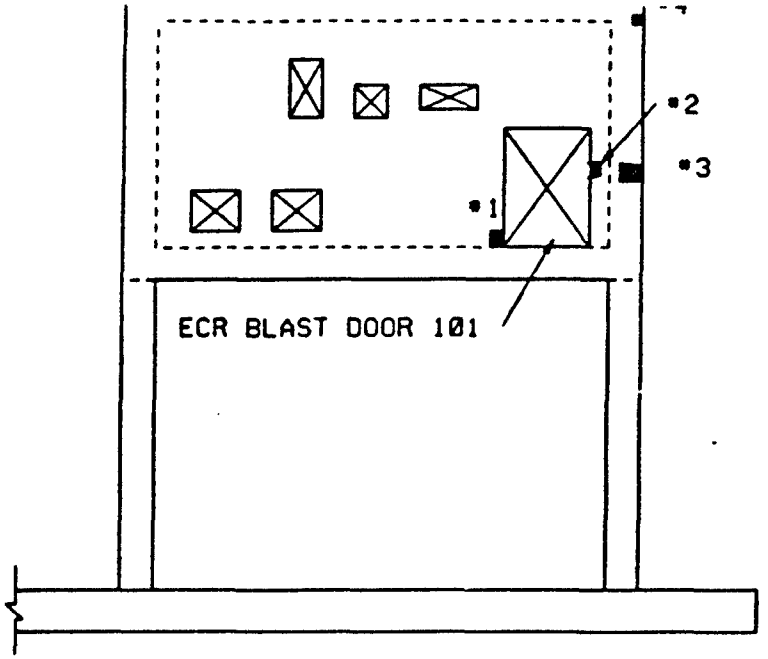

▭ DEFECTIVE AREA

FIGURE 7 ECR SOUTH ELEVATION

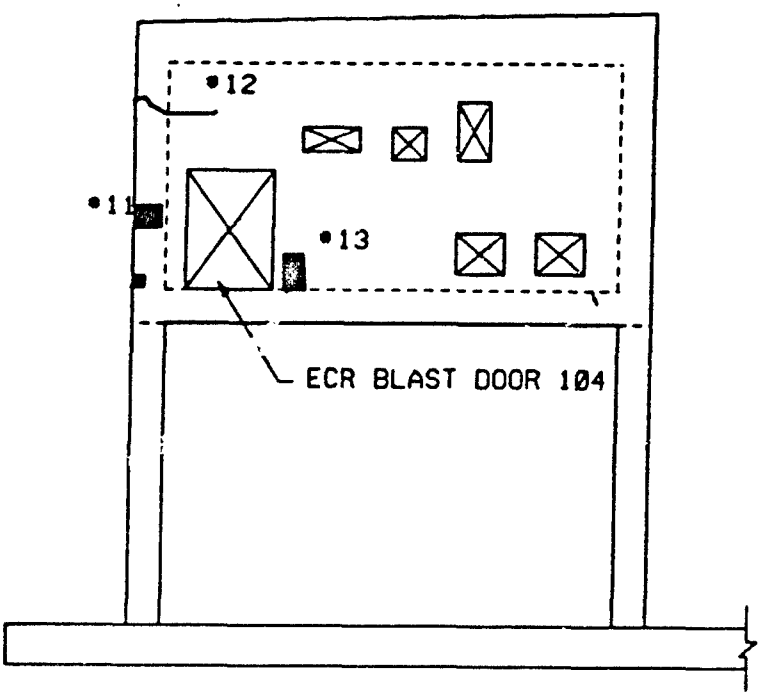

FIGURE 8 ECR NORTH ELEVATION

tain. This uncertainty was unacceptable in view of the ECRs critical role in the destruction process. PEO Chem Dml called upon USAEDH to evaluate the situation and recommend steps to be taken that would ensure that the ECRs would function as designed and as if they had been properly constructed.

CHRONOLOGY OF EVALUATION AND REPAIRS

General:

Initial evaluation of the ECRs began in late April 1987. USAEDH and the Construction Contractor prepared independent reports on the visible defects. An Ad-Hoc committee of experts from both private industry and government agencies was created to establish procedures to repair the deficiencies. The committee included senior personnel with expertise in Non-Destructive Testing (NDT), concrete repair/materials, quality assurance, and structural engineering. Represented on the committee in addition to USAEDH and PEO-Chem Dml were specialist from the Ralph M. Parsons Company, Pasadena, CA. and from the U.S. Army Waterways Experiment Station, Vicksburg, MS. The committee met in early May of 1987 and developed recommendations as to NDT, repair methods, and quality assurance for repair of the ECR structures. Reference 2 contains a complete record of the evaluation and repair of the ECRs. The committee recommendations will be discussed in the following paragraphs.

Evaluation Criteria:

The criteria established for repair of the ECR structures was straightforward: The method of repair must result in final quality equal to that which would have been provided if no problems had occurred during construction. The selected NDT procedures and repairs must eliminate any uncertainty in performance resulting from the deficient concrete. Furthermore, any suspect concrete, which was not accessible to NDT, would have to be removed. The final product of the committee were recommendations describing acceptable procedures for testing, repair, and quality assurance. These recommendations when properly implemented, provided the basis to certify that the ECRs would meet the original intent of the design and provide performance equivalent to new construction.

Evaluation Results:

Testing: The NDT testing method recommended by the committee was Ultrasonic Testing (UT). The pulse velocity (pitch-catch) UT procedure is a standard method of in-situ evaluation of concrete structures. The UT examinations can be made very rapidly and offer a great amount of versatility thus creating the ability to address many different testing situations. Ultrasonic Testing was selected over radiographic techniques. Radiographic Testing (RT) was not acceptable because the ECR wall thickness of 2'-1" was near the maximum range of standard radiographic equipment. Additionally, it was noted that radiography fails to detect internal flaws in certain orientations, and could be inconclusive. The committee also recommended that the entire surface area of the deficient concrete placement be tested initially followed by detailed emphasis on the known defective areas. After all deficient areas had been located and repaired a follow up UT of all the repairs was recommended to assure the success of the repair. In addition to UT examination, NDT testing was

also recommended to evaluate the in-situ concrete strength as well as the strength of repaired areas.

Repair: Repair materials proposed by the Contractor were "Sika Products". Sika products include a family of grouts, mortars and epoxy materials known to have excellent performance records. The committee made recommendations for repair of each defective area based on the use of these products. In general the committee recommended that shallow patches be made with a latex modified mortar, deep repairs made with a pre-mixed concrete (Quik Crete 6000), and repairs around embedded items with pourable grout or by pressure injection.

Quality Assurance: The Contractor selected the firm of Wiss, Janney, Elstner (WJE), Dallas, TX. to execute the testing. The Committee recommended that all initial UT examinations be conducted in the presence of USAEDH, USAEPOD and the USAEWES NDT expert. WJE was required to document results of all UT examinations (Reference 3). When defects were identified either visually or by UT they were to be removed. No repairs were initiated until the results were inspected by USAEWES and USAEDH. In addition, preparation of repair materials and the repair itself were recommended to be conducted in the presence of USAEWES, USAEDH and the representative of Bonded Materials Corporation (The Sika Product Distributor). This was done to assure that manufacturers recommendations would be followed correctly. All repaired defects would then be rechecked with UT to verify the quality of the work.

Initial NDT & Repair Procedure Planning:

On 28 May 1987 initial NDT of the ECRs began on Johnston Island. The ECRs had been marked off by the Contractor on 1'-6" grids using a transit. NDT readings were, as a minimum, taken at each grid intersection. In areas where the concrete appeared on the surface to be questionable, tests on a much closer grid were taken. The center wall between the ECRs was tested on a 6-inch grid over its entire surface. Over 1000 UT shots were taken over a 5 day period during the first phase of testing. In general the initial testing indicated that there was a lack of bond and probably voids behind many of the frames and embeds. Additionally, several areas of shallow subsurface defects were detected. The suspect material was removed and the area retested. All cold joints were tested. The UT results revealed that visible cold joints were either shallow joints that could be removed or that there was adequate bond through the joint.

Performance of Repair:

All defective areas visible and detected by UT were re-inspected by USAEWES, USAEDH, the Bonded materials representative, and the contractor to assure that the repair procedures, which had been approved and assigned to each defective area, were properly prepared for the correct repair material. After the required preparation and approval, sample defect areas were selected for repair so that the USAEWES material specialist and the Bonded Material representative could ensure that the contractor's personnel were properly trained in the use of the repair materials and surface preparation procedures. Trial mixes of the "Quik Crete" repair material were made to ensure that the material would be workable/flowable and its shrinkage properties limited. Sample areas which were selected for repairs were formed and repaired by the

contractor's personnel. Repairs made with Quik Crete, latex mortar and pourable grout were completed. In general the repairs were made without incident. Repaired areas were NDT tested after 3 days and found to be of higher strength than the in-situ concrete.

Final NDT:

Final NDT on the repaired ECR structure was performed between 29 June and 2 July 1987 by WJE. The testing team that performed the initial examination performed the post-testing. Repairs to all UT detected and visually observed defective areas had been completed. As previously defined by the repair committee, all patched regions were tested to ensure that proper bonding of the repair material and required quality had been achieved. Approximately 600 post-UT examinations were made on the repaired areas. All tested locations exhibited signals interpreted to be indicative of sound quality concrete. All repairs were judged to be adequately bonded and integral with the substrate concrete.

Ultrasonic testing by the through-transmission technique has been utilized for over 30 years for the nondestructive evaluation of concrete quality and uniformity. Certain statistical interpretations based on measured readings can provide valuable guidance in assessing the concrete tested. Research has indicated that good quality site cast concrete, placed from a single batch of material, would be expected to have a pulse velocity coefficient of variation of about 1.5 percent. Similarly, for concrete cast from several loads or trucks of concrete, a coefficient of variation of 2.5 percent would represent good construction standards. A corresponding value for an entire structure would be about 5 to 9 percent (Reference 3). Coefficient of variations for both the pre- and post- tests are shown in Tables 4 and 5 respectively. The JACADS ECRs represent a structure cast from several trucks of material and the pulse velocity coefficient of variation after all repairs were completed was 2.5 percent based on 600 test shots. It is concluded from these results that the repaired ECR structure is representative of good original construction standards.

Ultrasonic tests were performed on one representative concrete test cylinder. The pulse velocity readings taken on this cylinder were comparable to the readings taken in the ECR before and after each test. This indicated that the in-situ strength of the concrete was comparable to the cylinder strength. The cylinder test results indicate that compressive strengths of the ECR placement exceeds the contract requirement of 4000 psi. Since the UT examinations and the cylinder tests both indicated that the in-situ strength of the concrete was in excess of contract requirements, no destructive or further nondestructive testing to determine in-situ strength was performed.

Pressure Test Results:

The primary means of validating the performance of the ECRs was a pneumatic pressure test. This test serves not only as a means of testing the structure's integrity acting as a pressure vessel, but also provides an indication of the structure's load carrying capability. The pressure test is included as part of the construction contractors required acceptance testing.

TABLE 4 - SUMMARY OF PHASE I ULTRASONIC TESTS FOR ALL SUPPLEMENTAL LOCATIONS

LOCATION	No. of Shots	Appendix-B Table No.	Avg. Signal Amplitude mV	Avg. Pulse Velocity fps	Coefficient of Variation %
Detail A	88	2a	9.0	12,590	2.2
Detail B	41	3a	9.5	12,680	1.9
Detail C	19	4a	2.5	13,570	3.3
Detail D	27	5a	4.2	13,200	2.8
Detail E	39	6a	8.5	12,840	2.4
Detail F/G (lower)	65	7a	5.0	12,470	7.5
Detail F/G (upper)	40	8a	8.8	12,750	3.3
Detail H	44	9a	7.2	12,840	5.2
Detail I (Segment a)	21	10a	4.3	13,160	3.4
Detail I (Segment b)	47	11a	8.3	12,830	4.9
Detail I (Segment c)	31	12a	9.9	12,970	2.2
Detail J	58	13a	8.6	12,970	2.6
Detail K	75	14a	6.6	12,910	2.8
Ceiling (North ECR)	29	15a	4.9	13,070	1.7
Ceiling (South ECR)	26	16a	1.1	13,200	1.5

TABLE 5 - SUMMARY OF PHASE II ULTRASONIC TESTS FOR ALL SUPPLEMENTAL LOCATIONS

LOCATION	No. of Shots	Appendix-B Table No.	Avg. Signal Amplitude MV	Avg. Pulse Velocity fps	Coefficient of Variation %
Detail A	73	26	12.8	12,790	1.9
Detail B	41	36	13.6	12,850	1.9
Detail C	19	46	2.1	12,780	4.5
Detail D	24	56	12.0	12,980	1.5
Detail E	21	66	12.7	12,770	1.2
Detail F/G (lower)	78	76	5.0	12,990	2.5
Detail F/G (upper)	42	86	5.8	12,550	2.3
Detail H	50	96	5.8	12,930	1.9
Detail I (Segment a)	32	106	8.8	13,150	3.6
Detail I (Segment b)	55	116	6.0	12,930	2.1
Detail I (Segment c)	29	126	6.2	12,930	2.7
Detail J	44	136	6.0	12,870	2.4
Detail K	25	146	5.7	12,991	3.1
Ceiling (North ECR)	45	156	6.0	13,150	2.0
Ceiling (South ECR)	45	166	3.1	12,840	2.7

After completion of follow up UT testing of the repaired ECRs, the Contractor began preparations for the pneumatic pressure test. These test were performed between 23 and 25 September 1987. The results of these test were successful and the performance of the structures was significantly better than required by the contract specifications.

Conclusions:

Repair activities to correct the concrete placement deficiencies have been successfully completed. Intensive nondestructive testing confirmed that the repaired ECR structures meet or exceed the quality and material performance standards required for the intended explosive containment function. The pneumatic pressure test has shown that the vapor leakage rate of the as-built ECR structure is much less than the allowable specified by design. It is concluded that the JACADS ECRs have been constructed in accordance with the intent of the design, and can be expected to meet all performance requirements defined by the original load conditions.

REFERENCES

1. The Design of Blast Containment Rooms For Demilitarization Of Chemical Munitions, LaHoud, P.M., 21st. DDESB Seminar Vol. I dtd. August 1984.

2. Final Report For Repair and Acceptance of The Explosive Containment Room (ECR) Structures, HNDED-CS-88-2 dtd. Feb. 1988, Ross, B.L. and LaHoud, P.M.

3. Wiss, Janney, Elstner Associates, Inc. Final Report on Ultrasonic Testing of the ECRs at Johnston Island.

4. Chemical Demilitarization : Disposal of the Most Hazardous Wastes, Scott, J.A. and Rife, Richard, 21st. DDESB Seminar Vol. II dtd. August 1984.

OPPORTUNITIES FOR TECHNOLOGY TRANSFER FROM THE CHEMICAL STOCKPILE DISPOSAL PROGRAM

prepared for

TWENTY-THIRD DOD EXPLOSIVES SAFETY SEMINAR

August 9-11, 1988

presented by

JOHN A. SCOTT

The Ralph M. Parsons Company
Pasadena, California

coauthors:

Dr. R. H. Jolley
Ms. Mary Brown
Mr. Art Bigley
Mr. Tom Archer
The Ralph M. Parsons Company

OPPORTUNITIES FOR TECHNOLOGY TRANSFER FROM THE CHEMICAL STOCKPILE DISPOSAL PROGRAM

Rockets, bombs, mines, and projectiles containing lethal chemical agents have been part of the U.S. weapons stockpile for many years. These weapons have gone through several evolutions since their inception in the WWI period. The current munitions were developed in the 1950s and 1960s and are often referred to as the unitary stockpile. Unitary is defined as the lethal agent being complete and ready in single component form. As these unitary munitions have aged, their effectiveness has decreased as a result of a combination of chemical effects on the lethal agent and the accompanying interaction of the agent with its container. In addition, battlefield delivery systems and employment tactics have changed; thus, some weapons are obsolete.

The U.S. Army maintains chemical weapons for the armed forces at eight continental U.S. locations (shown in Figure 1). In addition, two other sites, one in Western Europe and one in the Pacific Ocean at Johnston Atoll, contain a portion of the stockpile. The FY 1986 Defense Authorization Act (Public Law 99-145) directed the Secretary of Defense to carry out the destruction of lethal chemical agents and munitions. The law specifically directs destruction in a manner that is safe for the workers, the public, and the environment.

The objectives of this paper are to familiarize the reader with the technology being applied to chemical weapons destruction and to highlight specific features of the technology that have application to other programs. This technology is significant because its features represent a safe and environmentally acceptable technology application for a plant designed to destroy extremely toxic material as well as explosives and propellants. This paper discusses the following four features of the technology:

(1) Process system.
(2) Control of hazardous vapors and dust.
(3) Waste handling.
(4) Adherence to the National Environmental Regulations.

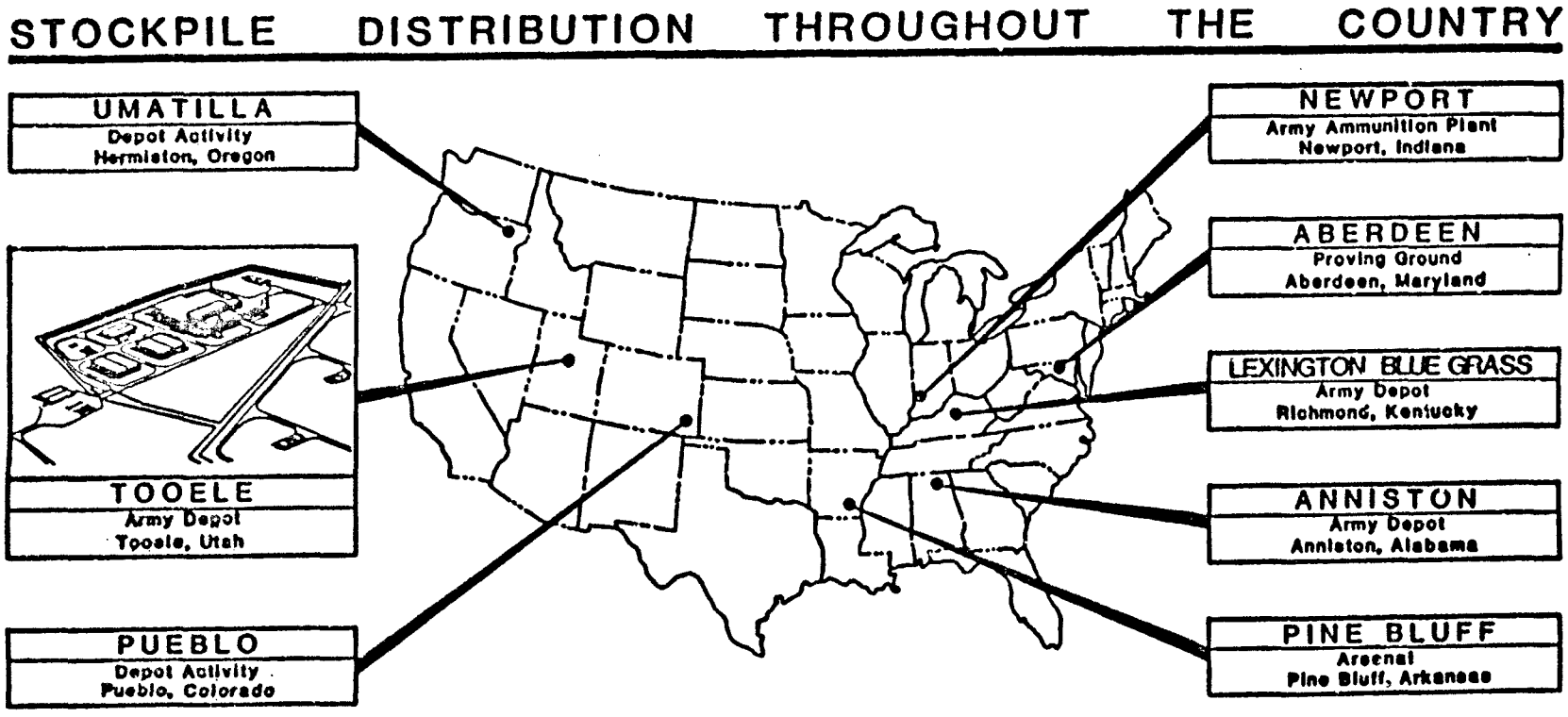

Figure 1 - CSDP Stockpile Sites

I. THE PROCESS SYSTEM

A. BACKGROUND

The Chemical Stockpile Disposal Program (CSDP) inventories at the various storage sites differ from one another. In total, rockets, bombs, land mines, projectiles, and bulk containers make up the existing inventory. Several of these munitions contain propellants and some contain explosives, but all munitions hold varying amounts of chemical agents. The types may be one of the nerve agents or one of a number of mustard gas blister agents. The munitions are fabricated of metal, and almost all are palletized with wood and metal strapping that must also be processed.

B. TECHNOLOGY

The major processing components of a CSDP plant are illustrated in Figure 2. These components have been tested at the Army's Chemical Agent Munition Disposal System (CAMDS) at the Tooele Army Depot, Utah. The engineering and design of a plant using these components were developed for the Johnston Atoll Chemical Agent Disposal System (JACADS) by The Ralph M. Parsons Company under the technical direction of the U.S. Army Toxic and Hazardous Materials Agency and U.S. Army Corps of Engineers, Huntsville Division. The basic concept of the demilitarization plant operation is to physically segregate the liquid agent, the energetics, the dunnage, and the munition metal for controlled incineration and decontamination using furnaces specifically adapted for the processing of each of these components.

The demilitarization equipment that effects the physical separation of the various munition components includes a variety of mechanical demilitarization machines. Rockets are processed in the explosive containment room (ECR) with specific demilitarization equipment. The rocket is accessed and agent drained at a rocket drain station while still contained in the fiberglass shipping tube and then sheared into five separate pieces using the rocket shear machine (RSM). Projectiles, or mortars, are conveyed to the ECR where the fuzes (or nose closures) and energetics are automatically removed by the projectile/mortar demilitarization (PMD) machine. Subsequently, the multipurpose demilitarization machine (MDM) removes the burster well, drains the agent, and then replaces the burster well. Bulk containers such as bombs and ton containers are conveyed to the bulk drain station (BDS) where the containers are accessed by a punch and drain machine, and the agent is removed. Land mines are unpacked manually using a glovebox, and the mine is conveyed into the ECR where the mine body is accessed, the agent is drained, and the energetic is removed from the mine body using the mine machine.

After separation of the explosives, propellants, and liquid agents, each component of the munition is ready for individual processing. Liquid agent that is drained from each munition is stored in tanks in the toxic cubical and subsequently combusted with air in the liquid incinerator (LIC) furnace at a temperature of 2,200 degrees F. Energetics such as bursters, propellants, and fuzes are processed in the deactivation furnace system (DFS) at a temperature

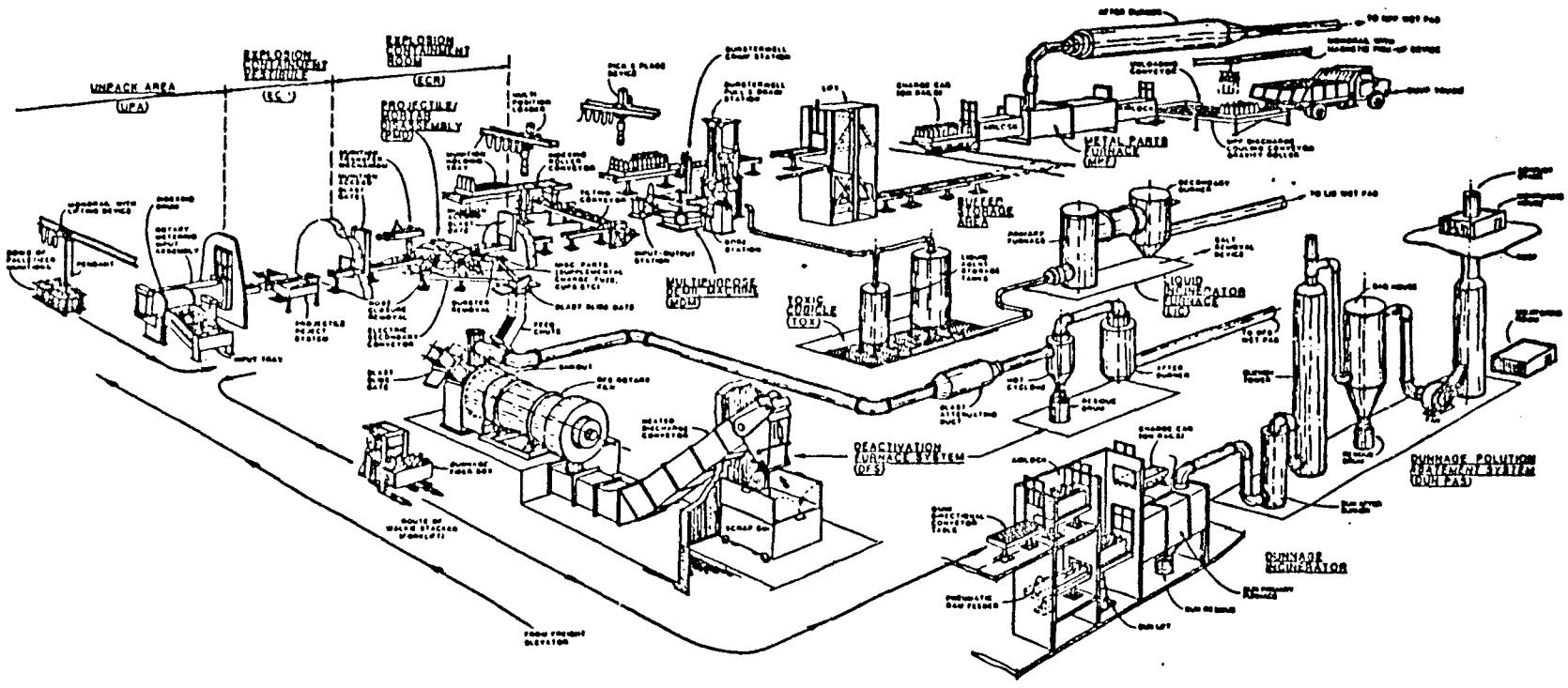

Figure 2 - Major Processing Compoments for Munitions

of 1,500 degrees F. The munition bodies, after draining the agent from them, are placed on racks and processed in the metal parts furnace (MPF) where residual agent is combusted, and the munition metal is decontaminated by exposure to a minimum temperature of 1,000 degrees F for a minimum of 15 minutes. Dunnage and miscellaneous contaminated and uncontaminated waste materials are placed in the dunnage incinerator (DUN) furnace where combustible material is incinerated and metal is decontaminated.

The combustion of the liquid agents produces acid gas components such as sulfur oxides, hydrogen chloride, hydrogen fluoride, and phosphorus oxides that require a special wet pollution abatement system (PAS) to effectively remove these components before release to the atmosphere. The equipment utilized in a wet PAS include the following four major elements:

(1) A quench tower is first used to reduce the temperature of the furnace exhaust gas, from about 2,000 degrees F to a near saturated gas at about 180 degrees F.

(2) The quenched exhaust is next passed through a venturi scrubber with a relatively high pressure drop to remove a major portion of the particulates larger than 0.4 micron and to remove a portion of the acid gas constituents.

(3) The venturi exhaust gas combined with the liquid brine from both the quench tower and the venturi scrubber are then directed to a packed tower for additional acid gas removal.

(4) The exhaust gas from the packed tower is drawn through a demister to remove the fine phosphoric acid mist derived from the nerve agents.

Air movement for each PAS and its furnaces is provided by dedicated induced draft fans with the exhaust gases vented to the atmosphere through a common stack.

The acid gas constituents are removed by their reaction with a solution of sodium hydroxide to form inorganic salts. Brine solutions from each of the wet PASs are processed in a brine reduction area (BRA) where water is evaporated to leave salts, which are packaged in sealed containers for disposal. A CSDP plant is designed for zero liquid effluent. The salts represent the largest volume of residue to be disposed of in the residue handling program.

The DUN furnace processes wood and other combustibles with little or no agent entrained. The protective clothing used in the CSDP plants is somewhat unique because it contains chlorine. (Provision is made to add sodium hydroxide to the quench tower when processing protective clothing if acid gases are present in the offgas.) The exhaust gas from the DUN is quenched to approximately 350 degrees F. and the entrained particulates are captured in a baghouse.

II. FACILITY VENTILATION SYSTEM DESIGN

A. BACKGROUND

Today the environment that we live in is being polluted from many sources. Much of this pollution is in the form of hazardous liquids, gases, and/or powders. The control of the hazardous vapors or dust released during chemical neutralization is described in this section. The specialized environmental system presented here can be applied to many operations where hazardous materials are being handled and/or processed.

In the CSDP plants, the majority of hazardous material emissions occur at the start of the process when transferring the hazardous chemical from the munitions (or storage containers) to the furnace for thermal destruction. At this point, the release of chemical vapors becomes difficult to control. To control these releases, an enclosure is placed around the hazardous waste processing plant, and a unique ventilation system is installed to capture and remove the hazardous material released from within the enclosure (building).

B. METHODOLOGY

To maintain the protective envelope within the building and to protect the personnel who are working in the building, the ventilated areas are classified into hazardous categories, Category A being the most hazardous and Category E being the least hazardous or safest area:

Category	Degree of Contamination
A	Routine contamination, either liquid or vapor
B	High probability of vapor contamination resulting from routine operation
C	Low probability of vapor contamination
D	Unlikely to have contamination
E	Maintained to be free of possible contamination

To protect the areas of probable contamination, a parallel/cascade ventilation system has been developed. The system uses 100 percent outside air with 100 percent exhaust air. To avoid reintroducing hazardous agent into the process areas, no air is recirculated. The outside supply air passes through cooling and heating coils to maintain the design temperature and humidity within the building. Air is supplied to Category C areas and maintained by means of manual balancing dampers at a desired negative pressure. The air is then transferred to areas of successively more contamination potential by virtue of the fact that such areas are held at successively more negative pressure. Air supplied to a Category C area is transferred to a Category B area and then to the most hazardous area, Category A.

Stationary manual balancing dampers located in transfer ducts are used to achieve these pressure differences between process areas. The exhaust blower in the filtration system serves as the driving force for the flow of air through the process areas. Automatically controlled balancing dampers are not used to avoid potential "searching" by the dampers, creating a possible pressurization within the room.

Isolation valves are provided in the transfer ducts between process areas subject to contamination in order to preclude agent migration. These valves have an extremely low leakage rate and are capable of closure from the control room in the event of an emergency, thereby preventing the possible spread of hazardous material from one process area to another. In addition, if the material is potentially explosive, blast valves are provided in the containment walls of the process areas where a blast could occur. The blast valves are cast into the wall and normally allow ventilation air to cascade from one process area to the next. If an explosion occurs, the blast wave closes the valve within 3 milliseconds, isolating the area from the rest of the building.

To ensure that the vapors are captured by the ventilation air to be later deposited in the exhaust filters, each of the probable contaminated areas is ventilated by the air change method as follows:

(1) Category A: 20 air changes per hour
(2) Category B: 10 air changes per hour
(3) Category C: 6 air changes per hour

The process areas with a high potential for contamination are ventilated at a higher air change rate, ensuring capture of hazardous vapors and later removal through the filtering system. The Category D areas use the standard industrial ventilation requirements for the intended service. Category E areas are to be maintained free of vapors through positive pressurization of the area with all outside supply air passed through carbon filters. This ensures that a safe environment for the personnel within the Category E area is maintained if hazardous chemicals are accidentally released to the atmosphere.

To protect the environment, all the exhaust air from Category C through A areas is filtered through the exhaust/filtering units. Exhaust air is pulled through welded ductwork to the exhaust/filtering units where it passes through a series of nine filter stages. The first filter stage, a media particulate filter rated at 80 percent based on ASHRAE Standard 52-76, removes any gross particulate that may be present. The second stage, a high-efficiency particulate air (HEPA) filter, removes the fine particulates down to 0.3 micron in size to prevent plugging of the carbon filters. Then six stages of activated carbon filters are used to remove any hazardous chemicals in the air; the six filters give a 1.5-second retention time for the air passing through the carbon filters. The final (ninth) stage is another HEPA filter, which collects any fines that may erode from the carbon filter stages. A centrifugal exhaust blower in each filter unit serves as the prime mover of the exhaust air. These blowers are provided with variable speed electric motors in order to compensate for differential loading of the filters during

their service life and to maintain a constant airflow rate through the building. After filtering, the exhaust air is discharged to the atmosphere through a stack.

The furnace room ventilation air is always exhausted to the exhaust filtration system before release to the atmosphere. Because the furnace gives off heat to the room, the room ambient air is allowed to rise to a maximum of 125 degrees F while the furnace is in operation. The outside air dampers will be in full open position when the furnace is operating at full capacity. The room ventilation will be a constant flow to the exhaust filters with only the furnace combustion air blower varying the quantity of outside supply air. When the combustion air blower is activated, the room pressure will drop below a set point modulating the outside air damper to allow the proper quantity of air to satisfy both combustion and room ventilation requirements while maintaining the desired room pressure.

Another area, the control room, is classified as a Category E area. This area is maintained at a positive pressure. The control room is maintained as a safe area so that if an emergency occurs, the plant operating personnel can monitor the process and bring the plant to a safe shutdown. Outside air enters the control room system through a weather louver and immediately mixes with the return air stream. Next, the mixed air enters the air handling unit (cooling and heating coils) using a high-pressure centrifugal fan that discharges to a carbon filter unit. The air passes through a series of nine stages of filtering as described previously for the process area exhaust filters. This air then is supplied to the control room and its support areas.

Category D areas use standard industrial ventilation because they are unoccupied by either personnel or agent. The Category D areas include mechanical equipment rooms and the electrical rooms. The outside air is supplied through a roughing filter (prefilter) and then exhausted through roof or wall exhaust fans directly to the atmosphere.

A parallel/cascade system will function properly only if the exhaust filtration system maintains a constant flow. All the room pressures and flows are predetermined and established during building balancing by the use of manual balancing dampers. All air from Category A, B, and C areas goes through the exhaust filtering system before release to the atmosphere.

The unique ventilation system combines a variety of specialized technical considerations to effectively control a hazardous material process and provide a safe working environment. The following specialized technical considerations are included:

(1) A once-through (100% outside air) ventilation system eliminates the possible recycle of hazardous material.

(2) Redundant filter stages treat all the air exhausted from the potentially contaminated process areas.

(3) The relative contamination potential of each process area is identified.

(4) Ventilation air is cascaded from process areas with the least potential for contamination to areas with the highest potential for contamination.

(5) Process areas with the highest potential for contamination are maintained at the highest negative room pressure.

(6) The ventilation (air change) rate increases as the potential for contamination increases.

(7) In the event of an emergency, each individual process area can be isolated with extremely low leakage valves to prevent the spread of contamination. Where the possibility of explosion exists, blast valves are also provided to contain the blast force.

(8) Hazardous chemical alarms are provided in the process areas to warn operators of process area contamination.

(9) Hazardous chemical alarms are provided between carbon filter stages to inform the operators when a chemical breakthrough occurs and carbon filter replacement is required.

(10) Variable speed exhaust blowers are used to maintain a constant airflow rate and process area negative pressure.

(11) The control room is maintained at a positive pressure so as to be free of hazardous material.

III. WASTE HANDLING CONCEPTS

A. BACKGROUND

The design of the CSDP facilities is such that process waste streams will be limited to solids. As noted on the overall process flow scheme in Figure 2, solids will be generated by the following sources:

(1) MPF scrap.
(2) DFS residue and scrap.
(3) LIC residue.
(4) DUN scrap and ash.
(5) BRA salts.

The total quantity of solid wastes generated is specific tc a particular facility and its munition stockpile. The various solid wastes, with the exception of metal munition casings or packing materials, will be tested for the characteristics of hazardous wastes as defined under the Resource Conservation and Recovery Act (RCRA). The solid wastes will be classified as hazardous only if they exhibit those characteristics. The munition casings will be considered containers under RCRA, and the thermal decontamination that they will be subjected to will meet or exceed the RCRA requirement for triple rinsing to remove hazardous residues.

Requirements for handling, storing, and disposing of hazardous waste are mandated in 40 CFR 262 through 265. These requirements are quite specific and require, among other things, a comprehensive document audit trail for all hazardous wastes. These requirements, when combined with the actual disposal costs for hazardous wastes, are a significant cost item for any project.

In view of the above, an evaluation was performed to quantify process solid waste generation and develop baseline waste handling and disposal concepts to support the RCRA permitting activities. In addition, waste minimization options were evaluated that could reduce the solid waste handling requirements and subsequent disposal costs.

B. METHODOLOGY

The process-generated solid wastes from the various furnace systems were quantified for the eight facilities considered under the CSDP. The data was used as the basis for the solid waste handling and disposal evaluation. The characteristics of the solid wastes as used in this analysis are presented in Table 1 for the major solid waste sources. The classification of the solid waste as either hazardous or nonhazardous has been based on existing environmental test data and on the current environmental permitting data, as applicable. Most of the solid waste is assumed to be hazardous waste with the exception of munition bodies and containers. Specifically, munition bodies and the mine drums are considered as containers and will not be subject to RCRA regulations after decontamination in the MPF. Other waste sources may be classified as nonhazardous when actual analysis is performed.

Table 1 - Summary of Solid Waste Characteristics

Major Solid Waste Source	Description	Characterization
MPF	Munition bodies	Nonhazardous
DFS	Rocket scrap	Hazardous
	Mine scrap	Nonhazardous
	Burster/fuze scrap	Hazardous
	Cyclone ash	Hazardous
	Slagging afterburner (AFB) solids	Hazardous
LIC	Salt-removal discharge solids	Hazardous
DUN	Scrap/ash	Hazardous
	Mine drums	Nonhazardous
	Baghouse ash	Hazardous
BRA	BRA salts	Hazardous

Testing for characteristics of hazardous wastes for all process-generated solid wastes is planned. It is possible that all waste streams will not exhibit such characteristics. If this is found to be the case, then the requirements for their handling and disposal would be less stringent than the procedures identified in this analysis. Disposal costs would be reduced accordingly.

Table 2 presents the total process wastes generated at each facility.

Table 2 - Summary of Total Process Solid Waste Generated[a]

Facility	Weight (tons)	Volume (ft^3)
Aberdeen Proving Ground[b]	NA	NA
Anniston Army Depot	19,158	548,916
Lexington-Blue Grass Army Depot	3,659	165,783
Newport Army Ammunition Plant[b]	NA	NA
Pine Bluff Arsenal	13,176	741,023
Pueblo Depot Activity	25,500	550,211
Tooele Army Depot	61,761	2,344,758
Umatilla Depot Activity	17,558	753,029

[a]Total process solid wastes includes protective clothing and charcoal residue/ ash, in addition to munition-specific solid wastes.
[b]NA = not available because the inventory is classified.

The basic solid waste handling plan requires the process-generated solid wastes to be collected in individual collection bins or containers at their sources. As previously noted, there are four major sources of solid waste, excluding that from the LIC, which is expected to generate little or no solid waste. The DFS and DUN each have two collection points. Table 3 presents an overview of the collection bins or containers that will be used to collect the solid waste from the various sources. Where possible, all hazardous waste will be collected in lined containers to minimize transfer operational problems. The scrap and ash from the DFS and DUN primary chambers will be at a relatively high temperature so that collection in lined containers is not feasible.

All collection bins, with the exception of the MPF transport container, will be transferred to a residue handling area (RHA) by forklift. In the RHA, the contents of the lined bins will be weighed, inventoried, and transferred to dedicated lined transport containers for movement offsite. Prior to movement

Table 3 - Summary of Collection Containers by Source

Major Source	Collection Container Description
DFS	
Heated discharge conveyor scrap[a]	Metal scrap bin, 5 ft long x 5 ft wide x 4 ft high, with bottom discharge provisions (70-ft^3 or 1-ton capacity).
Cyclone ash	Lined 55-gal drum (7.2-ft^3 capacity).
MPF	
Munition bodies	Transport container, 20 ft long x 8 ft wide x 5 ft high, rolloff type (540-ft^3 or 10-ton capacity).
LIC	
Solids from salt removal system	Lined 55-gal drum (7.2-ft^3 capacity).
DUN	
Primary chamber scrap[a]	Metal scrap bin, 5 ft long x 5 ft wide x 4 ft high, with bottom discharge provisions (70-ft^3 or 1-ton capacity).
Baghouse ash/salts	Lined 55-gal drum (7.2-ft^3 capacity).
BRA	
Salts	Lined container, 3 ft long x 3 ft wide x 3 ft high.

[a]Scrap to be placed in a supersack (70 ft^3) at the scrap transfer hopper.

offsite, the transport container liner will be sealed, and a tarpaulin will be placed over the top of the container to prevent liquids from collecting in the container during transporting to the approved disposal site. All RCRA-required manifests will be completed at the RHA.

The potentially hot scrap/ash will be transferred to the RHA for initial cooling. The contents will then be transferred by hopper to a supersack. Individual supersacks will be used for the DFS and DUN scrap. After filling

the supersack, it will be closed, weighed, inventoried, and transferred to the appropriate transport container for eventual transfer offsite.

Metal parts from the MPF will be placed directly in a transport container for movement directly offsite. The transport container will be located near the MPF cooling area so that the munitions can be placed directly into the transport container from their trays.

Transport containers will be identical for all applications. Basically, these units will be commercially available, 10-ton (20-yd^3) capacity, rolloff containers. Movement of these containers offsite will require the use of standard commercial trucks designed for rolloff containers. All onsite movement will be performed by site personnel to minimize the need for subcontractors to enter the high security facility. Provisions to transfer the transport containers to designated disposal operators have been made. All transport containers will be moved offsite to this transfer facility to await pickup. Permitting will not be required for this transfer facility as long as the containers are moved within 10 days or less. The contents of the transport containers will be disposed of at a nonhazardous or hazardous waste disposal facility, depending on the classification of the waste. Metal scrap from the MPF will be either sent to a nonhazardous landfill or sold as scrap metal. In all cases, the transport containers will be returned to the transfer facility.

An analysis was performed to determine whether volume reduction is a viable concept for the CSDP application. Disposal costs for solid wastes are typically on a mass (ton) or volume (cubic yard) basis, whichever is greater. Accordingly, there could be economic incentives to reduce the volume of waste for solids with densities less than about 74 lb/ft^3. At 74 lb/ft^3, 1 ton of solid waste will occupy about 1 yd^3. In addition, volume reduction could reduce transportation costs because the total number of containers requiring disposal would decrease.

IV. ADHERENCE TO ENVIRONMENTAL REGULATIONS

A. BACKGROUND

The National Environmental Regulations are our basic national charter for protection of the environment. They establish policy, set goals, and provide means for carrying out the policy. Federal agencies, including the Department of the Army, must comply with these regulations. Environmental Regulations must be integrated early in the planning phase to ensure that planning and decisions reflect environmental values to avoid delays later in the design and prevent potential conflicts. Environmental regulations become a fundamental design input similar to building and construction codes. The Army has outlined its approach to environmental compliance in Army Regulation 200-2, "Environmental Effects of Army Actions." The CSDP in turn has adopted the Environmental Regulation philosophy in accordance with AR 200-2 into the basic design concepts.

Environmental regulations may be broken down into three major areas of concern: air, water, and solids disposal. As the current stockpile of lethal chemical agents are demilitarized, all three areas of concern must be considered. Environmental regulations enters every phase of the CSDP from the

start of construction through facility closure and from the moment the munition enters the demilitarization area until its decontaminated metal parts and incinerator ash are ultimately disposed of. The CSDP sites will be permitted to operate under the Resource Conservation and Recovery Act (RCRA), the Clean Air Act (CAA), and the Toxic Substance Control Act (TSCA).

B. APPLICATION METHODOLOGY

Environmental compliance involves every aspect of the program. The munitions are transported over secure roads in vehicles that provide protection for the munitions from accidental spills or leaks. Emergency response plans as outlined in RCRA provide the checklist to respond to any foreseeable incident.

Once inside the Munitions Demilitarization Building (MDB), means of containing vapors, liquid emissions, and solids are provided. These means include blast protection, cascade air filtration, liquids containment, and solid waste handling. All agent and agent-contaminated components are either neutralized by chemical decontamination or incineration. Spent decontamination solutions, as well as all liquid waste generated within the facility, are incinerated. No liquid effluents will be generated at the facilities. Liquids containment includes storm water. Storm water is collected in a pond, tested, and either released if clean or treated if hazardous wastes are detected.

The various waste components and liquids are fed to one of four types of RCRA permitted and tested furnaces. The ash and residues from these furnaces will be collected in bag-lined containers, sealed, and stored in a weather-protected permitted area until ultimate disposal in an RCRA permitted landfill. The metal parts from the munitions are considered waste containers and are subject to complete decontamination prior to being landfilled or recycled through a metal scrap vendor.

The furnaces operate at negative pressure to prevent migration of hazardous fumes to the atmosphere. The combustion gases enter PASs where CAA, TSCA, and RCRA regulated gases and particulates are removed from the effluent prior to discharge to the atmosphere. The brines generated in the wet PASs are dried to minimize the volume of waste to be landfilled. The salts are collected in bags, sealed, and stored with the incinerator residues prior to disposal in an RCRA landfill.

Upon completion of the demilitarization, the facility will be "clean closed." All agent-contaminated machines, pipes, tanks, etc., will be chemically decontaminated and incinerated. Filter systems, sumps, floors, walls, etc., will be decontaminated and removed where possible for disposal in the furnaces. Ultimately, a mobile furnace will be brought in to thermally decontaminate the furnaces and PASs. All closure wastes will be disposed of in a RCRA permitted landfill.

Two key systems are discussed further: liquids containment, which is also commonly called "secondary containment," and polychlorinated biphenols (PCB) disposal in the DFS.

1. Secondary Containment Systems

Secondary containment systems must be designed, installed, and operated in accordance with the RCRA regulations in 40 CFR 264.193 and 270.16. The systems must prevent any migration of RCRA regulated wastes out of the system at any time and must be capable of detecting and collecting releases and accumulated liquids until the collected material is removed. Secondary containment systems must be constructed of compatible materials, placed on an acceptable foundation or base, provided with a leak-detection system, and sloped or otherwise designed to remove spills or leaked wastes.

Secondary containment is applied to all process buildings. The MDB, Process and Utility Building (PUB), and BRA will be constructed so that the lowest elevation in the building is higher than the elevation outside the building. The floors in the individual areas will be sloped to provide drainage to a trench or collection sump. The floor will be sealed to provide an impervious base to any spilled material. Six-inch curbs (minimum) prevent migration into noncontaminated areas as well as providing additional containment volume. Containment of the liquid wastes must be the greater of 10 percent of the container volume capacity (tanks, piping, etc.) or the largest container in that area. The only exception to this is the agent collection tank room of the toxic cubicle. DOD 6055.90-STD is stricter and states that a containment dike designed to hold the total contents of the waste system plus 10 percent of the volume shall be placed around aboveground liquid water systems.

The collection sumps serve as the primary means of containment. The sumps are classified as primary and secondary collection devices. Primary sumps are used in areas of regular washdown. Each sump is constructed of epoxy-coated welded steel. A liquid level sensor in the sump activates a sump pump to drain the waste liquid to the holding tanks. An alarm or signal is activated to indicate the presence of liquid. The sump is surrounded by a cast-in-place, epoxy-coated external concrete liner with an air gap in between. This external liner provides secondary containment to the primary sump. A liquid sensor wired to a visual and audible alarm is located in the bottom of the sump external liner to indicate if the primary containment device has failed.

Secondary sumps are of welded steel construction, coated with epoxy, and supported by a concrete base. A sump pump, level sensor, and alarm complete the secondary containment system. The secondary sumps provide containment for hazardous waste tank systems in the event of a spill, leak, or failure. In all cases, the liquids will be removed and the area decontaminated within 24 hours of detection.

2. PCB Disposal

Some M55 rockets contain up to 50 milligrams per kilogram of PCB in the shipping/firing tubes. The EPA under 40 CFR 761.70 of the TSCA requires that PCB contaminated waste be disposed of by incineration. The CSDP DFS and PAS have been designed in accordance with these regulations (RCRA and CAA) to incinerate the M55 shipping/firing tubes.

To comply with TSCA, the DFS has been designed to provide:

(1) A 2-second dwell time in the afterburner.

(2) An AFB operating temperature of 2,200 degrees F (2,192 ±212 degrees F is required).

(3) 15 percent excess air above stoichiometry (3 percent is required).

(4) Continuous monitoring for oxygen (O_2), carbon monoxide (CO), and combustion temperature.

(5) A wet scrubbing system to remove hydrogen chloride (HCl) from the exhaust gas.

Operating requirements achievable in the DFS and PAS include:

(1) Mass emissions from the stack of less than 0.001 gram of PCB per 1,000 grams of PCB feed.

(2) Combustion efficiency of 99.99 percent relative to CO.

(3) Hydrogen chloride stack emissions limited to 4 pounds per hour (RCRA 40 CFR 264.343) or less.

(4) Particulate matter stack emissions limited to 180 milligrams per dry standard cubic meter (RCRA 40 CFR 264.343).

(5) Maintaining the furnace at negative pressure relative to the room.

(6) Sulfur dioxide, carbon monoxide, nitrogen oxides, and lead emissions limited so as not to exceed the National Ambient Air Quality Standard (NAAQS).

The National Environmental Policy Act strongly influences the design of almost every industrial plant being built. Our national concern over clean air and water along with waste disposal is translated into design criteria. The CSDP has taken these criteria and produced specific designs to ensure compliance with the spirit and letter of the NEPA.

ACRONYMS AND ABBREVIATIONS

AFB	afterburner
ASHRAE	American Society of Heating, Refrigerating, and Air-Conditioning Engineers
BDS	bulk drain station
BRA	brine reduction area
CAA	Clean Air Act
CAMDS	Chemical Agent Munition Disposal System
CFR	Code of Federal Regulations
CSDP	Chemical Stockpile Disposal Program
DFS	deactivation furnace system
DUN	dunnage incinerator
ECR	explosive containment room
HEPA	high-efficiency particulate air (filter)
JACADS	Johnston Atoll Chemical Agent Disposal System
LIC	liquid incinerator
MDB	Munitions Demilitarization Building
MDM	multipurpose demilitarization machine
MPF	metal parts furnace
NAAQS	National Ambient Air Quality Standard
PAS	pollution abatement system
PCB	polychlorinated biphenyl
PMD	projectile/mortar disassembly
RCRA	Resource Conservation and Recovery Act
RHA	residue handling area
RSM	rocket shear machine
TSCA	Toxic Substances Control Act

SUPPRESSION OF SYMPATHETIC DETONATION IN STACKS OF 500 POUND BOMBS

Mr Gary Parsons, Mr Larry Pitts, Capt Pamela Summers and Mr Greg Glenn
Air Force Armament Laboratory, Eglin AFB, FL.

Large quantities of hazard class 1.1 munitions are in military service inventories. Because this class of munitions is mass detonating it imposes the greatest restriction on quantity distance (Q/D) criteria. In fact, at many Air Force installations quantities of class 1.1 munitions are below operational needs because there is not adequate land area to space facilities at safe separation distance. Figure 1 shows a typical Air Force Tactical Fighter Wing in West Germany. Note the close proximity of the ammunition storage area to German residences and base facilities.

While reduction of munition stockpiles is perhaps the most simple way to meet Q/D standards; it does impact readiness. In cases where a high level of readiness is essential, local commanders use waivers to allow deviations from standard storage procedure. A waiver is an agreement to accept risk. Secretary of Air Force policy--not to permit new construction under conditions where waivers to Q/D are in place--has forced many base commanders to reassess their munition storage posture.

Of all the munitions used by tactical forces, MK-80 series general purpose bombs constitute the biggest problem. Required quantities of bombs are large and high explosive quantities in each bomb produce strong shocks and high velocity fragments that readily detonate adjacent munitions. Figure 2 shows

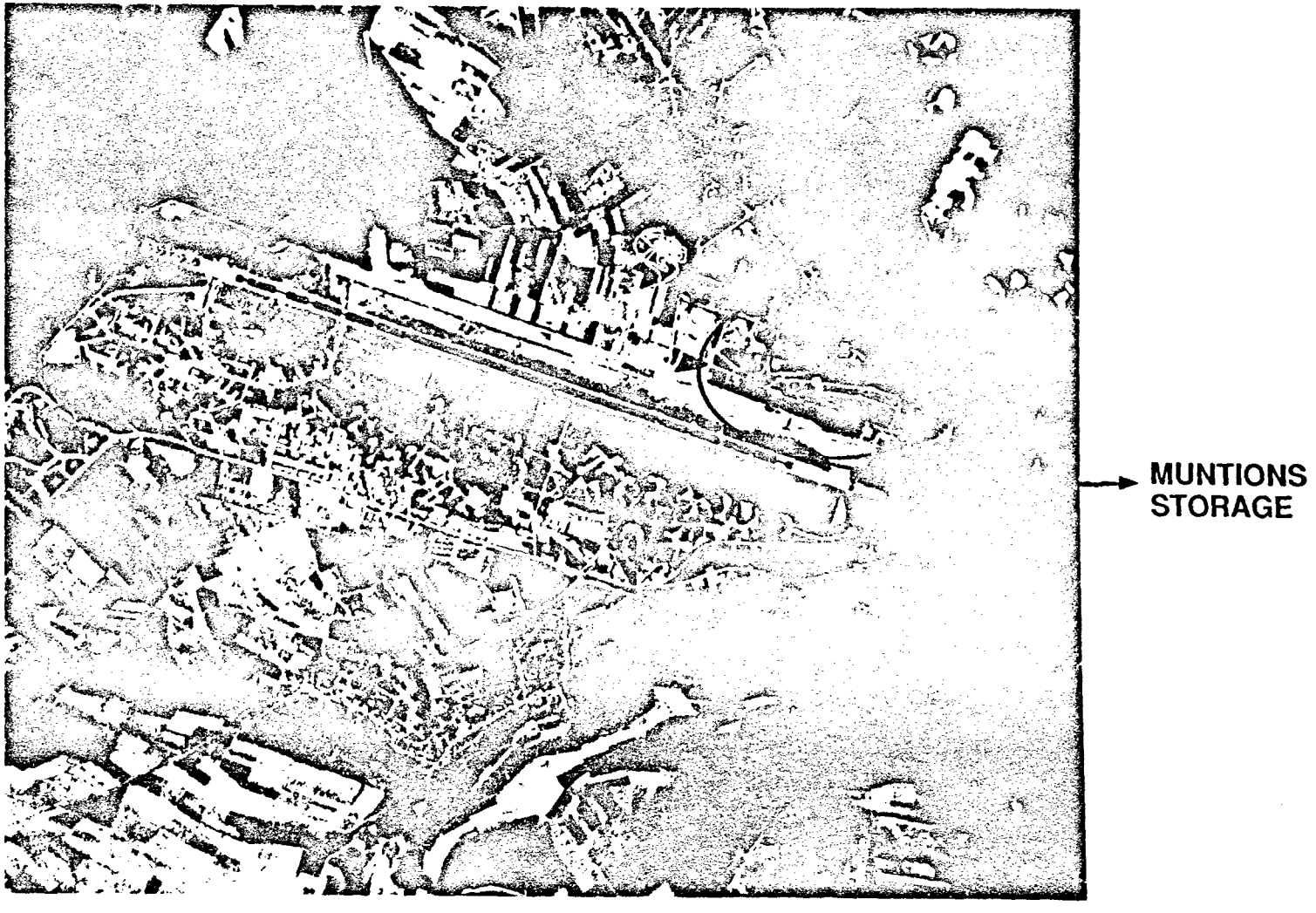

FIGURE 1. SPANGDAHLEM AB, WEST GERMANY

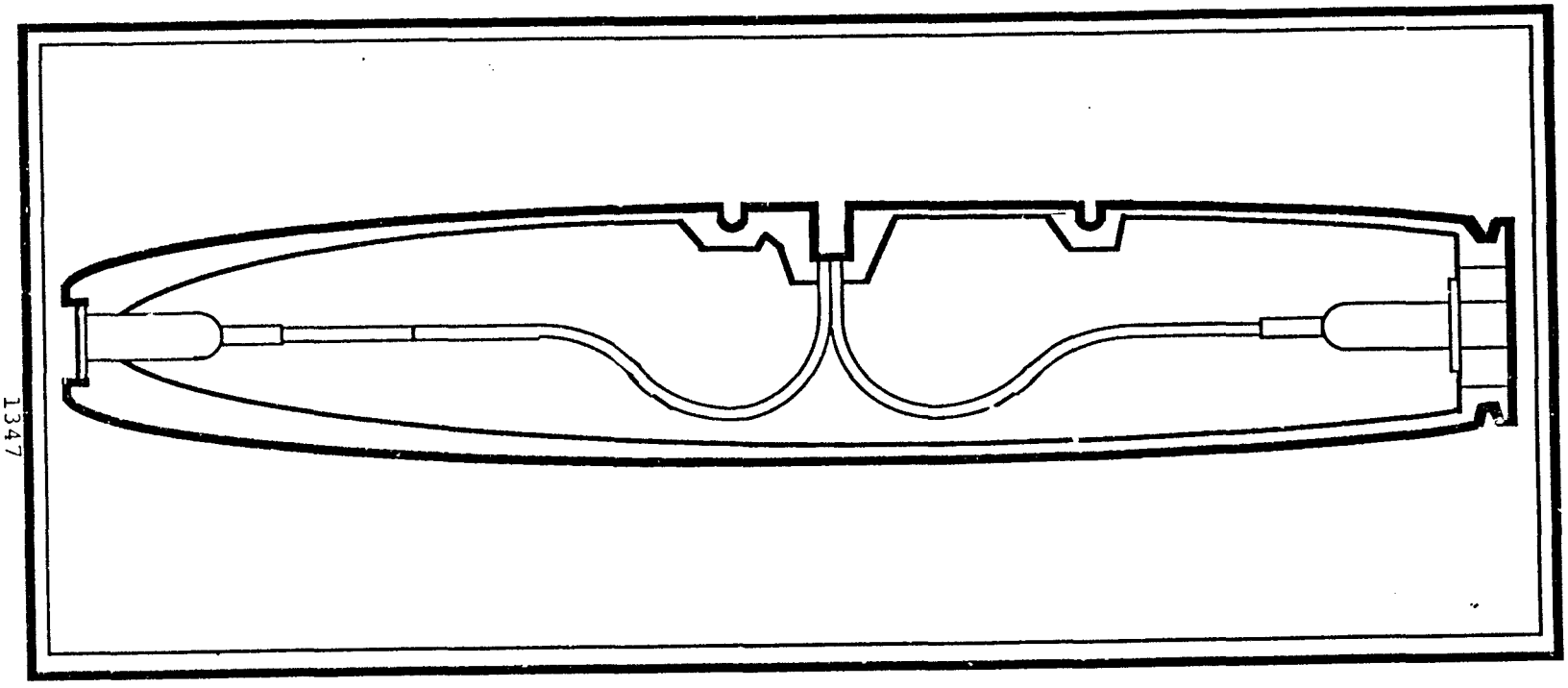

FIGURE 2. MK 82 500 POUND BOMB WITH 190 POUNDS OF TRITONAL EXPLOSIVE

a cross section of the MK-82 bomb. The explosive fill is tritonal, a mixture of TNT and aluminum. In 1984 the Air Force Armament Laboratory at Eglin AFB FL undertook a project to eliminate the mass detonation features of bombs. Our approach was to replace the tritonal fill with a less sensitive explosive and modify the bomb storage pallets to defocus the energy release from detonation of a single bomb. This presentation deals with the development of a new explosive fill, called AFX-1100, and the design of a special pallet that attenuates fragment and shock transmission loads. Further information on the properties of AFX-1100 may be found in Reference 1.

Table 1 shows the formula and explosive properties of AFX-1100. The explosive is basically tritonal that has been desensitized by the addition of a special wax mixture. The wax and TNT form a stable emulsion that causes the AFX-1100 to become sufficiently viscous to suspend the aluminum and wax homogeneously.

To assess the shock sensitivity of AFX-1100 we have conducted gap tests in the various configurations shown in Figure 3. For each gap test configuration, peak pressure is a function of the thickness of the plexiglas attenuator between the donor and acceptor and the size of the donor. Positive phase duration is a function of the size of the gap test assembly. The 8" diameter gap test was designed to simulate the pressure/time profile we would expect in bomb to bomb propagation (Reference 2).

TABLE 1. EXPLOSIVE FORMULA AND PROPERTIES

AFX-1100 COMPOSITION	SMALL-SCALE TESTING RESULTS	

• TNT AND WAX EMULSION
  • 66% TNT
  • 16% OD2 WAX - ACTS AS DESENSITIZER
  • 85% OZOKERITE WAX
  • 14% NITROCELLULOSE
  • 1% LECITHIN
  • 18% ALUMINUM
	TEST	RESULTS

	DSC	ONSET - 257° C PEAK - 273° C
	DROP HAMMER (5 kg)	P_{50} ~ 200.5cm
	CRT	.48 cm^3 / gm @ 120° C FOR 48 HRS
	Tc	250 °C ± 1
	Eact	39500 cal / mole
	CRITICAL DIAMETER	19.1 mm < D_c < 25.4 mm

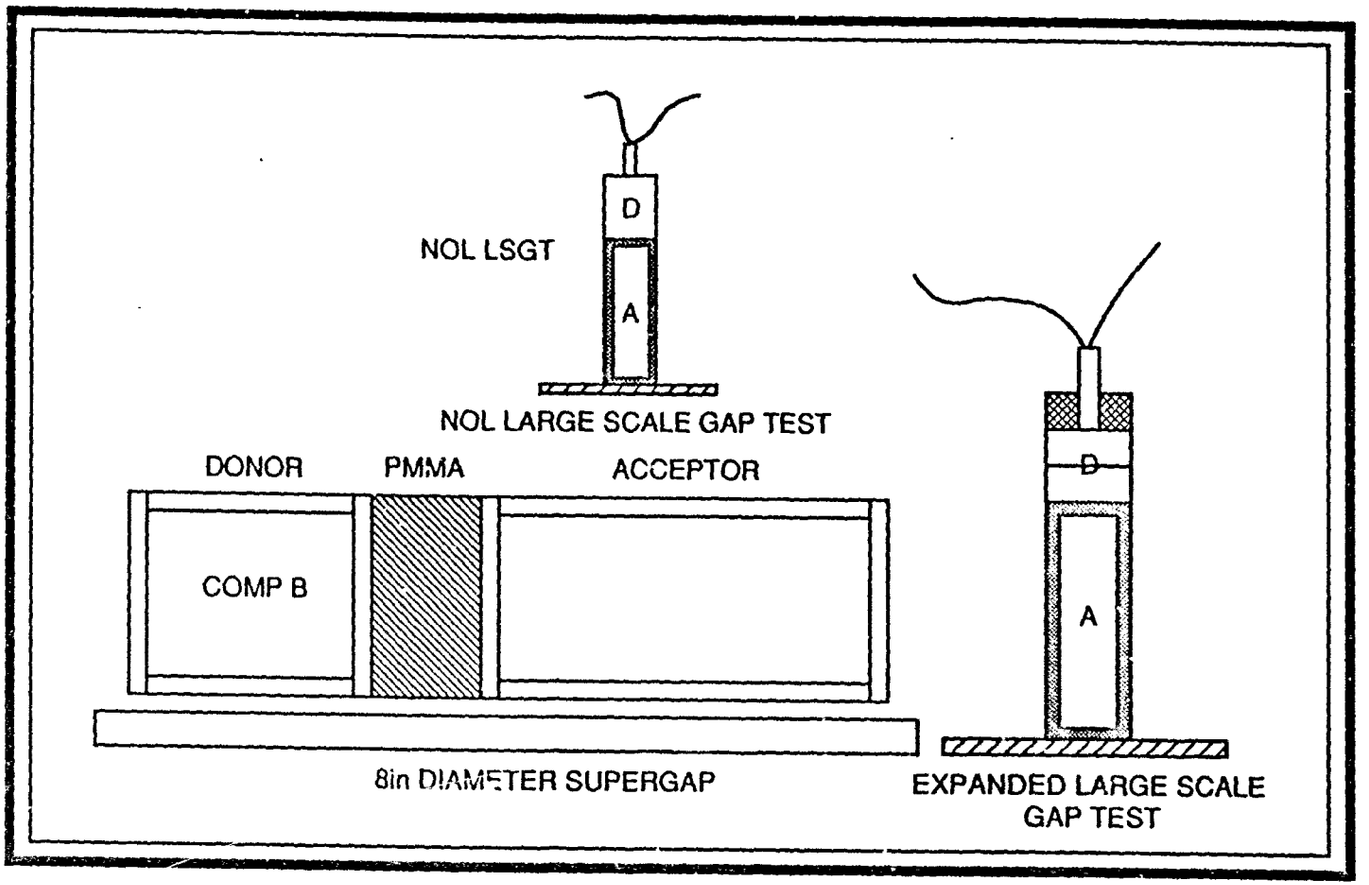

FIGURE 3. RELATIVE SIZE OF VARIOUS GAP TESTS USED TO MEASURE SHOCK SENSITIVITY

Wax is an extremely effective desensitizer. Figure 4 compares the shock sensitivity of AFX-1100 tritonal and PBX 9502. These data are reported in Reference 3. Of special interest is the difference at large diameters. AFX-1100 shows little increase in shock sensitivity even for long duration shocks similar to those transmitted in bomb to bomb geometries.

Figure 5 shows a linear array of MK-82 bombs filled with AFX 1100. Only the donor detonated. In fact, we have never observed propagation between rounds in two dimensional arrays even when spacing was varied from contact to 10 feet. In three dimensional arrays (Figure 6) confinement from adjacent bombs does focus energy preferentially and we have consistently observed detonation of diagonal acceptors. Additional protection was essential and the question became how much protection and what material should be used. The 8" gap test was used to evaluate the shock attenuation features of various materials. Table 2 shows that wood is equal to or better than plexiglas, concrete, aluminum, and steel on a volume basis and far better than most materials on a weight basis. These tests were done using a composition B donor and tritonal acceptors, consequently, we would expect to use less wood between AFX-1100 donors and acceptors since the donor produces lower detonation pressure and the acceptor is less sensitive.

Hydrocodes were used to provide an indication of the relative value of wood and layers of wood and air as shock attenuators. The geometric arrangement for these calculations is shown in Figure 7. We were interested in not only reducing the peak transmitted pressure but also increasing the rise time

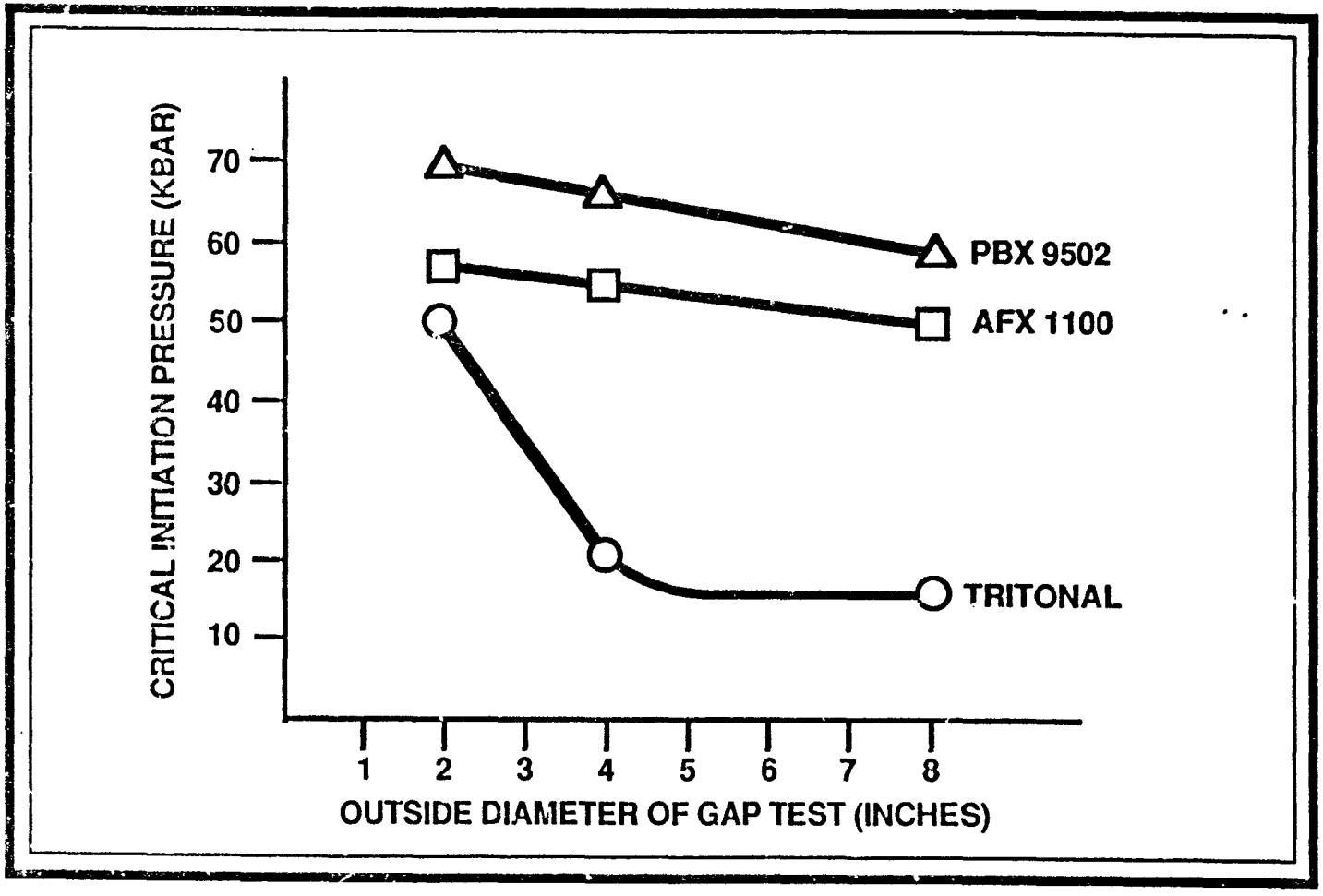

FIGURE 4. SHOCK SENSITIVITY OF THREE EXPLOSIVES MEASURED AT DIFFERENT CHARGE DIAMETERS

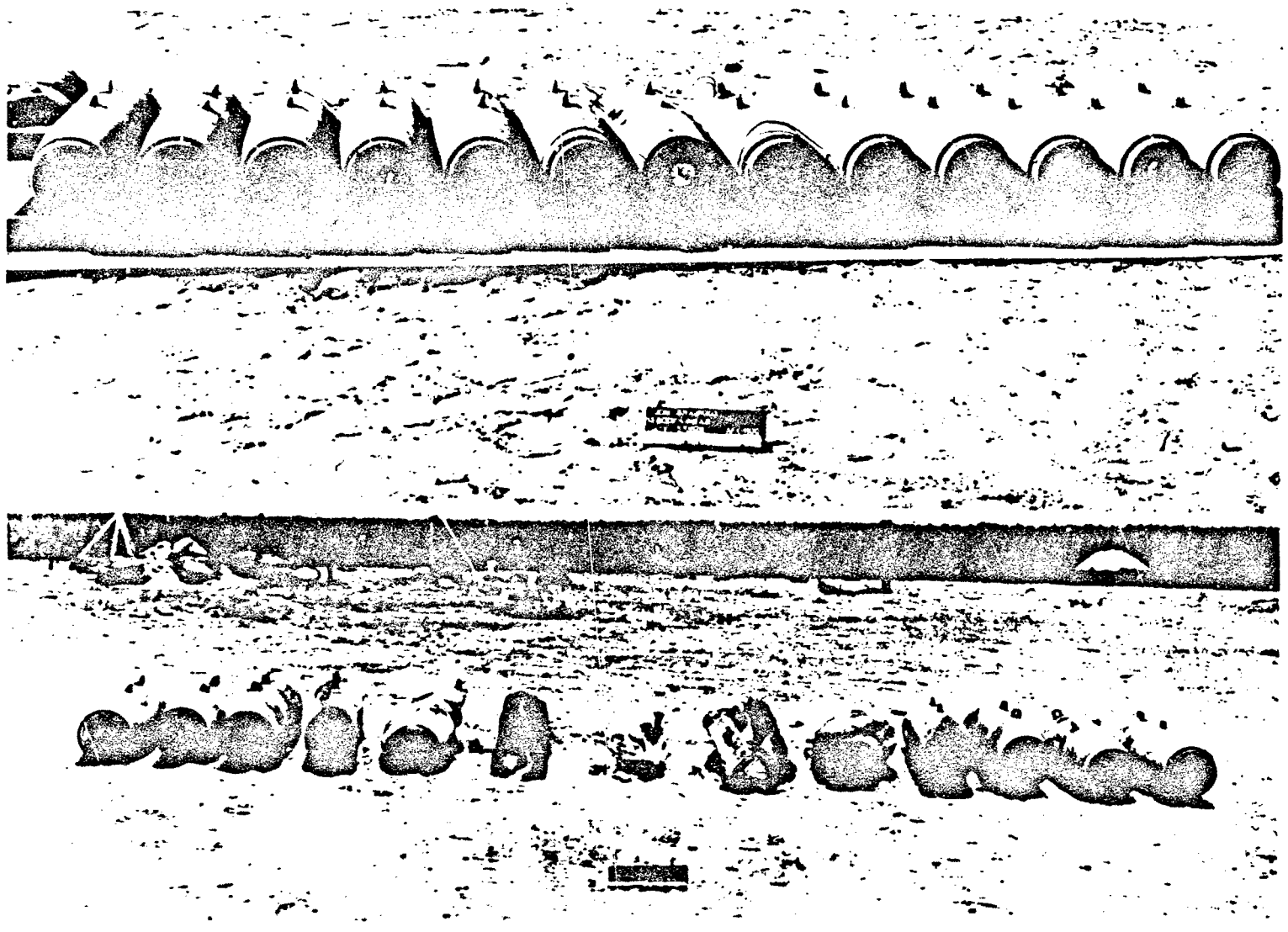

FIGURE 5. PRE AND POST TEST VIEW OF 13 BOMB LINEAR ARRAY

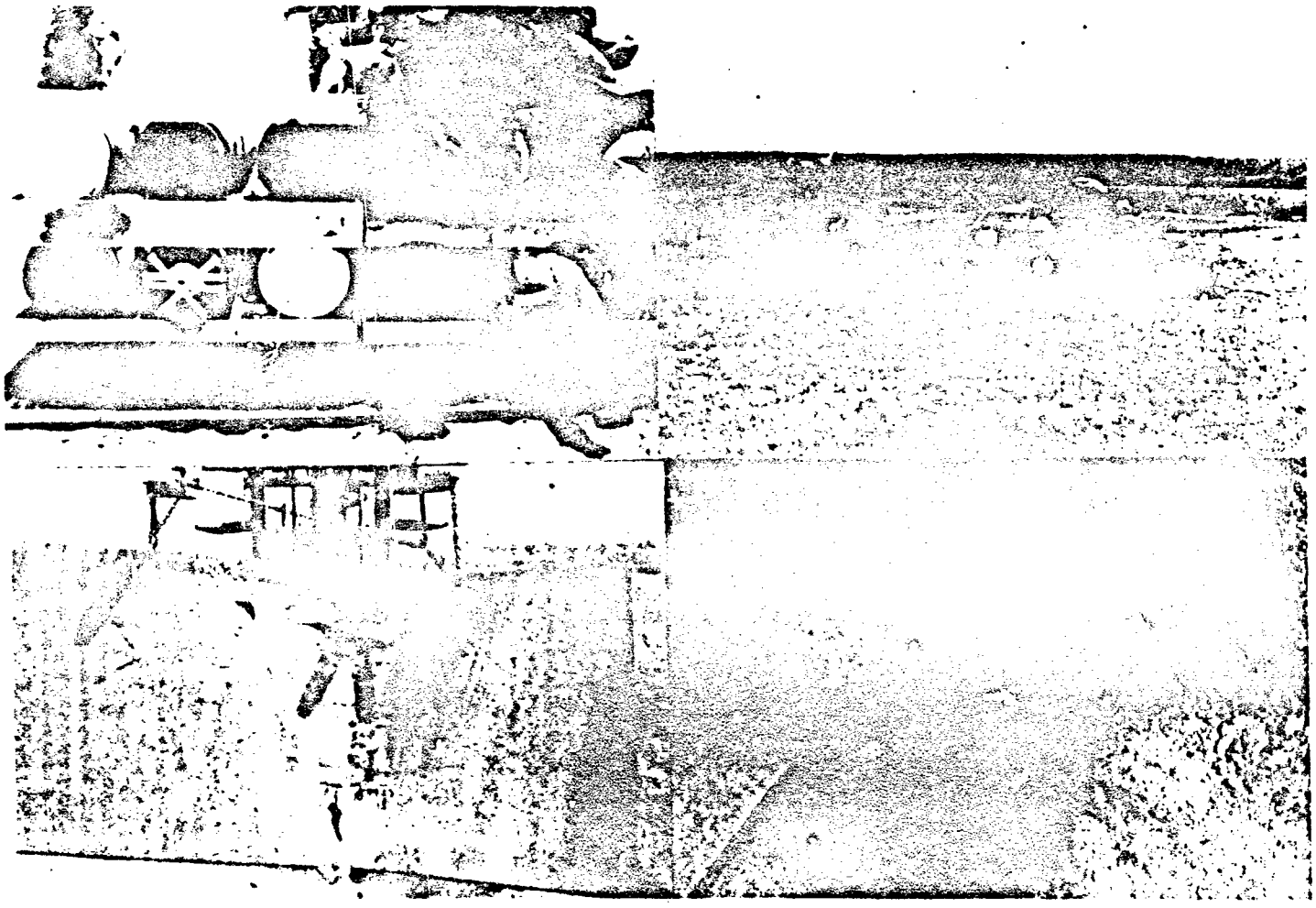

FIGURE 6. THREE DIMENSIONAL ARRAY OF BCMBS IN AFX - 1100 PALLET TEST

TABLE 2. RELATIVE RANKING OF SHOCK ATTENUATORS

MATERIAL	THICKNESS (T) (IN)	DENSITY (ρ)	RANK (ρ) (T)
PINE	5.5	0.6	3.3
POLYETHYLENE	6.0	0.9	5.4
WATER	7.0	1.0	7.0
PLEXIGLAS	6.0	1.2	7.2
CONCRETE	5.4	2.4	13
GLASS	8.9	2.2	20
STEEL	6.0	7.8	47

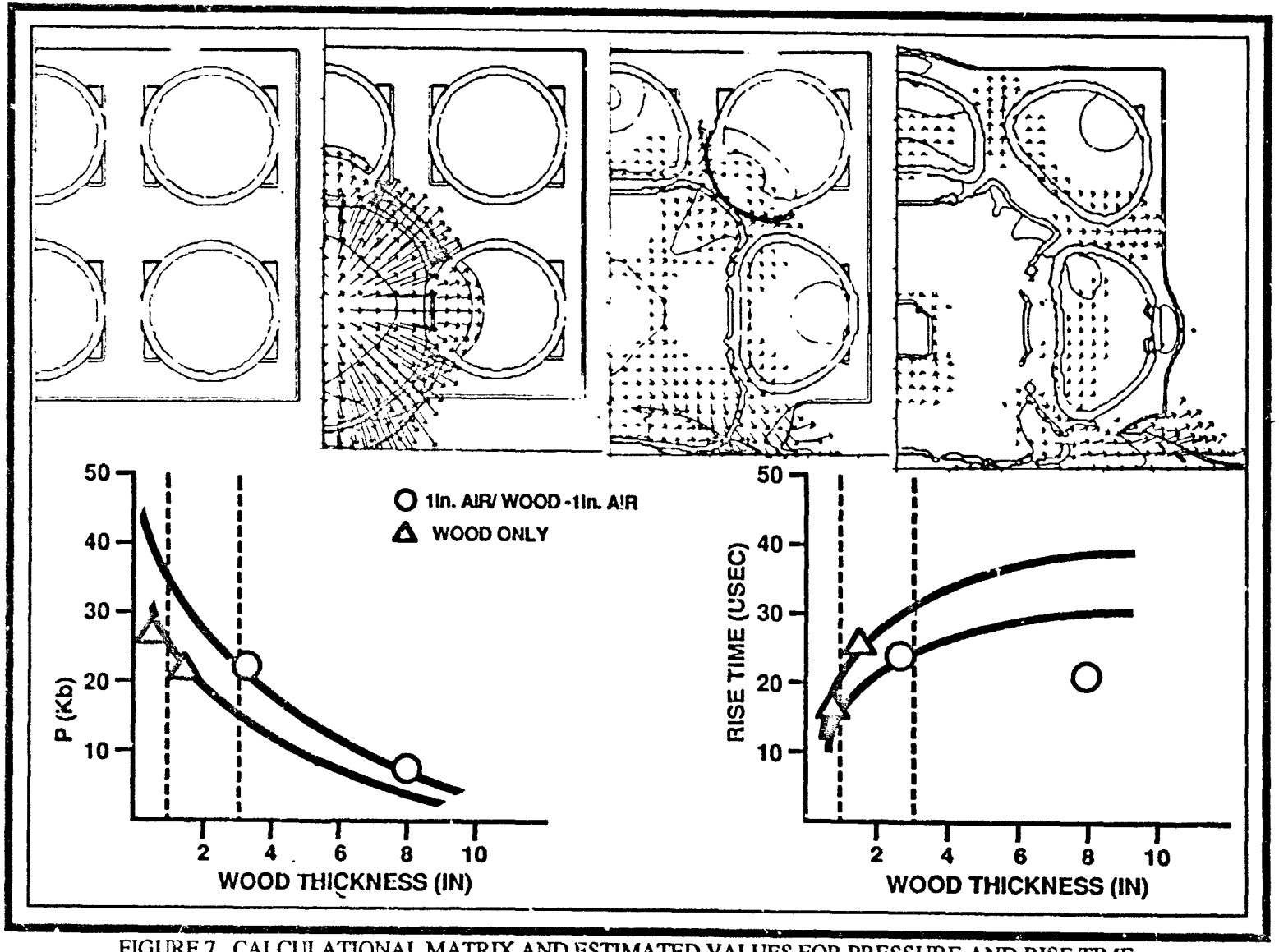

FIGURE 7. CALCULATIONAL MATRIX AND ESTIMATED VALUES FOR PRESSURE AND RISE TIME VERSUS WOOD AND AIR LAYER THICKNESS

since experimental evidence suggests that sub-detonative shocks are a mechanism for desensitization (Reference 4). These calculations were performed with tritonal donors and acceptors because the equation of state for explosive products and unreacted tritonal are known. We assumed the relative order of effects would be consistent with AFX-1100 explosive samples, and conducted a series of experiments using AFX-1100 filled donors and acceptors to establish the required quantity of wood to suppress sympathetic detonation.

The experimental setup is shown in Figure 8. Measurement of the transmitted pressures was accomplished by installation of carbon gauges. The measured threshold pressure of 43 Kbar is quite close to the value estimated from the 8" gap test (Figure 4). Using these data, several prototype wood pallets (Figure 9) were designed, fabricated, and tested, according to the arrangement shown in Figure 10. While none of the acceptors detonated in any of these tests the pallet providing 4 1/2-inch plywood spacing between bombs provided the greatest amount of protection to the acceptor bombs. Damage to the acceptors was attributed to mechanical loads applied by the donor. There was no evidence of bomb failure due to explosive reaction in the acceptors. Table 3 shows the explosive yield for the various pallets tested in the configuration shown in the previous figure. The yield is not significantly different for the various designs. Sympathetic detonation did not occur. With selection of the 4 1/2-inch wood pallet as baseline, additional tests were conducted to verify that increasing confinement would not produce a more violent response in the acceptors nearest the donor. Figure 11 shows that additional layers of inert bombs did not affect the outcome.

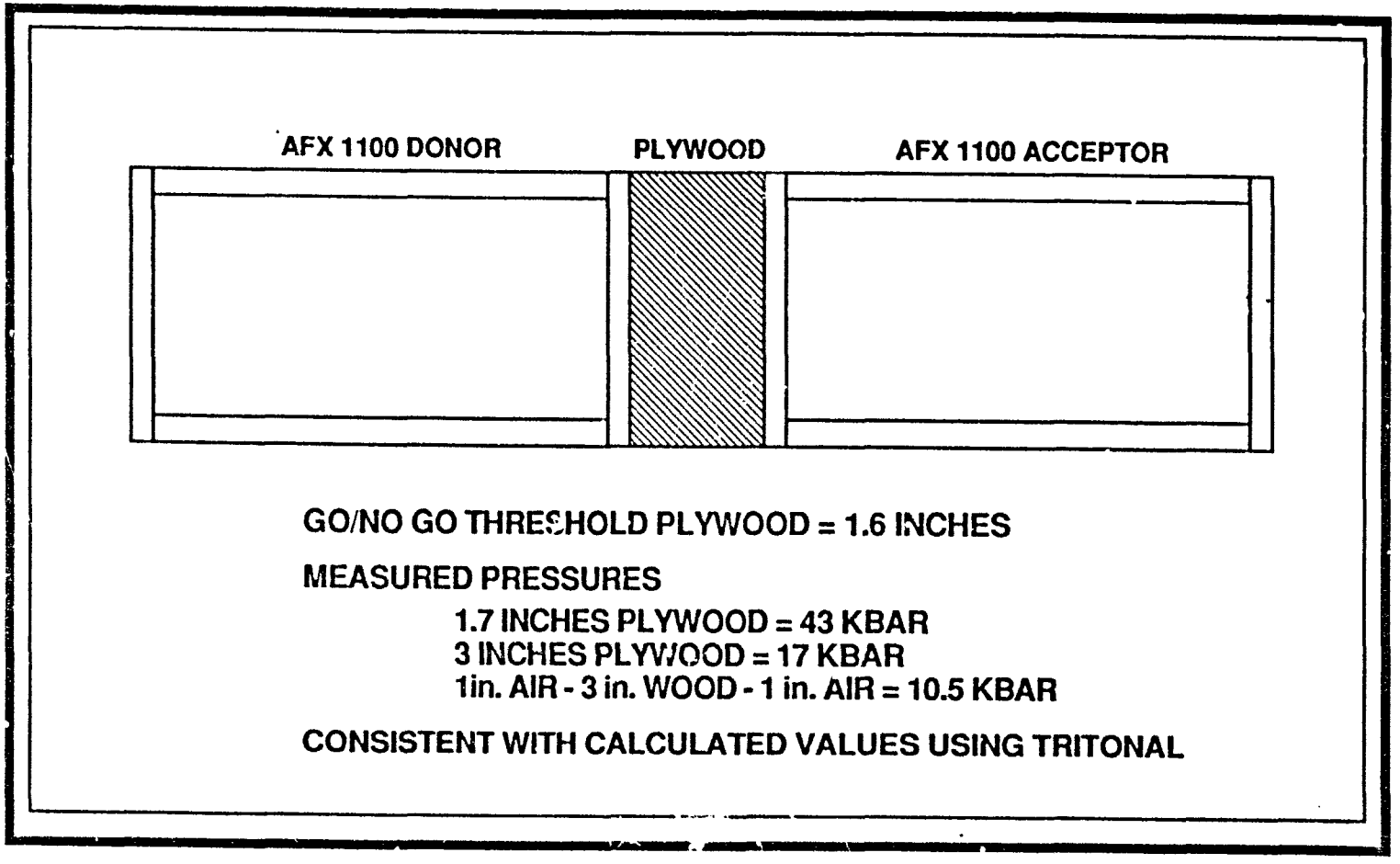

FIGURE 8. EXPERMENTAL SETUP FOR VALIDATING SHOCK ATTENUATION FEATURE OF WOOD

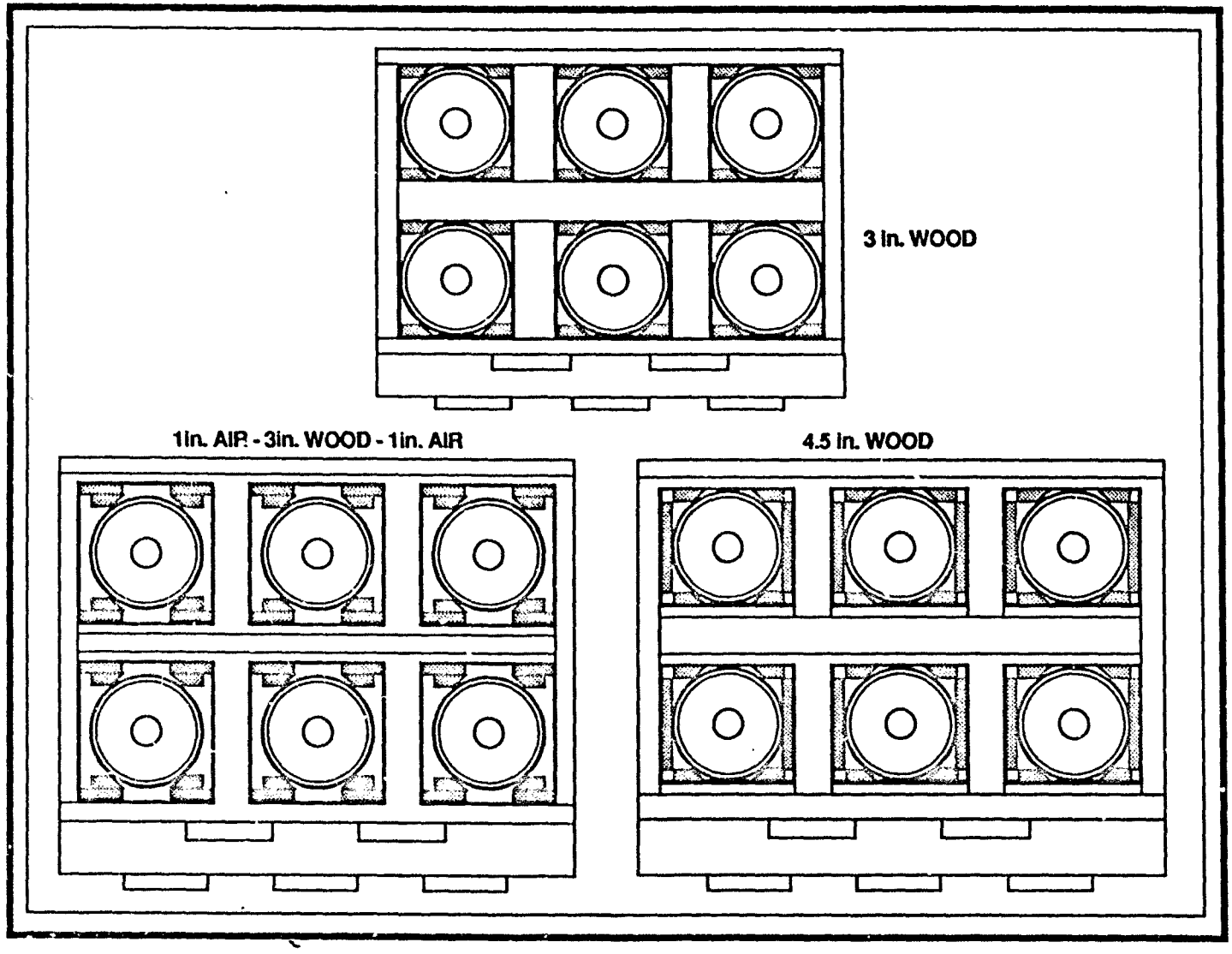

FIGURE 9. PROTOTYPE WOOD PALLET DESIGNS

FIGURE 10. TEST SETUP TO EVALUATE PROTOTYPE PALLETS (DONOR IS BOTTOM CENTER, FIVE ACCEPTORS ARE ARRANGED ACCORDING TO THEIR POSITION AROUND THE DONOR)

TABLE 3. ESTIMATED YIELD (LBs OF TNT) FROM SYMPATHETIC DETONATION TESTS

CONFIGURATION		# LIVE BOMBS	YIELD
3" BASELINE	(N)	1	230
3"	(N)	6	280
1" - 3" - 1"	(N)	6	270
4.5"	(N)	6	230
4.5"	(T)	6	180
4.5"	(T)	6	170

(N) - NOSE INITIATION (T) - TAIL INITIATION

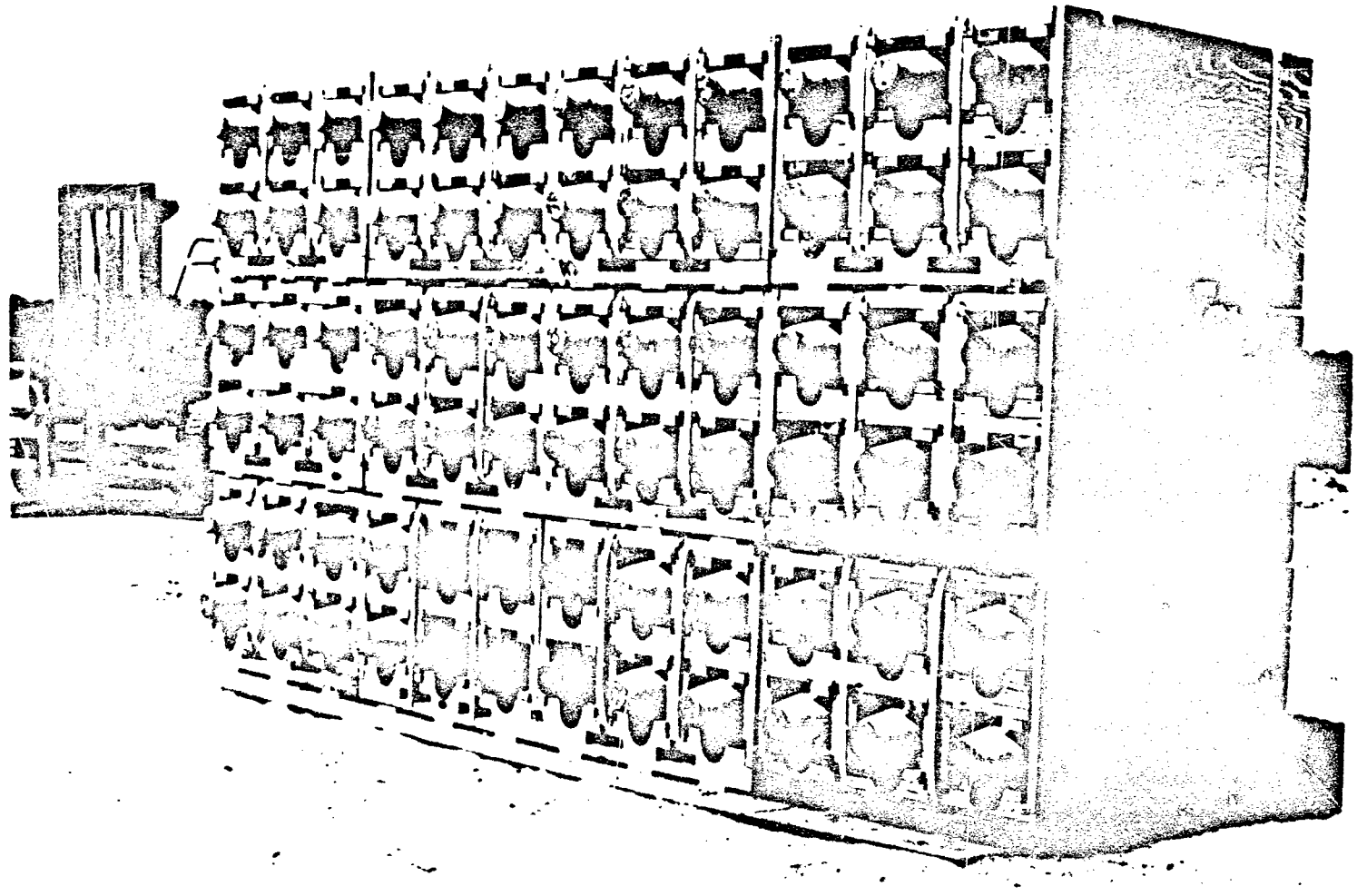

FIGURE 11. INCREASING CONFINEMENT BY ADDITIONAL INERT BOMBS

Hazard classification under TB 700-2 requires that stacks of munitions be evaluated for sympathetic detonation and cook-off. Following discussions with members of the safety community, we concluded that the donor bomb should have at least two layers of live bombs around it. Thus our center stack would include a core of 24 live bombs. In addition, at least one full pallet of bombs should be positioned fore and aft of the donor and aligned with the donor. To maintain symmetry we increased the number to nine live bombs fore and aft. This assembly was then surrounded by pallets of inert bombs sufficient to insure that 1 meter of confinement would be simulated. Figure 12 shows the finished assembly.

Detonation of the donor shattered large portions of wooden pallets and scattered live and inert bombs. A slow developing fire gradually progressed through the debris and AFX-1100 filled bombs cooked off over a period of several hours. A post test view of the test arena is shown in Figure 13. Of 42 live bombs used in this test, one was deliberately detonated, the remaining 41 were recovered. Nineteen bombs cooked off and of the nineteen, 3 ruptured and 16 vented out of the fuzewells. Interestingly, concrete filled bombs reacted more violently than the explosive filled items, presumably, because they are sealed with heavy nose and nail plates, and consequently, reach higher internal pressure prior to failure.

A second requirement for hazard classification is munition response in bonfire. Our interpretation of TB 700-2 called for 30 live bombs, contained in 5 pallets arranged as shown in Figure 14. Wood was stacked under the

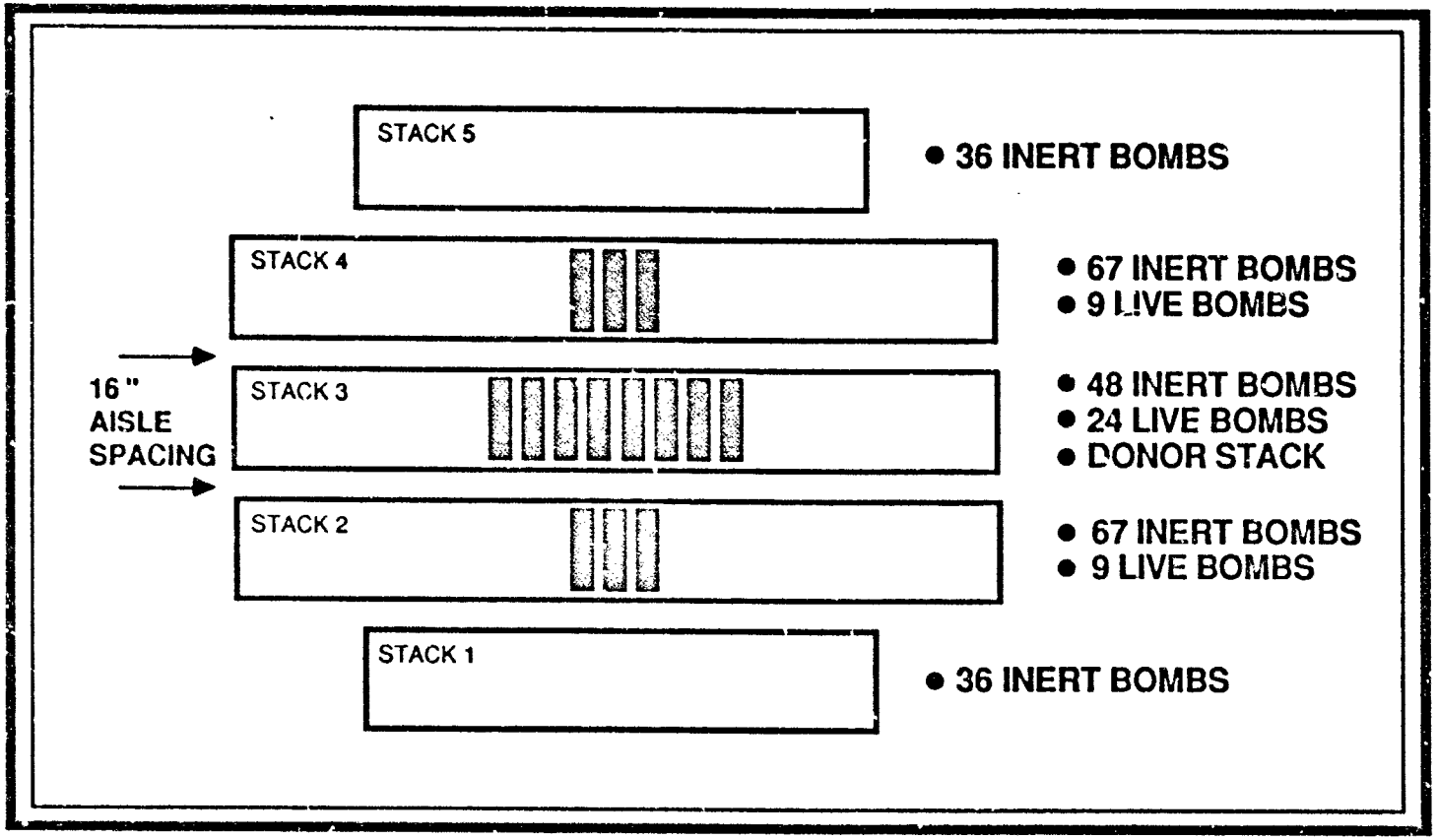

FIGURE 12. SCHEMATIC OF PALLET ASSEMBLY FOR STACK TEST

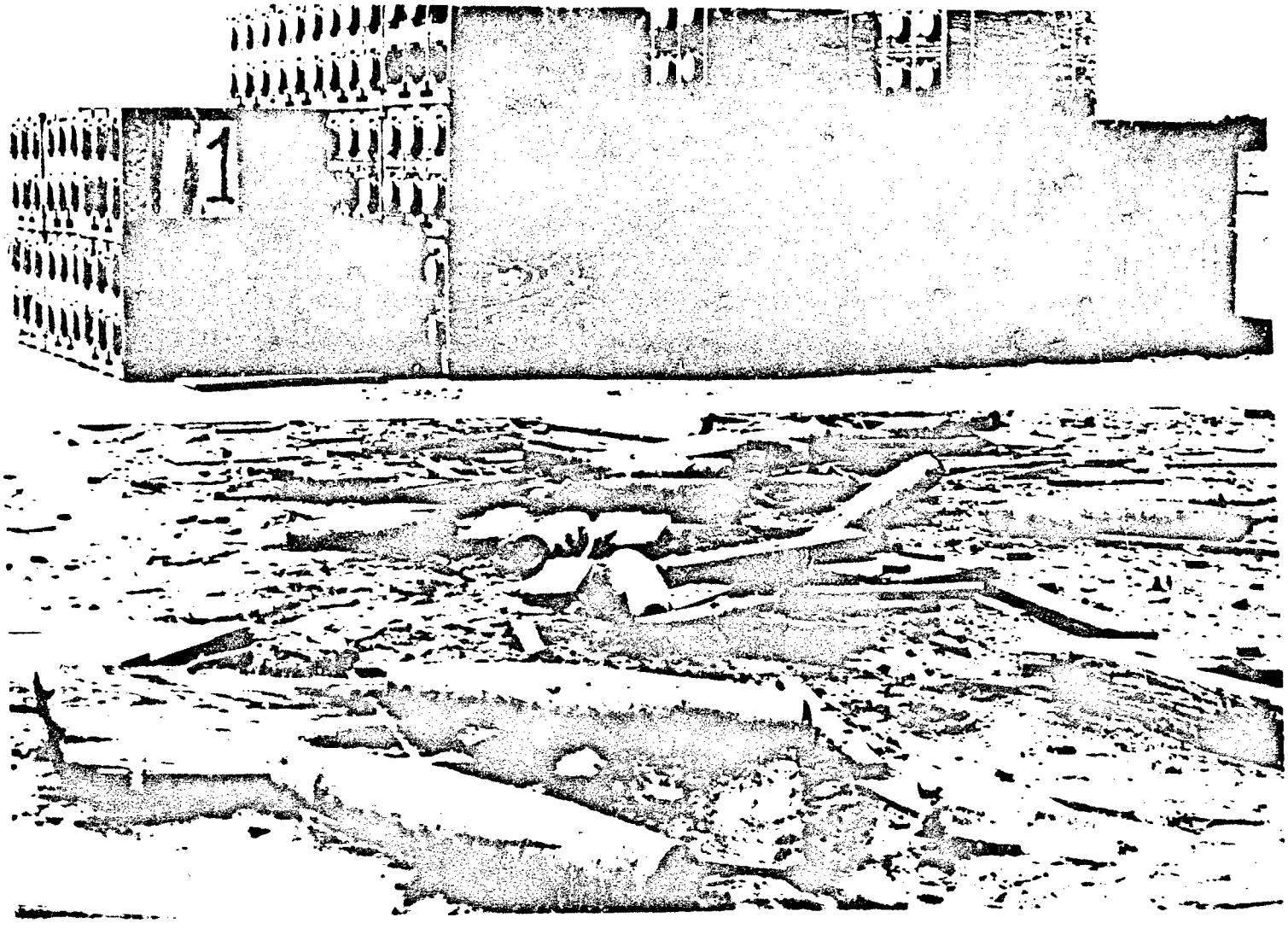

FIGURE 13. PRE AND POST TEST VIEW OF BOMB STACK

pallets and at least 1 meter on all sides and the top. Diesel fuel was poured at several sites within the assembly and thermite grenades were used to ignite the fuel. This fire develops very rapidly and the initial cook-off occurred 7 minutes after ignition. Reactions continued for 20 minutes. Twenty-eight bombs failed by venting through the fuze liner and two bombs failed by rupture of the skin along the seam.

In summary, we have demonstrated a very effective method of desensitizing a TNT based explosive. Not only is shock sensitivity reduced even in large diameters but no violent reactions occur in fast cook-off. A major concern early in this development was that deflagation to detonation would occur in large scale sympathetic detonation tests even though the AFX-1100 was less sensitive to direct shock initiation. It was speculated that deformation and crush-up of bombs adjacent to the donor would produce internal pressures that favor a rapid buildup. This was not observed in MK-82 bombs. Scaling to larger sizes, such as 2000 pound bombs, could produce a different response. The process for selection of a material for bomb pallets and design of those pallets was successful. Future plans include a new subscale design that better simulates MK-82 bomb geometry and equation of state characterization for AFX-1100 to improve hydrocode simulation. These tools should facilitate the evaluation of new materials for pallet construction so that lightweight, non-combustible alternatives to wood may be used.

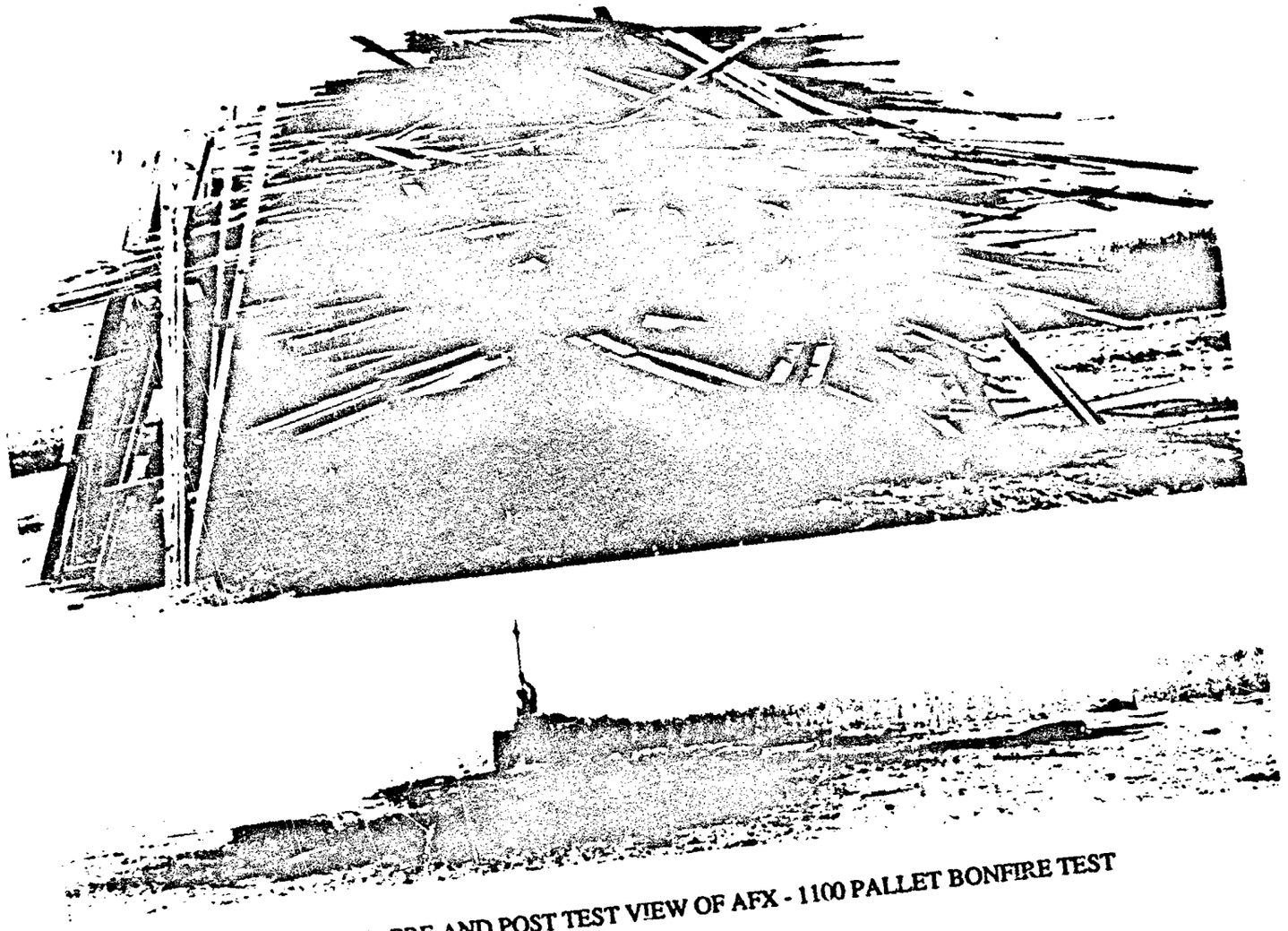

FIGURE 14. PRE AND POST TEST VIEW OF AFX - 1100 PALLET BONFIRE TEST

SUMMARY

DESENSITIZATION OF TNT BY EMULSIFYING WAXES IS EFFECTIVE WITHOUT INCREASING FAILURE DIAMETER

HYDROCODES PREDICT SHOCK TRANSMISSION FROM DONORS TO ACCEPTORS

EXPERIMENTAL MODELS WERE USED TO VALIDATE THE PREDICTIONS AND DESIGN A STORAGE PALLET

THE COMBINATION OF A LESS SENSITIVE FILL AND STORAGE PALLET PERMITS 500 POUND BOMBS TO BE STORED AS HAZARD CLASS 1.2 ITEMS

ACKNOWLEDGMENTS

The authors gratefully acknowledge the assistance of Mr Rick Strama of the 3246th Test Wing for supervision of the large scale test phase. Mr George Lambert conducted the subscale tests. Mr Steve Aubert developed the AFX-1100 formulation, and Capt Tony Taliancich designed the wooden pallets. Dr Joseph C. Foster, Jr., and Capt Keith Forbes conducted the study to evaluate shock attenuation of different materials. Mr John Osborne of Orlando Technology Inc. performed the hydrocode calculations for prototype pallets.

REFERENCES

1. Stephen A. Aubert, Sara J. Massey, and John D. Coriey, Desensitization of Tritonal with Wax Emulsions, AFATL-TR-88-32, Eglin AFB, FL, May 1988.

2. Joseph C. Foster, Jr., Michael E. Gunger, Bob G. Craig, and Gary H. Parsons. Suppression of Sympathetic Detonation, Minutes of the Twenty-First Explosive Safety Seminar. VOL I, pp 813-837.

3. Stephen A. Aubert, Joseph G. Glenn, and Gary H. Parsons. Shock Sensitivity of AFX-1100, a Desensitized Tritonal Fill, (AFATL TR to, be published).

4. A. W. Campbell and J. R. Travis, The Shock Desensitization of PBX 9404 and Composition B-3. Eighth Symposium (International) on Detonation, Albuquerque NM. July 15-19, 1985. NSWC MP 86-194, pp 1057-1068.

The Propagation Law of Air Shock Wave for Earth Overlaid Explosive Storehouse

Li Zheng Wang Zhongqin

ABSTRACT

We have made a series of tests that some earth overlaid explosive storehouses were blasted to investigate the safety distance under the condition of an earth overlaid explosive storehouse blasting. We have found out the propagation law of air shock wave by measuring the values of the overpressure of shock wave in every direction of the test explosive storehouse with piezocrystal transducers during blasting. We found that the overpressure of the shock wave due to the explosive storehouse blasting had an obvious direction distribution. When the scale distance defined as $\bar{R}=R/W^{1/3}$ between two explosive storehouses side by side was in the range of 0.5 to 5 $(m/kg^{1/3})$ the values of the overpressure were 18% to 52% of the values due to ground blasting. So the safety distance between two earth overlaid explosive storehouses could be reduced by 68% to 32% compared with that in the case of ground explosive storehouses.

I. Introduction

The explosive storehouses were often built on hillsides by excavating a given mass of earth or and rock making use of

the natural terrain as a defence. The hind wall of this sort of explosive storehouse was very close to hill body. The front wall of the storehouse was retaining wall made of rubbles and overlaid with earth 1 meter thick on the top of the wall and the overlaid soil was thicker and thicker in measure as a slope at the rate of 1:1 from the top of the wall down to ground. The roof was made of reinforced concrete overlaid with earth 0.5 meter thick on the surface of the roofing and with soil on the field outside the roof. There was traffic passage 6 meters in width outside each of the two brick built gables and there were earth embankments outside the passages which their length was the same as the width of the storehouse, i. e. the length of the gable. The embankments were as high as the top of the gables. The function of the overlaying earth was as follows: (1) to weaken the influence of air shock wave on environ ment while the storehouse itself was blasting, (2) to enhance its ability to protect against blast-flying stones and to weaken the shock wave acting on the roof in some degree in the case of other adjacent storehouse blasting.

In order to study the propagation law of the air shock wave due to earth overlaid explosive storehouse blasting, three reduced scales of tests which the ratio of the charge weight to the charge house volume was in the range of 0.08 to 0.12 Ton/m^3 were conducted according to the law of conformity of explosion.

II. Test

We had four measuring lines along the o-degree, 45-degree,

90-degree (or 75-degree and 115-degree in the light of specific topography of the test field), and 180-degree directions of the storehouse respectively in consideration of the symmetry of shock wave flowing field and that the shock wave distribution over the whole field outside the storehouse might be not necessarily the same or uniform. There were 10 to 13 measuring sites in the o-degree direction and 45-degree direction separately which the measure range was from 0.2 kg/cm^2 to 20 kg/cm^2 . There were about 10 measuring sites placed in the 90-degree direction and only 4 to 10 measuring sites placed in the 180-degree direction because of the slope (see Fig.1).

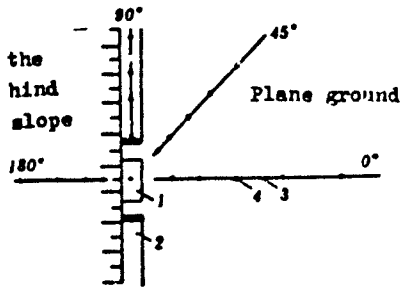

1. the explosive storehouse
2. the earth embankment
3. the measuring lines
4. the placed measuring sites

Fig.1 The sketch figure of the arrangement for the measure sites

In order to rise the overpressure measuring accuracy,we made use of Swiss Kistler transducers and 901, 931 types of piezocrystal transducers made in the Mechanical Institude of Chinese Academy of Science and SBR-1 type of double oscillographes. The work frequency of the measure system was 100kc. In addition, because we had a little difficulty with using piezocrystal transducers all in tests dur to the greater needs in quantity in

every test, so we also made use of BPR-2 measure system partly. The BPR-2 piezometer is a resistance-strain piezometer and its natural frequency is about 30kc. We used BPR-2 piezometers with Y6D-3A dynamical strain amplifiers and the natural frequency of the whole measure system is 1.5kc. Fig.2 shows the comparison between the accuracy of the piezocrystal measure system and that of the strain measure system.

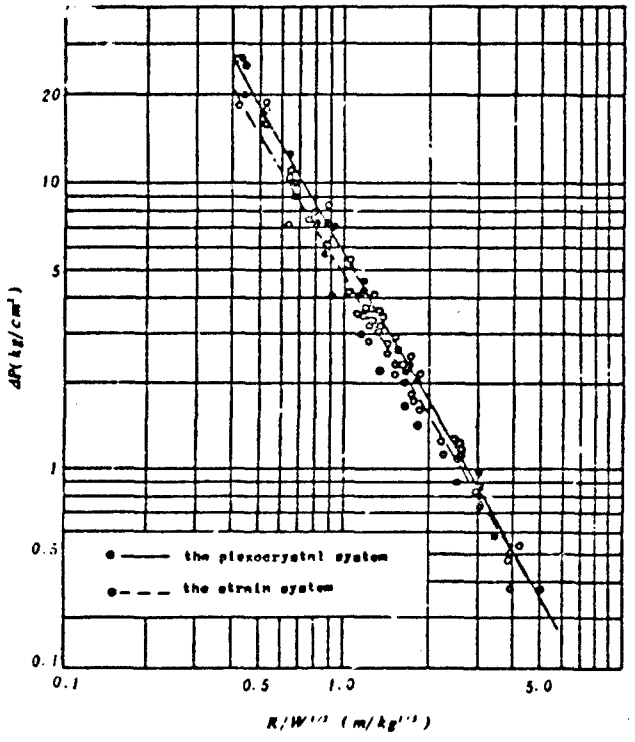

FTg-2 The test results of the overpressure of air shock wave by using the piezocrystal measure system and the strain measure system along with the 0-degree direction line

In order to compare our test results with the results in other test conditions and make our test results be of universal significance, we made corrections for all the test data of ours in accordance with the condition of standard air.

$$\left.\begin{array}{ll} \text{pressure} & \Delta P = \left(\frac{P_0}{P_0'}\right)\Delta P' = f_p \Delta P' \\ \text{distance} & R = \left(\frac{P_0'}{P_0}\right)^{1/3} R' = f_s R' \\ \text{time} & t = \left(\frac{P_0'}{P_0}\right)^{1/3}\left(\frac{T_0'}{T_0}\right)^{1/2} t' = f_t t' \\ \text{impulse} & I = \left(\frac{P_0}{P_0'}\right)\left(\frac{I_0'}{I_0}\right)^{1/3} I' = f_i I' \end{array}\right\} \quad (1)$$

where, P_0—the standard atmospheric pressure (the pressure of mercury 760 mm in height), T_0—the absolute temperature in the case of standard air ($=288.16^\circ K$ or $15^\circ c$), I_0 — the impulse in the case of standard air, P_0' , T_0' , I_0' —the atm. prassure, the absolute temp., the impulse respectively in the case of the test air field, f_p, f_s, f_t, f_i — the meteorotogical correction coefficients of the pressure, the dist, the time, the impulse separately.

The slope of the hillsides ranged between 21-degree and 39-degree in the actual tests. The energy releasing space for the blasting charge would vary with the slope. So the explosive blasting energy should be corrected to take count of the influence of the slope besides the above meteorological corrections, We chose 30-degree slope as a standard one and the correction formula for the charge load is as follows:

$$W = \frac{150}{180 - a} W' = f_w W' \quad (2)$$

where, W' — the actual charge load, W—the corrected charge load, α —the hillside slope, f_e —the energy correction coefficient ($=150^\circ/(180^\circ-\alpha)$).

III. The Propagation Law of the Air Shock Wave for the Earth Overlaid Explosive Storehouse

1. Dimensional Analysis

We had deduced the general relation about the overpressure of air shock wave and the general relation about the positive pressure time duration by means of dimension al analysis.First, we analyzed the function relations of the dominant characteristic parameters and the undetermined parameters from the explosion dynamical viewpoint. If W is the blast energy of TNT in the earth overlaid storehouse, P_0 and ρ_0 are the pressure and density of the air around the TNT charge respectively, R is the distance between the charge center and one of the measure sites, ΔP is the overpressure, and τ is the positive time duration at the site in R distance, then the dominant explosion dynamical characteristic parameters are W, P_0, ρ_0. R is a varible. And ΔP, τ are the undetermined parameters. The functional relation of these parameters can be described as follows:

$$\Delta P, \tau = f(W, P_0, \rho_0, R) \qquad (3)$$

According to π Law, the dimensionless relation of ΔP and R can be deduced as follows:

$$\frac{\Delta P}{P_0} = f\left(\frac{R}{\left(\frac{W}{P_0}\right)^{1/3}}\right) \qquad (4)$$

And the dimensionless relation of τ and R can be deduced as follows:

$$\frac{\tau}{W^{1/3}P_0^{-5/6}\rho_0^{1/3}} = f\left(\frac{R}{\left(\frac{W}{P_0}\right)^{1/3}}\right) \qquad (5)$$

In the case of standard state, $P_0=1$, $\rho_0=1$, then,

$$\Delta P = f\left(\frac{R}{W^{1/3}}\right) \qquad (6)$$

$$\tau/W^{1/3} = f(R/W^{1/3}) \qquad (7)$$

In addition, we built np the empirical formulae in different direction (or angle) lines, so the parameter of angle was not contained in the dimensionless formulae.

2. Empirical Formulae

We found by test that the function relations of ΔP, $\tau/W^{1/3}$ and $R/W^{1/3}$ were of linearity in first approximation on hyperlogarithm coordinates when the scale distance $\bar{R}$ ($= R/W^{1/3}$) was in the range of 4 to 50 $m/Ton^{1/3}$ So the formulae can be expressed as single term forms:

$$\Delta P = K_1(R/W^{1/3})^{-a_1} \qquad (8)$$

$$\frac{\tau}{W^{1/3}} = K_1\left(\frac{R}{W^{1/3}}\right)^{a_1} \qquad (9)$$

where, ΔP (kg/cm^2) —the incidence overpressure of shock wave in different directions of the earth overlaid storehouse, R(m) — the distance from the blast center to the measure site, W(kg)— the total chage load (TNT in bulk and the density was $0.85g/cm^3$), K_1, a_1 — factors shown in table 1, τ (ms) — the positive pressure time duration, K_1, a_1 —factors shown in table 2.

table 1

measure system	line direction	site quant.	correlation factor r	K_1	α_1
BPR-2 system	0°	60	-0.9893	4.8598	1.6480
	45°	42	-0.9738	3.1771	1.3914
	90°	44	-0.9427	3.8731	1.5127
	180°	10	-0.9524	8.6848	2.4041
piezocrystal system	0°	33	-0.9913	5.5200	1.7217

table 2

measure system	line direction	site quant.	correlation factor r	K_1	α_1
BPR-2 system	0°	39	0.9348	0.5794	0.8102
	45°	27	0.9218	0.5542	0.7774
	90°	29	0.8909	0.5251	0.7834

The overpressure formula can be more accurately expressed as a trinomial as follows:

$$\Delta P = A\left(\frac{1}{\bar{R}}\right)^{\prime} + B\left(\frac{1}{\bar{R}}\right)^{\prime} + C\left(\frac{1}{\bar{R}}\right)^{\prime} \qquad (10)$$

where, $\bar{R}$ $(m/kg^{1/3})$ — the scale distance, A, B, C — factors shown in table 3 determined by means of least square method according to the dimension al analysis.

table 3

direction / factor	0°	45°	90°	180°
A	0.826	0.970	0.678	0.850
B	4.863	3.272	5.233	3.805
C	-0.636	-0.946	-1.608	3.295
R($m/kg^{1/3}$)	0.4～5	0.4～6	0.4～5	0.7～2.5

3. Test Result Analyses

A. Overpressure

The calculated results of table 1 are shown in Fig. 3. It can be seen from Fig. 3 that the lines of ΔP versus $\bar{R}$ in the directions of 0-degree, 45-degree, and 90-degree intersect at one point when ΔP is $0.25kg/cm^2$ and the scale distance $\bar{R}$ is $6.0m/kg^{1/3}$, but the values of the overpressure in 0-degree direction take the first place, the values in 90-degree direction take the second place and the values in 45-degree direction take the third place in the range of $\Delta P > 0.25kg/cm^2$.

The above results are also described as isobaric lines shoun in Fig.4. From Fig.4, we can find that the values of ΔP in 0-degree direction were so great as to form convexes and the values of ΔP in 45-degree direction were so small as to form concaves when $\Delta P > 2kg/cm^2$, but the isobaric lines of the two directions are much like semicircular when $\Delta P < 0.5kg/cm^2$ in

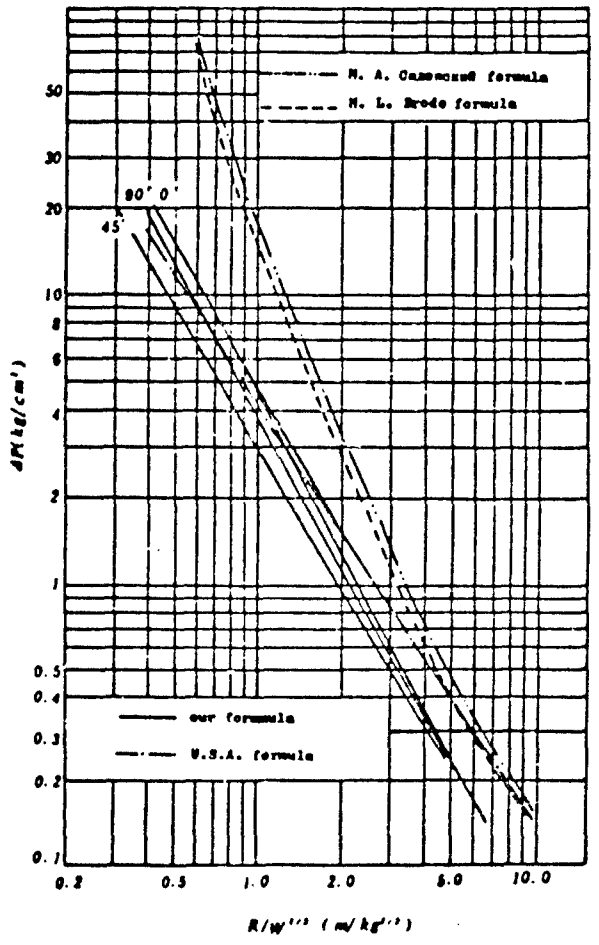

Fig. 3

The comparison of the overpressure attenuation laws of the earth overlaid storehouse blasting and the exposed blasting on ground

the range of 0 to 90-degree. The shock wave propagated along the slope up and behind the storehouse during the just initial post-explosion period because the roof and the brick built wall of the storehouse were first blasted. So, as regards the 180-degree direction, when $\Delta P > 2\ kg/cm^2$, the values of ΔP were greater than that in 0-degree direction and the isobaric lines formed larger convexes than that in the case of 0-degree direction because of the above case and the reflection action of shock wave at retaining wall. The shock wave broke through

the front rubble built wall in 0-degree direction just after the initial period and then the over-pressure in 180-degree direction went down very quickly and the isobaric lines in 180-degree became elliptical when the values of ΔP went down to $1kg/cm^2$ or less than that value.

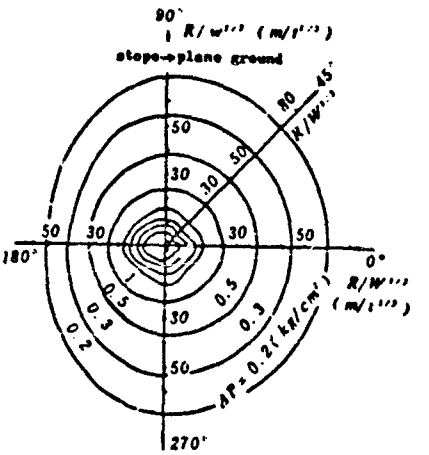

Fig.4 The isobraic lines at different scale distances due to the blasting of earthe overlaid storehouse

Considering that a pit would be formed under the condition of ground explosion and that the slope was 30 degrees, we revised the U.S.S.R. M.A. Садовский trinomial and the U.S.A. L. Brode trinomial. We took the revised factor for energy to be 1.75 × 1.21=2.1 and then calculated the coefficients of the overpressure formulae. In addition, the blast test of the earth overlaid storehouse with steel areh roof truss had be conducted in U.S.A. and we formulated the test data in the open direction of the storehouse to make comparisons. The specific forms of the formulae are as follows:

M. A. Садовский formula: $$\Delta P = \frac{0.97}{\bar{R}} + \frac{4.18}{\bar{R}^2} + \frac{13.65}{\bar{R}^3}$$

H. L. Brode formula: $$\Delta P = \frac{1.2486}{\bar{R}} + \frac{2.3860}{\bar{R}^2} + \frac{12.285}{\bar{R}^3} - 0.019$$

the U.S.A. earth overlaid storehouse formula (in the open direction): $$\Delta P = 4.2424(\bar{R})^{-1.4399}$$

the formula of ours (in the 0-degree direction): $$\Delta P = 4.8598(\bar{R})^{-1.4440}$$ (11)

The meaning and unit of each of the signs in these formulae are the same as that in the above parts of this paper.

The calculation lines of formulae (11) are shown in Fig. 3. From Fig.3 we can find that the values of overpressure due to ground blast take the first place and that of U.S.A. earth overlaid storehouse take the second place. The values of our test are larger than that of U.S.A. earth overlaid storehouse in the case of $\bar{R}<1.5m/kg^{1/3}$ and less than that of U.S.A. test in the case of $\bar{R}<1.50m/kg^{1/3}$.

Now we discuss the directivity of the overpressure of earth overlaid storehouse. If we compare the values of ΔP in 90-degree direction and 0-degree direction of the earth overlaid storehouse with the values ΔP_{ground} calculated by H.L.Brode formula from ground blast test, we can find that the values of ΔP are much less than the values of ΔP_{ground} because the storehouse construction and the overlaid earth of the earth overlaid storehouse formed a restrained blast, and that the ratio ($\Delta P/\Delta P_{ground}$) of ΔP to ΔP_{ground} goes up with the increasing of the value of the scale distance $R/W^{1/3}$. In the case of $R/W^{1/3} = 5.0$ to $0.5\ m/kg^{1/3}$, the ratio of $\Delta P/\Delta P_{ground}$ goes down very quickly but tends to constancy in the case of $R/W^{1/3} \geq 6.0\ m/kg^{1/3}$. The relations of $\Delta P/\Delta P_{ground}$ and $R/W^{1/3}$ are shown in Fig. 5.

If we place the earth overlaid storehouses in such being the case that the scale distance $R/W^{1/3}$ ranges from $1.30\ m/kg^{1/3}$ to $2.0m/kg^{1/3}$, the ΔP in 90-degree direction would be in the range from 0.1818 ΔP_{ground} to 0.4820 ΔP_{ground} . It means that the safety distance between the adjacent earth overlaid storehouses

wonld be only 0.326 to 0.619 times the safety distance under the condition of ground explosion, i.e. the safety distance under the condition of earth overlaid storehouse blasting could decrease by 68% to 32% comparied with ground blasting. Because the overpressure in 0-degree direction is greater than that in 90-degree direction and the main acting field for blast-flying stones is also along the 0-degree direction, so it is more reasonable that the adjacent storehouses should sit side by side along the 90 degrees - line.

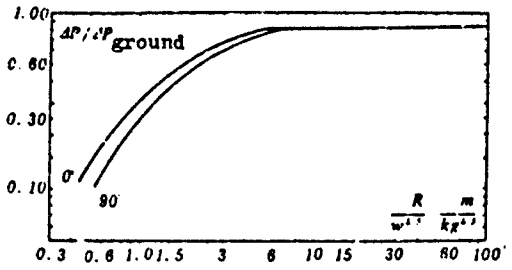

Fig.5 P/ P_{ground} versus $R/W^{1/3}$

B. the Positive Pressure Time Duration of Shock Wave The relations of positive pressure time duration and scale distance from the ground blast test, the U.S.A. earth overlaid storehouse blast test and our test are shown in Fig.6. From Fig.6, we can find that the positive pressure time duration in 0-degree direction takes the first place, and that in 45-degree direction takes the second place, and that in 90-degree direction takes the last place.

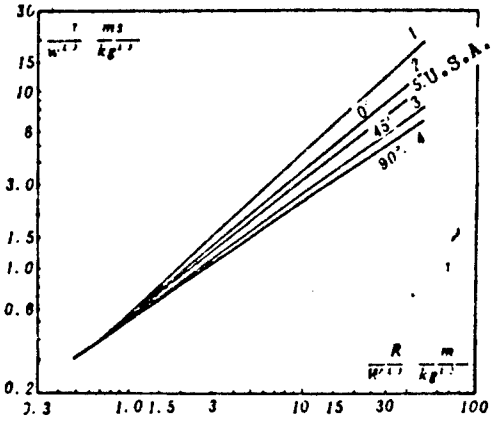

Fig 6 $\frac{t}{W^{1/3}}$ versus $\frac{R}{W^{1/3}}$

The positive pressure

acting time from the gronnd blast test is greater than that from our earth overlaid storehouse blast test by comparison. But.the positive time duration in the open direction of the U.S.A.earth overlaid storehouse is little less than that in the 0-degree direction of our earth overlaid storehouse.

IV. Conclusion

1. The values of overpressure of shock wave in the 0-degree direction, 45-degree direction, 90-degree direction of our earth overlaid storehouse are less than that from ground blasting, and are approximate to the values in the open direction of U.S.A. earth overlaid storehouse. The formulae about the overpressure of shock wave of earth overlaid storehouse can be used in engineering designs.

2. It is worth while paying attention to the directivity of the distribution of shock wave of the earth overlaid storehouse. The overpressure ΔP in the 90-degree direction of the earth overlaid storehouse is only 0.13 to 0.48 ΔP_{ground} in the case of $R/W^{1/3} = 1.3 \sim 2.0 m/kg^{1/3}$ due to the influence of the overlaying earth and the constructure of the earth overlaid storehouse on blast wave. It means that the safety distance between the adjacent earth overlaid storehouses could be shortened by 32% to 68%, and this proves that the placement of the storehouses along the 90 degrees-line is very reasonable. We should make full use of the distribution characteristic of the overpressure of shock wave of the earth overlaid storehouse to save field in engineering designs.

LA-UR 88-2533

Los Alamos National Laboratory is operated by the University of California for the United States Department of Energy under contract W-7405-ENG-36.

TITLE: MK-82 BOMB CHARACTERIZATION FOR THE SYMPATHETIC DETONATION STUDY

AUTHOR(S): Roy A. Lucht and Lawrence W. Hantel

SUBMITTED TO: Twenty-third DoD Explosives Safety Seminar
August 9-11, 1988
Atlanta, Georgia

Los Alamos National Laboratory
Los Alamos, New Mexico 87545

FORM NO 836 R4
ST NO 2629 5/81

MK-82 BOMB CHARACTERIZATION for the SYMPATHETIC DETONATION STUDY

by

Roy A. Lucht
and
Lawrence W. Hantel

ABSTRACT

Optical, radiographic, and electronic pin techniques were used to evaluate the fragmentation of tail- and side-initiated MK-82 MOD 1 general purpose bombs. They were found to contain large voids, randomly located from bomb to bomb, in the Tritonal explosive fill. Characteristics of the void-side performance of the bomb were found to be as much as 10% different from the nonvoid side and were much less reproducible than the characteristics of the nonvoid side. The data collected will be useful in evaluating sympathetic detonation mitigation systems designed for use with the bombs.

I. INTRODUCTION

The U.S. Air Force is involved in an insensitive munitions study, part of which includes an assessment of how to prevent sympathetic detonation of stored conventional munitions by means of mechanical suppressants. The Los Alamos National Laboratory has been participating in this effort since FY1986 with funds provided by AD/XR-3, Eglin Air Force Base, Florida.

The Los Alamos approach to the problem of sympathetic detonation is different from the traditional approach. Traditionally, large-scale tests of bomb arrays are conducted to statistically determine the efficacy of the proposed solution. However, if 20 or more bombs are involved in each test, the cost per test eliminates the possibility of large-number statistics. In addition, because of the threshold nature of the sympathetic detonation problem, we cannot infer that several successful large-scale tests will eliminate the possibility of future system failure. In sympathetic detonation testing, as with all explosives sensitivity testing, there is a region of input stimulus over which either a detonation or no reaction may occur. The simple case of explosive detonation caused by fragment impact is illustrated schematically in Fig. 1. A fragment with velocity in the range of v_1 to v_2 may or may not cause detonation on any given experiment. If the velocity is below v_1, detonations do not occur and if it is above v_2, they always occur. A small number of large-scale tests cannot be used effectively to calibrate such effects. The Los Alamos approach is to determine threshold values for detonation from various stimuli, then mitigation

schemes can be evaluated as to their ability to reduce the input stimuli to well below the threshold values.

Sympathetic detonation can be caused by a number of processes including fragment impact, shock transmission through a physical suppression system, or heating caused by physical distortion of acceptor bombs. As a first step to evaluating sympathetic detonation of MK-82 systems, we will characterize the donor to determine the worst-case fragments, shock strengths, etc. The second step is to determine acceptor thresholds for detonation, and the third step is to design and evaluate mitigation schemes for their capability to reduce the output to values well below the acceptor threshold levels. In this paper, we report the MK-82 donor characteristics of fragments close to the bomb, where they could be expected to affect acceptor bomb response.

II. EXPERIMENTAL RESULTS

MK-82 bombs contain about 87 kg of Tritonal explosive (80 wt% TNT/20 wt% Al). It is not an ideal system to characterize, from an explosives viewpoint, because the cast Tritonal fill is not homogeneous and contains large shrinkage voids. A typical void occupies 3 to 5% of the explosive cross section and is lined by TNT crystals. The void was generally within 10 to 25 mm of the bomb case. To characterize donor output, it was important to know where the void area was and to measure what effect it might have on fragment characteristics, as compared with those produced on the nonvoid side.

Because we needed to establish the void location for each shot, every MK-82 bomb was radiographed before being fired. Orthogonal views were taken to precisely determine the void location with respect to lifting lugs. The void side of the bomb was then oriented appropriately for each shot.

Three series of experiments have been completed. The first series consisted of tail-initiated bombs, in which tests, the primary diagnostic technique was radiography. The second series used tail-initiated bombs with streak and image intensifier cameras. The third series used side-initiated bombs and radiography. Electronic pins were used on all shots. For the tail-initiated bombs, the fuze well was packed with 125 mm of Composition C. A detonator and a booster were used to detonate the Composition C on the bomb axis. For the side-initiated bombs, a 50-mm-long by 50-mm-diameter cylinder of HMX-based explosive was pressed onto the side of the bomb with a thin layer of PETN-based soft explosive used to fill in the area between the flat explosive cylinder face and the curving case.

A typical shot setup for the first series of experiments is shown in Fig. 2. At the far right, behind the sandbags, are the x-ray heads that operate remotely from the Marx banks (beyond the picture). The sandbox to the right center protects the x-ray heads and holds lead shades used to separate the two beams. The bomb is in the center, laying on a wooden table well below ground level. It is surrounded by sandboxes to protect equipment from fragments. At the far left are the film cassettes. A sheet of Plexiglas is placed at a 45° angle to the

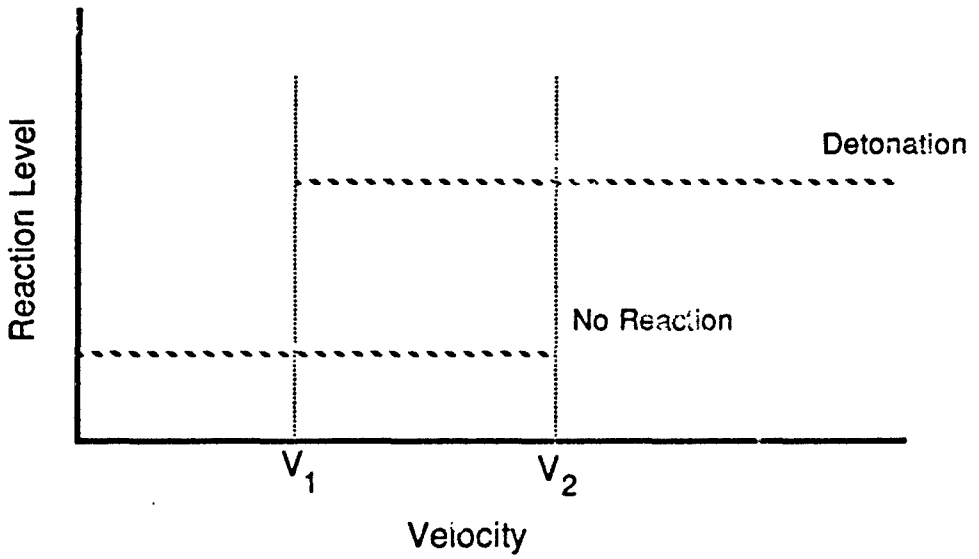

Fig. 1. Explosive reaction level versus fragment impact velocity for typical fragment impact sensitivity test.

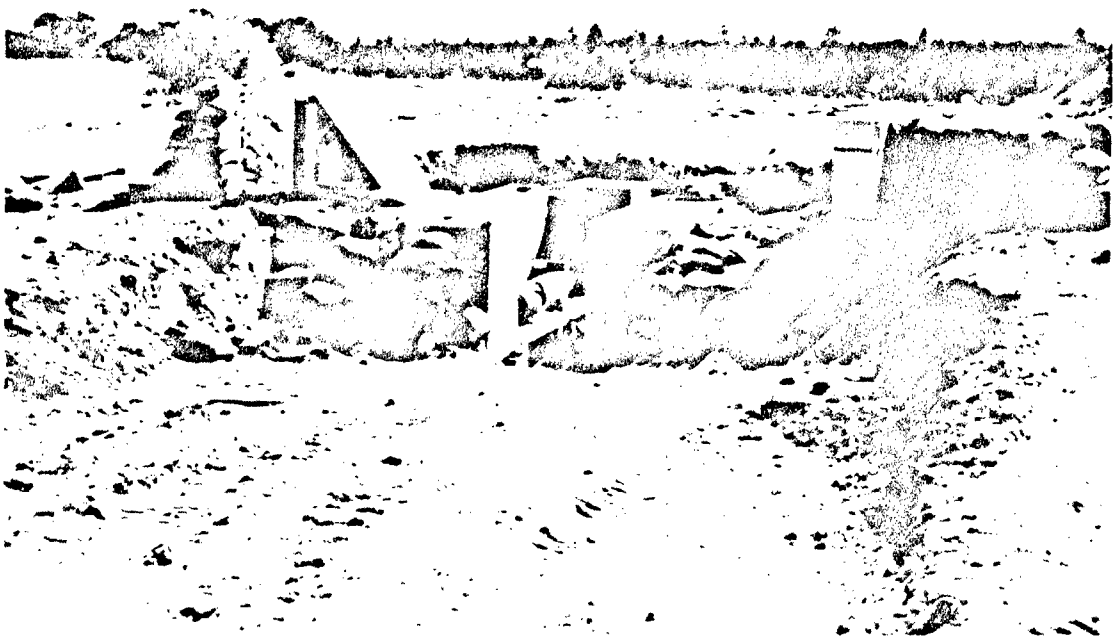

Fig. 2. Typical shot setup for MK-82 bomb characterization study.

cassettes to deflect the blast wave. The sandbags behind the cassettes slow them after they are launched by the bomb blast.

We were interested in early bomb-case motion to verify that the bomb detonated high order and to see if the initial motion was different on the void and nonvoid sides. Linear electronic-pin arrays were used to record a phase velocity down the bomb axis. These pins were located in a straight line on the outside surface of the bomb case at known distances from the tail. When the case started to move because of the shock driven by the detonation wave, the pins shorted out and produced timing signals. These arrays gave phase velocities in excess of Tritonal detonation velocity (6.5 mm/μs), which means that in each case the bomb detonated high order. The velocities were determined from least squares fits to the distance/time data as shown for Shot R0643 in Fig. 3.

Because some data sets contained only three or four data points, improved signal-to-noise ratio was achieved by combining like data sets and calculating least squares fits. The results for the nonvoid and void sides are shown in Figs. 4 and 5, respectively. Circled data points were not included in the fits. A statistically real difference in the two sides is evident. The phase velocity is 1% slower on the void side and the wave on the void side is delayed 4 μs at 150 μs, with respect to the wave on the nonvoid side. Although these differences are real, they are too small to be considered a significant difference in bomb performance.

Hexagonal electronic capped-pin arrays were used on Shots R0646 and R0647 to record the first few centimeters of bomb case expansion. Seven capped pins were mounted in a Plexiglas block in a centered-hexagonal configuration with 12.7 mm being the maximum distance between pin axes. The pins in an array were staggered radially out from the bomb case with the first pin touching the case and the last pin about 64 mm away. As the case accelerates radially out, the pins are successively shorted, giving a distance/time profile. Three arrays were used on Shot R0646, all located 635 mm from the bomb tail and at 90° intervals around the bomb (one over the void area, one 90° around the bomb, and the third 180° from the void). For Shot R0647, two arrays were located 635 mm from the bomb tail: one over the void area and the other 180° away. The third array was located over the void but an additional 119 mm down the bomb axis.

Figure 6 shows all data from the six arrays. The nonvoid data from both shots are nearly identical, whereas the void data lie on both sides of the nonvoid data. This points out the early motion shot-to-shot reproducibility problem created by the inhomogeneous explosive fill. These early case motion data provoked us to attempt several cylinder tests with the MK-82 bomb. Shots C5973 and C5977 produced excellent data. A smear camera and an image intensifier camera array were used on both shots to evaluate case motion optically, simultaneously on the void and nonvoid sides of the same bomb. Smear camera data from Shot C5973 are shown in Fig. 7 and image intensifier camera data from Shot C5977 are shown in Fig. 8.

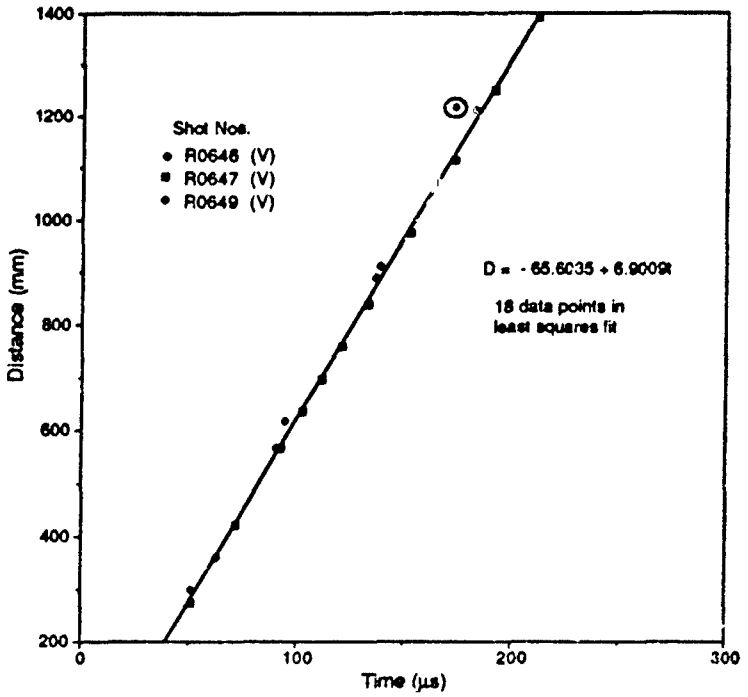

Fig. 5. All distance/time data for void case expansion.

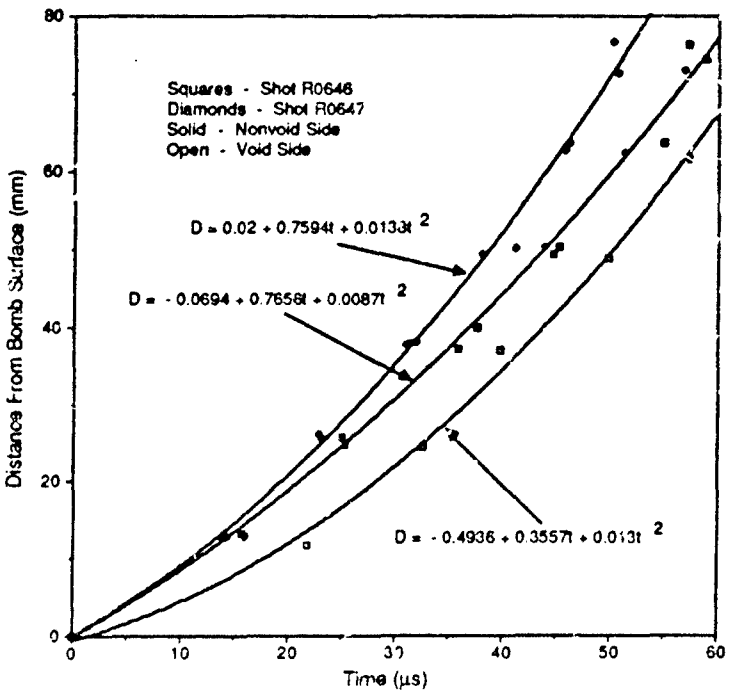

Fig. 6. Data from six capped-pin arrays, Shots R0646 and R0647.

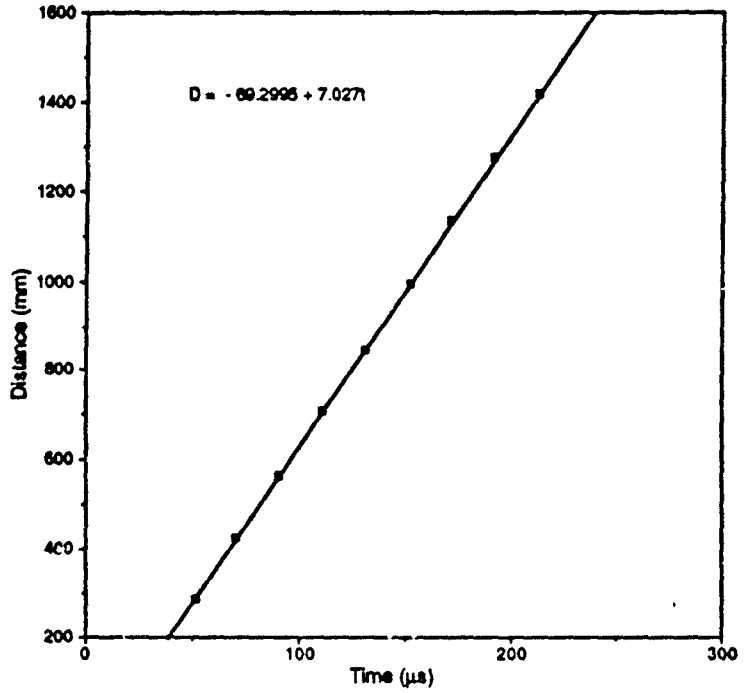

Fig. 3. Distance/time data for nonvoid case expansion, Shot R0643.

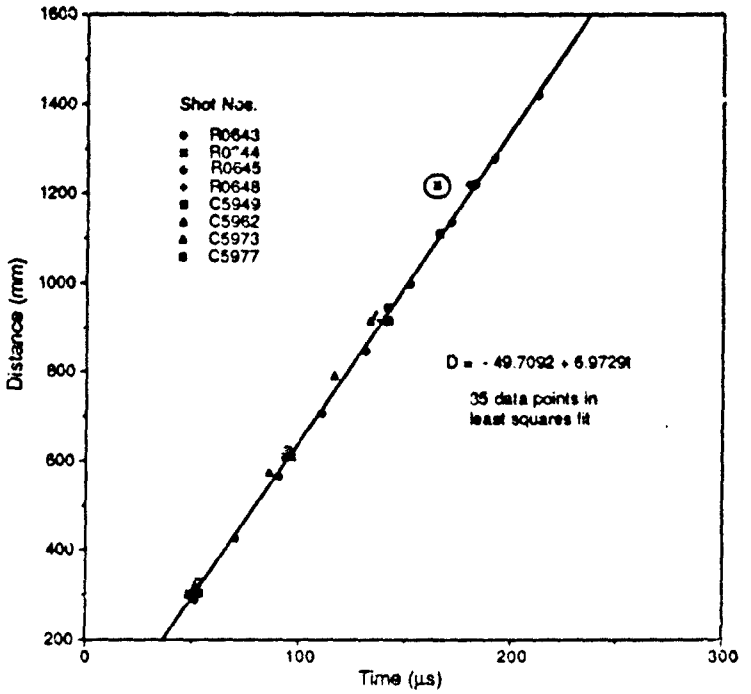

Fig. 4. All distance/time data for nonvoid case expansion.

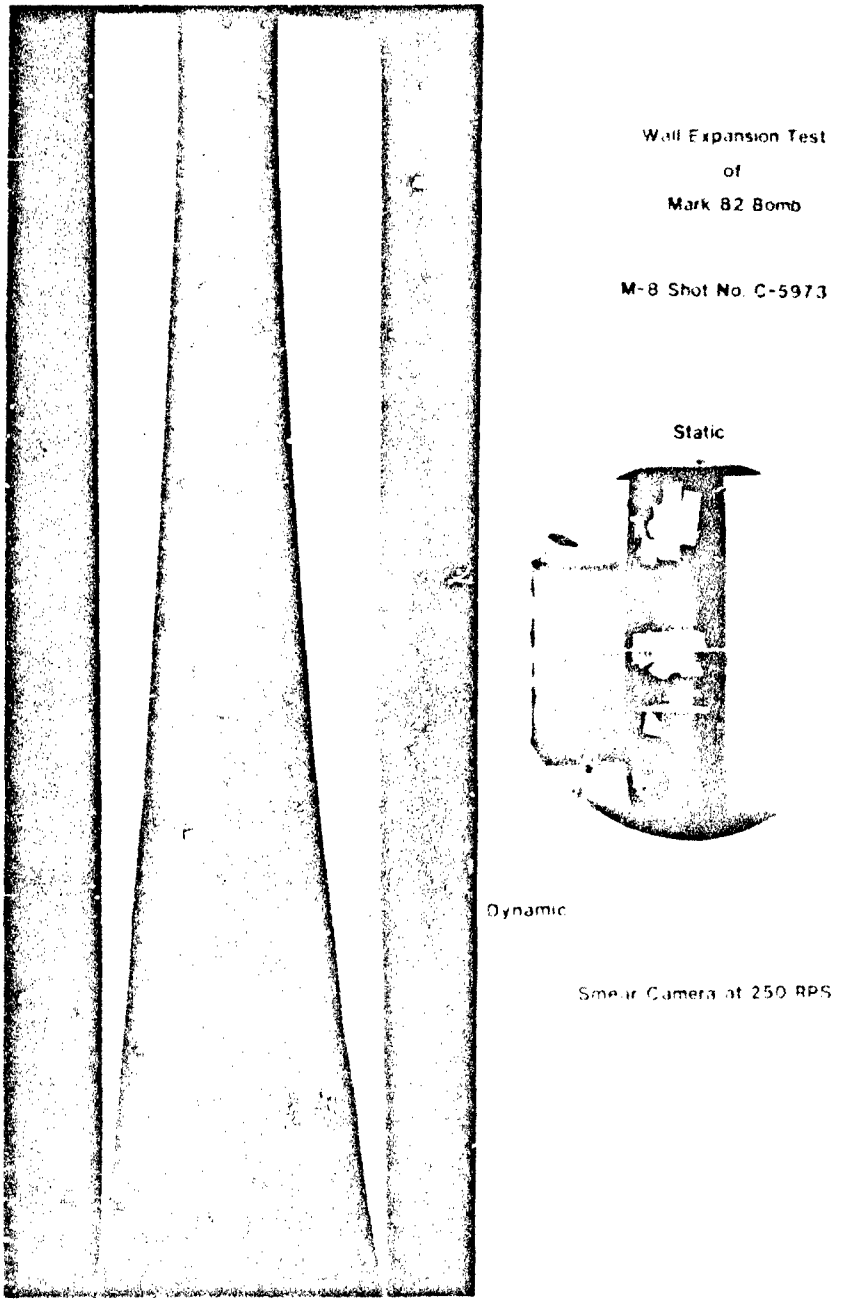

Fig. 7. Smear camera record for MK-82 void- and nonvoid-wall expansions (Shot C5973). The slit is 635 mm from the bomb tail with the nonvoid side on the left and the void side on the right.

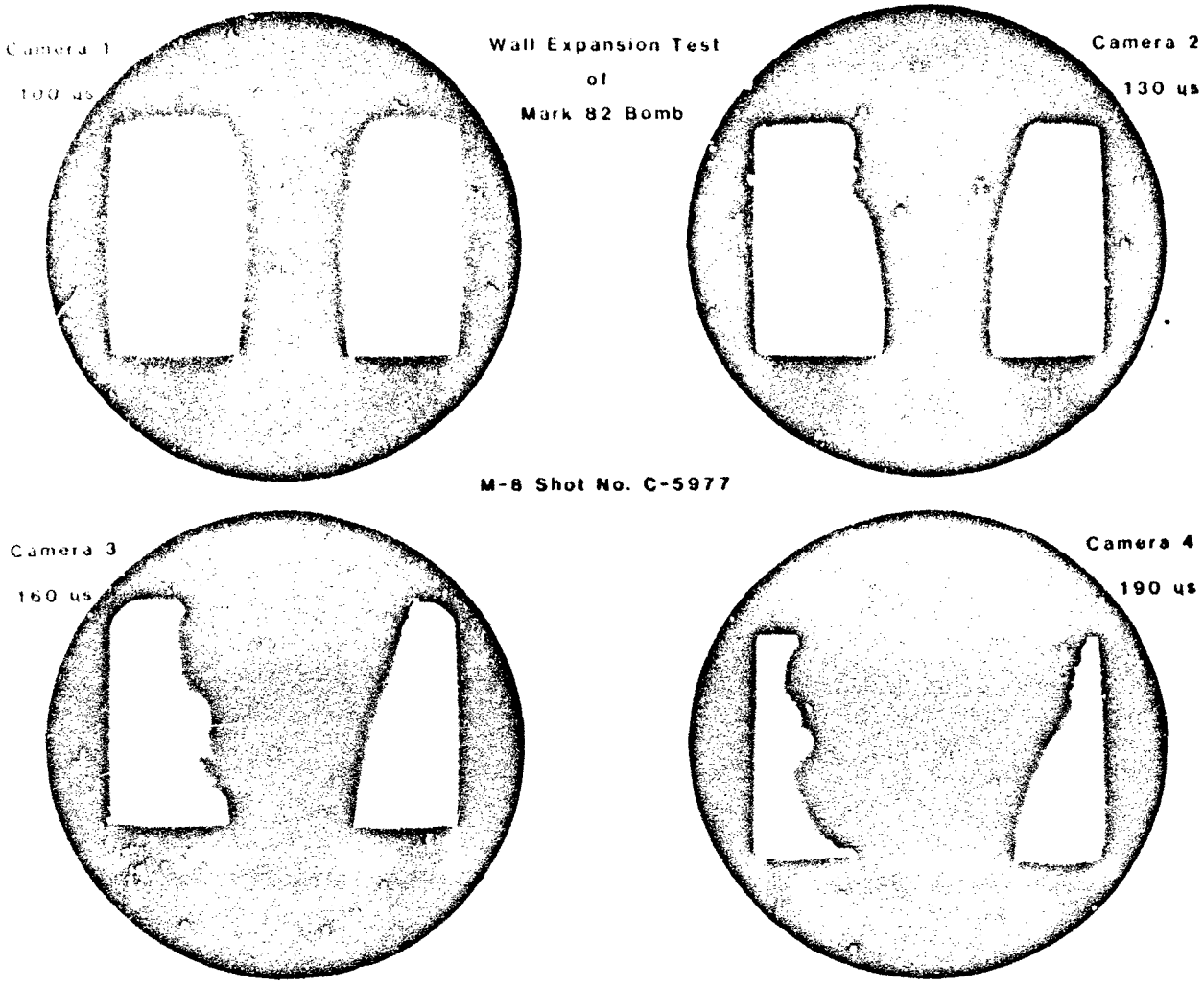

Fig. 8. Image intensifier photographs of MK-82 wall expansion (Shot C5977). The nonvoid side is on the left and the void side is on the right.

Streak camera data can best be displayed on distance/time plots. This is done for the two most successful shots in Fig. 9. Also displayed in Fig. 9 are all the hexagonal capped-pin array data. For all early case motion data taken, all nonvoid-side data were consistent. All void-side data were also consistent (with somewhat larger scatter) with the exception of the data of Shot R0647, which fell above the nonvoid data. All other void-side data fell below the nonvoid-side data. Because the location and size of the void are so nonreproducible, void-side expansion can be expected to vary greatly from bomb to bomb and from spot to spot for a given bomb.

The physical processes creating the pressure that drives the bomb case may be considerably different for the void and nonvoid sides. One hypothesis is that the detonation wave is fully supported and creates a high pressure at the steel case as it passes. This high pressure is maintained by the large bulk of explosive behind the steel and drives the steel at an initially high acceleration. The acceleration drops slowly but continuously as the expansion of the detonation products proceeds and the pressure drops correspondingly. On the void side, the initially high acceleration should be short lived because the gaseous detonation products can expand into the void, dropping the pressure. Case expansion then proceeds at a slower rate for a while. The products expanding into the void will collide with products from explosive from the other side of the void (the center of the bomb), causing the wave to reflect and the pressure to increase greatly. This high-pressure region then expands and catches up to the case, causing significant late-time acceleration. This is precisely the behavior seen in the data. All the data (except void-side data from R0647) show void and nonvoid-side expansion overlapping (i.e., identical acceleration) for about the first 5 μs. Then the nonvoid side case moves ahead of the void-side case until about 40 μs. Around 40 μs (depending on the void geometry of the given shot), the void-side case experiences higher acceleration than the nonvoid-side case and eventually passes it up. Evidence for this is seen in the higher fragment velocities measured from the flash radiographs discussed later in this paper. The x-t trajectories of the void- and nonvoid-side cases must cross shortly after fragmentation occurs but out of the smear camera view. If the first derivatives are taken of the least squares fits, velocities can be calculated at 80 μs. Fragmentation has usually occurred by 80 μs, and this is about the limit of where the least squares fit can be trusted. This was done yielding the following average velocities:

$$V(80\ \mu s) = 2.14\ mm/\mu s, \quad \text{void;}$$
$$V(80\ \mu s) = 1.92\ mm/\mu s, \quad \text{nonvoid.}$$

The difference in velocities is about 10%, which agrees well with the velocities obtained from the radiographic data. The fragment velocities from the radiographic data are slightly higher than these, which is understandable because some positive acceleration can be expected even after the case fragments. Acceleration stops or becomes negative only after the detonation products pass the fragments and produce equal pressure on all sides.

The streak camera data could also be used to determine when the case ruptured at the slit position (635 mm from the tail). Several of the image

intensifier frames were also used to determine time and axial positions where the case ruptured. The fragmentation positions and times were highly variable. The only conclusion that can be drawn is that fragmentation is highly variable from point to point on a given bomb and does not correlate well with void position. This conclusion is also indicated by the large variety of fragment sizes and shapes observed in the flash radiographs. Fragmentation effects may be dictated more by random flaws in the steel case than by physical processes in the explosive. Also, once the case breaks at a given point, adjacent case material is subjected to radically different stresses; thus adjacent case pieces can fragment at very different radial expansion positions.

Good dynamic radiographs were obtained from five tail-initiated shots. Two dynamic radiographs were taken of each shot; the first one was taken several hundred microseconds after the detonator in the bomb tail was fired, and the second one, a hundred or so microseconds later. The times were chosen so that the radiographs were taken after the bomb case was completely fragmented and the maximum fragment velocity obtained. The two radiographs allowed us to record the bomb fragments at two distinct times and displacements, from which the fragments' velocities could be determined. Careful geometric measurements and still radiographs with fiducials provided crosschecked position references for the dynamic radiographs.

Figure 10 is an example of the dynamic radiographs (Shot R0649), and Table 1 lists the data measured from the radiographs. Because the fragments are from an expanding cylinder, only the leading fragments radiographed can be assumed to have a low- or zero- "Z" velocity component. In this Cartesian coordinate system, the "X" and "Y" components define a vertical plane above the bomb, where "X" is parallel to the bomb axis, "Y" is vertical, and "Z" is parallel to the direction of the x-ray beam propagation. Thus, for the radiograph to be useful, it is mandatory that leading-edge fragments can be identified in both exposures. Because the fragments are irregularly shaped and tumbling, the cross-sectional areas can be considerably different at the two times viewed in the experiment. The area values indicate the visible range of sizes, showing no obvious large difference between the observed fragments from the void and nonvoid sides.

The radiographic analyses for all the shots included some very small, fast particles, and some particles well below the leading edge, where they may have significant "Z" component velocities that cannot be resolved. To compare void- and nonvoid-side performances, only fragments representing large leading-edge fragment motion should be considered. Because they are large, these fragments represent the bomb case motion best and have the most consistent velocities. Thus, an analysis was performed in which the large leading-edge fragments were chosen without regard to their velocities, from all experiments, and their velocities averaged. The averages included 8 fragments for the void side and 19 for the nonvoid side. The results are

$V = 2.215 \pm 0.005$ mm/μs, void, and;
$V = 1.947 \pm 0.018$ mm/μs, nonvoid.

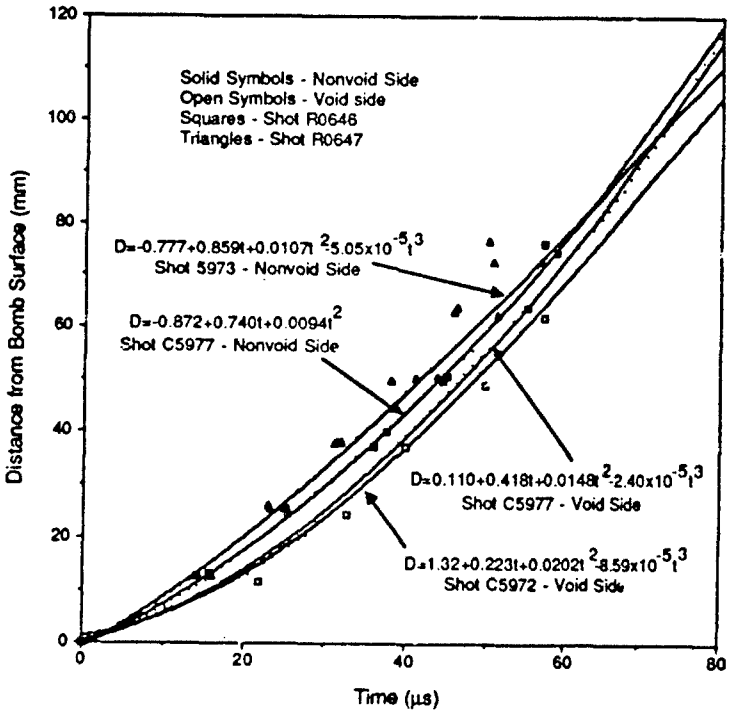

Fig. 9. Distance/time data from smear camera Shots C5973 and C5977 and from capped-pin array Shots R0646 and R0647.

Fig. 10. Dynamic radiographs of MK-82 bomb fragments from nonvoid side (Shot R0649). Bottom radiograph at 631 μs; top one at 727 μs.

TABLE I

FRAGMENT AREAS, VELOCITIES, AND ANGLES FOR SHOT R0649

Fragment Number	Film I Area (cm^2)	Film II Area (cm^2)	V(x) (mm/μs)	V(y) (mm/μs)	V (mm/μs)	Ø (degrees)
1	21.50	21.68	0.25	2.09	2.11	6.80
2	9.19	7.86	0.06	2.17	2.17	1.67
3	5.27	3.35[a]	0.24	1.96	1.97	6.96
4	3.36	2.70	0.29	1.71	1.73	9.55
5	3.20	5.51	0.38	1.85	1.88	10.96
6	6.44[b]	4.42[b]	0.26	1.82	1.84	7.98
7	6.46[b]	6.72[b]	0.50	1.97	2.04	14.18
8	12.56[a]	13.72	0.22	2.21	2.22	5 64
9	0.71	0.89	0.37	2.05	2.09	10.08
10	3.22	5.20	0.24	1.85	1.86	7.33
11	2.23	3.43	0.14	1.84	1.85	4.34

[a] Off edge of film.

[b] Long-fragment, arbitrary cutoff point.

V(av) = 1.98 ± 0.156 mm/μs

Ø(av) = 7.77 ± 3.392 °

Even if velocities two standard deviations closer are considered, the void-side fragments still have velocities at least 10% larger than nonvoid-side fragments. This agrees well with the streak camera data described above. Although this is statistically accurate, the difference is not large enough to be a major consideration when suppressant systems are designed, because velocities should be decreased much more than 10% below threshold levels.

Six side-initiated shots have been fired. Shot setup was almost identical to that shown in Fig. 2 for the tail-initiated shots except for the initiation scheme. A high-explosive cylinder (booster) was placed at the center of the bomb axially and on the side facing down (bottom of a bomb lying horizontally). For two of these shots, the voids were at the top of the bomb; for three, the voids were positioned to one side, and for one shot, the voids were at the bottom. In all experiments, linear pin arrays were used. Each array was positioned on a side of the bomb parallel to the bomb axis. Three or four linear arrays were used in each experiment. For reference, pin angles are measured from the bomb axis with vertical up being zero. Thus, pins that ran along the bottom are referred to as 180° data, along the side (in a horizontal plane through the bomb axis) as 90° data, and near the top of the bomb as 20° to 35° data. Pins could not be placed along the top (0°), because they might interfere with the radiographic analysis. Straight-line distances through the explosive between the explosive-bomb case interface above the booster (180° and axial center) and each pin (any angle and axial distance) were calculated and plotted versus pin arrival times. Good pin data were obtained for every shot. From

these data, detonation velocity and detonation wave corner-turning effects could be determined.

The linear pin array data were plotted for each array for all six experiments and linear least squares fits were calculated. The slopes of the lines correspond to wave velocities, most of which agree well with Tritonal detonation velocity. For Shot R0663, the void area was at the bottom of the bomb, adjacent to the detonation center. This shot failed to detonate, and the pin data showed the wave dying out away from the initiation point. This failure was probably caused by the layer of explosive between the bomb case and the void being too thin to sustain a detonation.

One linear pin array on each bomb ran along the bottom of the bomb (180° data) past the detonation center. For this configuration, the detonation wave must turn through essentially 90° before the data can be expected to show detonation velocity. Thus, the first several points can be expected to be slow and show significant scatter. This is just what is observed. If only the last several points are considered, the wave has had sufficient time to turn the corner and come up to detonation velocity.

A summary of the slopes from linear pin arrays for all side-initiated bombs show considerable scatter; however, trends are obvious. In general, waves that do not pass through a void have a velocity near the measured Tritonal velocity. Waves that do pass through or near a void appear to be faster. Limited core samples of a bomb yield significantly varying aluminum concentrations in the Tritonal. Specifically, some of the explosive near the void appears to be almost pure TNT. A detonation wave passing through a region of low aluminum concentration will be considerably faster than one through a region of high aluminum concentration, because the TNT velocity is 7% faster than Tritonal velocity.

Note that these determinations of velocity are different than the standard rate stick experimental technique. With the rate stick method, times of wave arrival are measured at different points along a straight line. Here, each distance-time data point represents a different wave direction. Considering this, these data are remarkably linear.

A typical statistical technique to increase signal-to-noise ratio is to combine like data sets. The difficulty here is due to changing reference times. Reference times can change from experiment to experiment and from array to array for a variety of reasons. The detonator cables for this experiment are about 300 ft long, and ring-up time can shift. The thickness of the soft explosive used and its contact with the bomb case can change from experiment to experiment. These and other system variations would normally amount to less than one or two microseconds' difference. The main cause of changing reference times is believed to be bomb-to-bomb variability, variations in explosive composition within a bomb, and whether or not the wave passes near or through a void.

A good time to use as a reference for comparisons is the time from each linear least squares fit at which the distance (x) is zero. This can be viewed as a

starting time (i.e., delay time) for each wave corresponding to a single data set. These intercept times were averaged for each group of like data sets (90° data adjacent to a nonvoid side), and each data set was then shifted a constant time interval so that its new intercept was equal to the average. Least squares fits were then calculated for the entire group of data. An example is shown in Fig. 11. A summary of all the side-initiated pin data follows in Table II.

TABLE II

SIDE-INITIATED PIN DATA

Configuration	Number of Data Points	X=0 Intercept (μs)	Velocity (mm/μs)
35° nonvoid	22	22.4	6.248
20-35° void	16	21.0	6.600
90° nonvoid	28	23.3	6.534
90° void	22	30.8	6.717
180° nonvoid	19	26.3	6.549
180° void	detonation failed		

There were 38 data points available for the 180° nonvoid case; however, only the latest 19 were used to allow the detonation to come up to speed, as shown in Fig. 12. The time required to attain detonation velocity explains the large x intercept for this configuration. The only other anomalously large intercept is for the 90° void case and may correspond to an induction time for passing through or around the void. However, this is contradictory to the higher observed velocity for this case. A similar result is not observed for the 20-35° void case probably because, at these angles, the wave only grazes the void area. All velocities appear reasonable, although the velocity for the 35° nonvoid case is smaller than expected.

Useful radiographs were obtained on four side-initiated experiments: two with the voids up (voids at 0° position) and two with the voids on the side (90° position). The data were analyzed in the same way as those for the tail-initiated experiments. After fragment velocities and areas were determined, leading-edge fragments were selected and their velocities and areas were averaged for each experiment and for the two types of experiments giving the results in Table III.

R0662 is difficult to interpret because almost all of both dynamic radiographs are covered with fragments; thus it is impossible to prove that the top fragments are leading fragments and that no fragments were above the radiographs. If this were the case, then the average velocity of 1.91 mm/μs would be a lower bound. Even with this caveat, the void-side fragment velocities are at least 10% higher than the nonvoid side fragments. This is essentially the same result as the tail-initiated series.

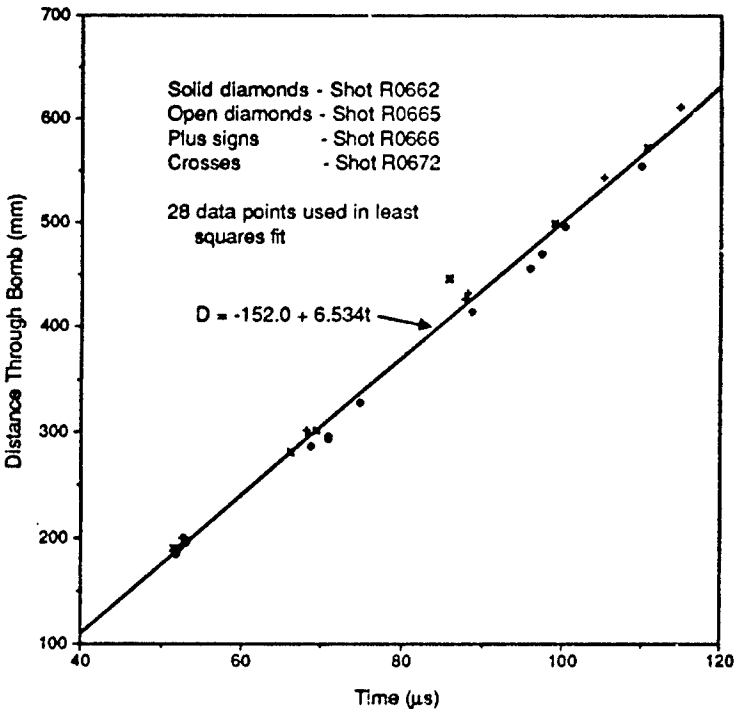

Fig. 11. Data from four linear pin arrays at 90° to the vertical on a nonvoid side, Shots R0662, R0665, R0666, and R0672.

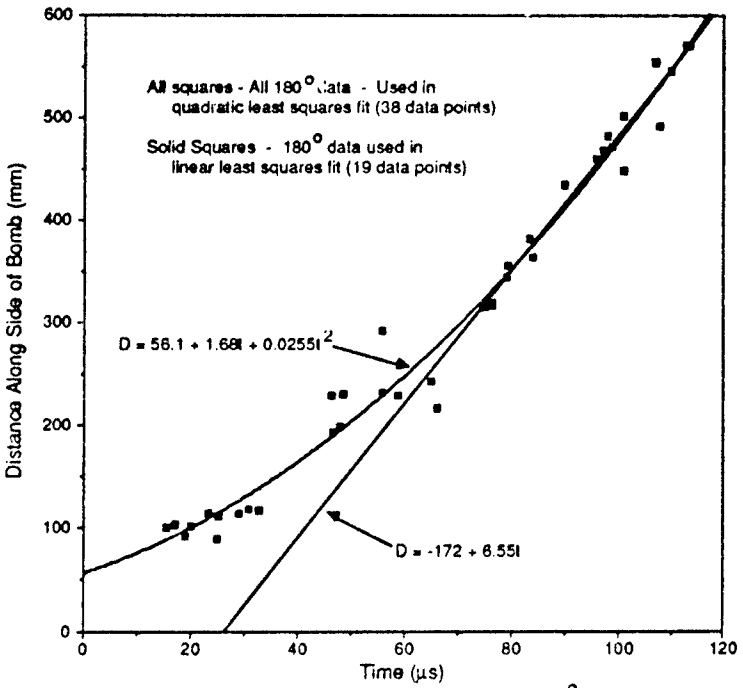

Fig. 12. Data from all side-initiated shots at 180° to the vertical (bottom of bomb), nonvoid side.

TABLE III

LEADING-EDGE FRAGMENT DATA

Experiment	Velocity (mm/μs)	Area (cm^2)	Number of Fragments	Configuration
R0662	1.91± 0.25	1.51 ± 1.07	8	Void Up
R0665	1.87 ± 0.11	2.86 ± 1.28	3	Nonvoid Up
R0666	1.85 ± 0.12	6.17 ± 2.59	6	Nonvoid Up
R0672	2.23 ± 0.28	2.82 ± 2.09	9	Void Up
R0662&R0672	2.08 ± 0.31	2.21 ± 1.80	17	Void Up
R0665&R0666	1.86 ± 0.11	6.06 ± 2.72	9	Nonvoid Up

Fragment sizes are more difficult to evaluate, because only areas of well-defined isolated fragments were measured, whereas areas of fragments in clusters could not be measured. Thus any conclusions made from averages of measured fragment areas are subject to question. The general impression after viewing the radiographs is that fragment sizes for the tail-initiated case were about the same size for the void and nonvoid sides; however, for the side-initiated case, the nonvoid-side fragments are about twice the size of the void-side fragments. The major difference in the experiments is that for the tail-initiated case, the detonation wave propagation vector is basically parallel to the bomb case; whereas, for the side-initiated case, it is orthogonal at the center and moves toward parallel at the ends of the bomb. Why the case should be more severely shattered in the void-side-initiated case is unknown; however, it may be due to collision of waves traveling in opposite directions in the thin section of Tritonal between the case and the void. Also, a subjective survey of the radiographs shows a larger variety of fragment sizes and velocities for the side-initiated cases than was observed for the tail-initiated bombs.This is reasonable because orthogonal waves often cause a plate to spall as well as fragment.

III. CONCLUSIONS

Statistically significant differences were observed in the behavior of the void side of the bomb compared with the nonvoid side for both tail- and side-initiated MK-82 bombs. In addition, differences were observed in the initial acceleration of the bomb case, which could result in different pressures being transmitted into close objects such as material intended to mitigate sympathetic detonation. Although average differences in fragment velocity of at least 10% were observed, individual high-velocity fragments can be generated from either the void or nonvoid sides. A nonstatistical survey of the fragment data indicates that only a few fragments with areas of a few square centimeters have velocities above 2.4 mm/μs. Thus if a suppressant system can be developed that reduces the velocities of these fragments to below the initiation threshold, a fragment-induced sympathetic detonation should not propagate through a stack of bombs.

ACKNOWLEDGMENTS

Many scientists and technicians contributed to this work, and the major contributors are listed here. Richard Garcia was firing-site leader for the flash-radiography experiments. He was assisted by Walter Quintana and Max Avila. Dan Hughes was firing-site leader for the streak camera experiments and was assisted by Tommy Herrera and Ken Uher. Jerry Langner analyzed the radiographs for fragment velocity and size, and Warner Miller read the streak and image intensifier films and produced position-time data from them.

This research was funded by the U. S. Air Force, Project Number DTC-7-419, which corresponds to Los Alamos Proposal Number DPS-87-29. The Air Force Program Manager is Mr. Joseph Jenus, AD/XR-3, Eglin AFB, FL 32542.

DRAGON MISSILE WARHEAD SYMPATHETIC DETONATION ANALYSIS AND TEST RESULTS

by

Verence D. Moore
Naval Surface Warfare Center
10901 New Hampshire Avenue
Silver Spring, MD 20903-5000

INTRODUCTION

This task was performed for the Systems Engineering Branch, Naval Surface Warfare Center, as part of the development program for the DRAGON missile to satisfy the U. S. Navy's Weapon System Explosives Safety Review Board (WSESRB) approval for service use of this version of the weapon system aboard naval vessels. The work was performed as part of the Navy's Insensitive Munitions Effort, that requires sympathetic detonation assessment or testing for all energetic materials carried aboard naval vessels.

The study's objectives were to determine the likelihood of sympathetic detonation, the maximum credible event (MCE) and, if necessary, recommend possible handling procedure changes and/or inhibitor/shield designs (feasible solutions) for reducing the MCE's.

The system evaluated in this study is the DRAGON missile warhead, which is stored in an environmentally-protected launch container; it is shipped in a wooden shipping container.

SYMPATHETIC DETONATION EVALUATION

The general missile configuration considered in the sympathetic detonation evaluation is one missile stored in a wooden shipping container. Pertinent material dimensions/properties required for the sympathetic detonation evaluation are presented in Table 1.

Table 2 lists the donor/acceptor combinations considered and the pressure thresholds necessary to sympathetically detonate the acceptor.

TABLE 1. DRAGON MISSILE'S WARHEAD DESCRIPTIVE DATA

DRAGON WARHEAD	
Explosive	Octol 75/25 (HMX/TNT)
TNT Equivalent (estimate), kg explosive/kg TNT	1.0
Explosive Density, kg/m^3 (lb/in^3)	1800 (0.0650)
Case Density, kg/m^3 (lb/in^3)	2800 (0.10)
Explosive Sound Speed, m/s (ft/s)	3140 (10300)
NOL Large Scale Gap Test Value, cards (kbars)	195 (20)
Explosive Mass, kg (lb)	1.71 (3.78)
Total Warhead Mass, kg (lb)	2.67 (5.88)
Diameter, mm (in)	122 (4.80)
Length, mm (in)	222 (8.74)
LAUNCH TUBE	
Material	Fiberglass
Thickness, mm (in)	1.0 (0.4)
Density, kg/m^3 (lb/in^3)	1900 (0.068)

TABLE 2. SYMPATHETIC DETONATION PREDICTIONS FOR THE DRAGON MISSILE

Configuration*	Acceptor	Detonation Threshold** GPa (kbars)	Fragment induced Overpressure+ GPa (kbars)	Sympathetic Detonation
1. Two Bare Missiles	W/H Adjacent	2.0 (20)	5.6 (56)	Yes
2. Stack of Missiles in Wooden S/C++	W/H Adjacent	2.0 (20)	1.8 (18)	Marginal

*Donor is the Warhead (W/H).

**NOL Large Scale Gap Test data was used to establish the threshold for detonation.

+Shock induced pressures need not be considered. At the separation distance for these configurations, the shock induced induced pressures are below the detonation threshold for the weapon system.

++S/C represents shipping container.

Shock induced pressures in the acceptor explosives were calculated in the following manner. The donor was assumed to be a spherical charge. UTE (Unified Theory of Explosions)[1,2] calculations provided normally reflected pressure estimates at the acceptor position. Shielding effects of the intervening material were ignored, this results in the highest loads being calculated. The inclusion of the intervening materials as mass surrounds in the UTE computations does not appreciably change the reflected pressures calculated. The reflected pressures computed at the charge-surface-to-charge-surface separation distance were assumed equal to the induced pressures in the acceptors.

Fragment induced pressures in the acceptor materials were computed in the following way.

The maximum donor fragment velocity, calculated by using the computer program FEN (Fragment Energy and Number),[2] was used as the initial fragment velocity in the direction normal to the charge cylindrical surface. The computer program FEN computes the fragment energy and numerical areal distributions for naturally fragmenting cased explosives.

The velocity determined above was then used in the following formula to estimate the pressure induced by the fragment impact in the acceptor material:

$$P = \rho * c * v / K_i$$

where:

P = pressure induced in the acceptor
ρ = initial density of acceptor material (see Table 1)
c = sound speed in acceptor material (see Table 1)
v = initial fragment velocity as determined above
k_i = factor representing reduction in fragment velocity for configuration i in Table 2 due to conservation of momentum between donor fragments and material shielding acceptor explosive/propellant

The above equation was obtained from the Rankine-Hugoniot equation for momentum.

$$p - p_o = \rho_o * u_s * u_p$$

where:

ρ_o = the density in undisturbed flow
u_s = shock velocity
u_p = particle velocity

The following assumptions were made:

(1) That the peak pressure P induced in the acceptor is equal to the peak reflected overpressure $p-p_o$.
(2) That the sound speed c is a good approximation for u_s.
(3) That the final fragment velocity v_2 is a good approximation for u_p. The Rankine-Hugoniot equation then becomes:

$$P = \rho * c * v_2$$

Finally, using the conservation of momentum equation:

$$m_1 v = (m_1 + m_2) v_2$$

and assuming an equal cross sectional area A for all masses, it can be shown that:

$$v_2 = v/K$$

where:

$K = (\rho_1 * t_1 * + \rho_2 * t_2)/\rho_1 * t_1$
m_1 = the mass of donor fragment
m_2 = the mass of the material shielding the acceptor
$m = \rho * t * A$
ρ = density
t = thickness

The results shown in Table 2 indicate a marginal result for fragment induced sympathetic detonation for the rounds in the wooden shipping containers. As a result of this study, a series of sympathetic detonation tests were performed. The purpose of these tests were to determine the actual sympathetic detonation characteristics of DRAGON missile warheads in their launch tubes and shipping containers given the detonation of one warhead in its design mode. (It must be remembered that the rocket motor contributions were not considered in this study.)

TEST PROGRAM

APPROACH

The test program consisted of three firings. Two shots examined the configuration of one donor and two acceptor warheads. The third shot consisted of a single warhead detonated in its design mode. For all shots, the warheads were in their launch tubes and shipping container.

TEST DESCRIPTION

The airblast gauge locations utilized throughout the test series are shown in Figure 1. The warheads were detonated at a height of five feet above ground zero. Detailed descriptions of the test requirements and general test procedures are presented in the following sections.

AIRBLAST GAUGES

Airblast measurements were made along two radials with five gauges per radial. The gauge locations were chosen to span a nominal range of 4 to 100 psi for the detonation of three DRAGON warheads. Table 3 presents the airblast gauge locations and the predicted airblast results for the detonation of one, two, and three DRAGON warheads. These predictions assume a uniform spherical charge--not a directed energy detonation. Figure 1 shows the airblast array for this test series. The gauges were mounted flush with the ground. All signals were recorded on a magnetic tape recorder.

The analog tape records were digitized with the R15 Data Reduction, and computer processed readouts were analyzed to determine the sympathetic detonation effects. Figure 2 shows a block diagram for the data acquisition and reduction system.

TABLE 3 AIRBLAST GAUGE LOCATIONS AND PREDICTED PRESSURES

RANGE	PRESSURE IN PSI FOR		
(feet)	ONE WARHEAD	TWO WARHEADS	THREE WARHEADS
8.0	40.7	71.2	99.7
12.0	18.9	30.2	39.6
15.0	13.0	20.2	26.8
30.0	4.7	6.7	8.3
50.0	2.4	3.4	4.1

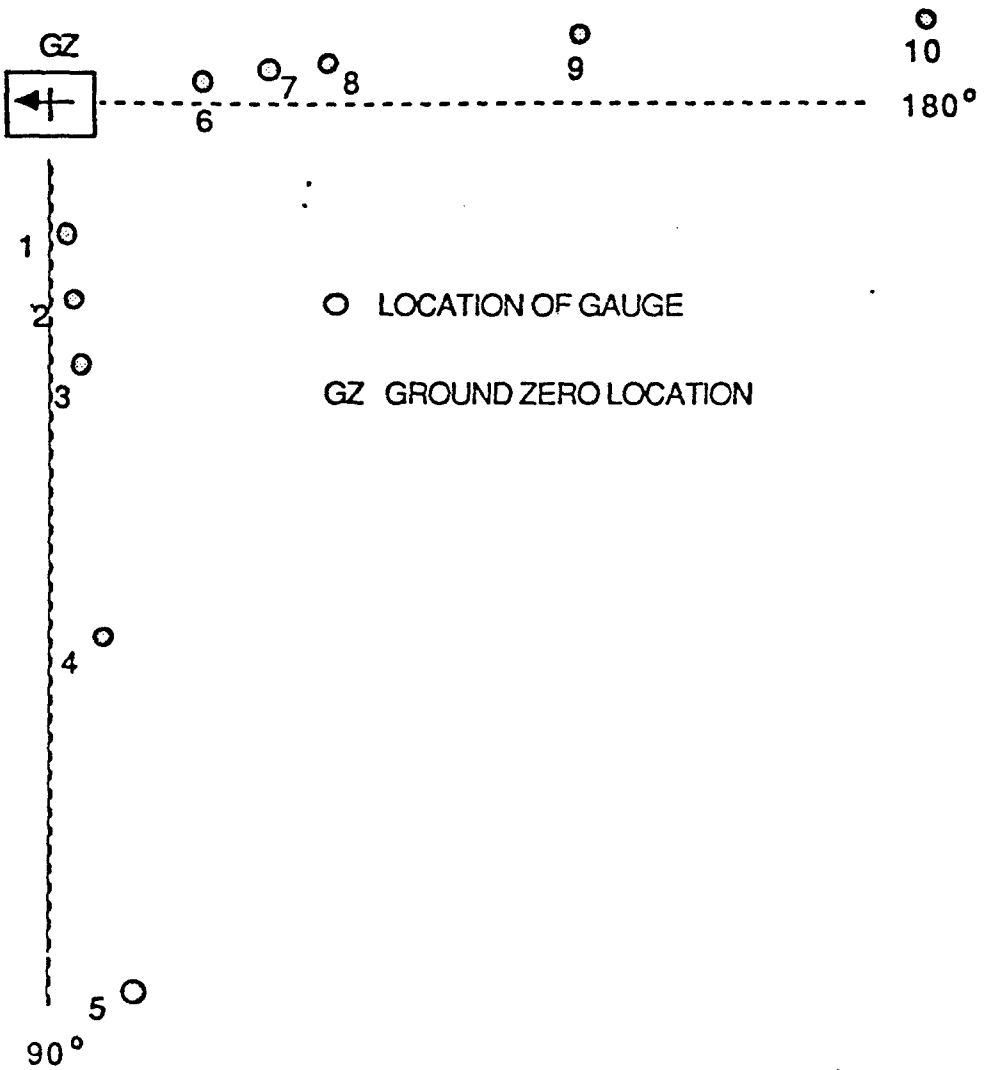

FIGURE 1 DIAGRAM OF GAUGE LINES USED IN TESTS

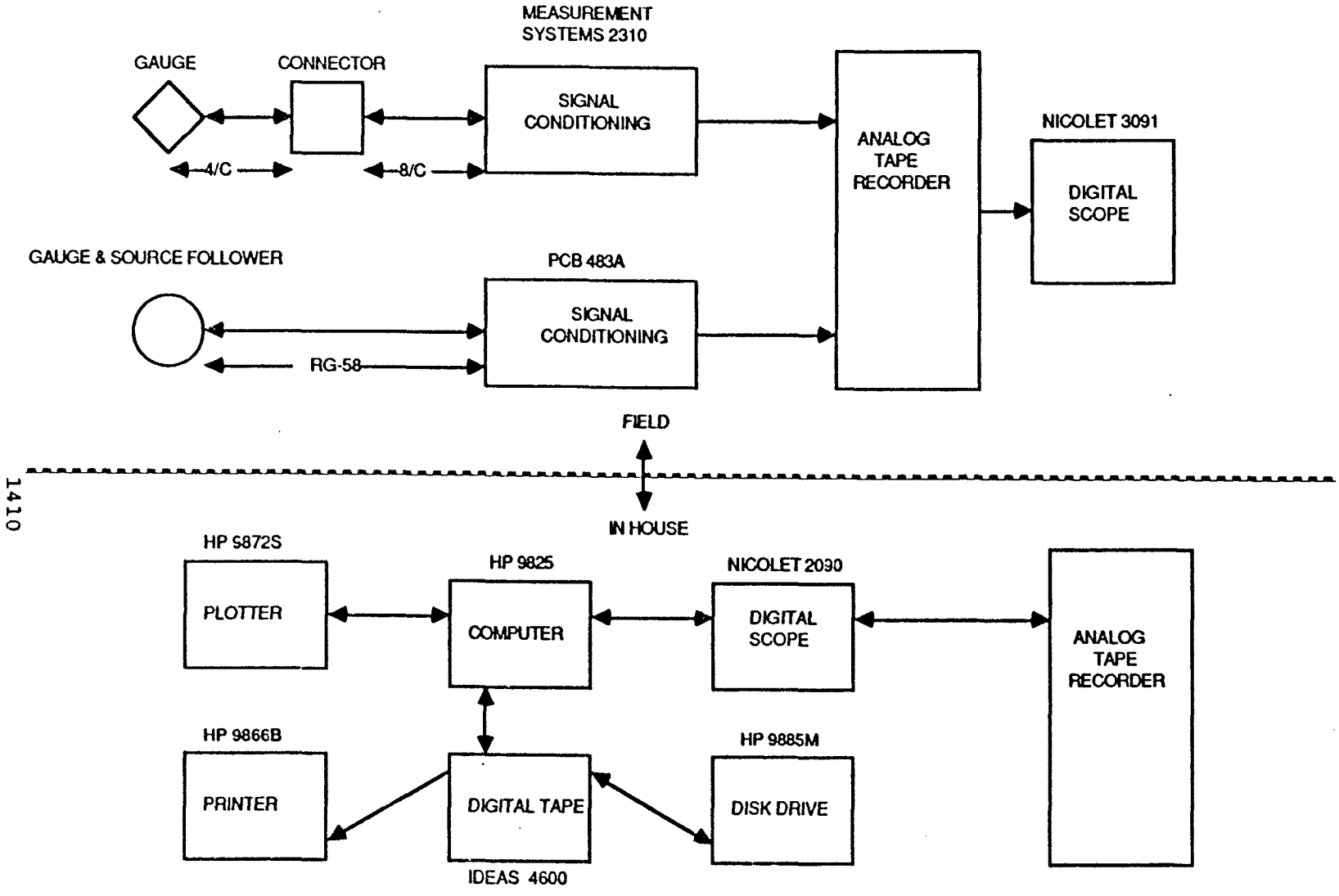

FIGURE 2. SIGNAL FLOW CHART

PHOTOGRAPHY

Each event was recorded photographically at three camera speeds ranging from 7000 pictures per seconds (pps) to 40,000 pps. The 20,000, and 40,000 pps cameras were also used to assess sympathetic detonation.

RESULTS

GENERAL OBSERVATIONS

There was no doubt that the donor warhead detonated high order for all three shots of the test series. None of the acceptor warheads sympathetically detonated. This result was verified by the airblast data (as shown in Table 4) and the fact that all four of the acceptor warheads were recovered after the tests.

SHOT SUMMARY

Shot 1. The test configuration for the first shot is shown in Figure 3. The donor warhead was detonated in its normal/design mode. All ten channels of pressure gauge data contained usable data.

Shot 2. The configuration for the second shot is also shown in Figure 3 The donor warhead was detonated in its normal mode. Nine of the ten channels of pressure data contained usable data. Examination of the test area after the test turned up both acceptor warheads intact. This demonstrated that the acceptor warheads did not detonate.

Shot 3. The configuration for the third shot is shown in Figure 3. The donor warhead was detonated in its normal mode. Post test examination of the test area turned up both acceptor warheads. This again showed that the acceptors did not sympathetically detonate. All ten channels of pressure gauge data contained usable data.

AIRBLAST RESULTS

Figure 4 compares the airblast produced by the single warhead detonation (shot 1) with that produced by the three warhead stack shots (shots 2 and 3). Figure 4A shows the results off the side of the warhead (positions 1-5) while Figure 4B shows the results off the tail (positions 6-10). Close-in, the stack shots produce airblast that is lower than the singe warhead detonation. This is due to the shielding effects of the added masses of the extra shipping containers and launch tubes. Farther out, the airblast pressures are nearly identical. Also shown in these figures are a comparison of the predicted pressures presented in Table 3 with the actual measured pressure-distance curves.

TABLE 4A. DRAGON SINGLE WARHEAD DETONATION

SHOT NUMBER	POSITION NUMBER	RANGE (feet)	PEAK PRESSURE (psi)	POSITIVE DURATION (ms)	POSITIVE IMPULSE (psi-ms)
1	1	8.00	33.2	1.60	22.44
1	2	12.00	21.0	1.52	14.23
1	3	15.20	13.1	4.08	12.75
1	4	30.15	6.3	5.80	8.99
1	5	50.25	3.2	4.92	5.69
1	6	8.00	34.0	2.20	23.41
1	7	12.10	21.1	3.32	18.82
1	8	15.10	16.2	3.64	14.52
1	9	30.05	7.4	5.96	8.81
1	10	50.04	3.3	6.88	6.00

TABLE 4B. DRAGON THREE WARHEAD STACK DETONATIONS

SHOT NUMBER	POSITION NUMBER	RANGE (feet)	PEAK PRESSURE (psi)	POSITIVE DURATION (ms)	POSITIVE IMPULSE (psi-ms)
2	1	8.00	31.0	2.04	33.25
2	2	12.00	- - -	1.44	- - -
2	3	15.20	15.5	3.64	14.79
2	4	30.15	7.7	4.84	10.46
2	5	50.25	3.8	4.96	6.49
2	6	8.00	29.6	2.19	32.40
2	7	12.10	19.3	3.32	23.27
2	8	15.10	14.2	4.12	13.62
2	9	30.05	6.3	5.56	8.25
2	10	50.04	2.9	6.48	5.31

SHOT NUMBER	POSITION NUMBER	RANGE (feet)	PEAK PRESSURE (psi)	POSITIVE DURATION (ms)	POSITIVE IMPULSE (psi-ms)
3	1	8.00	29.2	3.16	34.00
3	2	12.00	16.9	3.44	21.70
3	3	15.20	12.3	3.72	16.15
3	4	30.15	8.1	4.72	10.35
3	5	50.25	3.9	5.16	6.41
3	6	8.00	33.2	1.64	15.22
3	7	12.10	22.2	3.64	19.09
3	8	15.10	18.6	4.00	14.07
3	9	30.05	6.3	5.14	6.47
3	10	50.04	3.0	6.20	5.24

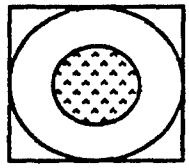

DESIGN MODE INITIATION

SETUP FOR TEST1

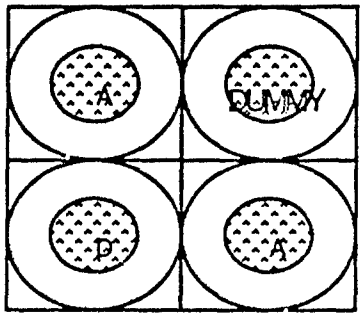

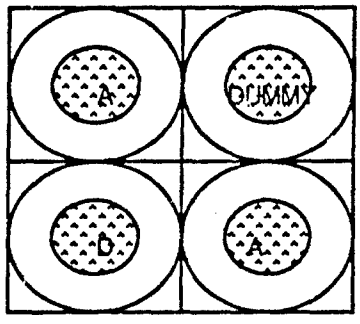

A=Acceptor
D=Donor

SETUP FOR TESTS 2 AND 3

FIGURE 3. SHIPPING CONTAINER/LAUNCH TUBE CONFIGURATIONS FOR DRAGON TESTS

FIGURE 4A. DRAGON WARHEAD TESTS--PRESSURES OFF THE SIDE

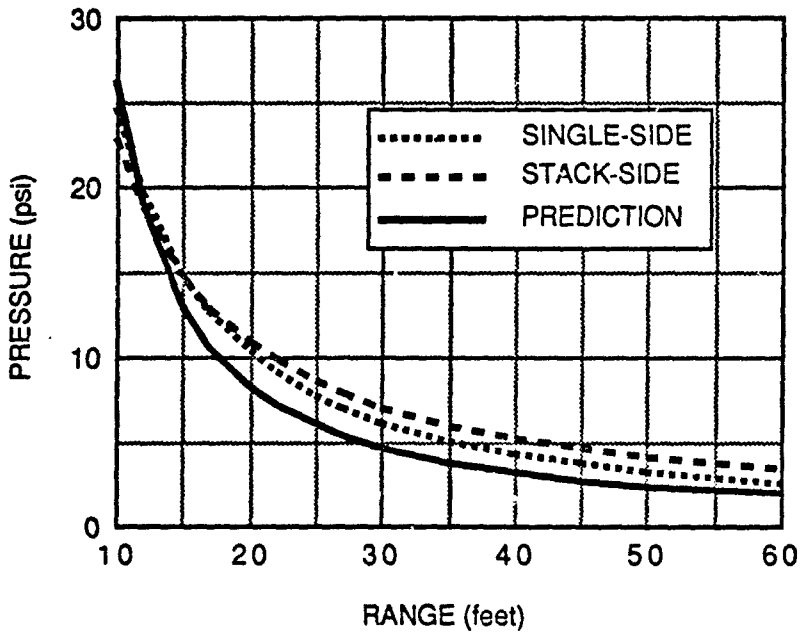

FIGURE 4B. DRAGON WARHEAD TEST--PRESSURES OFF THE END

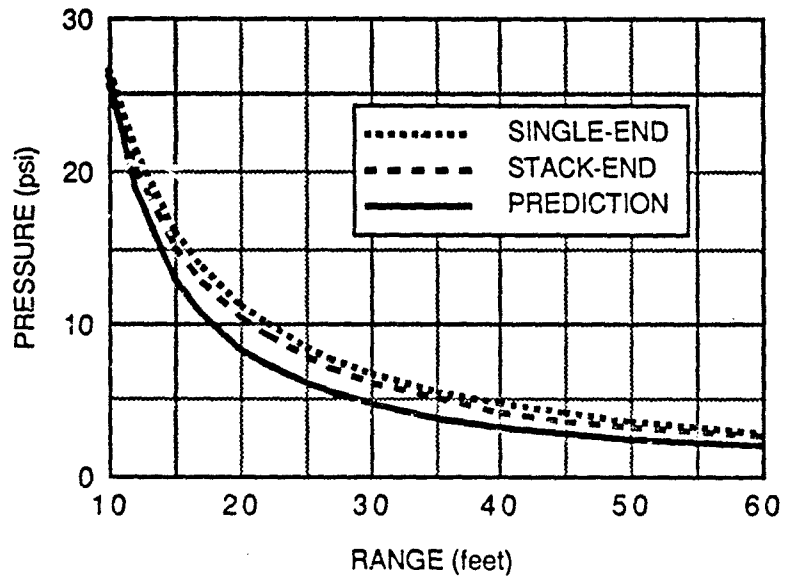

Thus, based on the measured airblast results, it is concluded that only the donor warhead detonated. None of the acceptors contributed to the reaction.

SUMMARY

The results from the tests indicate that the wooden shipping containers are a good fragment shield for the warheads. Only one of the acceptor warheads showed signs of being hit by a fragment--which indicates that the shipping containers were effective at stopping the fragments from the donor warheads.

The airblast predictions for a one-warhead detonation were a reasonable match for the measured results--another indication that only one warhead detonated.

REFERENCES

1. Porzel, F. B., "Technology Base of the Navy Explosives Safety Improvement Program," Minutes of the Nineteenth Explosives Safety Seminar, Department of Defense Explosives Safety Board, Los Angeles, CA, September 1980.

2. Porzel, F. B., Introduction to a Unified Theory of Explosions (UTE), NOL TR 72-209, 15 September 1972.

DESIGN BLAST LOADS FOR ABOVEGROUND STORAGE TANKS

by
W.A. Keenan and P.C. Wager
Naval Civil Engineering Laboratory
Port Hueneme, CA 93043

PURPOSE

This paper presents the procedure for calculating the design blast overpressure-time curves for the shell and roof of an aboveground storage tank due to the shock wave generated by an unconfined hemispherical surface burst explosion in the vicinity of the tank.

BACKGROUND

In 1988 the Naval Civil Engineering Laboratory developed the basis of design for aboveground fuel storage tanks (50,000 barrel) that can be safely located at public traffic route distance (K=24/30) from explosives sites (Ref 1). The maximum credible event (MCE) at the site is an accidental explosion involving mass detonation of Mark 81 bombs stored in three boxcars. The MCE is equivalent to 150,000 lb TNT. The tanks store either JP-5 fuel or diesel marine fuel.

The tank is a vertical cone roof tank, 110 feet diameter and 34 feet high. The shell and roof are constructed of welded steel plate designed to resist the blast overpressures. The shell is reinforced with a series of ring stiffeners to prevent shell buckling and shielded with precast concrete panels on the face toward the explosives site. The panels protect the structural steel shell and prevent fuel leakage from flying fragments and debris. The shield, along with the internal floating pan, also controls the hazard of secondary explosions inside the tank above the pan and outside the tank above the diked area.

One element of the basis of design for the fuel storage tank is the design blast loads which is the subject of this paper.

TANK AND LOAD PARAMETERS

Figure 1 defines the notation used to describe the geometry of an aboveground, fixed-roof, storage tank and location of the maximum credible explosion (MCE). The tank has a diameter, D, and height, H. The term R_o is the horizontal distance from the MCE to the nearest point on the tank (n = 1). The distance, R (ft), from the MCE to any other point n is,

$$R = R_o + x \qquad (1)$$

where

$$x = 0.5D\,(1-\cos\theta) \qquad (1a)$$

θ = angle of incidence of the shock wave or angle measured from line normal to shock front (Figure 1) (1b)

Figures 2a and 2b define the notation used to describe the design blast overpressure as a function of time at any point, n, on the shell or roof of the tank. Zero time is the instant when the incident shock wave first strikes the tank. This occurs when the shock wave reaches the first node, n = 1. The procedures used to calculate the design blast loads for each tank surface are described below, based on information in References 1 through 4, but adjusted for a right vertical cylinder.

DESIGN BLAST LOAD ON TANK WALL

Figure 2a defines the notation used to describe the design blast load on the shell of a fixed-roof tank. The load prediction method depends upon whether the point of interest is on the forward or leeward face of the tank.

Forward Face ($0° \leq \theta < 90°$)

The incident shock wave reaches node n at arrival time, t_d (msec),

$$t_d = x/U \tag{2}$$

where

x = distance from node n = 1 obtained from Equation 1a for given value of θ and D, ft (2a)

U = velocity of incident shock wave obtained from Figure 2-15 of Reference 2 (ft/msec) or (2b)

$$U = 1.117 \sqrt{1 + 6P_{so}/(7x14.7)} \text{ , ft/msec} \tag{2c}$$

When the incident shock wave reaches node n at time t_d, the local overpressure rises instantaneously from zero to the peak reflected overpressure, P_{d2} (psi),

$$P_{d2} = C_r P_{so} \tag{3}$$

where

P_{so} = peak incident blast overpressure obtained from Figure 2-15 of Reference 2 for a given value of $R/W^{1/3}$, psi. (3a)

$C_r = P_r/P_{so}$ = reflection coefficient obtained from Figure 2-193 of Reference 2 for given values of P_{so} and θ, provided $45° \leq \theta \leq 90°$ (3b)

$$C_r = 2\left[\frac{7 \text{ X } 14.7 + 4\ P_{so}}{7 \text{ X } 14.7 + P_{so}}\right], \text{ provided } \theta \leq 45° \quad (3c)$$

P_r = peak reflected blast overpressure, psi

W = design explosive weight, lbs TNT equivalent

At the instant when the reflected blast wave is formed at point n, a rarefaction wave forms at the top of the tank shell and travels vertically toward the bottom of the tank at the velocity of sound, C_{refl} at the reflected overpressure. Within a short time, called the clearing time, t_c (msec), the rarefaction wave enfeebles the reflected blast wave and reduces the overpressure to the stagnation overpressure, P_c (psi).

$$t_c = 3S/C_{refl} \quad (4)$$

where

S = H = height of tank, ft. (4a)

$$C_{refl} = 0.422\sqrt{\frac{1.088\ P_{so}^2 + 70\ P_{so} + 720}{102.9 + 6P_{so}}}, \text{ ft/msec,} \quad (4b)$$

obtained from Figure 3.21 of Reference 3.

The stagnation overpressure, P_c (psi), at time t_c is:

$$P_c = P_{d1}\left[1 - t_c/t_o\right] e^{-\alpha\, t_c/t_o} \quad (5)$$

where

$$P_{d1} = P_{so} + C_D\, q_o \quad (5a)$$

C_D = drag coefficient obtained from Figure 3.63c of Reference 3 because for $P_{so} < 10$ psi the Mach number $M < 0.4$ for most aboveground storage tanks (Figure 3.64 of Reference 3), and the Reynolds number, $R_e = UD/\nu > 5\times10^5$ (Figure 3.65 of Reference 3) where ν is the viscosity of air in the incident shock wave. (5b)

$$q_o = 14.7 \left[\frac{(5/14)\ (P_{so}/14.7)^2}{1 + (1/7)\ (P_{so}/14.7)} \right], \text{ psi, which is the} \qquad (5c)$$

peak dynamics pressure given by Equation 3.7b of Reference 3 for $P_{so} \leq 10$ psi.

α = Exponential decay factor

The exponential decay factor, α, is calculated so that the area under the pressure-time curve equals the total impulse, i_t (psi-msec), due to the combined incident plus drag overpressures or,

$$i_t = \int_o^{t_o} (P_{so} + C_D\ q_o)\ (1 - t/t_o)^{-\alpha t/t_o}\ dt \qquad (5d)$$

where

$i_t = i_s + i_D$ = total impluse, psi - msec

i_s = total impulse in the incident shock wave from Figure 2-15 of Reference 2, psi-msec

$$i_D = \int_o^{t_o} C_D\ q\ dt = \text{total impulse from air drag, psi-msec.}$$

q = dynamic overpressure from Figure 3.24 of Reference 3, psi

The time duration of the positive blast overpressure, t_o (msec), is:

$$t_o = C_1\ W^{1/3} \qquad (6)$$

where

$C_1 = t_o/W^{1/3}$ = scaled time duration of the incident blast overpressure, obtained from Figure 2-15 of of Reference 2 for a given value of $R/W^{1/3}$, msec/lb$^{1/3}$. (6a)

W = design explosive weight, lbs TNT equivalent

The design blast load, P (psi), decays linearly with time for $t_d \leq t \leq t_c + t_d$ so that:

$$P = P_{d2} \left[1 - (1 - P_c/P_{d2})\ (t/t_c - t_d/t_c) \right] \qquad (7)$$

The design blast load, P (psi), decays exponentially with time for $t_c + t_d \leq t \leq t_o + t_d$ so that:

$$P = P_{d1} \left[1 - t/t_o \right] e^{-\alpha\, t/t_o} \qquad (8)$$

Leeward Face ($90° \leq \theta \leq 180°$)

The incident shock wave reaches node n at the arrival time, t_d (msec), given by,

$$t_d = x/U \qquad (2)$$

When the incident shock wave reaches point n, the local overpressure rises instantaneously at time t_d from zero to the peak leeward overpressure, P_{d3} (psi), given by,

$$P_{d3} = P_{so} \left[1.5 - \theta/180 \right] \qquad (9)$$

Within a short time, called the clearing time, diffracted shock waves on the leeward face reduce the peak overpressure to the drag overpressure. The clearing time, t_c (msec), is:

$$t_c = (3\, S/C_{ref1})\ (\theta/90) \qquad (10)$$

where

$$S = H = \text{height of tank, ft.} \qquad (4a)$$

$$C_{ref1} = 0.422 \sqrt{\frac{1.088\, P_{so}^{\,2} + 70\, P_{so} + 720}{102.9 + 6\, P_{so}}}\ , \text{ ft/sec} \qquad (4b)$$

The drag overpressure, P_c (psi), at clearing time t_c is:

$$P_c = P_{d1} \left[1 - t_c/t_o \right] e^{-\alpha\, t_o/t_c} \qquad (5)$$

The time duration of the positive blast overpressure, t_o (msec), is:

$$t_o = C_1\, W^{1/3} \qquad (6)$$

The design blast load, P (psi), decays linearly with time for $t_d \leq t \leq t_c + t_d$ so that:

$$P = P_{d3} \left[1 - (1 - P_c/P_{d3})\ (t/t_c - t_d/t_c) \right] \qquad (11)$$

The design blast load, P (psi), decays exponentially with time for $t_c + t_d \leq t \leq t_o + t_d$ so that:

$$P = P_{d1} \left[1 - t/t_o \right] e^{- \alpha \, t/t_o} \qquad (8)$$

DESIGN BLAST LOAD ON ROOF

Figure 2b defines the notation used to describe the design blast load on the roof of a fixed-roof tank. The load prediction method is developed for a point on the roof, a roof strip parallel to the shock front, and a roof strip normal to the shock front. These conditions cover the blast loadings needed to design the girders, rafters, skin, and columns of the roof system.

Point on the Roof

The incident shock wave reaches point n at arrival time, t_d (msec),

$$t_d = x/U \qquad (2)$$

When the incident shock wave reaches point n, the local overpressure on the roof rises instantaneously at time t_d from zero to the peak drag overpressure, P_{d1} (psi), given by

$$P_{d1} = P_{so} + C_D \, q_o \qquad (5a)$$

where

P_{so} = peak incident blast overpressure obtained from Figure 2-15 of Reference 2 for a given value of $R/W^{1/3}$, psi. (3a)

C_D = drag coefficient obtained from Figure D-13 of Reference 4. (12)

$$q_o = 14.7 \left[\frac{(5/14) \, (P_{so}/14.7)^2}{1 + (1/7) \, (P_{so}/14.7)} \right], \text{ psi, which is the} \qquad (5c)$$

peak dynamics pressure given by Equation 3.7b of Reference 3 for $P_{so} \leq 10$ psi.

The time duration of the positive blast overpressure, t_o (msec), is:

$$t_o = C_1 \, W^{1/3} \qquad (6)$$

The design blast load, P (psi), decays exponentially with time for $t_c + t_d \leq t \leq t_o + t_d$ so that:

$$P = P_{d1}\left[1 - t/t_o\right] e^{-\alpha t/t_o} \qquad (8)$$

Roof Strip Parallel to Shock Front

Procedures for calculating the design blast loads on roof strips parallel to the shock front are identical to the procedures outlined above for a point on the roof.

Roof Strip Normal to Shock Front

The incident shock wave reaches the mid-point of strip n at arrival time, t_d (msec)

$$t_d = x/U \qquad (2)$$

where

x = distance from point n = 1 to point at mid-length of the strip, ft. (13)

$$U = 1.117\sqrt{1 + 6\,P_{so}/[7(14.7)]}\ , \quad \text{ft/msec} \qquad (2c)$$

The average blast overpressure on the strip begins to rise at time $t_d - t_\ell/2$, where

$$t_\ell = \ell/U \qquad (14)$$

where

ℓ = length of strip normal to shock front, ft (14a)

The time duration of the positive blast overpressure, t_o (msec), is:

$$t_o = C_1 W^{1/3} \qquad (6)$$

The average blast overpressure on the strip rises linearly with time. At time $t_d + t_\ell/2$, the overpressure reaches the peak drag overpressure, P_c (psi),

$$P_c = P_{d1}\left[1 - (t_d + t_\ell/2)/t_o\right] e^{-\alpha\,(t_o + t_\ell/2)/t_o} \qquad (15)$$

where

$$P_{d1} = P_{so} + C_D\, q_o \qquad (5a)$$

P_{so} = peak incident blast overpressure obtained from Figure 2-15 of Reference 2 for a given value of $R/W^{1/3}$, psi (3a)

C_D = drag coefficient obtained from Figure D-13 of Reference 4 based on the location of the centroid of the strip (16)

$$q_o = 14.7 \left[\frac{(5/14)\ (P_{so}/14.7)^2}{1 + (1/7)\ (P_{so}/14.7)} \right], \text{ psi, which is the peak dynamics pressure given by Equation 3.7b of Reference 3 for } P_{so} \leq 10 \text{ psi.} \quad (5c)$$

α = Exponential decay factor (see Equation 5d)

The design blast load, P (psi), decays exponentially with time for $t_c + t_d \leq t \leq t_o + t_d$ so that:

$$P = P_{d1} \left[1 - t/t_o \right] e^{-\alpha\, t/t_o} \quad (8)$$

SAMPLE PROBLEM

An aboveground, fixed-roof, storage tank is located 1,300 feet from an explosives handling area. The maximum credible explosion (MCE) at the area is equivalent to an unconfined hemispherical surface burst of 150,000 lb TNT. For the purpose of calculating design blast loads on the tank, the design explosive weight, W (lb TNT), is,

$$W = 1.2 \times 150{,}000 = 180{,}000 \text{ lb}$$

where the factor 1.2 is a safety factor required by NAVFAC P-397 to account for uncertainties in the structural design process.

The tank is 110 feet in diameter and 34 feet high. Therefore, the design blast loads are based on the following parameters:

$W = 180{,}000$ lb

$R_o = 1{,}300$ feet

$D = 110$ feet

$H = 34$ feet

Design Blast Loads For Tank Wall

The incident shock wave parameters at the tank are presented in Table 1. The design blast load parameters for the tank shell are given in Table 2. The overpressure-time curves for n = 1,2,... 13 on the tank

shell are presented in Figure 3. The distribution of the design blast load on the tank shell at various times is presented in Figure 4. Information in these tables and Figures is calculated using the above equations for locations on a tank shell.

Design Blast Loads For Tank Roof

The design blast load parameters for the tank roof are given in Table 3. The overpressure-time curves for individual roof points, individual roof strips parallel to the shock front, and individual roof strips normal to the shock front are presented in Figure 5. Information in these tables and Figures is calculated using the above equations for locations on a tank roof.

REFERENCES

1. Naval Civil Engineering Laboratory. Technical Note N-1785: Basis of Design for Aboveground Storage Tanks (50,000 Barrel) at Public Traffic Route Distance, by W.A. Keenan and T.J. Holland. Port Hueneme, CA. 93043. May 1988.

2. U.S. Army Armament Research, Development, and Engineering Center. Special Publication ARLCD-SP-84001: "Structures to Resist Effects of Acidental Explosions", Vol II: "Blast, Fragment, Shock Loads, "by H. Ayvazoyan, M. Dede, & N. Dobbs (Ammaum & Whitment Engineers, N.Y.) Picatinny Arsenal, NJ. Dec 1986.

3 U.S. Army Corps of Engineers. Manual EM 1110-345-413: Design of Structures to Resist the Effects of Atomic Weapons. July 1959.

4 Armour Research Foundation of Illinois Institute of Technology DASA 1154: Blast Effects on Buildings and Structures - Operation of Six-Foot and Two-Foot Shock Tubes, Final Test Report No. 16: Blast Effects on Tank Structures, by G. Nagumo. Contract No. AF 29(601)-796.

Table 1. Incident Shock Wave Parameters at Fuel Storage Tank

Tank Node Point n (--)	Tank Node Angle θ (deg)[a]	$\Delta X = X_n - X_{n-1}$ (ft)	Distance From Node 1 X (ft)	Distance From Explosion R (ft)[b]	Scaled Distance $R/W^{1/3}$ ($ft/lb^{1/3}$)	Incident Shock Velocity U (ft/msec)	$\Delta t = \Delta x/U$ (msec)	Arrival Time $t_d = t_{n-1} + \Delta t$ (msec)	Incident Shock Pressure P_{so} (psi)	Peak Dynamic Pressure q_o (psi)
1	0	1.9	0	1300	23.0	1.20	0	0	2.43	0.14
2	15	5.5	1.9	1302	23.1	1.20	1.6	1.6	2.43	0.14
3	30	8.7	7.4	1307	23.2	1.20	4.6	6.2	2.42	0.14
4	45	11.4	16.1	1316	23.3	1.20	7.3	13.5	2.40	0.14
5	60	13.3	27.5	1327	23.5	1.19	9.6	23.1	2.38	0.13
6	75	14.2	40.8	1341	23.8	1.19	11.2	34.3	2.36	0.13
7	90	14.8	55.0	1355	24.0	1.19	11.9	46.2	2.34	0.13
8	105	12.7	69.8	1370	24.3	1.19	12.4	58.6	2.32	0.13
9	120	11.4	82.5	1383	24.5	1.19	10.8	69.4	2.30	0.13
10	135	8.7	93.9	1394	24.7	1.18	9.7	79.1	2.27	0.12
11	150	5.5	102.6	1403	24.9	1.18	7.4	86.5	2.24	0.12
12	165	1.9	108.1	1408	25.0	1.18	4.7	91.2	2.22	0.12
13	180		110.0	1410	25.1	1.18	1.6	92.8	2.20	0.12

[a] Measured from line normal to shock front as shown in Figure 1.

[b] Equation 1 for R_o = 1300 ft and D = 110 ft.

Table 2. Design Blast Load Parameters for Tank Wall[a]

Tank Node Point n (--)	Tank Node Angle θ (deg)	Incident Shock Pressure P_{so} (psi)	Reflection Factor $C_r = P_r/P_{so}$ (--)	Peak Reflected Pressure P_{d2} (psi)	Sound Velocity C_{ref} (ft/msec)	Clearing Time t_c (msec)	$t_d + t_c$ (msec)	Drag Coeff. C_D (--)	Peak Pressure P_{d1} (psi)	Time Decay Factor α (--)
1	0	2.43	2.14	5.20	1.17	82	82	1.00	2.57	0.601
2	15	2.43	2.14	5.20	1.17	82	84	0.73	2.53	0.600
3	30	2.42	2.14	5.18	1.17	82	88	0.08	2.43	0.516
4	45	2.40	2.14	5.14	1.17	82	96	-0.80	2.29	0.472
5	60	2.38	2.90	6.90	1.16	83	106	-1.55	2.18	0.432
6	75	2.36	1.90	4.48	1.16	83	117	-1.96	2.11	0.434
7	90	2.34	1.00	2.34	1.16	83	129	-1.88	2.10	0.472
8	105	2.32	--	--	1.16	97	156	-1.34	2.15	0.515
9	120	2.30	--	--	1.16	110	179	-0.50	2.24	0.610
10	135	2.27	--	--	1.16	124	203	-0.50	2.21	0.602
11	150	2.24	--	--	1.16	138	225	-0.50	2.18	0.600
12	165	2.22	--	--	1.16	152	243	-0.50	2.16	0.560
13	180	2.20	--	--	1.16	165	258	-0.50	2.14	0.561

[a]See Figures 1 and 2a for notation.

Table 3. Design Blast Load Parameters for Tank Roof[a]

Tank Point/ Strip n (--)	Incident Shock Pressure P_{so} (psi)	Strip Length Normal to Shock Front ℓ (ft)	Shock Front Arrival Time t_d (msec)	Time for Shock Front to Traverse Strip t_ℓ (msec)	$t_d - t_\ell/2$ (msec)	$t_d + t_\ell/2$ (msec)	Drag Coeff. C_D (--)	Peak Pressure P_{d1} (psi)	Time Decay Factor α (--)
Points and Strips Parallel to Shock Front									
1	2.38	---	23.0	---	---	---	-0.96	2.25	0.512
7	2.34	---	46.0	---	---	---	-1.00	2.21	0.519
13	2.30	---	70.0	---	---	---	-0.50	2.24	0.610
Strips Normal to Shock Front									
1	2.38	55	23.0	45.8	0	46	-0.96	2.25	0.432
7	2.34	110	46.0	92.4	0	92	-1.00	2.21	0.433
13	2.30	55	70.0	46.6	47	93	-0.50	2.24	0.512

[a]See Figures 1 and 2b for notation.

Table 3. (Continued).[a]

Tank Point/ Strip n (--)	Incident Shock Pressure P_{so} (psi)	Clearing Pressure P_c (psi)	Scaled Duration $t_o/W^{1/3}$ (msec/lb$^{1/3}$)	Duration Incident Pressure t_o (msec)	$t_d + t_o$ (msec)	Scaled Incident Impulse $i_s/W^{1/3}$ (psi-msec/lb$^{1/3}$)	Incident Impulse i_s (psi-msec)
Points and Strips Parallel to Shock Front							
1	2.38	--	3.62	204	227	3.60	203
7	2.34	--	3.65	206	252	3.54	200
13	2.30	--	3.68	208	278	3.46	195
Strips Normal to Shock Front							
1	2.38	1.90	3.62	204	227	3.60	203
7	2.34	1.56	3.65	206	252	3.54	200
13	2.30	1.88	3.68	208	278	3.46	195

[a]See Figures 1 and 2b for notation.

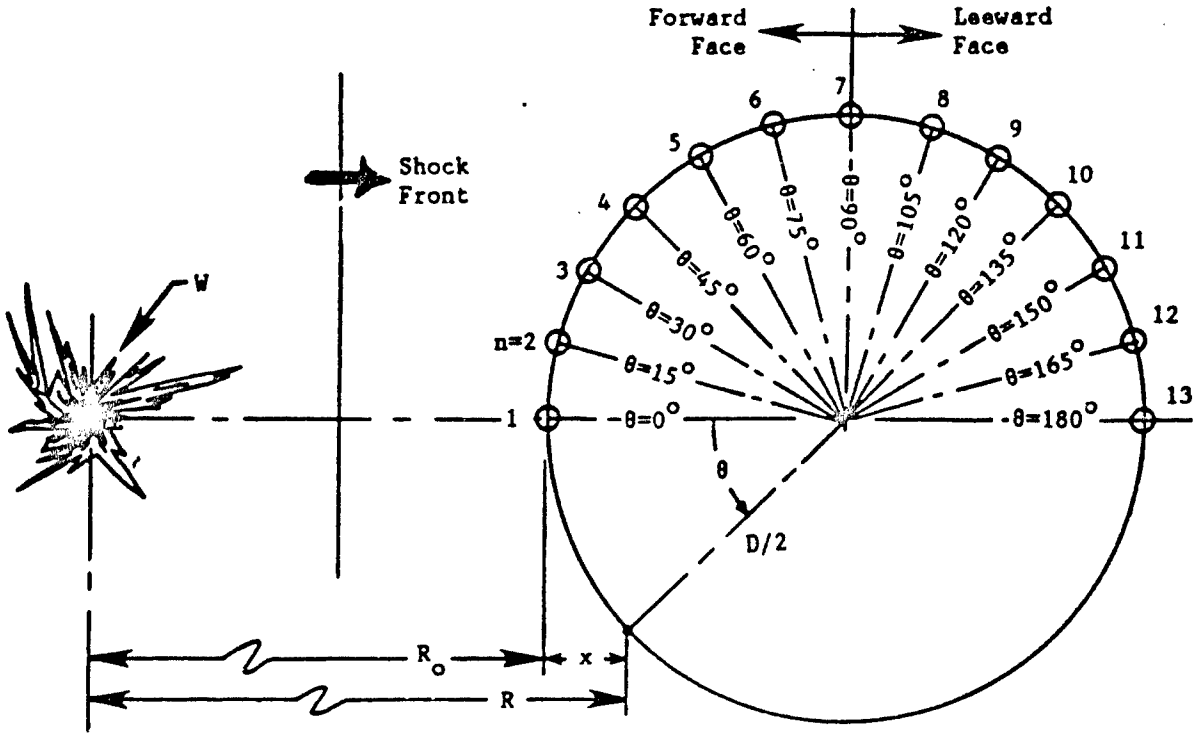

Plan View

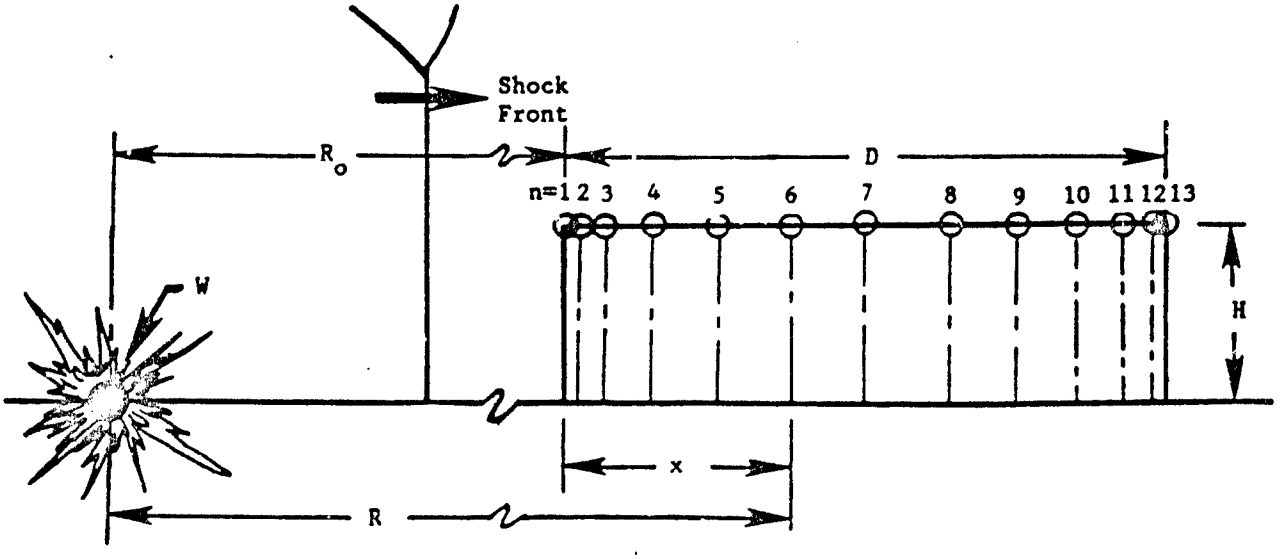

Elevation View

Figure 1. Notation for tank geometry and MCE explosion.

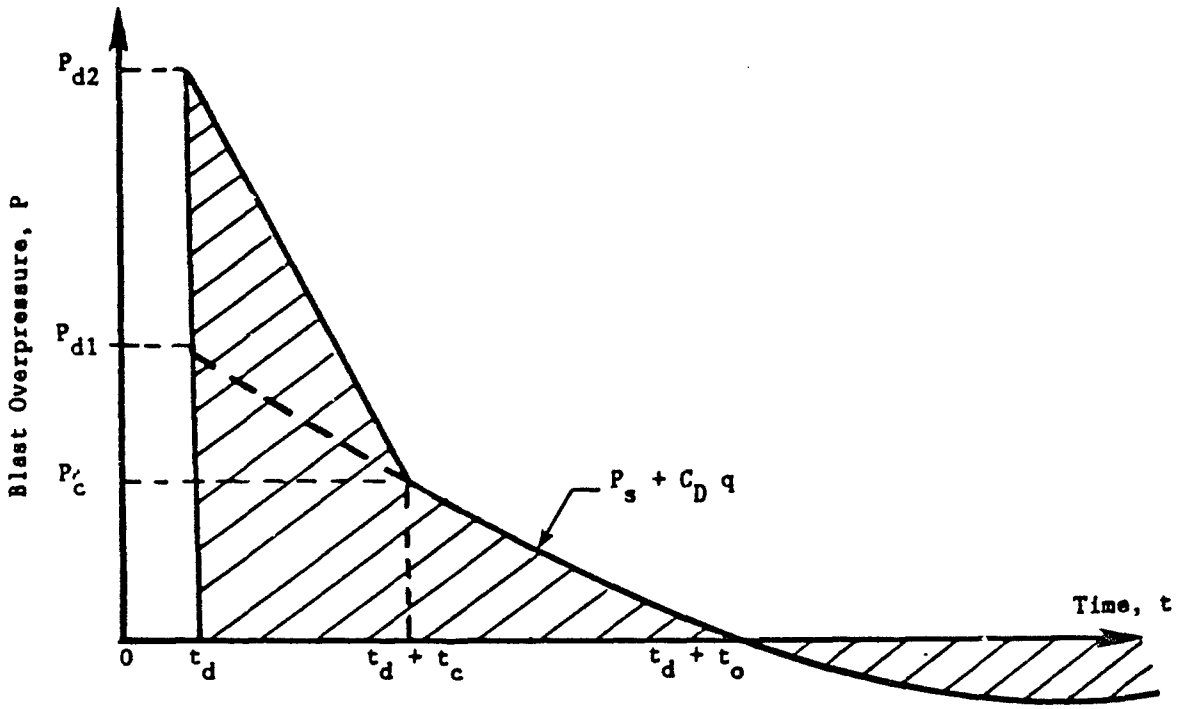

(a) Design blast load at nodes on forward face, $0° \leq \theta < 90°$.

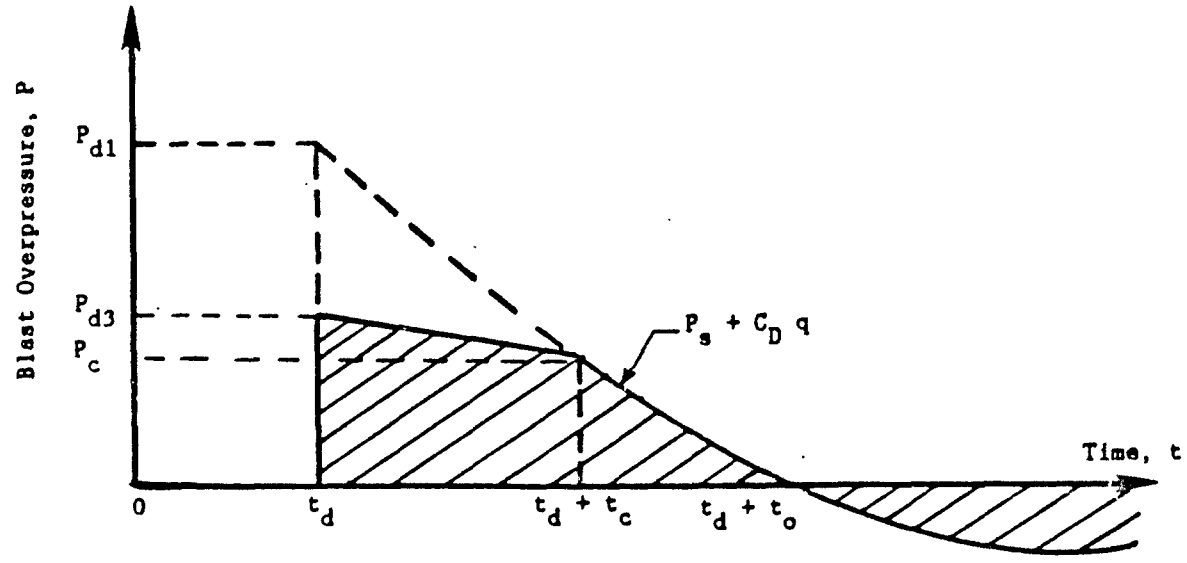

(b) Design blast load at nodes on leeward face, $90° \leq \theta \leq 180°$.

Figure 2a. Notation for design blast loads on tank wall.

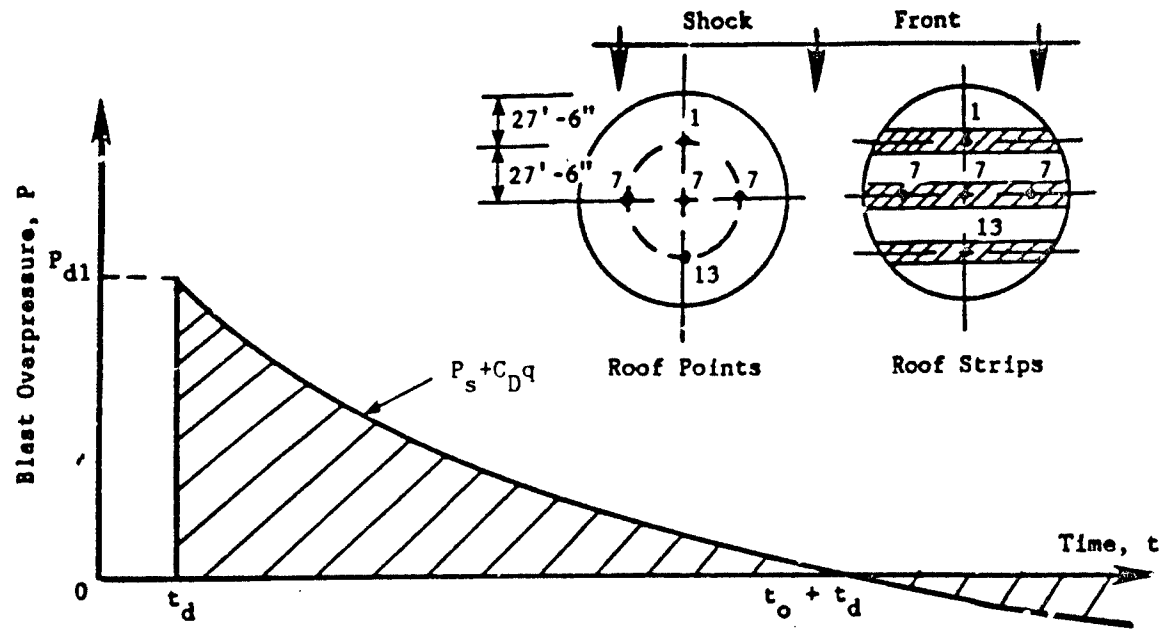

(a) Design blast loads for points on roof and for roof strips parallel to shock front.

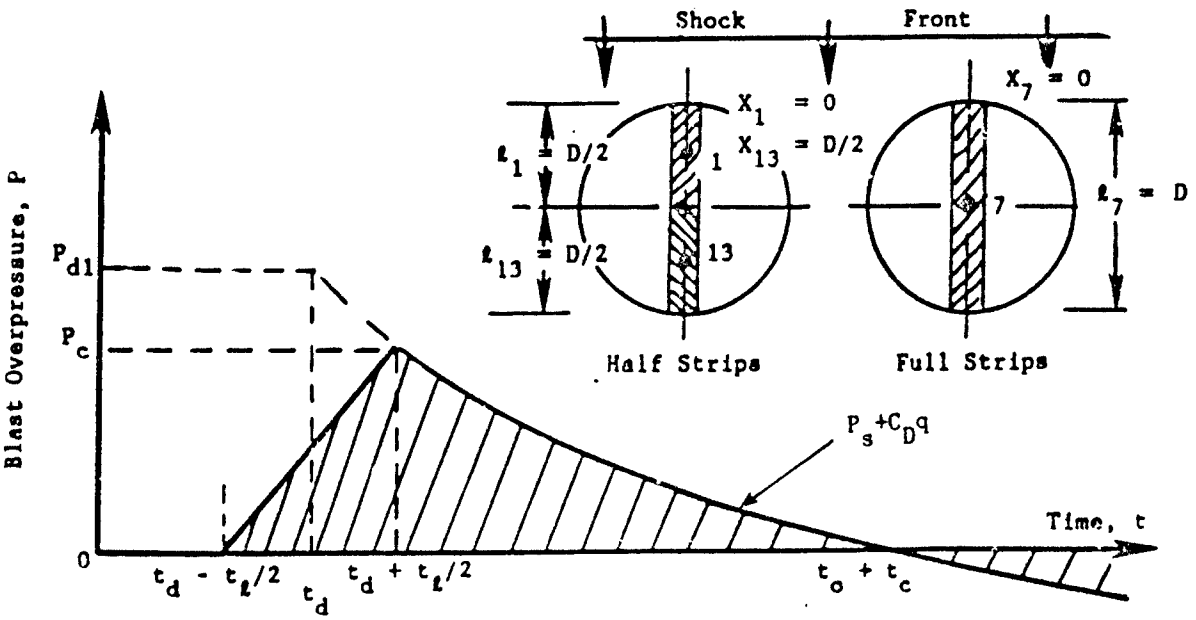

(b) Design blast loads for roof strips normal to shock front.

Figure 2b. Notation for design blast loads on tank roof.

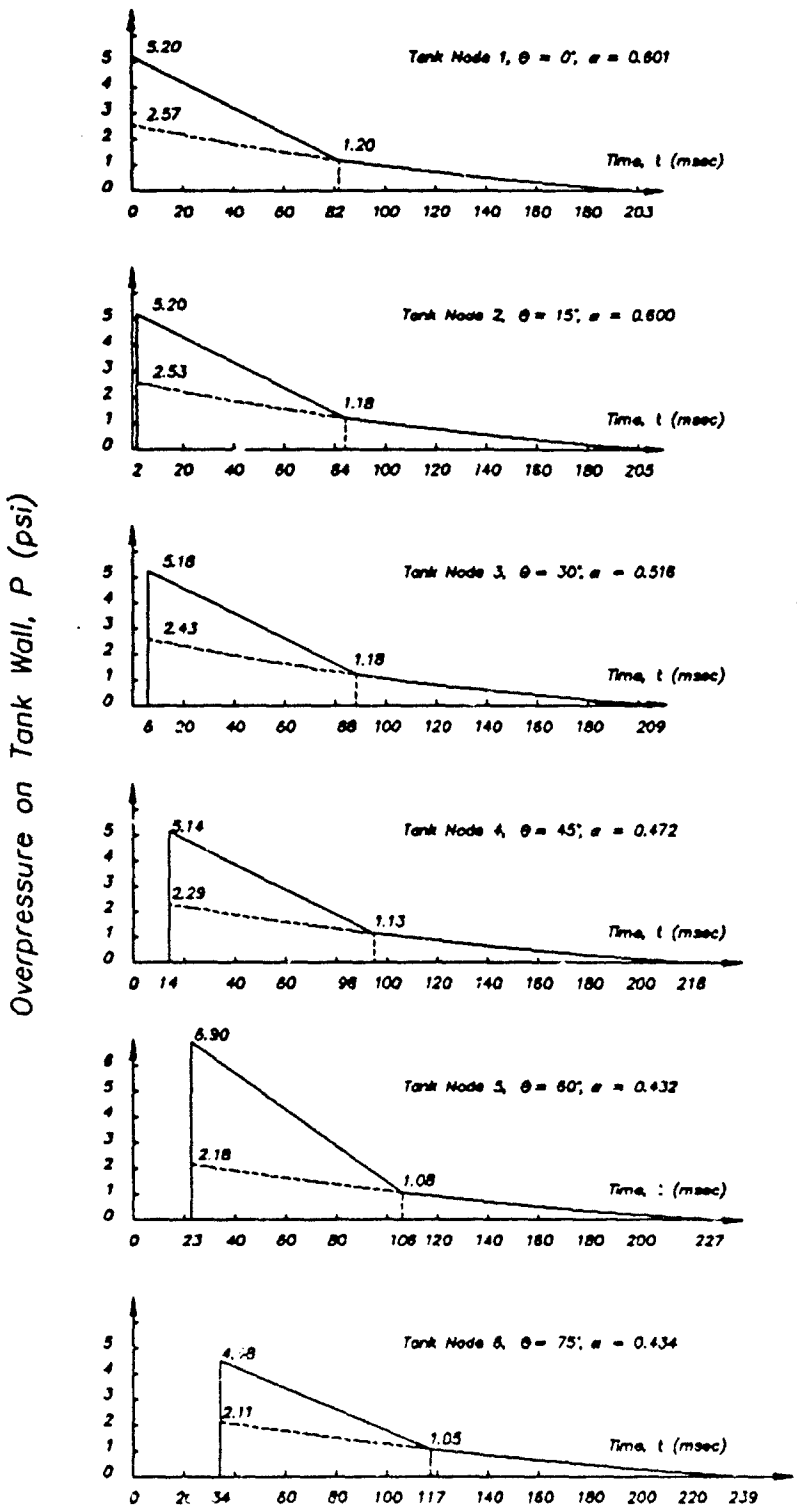

Figure 3a. Design blast overpressure-time curves for tank wall: n= 1, 2, 3, 4, 5, 6, and θ= 0°, 15°, 30°, 45°, 60°, 75°.

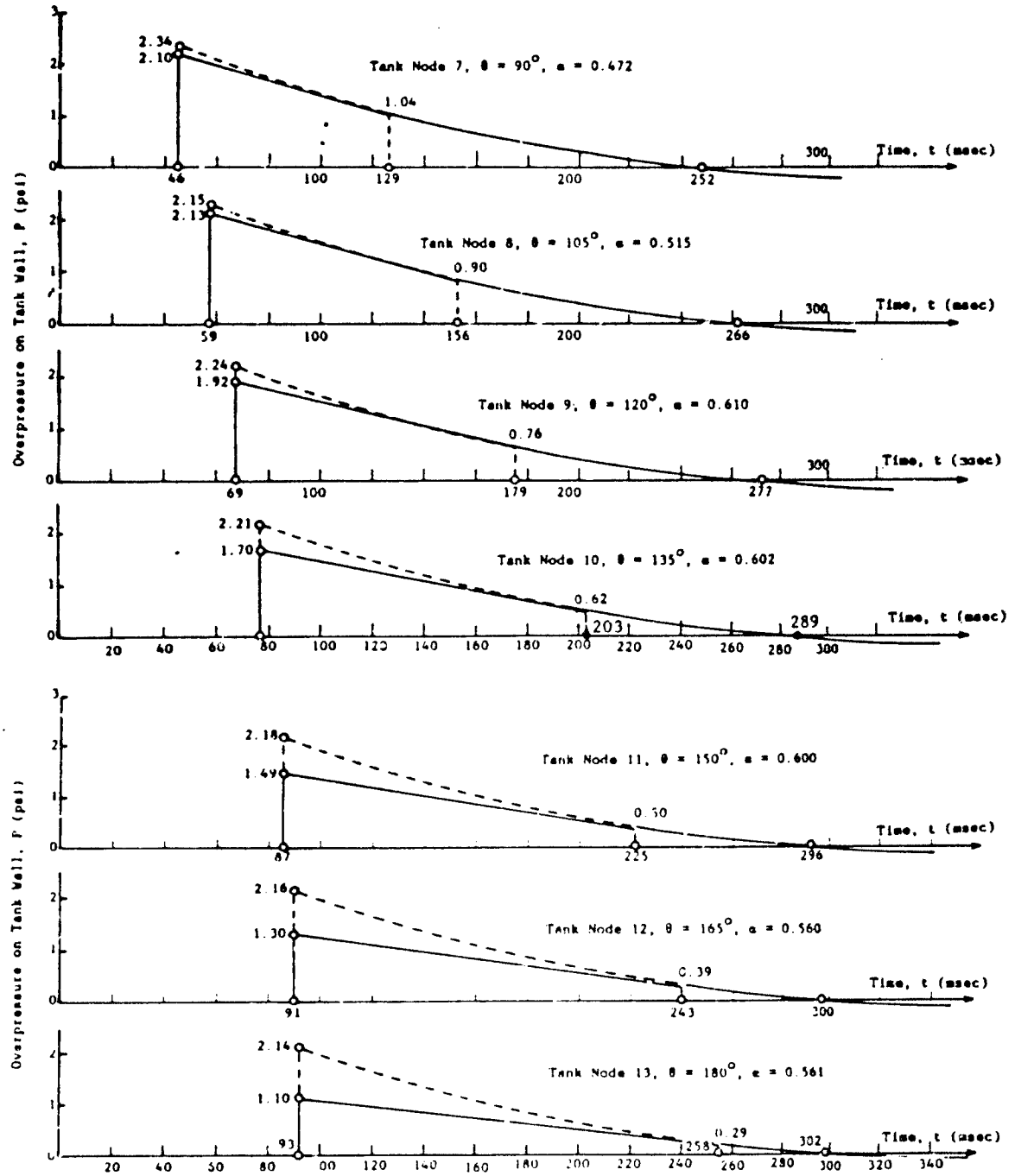

Figure 3b. Design blast overpressure-time curves for tank wall: n= 7, 8, 9, 10, 11, 12, 13, and θ= 90°, 105°, 120°, 135°, 150°, 165°, 180°.

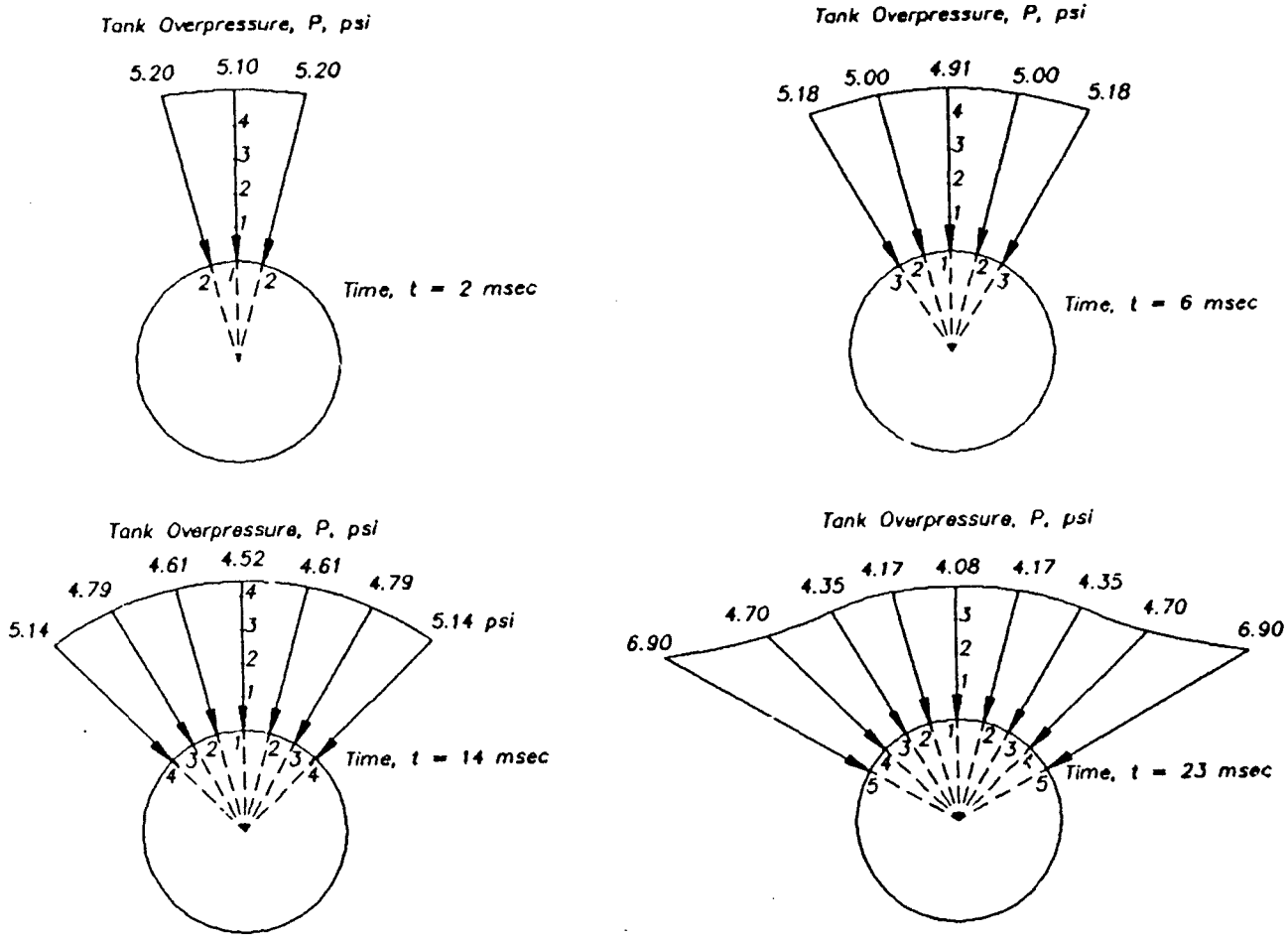

Figure 4a. Distribution of design blast load on tank wall: time, t= 2, 6, 14, and 23 msec.

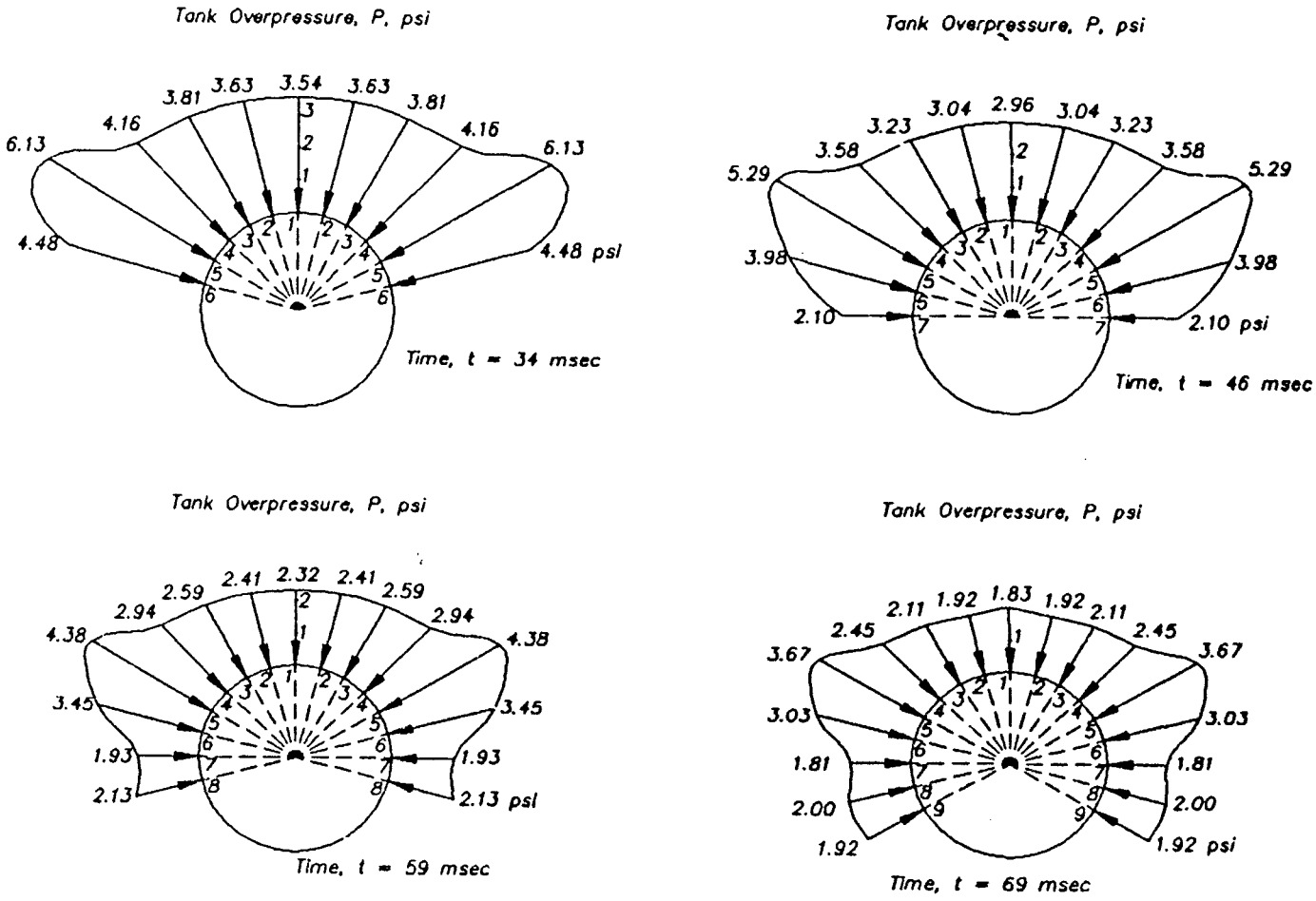

Figure 4b. Distribution of design blast load on tank wall: time, t= 34, 46, 59, 69 msec.

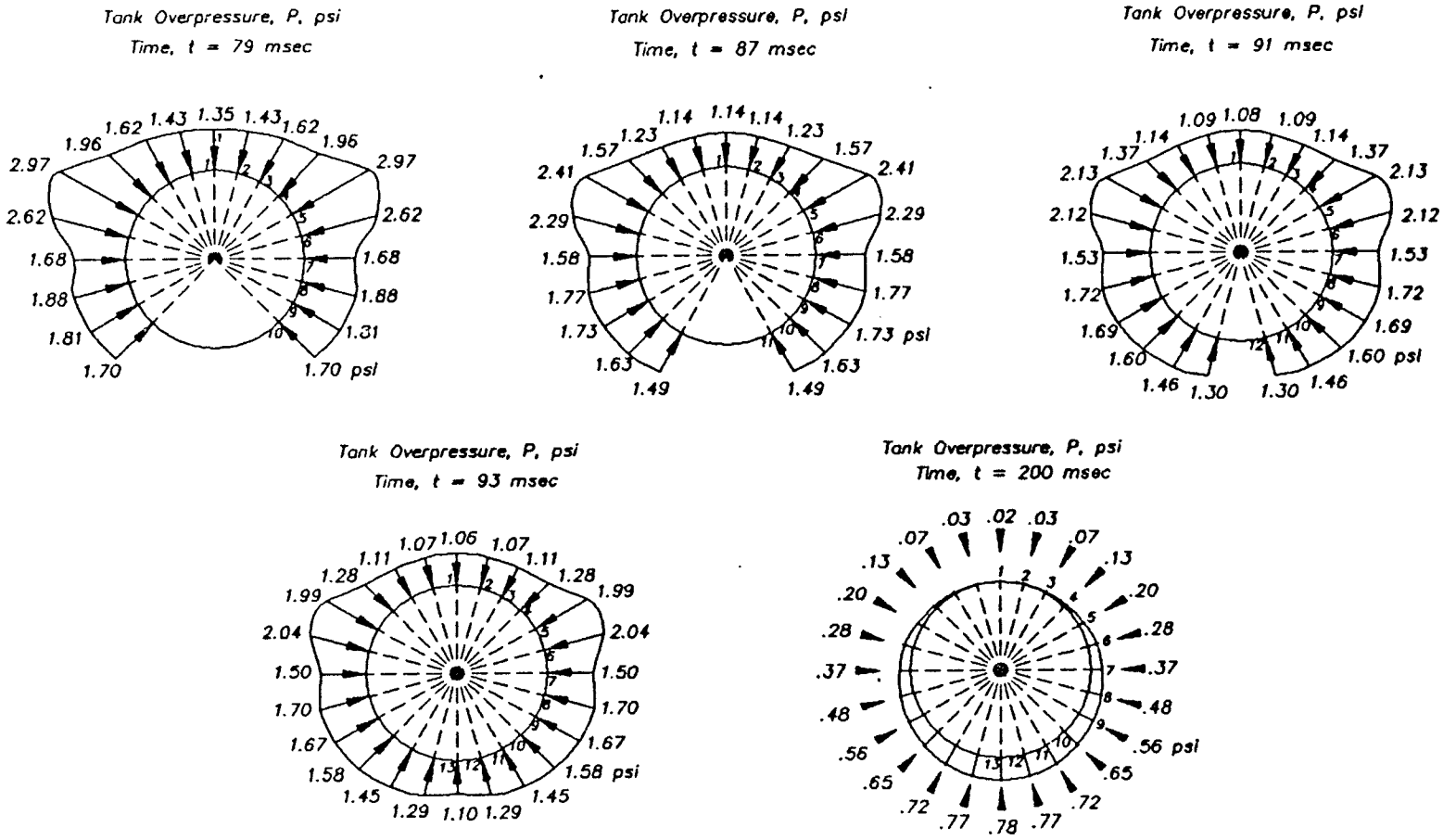

Figure 4c. Distribution of design blast load on tank wall: time, t= 79, 87, 91, 93, and 200 msec.

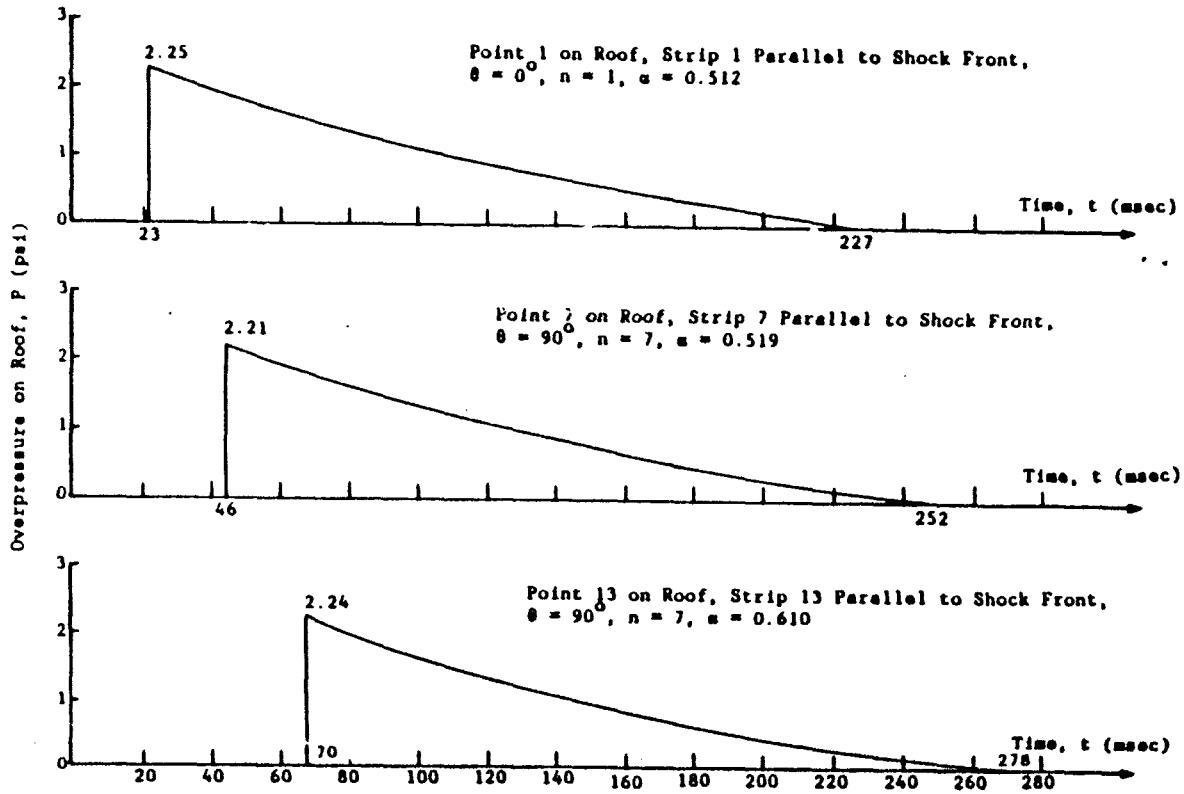

Figure 5a. Design blast overpressure-time curves for points on roof and roof strips parallel to shock front: n= 1, 7, 13 and θ= 0°, 90°, 180°.

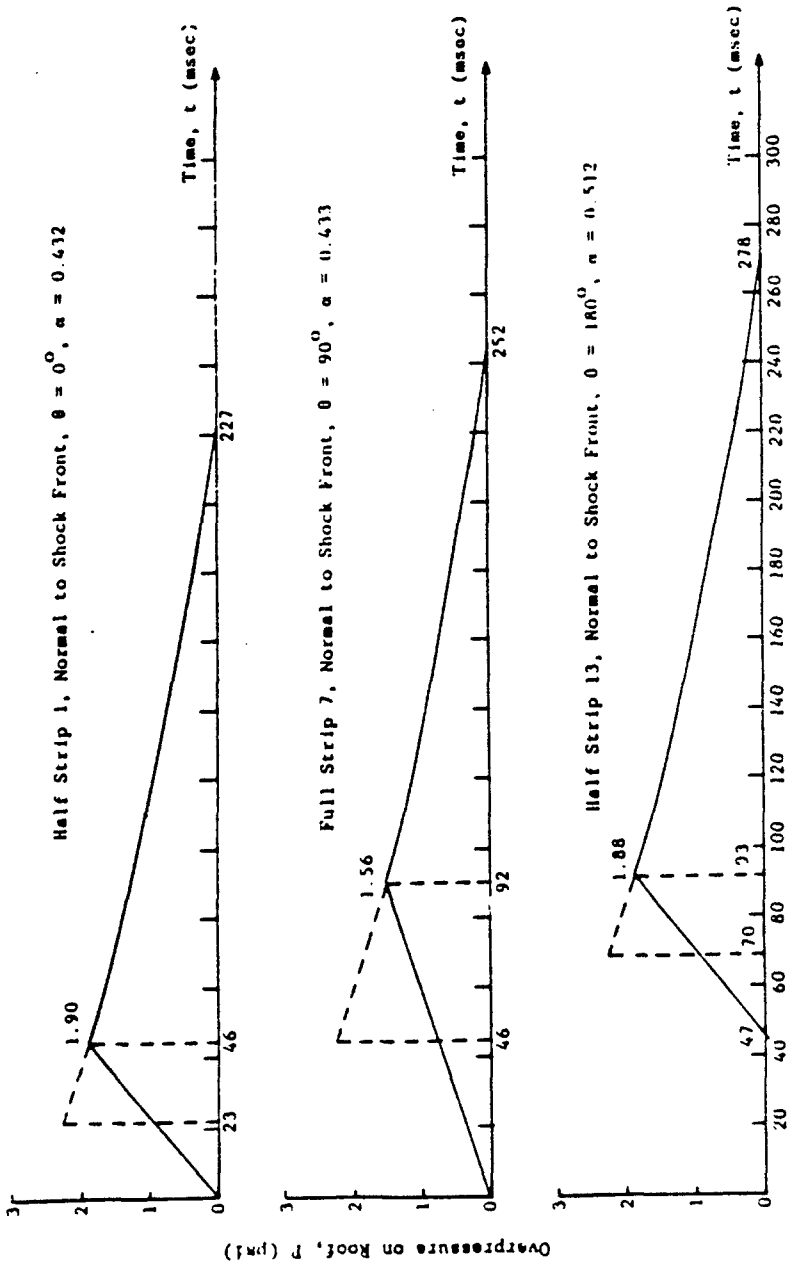

Figure 5b. Design blast overpressure-time curves for roof strips normal to shock front: half strip for n= 1, 13 and θ= 0°, 180°, and full strips for n= 7 and θ= 90°.

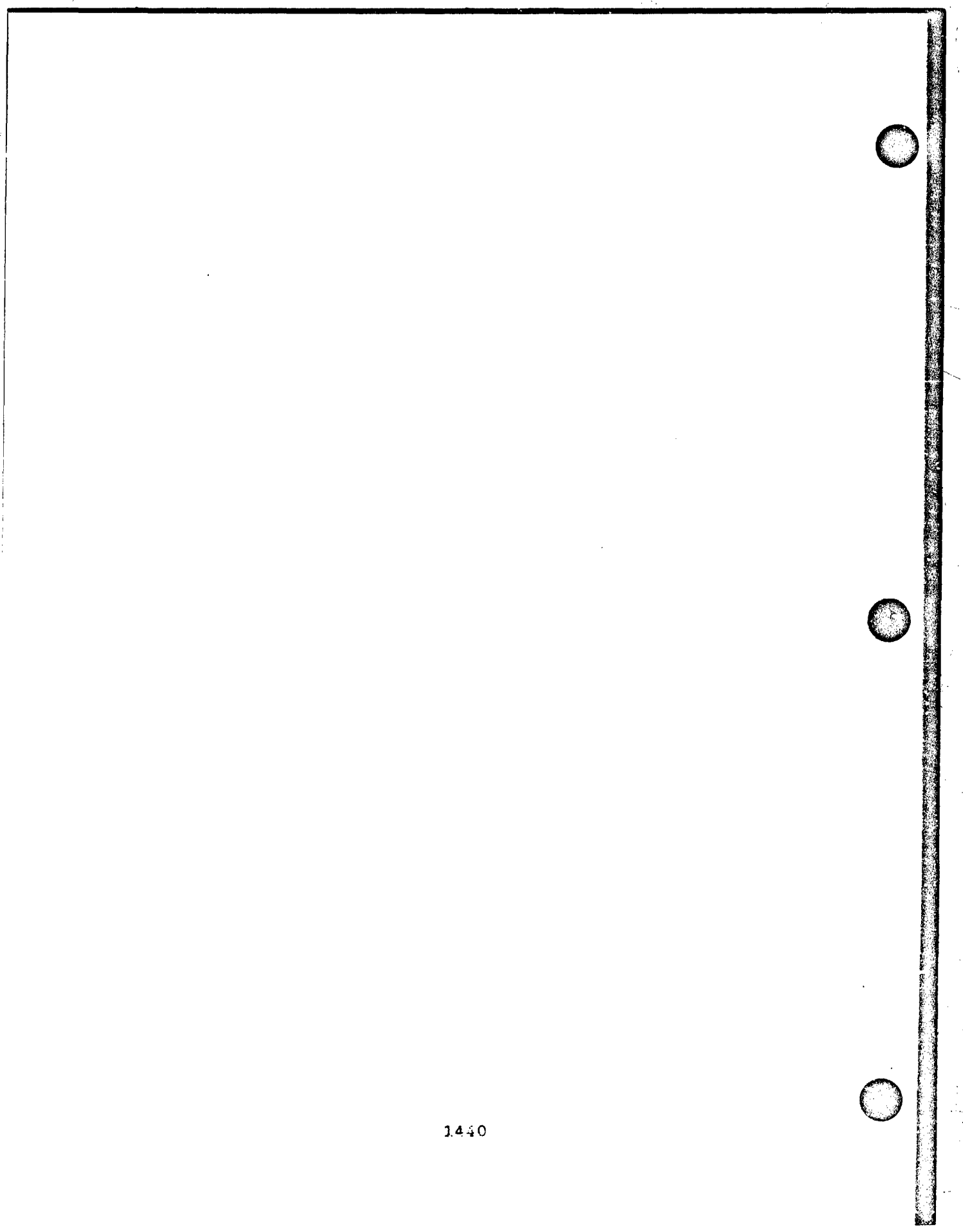

NELSON & WATT

TITLE: Analysis of Internal Blast Loads in Vented Chambers

*Donald H. Nelson, Mr., James M. Watt, Mr.
US Army Engineer Waterways Experiment Station
Vicksburg, MS 39180

ABSTRACT: Structural loads from internal explosions are very complex and in some cases difficult to predict. In a non-vented room or chamber, a detonated high explosive charge produces high temperature gas products and numerous shock reflections. These conditions combine to produce an excessively high blast loading. These loads can be several times greater and act in different directions than conventional design loads. This loading condition results in costly, heavily reinforced structural designs. In an effort to reduce the excessive internal loads, designers have considered the use of venting through glass windows and other frangible openings.

This paper presents recent test results of internal blasts at a high vent area ratio and compares the results with three methods for calculating internal blast loads. Two of the methods simplify the calculational procedure by neglecting multiple shock reflections. This neglect, though justified under certain conditions, may affect the accuracy of these methods at high vent area ratios when multiple shock reflections dominate the loading. The third method attempts to account for these multiple shock reflections and will be very useful for calculating loads for which multiple shock reflections are dominant.

BIOGRAPHY: Donald H. Nelson

PRESENT ASSIGNMENT: 1985 - Present, Research Structural Engineer, US Army Engineer Waterways Experiment Station, Vicksburg, MS. Conducts research on structural response to military weapons effects and terrorist attack.

PAST EXPERIENCE: 1981 - 1985, Structural Engineer, Bechtel Power Corporation, Grand Gulf Nuclear Power Station, Port Gibson, MS. Designed seismic supports for mechanical equipment and HVAC ductwork.

DEGREE HELD: B.S. in Civil Engineering from Louisiana Tech University.

Analysis of Internal Blast Loads in Vented Chambers

*Donald H. Nelson, Mr.
James M. Watt, Mr.
US Army Engineer Waterways Experiment Station
P.O. Box 631
Vicksburg, Mississippi 39180-0631

INTRODUCTION

The design of chambers capable of resisting internal blasts has been the subject of much research in recent years. Attention has been focused, however, not so much on the design of the structural members themselves but on load definition. If the loading from an internal blast can be predicted with confidence, the design of the structure itself is straightforward. Internal blast loads, unfortunately, are very complex and in some cases difficult to predict.

In a non-vented room or chamber, a detonated high explosive charge produces high temperature gas products and numerous shock reflections. These conditions combine to produce an excessively high blast loading. As a result, a non-vented chamber designed to survive internal blasts must behave as a pressure vessel capable of resisting long duration, quasi-static loads. These loads can be several times greater and act in different directions than conventional design loads. This loading condition results in costly, heavily reinforced structural designs. In an effort to reduce the excessive internal loads, designers have considered the use of venting through glass windows and other frangible openings.

Venting reduces the internal blast loading in chambers by allowing the explosion to escape into non-critical areas through openings in the chamber walls. This can result in a significant reduction in internal blast loads compared to non-vented chambers. However, there remains the problem of calculating the internal loads within the chamber so that the reduction in loading can be accounted for in the design. Load calculation is relatively simple for non-vented chambers, but becomes more complicated with the addition of venting.

The degree of venting provided in a chamber is expressed in terms of the vent area ratio, defined in this paper as the ratio of the total vent area to the total volume of the chamber. As the vent area ratio is increased for a particular explosive weight, the magnitude of the internal blast loads decreases. Internal blast load calculational methods (Reference 1,2, and 3), based on empirical formulae, work well at low to moderate vent area ratios when gas pressure dominates the internal loads, but may become less accurate as the vent area ratio becomes high. There is a need for verifying calculational procedures for internal blast loads at high vent area ratios.

This paper presents recent test results of internal blasts at a high vent area ratio and compares the results with three methods for

calculating internal blast loads. Two of the methods simplify the calculational procedure by neglecting multiple shock reflections. This neglect, though justified under certain conditions, may affect the accuracy of these methods at high vent area ratios when multiple shock reflections dominate the loading. The third method, however, attempts to account for these multiple shock reflections and will be very useful for calculating internal blast loads for which shock pressures are dominant.

EFFECT OF VENTING ON INTERNAL BLAST LOADS

There are a number of parameters which determine the internal blast loading characteristics in a chamber (Reference 1). The presence of venting can have a significant influence on the reduction of the internal loading. However, the vent area ratio is not the only parameter which defines the venting process. In most practical situations, vent areas will be closed by some type of panel for weather protection and security. It is necessary to consider what type of panel is being used to cover the vent opening (Reference 2). A window, for example, is a vent opening with a glass panel.

For a given chamber, explosive weight, and vent area ratio, the internal loading increases as the mass of the panel is increased (Reference 2). Lightweight, frangible panels will reflect some shock waves back into the chamber before venting is initiated through the opening. It will be shown that for the vent area and charge weight to room volume ratios used in these tests, the shock waves reflected from the glass panel represented a high percentage of the total internal loading. Since venting can not begin until panels are forced out of the vent openings, panels should be as lightweight as possible to minimize their effect on internal loads. Massive panels can delay venting long enough that the load reduction benefit of high vent area ratios is lost.

An internal blast loading typically consists of gas pressure from the explosive combustion products and multiple shock pressures from the detonation and the reflecting surfaces. Shock pressures are easily discernible in the pressure-time histories as rapidly rising spikes of pressure which decay exponentially. Gas pressure is recognizable as a relatively slow rising, long duration swell on which the numerous reflected shock pressures are superimposed.

A typical pressure-time history from a non-vented internal blast is shown in Figure 1a. In the absence of venting, a long duration quasi-static gas pressure results which decays very slowly as the room cools back to ambient temperature. This type of loading is described as quasi-static because the duration of the maximum gas pressure is very long relative to the fundamental response frequency of most structural members (References 1 and 4).

The effect of several ranges of venting on internal load characteristics is presented in Figures 1b through 1d. For these cases the vent openings do not have panels and the charge weight to room volume ratio is constant. In Figure 1b the effect of a low vent area ratio is illustrated. Though there is a noticeable reduction in gas pressure

duration, the loading can generally still be considered as quasi-static in most structural designs. In both the non-vented and low vent area ratio cases the shock pressures are a very small part of the total pressure-time history. For this reason, the methods which neglect multiple shock pressures do not sacrifice accuracy. Accurate prediction of the maximum gas pressure, the initial shock pressure, and the load duration is sufficient to describe such load cases for most structural design purposes.

As the vent area ratio is increased from low to moderate, the duration of the gas pressure is reduced further and, because a large part of the gas is expanding through the opening without being confined in the chamber, the peak gas pressure begins to decrease as shown in Figure 1c. The calculational methods which neglect multiple shock pressures may still predict quite accurately the impulse of such load cases, however, the shape of the simplified triangulated load function may deviate from the actual loading. As the vent area ratio is increased further, the gas pressure contribution to the total pressure-time history will decrease and the multiple shock pressure contribution will increase. The vent area ratio can be increased to a point where gas pressure will not develop due to lack of confinement and the internal load will be comprised primarily of multiple shock pressures. A pressure-time history of this type is shown in Figure 1d. The calculational methods which neglect multiple shock reflections attempt to make up for this neglect by substituting a rapidly decaying pseudo-gas pressure when calculating such loads.

A phenomenon that occurs at high vent area ratios is the variation of the blast loading from point to point throughout the chamber. This variation occurs because the shock pressures are dimensionally dependent. That is, shock pressures vary according to the explosive type and weight, the location of the explosive, the shape and dimensions of the chamber, and the size and location of the vent area. Conversely, when gas pressure is dominant at low to moderate vent area ratios, the internal loading is much more uniform throughout the chamber. Gas pressure is less dependent on the shape of the chamber and the location of the explosive and more dependent on the explosive type and weight, the volume of the chamber, and the venting parameters. Calculational methods which neglect multiple shock pressures do not accurately reproduce the variation of loading throughout a chamber when multiple shock pressures are dominant.

TEST CONFIGURATIONS

The two chamber configurations used in this test series had the following similar parameters: the explosive type, weight and location, the chamber dimensions, the vent area ratio, the vent area location, and the gage locations on the walls. As shown in Figure 2, the chamber was 12 1/2 ft. wide by 18 1/2 ft. long by 11 ft.-4 in. high for a total volume of approximately 2600 cf. The hemispherical charge was 5 lbs. of C-4 explosive and was located in the center of the chamber 24 inches

above the floor. One vent opening, 10 ft. high by 12 ft. wide, was located in one end of the chamber. Six interface pressure gages were located as shown in Figure 3 on the backwall directly opposite the vent opening. The vent area ratio was 0.046 $ft.^{-1}$.

In the first test, the charge was detonated in the chamber with the vent area open. The second test differed only in that a frangible glass panel was placed in the vent opening. The glass panels weighed approximately 6.5 psf. Using Reference 5, these test configurations could be described as a barrier structure with one wall removed or frangible or as a containment structure with nearly full venting. In any of these cases the manual recognizes that gas pressure may not develop.

CALCULATIONAL METHODS

Three methods were used to calculate the internal blast loads for comparison to the test data. All three methods are programmed for use on IBM compatible microcomputers. The first calculational method is described in the Army technical manual TM 5-855-1, "Fundamentals of Protective Design for Conventional Weapons" (Reference 1). This method has been developed into the computer code CONWEP by the USAE Waterways Experiment Station. Using CONWEP, the initial reflected shock pressure is first calculated at a desired target point within the chamber. The input for reflected shock pressure is the high-explosive charge type and weight, and the distance from the charge to the target point. Next, the maximum gas pressure and duration are calculated. Inputs for this calculation are the charge type and weight, the chamber volume, the total vent area, and the vent area ratio. Using the impulses calculated for the shock and gas pressure, two equivalent triangular loads are constructed and combined to represent the total internal blast load (Figure 4). Because CONWEP neglects multiple shock pressures, a rapidly decaying pseudo-gas pressure is substituted for multiple shock pressures at high vent area ratios. Furthermore, CONWEP does not model vent opening panels and was not used to calculate loads for Test 2. CONWEP will usually yield good predictions for non-vented chambers and for chambers with open venting (no panels) if gas pressure develops and dominates the loading.

The second calculational method was the computer code REDIPT developed by the Naval Civil Engineering Laboratory (Reference 2). REDIPT uses a gas pressure model similar to CONWEP but, in addition, has the capability to simulate a variable vent opening, such as one covered by a frangible panel which requires a finite amount of time to accelerate away from the opening before full venting can occur. Like CONWEP, REDIPT also neglects multiple shock pressures and substitutes a rapidly decaying pseudo-gas pressure at high vent area ratios. REDIPT does not calculate shock pressures. Normally, the initial shock at the target point is calculated by some other means as an equivalent triangular loading. REDIPT is then used to calculate an equivalent gas pressure triangular loading. The REDIPT calculation for Tests 1 and 2 includes the same

initial shock calculated by CONWEP for Test 1. The equivalent shock and gas pressure triangular loads are combined to represent the total internal blast loading. REDIPT will yield good results for non-vented chambers and for chambers with open and/or paneled vent areas at most vent area ratios.

The third calculational method was the computer code BLASTINW first developed by the USAE Waterways Experiment Station and later revised under contract by Applied Research Associates, Inc. (Reference 3). BLASTINW was designed for calculating gas pressure and multiple shock reflections in a non-vented rectangular chamber. BLASTINW calculates gas and multiple shock pressures independently and then combines the results. Since gas pressure did not develop during Tests 1 and 2, the gas pressure portion of the calculation was suppressed to obtain only shock pressures. BLASTINW will calculate the load functions at twenty selected target points in the chamber and will allow the non-simultaneous detonation of up to twenty explosive charges.

Unlike CONWEP and REDIPT, which describe the chamber only in terms of volume, BLASTINW requires the dimensions of the non-vented rectangular chamber and the location of the explosive as explicit inputs. This feature of BLASTINW allows flexibility for adapting the analysis to accommodate various geometric features of a specific chamber. This also permits the designer to manipulate BLASTINW to obtain multiple shock pressure predictions for a rectangular chamber having less than six sides. For example, to correctly model the Test 1 and 2 chamber configurations, it was necessary to describe one wall of the BLASTINW model as a large open vent area through which shock waves could escape. Since BLASTINW will not explicitly allow an open vent area in the analytical model, this problem was solved by modifying the BLASTINW chamber dimension inputs. The 10 ft. by 12 ft. vent area of the test chamber was approximately equal to the entire frontwall on which it was located. To simulate this vent area in BLASTINW the 18'-6" test chamber sidewall dimension perpendicular to the open vent area was replaced with a fictitious 200 ft. dimension (Figure 5). This prevented significant shock reflections from the frontwall from reaching the backwall in the BLASTINW calculation. The actual location of the explosive in the test chamber, 9 ft.- 6 in. from the backwall, was not modified in the analytical model. The target point locations selected in the BLASTINW model were identical to the backwall pressure gage locations of the test chamber. This BLASTINW model effectively simulated the shock pressures escaping through the open vent area in Test 1 and thus allowed direct comparison with the pressure gage test data.

To determine the blast loading at target points in Test 2, an approach was required using BLASTINW twice and a few manual calculations. Test 2 is the case in which a boundary wall exists for a short time and is then blown away. The chamber boundary dimensions once entered in BLASTINW for a particular run cannot be changed. Therefore, a single run of BLASTINW could not calculate the target point loadings for this two stage behavior. The expected loads of Test 2 were bounded by the

following two load cases, both of which were calculated separately using BLASTINW. Case 1, the lower bound, a large open vent area and no gas pressure, was the same configuration modeled for Test 1. Case 2, the upper bound, was a non-vented chamber with the gas pressure calculation deleted. Case 2 produced only the shock loads in the non-vented chamber. After determining Case 1 and 2 blast loads with BLASTINW, an interpolation method was used at each target point to determine the Test 2 load predictions. First, the load calculation for Case 1 was subtracted from the load calculation for Case 2. This difference represented the total increase in shock load captured in Case 2 relative to Case 1. The problem then was to determine what portion of this difference in shock loading would be captured in a chamber configured as in Test 2, where the vent opening was closed by a lightweight, frangible glass panel. By considering the time to failure of the glass panel (15 msec), plus the length of time required for a shock wave with a ray path of three reflections to travel from the center of the glass panel to the center of the backwall (22 msec), the influence of the glass panel on the backwall loading was assumed negligible after 37 msec. The interpolation was completed by truncating the difference between the Case 1 and 2 loads at 37 msec and then superimposing this truncated load function onto the Case 1 load to obtain the predictions for Test 2.

DISCUSSION OF TEST RESULTS

The pressure-time histories from both tests are shown in Figures 6 through 8. Because of the addition of the glass panel there is an increase in mid to late time (15 to 40 msec) shock reflections in Test 2 compared to Test 1. There is no indication of gas pressure within the chamber in any of the pressure records. The glass panel in Test 2 did not delay venting long enough for gas pressure to develop. High speed photography showed the glass was probably capable of reflecting shock waves back into the room for at least 15 msec after detonation.

The reliability of the test data is indicated by the excellent agreement of the pressure records between zero and 15 msec for each gage in both tests. After 15 msec the arrival of the glass panel shock reflections in Test 2 cause the pressure records to differ. The addition of the glass panels caused an average twofold increase in the maximum impulse in Test 2 over Test 1. This demonstrates the importance of including the effect of lightweight frangible panels on internal blast loads. The variation in impulse from gage to gage existed because a dominant gas pressure did not develop to equalize the loading throughout the chamber. The relatively high load recorded at gage IP-4 is due to symmetry of the gage with respect to the charge and the chamber.

COMPARISON OF CALCULATIONS TO TEST 1 RESULTS

In Figure 9 the CONWEP and REDIPT calculated blast loadings are compared to the average backwall data records from Test 1. Calculation of the positive blast load duration by REDIPT is good. Maximum impulse

comparisons, Figure 9, reveal that CONWEP and REDIPT differ from the average maximum measured impulse in Test 1 by factors of 0.78 and 1.12, respectively. In Figure 10 the BLASTINW pressure calculation for gage IP-5 is seen to bear the same characteristics as the test data. Both records have high pressure shocks between 3 and 10 msec followed by numerous low shock pressures beginning at approximately 12 msec. There is a distinct time lag, however, between the calculated shock pressures and the test data after 10 msec. This timing problem is associated with two assumptions made in the BLASTINW code. First, BLASTINW assumes the air density does not change in the chamber during the explosion and, secondly, BLASTINW neglects mach stem effects on the arrival times and peak pressures of all but the direct and first order rays. When an explosive is first detonated the initial shock wave travels out ahead of the explosive products and therefore is not effected by a change in air density. Accordingly, for up to 5 msec BLASTINW and the test data agree very well on the arrival times of the shock pressures reaching the gages. After the explosive products have expanded, all shock reflections travel through a more dense medium. This results in higher shock wave velocities than are calculated by BLASTINW. In Figure 11 the average BLASTINW backwall load is compared with the average backwall test data. The time lag of the maximum impulse is evident. Except for the timing differences, which would probably not be significant for most structural design calculations, the agreement between the calculated and measured impulse-time histories in Test 1 is excellent. The calculated average maximum impulse differs from the measured average maximum impulse by a factor of only 0.98.

COMPARISON OF CALCULATIONS TO TEST 2 RESULTS

In Test 2 the REDIPT calculation is slightly lower than the measured loading. Comparison of the REDIPT calculated average pressure and the average test data from the backwall is shown in Figure 12. The calculated maximum average impulse on the backwall in Figure 12 differs from the test data by a factor of 0.89.

The BLASTINW calculation for gage IP-5 is compared to the test data in Figure 13. Again timing differences are evident after 10 msec. The interpolation method using upper and lower bounds calculated with BLASTINW reproduced the shock reflections from the glass panel and resulted in good agreement of the maximum impulses. Calculated and measured average backwall loadings compare very well in Figure 14. The calculated and measured maximum impulses differed by only a factor of 1.03.

CONCLUSIONS

Using a microcomputer structural designers can (with some manipulation) calculate internal blast loadings in rectangular chambers quickly and with good accuracy at high vent area ratios including the effect of frangible panels. The three methods considered in this report, CONWEP, REDIPT, and BLASTINW, should all give comparable results for

chambers at low to moderate vent area ratios, when gas pressure dominates the internal blast loading. At high vent area ratios, when multiple shock reflections dominate the internal blast loading, BLASTINW and REDIPT produce more accurate predictions. BLASTINW can reproduce the variation in loading in a chamber when the load is dominated by shock pressures. BLASTINW may also be useful for calculating loads for enclosures with more than one wall removed. BLASTINW is currently being modified to account for changes in the chamber air density which will result in improved shock reflection calculations. However, the results obtained using the current version of BLASTINW are sufficient for accurately determining the internal load at high vent area ratios. All

ACKNOWLEDGMENTS

This investigation was sponsored by the US Department of State, Physical Security Division under the direction of Mr. Pat Fitzgerald. Technical monitors for the Department of State were Messrs. William Philo and Gerald Meyers. This work was performed by the US Army Engineer Waterways Experiment Station (WES), Structures Laboratory, Structural Mechanics Division. Project Manager was Mr. James M. Watt and Project Engineer was Mr. Donald H. Nelson.

The authors thank Mr. Gordon W. McMahon, Explosive Effects Division, (WES) for his technical assistance throughout the course of this research. The cooperation of the authorities at WES that permitted the preparation of this paper is appreciated.

REFERENCES

1. "Fundamentals of Protective Design for Conventional Weapons", Technical Manual (TM) 5-855-1, Department of the Army, Washington, D.C.

2. Tancreto, J. E., and Helseth, E. S., "Effect of Frangible Panels on Internal Gas Pressures", Naval Civil Engineering Laboratory, Port Hueneme, California, March 1987.

3. Britt, J. R., Drake, J. L., Cobb, M. B., Mobley, J. P., "Blastinw User's Manual", Applied Research Associates, Inc., Vicksburg, Mississippi, April 1986.

4. Biggs, John M., "Introduction to Structural Dynamics," McGraw-Hill Book Company, New York, 1964.

5. "Structures to Resist the Effects of Accidental Explosions", Volume 2, Special Publication ARLCD-SP-84001, U.S. Army Armament Research, Development and Engineering Center, Picatinny Arsenal, New Jersey, December 1987.

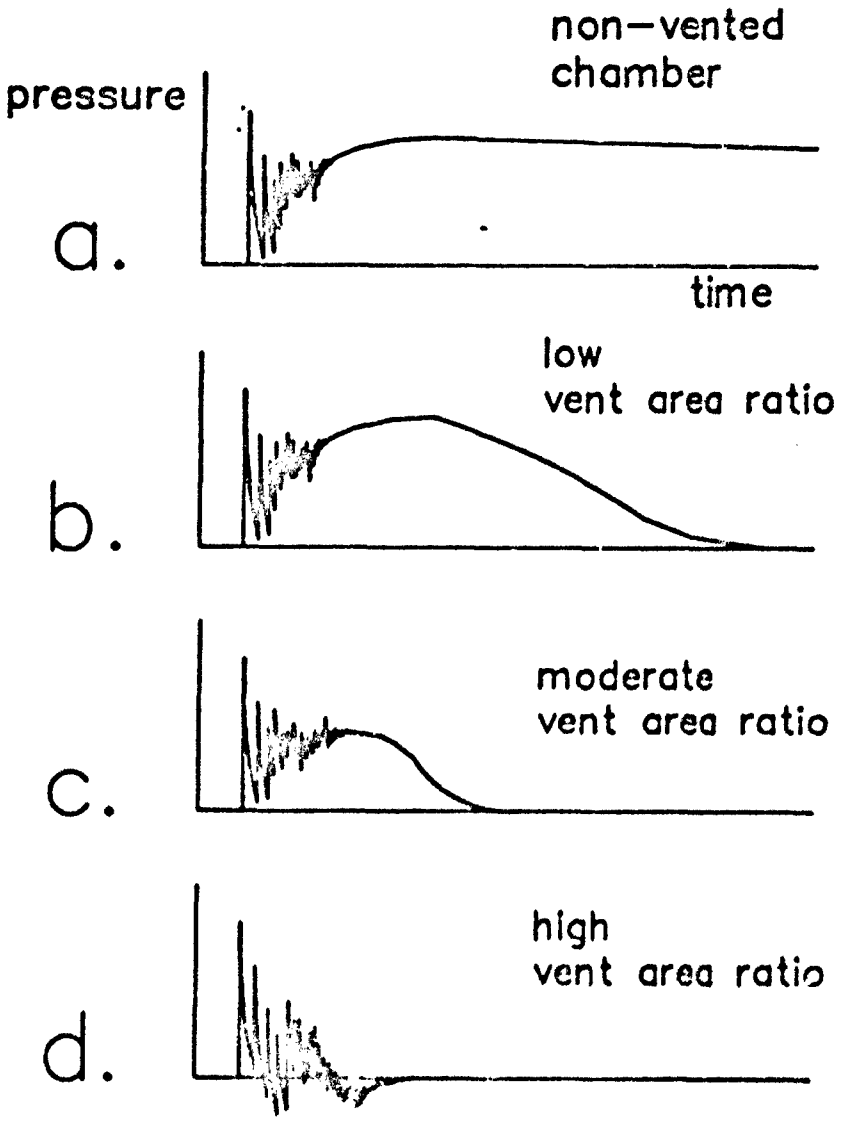

Figure 1. Effect of venting on internal blast load characteristics

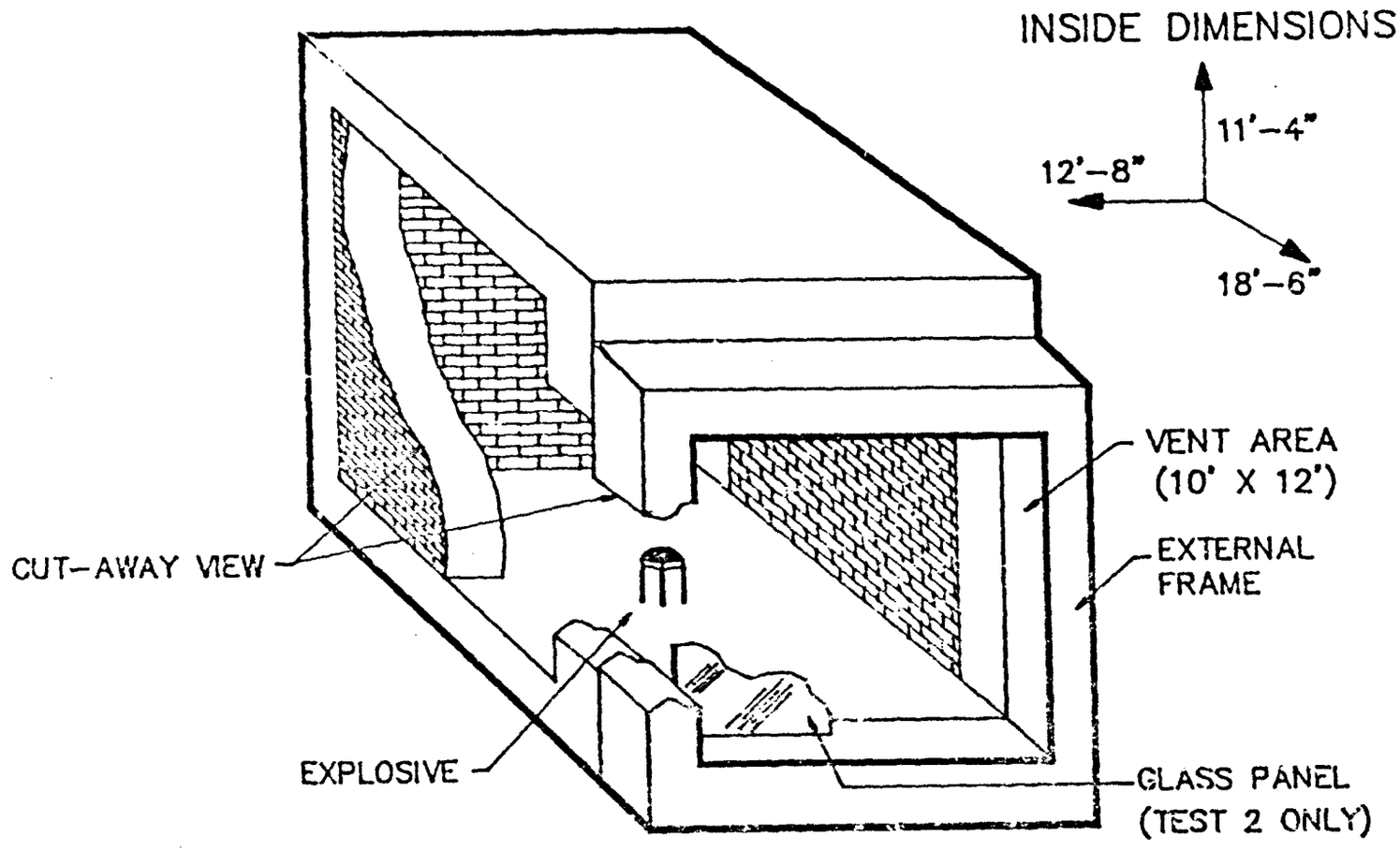

Figure 2. Full–scale test chamber dimensions and details

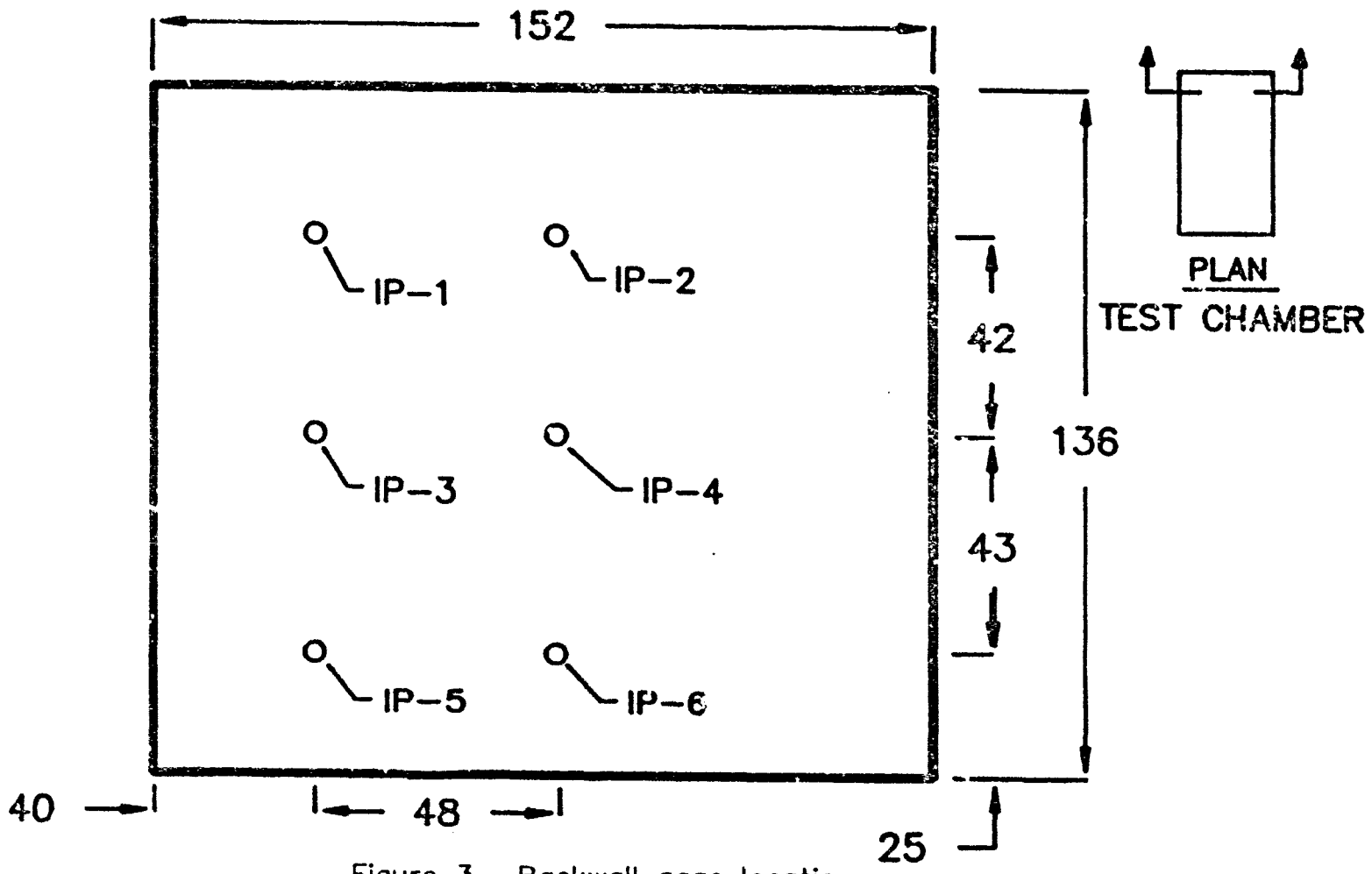

Figure 3. Backwall gage locations

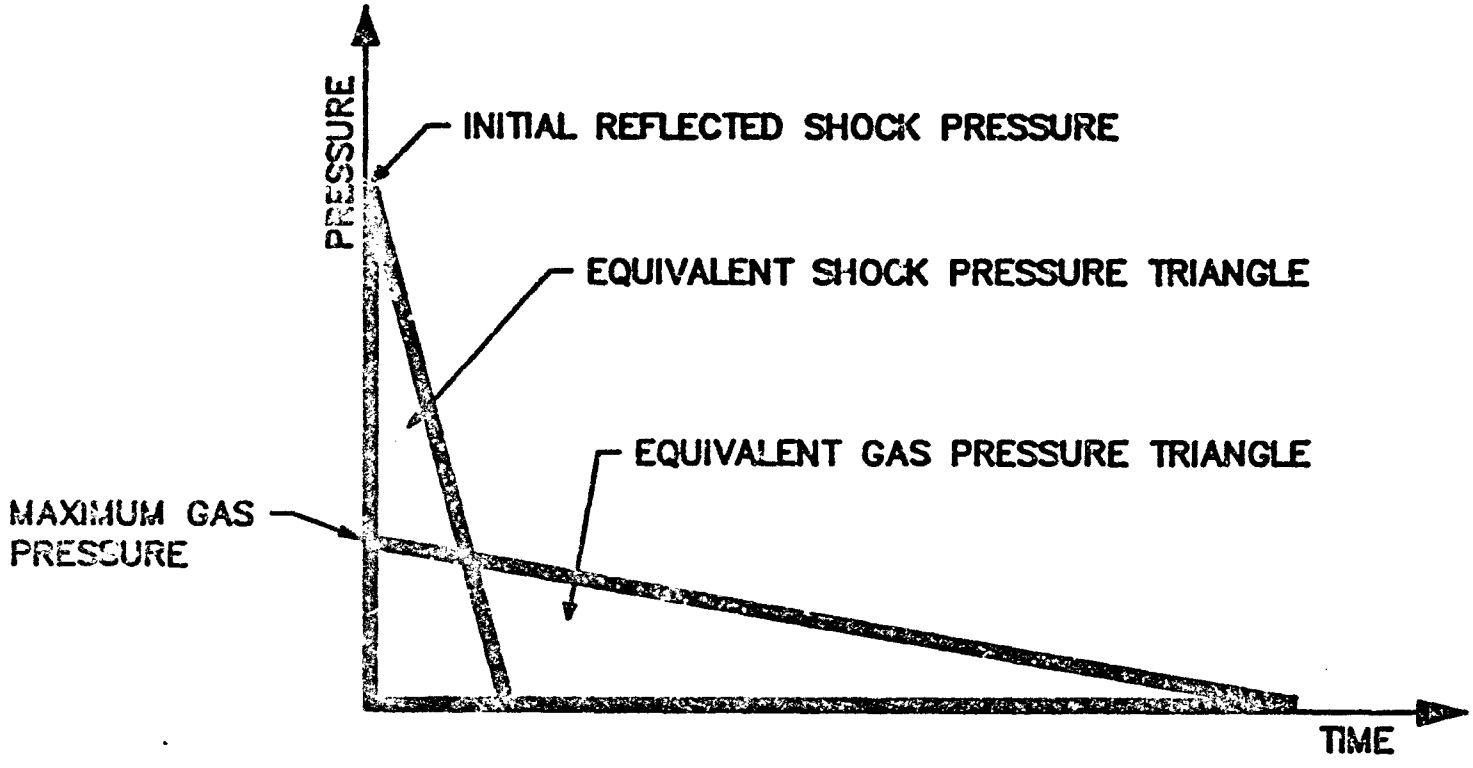

Figure 4. Typical equivalent triangular load function

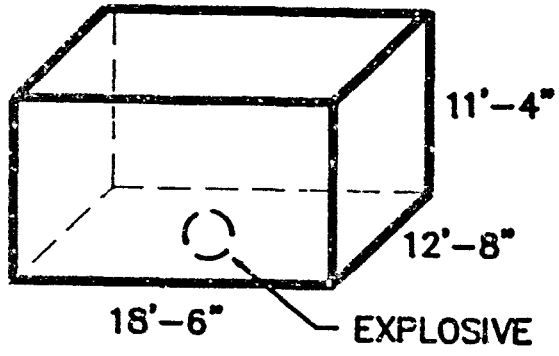

ACTUAL INSIDE DIMENSIONS

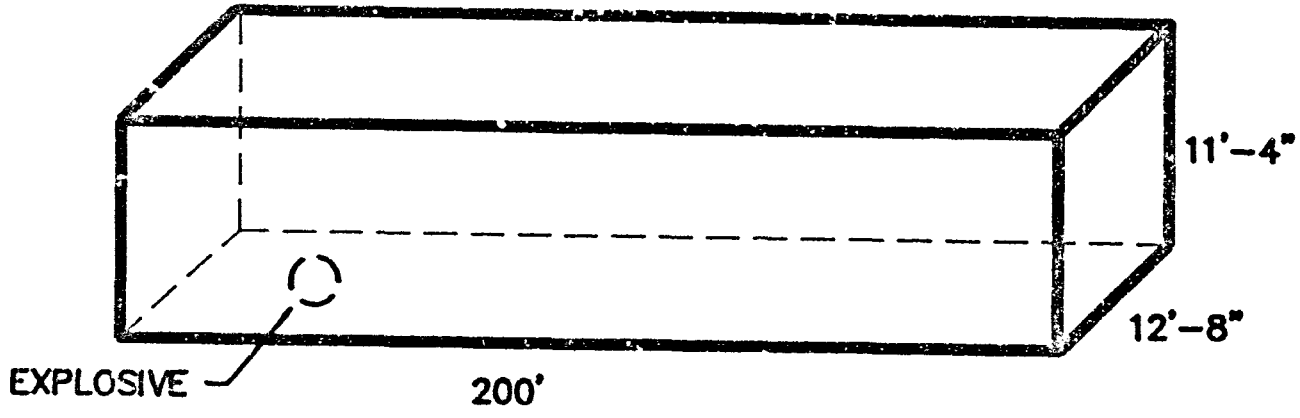

Figure 5. BLASTINW model inside dimensions (Test 1)

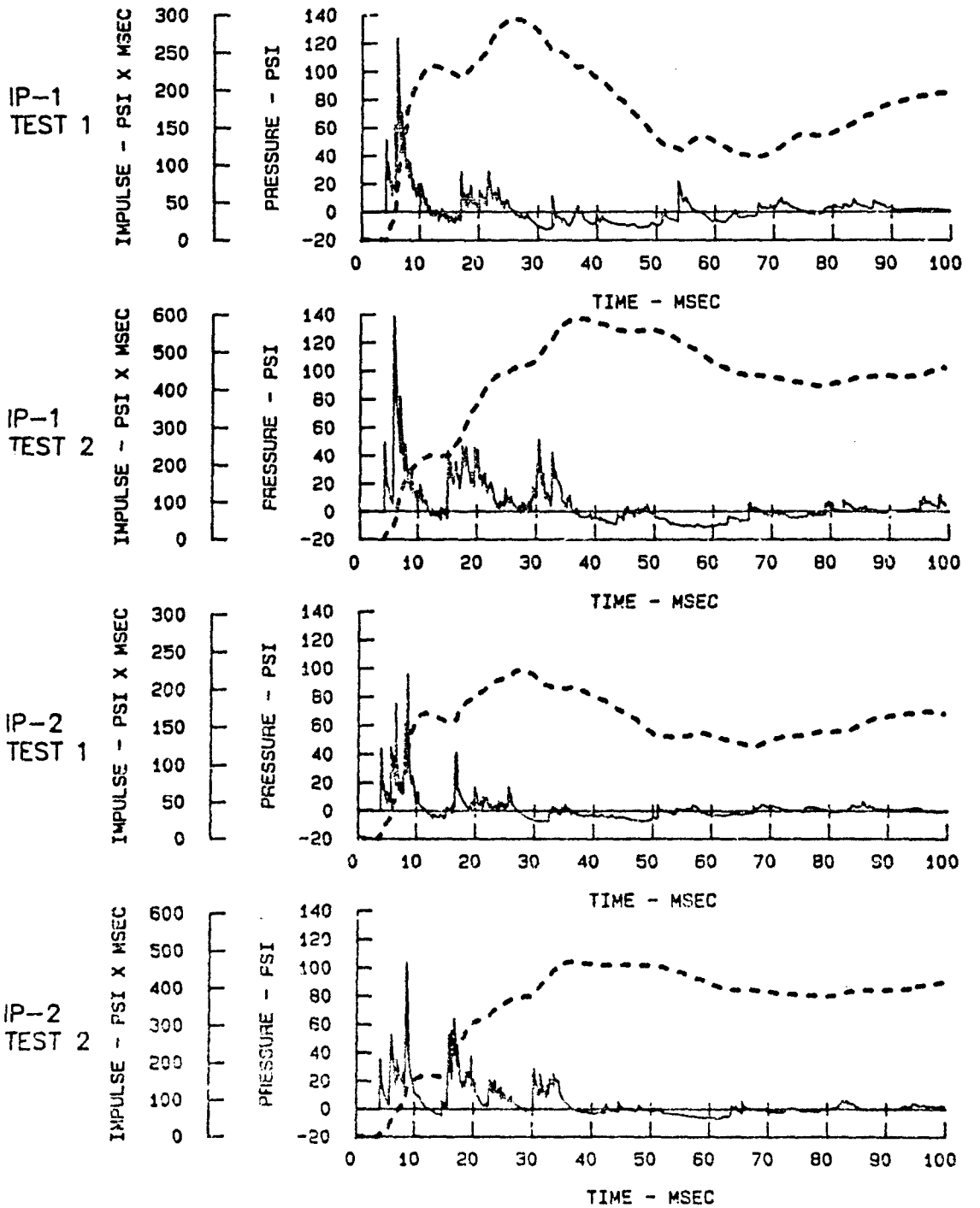

Figure 6. Test data for gages IP–1 and IP–2 from Tests 1 and 2.

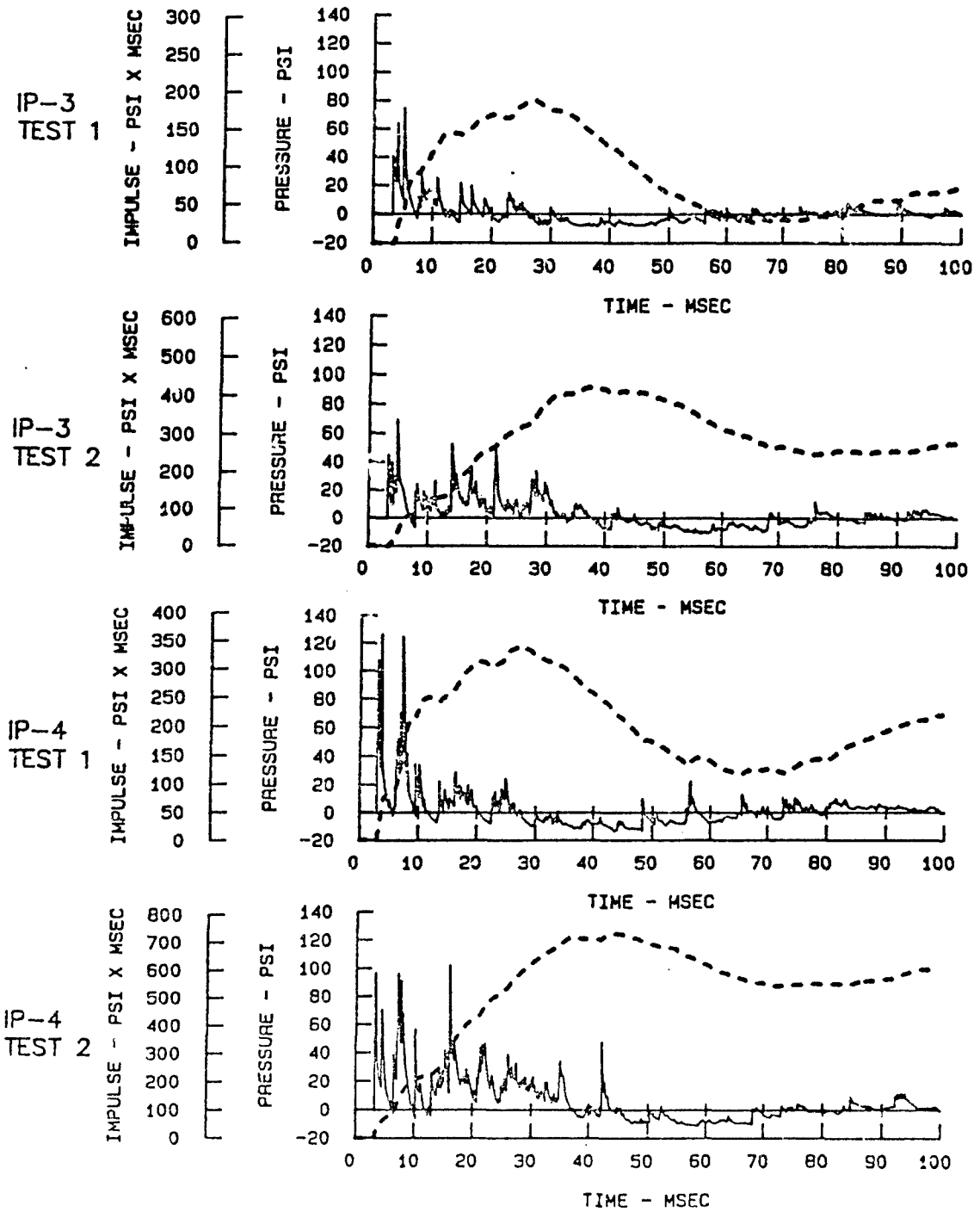

Figure 7. Test data for gages IP–3 and IP–4 from Tests 1 and 2.

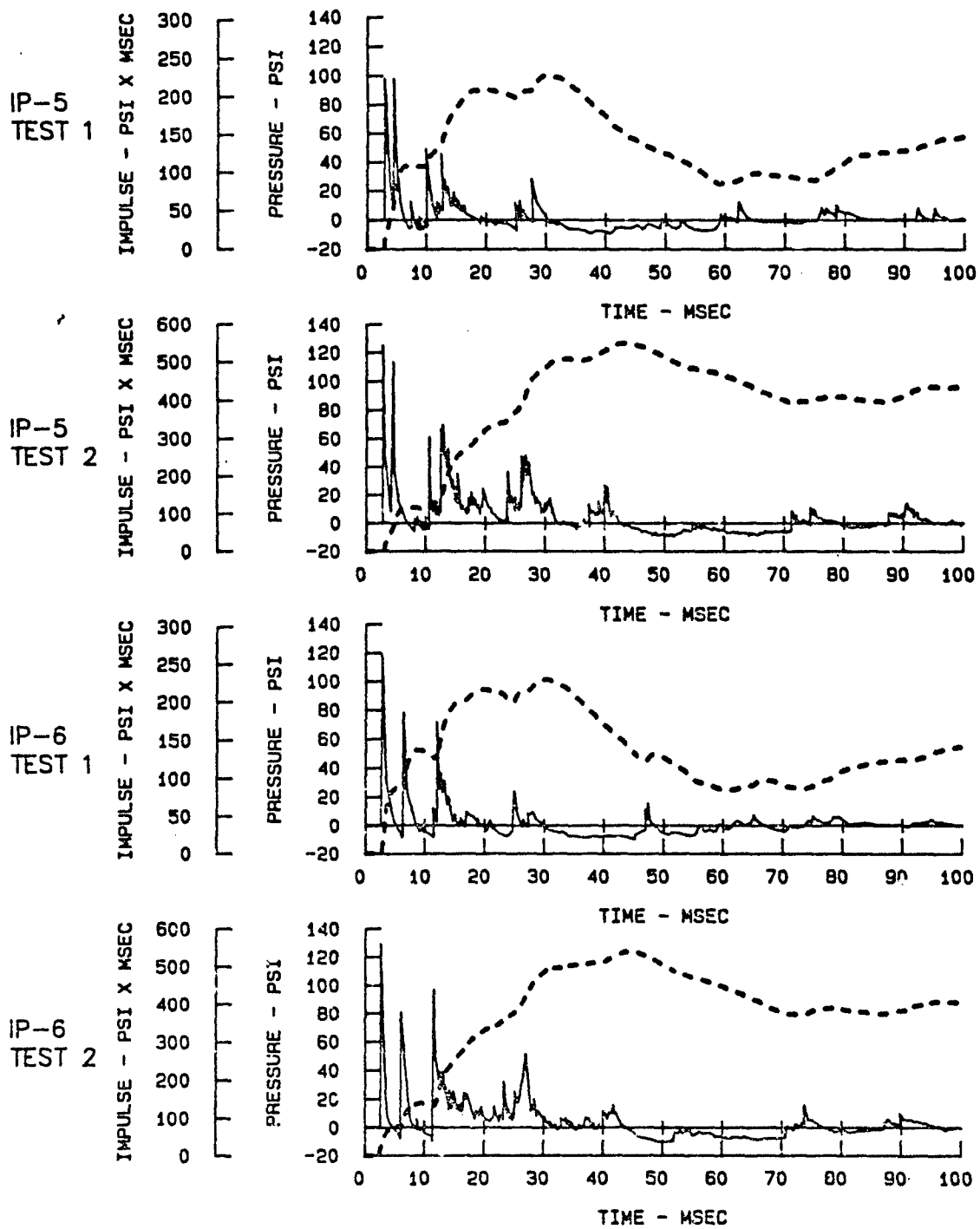

Figure 8. Test data for gages IP-5 and IP-6 from Tests 1 and 2.

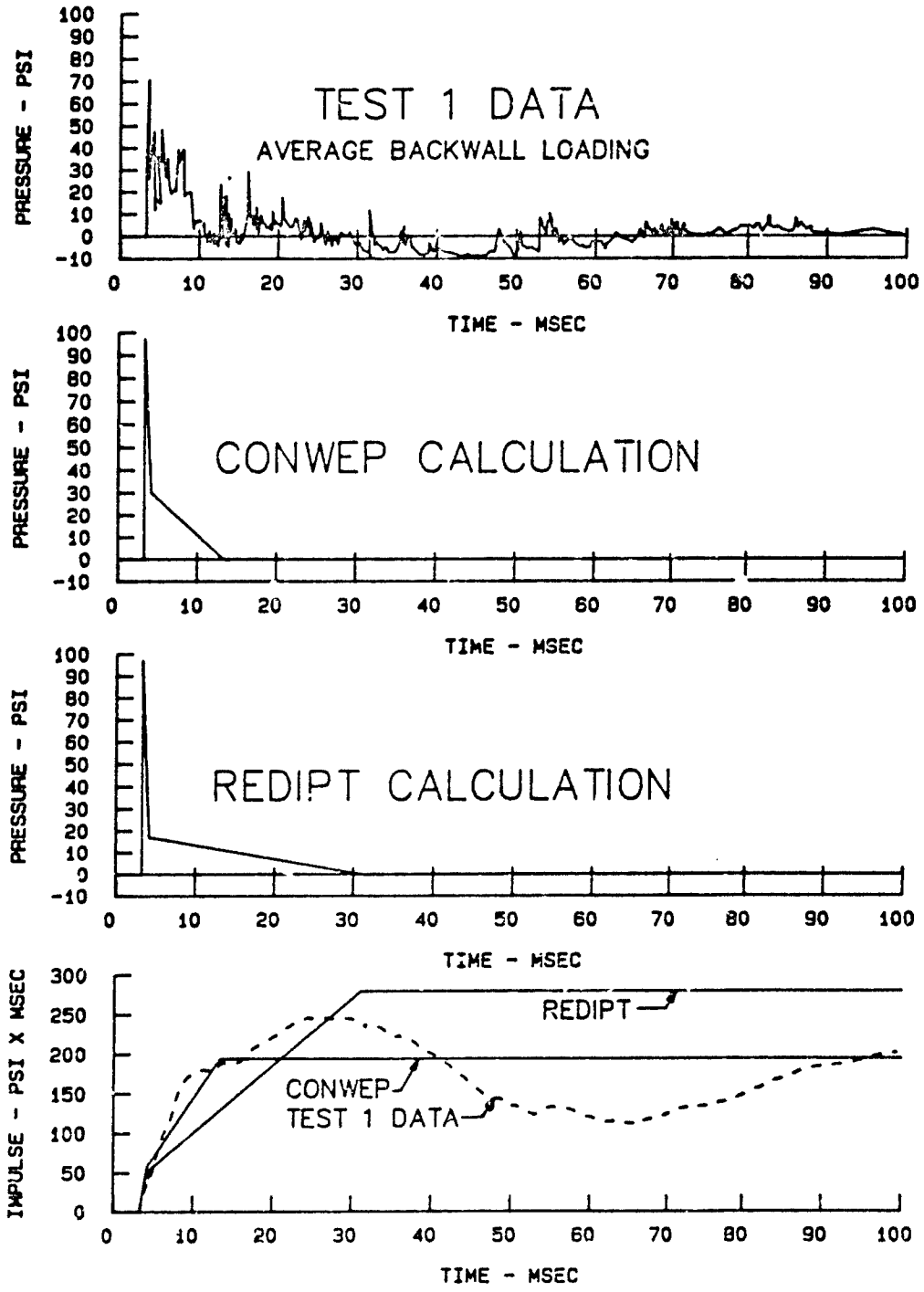

Figure 9. Comparison of CONWEP and REDIPT calculations with Test 1 data

TEST 1
COMPARISON OF IP-5 TEST DATA
TO BLASTINW CALCULATIONS

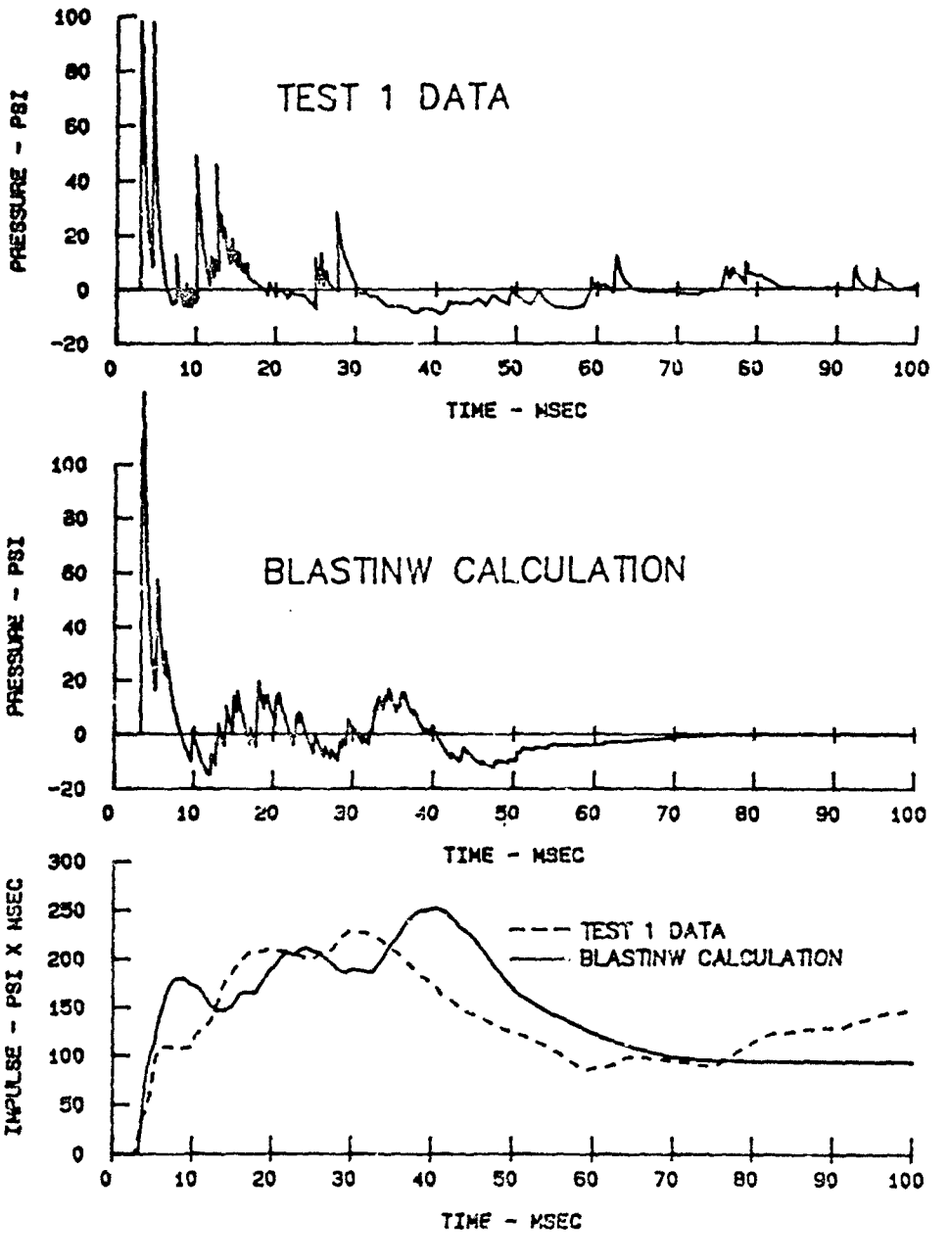

Figure 10. Comparison of gage IP-5 test data to BLASTINW calculation (Test 1)

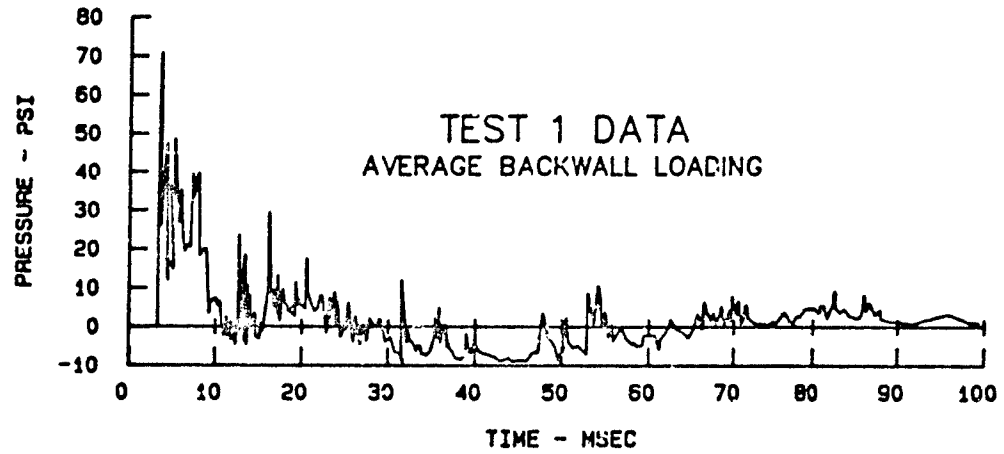

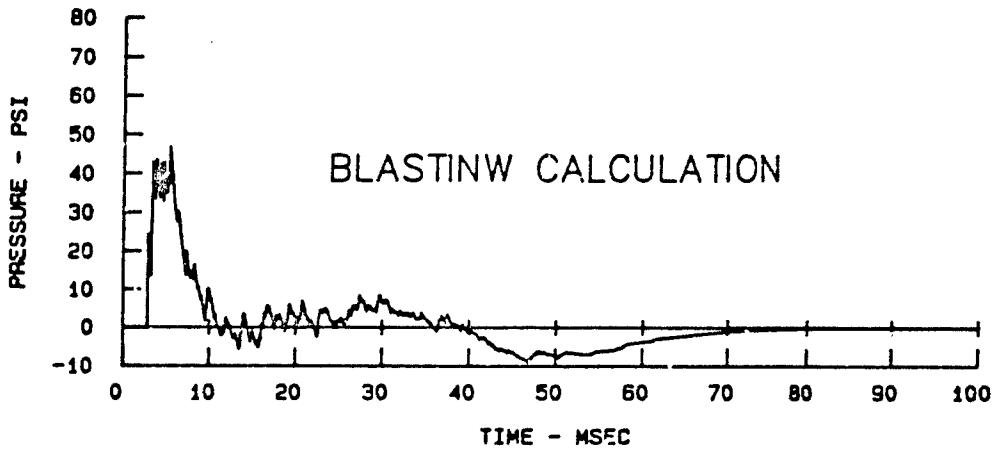

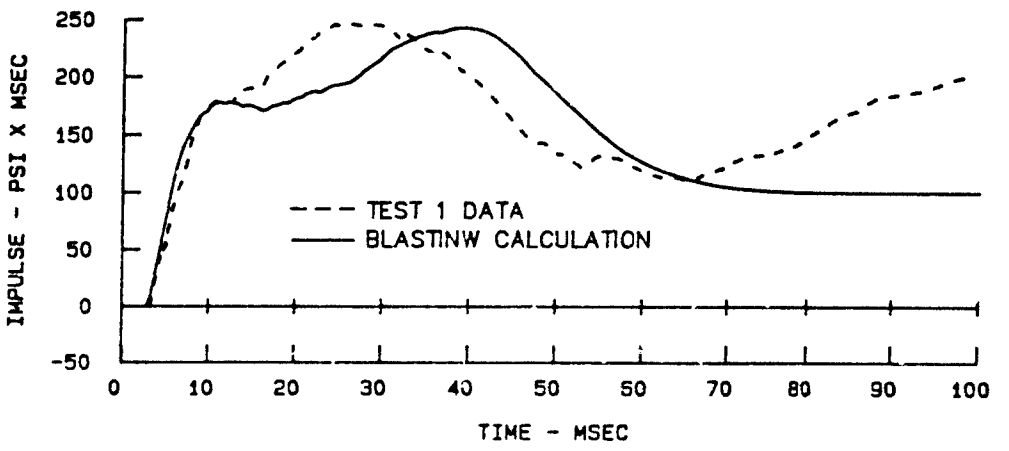

Figure 11. Comporison of BLASTINW calculations with Test 1 data

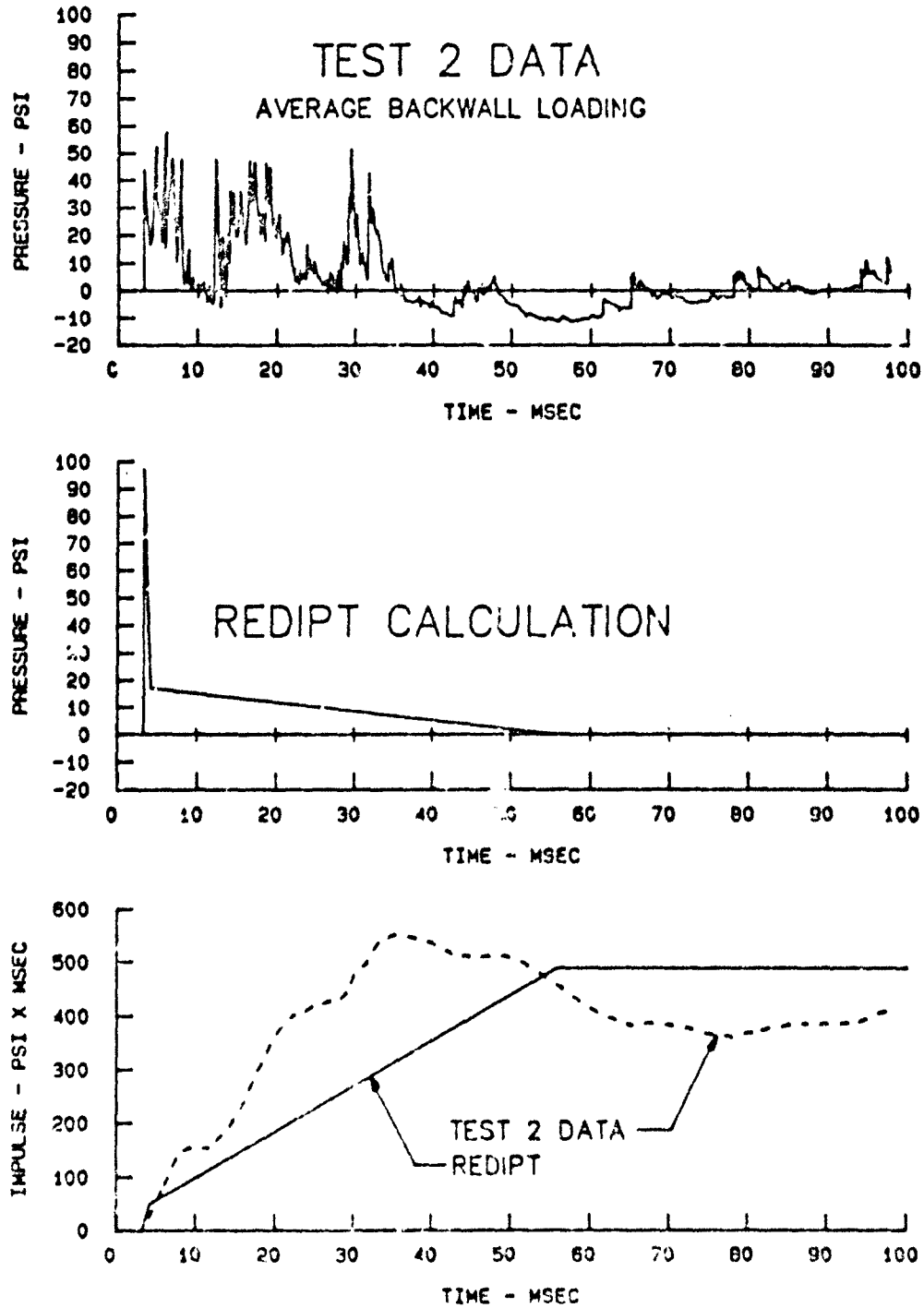

Figure 12. Comparison of REDIPT calculation with Test 2 data

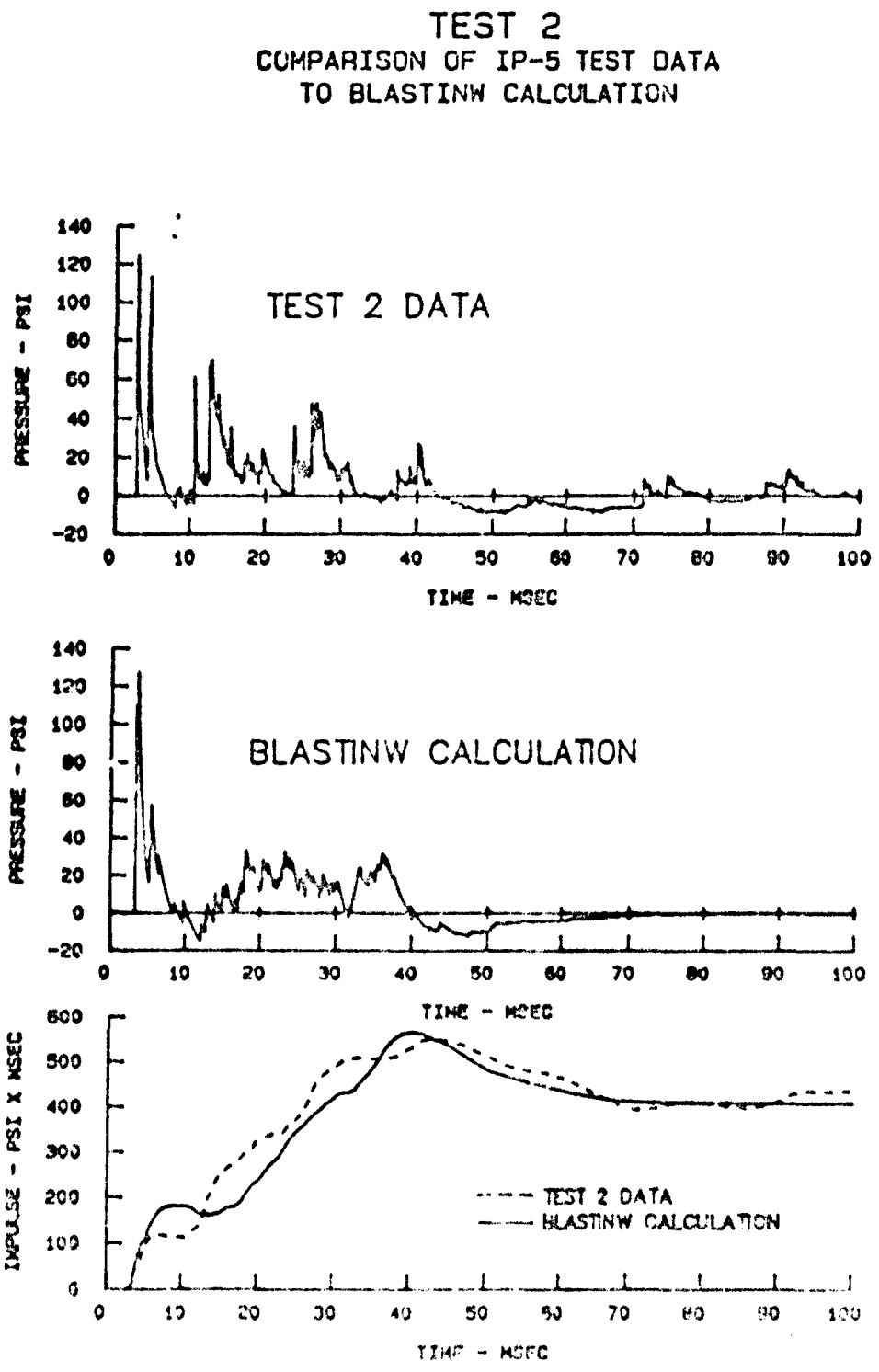

Figure 13. Comparison of gage IP-5 test data to BLASTINW calculation (Test 2)

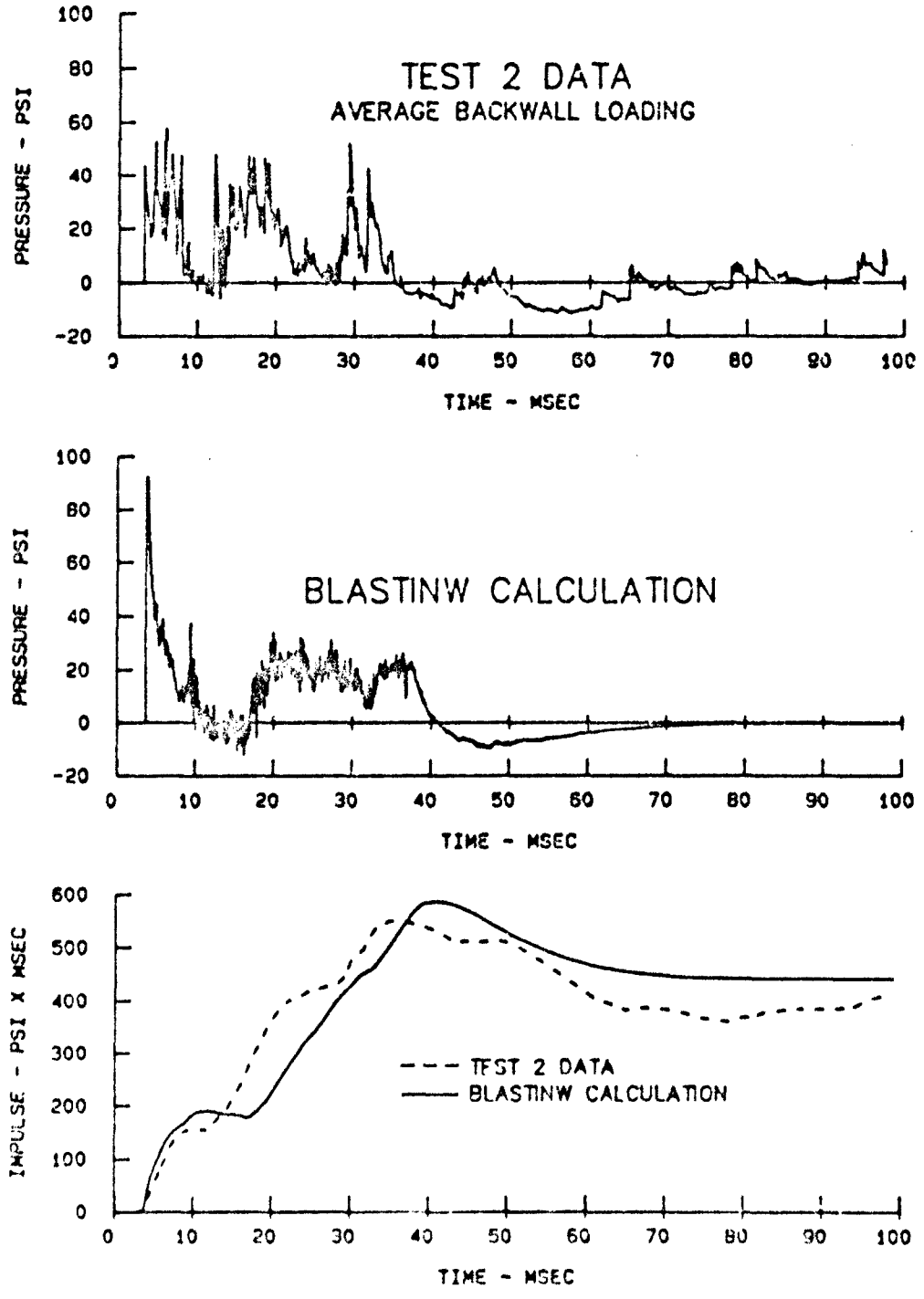

Figure 14. Comparison of BLASTINW calculations with Test 2 data

BLAST PRESSURE MEASUREMENTS IN CONTAINMENT TEST CELLS

by

Edward D. Esparza
Robert E. White
Southwest Research Institute
San Antonio, Texas

23rd Department of Defense Explosives Safety Seminar
9-11 August 1988

ABSTRACT

Three cylindrical test cells, approximately 14.5 ft in diameter and 24 ft long, were built at the DOE Mound Operation for testing up to 10 pounds of high explosives in a fully contained manner. A series of tests using spherical charges ranging from 2.5 to 12.5 pounds (TNT equivalent) were conducted by Southwest Research Institute to qualify each test cell for daily use. One of the major objectives of these tests was the measurement of the air blast and quasi-static gas pressure loads generated by the high explosive charges detonated at various locations in the test cells. Reflected blast pressure amplitudes as high as 6,000 psig and quasi-static gas pressures as high as 40 psig were measured. This paper presents an overview of the test program, a brief description of the test cells, details of the pressure measurement systems, examples of data traces, and comparison of the measured pressures with the pretest predictions.

INTRODUCTION

A series of qualification tests were conducted by Southwest Research Institute (SwRI) in three containment test cells fabricated for the Mound Operation of the Department of Energy at Miamisburg, Ohio. Mound is operated by the Monsanto Research Corporation (MRC). The three test fire-cells are the chief features of the new Component Test Facility (CTF) which also includes camera, preparation and control rooms, and a unified surge tank system to vent the cells and filter explosion products. An administrative wing of the CTF houses support-type functions to the testing operations. Figure 1 shows a layout of the CTF building and Figure 2 is a schematic of the test cells and surge tanks systems. For more details concerning the design of the CTF, the design and fabrication of the test cells, and the operation details of this facility, see Reference 1 which is being presented in another session at this seminar.

The purpose of the tests conducted by SwRI was to provide MRC with load and response experimental data for their use in qualifying the test cells for daily use with charges up to 10 lb. Thus, the objectives of the tests were to record transient strains, pressures, accelerations and temperatures resulting from internal detonations for each cell. In addition, seismic and acoustic sound levels were recorded for evaluation by MRC of architectural and sound-proofing qualifications. The testing services performed by SwRI were accomplished by detonating spherical charges within each cell and measuring the transients for obtaining blast loads and the structural response. Generally, the recorded data was processed and delivered to MRC for their use in determining if structural, seismic and acoustic criteria were met as part of the qualification process. Details of the SwRI tests are provided in Reference 2.

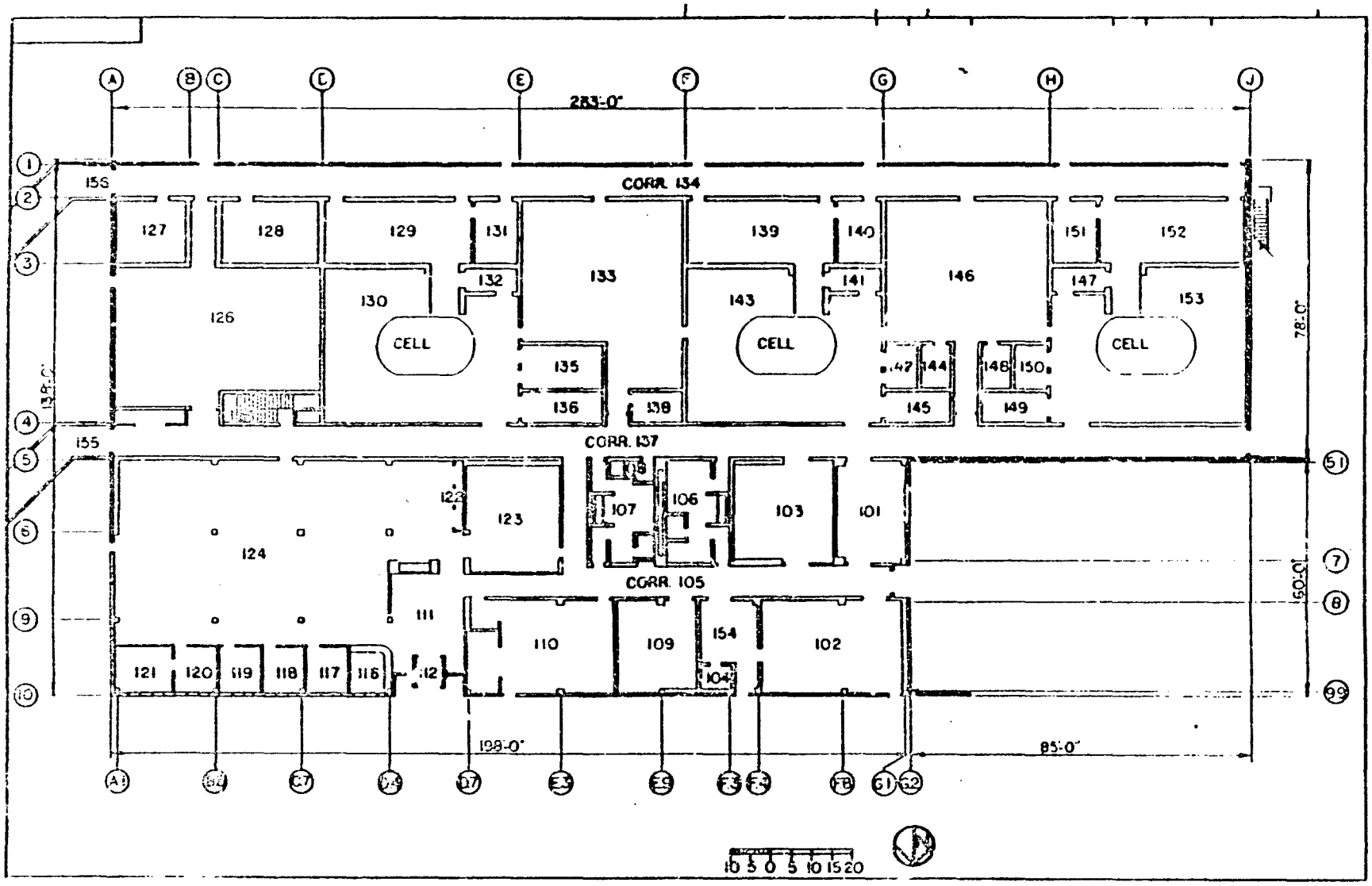

1467

Figure 1. Component Test Facility Layout

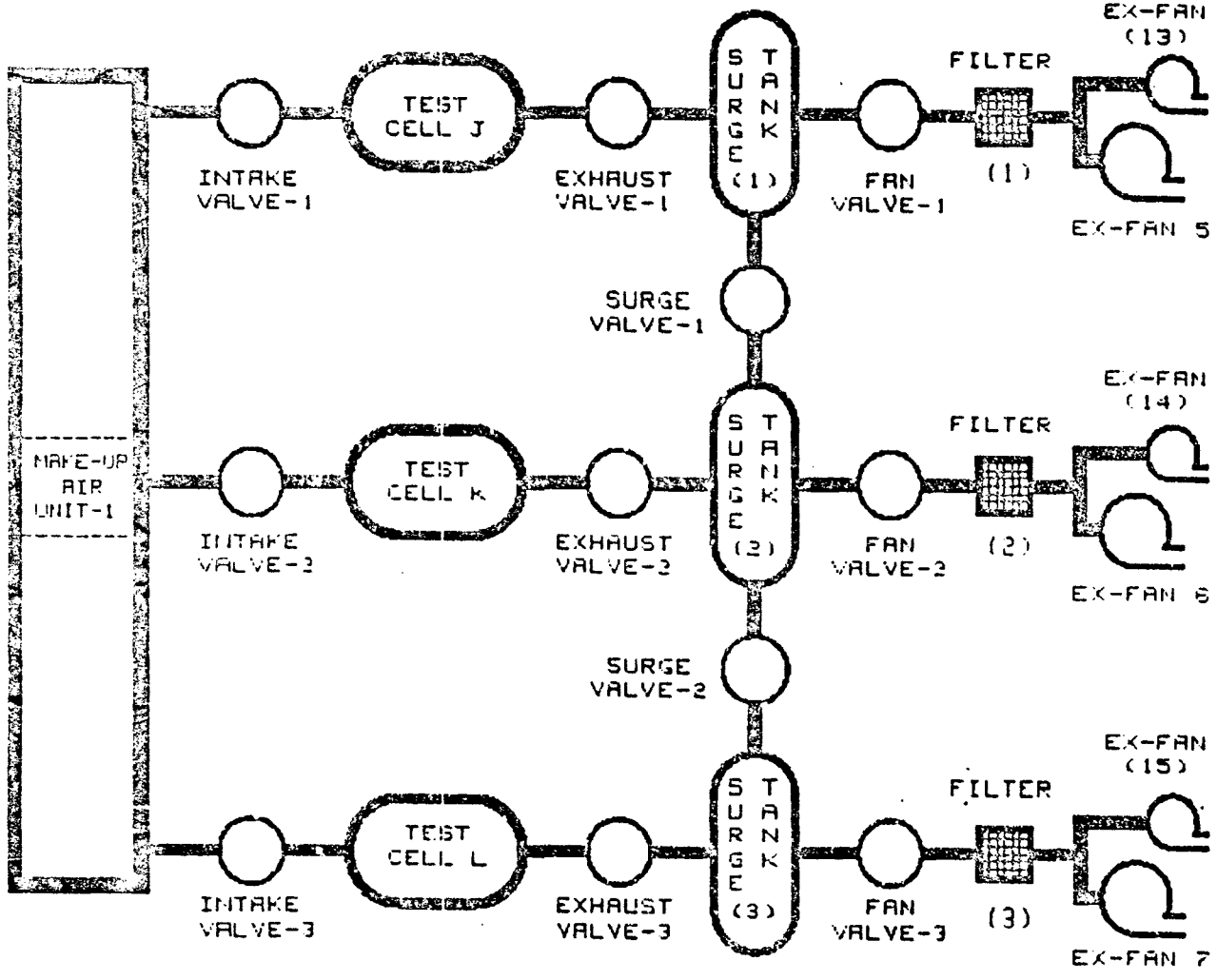

Figure 2. Schematic of Test Cells and Surge Tanks System

OVERVIEW OF TEST PROGRAM

The three test fire cells are virtually identical horizontal cylinders with elliptical heads having a gross diameter of 14 feet 6 inches and a length of 24 feet. The contained free volume of each cell is approximately 3,000 cubic feet. Each test fire cell is rigidly mounted to a concrete foundation which is 40 feet long, 15 feet wide, and 6 feet deep. The entire mass of the test cell/foundation is roughly 800,000 pounds. Each test fire cell has a 3 foot 6 inch by 7 foot manway with an automated doorway for entry. Other penetrations to the test fire cells include a large number of camera view ports, and instrumentation and air nozzles.

Other significant features of the test fire cells are a 5/8 inch thick fragment protection liner and a 5/8 inch thick steel floor installed over a concrete mat to create a flat working floor inside the cell. Head and shell thicknesses are 1.75 inches minimum SA-516 grade 70 steel. The test fire cells were built to ASME Section VIII Division 1 rules and have been hydrostatically tested to 660 psig. Working pressure rating is 340 psig.

Seventeen tests were conducted in the three cells. Explosive charges of C-4 were formed by weighing the appropriate quantity and molding spheres equivalent to 2.5, 5.0, 7.5, 10.0, and 12.5 lb of TNT. Equivalent weights were computed using heat of detonations taken from Reference 3. Three charge locations were selected by MRC for use on the tests, all on the horizontal center plane of a cell. One gas pressure transducer location and eight blast pressure transducer locations in each cell were designated to monitor the blast loads. However, on any given test, only three blast pressure transducers and one gas pressure transducer were installed and recorded. The locations of the blast pressure transducers, shown in Figure 3, were sometimes changed from test to test depending on the charge location. Figure 4 shows the three charge locations. The test sequence followed was:

Cell No.	Charge Location	Charge Weight (lb)
1	A	2.5
		5.0
		10.0
		12.5
	B	7.5
		10.0
	C	10.0
2	A	5.0
		10.0
		12.5
	B	10.0
	C	10.0
3	A	5.0
		10.0
		12.5
	B	10.0
	C	10.0

DESCRIPTION OF PRESSURE MEASUREMENT SYSTEMS

Two types of transducers were used, one for measuring the quasi-static gas pressures and another for measuring the reflected blast pressures. The gas pressure within the test cells was measured with a Kulite Model HEM-375 transducer which has static pressure response. This piezo resistive pressure gage has a nominal resonant frequency of 0 to 20 kHz and a pressure range of 1,000 psi, high enough to withstand blast pressure transients it could be exposed to and low enough to provide good resolution, even for the lower gas pressures expected. An acoustic filter was used to decouple most of the high-amplitude, high-frequency blast pressure pulses present before the gas pressure builds up within the chamber after a detonation. The acoustic filter consisted of a threaded adaptor with multiple ports and a small volume in front of the transducer diaphragm. The fill time of this volume, which is the effective rise time of the

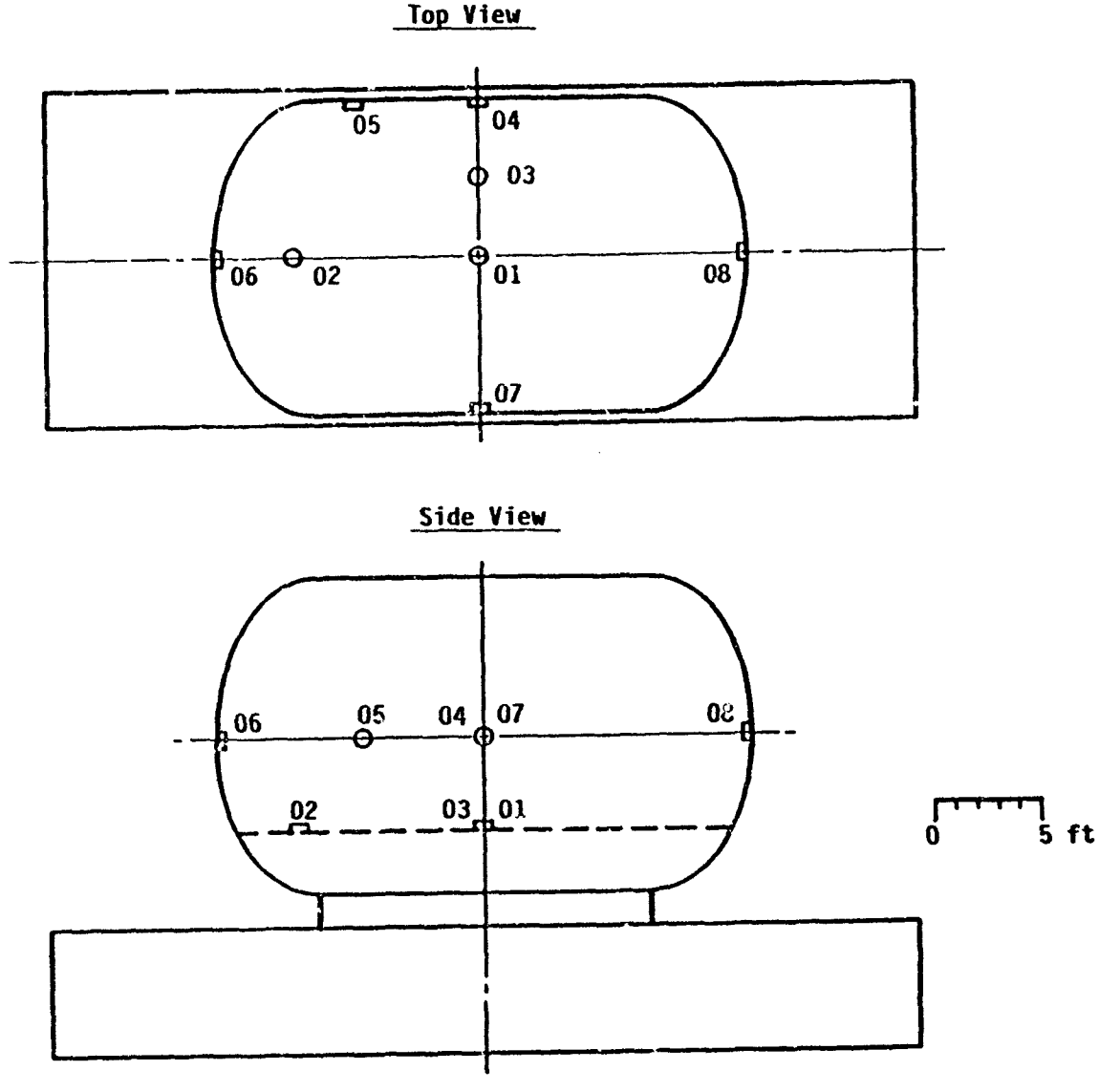

Figure 3. Blast Pressure Transducer Locations

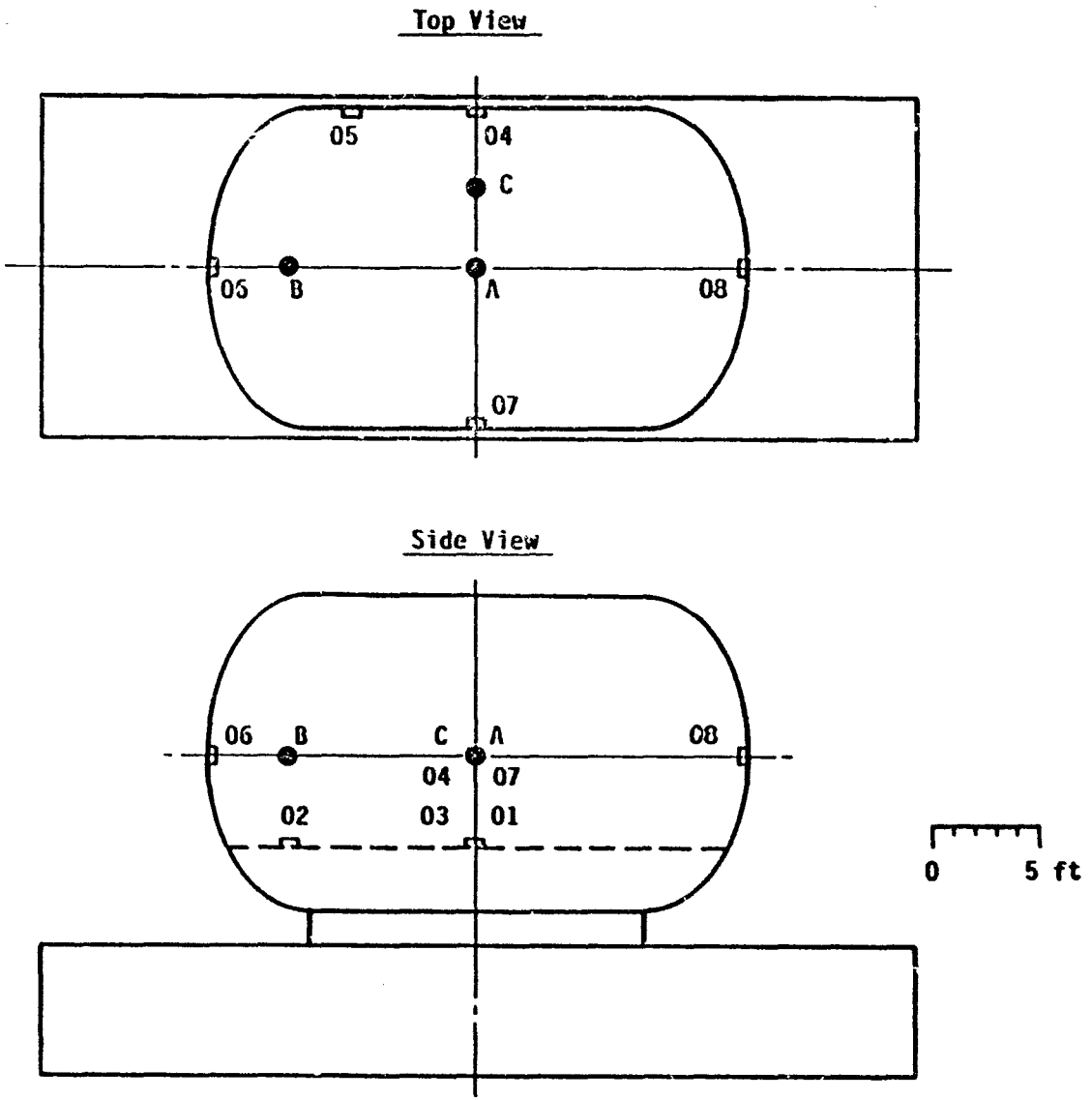

Figure 4. Explosive Charge Locations

protected sensor, was designed to be about 250 microseconds. This value was slow enough to filter the blast pressure pulses and fast enough to record the gas pressure rise. The data recorded showed that the gas pressures took as much as 20 milliseconds to reach a peak. Therefore, the acoustic filter worked as designed.

The reflected blast pressure measurements were made with PCB Piezotronics Series 102 pressure transducers. These piezoelectric gages use an acceleration compensated, quartz sensing element coupled to a miniature source follower within the body of the transducer. Power and signal amplification were provided by PCB Model 494A06, six channel units. The gas and blast pressure-time histories were recorded on magnetic tape using a Honeywell Model 101, Wideband II, FM tape recorder at a band width of 0-500 kHz (+1, - 3dB).

The data were processed at the test site in sets of four data channels using two Nicolet transient recorders for digitizing. The digital data were transferred from the transient recorder memory via a CAMAC data buss to a DEC 11/23 computer located at the test facility. Final data processing and plotting were then accomplished upon return to SwRI with a DEC 11/70 computer. Figure 5 shows a block diagram of the pressure data record/reduction system.

SUMMARY OF PRESSURE DATA AND DISCUSSION

An internal gas pressure measurement was successfully made in each cell for each test. Two examples of gas pressures measured are shown in Figure 6. In this case, two traces from tests using 12.5 lb charges at location A are presented to show the repeatability and self-consistency of the data. A summary of the peak gas pressure measured is presented in Table 1. For each charge weight used, the average gas pressure is given. In parentheses, the corresponding pretest predictions made using Reference 4 to set up the instrumentation are also given. In some cases, the average pressure is from only one measurement. For the 10 lb case, nine measurements were taken. As expected, no difference was found in amplitude in

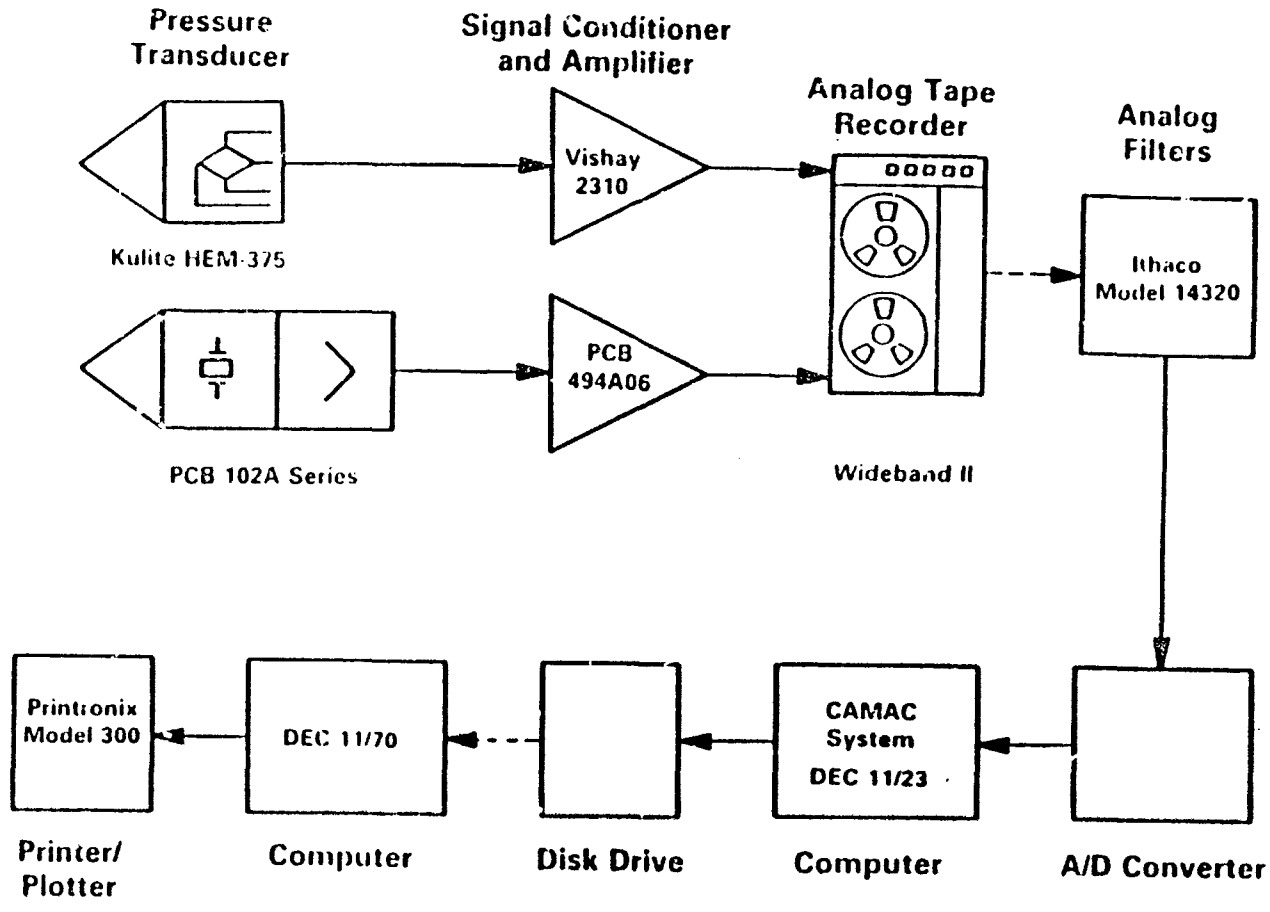

Figure 5. Data Recording and Processing System

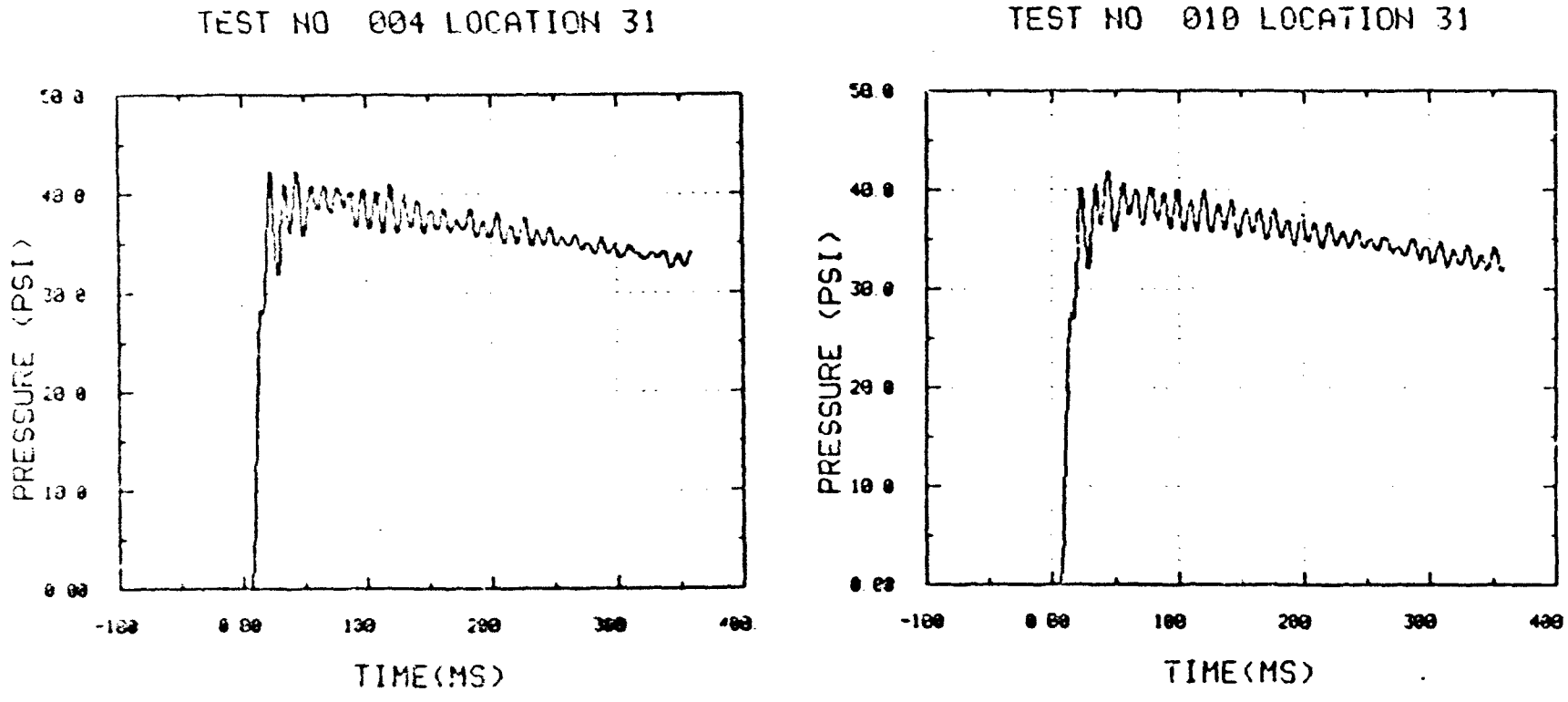

Figure 6. Gas Pressures From 12.5 lb Charge at Location A

that series due to charge location. Generally, the measured peak data were slightly lower than the pretest prediction.

Table 1. Summary of Gas Pressure Data

W (lb)	P (psi)	Charge Location	No. of Tests
2.5	8.4 (11.0)	A	1
5.0	16.7 (20.0)	A	3
7.5	24.3 (28.0)	B	1
10.0	32.0 (35.0)	A,B,C	9
12.5	38.7 (40.0)	A	3

As indicated previously, three blast pressure measurements were made on each test. On each test, a measurement was made on the floor directly below the charge. The other two measurements were made on the side locations using adapters in the existing camera viewports. Generally, for transducers located less than 7 ft from the charge, the pretest predictions were made using the TNT free air curves in Reference 4. At these close distances, no major enhancements from reflections on the floor were expected. For transducers more distant than 7 ft, the floor reflections were expected to enhance the pressure and impulse. Therefore, a factor of 2 was used on the charge weight to compute scaled distances. The peak reflected blast pressures and impulses are summarized in Table 2. The values for P and I are averages for 1 to 9 separate measurements depending on charge size and transducer location. Generally, the data for the closer scaled distances were in good agreement with the pretest predictions used to set up the instrumentation. However, for the more distant scaled distances, considerable enhancement on the peak reflected pressures and impulses from the floor and other surfaces was observed. In some instances, the impulse was 10 times larger, considerably higher than the 1.75 factor used by many in the literature to account for multiple reflections of contained detonations. The impulses listed in Table 2 were obtained from the pressure traces integrated out to 8 milliseconds. In some cases, the impulse at some of the more distant sensing locations were slightly larger than at the closer locations.

Table 2. Blast Pressure and Impulses

W (lb TNT)	R (ft)	Z ($ft/lb^{1/3}$)	P_r (psi)		I_r (psi - ms)	
2.5	4.0	2.9	521	(370)	76	(71)
	6.9	5.1	109	(95)		
	11.6	6.8*	164	(45)*	130	(40)*
5.0	4.0	2.3	960	(1000)	102	(111)
	6.9	4.0	224	(165)	121	(67)
	11.6	5.4*	235	(85)*	204	(60)*
7.5	3.0	1.5	3950	(3200)	350	(215)
	4.0	3.6	1440	(1550)	175	(147)
	20.0	8.1*	388	(29)*	400	(44)*
10.0	3.0	1.4	3640	(3900)	350	(260)
	4.0	1.8	2010	(2100)	224	(172)
	6.9	3.2	501	(300)	205	(108)
	10.7	3.9*	216	(180)*	452	(109)*
	11.6	4.3*	330	(145)*	313	(100)*
	20.0	7.4*	494	(37)*	536	(54)*
12.5	4.0	1.7	2760	(2300)	340	(209)
	6.9	3.0	513	(350)	288	(119)
	11.6	4.0*	413	(170)*	368	(114)*

* Used 2W to compute Z and obtain P and I from Ref. 4

Examples of the closer blast pressure measurements are given in Figures 7 and 8. Examples of the enhancement on the peak pressure and the multiple peaks recorded at the more distant sensor locations are presented in Figures 9, 10 and 11. These figures also depict quite well the repeatability of the blast pressure data recorded on this project.

CLOSURE

Three containment cells at the DOE Mound operation were successfully tested by SwRI. Seventeen tests were performed in which three blast pressure measurements and one gas pressure measurement were made on each test within the cells. The data recorded were self-consistent and quite repeatable. Peak gas pressures measured were close to the values expected before the tests. For blast measurements near the charge, the peak reflected pressures and impulses were as expected and compared well with free air values from standard TNT curves. For blast measurements further away from

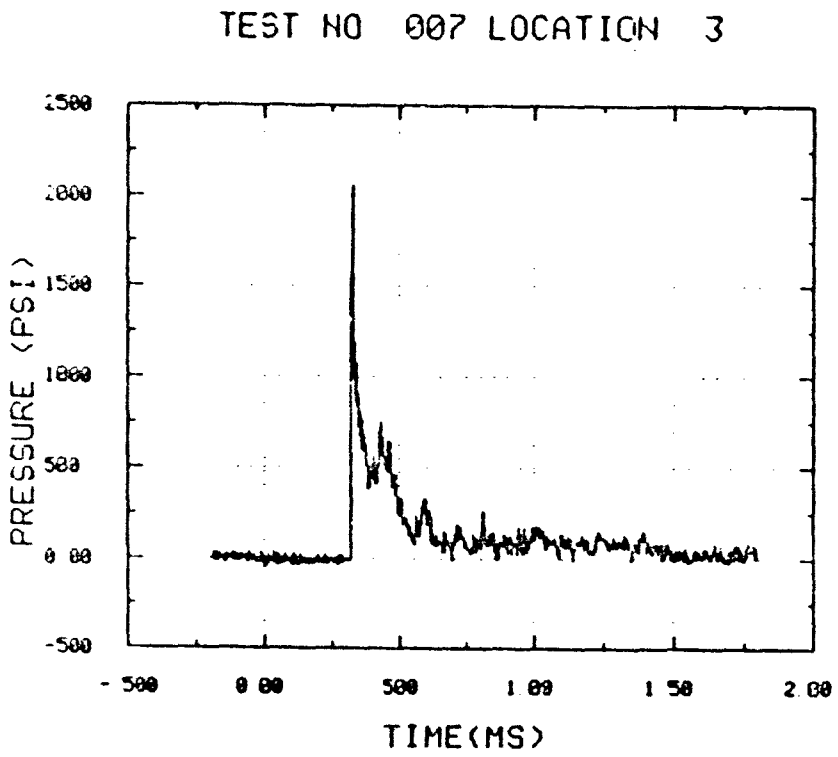

Figure 7. Blast Pressure From 10.0 lb Charge at Location C

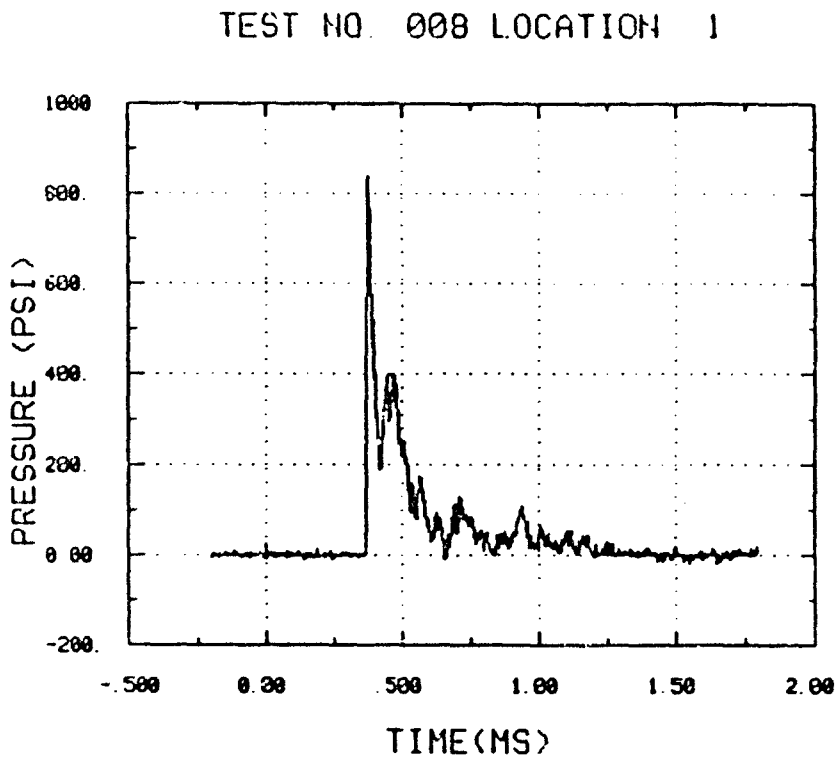

Figure 8. Blast Pressure From 5.0 lb Charge at Location A

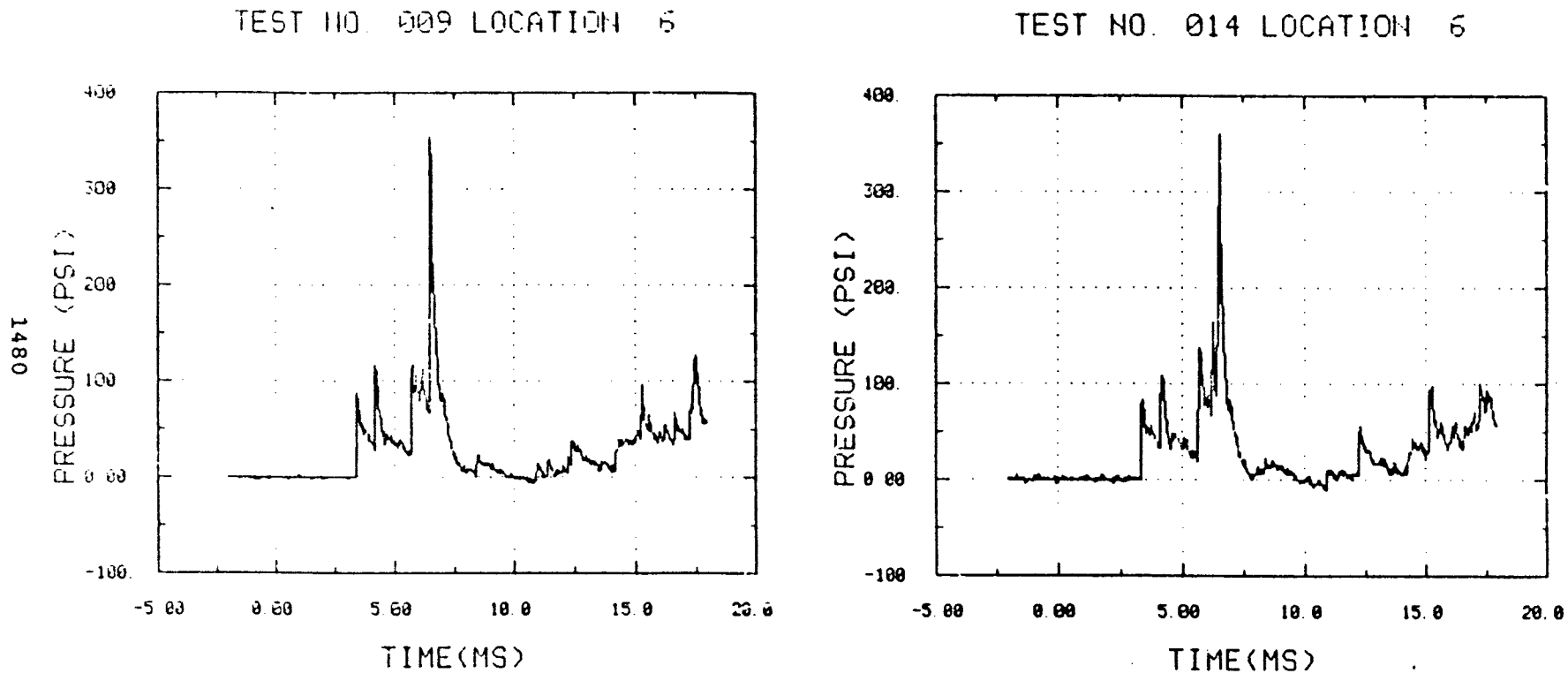

1480

Figure 9. Blast Pressure From 10 lb Charge at Location A

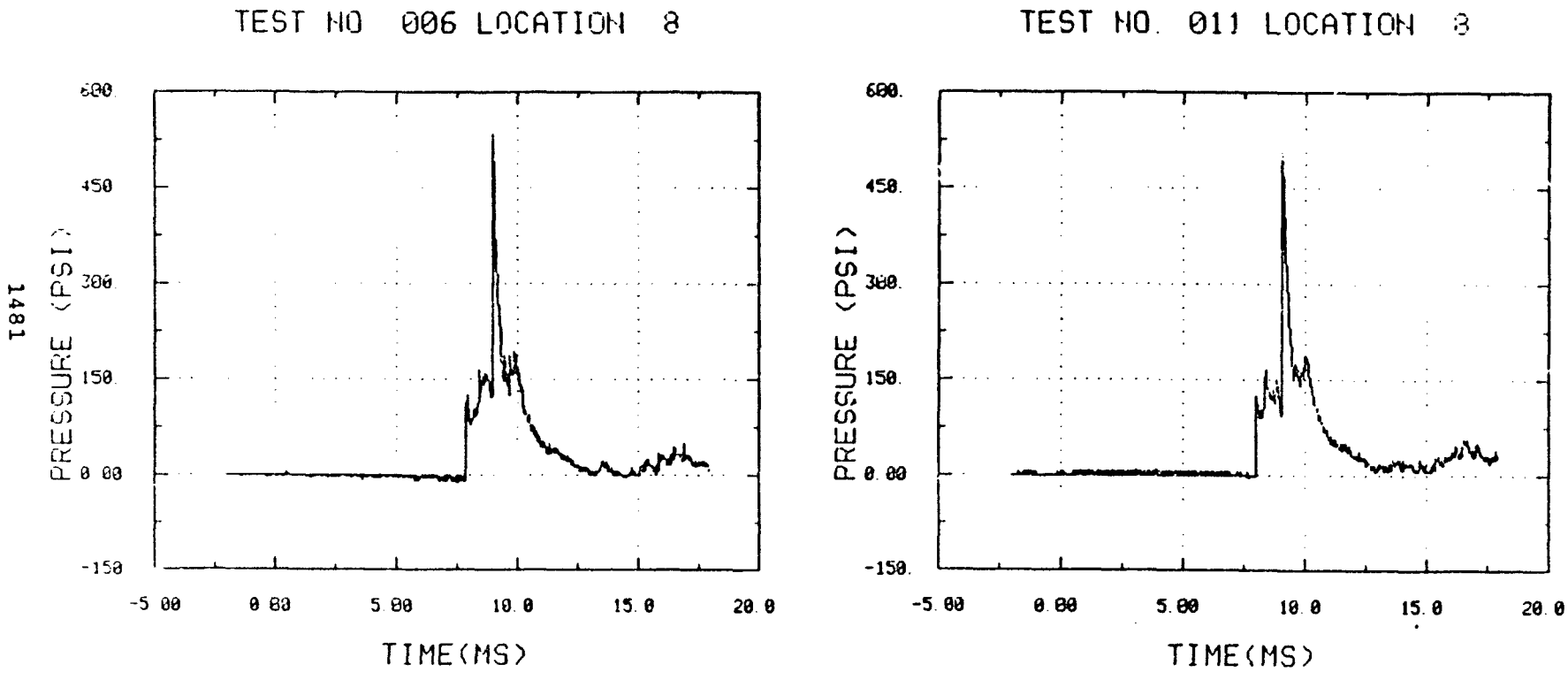

1481

Figure 10. Blast Pressure From 10 lb Charge at Location B

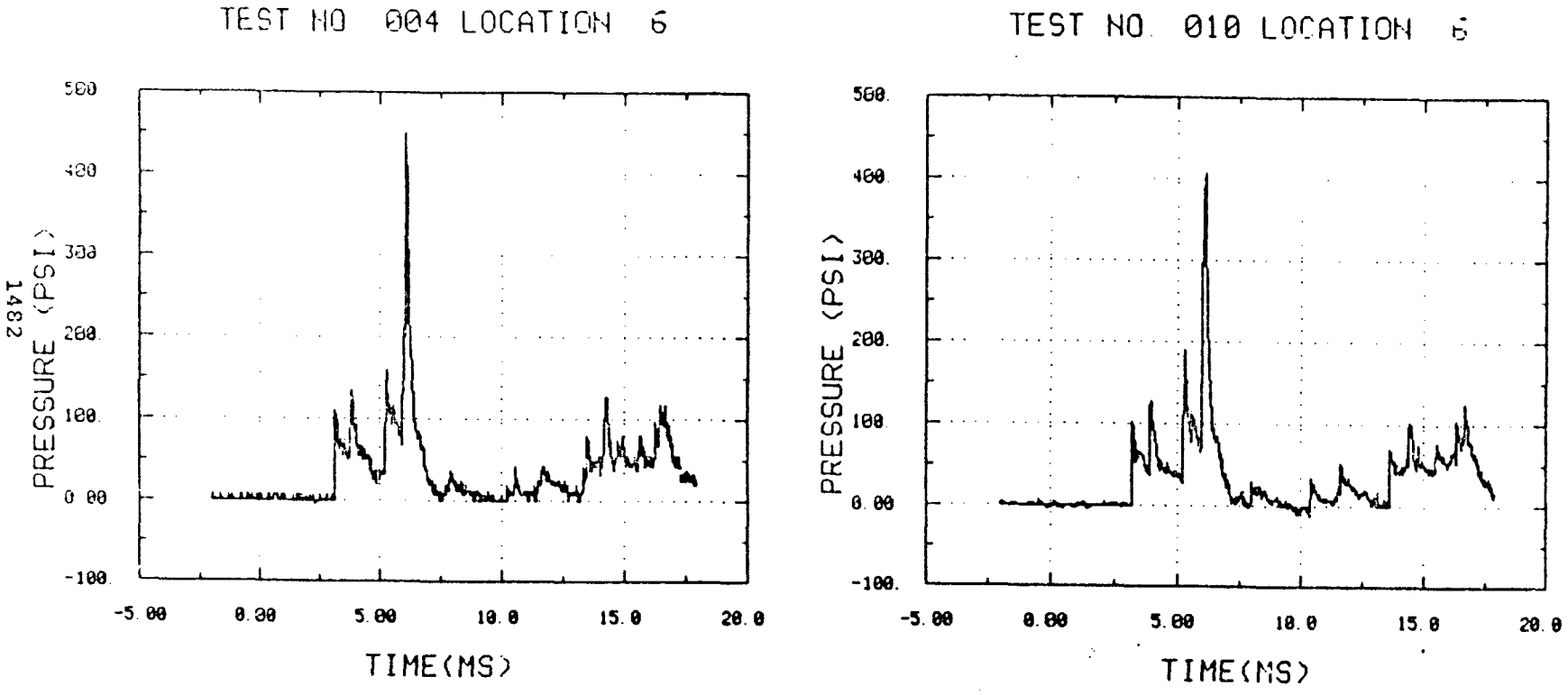

Figure 11. Blast Pressure From 12.5 lb Charge at Location A

the charge, peak reflected pressures and impulses were generally enhanced, in some cases by as much as 10 to 14 times. In some instances, these impulses were slightly larger than those at closer sensing locations in the same test.

ACKNOWLEDGEMENTS

The material for this paper was based on the results obtained by SwRI during a test project performed for the Monsanto Research Corporation at DOE Mound. The authors thank Mr. Stephen Rau of MRC and Mr. Marvin Ringer of Monsanto Company for advice, assistance and guidance in the performance of the project. The authors also thank Mr. Gerard Friesenhan of SwRI for his data system engineering and SwRI for providing the resources to prepare and present this paper.

REFERENCES

1. Stephen Rau, "Explosive Component Test Facility Test Fire Cells," 23rd Explosives Safety Seminar, Atlanta, Georgia, 1988.

2. White, R.E., "Component Test Facility Test Cell Qualification Test Program," SwRI Project 06-1452 Final Report, September 1987.

3. Explosives Handbook: Properties of Chemical Explosives and Explosives Simulants, LLNL Report No. UCRL-52977, Livermore, California, 1985.

4. A Manual for the Prediction of Blast and Fragment Loadings on Structures, U.S. DOE, DOE/TIC-11268, 1980.

BLAST WAVE PENETRATION INTO CUBICLES

Y. Kivity and A. Kalkstein

Rafael Ballistics Center
P.O.Box 2250, Haifa, Israel.

23rd DoD Explosives Safety Seminar,
9-11 August 1988, Atlanta, Georgia.

ABSTRACT

This work presents a preliminary computational study of blast wave penetration into cubicles. For simplicity, the cubicles are assumed to be cylindrical, with an axisymmetric circular opening on the side. A spherical explosive charge is assumed to be detonated outside the cubicle along the axis of symmetry, so that the entire problem is amenable to calculation by two- dimensional hydrocodes. In this study we employed the PISCES 2DELK code with its Eulerian processor to handle the complex wave reflections from the walls. Several cases were calculated, to assess the effects of the cubicle opening area and the presence of an opening cover. The results are presented in the form of wall impulse and pressure time-histories.

INTRODUCTION

The blast loading of vented structures as a result of internal explosions has received considerable attention in the explosive safety literature. A simple working model and an extensive literature survey may be found in the paper by Anderson et al.[1]. In contrast, the problem of the internal loads resulting from an external explosion is much less treated. Kucher and Harrison [2] used two-dimensional hydrocode calculations to model the air shock filling of a cylindrical enclosure with a central opening. Comparison of their calculations with

the experimental results of Coulter [3] yielded a good agreement for the shock front position and the early pressure time-history at various locations. Kaplan [4] presented a survey of experimental results on the effects of openings on the structural loads. He concluded that openings can alter significantly the external loads on the structure, and can create severe loading in the interior (in the form of wall pressure or acceleration of free standing objects). It appears, therefore, that a detailed study of the complex wave phenomena due to blast wave penetration through openings is not unjustified.

The purpose of the present work is to provide an estimate of the internal wall loading of a cubicle due to the penetration of an external blast through an opening in the cubicle. In particular, the effect of a frangible panel or cover will also be examined. The number of cases studied is limited, and the work is intended to provide an assessment of the computational approach, rather than a compendium of results for a variety of cases.

STATEMENT OF THE PROBLEM

The approach of the present work is similar to that of ref. 2, i.e. detailed calculations of the flow problem for a typical situation encountered in the explosives safety practice. We chose the case of an explosive charge detonated outside a cubicle with an opening. Such a problem is amenable to modeling by two-dimensional (axisymmetric) flow codes under certain symmetry restrictions. The cubicle is assumed to be cylindrical, with a circular opening at one end, centered on the axis of symmetry. Furthermore, the explosive charge is assumed to be spherical in shape, with its center lying on the symmetry axis. Fig. 1 gives a schematic of the problem. The modeling used here is very similar to the one employed in a previous work [5]: The cubicle is chosen to have equal length and diameter. The parameters in the problem are:

V - the volume of the cubicle,

W - the energy of the explosive charge,

A - the area of the opening,

M - the areal mass density of the cover,

K - the distance of the charge from the front wall,

and the equations of state of the air and of the detonation products.

The specific values of the parameters in this study were similar to the ones in ref. [5]:The cubicle was taken as acylinder having equal height and diameter of 1.08m, so that the volume V was one cubic meter, the explosive yield W was taken as 4.5 MJ, representing a TNT charge of 1 Kg., and the charge distance from the front wall was 0.99m. Two cases of uncovered openings were calculated (A=0.10, and A=0.56 sq.m), and one case with a covered opening of 0.56 sq.m and an areal mass density of 10 Kg/sq.m.

THE COMPUTATIONAL MODEL

The numerical solution is obtained with the PISCES 2DELK program [6], using its second order Euler processor. The computational model consists of a quadrilateral grid 2.07m long and 1.02m wide, with a square mesh size of 0.03m. The cubicle, with a radius of 0.54m and a height of 1.08m is imbedded in the grid as shown in Fig. 2. The walls of the cubicle are defined either by setting a rigid wall boundary condition (as in the rear wall), or by declaring certain grid cells to be wall boundaries (front and side walls). The axis of symmetry is also defined as a rigid wall. To save computer resources, we assume complete symmetry with respect to a plane perpendicular to the axis of symmetry and passing through the center of the spherical charge. This is strictly correct only for a limited period of time, (the time it takes the reflected wave from the front wall to reach this symmetry plane), but it may be regarded as a reasonable engineering approximation for longer times. The side grid boundary is defined by a "continuative flow" condition, which minimizes reflections from the boundary, thus simulating an infinite medium.

The charge is simulated by a sphere of dense hot gas, having the energy and mass of the explosive, but at a lower density of 25 Kg/cu.m. This approximation was used in a similar study [5], and was found to have a negligible effect on the long term wall impulse (an eightfold increase of the density affected the impulse by less than 5%).

The air and the dense hot gas were represented by an ideal gas equation of state. The ratio of specific heat coefficients was 1.40 for both gases.

The calculations reported here consumed about 25 hours per case on a MicroVax II computer.

RESULTS AND DISCUSSION

The results are displayed by velocity vector plots at selected times, and by time-history plots of various variables, at selected locations. The most relevant variables are pressure, wall impulse, and wall average pressure.

As an example, results for the uncovered opening case A= 0.10 sq.m are shown in Fig. 3. Prior to impingement on the structure (Fig. 3a) the air shock wave is almost spherical, as is evident from the shape of the interface between the air and the hot gas representing the detonation products. The small deviation from sphericity is a result of the coarse mesh and the fact that initially the hot gas sphere occupied very few cells across its radius. Two shock waves may be observed, one propagating in the air ahead of the interface, and the other within the hot gas sphere. The latter results from reflections within the hot gas sphere.

Fig. 3b shows further propagation of the shock wave in the air, both within the structure and around it. Due to reflections from the wall, the hot gas forms a jet-like shape. Inside the structure, a vortex starts to form, as a result of shock wave curvature. A similar effect was pointed out in ref.2.

Fig. 3c Shows the evolution of the flow at a later time. The vortex inside the cubicle is much stronger; There is a reverse flow from the cubicle opening outwards, and an inflow from the upper "continuative flow" boundary. This inflow is a result of the suction generated earlier, following the strong explosion.

A velocity vector plot for the case with a covered opening is shown in Fig. 4, at a time of 7 ms after detonation. this time the cover has already moved about 0.2 m inside the cubicle. Previous inflow and internal reflections have filled the cubicle and increased its pressure, so that at this time the internal pressure is higher than the outer pressure, and air is escaping from the cubicle.

The cover is modeled here as a moving rigid body, and its motion is governed by Newton's Law. This modeling is valid only for the early phase of the motion of a frangible panel, which is expected to break up eventually because of asymmetrical loading. This modeling, however, is adequate for assessing the effect of the cover in preventing the direct shock inside the structure, and in the general reduction of the internal loading, as will be discussed below.

The sets of fig.'s 5,6 and 7 are time-histories of backwall average pressure, backwall impulse and cubicle center pressure, respectively. Each set gives the behavior of a variable for the three cases studied: (a) an uncovered opening with A=0.56 sq.m, (b) an uncovered opening with A = 0.10 sq.m and (c) a frangible panel with A = 0.56 sq.m and areal mass density of 10 Kg/sq.m.

The backwall average pressure is shown in Fig.s 5. The small opening cubicle case has peak overpressure of 0.12 MPa, compared to 0.6 MPa for the large opening case. Note that the ratio of the peak values is very close to the ratio of the opening areas. The time to the peak is shorter by about 0.4 ms for the larger opening, since the blast wave is not impeded. The subsequent peaks exhibit a reverse behavior: The small opening case vents more slowly, and so its secondary peaks are higher than those of the large opening. The backwall average pressure for the covered case has a significantly different behavior. Because of the impeding behavior of the cover, the first peak is very low, about 0.027 MPa only. However, the cubicle continues to fill up, and a somewhat higher peak is attained at a later time, when sufficient clearance between the cover and the front wall has been generated.

The backwall specific impulse (i.e. impulse divided by wall area) is shown in Fig.'s 6. The impulse is obtained from the average pressure curves by time integration. The large opening impulse builds up rapidly to a value of about 0.48 MPa-ms, and then decays due to venting (Fig. 6b). The small opening impulse builds up slowly, with moderate decay due to venting (Fig. 6a). The small opening case was not continued sufficient time for maximum wall impulse to be attained, but it appears that it would attain a value of at least 0.23 MPa-ms. Clearly, the opening size effect on the impulse is less significant than on the peak pressure. The impulse for the covered opening case (Fig. 6c) was much smaller than the uncovered cases, as expected from the pressure curve of Fig. 5c.

The pressure time-history at the center of the cubicle is shown in Fig.'s 7 for the three cases. (These curves are absolute pressure, in contrast with the over-pressure curves of Fig.'s 5). The curves exhibit a typical behavior of pressure time-histories inside closed structures, duer to the complex wave reflections from walls. In this case of an axisymmetric flow, the axis of symmetry contributes also to wave reflections. The calculated peaks may be affected by the particular choice of numerical parameters in the calculation. The uncovered opening cases have peak values of 0.27 and 0.45 MPa for the small and the large openings, respectively. The covered opening peak is about 0.13-0.14 MPa only. The pressure curve goes down to zero when the rigid panel crosses the center of the cubicle, at a time of 18.2 ms.

CONCLUSIONS

A computational model for the penetration of a blast wave into structures with openings was presented. The model is based on using an Eulerian code for solving the flow equations numerically.

The results of the few examples calculated so far show that the opening size affects both the peak wall pressure and the impulse build-up time.The effect of frangible panels is very pronounced and may reduce the initial impulse (and the peak pressure) markedly. Some of the calculations should be continued for a longer time, to obtain more complete data.

The exploratory runs of the present study indicate that the model is a feasible tool for a more complete study, covering a wide range of the parameters involved. However, the use of a more powerful computer would be desirable, to make run times more practical.

REFERENCES

[1] Anderson, C.E. et al.: "Quasi-Static Pressure, Duration and Impulse for Explosions in Structures". Int. J. Mech. Sci., Vol. 25, No. 6, p. 455-464, (1983).

[2] Kucher, V. and Harrison, J.: "Air Shock Filling of a Model Room". BRL Report No. 2011, September 1977. (AD #A044798).

[3] Coulter, G.A.: "Air Shock Filling of Model Rooms", BRL Report No. 1916, March 1968.(AD #670937).

[4] Kaplan, K.: "Effects on Structural Loading of Blast Leakage into Structures". Proceedings of the 18th Explosives Safety Seminar, San-Antonio, Texas, September 1978.

[5] Kivity, Y. and Feller, S.: "Blast Venting from a Cubicle". Proceedings of the 22nd Explosives Safety Seminar, Anaheim, California, August 1986.

[6] Hancock, S.L.: "PISCES 2DELK Theoretical Manual", Physics International Company, San-Leandre, California, August 1985.

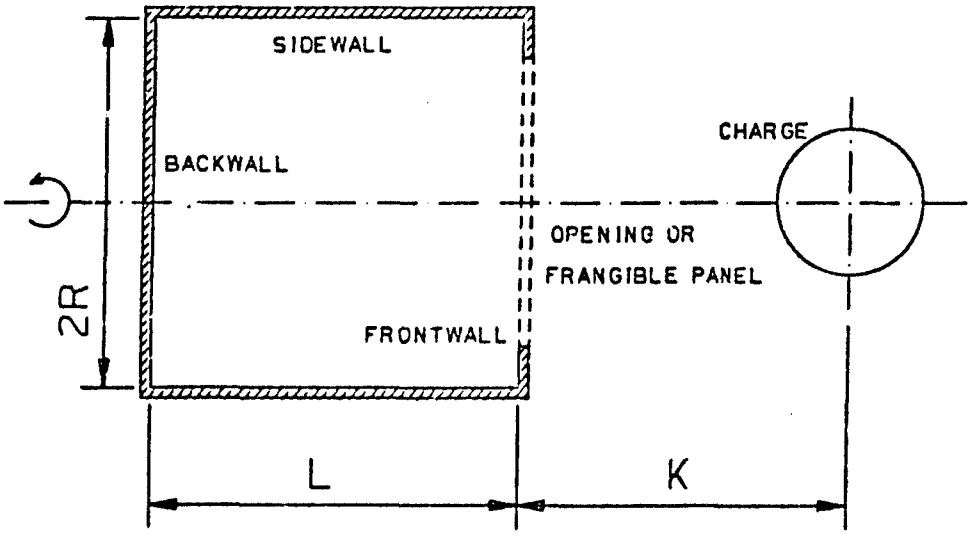

FIG. 1 : SCHEMATIC OF PROBLEM SETUP.

2R = L = 1.08 M (VOLUME = 1 M^3)

K = 0.99 M

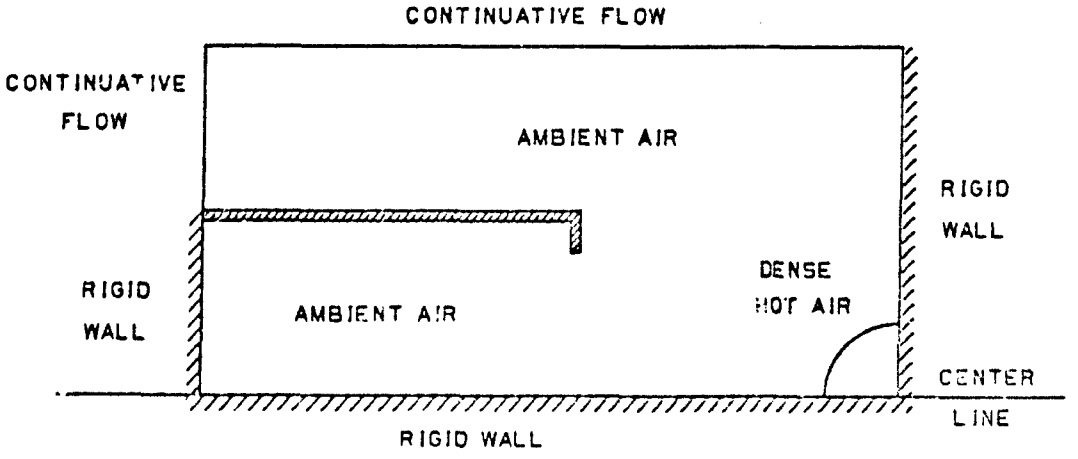

FIG. 2 : THE COMPUTATIONAL GRID.

1.02 M X 2.07 M (34 X 69 CELLS).

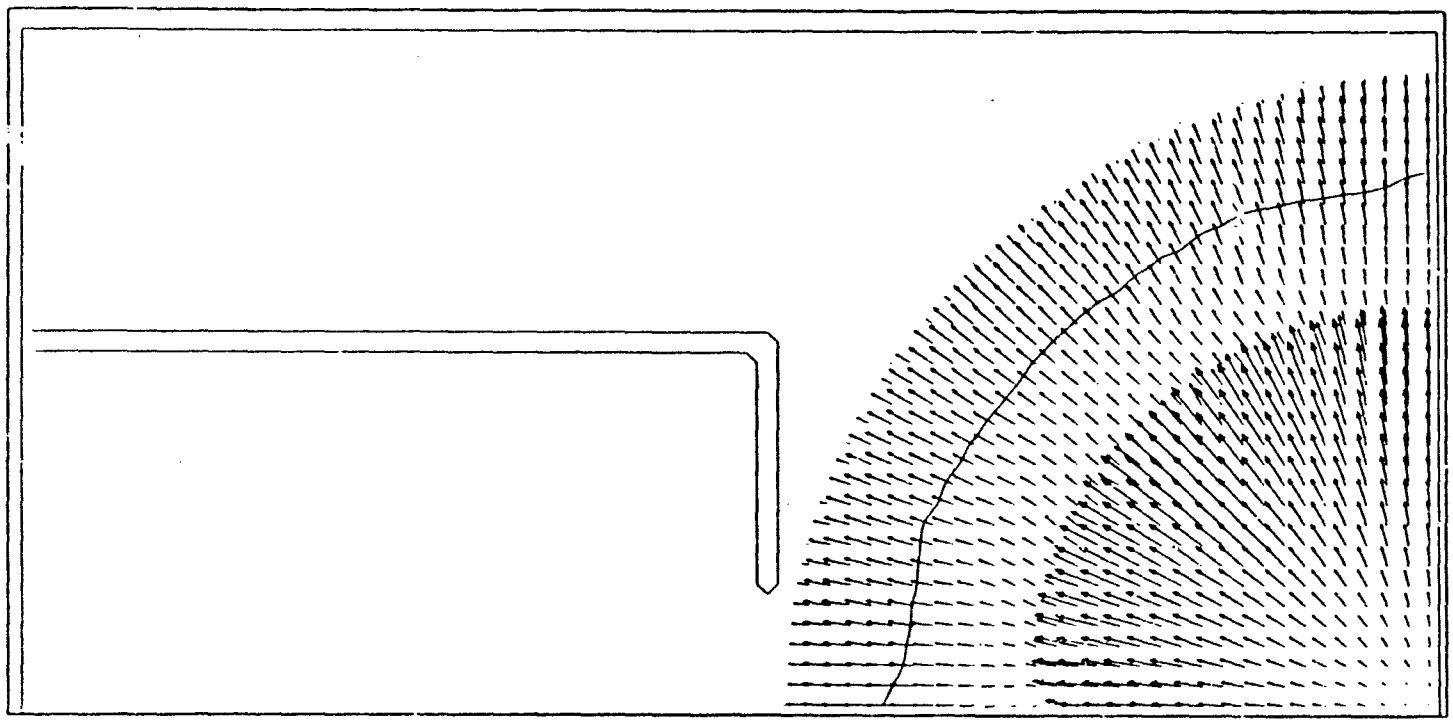

Fig 3a: Velocity Vector Plot at t=0.4689ms
(Opening radius = 0.18m)

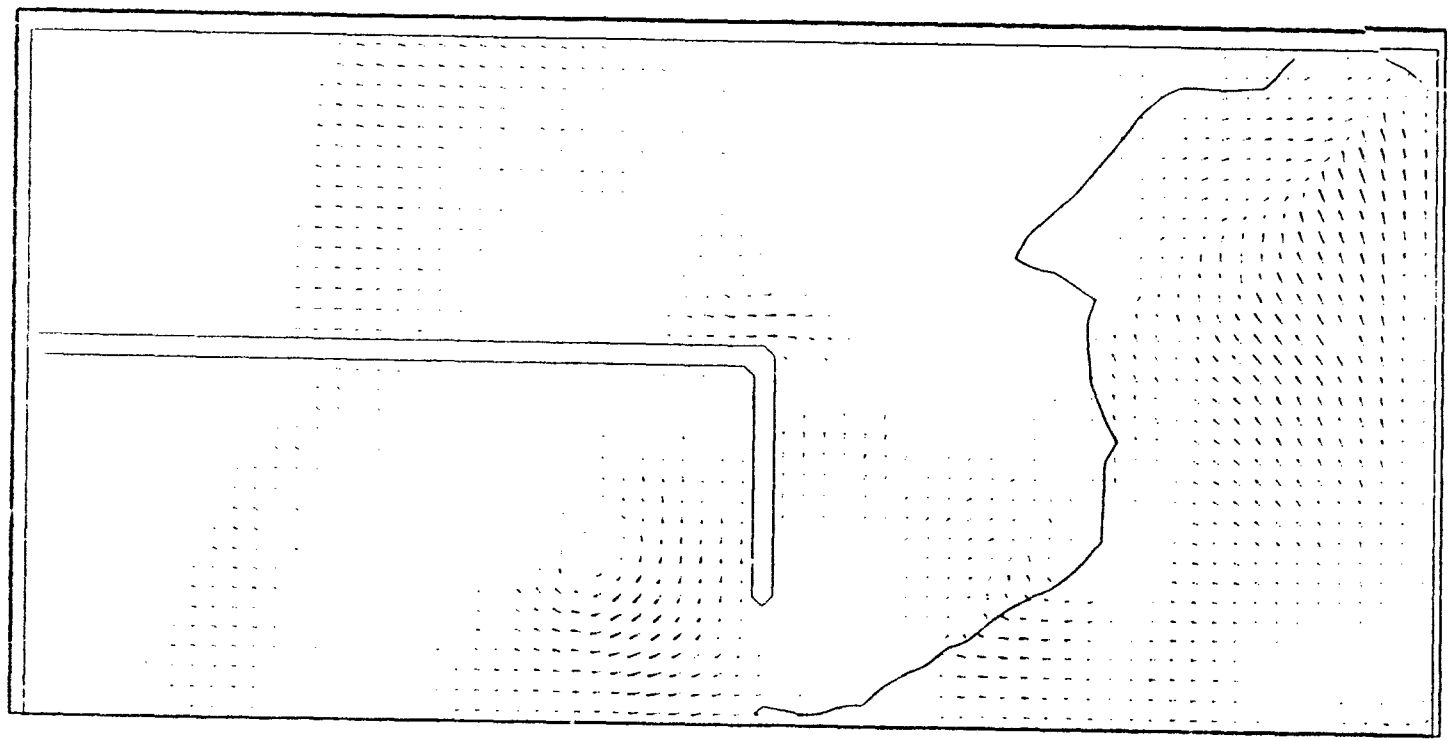

Fig 3b: Velocity Vector Plot at t=1.854ms
(Opening radius = 0.18m)

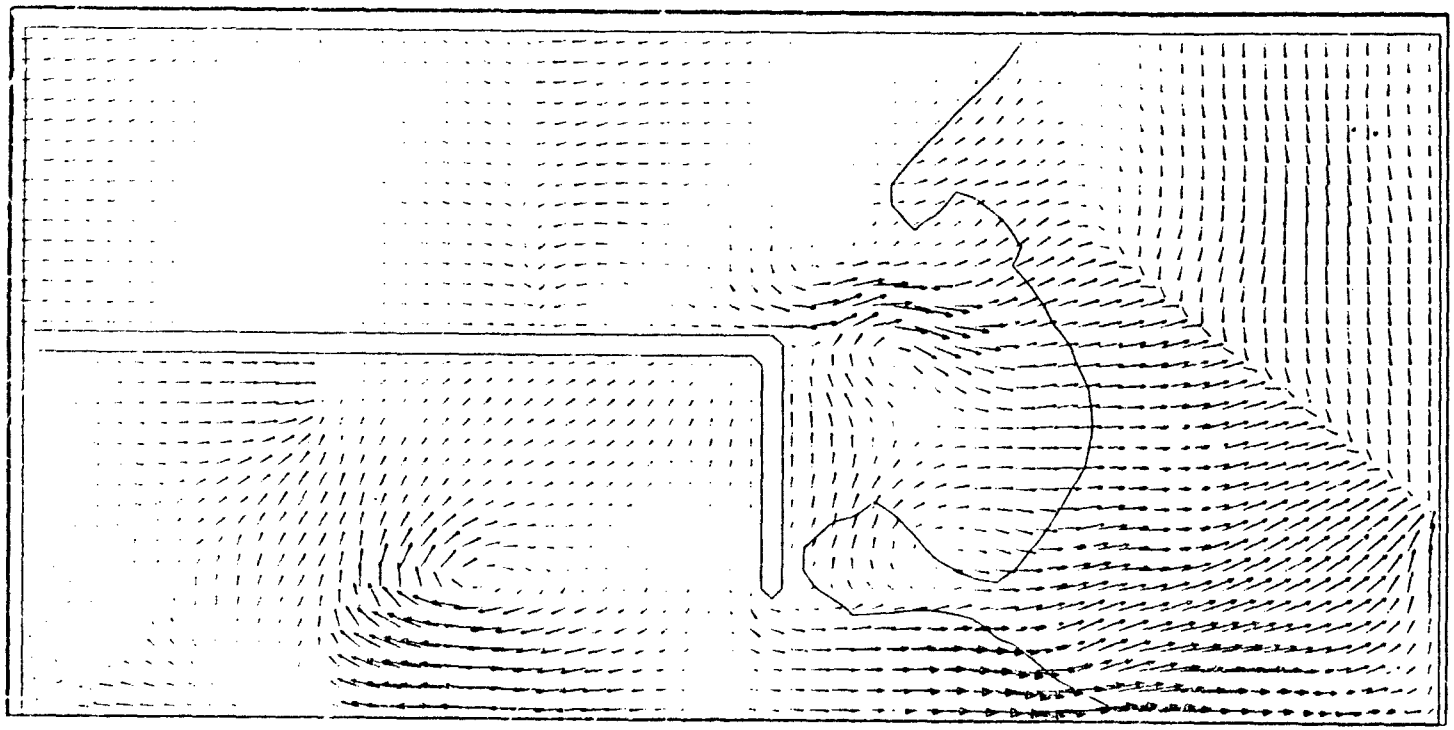

Fig 3c: Velocity Vector Plot at t=3.636ms
(Opening radius = 0.18m)

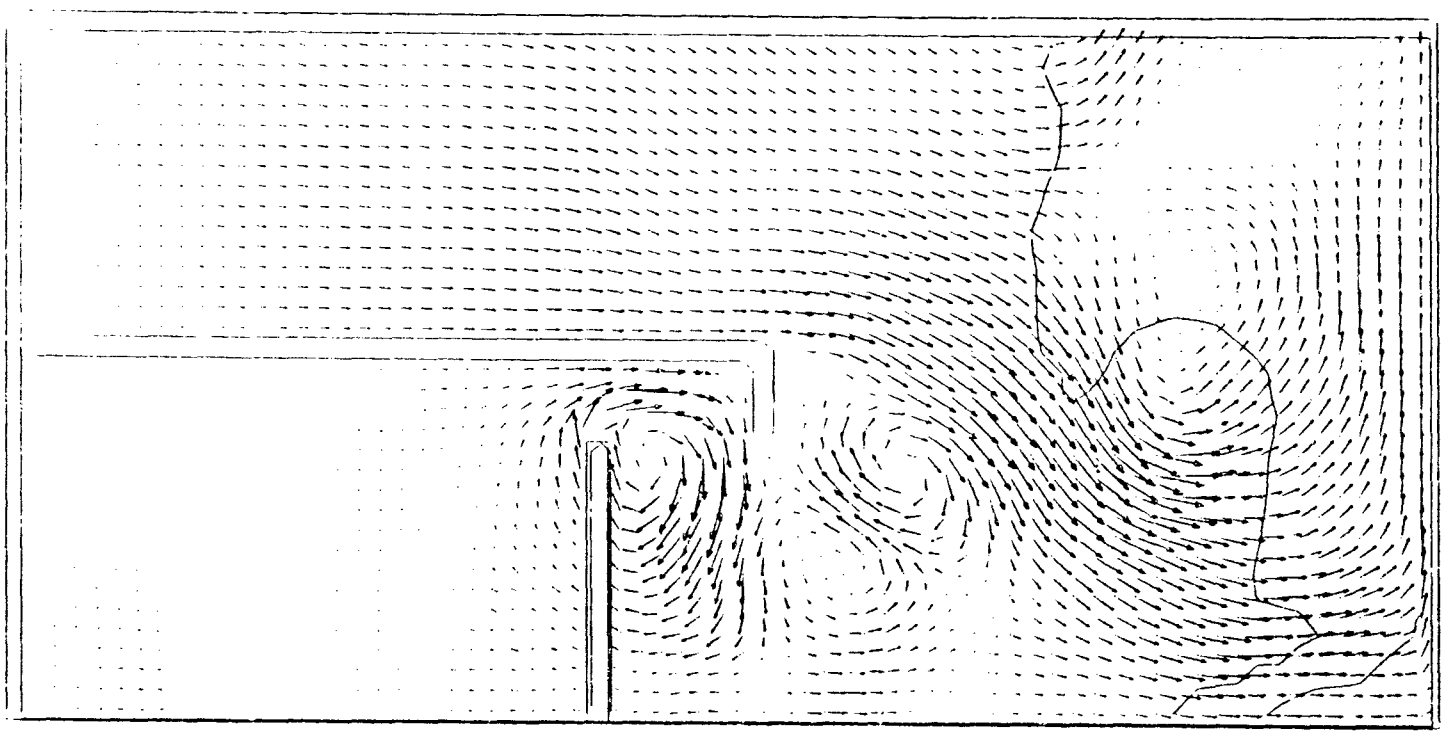

Fig 4: Velocity Vector Plot at t=6.977ms
(With a frangible panel having a radius of 0.42m)

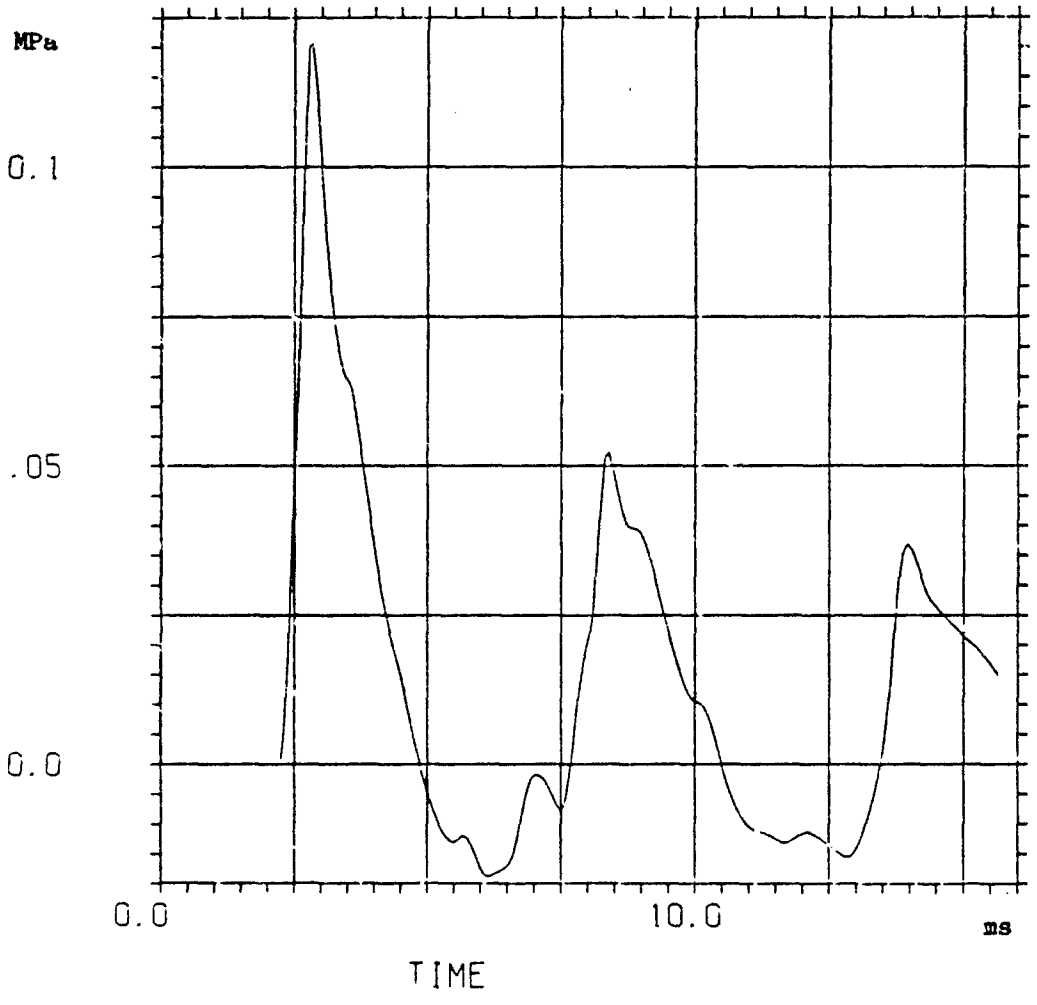

Fig 5a: Backwall Average Pressure
(Opening radius = 0.18m)

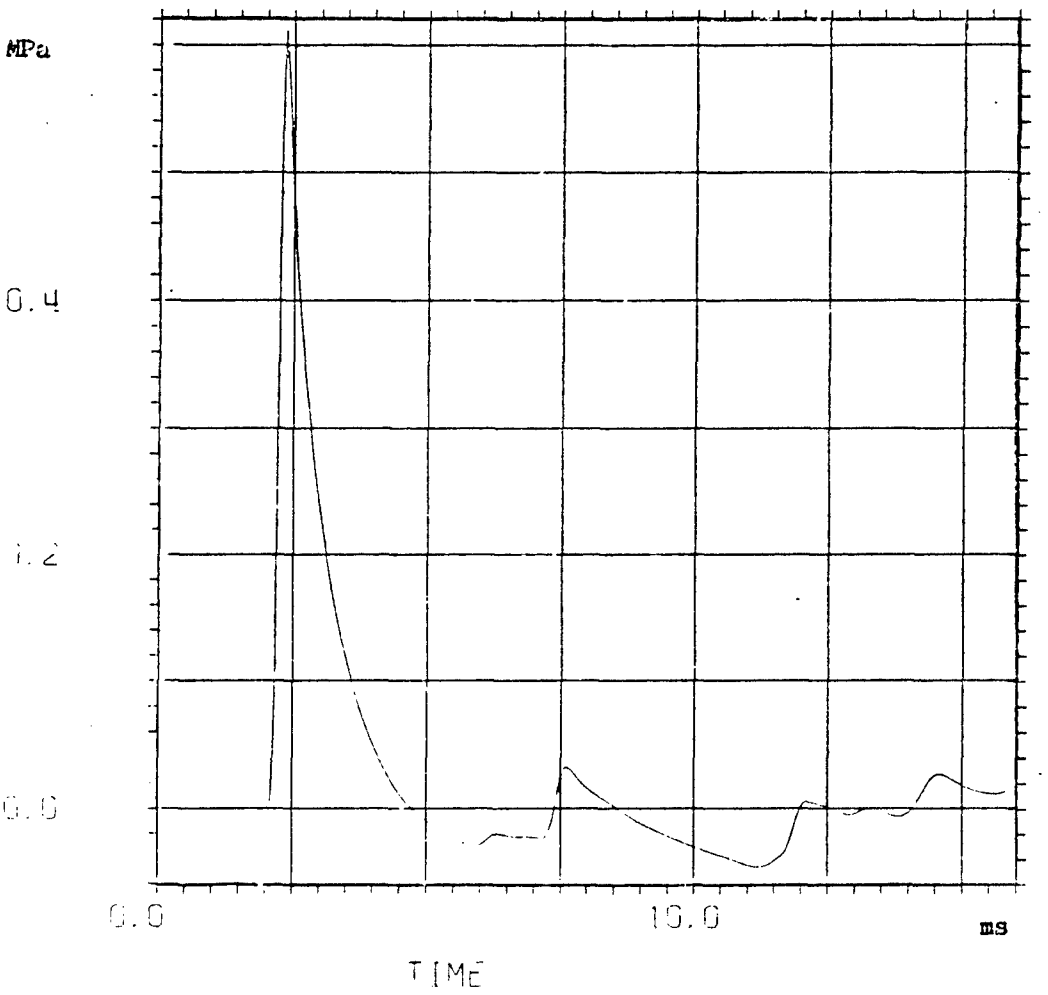

Fig 5b: Backwall Average Pressure
(Opening radius = 0.42m)

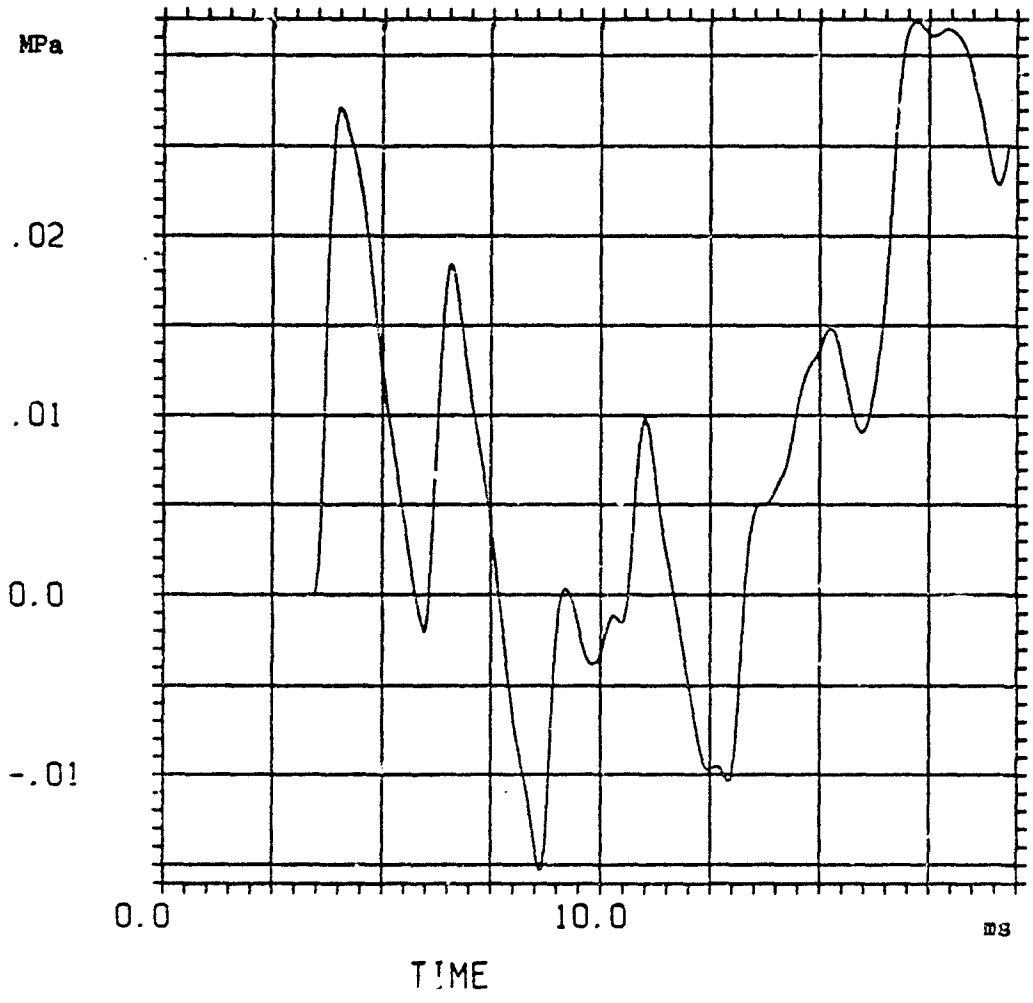

Fig 5c: Backwall Average Pressure
(With a frangible panel having a radius of 0.42m)

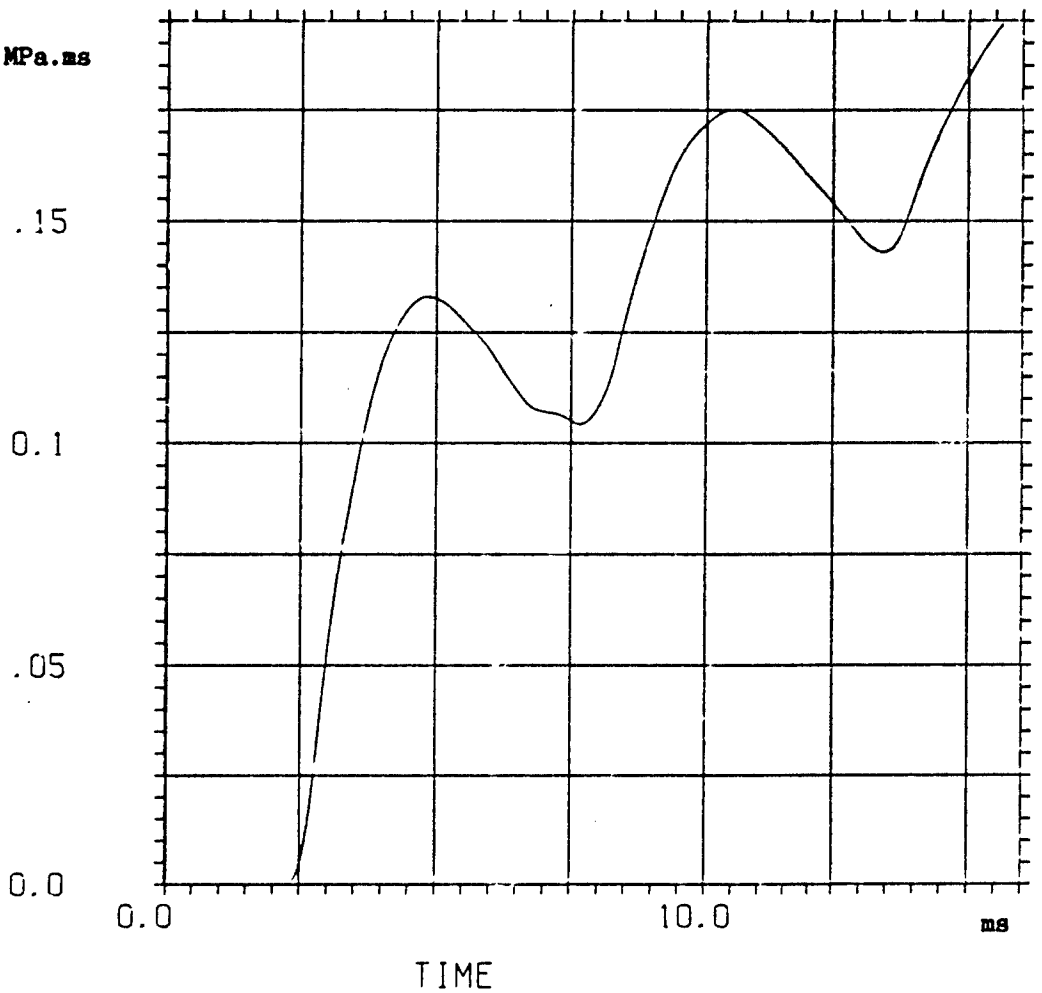

Fig 6a: Backwall Average Impulse
(Opening radius = 0.18m)

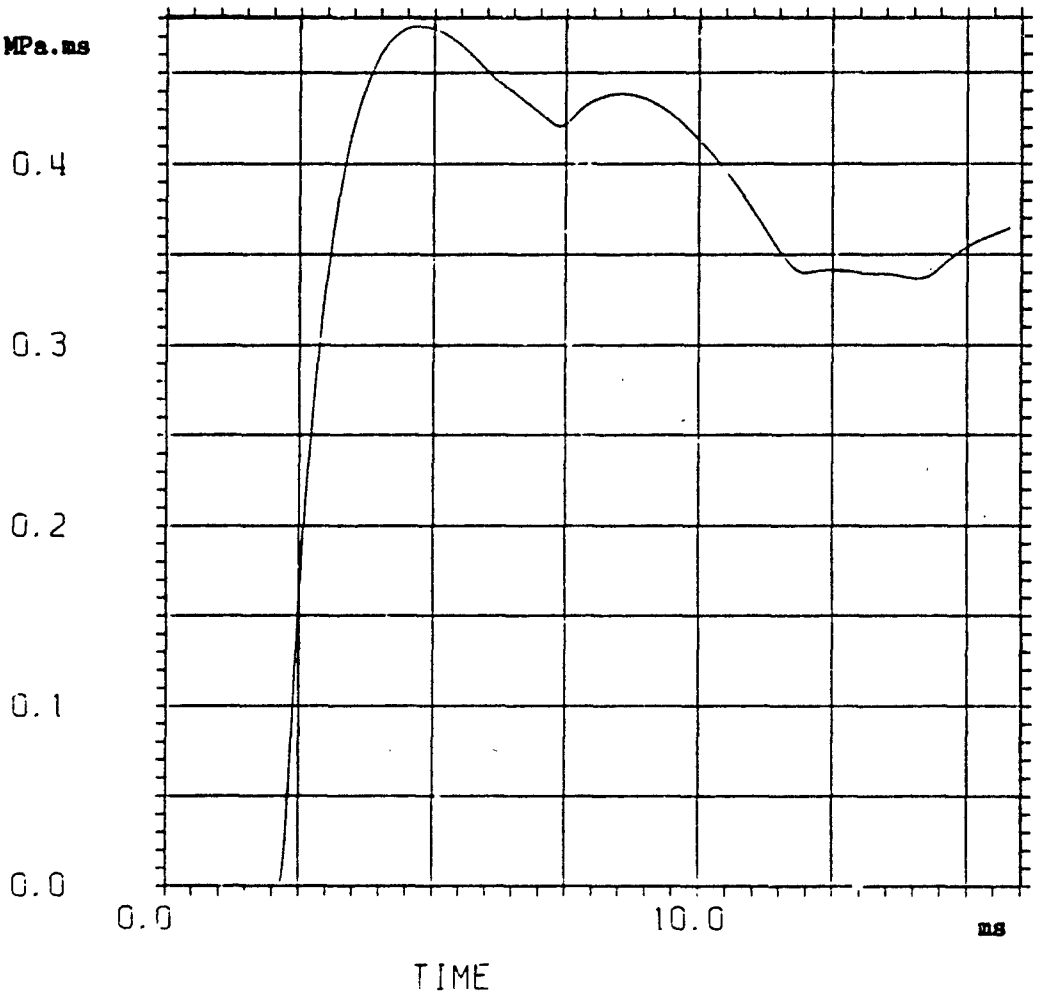

Fig 6b: Backwall Average Impulse
(Opening radius = 0.42m)

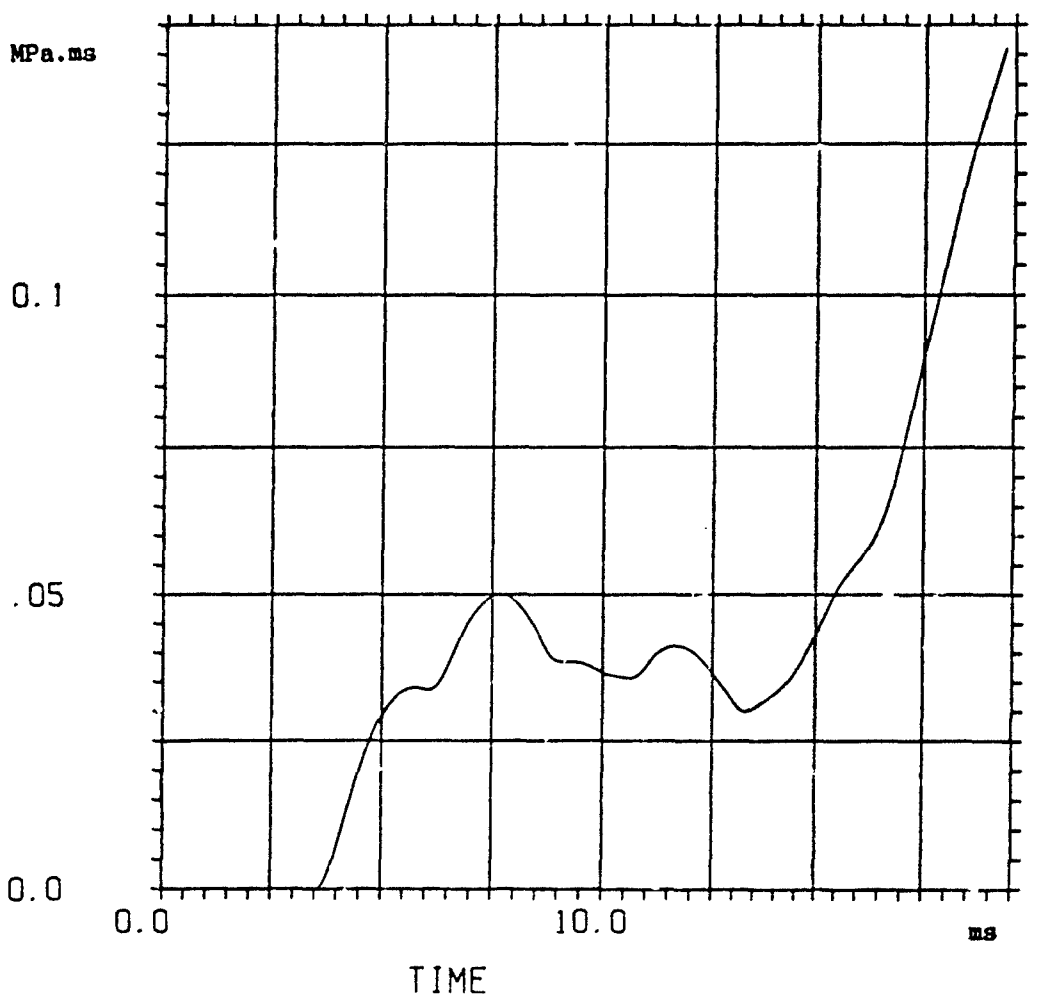

Fig 6c: Backwall Average Impulse
(With a frangible panel having a radius of 0.42m)

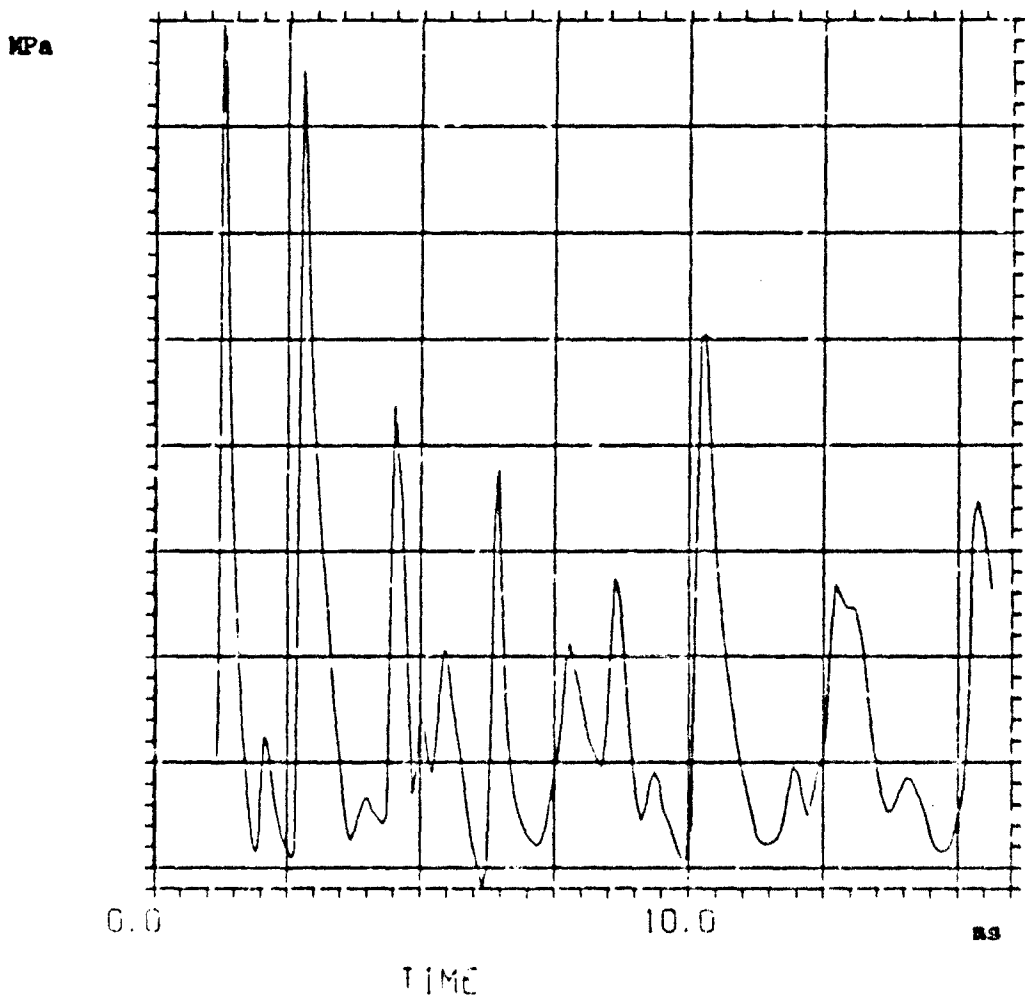

Fig 7a: Pressure Time History at the center of the cubicle
(Opening radius = 0.18m)

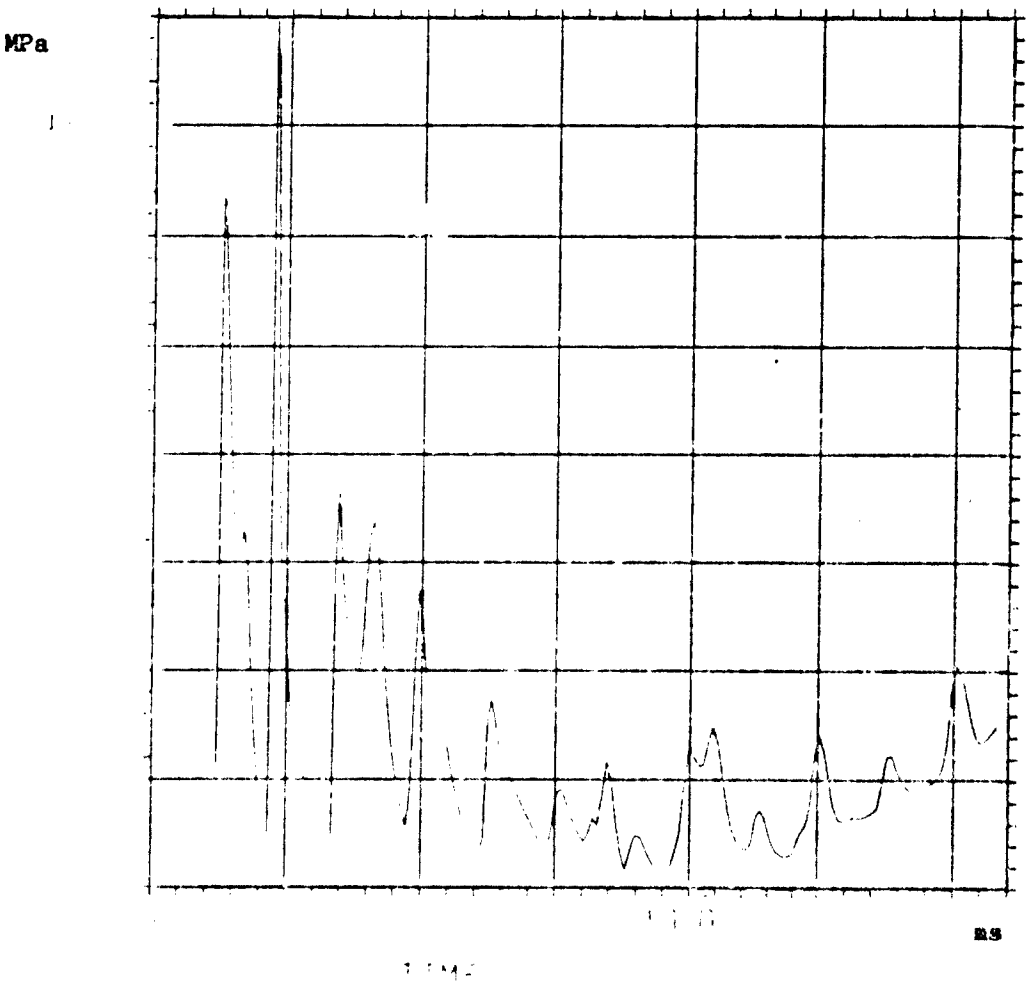

Fig 7b: Pressure Time History at the center of the cubicle
(Opening radius = 0.42m)

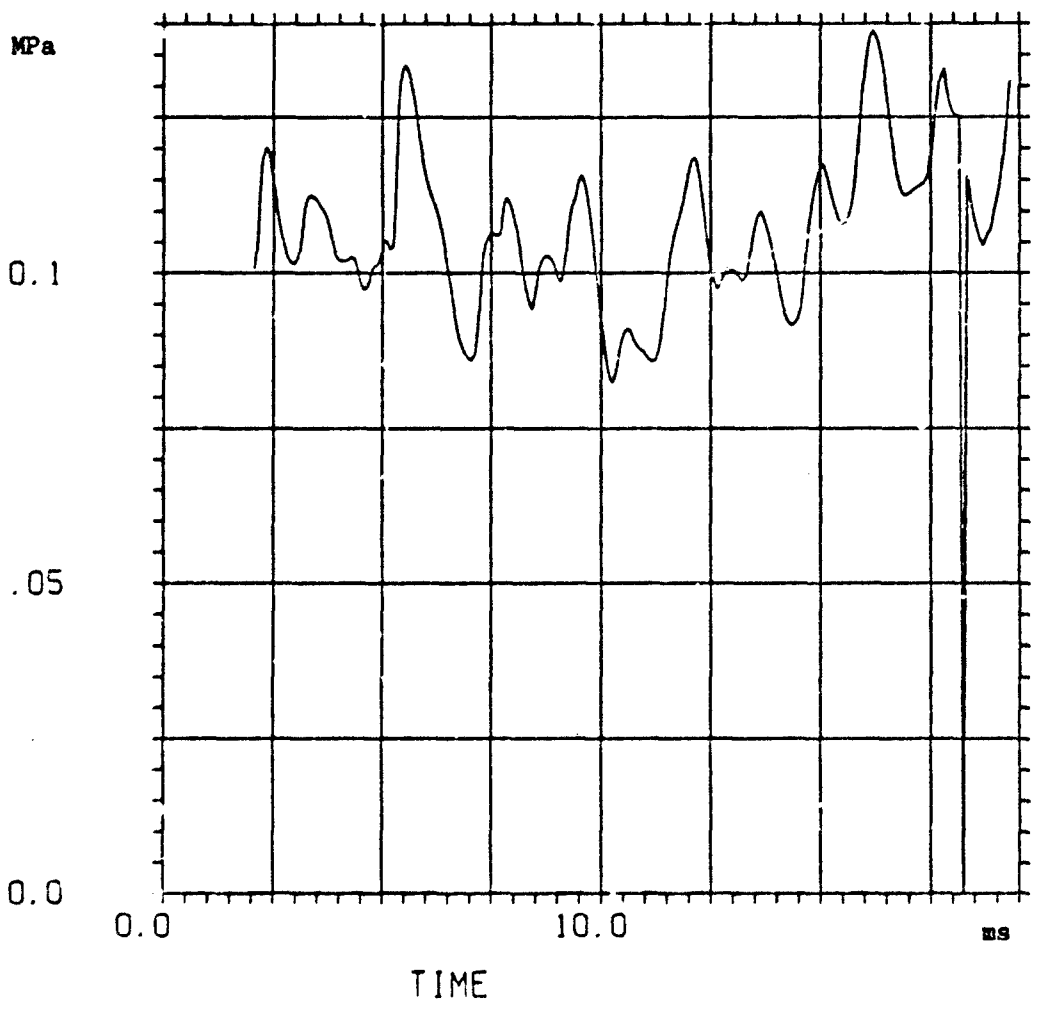

Fig 7c: Pressure Time History at the center of the cubicle
(With a frangible panel having a radius of 0.42m)

PROOF TEST OF AN AMMUNITION MAGAZINE HEADWALL AND DOOR USING HEST

BY

ARNFINN JENSSEN
NORWEGIAN DEFENCE CONSTRUCTION SERVICE
OSLO MIL/AKERSHUS
NORWAY

PRESENTED TO THE TWENTY-THIRD DOD EXPLOSIVES SAFETY SEMINAR
HYATT REGENCY HOTEL
ATLANTA, GEORGIA
9 - 11 AUGUST 1988

ABSTRACT

A proof test of an ammunition-magazine headwall and door is described. Above-ground ammunition magazines designed according to the NATO Safety Principles have to survive a specified design environment. The headwall and door have to withstand a blast overpressure of 700 kPa with an impulse of 28 kPa • s and a one kilogram piece of concrete with a velocity of 300 m/s. The High Explosives Simulation Technique (HEST) simulated the blast, and a 105 mm howitzer fired a sabot containing a concrete rod.

The paper describes the development of the VERTICAL HEST and how the necessary overburden and charge weight were determined using the tube technique.

The paper concludes that the VERTICAL HEST is suitable as a tool for proof testing and that safety distances are so small that the test can be carried out "in situ" in existing or new magazine areas. The VERTICAL HEST can therefore be used routinely as a part of the construction contracts for quality assurance.

CONTENTS

ILLUSTRATIONS

Table

1. INTRODUCTION

Recent safety regulations require that ammunition magazines be designed and sited to prevent propagation of detonation and spreading of fires from magazine to magazine if an accident occurs in one magazine.

NATO Safety Principles for the Storage of Ammunition and Explosives, AC/258-D/258, also states the design load for roof, side walls, and headwall (including the door) of acceptor magazines for different distances to donor magazines and the net explosives content (NEC) of neighboring donor magazines. National regulations may limit the NEC.

Distance, NEC, and orientation of the acceptor magazine to the donor magazine are the dominating parameters that determine the design load. Such loads can be determined case by case, but standardization requirements have led to a limited number of combinations (distance, NEC, and orientation). The end product has been a "standard" ammunition magazine, often of the igloo type (semicircular arch).

The use of pallets and containers has led to a requirement for larger doors and also rectangular cross section of magazines to allow more efficent use of floor space. A new 180 m^2 earth-covered magazine was designed to meet these new operational requirements and the following design loads for the headwall and door:

Air blast

Overpressure:	700 kPa
Duration (positive phase):	80 ms
Impulse:	28 kPa · s

Impact load

Mass:	1 kg concrete
Velocity:	300 m/s

As part of the quality assurance, it was decided to test the headwall and door. To save money a shortened magazine was built on a test site. The HEST (High Explosives Simulation Technique) was selected as a loading method.

2. OBJECTIVE AND JUSTIFICATION

The primary objective of the test was to investigate whether the headwall and door could resist the specified design load without being unduly strong.

The use of magazines that do not resist the design load may result in the total loss of assets in the magazine area (historically this has happened) and more damage to the surrounding area. On the other hand, an unduly strong magazine costs more than is necessary.

A secondary objective was to determine if the HEST could be used safely within a magazine area to allow "in situ" tests of magazines as part of the quality-assurance procedure. If magazines can be tested "in situ", the construction of a magazine only for testing can be avoided. It will also make it feasible for contracting and safety authorities to proof test "as built" structures at random before they are handed over to the user.

3. DESCRIPTION

The new box-shaped, earth-covered ammunition magazine is identified as "Overdekket ammunisjonshus - 180 m^2". A list of pertinent drawings is in Table 1. Applicable drawings are presented in Appendix A. Photographs are presented in Appendix B.

The design of the back wall, side walls, and roof is adapted from a German/US design (Ammunition storage, Munitions Lagerhaus, Typ MLH 180B). The front part of the magazine is of a standard Norwegian design with a short passageway between the blast/debris door and the fire door.

It is not practical to mount gaskets on the blast door to seal it sufficiently to avoid humid air leaking into the magazine. The fire door therefore serves as a "gas tight" door and also, together with the passageway, as heat/frost insulation.

A dehumidification unit is in a small room above the passageway. This room also serves as a fire and blast trap, avoiding costly blast valves in the headwall. The side walls in the passageway serve as load-bearing walls supporting the blast-door frame.

4. PREDICTIONS

This section presents the results expected from the proof testing of the headwall and door of an earth-covered ammunition magazine (earth-covered ammunition magazine - 180 m^2)

The main objective for the predictions here is to establish a basis for instrument settings. As a result, no attempt is made to validate the detailed design. That is the objective of the proof test.

TABLE I DRAWINGS

CONCRETE DRAWINGS

DRAWING NUMBER	DATE
A - 8601 - 1	22.05.86
A - 8601 - 2	22.05.86
A - 8601 - 3	22.05.86
A - 8601 - 4	22.05.86
A - 8601 - 5	22.05.86
A - 8601 - 6	22.05.86

STEEL DOOR DRAWINGS

DRAWING NUMBER	DATE
A - 8124 BL. 1 D	20.08.87
A - 8124 BL. 2 D	21.08.87
A - 8124 BL. 3 D	20.08.87
A - 8124 BL. 4 D	12.08.87
A - 8124 BL. 5 D	20.08.87
A - 8124 BL. 6 D	25.08.87

4.1 HEADWALL

4.1.1 Geometry and material properties

The overall geometry of the headwall is shown in Appendix A, Drawings 2 and 3. For simplified calculations, the headwall can be regarded as three rectangular slabs.

Without performing three-dimensional Finite Element Method (FEM) program calculations, it is difficult to get accurate results for deflections and strains. This uncertainty is due to whether or not the headwall slabs should be considered simply supported or fixed along their edges. A simplified sensitivity analysis is performed on the edge boundary condition, and expected results are given based on arguments in Section 4.3

The slabs on each side of the door will be critical, and thus, are treated here as follows:

Length: 1720 mm = 67.7" = 5.64'

Height: 4250 mm = 167.3" = 13.94'

Thickness: 400 mm = 15.75"

Concrete: C25; f'c = 3550 psi

Dynamic Increase Factor: 1.25; fdc' = 4400 psi

Reinforcement: KS 400, fy = 56 800 psi

Dynamic Increase Factor: 1.2; fdy = 68200 psi

No safety factors are applied because of the objective of the predicted results.

The geometry of the reinforcement used is as follows:

	Diameter		Spacing*			
	bar #	cal. mm	constr. mm	constr. mm	calculation in	mm	depth in
Blast side:							
Horizontal	5	15.31	16	150	5.82	142	1.5
Vertical	4	12.14	12	300	13.23	324	1.0
Tension side:							
Horizontal	5	15.31	16	150	5.82	142	1.5
Vertical	4	12.24	12	300	13.23	324	1.0

* Spacing adjusted because of variation between bar # terminology and Norwegian sizes, giving correct steel area.

4.1.2 Analysis

The computerized version of TM5 - 1300 (1969-version), BARCS, was used to perform the calculations and a sensitivity analysis to the boundary condition. Within the most likely "positive moment span," we get the following expected results:

Deflection: 0.025 - 0.1 inch (0.61-2.45 mm)

Strain: $1200 \cdot 10^{-6}$ - $4800 \cdot 10^{-6}$

Natural period: 3.5 - 5.0 ms

These predictions are based on an assumption (see Section 4.3) that the wall is almost fully fixed at the supports. The deflection would be 0.7 inch (17.15 mm) if the slab was simply supported.

4.2 STEEL DOOR

4.2.1 Geometry and material properties

The overall geometry of the steel door is shown on Drawings 10-13. As can be seen, the door is built up by vertical beams welded together flange to flange. The door is simply supported along all four edges.

Because of the relatively large horizontal span, each bean close to the center will get very little support from the beam next to it. This means that the response of a single beam will be representative for the maximum deflection to be expected.

Thus, we have a beam, simply supported at each end, with a total span of 2940 mm (115.75 inches). The beam is a NS HE-160B, having a flange width of 160 mm, a height of 160 mm, a web thickness of 8 mm, and a flange thickness of 13 mm. Its geometrical and material properties are as follows:

Moment of inertia: $I = 59.8\ in^4$

Weight: $M = 2.39$ lb/in

Steel quality: St - 37 - 2

Fy = 29000 psi

Fay = Fy · 1.1 = 31900 psi (average yield)

Fu = 53600 psi

Fau = Fu · 1.1 = 58960 psi (average ultimate)

Dynamic load factor is equal to 1.1:

Fdy - 35100 psi

Fdu = 64869 psi

4.2.2 Analysis

The analysis is performed according to John Healey et al., "Design of steel structures to resist the effects of HE explosions," Amman and Whitney, Aug. 1975.

The following are the results of the analysis and represent the maximum (midspan) results:

Deflection: = 0.64 inch (15.68 mm)

Strain: = $1450 \cdot 10^{-6}$

Natural period: Tn = 161 ms

4.3 DISCUSSION

4.3.1 Uncertainties

Prediction of the response of structures subjected to blast loading involves several uncertainties. In these predictions, the most uncertain factor is the boundary condition of the concrete headwall. As a result of the sensitivity analysis, it is concluded that the wall will respond almost as will a wall with fixed supports. This conclusion is based on the maximum concrete stress for the wall when it is fixed. The maximum stress is only slightly above fdc'. Taking this and the time from pouring to test into account, formation of plastic hinges seems unlikely.

4.3.2 Recommended gauge positions

The predictions are for wall and door centers (maximum response). It is recommended that at least two (if possible, three) displacement gauges be at each of these positions.

5. HEST DESIGN

The most convincing proof tests would be to build full-scale ammunition magazines, site them according to realistic siting situations, load them with the specified NEC, prime and detonate one magazine (donor), and observe what happens to the acceptor magazines and their contents. This might have to be repeated for different soil conditions (dry sand, saturated clay, rock). Examples of such full-scale tests are the ESKIMO I, II, and III tests.

A full-scale test requires a large test site, since noise from the detonation might cause window damage out to several kilometers. "In situ" testing is therefore often not possible. The cost of a full-scale test is also high and prevents routine quality-assurance tests from being carried out.

5.1 EARLIER HEST TESTS

Many load-simulation devices have been proposed and tested over the years. Some are described in reference 2. Of particular interest in reference 2 is a paper entitled "A status and capability report on nuclear airblast simulation using HEST." Reference 3 describes a test using HEST where the required peak overpressure was 350 kPa (50 psi).

GRABS (Giant Reusable Airblast Simulator) described in reference 1 and DABS (Dynamic Airblast Simulator) described in reference 4 are variants of HEST.

The FOAM HEST was used to load the roof of an ammunition-storage magazine with a load of 5600 kPa (800 psi) and 17.5 kPa · s (2500 psi · ms). The plan for this test is described in reference 5.

An example of how the HEST is applied and notations used is shown in Figure 1.

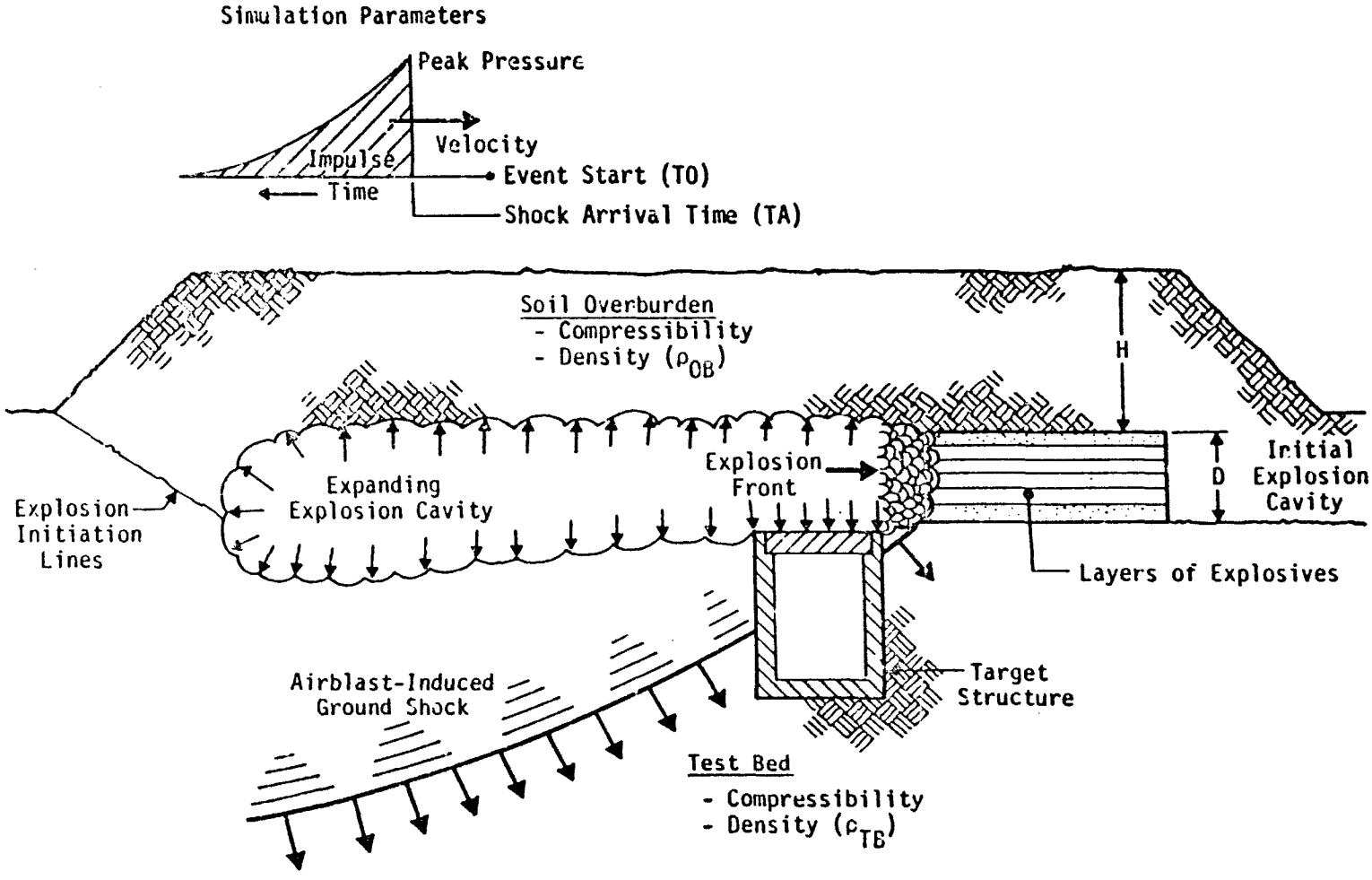

Figure 1. HEST. Use and notations.

5.2 COMPUTER CODE CALCULATIONS

Mr. Edward Seusy, at the Air Force Weapons Laboratory, has developed a HEST design lockup code. The HEST design is done iteratively, changing the loading density (cavity depth, charge weight) and overburden height, until an acceptable match to the described pressure-time history is found.

The lockup code is not validated for a VERTICAL HEST planned to be used to load the headwall and door of the new ammunition magazine. Nevertheless, the code was used for a preliminary design. These calculations and practical considerations resulted in a chosen "cavity depth" of 1.8 m.

5.3 THE TUBE TECHNIQUE

The peak pressure and gas pressure (chamber pressure) in a closed or partly closed vessel is basically determined by the loading density: kilos of HE per m^3. The impulse, on the other hand, is determined by the speed at which the reaction products are vented (pressure release). For the HEST, the venting is primarily determined by the mass of the overburden.

In principle, a one-dimensional physical model can therefore be used to determine the cavity depth (D) and overburden (H) to obtain the desired chamber pressure and impulse. (In fact, the lockup code is also a one-dimensional model.) Two tubes as shown in Figure 2 were used to determine

- Loading density.
- Depth of overburden.

The tubes (Figure 2) were used in a horizontal position to simulate a VERTICAL HEST.

Five blast gauges were installed in a flange plate at the end of the tube. This plate simulates the door and headwall of the ammunition magazine. The results from these tests and some other test results are presented in Figure 3.

Figure 4 shows results for low loading densities. The observed impulse versus depth of overburden is shown in Figure 5. One observation made early in the test series was that the tube should not extend outside the overburden because that would influence the observed impulse dramatically.

Based on these findings, the following were decided:

- Loading density: 0.22 kg/m^3
  Using Detonex 80, a Swiss detonating cord with 80 gram PETN per metre.

- Depth of sand overburden (1610 kg/m^3): 0.5 m.

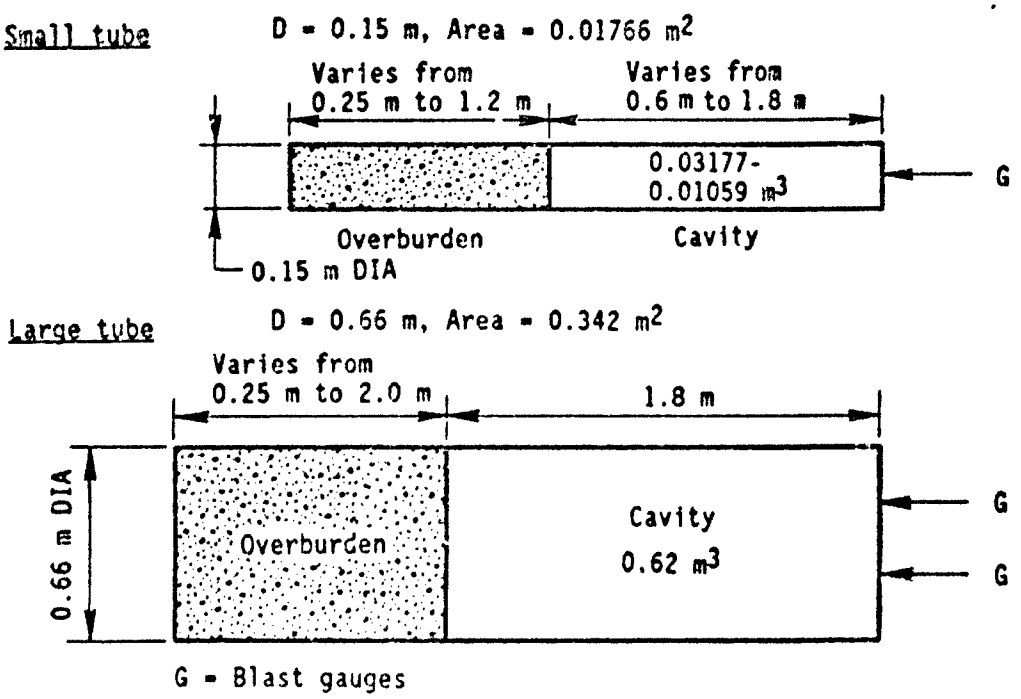

Figure 2. Small and large tube

The linear scale of the tube tests is 1:1 in the axial direction, which is the direction normal to the headwall. In a plane parallel to the headwall, however, the scale is small (1:53 and 1:12). The volume is also small, and the distribution of the primacord could not be simulated correctly, although the loading density was correct. The recorded pressure-time history at the end of the tube simulating the headwall differed across the tube.

Three recordings taken from the same shot in the small tube are shown in Figure 6. These uncertainties led to a decision to conduct a "mini wall" test before the proof test of the ammunition-magazine headwall and door to validate the results from the tube tests.

5.4 VALIDATION USING "MINI WALL"

The "mini wall" (4.1 m × 2.8 m) was built adjacent to the ammunition magazine. The layout at the test site is shown in Figure 7. The two structures and the primacord array are depicted in Appendix B. A sketch of the cavity and overburden is presented in Figure 8. Fifty-five metres of Detonex 80 (4.4 kg PETN), divided into 20 strings hung from the roof in the middle of the 19,95 m^3 cavity, were used.

Eleven pressure gauges were mounted in the wall at similar locations as the pressure gauges in the magazine headwall. A recorded pressure-time history is shown in Figure 9.

There was some scatter in the results with a somewhat low impulse but fairly accurate chamber pressure and positive duration. On the whole, the "mini wall" test showed satisfactory results.

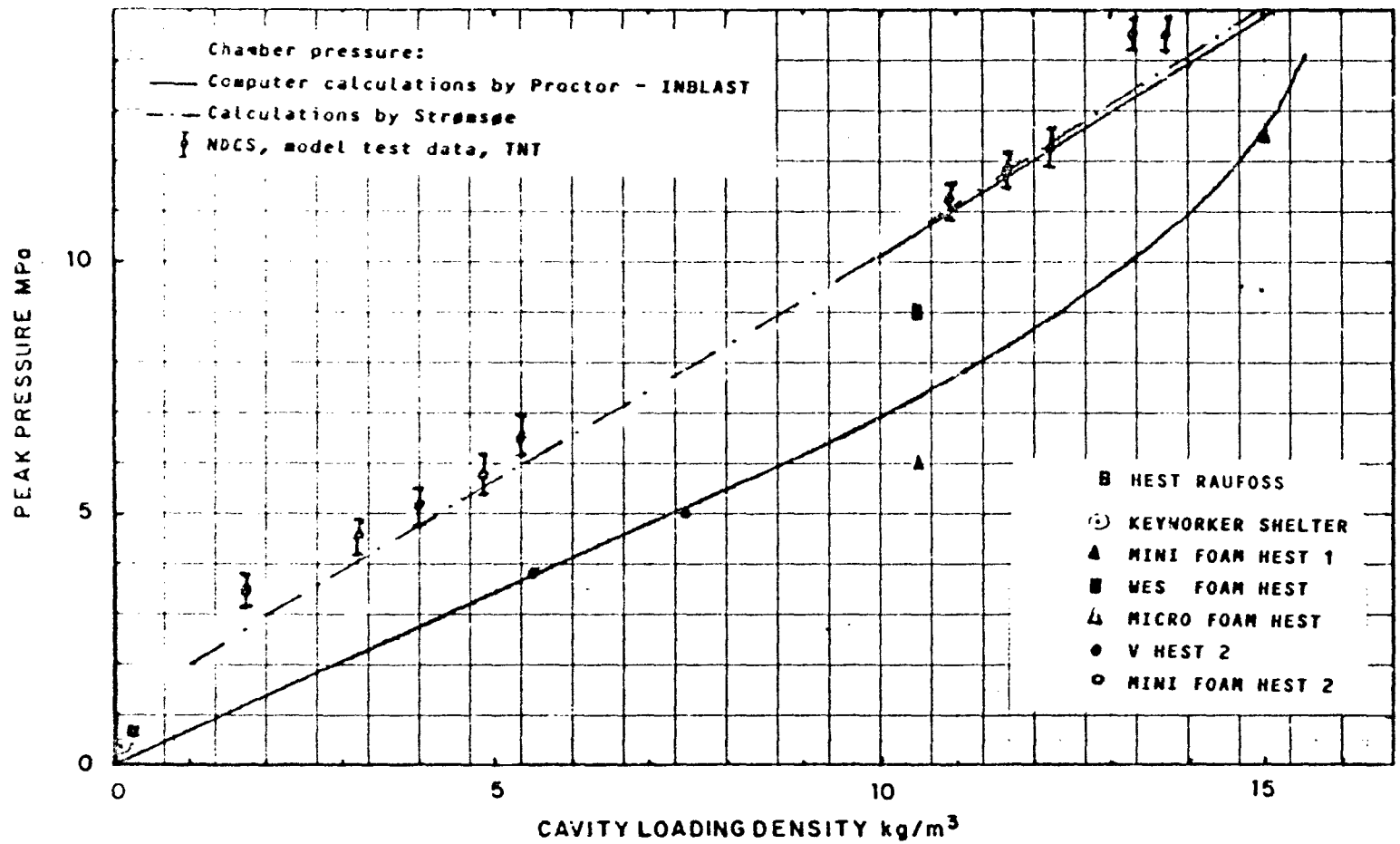

Figure 3. Chamber pressure versus loading density.

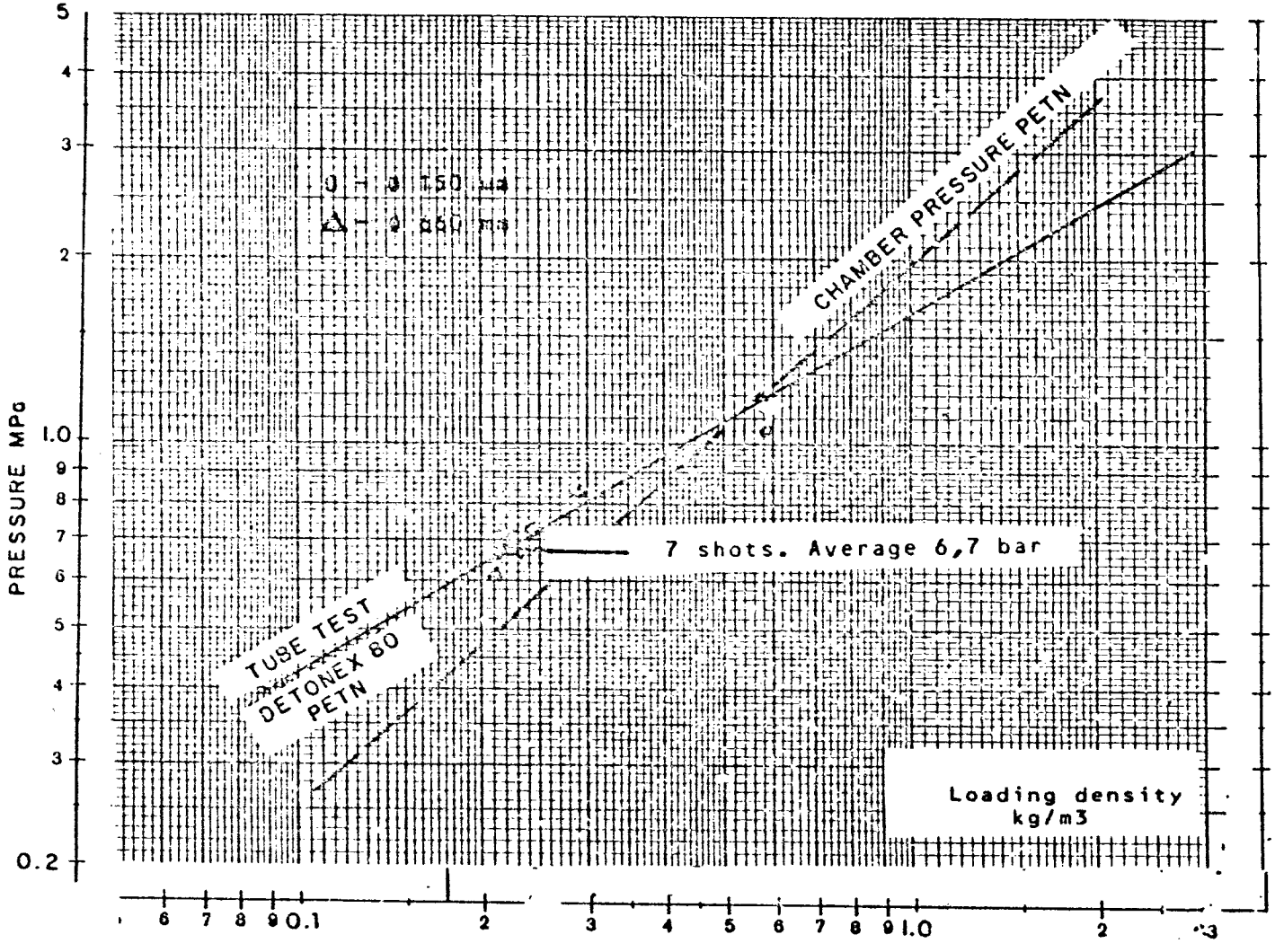

Figure 4. Chamber pressure versus loading density.

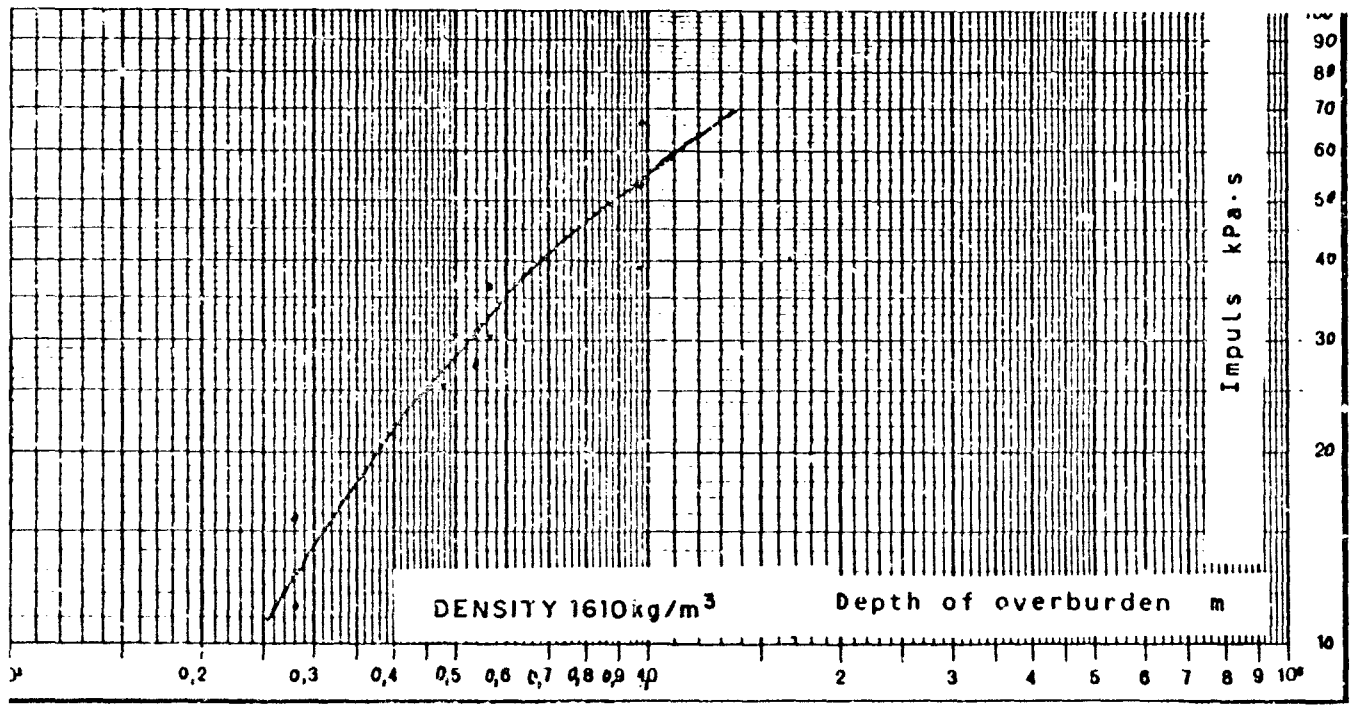

Figure 5. Impulse versus depth of overburden.

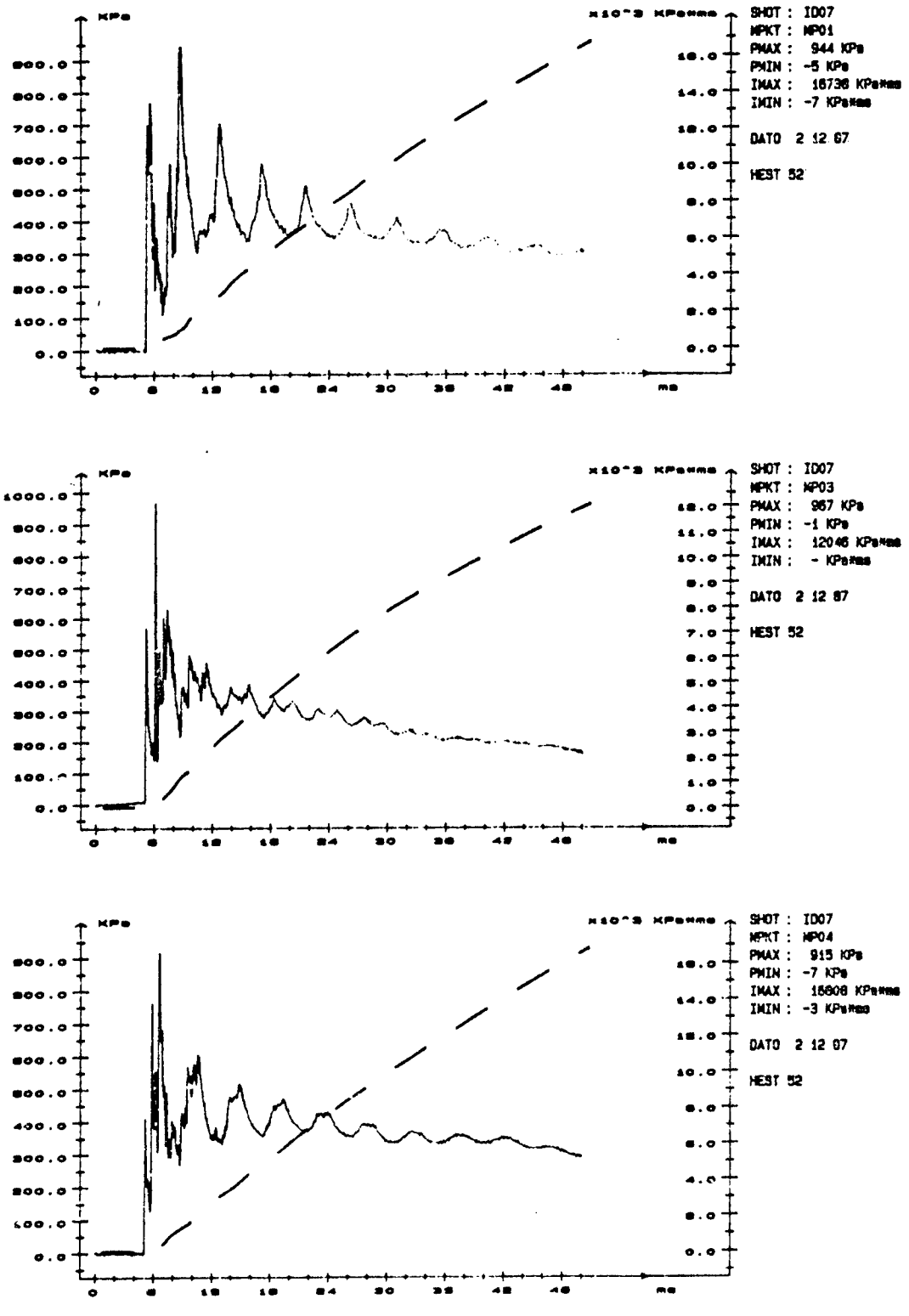

Figure 6. Pressure time histories in the small tube.

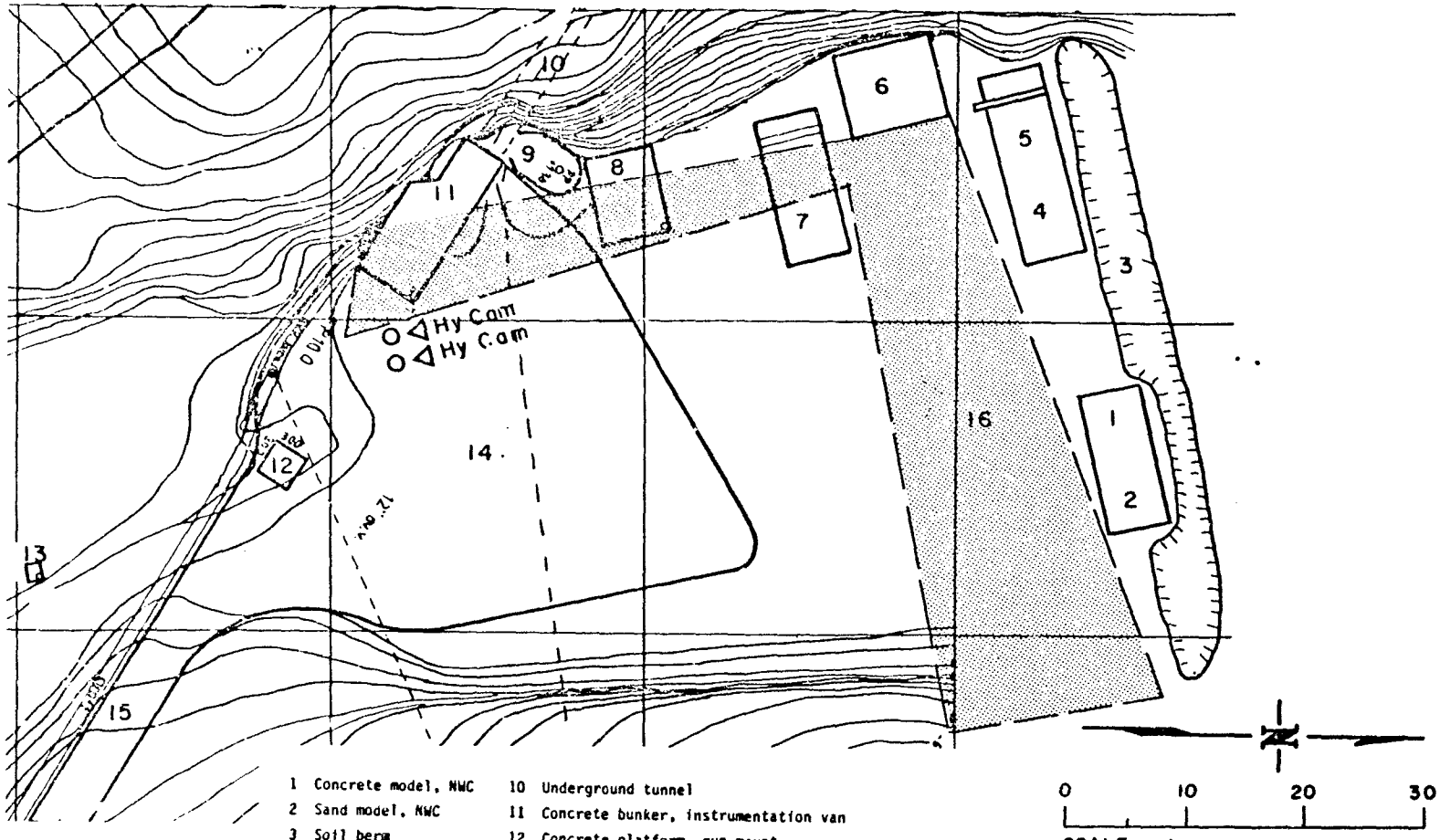

1 Concrete model, NWC
2 Sand model, NWC
3 Soil berm
4 Concrete platform
5 Miniwall
6 Ammunition magazine
7 Concrete platform
8 Concrete bunker
9 Concrete bunker
10 Underground tunnel
11 Concrete bunker, instrumentation van
12 Concrete platform, gun mount
13 Observation bunker, concrete
14 Asphalt pad
15 Access road
16 Shaded area shows main debris sectors for the headwall test

Figure 7. Layout at the test site.

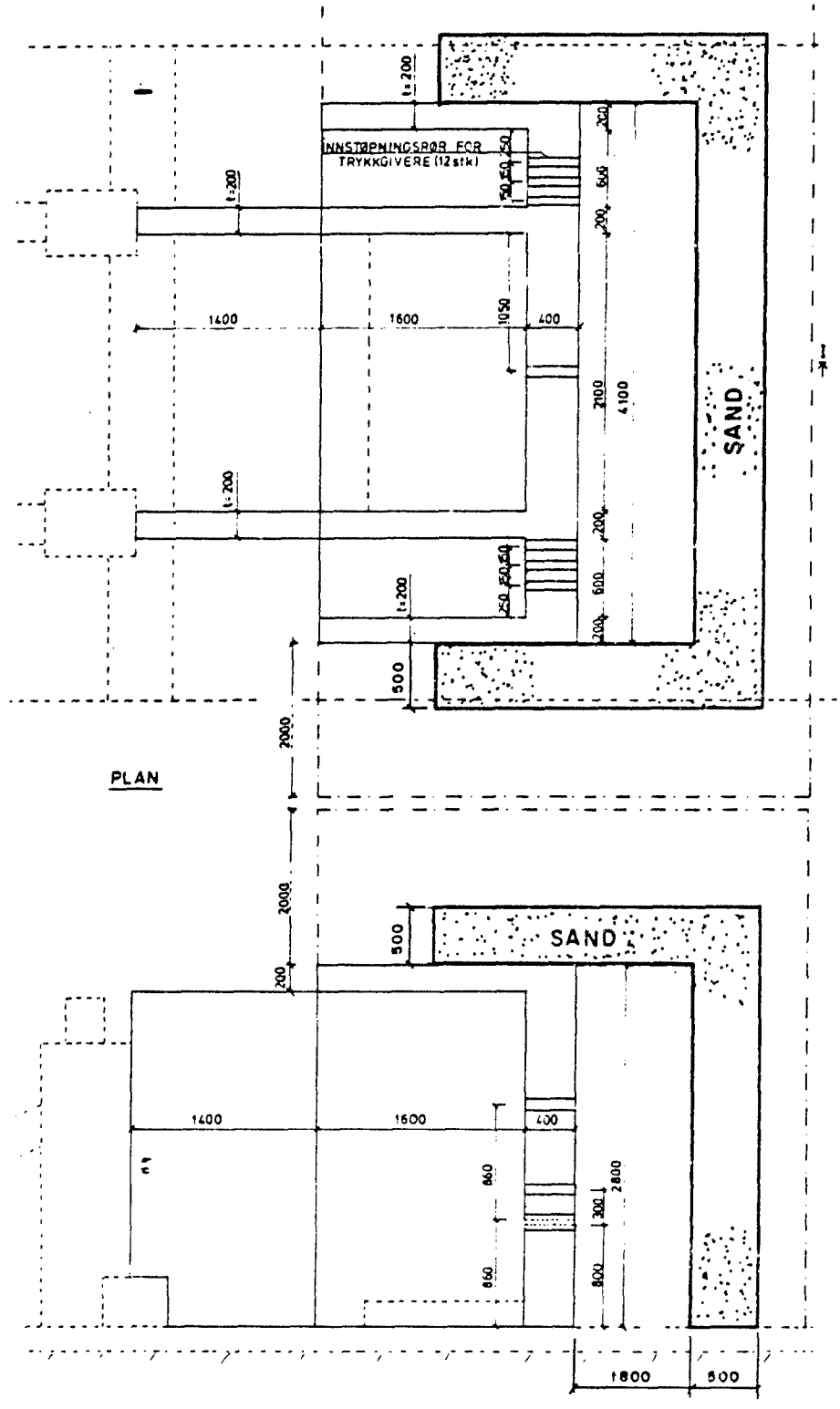

Figure 8. Sketch of cavity and overburden "mini wall".

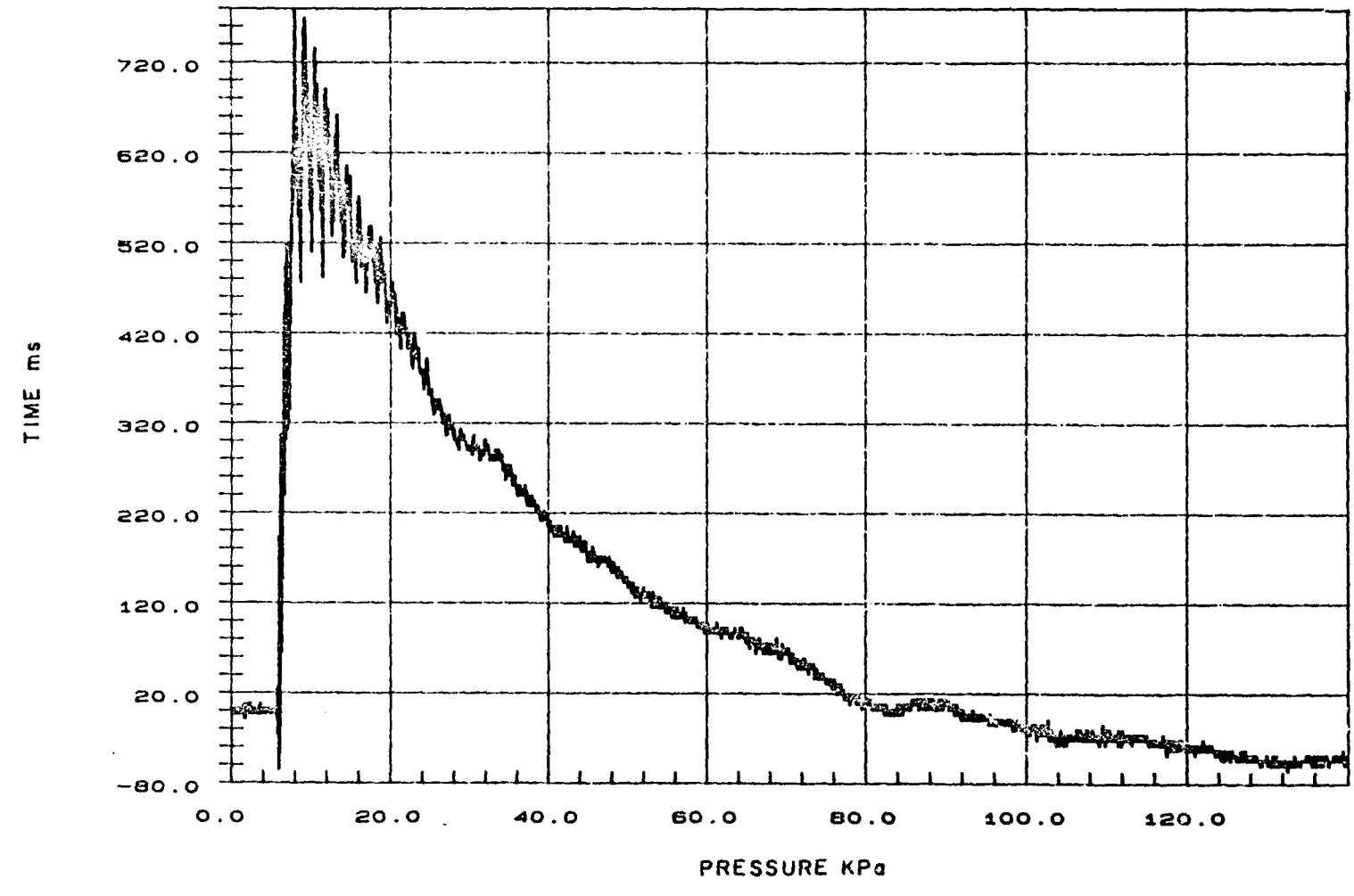

Figure 9. Recorded pressure time history - "mini wall".

5.5 FINAL DESIGN

Based on the results from the "mini wall" test, it was decided to go on with the same cavity depth, loading density, and overburden for the magazine test.

6. TEST SETUP

A sketch of the test setup with cavity and overburden is shown in Figure 10. Eleven pressure gauges were mounted in the headwall and four strain gauges on the door. External cameras are shown in Figure 7.

The explosive charge consisted of 44 strings of Detonex 80, each 5.5 m long. The total weight of PETN was 19.6 kg. The string arrangement is depicted in Appendix B.

7. RESULTS OF HEST TEST

7.1 LOAD

The blast load observed varied a little over the headwall surface, but a good representation of the pressure-time history is shown in Figure 11. Again the impulse is low-about 22 kPa • s instead of 28 kPa • s.

7.2 RESPONSE OF THE CONCRETE STRUCTURE

No cracks were observed in the headwall. Some spalling was observed in the floor in front of the frame of the fire door. This was obviously cosmetic repair patches made by the contractor. Some hairline cracks were observed in the floor, starting from the side walls of the passageway that also provides load-carrying walls for the headwall.

7.3 DOOR RESPONSE

The fire door jammed slightly because of the concrete spalling in front of the door frame. The floors in the passageway and magazine are at the same level, which means that the tolerance between the floor and door is very small. A small doorstep (10 mm) is recommended mainly to avoid practical problems during daily operation.

The blast door had received a permanent midspan deflection of 25 mm. This is more than was calculated. The lower door frame (doorstep) was raised about 5 mm at midspan. After the test both leaves could be opened and closed without problems.

The strain gauge records showed that the door had yielded. These records also showed that the door had vibrated violently with the same frequency (about 1000 Hz) as the reverberation of the blast wave in the cavity. Since the natural frequency of the door in question is about 6 Hz, forced vibration with a frequency of about 1000 Hz will not do any harm to the main structure.

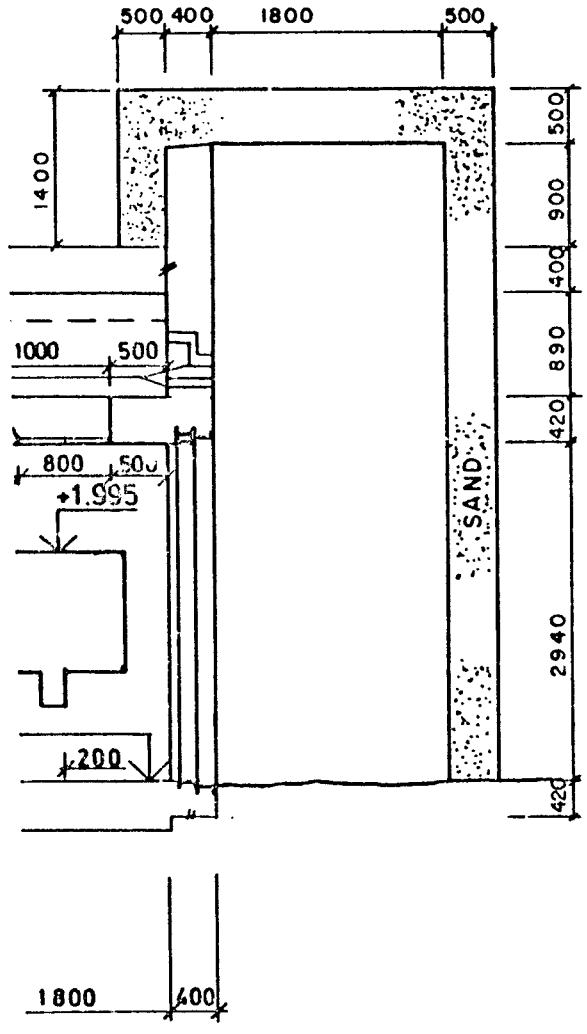

Section II-II

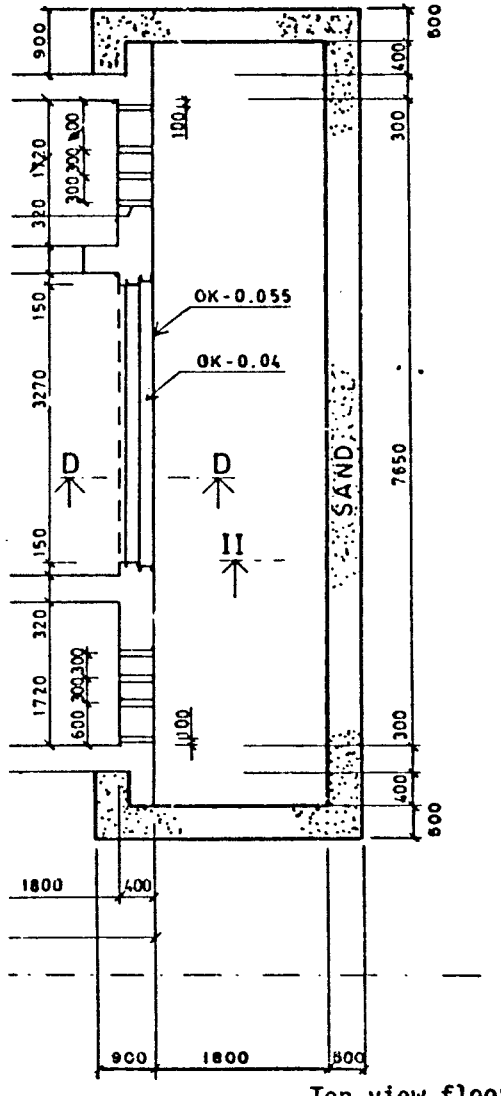

Top view floor

Figure 10. Cavity and overburden for magazine headwall test.

1527

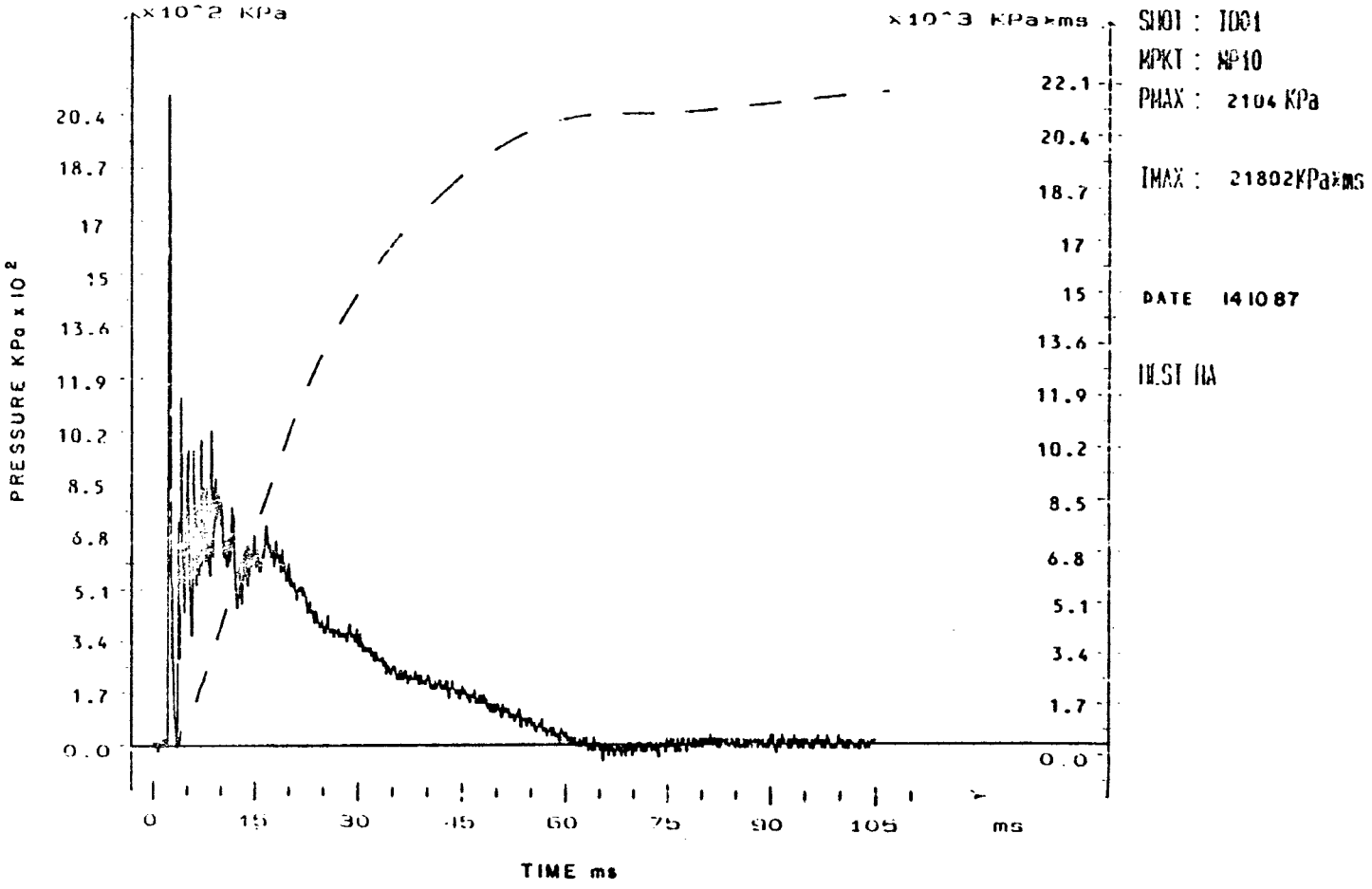

Figure 11. Recorded pressure - time history - headwall test.

Other doors with higher natural frequencies and hinges and locking mechanisms may be subjected to an unrealistic loading caused by reverberation when using the plain-air HEST.

7.4 BLAST TRAP

The room for the dehumidification unit acted perfectly as a blast trap (expansion chamber). The light hatch in the floor (roof of the passageway) showed no sign of damage, and the standing aluminium cylinders on the floor, located where the dehumidification unit will be mounted, had not tipped over or moved.

8. BLAST AND DEBRIS HAZARD

The debris throw, as seen by the technical cameras, is shown in Figures 12 and 13 for the "mini wall" and Figure 14 for the headwall test.

Based on the high-speed film, the maximum velocity of the overburden is about 28 m/s for both tests. The wooden framework was thrown out to a maximum of about 60 m to the front and side as shown by the shaded areas in Figure 7. The instrumentation van was located under a concrete roof (open bunker) as shown in Figure 7. Some personnel were also standing there. The noise was uncomfortable but tolerable. The debris is depicted in Appendix B.

9. DEBRIS LOAL TEST

9.1 TEST SETUP

To simulate a 1-kg piece of concrete with a velocity of 300 m/s, a 1-kg concrete "rod" was fired from a 105-mm howitzer using a sabot. A sketch of the concrete projectile and sabot is shown in Figure 15. The concrete rod was not reinforced and proved to be fairly weak. It was therefore replaced by an aluminium rod. The mass as of the rods and sabots are as follows:

Concrete rod:	0.886 ± 0.021 kg
Aluminium rod:	1.095 ± 0.020 kg
sabot total:	0.850 kg
sabot base plate:	0.610 kg

Some trial firings were conducted to establish the amount of propellant necessary to reach the correct velocity.

The velocity was measured using a Doppler radar. Figure 16 shows the velocity-distance diagram from one firing. It should be noted that the velocity of the rod drops faster than for a projectile. The muzzle velocity should not be used as the criterion velocity, but rather, the velocity at a distance corresponding to the firing range should be used.

After some experimentation, it was possible to obtain reproducible velocities between 290 m/s and 310 m/s at the 40-m range. A sketch of

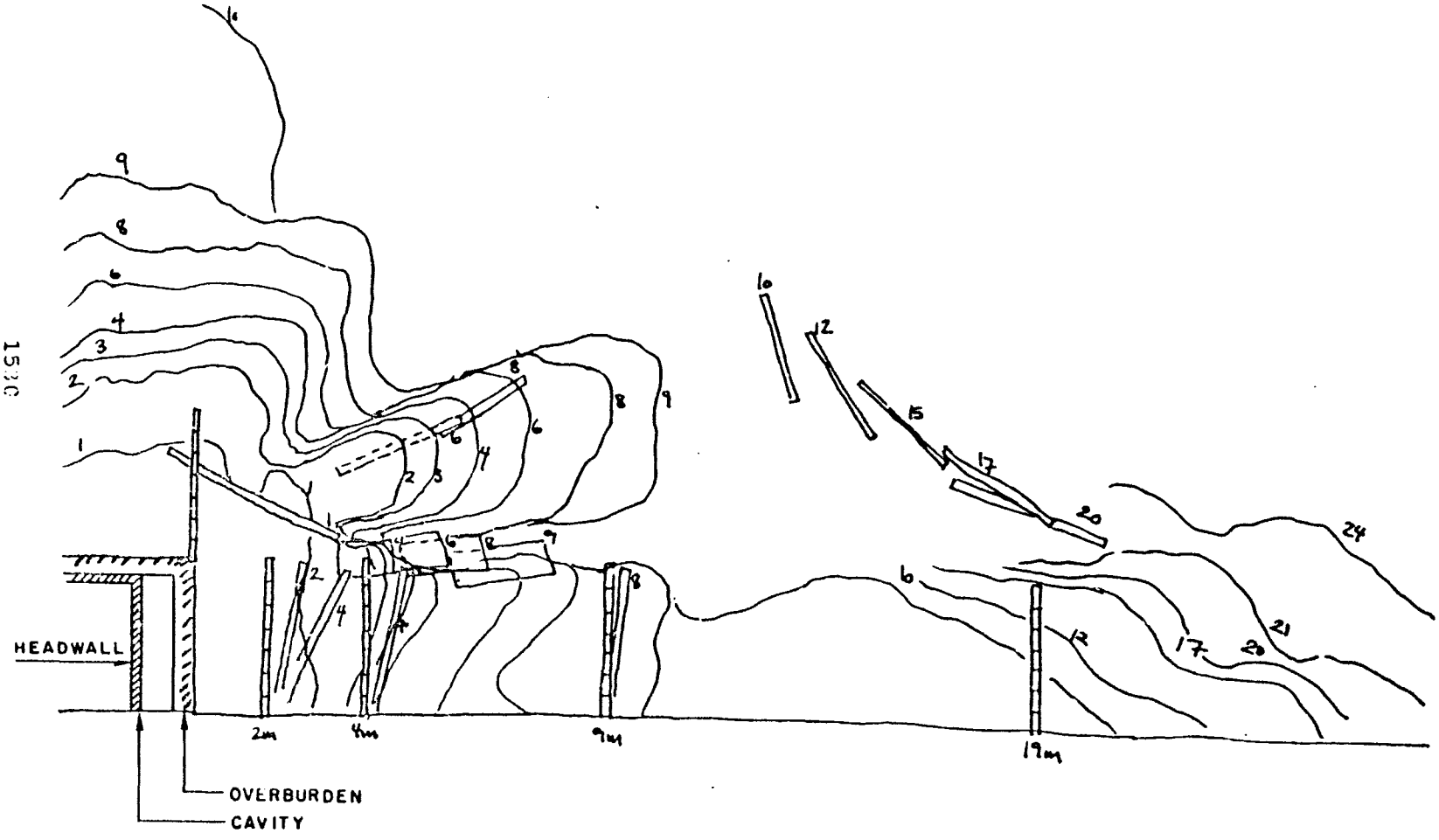

Figure 12. Mini wall-25 frames per second. Frame interval: 40 ms.

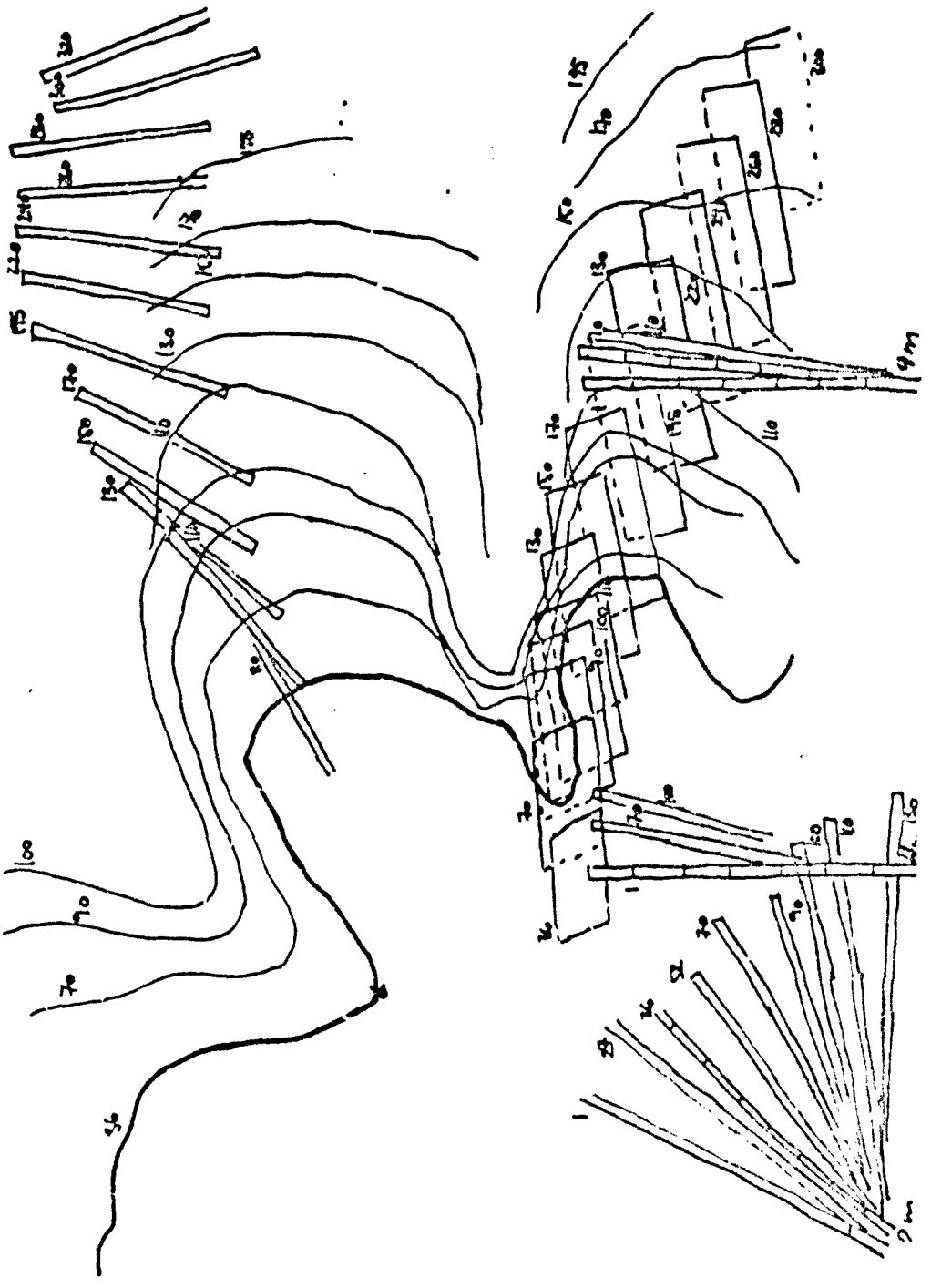

Figure 13. Mini wall-400 frames per second. Frame interval: 2.5 ms.

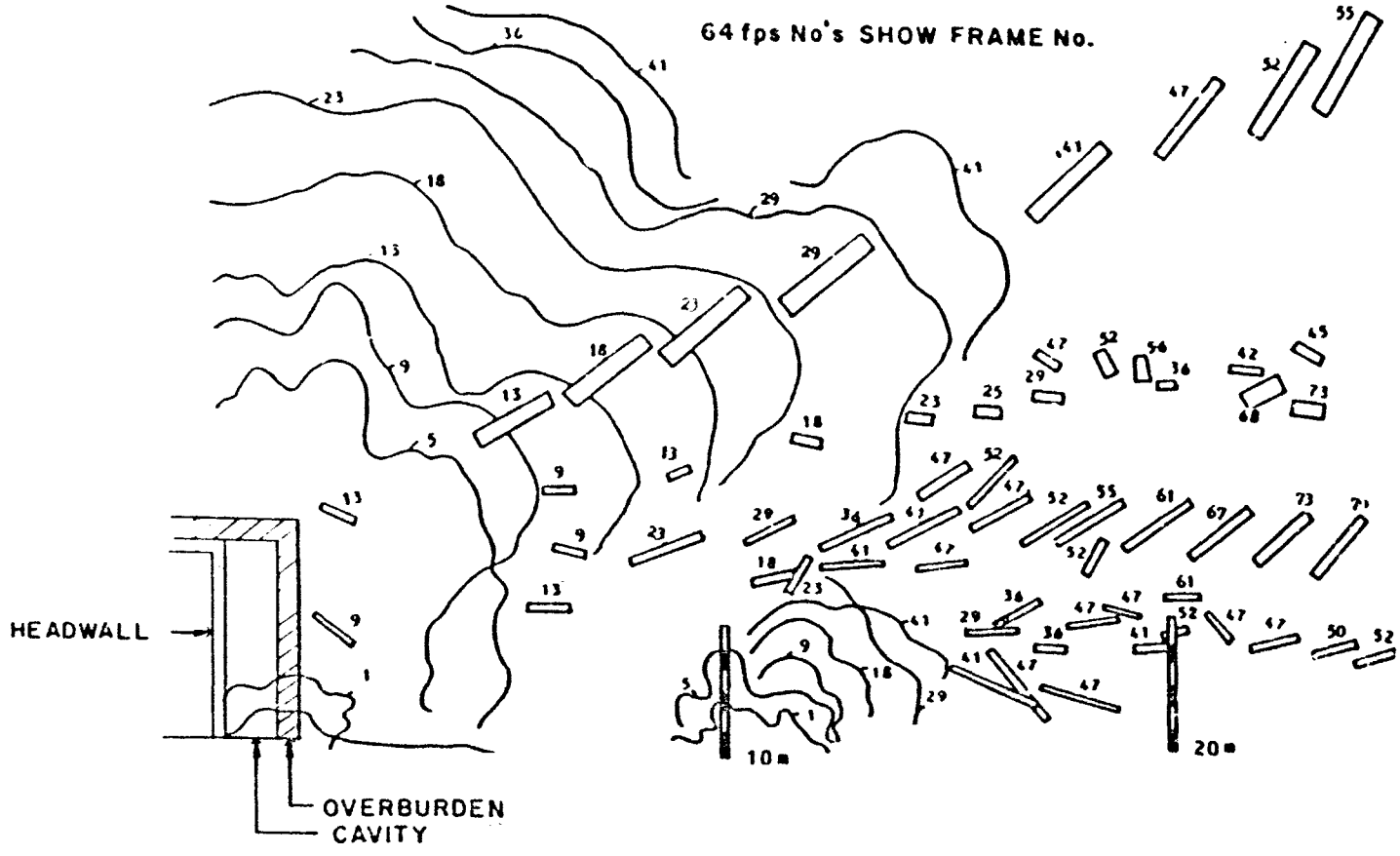

Figure 14. Headwall test-64 frames per second. Frame interval: 15.62 ms.

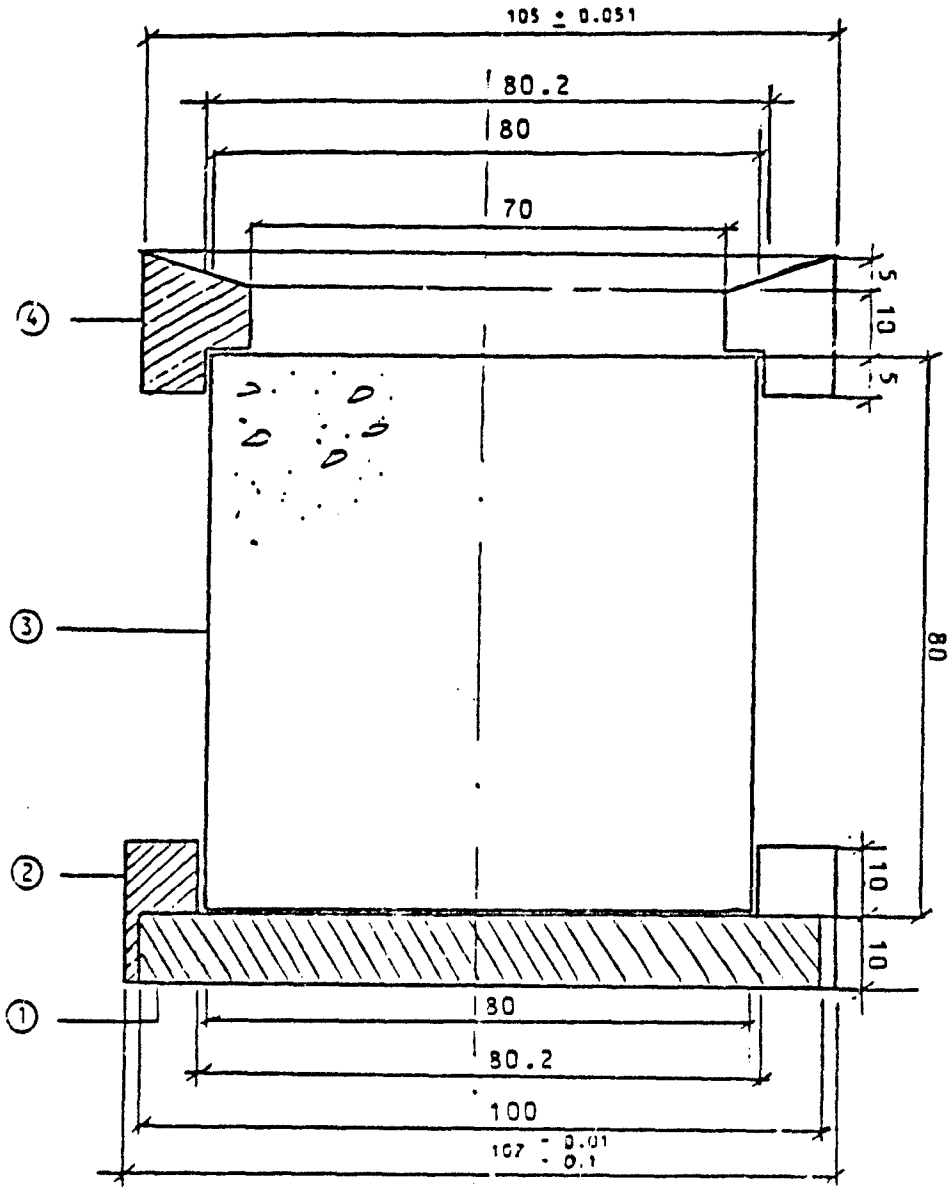

1 : Base plate steel
2 Telfon seal
3 Concrete projectile
4 Telfon seal and support - four parts

HEST PROJECTILE AND SABOT

Figure 15. Concrete rod and SABOT.

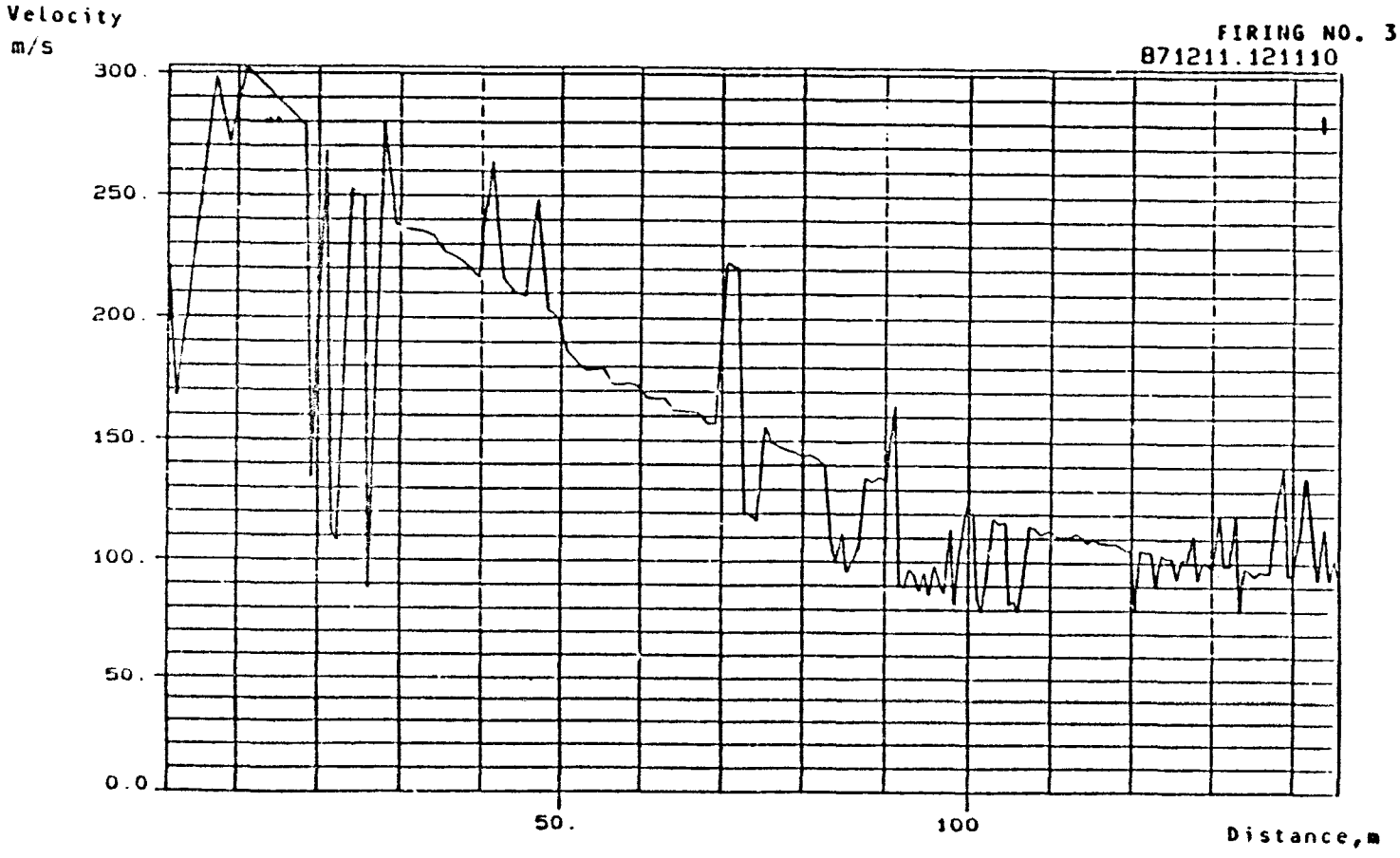

Figure 16. Velocity-distance diagram for aluminium projectile.

the test setup is shown in Figure 17. The howitzer and rod with sabot are depicted in Appendix B.

9.2 RESULTS

The concrete rods were crushed upon impact with the concrete wall. In fact, the sabot base plate did more damage, making a dent about 5 mm deep. The aluminium rods made a small crater in the wall about 200 mm in diameter and 40 mm deep. A circular plate was punched out of the outer skin of the blast door and pushed into the space between the outer and inner skin without damaging the inner skin. If an aluminium rod hit the door just where the locking mechanism is welded to the door, the lock mechanism might jam.

Damage to the wall and door is depicted in Appendix B.

10. CONCLUSIONS

a. The headwall withstood the defined load with a large margin. The rebar lacing in the floor and roof of the passageway could be removed. The door withstood the defined load with some permanent deformation. The room for the dehumidification unit worked as a blast trap as intended.

b. It was demonstrated that the VERTICAL HEST can be used "in situ" as a tool for proof testing or quality assurance.

c. Unreinforced concrete "projectiles" are not strong enough.

11. RECOMMENDATIONS

It is recommended that a VERTICAL HEST be standardized for the testing of magazine headwalls and doors such that HEST design using the lockup code or the tube technique for each test can be avoided. It is also recommended that proof- and quality-assurance testing be included in the NATO Safety Principles AC/258-D/258 as a requirement.

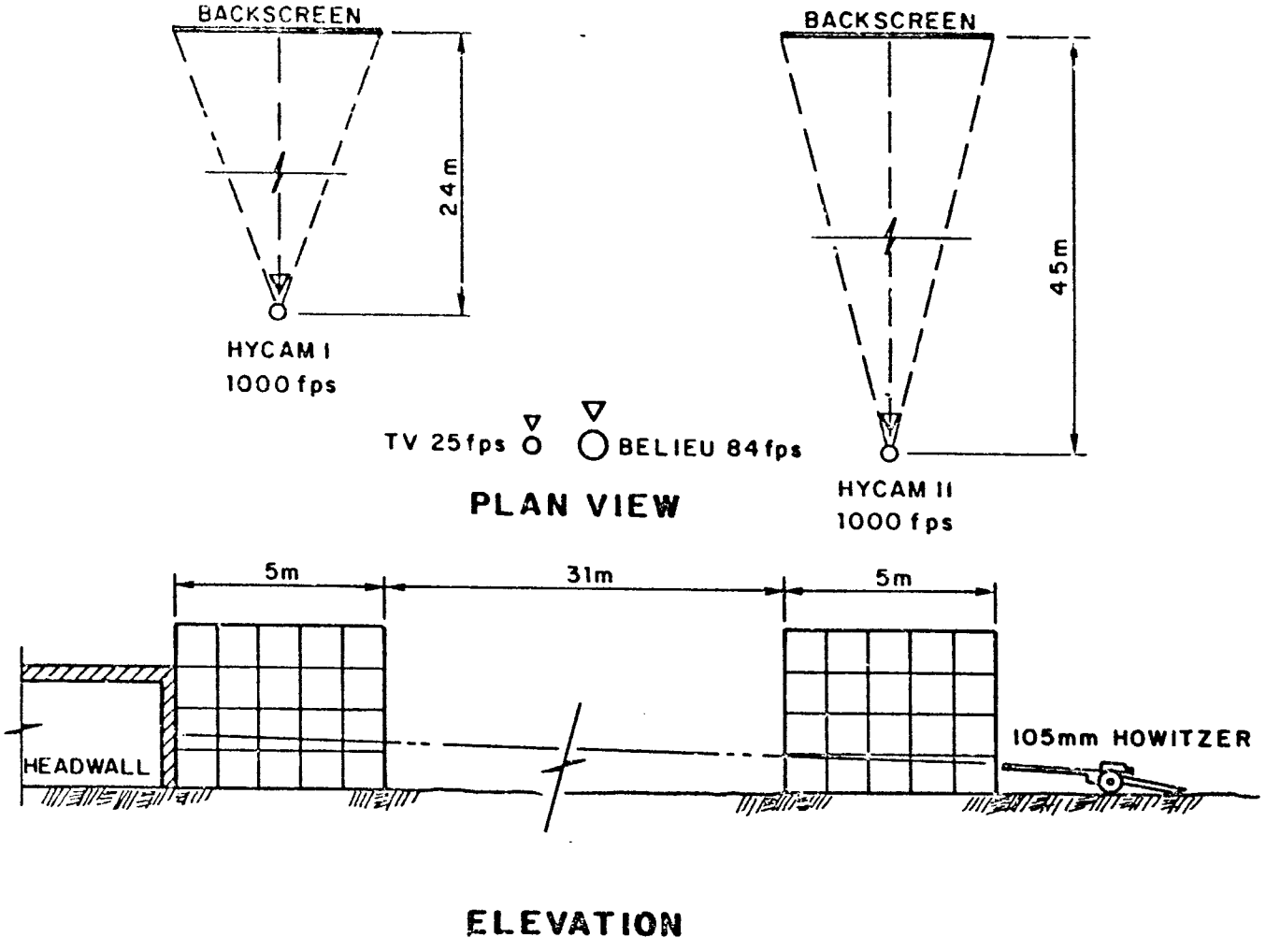

Figure 17. Headwall - horwitzer - cameras and backscreens.

REFERENCES

1. M.A. Plamondon: Utilization of the Grabs to Investigate Structure Media Interaction Phenomena Associated with Structures Buried in Soil. 4th International Symposium on Military Application of Blast Simulation (MABS). September 1974.

2. Proceedings of the nuclear blast and shock simulation symposium. November 1978.

3. S.C. Woodson, T.R. Slawson, and R.L. Holmes: Dynamic test of a corrugated steel keyworker blast shelter. Waterways Experiment Station, Technical Report SL-86-6. May 1986.

4. Airblast Simulator Design. AFWL-TR-77-106 Air Force Weapons Laboratory. July 1978.

5. Robert N. Murtha: The ESKIMO VII test plan. TM-51-83-12 Naval Civil Engineering Laboratory. August 1983.

APPENDIX A. DRAWINGS

"MINI WALL"

Drawing 1 "Mini wall"

AMMUNITION MAGAZINE

Drawing 2 Top view floor

Drawing 3 Section II - II

Drawing 4 Section I - I

Drawing 5 Side wall

Drawing 6 Section C - C

Drawing 7 Vertical projection, front wall

Drawing 8 Front view, section B - B

Drawing 9 Front view, section A - A

STEEL DOOR

Drawing 10 Steel door seen from outside

Drawing 11 Steel door seen from inside

Drawing 12 Door-leave

Drawing 13 Section A - A

A - 8601

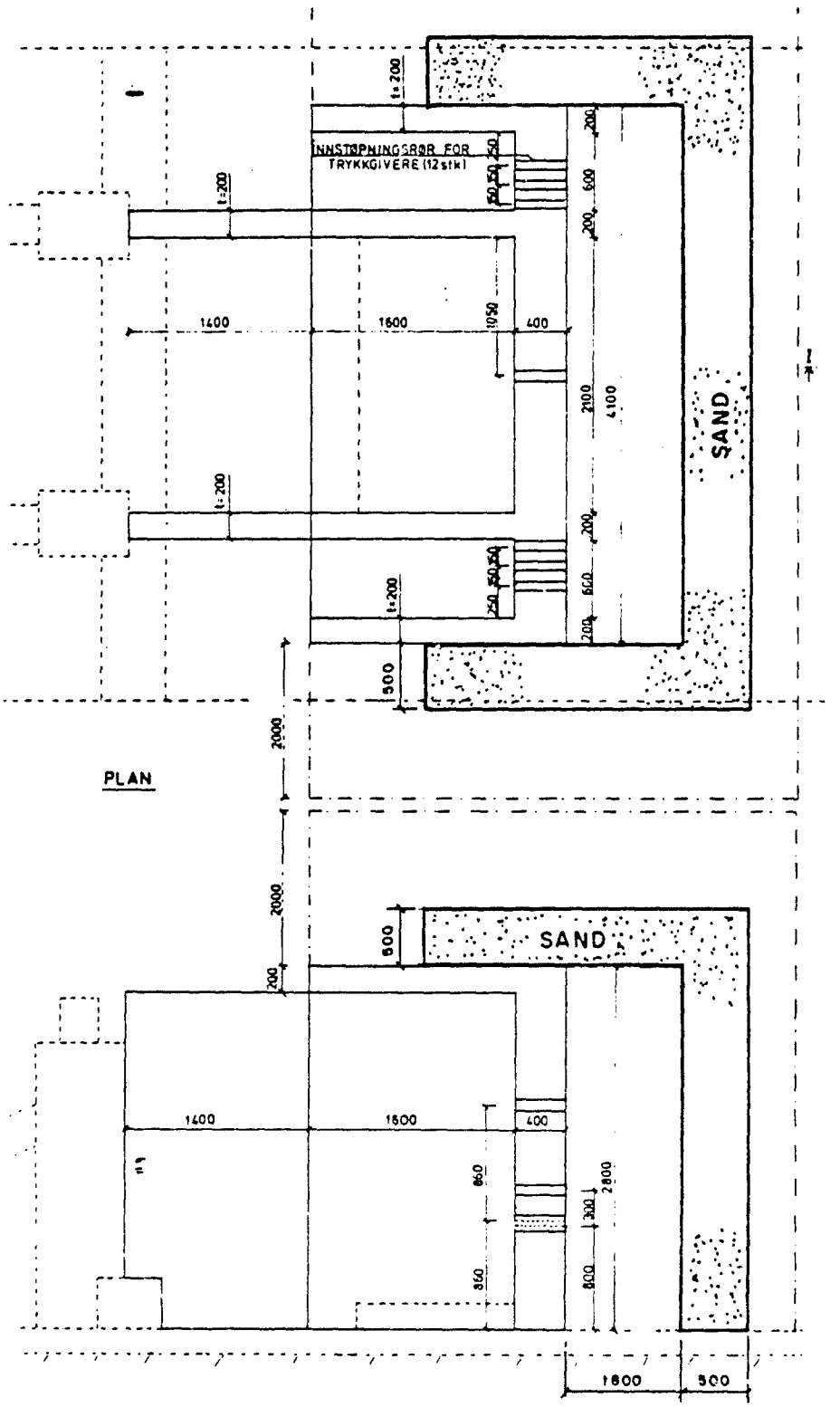

Drawing 1. Mini wall.

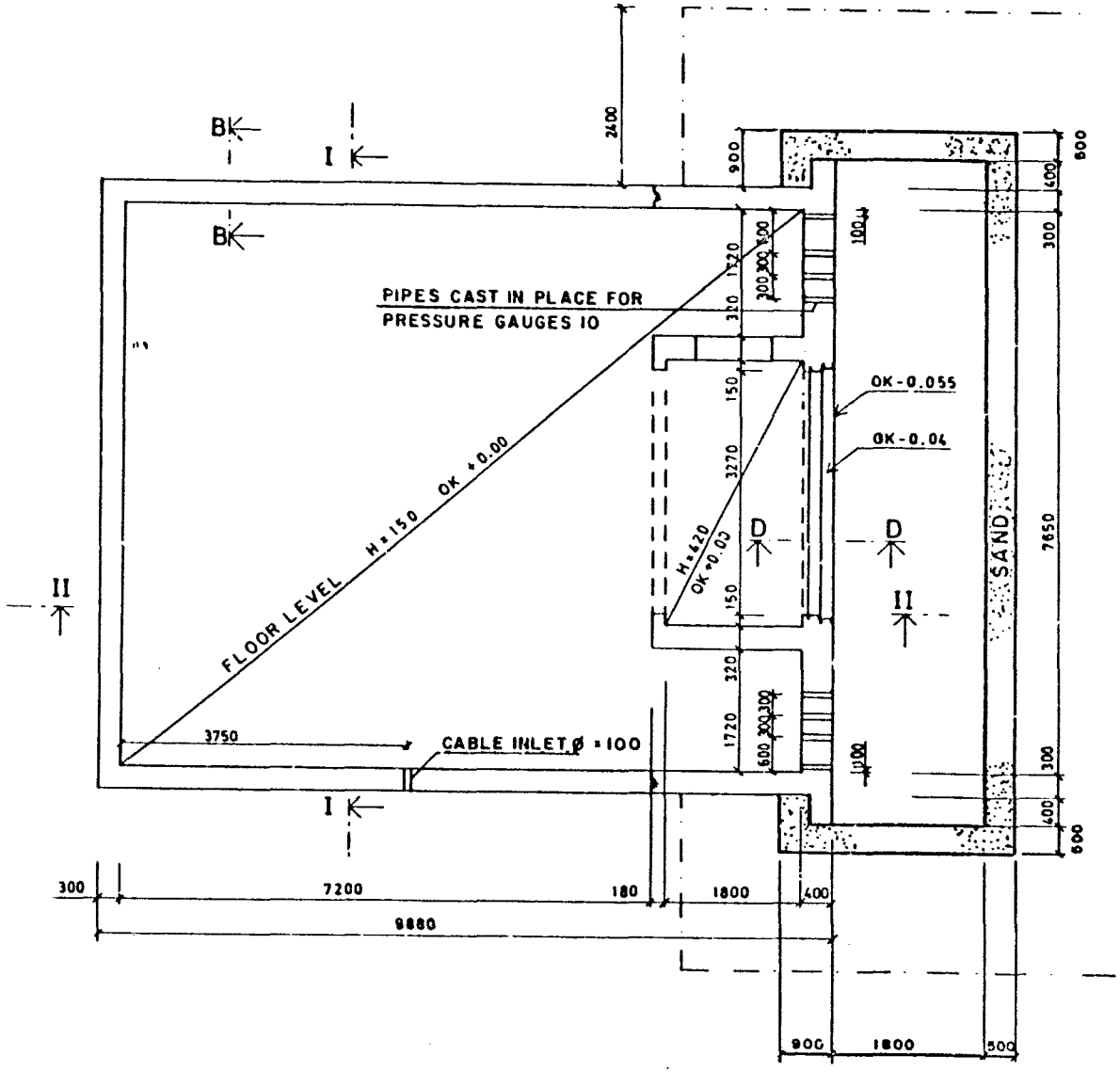

PLAN Drawing 2. Top view floor.

A - 8601 - 1

1540

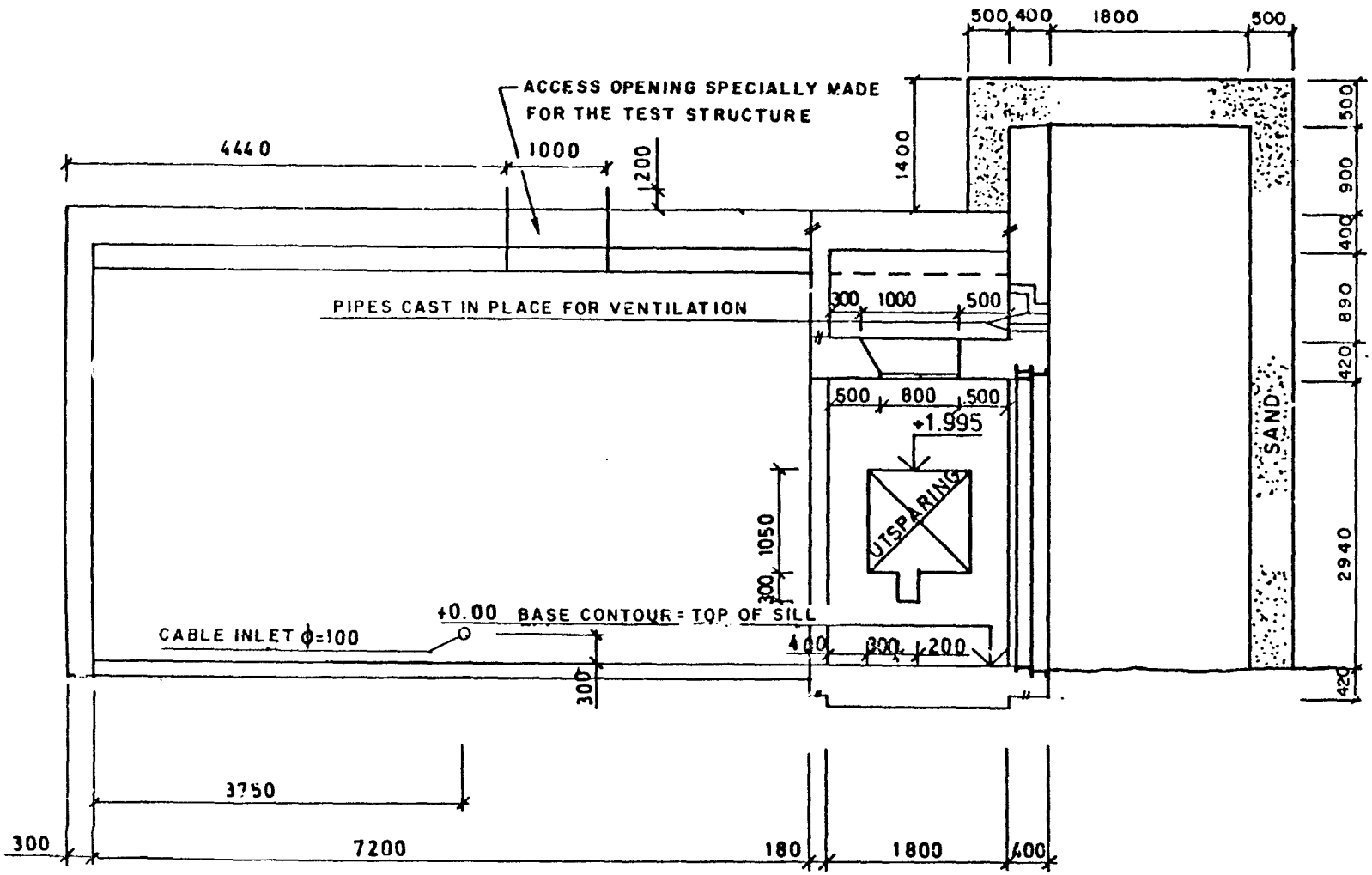

Drawing 3. Section II-II.

A - 8601 - 2

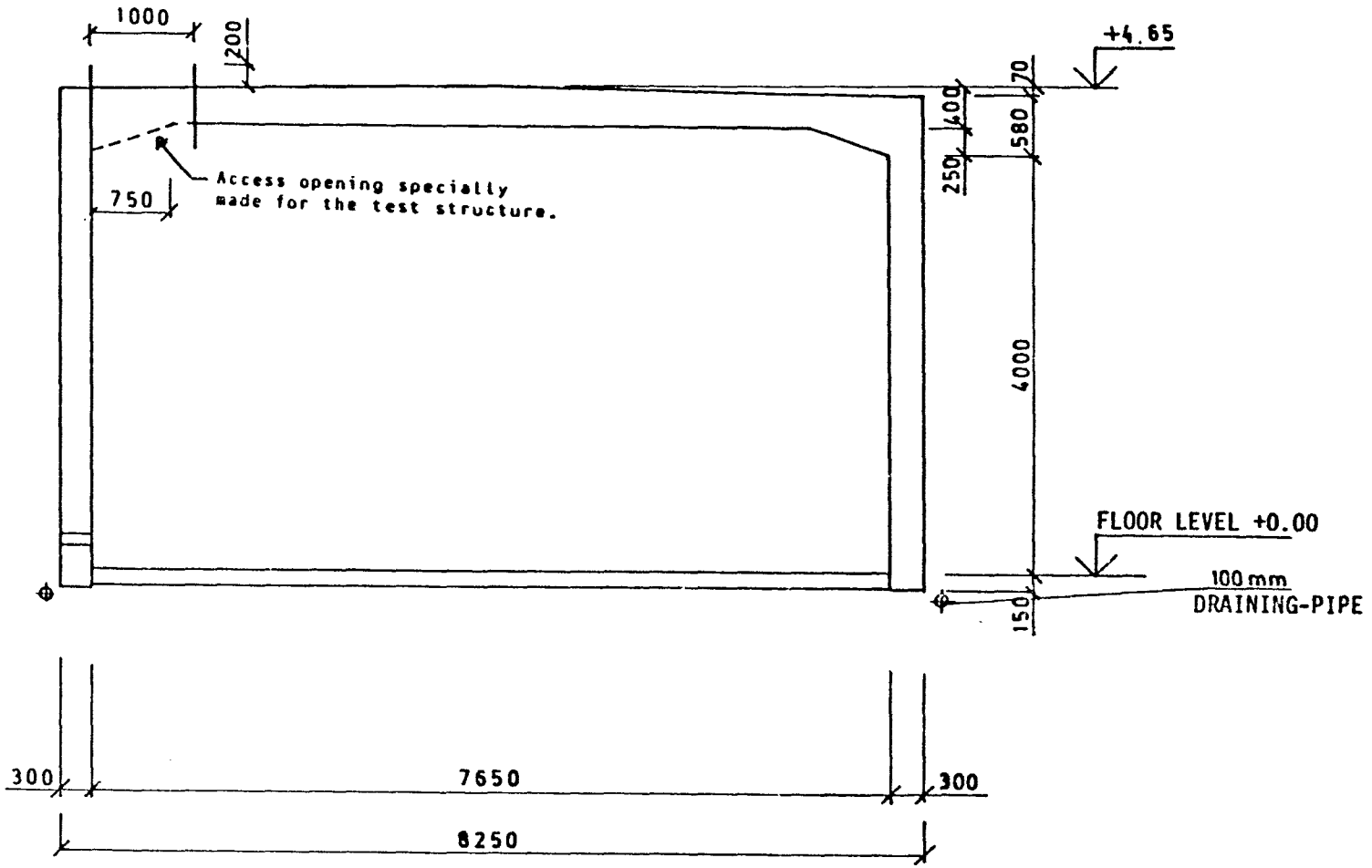

Drawing 4. Section I-I.

A - 8601 - 2

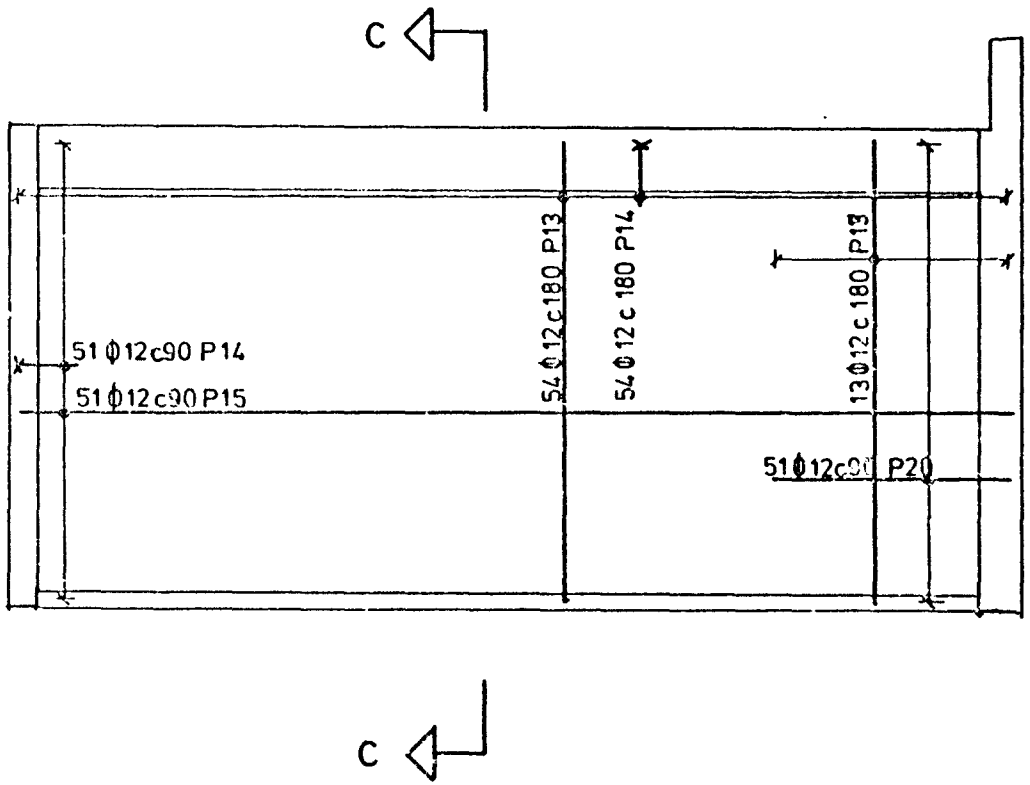

Drawing 5. Sidewall.

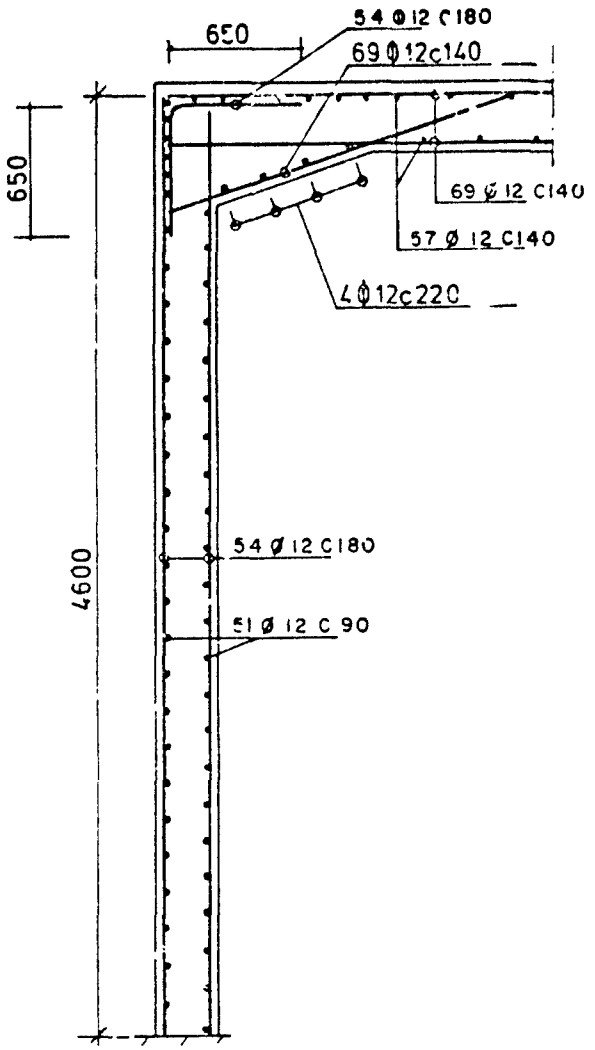

Drawing 6. Section C-C
1 : 25

A - 8601 - 5

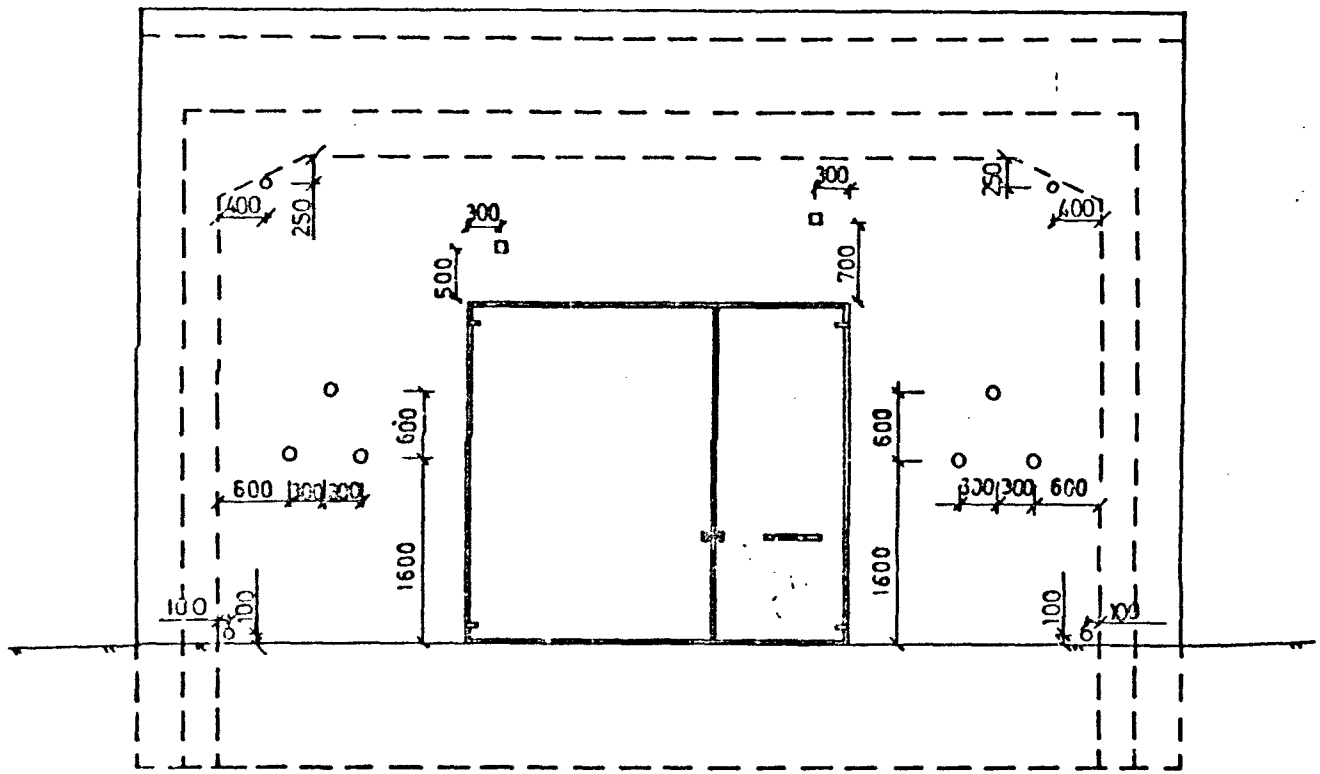

O BLAST GAUGE

□ VENTILATION OPENING

Drawing 7. Vertical projection, headwall.

A - 8601 - 2

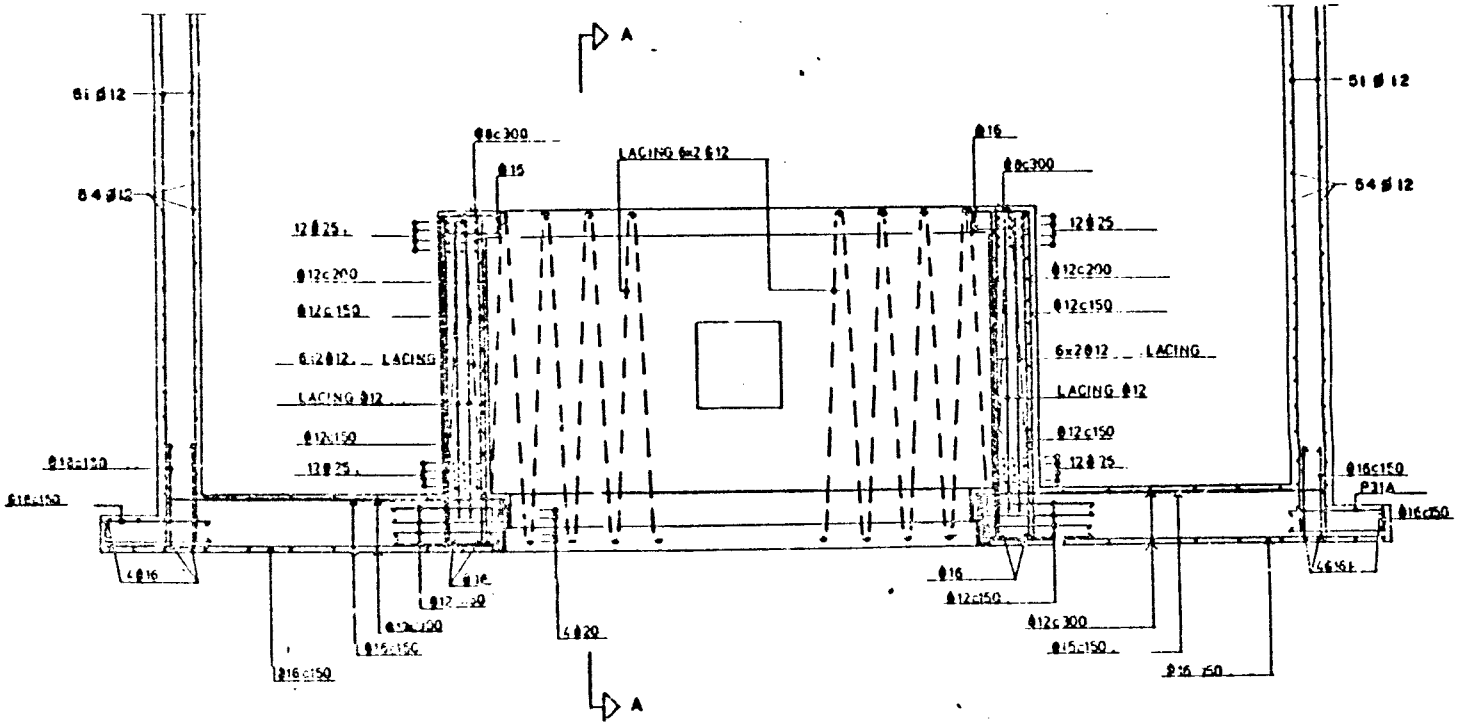

Drawing 8. Front view, Section B-B.

A - 8601 - 5

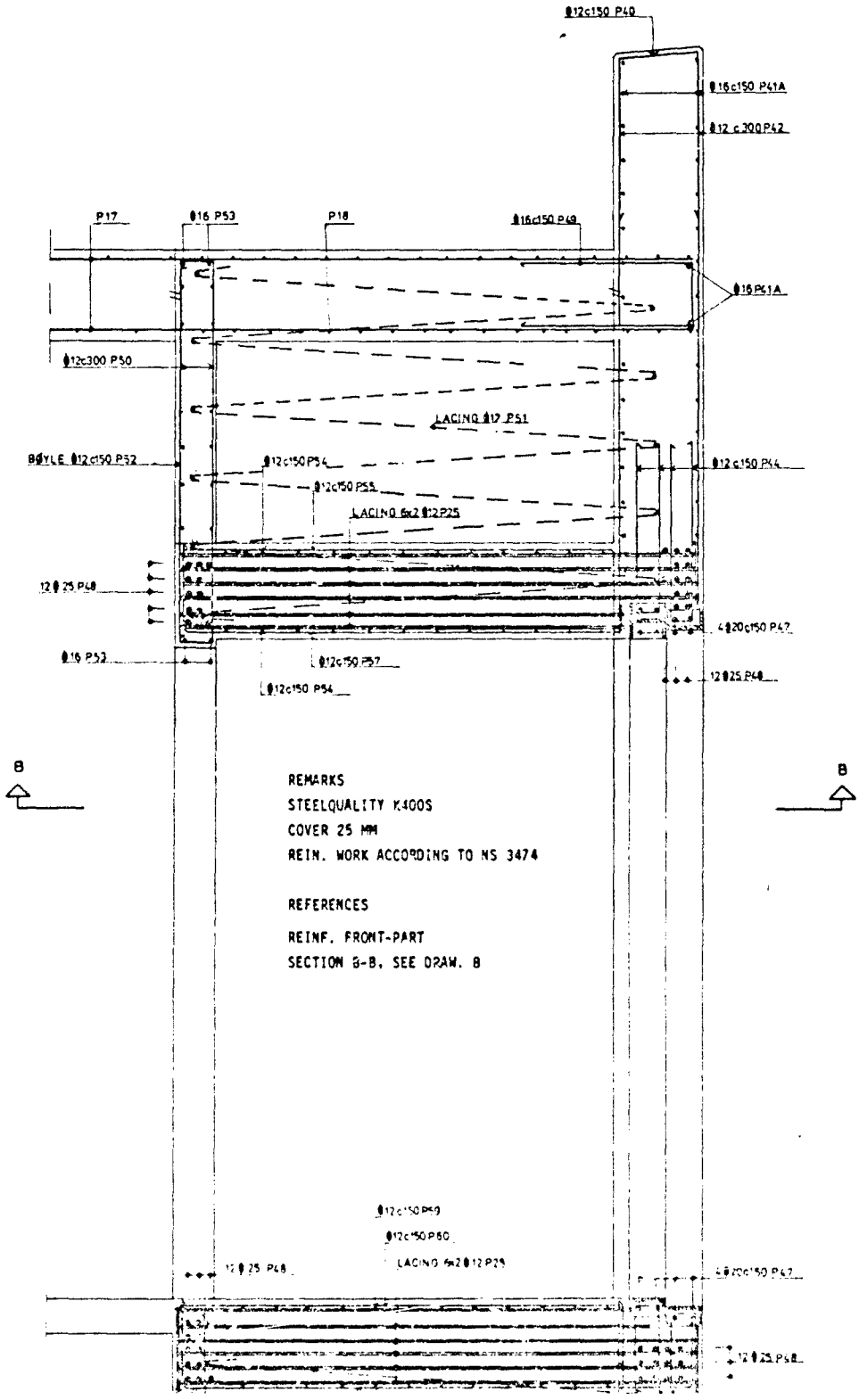

Drawing 9. Side view Section A-A.

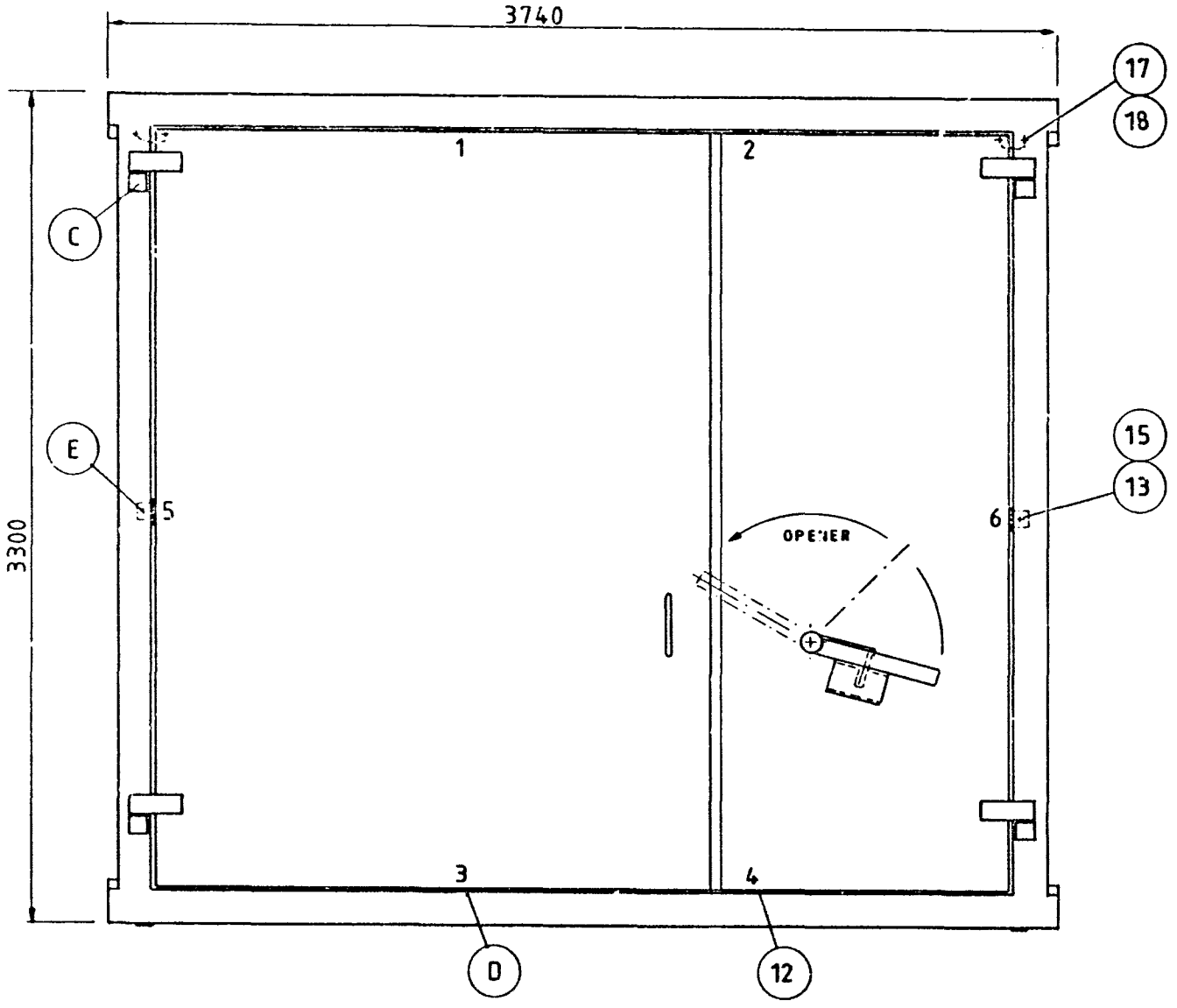

A - 8124 BL. 1 D

Drawing 10. Steel door seen from outside.

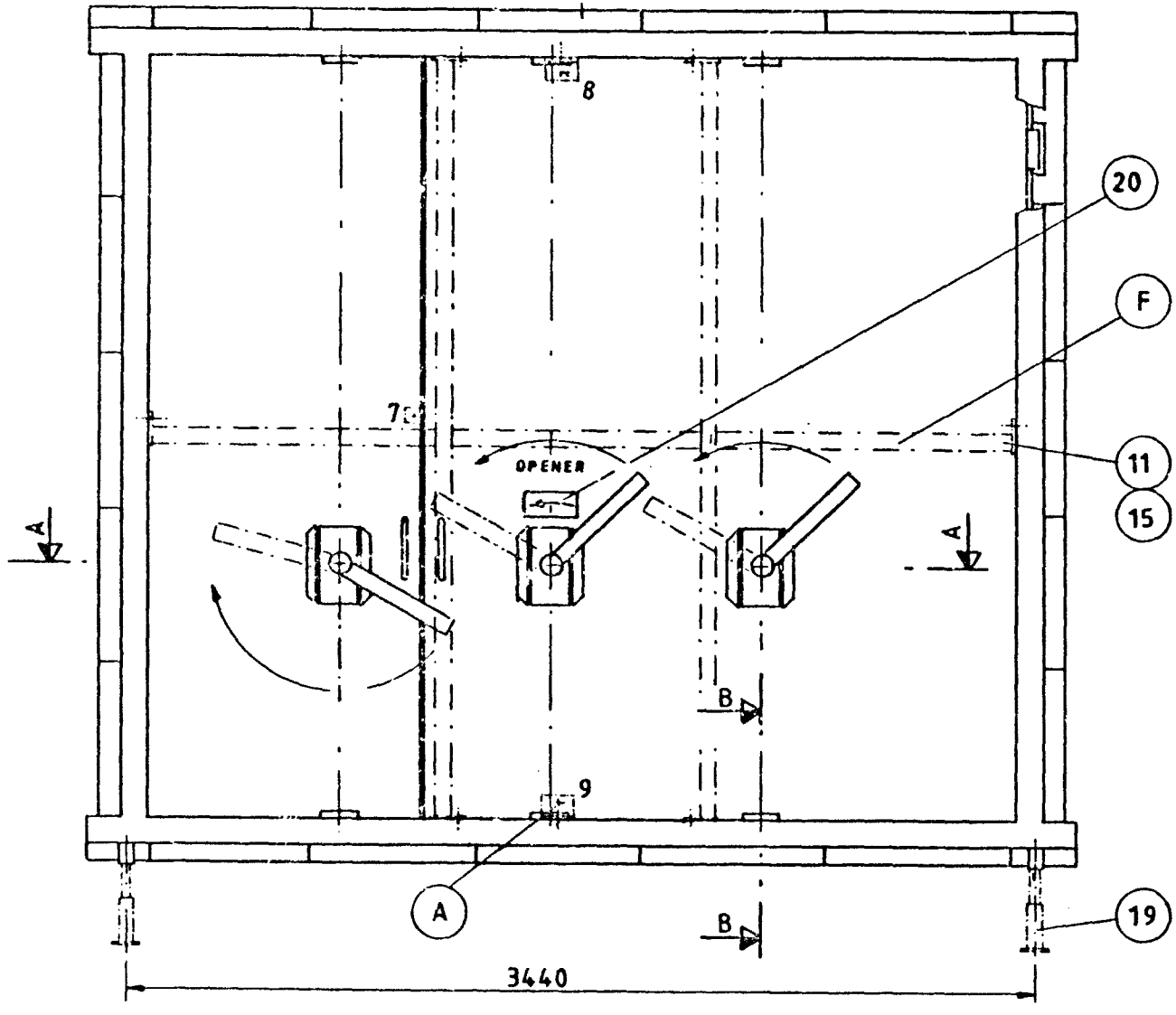

Drawing 11. Steel door seen from inside.

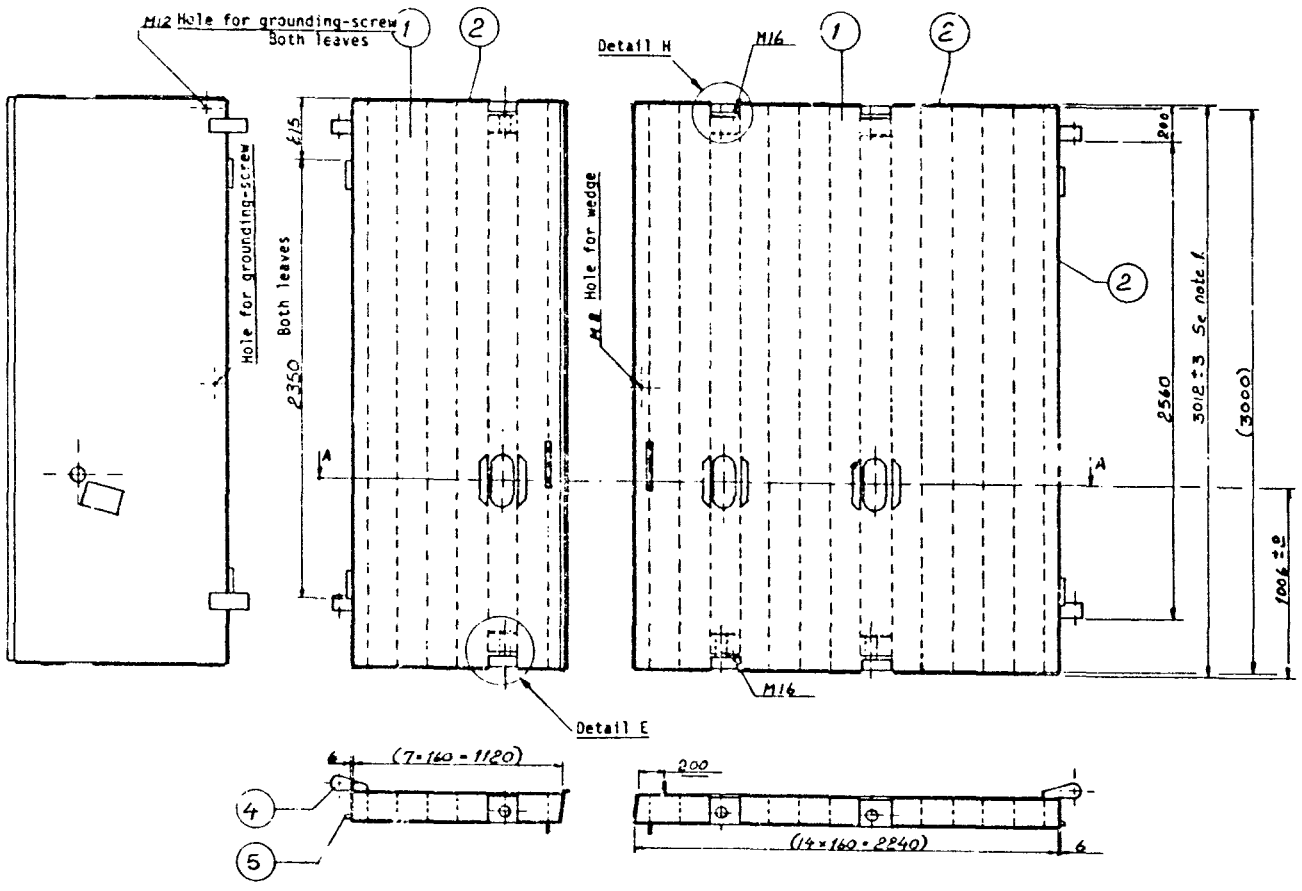

Drawing 12. Door-leave.

1550

A - 8124 BL. 2 D

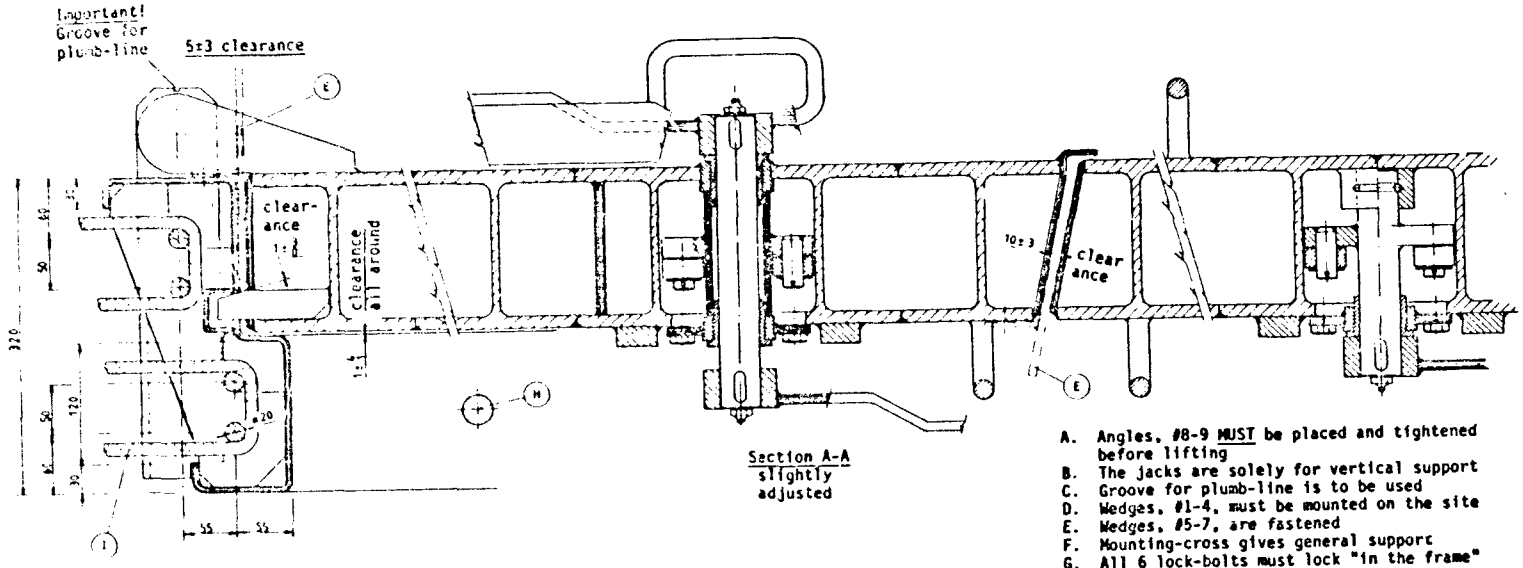

A. Angles, #8-9 MUST be placed and tightened before lifting
B. The jacks are solely for vertical support
C. Groove for plumb-line is to be used
D. Wedges, #1-4, must be mounted on the site
E. Wedges, #5-7, are fastened
F. Mounting-cross gives general support
G. All 6 lock-bolts must lock "in the frame"
H. 5 holes, Ø30, for after-injection
I. Reinforcement, delivered by contractor

Drawing 13. Section A-A.

A - 8124 BL. 1D

APPENDIX B. PHOTOGRAPHS

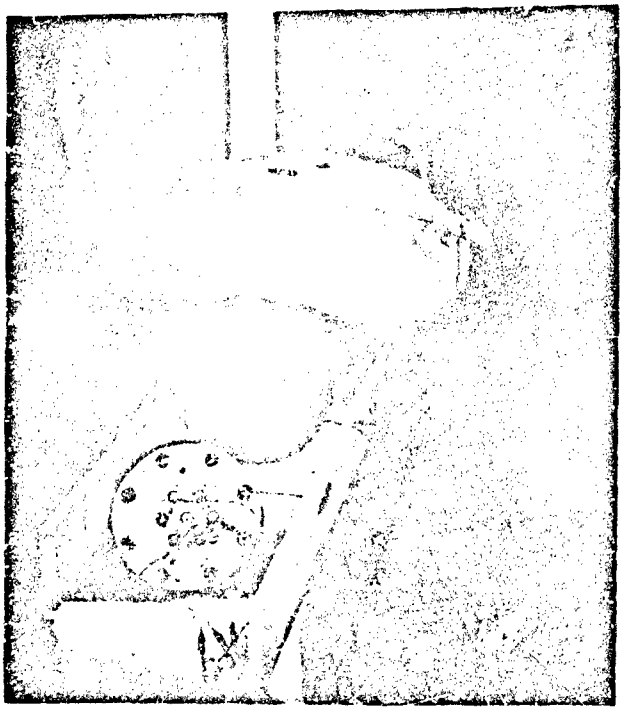

Small tube-diameter 150 mm -
showing 7 blast gauges in the flange plate
simulating the ammunition magazine headwall.

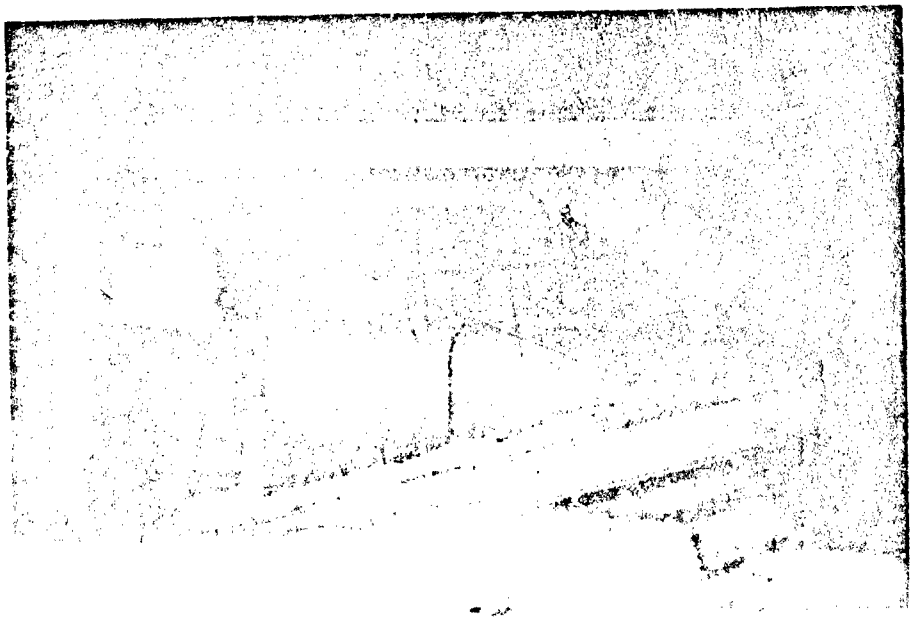

Large tube-diameter 660 mm -
showing sand filling tray above the part of the
tube simulating the overburden. Cavity at the left end.

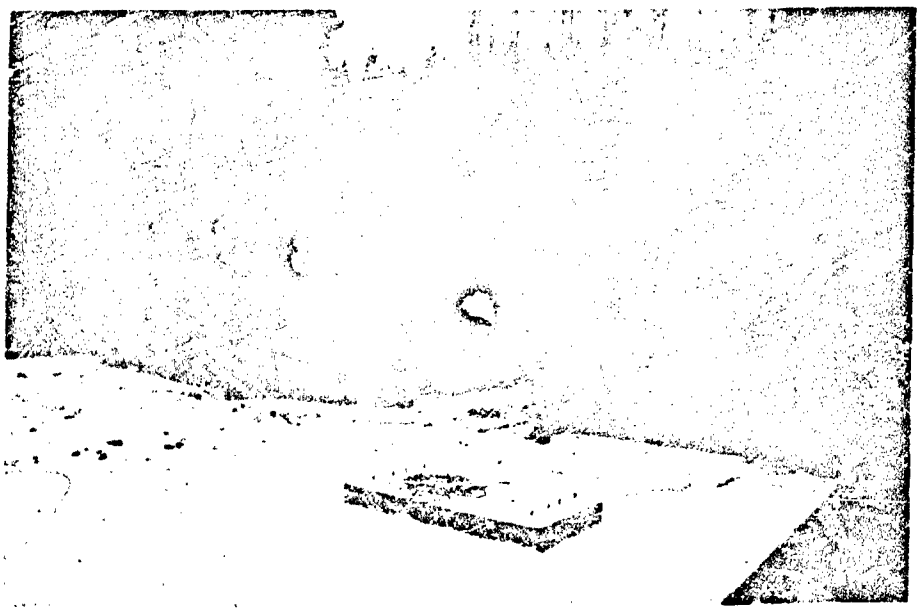

Ammunition magazine and mini wall side by side at the test site. See figure 7 for test setup.

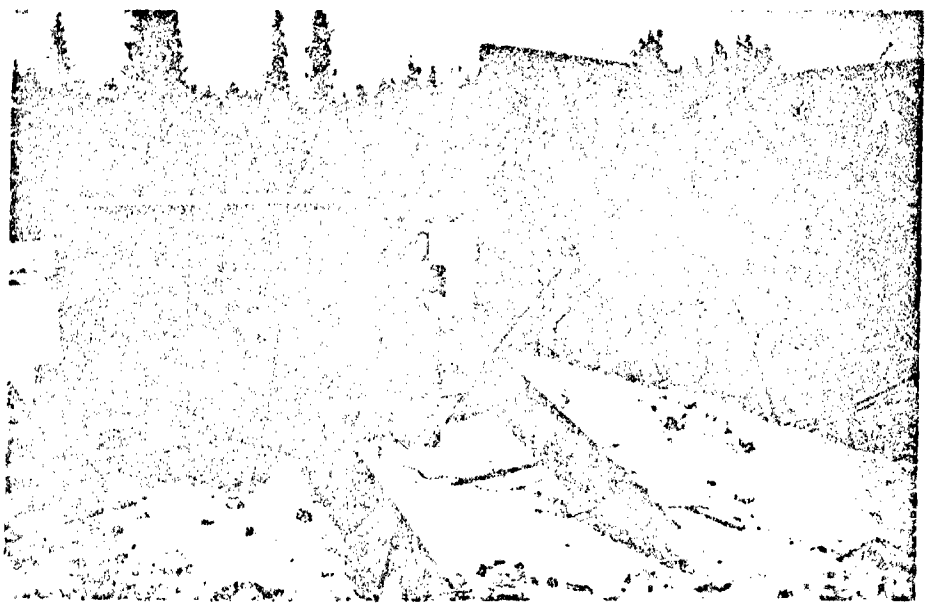

Support of miniwall.

Prima cord strings in the
"mini wall" cavity.

Mini wall just before shot showing
photopoles and cameras.

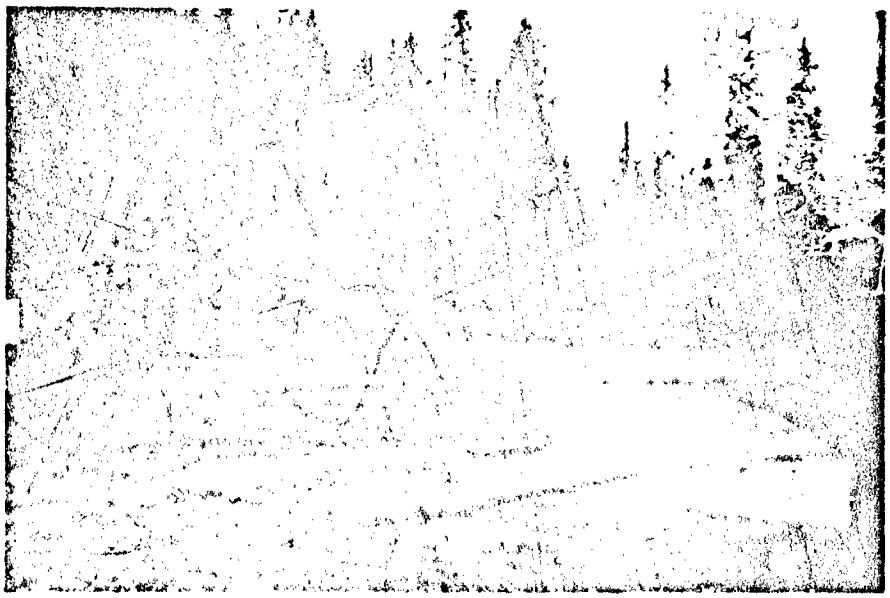

Mini wall shortly after firing.

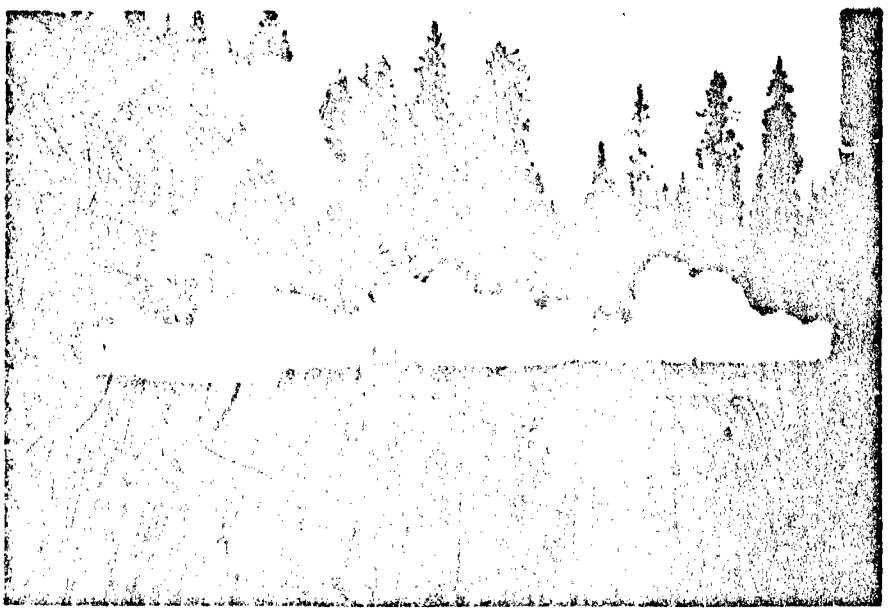

Overburden on the way back to the ground.

Experimenters on their way back to observe debris.

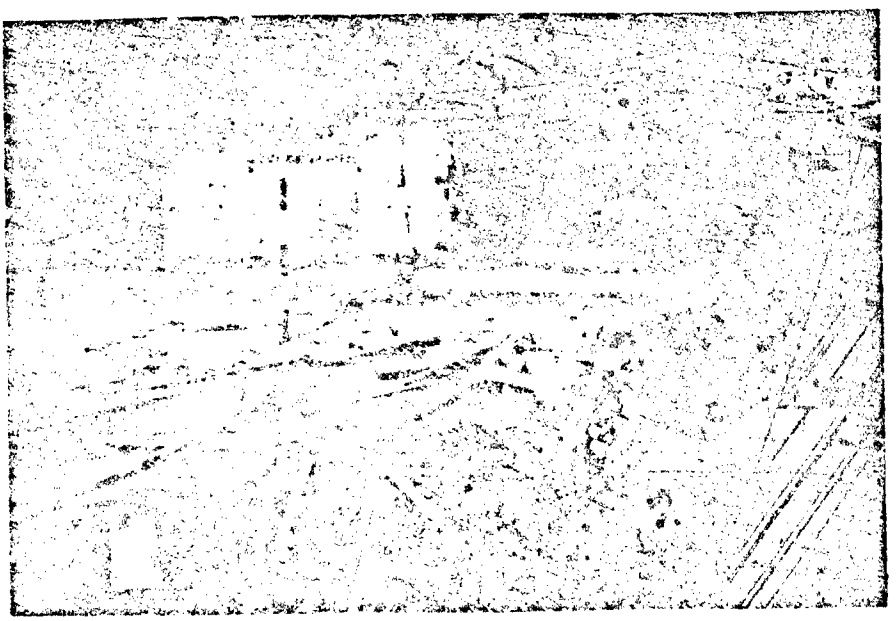

Debris in front of the mini wall.

VERTICAL HEST in front of magazine headwall.

Rain and debris.

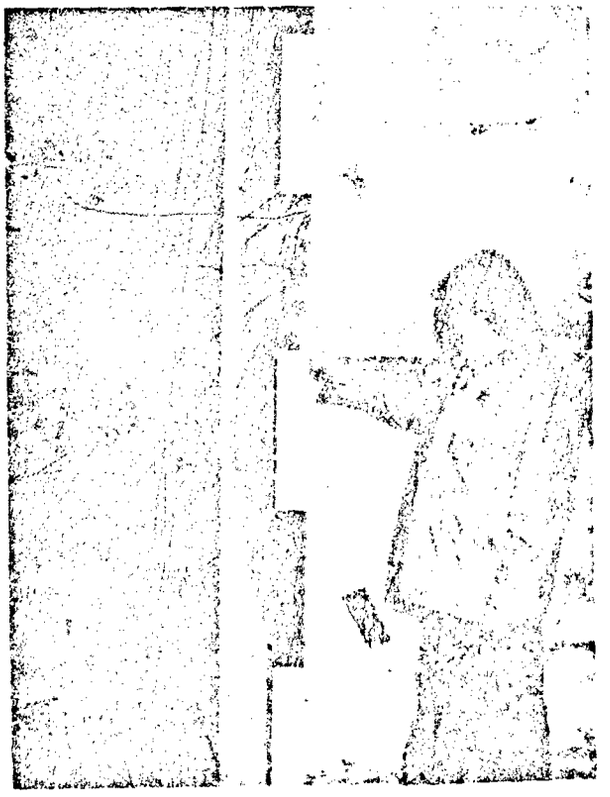

Permanent deformation
of magazine door.

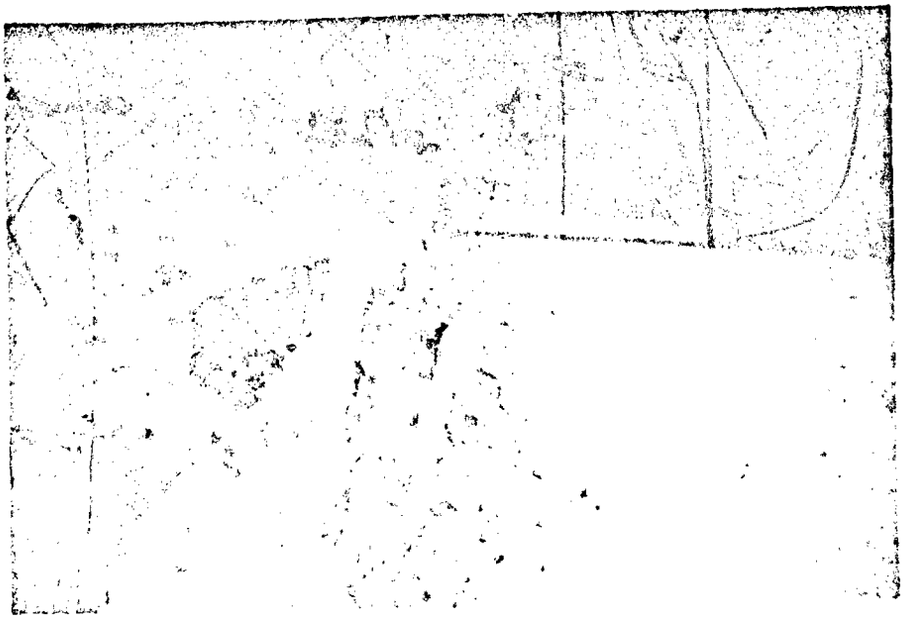

Spalling in front of fire door frame.

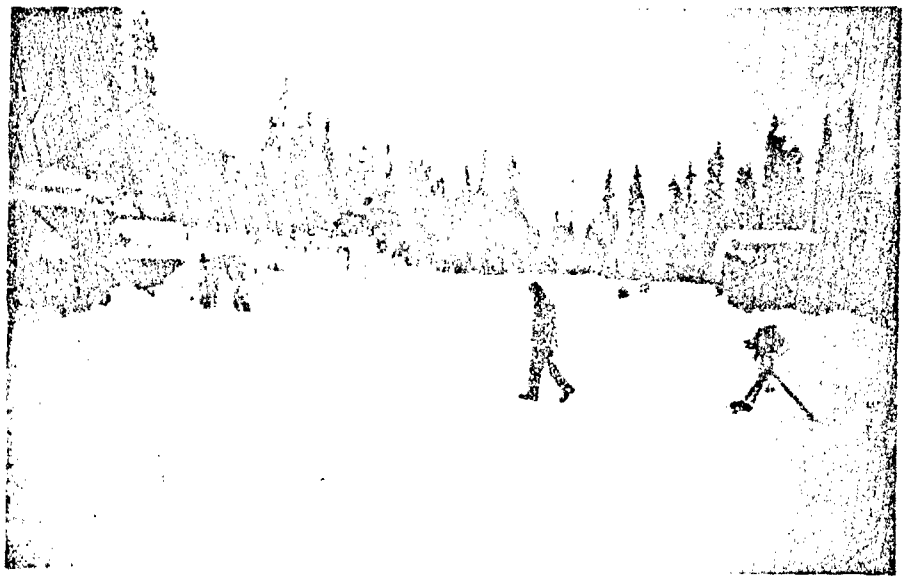

Ready for SABOT firing.

Experimenter with SABOT in his hand
ready to load the howitzer.

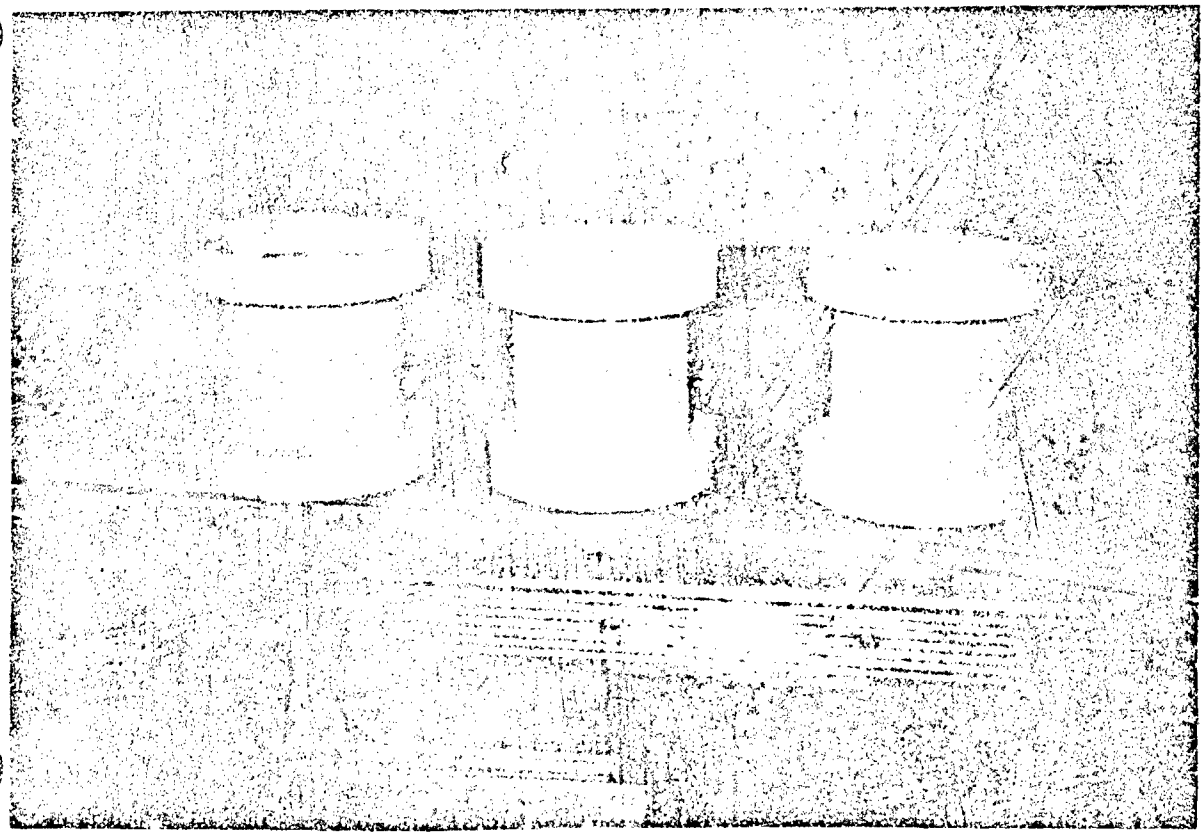

Concrete rods with SABOT.

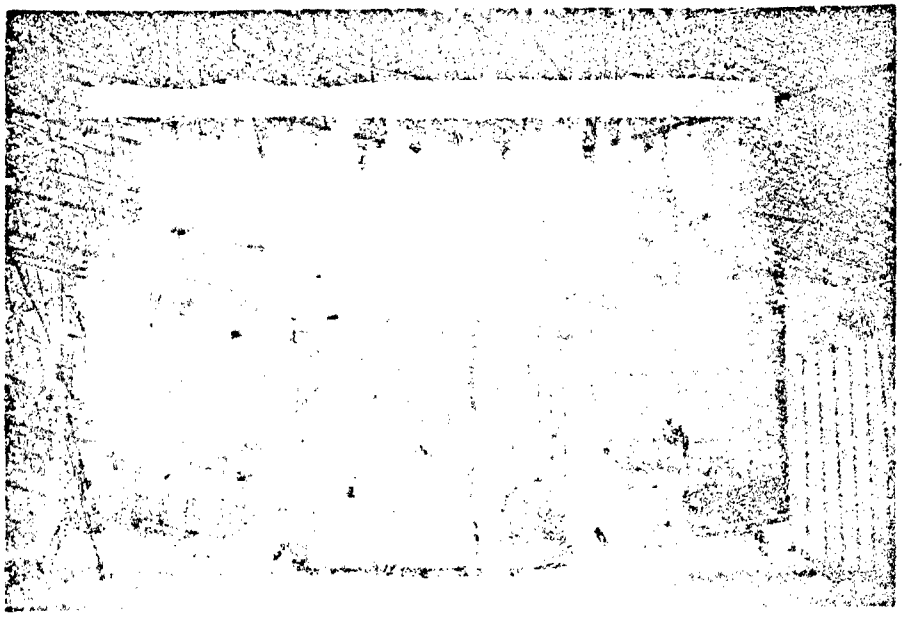

Target. Distance from howitzer - 41 m.

Dent in concrete wall caused by the base plate.

Crater in the concrete wall caused by the aluminium rod.

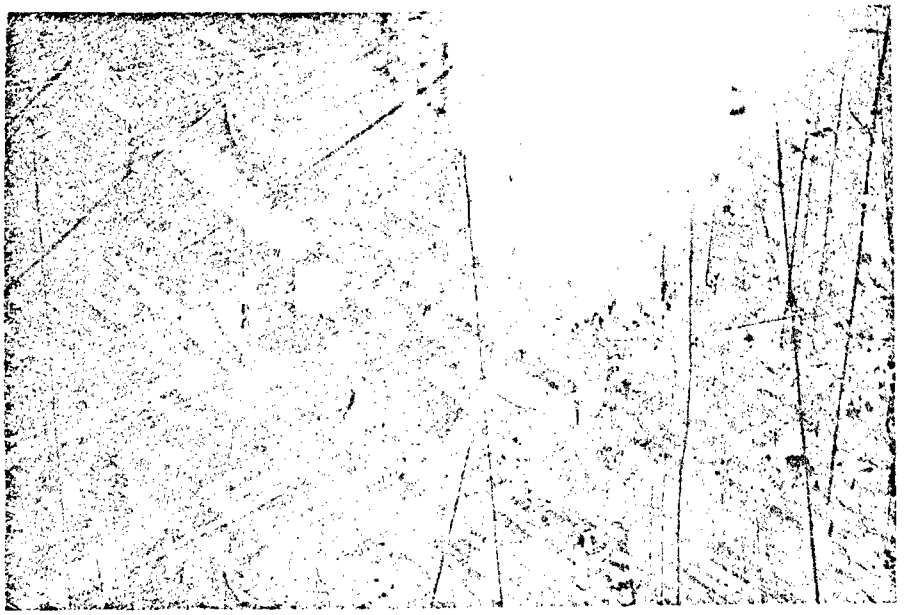

Crater depth is shown.

Dent in the door caused by the base plate.

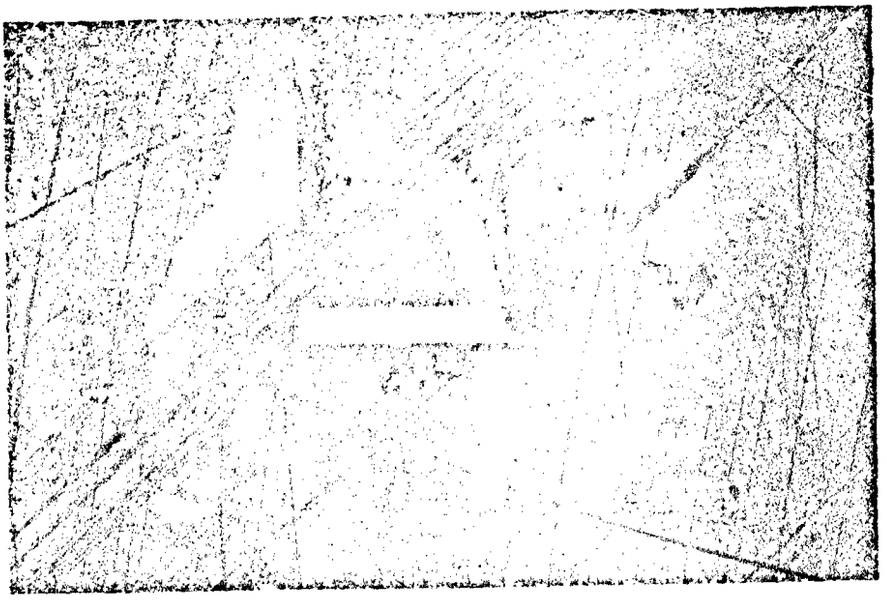

Hole in the front face of the door caused by the aluminium rod.

DYNAMIC TESTS OF REINFORCED CONCRETE SLABS

by

James E. Tancreto

Naval Civil Engineering Laboratory
Port Hueneme, California

for

23rd
Department of Defense
Explosives Safety Board
Seminar

Atlanta, Georgia
August 1988

DYNAMIC TESTS OF REINFORCED CONCRETE SLABS

by

James E. Tancreto

Naval Civil Engineering Laboratory
Port Hueneme, California

BACKGROUND

Design of conventionally reinforced concrete (R/C) slabs for blast loads had been limited to 2 degrees support rotation and to low and intermediate pressure design ranges by NAVFAC P-397 (Reference 1). Lacing was required for added ductility at design rotations of 2^{o} to 12^{o} (to prevent buckling of the compression steel and loss of bending capacity) and for close-in high pressure design ranges (to prevent breaching).

The revision to NAVFAC P-397 (see Reference 2) increases the allowable rotation of conventionally R/C slabs to 4^{o} when single leg stirrups (see Figure 1) are provided at a maximum spacing of d/2 (where d is the distance between top and bottom main steel reinforcing), and 8^{o} when sufficient tensile membrane resistance is provided. With tensile membrane action, stirrups are only required when necessary for shear or for close-in explosions. Lacing may still be used to maintain bending resistance at support rotations to 12^{o}.

Stirrups are required (regardless of rotation or type of resistance-flexural or membrane) for R/C slabs that must resist close-in explosions, (1.0 < scaled distance, Z < 3.0). Lacing reinforcement (see Figure 2) is required for very close-in explosions at scaled distances less than 1.0 from the explosive.

Additional data from dynamic tests were needed to verify the structural response of conventionally R/C slabs (a) with tensile membrane resistance, (b) under close-in loads, and (c) in bending, with stirrups (not lacing), to rotations of 4^{o} or more. It was believed that dynamic test data might also show that the allowable maximum spacing for single leg stirrups could be increased (from d/2) and that single leg stirrups are effective for resisting close-in explosions at scaled distances less than 1.0.

The Naval Civil Engineering Laboratory (NCEL) was funded by the Department of Defense Explosives Safety Board to conduct dynamic tests of R/C slabs to study the effect of the reinforcement on the dynamic response in these areas of interest. Ammann and Whitney Consulting Engineers planned (Reference 3) the initial test series (6 tests conducted in 1986 by the Terminal Effects Research and Analysis Group (TERA), New Mexico Tech, and NCEL). Five additional tests, planned by NCEL (Reference 4), will be conducted in September, 1988 using the original test setup at TERA.

TEST OBJECTIVES

The tests that have been conducted, and those that will be conducted this year, have been designed to verify the design criteria for slabs with tensile membrane resistance, and to investigate the effect of stirrup design on the response of R/C slabs at large support rotations ($> 4^{\circ}$) and for close-in explosions.

The specific test objectives were:

(a) Verify that R/C slabs with bending and adequate tensile membrane resistance may be designed for ultimate support rotations of 8°.

(b) Verify that R/C slabs with bending and adequate tensile membrane resistance only require stirrups where needed for shear resistance (and not for flexural ductility).

(c) Obtain data on the response of slabs with stirrup spacings at and greater than the maximum required by the revised criteria (Ref. 2). These data would add to the data base that might justify an increase in the maximum allowable spacing (d/2) of stirrups as now required by the revised criteria.

(d) Verify the breaching criteria for close-in explosions (lacing required at $Z < 1.0$ ft/lb$^{1/3}$ and stirrups required at $1.0 < Z < 3.0$). No shear steel required (for breaching) at $Z > 3.0$. Obtain data on slabs with stirrups and with no shear steel to justify a reduction in the scaled standoff distance required to prevent breaching.

SCOPE OF REPORT

This report will describe the test program, provide test results for the 6 slabs (out of 11 total) that have been tested, and give preliminary findings based on the tests of those 6 slabs. Final results and conclusions will be published after we have completed testing.

TEST PROGRAM

Test Planning. Table 1 shows the major variables for each of the test slabs. One laced slab (slab type II) was tested for comparison with the response of the conventionally R/C slabs. The major stirrup criteria design variables in the test program are stirrup spacing and the scaled distance of the explosive from the slab. The area of the stirrups was designed to resist the calculated shear loads. High steel percentages were used in slabs I, II, III, IV, and VI to obtain high shear stresses in the stirrups.

Slab types V, VII, and VIII were designed with lower, more common, steel percentages (including 0.15% - the minimum allowed in the revised criteria) to check the response of slabs with membrane resistance and little or no shear steel (stirrups) for added ductility. Stirrups were only provided in the lightly reinforced slabs if it was needed for shear. Slab type VIII needed shear steel near the supports (no stirrups were necessary in the middle 5' x 5'

square area). Since the scaled distances from the explosive to the top of the test slabs is always < 3, the revised criteria would require stirrups throughout the slab for breaching resistance to the close-in explosive charge. Stirrups were not provided, however, to fully test flexural response in membrane action and to obtain data that might reduce the stirrup requirements for breaching resistance.

Test Site. The tests were conducted by the TERA Group, New Mexico Tech, Socorro, New Mexico. TERA constructed the test fixture, test specimens, and the explosive charge, setup each test, and detonated the explosive charge. NCEL monitored the testing and provided the instrumentation.

Test Setup. The test setup is shown in Figure 3. A steel 7.5' x 7.5' x 8' deep cubicle is used to support the test slabs. The 10.5' x 10.5' test slabs are bolted to the top of the cubicle with a steel fixture that clamps the 1.5' perimeter of the slab. Oversize holes in the slab allow lateral slippage, but the clamping of the support structure develops the moment capacity of the slab at the supports. The slabs have an unsupported two way span of 7.5' x 7.5'. Tensile membrane action is developed by the 2-way square slab (a 2-way square slab supported on 4 sides develops an outside tensile ring that supports the in-plane tensile membrane forces - lateral restraint at the support is unnecessary). The dynamic loads are obtained from a spherical Composition C4 explosive charge suspended over the center of the slab. The steel support cubicle has a side access door that is closed during the test to prevent blast pressure from reaching the underside of the slab.

Test Specimens. The test specimen geometry is detailed in Table 2. Each R/C slab is 10' 6" x 10' 6" with a two-way unsupported span of 7'6" x 7' 6". The main (longitudinal) steel is #2 (metric equivalent) and #3 deformed bar with nominal yield strengths of 60 ksi. The wire reinforcement (ASTM designation W1, W2, and W3) was to be obtained with yield strengths of about 60 ksi (to be consistent with the design strengths for each slab). However, the wire obtained and used in slab types I and II was about one-half the design strength. Table 3 summarizes the steel reinforcement sizes and strengths. The concrete ultimate compression strength was about 4000 psi. Each slab type is described below.

Type I: the standard stirrup reinforced slab with 1% (each way, each face) longitudinal steel (#2 bar) at d/2 and W1 stirrups at each intersection of the longitudinal steel (stirrup spacing = d/2). This slab, and the type II laced slab, are used as the basis for measuring the performance of all other slabs (and their variation of parameters). T = 4.5", d = 3.1".

Type II: laced steel reinforced slab with 1% longitudinal steel at d/2. Method 3 (Reference 3; s = d, b = d/2) lacing reinforcement around every other intersection (spacing = d) of the main rebar. Equivalent to slab type I for shear steel diameter and spacing (d/2) and to slab type IV for spacing of lacing support of top and bottom main rebar (at every other intersection, spacing = d). The performance of slabs with stirrup reinforcement will be compared to the response of this that used lacing steel. T = 4.5", d = 3.0".

d) with slightly higher percentage (1.5%). The W3 stirrups are at each intersection (d). T = 4.5", d = 2.9".

Type III-L: similar to type III except that longitudinal steel is lapped in one direction (top and bottom).

Type IV: longitudinal reinforcing same as slab type I (1%, with spacing of d/2). However, the W2 stirrup spacing is at every other intersection of the longitudinal steel (at d vs. d/2 in the type I). The total area of stirrups in this slab is the same as that in the type I (the area of the W2 wire is twice the area of the W1 wire). T = 4.5", d = 3.1".

Type V: low steel percentage (0.31%) with #2's at 4" (d) and no shear steel (none required for shear). T = 6.0", d = 4.0".

Type V-L: similar to type V except that longitudinal steel is lapped in one direction (top and bottom).

Type VI: same steel spacings as in the slab type I but with about twice the steel percentage (used #3 bar vs. #2 bar in type I). Size of stirrups vary (W1 and W2) to match the calculated shear resistance (less shear steel area required in middle than near the supports). T = 4.5", d = 2.9".

Type VII: minimum allowable longitudinal steel (0.15%) with #3's at d spacing. No shear steel required. T = 9.6", d = 8.9".

Type VIII: low steel percentage (0.23%) with #3's at d spacing. W3 stirrups required for shear near supports with spacing of d/2 x d (d/2 spacing parallel to support). No stirrups in middle 5' x 5' square area. T = 8", d = 7.3".

Explosive Charge. The spherical Composition C4 charge weights and locations are shown in Table 4. The location and size were designed to obtain 4° to 10° support rotation and to vary the standoff scaled distance (for breaching effects). A TNT equivalency by weight of 1.13 (TNT weight = 1.13 x C4 weight) was used in the calculations of scaled distance and loads.

TEST RESULTS

The important response measurements are the maximum deflections and support rotations, the amount of spalling on the unloaded side of the slab, and observation of shear, breaching, and moment or tensile membrane failures. Table 5 summarizes the test results of the slabs that have been tested.

Support Rotations and Deflections. In all but one test, the support rotation of the slab exceeded 8°, (the allowable design rotation with tensile membrane resistance and without lacing shear steel). The heavily reinforced (2.5% main steel) type VI slab had a support rotation of 4.8°.

Table 6 compares the measured vs. calculated deflections and rotations. The predictions are based on load from the computer programs IMPRES (see Reference 2) and response from the computer program BARCS (Reference 5). The response was calculated as it would be when using the revised criteria (Reference 2). The measured deflections and support rotations were greater than calculated by up to 50%. This should not be unexpected when the design procedure for tensile membrane resistance is used for predicting actual deflections.

The design procedure in Reference 2 allows the use of a constant plastic resistance function to simplify the response calculation. The idealized design resistance function, shown in Figure 4, may be overestimated (with higher actual deflections) between 4° and 8° support rotation when moment resistance declines (because of crushing of compression concrete) and before tensile membrane resistance is developed . The tensile membrane resistance eventually exceeds the design resistance (at or before 8° rotation) and incremental deflections and rotations then become less than calculated. Tensile membrane resistance has been shown to be effective well beyond 12° support rotation. However because of the possibility of lower design resistance between about 4° and 8°, the maximum design support rotation was conservatively restricted to 8° (see Reference 2).

The greater deflection and rotation may also reflect higher test loads than predicted. It would only take an increase in impulse of 22% to account for 50% greater deflection and support rotation. Test pressure measurements near the slab were not reliable and were not used.

Spalling. Spalling was expected and occurred in all test slabs. The extent is shown in Table 5 in terms of the surface area that spalled. The depth of spalling was the thickness of the concrete cover plus the diameter of the outside longitudinal reinforcement.

The least amount of spalling occurred in slab type I with both the main rebar spacing and the stirrup spacing at the minimum tested spacings of d/2. Slab type V also had little spalling (2 x the type I spall area) even though it had large main rebar spacings and no shear steel. The greater charge standoff ($Z = 1.10$ vs. $Z < 0.70$ for the other tested slabs) was probably the main reason that spalling was low in the type V slab. Types II (laced) and IV, with shear steel that tied the main rebar at a spacing of d had moderate areas of spalling (3 times that of the type I).

The type VI slab had the same rebar and stirrup spacings as the type I, and twice the main steel area (#3 vs. #2 bar). Because of its high strength it deflected 1/2 as much of the type I. However, it had a spalled area about 4 times that of the type I. Slab type III, with large main rebar and stirrup spacing (d), had the largest spalled area (about 15 x the area of the type I).

The deflection of slabs I to V was about equal (around 10^{o}). Only the deflection of slab type VI was very different (4.8^{o}). The type VI slab, however, had one of the highest spalled areas. It appears that for deflection between 4^{o} and 12^{o}, the maximum deflection does not significantly affect spalling.

Load Resistance Failures. None of the tested slabs (types I - VI) were breached. Slab type V (without stirrups), did develop a 2.5' long concrete shear crack (parallel and about 1.5' from south support; centered between the east and west supports) with no failure of the main steel. The slab did not lose tensile membrane resistance, but was probably close to a breaching failure. The scaled standoff distance of the charge was 1.10 $ft/lb^{1/3}$, much closer than the 3.0 $ft/lb^{1/3}$ allowed without shear steel. No other failures (shear, bending or tensile membrane) were observed.

PRELIMINARY CONCLUSIONS

Preliminary conclusions, from test results of 6 slabs, in comparison with new criteria (Reference 2) are:

1. Tensile membrane design criteria verified
2. Breaching criteria are conservative. Stirrups were adequate for resisting breaching at $Z = 0.7\ ft/lb^{1/3}$. New criteria requires lacing at $Z < 1.0\ ft/lb^{1/3}$.
3. Stirrup spacings of d were adequate in slabs tested (vs. maximum spacing of d/2 in new criteria).
4. Spalling was reduced by reducing the spacing of main flexural steel. Lacing may not reduce spalling, especially when it ties main rebar at every other intersection (see lacing methods in Reference 2).
5. More dynamic tests are required to increase the parameter range of the data base and to develop statistical confidence in the results. Additional tests should be conducted to establish:

   (a) improved breaching criteria
   (b) allowable stirrup spacing (for flexural ductility and for shear)
   (c) allowable maximum rotation from flexural resistance with stirrups
   (d) ultimate rotation with tensile membrane resistance.

The 5 additional tests to be conducted in this summer will provide valuable additional data, but will not complete testing of the full range of variables. Additional data are also required to improve the statistical confidence limits.

REFERENCES

1. Structures to Resist the Effects of Accidental Explosions. Army TM 5-1300/Navy NAVFAC P-397/Air Force AFM 88-22. Washington, D.C., June 1969.

2. U.S. Army Armament Research, Development and Engineering Center. Special Publication ARLCD-SP-84001: Structures to Resist the Effects of Accidental Explosions. Dover N.J., Dec. 1988.

3. Ammann and Whitney Consulting Engineers. Test Plan to Verify Failure Criteria for Conventionally Reinforced Concrete Slabs. New York, NY., April 1985.

4. Naval Civil Engineering Laboratory. TM 51-88-02: FY88 Test Plan for Deflection Criteria of Reinforced Concrete Slabs under Blast Loads by J. E. Tancreto, Port Hueneme, CA., Jan. 1988.

5. Naval Civil Engineering Laboratory. TN 1494: Optimum Dynamic Design of Nonlinear Reinforced Concrete Slabs under Blast Loading by J. M. Ferritto, Port Hueneme, CA., July 1977.

Table 1. Major Test Parameters

SLAB TYPE (a)	MAIN STEEL AVERAGE % AGE	MAIN STEEL NOMINAL SPACING (b)	SHEAR STEEL SPACING (b)	CHARGE SCALED DISTANCE (c)	COMMENTS
I	1.06	d/2	d/2	0.69	STIRRUPS
II	1.09	d/2	d	0.74	LACING (Method 3)
III	1.52	d	d	0.65	STIRRUPS
IV	1.06	d/2	d	0.69	STIRRUPS
V	0.31	d		1.10	
VI	2.54	d/2	d/2	0.65	VARIABLE STIRRUPS
IIIb	1.18	2d/3	2d/3	0.67	STIRRUPS
III-L	1.18	2d/3	2d/3	0.67	STIRRUPS
V-L	0.23	3d/4		1.10	LAPPED MAIN STEEL
VII	0.15	d		1.00	LAPPED MAIN STEEL
VIII	0.23	d	d/2 x d	1.00	STIRRUPS AT SUPT

(a) Slabs I, II, III, IV, V, & VI have been tested.
Other slabs will be tested in Sept. 88.
(b) d is the avg. separation between top and bottom main steel.
(c) From center of explosive to top of slab (ft/lb^0.33).

Table 2. Test Specimen Geometry (a)

SLAB TYPE	THICK-NESS (in)	LONGITUDINAL REINFORCING: DIAMETER D (in)	LONGITUDINAL REINFORCING: SPACING (in)	d (b) (in)	AVERAGE STEEL %	SHEAR REINFORCING: DIAMETER (in)	SHEAR REINFORCING: SPACING (in)	SHEAR REINFORCING: TYPE (c)
I	4.5	0.25	1.5	3.1	1.06	0.113	1.5	STIRRUP
II	4.5	0.25	1.5	3.0	1.09	0.113	3.0	LACING
III	4.5	0.375	2.5	2.9	1.52	0.195	2.5	STIRRUP
IV	4.5	0.25	1.5	3.1	1.06	0.160	3.0	STIRRUP
V	6.0	0.25	4.0	4.0	0.31			NONE
VI	4.5	0.375	1.5	2.9	2.54	0.160	1.5	STIRRUP
						0.113	1.5	(d)
IIIb	4.5	0.375	2.5	3.75	1.18	0.195	2.5	STIRRUP
III-L(e)	4.5	0.375	2.5	3.75	1.18	0.195	2.5	STIRRUP
V-L(e)	6.0	0.25	4.0	5.38	0.23			NONE
VII	9.625	0.375	8.5	8.88	0.15			NONE
VIII	8.0	0.375	6.5	7.25	0.23	0.195	3.25 X 6.25	(f)

(a) As-built dimensions for Slabs I - VI.
Design dimensions for other slabs (to be tested in Sept. 88).
(b) Average distance between top and bottom steel. For all slabs except Slab V:
-The centerline of outside rebar is separated by do = (d + D).
-The centerline of inside rebar is separated by di = (d - D).
In slab V the rebar in both directions is separated by d.
(c) Stirrups at spacing shown each way (unless noted).
(d) 0.113" diam. stirrups in middle 3.5' x 3.5' square.
0.160 stirrups elsewhere.
(e) Longitudinal steel lapped.
(f) Short spacing parallel to support. No stirrups in middle 5' x 5' square.

Table 3. Reinforcement Properties

STEEL TYPE	DIAM (in)	AREA (si)	STRENGTH (ksi)			
			SLABS I & II		SLABS III - VIII	
			YIELD	ULTIMATE	YIELD	ULTIMATE
W1-WIRE	0.113	0.01	30.2	40.7	57.8	64.2
W2-WIRE	0.160	0.02	24.8	42.3	58.3	61.0
W3-WIRE	0.195	0.03	35.6	57.0	59.2	65.0
#2-BAR	0.250	0.05	74.5	97.3	74.5	97.3
#3-BAR	0.375	0.11	66.0	90.0	66.0	90.0

Table 4. Explosive Weight and Distance

SLAB TYPE	EXPLOSIVE WEIGHT C4 (lbs)	EXPLOSIVE WEIGHT TNT(a) (lbs)	DISTANCE (b) (ft)	SCALED DISTANCE (c)
I	60	67.8	2.83	0.69
II	60	67.8	3.00	0.74
III	60	67.8	2.67	0.65
IV	60	67.8	2.83	0.69
V	60	67.8	4.50	1.10
VI	60	67.8	2.67	0.65
IIIb	80	90.4	3.00	0.67
III-L	80	90.4	3.00	0.67
V-L	60	67.8	4.50	1.10
VII	80	90.4	4.50	1.00
VIII	80	90.4	4.50	1.00

(a) TNT Weight Equivalency = 1.13.
(b) Height of c.g. of spherical charge above slab.
(c) Scaled Distance, Z, ft/lb^(1/3)

Table 5. Summary of Response of Slabs

SLAB TYPE	MAXIMUM DEFL (in)	SUPPORT ROTATION (deg)	SPACING: MAIN STEEL	SPACING: SHEAR STEEL	SCALED DISTANCE (b)	SPALLED AREA (a) (sf)	FAILURES
I	8.0	10.1	d/2	d/2	0.69	2	
II	7.4	9.3	d	d	0.74	6	
III	8.4	10.5	d	d	0.65	27	
IV	9.8	12.2	d/2	d	0.69	6	
V	8.3	10.4	d		1.10	4	SHEAR (c)
VI	3.8	4.8	d/2	d/2	0.65	9	

(a) Approximate spalled surface area on bottom of slab. Area roughly centered in middle of slab. Depth of spalling equal to depth of cover + diam of outside longitudinal bar.
(b) Z, ft/(cube root of TNT equivalent weight)
(c) Vertical concrete shear crack (with vertical displacement), 2.5' long, parallel to support & about 1.25' from support. Steel unfailed, still effective in tensile membrane action.

Table 6. Calculated vs. Measured Deflection and Rotation

SLAB TYPE	ULTIMATE RESIST. psi	EFFECTIVE MASS (b)	BLAST INPULSE psi-ms	CALCULATED(a) DEFL in	CALCULATED(a) ROTATION degrees	MEASURED DEFL in	MEASURED ROTATION degrees	RATIO MEASURED/ CALCULATE
I	42	770	565	6.5	8.2	8.0	10.1	1.23
II	43	770	553	6.6	8.3	7.4	9.3	1.12
III	53	770	578	5.5	7.0	8.4	10.5	1.52
IV	42	770	565	6.5	8.2	9.8	12.2	1.50
V	21	1020	477	7.2	9.1	8.3	10.4	1.15
VI	89	770	578	3.5	4.4	3.8	4.8	1.07
IIIb	69	770	631	5.2	6.6			
III-L(d)	69	770	631	5.2	6.6			
V-L(d)	28	1020	477	5.4	6.8			
VII	47	1640	543	2.5	3.2			
VIII	50	1360	543	2.9	3.7			

(a) Calculated maximum deflection and rotation using computer program BARCS
(b) Effective unit mass = mass x load-mass Factor (psi-sqms/in)

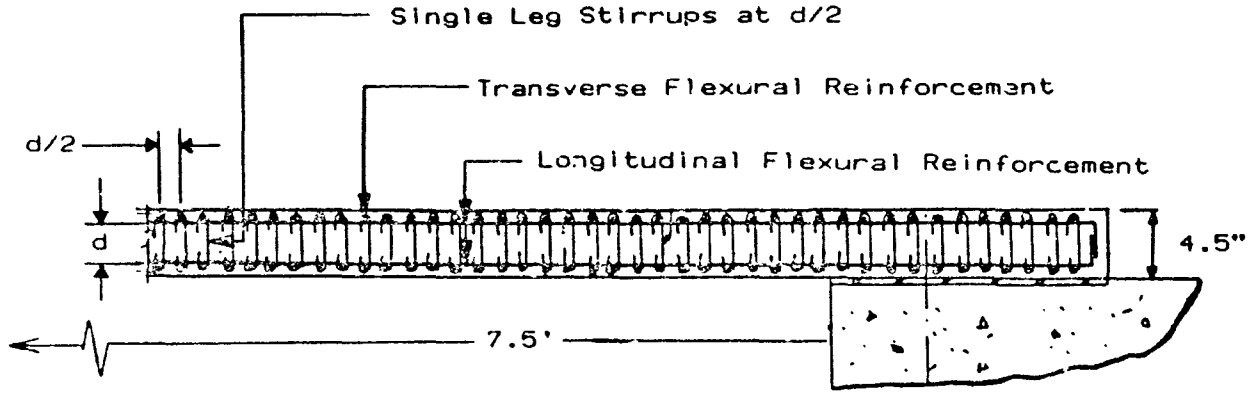

Figure 1. Typical Single Leg Stirrup Reinforcing (Slab Type I).

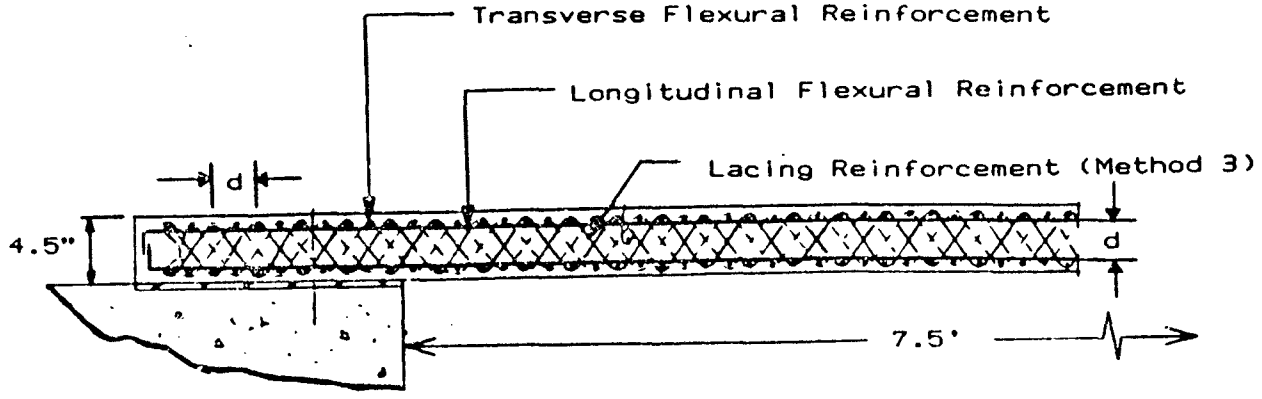

Figure 2. Typical Lacing Reinforcement (Slab Type II).

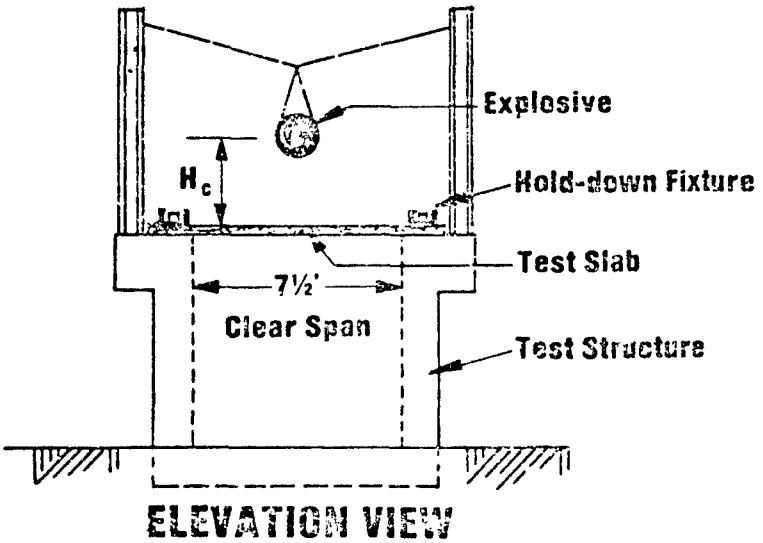

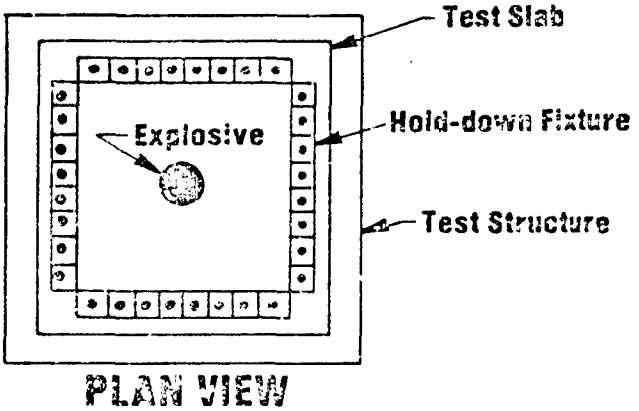

Figure 3. Test Setup

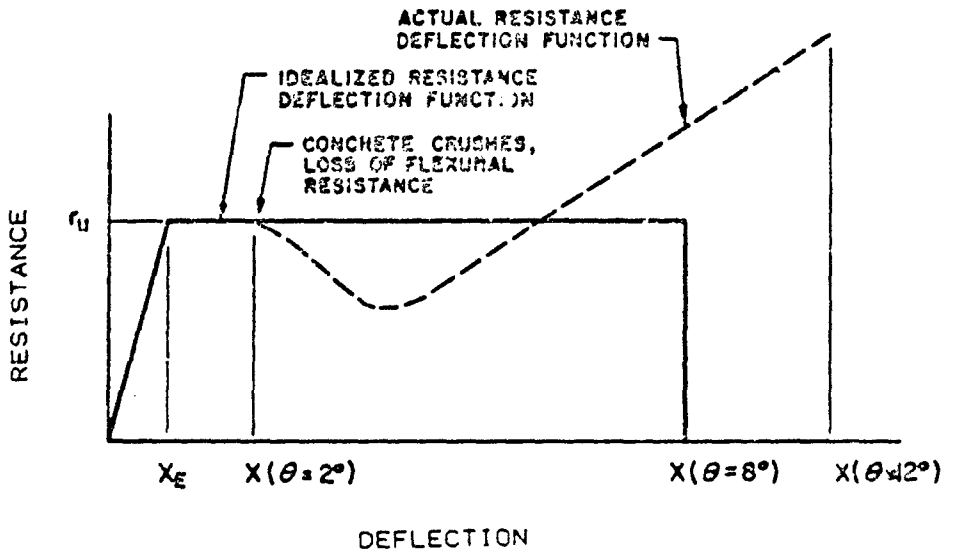

Figure 4. Design & Actual Tension Membrane Resistance & Deflection Function.

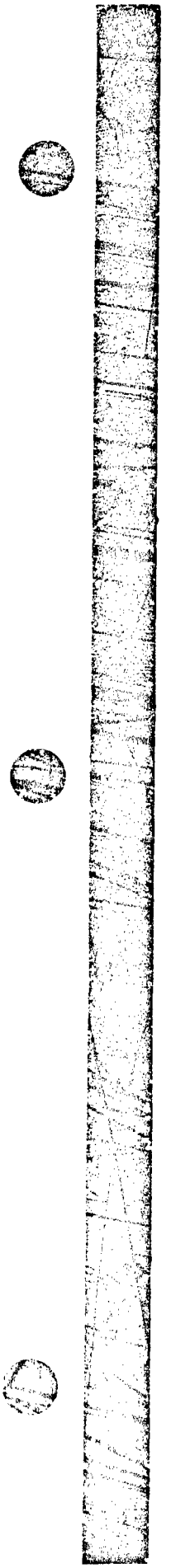

SEMIHARDENED BLAST DOOR/VALVE/WALL TEST SERIES

WALTER C. BUCHHOLTZ

AIR FORCE CIVIL ENGINEERING CENTER

TYNDALL AFB FLORIDA

ABSTRACT

This report is on a full scale test facility continuation of the half-scale blast tests conducted on simulated semihardened facility wall sections from October 1981 thru December 1984. A semihardened fifty foot by sixty foot facility was constructed at Tyndall AFB, Florida between July 1985 and June 1987 and tested from July to September 1987. There were eleven surface and three subsurface detonations with statically located conventional weapons. The surface weapon tests showed the effects on five blast doors, four different blast valves, a ventilation system with air filters, a 2'-7 1/2" (85 cm) bare wall and a 2'-1 1/2" (65 cm) wall protected with interior steel spall plate, precast concrete panels, Bitburg revetments, sand grid, sand berm and the bare wall. The subsurface tests showed the effects on 3'-3" (1.0 M) basement wall and a 2'-1 1/2" (65 cm) slab-on-grade concrete slab. During the subsurface tests, mannequins and office furniture were at strategic locations in the basement and ground floor.

INTRODUCTION

The objective of the semihardened blast door/valve/wall test series, was to provide data on the response of a reinforced concrete semihardened structure, blast doors, blast valves, and other components to a specific threat criteria. This data will be used to develop a cost-efficient design procedure, for a semihardened facility, to house critical personnel.

This full scale test series is a continuation of a half-scale, semihardened design criteria improvement series, conducted from September 1981 thru December 1985 at Tyndall AFB, Florida. This test series indicated that the percentage of reinforcing steel had little effect on the structural response when exposed to a design threat. The half-scaled tests also showed the addition of a sand berm, to the exterior of the structure, reduced the midspan deflections, and eliminated spalling from the interior mass surface. The addition of a steel spall plate on the interior wall surface contained the concrete spall. A summary of these tests was published as a technical report ESL-TR-85-32 "Semihardened Facility Design Criteria Improvements."

Extensive research programs have been performed to determine the survivability of blast doors and blast valves subjected to a

nuclear detonation. The responses of these components to a conventional weapon were largely unknown. It was uncertain if any of the currently available blast valves could function in the high pressure, short-duration and repeated air blast environment, as associated with conventional weapons effects.

TEST STRUCTURE

The semihardened structure of this test series was 60'-0 long and 50'-0 wide with a basement 30'-0 long and 50'-0 wide, which runs the entire width of the structure. There are two penthouses on the roof which house the blast valves. One penthouse is 37'-0 long and 16'-0 wide with eight compartments housing six blast valves, a blast screen and an open hole. The other penthouse is 9'-8" wide and 12'-0 long and has a blast valve and an air intake duct for the four chemical filters, and an air handling unit located on the first floor.

The basement floor and exterior walls are 3'-3" thick with 0.25% principal reinforcement and 0.10% transverse reinforcement in each face, with 0.12% shear ties, which will be the typical reinforcement for walls, floor and roofs through the remainder of this structure. The interior basement wall is 2'-1 1/2" thick with the same percentage of reinforcement. The basement ceiling and first floor is 8'-0 above the basement floor with half the slab 2'-1 1/2" thick and the other half 1'-5 3/4" thick, located under the alcove.

The first floor walls, which have a clear height of 13'-2", are 2'-1 1/2" thick except for the north wall, which has a thickness of 2'-7 1/2". The east wall has half the interior wall covered with an 11 gage steel spall plate, and the other half with 9 gage steel spall plate. The spall plate was to protect the chemical filters and the air handling unit, which is enclosed by a 12" interior wall supporting the penthouse above. The south wall was protected by 5 - 6" precast concrete panels, 4 Bitburg revetments 6'-7" high, or a polyethylene plastic honey combed sand grid filled with sand for a specific weapon detonation. The west exterior wall was protected by a 4'-7" high sand berm having a slope of 1:1.5. The west wall had six blast valves between the Luwa door and the sand berm. These valves consisted of two Batley, two Temet, one Luwa, and one Sheltec blast valves protected by a covered wing wall. The east wall had an unprotected 7 1/2" thick WES blast door, a two foot square escape hatch, and eight protected blast valve compartments. The south wall had a 4 1/2" thick WES door protected by a covered wing wall. The north wall had an opening into an alcove, which had two blast doors furnished by Temet USA and Security Systems Engineering Ltd. There was a steel plate partition between two columns and the south wall with a hung ceiling between the partition and the west wall.

The penthouse, located on the roof, has nine compartments. The air intake compartment for the gas filters has a room 7'-9" wide

and 8'-8" long, protected, by a Luwa blast valve and filter. The other eight compartments are 4'-0" wide and 11'-9" long separated by air tight 1/4 inch steel plate panels. These compartments are protected with one J.P. Sheltec blast valve, one Luwa blast valve, two Temet USA blast valves, two Batley blast valves, a two foot square open hole, and a blast screen with angles to deflect the blast. All eight compartments have a half-inch steel plate 4 inches in front of the blast valves or holes.

C & C Revetment chamber sections, 3'-0 wide, 4'-6" long, 2'-6" high and 3" thick, were erected in either one, three, or four sections high in front of the south wall. These sections had four different reinforcements: steel mesh, polypropylene fibers, steel mesh and polypropylene fibers, and steel mesh and steel fibers. All sections were bolted together with 2" x 1/4" steel straps. Some units had one anchor straps (unit 1 and 4), while others had two anchor straps (unit 2 and 3). After the sections were erected they were then filled with sand.

TEST DISCUSSION AND RESULTS

Between 8 July 1987 and 14 September 1987 we detonated 14 conventional weapons, all the same size, against the semihardened facility. Eleven events were static surface detonations, two were buried 12 feet and one was buried 6 feet. The buried weapons were at an angle of 70 degrees from horizontal.

The first test, Event 1, was against the east 2'-1 1/2" wall opposite the 7 1/2" WES door. During the test, the chemical filters and air handling unit were operating. The Luwa valve, in the air intake penthouse, had an exterior blast pressure of 59 psi and an interior pressure of 1.07psi. The door had an average exterior blast pressure of 4,000 psi with an interior pressure of 17 psi. The blast pressure knocked the WES door off its hinges and laid it in front of the opening on its face. The escape hatch, 32'-0 away, was opened by the blast and had fragment damage to the door. A bomb fragment hit the wing wall, changed directions, and hit the side of a precast panel that was in place on the south wall. The 7 1/2" WES door was then welded in place, and the escape hatch had a new locking device installed before the next test.

The second test, Event 2, was against the east wall opposite the escape hatch. This test was to determine the effects on the blast valves in the penthouse. All blast valves had external pressures between 200 and 300 psi with internal pressures less than 10 psi. The open hole internal pressure was 54 psi and the angle blast screen was 28 psi. The precast concrete panel on the south wall was knocked down by the blast. Other than fragmentation spall on the exterior of the east wall and wing wall, there was little other damage. The interior steel spall plates contained the spalled concrete. The 4 1/2" WES door on the south wall, was blown open and sustained some blast fragment damage to the opening mechanism.

The third test, Event 3, on the south wall determined the effects of the 6 inch precast wall panels, which was approximately 1 inch from the wall. All wall panels were knocked down and extensively damaged. There were two cracks along the top of the exterior wall with no exterior spall. The exterior wall pressure behind the wall panels, averaged 390 psi with a deflection of 1.64 inches. The interior wall had numerous cracks and one minor spall spot. The power outlet plug was knocked from the wall and some of the hung ceiling broke loose from its mount. The one section high C&C revetments were destroyed along with the unit that was three sections high with polypropylene fibers reinforcement. The other units in the first group that was 3 sections high with one anchor strap, did move away from the blast approximately 2 to 3 inches. The second and third group, that had two anchor straps, remained in place. All sections received extensive fragmentation damage.

Test 4, Event 7, was conducted against the west wall containing the Luwa door and six blast valves, which were protected by a wing wall. Because of the damage sustained by the 4 1/2 WES door and wall panel during Event 2, it was determined to have Event 7 next, in case we had another pretest failure on the door. To protect the blast gages on the south wall from fragmentation damage, the Bitburg revetments were installed. The Luwa door was constructed with 1/2-inch steel plates and filled with 7 1/2 inches of reinforced concrete. The door frame had narrow metal plates with anchor lugs protruding into the concrete wall. Fragments from the weapon perforated the thin concrete section around the door frame, and penetrated the edge of the door. The average exterior blast pressure at the edge of the door was 1460 psi with an interior pressure of 22 psi. The deflection of the door was 0.75 inches. The six blast valves had no fragment damage done to the valves. The average exterior blast pressure was 170 psi and the average interior blast pressure at the valve was 19 psi. There was some minor interior wall cracks around the blast valves. Unit 1 of the C&C revetments started leaning away from the weapon location, indicating a failure of the single anchor straps.

Test 5, Event 4, was conducted against the Bitburg revetments which were reset after the last test. The blast against the wall behind the revetments averaged 390 psi, with a peak wall deflection of 1.44 inches. Immediately above the revetments, the blast pressure averaged 1520 psi and at the roof level 350 psi. There was 2.0 square feet of spalled concrete on the exterior wall above the revetments, but none below the top of the revetments. The revetments were completely destroyed. The interior wall had more cracks, one concrete spaul spot, with portions of the hung ceiling falling.

Test 6, Event 5, was conducted against the sand grid, which was 6 inches from the wall. The blast pressure behind the sand grid averaged 390 psi, with a wall deflection of 1.44 inches, while above the sand grid the blast pressure averaged 1,520 psi. The

damage to the sand grid was noticable where the weapon was located. There was more cracking on the interior wall. Unit 1 of the C&C revetments, had only one section out of four remained standing, but leaning at approximately a 10 degree angle. Two sections failed during this test.

Test 7, Event 6, was conducted on a bare reinforced concrete wall 2' -1 1/2" thick and the 4 1/2 inch WES blast door. The blast pressure on the bare wall averaged 1,570 psi and had a peak deflection of 2.27 inches before it rebound and started to spall. There was a large area, 75 square feet, on the inside wall which spalled. The exterior wall also showed evidence of a large spall area. The 4 1/2 inch WES door had several fragmentation hits during the three previous tests. These three tests had an average outside blast pressure of 200 psi, an interior pressure of 4.3, with an average maximum deflection of 0.35 inches. This test, the weapon was closer to the door, and had an average exterior blast pressure of 225 psi, an interior pressure of 3.7 psi, and a peak deflection of 0.51 inches. Fragments from the weapon damaged the lower hinge and welded the base of the door to the frame under the locking device, preventing the door from opening. Therefore, after this test, there was only one door still operable that has been tested. Unit 1 of the C&C revetment was completely destroyed during this test. Units 2 and 3 received heavy fragmentation damage on the face, but continued to provide protection as a revetment.

Test 8, Event 9, was conducted on the west wall aginst a sand berm. The blast pressure against the exterior wall above the berm averaged 1,220 psi, while behind the burm the pressure averaged 240 psi. The peak deflection of the interior wall was 3.9 inches, which caused cracking along that wall. The exterior west wall had fragmentation spaul above the burm but none behind the berm. There was no damage to the berm, and could be reused several times.

Test 9, Event 8, tested the Temet door and the E.E. Systems Engineering door located in the alcove. The Temet USA door had an average exterior blast pressure of 170 psi, an interior pressure of 1.7 psi, and deflected 0.47 inches. The fragment damage consisted of shearing two of the three bolts on the top hinge connector bar. The E.E. Systems Engineering door, which was operating hydraulicly and 12 inches thick, with concrete fill between 2-1/2" thick steel plates, had no damage to it. The average external pressure was 300 psi, with an internal pressure of 5.0 psi and a deflection of 0.28 inches. Both doors continued to operate satisfactorly. Other than exterior fragmentation spall on the north and west wall there was no other damage.

Test 10, Event 10, was a surface detonation, conducted along the bare 2'-7 1/2" reinforced concrete north first floor wall and the 3'-3" basement wall. The average blast pressure on the first floor wall averaged 1,180 psi, with a deflection of 1.94 inches. The pressure against the exterior basement wall averaged 116 psi.

The Luwa blast valve in the penthouse had an external blast pressure of 40 psi and an internal pressure of 1.1 psi. There were spall cracks on the interior first floor wall and 35 square feet of concrete spall. There was no noticable interior basement wall cracks. The exterior exposed wall had a lot of fragmentation concrete spalling.

Test 11, Event 11, was the first buried detonation on the semihardened structure. The buried weapon was placed in the ground at 70 degrees from horizontal. This was to represent a bomb being aerial delivered. Event 11 was buried to a vertical depth of 6 feet to the center of gravity of the weapon. This located the weapon approximately the center of the north basement wall, opposite the alcove. The crater it formed was 36 feet in diameter and 8 feet deep. The blast pressure on the 3'-3" basement wall was approximately 390 psi with a peak deflection of 0.94 inches. The interior pressure was 0.18 psi. There was extensive cracking on the interior of the basement wall. There was no fragmentation spall on the exterior of the wall. In the basement we had cabinets, bookcases, desks, and mannequins, which were sitting, standing and lying down. One mannequin standing next to the exterior wall near the weapon, fell.

Test 12, Event 12, the second buried detonation on the north wall, opposite the penthouse, was at a depth of 12 feet vertically. The crater was 52 feet in diameter and at a depth of 10 feet. The center of gravity of the weapon was on line with the basement floor. A film of the detonation indicated the north side of the building raised a couple of inches, then fell back into place. The blast pressure on the exterior basement wall averaged 630 psi and had a peak deflection of 0.26 inches. The average interior basement pressure was 0.12 psi. There was substantially less interior wall cracks in this test than the previous test. The standing mannequin and bookcase, next to the exterior wall, fell.

Test 13, Event 14, the weapon, located in the archway to the alcove approximately 9'-6" from the center of the Temet USA door and E.E Systems Engineering door, was the last surface detonation. The average blast pressure on the doors was 6,320 psi, with an interior pressure at the doors of 32.7 psi. The interior pressure on the interior south wall was 8.5 psi. The E.E System Engineering door and frame was blown from the alcove wall, hitting and cracking a column, then rested intact near the second column 31 feet away. The interior of the door rested face-up with the bottom of the door away from the alcove. The Temet USA 3 inch thick steel door broke into three pieces. The twisted door frame and two door sections that rested in the 4'-7" wide hall at the 7 1/2" WES door moved 26 feet from its original position. The bottom section of door, near the outside wall, was thrown 23 feet near the chemical filter and air handler wall. The alcove exterior walls were blown out, along with its interior walls. The roof was extensively cracked over a 280 square foot area. There was one spall area in the basement ceiling under the

alcove. The 4 1/2 inch HES door, that could not be opened during the seventh test, was blown open. The duct work for the chemical filters and air handler was bent and portions removed. The interior steel partitions, between the columns and south wall were blown down along with the hung ceiling. The Luwa door remained closed even with two locking lugs of the original three locks in place.

Test 14, Event 13, was a 11'-0 buried detonation along the south wall. The floor was 2'-1 1/2" thick and a slab-on-grade. The view on the video film of the detonation showed the south wall being lifted approximately 2 feet then settling back to its original position. The crater was 46 feet in diameter and 10 feet deep. The average internal pressure was 0.20 psi. There was no additional visible wall, ceiling, floor nor roof cracks, nor spall areas. Next to the south wall a standing mannequin, a bookcase, wall clock and cabinet fell. All other furniture and mannequins remained in place.

CONCLUSIONS

A. The new wall design using 0.25 percent vertical reinforcement in both faces, performed very well. There were relatively small deflections, 1 to 4 inches measured in the 1/4 percent reinforced concrete wall. Shear ties are required in all semihardened structures.

B. The blast doors must be kept out of the line of sight of the weapon. Fragmentation severely damaged all doors, the hinges, locking devices, and frames, making the doors inoperable or breached.

C. All blast valves worked well during the first test, but failures were noted during other tests. Dust, concrete chips and fragments caused problems with the blast valve mechanism mainly with the spring steel that opened the valves after a test started to fail.

D. The sand berm worked best to prevent spall and can be used repeatedly. The sand grid was satisfactory for one or two detonations. The full height precast panels and Bitburg revetments prevented spall, but were severly damaged after one test and could not be reused.

E. The C&C sand filled box revetments worked extremely well and can be used for splinter protection of equipment and other facilities. They received several detonation blasts.

F. Spall plates on the interior of a shelter is very good protection in containing concrete spall.

G. Nothing should be placed on or next to an exterior wall.

H. A buried detonation provides less damage, due to blast and fragmentation, than a surface detonation.

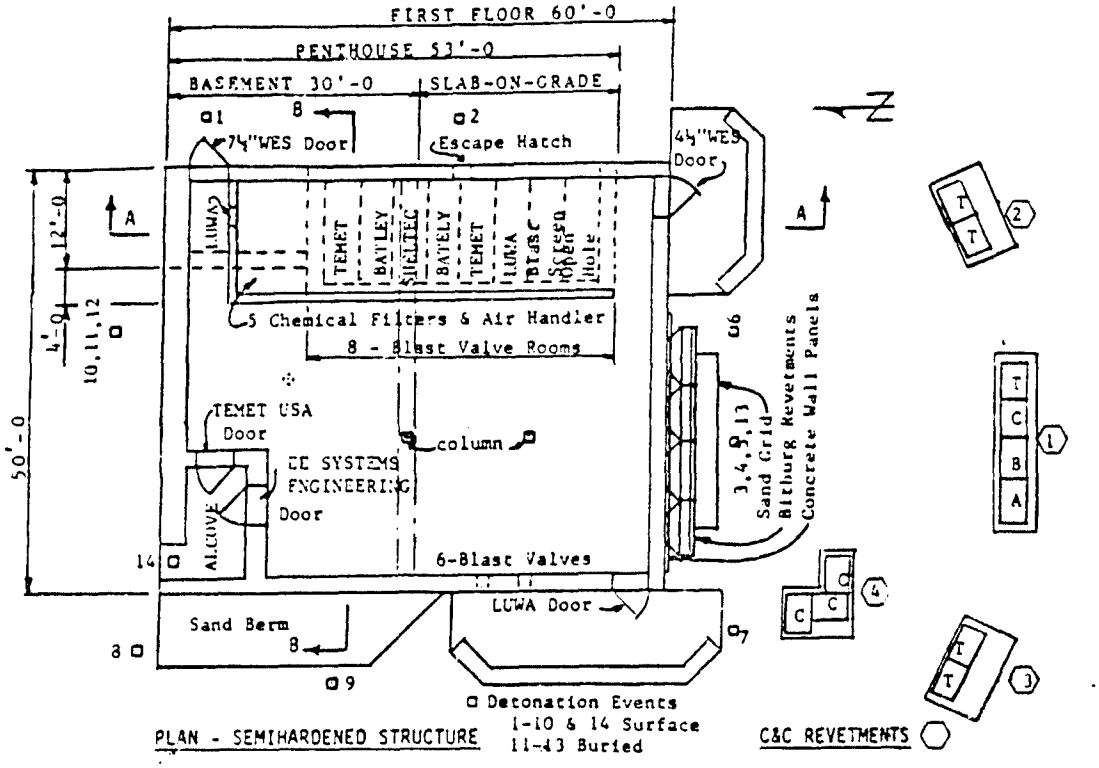

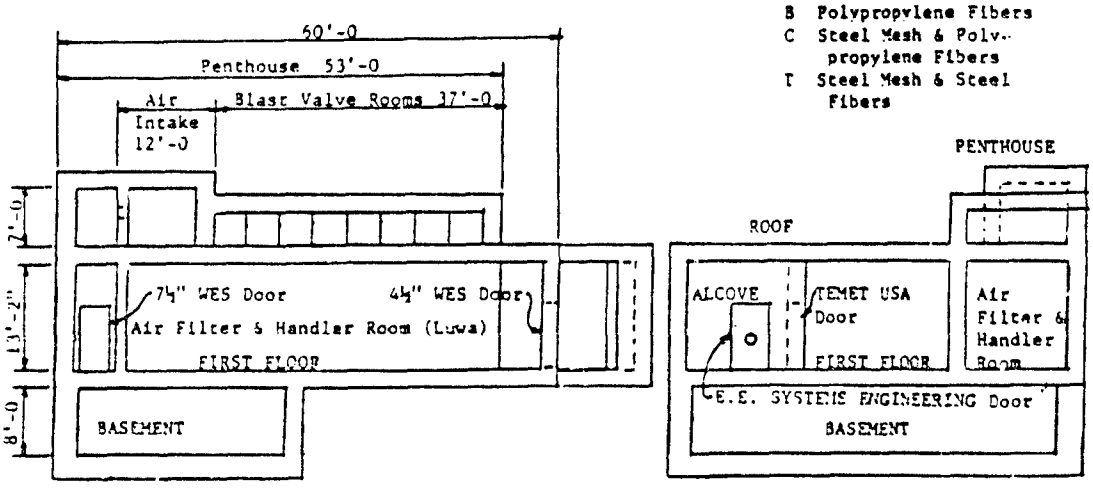

SEMIHARDENED TEST STRUCTURE

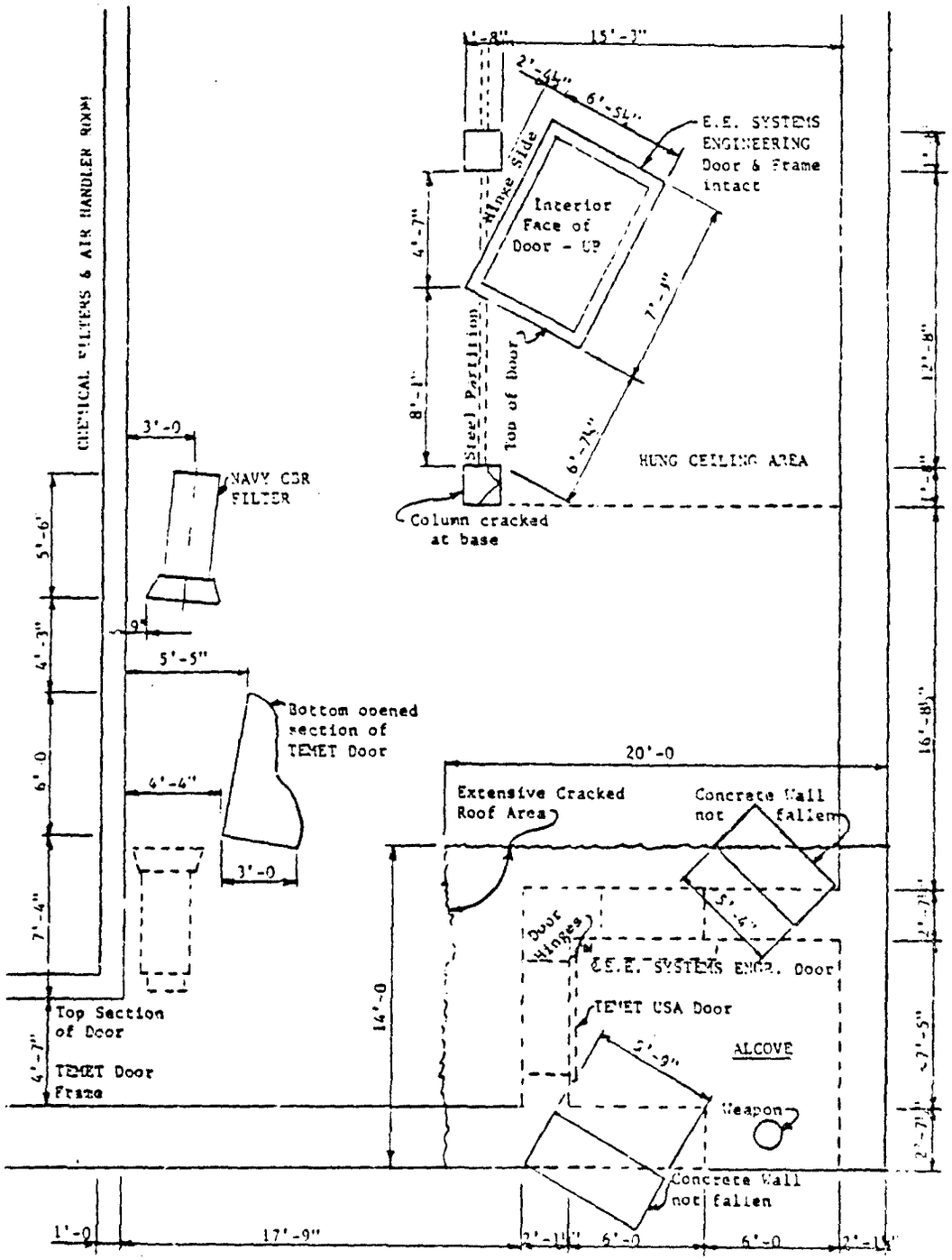

ALCOVE DAMAGE TO SEMIHARDENED TEST STRUCTURE

EVENT 14 - SEPTEMBER 2, 1987

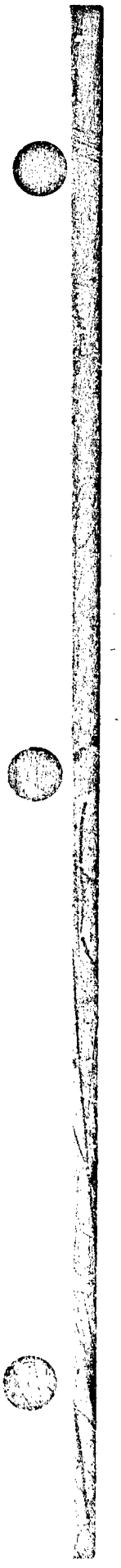

JET-FLOW FROM SHOCK TUBES

BY

Charles N. Kingery

Edmund Gion

U. S. Army Ballistic Research Laboratory

Aberdeen Proving Ground, MD 21005

ABSTRACT

This project was designed to map the magnitude and extent of the high velocity jet-flow exiting shock tubes. The flow was measured by installing stagnation probes along three blast lines and by supplementing these measurements with calibrated displacement cubes. The side-on and stagnation overpressures versus time were measured, and from that the side-on and stagnation impulses were calculated. The stagnation impulse showed a large drop in magnitude as the blast line was moved from the zero line to 1.5 and then to a 3-diameter off-set. A helium driver was used in the 2.54-cm diameter shock tube to simulate an explosion in a storage magazine. Results are presented in the form of stagnation impulse versus distance along the three blast lines. The significance of these findings is that the present quantity-distance criteria for munitions stored in underground magazines are based on side-on peak overpressure, but our results show that the peak stagnation pressure and impulse are much greater. At a distance where 10.3 kPa (1.5-psi) side-on pressure was measured, a 49.6 kPa (7.2-psi) stagnation pressure was measured. At the same distance, a side-on impulse was 12.6 kPa-ms (1.83 psi-ms), while the stagnation impulse was 139.0 kPa-ms (20.2 psi-ms)--a dramatic difference.

1. INTRODUCTION

1.1 Background. The peak overpressure exiting from shock tubes, underground munition storage site tunnel models, and full-scale sites has been documented and reported in Reference 1. The criterion for structural damage is peak side-on overpressure.[2] Although it is well known that dynamic pressure and dynamic pressure impulse can be a primary damage mechanism, little is known about the propagation of dynamic pressure outside of a tube or tunnel. The dynamic pressure may cause more damage than the peak side-on overpressure. It is for this reason that the current program has been conducted by the BRL with funding from the DOD Explosives Safety Board.

1.2 Objectives. It is well known that a narrow, high velocity flow exits shock tubes,[3] but the extent and magnitude are not well documented. One of the objectives of this study was to document the dynamic pressure and impulse propagating outside the tube along the zero degree axis. A second objective was to determine the width of the jet-flow by establishing off-set blast lines in units of tunnel diameter. The first blast line was along the zero axis; the second blast line was off-set 1.5 tunnel diameters; and the third line was off-set 3 tunnel diameters. We comment here that stagnation pressure impulse is taken to be equivalent to the dynamic pressure impulse because the side-on pressure impulse was found to be relatively insignificant in comparison.

A second method planned for mapping the magnitudes and extent of the jet-flow was to place small cubes of different density material in and out of the flow path and, from the measured displacement, to calculate the dynamic pressure impulse.

2. TEST PROCEDURES

2.1 Shock tube description. In order to conduct the experimental program in a controlled environment, a large open area in a BRL warehouse was established as the test site. A platform of 2.54 cm plywood on 5-cm by 15-cm (2 in x 6 in) wooden studs was constructed to facilitate gauge mounting and cable runs. A 2.54-cm (1-in) inside diameter, steel shock tube was selected because it would be operative indoors without resorting to remote control. A sketch of the tube is shown in Figure 1. The driver section of the tube was 150 cm (59 in), and the driven section was 133 cm (52.5 in.). The wall thickness of the tube was 1.27 cm. If we consider a full size tunnel diameter of five meters, then this tube is a 1:197 scale.

2.2 Instrumentation description. A schematic of the data acquisition-reduction system is given in Figure 2. Quartz piezoelectric transducers were used to record both the side-on overpressure and stagnation pressure versus time. The transducers are coupled through a power supply and data amplifiers to a digitizing oscilloscope. On-site comparisons of the results were made directly from the hard copies of the pressure versus time records. Final data processing and generation of the overpressure and stagnation impulse versus time were completed with the computer, printer, and plotter.

The stagnation pressure was recorded using a stagnation probe, as shown in Figure 3. This type of transducer has been used successfully in many shock tube experiments. Because of the steel wool placed inside the probe to dampen reflections, there is a finite rise-time associated with the recorded stagnation pressure versus time record. This does not affect the primary flow measurements because of the long duration.

2.3 Transducer layout. It was surmised that the jet-flow extended a considerable distance beyond the tunnel exit but was rather narrow. Therefore, rather than mapping the area along different radial lines extending from the tunnel entrance--i.e. 0, 5, 10, 15 degrees--the decision was made to map with parallel lines. The parallel lines established were a zero off-set, 1.5 tube diameter off-set, and a 3.0 tube diameter off-set. The off-sets and transducer locations are shown in Figure 4. In reality, the off-sets were achieved by moving the shock tube rather than by establishing new gauge lines. The location of the transducers was planned to produce a peak side-on overpressure of 5 kPa to 8 kPa at the last station for the different exit pressures. That is 35 diameters for the 500 kPa exit pressure, 48 diameters for the 900 kPa exit pressure, and 72 diameters for the 1,800 kPa exit pressure. The side-on and stagnation pressure both could not be made at each station on the same test; consequently, after one test, they were alternated, and a second test was conducted.

2.4 Cube displacement method. One method for measuring the flow effects is to measure the displacement of objects having known volume and density. A relationship between dynamic pressure impulse, displacement initial velocity, and cube parameters can be summed up in the following equation.[4]

$$\Delta I_s = (w/C_D A g)\sqrt{-\frac{D}{C}} \qquad (1)$$

when

ΔI_s = stagnation pressure impulse,* psi-sec
w = weight, lb
C_D = 1.2
A = cube face area, in^2
g = 32.17 ft/s^2
C = D/V_0^2, sec^2/ft**
D = displacement, ft
V_0^2 = initial velocity, squared ft^2/s^2

For a given cube, w, C_D, A, g, and $\sqrt{C}$ can be lumped into one constant

and Equation 1 becomes:

$$\Delta I_s = k \sqrt{D} \qquad (2)$$

Along the zero off-set line, the stagnation impulse (ΔI_s) has been documented; therefore, when the displacements for specific cubes are determined, the constant, k, can be obtained from

$$k = \Delta I_s / \sqrt{D}$$

The values of k for the different cube materials will be given later.

---

*Stagnation pressure impulse and dynamic pressure impulse are considered the same in this report.

**C was determined to be a constant based on the model described in Reference 4.

3. RESULTS

3.1 Jet-flow generation. The jet-flow measured outside of a shock tube is a function of gas dynamics occurring within the driver section and driven section. In Figure 5, a wave diagram has been constructed to show the complicated interaction of the different gases and rarefaction waves. Because the density of the gas within the driver is important, helium was chosen as the driver gas to match as closely as possible the density of the driver gas when an explosion occurs in a storage chamber.

3.2 Transducer measurements. The peak side-on overpressure and stagnation pressure were both measured at the tube exit and along the zero and off-set lines, but, because of reflections and blockage, they were not measured on the same shot. The primary objective of this program was to document the magnitude and extent of the jet-flow, and, therefore, most of the effort was expended in documenting the stagnation impulse. The station locations are shown in Figure 4. The two transducer stations not shown in Figure 4 are Station T-1 , located in the side wall of the tube at 2.54 cm from the end to measure the exit pressure and impulse--and Station S-1 , a pitot-tube-type stagnation gauge with the sensing end 0.6 cm inside the exit to record the stagnation pressure and impulse versus time exiting the tube. A sketch of gauge and location is shown in Figure 6.

3.2.1 Results along the zero line. The stagnation impulses (ΔI_s) measured along the zero off-set line are listed in Table 1. The values were first adjusted to account for variations in the exit impulse I_w. Exit impulse values of 1,500 kPa-ms, 5,000 kPa-ms, and 11,000 kPa-ms were selected as normalizing values. Therefore, if a stagnation impulse was

measured from an exit impulse of 1,400 kPa-ms, it was multiplied by I_w 1,500/I_w 1,400 or 1.07 to bring it up to the norm. The values listed in Table 1 are average values from more than one test, and are plotted in Figure 7.

It was noted that the stagnation impulse (ΔI_s) values appeared to increase in proportion to the increase in the exit impulse I_w. The ratio of stagnation impulse (ΔI_s) along the zero off-set line to exit side-on impulse I_w are also listed in Table 1. The ratios $\Delta I_s/I_w$ listed in Table 1 are plotted in Figure 8 as $\Delta I_s/I_w$ versus R/D_T. The results can be represented by a single curve, with the exception of R/D_T of 10, where the 11,000 I_w value is lower than that for the other exit conditions. Based on this curve, values of (ΔI_s) along the zero line can be predicted for any side-on exit impulse ranging from 1,500 to 11,000 kPa-ms.

3.2.2 Results along the 1.5-diameter line. The stagnation impulses measured along the 1.5-diameter line for the three different pressure levels are listed in Table 2. The values are plotted in Figure 9. The stagnation impulses versus distance for the three pressure levels show similar trends, but the values of $\Delta I_s/I_w$ do not blend into a single curve when plotted as impulse ratios versus distance. Compared to the zero line, the curves in Figure 9 for the three input impulses show a dramatic decrease in stagnation impulse at the close-in stations 6.5, 10, and 15. Beyond station 23, the three curves show attenuation of impulse with distance. Beyond station 35, values of stagnation impulse at the 1.5 diameter off-set appear to be the same as those measured along the zero line.

3.2.3. Results along the 3.0 Diameter Line. The stagnation impulses measured along the 3.0 diameter line are listed in Table 3. These values are plotted in Figure 10. The 3.0

diameter line, when compared to the zero line, shows even a greater attenuation of stagnation impulse. If we look at station 10, we can see that, for the low pressure shots, the values are 479 kPa-ms for the zero line, 72 kPa-ms for the 1.5-diameter line, and 20 kPa-ms for the 3.0 diameter line. This shows that, with an off-set of only three diameters, the stagnation impulse is only four percent of the zero line values. These differences become even greater as we approach the tunnel exit.

3.3 Cube displacement measurements. In an effort to precisely map the jet-flow without establishing more blast lines, it was suggested that small cubes of different density material be used in place of stagnation probes. As shown in Equation 2, if the stagnation impulse and displacement are known, the constant, k, can be determined, and the cube can be considered calibrated. Now, if the cubes are placed at off-set locations of 4, 5, 6, 7, 8, 9, or 10 diameters from the measured displacement, the stagnation impulse can be calculated.

3.3.1. Cube calibration. Cubes of two different sizes and three different materials were manufactured. They were steel, aluminum, and wood, sized one-inch and three-eighths-inch. The average weight of the three-eighths-inch steel cubes was 6.639 g; aluminum was 2.371 g; and wood was 0.5563 g. The one-inch steel cubes weighed 125.9 g; the aluminum was 45.0 g and the wood was 10.5 g. After the stagnation pressure versus distance was established along the zero line, then the cubes were placed at selected distances along the zero line, the shock tube was fired, and the displacements were measured. Care was taken to see that the cubes did not interfere with each other and that measurable displacements were obtained. From the blast line stagnation impulse, $\triangle I_s$, at a specific distance, and the cube displacement, D, from that location, a relationship was established where $k = \triangle I_s/\sqrt{D}$. Because of the smallness of

the shock tube and the sharp drop in ΔI_s values from the zero line to the three-diameter off-set, the three-eighths-inch cubes were used for most of the off-set measurements. A value of

$$k = .0202 \frac{psi\text{-}s}{ft.1/2} \quad \text{or} \quad 0.252 \frac{kPa\text{-}s}{m1/2}$$

was established for the three-eighths-inch steel cubes, and

$$k = .0061 \frac{psi\text{-}s}{ft.1/2} \quad \text{or} \quad .076 \frac{kPa\text{-}s}{m1/2}$$

was established for the three-eighths-inch aluminum cubes. The constant, k, can be substituted in Equation 2 to determine the stagnation impulse at the off-set position.

3.3.2 Cube impulse measurements. The stagnation impulse values based on cube displacements for various off-set distances are listed in Table 4. Note that the distances along the zero line are different from those in Table 3 because a grid was established consisting of 0.3048 metre squares (one-foot squares) to assist in measuring displacement distances. From the cube displacements the impulses were calculated for various off-sets at selected distances in front of the tube for specific exit conditions. The cube displacements were determined for the 1,500 kPa-ms exit impulse. When the off-set impulses ΔI_s for a given distance in front of the tube was plotted on semi-log paper as ΔI_s versus off-set, they fell along a straight line, which means that the decay from the zero line outward is exponential. At the close-in station, the slope is very steep, but it becomes less steep as the distance in front of the tube increases. An illustration of this trend is shown in Figure 11, where the data for 12, 24, and 36 diameters in front of the tube are plotted as ΔI_s versus off-set.

4. CONCLUSIONS

4.1 Magnitude and extent of jet-flow. Based on the transducer measurements, it can be concluded that the jet-flow exiting from the shock tube is a high velocity flow, a very turbulent flow and a relatively narrow jet, and can add significantly to target loading. The magnitude in terms of stagnation impulse is a function of the exit energy or side-on impulse. One would also expect a correlation with the stagnation impulse exiting the tube, but this was difficult to measure because of blockage.

4.2 Side-on and stagnation peak overpressures. A comparison has been made between the side-on peak overpressure measured at the gage station and the stagnation peak overpressure. The values are listed in Table 5. In the table, it can be seen that, along the zero line for an average value of ΔP of 4.5 psi side-on, the stagnation pressure is 35 psi; for ΔP of 2.5 psi, the Pstag is 17 psi; for ΔP of 1.5 psi, the Pstag is 7.2 psi; and for ΔP of 0.8 psi, the Pstag is 1.6 psi. These values are based on a helium gas driver, and the flow characteristic of the jet generated from these tests may not be the same as that generated from field tests with explosives detonated in the storage chamber.

5. REFERENCES

1. Kingery, Charles N., Survey of Airblast Data Related to Underground Munition Storage Sites, BRL Technical Report to be Published.

2. Ammunition and Explosives Safety Standards, DOD Manual 6055.9-STD, July 1984.

3. James, D. J., An Investigation of the Pressure Waves Propagated from the Opened End of a 30"x18" Shock Tube, AWRE Report 0-60/65, AWRE, England, September 1965.

4. Ethridge, N. H., Use of Displacements of Cubes as a Measure of Blast, Unpublished report, Aberdeen Research Center, Aberdeen, MD., _____ 1987.

TABLE 1. Stagnation Impulse along the Zero Line.

Dist.	I_w=1,500 kPa-ms		I_w=5,000 kPa-ms		I_w=11,000 kPa-ms	
R/DT	ΔI_s kPa-ms	$\Delta I_s/I_w$	ΔI_s kPa-ms	$\Delta I_s/I_w$	ΔI_s kPa-ms	$\Delta I_s/I_w$
4.5	959	0.639	...	...	...	...
6.5	518	0.345	1,863	0.373	3,627	0.330
10.0	479	0.319	1,566	0.313	2,407	0.219
15.0	296	0.197	1,137	0.227	2,233	0.204
23.0	142	0.095	460	0.092	1,212	0.110
35.0	54	0.036	172	0.034	478	0.044
48.0	17	0.011	43	0.009	126	0.012
54.0	17	0.011	...	...	135	0.012
60.0	17	0.011	41	0.008	126	0.012

TABLE 2. Stagnation Impulse along the 1.5-Diameter Off-set Line.

Dist.	I_w=1,500 kPa-ms		I_w=5,000 kPa-ms		I_w=11,000 kPa-ms	
R/DT	ΔI_s kPa-ms	$\Delta I_s/I_w$	ΔI_s kPa-ms	$\Delta I_s/I_w$	ΔI_s kPa-ms	$\Delta I_s/I_w$
4.5	49	0.032	155	0.031	...	...
6.5	87	0.058	117	0.023	368	0.034
10.0	72	0.048	192	0.039	511	0.047
15.0	86	0.057	270	0.054	608	0.055
23.0	99	0.066	153	0.031	518	0.047
35.0	25	0.017	160	0.032	368	0.034
54.0	4	0.009	72	0.015	133	0.012
100.0	...	...	...	...	...	...

TABLE 3. Stagnation Impulse along the 3.0-Diameter Off-set Line.

Dist.	I_w=1,500 kPa-ms		I_w=5,000 kPa-ms		I_w=11,000 kPa-ms	
R/D_T	ΔI_s kPa-ms	$\Delta I_s/I_w$	ΔI_s kPa-ms	$\Delta I_s/I_w$	ΔI_s kPa-ms	$\Delta I_s/I_w$
4.5	1	0.0006	34	0.0067	...	...
6.5	1	0.0006	31	0.0062	62	0.0056
10.0	20	0.0133	50	0.0099	60	0.0054
15.0	27	0.0180	44	0.0088	85	0.0074
23.0	50	0.0335	63	0.0103	188	0.0177
35.0	34	0.0227	131	0.0262	158	0.0144
54.0	5	0.0031	41	0.0092	123	0.0115
100.0	...	...	...	...	23	0.0020

TABLE 4. Stagnation Impulse Versus Off-set for I_w = 1,500 kPa-ms.

Distance along zero-line dia.	Impulse - kPa-ms						
	Off-set diameters						
	0.	1.5	3.0	4.0	5.0	6.0	7.0
12	400	95	22	9.5	...	...	...
18	220	115	67	40	26	17	11
24	142	87	55	40	29	22	16
30	75	55	41	34	28	23	19
36	52	38	28	23	19	15	13
44	38	32	27	24	22	20	17
54	17	15	13	...	...	...	...

TABLE 5. Side-on and Stagnation Peak Overpressure.

		Off-Set			
		0	1.5	3.0	
Distance dia. (in.)	ΔP psi	P_{stag} psi	P_{stag} psi	P_{stag} psi	P_w psi
10	4.0	32.7	14.0	5.0	73
15	2.3	14.5	11.0	3.0	"
23	1.3	7.3	10.0	3.0	"
35	0.7	1.5	2.7	1.5	"
10	8.0	44.0	20.0	11.0	145
15	4.6	29.0	15.0	5.0	"
23	2.6	22.0	20.0	6.0	"
35	1.5	7.0	7.0	5.0	"
54	0.9	1.7	1.7	1.7	"
10	14.7	55.0	44.0	27.0	275
15	8.6	58.0	54.0	15.0	"
23	4.8	43.0	29.0	22.0	"
35	2.7	15.0	15.0	9.0	"
54	1.6	7.3	4.0	4.0	"

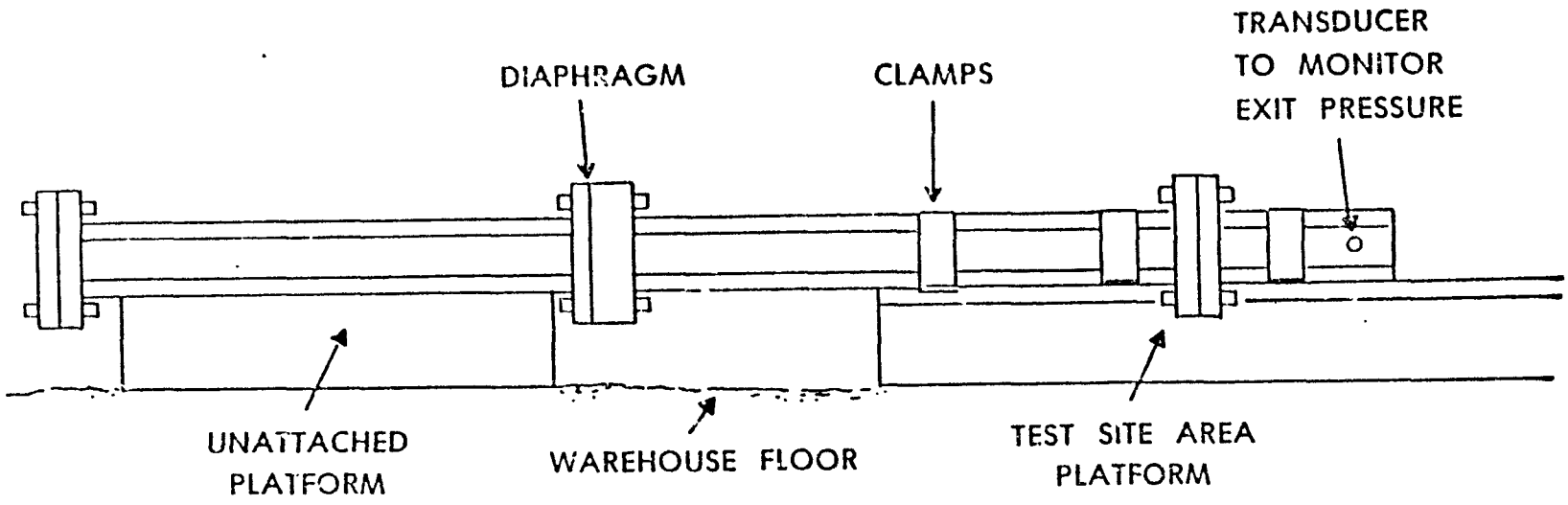

Figure 1. Sketch of 2.54-cm inside diameter shock tube.

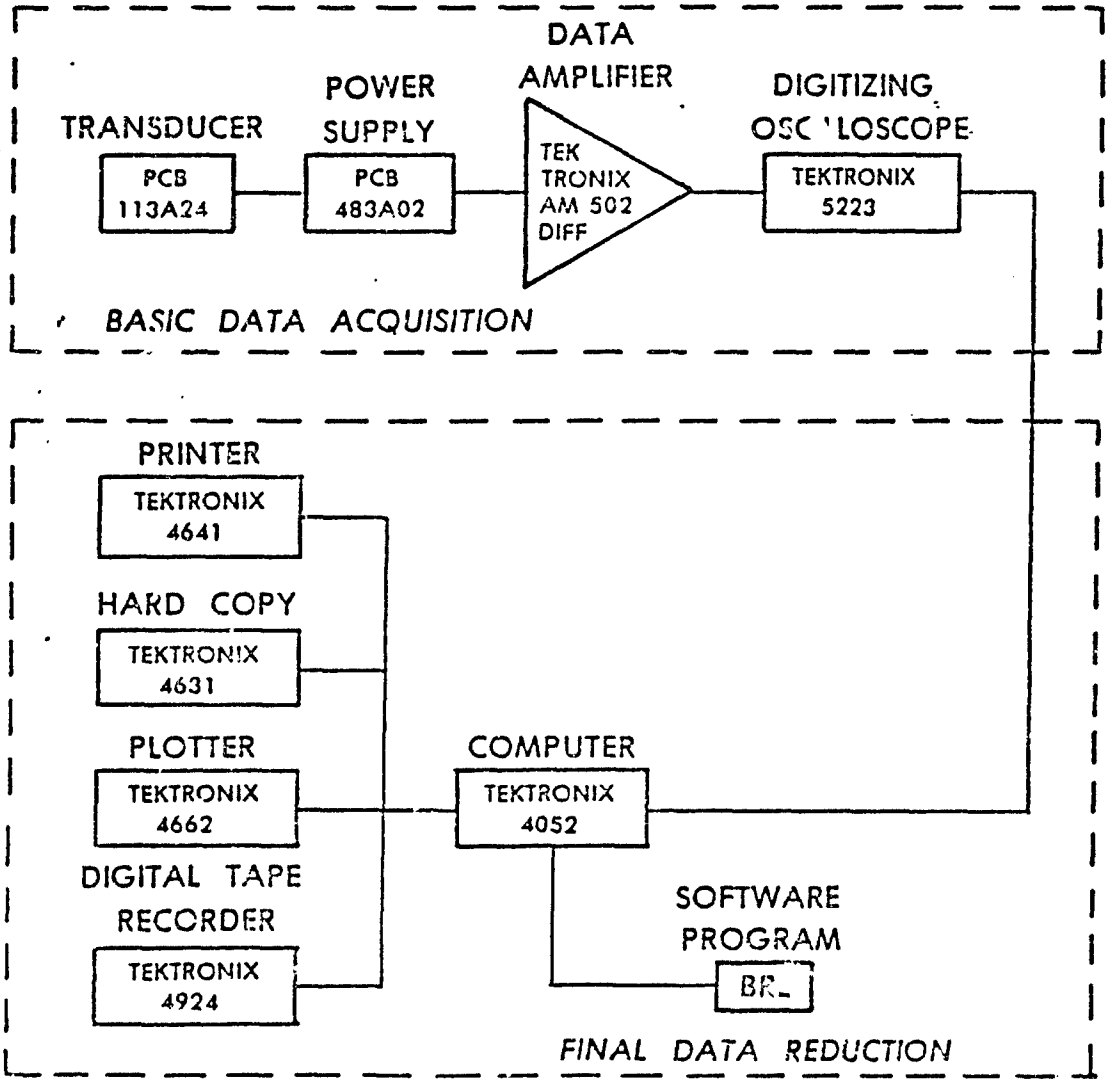

Figure 2. Schematic of data acquisition-reduction system.

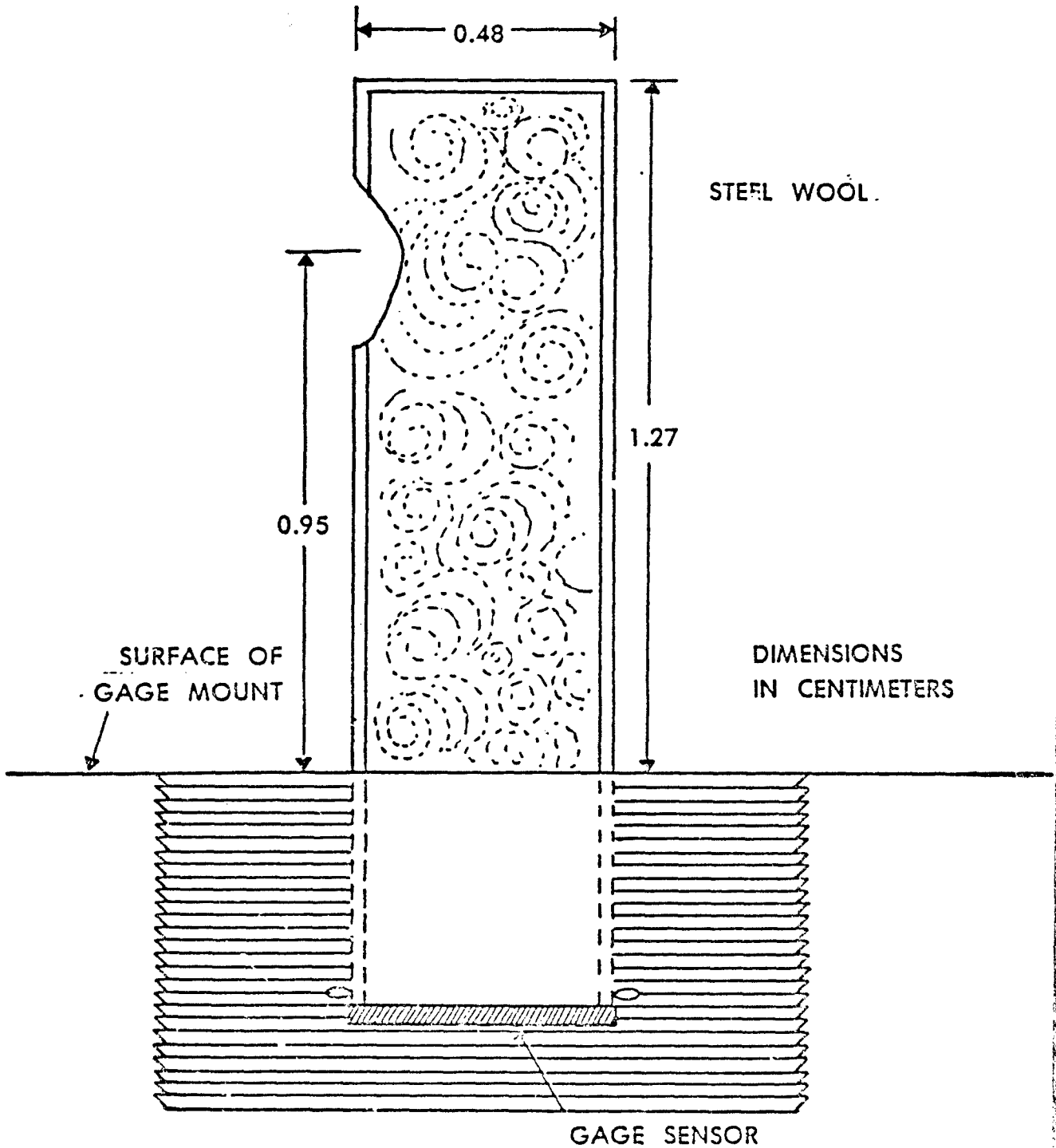

Figure 3. Sketch of stagnation probe.

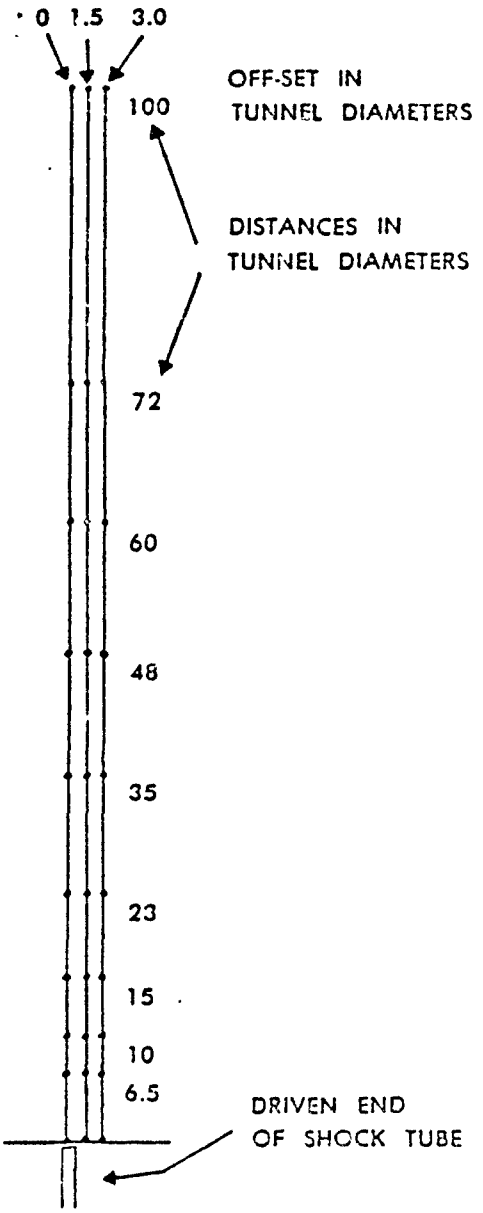

Figure 4. Transducer layout.

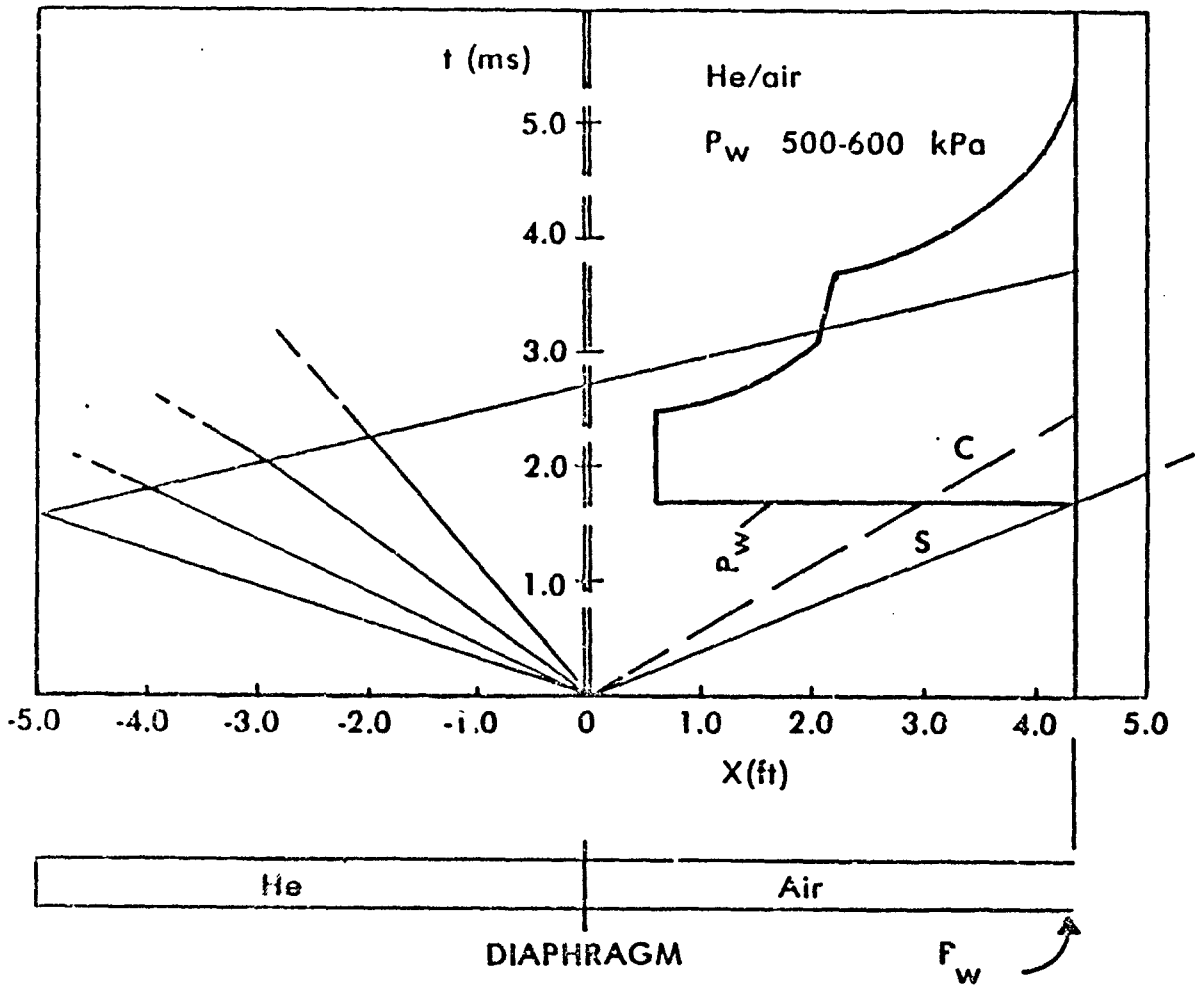

Figure 5. Wave diagram for exit pressure.

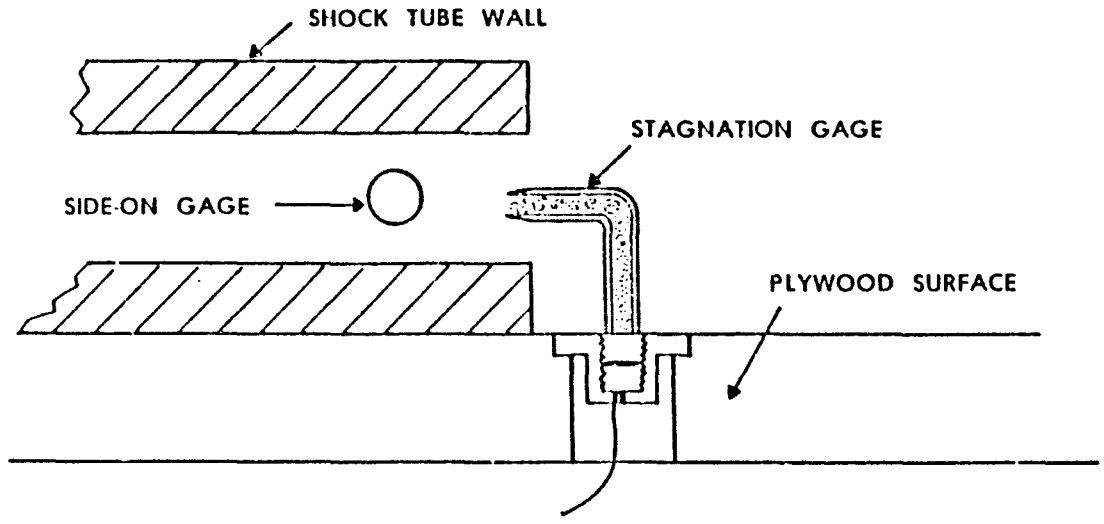

Figure 6. Sketch of stagnation gauge and location.

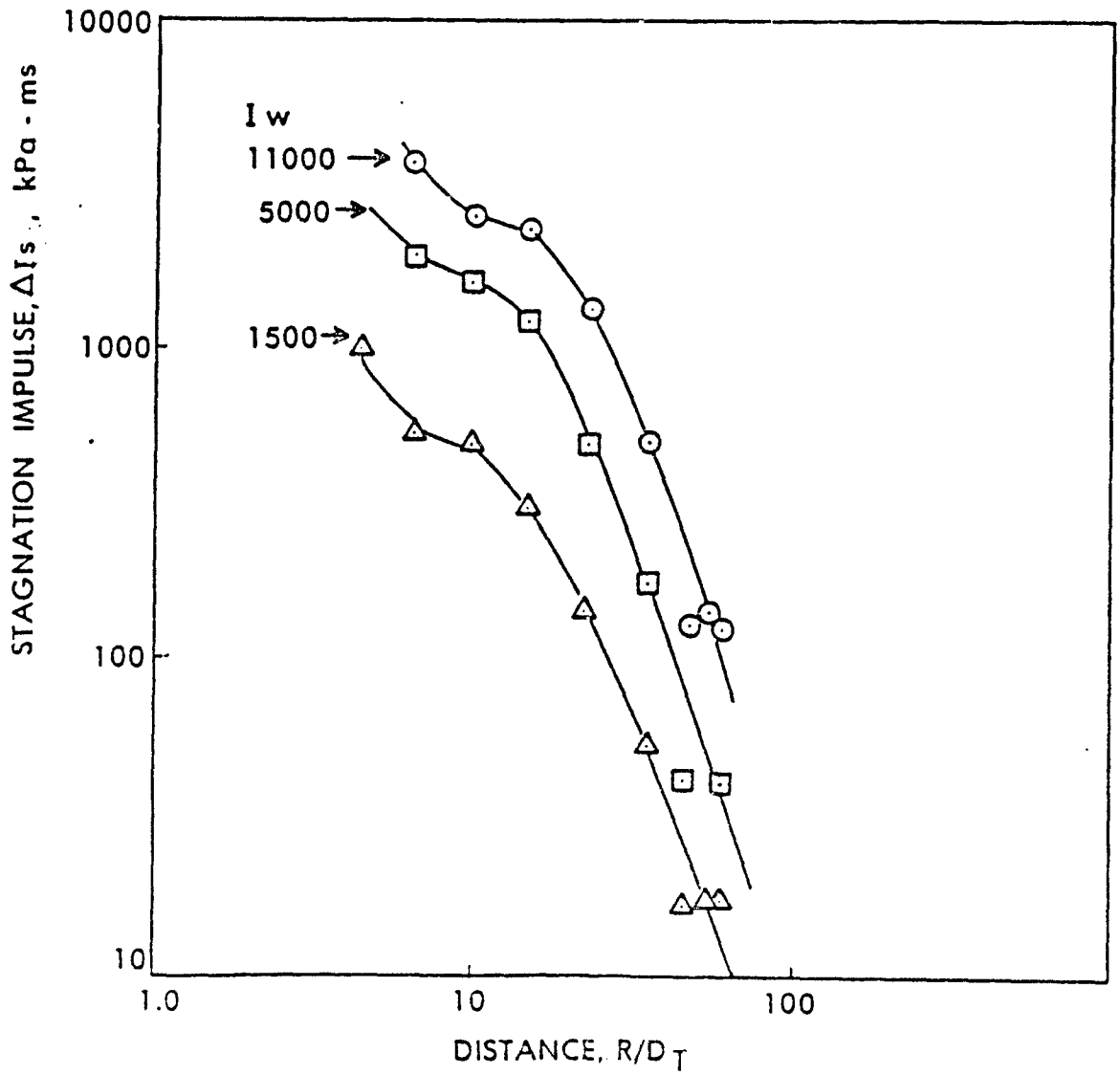

Figure 7. Stagnation impulse, (Δ Is), versus range (R) over tunnel diameter (DT) along the zero line for three exit impulses Iw.

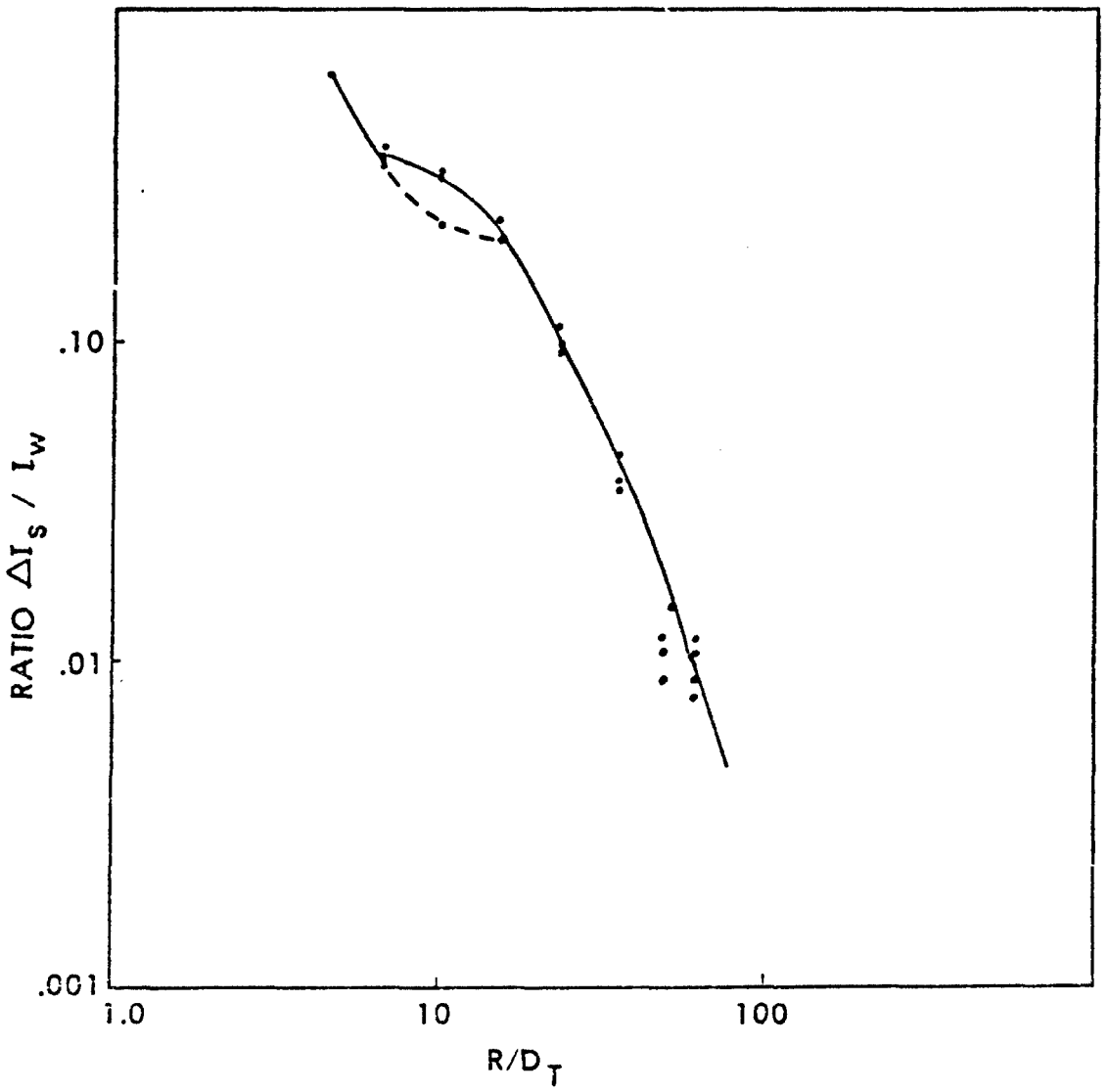

Figure 8. Ratio $\Delta I_s/I_w$ versus R/D_T.

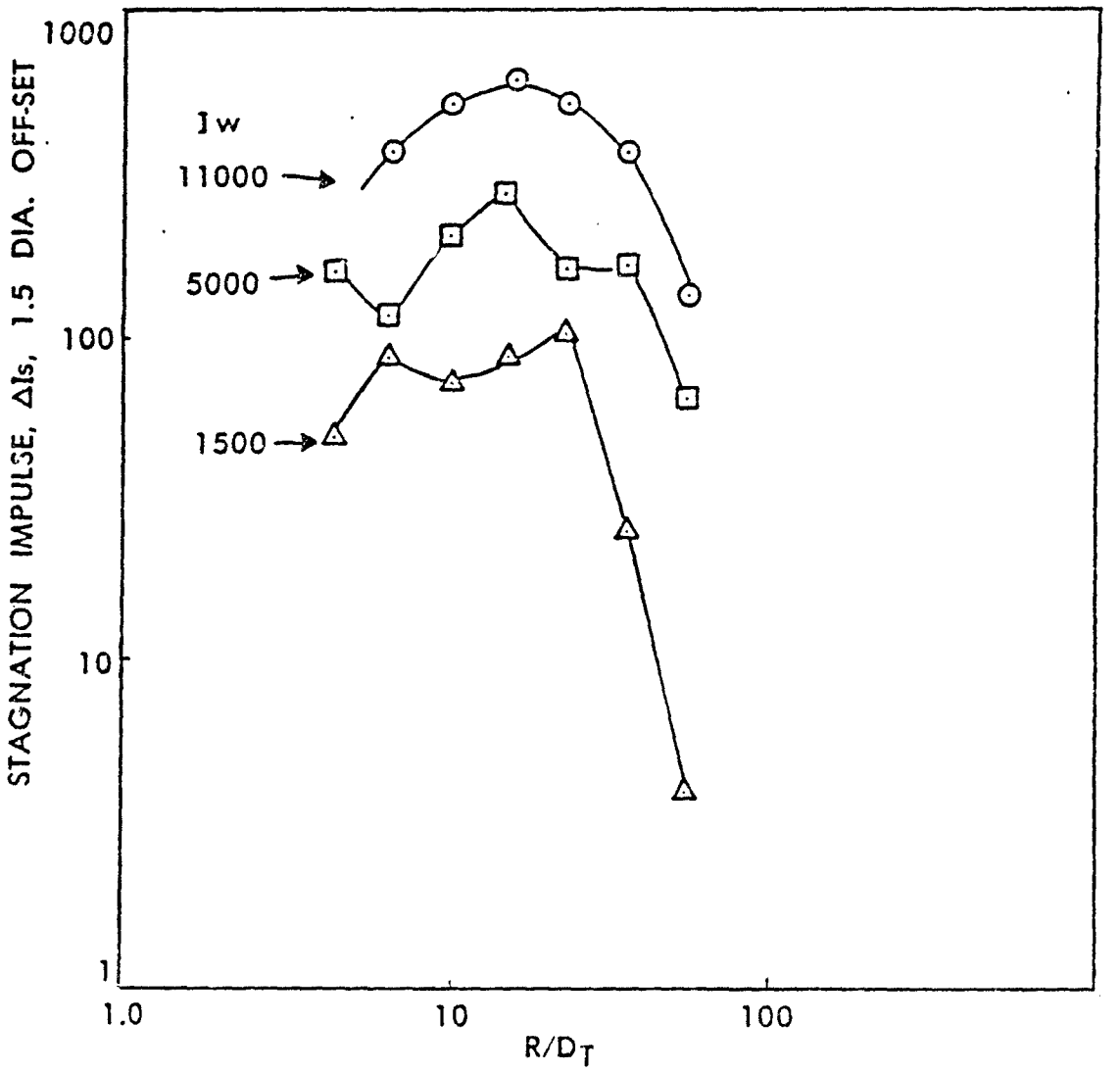

Figure 9. Stagnation impulse ($\triangle I_S$) versus range (R) over tunnel diameter (D_T), along the 1.5-diameter off-set line for three exit impulses(I_W).

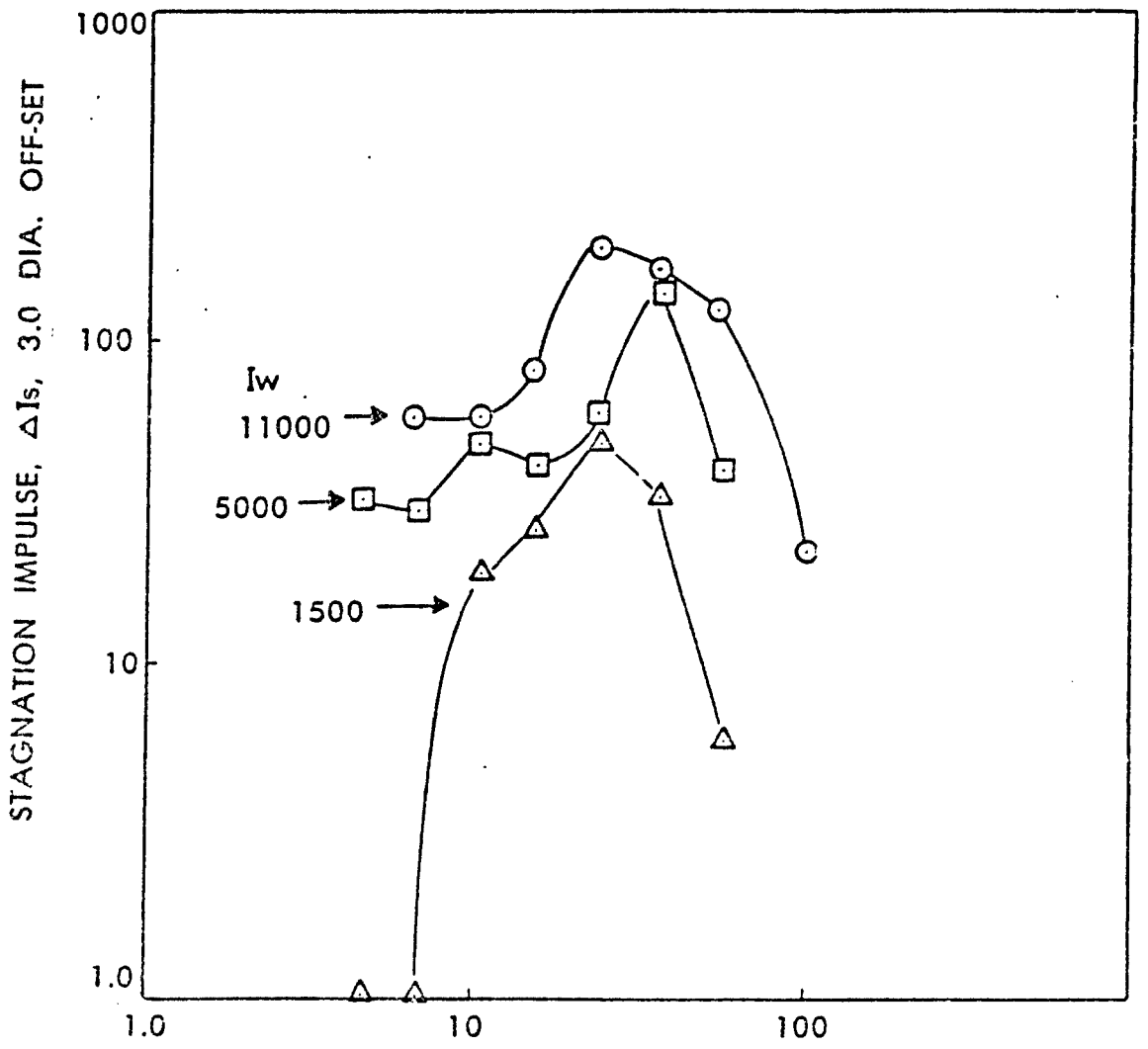

Figure 10. Stagnation impulse (ΔI_3), versus range (R) over tunnel diameter (D_T) along the 3.0-diameter off-set line for three exit impulses (I_w).

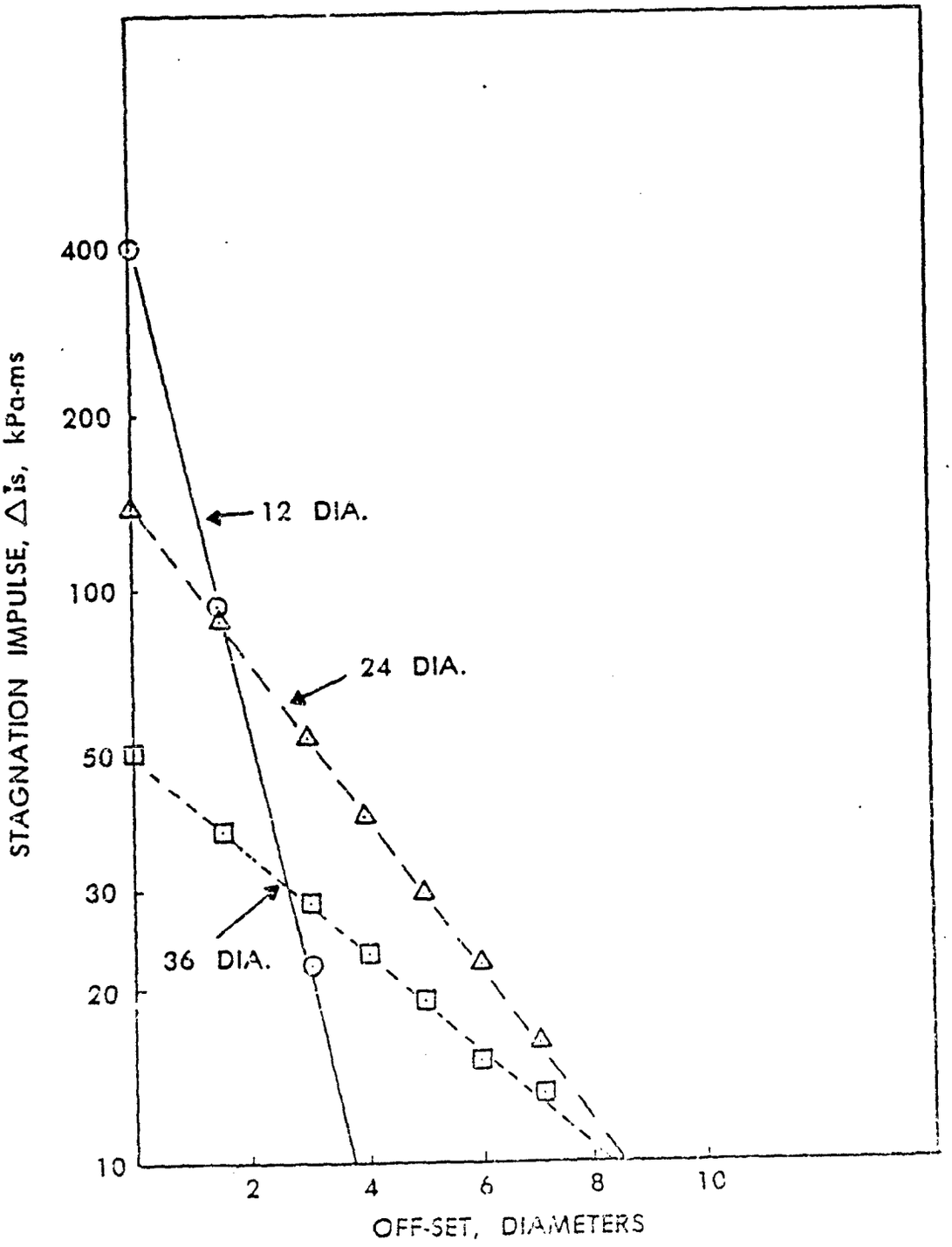

Figure 11. Stagnation impulse versus off-set.

SURVEY OF AIRBLAST DATA RELATED TO UNDERGROUND MUNITION STORAGE SITES

Charles N. Kingery
Terminal Ballistics Division
U.S. Army Ballistic Research Laboratory
Aberdeen Proving Ground, Maryland 21005-5066

ABSTRACT

This paper represents results of an in-depth review of the research, both experimental and theoretical, related to the problem of establishing a quantity-distance criteria for accidental explosions occurring in underground munition storage sites.

Six different methods proposed for calculating the safe inhabited building distance were reviewed. Using the same loading density and site configuration, distances were calculated and comparisons were made. The present standard published in the DDESB Safety Manual appears overly conservative while one of the methods proposed by a Norwegian report is under-conservative.

Three of the six methods relied on results obtained from research conducted with small scale models of underground storage sites. The other three methods are based on an empirical approach where the origin and methodology for the equations are not clear.

The weaknesses in all methods are discussed and a recommendation is made for what the author considers the best method.

1. INTRODUCTION

1.1 Background. The peak overpressure associated with a blast wave, propagating from an accidental explosion in an underground munition storage site, is the damaging mechanism that governs the distance at which inhabited buildings may be located. There is a range of peak overpressure, from 50 millibars (0.725 psi) to 86 millibars (1.2 psi), which has been established as the criterion for acceptable damage to an inhabited building. NATO countries, in general, use the 50 millibars while the United States use 86 millibars. There are also different methods used to predict the distance one might expect these peak overpressures. These differences in the peak overpressure for acceptable damage and the methods for predicting the distance at which this pressure would occur are of primary interest to this report.

1.2 Objectives. The objectives of this study are to determine the rationale for current criteria for both the U.S. and NATO countries, to assess weaknesses in the different approaches, and to establish a new recommendation based on scientific experiments and theoretical calculations.

2. RESULTS

2.1 Literature Search. An extensive literature search was made and a total of 24 reports reviewed in detail. These are listed as References 1-24. These reports included small scale and shock tube experiments, and computer calculations.

2.2 Chamber Pressure and Exit Pressure. The various parameters that govern the blast propagation outside of an underground tunnel are the storage chamber dimensions and volume, passageway dimensions and volume, mass and type of explosive stored, exit pressure, tunnel diameter, and the angle off of the zero-degree axis.

The mass of explosive and volume of the storage chamber are needed to establish the loading density. One of the Norwegian reports[5] concentrated on the build-up of pressure in the storage chamber by measuring the pressure versus time for different loading densities, types of explosive, and vent areas. The experimental results compared quite well with the output from Proctor's INBLAST computer code.[6] Although the chamber pressure is one of the important parameters and depends on loading density, early equations, developed to predict the exit pressure from the tunnel, used loading density rather than chamber pressure.[7] The equation established for predicting the exit pressure is approximated by

$$P_w \simeq 24(Q/V_c)^{0.66}, \qquad (1)$$

where

P_w = exit pressure, bars

Q = explosive mass, kg

V_t = total volume, m^3.

In English units, the equation becomes

$$P_w = 2172\ (W/V_t)0.66, \tag{2}$$

where P_w = exit pressure in psi,

W = explosive mass in lbs,

and V_t = total volume in ft^3.

When the passageway or exit tunnel cross-section is smaller than the chamber cross-section, then an attenuation of the shock was considered and other equations for P_w were developed.[7]

$$P_w = 12.1\ (Q/V_t)^{0.607}\ (A_j/A_c)^{0.19}, \tag{3}$$

where A_j = area of exit tunnel,

A_c = area of storage chamber at exit

(See Figure 1),

and P_w = bar, Q = kg, and $V_t = m^3$.

In English units, the equation becomes

$$P_w = 943\ (W/V_t)^{.607}\ (A_j/A_c)^{0.19}, \tag{4}$$

where P_w = psi, W = lbs, and $V_t = ft^3$.

In Reference 17, a new equation was developed to predict the exit pressure P_w. This equation is:

$$P_w = 16.4\ (Q/V_t)^{0.54}\ (A_j/A_c)^{0.24}. \tag{5}$$

As can be seen, this is a variation of Equation 3. A comparison of Equations 3 and 5 shows that at the lower loading densities, Equation 5 predicts higher values for P_w, while at higher loading densities ($Q/V_t > 30$), Equation 3 predicts higher values of P_w.

Equation 3			Equation 5		
Q/V_t	A_j/A_c	P_w	Q/V_t	A_j/A_c	P_w
10	.23	37	10	.23	40
30	.23	72	30	.23	72
50	.23	98	50	.23	95
100	.23	150	100	.23	138

A method developed at BRL considers the total volume pressure P_V as the governing parameter rather than the loading density. Of course, the loading density and type of explosive must be known in order to determine the total volume pressure (P_V). The INBLAST computer code is an excellent way to predict the chamber pressure for a given explosive and storage density. In the BRL method, the total volume is used in the equation and the same attenuation factor using A_j/A_c also appears in the equation, as follows:

$$P_w = 1.1 \ (P_V)^{0.83} \ (A_j/A_c)^{0.19}, \tag{6}$$

where P_w and P_V are in bars.

In English units, this translates to:

$$P_w = 1.733 \ (P_V)^{0.83} \ (A_j/A_c)^{0.19} \tag{7}$$

where P_w and P_V are in psi.

A plot of P_V (psi) versus w/V_t (lb/ft^3) is presented in Figure 2 for both TNT and PETN. This is to illustrate that the chamber pressure for each specific explosive should be calculated rather than using a TNT equivalence factor. In this illustration, PETN shows a lower efficiency than TNT at the low loading densities, but becomes higher above a loading density of 0.08 lbs/ft^3. The total volume pressures as a function of loading density for various explosives are listed in Table 1. This table was taken from Reference 19.

When Equation 6 is compared with Equation 5, the values of the predicted exit pressures for Equation 6 are larger at the higher loading densities.

TABLE 1. Static Overpressure as a Function of Loading Density from Explosions in Confined Spaces

STATIC OVERPRESSURE (P_{V_t}) psi

w/v_t (lbs/ft^3)	TNT	Pentolite	Comp B	Tritonal	H-6	HBX-1	HBX-3	RDX	PETN	Tetryl	Worse Case Unknown
1×10^{-4}	1.36	1.05	1.08	1.67	1.57	1.54	1.86	0.85	0.74	1.11	1.86
1.5	2.04	1.57	1.62	2.49	2.36	2.31	2.79	1.27	1.10	1.66	2.79
2.0	2.71	2.09	2.16	3.32	3.14	3.08	3.71	1.69	1.47	2.21	3.71
4.0	5.40	4.17	4.31	6.61	6.25	6.14	7.39	3.38	2.93	4.41	7.39
6.0	8.09	6.24	6.45	9.85	9.32	9.16	11.0	5.05	4.39	6.60	11.0
8.0	10.7	8.30	8.58	13.0	12.3	12.1	14.4	6.73	5.84	8.78	14.4
1×10^{-3}	13.3	10.3	10.7	16.1	15.2	15.0	17.8	8.39	7.29	10.9	17.8
1.5	19.5	15.2	15.7	23.4	22.2	21.9	25.8	12.5	10.9	16.1	25.8
2.0	25.4	20.0	20.6	30.3	28.8	28.4	33.3	16.4	14.3	21.1	33.3
4.0	47.0	37.4	38.6	55.3	52.8	52.1	60.4	31.2	27.3	39.4	60.4
6.0	66.6	53.4	55.2	77.6	74.3	73.4	84.4	44.8	39.3	56.1	84.4
8.0	85.0	68.4	70.7	98.2	94.2	93.2	106.2	57.7	50.6	71.8	106.2
1×10^{-2}	102.4	82.7	85.6	117.4	112.8	111.7	126.4	70.1	61.4	86.8	126.4
1.5	142.7	116.1	120.5	160.8	155.1	154.0	171.2	99.5	87.0	122.0	171.2
2.0	179.9	147.1	153.1	199.4	193.1	192.2	210.2	127.3	111.0	154.7	210.2
4.0	242.3	257.9	267.6	272.4	283.8	277.7	285.9	229.1	198.4	265.3	285.4
6.0	282.9	317.5	324.8	323.0	340.3	334.2	316.2	323.2	278.2	321.7	340.3
8.0	323.9	372.3	381.6	364.2	385.0	381.0	341.3	413.3	354.3	377.8	413.3
1×10^{-1}	367.6	427.0	438.2	402.7	426.7	425.3	384.3	482.9	428.2	433.7	482.9
1.5	475.6	563.2	579.0	492.3	524.2	530.4	489.5	649.4	607.8	573.0	649.4
2.0	582.6	699.0	717.7	577.4	617.1	631.5	592.8	815.8	770.4	711.9	815.8
4.0	1007	1241	1268	903.7	1023	1024	986.2	1482	1390	1261	1482
6.0	1430	1780	1816	1223	1449	1410	1355	2148	2009	1807	2148
8.0	1853	2318	2364	1541	1874	1811	1724	2814	2629	2352	2814
1×10^{0}	2275	2857	2911	1859	2299	2210	2093	3481	3248	2898	3481
1.5	3331	4202	4279	2650	3361	3230	3018	5146	4797	4260	5146
2.0	4386	5548	5647	3441	4423	4251	3942	6812	6346	5623	6812

Equation 5		Equation 6
Q/V_t	P_w, bar	P_w, bar
10	40	38
30	72	90
50	95	137
100	138	250

This increase in the value of the exit pressure may be justified because it can be seen in Figure 2 that as the loading density increases, the chamber pressure, P_v, increases quite rapidly.

2.3 Outside Pressure. A method for predicting the pressure propagating outside of the tunnel exit and along different radials was developed and presented in Reference 10. The basic equation is presented as follows:

$$\Delta P/P_w = 1.24\ (R/D_t)^{-1.35}/\left[1 + (\theta/56)^2\right], \qquad (8)$$

where ΔP = pressure at target in bar or psi,

P_w = exit pressure in bar or psi,

R = distance to target in m or ft,

D_t = tunnel diameter in m or ft,

and θ = angle in degrees, off zero axis.

Equation 8 has been plotted in Figure 3, along with data points taken from experiments reported in References 10, 11, and 14-17. It is interesting to note that data from References 11 and 14-16 were generated from shock waves exiting from shock tubes.

In practical use, the desired parameter is the distance R at which a selected pressure would occur. Therefore, Equation 8 may be rewritten as:

$$R = D_t\left(\frac{\Delta P}{1.24\ P_w}\right)^{-0.74}\left[1 + \frac{\theta}{56}^2\right]^{-0.74}. \qquad (9)$$

These equations were developed by the Norwegians and presented in Reference 10. The distance R_o along the zero line for a given pressure may be multiplied by the attenuation factor,

$$AF = \left[1 + \left(\frac{\theta}{56}\right)^2\right]^{-0.74},$$

to obtain the distance along any radial at which the same given pressure might be expected. This attenuation factor AF is plotted versus angle off the zero axis in Figure 4. The dashed lines in Figure 4 represent the present attenuation system where sectors are used rather than a continuous attenuation.

A second method was proposed by the Norwegians.[17] In this report, equation in the form of Equation 8 was presented.

$$P/P_w = (1.2987\ R/D_t)^{-1.2987}(kn), \tag{10}$$

where kn is an attenuation factor for different sectors. 0^o-30^o: kn = 1 and 30^o-60^o: kn = 0.74.

If we put Equation 10 into the form of Equation 9, then we have:

$$R = D_t\ (0.77)\ (P_w/\ P)^{0.77}(kn). \tag{11}$$

When values of R/D_t and P/P_w from this equation are compared with Figure 3, they fall below the curve established for Equation 8. The attenuation factors for distance k versus angle sectors are 0-30: kn = 1, 30-60: kn = 0.89, 60-90: kn = 0.67, 90-120: kn = 0.5, and 120-180: kn = 0.25.

Equations 10 and 11 were developed from small scale experiments and the data falls along the calculated curve, but it is recommended in this report that Equation 9 be used to calculate the distance at which selected peak overpressures should occur. This recommendation is based on the fit of data from other sources as shown in Figure 3.

2.4 Other Methods Considered. There are two other methods that were proposed for consideration as criteria for predicting the distance at which an inhabited building could be located.

The first method was submitted by the Norwegians.[20] The basic equation to predict the distance to expect a peak shock pressure of 50 mbar is as follows:

$$R_o = 18.8\ (Q/V)^{0.265}\ (Q/nk)^{0.283}, \tag{12}$$

where

Q = explosive mass in kilograms,

V = volume of storage chamber, m^3,

n = 1 when storage site has only one exit, or when there are more than one and the blast waves interact.

n = 2 when there are more than two exits and the blast waves are not expected to interact.

k = 3 if the branch passageway between the storage chamber and the main passageway has the following characteristics:

- crosssectional area is not greater than 1/2 the main passageway area,
- length is not less than 2/3 of the required interval, and
- the angle between main passageway and branch passageway is within the interval of 60° to 120°.

k = 1 for all other cases.

Equation 12 covers the section 0° to 30°. For sector 30° to 60°, the constant 18.8 is reduced to 16.9; from 60° to 90°, 18.8 becomes 12.5; from 90° to 120°, 18.8 becomes 8.1; and for 120° to 180°, the constant 18.8 is reduced to 4.7. These attenuation factors for distance are the same as the dashed lines in Figure 4. A comparison of this method with other methods will be presented later in this report.

A second method which is quite similar to the one just discussed was proposed by Paul Price, DOD Explosives Safety Board.[21] This equation is presented as follows:

$$R_o = F_y\,(W/V)^{0.265}\,(W/nk)^{X_y}, \tag{13}$$

where F_y is a function of explosive mass,

X_y is a function of explosive mass,

W = explosive mass in pounds, lbs,

and V = volume of storage chamber, ft^3.

n and k have the same definition as given in the previous method.

When calculating R_o for various charge masses, these factors are listed below:

0-100000		100000-250000		250000-500000	
F_y	X_y	F_y	X_y	F_y	X_y
92	0.283	5.29	0.531	115	0.283

This calculation for R_o includes the 0^o to 30^o sector. For the other sectors, use the dashed line attenuation factors given in Figure 4.

Both of these methods have certain requirements which must be met. The first method states that the cross-section of the main passageway must not be larger in cross-section than 20 m^2, the tunnel roughness must be at least 5%, and the length of the passageway must be at least 100 meters. There are no corrections given for smaller area tunnels, shorter tunnels, or longer tunnels.

The method proposed by Paul Price does not specify tunnel cross-sectional area, but states that if the tunnel is longer than 330 feet, then reduce the distance R_o by 23%.

A third method for comparison is the current one in Reference 22. Distances in this standard are based on the equation:

$$R_o = 76(W_t)^{1/3}, \tag{14}$$

where $W_r = W/nk$.

n and k are similar to previous description.

R_o = range, ft, and

W = explosive stored, lbs.

The loading density, chamber volume, and passageway length or diameter are not required for this method of calculation.

3. COMPARISON OF RESULTS

3.1 Description of Method.

3.1.1 Method 1. This method is published in the current safety manual[22] and will be presented to show that in most test cases, it is very conservative. Equation 14 is used in Method 1.

$$R_o \text{ (ft)} = 76 \, (W_r/nk)^{1/3},$$

where R_o is the inhabited building distance for the 0^o-30^o sector (1.2 psi or 2.8 mbar).

3.1.2 Method 2. Method 2 was proposed by the Norwegians in Reference 20. In Method 2, Equation 12 is used as:

$$R_o \text{ (m)} = 18.8 \, (Q/V)^{0.265} (Q/nk)^{0.283}$$

This method was detailed in Section 2.4 above.

3.1.3 Method 3. This method is similar to Method 2, with the exception of a change in constants and exponents depending on the change in mass. In Method 3, Equation 13 is used.

$$R_o \text{ (ft)} = 92 \, (W/V)^{0.265} (W/nk)^{0.283}$$

This equation is used for a W of 0 to 100000 lbs. Here again, R_o applies to the 0^o to 30^o sector.

3.1.4 Method 4. This method is one proposed in Reference 7. It requires the geometry of the storage site and mass of explosive in order to calculate the exit pressure, P_w, and a second equation is used to calculate R_o. The first, Equation 4, is

$$P_w \text{ (psi)} = 943 \, (W/V_t)^{0.607} (A_j/A_c)^{0.19},$$

then Equation 9 in English units is:

$$R_o \text{ (ft)} = D_T \, (1.173)(\Delta P/P_w)^{-0.74},$$

then attenuation factors are applied for the different radials as presented in Figure 4.

3.1.5 Method 5. This method was also developed by the Norwegians.[17] Equation 5 in English units becomes:

$$P_w \text{ (psi)} = 1064 \, (W/V_t)^{0.54}(A_j/A_c)^{0.24};$$

then Equation 11 becomes:

$$R_o \text{ (ft)} = D_t \, (0.77)(P_w/\Delta P)^{0.77}$$

where R_o is used for the 0° to 30° sector. For 30°-60°, use 0.89 R_o, 60°-90° use 0.67 R_o, for 90°-120° use 0.50 R_o, and for 120° to 180° use 0.25 R_o.

3.1.6 Method 6. This method was developed at BRL and is being proposed as a new criterion for predicting the distance at which a specific peak overpressure should occur. The major difference in this method is that the pressure in the overall chamber and tunnel volume is used in Equation 7 rather than loading density.

$$P_w \text{ (psi)} = 1.733 \, (P_{V_t})^{0.83}(A_j/A_c)0^{.19}.$$

Then Equation 9, in English units, is:

$$R_o \text{ (ft)} = D_t \, (1.173)(\Delta P/P_w)^{-0.74}.$$

3.2 Comparision of Methods. A comparision of the six methods will be made where the initial storage site parameters are the same, so that a direct comparison can be made. We will assume there is only one tunnel exit, then n = 1 and the criteria are met to make k = 1. The exit tunnel diameter is 16.6 feet and calculations will be made for the distance to 1.2 psi and 0.725 psi (50 mbar). The ratio A_j/A_c from Figure 1 is 0.23.

3.2.1 Comparision of Six Methods - Increase in Charge Mass. In Table 2, the volume of the storage chamber and the passageway tunnel remained constant while the amount of explosive was increased from 2204 lbs to 11020 lbs, an increase of five times. The increase in distance ranged from a factor of 1.71 to 2.41. With the exception of Method 1, the spread of distances for the five other methods is within ± 11%.

TABLE 2. Comparison of Six Methods - Increase in Charge Mass

Method	Charge Mass W (lbs)	Loading Density W/V_c (lbs/ft^3)	W/V_t (lbs/ft^3)	1.20 psi R_o-ft	0.725 psi R_o-ft	P_w psi
1	2204	0.062	0.021	989	--	--
2	2204	0.062	0.021	--	436	--
3	2204	0.062	0.021	389	--	--
4	2204	0.062	0.021	386	561	68
5	2204	0.062	0.021	364	537	93
6	2204	0.062	0.021	444	644	82
1	11020	0.312	0.105	1691	--	--
2	11020	0.312	0.105	--	1052	--
3	11020	0.312	0.105	941	--	--
4	11020	0.312	0.105	797	1157	181
5	11020	0.312	0.105	709	1045	221
6	11020	0.312	0.105	800	1162	182

NOTE: Storage site dimensions constant.

3.2.2. Increase in Chamber Volume and Explosive Mass. In Table 3, the amount of explosive was increased by a factor of 10, and the chamber volume was increased by a factor of 10, so the loading density remained the same (0.624). The volume of the tunnel passageway was increased approximately 30%. This changed the loading density of the total volume from 0.211 to 0.499. The distances calculated for 1.2 and 0.725 psi at the 0.211 loading density are within ± 7% with the exception of Method 1. When the loading density of the total volume was changed to 0.499, the spread of distances increased to ± 20%. Methods 4-6 are usually quite consistent in that Method 5 calculates values that are less than the other two.

TABLE 3. Comparison of Six Methods - Increase in Charge Mass and Total Volume

Method	Charge Mass W (lbs)	Loading Density W/V_c (lbs/ft^3)	W/V_t (lbs/ft^3)	1.20 psi R_o-ft	0.725 psi R_o-ft	P_w psi
1	22040	0.624	0.211	2131	—	—
2	22040	0.624	0.211	—	1539	—
3	22040	0.624	0.211	1379	—	—
4	22040	0.624	0.211	1092	1586	277
5	22040	0.624	0.211	947	1397	322
6	22040	0.624	0.211	1080	1569	273
1	220400	0.624	0.499	4590	—	—
2	220400	0.624	0.499	—	2952	—
3	220400	0.624	0.499	2470	—	—
4	220400	0.624	0.499	1607	2334	467
5	220400	0.624	0.499	1356	1999	513
6	220400	0.624	0.499	1617	2348	471

NOTE: Explosive mass and chamber volume increased 10 times and total volume increased 4 times.

3.2.3 Comparision of Six Methods - Decrease in Tunnel Diameter. In table 4, the explosive mass was increased to 500000 lbs. The loading density of the chamber and total volume remained the same. The only difference is in the diameter of the exit tunnel. Here you can see that Methods 1-3, which do not use the tunnel diameter in their equations, have the same calculated distance, while Methods 4-6 show a reduction in distance of approximately 39%, which corresponds to the reduction in tunnel diameter.

Table 4. Comparision of Six Methods - Decrease in Tunnel Diameter

Method	Charge Mass W (lbs)	Loading Density W/V_c (lbs/ft^3)	Loading Density W/V_t (lbs/ft^3)	1.20 psi R_o-ft	0.725 psi R_o-ft	P_w psi	Tunnel Diameter (ft)
1	500000	6.24	4.99	6032	—	—	16.6
2	500000	6.24	4.99	--	6790	—	
3	500000	6.24	4.99	7609	—	—	
4	500000	6.24	4.99	4519	6561	1888	
5	500000	6.24	4.99	3535	5211	1780	
6	500000	6.24	4.99	6310	9161	2964	
1	500000	6.24	4.99	6032	—	--	10.0
2	500000	6.24	4.99	--	6790	--	
3	500000	6.24	4.99	7609	—	—	
4	500000	6.24	4.99	2722	3952	1888	
5	500000	6.24	4.99	2129	3139	1780	
6	500000	6.24	4.99	3800	5518	2964	

3.3 Tunnel Junctions. When there are two exit tunnels and they are separated enough so that there is no enhancement between them, in Equation 13 the value of n becomes 2. When Method 3 is used to calculate values in Table 2 for an explosive mass of 11020 lbs and a loading density of 0.312 lbs/ft^3, then R_o was calculated as 941 feet. If a value of n = 2 is used in Equation 13, the distance is reduced to 767 feet.

It is suggested by the author that a new approach be taken when there are tunnel branches or junctions. This new method would reduce the transmitted pressure by factors based on shock tube experiments. These reduction factors are presented in Figure 5 and are based on data in Reference 23. The 90° tunnel junction data do not follow a simple equation and, therefore, the curve presented in Figure 6 should be used.

If we make a comparison between Methods 3 and 6 and assume a Y junction in the tunnel system that gives two exit tunnels that do not cause any exterior enhancement, then the inhabited building distance will change as follows. Using the 11020 lbs in Table 2, the distance using Method 3 is 941 feet. If we use n = 2 in Equation 13, this distance reduces to 767 feet. This is a reduction of approximately 18%.

Now using Equation 7 to calculate P_w, we find P_w equal to 182 psi. With a Y junction as shown in Figure 5c, P_w would be multiplied by 0.65 to become 118 psi. With P_w equal to 118 in Equation 9, the inhabited building distance reduces from 800 feet down to 581 feet. This is a reduction of 27%.

This implies that using n = 2 may be conservative and that the 941 feet should reduce to 687 feet rather than 767 feet.

It should also be noted that with a tunnel junction as shown in Figure 5a, there would be different exit pressures at the end of the two tunnels. The inhabited building distance would also be different in front of the two exits.

The reduction in pressure propagating through the different junctions applies only if the tunnel cross sectioned area of each branch remains the same. In configurations where there is a reduction or increase in the cross section area of the tunnel, then these conditions should be treated on an individual basis.

An extensive series of tests were conducted by Switzerland.[24] The values given in Figure 5 compare quite well with the results reported in Reference 24. The BRL value of transmitted pressure of 0.80 P_s in Figure 5a compares with a Reference 24 value of 0.83 P_s.

The side tunnel (Figure 5a) values from Reference 24 are plotted in Figure 6 along with the BRL-generated curve. The 90° dead-end tunnel (Figure 5b) value for the transmitted shock is 0.7 P_s, while the Reference 24 value shows a spread of 0.57 P_s to 0.68 P_s, which appears to be partially a function of incident pressure. The Y junction transmitted pressure values from Reference 24 for equal to 15° through 90° range from 0.65 P_s at 14.5 psi down to 0.58 P_s at 130 psi. This compares with a value of 0.65 P_s developed in Figure 5c from BRL data in Reference 23.

4. CONCLUSIONS

4.1 Weaknesses. It is impossible to establish one or two equations that will be universally accepted and that fit all underground storage sites. This report has presented, discussed, and compared the results of six methods proposed for determining the safe, inhabited building distance. All methods have certain weaknesses, some more than others. In the opinion of the author, certain parameters should be known. These are as follows:

- Storage Chamber Volume
- Exit Tunnel Volume
- Loading Density
- Explosive Distribution and Containment
- Chamber Pressure for Specific Explosives
- Chamber Diameter
- Tunnel Diameter
- Tunnel Junctions (If any.)
- Tunnel Roughness
- Terrain Outside of Tunnel

All of these variables will affect in some way the overpressure propagated outside of the tunnel. One other variable not dealt with is the location, confinement, and point of initiation of the explosive source. The major portion of scaled model tests has been conducted with linear charges placed along the centerline of the chamber or near spherical charges placed near the entrance to the storage chamber. When in a real storage scenario, there will be pallets and boxes of munitions stored throughout the chamber and on the floor. Most of the munitions will have some kind of containment, from the thin skin of rocket motors to the thick casing of general purpose bombs. The effect of containment on the build-up of gas pressure within the storage chamber has not been fully addressed.

4.2 Recommendations. It has been shown that Methods 4 or 6 give the most consistent values, and the inhabited building distances vary only a few percent in the medium loading densities, i.e., less than 0.624 lb/ft^3. At the higher loading densities, it is recommended that Method 6 be used in any prediction calculation. It can be seen in Figure 2 that using the loading density (W/V_t) as an input parameter in Equation 4 will give different exit pressures, than using the static pressure (P_{V_t}), which is based on (W/V_t) as the input parameter in Equation 7.

Having available this list of nine variables, there is still no assurance that a precise prediction can be made. The methods presented here should be used as guides and not for planning and construction of new sites. When planning the location of a new site, it is recommended that a scaled model of the site be constructed and tests conducted to determine the range for inhabited buildings. This is also true where there may be a controversy over a specific, existing site.

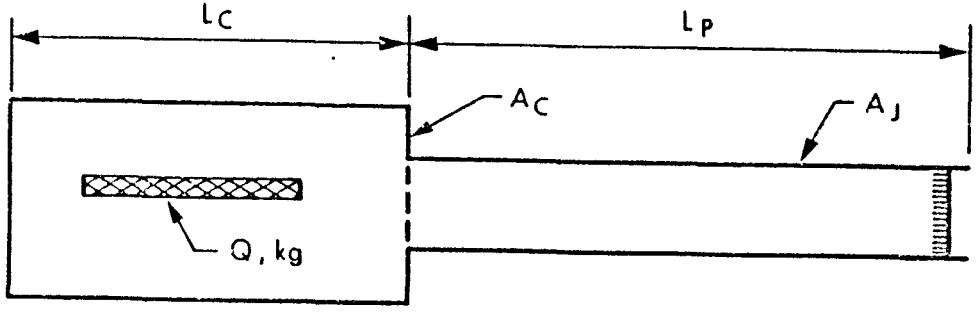

$V_C = A_C \times L_C$, m^3 $\qquad$ Q/V_C = CHAMBER LOADING DENSITY, kg/m^3

$V_P = A_J \times L_P$, m^3 $\qquad$ Q/V_T = TOTAL VOLUME LOADING DENSITY, kg/m^3

$V_T = V_C + V_P$, m^3 $\qquad$ $kg/m^3 \times 0.0624 = lbs/ft^3$

Figure 1. Storage Site Considerations

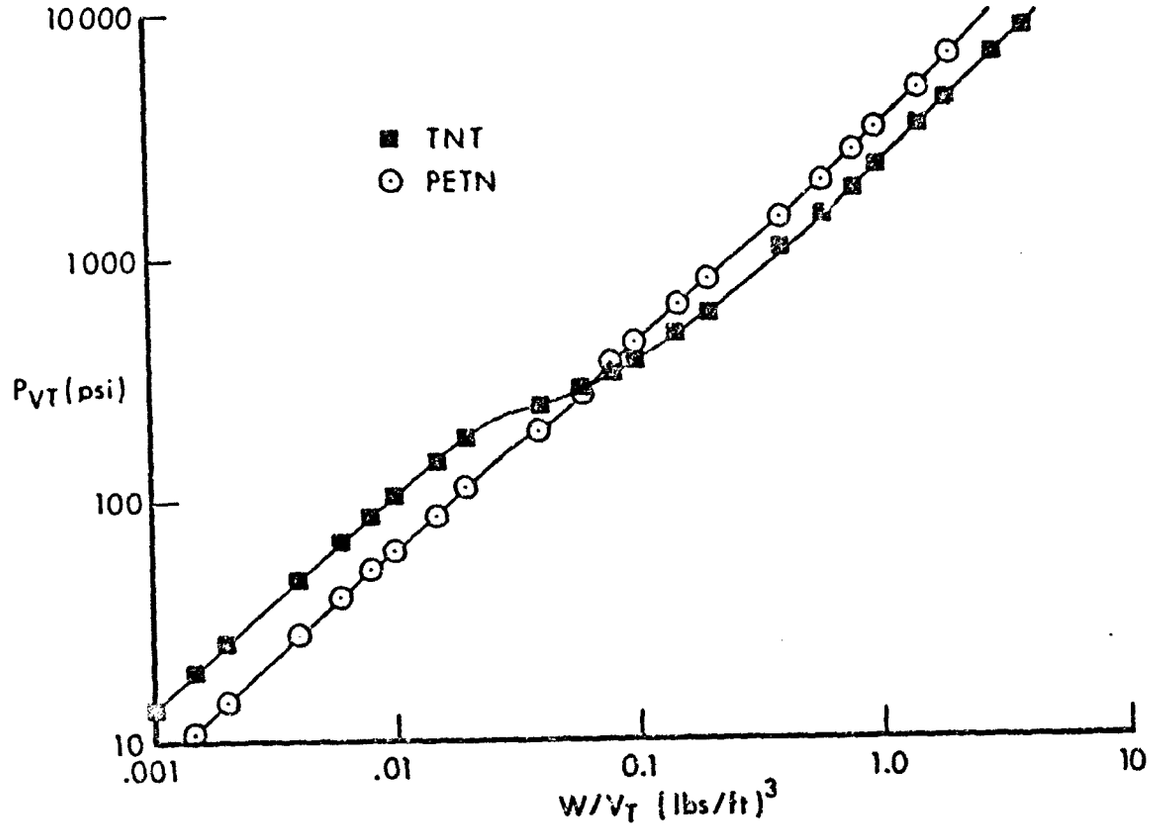

Figure 2. Chamber Pressure (P_{VT}) versus Loading Density (W/V_T)

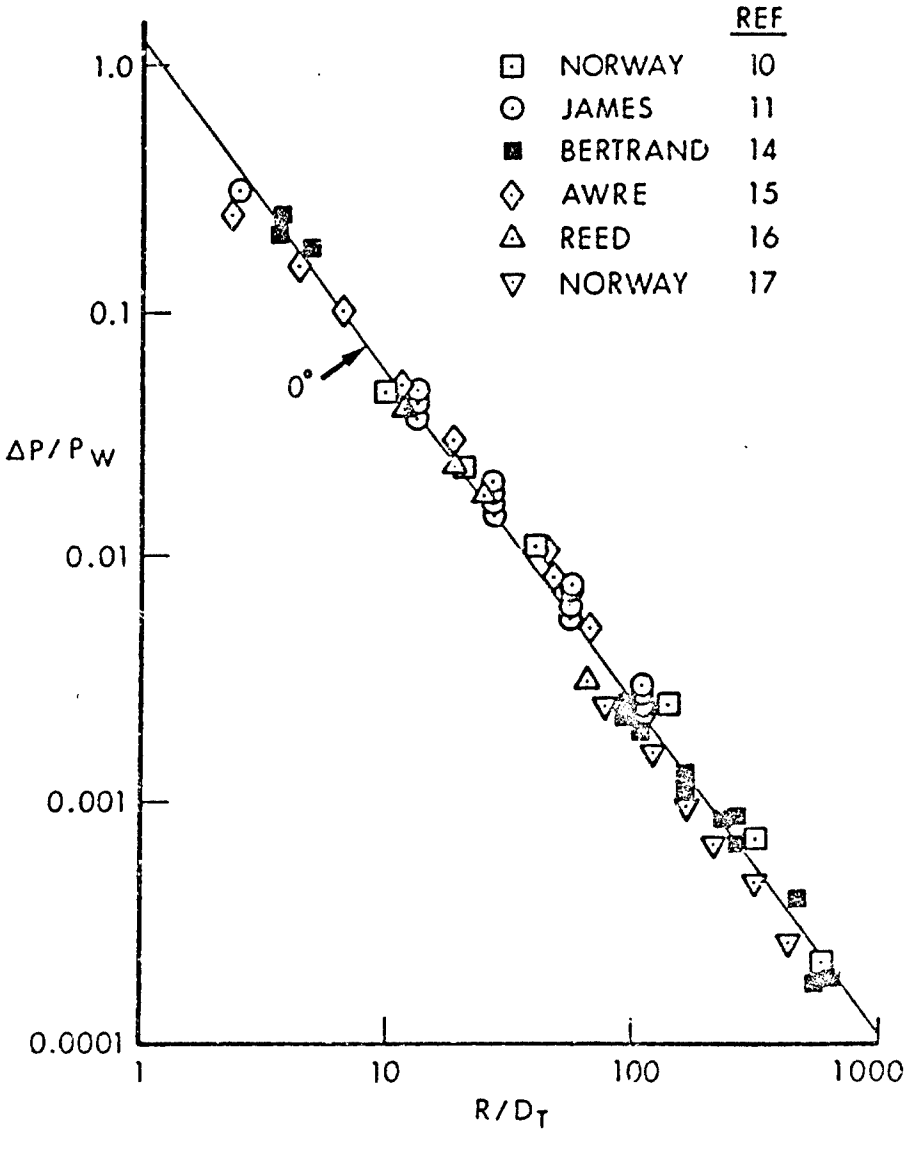

Figure 3. P/P_W versus R/D_T Along Different Radials

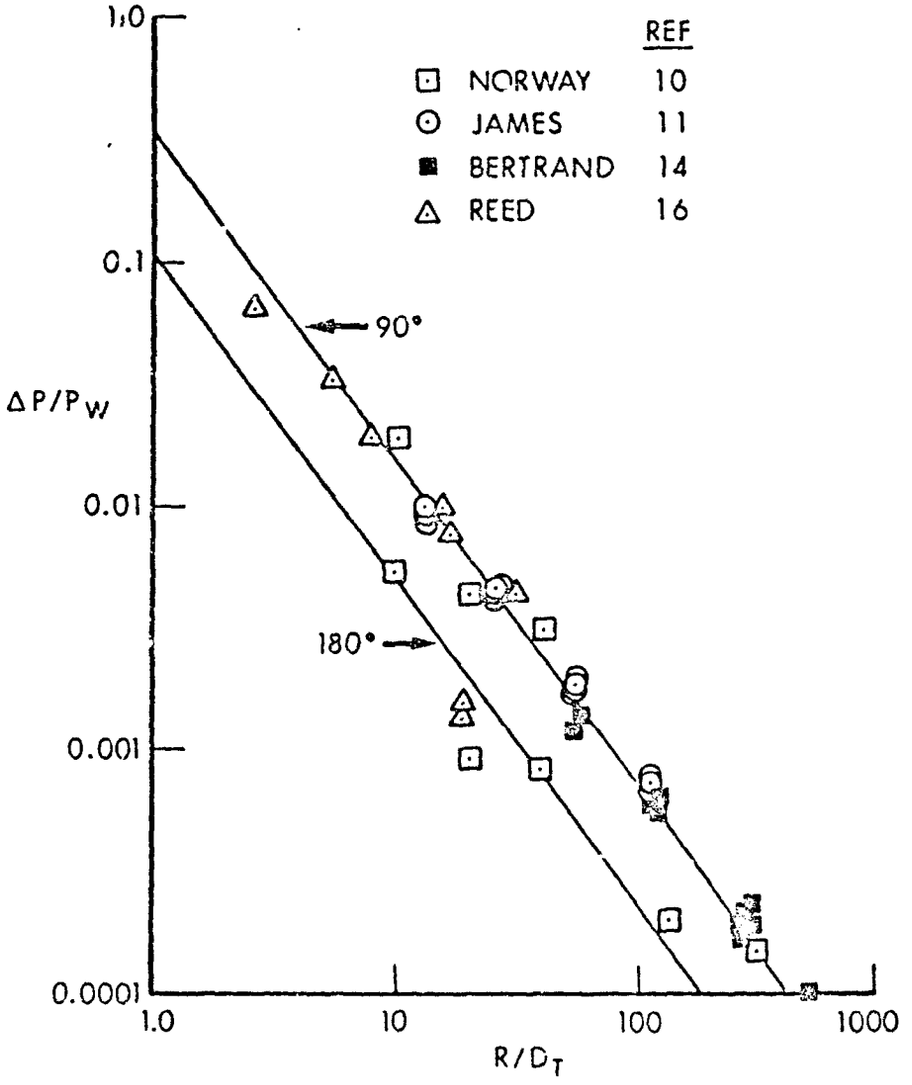

Figure 3. P/P_W versus R/D_T Along Different Radials (continued)

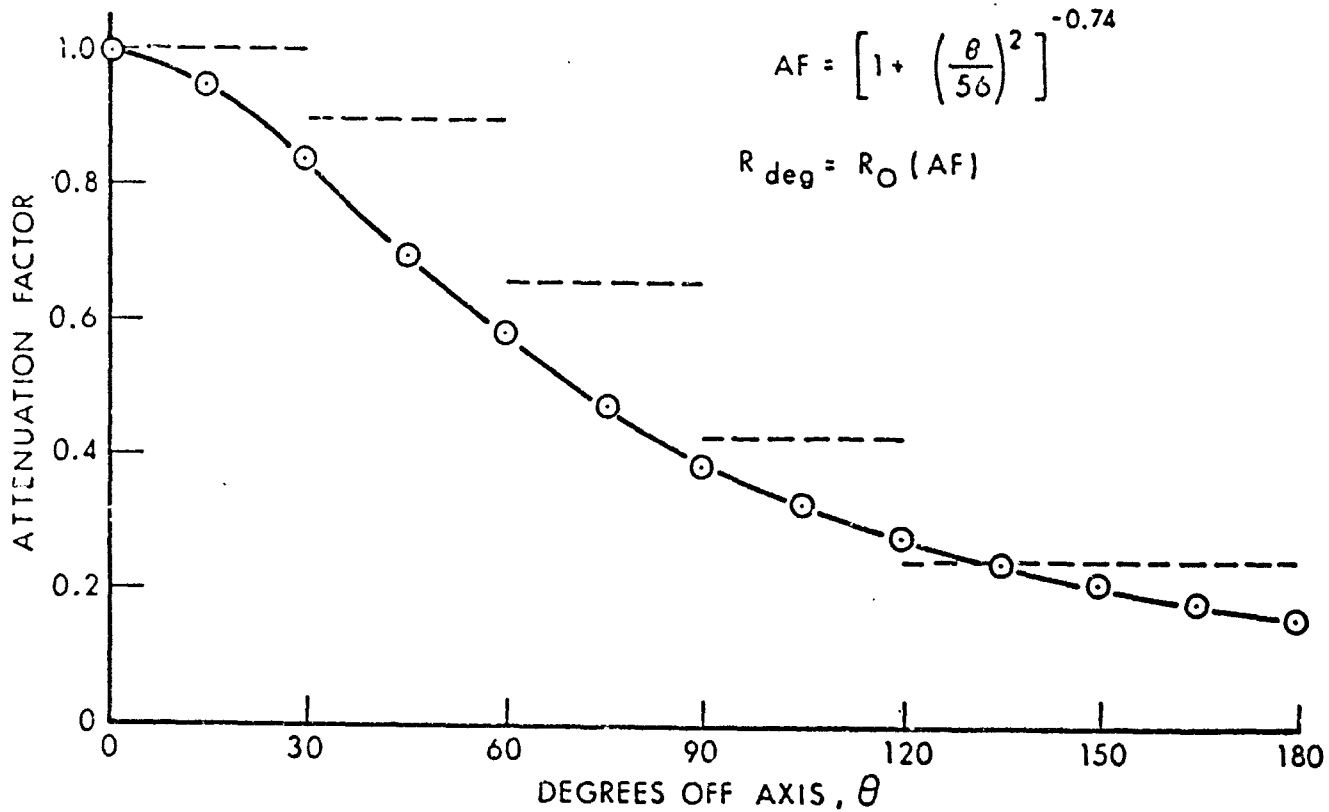

Figure 4. Attenuation Factor versus Degrees Off-Axis

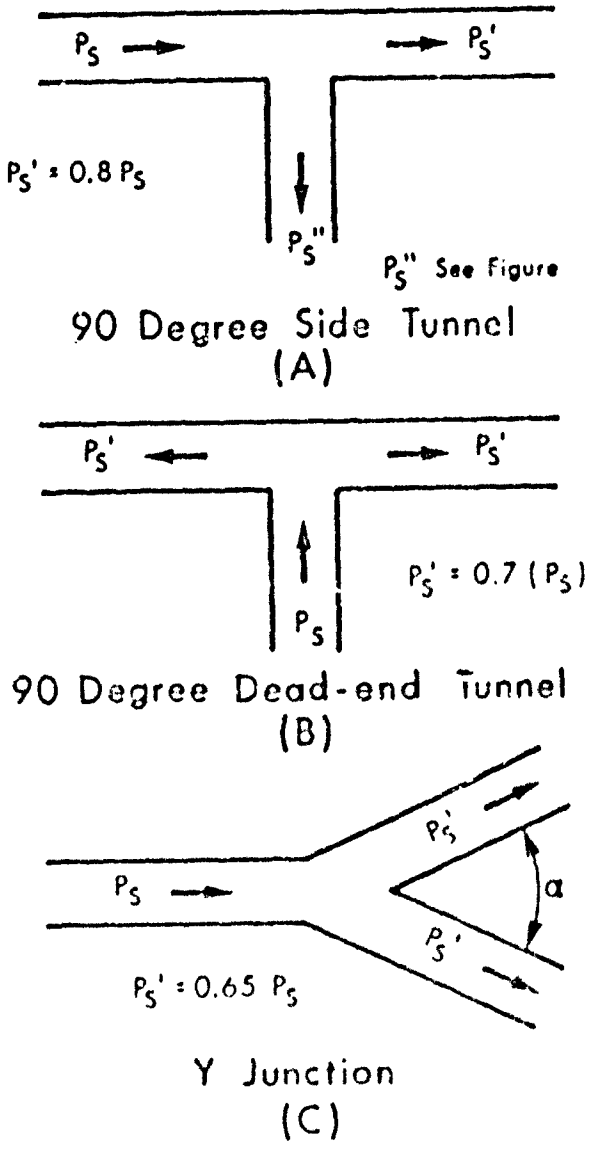

Figure 5. Transmitted Pressure versus Input Pressure for Various Tunnel Junctions

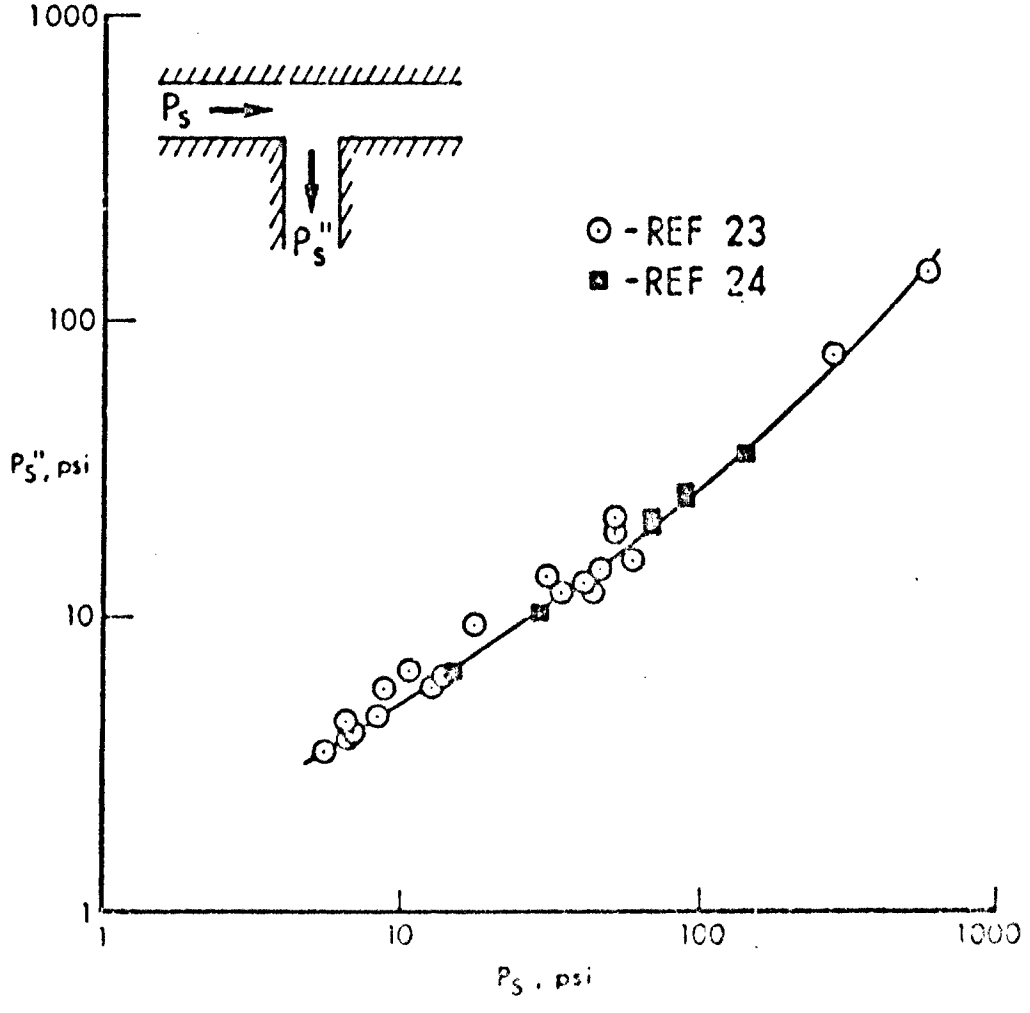

Figure 6. Incident versus Transmitted Shock Overpressure for Tunnel Joined to an Equal Area Tunnel

REFERENCES

1. D.R. Curran, "Underground Storage of Ammunition Experiments Concerning Accidental Detonations in an Underground Chamber," NDRE Report X-111, May 1966.

2. Arne Skjeltrope, "Underground Ammunition Storage-Model Tests to Investigate External Safety Distances," NDRC Report 36/67, August 1967.

3. G. Fredrikson, A. Jenssen, and S. Johnsen, "Underground Ammunition Storage Blast Effects from Accidental Explosions," NDLS Report 50/70, December 1970.

4. A. Skjeltrope, T. Hegdahl, and R. Jenssen, "Underground Ammunition Storage, Report 1, Test Programme, Instrumentation, and Data Reduction," NDSC Report 80/72, September 1975.

5. A. Skjeltrope, T. Hegdahl, and R. Jenssen, "Underground Ammunition Storage, Blast Propagation in Tunnel Systems. Report IIA, Chamber Pressures," NDRC Report 79/72, September 1975.

6. J. Proctor and W. Filler, "A Computerized Technique for Blast Loads and Confined Explosions," Proceedings of Fourteenth Annual Explosive Safety Seminar, 1972.

7. A. Skjeltrope, T. Hegdahl, and R. Jenssen, "Underground Ammunition Storage, Blast Propagation in the Tunnel System, Single Chamber Storage, Variable Tunnel Diameter and Variable Chamber Volume," NDSC Report 81/72, June 1975.

8. A. Skjeltrope, T. Hegdahl, and R. Jenssen, "Underground Ammunition Storage, Blast Propagation in the Tunnel System, Connected Chamber Storage, Variable Chamber Volume, and Variable Angle Between Branch and Main Passageway," NDSC Report 82/72, November 1978.

9. A. Skjeltrope, T. Hegdahl, and R. Jenssen, "Underground Ammunition Storage, Blast Propagation in the Tunnel System, Connected Chamber Storage, Blast Load on Doors in Three Sites," NDSC Report 83/72, 1975.

10. A. Skjeltrope, T. Hegdahl, and R. Jenssen, "Blast Propagation Outside a Typical Ammunition Storage Site," Proceedings of the Fifth International Symposium on Military Applications of Blast Simulators," Stockholm, May 1977.

11. D.J. James, "An Investigation of the Pressure Waves Propagated from the Opened End of a 30" x 18" Shock Tube," AWRE Report 0-60/65, AWRE, England, September 1965.

12. J.W. Reed, "Environmental Air Blast Around Large Shock Tubes," Proceedings 1, MABSA, Sect II.4, September 1985.

REFERENCES (Continued)

13. C.F. Millington and N.J.U. Rees, "A Reassessment on an Existing Underground Explosives Storage Facility in the UK," Minutes of the 20th Explosives Safety Seminar, Vol II, August 1982.

14. B. Bertrand and W. Matthews, "Overpressure and Duration of Shock Waves Emerging from Open-Ended Shock Tubes," BRL Memo Report 1724, November 1965.

15. W.S.W. Mawbey, "A Scaled Model Investigation of the Flow from the Open End of a Shock Tube of Rectangular Cross Section," AWRE-61/65, August 1965.

16. Jack W. Reed, "Microbaragraph Measurements Around the Large French Blast Simulator," Sandia National Laboratory Report, Albuquerque, NM, draft copy.

17. Einar S. Helseth, "Blast Effects from Accidental Explosions," NDCS Report NR 174/85, November 1985.

18. D.R. Smith, "Effects of Explosions in Underground Magazines," draft copy, Waterways Experiment Station, April 1979.

19. M.M. Swisdak, "Explosion Effects and Properties, Part 1-Explosions in Air," NSWC-WOL, TR 75-116, October 1975.

20. Annex A to NO (UST) 1WP/8, 8 Mar 34.

21. Draft Proposal-Paul Price, Explosive Safety Board.

22. "Ammunition and Explosives Safety Standards," DOD 6055.9-STD.

23. Shock Tube Facility Staff, "Information Summary of Blast Patterns in Tunnels and Chambers," BRL Memo Report 1390, March 1962.

24. Ed Binggeli, "Blast Wave Propagation in Branched Tunnels," HC Laboratory, Spiez, Switzerland, Proceedings Vol 1, Military Applications of Blast Simulators, Canada, July 1981.

ABSTRACT

SIMULATION TECHNIQUES FOR THE PREDICTION OF BLAST FROM UNDERGROUND MUNITIONS STORAGE FACILITIES

by

George A. Coulter
Gerald Bulmash
Charles N. Kingery

Results are presented from a series of shock tube and 1:50 scale model high explosive (PETN) tunnel tests, designed to simulate underground chamber/tunnel explosions. The models consisted of straight and smooth chamber/tunnel configurations with converging area changes. The experimental data are compared with predictions from a modified INBLAST computer code to which was added the blast wave propagation along the tunnel. Modifications were made either by the addition to INBLAST of shock tube equations for converging area change at the diaphragm or by addition of the BRL-Q1D one-dimensional hydrocode. Effects of baffle induced tunnel area changes were included in the hydrocode when needed. Otherwise, the algebraic shock tube equations were used. The field test, in addition to internal blast pressure, measured the exit field pressures as a function of the chamber charge loading density. The free-field blast pressure was measured as a function of radial distance and angle of propagation with respect to the tunnel's long axis. Results were found to be consistent with those found in the literature. Data from the test results will be incorporated into the quantity-distance standards for underground storage of munitions. This will result in a more comprehensive data base for airblast effects from ordnance.

I. INTRODUCTION

This paper is a report of research completed for the Department of Defense Explosives Safety Board (DDESB) to help characterize airblast hazards for determining quantity-distance (Q-D) standards for ordnance. The Ballistic Research Laboratory (BRL) was tasked to conduct, analyze, and report shock tube and field experiments simulating explosions of munitions in underground storage facilities. The results were to be compared with predictions for external airblast effects from empirical models found in the literature.

In particular, the INBLAST computer code (Reference 1) was to be modified to include blast propagation down tunnels. Also, scale model field tests were to be conducted to improve the empirical model for airblast effects external to the exit tunnel to the storage facility. Finally, improved Q-D standards (for airblast effects) were to be proposed for the underground storage of munitions, if needed.

II. TEST PROCEDURES

Two types of test programs were set up at BRL to meet the desired objectives. A smooth steel pipe chamber/tunnel, 1:50 scale model of a storage facility was constructed. The model was operated as a converging shock tube. Helium was used as a driver gas in order to best simulate the sound speed ratio of detonated TNT explosive. The second test series was held on a field range. A similar model was used, but the driver was operated with PRIMACORD (PETN) explosive (Reference 2) instead of helium.

A. Shock Tube Model

The 1:50 scale shock tube model is shown sketched in Figure 1. A straight chamber/tunnel configuration with a single area change was chosen for simplicity. Construction was of thick wall, smooth steel pipes. Since it was to be operated indoors, a dump tank was added at the end of the test tunnel. Pertinent dimensions and ratios are listed in the figure. Quartz pressure transducers were used for both the shock tube and field tests. Helium driver gas was chosen so as to match the sound speed of the gas mixture from the exploded TNT to be simulated for this test series. Diaphragms, at the converging test section, of mylar, aluminum, and copper were used to contain the driver pressure until self-rupture occurred. This determined the pressure that was obtained in the tunnel section of the model. Baffles were inserted in the test tunnel during the test to determine the feasibility of using baffles to attenuate the blast in the tunnel.

B. Field Model

The shock tube model was modified slightly and moved to the outdoor firing range. See Figure 2 for a sketch of the field layout. Pressure transducers were placed in flush ground mounts along 0, 45, 90, and 135 degree radials from the open tunnel exit. The PRIMACORD was cut in lengths, bundled, and centered along the axis of the driver chamber. Detonation of the explosive was from the end near the back of the driver.

The charge was varied on one shot by placing a single charge of C-4 near the center of the driver and on-axis. It was thought that charge placement in the driver might affect the blast wave created within the tunnel of the model.

A Tektronix Model 5223 digital recording system was used for the shock tube experiments since only a few recording channels were needed. An analog FM Honeywell 101 tape recording system was used for the larger number of channels needed on the field shots. Final data processing was completed by the use of a Tektronix 4051 computer and software developed at BRL.

III. RESULTS

A. Shock Tube

Simulation in the shock tube ranged, for the chamber loading density, Q/Vc, of 0.36 to 3.4 kg/m3. The quasi-static chamber pressure produced was from 1,300 to 4600 kPa. The initial series of shots was for an unobstructed tunnel. A second series of shots repeated the first, but baffles were placed at 27 and 36 tunnel diameters distance along the tunnel before the shots.

The attenuation between 25 and 45 diameters, without baffles, was measured to be 0.5 to 3.5 percent including any transducer calibration error. With two baffles in place, each blocked 26.2 percent, the shock front attenuation was measured to be between 7.5 and 10.3 percent. With two baffles each blocked 50 percent, the attenuation increased to 39.7 to 43.1 percent, including the smooth wall effects in the unobstructed tests already noted. A more complete baffle/attenuation program is needed to determine correct baffle location to maximize the baffles' efficiency. Figures 3 and 4 show sample records from the shock tube test section. Note that the records have a second major peak caused by reflection from the entrance throat to the dump tank. This should be ignored.

Although the two baffles blocked 50 percent each, did cause substantial attenuation, this much blockage of an access tunnel to an underground facility may not be practical at all.

B. Field Tests

Figures 5 and 6 are photographs of the field model showing the explosive chamber end and the blast lines outside of the tunnel exit, respectively. Figure 7 shows the centering device used for loading the bundle of PRIMACORD in the driver chamber. Figures 8 and 9 show the post-shot damage to the packed sand firing site surface. Some cratering occurred near the exit, and a soot path extended along the 0 degree-line during the higher loading density shots.

Figure 10 displays some pressure-time records from the driver chamber, the test tunnel, and from the ground stations outside the exit from the tunnel. The record from Station C-2, from the driver chamber, shows large reflection pressure spikes as the blast wave from the detonated PRIMACORD reflects within the chamber. There is a pressure decrease, then it builds

back up to some average quasi-static value of fill pressure. The pressure then decays by expanding into the tunnel and out the tunnel exit. Stations T-1 and T-2 give records similar in profile to that seen from the driver chamber, although reduced in pressure. The remaining records shown are from the exterior free-field blast lines. Notice the variation in record shapes in going from the 0 degree-line to the other lines. The transducers had been installed so as to record equal pressures for similar stations for all blast lines. The four pressure levels chosen were 70, 24, 12, and 5 kPa. To maintain the same levels for all shots as the loading density was changed, the distance of the stations was increased for increasing charge density.

More discussion of the results is given in the Analysis Section.

IV. ANALYSIS

Modifications to INBLAST are given; predictions are compared to the shock tube experiments and to the model chamber/tunnel (with PETN and C-4) explosive field data.

A. Modification to INBLAST

The Internal Blast Damage Mechanisms Computer Program (INBLAST) developed at Naval Ordnance Laboratory describes the blast loading characteristics of the detonation of a high explosive internal to a structure. See Reference 1 for documentation. In the present application, INBLAST was modified to include shock tube equations which included area change (Reference 4). A short smooth tunnel was assumed (< 35 diameters) so viscous effects might be neglected. The modification was used in the following way.

The INBLAST code is used to compute the maximum internal gas pressure in the storage chamber for the detonation of the given stored munitions. The computed (quasi-static) storage chamber pressure is assumed to act like a shock tube driver pressure.This will create a blast wave in the access tunnel system. The shock wave equations are solved by an iteration method to predict the tunnel pressure, Pw. These equations are listed as Equations 1-5.

$$gP41/P21=[1-(B*U21/2*A41)(g)\exp(-1/C)]\exp(-C), \quad (1)$$

$$g=[(2+B*M5^2)/(2+B*Me^2)]\exp(C/2)*[(2+B*Me^2)/(2+B*M5^2)]\exp(C), \quad (2)$$

$$M5(S4/S1)=Me[(2+B*M5^2)/(2+B*Me^2)]\exp(D), \quad (3)$$

$$M3=U21/[A41(g)\exp(1/C)-U21*B/2], \quad (4)$$

and

$$U21=(P21-1)/k1[E(F*P21+1)]\exp(1/2). \quad (5)$$

Where, $B=k4-1$, $C=2k4/(k4-1)$, $D=(k4+1)/2(k4-1)$,

$E=(k1-1)/2k1$, and $F=(k1+1)/(k1-1)$.

Values of parameters calculated from the INBLAST program are the chamber pressure ratio P41, chamber sound speed ratio A41, ratio of specific heats for the chamber, k4, and for ambient air, k1. Also the cross section of the chamber to the cross section of the tunnel ratio, S4/S1. For the case of most interest for strong shocks, the Mach number Me=1, at the chamber/tunnel area change and the factor g depends only on S4/S1 and k4. Equation 6 gives the tunnel pressure Pw.

$$Pw=P1(P21-1) \qquad (6)$$

The modification to INBLAST could be made to include steep decaying waves by including a hydrocode calculation instead of the algebraic equations discussed. For example, the BRL-QID (Reference 5) might be used for the addition if needed. Predictions from the INBLAST/shock tube method and two other methods obtained from fitting published field data are shown in Table 1. Equation 7 was used from Reference 6 and Equation 8 from Reference 7 to make the comparisons shown for tunnel pressure Pw.

$$Pw=12.1(Q/Vt)\exp(0.607)*(Aj/Ac)\exp(0.19) \qquad (7)$$

and

$$Pw=1.10(Pvt)\exp(0.83)*(Aj/Ac)\exp(0.19), \qquad (8)$$

where the pressures Pw and Pvt are both in bars. Aj/Ac is the area ratio of the tunnel to storage chamber areas. Equation 8 takes into account different kinds of explosives. Equation 7 does not.

TABLE 1. COMPARISON OF SMOOTH WALL SHOCK TUBE RESULTS WITH PREDICTIONS

Shot Number	Simulated Charge-TNT Q,kg	Charge Density Q/Vc,kg/m3	Charge Density Q/Vt,kg/m3	Chamber Pressure Pc,kPa	Area Ratio Aj/Ac	Tunnel Pressure Pw, kPa Eq.7	Eq.8	INBL	BRL
5	0.0185	0.196	0.137	814	0.16	256	348	538	439
4	0.0424	0.450	0.315	1448	0.16	424	611	779	660
6	0.1600	1.700	1.188	2696	0.16	948	1010	1028	1006
7	0.4240	4.500	3.148	5454	0.16	1683	1694	1566	1560

Notes:
(1) Results in bars from the equations have been converted to kPa: 1 bar equals 100 kPa.
(2) Ambient pressure, P1= 102.73 kPa.

B. Comparison of Field Test Results

Equations 7 and 8 above were used also to predict the tunnel pressure for all the field shots. Table 2 shows these comparisons.

TABLE 2. COMPARISON OF FIELD RESULTS WITH PREDICTIONS

Shot Number	Charge Q,kg	Density Q/Vc,kg/m3	Density Q/Vt,kg/m3	Pressure Pvt,kPa Ref. 8	Area Ratio Aj/Ac	Tunnel Pressure Pw,kPa Eq. 7	Pw,kPa Eq 8	Pw,kPa Exp.
1	0.0332	0.3562	0.2912	710	0.16	404	395	475
2	0.0634	0.680	0.556	1200	0.16	598	611	765
3	0.1359	1.458	1.192	2300	0.16	950	1048	1103
4	0.3170	3.401	2.780	4700	0.16	1589	1897	1551
5	0.3670	3.938	3.219	5700	0.16	1737	2226	4100

* Tests 1,2,3, and 4 are with PRIMACORD; Test 5 is with C-4.

The spread in values for Pw appears reasonable except for the C-4 shot. It appears in this shot that large internal reflections within the driver chamber propagated down the tunnel, and also outside the tunnel exit.

C. Prediction of Blast Outside the Tunnel

Given the predicted value of Pw inside the tunnel, the blast outside the tunnel is predicted from Reference 8 by Equation 9.

$$\text{delta } P/Pw = 1.24\ (R/Dt)\exp(-1.35)/[1+(\text{theta}/56)\exp(2)], \qquad (9)$$

where delta P/Pw is the ratio of free-field blast pressure to the exit pressure at a radial distance to tunnel diameter ratio, R/Dt, for a radial of angle theta degrees measured from the long axis of the tunnel. A useful form of Equation 9 for the zero degree line is given as Equation 10.

$$Ro = 1.173\ Dt*(\text{delta } P/Pw)\exp(-0.74). \qquad (10)$$

5

Figures 11-14 show the data from the field shots plotted with values predicted by Equation 9. The data generally fall somewhat higher than predicted except for the 135 degree line where the data are lower. Pressures from the 135 degree line are influenced greatly by the tunnel's end topography and the pressure in this case may well be low because of the sandbag/end flange combination at the tunnel exit.

V. SUMMARY AND CONCLUSIONS

Results have been presented from a series of shock tube and field tests which were used to model blast effects expected from explosions in underground storage facilities. Pressure-time records have been shown to illustrate the blast pressure effects for both inside and outside a storage facility.

Comparisons were made with currently used methods to predict these blast effects. Generally, the methods used were satisfactory. It should be noted that the charge location and charge shape within a given storage chamber appear to hamper accurate blast prediction inside the tunnel. This in turn, affects the predictions outside the tunnel.

A preliminary effort was made to attenuate the blast wave within the tunnel by use of baffles. It was necessary to add two baffles which were 50 percent blocked each in order to obtain about 40 percent attenuation over a travel of 20 tunnel diameters. It was felt that a tunnel blocked this amount would not be practical in a full size storage facility.

A more complete discussion of these results may be found in the complete report of this research, Reference 9.

In conclusion, the INBLAST or similar code may be used to predict the pressure in the storage chamber from an explosion of the stored munitions. Then the equations of either Skjeltorp (Reference 6) or Kingery (Reference 7) may be used to predict the blast pressure at the end of the access tunnel. The free-field blast pressure outside the tunnel's exit may be predicted along the desired radials at various distances by using the equations given by Skjeltorp and others (Reference 8).

It is recommended that for studies of attenuation devices, a shock tube simulation technique be used to narrow the number of choices. The most promising methods could then be built into models of particular storage facilities, either planned or in existence, to be used in further field testing. Results from the field tests could then be applied to the full-size storage facilities selected for appraisal.

REFERENCES

1. Procter, James F., "Internal Blast Damage Mechanisms Computer Program," Naval Ordnance Laboratory Technical Report NOLTR 72-231, 31 August 1972.

2. "Primacord Detonating Cord Handbook," Ensign Bickford Co., Simsbury, Connecticut 06070, Ninth printing 1963.

3. "Quartz Sensors," PCB Piezotronics, Inc., Catalog 884, 1984.

4. Glass, I. I. and Hall, J. Gordon,"Handbook of Supersonic Aerodynamics, Section 18, Shock Tubes," NAVORD Report 1488 (Vol. 6), December 1959.

5. Opalka, Klaus O. and Mark, Andrew,"The BRL-QID Code: A Tool for the Numerical Simulation of Flows in Shock Tubes with Variable Cross-Sectional Area," Ballistic Research Laboratory Technical Report BRL-TR-2763, October 1986.

6. Skjeltorp, A. T., Hegdahl, T., and Jenssen, A., "Underground Ammunition Storage, Blast Propagation in the Tunnel System, Report III A," Norwegian Defence Construction Service Office of Test and Development, Fortifikatorisk Notat nr. 81/72.

7. Kingery, Charles N., "Survey of Airblast Data Related to Underground Munitions Storage Sites," Ballistic Research Laboratory Technical report. To be published.

8. Skjeltorp, A. T., Jenssen, A., and Rinnan, A., "Blast Propagation Outside a Typical Ammunition Storage Site, MABS 5, Stockholm, Sweden, May 22-26, 1977.

9. Coulter, George A., Bulmash Gerald, and Kingery, Charles N., "Simulation Techniques for the Prediction of Blast from Underground Munitions Storage Facilities," Ballistic Research Laboratory Memorandum report. To be published.

NOTES ~

1. ALL SECTIONS ARE SMOOTH WALL PIPE
2. NOT TO SCALE
3. DUMP TANK USED INDOORS

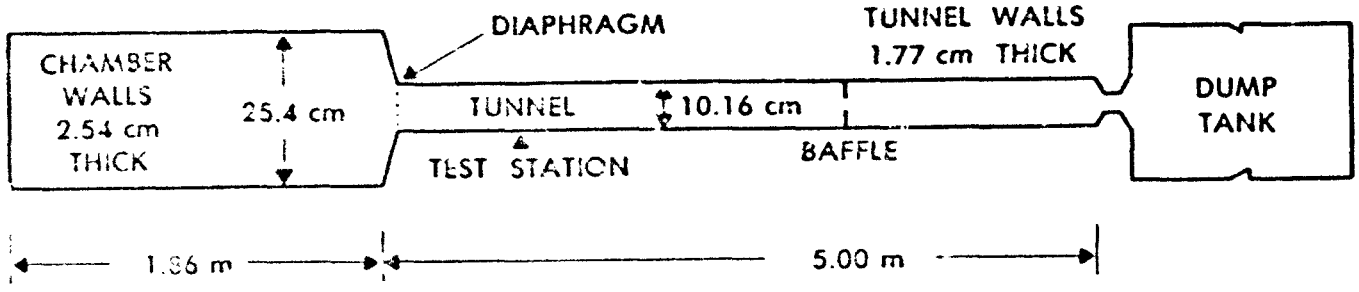

CHAMBER / TUNNEL	BAFFLE STATIONS	TEST STATIONS
$\frac{\text{TUNNEL AREA}}{\text{CHAMBER AREA}} = 0.16$	27 TUNNEL DIA.	20 TUNNEL DIA.
	36	25
		30
		33
		45

CHAMBER VOLUME = 0.0942 m^3

TUNNEL VOLUME = 0.0405 m^3 (FOR 5 m)

TOTAL VOLUME = 0.1347 m^3

FIGURE 1. 1:50 Scale Shock Tube Model

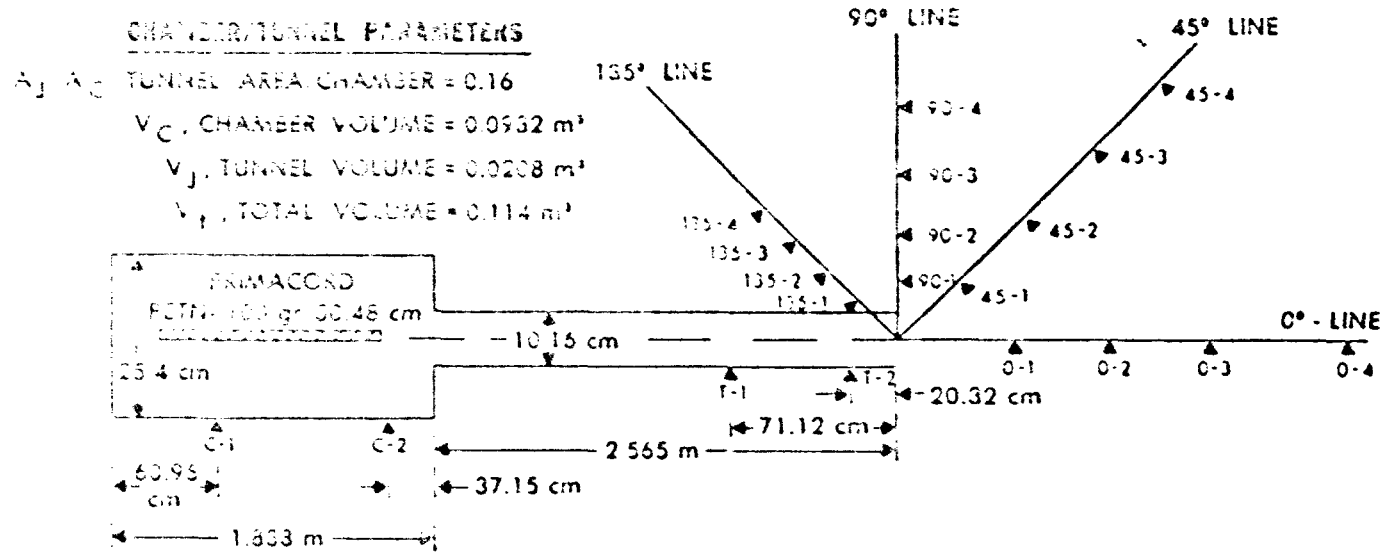

CHAMBER LOADING DENSITY

0.36 - 3.40 kg m⁻³;
CHARGE CENTERED

FIELD STATIONS

FOUR STATIONS . . .ON EACH LINE: COVERING RANGES GIVING HEAVY DAMAGE TO INHABITED BUILDING DISTANCES

FIGURE 2. Tunnel Configuration for Field Shots

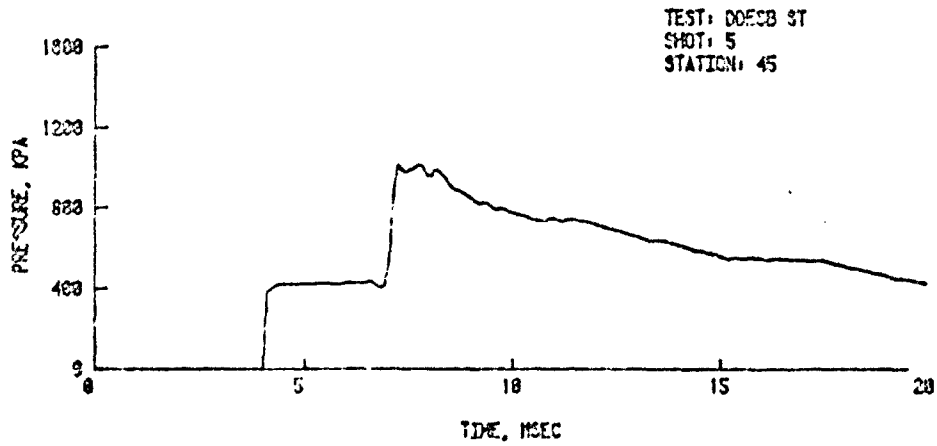

A. NO BAFFLES

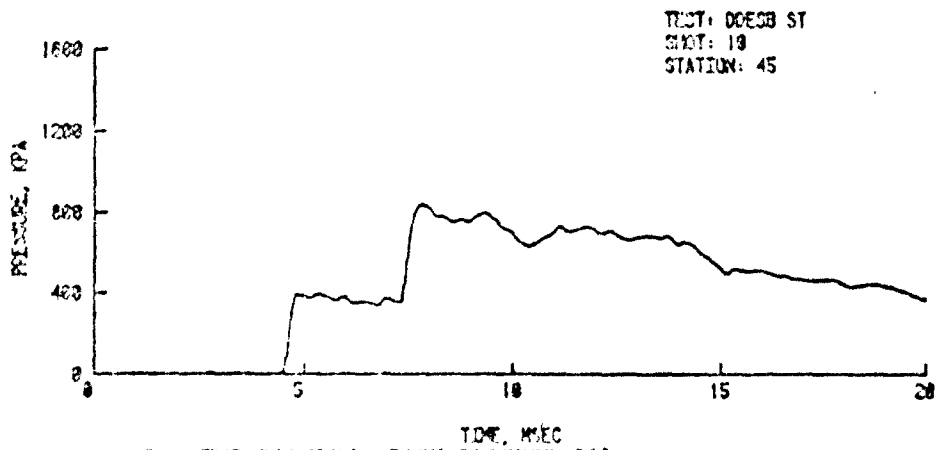

B. TWO BAFFLES, EACH BLOCKED 26%

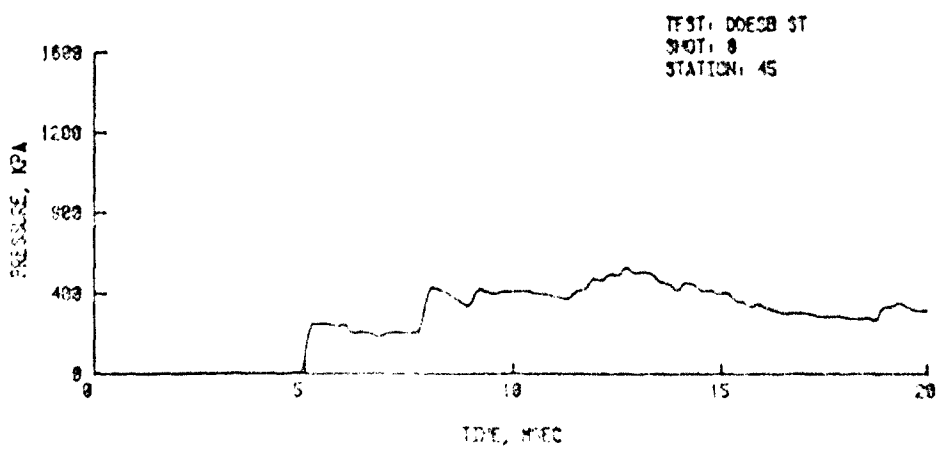

C. TWO BAFFLES, EACH BLOCKED 50%

FIGURE 3. Attenuation Over 3½ Test Section Diameters, Average Driver Pressure 814 kPa

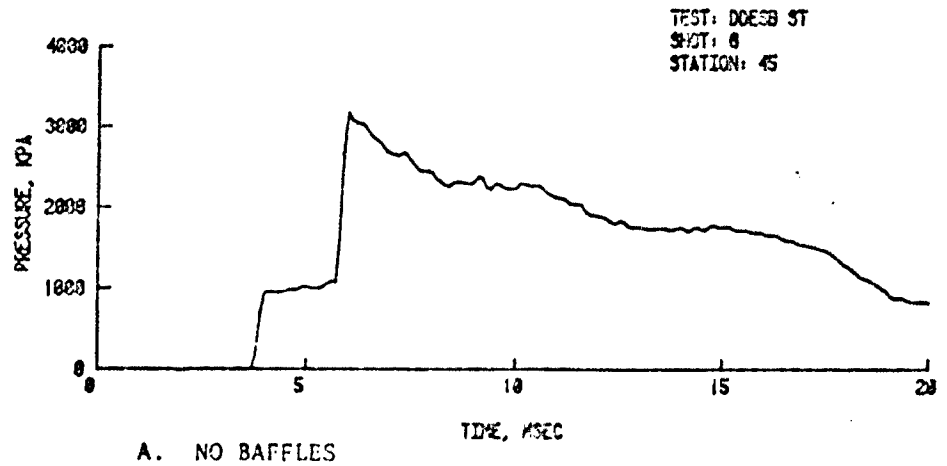

A. NO BAFFLES

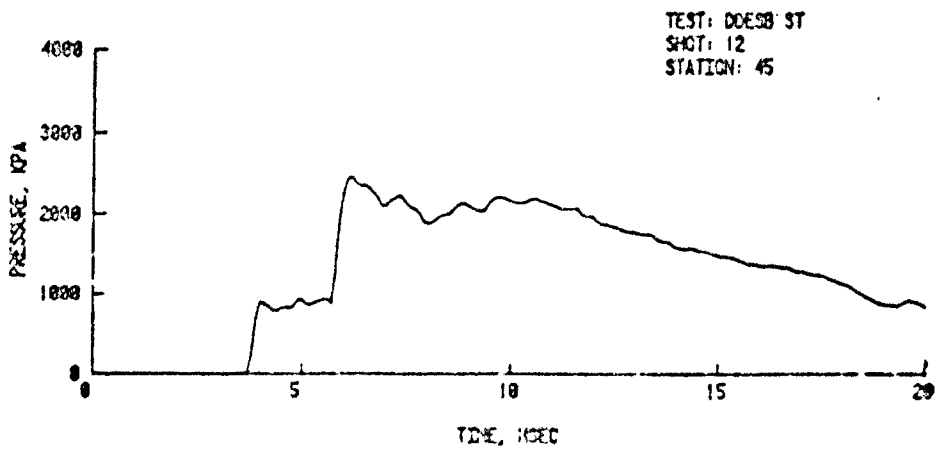

B. TWO BAFFLES, EACH BLOCKED 26%

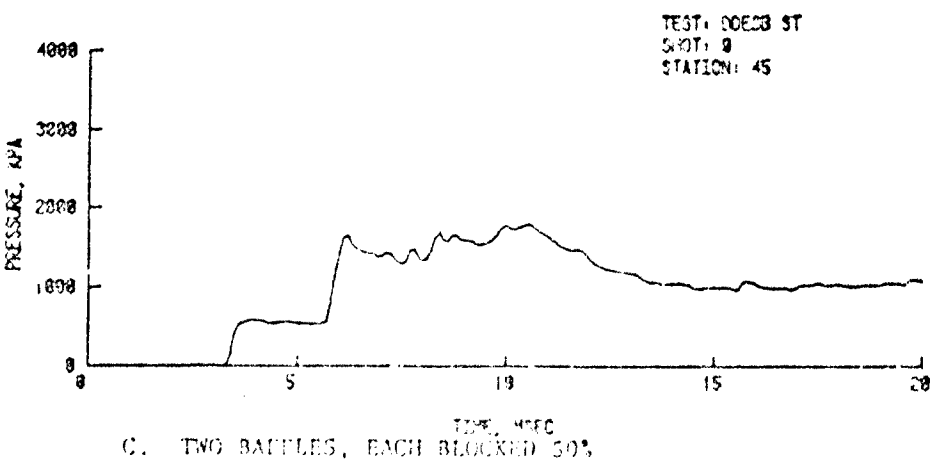

C. TWO BAFFLES, EACH BLOCKED 50%

FIGURE 4. Attenuation Over 45 Test Section Diameters, Ave. to Driver Pressure (P53 Psi)

FIGURE 5. View of Chamber of Field Model.

FIGURE 5. View of Tunnel Exit and Gage Stations.

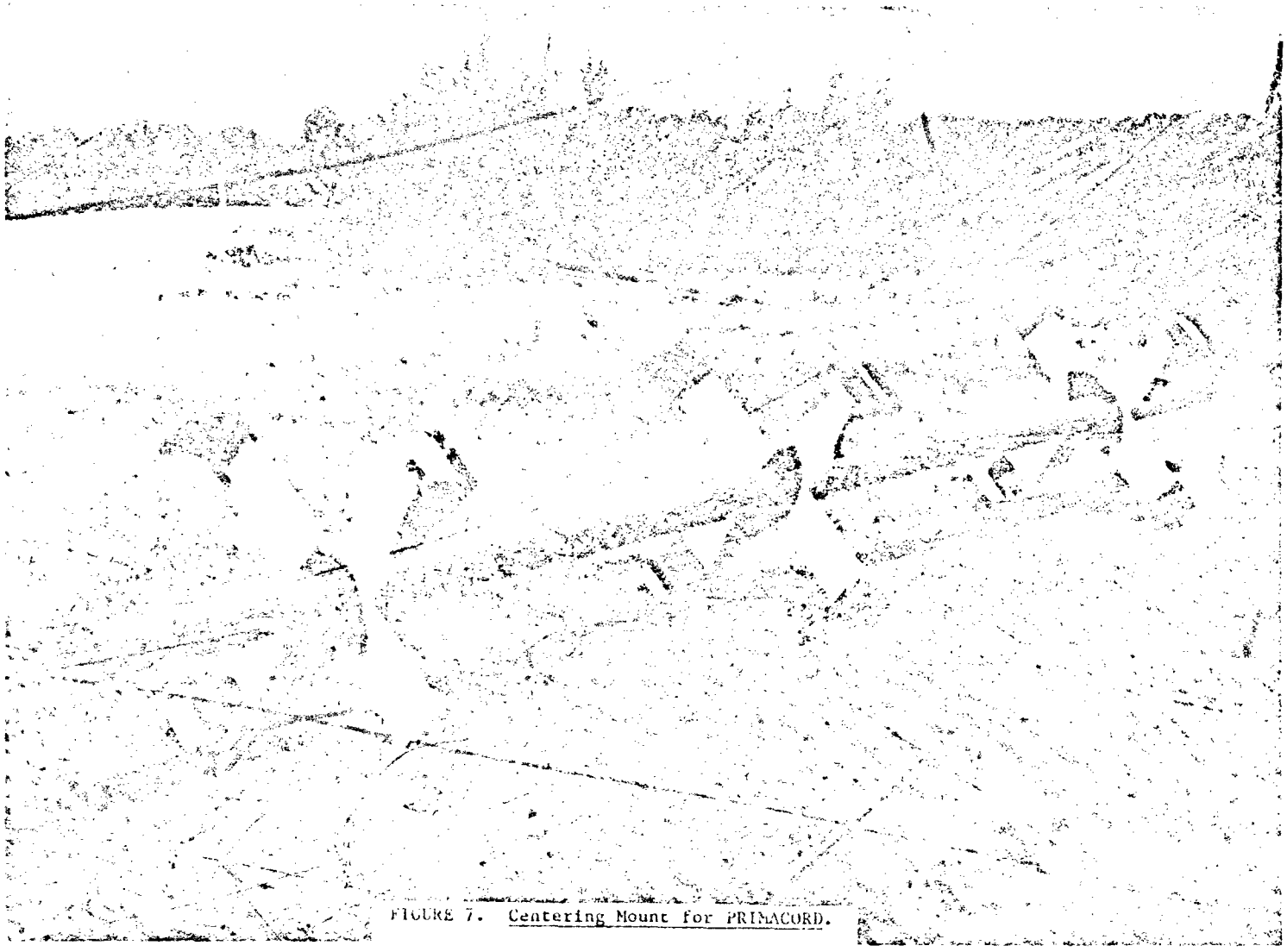

FIGURE 7. Centering Mount for PRIMACORD.

FIGURE 6. Post-shot View Along 0° Line.

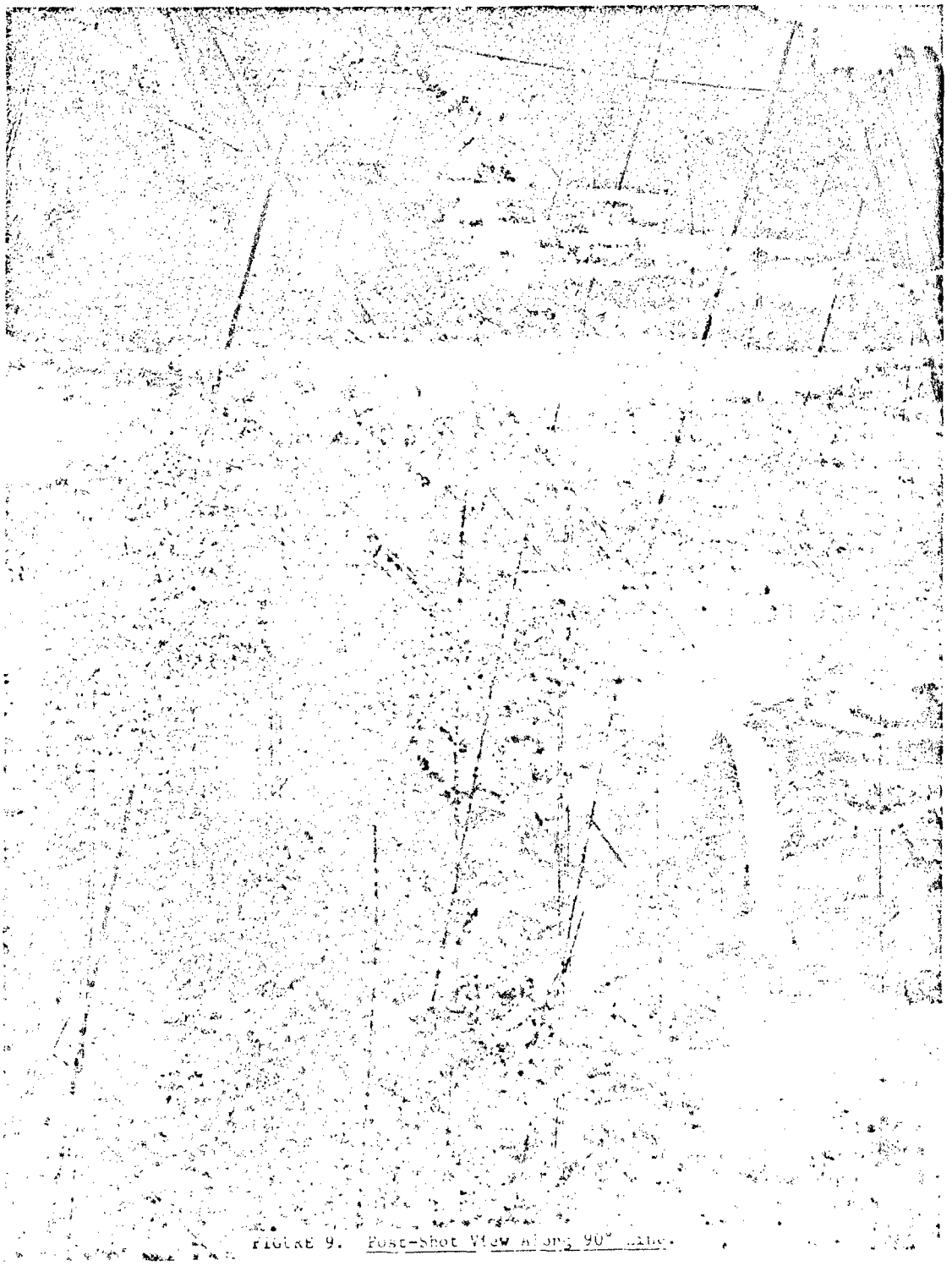

FIGURE 9. Post-Shot View along 90° Line.

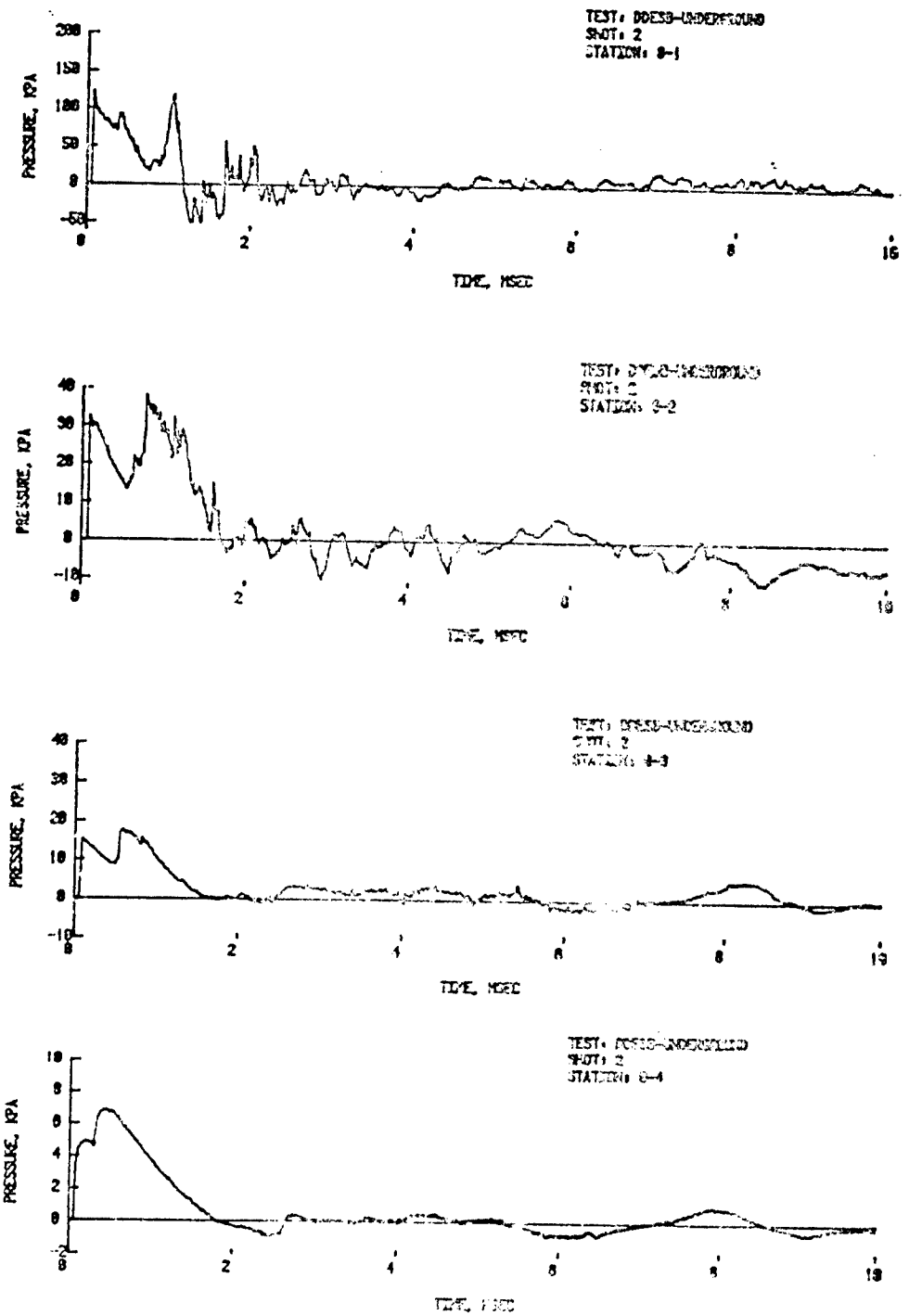

FIGURE 10. Pressure-Time Records From Field Test (Cont)

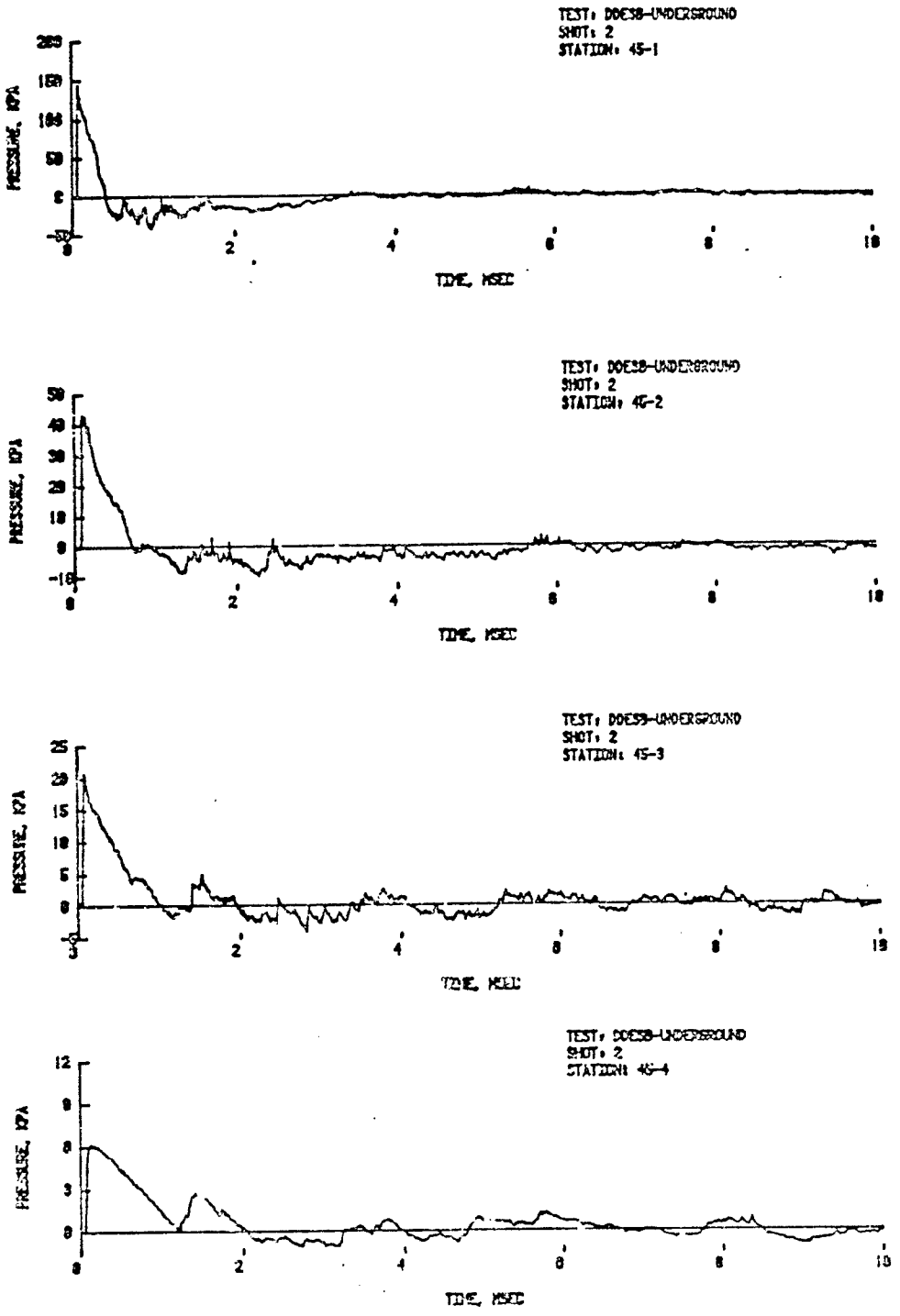

FIGURE 10. Pressure-Time Records From Field Test

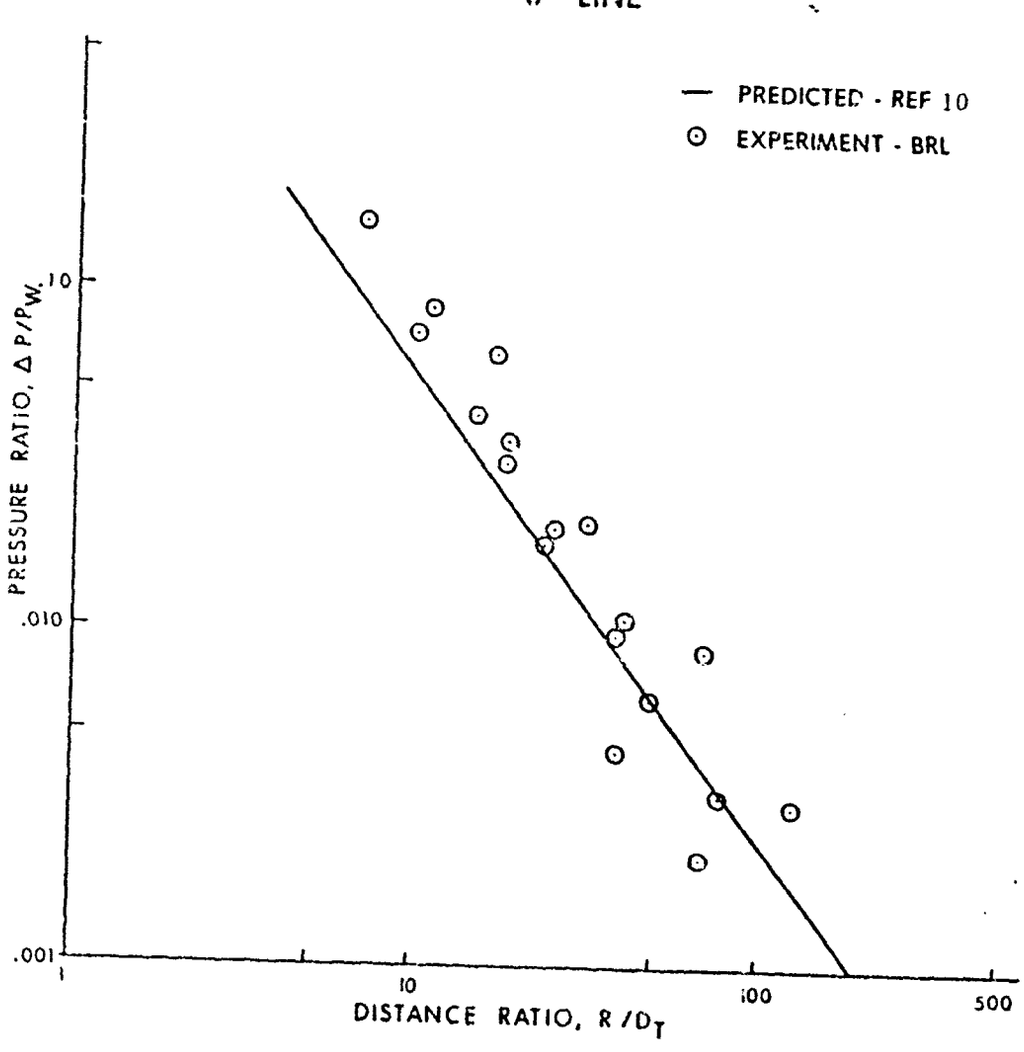

FIGURE 11. Pressure on 0^{o} Line Outside Tunnel

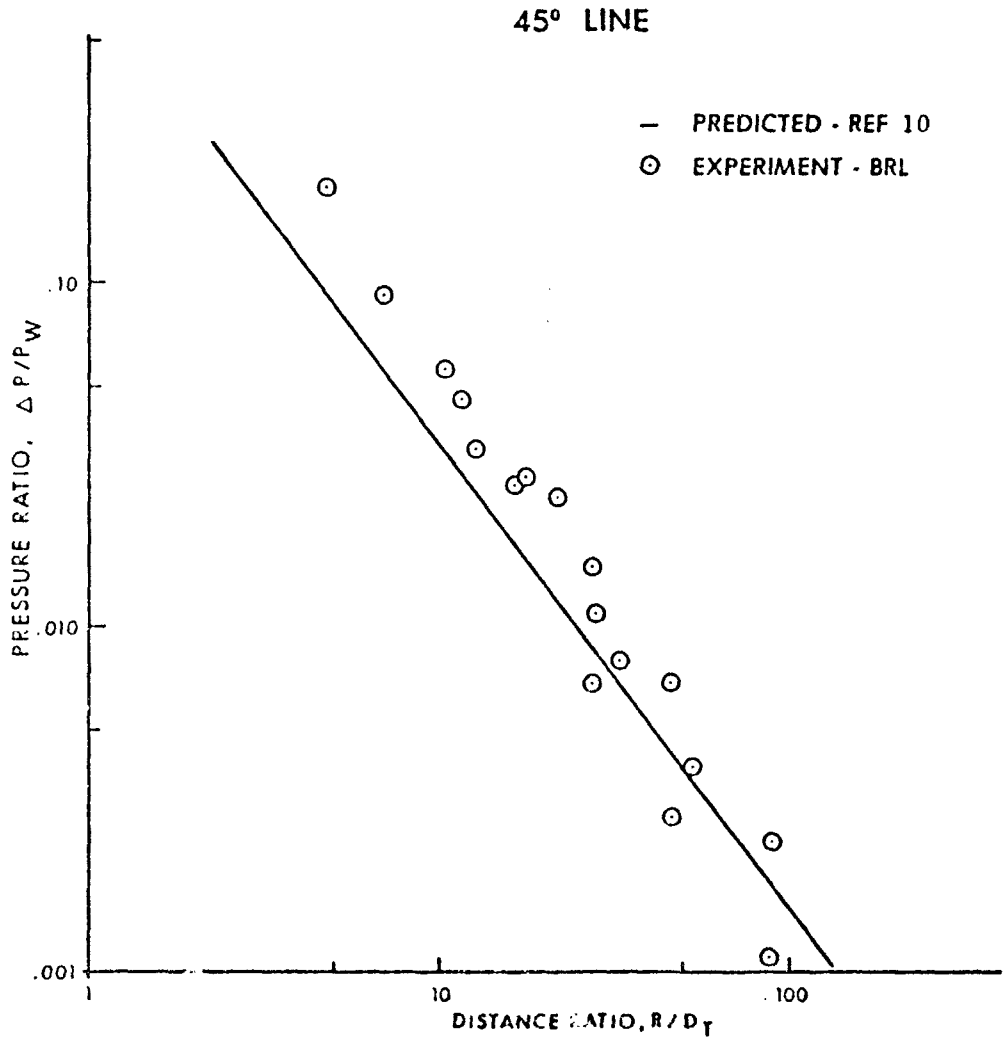

FIGURE 12. Pressure on 45° Line Outside Tunnel

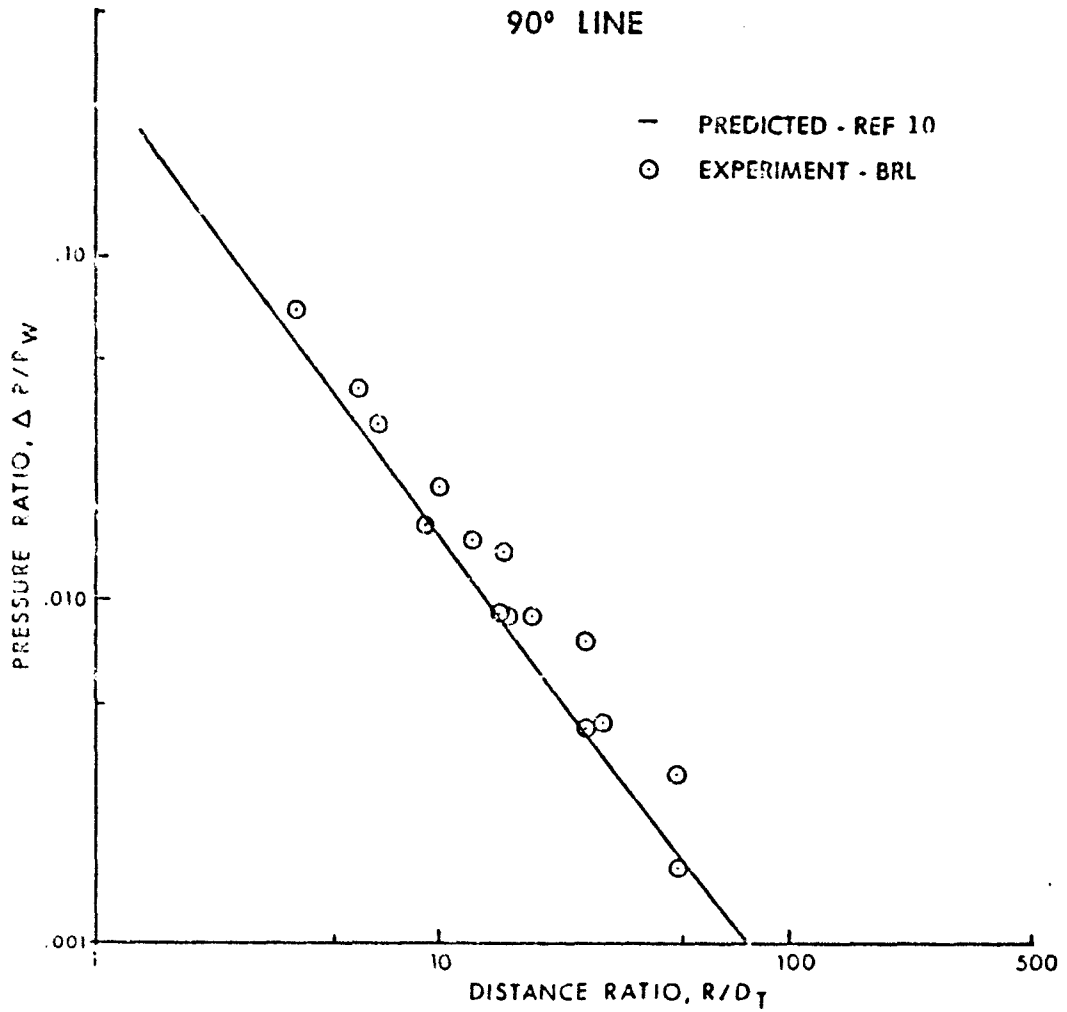

FIGURE 13. Pressure on 90° Line Outside Tunnel

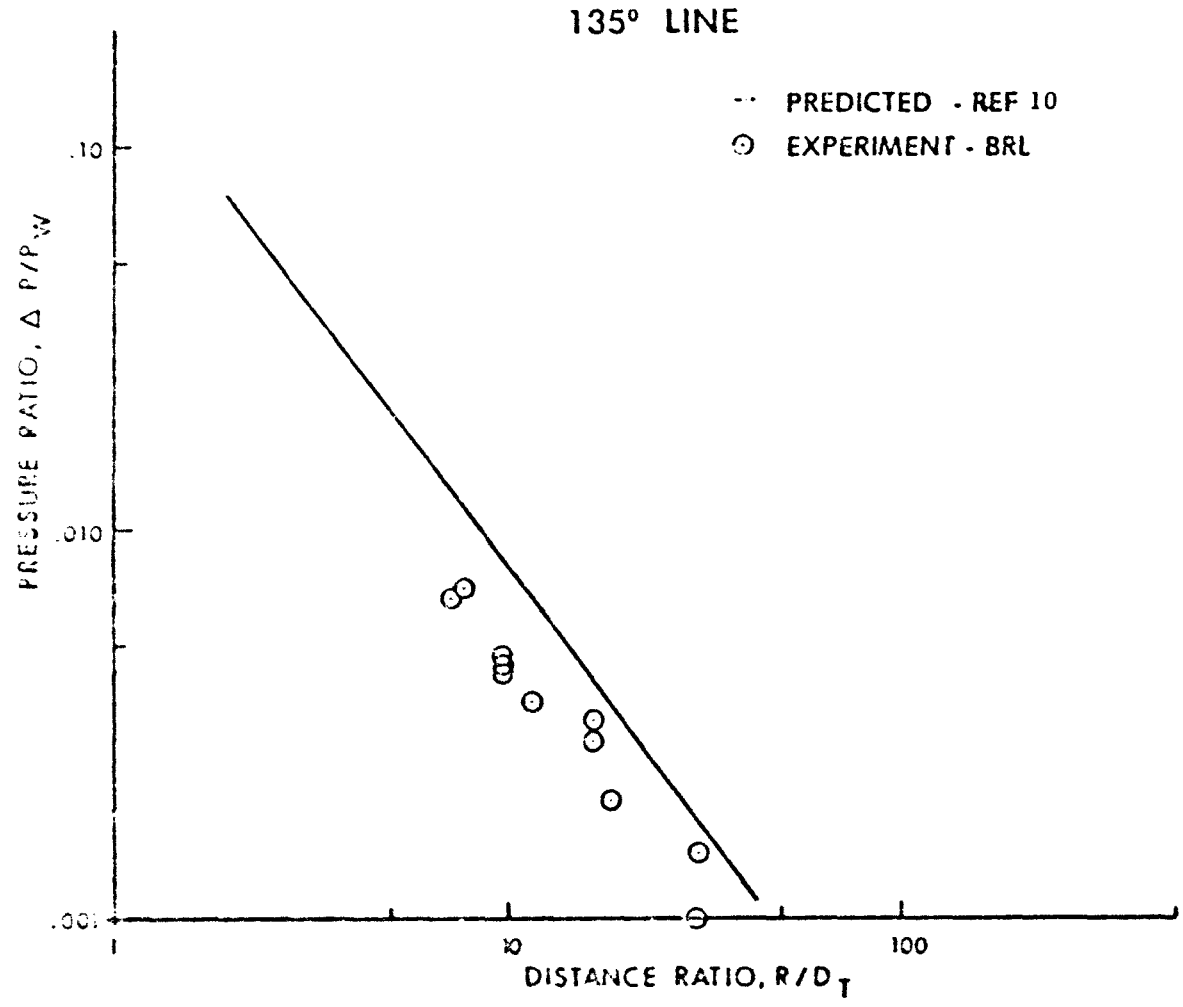

FIGURE 14. Pressure on 135° Line Outside Tunnel

TWENTY-THIRD DOD EXPLOSIVES SAFETY SEMINAR

9 - 11 AUGUST 1988 - ATLANTA - USA

UN 1.5 ARTICLES : WHAT ARE THE STAKES ?

by Jean Gabriel GOLIGER*

The paper reminds what type of articles is concerned by the new UN label 1.5 : these are articles intended to function by detonation, such as bombs, torpedoes, warheads or shaped charges. The paper, then, explains why a 1.5 hazard division is useful and why other hazard divisions are inadequate when new articles of such a type, presenting less hazards than existing ones, are offered to transport. Technical definition of 1.5 article as it is presently proposed is given in the paper. At last, the possible advantages that the public safety and the shipper can expect during a ground, air or sea transportation, through the use of the 1.5 Article Label, are listed.

* SNPE-GTS - P.O. BOX N° 2 - 91710 VERT LE PETIT - FRANCE
TELEX 604479 POUDRES F
TELECOPY (33) (1) 64.93.41.45

Since some years, the United Nations group of Experts on Explosives (GEX) has been debating of a new kind of items : 1.5 articles. The UN GEX is treating only of transportation, and not of storage. The results of the agreements are incorporated in recommandations, so called "Orange books" after an approval by the Committee of Experts on The Transport of Dangerous Goods. Presently the Orange Books are in three volumes. Most of the elements of Orange Books are then incorporated in the different international regulations of Transport.

Firstly, I shall describe the situation before the creation of 1.5. articles ; I shall recall what type of articles is concerned by the 1.5. Hazard Division and how they are defined today. Then I shall show the advantage of the creation of 1.5 articles for public safety. Finally I shall list the advantages that the manufacturers and users can expect from it.

SITUATION BEFORE THE CREATION OF 1.5 ARTICLES

The concerned articles are intended to function by detonation. They are, for example, bombs, torpedoes, warheads, shaped charges. In the present UN classification flow chart, they should undergo the series 6 trials. The 6a (single package) test and 6b (stack) test require that one article be functionaly detonated. An article near the center of the package is caused to function in the designed mode : detonation. As they are made to do so, obviously the initiated article detonates.

Depending on the mass of high explosive contained in one article and depending on the propagation from one article to the next one, then, from one package to the next one, we result in a 1.1, 1.2, 1.4 or 1.4S Hazard Division. In fact, as soon as an article contains more than 0.500 kg of high explosive it is inevitably at least in 1.2, and as soon as it contains more than a few kilograms of high explosive it is in 1.1, this being solely due to the effect of the unitary detonation of one article whatever its sensitivity may be. As a result, only small articles or, more precisely, articles containing small quantities of high explosives, can arrive in 1.4 or 1.4 S.

A priori, the design of most of the existing detonating articles is consistent with their classification in Division 1.1. Moreover, various transport accidents have indicated that there was, indeed, a risk of detonation for the 1.1 products specifically when there is an external fire.

The type of articles concerned by the 1.5 label is detonating articles, presently, classified and transported in 1.1 and 1.2 and of average or large content of high explosive.

DEFINITION OF 1.5 ARTICLES

Today, the hazards offered by this type of articles are no longer a fatality. Today we know how to make new articles of the same use which are far more safe in transport.

These articles are to be substituted,in major cases to existing articles. The guarantee of an increased safety is based on the use of low reactivity and sensitivity high explosives and on a new design. UN Committee of Expert has adopted the following definitions in December 1986, introducing articles in division 1.5, which, before this, comprised only substances.

"Division 1.5 very insensitive substances and articles

This division comprises :

(a) Substances which have a mass explosion hazard but are so insensitive that there is very little probability of initiation or of transition from burning to detonation under normal conditions of transport.

NOTE : The probability of transition from burning to detonation is greater when large quantities are carried in a ship.

(b) Articles which contain only extremely insensitive detonating substances and which demonstrate a negligible probability of accidental initiation or propagation.

NOTE : The risk from articles of Division 1.5 is limited to the explosion of a single article."

After this first step, UN GEX is debating on a second step, the technical definition and the separation rules of 1.5 Articles.

Assignment of articles in 1.5 Division is proposed on mandatory tests called series 7. The proposal on Series 7 to be debated at the twenty-eighth session of the GEX, 1 - 5 August 1988, results from an unformal meeting which was held in PARIS in JANUARY 1988, and will be presented by the Expert of France.

I present some elements of this proposal hereafter.

Firstly, tests and severe criteria on articles bring a first guarantee. But we know that tests on articles can be fallacious. The definition of the 1.5 articles therefore provides a second guarantee : the exclusive use of substances with limited sensitivity and reactivity, i.e. Extremely Insensitive Detonating Substances (E I D S).

Tests on substances are Cap test, Gap test, External Fire Test, Slow Cook-off Test and either the friability test, or Susan and Bullet Impact Tests. The Friability Test procedure is given here after in Annex 1.

Tests on articles are External Fire, Slow Cook-off, Bullet Impact and Propagation Tests.

For every one of these tests severe criteria are proposed : for examples on articles, no detonation must be obtained at the External Fire, Slow Cook-off and Bullet Impact Tests ; no propagation between two like articles can be obtained, if one of them is deliberately initiated in detonation.

TABLE 1 shows the details of proposed Tests and Criteria

ADVANTAGES FOR PUBLIC SAFETY

Whatever the scenarios of a transport accident may be, it can be asserted that the accidental detonation of a single article of this type, or numerous ones, is ruled out. This is a very clear advantage for public safety. Substitution of existing transport of products with a certain degree of hazard, by transport of far safer products means considerable improvement. The UN group of Experts on Explosives must be congratulated, not only on following up what exists, but even encouraging professionals to design articles which are safer in transport for the future.

ADVANTAGES FOR MANUFACTURERS AND USERS

In order for this advantage to be evident in the field, these products must exist and be transported in the place of existing products. What advantages can manufacturers and users expect from 1.5. articles ? These new products will cost money in order to be designed and tested. Industry must have an advantage in return, material encouragements. From my part, I can see four quite tangible ones.

The fact of transporting these articles in 1.5 will, on its own, make this much easier. Whoever has sought to find a transport charter cannot ignore the difficulty in having a 1.1 cargo transported.

Here is a first encouragement. Second encouragement, the mixing of 1.5. Articles with 1.2 and 1.3 should result in remaining within these same divisions without going up to 1.1 It goes without saying that the creation of an N compatibility group for 1.5 Articles should not complicate the task of the carriers. Versus groups C, D and E, N should be fully compatible.

Third encouragement, air transport by civil cargo aircraft should become feasible for the 1.5 Articles, the characteristics of these products fully warranting that this is reasonnable.

Finally and last possible encouragement, why not envisage an alleviation of the land transport requirements. In order for class 1 products, with low hazard such as 1.5, 1.4 and 1.4S to develop, it is indispensable that these divisions be accompanied by an alleviation of the requirements.

CONCLUSIONS

Even if the UN Group of Experts does not define the procedures for each mode of transport the members of the group cannot stand aside from this problem, so I shall finish this paper by a personal wish. I wish that in the coming years the UN Committee of Experts on The Transport of Dangerous goods can contribute to a genuine promotion of moderate hazard, class 1 products, such as 1.4., 1.4S and 1.5. through alleviation of the transport requirements, even if it is necessary to be even more sure of the validity of these classifications.

TABLE 1- PROPOSED TESTS FOR A UN 1.5 CANDIDATE ARTICLE

Test Series	Test Type	Test No	Name of test	Details and Criteria to be accepted as 1.5. Article
			TESTS ON SUBSTANCES USED IN THE ARTICLE	
7	(a)		EIDS Cap Test	UN Test 5 (a) - No detonation
7	(b)		EIDS Gap Test	Diameter 95 mm - No detonation at a gap of 70 mm
7	(c)	(i)	Susan Test	Under 10 % of TNT equivalency
		(ii)	Friability Test	Under 15 MPa/ms at 150 m/s
7	(d)	(i)	EIDS Bullet Impact Test	Bullet diameter 12.7 mm - No explosion and No detonation
		(ii)	Friability Test	Under 15 MPa/ms at 150 m/s
7	(e)		EIDS External Fire Test	No detonation - No violent reaction
7	(f)		EIDS Slow Cook-off Test	(3.3°C per hour) - No detonation - No violent reaction
			TESTS ON ARTICLE	
7	(g)		1.5 Article External Fire Test	Identical to UN 6 (c) test - Must be not 1.1, nor 1.2, nor 1.3
7	(h)		1.5 Article Slow Cook-off Test	No reaction more severe than burning
7	(i)		1.5 Article Bullet Impact Test	Bullet diameter 12.7 mm - No detonation
7	(j)		1.5 Article Propagation Test	No detonation of the acceptor

THE LICENSING OF PORTS AND HARBOURS HANDLING EXPLOSIVES

G E Williamson, Health and Safety Executive, UK

SUMMARY

1. This paper sets out to describe Regulations made in 1987 which require among other things the licensing of all ports and other places around the coastline of Great Britain where explosives, both commercial and military, are handled. The approaches adopted in setting explosives limits considered tolerable in licensing terms could have application for other inter-modal handling operations.

2. Although based on legal requirements, the paper is not intended to be an authoritative interpretation of the law; such interpretation can only be made by the courts. Indeed, the intention has been to give no more than a brief overview sufficient to put the new licensing provisions into perspective.

INTRODUCTION

3. Up until 1 June 1987, the carriage and handling of explosives in harbours around Great Britain was controlled by a large number of individual byelaws, or else by the Conveyance in Harbours of Military Explosives Regulations 1977. The byelaws were made under the Explosives Acts 1875 and 1923. Similar provisions covered petroleum spirit and other dangerous substances.

4. The explosives byelaws were generally framed along the lines of a model set of terms and would normally include quantity limits based on the advice of appropriate Government Departments following on-site surveys.

5. But that approach fell, along with the relevant statutory provisions and any byelaws made under them, when new regulations were made under the Health and Safety at Work etc Act 1974.

6. The new Regulations provided for a more comprehensive form of control, one concerned with all classes of dangerous substance and which could apply at a wider range of places than before, especially in relation to explosives.

NEW REGULATIONS

7. The Dangerous Substances in Harbour Areas Regulations 1987 (Statutory Instrument 1987 No.37) came into force on 1 June 1987. They control the carriage, loading, unloading and storage of all classes of dangerous substances in harbours and harbour areas in Great Britain. Few exceptions are made from the application of the Regulations; an important one in the context of this paper covers nuclear explosive devices and their components, subject in any case to other controls.

8. The definition of a dangerous substance is broadly based and includes for example any substance or article within a current definition of dangerous goods in the International Maritime Dangerous Goods Code (IMDG Code). It includes all conventional explosives, whether commercial or military and irrespective of hazard division or compatibility group.

9. The terms harbour and harbour area are also broadly defined. Harbour areas are controlled by statutory harbour authorities and harbours are not. Harbour areas may include areas of water outside the port itself. Harbours may include adjacent land and buildings. The Regulations do not apply anywhere outside a harbour or harbour area except for the purposes of explosives licensing.

10. The Regulations include provisions which can apply to explosives just as they apply to any other dangerous substance. They also include provisions which apply specifically to explosives.

11. The general provisions cover such matters as:

- the advance notice required before dangerous substances can be brought into a harbour or harbour area;

- the powers of the Harbour Master to prohibit entry, require removal or regulate the handling of dangerous substances in view of the likely risks to health or safety;

- the marking and navigation of vessels, including the requirement to ensure that vessels carrying more than specified amounts of explosives are in a state of readiness to be moved at any time tidal conditions allow;

- the duties to handle dangerous substances safely and to take all necessary precautions to avoid fire or explosion, including the need to ensure that all persons handling them are properly trained;

- the requirement for freight containers from inland to be accompanied by a certificate certifying that they have been properly packed, and for all packages to be suitable for their purpose and properly labelled;

- the need for harbour authorities to prepare an emergency plan, the safety precautions to be taken by berth operators and the need to report untoward incidents;

- the storage of dangerous substances and the parking of road vehicles carrying them.

12. The specific provisions, set out in Part IX of the Regulations, include the licensing requirements described below and cover as well:

- the security of explosives and appointment of explosives security officers;

- the need for vessels and vehicles loaded with explosives to be taken out of harbours and harbour areas as soon as reasonably practicable;

- the safety of electro-explosive devices;

- the notification of deteriorated explosives and precautions to take;

- the requirement to keep, and then hold for 5 years, records of all explosives handled other than shop goods fireworks.

13. Practical guidance on means of compliance with certain of the Regulations and with relevant provisions of the Health and Safety at Work etc Act 1974 is given in an Approved Code of Practice. A guide to the Dangerous Substances in Harbour Areas Regulations 1987 has also been published by the Health and Safety Executive.

EXPLOSIVES LICENSING

14. The Dangerous Substances in Harbour Areas Regulations 1987 prohibit explosives from being brought into, carried or handled in a harbour or harbour area unless such activities are covered by an explosives licence granted by the Health and Safety Executive. In the same way, an explosives licence is also required for loading on board or unloading from a vessel of explosives when this occurs on any part of the coast or in the tidal waters of Great Britain or within territorial waters adjacent to Great Britain.

15. Certain exceptions are made from that general prohibition and its extension outside harbours and harbour areas. The exceptions include:

- explosives of Hazard Division 1.4 and most other explosives in amounts of upto 10 kilograms;
- explosives for immediate use by a vessel or to be dumped at sea as authorised;
- explosives of less than 1 tonne intended for immediate use in the harbour or harbour area itself;
- berths within a commercial explosives factory or magazine;
- explosives carried by a British or foreign warship;
- explosives carried by certain other vessels in the service of the Crown;
- explosives within the limits of certain naval dockyards or other military facilities specifically named.

16. Added to that, explosives may be handled in accordance with byelaws already in operation, and with the Conveyance in Harbours of Military Explosives Regulations 1977, until a licence has been issued or refused, or until 31 December 1991, provided that application for a licence has by now been made.

17. The Regulations do not prescribe the form or contents of the licence; that is left to the discretion of the Health and Safety Executive. The Executive may reject an application or may grant a licence subject to such conditions as it thinks fit; it may vary or revoke a licence at any time in writing. Provision is made for public consultation on proposals for licensing; the Health and Safety Executive has then to take account of any comments or objections made.

18. The Executive may grant provisional explosives licences in cases of urgency and for a period of upto 6 months.

LICENSING IN PRACTICE

19. During the first year the Regulations have been in operation, the Health and Safety Executive has received some 170 applications for explosives licences. Applications have ranged from ports already well established in the explosives trade and having existing byelaws - which could stand if appropriate until the end of 1991 - to smaller places not having that benefit and thus not permitted to handle explosives until a licence could be issued.

20. Priorities have been set to ensure so far as possible that adequate flows of explosives could be safety maintained. Most attention has been focussed onto the continuing movement of explosives to the Western Isles of Scotland, onto ports where development work had called into question the existing byelaw quantity limits and onto certain new-entrant ports. Good progress has been made.

21. In drafting licences, the aim has been to keep them as short as possible, to concentrate on two central issues. Firstly, the need to specify quite clearly the places within a harbour or harbour area where vessels may be anchored or berthed and the quantity limits which apply. Secondly, the safeguarding arrangements necessary to ensure that any developments in or around the harbour or other place are properly considered and if appropriate then taken into account in a licence revision.

22. Care has been taken to ensure licences do not repeat any provision made elsewhere, in particular in the parent legislation already outlind above, or in other relevant provisions such as those concerned with the carriage of explosives outside the harbour or harbour area, whether by sea, road or rail. But at the same time it is sensible to bear in mind the idea that one of the reasons for having a licensing system is to allow for flexibility and enable the licensing authority to impose requirements by way of licence conditions where the particular circumstances merit it.

23. The licence will show the relationship between the quantity limits set and the distances to be maintained between the explosives and any passenger vessel or any other explosives or person not connected with the handling operations. Separate limits are set for hazard division 1.1 and 1.5 explosives and those of HD 1.2 or 1.3; the potential need to reduce the specified limits where the explosives include those in compatibility groups A, B or F is covered. The licence will show the distances to be used in the preparation of safeguarding plans.

24. The licence will also include any special conditions applying to the quantity limits set. Such conditions might include the evacuation of certain buildings when explosives are being handled, they may set a limit on the frequency of explosives movements allowed through the place.

25. For the most part the quantity limits have been set on the basis of established consequence models for hazard division 1.1 explosives. Data collected in a detailed survey of the site can be fed directly into a portable computer and run on a spreadsheet to generate information about likely consequences which can then guide decisions about licensing. A particular advantage is the ability to immediately test and check the results being obtained.

26. Some places surveyed could not be licensed on that basis. The quantity limit derived from an assessment of consequences alone proved too low in operational terms. It has been possible however to generate broad brush frequencies for the initiation of explosives which may be expected to occur at some of the simpler handling facilities in particular locations. Consideration of the likely ranges of individual and societal risks involved, in the light of proposals made by the Health and Safety Executive in a paper on the tolerability of risk from nuclear power stations, provided further pointers towards licensable quantity limits.

27. The ability to consider the likely risks proved particularly useful in the provisional licensing of places for short term use pending the identification of more suitable, safer routes.

11 August 1988

TWENTY-THIRD DOD EXPLOSIVES SAFETY SEMINAR

SESSION: EXPLOSIVES SAFETY MANAGEMENT

TITLE OF PRESENTATION: U.S. ARMY EXPLOSIVES SAFETY MANAGEMENT/U.S. ARMY TECHNICAL CENTER FOR EXPLOSIVES SAFETY - OVERVIEW

PRESENTED BY: MR. GARY W. ABRISZ
CHIEF, LOGISTICS EXPLOSIVES SAFETY
DIVISION, U.S. ARMY TECHNICAL CENTER
FOR EXPLOSIVES SAFETY

Introduction:

Vu-graph #1

Good morning, I'm Gary Abrisz, the Chief of the Logistics Explosives Safety Division in the U.S. Army Technical Center for Explosives Safety.

Vu-graph #2

As Mr. Walker, the Deputy Assistant Secretary of the Army (Installations and Logistics) discussed in his keynote address on Tuesday, the Army developed an explosives safety management concept in 1987 and began implementation of the resulting program in 1988.

Vu-graph #3

The overall program relates to the three key elements shown here.

I'll discuss briefly the Department of Army Explosives Safety Council and the Executive Director for Explosives Safety to put the mission of the U.S. Army Technical Center for Explosives Safety into perspective and go into more detail on the U.S. Army Technical Center for Explosives Safety mission, responsibilities, and staffing.

Vu-graph #4

The Explosives Safety Council met for the first time in May of this year. This Council is made up of voting members from the major Army commands. The Director of Army Safety is designated as the Council Chairman.

This Council provides the major Army commands direct input into Army explosives safety policy formulation which they will be responsible to implement within their command.

Vu-graph #5

The Executive Director for Explosives Safety, currently Lieutenant General Hissong, provides for centralization in executing the Army's explosives safety mission. He is an extension of Headquarters, Department of the Army in exercising management and operational control of the new U.S. Army Technical Center for Explosives Safety.

Vu-graph #6

The U.S. Army Technical Center for Explosives Safety has the mission of providing assistance and technical services Army-wide.

The overall goal is to assure that personnel involved with ammunition and explosives functions operate in the safest environment possible, thus avoiding the loss of mission readiness through explosives accidents.

Vu-graph #7

We are located on Savanna Army Depot Activity, Savanna, Illinois and are an element of the U.S. Army Defense Ammunition Center and School at that location.

Vu-graph #8

The U.S. Army Technical Center for Explosives Safety as established has authority for day-to-day communications and interfaces throughout the explosives safety community to serve and assist in the various explosives safety missions.

Vu-graph #9

I will discuss briefly some of the U.S. Army Technical Center for Explosives Safety major responsibilities shown here, and you will see how those various interfaces are developed and maintained.

Again, we are a service and support organization for Headquarters, Department of the Army and the major Army commands Army-wide.

Vu-graph #10

The U.S. Army Technical Center for Explosives Safety is responsible to develop and maintain Army explosives safety standards. Currently, in this area of responsibility we have a revised Army regulation and a newly developed Department of the Army pamphlet. Both have been provided the major Army commands and other Army agencies for review and comment. We are directing our efforts to having final publications developed by the second quarter of fiscal year 1989.

The U.S. Army Technical Center for Explosives Safety has also assumed proponency for Technical Manual 9-1300-206, and will maintain it consistent with the newly developed Army regulation and the Department of the Army pamphlet.

Vu-graph #11

The U.S. Army Technical Center for Explosives Safety has a direct interface with the Department of Defense Explosives Safety Board. We are responsible to be the Army's final review and approval authority for explosives safety site and general construction plan being submitted to the Board for final review and approval.

Vu-graph #12

The U.S. Army Technical Center for Explosives Safety is also responsible to provide the Army's response to the Department of Defense Explosives Safety Board's explosives safety survey reports generating from the Board's surveys of Army installations and operations. We are to provide assistance to the major Army commands in identifying and accomplishing corrective actions when deficiencies are identified in the reports.

Vu-graph #13

The Army is currently developing guidelines for major Army commands implementation of explosives safety waiver management. The new Department of the Army pamphlet will contain the waiver program management requirements.

Vu-graph #14

This program will be not only for waiver management but also the management of Army exemptions to the ammunition and explosives safety standards. Proposed program management in both of these areas will be presented at the next meeting of the Department of the Army Explosives Safety Council for review and decision. Establishing appropriate levels of authority for waiver and exemption approvals in the Army is important to this task.

Revisit Vu-graph #9

For the U.S. Army Technical Center for Explosives Safety to accomplish the responsibilities just mentioned, as well as supporting Army-wide explosives safety training; managing a technical data base system and a technical library for the Army; maintaining cognizance and promoting research, development and application for explosives safety technology, and providing explosives accident/malfunction investigation assistance, all requires a multi-disciplined and professional staff.

Vu-graph #15

I'll briefly discuss the organization and staffing of the U.S. Army Technical Center for Explosives Safety.

To accomplish the assigned responsibilities, we are organized into three separate divisions and an overall director.

Vu-graph #16

The U.S. Army Technical Center for Explosives Safety has an authorized table of distribution and allowances of thirty-five positions. We have authority currently to fill thirty-one of the thirty-five. Currently twenty positions are filled, ten are in recruitment and five are in the final position classification processes.

Vu-graph #17

The Director of the organization will be a GM-340-15, Program Manager. There will be a scientific advisor in the organization to support, guide, and conduct special studies and scientific research in various problem areas requiring evaluations.

Vu-graph #18

The Logistics Explosives Safety Division personnel deal with ammunition and explosives safety concerns from the production base on through the complete life cycle. Areas such as transportation, storage maintenance, and demilitarization. This includes facilities used for ammunition and explosives storage and operations and the associated quantity distance and logistics functions. Accordingly, the logistics and safety disciplines are represented in this division.

Vu-graph #19

The Development and Production Division personnel deal directly with the production base and will provide support and assistance in accomplishing the explosives safety missions in that area. This involves participation in the research and development and the testing arenas.

Accordingly, you see the engineering disciplines are heavily represented in this division.

Vu-graph #20

The Program Management and Data Division personnel are responsible to acquire, catalog, organize, and store explosives and ammunition technical information. This will establish a data management system and a technical library for use by organizations Army-wide. They will interface Department of Defense-wide and with industry to develop the data bases required.

In addition, they will maintain and manage the resource management functions for the U.S. Army Technical Center for Explosives Safety.

Vu-graph #21

In summary, the U.S. Army Technical Center for Explosives Safety is to be a source of explosives and ammunition safety expertise and information. We are developing and expanding in that mission.

Vu-graph #22

Should you require assistance or have information in the explosives and ammunition safety area you wish to pass on or discuss, please contact us.

Thank you.

U.S. ARMY

EXPLOSIVES

SAFETY

PROGRAM

U.S. ARMY EXPLOSIVES SAFETY PROGRAM

MAR 87 - DIRECTOR OF THE ARMY STAFF (DAS) ESTABLISHED.

--GENERAL OFFICER STEERING COMMITTEE

--SPECIAL STUDY GROUP

APR 87 - DAS APPROVED CONCEPT

FEB 88 - DAS SIGNED PROGRAM DOCUMENT FOR IMPLEMENTATION

1687

EXPLOSIVES SAFETY MANAGEMENT

EXPLOSIVES SAFETY MANAGEMENT PLAN KEY ELEMENTS

- DA EXPLOSIVES SAFETY COUNCIL (DAESC)
- EXECUTIVE DIRECTOR FOR EXPLOSIVES SAFETY (EDES)
- U.S. ARMY TECHNICAL CENTER FOR EXPLOSIVES SAFETY (USATCES)

1688

THE DEPARTMENT OF THE ARMY EXPLOSIVES SAFETY COUNCIL (DAESC)

- PROVIDES ARSTAF AND MACOM PRIORITIZATION AND DECISION PROCESS
- DEVELOPMENT OF POLICY, PROCEDURES
- MEETS AT LEAST TWO TIMES A YEAR
- DIRECTOR OF ARMY SAFETY
- MACOM MEMBERS, COLONELS AND HIGHER, AND MACOM SAFETY DIRECTOR

THE EXECUTIVE DIRECTOR FOR EXPLOSIVES SAFETY (EDES)

- EXECUTES POLICY AND PRIORITIES DEVELOPED BY THE DAESC
- DEPUTY CG FOR MATERIAL READINESS OF AMC (DESIGNATED JUNE 1967 BY THE CHIEF OF STAFF OF ARMY)
- EXECUTIVE AGENT FOR ARMY EXPLOSIVES SAFETY
- EXECUTIVE DIRECTOR OF THE TECHNICAL CENTER FOR EXPLOSIVES SAFETY

1690

USATCES

MISSION STATEMENT

THE USATCES, UNDER THE DIRECTION OF THE EXECUTIVE DIRECTOR FOR EXPLOSIVES SAFETY, IS TO PROVIDE ASSISTANCE AND TECHNICAL SERVICES TO SUPPORT AND ENHANCE THE ARMY EXPLOSIVES SAFETY PROGRAM.

GOAL

TO PROVIDE THE BEST POSSIBLE ASSISTANCE AND GUIDANCE TO ENABLE ARMY ORGANIZATIONS TO CONTROL THE INHERENT RISKS OF AMMUNITION AND EXPLOSIVES AVOIDING THE LOSS OF MISSION READINESS THROUGH PERSONNEL INJURIES AND PROPERTY DAMAGE.

SAVANNA, IL

1692

USATCES

PRIMARY INTERFACES

DOD EXPLOSIVES SAFETY BOARD

ARMY STAFF

USASC

MAJOR ARMY COMMANDS

UNITS/INSTALLATIONS/AGENCIES

OTHER SERVICES

USATCES

RESPONSIBILITIES

- SERVE AND SUPPORT HQDA AND MACOM COMMANDERS ARMY-WIDE
- DEVELOP AND MAINTAIN ARMY EXPLOSIVES SAFETY STANDARDS
- PROVIDE ARMY APPROVAL AUTHORITY FOR DDESB SITE AND GENERAL CONSTRUCTION PLANS
- TRACK DDESB EXPLOSIVES SAFETY REPORTS
- TRACK EXPLOSIVES SAFETY WAIVERS/EXEMPTION REQUESTS
- IDENTIFY AND SUPPORT ARMY EXPLOSIVES SAFETY TRAINING NEEDS
- MAINTAIN COGNIZANCE AND PROMOTE RESEARCH, DEVELOPMENT, AND APPLICATION FOR EXPLOSIVES SAFETY TECHNOLOGY
- ESTABLISH A TECHNICAL DATA BASE MANAGEMENT SYSTEM AND TECHNICAL LIBRARY FOR THE ARMY
- PROVIDE ACCIDENT/MALFUNCTION INVESTIGATION ASSISTANCE

• ARMY EXPLOSIVES SAFETY STANDARDS DEVELOPMENT AND MAINTENANCE

- AR 385-64 (REVISED AS CONSOLIDATION)	AMMUNITION AND EXPLOSIVES SAFETY STANDARDS (FIRST IPR PROCESS REVIEW (IPR) 1-2 JUN 88) PUBLICATION OF REGULATION PROJECTED FOR 2D QTR FY 89 (CONSOLIDATION OF AR 385-26, AR 385-60, AR 385-64, AND AR 385-65) (COORDINATING DRAFT DISTRIBUTED FOR REVIEW 13 JUL 88)
- DA PAM 385-64	BEING DEVELOPED (FIRST IPR 1-2 JUN 88) PUBLICATION OF PAMPHLET PROJECTED FOR 2D QTR FY 89 (COORDINATING DRAFT DISTRIBUTED FOR REVIEW 13 JUL 88)
- TM 9-1300-206	AMMUNITION AND EXPLOSIVES SAFETY STANDARDS (PROPONENT)

1665

DDESB SITE AND GENERAL CONSTRUCTION PLAN SUBMISSIONS

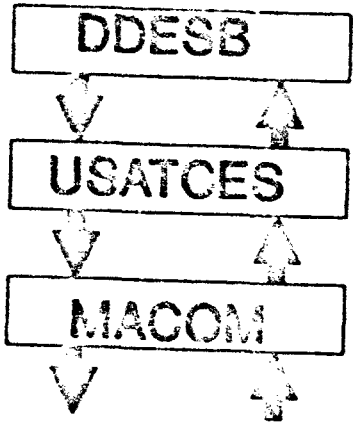

REVIEW

RETURN

DDESB EXPLOSIVES SAFETY SURVEY REPORTS

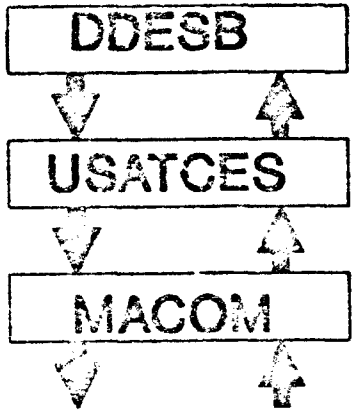

REVIEW

RETURN

• EXPLOSIVES SAFETY WAIVERS PROGRAM MANAGEMENT

- MACOM COMMANDER AUTHORITY
  -- ESTABLISHING ARMY GUIDELINES ON WAIVER MGMT
- DA PAM 385-64 DRAFT
  -- STANDARD FORM
  -- WAIVER APPROVAL AUTHORITY LEVELS
  -- NEXT DAESC FOR DECISION

• EXPLOSIVES SAFETY EXEMPTION PROGRAM MANAGEMENT

- EXEMPTIONS - SECRETARY/UNDER SECRETARY OF THE ARMY AUTHORITY

  -- EUSA - SIX 2D INFANTRY DIVISION CAMPS (FY 88 MCA PROJ.)

✓ -- USAREUR - NORDENHAM, GE

✓ -- MTMC - MILITARY OCEAN TERMINAL SUNNY POINT

✓ -- USARSO - MINDI PIER

✓ -- USAREUR - NATO/HOST NATION EXPLOSIVES SAFETY CRITERIA

✓ -- USAREUR - WEILERBACH, GE

✓ IN PROGRESS

RESPONSIBILITIES

- SERVE AND SUPPORT HQDA AND MACOM COMMANDERS ARMY-WIDE
- DEVELOP AND MAINTAIN ARMY EXPLOSIVES SAFETY STANDARDS
- PROVIDE ARMY APPROVAL AUTHORITY FOR DDESB SITE AND GENERAL CONSTRUCTION PLANS
- TRACK DDESB EXPLOSIVES SAFETY REPORTS
- TRACK EXPLOSIVES SAFETY WAIVERS/EXEMPTION REQUESTS
- IDENTIFY AND SUPPORT ARMY EXPLOSIVES SAFETY TRAINING NEEDS
- MAINTAIN COGNIZANCE AND PROMOTE RESEARCH, DEVELOPMENT, AND APPLICATION FOR EXPLOSIVES SAFETY TECHNOLOGY
- ESTABLISH A TECHNICAL DATA BASE MANAGEMENT SYSTEM AND TECHNICAL LIBRARY FOR THE ARMY
- PROVIDE ACCIDENT/MALFUNCTION INVESTIGATION ASSISTANCE

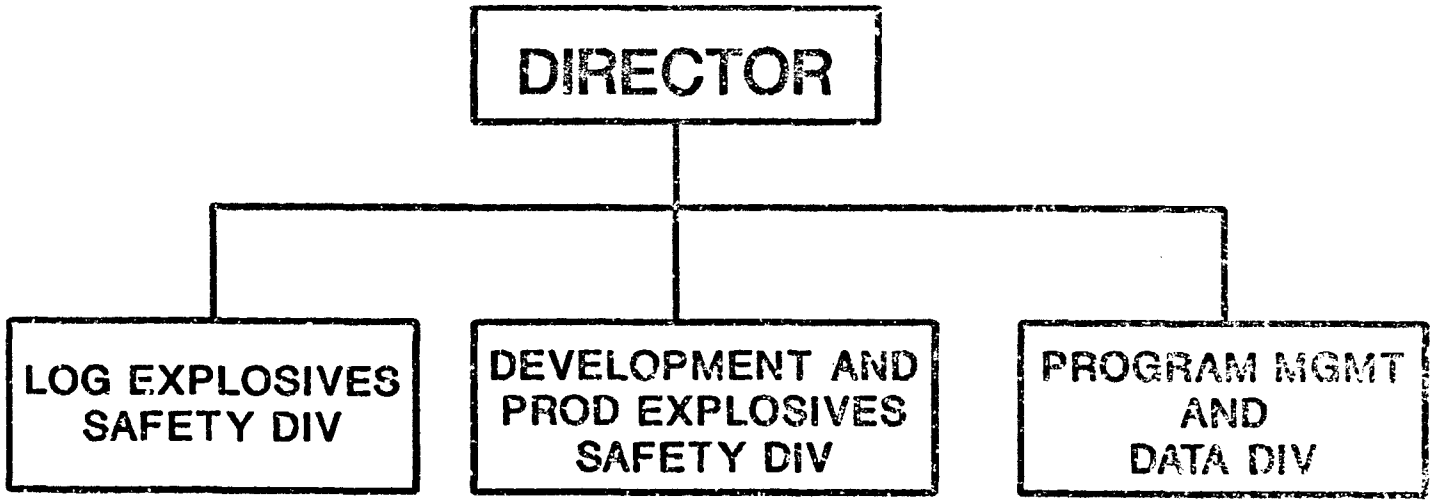
DIRECTOR
LOG EXPLOSIVES SAFETY DIV
DEVELOPMENT AND PROD EXPLOSIVES SAFETY DIV
PROGRAM MGMT AND DATA DIV

1701

USATCES STAFFING STATUS
35 POSITIONS AUTHORIZED ON TDA

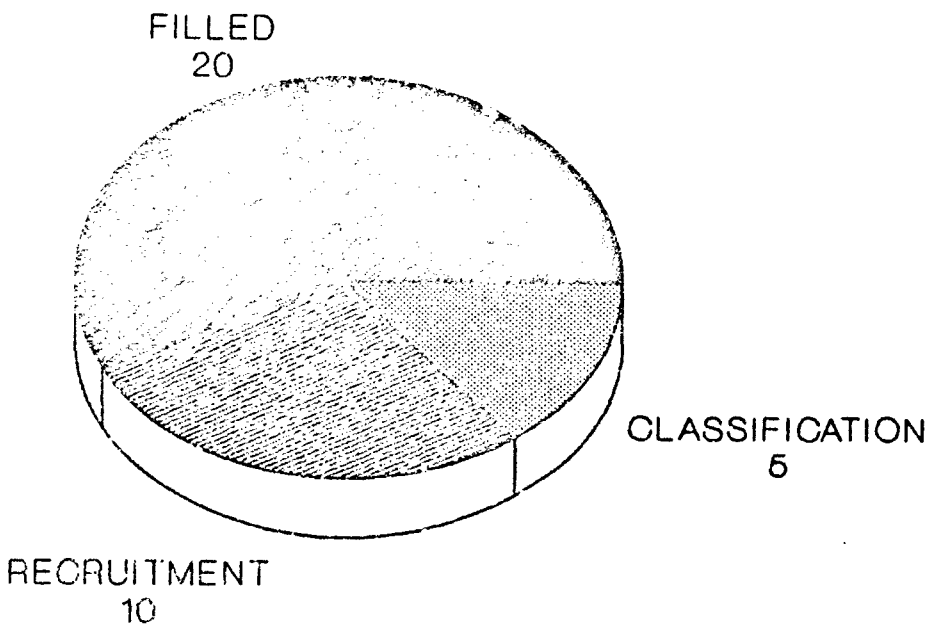

1702

USAFCES

OFFICE OF THE DIRECTOR

- ✓ 1-GM-15 DIRECTOR (PROGRAM MANAGER)
- ✓ 1-GM-14 SCIENTIFIC ADVISOR
- ✓ 1-GS-06 SECRETARY (STENOGRAPHER)

✓ HAVE NOT BEEN FILLED

1703

USATCES

LOGISTICS EXPLOSIVES SAFETY DIVISION

1704

1-GM-14 CHIEF (PROGRAM MANAGER)
1-GS-13 QASAS
1-GS-13 LOGISTICS MANAGEMENT SPECIALIST
1-GS-13 SAFETY AND OCCUPATIONAL HEALTH MANAGER
1-GS-12 QASAS
1-GS-12 SAFETY AND OCCUPATIONAL HEALTH SPECIALIST
1-GS-12 LOGISTICS MANAGEMENT SPECIALIST
1-GS-11 STORAGE SPECIALIST
1-GS-05 SECRETARY-STENOGRAPHER

✓ 1-GS-13 CIVIL ENGINEER
✓ 1-GS-05 COMPUTER ASSISTANT

✓ HAVE NOT BEEN FILLED

DEVELOPMENT AND PRODUCTION EXPLOSIVES SAFETY DIVISION

1705

1- GS- 13 SAFETY ENGINEER
1- GS- 13 QASAS
1- GS- 13 CHEMICAL ENGINEER
1- GS- 13 MECHANICAL ENGINEER
1- GS- 12 QASAS
1- GS- 11 INDUSTRIAL SPECIALIST (ORDNANCE)
1- GS- 05 COMPUTER ASSISTANT
1- GS- 04 CLERK- STENOGRAPHER

✓ 1- GM- 14 CHIEF (PROGRAM MANAGER)
✓ 1- GS- 13 INDUSTRIAL ENGINEER
✓ 1- GS- 12 SAFETY ENGINEER

✓ HAVE NOT BEEN FILLED

PROGRAM MANAGEMENT AND DATA DIVISION

1-GS-13 EXPLOSIVES SAFETY TECHNICAL DATA BASE COORDINATOR
1-GS-05 COMPUTER ASSISTANT
1-GS-04 CLERK-STENOGRAPHER

✓ 1-GM-14 CHIEF (PROGRAM MANAGER)
✓ 1-GS-13 PROGRAM ANALYST
✓ 1-GS-12 BUDGET ANALYST
✓ 1-GS-12 TECH-WRITER EDITOR
✓ 1-GS-12 COMPUTER PROGRAM ANALYST
✓ 1-GS-11 LIBRARIAN
✓ 1-GS-05 LIBRARIAN TECHNICIAN

✓ HAVE NOT BEEN FILLED

1706

USATCES

SUMMARY

THE USATCES IS A SOURCE OF EXPLOSIVES SAFETY TECHNICAL EXPERTISE AND INFORMATION IN SUPPORT OF AN ENHANCED ARMY EXPLOSIVES SAFETY PROGRAM.

1707

DIRECTOR
U.S. ARMY TECHNICAL CENTER FOR EXPLOSIVES SAFETY
ATTN: SMCAC-ES
SAVANNA, IL 61074-9639

AUTOVON: 585-8801
COMMERCIAL: (815) 273-8801

1708

RESPONSIBILITY AND ACCOUNTABILITY IN THE WORKPLACE

Robert H. Spotz
Naval Ordnance Station
Indian Head, Maryland

In reviewing all the successful management techniques I have used in over twenty-five years of managing potentially hazardous explosive and propellant operations, I find they fall into one of four categories [Encl (1)]:

- Clearly assign responsibility and accountability
- Tell people what you expect
- Teach people what they need to know
- Hold people accountable

I find these apply to organization as well as individuals.

In clearly assigning responsibility and accountability, we generally have a position description, performance objectives, job standards, and program plans [Encl (2)].

Every organization has what I call common denominators [Encl (3)]. For example, in an ordnance plant, the basic job is to make an excellent product, on time, within cost, and with safety of operations. The basic common denominators of the ordnance plant are quality, cost, schedules, and safety. It is important to clearly put these denominators in each position description. It is also mandatory to tie these common denominators from the job description into specific quantities for the annual performance objectives. For example, what level of rejects is outstanding, satisfactory and unsatisfactory?

In addition to job descriptions and performance objectives, program plans and weekly schedules can be valuable in telling people in more detail what is expected of them [Encl (4)]. Probably the most valuable training tool is a desk plan or training outline for the position. I had learned of this from a secretary who was temporarily filling in for the Technical Director's secretary. I asked how she knew what to do in the temporary job and she showed me the desk plan for that position. It was so simple yet so ingenious. Since that time I have developed desk plans for each position in every organization I have managed.

Examples of Training Outlines and Weekly Production Schedules are attached [Encls (5 & 6)].

In addition to common denominators, each organization has defined certain basic levels of responsibility. It is critical for employees to understand these levels of responsibility. Supervisors and managers are basic to every organization. However, I find that the responsibilities of each are not well understood. In the simplest form an individual is responsible for his own actions; a supervisor is responsible for his own actions as well as the subordinates. This basic concept or definition of responsibility is poorly understood. The success of an organization is critical to this concept being understood. Yet it seems to be a natural human instinct to try to put the responsibility for failure on to someone or something else. More often than I can remember, I was the single lowest person in the organization who freely admitted mistakes. Too often I had to analyze the facts and determine those subordinates who were also responsible. Generally no one volunteers.

Examples of some basic levels of responsibility are attached [Encl (7)].

Approved for public release; distribution unlimited.

In teaching people what they need to know I utilize [Encl (8)]:

- A training outline
- An individual training plan which highlights the weakness of the individual as compared to the position training outline
- An employee skill record which is used to monitor progress of employee skills compared to the skills necessary to perform the position [Encl (9)]

Other monitoring techniques are attached [Encl (10)].

To close the loop of good management, it is critical to provide positive and negative feedback to the subordinate. In general, supervision has a difficult time with this.

An effective system of providing feedback is attached [Encl (11)].

In summary, there are four good basic management principles [Encl (12)]:

- Clearly assign responsibility and accountability
- Tell people what you expect
- Teach people what they need to know
- Provide positive and negative feedback

These basic management principles form a circle. Omitting any one of them eventually destroys the organization.

GOOD BASIC MANAGEMENT PRINCIPLES

- Clearly assign responsibility and accountability
- Tell people what you expect
- Teach people what they need to know
- Hold people accountable

Enclosure (1)

CLEARLY ASSIGN RESPONSIBILITY AND ACCOUNTABILITY

- Position description
- Annual performance objectives
- Standards
- Program plan

Enclosure (2)

COMMON DENOMINATORS

- Cost
- Quality
- Schedules
- Safety
- Cleanliness

Enclosure (3)

TELL PEOPLE WHAT YOU EXPECT

- Annual performance objectives
- Training outline for position
- Weekly schedule
- Program plant
- Set example

Enclosure (4)

TRAINING OUTLINE FOR EACH POSITION

I. Indoctrination

II. Responsibilities

III. Documentation

IV. Hardware

V. Methods of operation

VI. Equipment familiarization

VII. Formal training

VIII. Branch policy

IX. Division policy

X. Department policy

Enclosure (5)

EXTRUDED PRODUCTS BRANCH (2021)
WEEKLY PRODUCTION SCHEDULE

FOR WEEK ENDING _____ OPERATOR RESPONSIBILITY _____

BLDG.	PROGRAM	JOB DESCRIPTION CHARGE NO.	MON	TUE	WED	THU	FRI	STANDARD	PROJECT ENGINEER

I ASSIGN OPERATIONAL RESPONSIBILITY (LIMITED TO SECTIONS 6.B.1 and 6.B.4) DEFINED IN INST 11016.10 AS INDICATED FOR BUILDINGS ASSIGNED TO ME.

_____
MANAGER, EXTRUDED PRODUCTS BRANCH

Enclosure (6)

CLARIFICATION OF RESPONSIBILITIES

- Individual
- Supervisor
- Manager
- Operator in charge
- Technical support
- Overall building responsibility
- Driver
  - — project leader
  - — lead shop

Enclosure (7)

TEACH PEOPLE WHAT THEY NEED TO KNOW

- Training outline for each position
- Individual training plan
- Importance to organization
- Employee skill record
- Monitor

EMPLOYEE SKILL RECORD

DEPARTMENT	DIVISION	BRANCH
LEGEND	WORK JOB	
P/U PHYSICALLY UNFIT NO EXPERIENCE IN INSTRUCTION GIVEN LIMITED SKILL FULLY QUALIFIED		
EMPLOYEES		

Enclosure (9)

MONITORING METHODS

- Weekly reports
- Monthly program status reports
- Program quarterly reviews
- Inspections by others
- Tours
- Corrective action reports
- Trend analysis
  — process control charts

PROVIDE POSITIVE AN NEGATIVE FEEDBACK

- Performance appraisal
- Routine reports
- Verbal
- Awards/punishment
- Trend analysis

Enclosure (11)

GOOD BASIC MANAGEMENT PRINCIPLES

- Clearly assign responsibility & accountability
- Tell people what you expect
- Teach people what they need to know
- Hold people accountable

Enclosure (12)

COMPARISON OF SELECTED SAFETY PROCEDURES ON THE HANDLING OF EXPLOSIVES IN TRANSITION FROM STORAGE TO IN-PROCESS STATUS

by

DONALD J. HILL, B.S., M.B.A.
DEFENSE CONTRACT ADMINISTRATION SERVICES
MANAGEMENT AREA - TWIN CITIES
ST. PAUL, MINNESOTA

at the

TWENTY-THIRD DoD EXPLOSIVES SAFETY SEMINAR
8-11 AUGUST 1988, ATLANTA, GEORGIA

ABSTRACT

Various methods and safety procedures are employed in the explosives manufacturing industry to assure the safe transition of 1.1 materials (DoD Hazard Classification/Division). Special handling, not applicable to either the storage or in-process status, may be required.

This presentation compares three options, which may be used, to assist in determining and making the best selection for your operation, in order to provide a competitive edge within the industry.

INTRODUCTION

The explosives manufacturing industry is in need of practical solutions with respect to explosives handling to enhance safety. If the price of safety becomes prohibitive, the competitive edge is lost and safety goals become no more than stumbling blocks to defense readiness.

To accomplish such a far-reaching goal, and yet abide by the explosives safety 'Cardinal Rule' of limiting exposures to the minimum number of personnel for the minimum amount of time and the minimum amount of hazardous material consistent with safe and efficient operations, requires substantial forethought and extensive technological development by the industry.

The procedures and apparatus utilized within the safety time-frame where 1.1 materials are removed from their resting place, in an explosives storage magazine, to that point where the

material is behind firewalls, operational shields, or barricades, on the operating line and 'in-process', is considered and discussed in this paper with the selected types of operational shields. No automatic remote controlled or robotic methods were reviewed or considered in making the following comparisons.

Various types of operational shields were initiall reviewed and evaluated in the development of this paper, however, for brevity, only three specific types are considered for discussion. These are:

The Line Service Boxes (LSB),

The Vented Suppressive Shielding Cart (VSSC) and,

The Manual Explosives Transport Vehicle (METV).

These three selections are believed to be generally representative of industry needs.

The criteria employed in the selection of operational shields for review and evaluation were: simplicity of design, flexibility toward use and cost.

LINE SERVICE BOXES (LSB)

DEVELOPMENT: The line service box reviewed and considered for this paper was developed by Honeywell, Inc., Minneapolis, MN. This particular type of operational shield was selected since it could easily be modified to be mobile in a single unit. As indicated in Figure 1, the LSB provides for the control of fragments and the partial suppression of over-pressure and heat-flux by

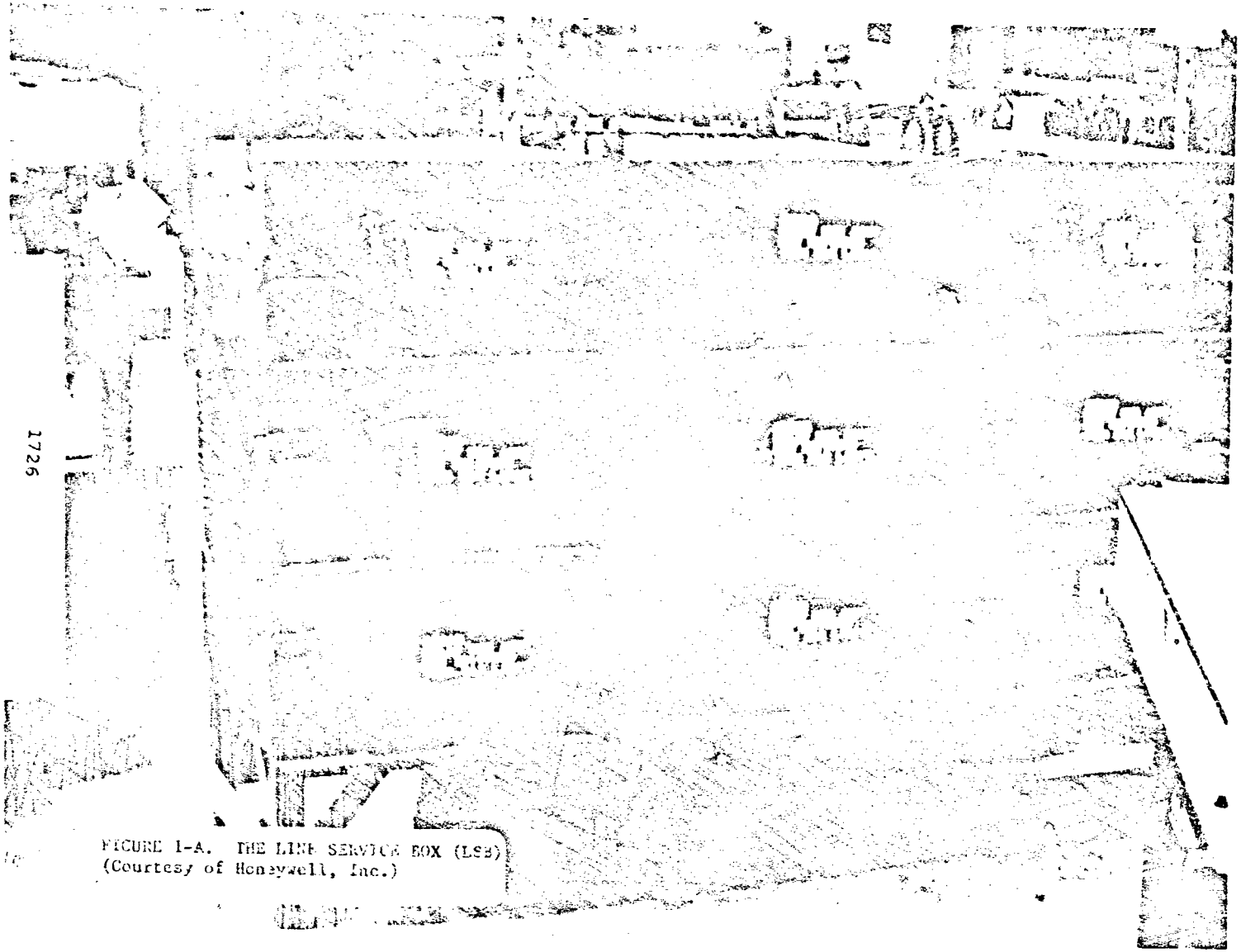

FIGURE I-A. THE LINE SERVICE BOX (LSB)
(Courtesy of Honeywell, Inc.)

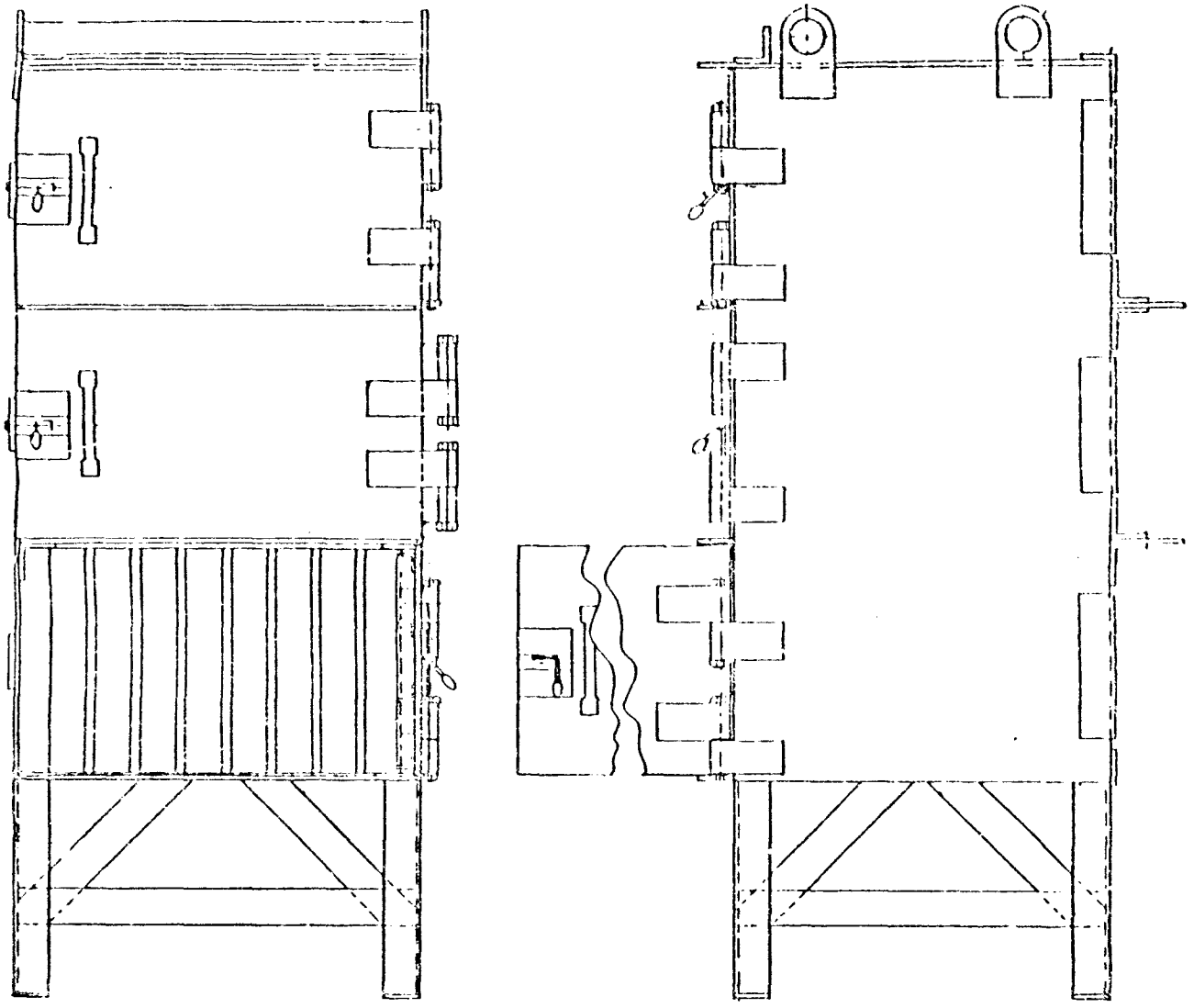

FIGURE 1-B. THE LINE SERVICE BOX (LSB)
SHOWING SINGLE UNIT CONSTRUCTION
(Courtesy of Honeywell, Inc.)

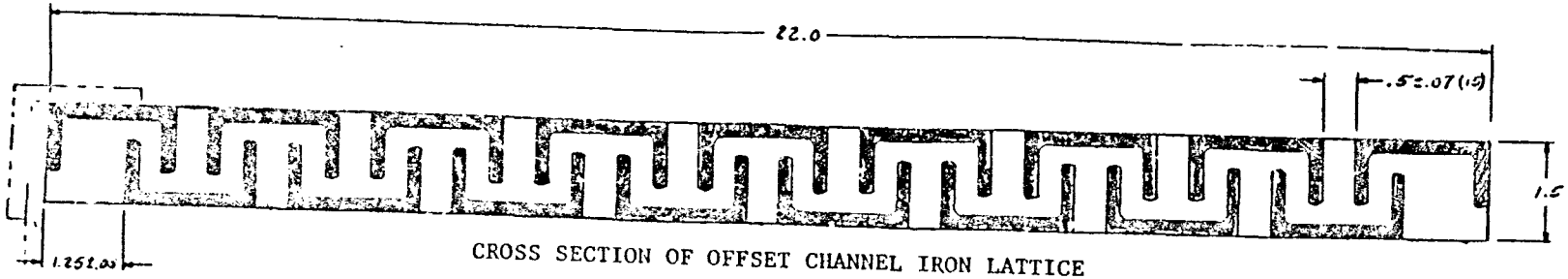

CROSS SECTION OF OFFSET CHANNEL IRON LATTICE

1728

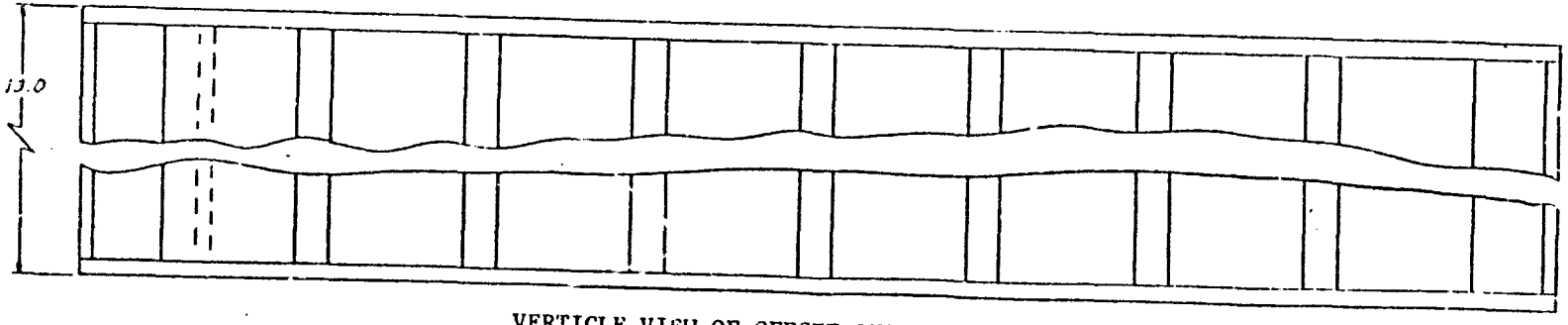

VERTICLE VIEW OF OFFSET CHANNEL IRON LATTICE

FIGURE 2. THE LINE SERVICE BOX (LSB)
SHOWING THF SUPPRESIVE SHIELD METHOD
(Courtesy of Honeywell, Inc.)

venting a blast to the rear through offset channel iron construction (see Figure 2).

DESCRIPTION: The LSB units are approximately 13 inches high by 22 1/2 inches wide by 20 inches deep. This unit was designed and constructed so as to contain two 50 caliber ammunition cans with space for hand access. The units are stacked three high to conserve space and are constructed of quarter-inch plate steel, angle and channel iron, one inch flat stock for hinges, and, hardened steel bolts for the hinge and retainer bolt.

TEST: The testing of the LSB resulted in the unit being certified to contain 8 grams of PBXN-5 materials. Tests determined that the door must be ground to fit to a close tolerance, so as to suppress and contain flame passage as much as possible. Also, an extended flange is provided above and below, in front and in back, to prevent flame passage from one unit to another, thus causing ignition/propagation. It was found that if the door was reinforced on the inside, that an increased amount of material could be contained.

VENTED SUPPRESSIVE SHIELDING CARTS (VSSC)

DEVELOPMENT: The VSSC concept of interlocking angle iron (for fragment shielding) and interlacing perforated steel plates and copper screen (for heat absorption) was developed as part of the U.S. ARMY Manufacturing Technology Program to protect personnel and equipment from explosive related incidents. A

VENTED SUPPRESIVE SHIELDING

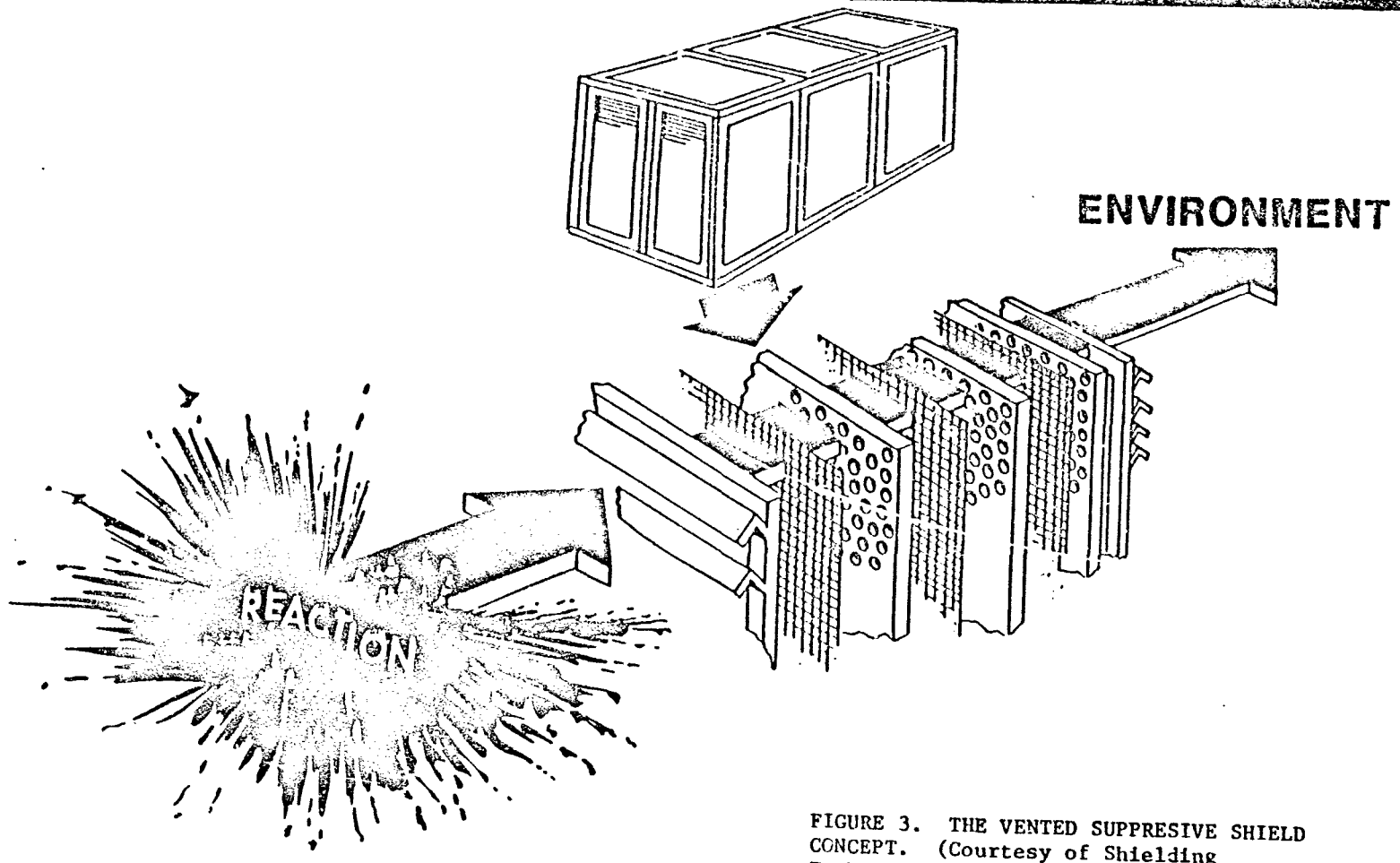

FIGURE 3. THE VENTED SUPPRESIVE SHIELD CONCEPT. (Courtesy of Shielding Technology, Inc., Bel Air, MD)

1730

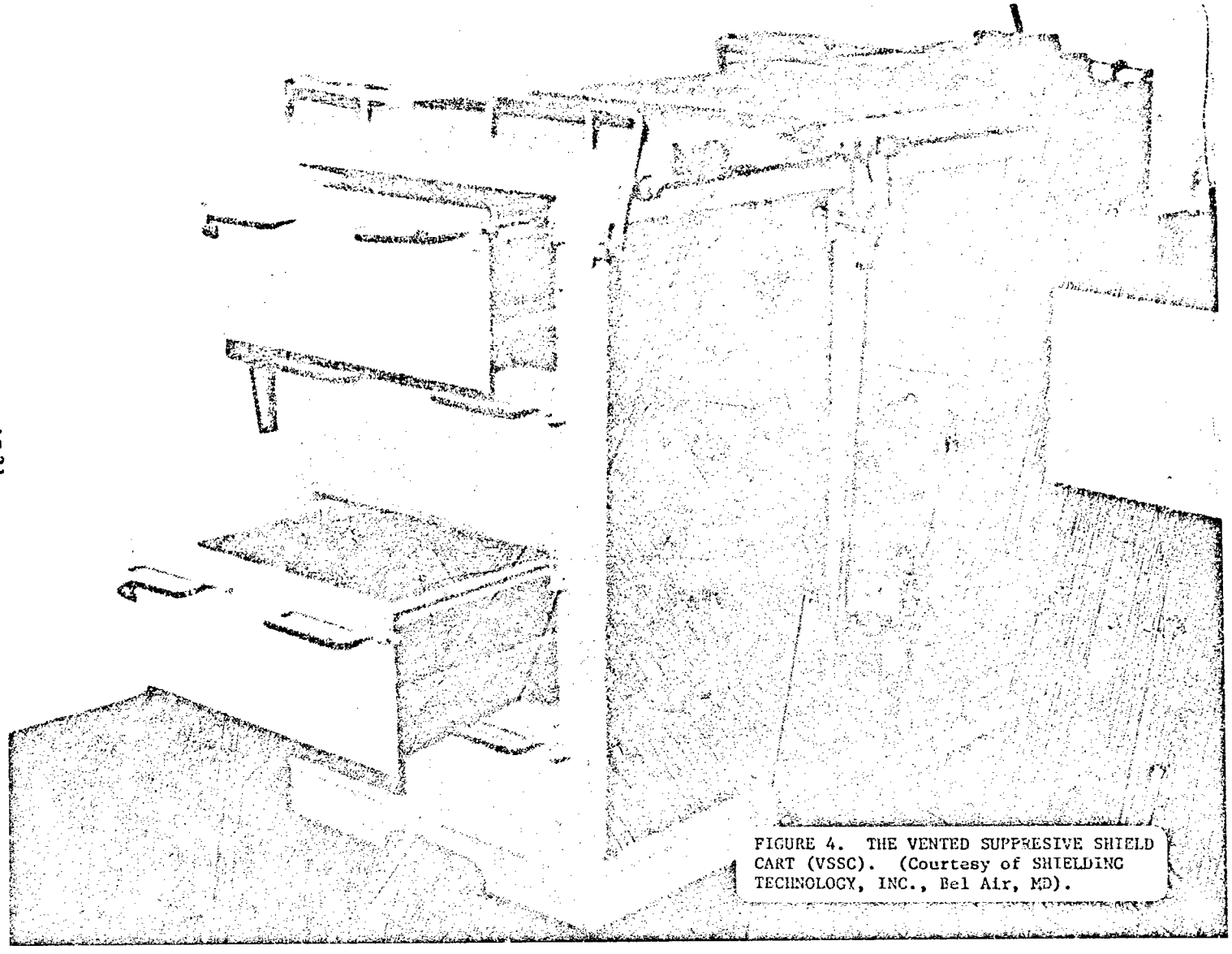

FIGURE 4. THE VENTED SUPPRESIVE SHIELD CART (VSSC). (Courtesy of SHIELDING TECHNOLOGY, INC., Bel Air, MD).

VSSC allows control of a blast by venting the explosion gas pressure and limiting the thermal hazard by cooling. This concept is depicted in Figure 3.

The VSSC appears to have the potential for being easily modified and adaptable to a variety of specific explosive handling operations. This adaptability is evidenced in the development of both a labyrinth wall and a mobile storage cart for transportation of materials.

DESCRIPTION: The mobile VSS Cart is shown in figure 4. The cart was specifically designed for moving 'in-process' ignitors to various work stations on an operating line in a production facility. In this mode, the cart is effective as both a transporter and line service box with four drawers on each side.

The VSSC, if used as a transporter and line service box, eliminates the exposure in the manually handling of an explosive material while transfering from a transporter to the line service box.

TEST: The testing of the VSSC resulted in the unit being certified to contain, and justify for use, approximately 4 lb. of Boron-Potassium Nitrate (BKNO3) or 4 lb. of Magnesium-Teflon-Viton (MTV).

In tests with 5 lbs. BKNO3, an initial short brilliant flash flame was observed to extend less than three feet to either side and four feet above the VSSC, which was followed by a white smoke cloud which quickly dissipated. In tests with 5 lbs. of MTV, the

flame was followed by thick black smoke which accompanied the burning for approximately five seconds before dissipating. No flame was observed at the operators station in front of the drawers for either test.

MANUAL EXPLOSIVES TRANSPORT VEHICLES (METV)

DEVELOPMENT: The METV and its conjoining storage barricade were developed at the Iowa AAP, Middletown, IA, and fabricated onsite by Mason & Hanger - Silas Mason Co., Inc. Although the storage barrricade is part of the safety system and used in conjunction with the METV, the emphasis and consideration of this paper is primarily on just the METV and its potential applications. The METV was designed to totally contain a blast.

DESCRIPTION: The METV, shown in Figure 5, is a 24 inch diameter spherical shaped all welded construction of one quarter inch thick, 310 low carbon stainless steel. The eight inch diameter gated opening is fitted with an interior 'horseshoe' hinge with a tang on the exterior for opening/closing and for loading/unloading. The eight inch opening is flanged for the purpose of connecting and locking the METV to the storage barricade. The sphere is mounted at the proper height on a tubular frame which is on four wheels. Inside the sphere, a bracket is provided to hold a tray and cups, which are all made up of conductive plastic. The METV was fabricated locally in the welding shop.

TEST: The testing of the METV resulted in the unit being

FIGURE 5-A. THE MANUAL EXPLOSIVES TRANSPORT VEHICLE (METV). Courtesy of MASON & HANGER - SILAS MASON CO., INC.

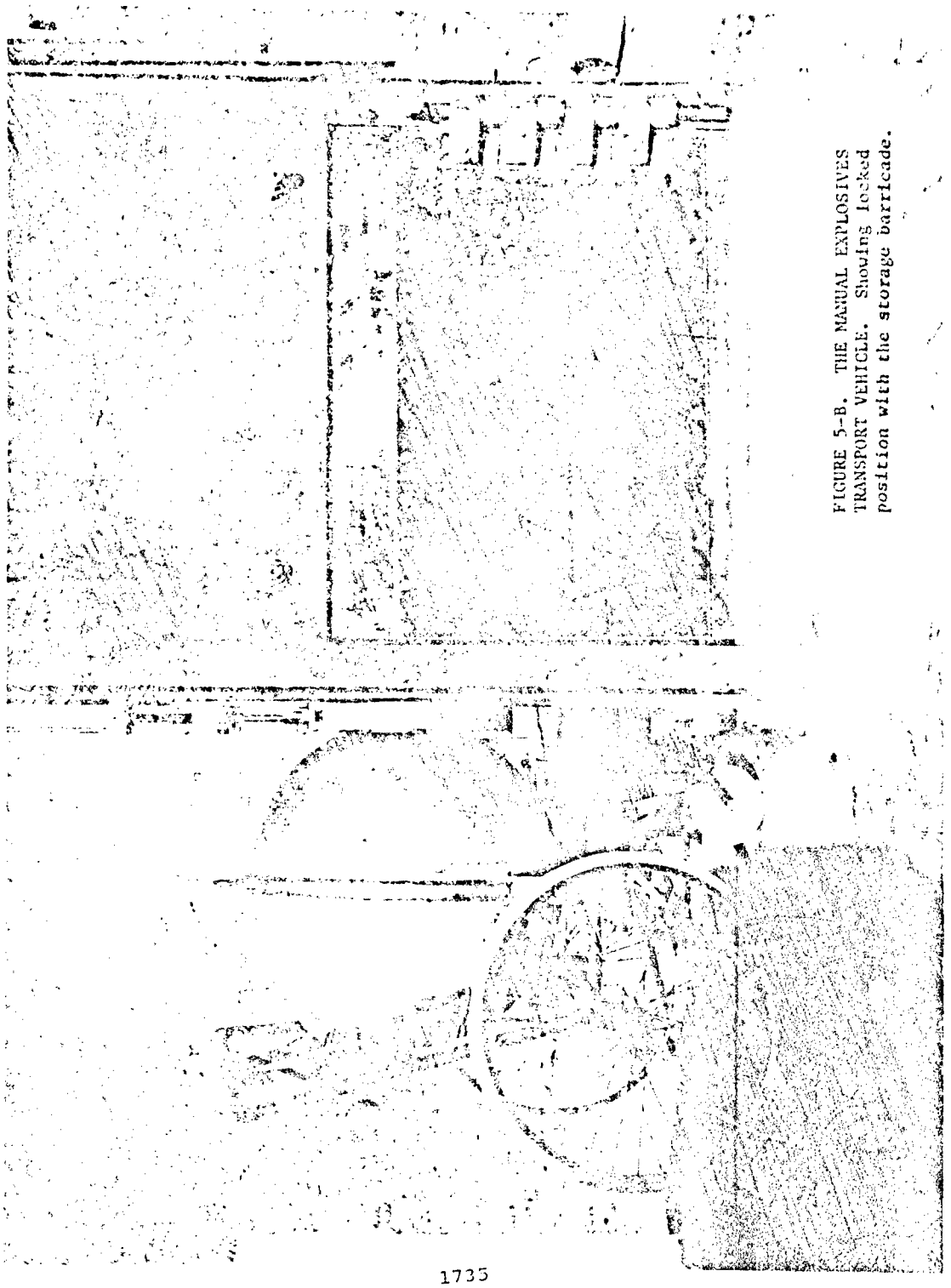

FIGURE 5-B. THE MANUAL EXPLOSIVES TRANSPORT VEHICLE. Showing locked position with the storage barricade.

certified to contain 20 ounces of NOL-130 primer mix. In one test, it took approximately 18 minutes for the pressure in the sphere to leak off, and in another test, a reading of 146 Db on the 'A' scale was noted and was recorded by the noise meter which was located at a distance of ten feet from the sphere test area.

The testing of the METV was in conjunction with tests on the storage barricade. The storage barricade was constructed of one-half inch steel plate, approximately 43 inches long, 31 inches wide, and eight feet tall with a five foot cap of three-eighths inch steel plate, making the total height of the barricade thirteen feet. The barricade is equipped with two large thirty inch by thirty-seven inch access doors. and is equipped with the connecting and locking device for hook-up with the METV. The storage barricade was certified to 20 ounces of NOL-130 primer mix. The storage barricade was fabricated locally in the welding shop.

SUMMARY AND CONCLUSION

Operational shields, regardless of design, should be prescribed rather than generally assigned to specific explosives handling operations. All shields should be tested and conform to MIL-STD-398 (Shields, Operational For Ammunition Operations, Criteria For Design of and Tests For Acceptance) requirements. Tests should be considered for operational shields which may qualify them for use with various materials, such as, explosives,

pyrotechnics, and propellants. The tests, in order to conform with, MIL-STD-398, should:

A. Prevent exposure to operating personnel of peak positive incident pressures above 2.3 psi or peak positive normal reflected pressure above 5.0 psi, with impulse noise levels that are reduced to 140 decibels or below.

B. Contain all fragmentation or direct the fragmentation away from areas, prevent secondary fragmentation, and prevent the movement, overturning, or structural deflection where personnel could be injured.

C. Limit exposure of personnel to a critical heat flux value based on the total time of exposure with operating personnel by locating a sufficient distance from the shield to assure their protection.

The operational shields considered in this paper were selected for their flexibility in use within the explosives industry. Each of the operational shields discussed could be modified or used 'as-is' for any number of explosives handling applications. The technology presently exists which can improve handling of explosives within the time-frame between 'storage' and 'in-process' status. Single handling units can act as both a transporter and as an on-line storage and provide specific levels of containment which agree with the explosives safety 'Cardinal Rule'.

FIGURE 6.

SYNOPSIS OF OPERATIONAL SHIELD COMPARISONS

	LINE SERVICE BOXES (LSB)	VENTILATED SUPPRESSIVE SHIELDING CART (VSSC)	MANUAL EXPLOSIVES TRANSPORT VEHICLE (METV)
CERTIFICATION -	Certified to: 8 grams PBXN-5	Certified to: 4 lb. BKNO3 or MTV	Certified to: 20 ounces MOL-130 primer mix
FABRICATION AND COSTS -	Local Fabrication- Low cost	Local Fabrication- Moderate cost	Local Fabrication- Moderate cost
HANDLING METHOD AND PROCEDURES -	Stationary- but could be made manually mobile	Manually mobile	Manually mobile
FRAGMENT RETENTION -	Total fragments contained	Total fragments contained	Total fragments contained
BLAST OVERPRESSURE SUPPRESSION -	Partially directed	Partially reduced	Partially reduced or eliminated
IMPULSE NOISE LEVEL REDUCTION -	Partially reduced- directed	Partially reduced	Partial to almost total reduction
HEAT FLUX SUPPRESSION -	Partially reduced- directed	Partially reduced- directed	Partial to almost total reduction

ACKNOWLEDGMENTS

The author wishes to sincerely thank the following parties, their organizations and their staff, for their assistance in the development of the paper: Mr. Tom Denison, Safety, Honeywell, Inc., Minneapolis, MN; Mr. Robert Haines, AMCCOM Safety, Iowa AAP, Middletown, IA; Mr. Mel Hudson, Engineer, NAVORD, Indian Head, MD; Dr. D. J. Katsanis, Engineer, Shielding Technology Inc., Bel Air, MD; Mr. R. Schum, Quality Assurance Division Chief, DCASMA-Twin Cities, St. Paul, MN; Mr. Joe Shannon, Safety, Mason & Hanger - Silas Mason Co., Inc., Iowa AAP, Middletown, IA; Mr. Pete Zakrzewski, Safety Engineer, DCASR-St. Louis, St. Louis, MO; and, members of the Field Safety Activity, U. S. ARMY MATERIAL COMMAND, Indiana AAP, Charlestown, IN.

REFERENCES

1. Federoff, Basil, T.; and, Sheffield, Oliver E.; assisted by Kaye, Seymour M; and, Management Science Associates, "Handling Explosives", Encyclopedia of Explosives and Related Items, Volume 7, Picatinny Arsenal, Dover, New Jersey, 1975.

2. Hudson, M.C.; Williams, C.; Katsanis, D.J.; and, Henderson, W.P., "Vented Suppressive Shielding in Pyrotechnic Operations", Minutes of the Twenty-second Explosives Safety Seminar, pp. 515-530, DDESB, 26-28 August 1986.

3. Greenberg, Brigadier General Paul L., "The Impact of Explosives Safety on readiness - The Price of Safety", Minutes of the Twenty-second Explosives Safety Seminar, pp. 799-803, DDESB, 26-28 August 1986

4. AMC-R 385-100, "Safety Manual", United States Army Material Command, Department of the Army, Alexandria, VA, August 1985.

5. DOD MIL-STD-398, Military Standard, "Shields, Operational for Ammunition Operations, Criteria for Design of and Tests for Acceptance", Department of Defense, Washington, D.C., 5 November 1976.

6. DOD 4145.26-M, "Contractors' Safety Manual for Ammunition and Explosives" Department of Defense, Office of the Secretary of Defense, Washington D.C. March 1986.

7. DOD 6055.9-STD, "Ammunition and Explosives Safety Standards", Department of Defense, Office of the Secretary of Defense, Washington, D.C., July 1984.

8. NFPA 495-1982, "Code for the Manufacture, Transportation, Storage and Use of Explosive Materials", National Fire Protection Association, Batterymarch Park, Quincy, MA, 1982.

9. TM 9-1300-214, "Military Explosives", Headquarters, Department of the Army, Washington, D.C., 20 September 1984.

EXPLOSIVES SAFETY IN THE TACTICAL ENVIRONMENT
PROBLEMS OF AMMUNITION STORAGE IN V CORPS

by
John S. Crossetto

Ammunition, like any other perishable commodity, has a life cycle. It is produced, inspected, packaged, transported, stored and, finally, either used or destroyed. During this progression the most static mode, storage, is commonly viewed as the safest and explosives safety regulations are developed reflecting static forms of protection. To avoid accidental functioning of the material or, failing that, loss of life or propagation, ammunition is protected from fire and lightning and is separated from objects requiring protection. Unfortunately, these regulations and assumptions do not fully account for the dynamics of storage in the tactical environment where the placement, configuration and handling of ammunition is based chiefly on the criterion of combat readiness.

The concept of readiness in this environment involves, among other considerations, the modelling of basic load ammunition to facilitate upload, detailed traffic plans for the rapid movement of ammunition off storage points, procedures of re-supply, serviceability of stocks, and explosives safety in the storage, handling, transportation and use of ammunition. Basic load ammunition, ammunition which the unit initially carries into battle, must be stored on or near the combat unit garrison and must be configured for quick upload and response. Certain sustainment stocks, based on war plans, must be available at forward storage locations and other Pre Positioned War Reserve (PPWR) must be stored farther to the rear. Moreover, basic load ammunition must be under the control of the combat units and these units must constantly exercise their readiness plans, including the upload of live ammunition onto tactical vehicles.

V Corps stores in excess of 103,400 short tons of ammunition in a variety of storage sites and locations from the French to the East German borders. Among these four dozen storage sites are four Prestock Points (PSP) storing both PPWR and modelled basic load, six Forward Storage Sites (FSTS) storing sustainment and barrier ammunition, eleven Basic Load Storage Areas (BLSA) storing both modelled and bulk basic load, four Quick Reaction Sites (QRS) designed specifically for the quick upload of modelled basic load ammunition, an Ammunition Supply Point (ASP), three Border Observation Posts, and eighteen uploaded armor parks (some located in or near densely populated installations and villages.)

Explosives safety management in this widely diverse and volatile atmosphere is highly centralized at V Corps Headquarters. The Safety Office, reporting directly to the Chief of Staff, licenses each storage location, reviews each license annually for compliance and encroachment, evaluates explosives safety waiver requests, serves on accident investigation boards for all Class A explosive accidents, submits construction site plans for DDESB approval, teaches basic explosives safety to over 50 safety officers and NCOs each month, and either develops or disseminates explosives safety policy for V Corps. The highest priority is given to coordination and cooperation between the V Corps Safety Office and the Quality Assurance Specialist (Ammunition Surveillance) (QASAS) organization to ensure that the using and storing units receive consistent and non-contradictory explosives safety guidance.

In addition to the explosives safety roles played by the V Corps Safety Office and the V Corps QASAS a significant, if subordinate, role is played by each of the ten Military Community (MILCOM) safety offices, by the three Division/Regimental safety offices, the 3D Support Command Safety Office, and by the ammunition personnel of the using and storing units. The MILCOM safety offices ensure that the storage sites and facilities are properly serviced by community engineers and coordinate with MILCOM Master Planners to prevent construction plans which may encroach on the sites. The Division/Regimental safety offices provide first-line explosives safety assistance to the tactical units both in their storage locations and in the field. The 3D Support Command Safety Office is the official custodian of Restricted Area Decrees (RAD) and provides first-line coordination with local German explosives authorities. Finally, it is the ammunition personnel from the using and storing units who must ensure the safe handling, storage, transportation and use of ammunition on a daily basis.

This explosives safety management system, for all its diversity, works. However, the problems which face explosives safety management in the tactical environment are not necessarily ones that can be solved in that environment. They are often the unexpected consequences of policy generated by DOD or DA headquarters, the research and developement community or quality control. In fact, if problems are unknowingly generated and left unsolved anywhere in the ammunition logistics or explosives safety community, these problems will eventually reach the tactical environment in magnified form. While clairvoyance can never be inserted into the logistician's job description, an awareness of tactical problems in the early stages of planning or regulation writing would lessen the impact of these unexpected consequences in the field.

The examples selected for discussion are intended to illustrate the nature and scope of the problem by focusing on the necessity for clear, concise, comprehensive regulations, the need for inspecting agencies to be thoroughly familiar with the regulations, the dramatic and immediate impact of new ammunition and equipment fielding, and the importance of a continuing reassessment of ammunition already in the field. Lack of clear regulations, readily available, is simply an invitation to non-compliance; confusion on the part of Army inspection teams (often disguising a relentless hunt for deficiencies as technical assistance) damages the bedrock of credibility on which compliance and cooperation rests; new equipment problems effect readiness as well as explosives safety; and the failure to continually reassess problem-ridden ammunition costs lives.

A clear, concise, comprehensive Army regulation is the most obvious requirement for the smooth operation of an explosives safety management system which contains trained explosives safety and surveillance professionals, professional soldiers with no formal training in explosives safety, and both German and American personnel. At present TM9-1300-206 comes closest to meeting this requirement but lies too far down the regulatory chain. DOD 6055.9-STD, reprinted as AR 385-64, passes none of these vital tests, contains virtually no field guidance, and often possesses a wide divergence between what is stated and what is actually meant. The requirement to protect construction workers at static storage areas with Intraline Separation Distance and the requirement to submit site plans for storage areas undergoing a reduction in explosive hazard are two recent examples of this divergence.

While the problem of a comprehensive Army regulation is being addressed by the newly created Technical Center for Explosives Safety, it is essential that any new regulation address the tactical environment. Unrealistic requirements, or requirements suited only for static CONUS storage, could fail the common sense test in the tactical environment. The Technical Center must rethink old assumptions, specifically address the tactical environment and provide the widest possible latitude for risk assessment at the MACOM level. The new regulation must not be a mere compilation of old policies.

It is essential, for example, that required distances in the new regulation be given in meters as well as feet, that weights be given in kilograms as well as pounds, and formulae presented in terms which are workable in Net Explosive Quantity (NEQ) as well as Net Explosive Weight (NEW). If 'buttoned up' uploaded tanks are required to have 20 meters separation from an inhabited building, some acknowledgement must be given to unit maintenance and serviceability inspections which require the rounds to be on the ground for short periods. If rounds are never allowed on the ground, the usefullness of the uploaded tank park evaporates. If local risk assessment is to determine the acceptable exposure risk, then the guidelines for that risk assessment should be clearly stated.

This same problem exists for the live ammunition upload exercise, the most common go-to-war exercise in the tactical environment. Training requires the simultaneous upload of ammunition from adjacent storage magazines to test load plans, loading times and trafficability in an authentic go-to-war context. This exercise is simply too essential to readiness to be curtailed yet no mention is made of the exercise in existing regulations. The present undercurrent of opinion in the explosives safety community is that some rules were made to be waived and that the tactical environment should operate on a soft cushion of waivers. V Corps Safety considers this growing sentiment to be the antithesis of explosives safety and will continue to fill the policy vacuum created by current regulations. V Corps is waiver free and intends to stay that way. We have yet to witness an explosives operation made more safe by a piece of paper which transfers responsibility for the risk from the explosives safety community to the waiving authority.

In USAREUR the regulation dilemma will remain complex. The German regulation, ZDv 34 series, particularly ZDv 34/230, is a model of clarity and precision but is not normally binding on US Forces and is not widely available in English translation. USAREUR Regulation 385-11 is woefully outdated and now used solely for licensing policy. The NATO document, AC/258-D/258, is binding on US Forces for exposed sites outside US controlled property and must be used in conjunction with the DOD standard/Army regulation for quantity-distance calculations.

While the regulation maze is an ongoing problem for personnel in USAREUR, it is a source of intense confusion for inspection teams from CONUS. Teams are often unfamiliar with NATO regulations, German legal restraints and the Restricted Area Decrees (RAD) governing storage on most V Corps sites. These RAD zones restrict land usage surrounding storage sites and serve much the same function as a perimeter fence at a CONUS installation. For example, RAD IV, the equivalent of our Inhabited Building Distance, might reflect the actual distance to an inhabited structure or merely the distance within which inhabited structures may not be built. Unfamiliarity with this system obviously affects the quality of inspection team observations and

recommendations. With the exception of hazard class 1.2 ammunition with a high assigned fragment distance, the NATO quantity-distance regulations tend to be significantly more restrictive than our own. What is absolutely certain is that the host nation will never restrict building (the legal consequence of a ESD zone) to provide protection from a hazard it does not accept. Once ammunition arrives in country, off-post protection will continue to be provided to German/NATO standards, not our own.

Another pressing problem in the rapidly changing tactical environment is the impact of new ammunition and equipment on explosives safety. The new family of 120mm sabot tank ammunition with the combustible cartridge case, for example, brought a reduction in hazard classification from 1.2 to 1.3 over the old 105mm round. However, when the new round was packed in the PA-118 lightweight metal container and fielded in USAREUR the old fragment hazard had been engineered back in and the hazard class returned to 1.2. While the elevation of hazard class may not have had a serious impact on static CONUS storage, it had a significant impact on the soldier in the field exposed to the hazard and on the ability of V Corps to store the ammunition closer to the tanks including, in some instances, in uploaded tank parks. (The storing of rounds close to tanks is a critical tactical consideration impacting on the decision to keep tanks uploaded in the first place.) The fielding of the Field Artillery Ammunition Support Vehicle (FAASV), requiring the removal of the grommet from the 155mm round prior to placing the round in the vehicle is a second example. The exposure of the rotating band and obturator during one-time use may not cause significant serviceability and safety problems, however damage to the vital components of the round during frequent uploading in the tactical environment does.

Failure to continually reassess problem-ridden ammunition became critical to V Corps in the summer of 1987 following the in-bore detonation of an M329A2 4.2 inch mortar round at Grafenwohr Training Area which killed one soldier and seriously injured several others. During the investigation of the accident it became clear to V Corps Safety that the round had been haunted by serious sticking problems since its inception and had long since failed to meet the Army requirements for an accurate, long-range, rapid-fire round. The round stuck so frequently in some cannons that realistic training was simply not possible. Moreover, the frequency of emergency procedures for firing and freeing stuck rounds invited non-compliance with safety evacuation requirements.

Although much of the investigation centered on the elusive cause of the detonation, still unknown, Safety focused its attention on the combat usefullness of a mortar round which required frequent re-indexing to seat the round, frequent kicking of the cannon to fire the round, elaborate swabbing techniques and even more elaborate techniques for freeing stuck rounds which could not be 'kicked' down range. A V Corps survey of its mortar platoons indicated that many mortarmen had long ago lost confidence in the M329A2 and that the sticking problems experienced by the mortar platoon on the day of the accident had become commonplace. Even in the unlikely event that the pressures of training were solely responsible for the stickers, the pressures of combat could surely be assumed to be greater. Timely reassessment of that problem-ridden round should have prevented that platoon from training with that round, even from the ground mount.

The tactical environment is not an aberation in the explosives safety community but rather the ultimate-use environment for which ammunition and weaponry is designed. Moreover, it is recognized throughout the tactical community that problems will continue to elude detection and correction prior to fielding and implementation and that the ultimate-use environment is also, inevitably, the ultimate-testing environment. It is, however, reasonable to conclude that an early and persistent awareness of the demands and requirements of the tactical situation would hasten the discovery of explosives safety problems and facilitate their resolution.

SCALE MODEL TUNNEL MAGAZINE TESTS
for
SAFE PRESSURE DISTANCE

by

James E. Tancreto

Naval Civil Engineering Laboratory
Port Hueneme, California

for

23rd
Department of Defense
Explosives Safety Board
Seminar

Atlanta, Georgia
August 1988

SCALE MODEL TUNNEL MAGAZINE TESTS FOR SAFE PRESSURE DISTANCE

James E. Tancreto
Research Structural Engineer
Naval Civil Engineering Laboratory
Port Hueneme, CA

1.0 INTRODUCTION

Tunnel magazine tests (such as those reported in References 1 and 2) and resulting empirical relationships for the external pressure environment from internal explosions show that the safety criteria in NAVSEA OP 5 (Reference 3) is very conservative for many tunnel magazines. These studies are now being considered by the Department of Defense Explosives Safety Board (DDESB) for revision of the existing criteria. The new criteria will account for the effect of the size (equivalent diameter) of the exit on pressures outside the tunnel. The Navy has many tunnels with multiple baffles in the exit tunnel that effectively reduce the equivalent exit diameter, until the baffles are ejected from the tunnel by the high pressures. The new criteria would not account for the effect of closing down the tunnel exit area with baffles that would fail. Tests with fixed baffles have shown that scaled distances of 30 to 40 $ft/lb^{1/3}$ (vs. the current criteria of 76 $ft/lb^{1/3}$ to the front of the magazine) would be possible. Tests were required to show the effect of "frangible" baffles. The debris hazard from the concrete baffles and headwall was also addressed by the test program, but is not covered in this paper.

2.0 OBJECTIVE

The test program was designed to determine the overpressure and debris hazard from an explosion in a tunnel magazine with and without "frangible" baffles in the exit tunnel.

This paper provides the test results for external overpressure vs. distance, direction, equivalent exit diameter, and charge density (explosive weight / tunnel volume, W/V).

3.0 TEST PROGRAM

The important variables were charge weight, the number of baffles, and the scale model size. Table 1 shows the scale model test specimen geometry. Table 2 shows the value of the basic test variables for each test setup. Three tests (1a, 1b, and 1c) were run with no headwall or baffles for comparison with the tunnel tests using baffles. A reusable 12 inch artillery gun barrel was used for multiple 1/15th scale model parameter tests and a 1/6th scale model was constructed for one test.

3.1 Test Site

The tests were conducted by the Terminal Effects Research and Analysis Group (TERA), New Mexico Institute of Mining and Technology, Socorro, New Mexico. Camera coverage was provided by TERA and pressure gage instrumentation and

recording were provided by the Naval Civil Engineering Laboratory (NCEL). The testing was located at the TERA West Valley test site. This site provided a large level surface for locating pressure gages and for debris recovery.

3.2 Test Structure

The scale model test structures used cylindrical tunnel x-sections instead of the normal arch section of Navy tunnels (see Figure 1). This allowed for simpler, less expensive construction with no expected loss in accuracy. The dimensions of the two scale model test structures are shown in Table 1 and in Figure 2 (1/15th scale), Figure 3 (1/6.43 scale), and Figure 4 (baffles and headwall). Table 2 shows the value of the variables in each test.

The scale model unreinforced concrete baffles were not structurally restrained. The headwall was restrained at the bottom by a heavy backup plate to simulate the actual construction (continuous pour, in excavation, to bedrock). The concrete mix design used model aggregate sizes based on a full scale maximum aggregate size of 1 inch. The mix gave a concrete compression strength of about 5000 psi. The headwall included scaled wire reinforcing (scaled diameter, equal strength, equal number) around the door to simulate the actual design. Scaled sheet metal doors were taped to the headwall.

Plywood walls were placed perpendicular to the tunnel (on the 90^{o} line) to provide a reflecting surface similar to the actual overburden. The wall was conservatively designed to be steeper than the normal overburden (producing stronger reflections to the front of the tunnel).

A 12 inch artillery gun barrel (4 inch minimum thick wall) was used in the 1/15th scale tunnel structure (Figure 2). The gun was strong enough to sustain repeated testing with the required 3, 6, and 12 lb. C4 explosive charges. A steel structural collar was welded around the open end and a plug, to prevent pressure leakage, was placed in the back end. No overburden was used, except at the back of the tunnel to help restrain the steel plug. The plug was partially driven into the sand fill by the pressures in each test (allowing insignificant pressure leakage) and then repositioned for the following test. An 80 foot long (40 feet to each side) by 12 foot high (see Figure 3) plywood reflecting wall was used to simulate tunnel overburden.

A 1 inch thick 28 inch diameter steel pipe was used to form the 1/6.43 (to be called 1/6th) scale model tunnel structure. Unreinforced concrete was used for the floor slab and between the pipe and a square form of heavy steel plate walls (2 inch thick x 34 inch high) and roof (6 inch thick x 5 feet wide). The steel forms were 3 inches (minimum) from the steel pipe (at the sidewall half-height and at the roof mid-width). The back of the tunnel was formed in a cut section of the natural rear ground slope. A minimum of 20 feet of uncompacted fill was used over and around the concrete and steel to obtain adequate containment of the loads. NAVFAC OP 5 regulations require an overburden depth of $3.5W^{1/3}$ (about 16 feet scale model) for no disruption of the surface soil and $0.5W^{1/3}$ (2-1/4 feet) for the structure to act as a tunnel for external pressure considerations. A 120 foot long (60 feet to each side) by 20 feet high (see Figure 4) plywood wall was used to simulate the reflecting properties of the face of the tunnel overburden.

3.3 Explosives

Composition C4 explosive was used in the 1/15th scale model tests and TNT was used in the 1/6th scale test. The center of gravity of the cylindrical explosives was in the center of the tunnel x-section and 1/4th the tunnel length from the rear of the tunnel. This had been determined to be a conservative location (pressures outside a tunnel are somewhat higher for charges located closer to the rear wall) for the amount and typical storage location of the explosive being simulated. Charges were detonated with NONEL cord and detonators. Multiple charges were detonated simultaneously.

The composition C4 was constructed in 3 lb. cylinders, 2.5 inches in diameter by 15 inches long. An external cylindrical wrap of lightweight welded wire mesh was used to maintain the shape. A wire cradle supported the charge at the proper height. The charge density of the setup (Charge weight, W, divided by tunnel volume, V) was varied by using three charge weights: three, six and 12 lb. An 8 inch spacing was maintained between ends of the explosive cylinders, when multiple 3 lb. charges were needed.

The 1/6th scale model explosive charge consisted of two aluminum clad (0.06 in thick) 40 lb. TNT cylinders. The 6 inch diameter by 32 inch long cylinders were separated by 32 inches. The thin casing was used in casting the charge and would have little effect (especially in the 1.2 psi range) on the pressures outside the tunnel. The charge was supported on a wood 2"x4" cradle.

3.4 Instrumentation

Pressure gages were used (except in tests 7a, 7b, and 7c) to obtain pressure - distance data in prescribed directions. High speed motion picture cameras were used to obtain debris launch velocity and angle data in all tests but 1a, 1b, and 1c (which had no headwall, baffles, or debris). Debris was recovered, except in tests 1a, 1b, and 1c, for analysis of the debris distribution and size characteristics. A witness panel was used in tests 7a, 7b and 7c to obtain additional data on the debris launch angle and debris density. Real time video camera coverage of the event and still photographs of the test setup before and after testing were also obtained. Only the overpressure data is discussed in this report. Debris data from the high speed cameras, and debris recovery will be given in other reports.

Pressure gages were located inside the tunnel exit, in the walls opposite each baffle location, and at selected lines and ranges on the level ground surface outside the tunnels. Gage mount locations are shown in Figures 5 and 6 for the two scale model setups. Locations were chosen to obtain a complete Pressure vs. Scaled Range relationship to the front (0° line) of the tunnels and to capture the relationship near 1.2 psi on the other lines (15°, 30°, 90°, and 180°). All gages were oriented for incident (side-on) pressures. Only piezoelectric gages were used for pressures over 80 psi. Piezoelectric and piezoresistive gages were used at other locations.

4.0 PRESSURE-DISTANCE DATA

Analog data, recorded on magnetic tape by NCEL, was digitized by TERA and plotted. The digitized data results included peak pressure and impulse. Only the peak pressure data is included in this report.

Tunnel external pressure data is a function of R/D (range divided by effective tunnel diameter. The peak pressure and scaled distance (R/D) data are given in Tables 3 through 7. Normally the non-dimensional ratio P/P_x (incident pressure at range R divided by the incident pressure at the tunnel exit) is plotted vs. R/D. However, since it was difficult to establish the exit pressure and because it was not necessary for the development of safe pressure-distance criteria, the peak incident overpresure, P, (not P/P_x) is plotted versus R/D. Theoretically, P/P_x is a function of R/D and one line could be used to show the relationship given by the three lines in Figures 7 and 8. However, since P_x is directly related to W/V, the criteria will be developed as a function of W/V (which we know much more accurately than P_x), and R/D (see Section 5.1).

Configuration 0 (basic tunnel with no baffles or headwall), 1/15th scale model test results on the 0° line are shown in Figure 7.

Configuration 2 (headwall and both baffles) and Configuration 1 (headwall and baffle 1 - Test 2 only), 0° line data are plotted in Figures 8 (1/15th scale) and 9 (1/6th scale). The 12 lb. Configurations 1 and 2 (Tests 2 and 4) results were combined when it was determined that the smaller baffle 2 (28% area reduction) had little or no effect on external pressure when used with baffle 1 (52% area reduction) and the headwall (54% area reduction). Figure 10 shows the 1/6th scale model results for pressures on different lines (15°, 30°, 90°, and 180°).

5.0 DATA ANALYSIS

5.1 Scaled Relationships

The pressure, P, outside a tunnel at range R, has been shown (see References 1 and 2) to be related to the pressure at the tunnel exit, P_x, and the equivalent diameter (diameter of a circle with the same area as the tunnel exit) by the power curve given in Equation 1 (note that the lower case characters in the following equations are constants that must be determined by the test data):

$$P/P_x = a(R/D)^b \qquad (1)$$

The exit pressure in this relationship is directly related to the chamber pressure, P_c as shown in Equation 2:

$$P_x = c(P_c)^d \qquad (2)$$

The chamber pressure is a function of charge density and is normally written as given in equation 3 (see Reference 4):

$$P_c = e(W/V)^f \qquad (3)$$

Combining Equations 2 and 3 gives:

$$P_x = g(W/V)^h \quad (4)$$

Since the test program was designed to obtain P at R for various W/V ratios, and since W/V was known and P_x is very difficult to measure, the criteria was developed in terms of W/V instead of P_x. The relationship, in terms of W, V, R, and D (from Equations 1 and 4) is:

$$P = ag(W/V)^h(R/D)^b \quad (5)$$

The pressure criteria for safe distance is fixed at 1.2 psi, therefore the design criteria for safe distance and allowable storage capacity can be related by:

$$(R/D)^b = j(W/V)^{-h} \quad \text{(where } j = \text{constant} = P/ag\text{)} \quad (6)$$

Equation 6 can be written to isolate the key parameter. For instance, the allowable storage capacity of a tunnel (with volume V and equivalent diameter D) and safe inhabited building distance R (1.2 psi range) is:

$$W = kV(R/D)^m \quad (7)$$

where k and m are constants to be determined from the test data.

5.2 TNT Equivalency

Composition C4 was used in the 1/15th scale tests, while TNT was used in the 1/6th scale test. Different explosives or equal weight develop different gas pressures and exit pressures. Quantity-distance relationships in NAVSEA OP 5 (Reference 3) are based on TNT. Therefore, the charge densities (W/V) of the C4 tests were corrected for the TNT weight equivalency of C4. NSWC used the computer program INBLAST (Reference 5) to calculate chamber pressure vs. W/V (for: $0.2 < W/V < 1.2$) for C4 and TNT. The results gave a constant TNT equivalency for C4 of 1.28 (TNT equivalent weight = 1.28 x C4 weight, for equal pressure) for the range of W/V in the tests.

6.0 RESULTS

The 0^o line (in line and directly to the front of the tunnel) normally records the highest pressure at any range. Following normal practice, the safe distance to the front of the tunnel, R_0, was established and the safe distances in other directions were determined as a ratio of R_0 (as a function of the angle). Results were determined for two exit configurations: with and without baffles (Configurations 2 and 0).

6.1 Pressure vs. R/D - 0 Degree Line

The peak pressure data shown in Tables 3 through 7 was used to determine the least squares best fit relationship to the power curve:

$$P = a(R/D)^b \quad (8)$$

for each W/V ratio (i.e. the 1/15th scale 3, 6, and 12 lb. tests and the 1/6th scale 96 lb. test). Figures 11 and 12 show typical (1/15th scale, 6 lb. test, W/V = 0.611) plotted data and the associated straight line best fit curves for: (a) all the data (Figure 11), and (b) the data around 1.2 psi (Figure 12). Although a good fit is obtained using all the data, a better fit can be obtained if only the data in the pressure range of interest is used. Therefore, data around 1.2 psi ($10 < P < 0.35$ psi, in the 1/15th scale tests; and $3.5 < P < 0.6$, in the 1/6 scale test) were used to determine the best fit R/D value at 1.2 psi (for each W/V value). The results are shown in Table 8.

6.2 Safe Inhabited Building Distance - R/D vs. W/V.

0 Degree Line. The results of the best fit statistical study for the R/D at which 1.2 psi occurs for each W/V are shown in Table 8 and plotted in Figure 13. The best fit power curve for safe distance from a tunnel without baffles (from Test 1a, 1b, and 1c data) is:

$$R/D = 114(W/V)^{0.31} \qquad \text{No Baffles}, \quad 0.3 < W(TNT)/V < 1.22$$

The best fit relationship for tunnels with baffles (from Test 2, 4, 5a, 5b, 6a, 6b, and 8 data) is:

$$R/D = 97(W/V)^{0.58} \qquad \text{With Baffles (see Section 6.3)}, \quad 0.3 < W(TNT)/V < 1.22$$

The plot in Figure 13 shows the effectiveness of the "frangible" baffles in reducing safe distance. The effect of the baffles decreases as charge density is increased (see the R/D ratios in the last column of Table 8). For example, at a W/V of 0.305 the baffles reduce the safe distance to 63% of the safe distance without baffles, but at a W/V of 1.22 the safe distance is 92% of the safe distance without baffles.

Directional Factors.

Best fit relationships were calculated for P vs. R/D (using all data points) in each direction (see the example best fit curve in Figure 11). The 1.2 psi R/D was calculated and compared with the best fit value on the 0^o line. Average ratios for R_a/R_0 (range on line 'a' divided by range on the 0^o line = C_a) were obtained for each line (15^o, 30^o, 90^o and 180^o). The safe range in any direction is obtained by multiplying R_0 by the appropriate angle direction factor, C_a. In general, the safe range at an angle, 'a', from the 0^o line is:

$$R_a = C_a R_0 \qquad (9)$$

Table 9 summarizes the data and directional factors for the tests without baffles. Table 10 summarizes the direction factors for the tests with baffles. Results are plotted and compared with Norwegian criteria in Figure 14.

The directional factors are higher in tests with baffles than in the tests without baffles and all tests produced higher directional factors than would be predicted by the Norwegian criteria. In addition the directional factors

in tests with baffles show a dependency on W/V. As W/V decreases the directional factors increase. This can probably be explained by the effect of the vertical plywood reflecting wall which is closer to the 1.2 psi pressure range for the smaller W/V ratios. Since the wall was very conservative when compared with normal tunnel magazine geometry, it is justifiable to smooth out the baffle test results by averaging the data over all tests. The 1/6th scale model test was expected to give the best directional results and is the only test used for the 180 degree line. The 180 degree line in the 1/15th scale test was not level nor did it model the terrain (see Figure 2).

Recommended design directional factors for the test tunnel geometries with baffles are shown in Figure 14.

6.3 Tunnel Geometry Limitations

Typical tunnels were used to design the test models. Some tunnels will not be within the limits of the tested variables and the results will not apply to them. The allowable explosive storage weight and safe distance are related to equivalent exit diameter, D, and total tunnel volume, V, in Equations 1 to 3 and Table 4. Therefore, variations in D and V are possible. However, other geometric parameters must meet the following requirements (within 10%):

(a) Two baffles, each with a minimum thickness of 4 ft.
(b) One baffle with minimum area = 0.5 x tunnel exit area.
(c) Other baffle with minimum area = 0.25 x tunnel exit area.
(d) Headwall with minimum thickness of 3.5 ft.
(e) Headwall door opening no greater than 96 sf.

7.0 CONCLUSIONS

Best fit peak pressure vs. scaled distance (R/D) relationships for $0.3 < W/V < 1.22$ have been developed for use in determining the safe inhabited building distance (for peak pressure) from specific Navy tunnels with or without baffles. Tunnels without baffles were shown to have a safe inhabited building distance (range for 1.2 psi) of about 65% of the current safe distance required by Reference 3 ($K = 76 ft/lb^{1/3}$). With baffles the safe distance is between 40 and 60% (depending on W/V) of the existing required safe distance. The new relationships are not directly related to the existing requirements because they are based on a power curve with R/D vs. W/V (Equation 6), whereas the existing criteria are based on free air relationships with $P = c(R/W^{1/3})^{a}$.

Use of the data in this report to determine the safe inhabited building distance from tunnels with or without baffles must be approved by the DDESB on a case by case basis. Best fit results have been shown. Until additional data is obtained, 90% confidence values (about 10% increase in safe distance) may be required.

REFERENCES

1. Norwegian Defence Construction Service. Technical Paper: Underground Ammunition Storage Magazines, Blast Effects from Accidental Explosions, by Einar S. Helseth and Arnfinn Jensen. Presented at the 22nd DDESB Seminar. Anaheim, CA. Aug. 1986.

2. Royal Swedish Fortifications Administration. Technical Paper: KLOTZ-Club Tests in Sweden, by Bengt E. Vretblad. Presented at the 22nd DDESB Seminar. Anaheim, CA. Aug. 1986.

3. Naval Sea Systems Command. Technical Manual NAVSEA OP 5, Volume 1: Ammunition and Explosives Ashore. Fourth Revision, Change 12, 15 Oct. 1984.

4. U.S. Army Armament Research, Development and Engineering Center. Special Publication ARLCD-SP-84001: Structures to Resist the Effects of Accidental Explosions. Volume III. Blast, Fragment, and Shock Loads. Dover N.J., Dec. 1988.

5. Naval Ordnance Laboratory. Technical Report: NOLTR 72-231 Internal Blast Damage Mechanisms Computer Program, by James F. Proctor, White Oak, MD August 1972.

Table 1. Tunnel Magazine Test Geometry

PARAMETER	UNITS	SCALE		
		Full	1/6.43	1/15
TUNNEL:				
DIAMETER, D (a)	FT	15	2.33	1
AREA	SF	177	4.28	0.785
LENGTH	FT	240	37.33	16
VOLUME	CF	42410	159.6	12.57
HEADWALL:				
THICKNESS	IN	43.0	6.7	2.9
OPEN AREA RATIO		0.46	0.46	0.46
DIAMETER, Dh (a)	FT	10.2	1.58	0.68
Dh/D		0.68	0.68	0.68
BAFFLE 1:				
THICKNESS	IN	48.0	7.5	3.2
SETBACK (b)	FT	14.4	2.25	0.97
OPEN AREA RATIO		0.48	0.48	0.48
DIAMETER, D1 (a)	FT	10.4	1.62	0.69
D1/D		0.69	0.69	0.69
BAFFLE 2:				
THICKNESS	IN	48.0	7.5	3.2
SETBACK (b)	FT	34.9	5.44	2.33
OPEN AREA RATIO		0.72	0.72	0.72
DIAMETER, D2 (a)	FT	12.7	1.98	0.85
D2/D		0.85	0.85	0.85

(a) Diameter of an equivalent circular open area.
(b) Distance of baffle from headwall

Table 2. Test Specimen Parameters

TEST	SCALE FACTOR	CONFIG. (a)	EXPLOSIVE TYPE	EXPLOSIVE WEIGHT lb	W/V lb/cf (b) C4	W/V lb/cf (b) TNT
1a	15	0	C4	3	0.239	0.305
1b	15	0	C4	6	0.477	0.611
1c	15	0	C4	12	0.955	1.222
2	15	1	C4	12	0.955	1.222
4	15	2	C4	12	0.955	1.222
5a	15	2	C4	6	0.477	0.611
5b	15	2	C4	6	0.477	0.611
6a	15	2	C4	3	0.239	0.305
6b	15	2	C4	3	0.239	0.305
7a (c)	15	3	C4	6	0.477	0.611
7b (c)	15	4	C4	6	0.477	0.611
7b (c)	15	2	C4	3	0.239	0.305
8	6.43	2	TNT	96	0.470	0.602

(a)

CONFIGURATION	GEOMETRY
0	No Headwall or Baffles
1	Headwall + Baffle 1
2	Headwall + Baffles 1 & 2
3	Baffles 1 & 2
4	Headwall only

(b) Based on TNT Gas Pressure Equivalency for C4 of 1.28 by weight.

(c) Only debris data recovered (not shown in this report).

Table 3. Pressure Data, Tests 1a, 1b, & 1c (a)
W = 3, 6, & 12 lbs C4, Configuration 0

-GAGE LOCATION--		----MEASURED C4 DATA----		
Line	Range	Pressure, P, psi		
deg	(b) ft	W=3#	W=6#	W=12#
0	-1.1	1344	1937	2062
0	-2.5	1454	1845	
0	2	591		1097
0	10	27.0	43.9	103
0	20	11.1	19.0	24.7
0	40	3.39	4.96	6.13
0	60	2.10	2.68	3.82
0	80	0.91	1.59	2.03
0	100	0.75	1.39	1.59
0	120	0.58	0.91	1.15
0	160	0.41	0.59	0.71
0	200	0.33	0.47	0.56
30	40		4.63	
30	60	1.56	2.80	3.25
30	80	1.29	1.83	2.01
30	100	0.74	1.02	1.52
30	120	0.49	0.71	0.89
90	20	4.45	6.53	8.37
90	40	1.67	1.75	3.31
90	60	0.54	1.13	1.91
90	80	0.32	0.81	1.14
90	100	0.27	0.52	0.75
180	30	0.64	0.49	0.50
180	40	0.54	0.4	0.46

(a) Test 1a: 3 lbs
Test 1b: 6 lbs
Test 1c: 12 lbs
Configuration 0: No baffles or headwall

(b) D = 1.00 ft. Therefore R/D = R ft/ft

Table 4. Pressure Data, Tests 6a and 6b
W = 3 lbs C4, Configuration 2

GAGE Line deg	LOCATION Range (a) ft	MEASURED C4 DATA Pressure, P, psi TEST 6a	TEST 6b	Pavg
0	-1.1	4482	4310	4396
0	-2.5	3398	4327	3863
0	10	14.6	13.8	14.2
0	20	4.55	6.69	5.62
0	40		1.60	1.60
0	60	0.80	0.82	0.81
0	80	0.46	0.48	0.47
0	100	0.37	0.41	0.39
0	120	0.31	0.33	0.32
0	160	0.23	0.21	0.22
0	200	0.18	0.20	0.19
30	40	2.42	1.85	2.14
30	60	1.11	0.96	1.03
30	80	0.85	0.72	0.79
30	100	0.53	0.46	0.50
30	120	0.38	0.37	0.37
90	20	3.84	3.72	3.78
90	40	1.19	2.10	1.64
90	60	0.54	0.52	0.53
90	80	0.46	0.59	0.53
90	100	0.33	0.29	0.31
180	30	0.32	0.35	0.34
180	40	0.33	0.25	0.29

(a) D = 1.00 ft. Therefore, R/D = R ft/ft

Table 5. Pressure Data, Tests 5a and 5b
W = 6 lbs C4, Configuration 2

GAGE Line deg	LOCATION Range (a) ft	MEASURED C4 DATA Pressure, P, psi TEST 5a	TEST 5b	Pavg
0	-1.1	4500	4602	4551
0	-2.5	3608	4070	3839
0	10	17.3	16.8	17.0
0	20	8.01	7.33	7.67
0	40	3.23	2.45	2.84
0	50		1.50	1.50
0	80	0.85	0.84	0.85
0	100	0.75	0.67	0.71
0	120	0.54	0.54	0.54
0	160	0.36	0.39	0.38
0	200	0.28	0.31	0.29
30	40	3.22		3.22
30	60		1.52	1.52
30	80	1.16	1.11	1.14
30	100	0.78	0.66	0.72
30	120	0.49	0.50	0.50
90	20	6.57	5.80	6.19
90	40	2.34	2.71	2.52
90	60	0.95	0.78	0.87
90	80	0.63	0.58	0.60
90	100	0.43	0.38	0.40
180	30	0.48	0.48	0.48
180	40	0.46	0.34	0.40

(a) D = 1.00 ft. Therefore, R/D = R ft/ft

Table 6. Pressure Data, Tests 2 and 4 (a)
W = 12 lbs C4, Configurations 1 & 2

GAGE LOCATION		MEASURED C4 DATA		
Line deg	Range (b) ft	Pressure, P, psi TEST 2	TEST 4	Pavg
0	-1.1	5014	6084	0.256
0	10	40.8	31.4	36.1
0	20	16.5	12.7	14.6
0	40	4.58	4.94	4.76
0	60	2.66	3.40	3.03
0	80	1.65	1.61	1.63
0	100	1.34	1.63	1.49
0	120	1.06	1.07	1.06
0	160	0.62	0.68	0.65
0	200	0.51	0.55	0.53
30	40		5.05	5.05
30	60	2.99	2.89	2.94
30	80	1.73	2.11	1.92
30	100	1.25	1.21	1.23
30	120	0.76	0.78	0.77
90	20	10.4	11.8	11.13
90	40	4.43	4.12	4.28
90	60	1.63	1.38	1.51
90	80	1.00	0.92	0.96
90	100	0.77	0.69	0.73
180	30	0.75		0.75
180	40	0.65	0.63	0.64

(a) Test 2 used Configuration 1 (Baffle 1 + Headwall)
Test 4 used Configuration 2 (Baffles 1&2 + Headwall)

(b) D = 1.00 ft. Therefore R/D = R ft/ft

Table 7. Scaled Pressure Data, Test 8
W = 96# TNT, Configuration 2

GAGE LOCATION			TNT DATA
Line deg	Range ft	P/D (a)	P psi
0	-2.56	-1.10	4334
0	-5.76	-2.47	3292
0	30	12.9	13.1
0	50	21.4	6.15
0	70	30.0	3.52
0	100	42.9	2.66
0	130	55.7	2.07
0	170	72.9	1.31
0	220	94.3	0.82
0	280	120.0	0.65
15	130	55.7	1.67
15	170	72.9	1.16
15	220	94.3	0.72
30	130	55.7	1.99
30	170	72.9	1.10
30	220	94.3	0.81
90	70	30.0	2.74
90	100	42.9	1.46
90	130	55.7	1.01
90	170	72.9	0.67
180	30	12.9	1.03
180	50	21.4	0.77
180	70	30.0	0.53
180	100	42.9	0.72

(a) D = 2-1/3 ft.

Table 8. 1.2 psi R/D vs. Charge Density (TNT).

Scale Factor	W lb	W/V(a) lb/cf	R/D (b) NO BAFFLES	R/D (b) WITH BAFFLES	R/D RATIO WITH/NO
15	3	0.305	77.3	48.4	0.63
15	6	0.611	102.7	69.5	0.68
15	12	1.222	118.7	108.8	0.92
6.43	96	0.602		76.7	

(a) W/V for 1/15th scale tests uses the TNT Equivalency (by weight) of C4 based on equal exit pressures (by NSWC program INBLAST). W(TNT) = 1.28W(C4)

(b) R/D at P = 1.2 psi from best fit power curve with P = f(R/D).

Table 9. Pressure Directional Factors
Tunnels without Baffles

TESTS	CHARGE WEIGHT lbs	W/V (a) lbs/cf	LINE (b) deg	R/D (c) ft/ft	DIRECTION FACTOR- EACH W/V (d)	DIRECTION FACTOR- AVG. (e)
1a	3	0.305	0	77.5	1	1
1b	6	0.611	0	103.5	1	
1c	12	1.222	0	117.3	1	
1a	3	0.305	30	74.8	0.97	0.93
1b	6	0.611	30	93.4	0.90	
1c	12	1.222	30	106.7	0.91	
1a	3	0.305	90	42.1	0.54	0.59
1b	6	0.611	90	57.8	0.56	
1c	12	1.222	90	77.1	0.66	

(a) W/V calculated for TNT equivalent explosive weights.
(b) Gage line measured in degrees from 0 degree (front) line.
(c) R/D at 1.2 psi from best fit line to all data from test(s).
(d) Directional Factor (R/D)/(R/D on 0 deg line) for each W/V.
(e) Average directional factor for all W/V on given line.

Table 10. Pressure Directional Factors
Tunnels with Baffles

TESTS	CHARGE WEIGHT lbs	W/V (a) lbs/cf	LINE (b) deg	R/D (c) ft/ft	DIRECTION FACTOR- EACH W/V (d)	DIRECTION FACTOR- AVG. (e)
6a & 6b	3	0.305	0	48.4	1	1
5a & 5b	6	0.611	0	69.5	1	
2 & 4	12	1.222	0	108.8	1	
8	96	0.602	0	76.7	1	
8	96	0.602	15	69.4	0.91	0.91
6a & 6b	3	0.305	30	57.1	1.18	1.02
5a & 5b	6	0.611	30	73.0	1.05	
2 & 4	12	1.222	30	98.9	0.91	
8	96	0.602	30	73.0	0.95	
6a & 6b	3	0.305	90	42.6	0.88	0.74
5a & 5b	6	0.611	90	53.8	0.77	
2 & 4	12	1.222	90	73.1	0.67	
8	96	0.602	90	49.9	0.65	
8	96	0.602	180	11.0	0.14	0.14

(a) W/V calculated for TNT equivalent explosive weights.
(b) Gage line measured in degrees from 0 degree (front) line.
(c) R/D at 1.2 psi from best fit line to all data from test(s).
(d) Directional Factor (R/D)/(R/D on 0 deg line) for each W/V.
(e) Average directional factor for all W/V on given line.

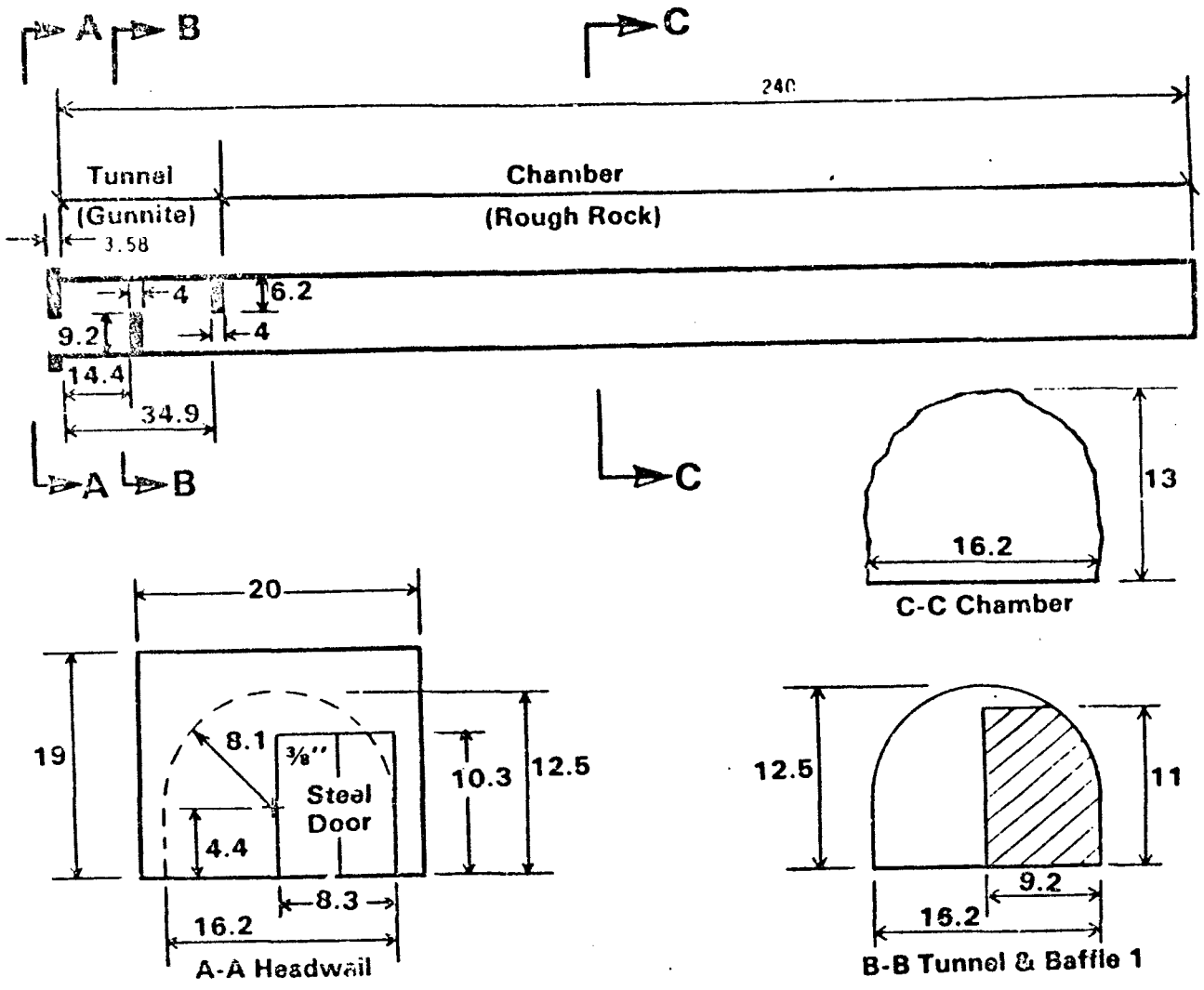

Figure 1. Typical Full Scale Tunnel Magazine Dimensions (feet).

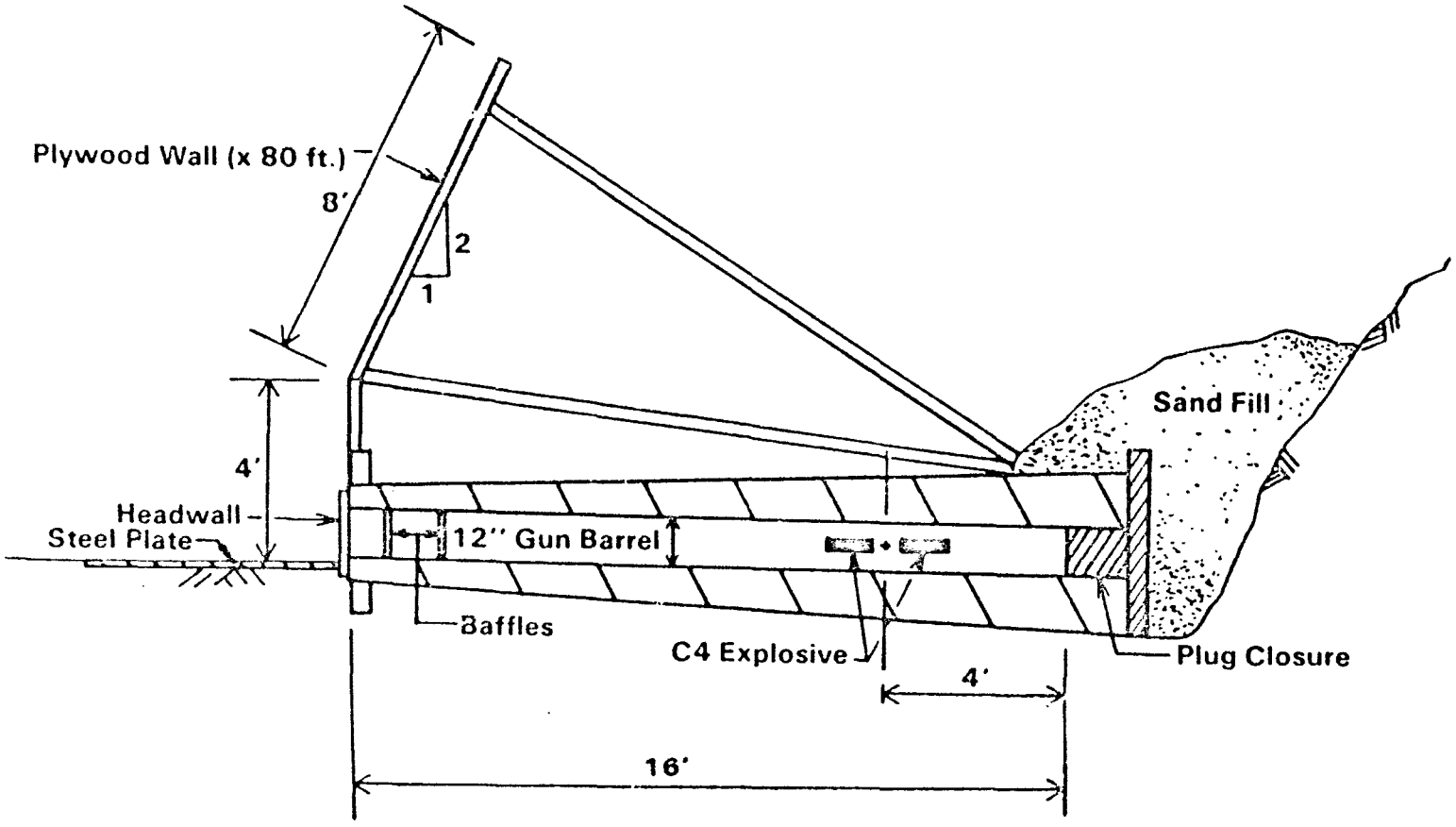

Figure 2. 1/15th Scale Model Tunnel Test Setup

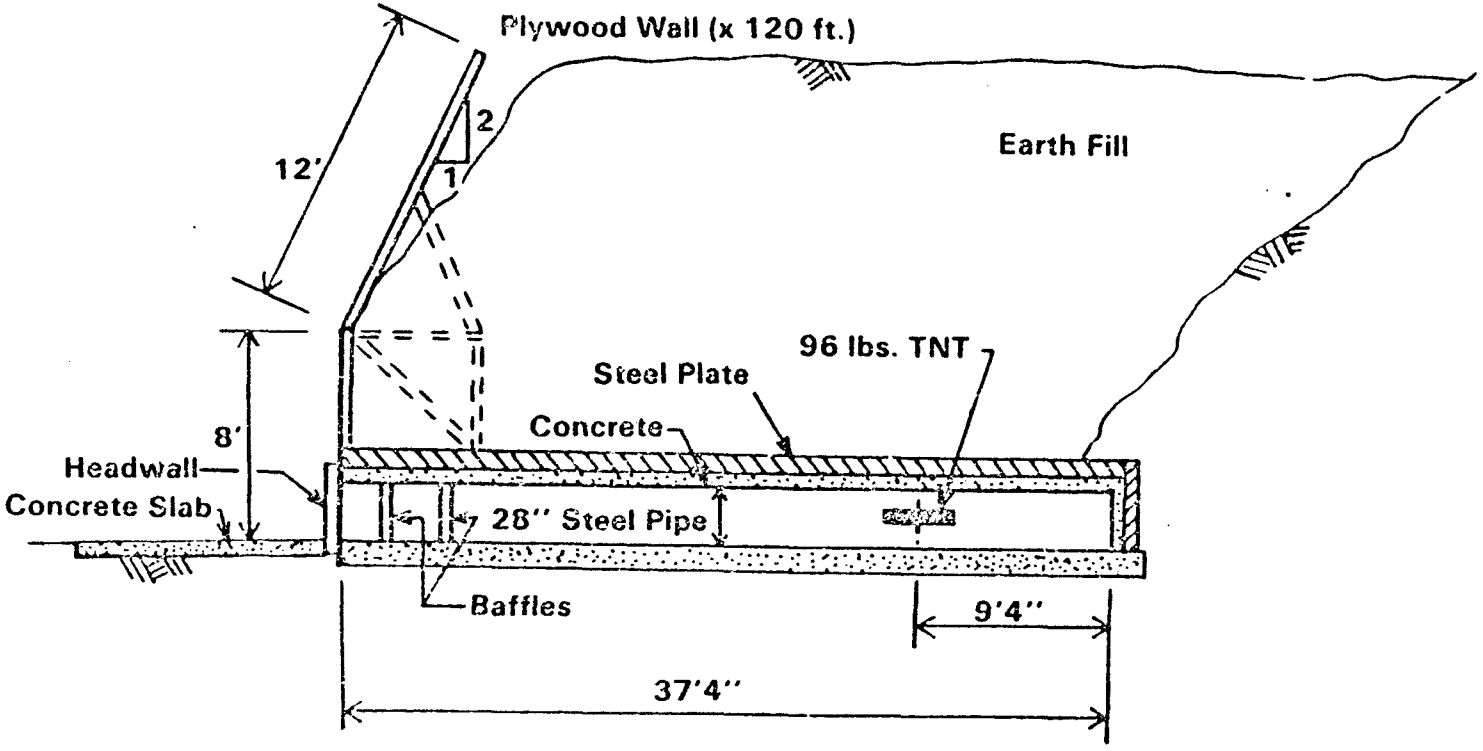

Figure 3. 1/6th Scale Model Tunnel Test Setup

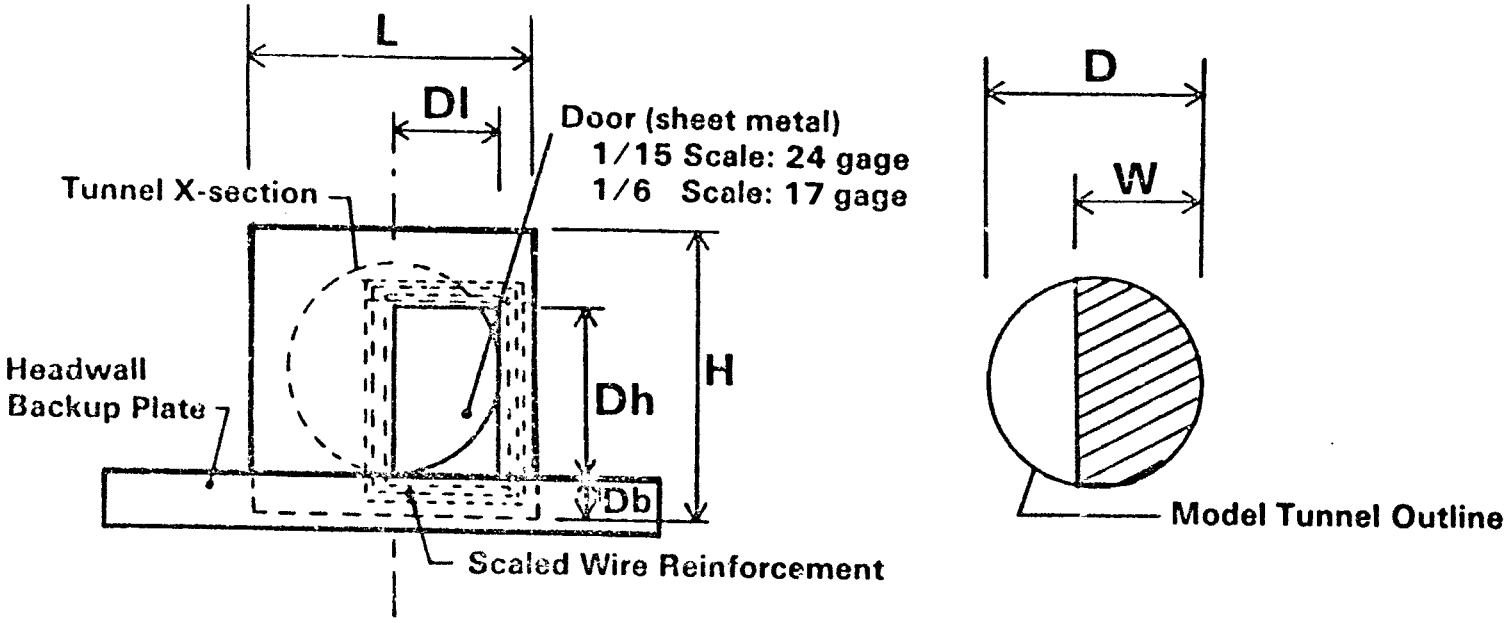

Headwall Dimensions

	Scale 1/15	Model 1/6
T	2.9"	6.7"
L=H	17.0	40.0
Dh	10.1	23.6
Dl	6.0	14.0
Db	2.5	5.9

Baffle Dimensions

	Scale 1/15	Model 1/6
T1=T2	3.2"	7.5"
w1	6.2	3.9
w2	15.5	9.1
D	12.0	28.0

Figure 4. Scale Model Headwall and Baffle Geometry

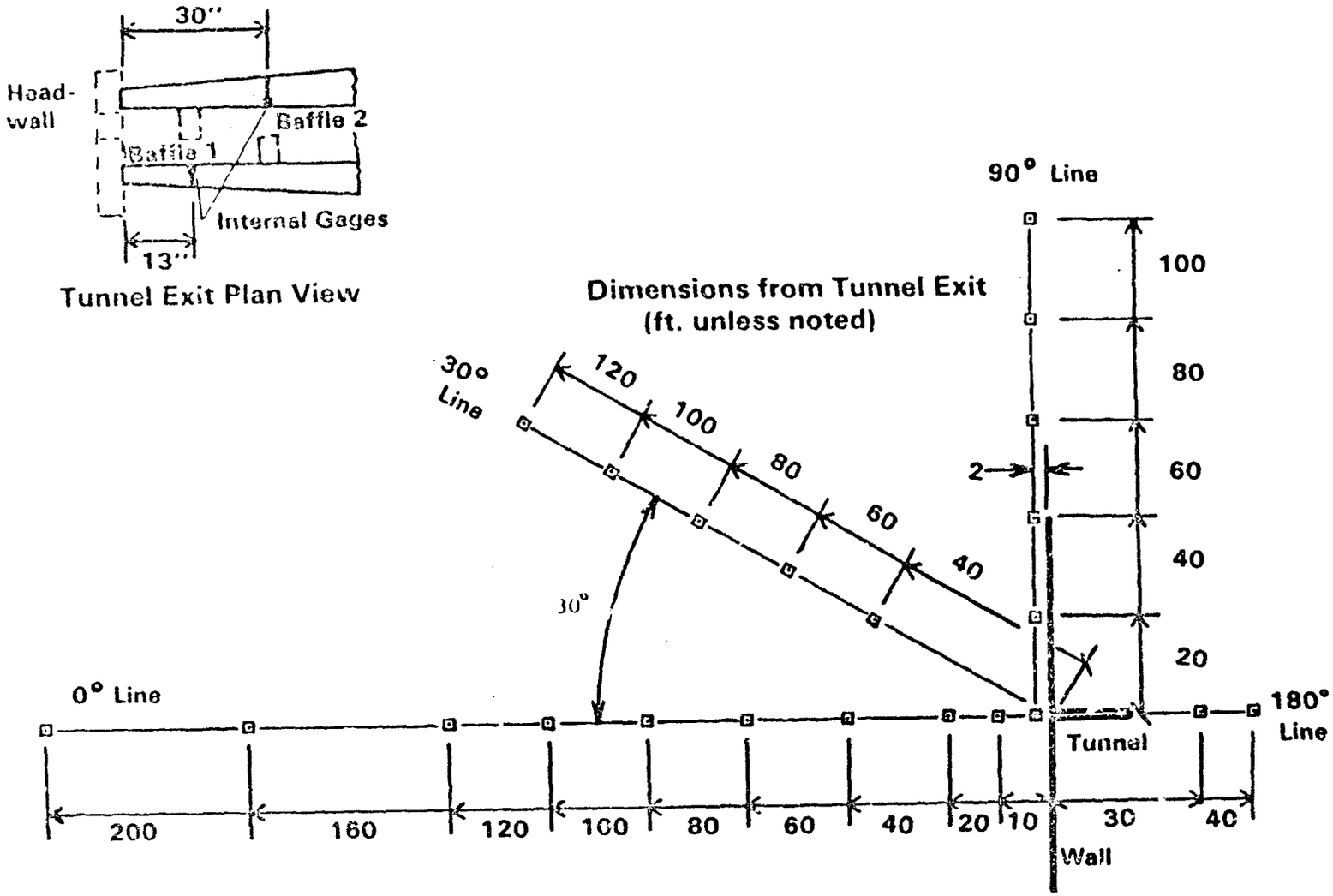

Figure 5. Pressure Gage Locations, 1/15th Scale Model

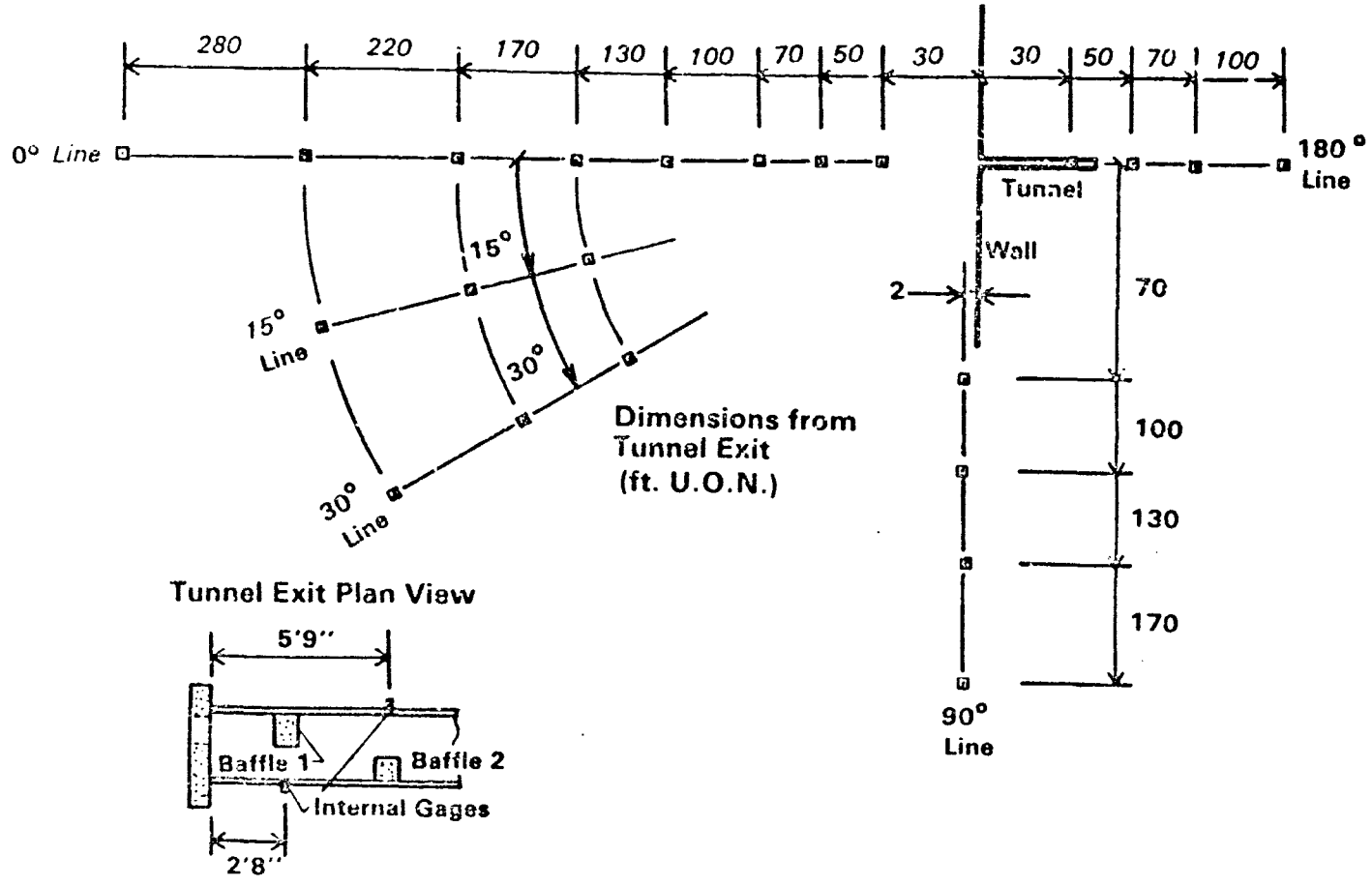

Figure 6. Pressure Gage Locations, 1/6th Scale Model

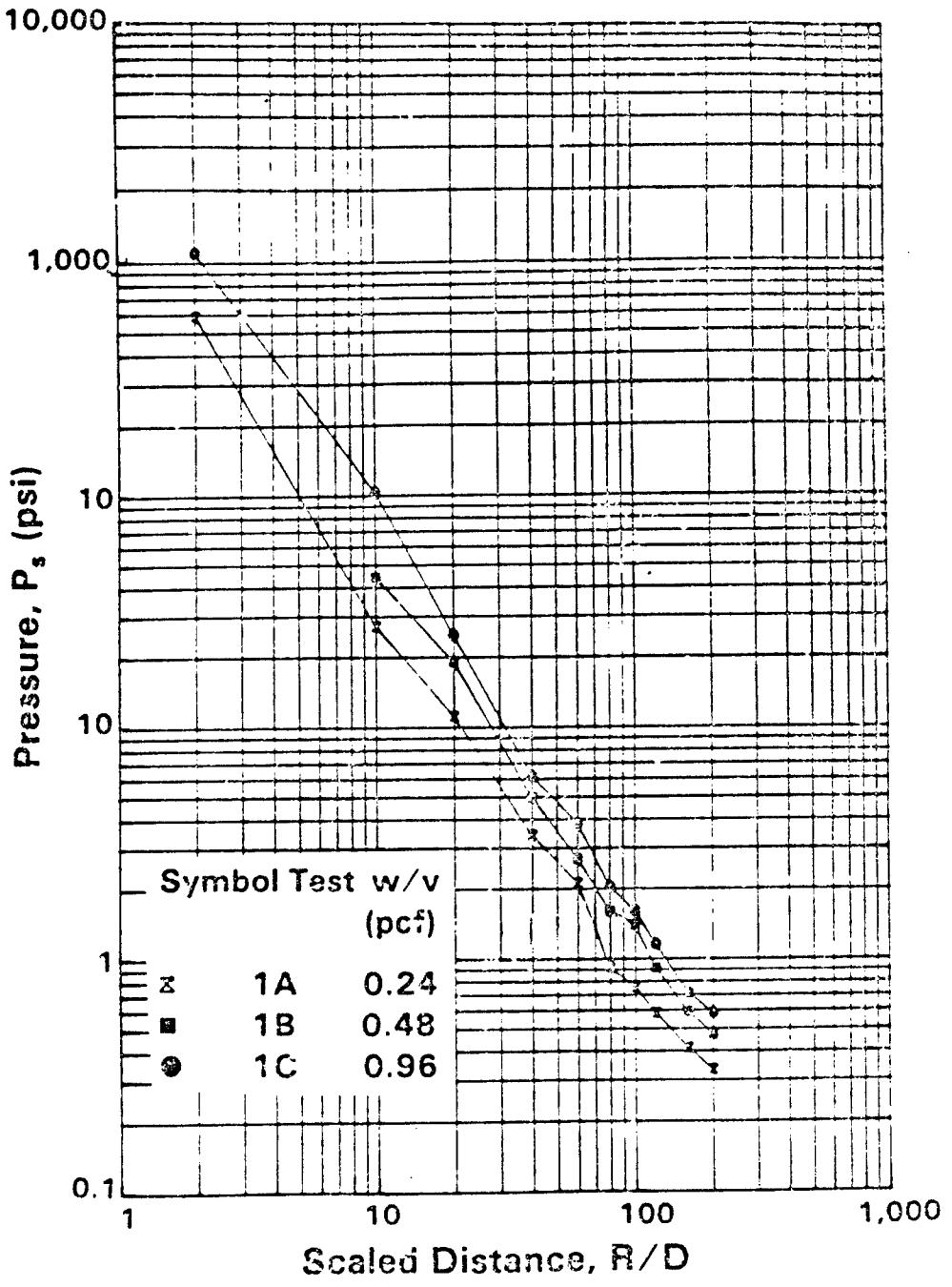

Figure 7. P vs. R/D, Configuration O, "O" Line, W=3, 6 & 12 lbs. C4

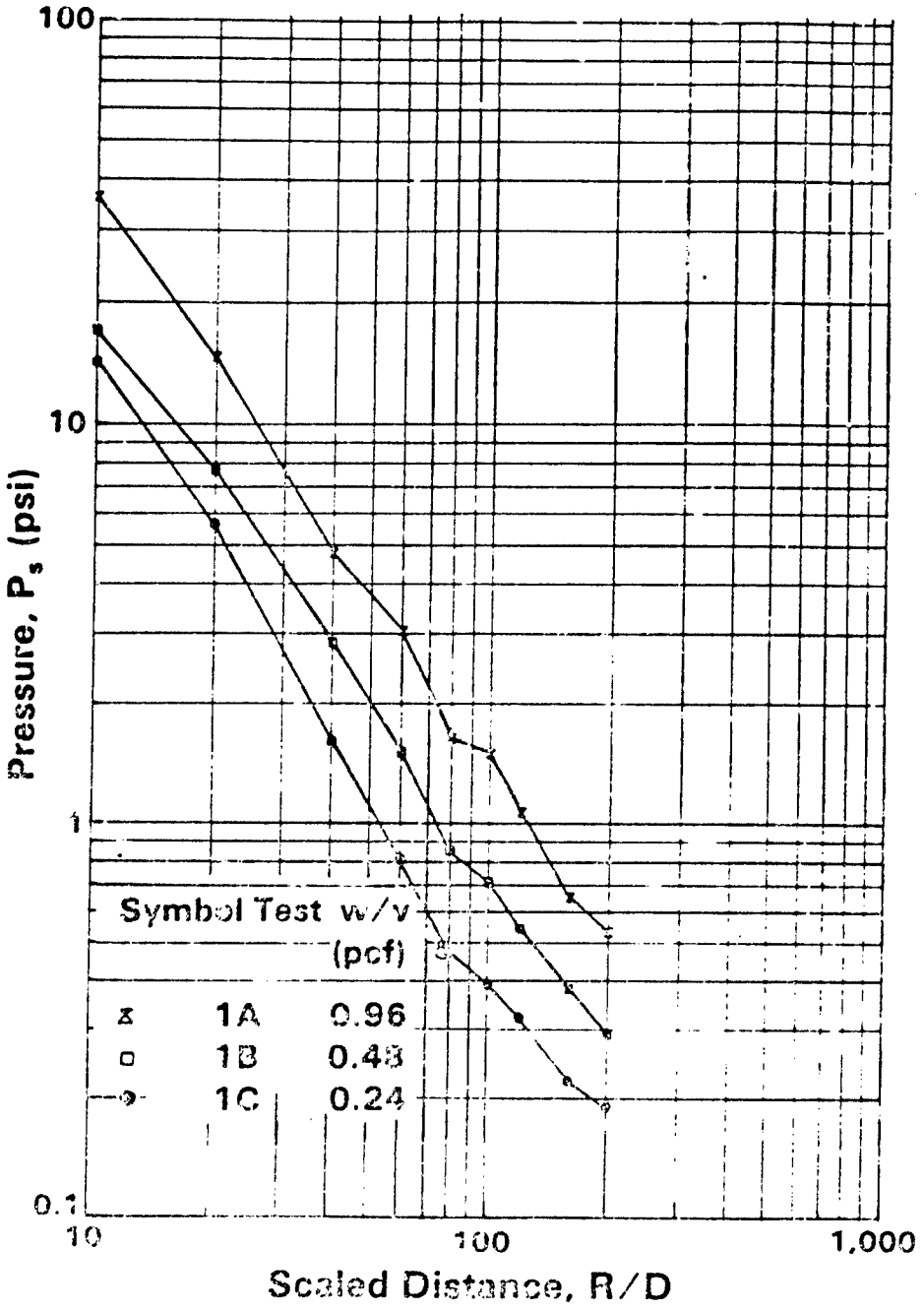

Figure 8. P vs R/D, Configuration 2, "O" Line, W=3, 6, & 12 lbs C4

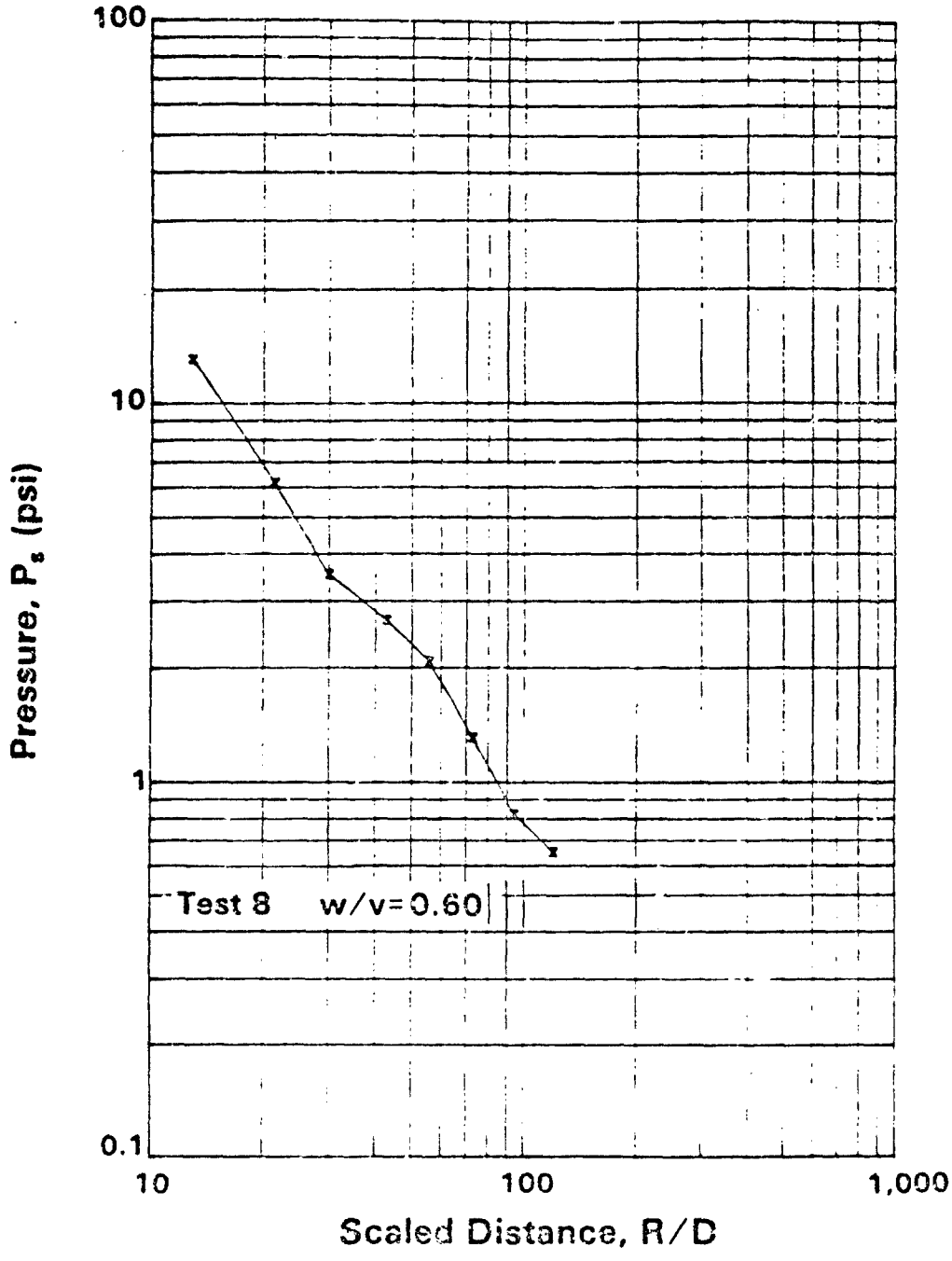

Figure 9. P vs R/D, Configuration 2, "O" Line, W=96 lbs. TNT

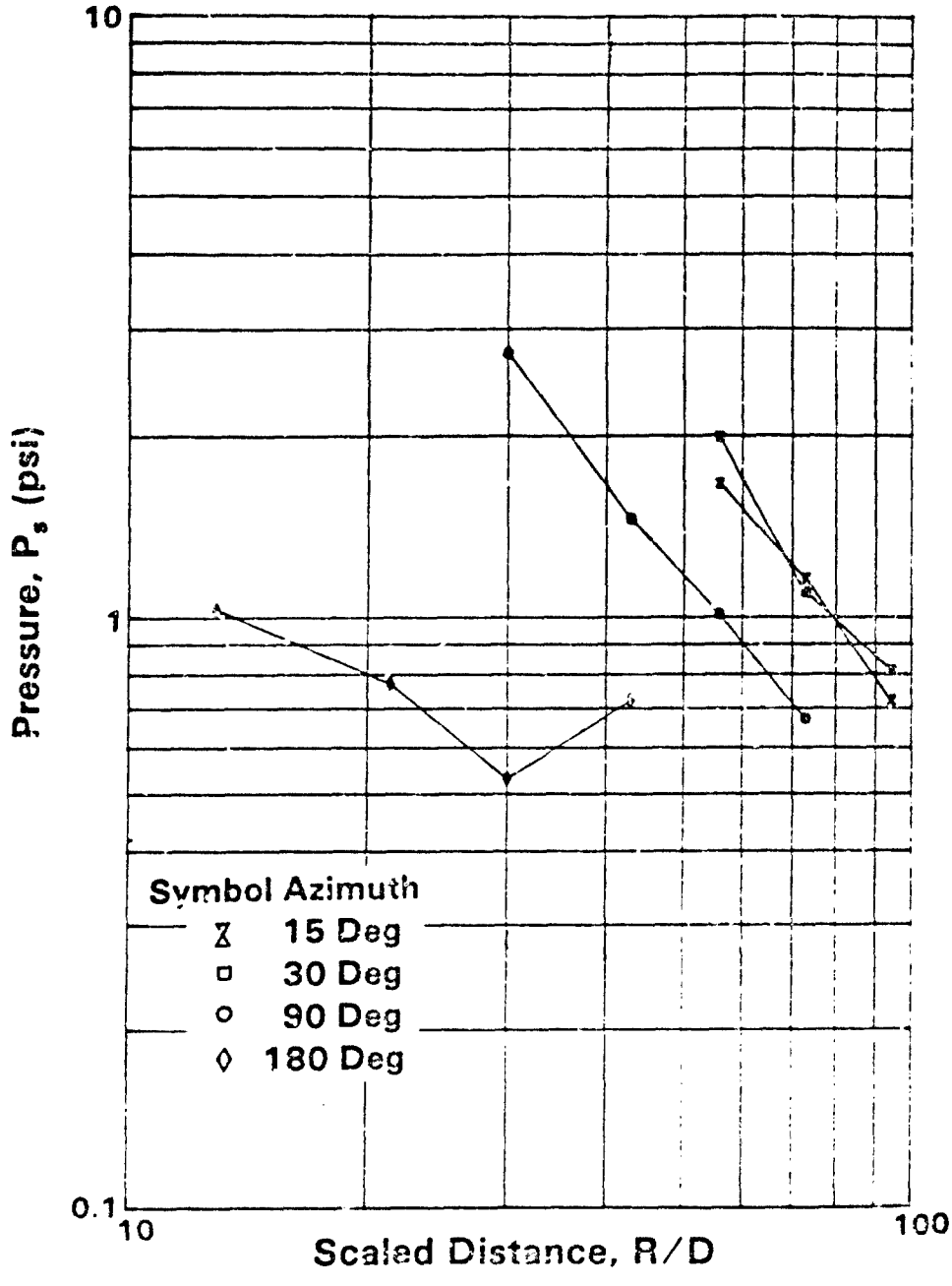

Figure 10. P vs R/D, Configuration 2, 15, 30, 90 & 180 Lines, W=96 lbs. TNT

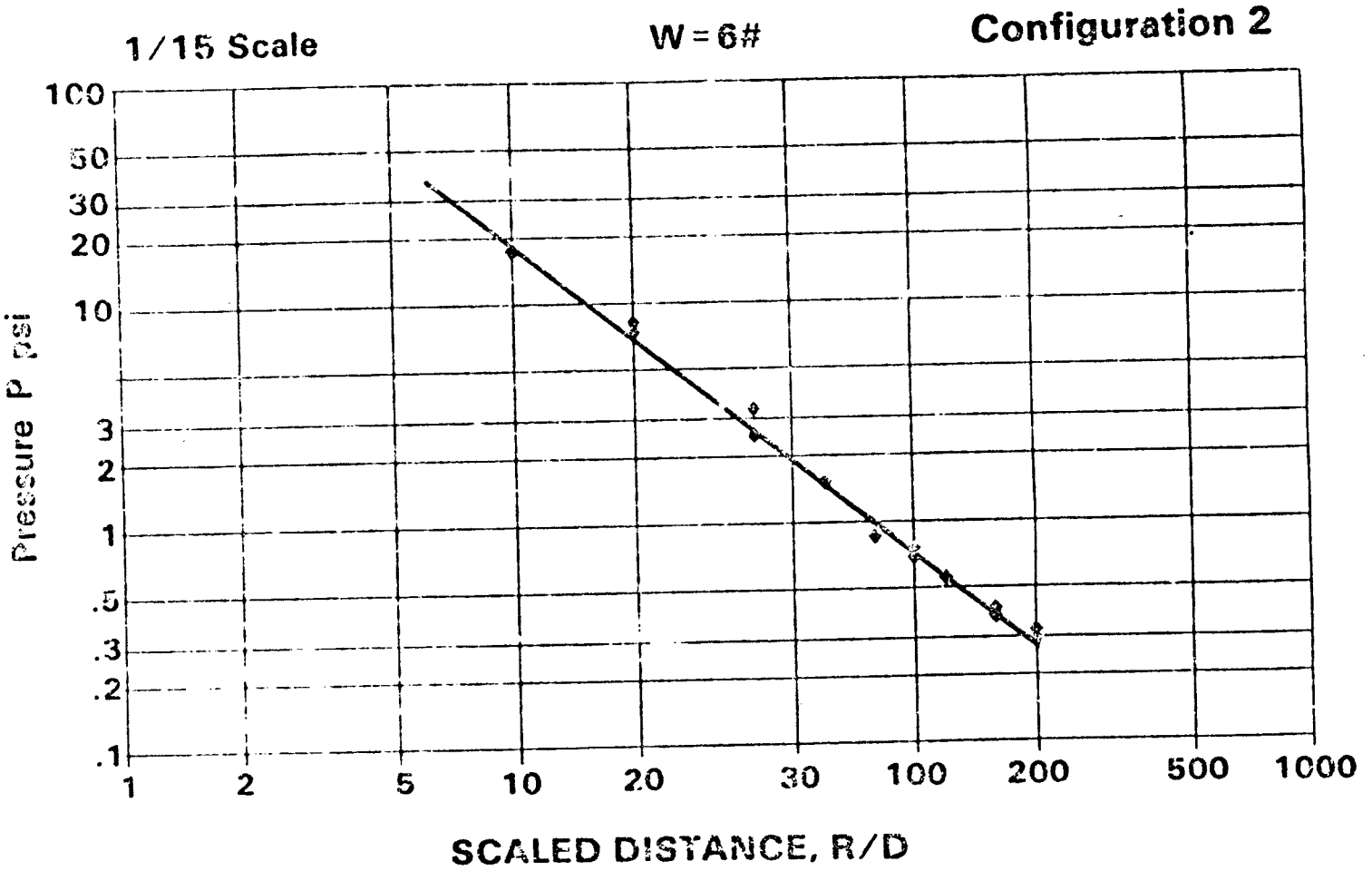

Figure 11. P vs. R/D, Best Fit Line, Configuration 2, W=6# C4

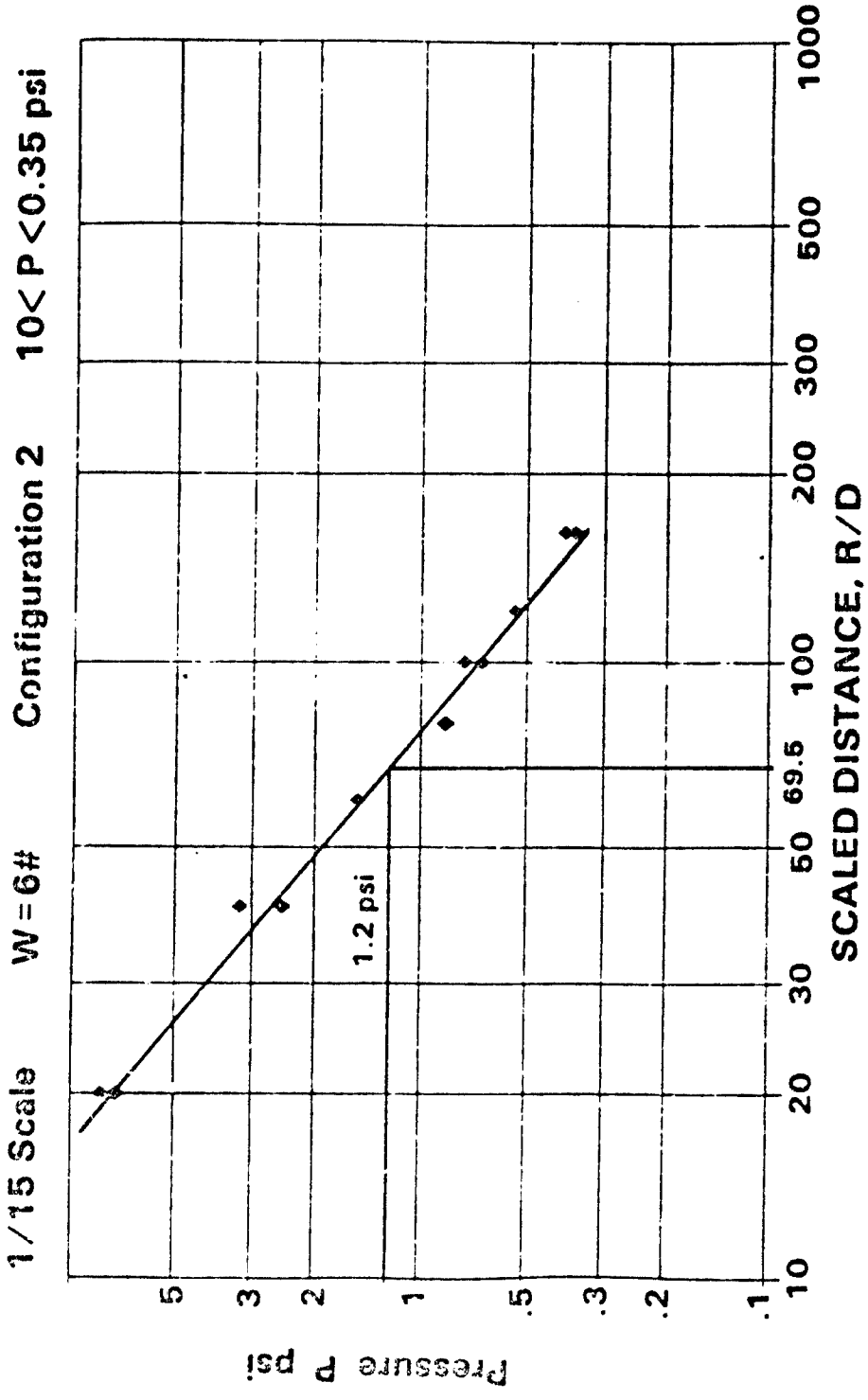

Figure 12. P vs. R/D, Best Fit Line, Configuration 2, W=64# C4, 10 P 0.35

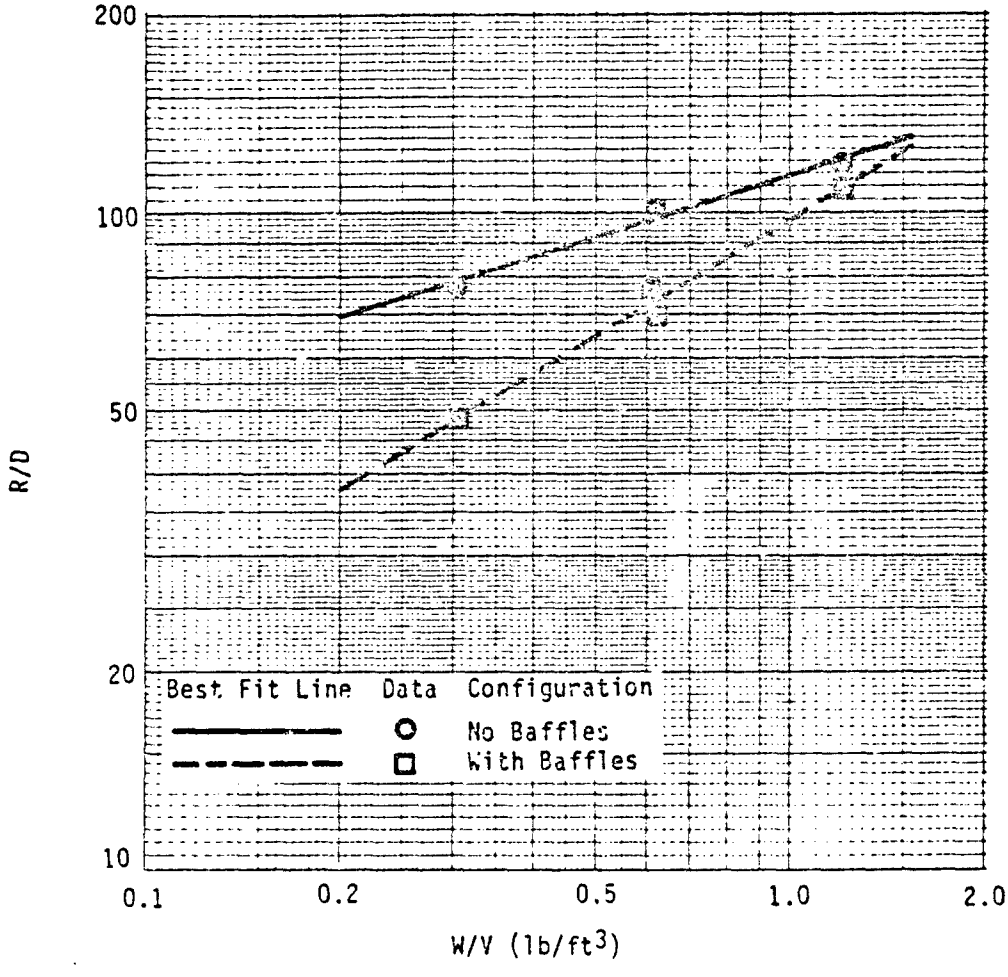

Figure 13. 1.2 psi R/D vs. W/V (With & Without Baffles)

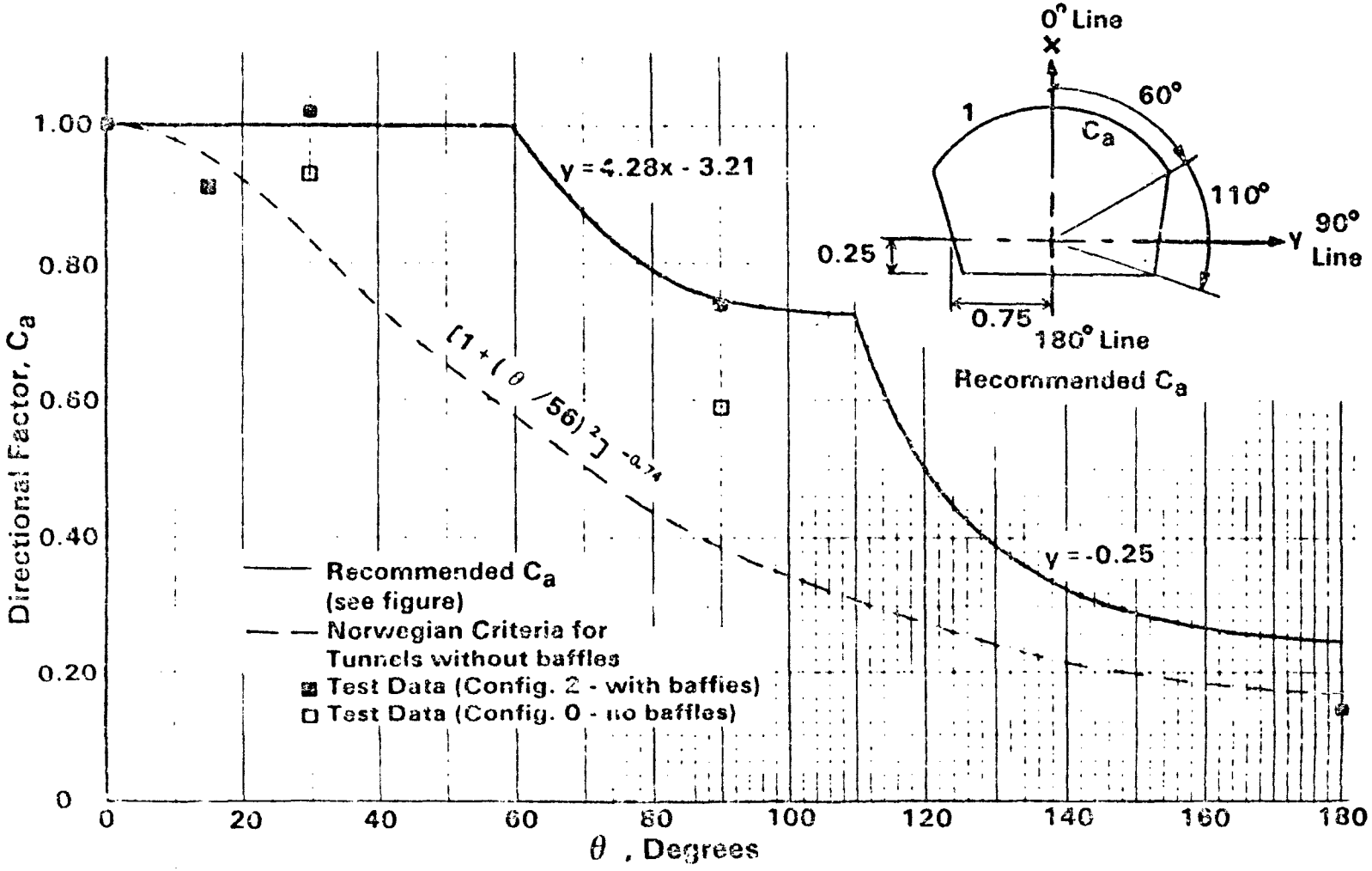

Figure 14. Directional Factors: Test Data and Recommended

WES UNDERGROUND MAGAZINE MODEL TESTS

by

C. E. Joachim and D. R. Smith

U.S. Army Corps of Engineer
Waterways Experiment Station
Vicksburg, Mississippi

Prepared for:

Department of Defense Explosive Safety Board
Twenty-Third DOD Explosives Safety Seminar
9-11 August 1988

WES UNDERGROUND MAGAZINE MODEL TESTS

C. E. Joachim and D. R. Smith
U.S. Army Engineer Waterways Experiment Station
Vicksburg, Mississippi

INTRODUCTION

The use of underground munition storage facilities offers many potential advantages over above-ground storage facilities, including controlled storage environments, reduced external hazards from accidental explosions, and greater protection of the munitions from military attacks or sabotage. However, the construction and use of underground magazines still requires the development of more realistic design safety criteria. These criteria must take into account the depth of chamber cover, minimum chamber spacing (for multiple chambered facilities), inhabited building and public road distances from the facility entrance, and other factors. The hazard ranges for an accidental explosion are also dependent upon site geologic media, configuration of the underground facility, the type and quantity of explosive, and the topography of the site.

Abundant analytical and experimental data exists on damage to rock (stress levels, fracturing, displacement, etc.) from well-coupled, concentrated charge detonations (from weapons effects testing), as well as from distributed charge detonations (from mining technology). Very little information is available, however, on rock damage from the type of detonation represented by an accidental explosion in an underground ammunition storage chamber; i.e., where the charge is distributed along the length of a long cavity containing a large, enclosed air volume.

Additional quantitative data was needed to relate the stress/strain levels in rock, as a function of range, to the detonation parameters that uniquely characterize an accidental detonation in this environment. Practical design standards can then be developed to insure protection of the contents in adjacent chambers of a multi-chamber facility, while minimizing the construction costs related to the chamber separation distances.

The WES program of underground magazine model tests, described in this paper, was designed to provide this data base. The work was sponsored by the Department of Defense Explosive Safety Board.

OBJECTIVE

The primary purpose of the WES model study was to improve the state-of-the-art for prediction techniques used to establish underground explosive storage safety standards and design criteria. The main objective was to determine the spacing between underground storage chambers required to prevent a detonation in one chamber from sympathatically detonating explosives in an adjacent chamber. Secondary objectives were to establish the separation required to minimize damage to contents in adjacent chambers, and the standoff distances from the facility required to protect inhabited buildings from external airblast propagating from the portal.

TEST DESIGN

The WES model consisted of a single storage chamber and access tunnel embedded in a granite-matching grout block. The dimensions of the storage chamber corresponded to a 1:75 scale model of a generic underground magazine. The test chamber was 9.7 cm in diameter by 1.15 m long, and modeled a full-scale magazine 7.3 m in diameter by 86 m long. Similarly, the model access tunnel, 6.8 cm diameter by 1.07 m long, represented a full scale tunnel 5.1 m diameter and 80 m in length. The corresponding chamber volumes were 0.00844 m^3 (8,440 cm^3) in the model and 3560 m^3 in the full scale. Cross-sections along and perpendicular to the chamber centerline are shown in Figures 1 and 2.

Surrounding the model storage chamber in radial arrays were six accelerometers and eight strain gages (Figure 2). The distance between the center of the chamber and each ground motion gage is given in Table 1. The external airblast gages were placed along a 0-degree line extending directly out from the access tunnel portal, and on three "off-axis" lines at 30, 45, and 60 degrees from the extended tunnel centerline (Figure 3). The ranges of the airblast gages from the tunnel exit are presented in Table 2.

CONSTRUCTION

The model chamber and tunnel were formed in a 20 m^3 block of reinforced cement grout. The grout was designed to approximate the strength properties of granite. The storage chamber and access tunnel were formed with smooth-wall steel tubing and suspended by wire within the block form. Steel reinforcing rods were used to prevent stress concentrations from cracking the block.

Thermodynamic calculations indicated that high internal thermal stresses might crack the grout block, if it was formed in a single pour. Therefore three separate pours were made, with the previous pours being coated with epoxy to minimize the effects of cold joints. During the second pour, thin-wall copper tubes were inserted for later gage placement. To insure bonding of the strain gages to the test block, the vertical tubes over the center of the storage chamber were removed after the third pour reached an initial set. The vertical holes were filled with the same grout mix used to fabricate the test block, and accelerometer and strain gage columns were then inserted into the grout-filled holes and the displaced grout removed.

INSTRUMENTATION

The selection of accelerometer gage ranges was based on an extrapolation of shock data from previous tests involving both spherical and cylindrical decoupled charges (Herbst, 1961; Atchison, 1964, Perret, 1968; and Drake, 1974). The accelerometers were placed in high-strength, watertight canisters. The lowest natural frequency of the canisters was experimentally determined to be 32,000 Hz, which was compatible with the frequency of the recording system. The mounting bases were sufficiently strong to eliminate any base-induced strain which could degrade the accelerometer signal. The locations of the accelerometers are given in Table 1. Gage numbers are keyed to the numbers shown in Figure 2.

Strain measurements were made with eight waterproofed strain gages bonded to a single 4.8-cm diameter grout column. The strain gages were 0.635-cm long, 350-OHM foil gages, with a gage factor of 2.14 at 75 degrees F. The grout column was cast with the same mix used in the

model to ensure matching properties. The properties of the grout are given in Table 3. The locations of the strain gages are given in Table 1.

The selection of airblast gages was based on the expected airblast frequencies and amplitudes. In addition, the gages needed to have negligible lateral sensitivity in order to minimize the effects of lateral acceleration of the grout around the chamber induced by dilatation of the chamber by the detonation. Sufficient airblast data were available to predict frequency and amplitude (Westine, 1969; Fredricksen, 1970; Skjeltorp, 1975 A and 1975 B; and Gurke, 1977).

Airblast gage location data are given in Table 2. The gage numbers are keyed to numbers shown in Figure 3.

CHAMBER CHARGE LOADINGS

The explosive used in all tests was PETN detonating cord. The charges were assembled by taping the required number of strands of det cord together, and were detonated from the portal end. The burn rate (8,300 mps) was fast enough to produce the desired cylindrically-expanding ground shock. In addition, experimental data and theoretical techniques were available to accurately predict the equilibrium pressure developed in the charge chamber by a PETN detonation (Porzel, 1969; Fredricksen, 1970; Kriebel, 1972; Proctor, 1974; and Gurke, 1977).

The test program was performed in three phases. Phase 1 was designed primarily to obtain ground shock and motion data in the simulated rock environment around the chamber. At least one airblast gage was monitored during each test, however. Chamber loading densities of 1.6, 4.8, 16.0, and 32.0 kg/m^3 were used for these tests, with several tests conducted at each density.

Phase 2 was designed to provide external airblast pressure data. It consisted of a total of 51 tests conducted at loading densities of 1.6, 3.2, 4.5, 5.9, and 7.4 kg/m^3. Phase 3 consisted of a single test at a loading density of 405 kg/m^3. While catastrophic failure of the model was anticipated, peak strains were successfully measured during the propagation of the initial stress wave, before breakup of the grout block occurred.

RESULTS

Shock and Stress Measurements

Analog time histories were digitized on an analog-to-digital converter and processed on the WES GE-635 computer. Acceleration records were numerically integrated to obtain particle velocities. Peak velocity, strain, and airblast pressure data are listed in Tables 4, 5, and 6.

Peak particle velocities at each range were averaged, and then normalized to the chamber loading density. In Figure 4, the normalized velocities are plotted as a function of distance factor R/D, where R is the radial distance from the center of the cavity to the measurement point and D is the equivalent hydraulic diameter of the storage chamber. The data scatter is consistent with that typically obtained in ground motion investigations. Peak velocities in the model are slightly less than would be predicted with previous data from explosions in 0.6-m diameter cavities in sandstone and heavily jointed granite (Amend, 1977).

The equivalent hydraulic diameter (in meters) of a tunnel or chamber is

$$D = 2\,(A/\pi)^{1/2} \qquad (1)$$

where A is the cross-sectional area, m^2.

For the normalized particle velocities (Figure 4) obtained for loading densities of 1.6 and 16.0 kg/m^3, it can be seen that an order of magnitude increase in loading density did not produce a significant difference in the normalized data. However, a further increase in loading density to 32.0 kg/m^3 almost doubles the normalized particle velocity.

Peak strain was calculated from peak particle velocity by using the one-dimensional approximation

$$E = V/C \qquad (2)$$

where E is the peak strain, μin./inch or μm/m

V is the peak particle velocity, m/sec

and C is the compressional wave velocity, m/sec

The peak strain data (Table 5) and the peak strains calculated from the peak velocity measurements are shown in Figure 5. The legend gives symbols for calculated (V/C) and measured (Ξ) data. The scatter in the data is consistent with typical variations in strain and/or velocity measurements. It should be noted that the strain measurements were derived from a vertical gage array, whereas the particle velocity data were obtained from a horizontal array. The extent of agreement between the two data sets demonstrates that there were no apparent directional anomalies.

Strain measurements were made at ranges of 2.5 to 15.6 chamber diameters from the center of the cavity. As shown in Figure 5, these data are complimented by similar data from Bureau of Mines tests (Atchison, 1964), in which gages were located between 14 and 204 cavity diameters from the source. As demonstrated by Drake (1974), the attenuation in the Bureau of Mines data is dominated by spherical decay, while the close-in data attenuates cylindrically, transitioning to spherical attention at an R/D value of about 6.0, which corresponds to a radial distance equal to one-half the chamber length. The rate of peak strain decay in the cylindrical and spherical regions is $R^{-1/2}$ and R^{-2}, respectively. A curve which provides an upper bound to the peak strain data for this test geometry is also shown in Figure 5.

In summary, these results indicate that the upper bound of the peak free-field strain produced by an explosion in an arbitrary cylindrical cavity can be determined. The study also showed that the transition from cylindrical to spherical attenuation will occur at radial distances on the order of one-half the chamber length. Using the results of the WES and previous tests, the upper bound equations are

$$E/Q = 50 \times 10^{-6} (R/D)^{-1/2}; \quad \text{for } R < L/2 \qquad (3)$$

and

$$E/Q = 6.94 \times 10^{-6} (2\,L/D)^{1.5} (R/D)^{-2}; \quad \text{for } R > L/2 \qquad (4)$$

where Q is the loading density, kg/m^3.

Air Blast Measurements

The peak free-field airblast pressure data are given in Table 6. The average peak values measured at each gage station are presented in Figures 6 through 9 as a function of exit pressure (P_e), the access tunnel equivalent hydraulic diameter (D), and range (R). The exit

pressure at the portal (in pascals) was determined from the following relation (Skjeltorp, 1968):

$$P_e = 1.21E + 06\ (W/V_t)^{0.61}\ (A_j/A_c)^{0.19} \qquad (5)$$

for $0.11 < A_j/A_c < 0.45$

where W is the total TNT-equivalent charge weight, kg

V_t is the total air volume (chamber + access tunnel), m^3,

A_j is the cross-sectional area of the access tunnel, m^2,

and A_c is the cross-sectional area of the storage chamber, m^2.

The external airblast pressures plotted in Figures 6 through 9 were normalized with exit pressures calculated using Equation 5.

Substantial scatter exists in all the airblast data. Low-strength shocks, produced by low loading densities, may have been substantially attenuated by small degrees of wall roughness. This could have produced lower exit pressures than predicted and, consequently, larger attenuation in the blast wave as it propagated outside the portal. These effects are nonlinearly related to the loading density. Since the loading density is used to calculate the exit pressure without considering the wall roughness effects, some data scatter was probably due to this nonlinearity. Gurke (1977) reported similar results for low loading densities.

Skjeltorp (1975 A) has developed the following non-dimensional airblast pressure-distance relation as an upper bound:

$$P/Pe = 1.24\ \{(R/D)^{-1.35}\}\ /\ \{1 + (\Theta/56\ )^2\} \qquad (6)$$

where Θ is the angle measured from the extended tunnel centerline (in degrees) and D is the access tunnel diameter (in meters). As can be seen in Figures 6 through 9, the curve computed with this equation effectively forms an upper bound to the WES model airblast data. The dimensionless form of Equation 6 provides a method for scaling tests in a similar geometry over a wide range of loading densities. It also provides a method for predicting required standoff distances as a function of the blast pressure damage threshold for various types of structures.

ANALYSIS

Chamber Spacing

Within an underground storage facility, the spacing between storage chambers must be sufficient to prevent explosive communication resulting from catastrophic wall failure or rock spalling. The level of damage to unlined tunnels, produced by the stress field from by an external explosion, can be related to the strain developed at the tunnel wall. Catastrophic failure (enough to cause tunnel closure) may occur if the strain at the tunnel wall is greater than 4×10^{-3}. It is also possible that high velocity rock spalls from such a failure could impact munitions in the chamber with sufficient forces to initiate a detonation. Minor surface damage to the walls may occur at strain magnitudes less than 4×10^{-3}. To preclude damage to the contents of adjacent storage chambers in an underground magazine, the spacing between chambers should be large enough to prevent any wall surface damage.

Manipulating Equations 3 and 4, we get the following:

$$R/D = 2.50 \times 10^{-9} (Q/E)^2; \quad \text{for } R < L/2 \qquad (7)$$

and $$R/D = 2.63 \times 10^{-3} (2\ L/D)^{0.75} (Q/E)^{1/2}; \quad \text{for } R > L/2 \qquad (8)$$

Substituting the strain threshold for catastrophic failure into Equations 7 and 8 we get

$$R/D = 1.56 \times 10^{-4} Q^2; \quad \text{for } R < L/2 \qquad (9)$$

and $$R/D = 4.17 \times 10^{-2} (2\ L/D)^{0.75} Q^{1/2} \quad \text{for } R > L/2 \qquad (10)$$

The chamber spacing required to prevent spall-induced sympathetic detonations can be obtained from Equations 7 and 8, if the spall velocity, V_{sp}, required to initiate the contents of the adjacent chamber is known. Using Equation 2, the peak spall strain can be approximated as

$$E = V_{sp}/2C \qquad (11)$$

Substituting for strain in Equations 7 and 8, the chamber separation required to insure that rock spall cannot initiate a detonation in an adjacent magazine is given by

$$R/D = 1 \times 10\text{-}8 (QC/V_{sp})^2 \quad \text{for } R < L/2 \qquad (12)$$

and $$R/D = 3.73 \times 10^{-3} (2L/D)^{0.75} (QC/V_{sp})^{1/2}; \quad \text{for } R > L/2 \qquad (13)$$

At low loading densities, the chamber spacing will be determined by Equations 9 or 12, which are within the region of cylindrical shock attenuation. As the loading density is increased, the required spacing will obviously increase. Above some threshold loading density, the chamber spacing is determined by Equation 10 or 13, which are based on spherical decay. In this region, the standoff distance increases with a corresponding increase in loading density, chamber length or a decrease in chamber radius.

In most cases, the minimum chamber spacing will be determined by catastrophic wall failure, because the spall velocity required to initiate many explosives is typically on the order of 120 m/sec. This spall velocity corresponds to a wall strain which is well above the threshold for catastrophic wall failure. Spalling dominates only when sensitive explosives (initiated by very low spall velocities) are stored in the adjacent chamber. As an example, for a storage chamber in granite (assume C = 4,600 m/sec), spalling dominates only if the impact sensitivity of the contents is less than 37 m/sec.

The equation (converted to metric units) used in the the Department of Defense Ammunition and Explosives Safety Standards Manual (DOD 6055.9-STD, 1984) to determine the chamber separation required to prevent sympathetic detonations in adjacent chambers is

$$D_{cp} = 0.60\ W^{1/3} \qquad (14)$$

where D_{cp} is the separation distance, m

and W is the total TNT-equivalent charge weight of the magazine contents, in kg.

It is difficult to make a general comparison between the values given by Equation 14 and those developed earlier in this paper, because Equation 14 does not explicitly address the geometric, spall velocity, medium properties, or nonlinear decoupling effects. However, the equations can be compared by assuming a design geometry and values for the loading density and spall velocity. For comparison purposes, the following values were assumed:

Chamber length -	79.9 m
Chamber diameter -	7.46 m
Spall velocity required for initiation of contents -	120 m/sec
Wave speed of rock -	4573 m/sec

These dimensions are consistent with full-scale designs of underground magazines constructed in Europe. The required standoff distances between chambers, as predicted by the above equations for spall, tunnel closure, and the current safety standards, are presented in Table 7 for loading densities between 1.6 and 400 kg/m^3.

The predictions given in Table 7 indicate that the current safety standards for chamber separation to prevent sympathetic detonation in adjacent chambers are very conservative. In this example, a loading density of more than 112 kg/m^3 would be required to generate a spall velocity of 120 m/sec in the tunnel wall. According to Equations 9 and 10, zero chamber separation is required to prevent tunnel closure if the loading density is below 64 kg/m^3. This is because loading densities less than 64 kg/m^3 produce strains at the chamber wall that are less than the incident strain normally required (4×10^{-3}) to produce wall failure. Based on structural considerations alone, however, a chamber separation of at least one-fourth the chamber diameter is recommended.

Damage to the chamber contents may occur if the strain at the chamber wall is sufficient to induce intermittent wall damage; i.e., peak strains greater than 4×10^{-4}. Substituting for strain in Equations 7 and 8, the minimum spacing required between storage chambers to prevent damage to the contents is given by

$$R/D = 0.0156\ (Q)^2 \qquad \text{for } R < L/2 \qquad (15)$$

$$R/D = 0.132\ (2\ L/D)^{0.75}\ (Q)^{1/2} \qquad \text{for } R > L/2 \qquad (16)$$

According to DOD 6055.9-STD (1984), the chamber separation (D_{cd}) required to prevent damage to stored ammunition can be calculated by the following formulas (converted to metric):

$$D_{cd} = 1.39\ W^{1/3} \quad \text{(Sandstone)} \qquad (17)$$

$$D_{cd} = 1.71\ W^{1/3} \quad \text{(Limestone)} \qquad (18)$$

$$D_{cd} = 1.98\ W^{1/3} \quad \text{(Granite)} \qquad (19)$$

Table 8 compares separation distances to prevent munition damage for different loading densities.

Based on these results, the current safety standards appear to be conservative for most magazine geometries.

Airblast

The equations developed by Skjeltrop (1975 A) have been used to predict peak tunnel exit pressures for the test geometry and range of loading densities addressed in this study, and the external pressures as a function of the exit pressure, tunnel diameter, and range from the exit. Equations 5 and 6 provide an effective upper bound to the measured peak pressure data.

The airblast standoff distance required by DOD 6055.9-STD (1984) is determined by the following equation:

$$D\theta = C\theta \ W^{1/3} \qquad (20)$$

where $D\theta$ is the required standoff distance along a line which is offset θ degrees from the extended centerline and

W is the net explosive weight (kg)

$C\theta$ is a constant functionally dependent on direction.

The following values are assumed for a general comparison of the required standoff distance and Equation 6:.

Chamber diameter -	7.26 m
Chamber length -	86.0 m
Access tunnel diameter -	5.09 m
Access tunnel length -	80.0 m

The standoff distances required by the DDESB DOD 6055.9-STD (1984) for inhabited areas is compared to the distances calculated by Equation 6 in Table 9. The results indicate that the current safety standards are very conservative at small loading densities. For higher loading densities, the current standards are reasonably accurate along the extended tunnel centerline, but are still conservative in the off-axis directions.

CONCLUSIONS

The results of this study provide a quantitative data base for designing multi-chamber underground munition storage facilties with a minimum safe spacing between chambers to prevent sympathetic detonations or damage to the contents of an adjacent chamber, if an accidental explosion occurs. The results also indicate that current design standards may be highly conservative for low loading densities, and slightly conservative for high loading densitites. Based on the test results, the external airblast safety ranges for inhabited buildings

recommended by present safety standards appear to be similarly conservative, particularly for low loading densities.

ACKNOWLEDGEMENT

The permission of the Chief of Engineers to publish this paper is greatly acknowledged.

REFERENCES

Amend, Joseph H., "HAVE HOST Cylindrical In Situ Test (CIST) Data Analysis and Material Model Report," Technical Note No. DE-TN-77-005, U.S. Air Force Weapons Laboratory, Kirtland AFB, NM, 1977.

Atchison, T. C., Duvall, W. I., and Pugliese, J. M., "Effects of Decoupling on Explosion-Generated Strain Pulses in Rock," Report of Investigations RI-6333, U.S. Bureau of Mines, Washington, DC, 1964.

Drake, James L., "Decoupling of Ground Shock from Explosions in Rock Cavities," Miscellaneous Paper No. 74-1, U.S. Army Engineer Waterways Experiment Station, Vicksburg, MS, 1974.

Fredricksen, G., and Jenssen, A., "Underground Ammunition Storage," Report No. 59/70, Norwegian Defence Construction Service, Oslo, Norway, 1970.

Gurke, G., and Scheklinski, G., "Underground Ammunition Storage Model Tests," Report E 12/77, Ernst-Mach Institute, Freiburg, Germany, 1977.

Herbst, R. F., Werth, G. C., and Springer, D. L., "Use of Large Cavities to Reduce Seismic Waves from Underground Explosions," Vol 66, No 3, Journal of Geophysical Research, 1961.

Perret, W. R., "Free Field Ground Motion Study, Project Sterling," Research Report SC-RR-68-410, Sandia Laboratories, Albuquerque, NM, 1968.

Skjeltorp, A. T., "One-Dimensional Blast Wave Propagation," Report No. 48/69, 1968, Norwegian Defence Construction Service, Oslo, Norway.

Skjeltorp, A. T., Hegdahl, T., and Jenssen, A., "Underground Ammunition Storage, I, IIA, IIIA, IVA, and VA," Report Nos. 80/72, 81/72, 83/72, 84/72, Norwegian Defence Construction Service, Oslo, Norway, 1975 A.

Skjeltorp, A. T., "Airblast Propagation through Tunnels and the Effects of Wall Roughness," Report No. 103/75, Norwegian Defence Construction Service, Oslo, Norway, 1975 B.

Westine, Peter S., "The Blast Field about the Muzzle of Guns," paper presented at 39th Symposium on Shock and Vibration, Pacific Grove, CA, 1969.

Table 1

Distance Between the Center of the Storage Chamber and Ground Motion Sensors

Accelerometers		Strain Gages	
Gage Number	Distance cm	Gage Number	Distance cm
1	25.3	8	34.5
2	50.3	9	44.5
3	92.4	10	54.6
4	151.	11	64.9
5	42.1	12	75.0
6	58.8	13	85.1
7	24.1	14	95.4

Table 2

Location of Airblast Canisters with Respect to the Portal and the Extended Centerline

Canister Number	Angle from Extended Centerline degrees	Radial Distance from Portal cm
1	0	22.9
2	0	45.7
3	0	75.2
4	0	304.9
5	30	91.5
6	30	152.4
7	30	243.9
8	45	61.0
9	45	106.7
10	45	152.4
11	45	213.4
12	60	30.5
13	60	76.2
14	60	152.4

Table 3

Experimentally Determined Grout Properties
(average values from six specimens)

Specific Gravity	2.19
Compressional Wave Velocity (m/sec)	3,949.4
Shear Wave Velocity (m/sec)	2,553
Shear Wave Velocity/Compressional Velocity	0.647
Young's Modulus (N/mm^2)	32,590
Shear Modulus (N/mm^2)	14,280
Bulk Modulus (N/mm^2)	15,180
LAME Constant (N/mm^2)	5,657
Poisson's Ratio	0.140

Table 4

Peak Particle Velocities as a Function of Loading Density and Range

Loading Density kg/m^3	Particle Velocity m/sec					
	Gage Ranges (cm):					
	25.3	42.1	50.3	58.8	92.4	151
1.6	0.14	0.070	0.061	--	0.012	0.0098
	0.19	0.055	0.088	--	0.021	0.015
	0.085	0.11	0.040	0.055	0.0085	0.0091
4.8	0.30	0.21	0.17	--	0.055	0.030
	0.43	0.22	0.19	0.12	0.076	0.049
	0.37	0.23	0.22	0.14	0.067	0.046
	0.30	0.22	0.14	0.11	0.061	0.037
16.0	0.98	0.73	0.34	0.30	0.21	0.070
	1.07	0.49	0.61	0.44	0.18	0.061
	1.49	0.91	0.37	0.49	0.076	0.085
	1.46	0.61	0.52	0.79	0.17	--
32.0	3.54	1.37	--	--	--	0.37
	3.35	1.98	2.13	2.20	1.10	0.40
	3.35	1.98	2.74	2.13	--	0.70

Table 5

Peak Strain as a Function of Loading Density and Gage Range

Loading Density kg/m^3	Peak Strain μin./in.							
	Gage Range (cm):							
	24.1	34.5	44.5	54.6	64.9	75.0	85.1	95.4
1.6	54	69	38	40	33	23	23	16
	40	78	25	--	--	--	--	--
	40	107	30	37	20	14	--	--
	34	20	20	12	18	13	8	8
4.8	119	--	86	49	52	53	22	12
	97	94	43	33	33	27	25	--
	139	109	102	63	61	54	41	33
16.0	373	224	261	--	71	41	39	28
	240	229	155	--	54	42	24	26
	310	271	206	44	32	22	30	21
	347	237	250	47	43	58	25	31
32.0	560	626	465	224	149	86	70	68
	772	--	633	291	290	145	137	63
	984	956	767	528	--	--	--	--
405	--	--	7000	7100	7800	4985	3850	2420
			9000*	5800*	5900*	4800*		

* Obtained from a second strain gage column used only on that test.

Table 6

Peak Measured Airblast Pressures Versus Angle from the Extended Centerline of the Access Tunnel

Loading Density kg/m^3	Radial Distance from Portal m	Peak Airblast Pressure kPa			
		Angle from Tunnel Centerline:			
		0°	30°	45°	60°
1.6	0.23	172	--	--	--
1.6	0.23	159	--	--	--
1.6	0.23	193	--	--	--
1.6	0.23	163	--	--	--
1.6	0.30	--	--	--	34
1.6	0.30	--	--	--	29.3
1.6	0.61	--	--	6.9	--
1.6	0.61	--	--	6.2	--
1.6	0.76	--	--	--	4.5
1.6	0.91	--	6.3	--	--
1.6	0.91	--	5.2	--	--
1.6	1.07	--	--	6.9	--
1.6	1.07	--	--	5.2	--
1.6	1.07	--	--	4.4	--
1.6	1.52	--	5.7	--	4.8
1.6	1.52	--	4.5	--	4.7
1.6	1.52	--	--	--	4.7
1.6	2.13	--	--	4.0	--
1.6	2.13	--	--	2.8	--
1.6	2.13	--	--	2.8	--
1.6	2.44	--	4.3	--	--
1.6	2.44	--	3.7	--	--
1.6	2.44	--	2.1	--	--
1.6	3.05	1.4	--	--	--
1.6	3.05	1.9	--	--	--
1.6	3.05	1.5	--	--	--
1.6	3.05	1.6	--	--	--

(Continued)

Table 6

Peak Measured Airblast Pressures Versus Angle from the Extended Centerline of the Access Tunnel

Loading Density kg/m^3	Radial Distance from Portal m	Peak Airblast Pressure kPa			
		Angle from Tunnel Centerline:			
		0°	30°	45°	60°
3.0	0.30	--	--	--	68
3.0	0.61	--	--	13.0	--
3.0	0.61	--	--	15.5	--
3.0	0.76	--	--	--	7.45
3.0	0.76	--	--	--	7.6
3.0	0.91	--	12	--	--
3.0	0.91	--	13	--	--
3.0	1.07	--	--	13	--
3.0	1.07	--	--	14.3	--
3.0	1.52	--	9.7	--	6.3
3.0	1.52	--	10.8	--	5.5
3.0	2.13	--	--	4.9	--
3.0	2.13	--	--	4.8	--
3.0	3.05	5.6	--	--	--
3.0	3.05	3.2	--	--	--
3.0	3.05	2.0	--	--	--
3.0	3.05	2.2	--	--	--
4.5	0.23	296	--	--	--
4.5	0.23	317	--	--	--
4.5	0.23	331	--	--	--
4.5	0.23	276	--	--	--
4.5	0.30	--	--	--	238
4.5	0.30	--	--	--	252
4.5	0.61	--	--	57	--
4.5	0.61	--	--	52	--
4.5	0.76	--	--	--	26.5

(Continued)

Table 6

Peak Measured Airblast Pressures Versus Angle from the Extended Centerline of the Access Tunnel

Loading Density kg/m^3	Radial Distance from Portal m	Peak Airblast Pressure kPa			
		Angle from Tunnel Centerline:			
		0°	30°	45°	60°
4.5	0.91	--	30.0	--	--
4.5	0.91	--	34	--	--
4.5	1.07	--	--	21	--
4.5	1.07	--	--	18	--
4.5	1.52	--	10	7.38	6.9
4.5	1.52	--	10	7.45	6.9
4.5	2.13	--	--	5.5	--
4.5	2.13	--	--	5.2	--
4.5	2.44	--	5.9	--	--
4.5	2.44	--	5.4	--	--
4.5	3.05	6.8	--	--	--
4.5	3.05	9.03	--	--	--
4.5	3.05	1.5	--	--	--
4.5	3.05	7.24	--	--	--
5.9	0.61	--	--	77.2	--
5.9	0.61	--	--	50	--
5.9	0.76	--	--	--	32.3
5.9	0.76	--	--	--	26
5.9	0.91	--	33	--	--
5.9	0.91	--	40	--	--
5.9	1.07	--	--	27.4	--
5.9	1.07	--	--	26.5	--
5.9	1.52	--	16.4	12.8	10
5.9	1.52	--	17	11	10.6
5.9	2.13	--	--	10.8	--
5.9	2.13	--	--	8.62	--
5.9	2.44	--	11	--	--
5.9	2.44	--	11.0	--	--

(Continued)

Table 6

Peak Measured Airblast Pressures Versus Angle from the Extended Centerline of the Access Tunnel

Loading Density kg/m^3	Radial Distance from Portal m	Peak Airblast Pressure kPa			
		Angle from Tunnel Centerline:			
		0°	30°	45°	60°
7.4	0.61	--	--	86.2	--
7.4	0.76	--	--	--	36.2
7.4	0.91	--	58	--	--
7.4	1.07	--	--	37	--
7.4	1.52	--	25	23	18
7.4	2.13	--	25	23	21
15.5	0.23	483	--	--	--
15.5	0.45	259	--	--	--
15.5	0.45	276	--	--	--
15.5	0.76	166	--	--	--
15.5	0.76	124	--	--	--
15.5	3.05	25.9	--	--	--
31.2	0.76	379	--	--	--
31.2	3.05	46	--	--	--
31.2	3.05	43	--	--	--
31.2	3.05	47	--	--	--

(Concluded)

Table 7

Chamber Separation Distance Required to Prevent Sympathetic Detonations--Comparison of Derived (Recommended) Values with Current Safety Standard

Loading Density kg/m^3	Chamber Separation		
	Spalling m	Tunnel Closure m	Safety Standard m
1.6	0	0	11.05
3.2	0	0	13.92
4.8	0	0	15.94
8.0	0	0	18.89
16.0	0	0	23.80
32.0	0	0	29.99
64.0	0	4.77	37.79
96.0	0	10.73	43.26
160.0	2.69	29.81	51.28
240.0	6.05	47.98	58.70
320.0	10.75	55.40	64.61
400.0	16.88	62.02	69.60

Table 8

Chamber Separation Required to Present Damage to Adjacent Chamber Contents--Comparison of Derived (Recommended) Value with Current Safety Standard

Loading Density kg/m^3	Chamber Separation	
	Recommended m	Safety Standards m
1.6	0	36.83
3.2	0	46.40
4.8	0	53.12
8.0	7.45	62.98
16.0	29.81	79.35
32.0	55.46	99.97
64.0	78.43	125.95
96.0	96.06	114.18
160.0	124.01	170.05
240.0	151.88	195.69
320.0	175.38	215.38
400.0	196.32	232.01

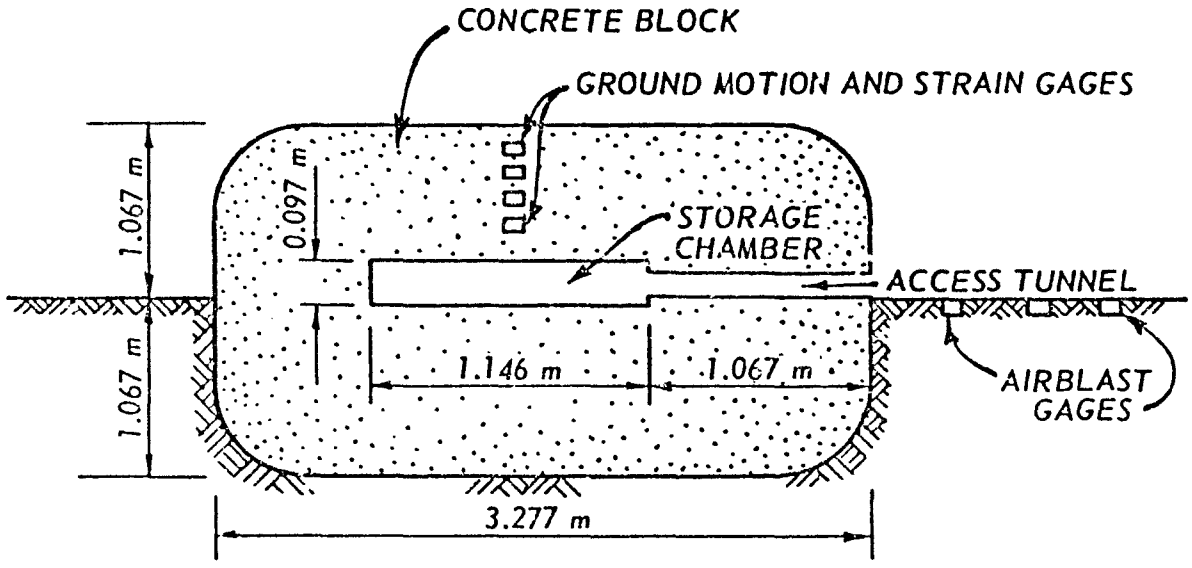

Figure 1. Schematic of underground storage facility model.

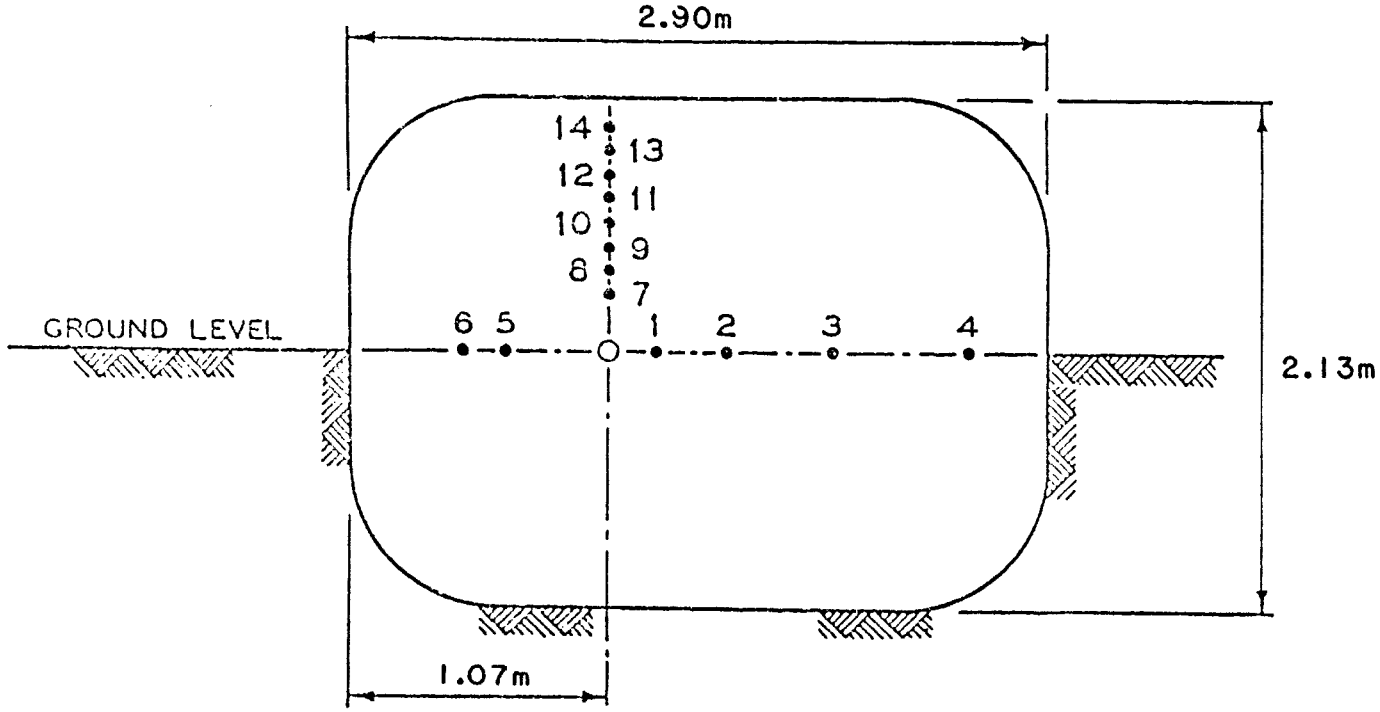

Figure 2. Vertical cross-section of model (normal to chamber/tunnel axis), showing location of the ground motion gages.

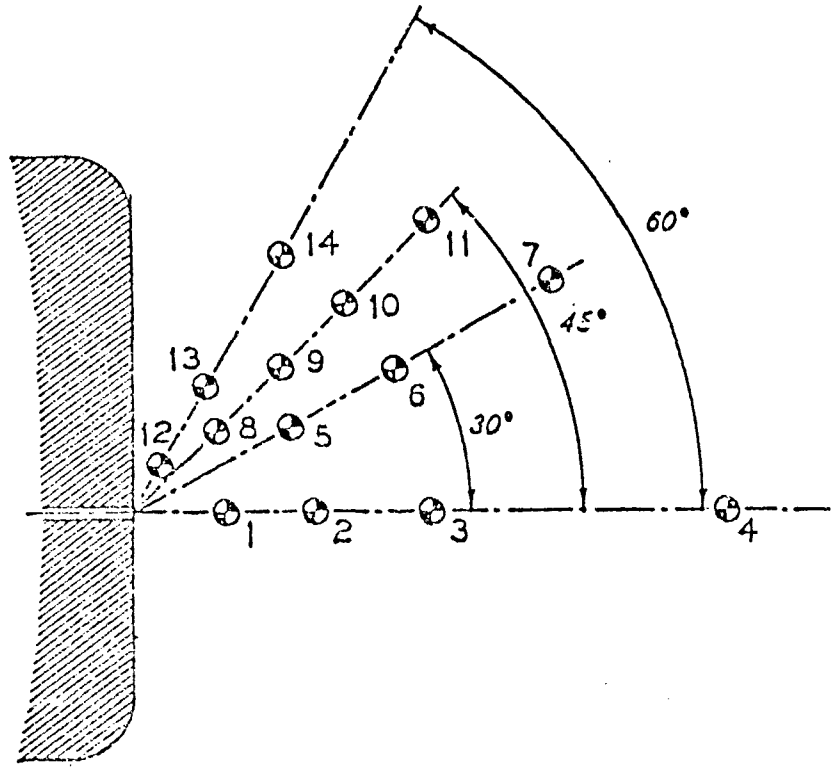

Figure 3. Plan view of model, showing location of external airblast pressure gages.

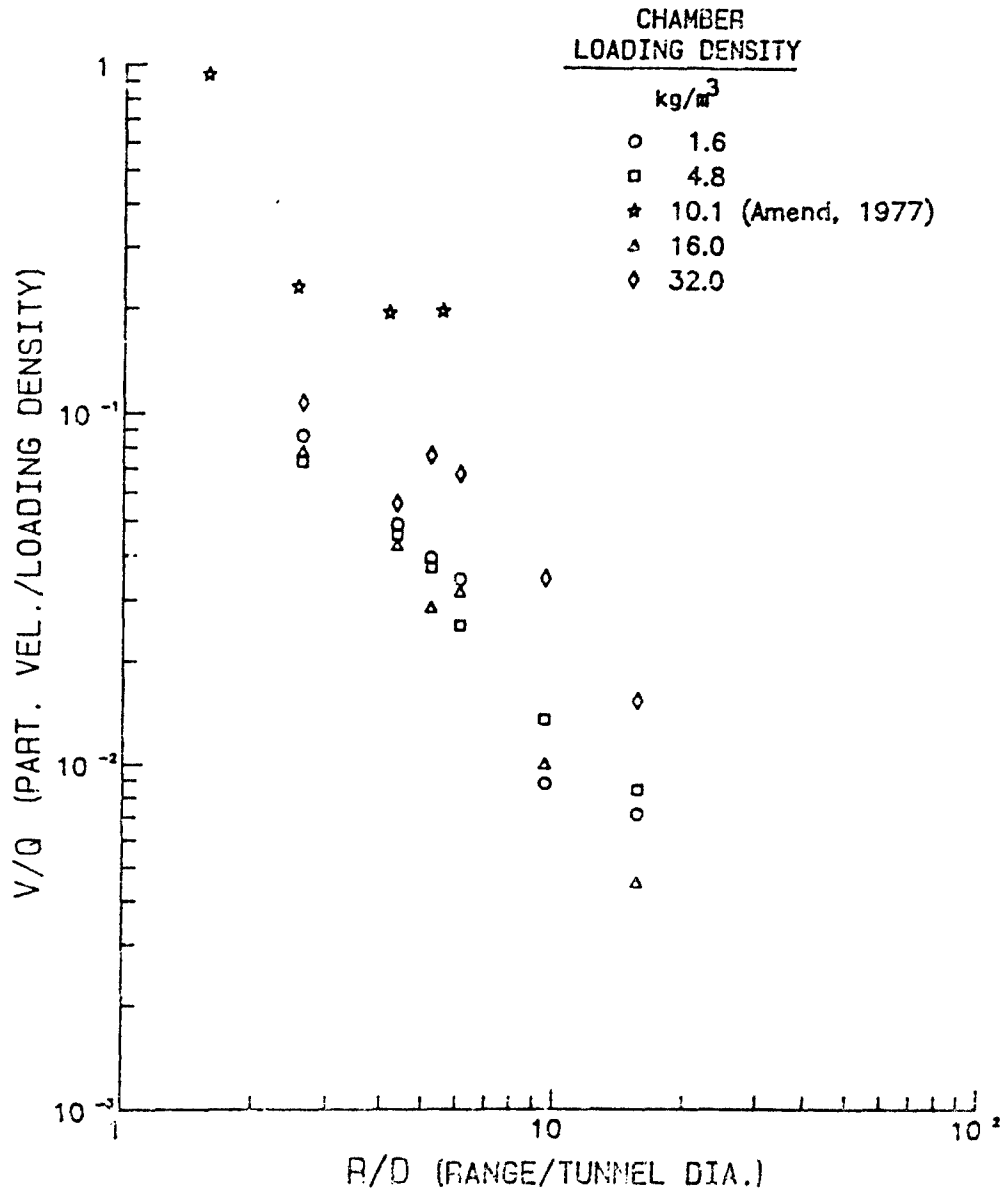

Figure 4. Normalized peak particle velocity versus dimensionless distance from center of chamber.

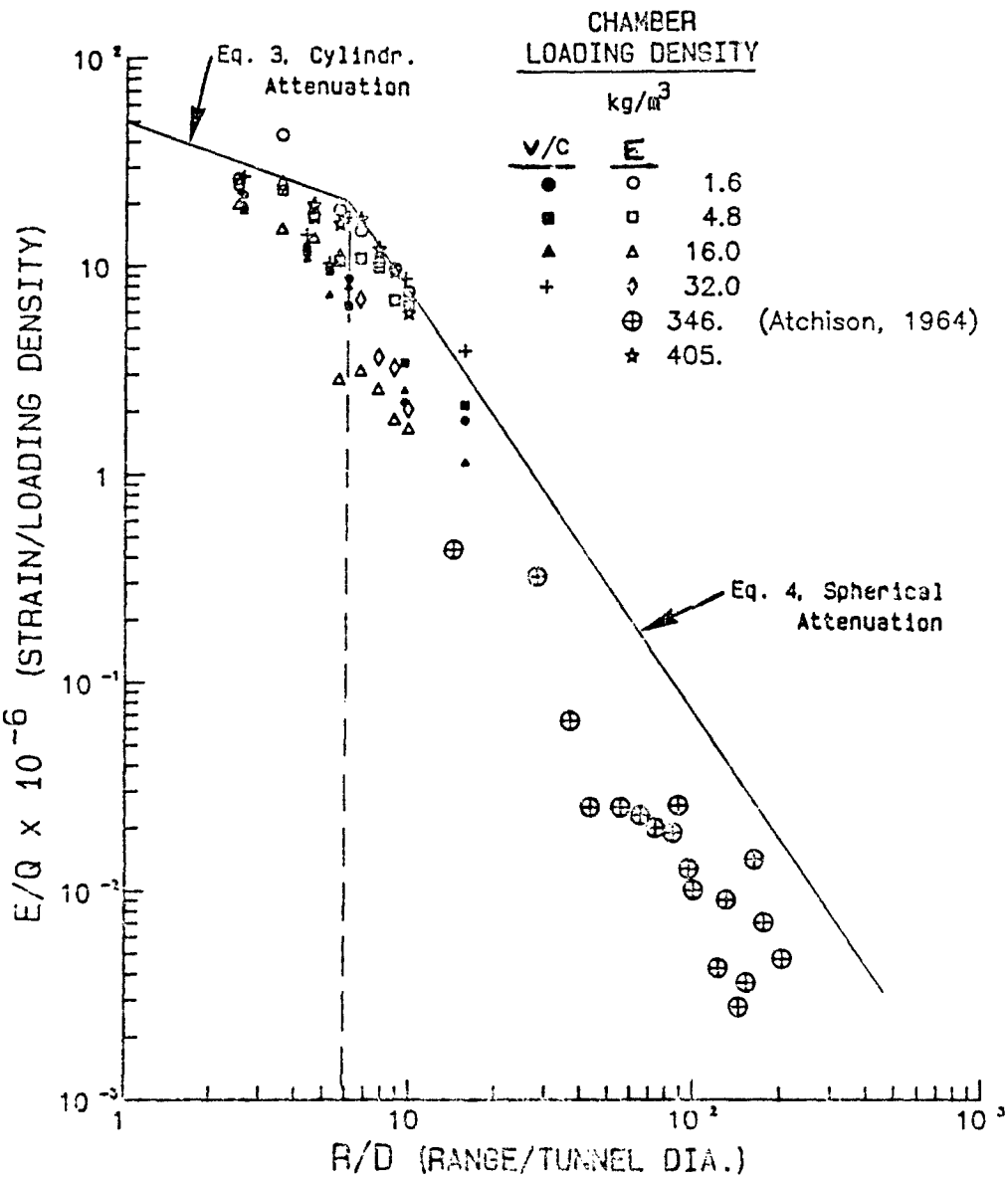

Figure 5. Normalized strain data as a function of dimensionless distance.

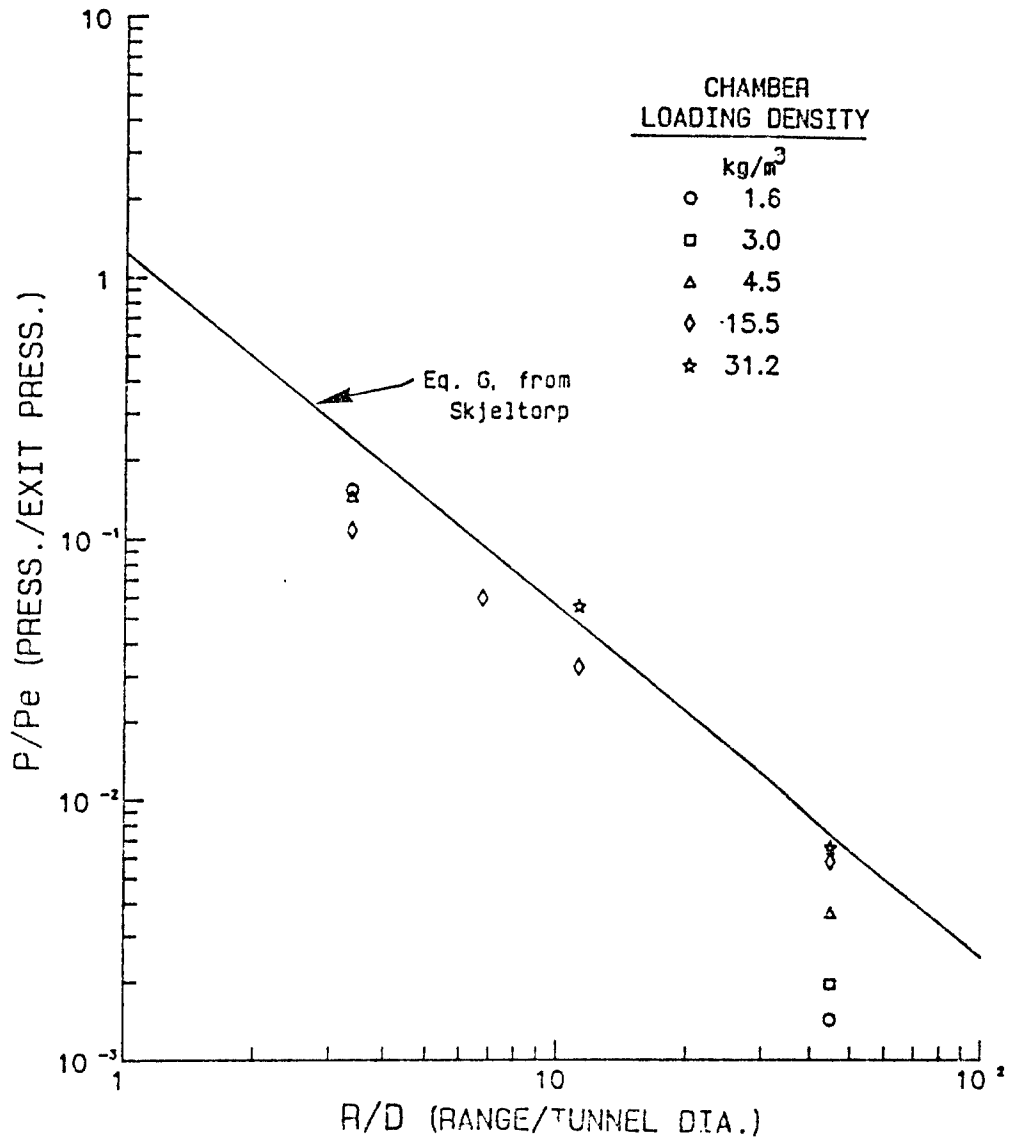

Figure 6. Normalized airblast pressure along the extended tunnel centerline as a function of dimensionless distance.

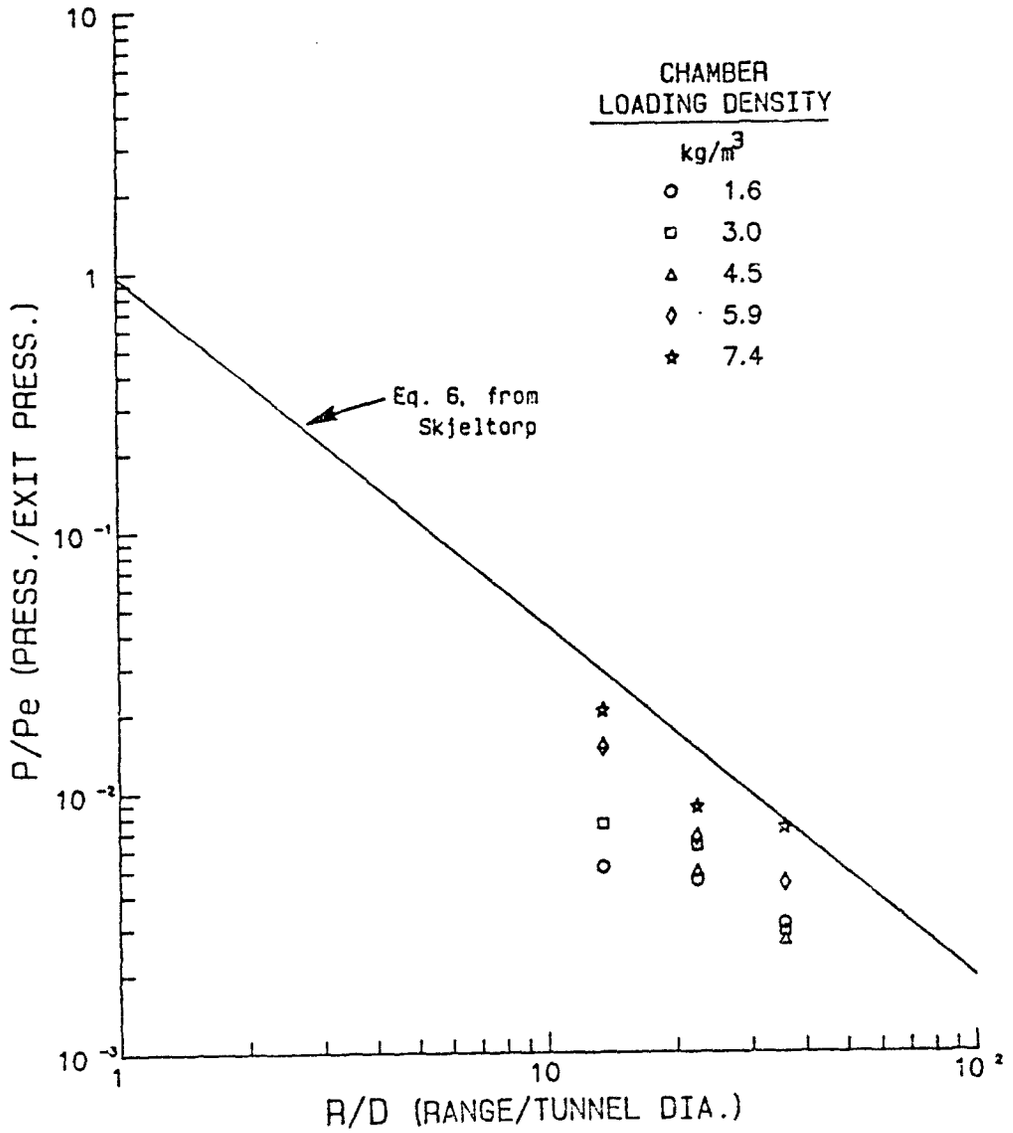

Figure 7. Normalized external airblast pressure 30° from extended tunnel centerline as a function of dimensionless distance.

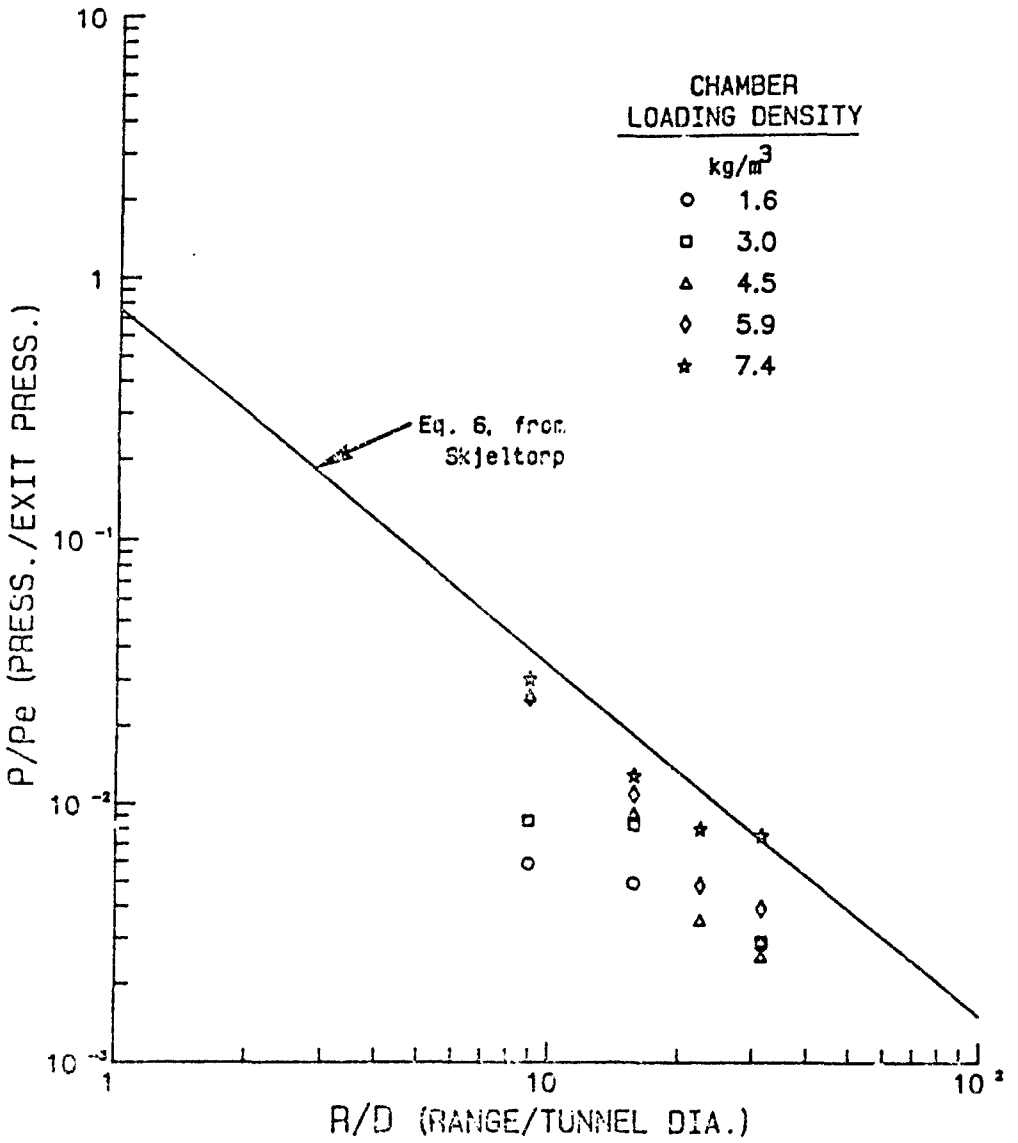

Figure 8. Normalized external airblast pressure 45° from extended tunnel centerline as a function of dimensionless distance.

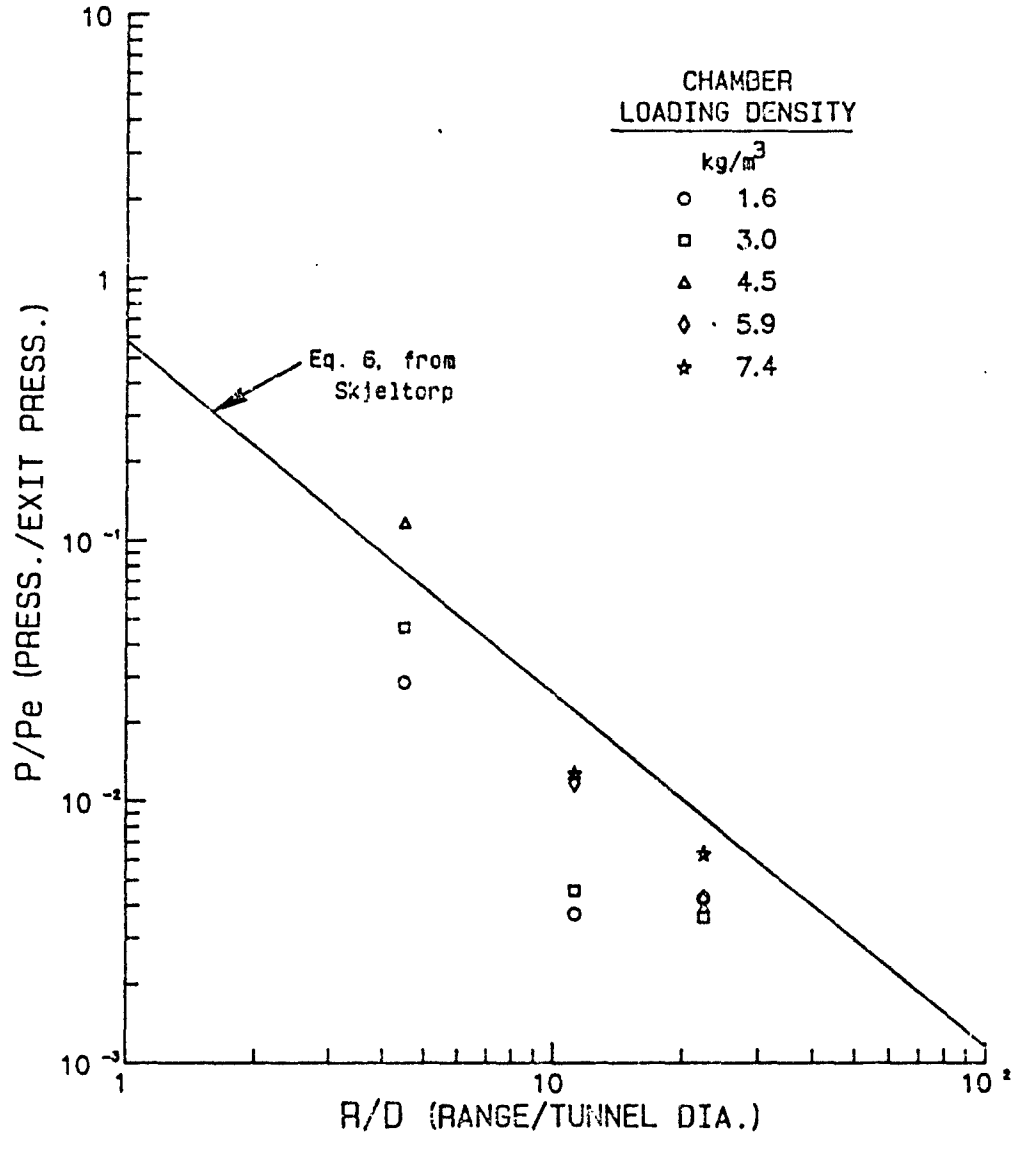

Figure 9. Normalized external airblast pressure 60° from extended tunnel centerline as a function of dimensionless distance.

UNDERGROUND STORAGE IN UNLINED ROCK TUNNELS: ROCK MECHANICS CONSIDERATIONS IN ESTIMATING DAMAGE LEVELS

William J. Johnson, Geophysicist and Project Manager
Arnon Rozen, Head - Protective Design Group
Paul C. Rizzo Associates, Inc.
Pittsburgh, Pennsylvania

ABSTRACT

The most commonly applied means of designing an unlined underground opening in rock to resist underground blast loads from an external detonation is to use empirical relationships of damage versus size of charge and distance developed during the 1950's. However, these relationships do not adequately consider the quality of the rock mass. Previously unpublished test data have been reviewed and a means developed to incorporate rock quality in the estimation of probable damage using a correction factor to peak particle velocity based on RQD. These results represent a first step in the use of rock mass characteristics to define probable damage levels from underground blast loadings, but a considerable amount of new data would be required if all possible means of characterizing a rock mass are to be considered.

INTRODUCTION

Underground siting of industrial, commercial, and defense installations is becoming increasingly popular based on both economic and environmental considerations. When these underground installations are used to store highly hazardous materials or used for safe ammunitions storage, they must be designed to resist the expected levels of dynamic ground motions caused by either an external detonation above them or an internal detonation within an adjacent cavern.

A substantial amount of work to evaluate the effects of blasts and blast propagation phenomena within tunnels through studies of underground ammunition storage magazines has been done by the Norwegian Defense Construction Service (Skjeltorp et al., 1975a, 1975b; Helseth and Jenssen, 1986). This excellent work has been directed mainly towards blast propagation in various tunnel systems and the related aboveground safety-distance determinations as dependent on explosive quantities. Comparable work has not been published for prediction of the effects of external blasts.

In order to achieve a safe design, it is necessary for the engineer to be able to predict the ground motions and to establish the damage criteria. The two major analytical methods available to engineers, numerical and empirical, have severe limitations. The highly developed numerical codes with their multi-parameter rock (or soil) models call for a large amount of site-specific data which are usually unavailable, and the costs required to obtain them are often too high to justify the use of comprehensive dynamic analyses. Purely empirical methods suffer similarly because the data base for their development is limited and the relationships derived may be overgeneralized.

The purpose of this paper is to present some practical engineering relationships to be used in estimating the damage levels along the unlined rock surface of tunnels due to underground detonations by rock-penetrating weapons or explosions in adjacent storage chambers. The intent of this work is to complement work done by the Norwegians in evaluating underground inter-magazine phenomena, especially in jointed, soft and medium-strength rocks. Damage levels are correlated with the detonation input in the form of expected ground motions and the cracking and fall of stones from the tunnel walls.

The basis for the empirical relationships presented in this paper are previous studies and unpublished experimental data gathered by one of the authors (A. Rozen). As such, the relationships presented are considered to represent an improvement over previous presentations, but it is emphasized that the available data base is not complete enough to confidently predict tunnel behavior under all possible site conditions. Accordingly, the empirical approach presented herein is suggested as being appropriate for a preliminary analysis in a feasibility study stage of a project.

UNLINED TUNNEL CONDITIONS

Unlined tunnels used to be commonly specified if sound rock conditions were present, but today many designers prefer to specify a minimum thickness of shotcrete even in good rock. The use of shotcrete improves the safety and stability of the opening by minimizing stone-falls, preventing weathering, sealing open cracks and joints, adhering loose material to the rock mass, etc.

In the discussion that follows, the term "unlined tunnel" includes also tunnels with spot shotcrete up to 5 centimeters in thickness, continuous shotcrete up to 2.5 centimeters thick and spot bolting.

Thicker continuous shotcrete (reinforced or unreinforced) of 7.5 cms and above, and continuous-pattern rock bolting should be treated as lined tunnels, as the structural behavior of the liner and the relative stiffness of the lining system and the surrounding rock mass substantially influence the potential for damage.

DAMAGE MECHANISMS

Damage mechanisms from underground detonations in unlined rock tunnels are a function of the mechanical properties of the rock mass and the local breakage and deformations caused during the construction period as affected by the construction method. Every construction method used to excavate an opening in rock produces some damaged or loosened rock surrounding the excavated opening, and every excavated rock cavity is therefore surrounded by a zone of relatively weak rock. The extent of the damage, both as related to the propagation of damage into the rock mass and the type of damage (loosening of existing joints, opening of new cracks, etc.) is a function of the tunnel geology and history. In particular, the vibratory motions caused by propagating shock waves can trigger movements such as slabbing of already overstressed zones or along loosened gouge-coated joints.

A vivid description of the damage patterns caused by underground detonations was given by Engineering Research Associates (ERA, 1953). The series of tests involved detonation of 145 kilograms to 145 tons of TNT located above and slightly off axis from tunnels of two to ten meters in diameter in sandstone, limestone, and granite.

The damage was classified into four zones (Figure 1). Zone 1 was defined as a complete cave-in or a "tight closure" of the opening with an upward crater or "chimney" reaching the ground surface. Zone 2 was characterized as having "heavy damage" or "general failure" including large joint movements, opening of many new cracks, and high-speed ejection of loose stones of all sizes, including heavy ones. Zone 3 was defined as "medium damage" or "local failure" and was similar to the damage in Zone 2 but with smaller initial velocities imparted to the falling stones, small movements of stones in general, and smaller mass per impact in particular. Zone 4 was defined as "light damage" or "intermittent failure" and involved smaller stones falling at lower speeds or even "free fall", some sliding along existing joints, some opening of new cracks, fall of already loose stones, etc.

The importance of the natural rock discontinuities, such as joints, fractures, seams, and faults, becomes more significant as the observer moves from Zone 1 to Zone 4. The natural discontinuities tend to reduce the stiffness and the strength of the rock mass as compared to those for the intact rock, and the vibratory motions caused by the detonation tend to trigger motions or instability of joints already in a loosened condition. At relatively small levels of vibration, damage mechanisms are controlled by natural and man-induced fracturing immediately adjacent to the underground opening.

CRITERIA FOR SELECTING GROUND MOTION PARAMETERS AS INDICATIVE OF TUNNEL DAMAGE

As discussed by Dowding and Rozen (1978), the use of peak ground motion as a damage index is still an accepted practice. The three measured or calculated ground motion indices are peak ground acceleration, peak particle velocity, and peak displacement, but strain is becoming a fourth parameter which has been used successfully to relate ground motion to damage.

In addition to the peak ground motion values, the frequency content of the vibratory motion as defined by response spectra, is also important in assessing damage potential. High frequency vibrations, which are normally related to blasting effects, contribute to the possibility of relative displacement between rock blocks along planes of weakness. As such, the high frequency components which tend to concentrate the transient stresses may control the local spalling of rock. Fortunately, the attenuation of the high frequency component of ground vibration is faster than the rest of the motion.

Available data does not permit us, even today, to prefer a certain peak motion parameter as being the best indicator of damage, as all correlations have a significant amount of uncertainty and scatter. At present, peak particle velocity is the parameter preferred by those dealing with blast vibrations, while peak acceleration is usually used by earthquake engineers. Displacements are not commonly assessed because the sensors used to record vibrations are normally based on measuring accelerations or velocities, making

it necessary to mathematically calculate displacements, a process which may produce baseline errors. Hendron (1977) emphasized the use of strains as a better damage measure. Strain may be measured directly as an independent variable, as done during the ERA (1953) tests, but in many cases it is a common practice to estimate S (strain) using:

$$S = V/C \qquad (1)$$

where: S = strain, percent
V = particle velocity in m/sec
C = seismic velocity in m/sec

The circumferential strains, which lead to damage, can be calculated both from the compression wave propagation velocity, as is the practice in the evaluation of blast vibrations or from shear and Raleigh waves, as is common in earthquake engineering. Given the possibilities for using different ground motion parameters, it is recommended that the prudent analyst use more than a single measure, and after comparing the various results the analyst should use his experience to judge which one best fits the specific case.

RECOMMENDED RELATIONSHIPS

Peak acceleration data based on the ERA (1953) tests were presented by the U.S. Army Engineers (USAE, 1961) in the form of:

$$A = 0.005 \left(\frac{R}{W^{1/3}}\right)^{-3.9} \times \frac{C^2}{W^{1/3}} \qquad (2)$$

where: A = peak acceleration in g
R = range in meters
W = charge weight in kg
C = seismic velocity in m/sec

A set of tests was carried out during the 1980s, using 500 kilograms TNT charges (Rozen, 1985). These tests were conducted in soft limestone and chalk formations and suggested a somewhat more conservative correlation:

$$A = 0.006\left(\frac{R}{W^{1/3}}\right)^{-3.6} \times \frac{C^2}{W^{1/3}} \qquad (3)$$

It is of importance to note that the peak acceleration was not defined as a function of the scaled distance alone and that both the rock mass properties as indicated by the seismic velocity and charge size are influencing factors, as shown in the C^2 and $W^{1/3}$ terms, respectively. Figures 2a and 2b present the attenuation of peak acceleration with distance for 500 kilograms TNT charges which were fully buried and coupled. It should be noted that for the case of an accident within an underground magazine, the expected coupling will be highly reduced, as the functional arrangement of ammunition stacks within the cavern usually calls for certain free space between the ammunition and the rock walls to assure service, handling, and inspection. Figure 3 presents a comparison between the ERA (1953) data and the new information presented here.

Peak particle velocity data from the ERA (1953) tests lead to:

$$V = 1143 \left(\frac{R}{W^{1/3}}\right)^{-2.8} \quad (4)$$

where: V = peak particle velocity in cm/sec

Again, the new tests conducted in soft chalk formations predict a slightly higher ground motion than the ERA (1953) tests.

$$V = 1200 \left(\frac{R}{W^{1/3}}\right)^{-2.7} \quad (5)$$

Figure 4 compares the attenuation of peak particle velocity with distance, comparing the ERA (1953) data with the new data gathered in chalk.

The peak displacement was also documented by the ERA (1953) data:

$$D = 9.13 \times W^{1/3} \left(R/W^{1/3}\right)^{-2.7} \quad (6)$$

where: D = peak displacement in cms

and the 1980's data from soft chalk are given by:

$$D = 13.78 \times W^{1/3} \times \left(R/W^{1/3}\right)^{-2.4} \quad (7)$$

These data are compared on Figure 5a, while the details of the attenuation in the soft chalk are presented on Figure 5b.

It should be noted that for all three ground motion parameters, the new results from soft chalk systematically indicate a larger ground motion for a given distance and charge size than the older data obtained from hard rock. It is not well established if the differences are dependent only on the rock and explosive characteristics or are also influenced by the differences in measuring techniques and instrumentation developed during the last 30 years. It is usually assumed that hard, competent rocks attenuate motion less than soft rocks, but the new results indicate an apparent contradiction.

As strains were not measured independently in the recent tests in chalk, all strains used for damage correlations were calculated based on Equation 1, where the seismic velocity was taken to be 800 meters per second.

The ERA (1953) data are given as:

$$S = 0.004 \left(\frac{R}{W^{1/3}}\right)^{-1.9} \text{ in cm/cm} \quad (8)$$

Both curves are plotted on Figure 6. In this case, the older data taken from hard rock are significantly more conservative at distances less than about 40 meters.

Dominant frequencies of the shock waves at varying distances for a given explosive charge can also be compared for both the ERA (1953) and recent data. As expected, both exhibit the phenomenon of a shift to lower

predominant frequencies for a given distance, but the recent data from soft rock indicates a significantly higher frequency content for a given charge and distance than for the ERA hard rock sites (Figure 7). This change in predominant frequency versus distance is also illustrated for the chalk site by means of smoothed response spectra of the ground motion at varying distances on a 500 kilogram charge (Figure 8).

DAMAGE CRITERIA

Once potential indicators of damage have been defined, it is necessary to relate them to actual damage to the tunnel. Emphasis has been placed on peak particle velocity as this is the most commonly applied parameter; it has the advantage of being essentially frequency-independent; and the problems associated with its use are common to whatever parameter is considered.

The main difficulty with the use of any of the existing indicator parameters to predict damage, as pointed out by Hendron (1977), Dowding and Rozen (1978), Owen and Scholl (1981), and others, is that absolute values of the parameters give only a general indication of the actual damage, i.e., the data exhibit a large scatter. Part of the problem is that the use of seismic velocity alone is a poor criteria for characterizing the mechanical properties of the rock mass. For example, the same particle velocity in an intact, soft rock might cause less damage than in a highly fractured, hard rock, even though the seismic velocity of both might be the same. Rock fracturing is an additional property that should be incorporated in evaluating the potential of a tunnel to blast damage.

As a first approximation, an attempt has been made to incorporate the concept of RQD (Deere, 1974) into the prediction of damage from blast loads. Using peak particle velocity as the indicator parameter, the use of an "effective" velocity to define damage is proposed. Rock tunnel damage indices for velocities in intact rock are provided in Table 1 as "effective" velocities. If the rock in which the underground opening has been excavated is not intact, i.e., has an RQD lower than 100, then the anticipated or measured particle velocity should be multiplied by a correction factor as shown on Figure 9. This correction factor, based on results from the tests in chalk, appears to have a least squares fit to the following relationship:

$$CF = (100/RQD)^{0.85} \qquad (9)$$

where CF is the correction factor and RQD is the rock quality designation. The form of this equation for RQD values of less than 50 is speculative. The least squares fit for RQD values greater than 50 may overpredict the correction factor for lower RQD values as shown as the upper bound curve on Figure 9. A linear extrapolation to lower RQD values as shown as the lower bound curve may be more appropriate, but this is highly judgmental. For this reason, the area between the lower and upper bound curves is shaded. The problem, however, may be mute, as it is unlikely that tunnels used for storage will be unlined if the RQD values are below 50.

As an example of a damage calculation, assume that the charge size and distance evaluation has been completed and a peak particle velocity of 20 centimeters per second has been derived. This number is essentially a valid indicator of damage (in this case lack of damage) as per Table 1, if the rock quality is excellent. If the RQD of the rock mass is 50, however, then the effective velocity is 36, which implies the fall of stones and minor tensile slabbing. For RQD values lower than 50, it is assumed that the tunnel is lined.

SUMMARY

Previously unpublished results of experiments to assess the stability of unlined openings in rock against blast loads have been used to reassess commonly used empirical relationships for tunnel design. These new data, taken from a chalk environment, indicate consistently higher values of ground motion for a given charge and distance than data obtained from earlier tests in hard rock (ERA, 1953). It is not clear if this discrepancy is due to the presence of chalk versus granite, sandstone, or limestone, or due to differences in measurement techniques. An important observation from the new tests, however, is that the quality of the rock mass is important in predicting damage.

Previously used empirical relationships to predict damage in an unlined rock opening from an underground blast (ERA, 1953) characterized the rock mass using only seismic velocity. Analysis of new data with detailed information on RQD indicates that knowledge of rock fracturing is also important if damage is to be reliably predicted. RQD has been used to derive a correction factor to the derivation of peak particle velocity as a damage indicator.

The use of RQD in predicting damage to an unlined rock opening is considered to represent an improvement over previously used empirical relationships. However, the use of RQD is only a first step in defining the rock mass. The use of other, more comprehensive relationships, such as those of Barton et al. (1974) or Bieniawski (1979), could lead to even better means of predicting damage. Unfortunately, most of the empirical data available, including data gathered for purposes of earthquake engineering as well as underground blasting, do not contain sufficiently detailed descriptions of the rock mass. A considerable amount of new data taken under highly controlled conditions will be required if any additional improvement to the means of predicting the blast damage in unlined tunnels is to be achieved.

REFERENCES

Barton, N., R. Lien, and J. Lunde, 1974, "Engineering Classification of Rock Masses for the Design of Tunnel Support," Rock Mechanics, Vol. 6, No. 9, pp. 183-236.

Bieniawski, Z. T., 1979, "Tunnel Design by Mass Classification," USAE-WES, Technical Report GL-79-19, AD-A076 540.

Cecil, D. S., 1976, "Correlations of Rock Bolt-Shotcrete Support and Rock Quality Parameters in Scandinavian Tunnels," Ph.D. Thesis, University of Illinois, Urbana.

Deere, D. U., 1974, "Technical Description of Rock Cores for Engineering Purposes," Rock and Engineering Geology, Vol. 1, No. 1, pp. 17-22.

Dowding and Rozen, 1978, "Damage to Rock Tunnels from Earthquake Shaking," Journal of the Geotechnical Engineering Division, ASCE, GT2, pp, 175-191.

Engineering Research Associates, 1953, "Underground Explosion Test Program," Final Report - Rock, U.S. Army Corps of Engineers, Sacramento District.

Helseth, E.S., A. Jenssen, 1986, "Underground Ammunition Storage Magazines, Blast Effects from Accidental Explosions," Norwegian Defense Construction Service, Oslo.

Hendron, A. J., 1977, "Engineering of Rock Blasting on Civil Projects," Structural and Geotechnical Mechanics, W. J. Hall, ed., Prentice Hall, Englewood Cliffs, N.J.

Owen, G. N., R. E. Scholl, 1981, "Earthquake Engineering of Large Underground Structures," FHWA/RD-80/195, PB 81-247918.

Rozen, A., 1985, Unpublished Test Results.

Skjeltorp, A. T., T. Hegdahl, A. Jenssen, 1975, "Underground Ammunition Storage, Blast Propagation in Tunnel System," Norwegian Defense Construction Service, Oslo.

U.S. Army Engineers, 1961, "Design of Underground Installation in Rock - Penetration and Explosion Effects," TM-5-857.

TABLE 1

ROCK TUNNEL DAMAGE INDICES

DESCRIPTION	EFFECTIVE PEAK PARTICLE VELOCITY (cm/sec)
No damage of unlined tunnel	≤20 (8)
No new fractures in intact rock	≤25 (10)
Fall of stones and minor tensile slabbing in unlined tunnel	30 to 55
Formation of new cracks and mainly tensile but some radial	above 60
Hairline cracking of shotcrete	above 90
Shearing cracking of shotcrete	above 120
Light damage or intermittent failure (Zone 4) in underground test series	90 to 180
Medium damage or local failure (Zone 3) in underground test series	180 to 330
Heavy damage or general failure (Zone 7) in underground test series	above 300

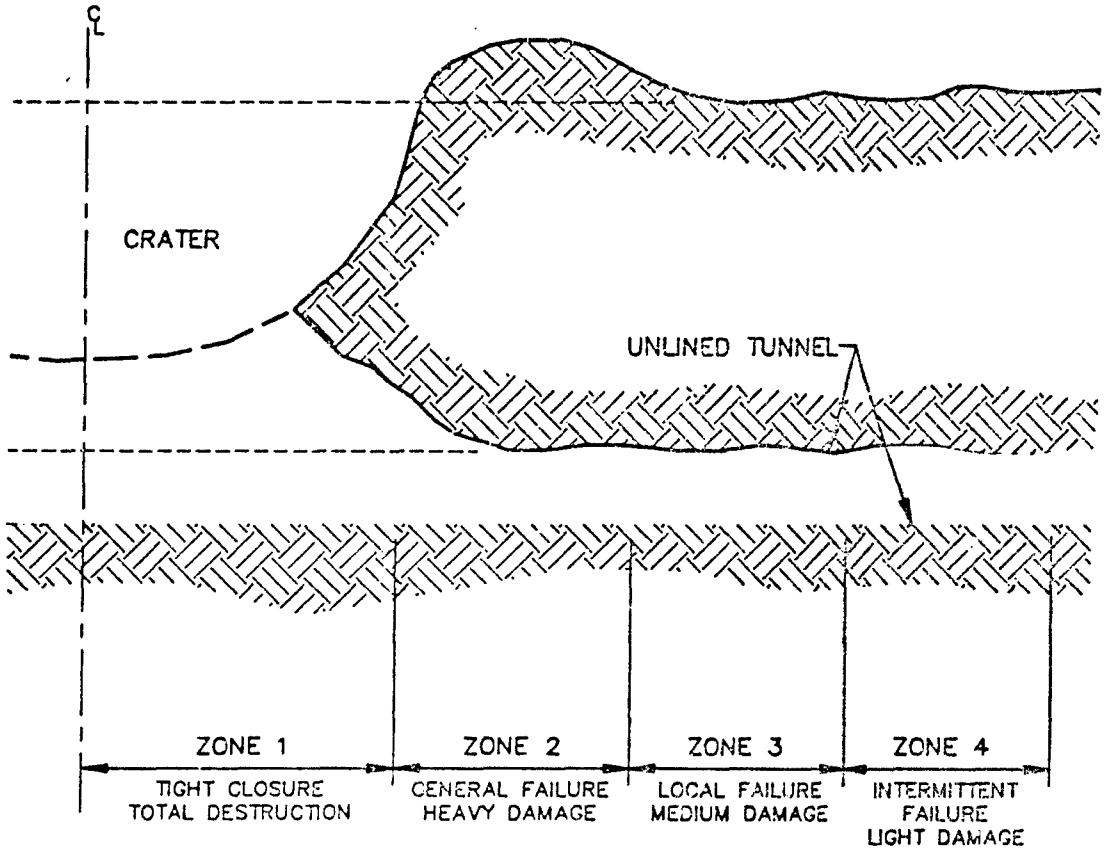

FIGURE 1: DAMAGE ZONES IN UNLINED TUNNEL TESTS.

(BASED ON ENGINEERING RESEARCH ASSOCIATES TEST PROGRAM)

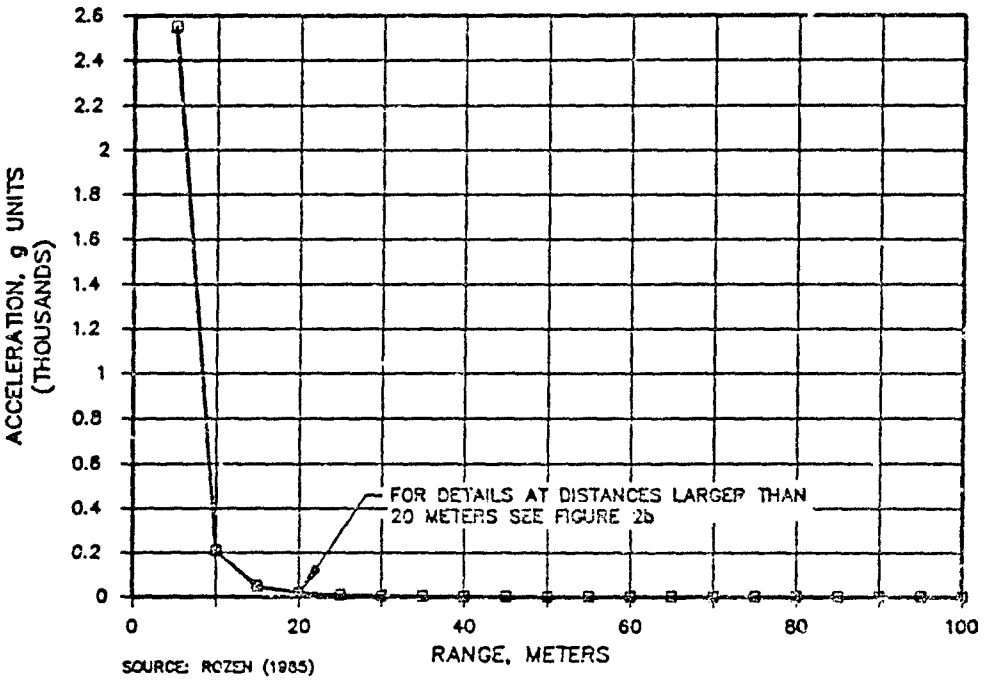

FIGURE 2a: ACCELERATION IN CHALK
500 kg TNT FULLY COUPLED

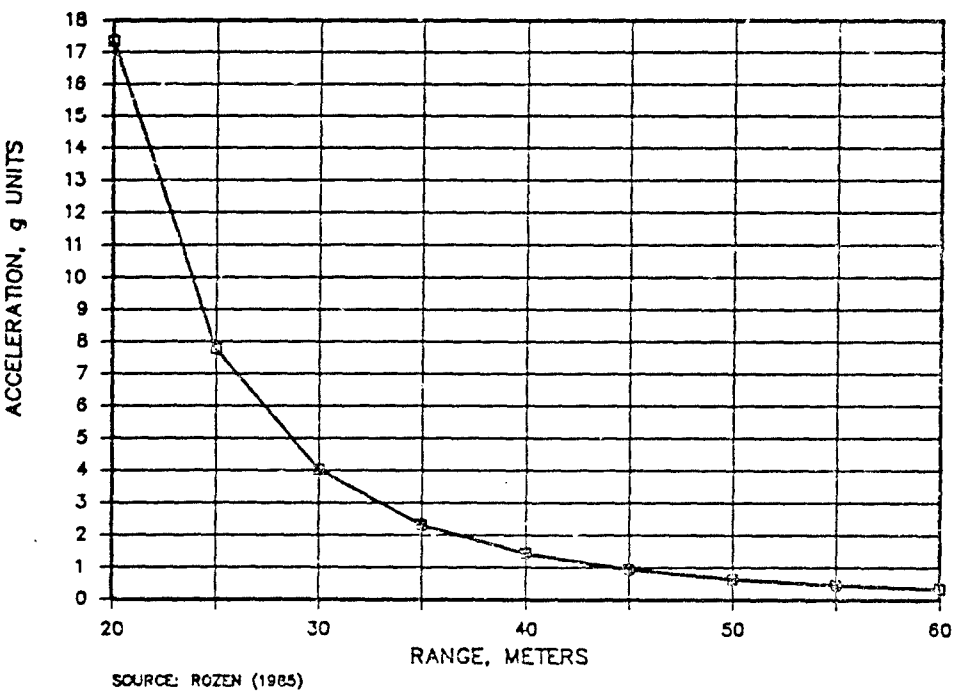

FIGURE 2b: ACCELERATION IN CHALK
500 kg TNT FULLY COUPLED

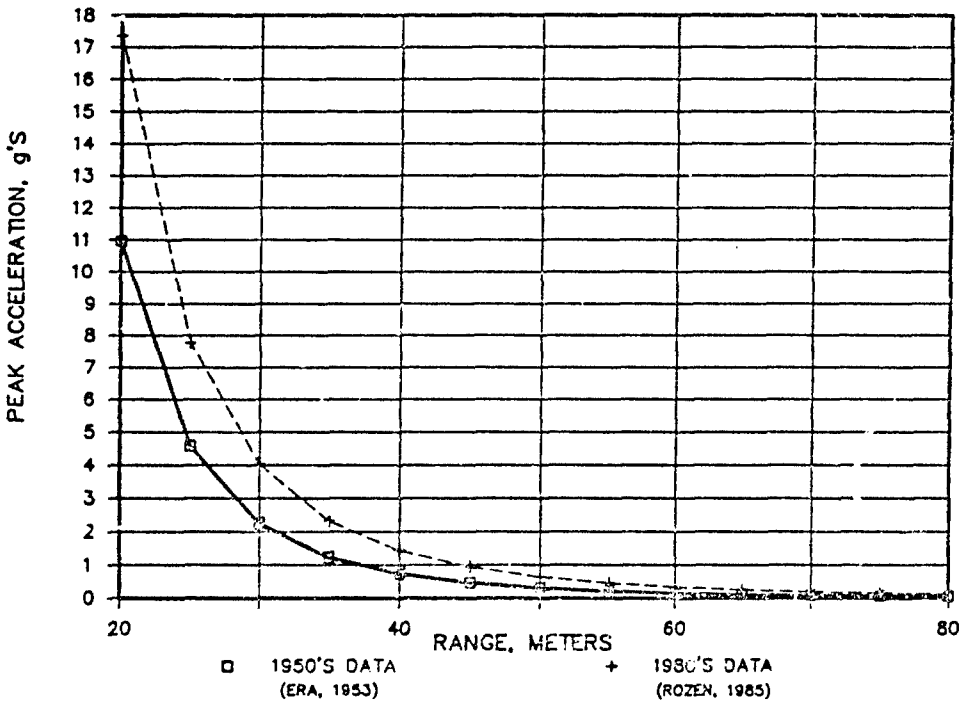

FIGURE 3: COMPARISON OF PEAK ACCELERATION
500 kgs TNT FULLY COUPLED

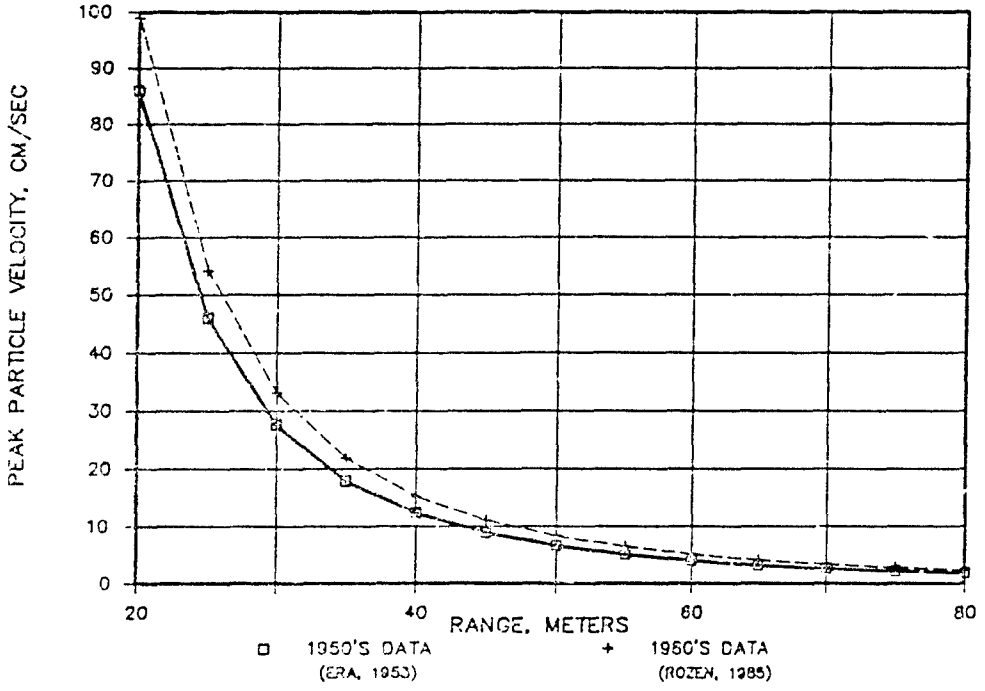

FIGURE 4: COMPARISON OF PEAK PARTICLE VELOCITY
500 kgs TNT FULLY COUPLED

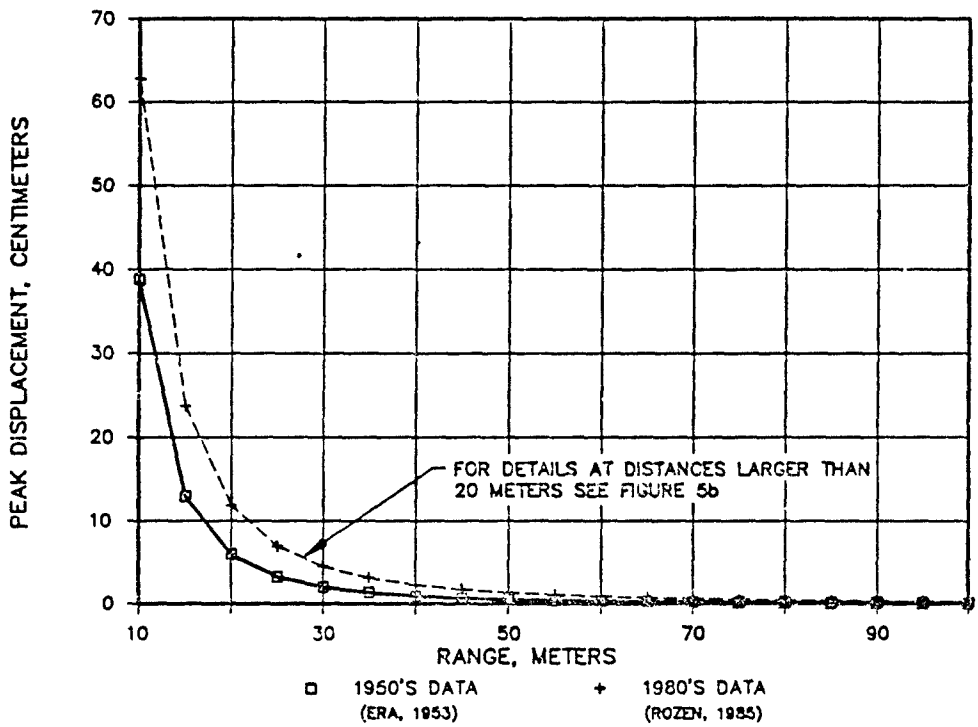

FIGURE 5a: COMPARISON OF PEAK DISPLACEMENT
500 kgs TNT FULLY COUPLED

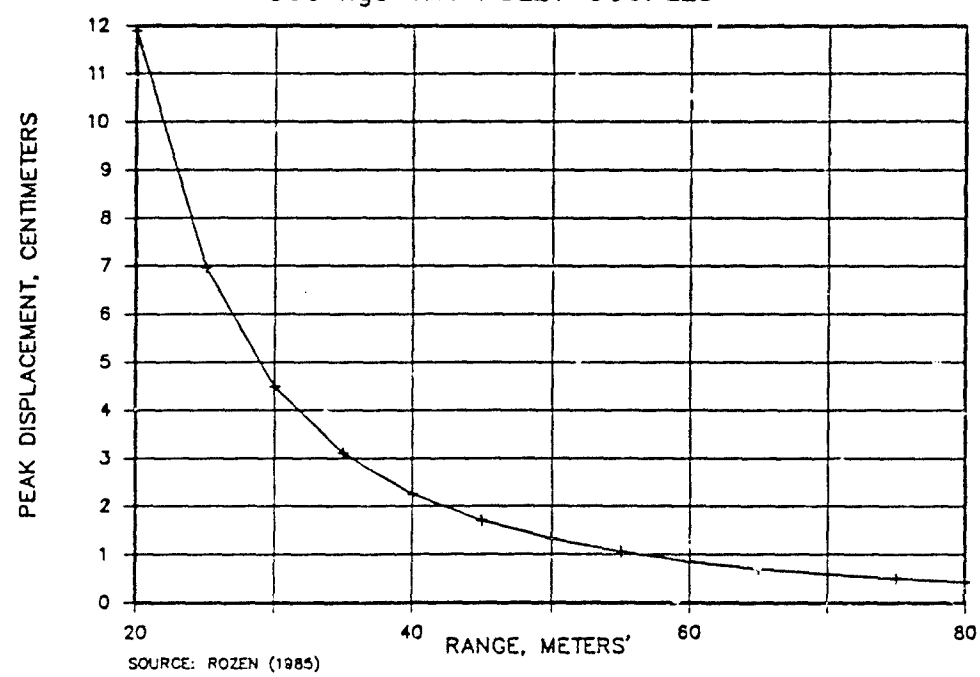

FIGURE 5b: PEAK DISPLACEMENT IN CHALK
500 kgs TNT FULLY COUPLED

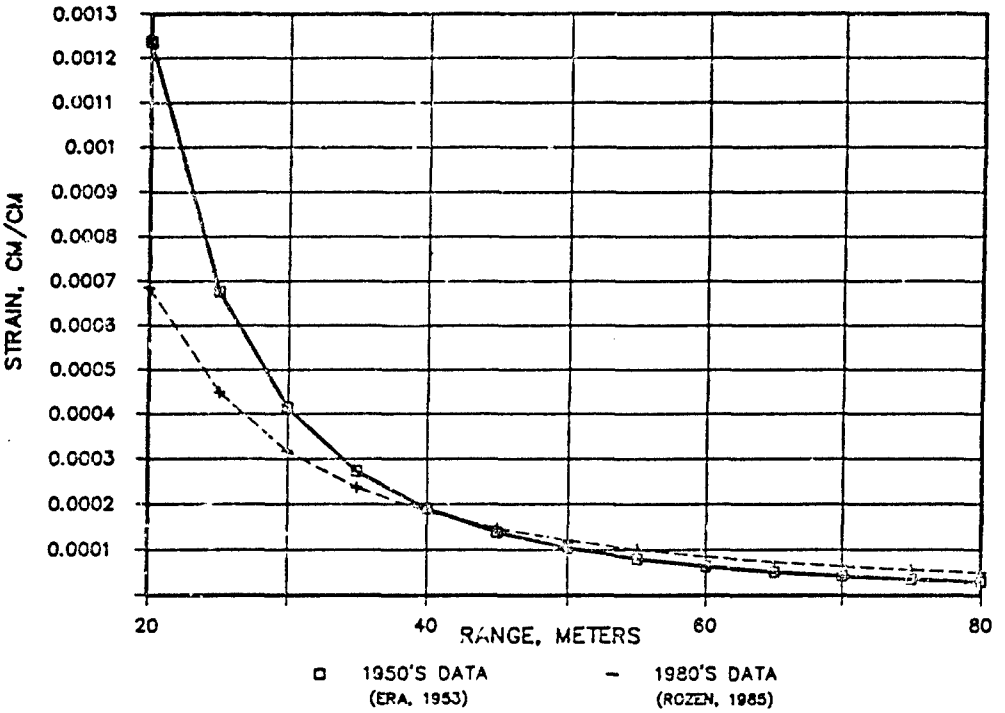

FIGURE 6: CALCULATED STRAIN IN CHALK
500 kgs TNT FULLY COUPLED

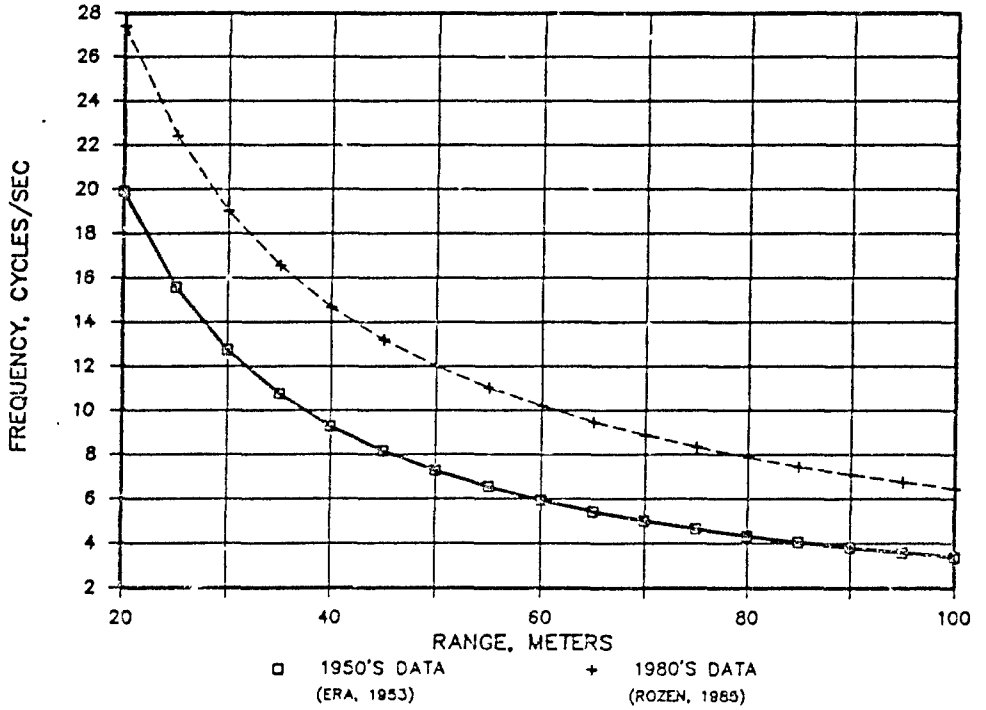

FIGURE 7: DOMINANT FREQUENCY VERSUS DISTANCE
500 kgs TNT FULLY COUPLED

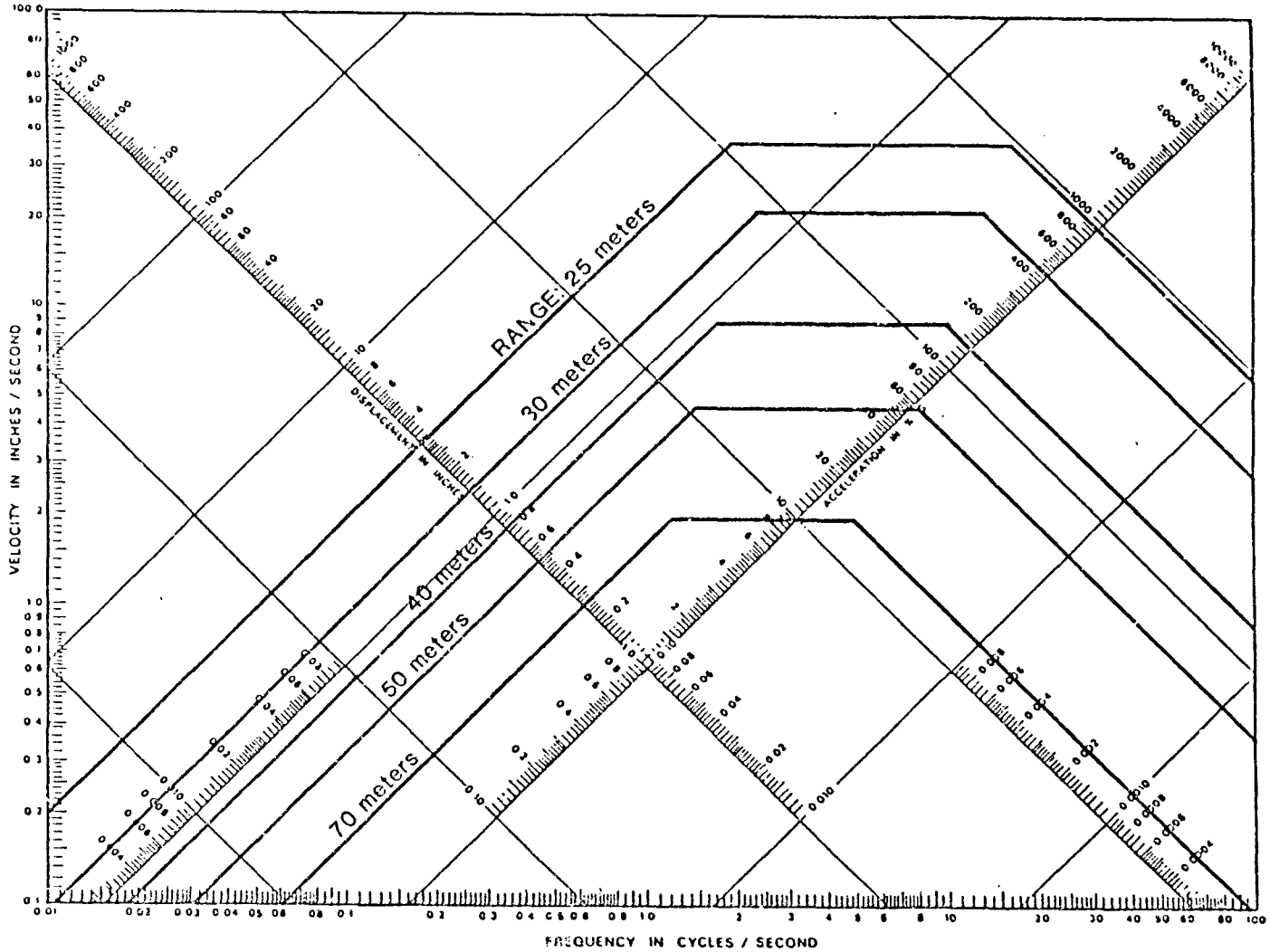

FIGURE 8: RESPONSE SPECTRUM FOR 500 kgs TNT IN CHALK

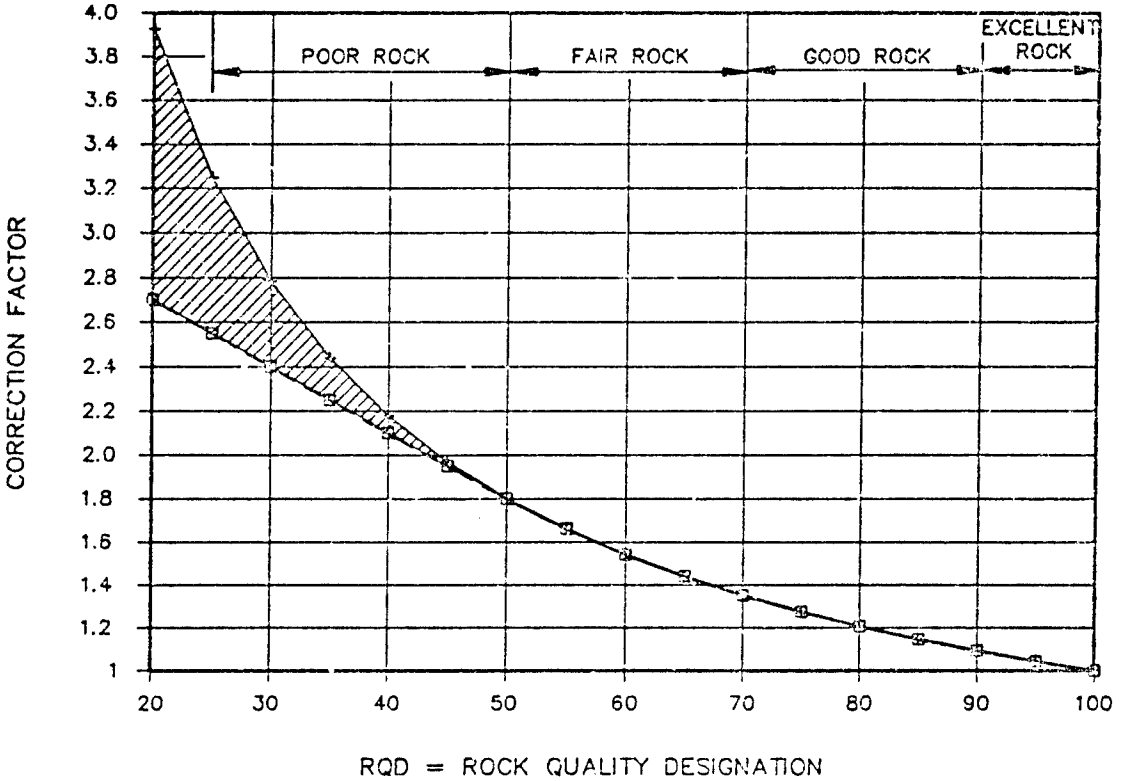

FIGURE 9: DAMAGE–CRITERIA CORRECTION FACTOR TO PEAK PARTICLE VELOCITY

EXPLOSIONS IN SOILS: THE EFFECTS OF SOIL PROPERTIES ON SHOCK ATTENUATION

William J. Johnson, Geophysicist and Project Manager
Arnon Rozen, Head - Protective Design Group
Paul C. Rizzo Associates, Inc.
Pittsburgh, Pennsylvania

ABSTRACT

The pioneering studies of soil attenuation from explosions conducted during WWII by C.W. Lampson deserve to be re-evaluated. Lampson's work provides average values of peak pressure for different charge sizes, couplings, distances, and soils which, based on the authors' experience in conducting similar experiments, stand the test of time very well. The current U.S. Army Engineer's Manual provides design loadings incorporating an undefined, but conservative factor of safety. A review of Lampson's original work provides some insight into this degree of conservatism.

The most critical factor in calculating shock loadings is soil type. The effect of soil in assessing the attenuation of ground motion from explosions is currently based on the engineer's interpretation of data in tabular form. Smooth curves for estimating the soil attenuation constants are presented which hopefully will somewhat facilitate the estimation of appropriate soil constants, both for Lampson's work and modern formulations.

INTRODUCTION

Military and other civil engineers around the world look to the U.S. Army Engineers' (USAE) Manual when they wish to design underground structures to withstand shock loadings from conventional detonations. A drawback to this manual, however, is that it does not provide an indication of the factor of safety associated with the designs. Classified experiments conducted by one of the authors (Rozen, 1986) indicate that the factor of safety associated with defining the peak pressure from an explosion propagating through soil may be rather high. Without compromising security, it can be stated, however, that the original work published by Lampson (1946) does provide reasonably good values of average pressure versus charge size, coupling, distance, and soil type. Given the type of monitoring equipment available at the time, Lampson's contribution to our understanding of shock wave propagation is remarkable.

Soil properties are the most important single variable governing the transmission and attenuation of a shock-induced pressure wave in soil for a given range and amount of explosives. This fact was first documented by Lampson (1946), who noted that different soil types could cause the peak pressure to vary by over two orders of magnitude, whereas coupling effects were found to be less than one order of magnitude. Additional studies published by Drake and Little (1983) and incorporated into the USAE manual

confirm the importance of soil properties. In particular, they note the critical role of moisture content of cohesive and loose granular soils, and of relative density for all granular soils.

Drake and Little (1983) incorporate soil properties into two variables within their attenuation formula. The Lampson relationship requires an estimation of one soil-related variable. Both approaches are limited to the data sets utilized, and a means to estimate their individual parameters are based on tables where soil types are compared to estimate the appropriate constants.

Additional, previously unpublished soil data have been incorporated with the published data sets and plotted so that smooth curves can be drawn through the data points. The purpose of this exercise has been to facilitate estimation of the soil parameters, both for Lampson's and Drake and Little's formulations. It is intended that these curves be used to obtain both best-estimate and recommended design pressures for specific loading conditions.

BACKGROUND - SIGNIFICANCE OF THE SOIL CONSTANTS

During World War II, the Committee of Passive Protection Against Bombing of the U.S. Army conducted a long series of in-situ tests in several soils at various locations within the U.S. (see Table 1). These data were summarized by Lampson (1946) who derived a semi-empirical relationship supported by similitude analysis which correlates pressure attenuation in the soil.

$$P = F \cdot E \cdot k \cdot \lambda^{-n} \qquad (1)$$

where: P = peak pressure, psi

F = coupling coefficient determined as a function of the the depth of burial of the charge

E = an energy factor determined by the type of explosive ($E = 1.0$ for TNT)

k = a constant characteristic of the soil

$\lambda = \frac{R}{W_o^{1/3}}$ = scaled distance, $ft/lbs^{1/3}$

n = an exponent which defines the attenuation rate

R = distance (range), feet

W_o = charge weight, pounds

According to Lampson's findings the attenuation rate was usually a constant ($n = 3$), except for very shallow detonations of less than $\frac{3}{2} W^{1/3}$ feet. At shallower depths, the attenuation becomes greater with n approaching approximately the value of 4. For the common cases with full coupling, n was taken to be 3.

It is important to emphasize that Lampson found that n is influenced by the charge's depth of burial independent of the soil characteristics. All the effects of the soil were presented in his equation by a single soil constant k.

Lampson's results were used by many engineers and, with slight modifications, were incorporated in the USAE (1946 and 1965). This manual was used as a major source of information and as a design guideline for both the U.S. and foreign armies. The next breakthrough was suggested by Drake and Little (1983) and incorporated in the updated version of the USAE Manual (1984).

Drake and Little (1983) suggest a set of equations to define the various ground shock inputs (pressure, impulse, displacement, particle velocity, and acceleration), but our discussion herein will concentrate only on the equation suggested to predict the peak ground pressure:

$$P = f \cdot (\rho c) \cdot 160 \left(\frac{R}{W^{1/3}}\right)^{-n} \qquad (2)$$

where: P = peak pressure, in psi
f = coupling factor
ρc = acoustic impedance of the soil, psi/ft/sec
ρ = mass density of the soil, lb/sec/ft^4
c = seismic velocity in the soil, ft/sec
R = distance (range), feet
W = charge weight, pounds
n = attenuation factor

In this equation, the attenuation factor, n, is not a constant and is dependent on the in-situ soil characteristics contrary to Lampson's findings as discussed above. The influence of the soil characteristics on the ground pressure is given, in the new case, by two variables (n and ρc) and not one as suggested by Lampson. As the values of n for various soils range from n = 1.5 in highly saturated and cohesive soils to n = 3.5 in dry and loose sand, highly diverse results are obtainable, depending on the subjective judgment of the analyst.

In spite of the different equation forms, the formulations of Lampson (1946) and Drake and Little (1983) are actually quite similar. The value of W in Equation 2 is simply $E \cdot W_o$ in Equation 1. The value of ρc in Equation 2 is approximately equivalent to the k value of Equation 1. The main conceptual difference between the two approaches thus lies in the incorporation by Drake and Little (1983) of the variable exponent n.

NEW DATA

One of the authors (Rozen, 1986) was responsible during the period from 1983 to 1985 for conducting a series of tests of soil attenuation, similar to those reported by Lampson (1946) and Drake and Little (1983). The soil characteristics and their attenuation characteristics are provided in Table 2. The data presented in Table 2 were chosen from three independent test series

conducted in Asia and Africa. A detailed description of the tests is classified due to the targets and weapons involved, but in all three cases several charges ranging from 5 kgs to 500 kgs of TNT were detonated at burial depths and fill conditions which assured full coupling.

Both pressure and acceleration sensors were buried in the free field and on the wall of the underground test structures. Measurements were taken at various scaled distances and soil conditions. The testing sites were used during both dry and wet seasons, although special efforts were made to use the sites while the soil was saturated.

These data also support the observations previously made that the rate of attenuation depends on the acoustic impedance and seismic velocity of the soil.

ESTIMATION OF SOIL ATTENUATION PARAMETER(S)

The basic method for estimating the soil constants in the USAE manual is by means of tables which present empirical data. With this presentation, it is necessary to interpolate and use considerable judgment in estimating soil attenuation characteristics. An attempt has been made to present smooth curves to facilitate the estimation of the different constants by incorporating the new data.

Both Lampson (1946) and Drake and Little (1983) provide a means to estimate their relative soil constants by means of tables, as provided for Lampson in Table 1. Lampson (1946), however, also suggested an analytical expression for the soil constant:

$$k = \frac{1}{25} \cdot \rho V^2 \qquad (3)$$

where: ρ = mass density of the soil, $\frac{\text{pounds per cubic inch}}{386 \text{ in per sec}^2}$

V = seismic velocity, in/sec

In many practical situations which the authors have encountered in the past, the only information available at the preliminary stage of a site evaluation has been seismic velocity known from geophysical studies at the site. Detailed information on the mass density becomes known only after comprehensive site exploration and laboratory testing. Hence, in many cases involving preliminary design, another expression relating the k factor to the seismic velocity is of interest. The use of a relationship involving only seismic velocity has the advantage that seismic velocity is a measurement of bulk soil properties, as opposed to the measurement of density, which many not be representative of the soil mass. However, as noted by Drake and Little (1983), velocity alone must be interpreted with extreme caution, if there is the possibility that the soil might be cemented.

The relationship between Lampson's soil constant k and seismic velocity, incorporating new data, is presented graphically on Figure 1.

The suggested best fit curve is given by:

$$k = 0.000459 \times V^{1.406} \quad (4)$$

where: V = seismic velocity, ft/sec.

Please note the different units for V in Equations 3 and 4.

The new data can also be compared with the data presented in the USAE manual to facilitate the estimation of ρc and n. Figure 2 compares seismic velocity with the attenuation factor n, while n is compared to acoustic impedance ρc on Figure 3. The soil types from the new data are indicated on both figures. The other points are taken from the USAE manual.

The effect of soil saturation is striking. For a small change in the attenuation factor, n, from 2.3 to 2.5, acoustic impedance drops from about 120 to 40 psi/ft/sec and seismic velocity drops from about 5,000 ft/sec to about 1,500 ft/sec. The new data basically reinforce previous interpretations. However, it is recommended that the USAE manual include soils with velocities in the range of 6,000 to 7,000 feet per second with an attenuation factor of 1.4 for heavy, saturated clays. Conversely, Lampson's original data indicate that an attenuation factor of 4 be allowed for shallow detonations in loose, dry sand.

The use of a continuous band instead of the individual data points is aimed at improving the selection of the attenuation factors by giving the analyst a wider choice of seismic velocities and guidelines as related to the variations in soil characteristics.

An important point to remember in estimating the effects of explosions on underground structures is that the attenuation factor must represent the average characteristics of the site through an entire year, considering that measurements of the seismic velocity or acoustic impedance may vary depending on the season. The situation becomes more delicate when dealing with a remote enemy target in which no measurements are available and soil data must be inferred based on general geographic and geologic information. The choice between the upper and lower boundaries is also dependent on the degree of conservatism and the analyst's viewpoint: attacker versus defender.

COMPARISON OF LAMPSON (1946) AND DRAKE AND LITTLE (1983)

A comparison between the USAE manual design data and Lampson's constant is provided in Table 3. Graphs comparing the predicted earth pressure from Lampson (1946) with the Drake and Little (1983) data incorporated in USAE manual are provided on Figure 4 for different soil types and scaled distances ($ft/lb^{1/3}$) and assuming a full coupling. For most cases, the predicted pressures are about a factor of 3 higher for the USAE manual than for Lampson (1946) at small scaled distances, but quickly are in excess of 5 for larger scaled distances. The examples for alluvium and wet, saturated clay exhibit essentially a constant ratio of about 6.5 at all scaled distances. The attenuation coefficient n is 3 for these cases, the same as Lampson's exponent.

The rationale for comparing the current USAE manual with older work is to provide engineers with an idea of the degree of conservatism associated with the USAE manual. Based on the authors' experience, Lampson (1946) predicts reasonable average values of pressures that could be expected from given charge sizes, distances, couplings, and soil types. The ratio between predicted values from the USAE manual and Lampson are thus considered to indicate the degree of conservatism in the manual. This is not a criticism of the USAE manual, as the values reported are intended for use in the design of underground structures, where factors of safety are required.

SUMMARY

This study presents a simplified method to estimate blast attenuation in various soil media based on test data compiled since World War II by the U.S. Army Corps of Engineers and updated by several tests carried out abroad during the early 1980's. Continuous bands for selection of the attenuation factor(s) and qualitative tendencies within the bands have been identified which it is hoped will facilitate selection of soil attenuation parameters.

Earth pressures as originally calculated by Lampson (1946) have been compared with those derived from the USAE manual to provide a rough estimate of the degree of conservatism associated with USAE manual. It is suggested that the current manual could be improved if factors of safety could be provided for the design values. Alternatively, the reporting of results of explosion tests in terms of average values of pressure or ground motion with an indication of the standard deviation could help engineers decide on the degree of conservatism and factors of safety associated with their particular structures.

REFERENCES

Drake, J.L. and C.D. Little, 1983, "Ground Shock from Penetrating Conventional Weapons," Symposium on the Interaction of Non-Nuclear Munitions with Structures, U.S. Air Force Academy, Colorado.

Lampson, C.W., 1946, "Effects of Impact and Explosion," Chapter 3: Explosions in Earth, NDRC-Div. 2, National Defense Research Committee, Washington, D.C.

Rozen, A., 1986, Unpublished data.

U.S. Army Engineers, 1946, "Fundamentals of Protective Design - Non-Nuclear," Washington, D.C.

U.S. Army Engineers, 1984, "Fundamentals of Protective Design for Conventional Weapons," Waterways Experiment Station, Vicksburg, Mississippi.

TABLE 1

TABULATION OF CONSTANTS FOR VARIOUS SOILS
(LAMPSON, 1946)

SOIL TYPE	SEISMIC VELOCITY (fps) MIN	SEISMIC VELOCITY (fps) MAX	SOIL CONSTANT k(psi) MIN	SOIL CONSTANT k(psi) MAX
Topsoil (light, dry)	600	900	262	590
Topsoil (moist, loamy silt)	1,000	1,300	812	1,370
Topsoil (clayey)	1,300	2,000	1,420	3,370
Topsoil (semi-consolidated sandy clay)	1,250	2,150	1,510	4,150
Wet Loam	--	2,500	--	5,600
Clay (dense wet, depending on depth)	3,000	5,900	8,850	34,100
Rubble or Gravel	1,970	2,600	6,400	11,100
Cemented Sand	2,300	3,200	9,700	12,600
Water-Saturated Sand	--	4,600	--	22,500
Sand	4,600	8,400	26,200	87,000
Sand Clay	3,200	3,800	10,000	13,900
Cemented Sand Clay	3,800	4,200	17,800	21,700
Clay, Clayey Sandstone	--	5,900	--	45,000
Loose Rock Talus	1,250	2,500	1,750	7,000
Weather-Fractured Rock	1,500	10,000	3,100	140,000
Weather-Fractured Shale	7,000	11,000	63,000	156,000
Weather-Fractured Sandstone	4,250	9,000	23,500	116,000
Granite (slightly seamed)	--	10,500	--	160,000
Limestone (massive)	16,400	20,200	390,000	590,000

TABLE 2

TEST DATA CONDUCTED IN VARIOUS CLAYEY DEPOSITS
DURING THE 1983 - 1985 PERIOD

	UNIT WEIGHT (lb/ft^3)	SEISMIC VELOCITY (ft/sec)	ACOUSTIC IMPEDANCE (psi/ft/sec)	ATTENUATION MINIMUM	ATTENUATION MAXIMUM	LAMPSON'S SOIL CONSTANT (psi)
Dry, sandy clay	110	1,100	26.1	2.6	2.7	1,155
Wet, sandy clay	115	1,200	29.8	2.7	2.8	1,438
Wet clay	120	1,300	33.7	2.6	2.7	1,760
Wet, silty clay	115	3,000	74.5	2.5	--	8,984
Wet clay	117	3,500	88.4	2.4	2.5	12,441
Saturated sandy clay	120	4,800	124.3	2.25	2.5	24,000
Saturated stiff clay	120	5,200	134.7	1.9	2.1	28,167
Saturated silty clay	120	5,400	139.9	2	2.3	30,375
Saturated clay	125	5,900	159.2	1.5	1.7	37,771

TABLE 3

ESTIMATES OF LAMPSON'S SOIL CONSTANT FOR THE USAE SOILS

	UNIT WEIGHT (lb/ft^3)	SEISMIC VELOCITY (ft/sec)	LAMPSON'S K
Loose, dry sand and gravel with low relative density	90	600	280
Sandy loam, loose dry sands and backfill	100	1,000	870
Dense sand, high relative density	110	1,600	2,450
Wet sandy clay with air voids (greater than 4 percent)	120	1,800	3,400
Saturated sandy clays and sands with small amounts of air voids (less than 1 percent)	120	5,000	26,000
Heavy saturated clays and clay shales	125	>5,000	30,000

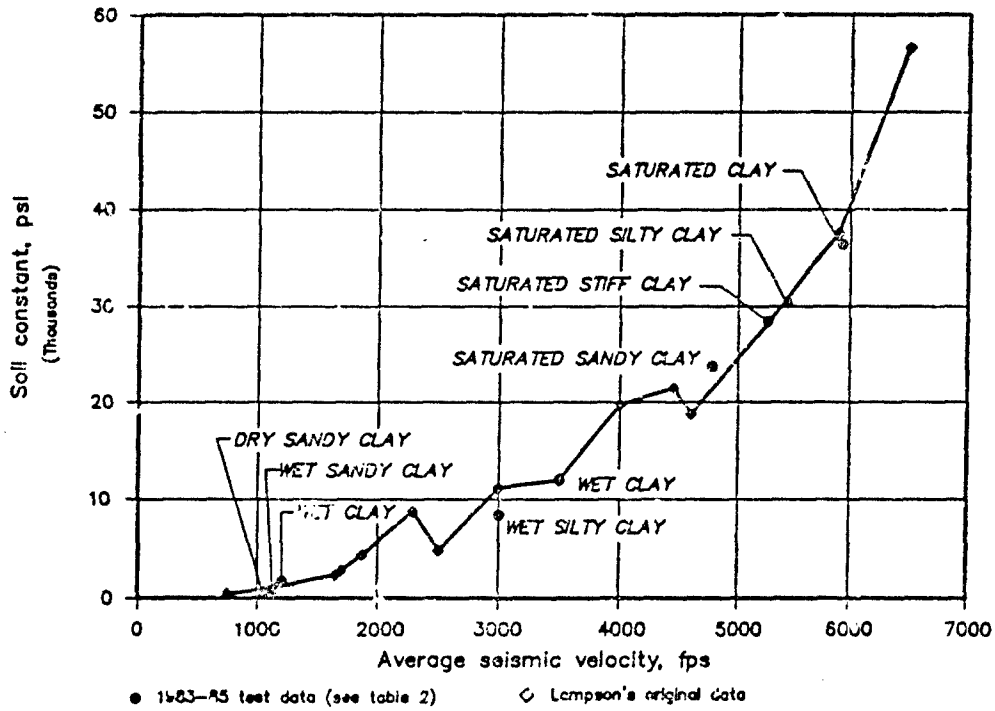

FIGURE 1: LAMPSON'S SOIL CONSTANT

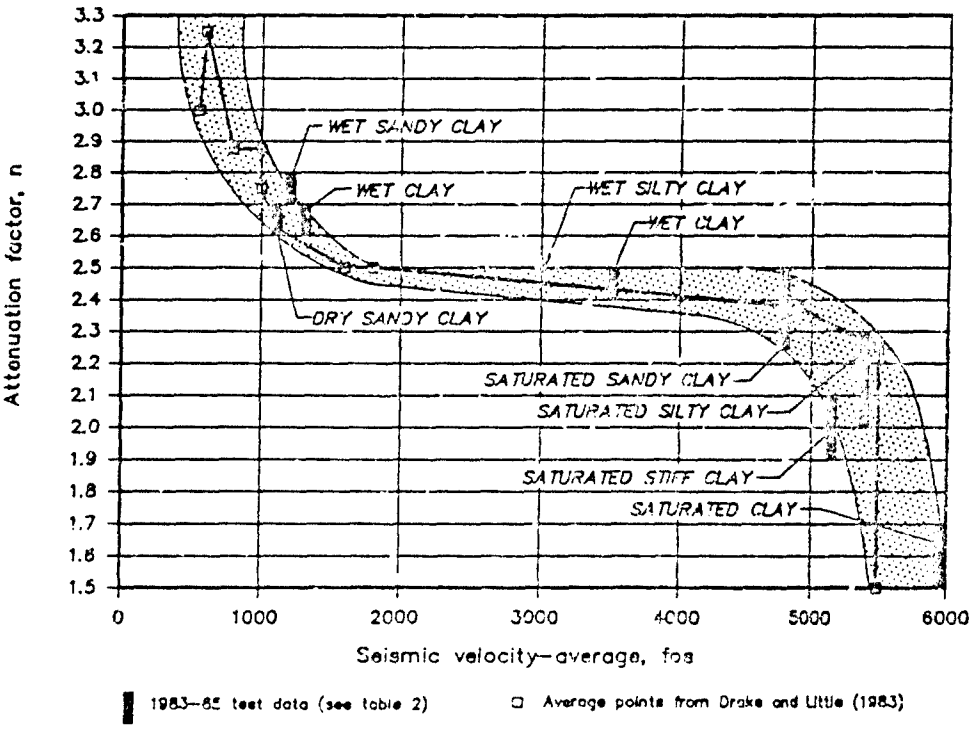

FIGURE 2: ATTENUATION FACTOR IN SOILS

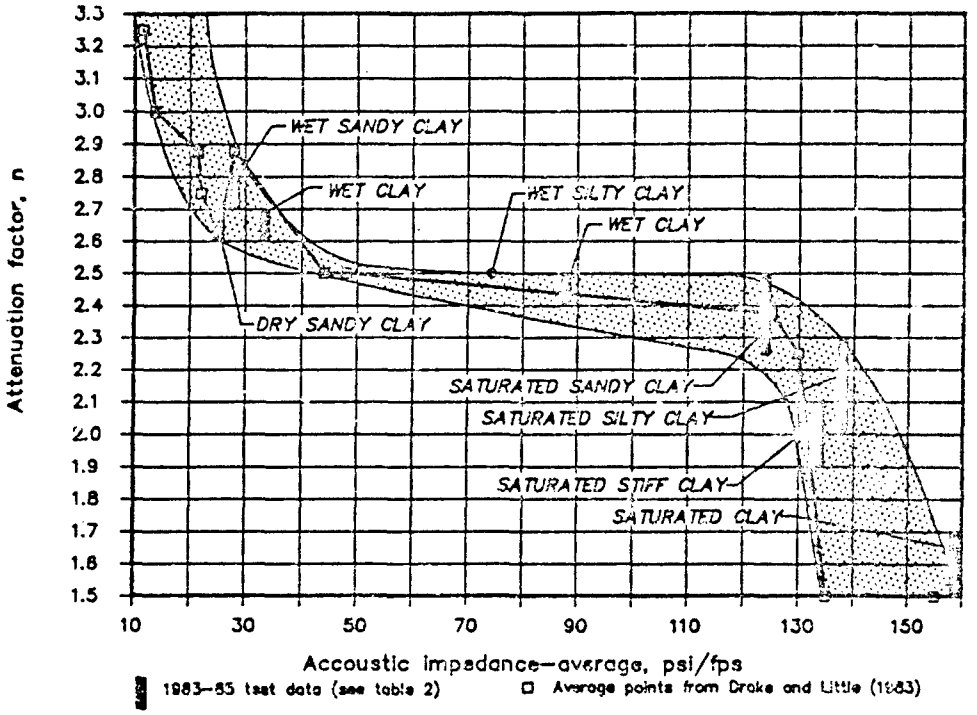

FIGURE 3: ATTENUATION FACTOR IN SOILS

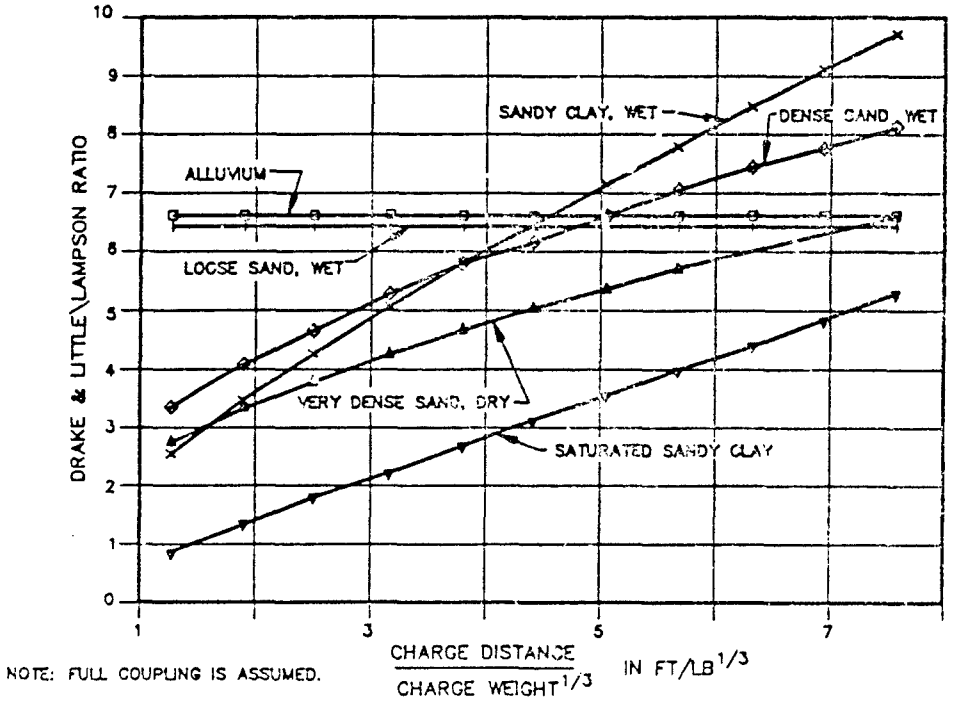

NOTE: FULL COUPLING IS ASSUMED.

FIGURE 4: COMPARISON OF LAMPSON (1946) WITH DRAKE AND LITTLE (1983) FOR CALCULATED PRESSURE

TOXICOLOGICAL AGENT PROTECTIVE ENSEMBLE

SELF-CONTAINED

(TAPES)

By Laurie Ann Kwiedorowicz

U.S. Army Armament Munitions and Chemical Command
Chemical Research Development and Engineering Center
Aberdeen Proving Ground, Maryland, 21010

DEVELOPMENT OF THE TOXICOLOGICAL AGENT PROTECTIVE ENSEMBLE-SELF-CONTAINED (TAPES) SYSTEM

BACKGROUND

Over the past decade, the U.S. Army has developed the need for a toxicological protective ensemble with a self-contained breathing apparatus (SCBA) for use in chemical agent environments Immediately Dangerous to Life and Health (IDLH). The existing Level A M3 protective ensemble uses a negative pressure respirator. The M3 ensemble was designed as a liquid protective ensemble for decontamination operations- not for IDLH atmospheres. Similarly, the Protective Outfit, Toxicological, Microclimate Controlled (POTMC) is another liquid protective ensemble intended for use by explosive ordinance personnel. The Department Of Defense Ammunition and Explosive Safety Standard, DOD 6055.9- STD, requires the use of a National Institute for Occupational Safety and Health (NIOSH) approved, full, facepiece, pressure demand respirator in IDLH atmospheres. In addition, the U.S. Army Armament, Munitions, and Chemical Regulation, AMC 385-131 R, requires the use of a NIOSH approved, positive pressure facepiece in IDLH environments.

Since the M3 suit and the POTMC do not meet the requirements of DOD 6055.9- STD, the U.S. Army developed the Demilitarization Protective Ensemble (DPE) for use at the Chemical Agent Munitions Disposal System (CAMDS) at Tooele Army Depot. The DPE is an encapsulated protective ensemble that uses an umbilical hose to supply air to the user. Because the 300 foot umbilical cord on the DPE was considered impractical for most depot operations, the

U.S. Army Chemical Research Development and Engineering Center (CRDEC) modified the DPE to include a back closure and a 60 minute, NIOSH approved, closed circuit SCBA. This modified system, called the Toxicological Agent Protective Ensemble- Self-Contained (TAPES), was developed to satisfy the immediate needs of the user community. TAPES is a system which is outside the Army's material acquisition decision process and will not be type-classified.

ENSEMBLE DESCRIPTION

The second generation of DPE equipment, called the TAPES system , provides an emergency need to the U.S. Army Armament Munitions Command (AMCCOM) community. The TAPES system provides up to 60 minutes of protection in IDLH environments (GB, VX, and GD). The system consists of the following components:

- o An encapsulated outer garment (similar to DPE)
- o An SCBA
- o A pressurization system
- o A cooling vest
- o A communication system

(a) Outergarment.

The outergarment totally encapsulates the wearer and all other ensemble components (except the boots and gloves). The outergarment was designed with side expansion panels which

minimize air pressure changes inside the suit (while it is inflated). The material used to construct the overgarment is 20 mil. chlorinated polyethylene (CPE) and the visor is made from polycarbonate.

Entry into the outergarment is made through a vertical opening using an extruded closure/ restraint zipper assembly. A two-track extruded plastic closure (EPC) and a restraint zipper make up the closure assembly. The EPC is made from CPE and has two parallel tracks that provide sealing. The EPC is closed by manually interfacing the mating halves together and is opened by an external pull tab. The zipper is heat sealed to the back of the EPC. Exposure to hazardous chemicals during depot operations is minimized by positioning the restraint zipper behind the EPC.

(b) Biopak 60 Rebreather.

A Biomarine Biopak 60 is used as the SCBA. An ice bath is used in conjunction with the rebreather in order to maintain dry, cool, breathing air. The Biopak 60 recirculates the majority of the wearer's exhaled air, permitting the unit to be lighter and more compact than open circuit equipment. The duration of wear is 60 minutes regardless of of the user's activity. Inward leakage of chemicals is prevented because the overgarment and the Biopak 60 are maintained at a slightly higher pressure than ambient. An alarm sounds when 25% of the respirator service air (15 minutes) is remaining. The NIOSH certified unit weighs 25

pounds fully charged with mask hoses. The unit can be worn for use in temperatures as low as -15 degrees F.

During any type of activity, the Biopak 60 provides a constant 2 liters/minute of air to the mask. Excess air is vented through a relief valve and used to provide positive suit pressure.

(c) Suit Pressurization System.

The suit pressurization system provides positive pressure within the TAPES system during operation. Three components make up the pressurization system: an inlet valve for initial garment pressurization, a volume accumulator to prevent pressure surges (due to volume changes), and an overpressure exhaust assembly that minimizes the operating pressure. After donning the suit, the inlet valve allows initial pressurization from an external air supply. Normal operating pressures within the suit range between 0.5 and 1.0 iwg. The volume accumulator minimizes internal pressure during operation. The accumulator is an area at the waist and back which expands whenever the user's activity reduces the internal suit volume. Therefore, air displaces to the accumulator and prevents a large increase in suit pressure. When the accumulator reaches full capacity, the overpressure exhaust fittings open to maintain a stable pressure inside the suit.

(d) Cool Vest.

A commercial cool vest, made by ILC Dover (Model 19), is

used for the cooling system. The vest contains an an ice/ water bag attached to a battery operated pump that circulates water from the ice bag to the vest and the back. The pocket containing the pump, ice bag, and bladder is worn on the chest so the rebreather can be worn over it (on the user's back).

(e) Communication System.

A personal communication system with a throat microphone (Loudmouth) is included to enhance face-to-face communications. The unit also contains a motion sensor and an emergency sound switch should the user be in trouble and unable to communicate. The Loudmouth communications system should be fully charged prior to its use.

SET UP AND SUPPLIES

Attachment 1 provides a recommended list of supplies and spare parts that must be purchased and kept in inventory if the TAPES system is to be operated and maintained. In addition, the following supplies should be kept on hand for emergency use (or training):

- o Crushed ice (10 lbs/ user)
- o Ready supply of breathing oxygen or pre-filled bottles
- o Ready supply of TAP boots (2 sizes too big)
- o Ready supply of TAP gloves
- o A portable air generator

- o Excess bags of rebreather scrubber material (sodasorb)
- o Dow lubricant
- o Charged 9 volt batteries for the communication system
- o Charged 8 volt ILC Dover gel type batteries for the cool vest.

OPERATION OF THE TAPES SYSTEM

(a) Donning the TAPES System.

The user must be fully dressed in Government issued TAP undergarments and coveralls. The wearer then dons a fully charged cool vest (with fully charged battery, ice, and water).

Prior to donning, the rebreather should be inspected and fresh sodasorb should be installed in the canister tray.

The cooling shroud on the breathing hose is hooked to the cooling vest.

The communication system is hooked to the rebreather harness (in the front) and the throat mike is installed at the neck. The communication system is turned on and the volume of the system is adjusted to the individual's preference.

The velcro strap which secures the breathing hoses is wound around the breathing hoses so the weight of the breathing hoses is carried evenly.

The oxygen valve on the rebreather is turned to the on position and the facepiece is fitted to the wearer's face. The wearer inhales into the mask several times to clear and verify

that the air supply is steady.

Immediately, the wearer bends over and, assisted by a dresser, steps into the overgarment (which is unfolded and unzipped). The overgarment is manually closed in the rear by the dresser.

The boots and gloves are put on the wearer by the dresser. Boots and gloves are taped to the overgarment using 4 " wide Government tape.

The suit is sealed and overpressurized by either a helium/air mixture or air depending on how the rear suit closure is to be certified. The dresser can use either soapy water or a hand held helium leak detector to check the adequacy of the rear seal.

The wearer is now ready to procede with toxic entry.

NOTE: Dressing procedures must be accomplished in pairs. Entry into hazardous areas is always done in pairs for safety considerations.

(b) Doffing the TAPES System.

After the wearer has exited a hazardous area, standard deconning procedures should be followed with heavy emphasis on the rear closure, armpit, and crotch areas.

After decontamination has been completed and the wearer is standing in his deconned overgarment (minus the boots and gloves left in the decon area), a dresser wearing "Level B" clothing will unzip the rear closure of the suit. The TAPES wearer pulls

his hands out of the arms of the suit and pushes his arms up and into the hood area to assist in removing the overgarment. Then, the wearer proceeds to roll the suit from the waist down, careful to roll with the clean side of the suit touching the wearer. Disposal of the suit is as required.

Since this suit was designed for a one-time use, the suit is always prepared for disposal after use.

(c) Emergency Operating Procedures.

In the event of air loss while wearing the TAPES system, the wearer should take the mask off and breath the clean air inside the overgarment. He should immediately exit the hazardous area and proceed with decontamination procedures.

Any time that contamination or tears of the suit material are observed, the wearer should exit the hazardous area immediately and proceed with decontamination procedures.

If the alarm sounds on the rebreather, it indicates that 15 minutes of service air is left. The wearer should exit the hazardous area and proceed with decontamination procedures.

MAINTENANCE AND FOLLOW ON TRAINING

Basic maintenance of the TAPES system is covered in the contractor's operation and maintenance manuals which will be distributed to U.S. Army depots during the fall of 1988. In addition, basic maintenance of the TAPES system is discussed and practiced during the current TAPES Familiarization courses

being conducted by Chemical Research Development and Engineering Center personnel (CRDEC). In-depth maintenance procedures are covered in the contractor manuals and training in this area is offered by the rebreather manufacturer (Biomarine) for a nominal price.

Substantial training is required by the local installations prior to the certification of the TAPES equipment for use in IDLH environments. This training should be accomplished locally via an approved training plan by the safety and surety authorities. Current TAPES users will be participating in additional training prior to certification during the fall of 1988. The logistics of procuring additional systems and spare parts is in the process of being established among the current U.S. Army depots.

SUMMARY

The TAPES system is now being issued for emergency depot, chemical demilitarization, or other nonroutine uses. This system is not intended as a replacement for the M3 Level A protective ensemble, but rather as a supplement when IDLH conditions do not permit the the use of the M3 suit. The actual determination of what constitutes a nonroutine emergency will be determined by the supervisor and the local authorities. The TAPES system is intended to bridge the current gap between existing Level A protective equipment and state of the art self-contained equipment that is in the beginning stages of development by U.S. Army personnel.

Authorization for use of the TAPES system is per AMC Regulation 385-131 (para. 4.1 (b)). Use of the TAPES is by the Director, AMC Field Safety Activity: Attention: AMXOS-C.

Recommended Purchases for Initial Inventory

	$Each	$Total
a. 10 spare cylinders for oxygen, #60-400	200	2000
b. 10 cases sodasorb 12 pkg/case #60-20012	48	480
c. 5 boxes disinfectant (100/box) #201-900G2	48	240
d. 2 Service Kits #400-450G1	340	680
e. 10 Scrubber foam #816004301	1.55	15.50
f 2 Transfil Valves #45-401	85	170
g. 2 spare parts kits #201-898G1	157	314
h. 3 silicone grease tubes DOW111	20	100
i. 15 antifog cloths #201-228	5	75
j. 20 thermaclear antifog inserts #37-000-001	7.50	150
k. 2 diaphragm assemblies #300-534G1	120	240
l. 2 grease & hose assemblies #200-574	75	150
m. 10 yoke o'rings #287001103	3.60	36
n. 10 scrubber cover O-rings #252545378	10.65	106.50
o. 10 scrubber canister O-rings #25217036	6	60

	Each	Total
p. 10 O-ring, mainline center section #H-6004	1	10
q. 1 video training #NS-VHS-1	20	20
r. 10 spare trays for canister #300-617-G1	80	800
s. 10 cool vest battery charges #CP29-0047	53	530
t. 10 cool vest battery packs #0000-25107	60	600
u. 2 repair kits-cool vest #0000-26463	50	100

The above items should be ordered to establish local inventories necessary to perform the training for the use of the equipment.

A. Items A-R should be ordered from: Rexnord Safety Products 45 Great Valley Parkway, Malvern PA, 19355, (215) 647-7200.

B. Items S-U should be ordered from: ILC Dover, P.O. Box 266, Frederica, DE., 19946, (302)-335-3911.

C. Additional communications systems (model LMPT-1 $360) can be ordered from: Earmark, Inc. 1125 Dixwell Avenue, Hamden, Conn 06514, (203) 777-2130.

D. If additional chemturion model 5101 garments are needed, they can be ordered from ILC Dover.

THE ESTIMATION AND PORTRAYAL OF INVOLUNTARY RISK TO AN INDIVIDUAL

Willard E. Fraize
Principal Engineer
Energy, Resource, and Environmental Systems Division
The MITRE Corporation
McLean, Virginia

for

Department of Defense
Twenty-Third Explosives Safety Seminar
Atlanta, Georgia

9-11 August 1988

. . . . . .

ABSTRACT

While a programmatic decision involving some risk to the public is usually made on the basis on community or societal risk -- that is, the total number of persons at risk -- an individual among the affected public is likely to be more concerned with his/her personal risk. Both measures of risk were analyzed for the Chemical Stockpile Disposal Program (CSDP). This paper describes the method for estimating and presenting risk to an individual at a specified distance from a potential accident site, whether at a fixed installation or along a transportation corridor. The concept of an individual risk curve, showing the probability of an individual's death as a function of distance from a site, is introduced and illustrated with data from the CSDP risk analysis. An alternative measure of individual risk -- the individual's 'time-at-risk' -- is defined and illustrated.

1.0 INTRODUCTION

1.1 The Chemical Stockpile Disposal Program

The U.S. Army was directed by Congress (Public Law 99-145) to destroy the nation's stockpile of lethal, unitary chemical agents and munitions in a manner which provides for maximum protection to the public. A comparative risk assessment of the several proposed alternatives for the Army's Chemical Stockpile Disposal Program (CSDP) was performed. The results of the risk analysis were used to support the selection of the environmentally preferred disposal alternative in the Final Programmatic Environmental Impact Statement (FPEIS) (U.S. Army, 1988). The results were also used as one of several factors considered by the Army in arriving at its Record of Decision of 23 February 1988 which stated the Army's decision to proceed with the on-site disposal alternative. A detailed description of the risk analysis methodology is reported elsewhere (U.S. Army, 1987; Perry, J. G. et al, 1988) and will not be covered in this paper.

The Chemical Stockpile consists of a wide range of munitions and bulk agent storage containers. Three chemical agent types are used: the persistent nerve agent, VX; the non-persistent nerve agent, GB; and, the persistent blister agents known as mustards and designated by the symbols H, HT, and HD.

The stockpile is currently stored in eight locations throughout the conterminous U.S. (CONUS): Anniston Army Depot (ANAD), Alabama; Aberdeen Proving Ground (APG), Maryland; Lexington Blue-Grass Army Depot (LBAD), Kentucky; Newport Army Ammunition Plant (NAAP), Indiana; Pine Bluff Arsenal (PBA), Arkansas; Pueblo Depot Activity (PUDA), Colorado; Tooele Army Depot (TEAD), Utah; and, Umatilla Depot Activity (UMDA), Oregon.

Of eight programmatic alternatives originally identified for the CSDP, only five were carried through the full scope of the risk analysis; those five are:

- The continued storage of the stockpile in its present locations (this is the "no-action" alternative required by the National Environmental Policy Act) [the CONTINUED STORAGE Alternative (STR)];
- On-site destruction of the stockpile at its present storage lotions [the ON-SITE Alternative (ONS)];
- Movement of the CONUS stocks to two regional disposal centers (at ANAD and TEAD) [the REGIONAL alternative (REG)];
- Movement of the CONUS stocks to one national disposal center (at TEAD) [the NATIONAL alternative (NAT)]; and,

- Movement of the stocks from two sites (APG and LBAD) by air to the national disposal site (TEAD) with the remainder of the stockpile destroyed on-site [the PARTIAL RELOCATION alternative (PRB)].

The other three CSDP alternatives, which will not be discussed in this paper, involve variations on the partial relocation alternative, including an option for water transport of the APG stockpile to Johnston Island in the Pacific Ocean.

1.2 Purpose of This Paper

The purpose of this paper is to describe the approach that was used in the estimation of risk posed by the CSDP to an individual who lives or works close enough to a CSDP storage or disposal site or transportation corridor to experience added risk as a result of CSDP activities.

1.3 Definition of Risk

In general, risk is a measure of the potential for exposure to unwanted events or consequences (e.g., injuries or fatalities). For purposes of the CSDP risk analysis and this paper, risk is defined as the expected impact on public safety as a result of the set of possible agent-releasing accidents associated with the storage, transporting, handling, and physical destruction (demilitarization) of the munitions and agent in the stockpile. Risk is measured by both the probability of a lethal event (potential accident) occurring and the number of public fatalities that might result if the event were to take place.

For purposes of this study, the term "public" excludes persons within the boundaries of the military installations.

When considering the risk to an individual, the measure of consequence is fixed: a lethal exposure to agent (i.e., the individual's death).

1.4 Perspectives of Risk

1.4.1 Individual vs. Community/Societal Risk

Both individual and community/societal perspectives of risk are considered, although the emphasis is on the latter. The risk to an individual is calculated by multiplying together the probabilities of each of the circumstances necessary to produce a fatality. The total risk to an individual is the sum of the individual risks posed by each identified accident scenario that could happen at the individual's location. To estimate the risk to the general population, the factors defining risk to

an individual must be applied to the total number of individuals potentially affected by any accident.

1.4.2 Voluntary vs. Involuntary Risk

The public on whom any risk associated with the CSDP will fall will view the imposed risk as involuntary risk, as opposed to the kind of risk that may be routinely and voluntarily accepted in the normal course of life. This difference in perspective will generally affect, in a negative way, the public's willingness to accept either the fact of added risk, regardless of how small the increment, or the credibility of its estimation. The public's skepticism and fear of the unknown, when it deals with involuntary risk (such as that due to the CSDP), will make the job of the presenter of risk results much more difficult. Attempts to compare risk analysis results with risk due to voluntary activities such as driving an automobile (where the risk-taker obtains a direct benefit -- mobility -- from his/her high risk activity) will usually fail to be convincing.

2.0 ANALYSIS OF INDIVIDUAL RISK

As noted above, risk can be viewed from two basic perspectives:

- Risk to an individual at a specified location; and
- Risk to the entire affected population (societal or community risk).

In the first case, risk to an individual is the probability that he or she will be lethally exposed to agent while at a fixed location. Risk to the affected population is the expected total number of individuals who might be lethally exposed by the event. Individual risk is a measure that addresses the individual's personal exposure. Societal/community risk is an extensive risk measure that may be more useful to a decision-maker who needs to assess total effects on the public.

An individual tends to view risk in very personal terms, such as the probability that an unwanted event will occur to him or to his family. Many risky activities or situations to which an individual is exposed are voluntary (e.g., a canoe ride) and their risk is accepted in return for the benefits the activity brings. Others (e.g., being struck by lightning) are "acts of God or nature" and the associated risk is generally accepted as a part of living. Still others (e.g., living near a nuclear power plant or along a rail route that carries hazardous chemicals) are viewed as involuntary, the result of man-made intrusions, and often are less willingly accepted. In this risk analysis, we are dealing with a man-made activity that the public may view as an imposed or involuntary risk. Risk comparable in character (not necessarily magnitude) to that potentially imposed by the CSDP might be that associated with living next to a chemical

plant processing hazardous chemicals or living along a transportation route carrying such materials.

Community or societal risk is, in effect, the aggregate of individual risk to which all members of the local population are exposed. Thus, individual risk is independent of the number of individuals at risk; community or societal risk is not.

2.1 Computation of Individual Risk

2.1.1 General Case

The risk to an individual can be estimated as the product of the probabilities of each of the circumstances necessary to cause the individual's death. This combined probability of occurrence is multiplied by the consequence to determine risk; in the individual case, consequence is always equal to 1 (the death of the individual), and so does not affect the risk value we calculate. Figure 1 illustrates the major factors affecting the risk to an individual posed by a potential release of chemical agent; these factors are:

- the probability that an accidental release will occur;
- the probability (along transportation corridors only) that a transport vehicle will be in the vicinity of the individual when the accident occurs;
- the probability of being downwind of the release;
- the probability of being within the plume width;
- the probability that an individual within a given lethality zone of the plume will die.

For the case of individual risk along a transportation corridor, the analysis is based on determining the route length over which an accident can occur and still affect an individual at a given location. This is equivalent to basing individual risk on exposure time. Basically, the analysis computes average individual risk along the transportation corridor, based on average distances, speeds, and exposure times along the route.

Whether along a transportation route or near a fixed site, the total risk to an individual is the sum of the individual risks posed by each identified accident scenario that could happen at the individual's location.

Concept:

The Probability of a Potential Individual Fatality Depends on Several Factors

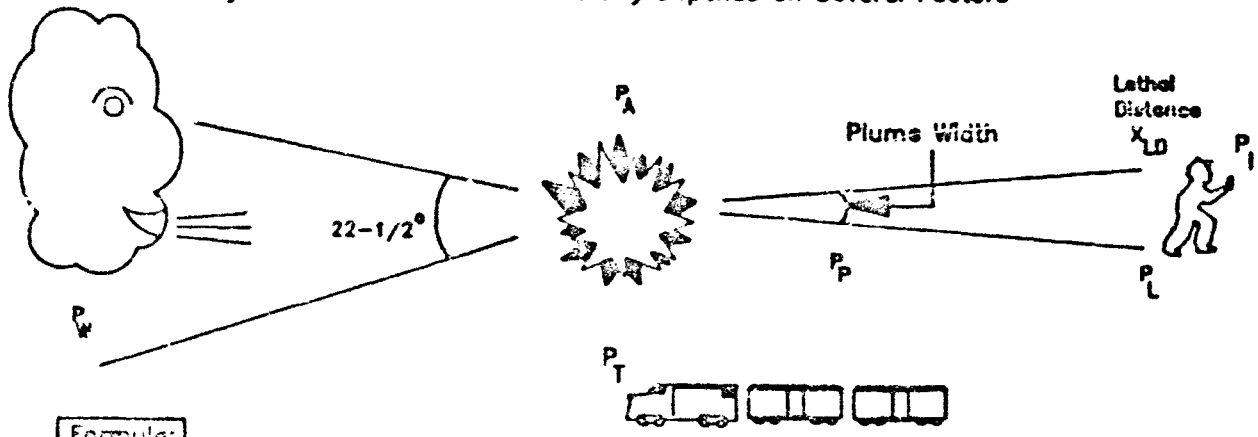

Formula:

$P_I = P_W \times P_A \times P_T \times P_P \times P_L$ Where:

P_I = Probability of an Individual Fatality
P_W = Probability of Wind Directed from an Appropriate Sector
P_A = Probability of an Accidental Release of Agent
P_T = Probability of a Train being Present (as applicable)
P_P = Probability of an Individual Being within the Plume Width
P_L = Probability of a Potential Fatality for an Individual within the Plume

Typical Data are:

$P_I = 0.06 \times P_A \times 1.0 \times 0.3 \times 0.2 = 0.004 \times P_A$

FIGURE 1. FACTORS IN THE ESTIMATION OF INDIVIDUAL RISK

2.1.2 Quantitative Illustration of Individual Risk

Referring to the factors defined in Figure 1, we see, first of all, that there is the probability that an accidental release will occur; this is the probability associated with the source term , and we will represent its value by the symbol, P_A. If the accident involves a transportation accident (a train is shown for illustration), then we must include the probability that the transport vehicle will be close enough to harm the individual when the accident occurs; call this probability, P_T. For the sake of this illustration, we will assume it has a value of 1. (Risk along a transportation route will be discussed in more detail below.) Now, given that there is a probability, $P_A \times P_T$, of accidental agent release in the vicinity of the individual, the next factor affecting the individual's risk is whether he is downwind of the accident. Assuming for the moment that the wind has equal probability of blowing from any of the 16 compass point directions (N, NNE, NE, ENE, etc.), then the probability of being downwind of the release can be represented by P_W, which has a value of 1 in 16, or approximately 0.06. The width of the potentially lethal portion of the atmospheric plume is approximately one-third of a compass sector. Therefore, if the individual is "downwind" of the accident, the probability of being within the plume width, P_P, is about 1 in 3, or 0.3. Finally, the individual must be close enough to the accident site so that potentially lethal dosages could reach him. "Close enough" in this case is determined by the atmospheric plume dispersion analysis. It is defined as the downwind distance to the "no-deaths" dosage for whatever chemical agent is involved. Since dosage increases as the individual is closer to the accident site and closer to the centerline of the agent plume, the probability of a fatality for an individual within the plume, P_L, which ranges from a value of 0 to 1 within the plume boundary, has an average value of, typically, 1 in 5, or 0.2. That is, of all the individuals within the plume, only about 20 percent would be fatalities, assuming the population were evenly distributed.

Putting all this together, we can calculate the probability of an individual's fatality, P_I, as follows:

$$P_I = P_A \times P_T \times P_W \times P_P \times P_L$$

$$= P_A \times 1.0 \times 0.06 \times 0.3 \times 0.2$$

$$= P_A \times 0.004$$

$$= P_A/250$$

This says that even if an accidental release does occur close enough to potentially harm an individual, the probability of the individual's death is on the order of 1/250th of the probability (P_A) that the accident will occur there in the first place, which, by itself, is usually an extremely small number. This, then, is the general method by which risk to the individual has been calculated.

2.1.3 Computation of Individual Risk Along a Transportation Route

Figure 2 introduces the additional considerations required when dealing with risk to an individual along a rail route or other transportation corridor. The factors affecting individual risk are the same as those discussed in conjunction with Figure 1, but a slightly more complicated calculation is required to estimate the probability of the accident occurring in a region that could affect the individual (i.e., the probability factors, P_i, and P_T discussed above). As shown in Figure 2, if an individual is located a distance, d, away from the rail route, and an accident produces a plume with a "no-deaths" hazard distance of length L, the individual could be killed if the accident occurred anywhere over a distance equal to 2 x Z, centered at the individual's location along the route.

To calculate the probability that an accident will occur within the relevant track segment, 2 x Z, (P_Z), we must account for:

- the probability, $p_A(t)$, of an accident per unit time (e.g., per hour) per train;
- the time, t, required for the train to traverse the track segment at 2 x Z;
- the number, N, of trains passing a given location.

Then:

$$P_Z = 2 \times p_A(t) \times t \times N.$$

However, since actuarial data on transportation accidents is provided to MITRE in terms of the probability of an accident per unit distance per train, $p_A(z)$, this analysis employs an equivalent expression for P_Z:

$$P_Z = 2 \times p_A(z) \times Z \times N.$$

Thus, the individual risk along a transportation route can be expressed either in terms of exposure time, t, or a hazard distance, 2 x Z, along the track, both of which are related to the distance the individual is from the route and the size of the potential accident. Time and distance are related to one another through the simple kinematic relationship involving the average train speed, v, which states that:

$$t = (2 \times Z)/v$$

For computational purposes, this risk analysis computes individual risk on the basis of lengths of track over which an accident can occur. As seen from the above, this is equivalent to basing individual risk on

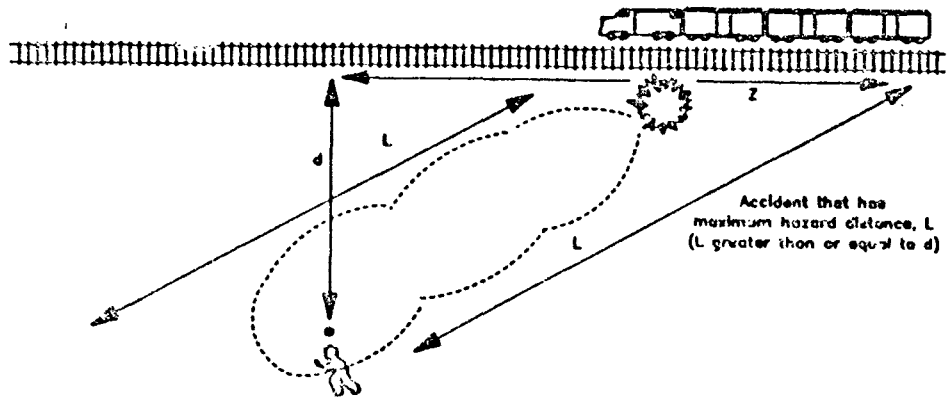

Risk to the individual, P_I, from an accident that has a 'no-deaths' hazard distance of L:

$$P_I = \left[\begin{array}{l}\text{Probability, } P_Z\text{, of} \\ \text{an accident within} \\ \text{a distance, } 2 \times Z\end{array}\right] \times \left[\begin{array}{l}\text{Probability of a} \\ \text{lethal exposure} \\ \text{to the resulting} \\ \text{plume (see Fig. 1)}\end{array}\right]$$

where:

$$P_Z = 2 \times \left[\begin{array}{l}\text{Probability, } P_A^{(t)}\text{,} \\ \text{of an accident per} \\ \text{unit time, per train}\end{array}\right] \times \left[\begin{array}{l}\text{Time, t, required} \\ \text{to travel a} \\ \text{distance, Z}\end{array}\right] \times \left[\begin{array}{l}\text{Number, N, of} \\ \text{trains passing} \\ \text{this location}\end{array}\right]$$

$$= 2 \times \left[\begin{array}{l}\text{Probability, } p_A^{(Z)}\text{,} \\ \text{of an accident per} \\ \text{unit distance, per} \\ \text{train}\end{array}\right] \times \left[\begin{array}{l}\text{Distance, Z, over} \\ \text{which a plume} \\ \text{of length, L, could} \\ \text{affect the individual}\end{array}\right] \times \left[\begin{array}{l}\text{Number, N, of} \\ \text{trains passing} \\ \text{this location}\end{array}\right]$$

- Estimation of risk due to that accident takes into account the occurrence anywhere within track length, 2 x Z
- Total individual risk is the sum of risks due to all accidents that can result in hazard distances greater than individual's distance from track

FIGURE 2. RISK TO AN INDIVIDUAL ALONG A TRANSPORTATION CORRIDOR

exposure time. To compute individual risk on the basis of lengths of track over which an accident can occur, it is assumed that the accident, if it occurs, could happen anywhere along the transportation route with equal probability. This is not strictly correct, given the variability of conditions along a rail corridor, but the best that can be assumed given the available data and the broad scope of the risk analysis.

2.2 Time-at-Risk Considerations

The probabilistic individual risk measures, discussed above in relation to Figure 2, account, implicitly, for the time during which an individual is exposed to risk from accidental chemical agent release. The computation of the individual risk curve accounts for the probability of individual accident scenarios occurring as well as the severity of the release (i.e., the position of the individual within the plume) and the likelihood that meteorological conditions (i.e., wind direction) will cause the plume to move over the individual.

However, for many individuals, the concept of individual risk may be more easily understood in terms of the individual's total time of exposure to risk, regardless of whether his/her actual risk varies during that period or is comparable to the actual risk borne by others. Accordingly, two time-related risk measures were introduced to the CSDP risk analysis:

- The total time-at-risk during the CSDP when an individual could be exposed if an accident were to occur;
- The total person-years-at-risk during the CSDP -- a measure equal to the time-at-risk times the number of people experiencing any risk (i.e., being within a zone that could encompass potentially lethal exposures, as defined by the 'no-deaths' plume length under worst-case meteorological conditions).

Since only time-at-risk deals with individual risk, we will not further discuss person-years-at-risk.

Time-at-risk is readily addressed at the storage/disposal sites since the appropriate time measure is simply the duration of disposal activities at a given site. These times vary from less than 1 year to over 4 years (i.e., 9000 to 35,000 hours), depending on the site. The actual disposal duration time at a given site cannot be stated because of the possibility of revealing classified data regarding stockpile size. By this measure, all individuals within a distance equal to the maximum possible (worst-case weather) 'no-deaths' plume length from a specific site should be considered 'at risk' for the same duration of time; outside this site-specific maximum distance, time-at-risk would be zero. Table 1 lists these maximum (worst-case) distances for each site and each applicable disposal alternative for the mitigated risk case, as reported in the FPEIS (U.S.

Army, 1988). An individual located within the stated distance of a given site could assume his/her time-at-risk to be the duration of disposal activity for a given disposal alternative.

Along transportation corridors, time-at-risk for an individual is dependent on the individual's location -- his/her distance from the transportation corridor. Table 2 lists the maximum worst-case plume lengths for the transportation corridors.

Figures 3 and 4 show time-at-risk along rail and air transportation corridors, respectively, in terms of hours of exposure per vehicle trip as a function of an individual's distance from the centerline of the corridor and the severity (worst-case 'no-deaths' plume length) of the worst identified potential accident for a given corridor (as determined from Table 2). To determine his/her time-at-risk for a given disposal alternative, an individual would need to do the following:

- identify which site stockpiles are to be transported along his/her portion of the corridor;
- determine the number of transporter trips (number of train-trips or aircraft-trips) required to move the stockpile for each site;
- estimate, with the aid of Table 2 and Figures 3 and 4, the time-at-risk per trip from each site;
- calculate the sum of total time-at-risk by the relation:

$$\text{TOTAL TIME-AT-RISK, } T = \sum_{\text{all sites}} (\text{time/trip})_{\text{site } j} * (\text{trips/stockpile})_{\text{site } j}$$

An approximate upper limit can be set on time-at-risk for both fixed site and transportation corridors:

- For fixed sites, the maximum time-at-risk is in the range of 4 years (35,000 hrs);
- For the regional (rail) corridors, the maximum number of trains is approximately 50, and the maximum hazard distance is in the 20 km range; an individual living within 10 km of the track carrying all 50 (or so) trains would experience a total time-at-risk of:

$$\text{MAX. TIME-AT-RISK (REG)} = (0.7 \text{ hr/train}) * (50 \text{ trains}) = 35 \text{ hr}$$

TABLE 1
MAXIMUM (WORST-CASE) HAZARD DISTANCES -- STORAGE/DISPOSAL SITES

SITE	MAXIMUM (WORST CASE) HAZARD DISTANCE (km) -- for a given Disposal Alternative -- STR	ONS	REG	NAT	PRB
ANAD	150.4	32.9	28.2	27.9	32.9
APG	17.4	4.4	44.6	44.6	11.5
LBAD	4.6	17.5	14.9	14.9	30.8
NAAP	304.2	15.5	6.1	6.1	15.5
PBA	85.2	32.9	183.8	183.8	32.9
PUDA	56.2	4.3	75.9	75.9	4.3
TEAD	108.0	32.9	27.9	27.9	32.9
UMDA	314.0	28.2	150.8	150.8	28.2

* * * * * * * *

TABLE 2
MAXIMUM (WORST-CASE) HAZARD DISTANCE -- TRANSPORTATION CORRIDORS

ORIGINATING SITE	MAXIMUM (WORST-CASE) HAZARD DISTANCE (km) -- for a given Disposal Alternative -- REG	NAT	PRB
ANAD	*****	19.1	*****
APG	2.3	2.3	2.3
LBAD	16.5	16.5	30.8
NAAP	8.6	8.6	*****
PBA	19.1	19.1	*****
PUDA	3.8	3.8	*****
UMDA	19.1	19.1	*****

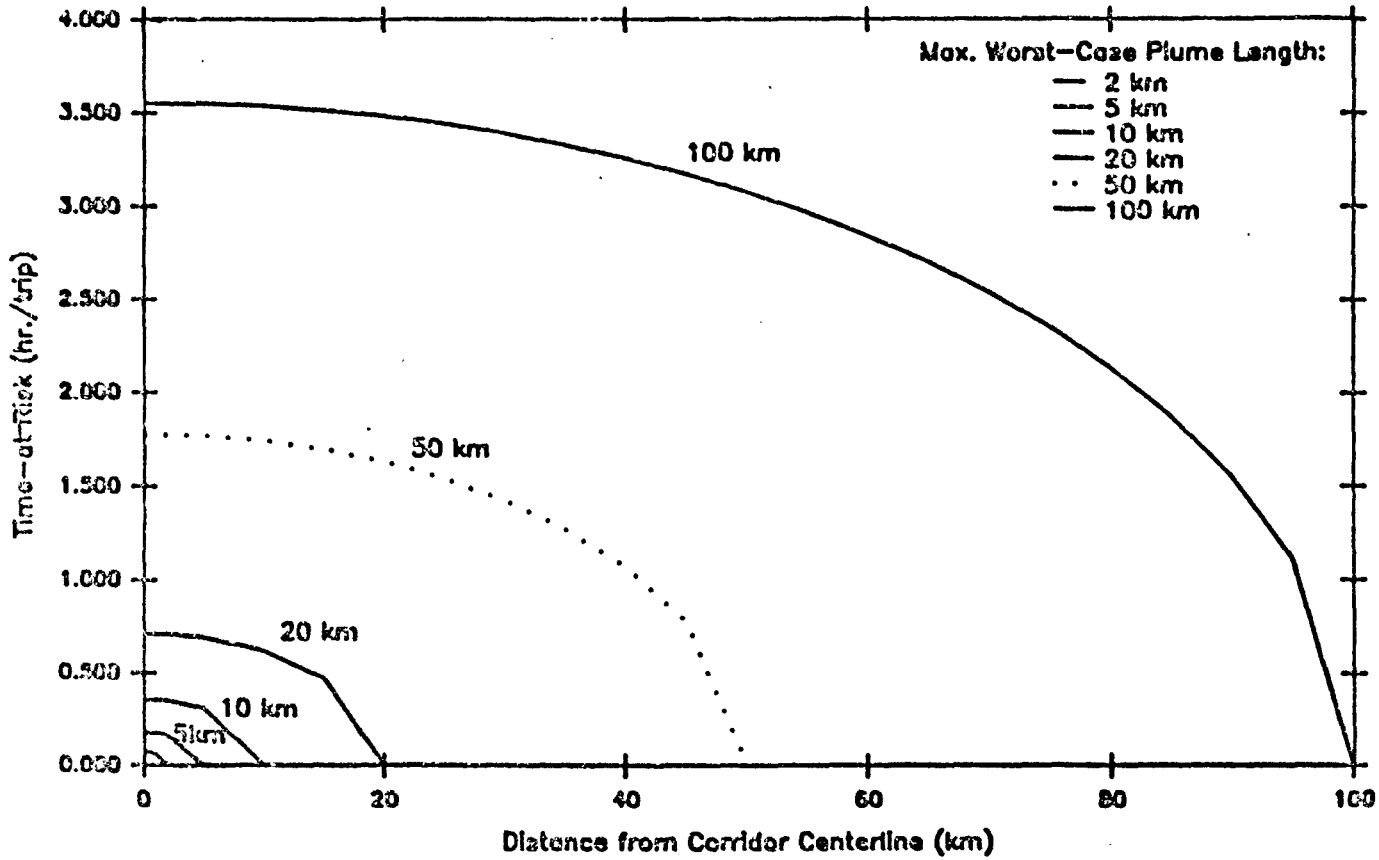

FIGURE 3. TIME-AT-RISK -- RAIL CORRIDORS
Hr. per Train Trip (35 mph)

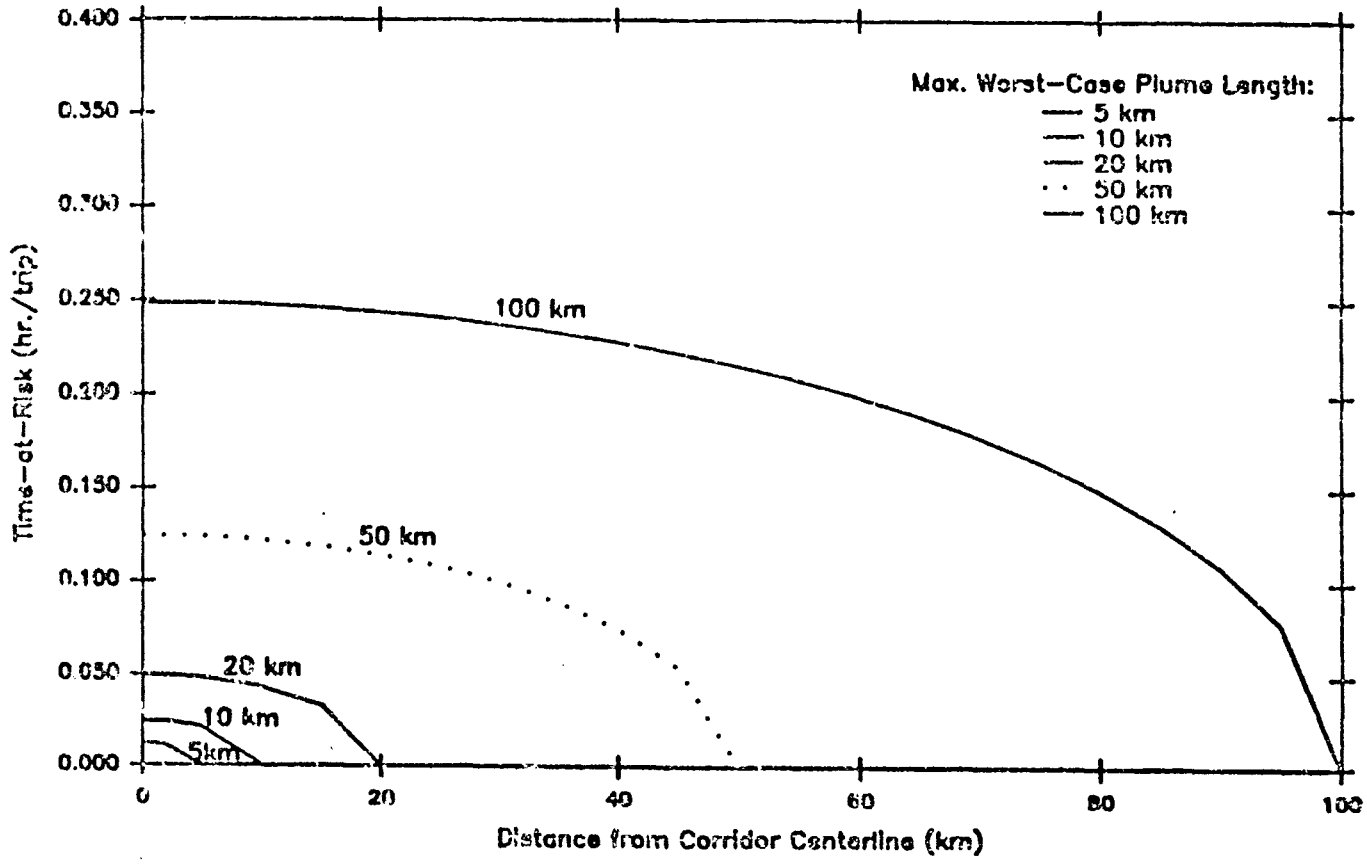

FIGURE 4. TIME-AT-RISK -- AIR CORRIDORS
Hr. per Aircraft Trip (500 mph)

- For the national (rail) corridors, the maximum hazard distance is also approximately 20 km. The maximum number of trains for this alternative is approximately 75, leading to:

  MAX. TIME-AT-RISK (NAT) = 53 hr

- For the partial relocation (air-mode) corridor, the maximum hazard distance is approximately 31 km, leading to a time-at-risk of approximately 0.07 hr/aircraft flight. The actual number of flights required to move the APG and LBAD stockpiles is classified; but, it can be said to be in the range of 900 - 1200 air-lifts for the APG stockpile and in the range of 1200 - 1500 air-lifts for the LBAD stockpile, yielding a total number of airlifts in the range of 2100 - 2700 for the combined air-lifted stockpile. Using 2500 air-lifts (which could consist of several flights each, but would not thereby add to an individual's time-at-risk) as as a rough indicator of air traffic intensity, we find that:

  MAX. TIME-AT-RISK (AIR MODE) =
  (0.07 hr/flight) * (2500 flights) = 175 hr

Thus, the time-at-risk for individuals along the transportation corridors is in the range of 100 hr. For individuals around a disposal site, time-at-risk is measured in the tens-of-thousands of hours -- a hundred-fold greater time than for those along the corridors.

2.3 Individual Risk Curve

2.3.1 General Description

The probabilistic description of individual risk is conveniently displayed by means of the individual risk curve, schematically represented by Figure 5. For each applicable accident scenario, the probability of an individual's death at a given distance from the site of the agent release is estimated, in the manner described in section 2.1, as the product of three basic terms: 1) the probability of the event occurring; 2) the probability of an individual being within the plume, given a uniform wind-rose (equal to the ratio of plume width to the perimeter of the circle designating the individual's given distance from the release site); and, 3) the fatality rate associated with the centerline dosage within the plume at a given distance from the release site. This product, determined for fixed distance increments of 0.1, 0.2, 0.5, 1.0, 2.0, etc. out to 100 km, is then summed for each distance value for all applicable potential accidents. The result is an individual risk curve, defining the probability of an individual's death as a function of distance from the site. A representative individual risk curve (drawn from the CSDP risk analysis for a specific site) is presented in Figure 6. Using this individual risk

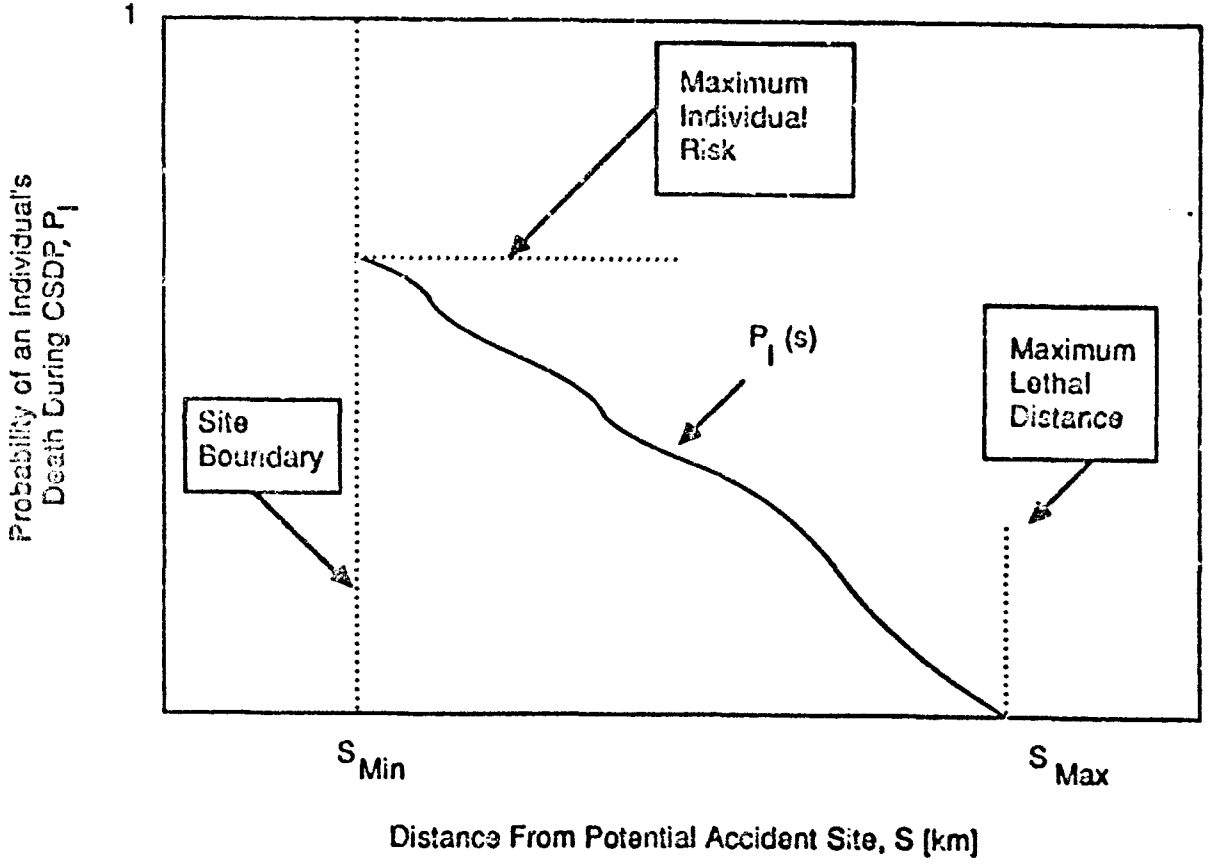

FIGURE 5. REPRESENTATIVE INDIVIDUAL RISK CURVE

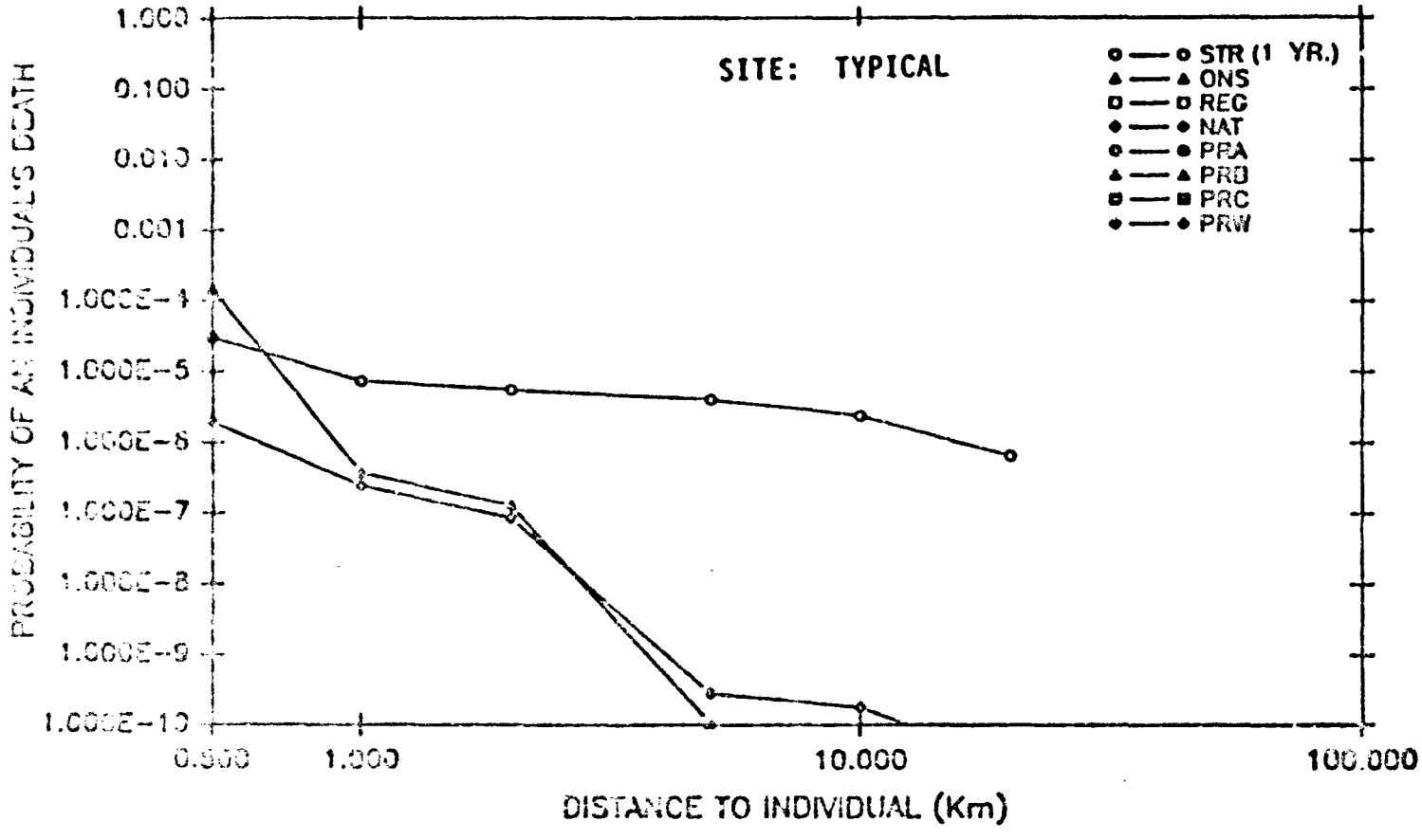

FIGURE 6. INDIVIDUAL RISK CURVES AT A TYPICAL SITE

curve as a guide, the following measures of risk to an individual at a given location were defined:

- **maximum individual risk**, equal to the probability of a fatal exposure at the site boundary (assumed to be 0.5 km from the on-site disposal/storage operations) or as close as 0.1 km to the centerline of a transportation corridor. This indicator is equal to the vertical intercept of the individual risk curve at the appropriate distance value (0.5 or 0.1 km); it is dependent only on the mix of potential accidents that could happen at the individual's location and, since it applies only to an individual, is independent of population density.

- **maximum lethal distance**, equal to the maximum downwind length (given by the 'no-deaths' dose) of the plume from the worst of all identified potential accidents under worst-case weather conditions at a specific location. Conversely, it is also the minimum distance an individual could be from a given site or transportation corridor and have no risk of lethal exposure during the disposal program. It is equal to the horizontal intercept of the individual risk curve at some minimum accepted level of credibility -- say, 1×10^{-10} per stockpile.

An individual living near a particular site can interpret his individual risk from a curve such as shown in Figure 6 in the following way. The vertical scale of the figure displays the probability of that individual's death during the course of the CSDP activities at the site (3 to 5 years for the disposal alternatives; 25 years for the continued storage option). The curves show that the individual's risk decreases steadily as his distance from the site (as read on the horizontal scale of the graph) increases. The minimum distance shown is 0.5 km, which, by assumption imposed on the analysis, is the minimum distance from chemical operations to the site boundary for any of the disposal/storage sites. Thus, the risk given by the figure is the maximum off-site (public) risk only. (Risk to on-post personnel is not within the scope of this analysis.)

Interpretation of the individual risk curve will proceed as follows. Consider first an individual who spent the entire duration of the CSDP located at the boundary of the site (at 0.5 km). For the applicable disposal alternatives, that individual would experience a chance of death during the CSDP of the value given by the vertical scale of the figure. If the individual lives farther away from the site center, his risk becomes progressively lower until finally the individual is beyond the point where the most severe accident is expected to cause any lethal impact and his risk of death becomes zero. The individual risk value at 0.5 km is the principal risk measure: maximum individual risk. The distance beyond which no lethal effects are expected for any applicable accident is the maximum lethal distance under most-likely meteorological conditions; not

shown is the other major risk measure for individual risk -- the maximum lethal distance which, as noted earlier, is based on the assumption of extreme conditions (meteorology, wind direction, and population density).

2.3.2 Individual Risk Results for The CSDP

For the CSDP, individual risk was found to vary widely from site to site and among the disposal alternatives. The regional and national disposal sites, TEAD and ANAD, pose highest risk to an individual on the basis of maximum individual risk (probability of an individual's death during the CSDP when at an assumed 0.5 km site boundary). On the basis of maximum lethal distance (the farthest plume reach of any identified accident under the worst-case meteorology), individual risk is highest at PBA, PUDA, and UMDA for the national and regional alternatives. For these three sites, the worst case hazard distance is the result of an aircraft crash into the short-term storage (holding) area while awaiting rail shipment. The fact that these scenarios do not pertain to other sites is due to the elimination of all accident scenarios for which the probability of occurrence during the CSDP is less than 10^{-8}. Since maximum individual risk incorporates probability data in its determination, it may be the preferred measure for individual risk, if only one measure were to be used.

In contrast to the individual risk data for a fixed site, risk to an individual along transportation corridors is calculated to within 0.1 km of the corridor centerline; the individual risk at this minimum distance is the value used in determining maximum individual risk for alternatives including off-site transportation. Maximum individual risk is negligible (less than 10^{-8}) along all the transportation corridors -- a conclusion consistent with the relatively low individual time-at-risk values discussed in section 3.5.1 below. However, maximum lethal distance values are not negligible for the transportation corridors and, in fact, for the LBAD - TEAD corridor (C5 aircraft), can exceed 50 km.

3.0 CONCLUSIONS AND RECOMMENDATIONS

The importance of using aggregated societal risk measures, representing the total risk experienced by all members of the affected community, as a basis for a programmatic decision among alternatives is generally acknowledged. The role of individual risk estimation is less clear. Two arguments for the estimation of individual risk can be suggested:

1. Some members of the public in the vicinity of a CSDP facility or transportation corridor are going to insist on knowing what impact the CSDP (or any other potentially risky program) could have on their personal risk, no matter how many or how severely other

members of the public might be affected. Individual risk computations will enable officials to answer such inquiries.

2. Individual risk estimation will enable the program manager to determine whether or not an acceptable level of societal/community risk arises at the expense of high risk borne by a relatively few people.

The effectiveness of risk management/mitigation efforts should be judged in terms of reductions in not only societal risk measures, but individual risk measures as well. Risk management/mitigation efforts which lead to reductions in societal risk by reducing the number of individuals affected could entail higher risk (e.g., through higher accident probability) for individuals closer to the site boundary or transportation corridor.

The probabilistic measures of individual risk (the risk curve and its intercepts: maximum individual risk and maximum lethal distance) are preferred over the time-based measure, maximum time-at-risk, because they contain more information, accounting for relative magnitude and probability of occurrence of all contributing accidents. However, maximum time-at-risk is the only risk measure appropriate to the question in the mind of that potentially affected individual who asks: "For how long must I and my family be away from home if we will accept no additional risk at all from the program?"

Lastly, individuals do not want to be told that their added risk is small in comparison with risks they voluntary expose themselves to in their daily lives. While it may be useful for the risk analyst and the government program managers/decision-makers to make such comparisons to assure themselves of the reasonableness of the imposed risk, communicating this information to the general public in a convincing way is unlikely to prove successful.

REFERENCES

U.S. Army Program Executive Office -- Program Manager for Chemical Demilitarization (1987), Risk Analysis in Support of the Chemical Stockpile Disposal Program, MTR87W00230, The MITRE Corporation, December 1987, SAPEO-CDE-IS-87014.

U.S. Army Program Executive Office -- Program Manager for Chemical Demilitarization (1988), Chemical Stockpile Disposal Program, Final Programmatic Environmental Impact Statement, January 1988.

Cutler, R. M., The Application of the D2PC Dispersion Model to Large Releases of Chemical Agent, presented at the Twenty-third DOD Explosives Safety Seminar, Atlanta, Georgia, 9-11 August 1988[a].

Cutler, R. M., The Treatment of Uncertainty in a Comparative Risk Assessment, presented at the Twenty-third DOD Explosives Safety Seminar, Atlanta, Georgia, 9-11 August 1988[b].

Perry, J. G. et al, Methodology Issues in the Application of Comparative Risk Assessment to the Chemical Stockpile Disposal Program, presented at the Twenty-third DOD Explosives Safety Seminar, Atlanta, Georgia, 9-11 August 1988.

THE PRESENTATION OF RISK TO THE PUBLIC
- ALTERNATIVE MEASURES AND FORMATS -

Willard E. Fraize
Principal Engineer
Energy, Resource, and Environmental Systems Division
The MITRE Corporation
McLean, Virginia

for

Department of Defense
Twenty-Third Explosives Safety Seminar
Atlanta, Georgia

9-11 August 1988

- - - - - - - - - - -

ABSTRACT

In support of the Chemical Stockpile Disposal Program (CSDP), an analysis was performed of the risk to the public due to the several disposal alternatives under consideration. Risk to the public was viewed from two perspectives: risk to the community or society at large; and, risk to any given individual depending on his location. Community/societal risk can be measured in several ways, including: the probability of one or more fatalities; the maximum number of fatalities; and, the expected value of fatalities, based on accident probability considerations. Individual risk can be expressed in terms of maximum lethal plume length (the distance beyond which no individual would experience a lethal dose) and the probability of an individual's death as a function of position from the accident site. In addition to the probability-based risk measures, two time-based risk measures are introduced: time-at-risk and person-years-at-risk. This paper describes each of these measures, discusses and evaluates the alternative means for their portrayal, and illustrates their use via reference to the CSDP risk analysis.

1.0 INTRODUCTION

The U.S. Army was directed by Congress (Public Law 99-145) to destroy the nation's stockpile of lethal, unitary chemical agents and munitions in a manner which provides for maximum protection to the public. This paper describes the alternative risk measures and the associated presentation formats that were used in the comparative assessment of risk for the several alternatives within the Army's Chemical Stockpile Disposal Program (CSDP).

1.1 The Chemical Stockpile Program

The Chemical Stockpile consists of a wide range of munitions and bulk agent storage containers. Three chemical agent types are used: the persistent nerve agent, VX; the non-persistent nerve agent, GB; and, the persistent blister agents known as mustards and designated by the symbols H, HT, and HD.

The stockpile is currently stored in eight locations throughout the conterminous U.S. (CONUS): Anniston Army Depot (ANAD), Alabama; Aberdeen Proving Ground (APG), Maryland; Lexington Blue-Grass Army Depot (LBAD), Kentucky; Newport Army Ammunition Plant (NAAP), Indiana; Pine Bluff Arsenal (PBA), Arkansas; Pueblo Depot Activity (PUDA), Colorado; Tooele Army Depot (TEAD), Utah; and, Umatilla Depot Activity (UMDA), Oregon.

Of eight programmatic alternatives originally identified for the CSDP, only five were carried through the full scope of the risk analysis; those five are:

- The continued storage of the stockpile in its present locations (this is the "no-action" alternative required by the National Environmental Policy Act) [the CONTINUED STORAGE Alternative (STR)];
- On-site destruction of the stockpile at its present storage lotions [the ON-SITE Alternative (ONS)];
- Movement of the CONUS stocks to two regional disposal centers (at ANAD and TEAD) [the REGIONAL alternative (REG)];
- Movement of the CONUS stocks to one national disposal center (at TEAD) [the NATIONAL alternative (NAT)]; and,
- Movement of the stocks from two sites (APG and LBAD) by air to the national disposal site (TEAD) with the remainder of the stockpile destroyed on-site [the PARTIAL RELOCATION alternative (PRB)].

The other three CSDP alternatives, which will not be discussed in this paper, involve variations on the partial relocation alternative, including an option for water transport of the APG stockpile to Johnston Island in the Pacific Ocean.

1.2 Purpose and Context of the CSDP Risk Analysis

The purpose of the CSDP risk analysis was to provide a consistent and quantitative basis for comparing the risks to the public for each of the disposal alternatives. The results of the risk analysis were used to support the selection of the environmentally preferred disposal alternative in the Final Programmatic Environmental Impact Statement (FPEIS) (U.S. Army, 1988). The results were also used as one of several factors considered by the Army in arriving at its Record of Decision of 23 February 1988 which stated the Army's decision to proceed with the on-site disposal alternative. A detailed description of the risk analysis methodology is reported elsewhere (U.S. Army, 1987; Perry, J. G. et al, 1988) and will not be covered in this paper.

1.3 Definition of Risk

In general, risk is a measure of the potential for exposure to unwanted events or consequences (e.g., injuries or fatalities). For purposes of the CSDP risk analysis and this paper, risk is defined as the expected impact on public safety as a result of the set of possible agent-releasing accidents associated with the storage, transporting, handling, and physical destruction (demilitarization) of the munitions and agent in the stockpile. Risk is measured by both the probability of a lethal event (potential accident) occurring and the number of public fatalities that might result if the event were to take place.

For purposes of this study, the term "public" excludes persons within the boundaries of the military installations.

1.4 Perspectives of Risk

Both individual and community/societal perspectives of risk are considered, although the emphasis is on the latter. The risk to an individual is calculated by multiplying together the probabilities of each of the circumstances necessary to produce a fatality. The total risk to an individual is the sum of the individual risks posed by each identified accident scenario that could happen at the individual's location. To estimate the risk to the general population, the factors defining risk to

an individual must be applied to the total number of individuals potentially affected by any accident.

The public on whom any risk associated with the CSDP will fall will view the imposed risk as involuntary risk, as opposed to the kind of risk that may be routinely and voluntarily accepted in the normal course of life. This difference in perspective will generally affect, in a negative way, the public's willingness to accept either the fact of added risk, regardless of how small the increment, or the credibility of its estimation. The public's skepticism and fear of the unknown, when it deals with involuntary risk (such as that due to the CSDP), will make the job of the presenter of risk results much more difficult. Attempts to compare risk analysis results with risk due to voluntary activities such as driving an automobile (where the risk-taker obtains a direct benefit -- mobility -- from his/her high risk activity) will usually fail to be convincing.

2.0 MEASURES OF RISK

2.1 Components of Risk

Risk may be described as the product of two quantities: the probability of the unwanted event occurring and the consequence to an individual or the public, if the event does occur.

The probability of a potential accident is a quantitative statement of the "odds" of that accident occurring during the course of the CSDP. For instance, analysis of the accident and all of the separate events leading up to it might show that the odds of the accident occurring at some time during the CSDP might be 1 in 200,000; we can express the probability of that event occurring in just that way -- 1 in 200,000 -- or in the following equivalent ways: 0.000005; 1/200,000; or, in scientific notation, 5×10^{-6}. For this analysis, the probability of an accident is expressed as the likelihood (or "odds") of its occurring once during the stockpile disposal program. The only exception is for long-term storage accidents where probability has been expressed as the likelihood of occurrence during a 25-year period (the assumed duration of the "no-action" alternative).

Since the results of this study were used to communicate information to the general public, we have, in most cases, used the term "probability" where, in a strictly technical sense, the term "frequency" would be used by statisticians. The term "frequency" might confuse some people when it is used to describe events that that have not occurred and are very unlikely ever to happen. Moreover, when the frequency values are very small, there is little difference between these and the probability values.

Generally, the consequence of a potential CSDP accident could be expressed by several measures, of which the most important are:

- size of the lethal plume produced by the accident, defined as the downwind distance to where the "exposure" (the product of agent concentration and time) equals the estimated minimum lethal value (the "no-deaths" hazard distance). Plume size depends on agent type, quantity, mode of release, and meteorological conditions.

- potential fatalities per event, as determined from plume size and direction, local population distribution (by distance and direction), and estimates of human response to chemical agent exposure.

For the CSDP risk analysis and in this paper, the preferred consequence measure is the latter one -- potential fatalities (per event) -- because it is best representative of potential impacts on the local population and is sensitive to its local density and distribution.

Figure 1 is a graphical portrayal of the two-dimensional nature of risk. Any potential accident can be displayed on such a graph, given an estimate of its two risk parameters: probability and consequence (here measured in terms of the length of the agent plume resulting from the accident). High risk events would fall in the upper right hand portion of such a chart; low risk events are those in the lower left of the chart. The dashed line symbolizes a typical site boundary around a CSDP installation, and serves to show that if an event's severity yields a plume length less than the distance to the site boundary, then the consequences of the event remain on-site and are of no immediate concern to the public. Of course, the Army and on-site personnel are concerned and can be affected by all events.

This risk analysis treats acute/lethal effects only, and is limited to consideration of airborne release of agent.

2.2 Societal/Community Risk Measures

If the set of accident scenarios which contribute to the risk for a given disposal alternative at a given location or site are sorted in decreasing order of consequence, as measured by potential fatalities per event, and the probability values for each accident are added cumulatively beginning with the highest consequence accident, then a plot of the resulting quantities, cumulative probability vs. potential fatalities, will define the societal or community cumulative risk curve for the alternative and location. If the accident scenarios applicable to all locations are combined into one data set, then the resulting cumulative risk curve is the programmatic risk curve for the alternative. A representative cumulative risk curve is shown in Figure 2. Using the cumulative risk curve in Figure 2 as a guide, three probability-based measures of societal or community risk, as used in the CSDP risk analysis, can be defined:

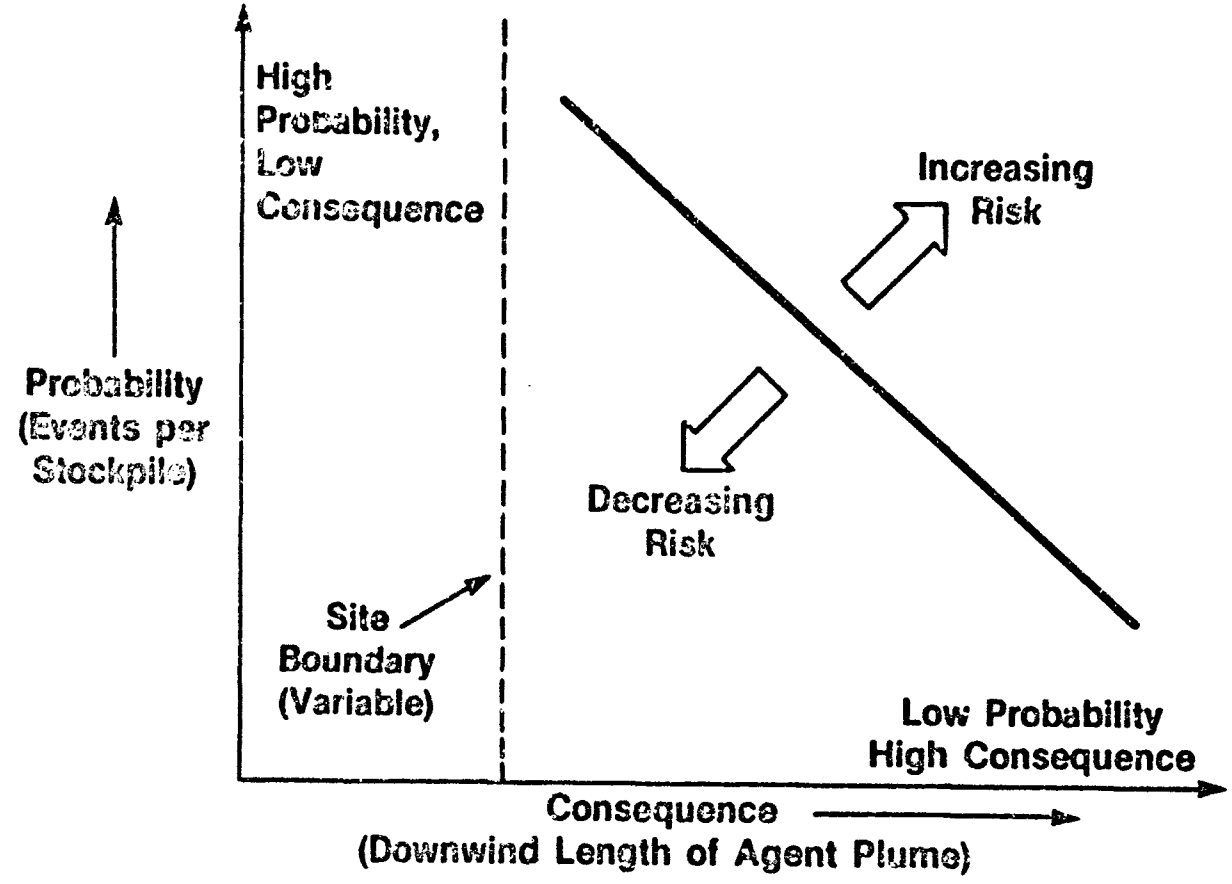

FIGURE 1. RISK AS MEASURED BY PROBABILITY AND CONSEQUENCE

- **probability of one or more fatalities**, a public risk indicator equal to the chance that there will be at least one fatality at a given site or for the nation as a whole during the CSDP. This measure is calculated by summing the probabilities of all accidents that could cause one or more fatalities. Included in this sum are all accidents for which the potential fatality estimate, based on assuming uniform population densities, is less than unity. (This means that that accident is expected to cause a fatality for only a fraction of the times it occurs; for the remaining fraction of occurrences, that event would not cause a fatality. For such accidents, the probability of occurrence is reduced so that only the fraction of events expected to cause a fatality are counted).

- **maximum number of fatalities**, equal to the maximum consequence of all accidents at a site or for the nation. This risk measure is based on worst-case weather conditions, actual population densities (1980 census data, as analyzed by Oak Ridge National Laboratories), and worst possible wind direction (i.e., plume striking the highest number of people without any allowance for preventive/emergency response measures).

- **expected fatalities**, equal to the sum of the risk contribution of all accidents at a site or for the nation, where risk for each accident is the potential fatality count (if the accident were to occur) multiplied by the probability of the accident occurring. Note that expected fatalities is proportional to the probability of a fatality-causing event occurring, and will nearly always be a small number -- well less than unity. For example, an accident with a potential fatality estimate of 12 and a probability of 10^{-6} (odds of 1 in a million of occurring during the CSDP) would have an expected fatality value of 12×10^{-6}. At the programmatic level, the expected fatalities value is the sum of the expected fatality contribution of several hundreds of potential events and might lie somewhere in the range of 10^{-3}, or 0.001. This typical value can be interpreted in the following way: The program can be expected to cause, on average, one fatality every 1000 times the program is executed; since the program consists of many events which could cause multiple fatalities, a more typical interpretation would be made up of several parts, such as: one fatality every 10,000 programs (expected fatality contribution of 1/10,000 = 0.0001) plus a 10-fatality event every 25,000 programs (contribution of 10/25,000 = 0.0004) plus a 100-fatality event every 200,000 programs (contributing 100/200,000 = 0.0005), for a total expected fatality value of 0.001.

In addition to the probability-based societal/community risk measures listed above, a time-based societal risk measure was defined:

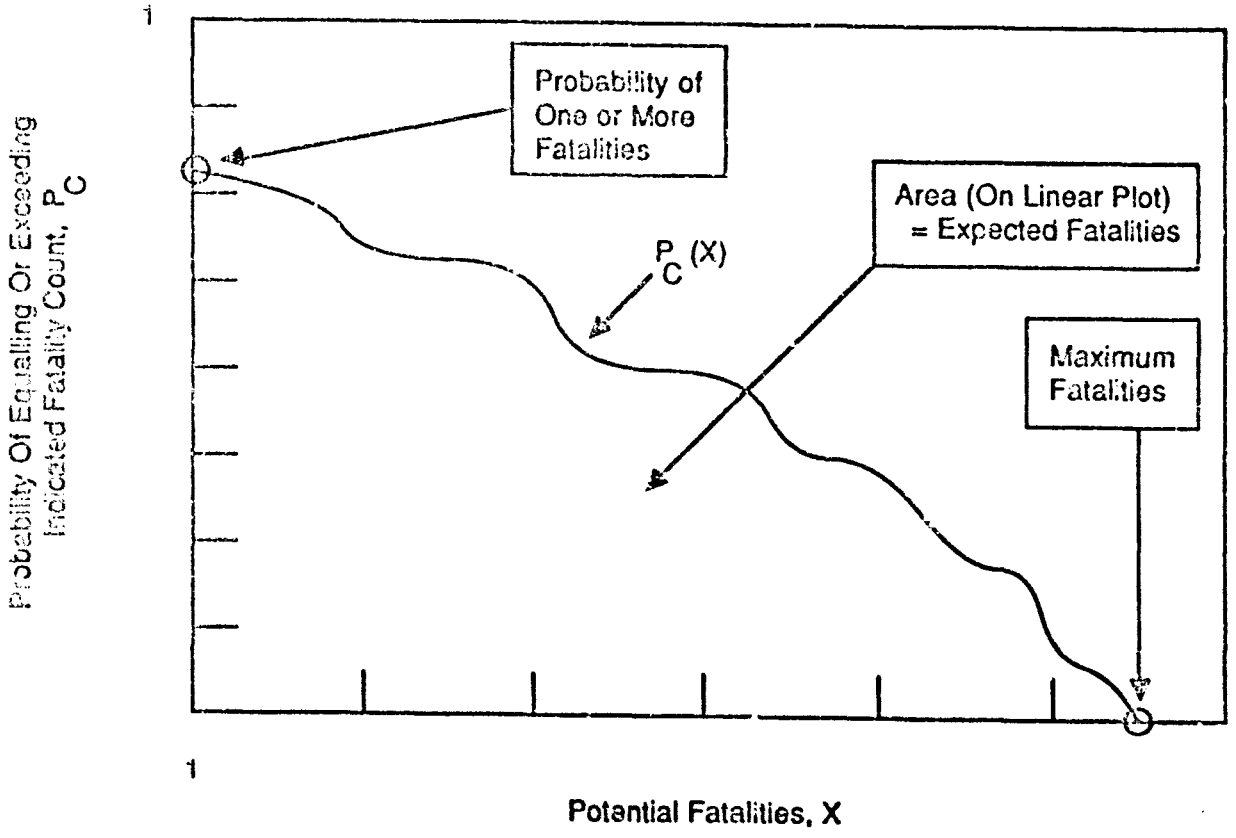

FIGURE 2. REPRESENTATIVE CUMULATIVE RISK CURVE (SOCIETAL RISK).

- person-years-at-risk, equal to the population living within all zones that could experience potentially lethal agent exposure multiplied by the time period over which that worst-case event could take place (typically, the duration of disposal operations at fixed sites or the time during which transport vehicles might be within lethal plume reach of population groups along the corridors). This measure does not account for the fact that individuals within the affected population groups who are farther from the potential accident site are at lower risk of suffering ill effects of exposure; all affected individuals are counted if they have any risk at all.

2.3 Individual Risk Measures

For the estimation of individual risk, a different approach is required. For each applicable accident scenario, the probability of an individual's death at a given distance from the site of the agent release is estimated as the product of three terms: 1) the probability of the event occurring; 2) the probability of an individual being within the plume, given a uniform wind-rose (equal to the ratio of plume width to the perimeter of the circle designating the individual's given distance from the release site); and, 3) the fatality rate associated with the centerline dosage within the plume at a given distance from the release site (see section 4.1.3). This product, determined for the fixed distance increments of 0.1, 0.2, 0.5, 1.0, 2.0, etc. out to 100 km, is then summed for each distance value for all applicable potential accidents. The result is an individual risk curve, defining the probability of an individuals' death as a function of distance from the site. A representative individual risk curve (for a specified site) is presented in Figure 3. Using the individual risk curve in Figure 3 as a guide, the following measures of risk to an individual at a given location were defined:

- maximum individual risk, equal to the probability of a fatal exposure at the site boundary (assumed to be 0.5 km from the on-site disposal/storage operations) or as close as 0.1 km to the centerline of a transportation corridor. This indicator is equal to the vertical intercept of the individual risk curve at the appropriate distance value (0.5 or 0.1 km); it is dependent only on the mix of potential accidents that could happen at the individual's location and, since it applies only to an individual, is independent of population density.

- maximum lethal distance, equal to the maximum downwind length (given by the 'no-deaths' dose) of the plume from the worst of all identified potential accidents under worst-case weather conditions at a specific location. Conversely, it is also the minimum distance an individual could be from a given site or transportation corridor and have no risk of lethal exposure during the disposal

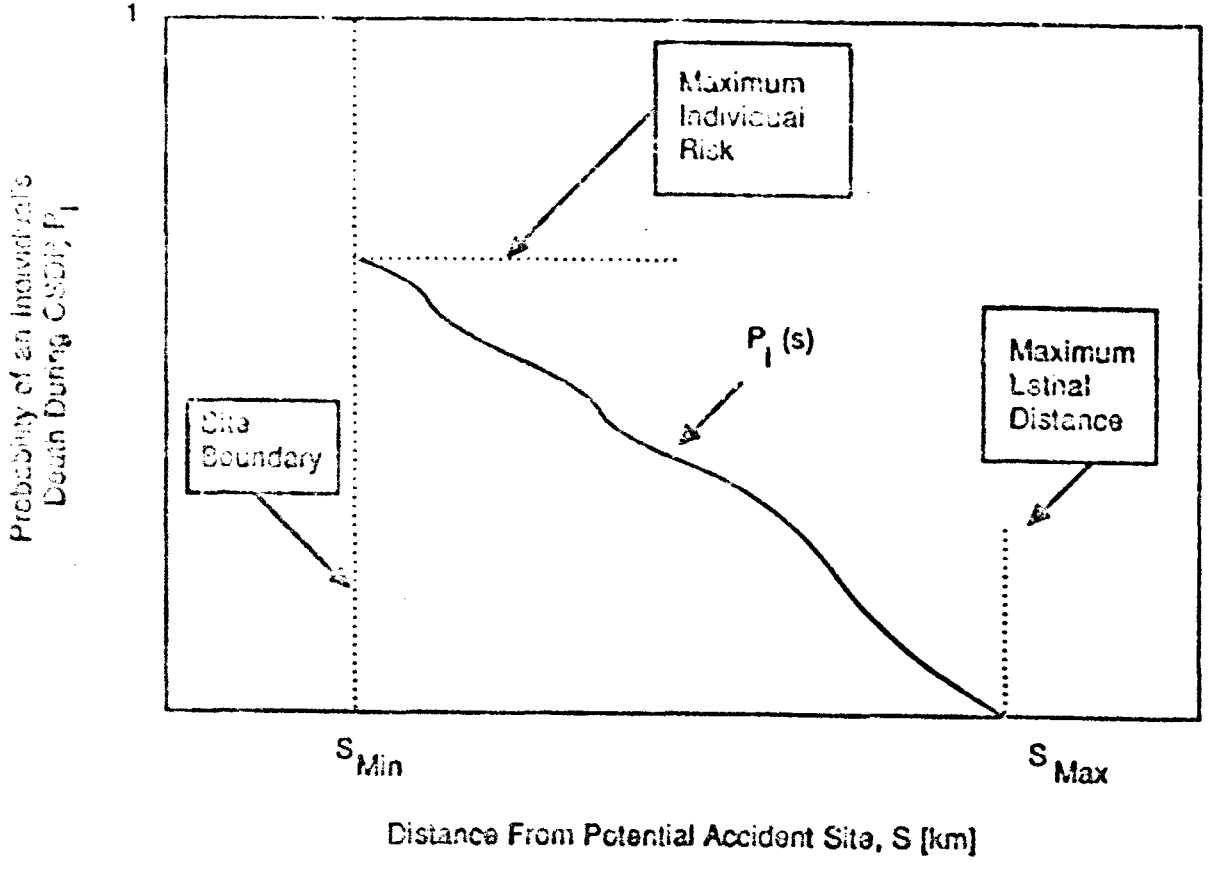

FIGURE 3. REPRESENTATIVE INDIVIDUAL RISK CURVE

program. It is equal to the horizontal intercept of the individual risk curve at some minimum accepted level of credibility -- say, 1 x 10^{-10} per stockpile.

In addition, the following time-based risk measure was defined to address those members of the public who were most concerned about whether and for how long they might be exposed to any risk at all, independent of magnitude (dose or probability):

- **maximum total time at risk**, representing the maximum length of time an individual could be at risk at a fixed location near a site or along a transportation corridor. For those living within a radius equal to or less than the maximum lethal hazard distance, the time at risk is the total time during which stockpile disposal activities will take place at that site, regardless of where the individual is located. For those individuals along the transportation corridors, the time depends on the distance from the rail line or air corridor; the maximum time is assumed to occur if the individual is located at a 0.1 km distance from the rail track or centerline of the air corridor. These persons are exposed to a hazard only when a train or aircraft is in the vicinity (defined as the maximum lethal hazard distance in either direction) of them. This time is summed for each agent-bearing train or aircraft that would pass by in each alternative. Since maximum lethal hazard distance is used in this determination, the worst-case meteorological conditions apply.

3.0 PRESENTATION OF RISK

The presentation of risk analysis results follows an extensive analysis effort which must begin with the definition of a set of potential accidents (scenarios) for the particular activity and location(s) of interest. Each accident must be described in terms of its probability of occurrence and its expected release of agent (by mode and amount of release). The validity of the risk analysis is highly dependent on the quality and comprehensiveness of the accident scenario data base. The computational procedure for determining aggregate risk measures is described in other papers at this seminar. In this section, we will briefly discuss the varied audience for the CSDP risk analysis results and will then describe the several means used for communicating those results.

3.1 Audiences to be Addressed

The risk analysis is intended to meet information needs of several audiences. The principal audiences are:

- Army decision-makers who must select a disposal alternative;
- local governments and community groups who need to understand and evaluate the potential impacts on their local populations;
- individuals who are concerned about their personal risk, given their locations with respect to storage sites, disposal sites, or transportation routes; and
- Army program managers responsible for implementing a disposal alternative, who must be aware of activities that have the potential for high risk to the public, and who must ensure that the CSDP is implemented safely.

Some of these audiences may be most concerned about community/societal risk -- that is, the total number of persons potentially affected by the program as a whole. Others may be concerned about identifying the major contributors to societal or community risk so they can do something about mitigating or managing it. Individuals are concerned about what the program means to them, personally, and may or may not be interested in community or societal risk.

3.2 Presentation Formats

Three formats for presenting risk in varying levels of detail are depicted by Figure 4:

Item A. Risk curves, which portray, for the full set of applicable accident scenarios:

- the probability of exceeding a given number of potential fatalities per event (vertical axis), against
- the potential fatalities per event (horizontal axis);
- the upper and lower bound estimates, as well as the mean (average) value, reflecting the uncertainty in the probability component of the risk curve -- the uncertainty range defining the 90% confidence limits; and
- the maximum potential fatalities, assuming worst-case meteorology, distributed population, and worst possible wind direction, shown as a dashed vertical line.

Risk curves depict the overall character of the set of identified accidents which make up the risk for a program alternative. A visual comparison of risk curves will not only reveal the relative differences in

A. RISK CURVE

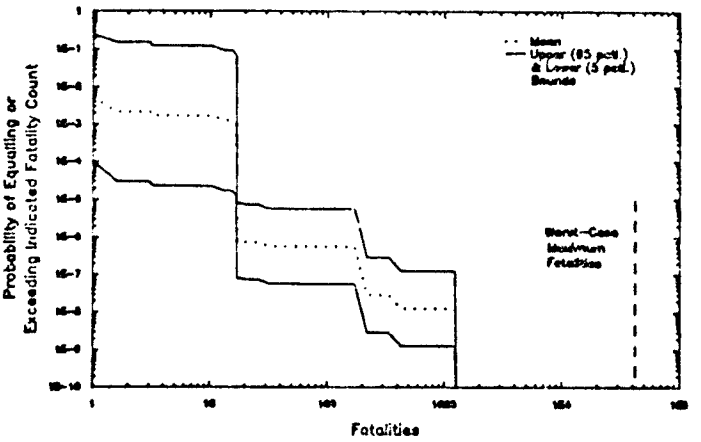

B. RISK PICTOGRAM

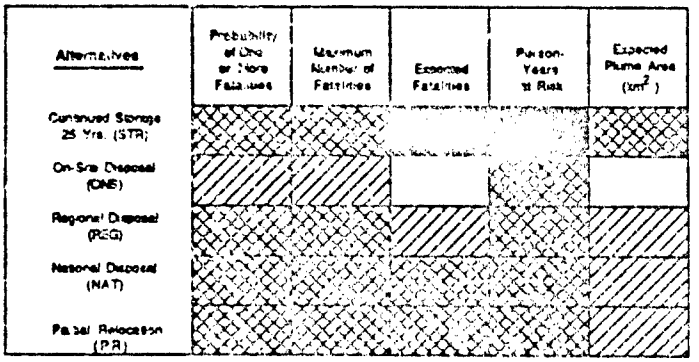

C. EXPECTED FATALITIES PLOT

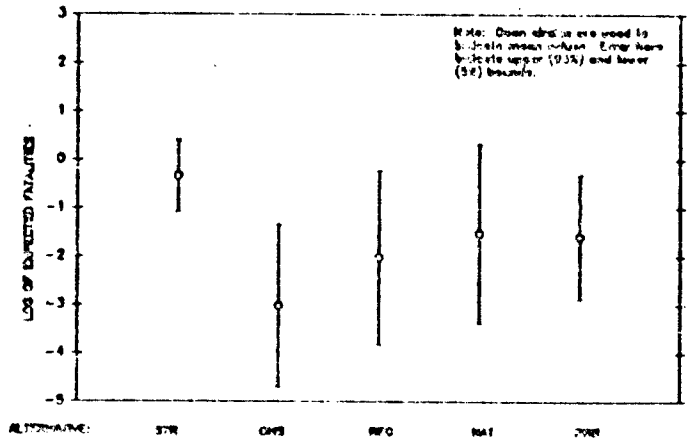

FIGURE 4. PORTRAYAL OF PUBLIC RISK -- 3 ALTERNATIVE FORMATS

overall risk of alternatives, indicated by the area under the risk curve (on linear plots only), but will also make apparent, for alternatives having comparable overall risk (area), the difference between alternatives dominated by high-probability/low-consequence accidents and those dominated by low-probability/high-consequence accidents.

An illustration of a cumulative risk curve, showing a number of sources of community/societal risk, is presented as Figure 5. Figure 5 serves not only to indicate historical precedent for use of cumulative risk curves but will also enable the reader to compare the results of the CSDP risk analysis with the risk reported for other types of societal risk. Note that the representative societal risk curves in Figure 5 are presented in terms of the (low) frequency that an accident of consequence equal to or greater than that given by the horizontal scale will occur during a recurring time period (one year); the CSDP cumulative risk curves, on the other hand, are expressed in terms of a probability that an accident of consequence equal to or greater than that given by the same horizontal scale will occur during the fixed (non-recurring) duration of the CSDP.

Item B. Risk pictograms, which display:

- a pictorial indicator (the darkness of the shading) of the relative magnitude of each of the measures of risk chosen for this analysis;
- a key to the numerical range represented by each of the shading values (not shown); and
- an array of data allowing comparison of risk at all sites for a given disposal alternative or, alternatively, comparison among alternatives for a given site (both approaches are used in this report).

Risk pictograms provide a visual impression of the relative magnitude of public risk for all combinations of alternatives and locations. They were chosen as the preferred vehicle for reporting risk results to the public in the FPEIS.

Item C. Expected fatalities plots, showing mean estimated values of expected fatalities, with uncertainty bands. The expected fatalities value is defined as the sum of the risk (probability times potential fatalities) for all applicable accidents. While this measure of risk is convenient and consistent, permitting the summing and disaggregation of the contributions to CSDP risk, it provides the least information of any of the risk measures. For example, it does not clearly show the relative contributions of low consequence/high probability accidents and high consequence/low probability accidents, which is often of great interest to the public. As illustrated in Figure 4, expected fatality data are presented in this report with error bars indicating the estimated uncertainty in the

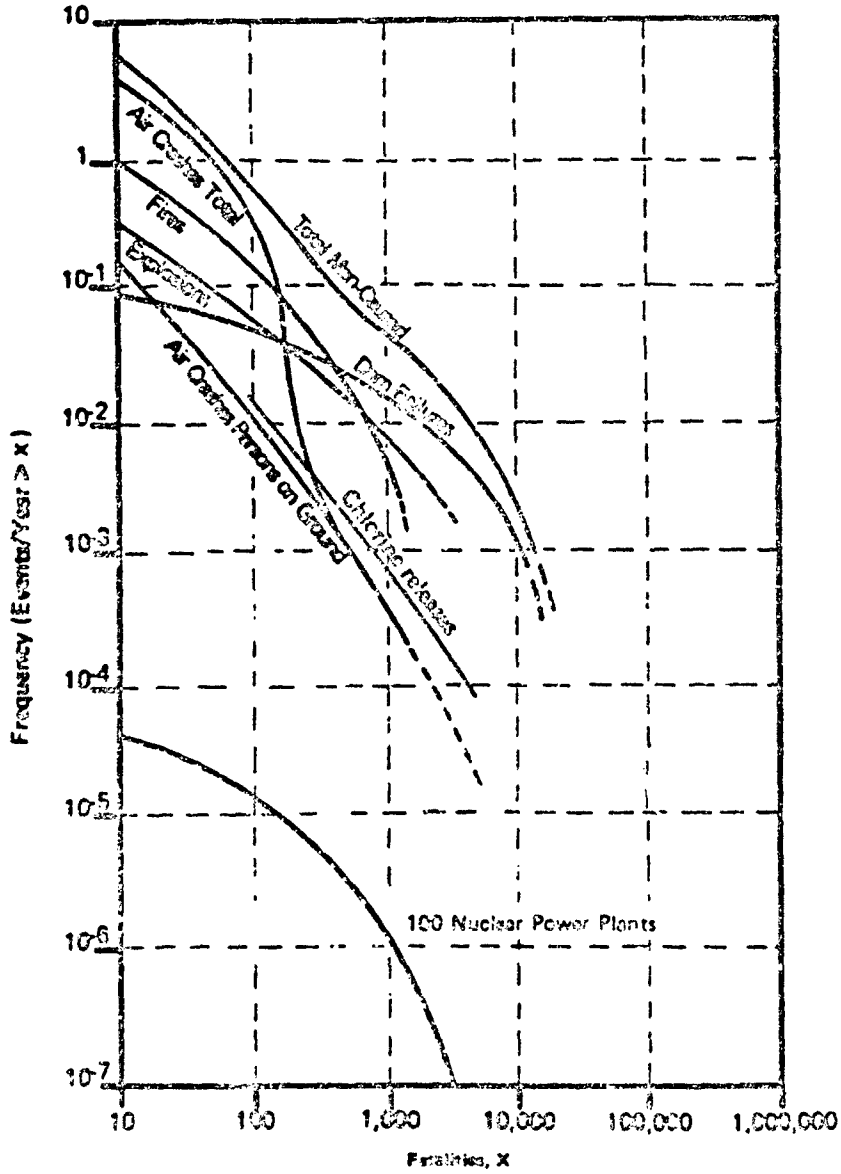

Comparisons of risks for fatalities. (From Reactor Safety Study, WASH-1400 (October 1975).)

FIGURE 5. EXAMPLE USE OF RISK CURVES

calculated value. The extremes of the error bars represent the 90% confidence limits -- that is, there is only a 10% probability that the actual expected fatalities value would fall outside the indicated range.

The three graphical presentation formats described above were the major means for portraying the results of the CSDP risk analysis. Examples of these and other supplementary formats are presented in section 4.0.

3.3 Dealing with Uncertainty

Uncertainties in the estimation of risk arise due to many causes, including the inadequacy of data, inaccuracies in modeling, and the incomplete identification and understanding of accident phenomena. Uncertainty can arise in the estimation of both probability and consequences. The methodology for the treatment of uncertainty in the risk analysis results is beyond the scope of this paper; it is, nevertheless, dealt with in detail by another paper at this seminar (R. M. Cutler, 1988). For presentation purposes, uncertainty can be indicated as a band about the mean on the risk curves (Item A, Figure 4) or as an error/uncertainty bar on the expected fatality plots (Item C, Figure 4). Uncertainty analysis can also be helpful in determining whether or not the difference in risk, as measured by expected fatalities, between two alternatives is statistically significant. An illustration of the role of uncertainty analysis in risk portrayal may be found in section 4.0.

4.0 SOME EXAMPLES FROM THE CSDP RISK ANALYSIS

4.1 Risk Curves

Risk curves contain the most detailed information of any of the alternative formats. However, risk curves do not reveal the contribution to overall risk of individual accident scenarios -- information that is of interest to the program manager who must take responsibility for managing risk by focussing on and mitigating those accident scenarios most contributing to risk; to do this, one needs a complete tabulation of individual accidents, characterized and ranked according to risk as measured by expected fatalities (i.e., the product of probability and potential fatalities). Such a detailed presentation was a part of the risk analysis results (classified SECRET), but is not included here because of the classification issue and the fact that it is beyond the scope of this paper.

Illustrations of risk curves to depict risk associated with the CSDP are found in Figures 6 and 7. Figure 6 displays risk for the on-site disposal alternative; this particular risk curve applies to the risk analysis results before mitigation efforts were applied (Mitigation of the

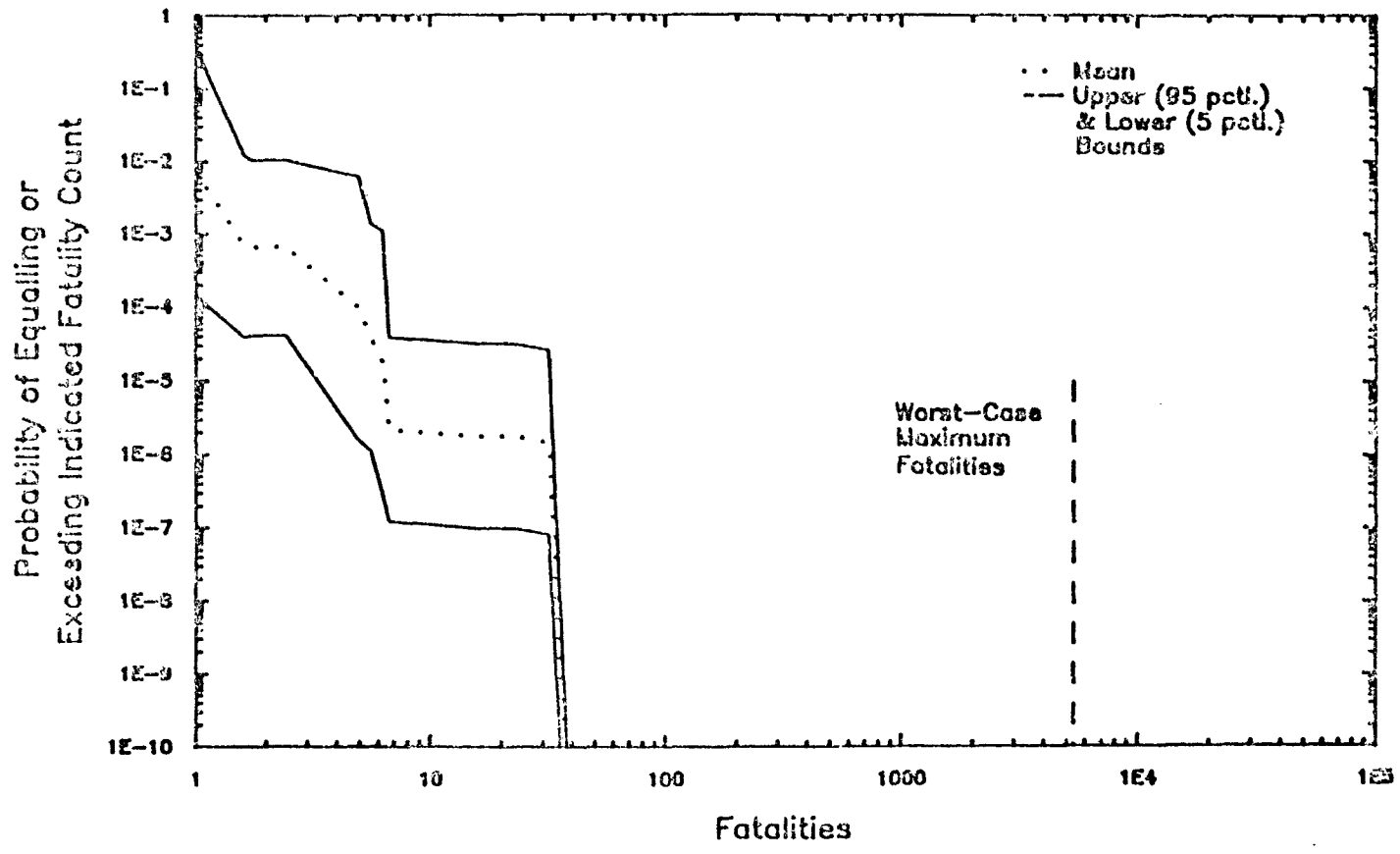

Note: This curve represents risk prior to implementation of mitigation measures; it is included for illustration of presentation format only.

FIGURE 6. CUMULATIVE RISK CURVE FOR THE ON-SITE DISPOSAL ALTERNATIVE
- with Uncertainty Bounds -

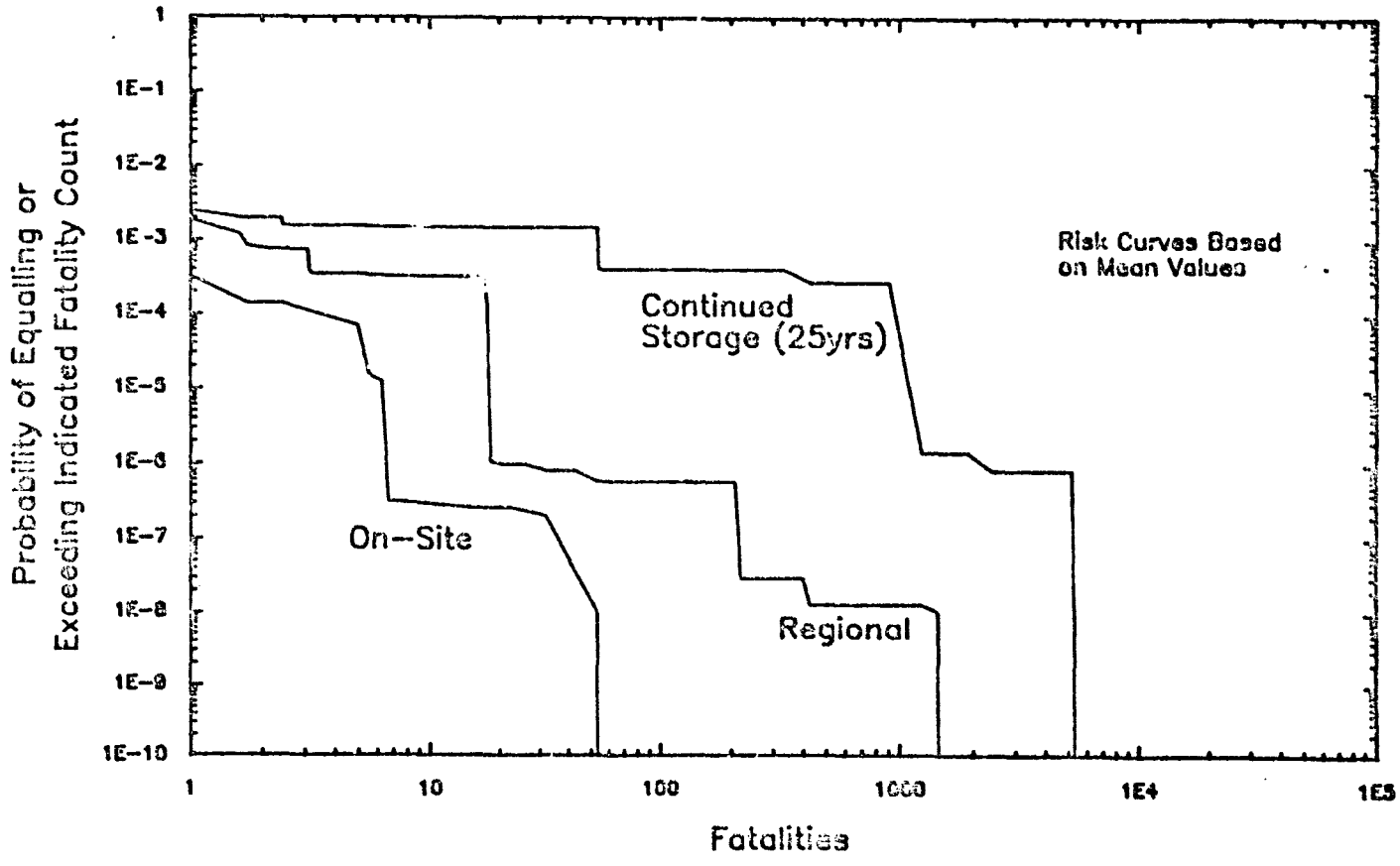

FIGURE 7. CUMULATIVE RISK CURVES FOR THREE CSDP ALTERNATIVES

CSDP risk is presented in another paper at this seminar (R. B. Perry and W. W. Duff, 1988). This curve shows the upper and lower uncertainty bounds as well as the mean value estimate for the risk curve. Focussing only on the mean value curve, we can see that the risk curve indicates a probability of nearly 1 in 100 that there will be at least one public fatality during the course of the CSDP, somewhere among the eight CONUS sites. (For the mitigated risk case, that probability of one-or-more-fatalities drops to about 1 in 3000). Figure 6 also indicates that for the most-likely meteorological conditions, the maximum fatalities to be expected from the most severe potential accident are in the range of 40 deaths. For worst-case meteorological conditions, the most severe accident could involve over 5000 fatalities; however, no probability can be assigned to this accident because its occurrence is dependent on the unknown probability of the worst-case weather occurring and on the lethal agent plume being directed in the worst possible direction (covering the most heavily populated regions). Showing the upper and lower bounds (at the 95 and 5 percentile levels, respectively) allows the reader to conclude that there is a 90% probability that the actual risk curve will lie between the upper and lower bound curves.

The same type of cumulative risk curve, but without uncertainty bounds is shown in Figure 7 wherein the risk curves represent the mean value of risk (expected fatalities) for three CSDP alternatives (chosen for illustration only, since the three encompass all activity categories considered in the risk analysis): Continued Storage; On-site Disposal; and Regional Disposal. The three risk curves show clearly the differences in general character of risk associated with the three alternatives:

- As seen by the relative areas under each curve, continued storage (for 25 years) poses highest overall risk (expected fatalities), and on-site disposal the least;
- Similarly, continued storage could lead to more (maximum) fatalities, by a factors of 100 over on-site disposal and 3 to 5 over regional disposal;
- For the three alternatives, the probability of one-or-more fatalities is within a factor of 10, with storage posing the greatest risk by that measure and on-site disposal the least.

4.2 Risk Pictogram

Figure 8 contains the risk pictogram which compares the five major CSDP alternatives on the basis of four of the major risk measures (defined above in sections 2.2 and 2.3) plus a fifth measure, expected plume area, introduced to assist in addressing ecological impact of the CSDP

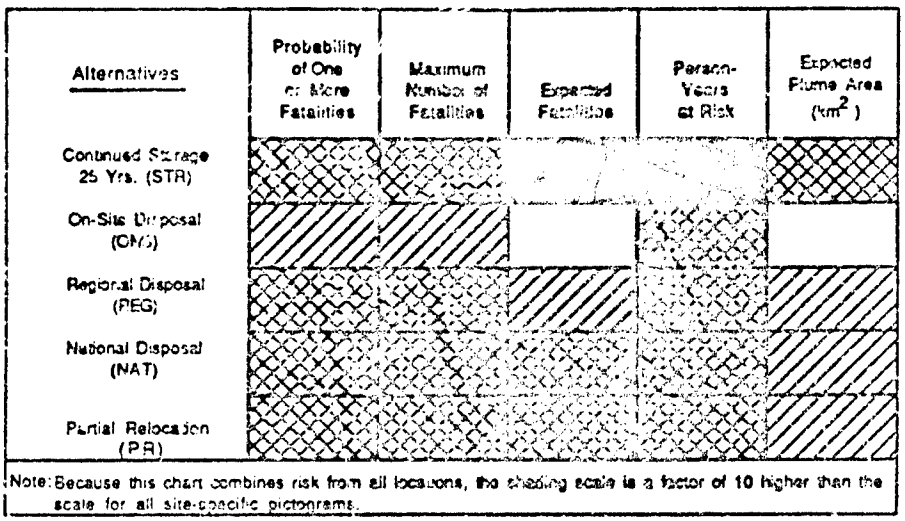

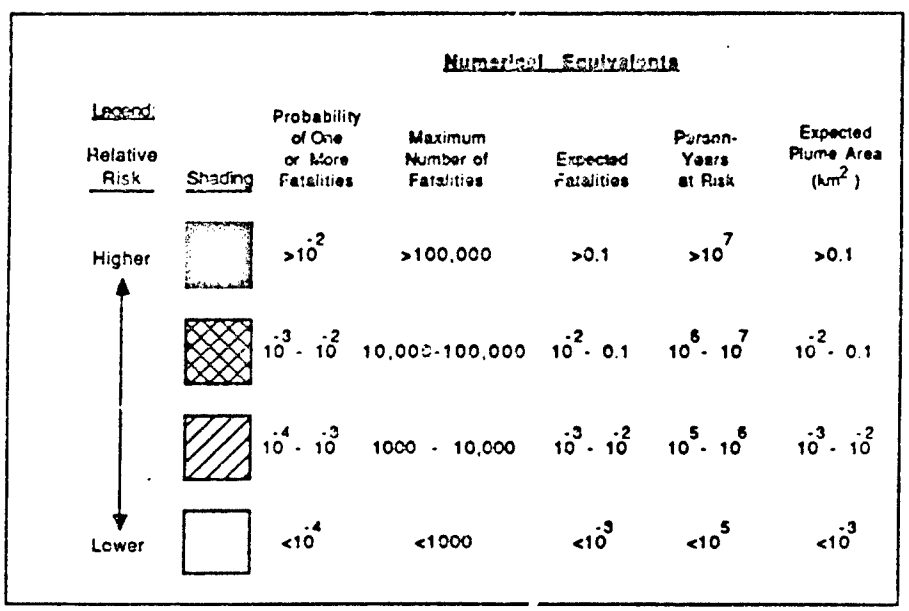

FIGURE 8. PICTOGRAM COMPARISON OF PROGRAMMATIC RISK FOR CSDP ALTERNATIVES
- All Locations Combined, with Mitigation -

alternatives. The four levels of shading are defined by numerical ranges in the block below the pictogram itself; darker shading signifies higher risk for each measure. The shadings assigned to each block in the pictogram are dictated simply by where the mean value for each risk parameter falls with respect to the numerical boundaries for each shading category. Hence, two alternatives could show shading differences one category apart when the actual mean values were very close to one another, as long as the two values fall on opposite sides of the shading category boundary. Since the numerical ranges for the shading categories are a factor of 10 wide, differences of two shading categories would indicate a difference in mean value of the risk measure in question of at least a factor 10 and as much as a factor of 1000 or more.

In Figure 8, the on-site disposal alternative is indicated to have the lowest value of risk for all measures except person-years-at-risk, for which it appears comparable to the other disposal alternatives (not including continued storage). Whether or not the difference in risk as indicated by the pictogram is significant can not be determined from the pictogram alone, but can and was addressed by the uncertainty analysis. The pictogram shows also that there is no significant difference in risk among the three alternatives involving off-site transportation (the so-called 'collocation' alternatives).

4.3 Expected Fatalities Plots

The expected fatalities values for each disposal alternative (the area under the respective cumulative risk curves) can be compared with one another on a simple 'error bar' plot as shown in Figure 9. The error bars indicate the upper and lower uncertainty bounds (estimated to be the 95 percentile and 5 percentile, respectively) which are the expected fatalities values based on the areas under the upper and lower bounds of the corresponding cumulative risk curve (see Figure 6 for the on-site disposal alternative). The alternative-defining acronyms along the horizontal axis of Figure 9 are defined in section 1.1.

Figure 9 shows that on-site disposal (ONS) has the lowest value for expected fatalities -- approximately 10^{-3} expected fatalities per CSDP stockpile -- of any alternative; but, the size of the uncertainty band relative to the differences between the mean values suggests the strong possibility that, given the estimate of uncertainty, the risk due to on-site disposal might actually be greater than that for one or more of the other alternatives; there appears to be little likelihood that the on-site disposal risk will be greater than the risk of continued storage for 25 years.

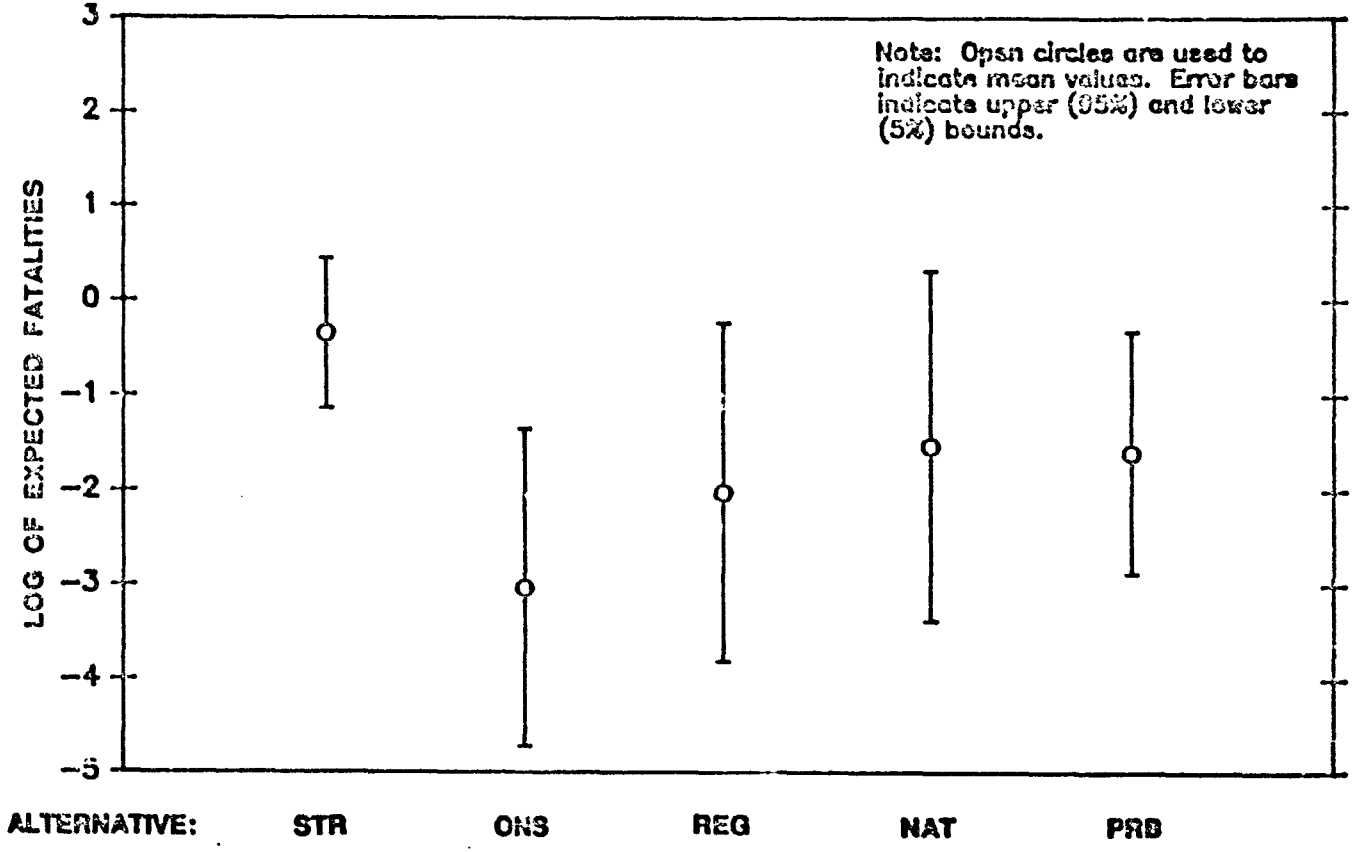

FIGURE 9. COMPARISON OF SOCIETAL RISK (EXPECTED FATALITIES) FOR PROGRAMMATIC ALTERNATIVES -- with Uncertainty Bounds

4.4 Portrayal of Uncertainty

For the five CSDP alternatives illustrated in Figure 9, an analysis of the uncertainty of differences between any two alternatives, using a method outlined in another paper at this seminar (R.M. Cutler, 1988), will yield estimates of the probability that the risk associated with one alternative will be greater than the risk of any other alternative. The results of this comparison are displayed in Table 1. An explanation of how to interpret the table is appended as a footnote to the table. Note that, according to Table 1, there is only a 1 percent chance that on site disposal risk will be greater than that associated with continued storage (25 years). However, the risk difference between on-site and regional disposal is noticeably less, as seen in Figure 9, and the results in Table 1 confirm this by showing that there is a 25 percent probability that on-site disposal risk is greater that regional disposal risk; conversely, there is a 75 percent probability that on-site risk is indeed less than regional disposal risk.

4.5 Person-Years-at-Risk

Figures 10 through 12 illustrate the CSDP risk using person-years-at-risk as the measure. The method for computing this risk measure is outlined in section 2.2. Figure 10 compares person-years-at-risk for the CSDP alternatives for all locations, including transportation corridors as appropriate. Continued storage (25 years) clearly dominates this risk measure because of the longer exposure time for this ('no-action') alternative and the severity of the credible accidents because of the large size of the inventory potentially releasable in an accident. On-site disposal indicates the lowest value for person-years-at-risk of all alternatives. Figure 11 shows person-years-at-risk for the transportation corridors only. On the basis of this parameter, regional disposal appears to be preferred by far. Note the very low value for the person-years-at-risk along the corridors (5,000 to 50,000) compared to the programmatic values which include the person-years-at-risk around the storage and disposal sites (2 million to 135 million). Lastly, Figure 12 shows person-years-at-risk as distributed among the disposal sites for the on-site disposal alternative. Values range from essentially zero, at PUDA, to over 1 million at PBA, with ANAD not far behind at 650,000.

TABLE 1. PROBABILITY OF RISK DIFFERENCES BETWEEN ALTERNATIVES [percent]*

Definition of Alternative Codes:

STR: Continued Storage
ONS: On-site Disposal
REG: Regional Disposal
NAT: National Disposal
PRB: Partial Relocation by Air

	PROBABILITY THAT RISK(ALT_i) > RISK(ALT_j)				
ALT_i \ ALT_j:	STR	ONS	REG	NAT	PRB
STR	0	99	92	83	91
ONS	1	0	25	16	4
REG	8	75	0	36	37
NAT	17	84	64	0	52
PRB	9	96	63	43	0

* Example: The probability that NAT (in row 4) is riskier than ONS (in column 2) is 84 percent. Conversely, the probability that ONS (in row 2) is riskier than NAT (in column 4) is 16 percent. Note that the two results, 84 percent and 16 percent, are complementary and total 100 percent. Thus, the "odds" that NAT is riskier than ONS are 84:16, or about 5:1. These results are based on comparisons of the means and ranges of computed "expected fatalities," after eliminating accident scenario contributions common to the two alternatives being compared (in order to obtain independently distributed data). Since some types of uncertainty have not been considered explicitly, mid-range probabilities (e.g., those between 30 percent and 70 percent) are not believed to substantiate conclusions that risks are different.

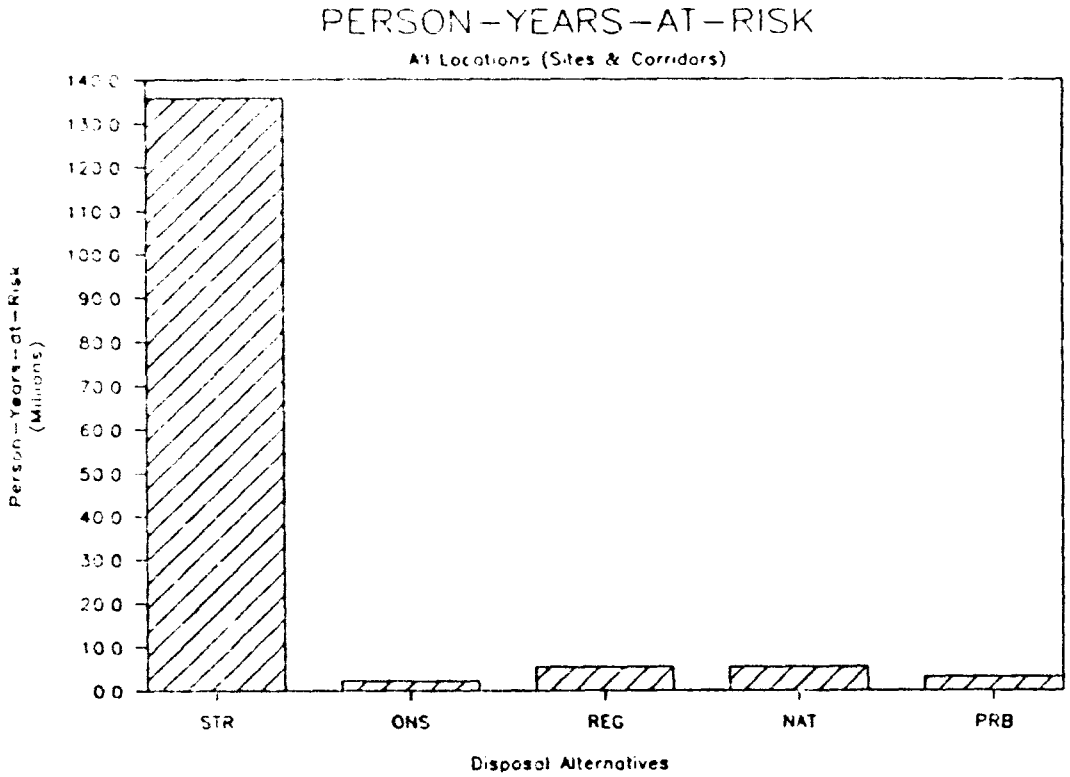

FIGURE 10. PERSON-YEARS-AT-RISK -- CSDP PROGRAMMATIC ALTERNATIVES
- All Locations (Sites and Transportation Corridors) -

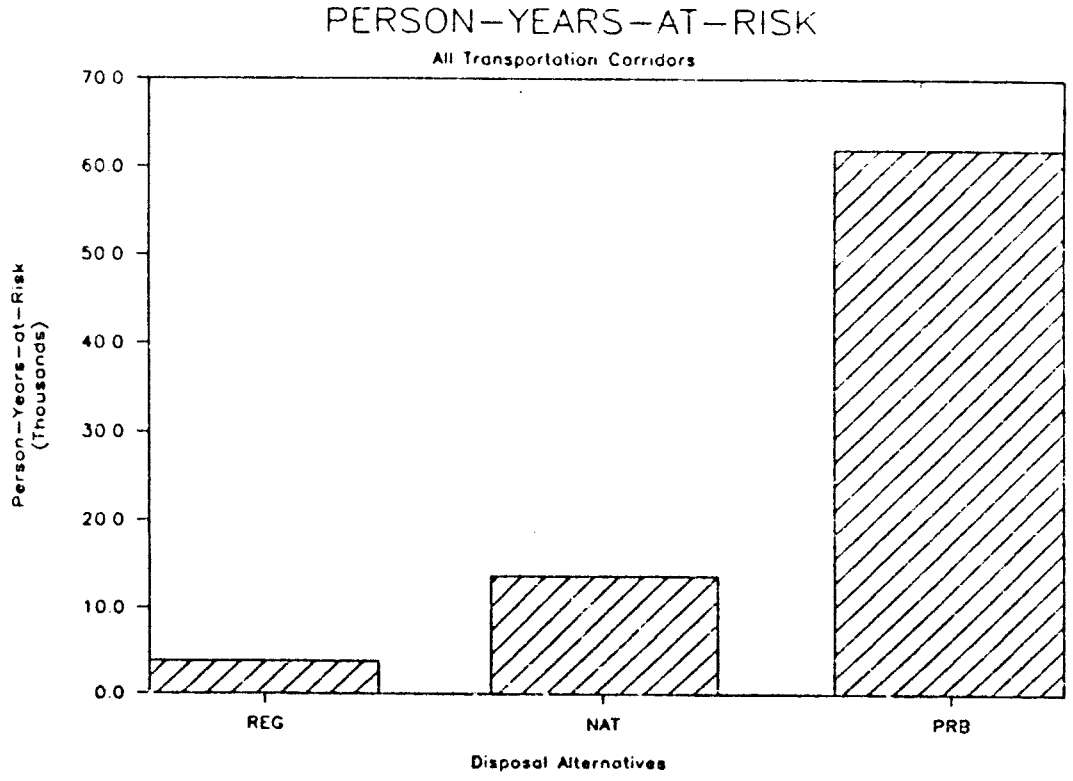

FIGURE 11. PERSON-YEARS-AT-RISK -- CSDP PROGRAMMATIC ALTERNATIVES
- Transportation Corridors -

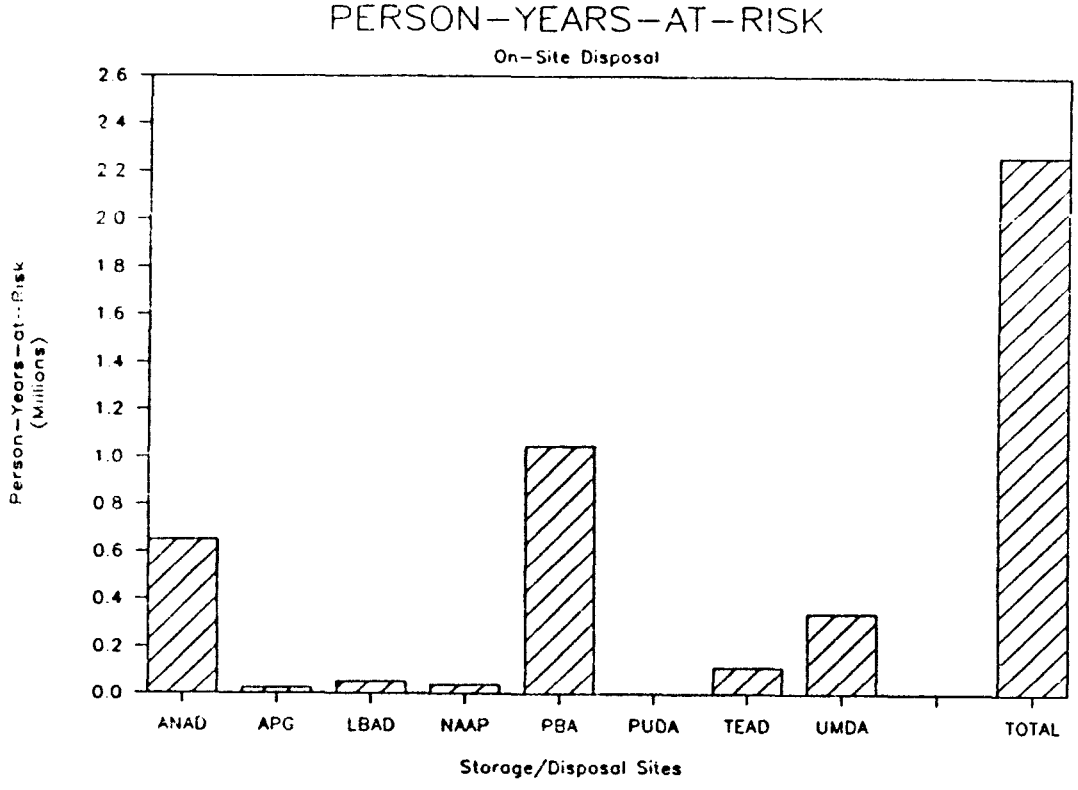

FIGURE 12. PERSON-YEARS-AT-RISK -- ON-SITE DISPOSAL
- by Disposal Site -

5.0 OBSERVATIONS AND RECOMMENDATIONS

This author has learned the hard way that the presentation of risk to a general audience is not an easy matter. What may be obvious to the risk analyst is by no means so to an audience not conditioned to think in terms of probabilistic descriptions of reality. Risk analysis, by its very nature must deal with the unknown; it is usually faced with the task of making predictions of future relative safety of complex systems on the basis of extrapolations of limited and, often, non-existing data. Risk is often dominated by very severe consequence but highly improbable events. Risk analysis must, therefore, be carried out with due respect for the inherent uncertainty in the base of relevant data and associated predictive models; similarly, the risk analyst must be conscious of the difficulty the general public will have in accepting and/or interpreting the predictions of risk where the potential consequences are well beyond anyone's experience and the probabilities are too low to be easily comprehended.

By way of guidelines that the author himself intends to pay greater head to the next time around and which, therefore, may be of value to others flirting with the need to carry out and present the results of risk analysis, the author offers the following recommendations:

- Know your audience. Be sure that the level of detail in both the execution and the presentation of the risk analysis matches the needs of the audience. The risk manager will want a risk-ranked detailed listing of individual accidents. The community leaders will want to know the societal impact on their locality and how it compares with risk imposed elsewhere, and may be best satisfied with credible graphical presentations such as the use of the pictogram. The risk analyst will appreciate best the cumulative risk curves and the presentation of uncertainty data. The program director who may have to chose between alternatives on the basis of relative risk may be most responsive to the risk curve and to the other risk measures that display expected values of risk according to the areas of interest (e.g., by site).

- Display the Uncertainty. A risk analysis which does not clearly indicate the level of uncertainty inherent in the process, whether due to data inadequacy, level of completeness, or methodology limitations, will lack for credibility and, more importantly, may be taken for more than it really is: a quantitative approximation of the public safety impact of a program or other set of activities. Deterministic comparisons of program alternatives without consideration of uncertainty can lead to the mistaken belief that one alternative is significantly less risky than another.

- Use Expected Fatalities as the Preferred Measure of Risk. Expected fatalities, while it may have an ominous label, is the most useful measure of societal risk because it best accounts for the consequences as experienced by the local affected population and because it reflects the estimated probability of lethal events occurring. Other measures, such as maximum hazard distance, may be used to supplement the portrayal and interpretation of risk, but they should not supplant the use of expected fatalities.

- Avoid Comparisons Between Voluntary and Involuntary Risk. Although the risk analyst might be tempted to calibrate the magnitude of risk of an imposed program (representing an involuntary exposure to risk) by comparing the risk with the levels of risk the public might routinely accept (voluntary exposure to risk) in return for the benefits offered, the comparison should be avoided. The general public usually perceives involuntary risk as being in a completely different category, and not an appropriate basis for comparison with the risk of a government program over which the individual has no control.

REFERENCES

U.S. Army Program Executive Office -- Program Manager for Chemical Demilitarization (1987), Risk Analysis in Support of the Chemical Stockpile Disposal Program, MTR87W00230, The MITRE Corporation, December 1987, SAPEO-CDE-IS-87014.

U.S. Army Program Executive Office -- Program Manager for Chemical Demilitarization (1988), Chemical Stockpile Disposal Program, Final Programmatic Environmental Impact Statement, January 1988.

Cutler, R. M., The Treatment of Uncertainty in a Comparative Risk Assessment, presented at the Twenty-third DOD Explosives Safety Seminar, Atlanta, Georgia, 9-11 August 1988.

Perry, R. B. and Duff, W. W., Risk Mitigation for the Chemical Stockpile Disposal Program: Identification of Opportunities and Estimation of Potential Benefits, presented at the Twenty-third DOD Explosives Safety Seminar, Atlanta, Georgia, 9-11 August 1988.

Perry, J. G. et al, Methodology Issues in the Application of Comparative Risk Assessment to the Chemical Stockpile Disposal Program, presented at the Twenty-third DOD Explosives Safety Seminar, Atlanta, Georgia, 9-11 August 1988.

GROUND MOTION MEASUREMENTS FROM A MUNITIONS STORAGE IGLOO DETONATION

by

G. W. McMahon, C. R. Welch, and J. K. Ingram

U.S. Army Corps of Engineers
Waterways Experiment Station
Vicksburg, Mississippi

Prepared for:

Department of Defense Explosive Safety Board
Twenty-Third DOD Explosives Safety Seminar
9-11 August 1988

1989

GROUND MOTION MEASUREMENTS FROM A MUNITIONS STORAGE IGLOO DETONATION

G. W. McMahon, C. R. Welch, and J. K. Ingram

U.S. Army Engineer Waterways Experiment Station
Vicksburg, Mississippi

1 INTRODUCTION

The U.S. Air Force has recently conducted a number of blast propagation tests with stacked bombs in simulated and actual munition storage igloos. The purpose of these tests was to validate buffer systems designed to prevent sympathetic detonations between adjacent bomb stacks. The particular test described in this paper was conducted in a full-scale storage igloo on 17 December 1986, at the Naval Weapons Center (NWC), China Lake, California. The basic purpose of the test was to verify the buffer performance results of previous tests conducted in simulated storage igloos (at Hill AFB, Utah).

The Waterways Experiment Station (WES) performed measurements of the internal and external (free-field) airblast pressure, as well as vertical and horizontal ground motions around the igloo. The ground motion measurements were included to determine if the igloo structure provided any blast containment effect on the resulting ground motion and airblast, compared to uncontained surface bursts using bare charges.

The following sections describe this test, and compare the igloo test results with those from uncontained surface bursts, and from a previous igloo test at the same site.

2 EXPERIMENT DESCRIPTION

The test igloo consisted of a corrugated steel semi-circular arch frame with a concrete floor and abutment, covered by 0.6 m of native soil on the top of the igloo and approximately 4 m on the sides and rear at ground level (see Figure 1). The inside dimensions of the igloo were 7.6 m wide by 18.0 m long. The test involved the detonation of a donor stack of forty-eight 2,000-lb MK-84 GP bombs, with a total explosive

weight of 20,600 kg of tritonal. A buffer, consisting of stacked pallets of 20-mm ammunition, separated the donor stack from an acceptor stack of 24 MK-84 bombs (see Figure 1).

Free-field airblast measurements were made along two radials from the center of the igloo; one along the igloo axis extending from the entrance, and the second along a line perpendicular to the first (see Figure 2). The last two gage locations along the radial extending from the axis of the igloo were rotated 23.5 degrees off the axis due to obstructions. Measurement stations were located from 120 m to 610 m from the igloo on both radials.

The ground motion measurements were made along the radial perpendicular to the igloo axis. The ground motion array consisted of six stations located at distances of 13.7 m to 416 m from the center of the igloo. Each station contained a vertical and a horizontal accelerometer in a single protective canister. The canisters were buried with their centers at a depth of 0.46 m below the surface.

3 RESULTS AND ANALYSIS

A post-test examination of the igloo area indicated that all 48 of the GP bombs in the donor stack detonated high order. In the acceptor stack, 12 bombs survived the test and 12 others either burned or detonated low order. There was no indication that any of the acceptor bombs detonated high order.

The airblast pressure-distance data from both radials are shown in Figure 3. At the closest measurement range (120 m from the igloo), the pressure along the end radial (outward extending from the door of the igloo) was about 50 percent higher than the data from the side radial. The data converges to approximately the same pressure level at the farthest airblast stations (610 m).

The difference in the airblast pressure-distance levels along the two radials can be related to the way the detonation initially vented from the igloo. The thin steel doors were the weakest part of the igloo

structure. Analysis of the high-speed film coverage showed significant jetting through the doorway of the igloo before the detonation vented through the top of the structure.

An analysis was made to determine the equivalent yield of a surface-tangent, hemispherical, TNT charge which would produce peak pressures matching those values measured at each airblast station. The results are presented in Figure 4. The analysis supports the conclusion that the initial jetting of the explosion out the door of the igloo strongly influenced the close-in gages. The equivalent charge weights calculated for stations along the side radial were much more consistent than those from the axial radial. At the close-in stations along the axial radial, however, the equivalent charge weights determined were up to 1.8 times the explosive weight of the 48 MK-84 bombs. At the farthest stations, the equivalent charge weights determined were closer to the actual charge weight on the igloo, with the side radial yielding approximately a 17,000-kg equivalent TNT source and the end radial yielding approximately a 21,000-kg equivalent TNT source.

A pressure-distance curve from a similar, previous test (Figure 5) on the same site did not exhibit the degree of difference between the side and end-on gage lines as seen on this test. The storage igloos were very similar, except that the igloo on the previous test was a concrete arch type and was slightly larger. Both igloos had roughly the same amount of soil cover. The main difference in the two tests was the charge weight, with the earlier test consisting of a donor stack of 64 and two acceptor stacks of 32 MK-84 bombs each. In this test the detonation of the donor stack propagated to both of the acceptor stacks, resulting in high order detonation of all 128 bombs in the igloo.

Because of the larger explosive yield, the igloo on the previous test provided less relative confinement of the detonation. The surrounding blast pressures were therefore probably less directionally sensitive than for the latest test. Given the fact that this directional sensitivity enhances the airblast along some radials, it can be argued that, for lower detonation yields, the presence of the igloo itself could increase the range of collateral damage in front of the

structure over that from a completely confined detonation, simply because of jetting from the entrance. Of course, this ignores any increase or decrease in debris-induced damage caused by the presence of the igloo.

The peak values recorded by the ground motion measurements are listed in Table 1. Acceleration and velocity wave forms are shown as stacked plots with a common time base in Figures 6-9. The velocities were determined by integrating the acceleration records, after appropriate base-line shift corrections. The ground motion wave forms are characterized by low-frequency, direct-induced motions with a superimposed high-frequency, airblast-induced motion which is typical for near-surface measurements. This phenomena is evident in the acceleration wave forms (Figures 6 and 7), but is better seen in the velocity wave forms (Figures 8 and 9). The airblast-induced motion arrives before the direct-induced motion up to the point of outrunning, which occurs at a range of approximately 61 m on this test (see Figure 10, which shows the times of airblast arrival and direct-induced ground motion arriva as functions of range).

The ground motion data from this test were compared with data from five uncontained high explosive tests conducted in similar soils. Table 2 lists the tests and pertinent test parameters. The charge weights ranged from 4,000 equivalent tons of TNT (Misty Picture Event) to 20 tons of TNT (Distant Plain Event 3). All of the tests employed surface-tangent charges, except Distant Plain 3, which was a half-buried spherical charge. It was included in this analysis because of its similarity in explosive yield to the igloo test, and because of the greater degree of shock coupling into the earth from the half-buried charge geometry.

Each of these tests contained motion data at various depths below the surface. The depths chosen for comparison to the igloo data were those closest to the scaled gage depths used on the igloo test. Figures 11 and 12 contain plots of scaled peak downward and peak horizontal (outward) accelerations for each test. The significant scatter observed is not uncommon for this type of measurement. The low values of scaled vertical acceleration seen in the close-in igloo data

(Figure 11) can be explained by the lower than expected airblast pressures on the side radial. In the region before the point of outrunning (approximately 2 $m/kg^{1/3}$), vertical downward accelerations are dominated by high-frequency airblast-induced motions. The igloo data are dominated by these high-frequency motions but are lower in magnitude because the airblast pressures have been shown to be less on the igloo test, for close-in ranges on the side radial, than what would normally be expected from an unconfined surface burst.

The peak vertical and horizontal velocities are plotted as a function of scaled range in Figures 13 and 14. The data from the igloo test is internally consistant with the entire data set. Note that the vertical velocity at the closest range was not plotted because its motion vector was upward, rather than downward.

The remaining five horizontal particle velocity measurements from the present igloo test fall within the data scatter from the bare explosive charge tests (Figure 14). Thus, no enhancement of the horizontal motions from the igloo can be inferred.

The igloo vertical particle velocity data at the close-in ranges fall slightly below the data from the other tests. At the farther ranges, the igloo vertical data is again within the data scatter of the earlier tests. The variation at the close-in ranges was probably caused by the perturbation of the airblast by the igloo, as mentioned earlier. Figure 8 illustrates this, in that the peak airblast-induced vertical velocity at the close-in stations was negligible, compared to the lower frequency, direct-induced vertical motion.

4 CONCLUSIONS

Airblast from the present igloo test was considerably altered at close-in ranges as a result of igloo containment. This effect caused the airblast to be increased along some radials, and decreased along other radials. The far-field airblast, however, showed less variation with direction, and was close to that expected from bare HE charges.

The effect of igloo containment on airblast becomes less pronounced as the contained explosive weight increases, and for practical values of explosive weight and igloo characteristics, may become negligible.

Peak horizontal particle velocities from the present igloo test fell within the scaled data from past bare HE surface events. Peak vertical particle velocities from the present igloo test in the far field also fell within the data scatter from previous bare explosive tests. Close-in igloo vertical particle velocities, however, were slightly below the other data. This is probably due to the perturbation of the airblast by the igloo.

It was initially believed that, while the containment afforded by the structure and soil cover over an explosion in an igloo structure would reduce the close-in airblast-induced ground shock, it would in fact increase the direct-induced motions by partially tamping the detonation, thereby increasing the energy coupling into the ground. This did not occur, however. There was apparently sufficient air volume in the igloo to allow expansion of the blast wave enough to compensate for the containment effect.

5 ACKNOWLEDGEMENTS

This test was sponsored by the Air Force Inspection and Safety Center, Norton AFB, under the guidance of LTC Ed Jacobs. Funding was directed from the Air Force Logistics Command, Hill AFB, and test responsibility and execution were handled by the Naval Weapons Center, China Lake, California, under the direction of Mr. Carl Halsey. We appreciate permission granted by the Office, Chief of Engineers to publish this paper.

REFERENCES

1. _____. November, 1986. "Fundamentals of Protective Design for Conventional Weapons," Technical Manual TM 5-8551, Department of the Army.

2. C. N. Kingery, G. Bulmash; "Airblast Parameters From TNT Spherical and Hemispherical Surface Burst"; Technical Report ARBRL-TR-02555, April 1984, Ballistic Research Laboratory, Aberdeen Proving Ground, Maryland.

3. J. K. Ingram, G. W. McMahon; "Ground Motion Data Report, Munition Storage Propagation Test"; Letter Report, February 1978.

4. D. W. Murrell; "Distant Plain Events 6 and 1A Project 3.02A, Earth Motion and Stress Measurements"; Technical Report N-70-14, September 1970, U.S. Army Engineer Waterways Experiment Station, Vicksburg, MS.

5. D. W. Murrell; "Operation Prairie Flat, Project TN 302: Earth Motion and Stress Measurements"; Technical Report N-72-2, February, 1972, U.S. Army Engineer Waterways Experiment Station, Vicksburg, MS.

6. J. K. Ingram; "Project Officers Final Report: Operation Distant Plain, Events 1, 2A, 3, 4, and 5; Project 3.02A, Earth Motion and Stress Measurements"; Technical Report N-71-3, May 1971, U.S. Army Engineer Waterways Experiment Station, Vicksburg, MS.

7. J. K. Ingram; "Project 9001: Ground Motion Measurements, Mill Race Event"; January 1982, U.S. Army Engineer Waterways Experiment Station, Vicksburg, MS.

8. D. D. Rickman, J. K. Ingram; "Misty Picture Ground Motion Measurements, Final Report"; Technical Report SL-88-5, February 1988, U.S. Army Engineer Waterways Experiment Station, Vicksburg, MS.

9. Langhaar, H. L. 1951. Dimensional Analysis and Theory of Models, John Wiley and Sons, New York.

10. R. J. Odello; "Ground Shock Effects from Accidental Explosions"; Technical Memorandum M-51-76-22, November 1976, Naval Civil Engineering Laboratory, Port Hueneme, California.

Table 1 Ground Motion Data†

Measurement No.	Sensing Direction	Gage Range (m)	Arrival Time		Acceleration		Velocity	
			Direct Induced (msec)	Airblast Induced (msec)	Pos* Peak (g's)	Neg** Peak (g's)	Pos Peak (m/sec)	Neg Peak (m/sec)
AV-14	Vertical	13.7	--	34.8	3100	---	42.7	---
AH-14	Horizontal	13.7	--	34.8	336	265	1.39	1.42
AV-27	Vertical	27.4	--	42	4.3	8.5	0.78	0.73
AH-27	Horizontal	27.4	--	42	3.8	1.3	0.87	0.41
AV-55	Vertical	54.8	--	91	3.3	4.9	0.47	0.34
AH-55	Horizontal	54.8	--	91	2.6	1.8	0.28	0.35
AV-111	Vertical	111.3	121	224	1.4	1.9	0.14	0.15
AH-111	Horizontal	111.3	121	224	0.74	1.3	0.084	0.088
AV-277	Vertical	277.4	190	681	0.91	2.8	0.023	0.076
AH-277	Horizontal	277.4	190	681	0.66	0.80	0.051	0.024
AV-416	Vertical	415.9	210	1069	0.56	0.72	0.010	0.028
AH-416	Horizontal	415.9	210	1069	0.36	0.68	0.022	0.010

* Positive = up motion for vertical gages; outward motion for horizontal gages.
** Negative = down motion for vertical gages; inward motion for horizontal gages.
† All measurements were made at 1.5 ft depth below ground surface.

Table 2 Large-Scale Unconfined Bare Charge Tests Compared to Igloo Test

Test Name	Explosive and Charge Weight	Equivalent Weight of TNT	Charge Geometry	Location and Soil Type	Equivalent Depth on IGLOO Test (m)
DISTANT PLAIN EVENT 3	TNT 20 tons	20 tons	Half-buried sphere	DRES[a] Sandy silty clay	0.49
PRAIRIE FLAT	TNT 500 tons	500 tons	Surface-tanget sphere	DRES Sandy silty clay	0.55
MILL RACE	ANFO 600 tons	500 tons	Capped surface-tangent cylinder	WSMR[b] Dry desert alluvium	0.37
MISTY PICTURE	ANFO 4800 tons	4000 tons	Surface-tangent Hemisphere	WSMR Dry desert alluvium	0.27[c], 0.55
DISTANT PLAIN EVENT 6	TNT 100 tons	100 tons	Surface-tangent Sphere	DRES Sandy Silty clay	0.28

a DRES - Defense Research Establishment Suffield, Canada.
b WSMR - White Sands Missile Range, New Mexico.
c Two data locations at 0.55 m equivalent depth.

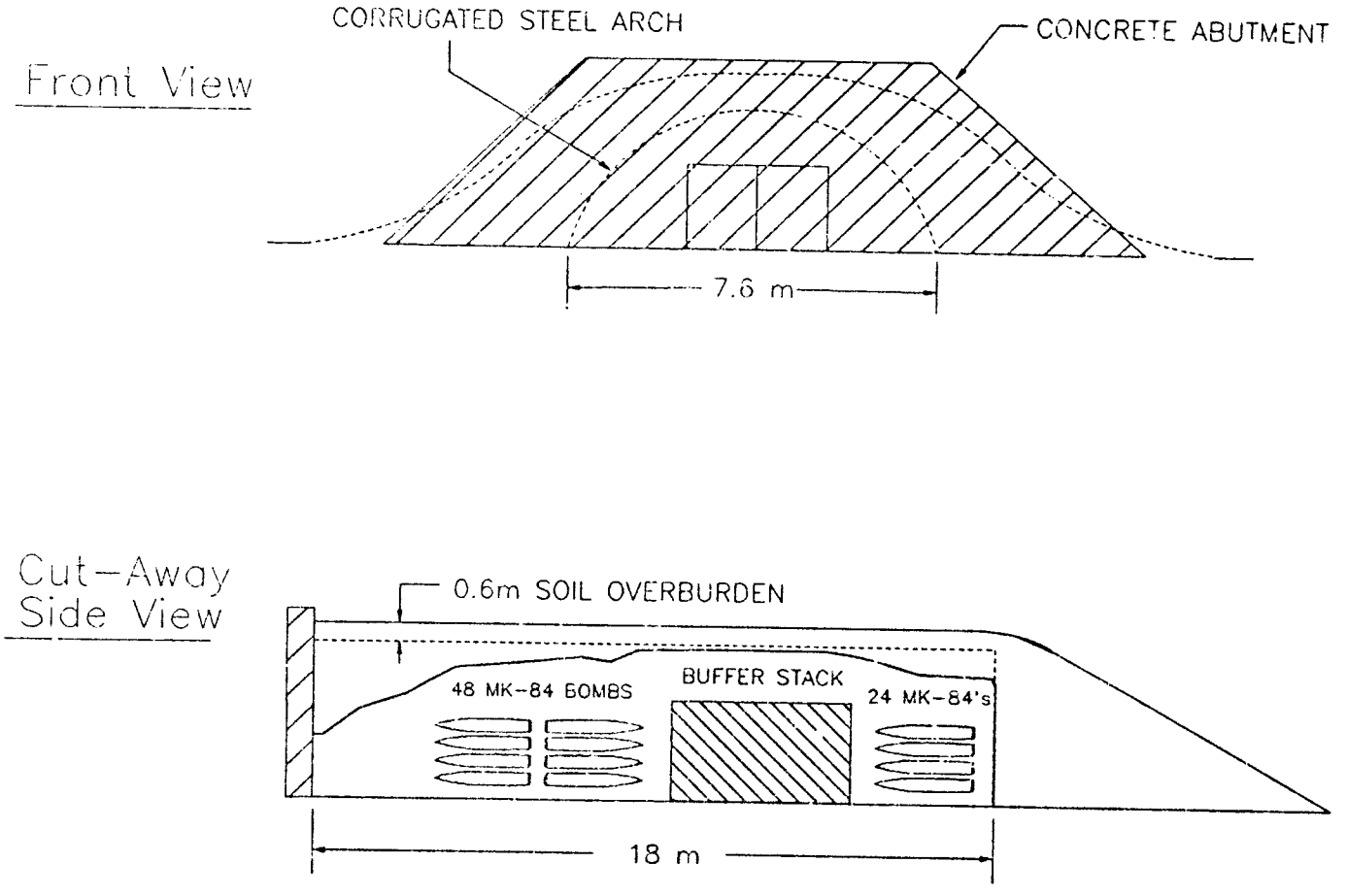

Figure 1. Igloo dimensions and charge arrangement.

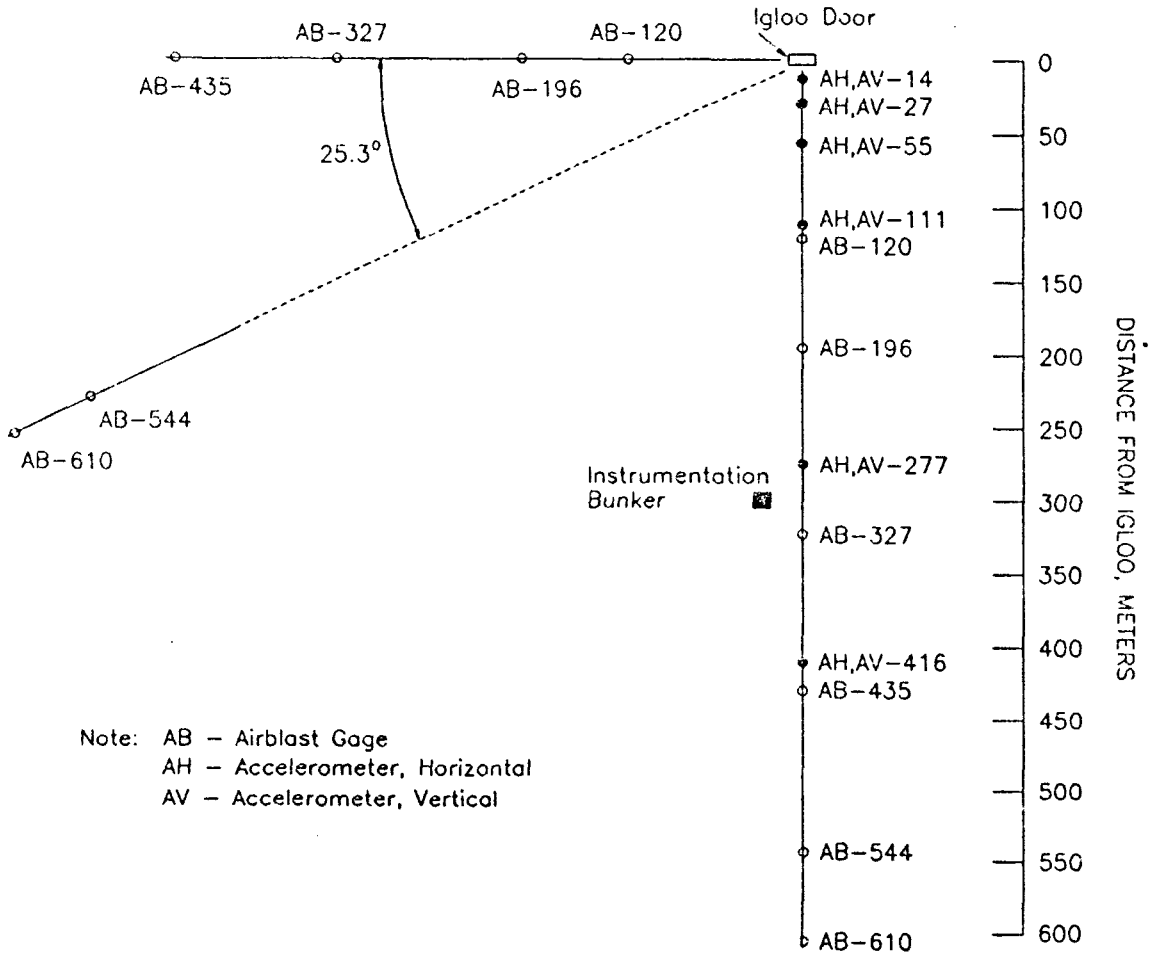

Figure 2. Ground motion and airblast measurement positions.

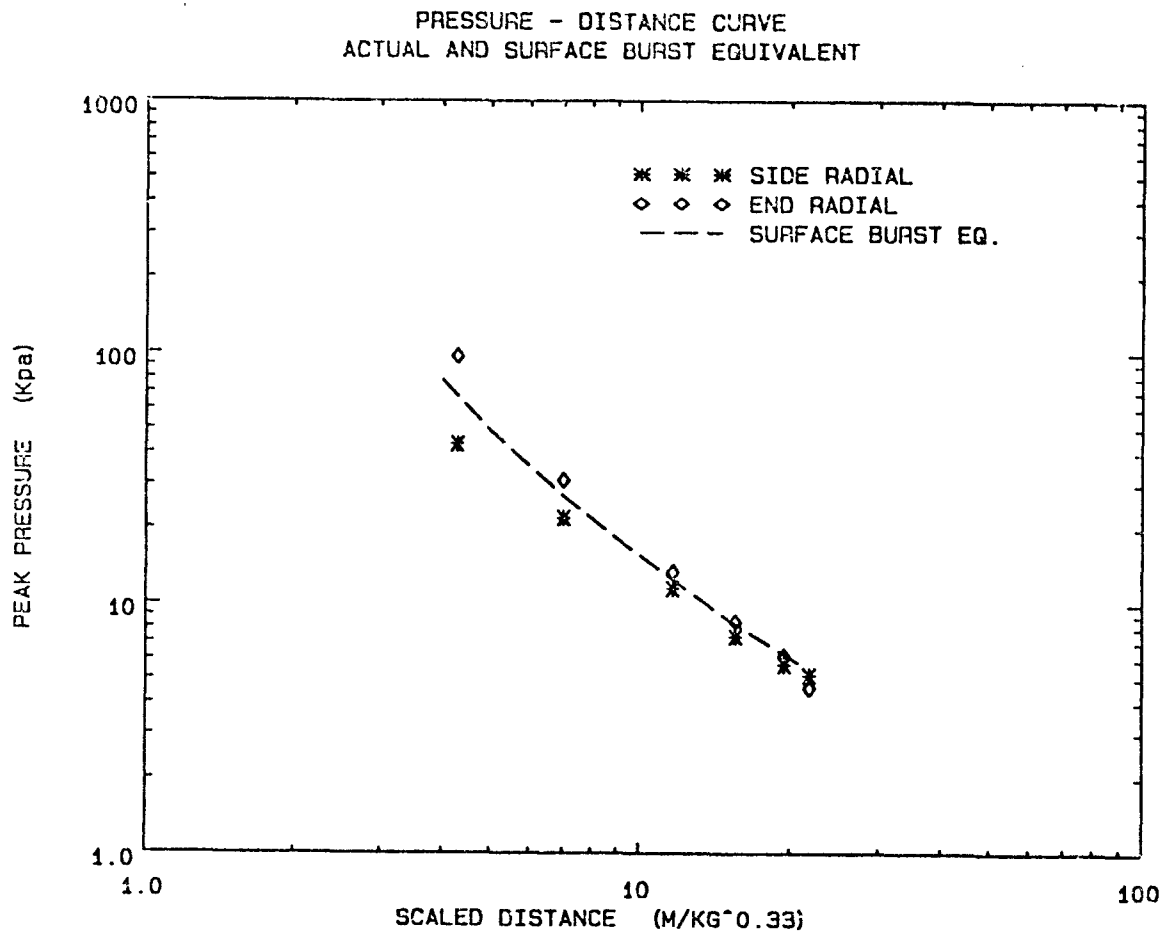

Figure 3. Pressure-distance data for both airblast radials shown with pressure-distance curve from an unconfined TNT equivalent of 48 MK-34 bombs.

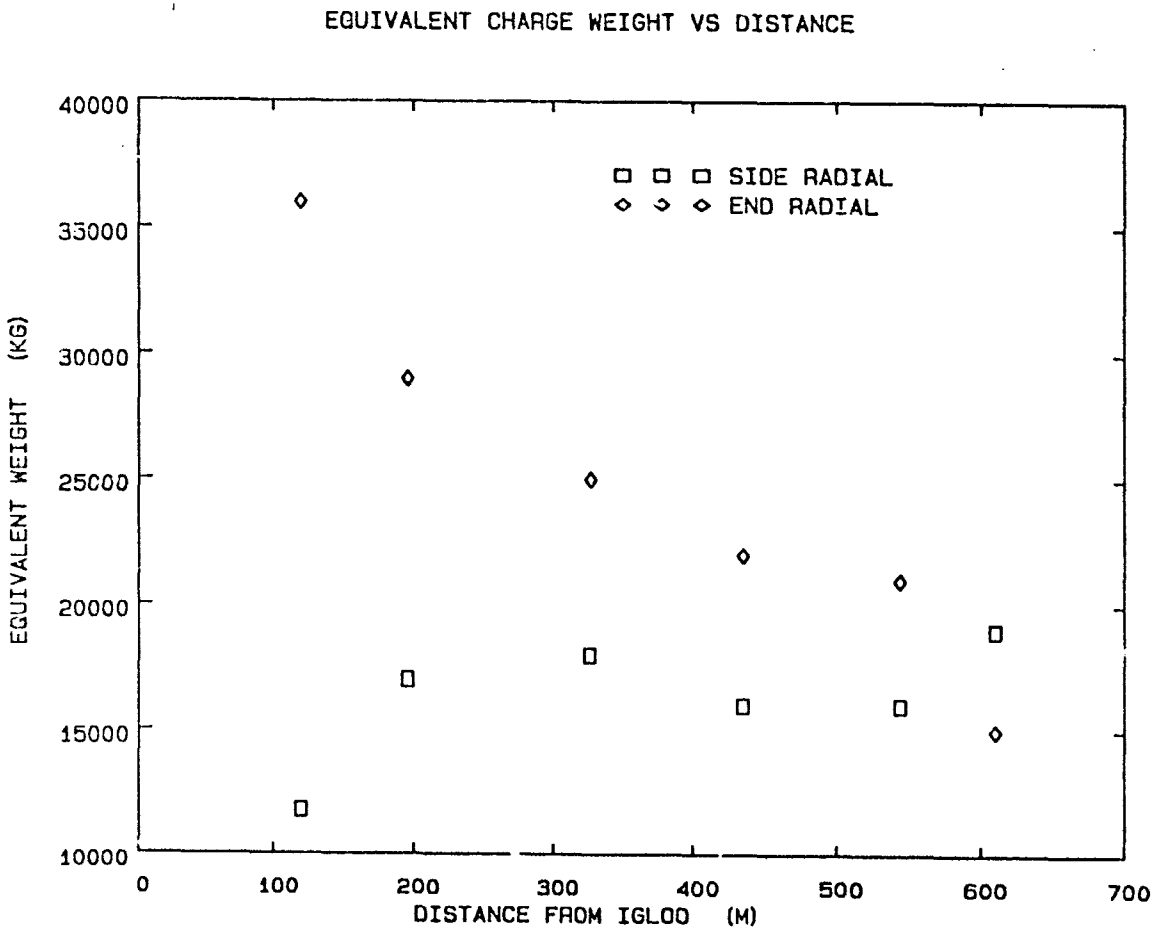

Figure 4. Calculated equivalent TNT hemispherical surface burst for both airblast radials based on measured pressure at each airblast station.

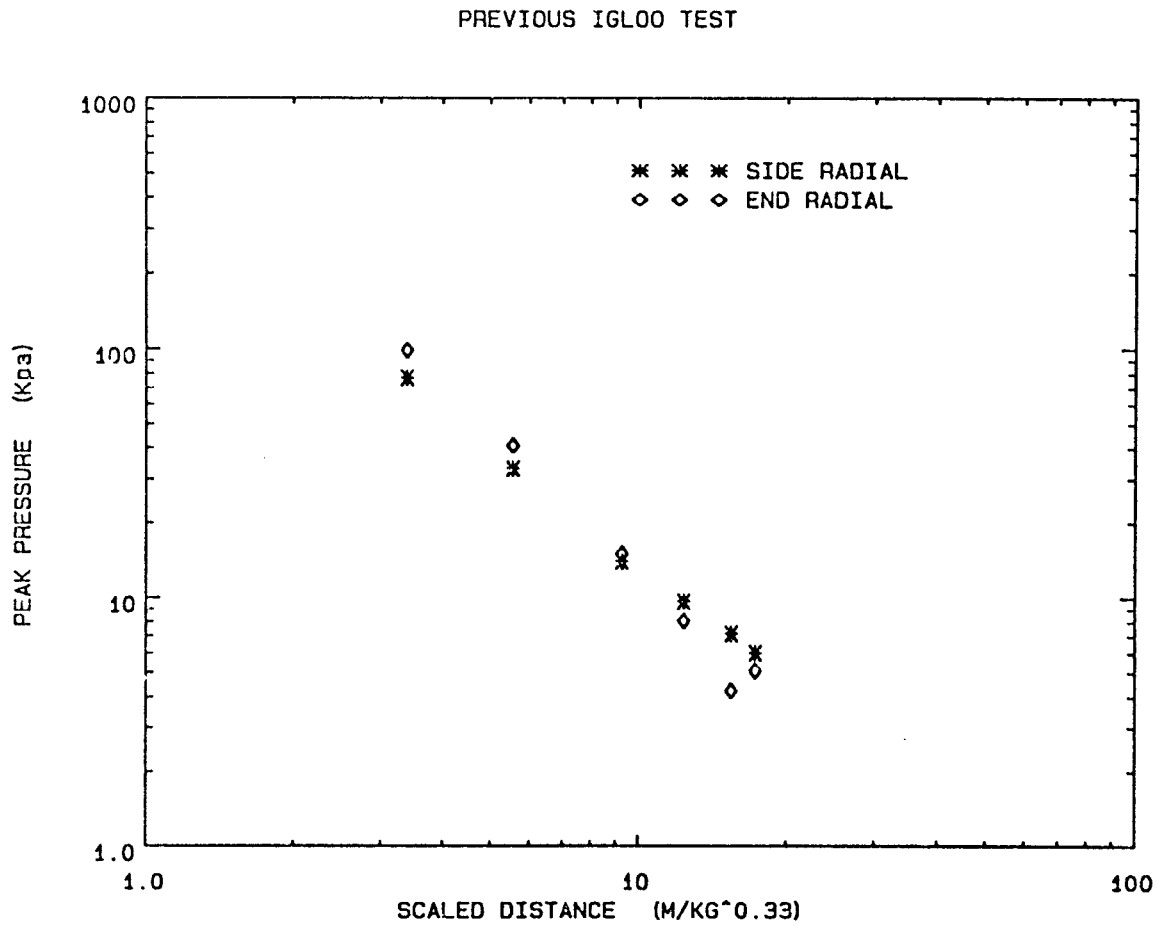

Figure 5. Pressure-distance data for both radials of a previous igloo test where 128 MK-84 GP bombs were detonated.

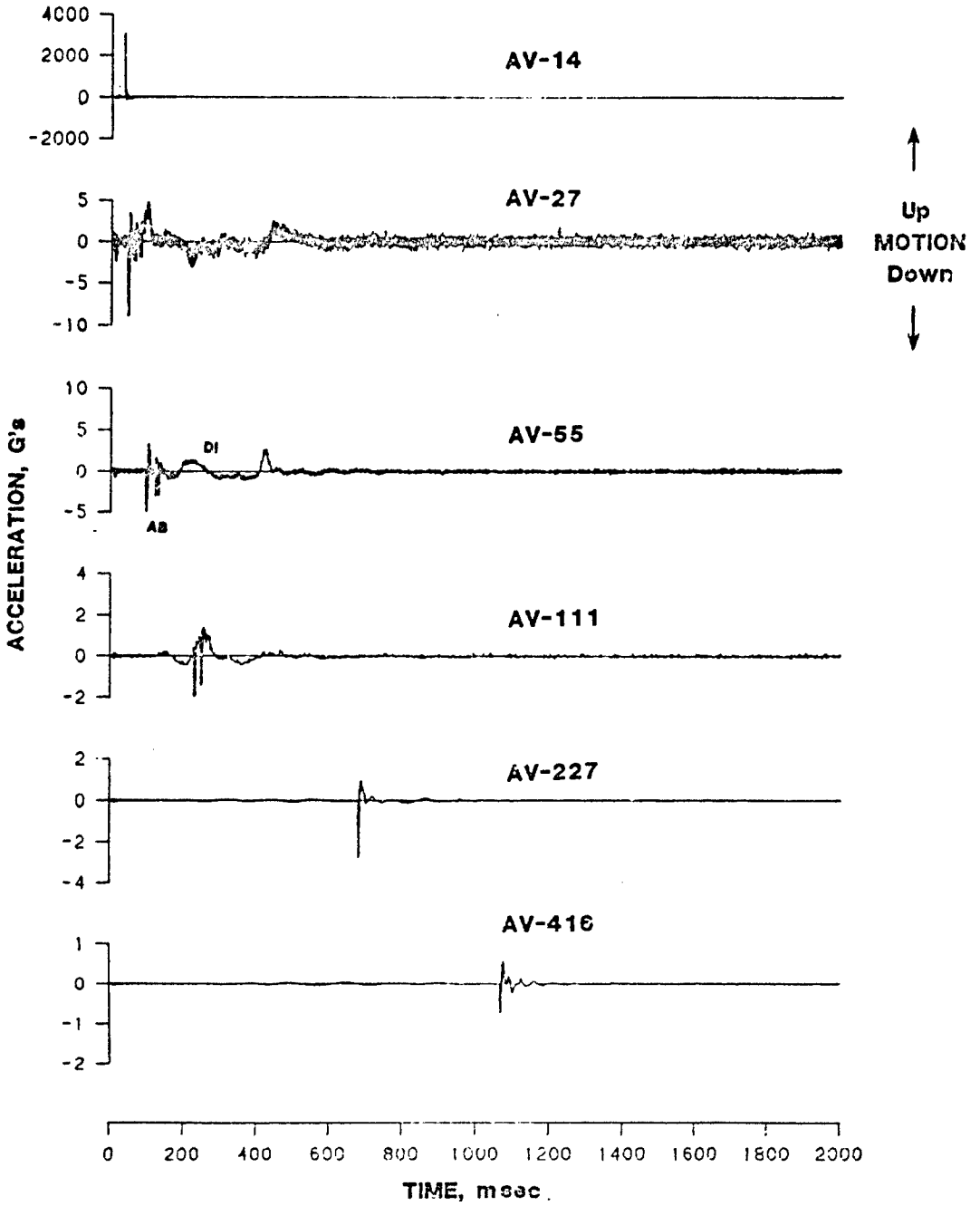

Figure 6. Vertical acceleration wave forms at each ground motion station plotted to a common time base. Direct-induced (DI) and airblast-induced (AB) portions of wave forms are identified.

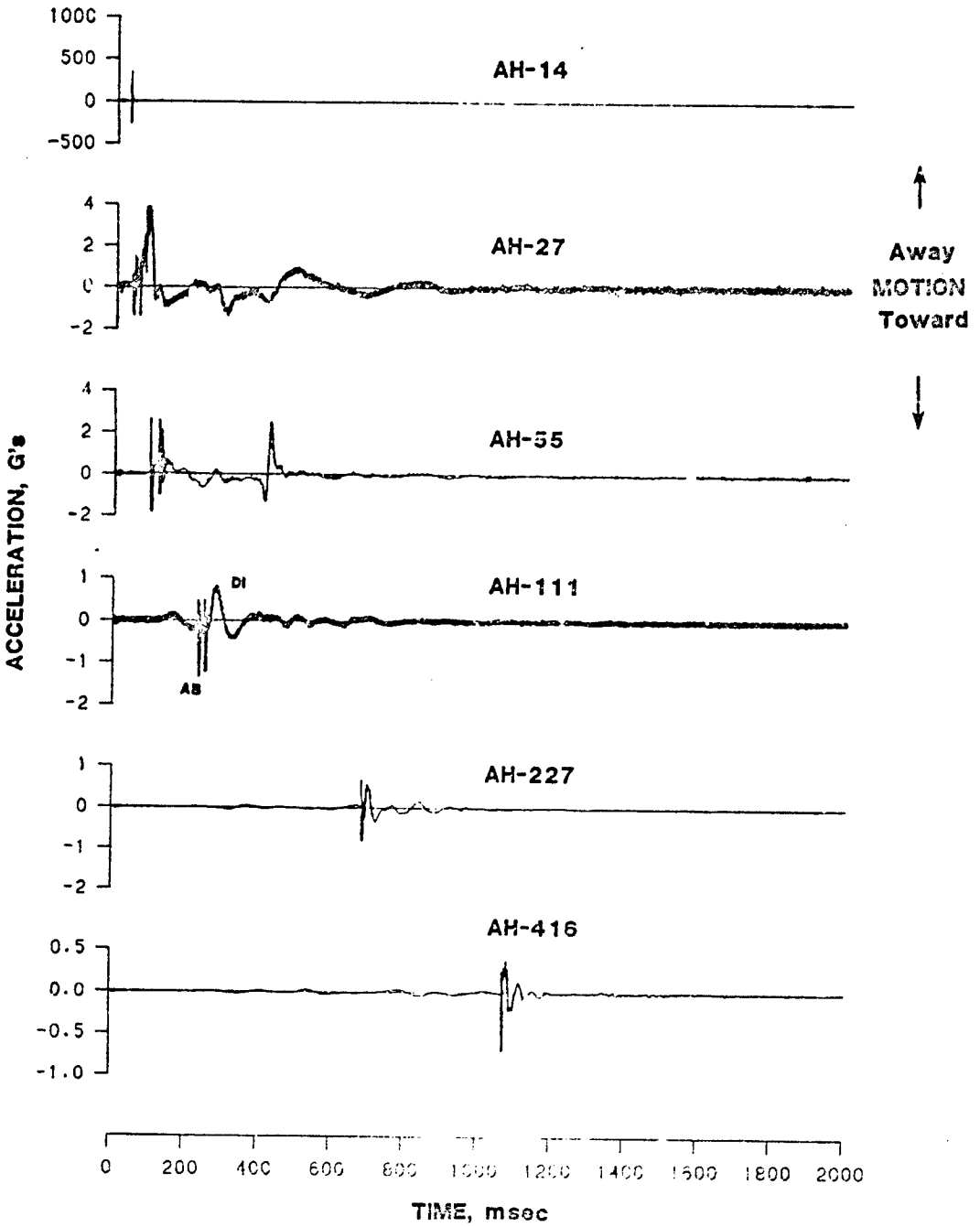

Figure 7. Horizontal acceleration wave forms plotted to a common time base.

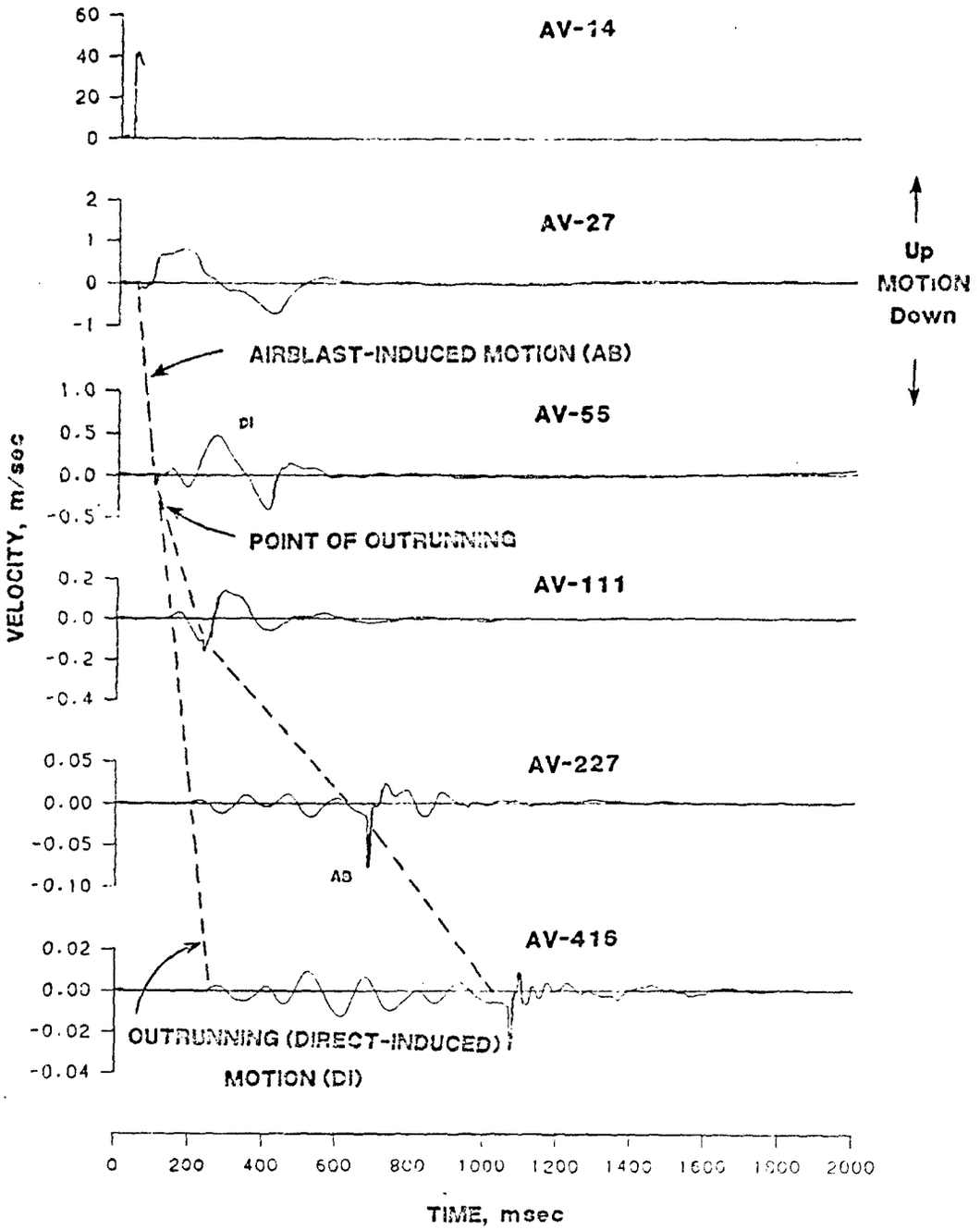

Figure 8. Vertical velocity wave forms (integrated vertical accelerations) plotted to a common time base. Point of outrunning is identified from time of arrival of direct-induced and airblast-induced motions.

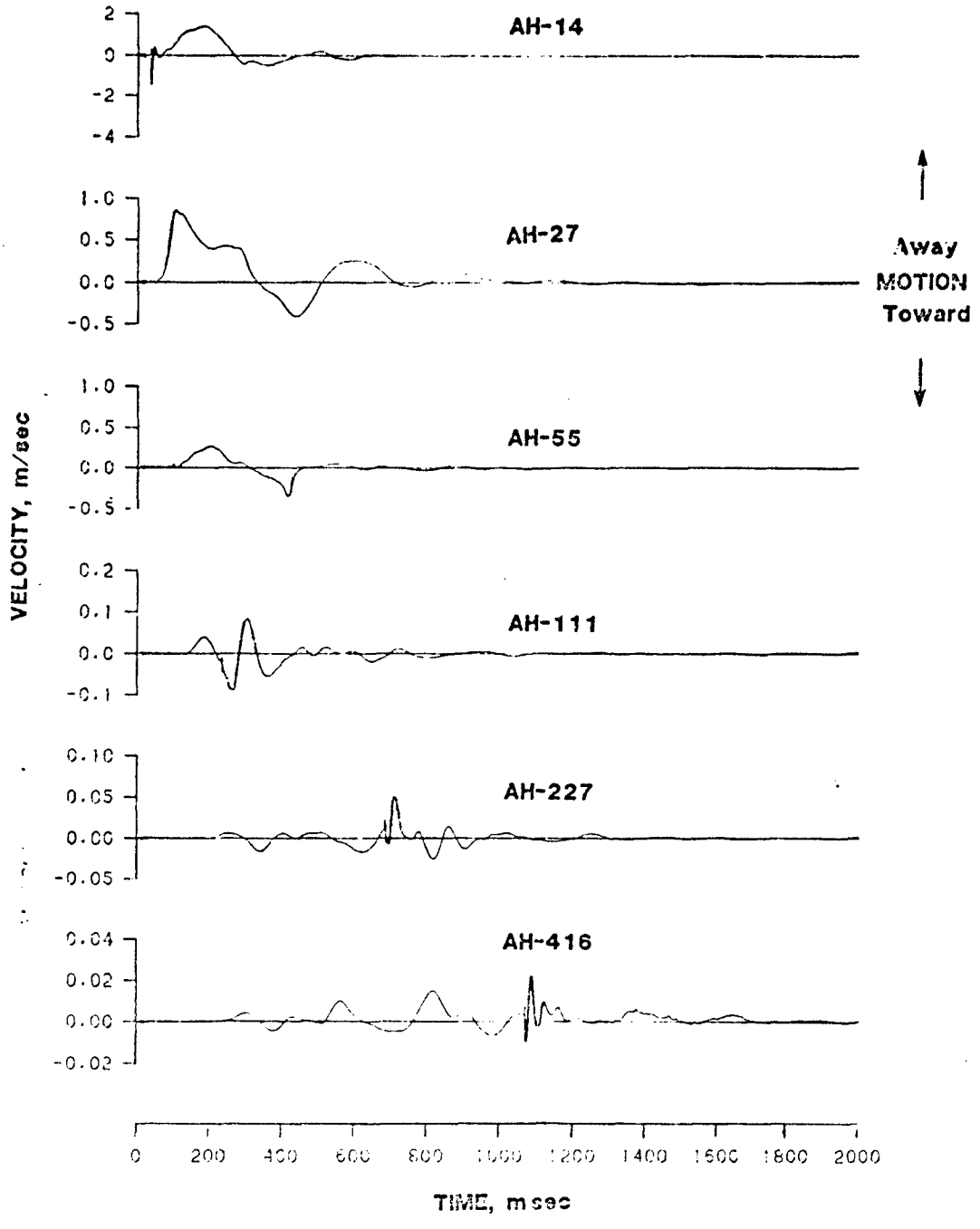

Figure 9. Horizontal velocity wave forms (integrated horizontal accelerations) plotted to a common time base.

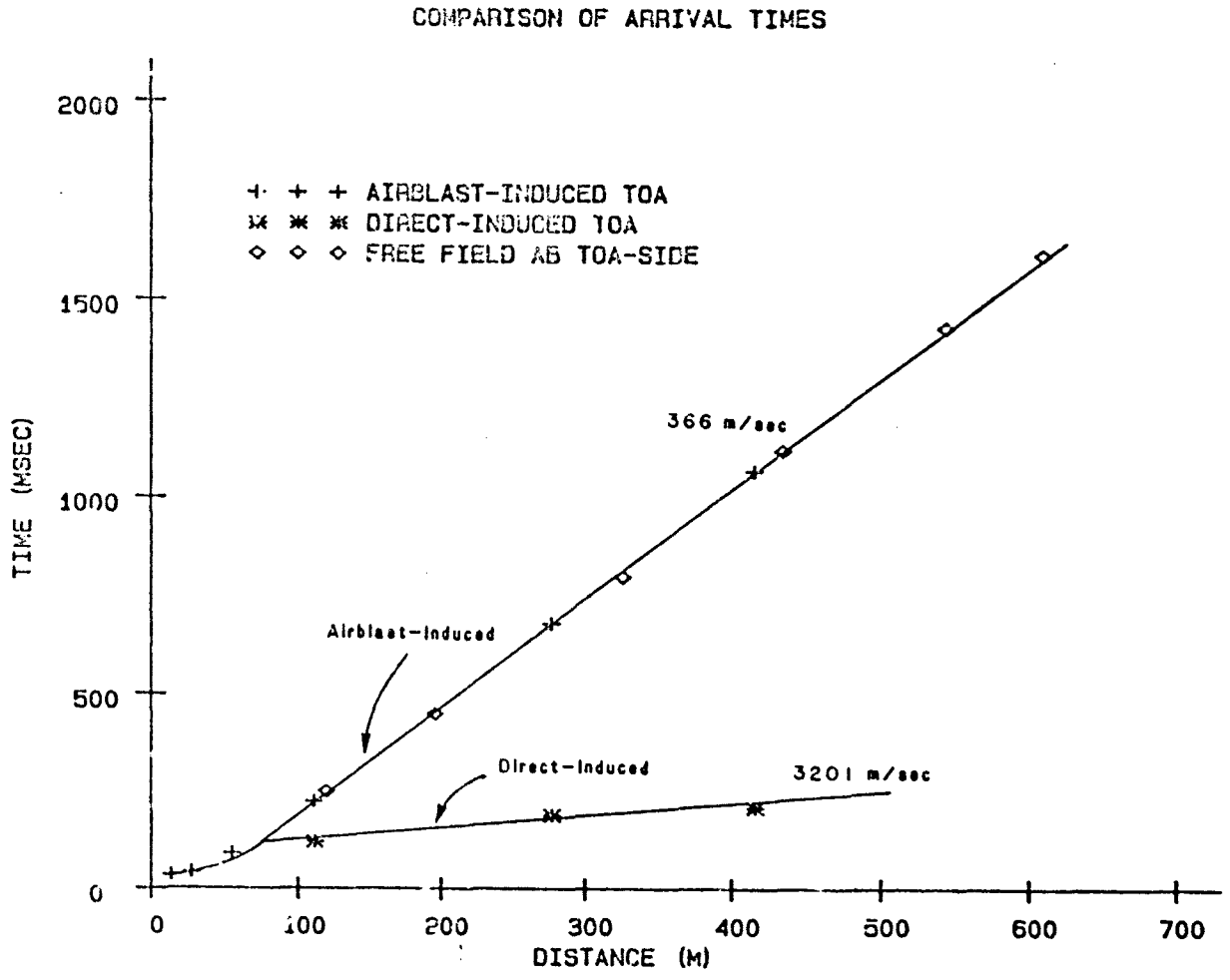

Figure 10. Comparison of direct-induced and airblast-induced arrival times with airblast arrival times.

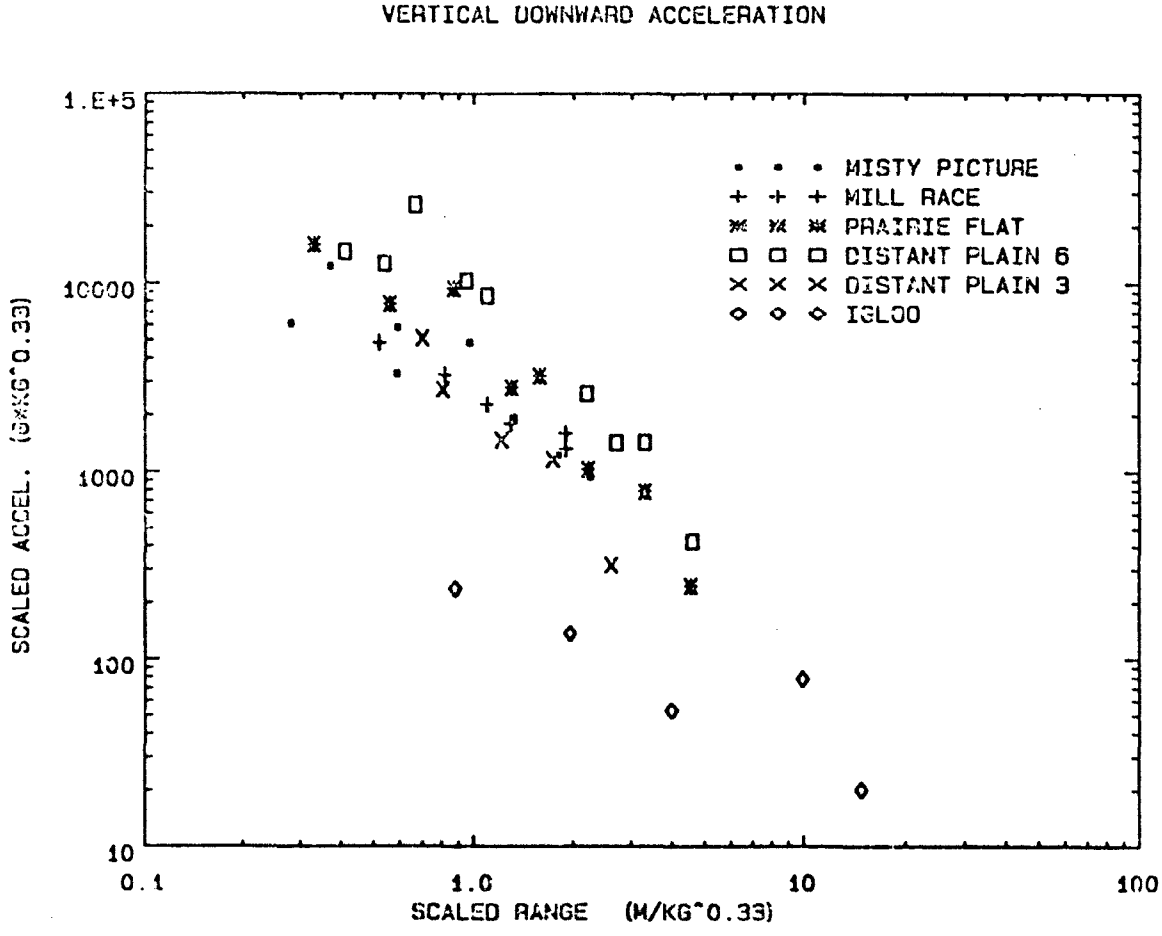

Figure 11. Comparison of igloo peak vertical downward acceleration data with data from unconfined bare charge tests.

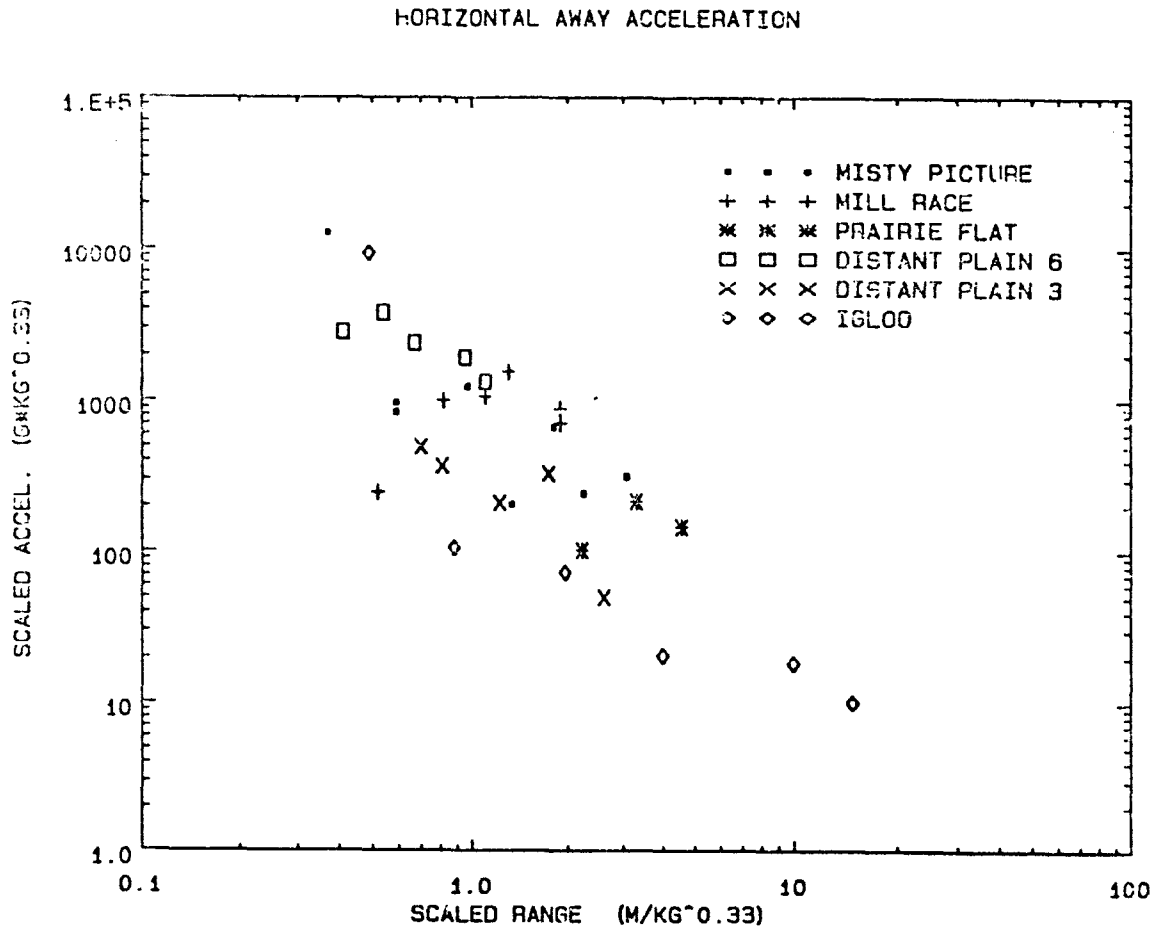

Figure 12. Comparison of igloo peak horizontal outward acceleration data with data from unconfined bare charge tests.

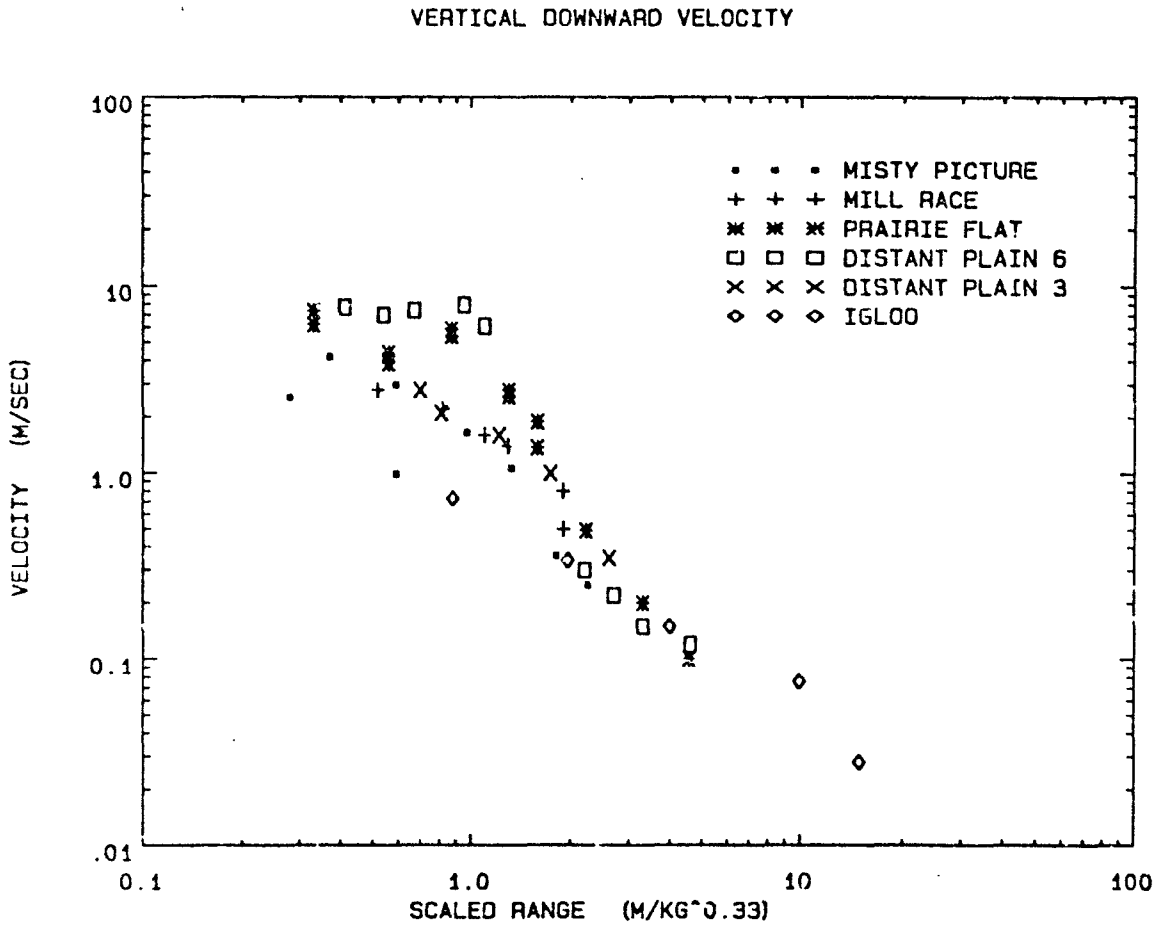

Figure 13. Comparison of igloo peak vertical downward velocity data with data from unconfined bare charge tests.

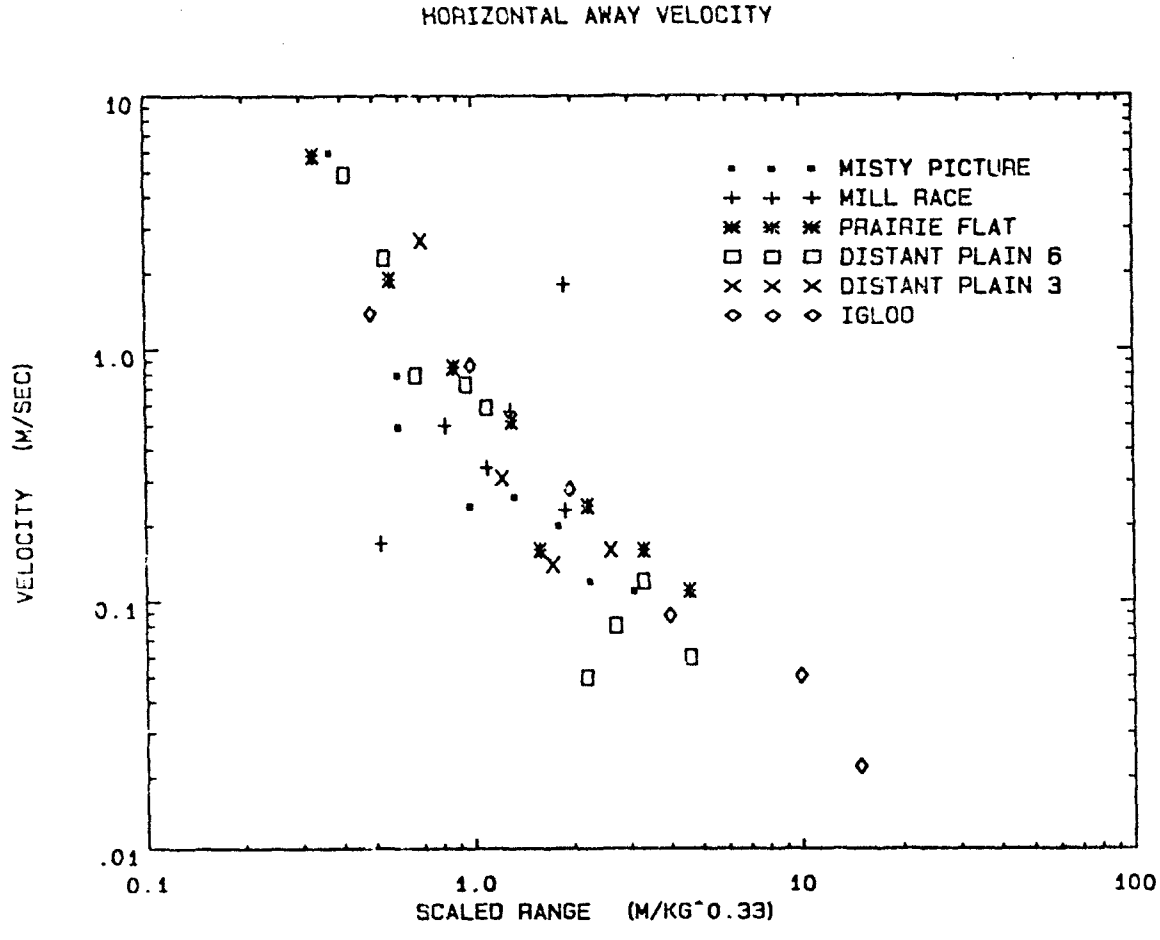

Figure 14. Comparison of igloo peak horizontal outward velocity data with data from unconfined bare charge tests.

Considerations Affecting Design and Response Time of High Speed Detection/Suppression Systems

Presented at the

23rd Annual DOD Explosives Safety Seminar

Hyatt Regency Hotel
Atlanta, Georgia
August 9-11, 1988

Kenneth Klapmeier, Bernhard Stinger, Robert Fillmore

Detector Electronics Corporation
6901 West 110th Street
Minneapolis, Minnesota 55438

Within the munitions manufacturing community, increasing attention is being given to the relationship between the burning characteristics of various pyrotechnic and propellant materials and the capability of the high speed detection and deluge systems used to protect personnel, equipment, and buildings from the hazards presented by munitions operations.

Recent tests have produced data that presents a much clearer picture of the actual response times needed for the high speed deluge systems to do an adequate job of protection. This has resulted both in revisions to the established standards and a requirement for response time testing of the actual systems.

AMCR 385-100 (AMC Safety Manual) has been revised and will be formally published soon. This revised standard will state a requirement for total system response time not to exceed 100 milliseconds (ms) for systems under 500 gallons per minute (gpm) total flow, and not to exceed 200 ms for systems over 500 gpm. Total system response time is defined as follows: time elapsed from detection to flow at the nozzle. The start time, or time zero, is to be designated as the time of total saturation of the optical flame detector. The stop time is defined as the detection of first water at the nozzle. This is usually the nozzle(s) closest to the hazard, or as determined by a hazard analysis. AMCR 385-100 will also mandate specific requirements for testing the response time of both new and existing installations.

Recent testing at ammunition plants and fire test facilities has pointed out dramatic differences in the response time of high speed detection systems. These differences are a function of the burning characteristics of the combustible material, detector location, and detector spacing. These findings could be extremely significant to existing installations and their ability not only to meet the specified response time requirement, but more importantly, to satisfactorily contain or suppress ignition incidents. Accurate total system response time testing may indicate a need for modification or revision of the system in order to comply with new requirements. Such testing will also provide data for comparison during annual inspections, or after a system has been inactive or has been modified.

The purpose of this paper is first, to discuss the various factors that affect the response time of the detection system. Second, the various instruments and methodology currently available for response time testing will be described, along with the theory of operation of the various instruments and a brief discussion of the advantages and limitations of each method. Factors affecting the response time of the deluge equipment portion of the system have been covered by other papers at this seminar.

Factors that affect the response time of an optical detection system can be broken down into internal and external components. The internal component typically includes the time required for

the control unit to respond to the signal from the optical sensor. This response time is usually a very repeatable and demonstrable characteristic of the system. Typically the response time that is stated in the manufacturer's specifications is the speed of response under what is called a "saturating condition". This means that the optical sensor is suddenly receiving an overwhelming amount of energy in the optical range to which it is sensitive. This causes the detector to produce its maximum level of output, which cannot be increased with greater levels of radiant energy.

The other factors that affect response time are external. These include flame size, distance between the fire and the detector, the presence of physical obstructions or other attenuating factors between the flame and the detector, and the composition of the material being burned. This is shown in Figure 1.

Typical UV Flame Detector

To better understand the individual factors affecting detection system response time, let us consider an example of a typical ultraviolet (UV) flame detection system.

The heart of the system is the detecting element itself. The Geiger-Mueller type sensor used in the detector produces a series of pulses in response to the presence of short wavelength UV radiation. The frequency of these pulses is directly proportional to the level of UV present. Figure 2 shows this relationship. The values shown on the Y axis pertain to detector output, which is the frequency of the counts per second (cps). The X axis shows the level of UV radiation in arbitrary linear units. Notice that there are two distinct regions to this curve. Near the origin, the line is linear. This means that doubling the level of UV also doubles the resultant detector output. As the level of detector output increases beyond approximately 200 cps, there is deviation from this trend. At these higher detector output levels, an incremental increase in UV radiation causes progressively smaller increases in detector output.

The controller analyzes the detector output and activates the appropriate control outputs in response to the presence of fire. Because sources of interference in the UV spectrum are few and well known, the only signal processing that is necessary involves determining whether the detector output level exceeds the selected sensitivity setting. At any given sensitivity setting, the time required to satisfy the alarm criteria increases as the frequency of detector output decreases.

Figure 3 shows the response time of two typical control units that are manufactured by Detector Electronics and used in the munitions industry. This chart plots the response time of the control units versus the count rate or signal strength from the UV

detector at several different sensitivity settings. As can be seen on the chart, minimum response time can be achieved when the control unit receives count rates of 1000 cps, which occurs when the detector is saturated by a high intensity UV source. Lower count rates produce proportionately slower response times. For example, reducing the detector output by a factor of two doubles the resulting response time. In addition, the fastest response time for a given controller will be achieved with the lowest cps, or highest sensitivity setting.

Sensor type has a significant influence on the magnitude of detector output when exposed to the UV radiation originating from actual fires. By using a detector whose sensitivity spectrum best matches the emission spectrum of the fire in question, the maximum output and therefore minimum response time can be achieved. Figure 4 shows the response time of two types of UV detectors manufactured by Detector Electronics and used in the munitions industry during fire tests with single base propellant. It is important to point out that the data plotted in this graph pertains only to the specific quantity and type of material used in this test as well as the distance between the detectors and the fire. A change in any one of these factors would produce different results, as will be elaborated later in this paper.

The positioning and number of detectors is also very important to the response time of the detection system. For the detector to see the fire, it is necessary for the fire to be within the field of view, or cone of vision of the detector. Therefore, we strongly suggest an arrangement where the detectors are placed along the walls or corners of the hazardous area for general coverage. These general coverage detectors are aimed with overlapping fields of view in order to eliminate any blind spots. Strategically positioned detectors placed in close proximity to likely points of fire origination are also recommended. Examples include placement of detectors as close as possible to sites such as a compression point in a shell loading operation or at a sewing machine in a bag loading operation.

Since the output of more than one detector can be tied together on a control unit, or zone of a given control unit, response time can be improved by having two detectors viewing the same hazardous area. Figure 5 shows the detector output of two detection systems viewing the same fire. These two systems are identical in all details except that the first system has two detectors per zone, while the other system has one detector per zone. The advantage is that when two detectors viewing the same area are connected to the same zone, their outputs are combined. The response time improvement realized by this technique is proportionate to the increase of the count rates.

The distance between the detector and the fire is one of the most significant factors affecting response time. As was pointed out earlier, minimum response time occurs when the detection system is exposed to a saturating source of radiation. However,

saturating levels of radiation rarely occur in the real world, unless large fires occur at close proximity to the detector. In most applications, the detector will be required to detect a fire at distances which vary from two or three feet to fifteen feet or more, depending on the size of the area to be protected and whether or not spot coverage detectors have been utilized. Since the fire must be detected while it is still small enough to enable successful suppression, the alarm must be signalled before the fire has reached a large size.

Test Results

Figure 6 shows the results of response time tests with ten grams of black powder using the DE1888N detector and R7404 Controller set for maximum sensitivity at various distances. Notice that the response time of 116.7 milliseconds at twenty feet is approximately four times longer than the 26.7 millisecond response at five feet. More significantly, we see that the intensity of UV is insufficient to trigger an alarm when the distance is increased to twenty-five feet. This is not to say that the system is incapable of response at this distance. Rather, the fire would have to grow to a larger size in order to be detected. Figure 7 shows test results with a DE1888N at fifteen feet, set for a moderately sensitive 24 cps alarm threshold with a variety of munitions materials. Here we see near minimum response times, indicating that these materials produced high intensity UV. This is partly the result of a larger quantity of material, but is most substantially the consequence of different combustion chemistries.

As can be seen, reaction times ranging from 20 to 100 milliseconds are typical for small munitions fires at distances of 10 to 15 feet. It is also evident that the response time increases at a rapid rate with respect to distance. This is due to the fact that all optical detectors operate under the inverse square law of optics, meaning that doubling the distance from a detector to the fire decreases the amount of ultraviolet energy the detector receives from the fire by a factor of 4. Similarly, halving the distance from a detector to the fire increases the output of the sensor module by a factor of 4. The significance of this increase in output can be seen in Figure 8. Here we see that an increase in detector output from 100 to 400 counts per second decreases response time from 140 milliseconds to 30 milliseconds.

Measuring Response Time

The different techniques for quantitative measurement of the response time of the optical fire detection system differ primarily in whether they are intended to measure only the internal or internal plus external components of the total response time. We have seen that the internal factors can easily be measured by triggering the detector with saturating levels of radiation. This type of measurement is well suited for

determining the minimum limits of response time imposed by the system hardware. This then provides the user with a best case scenario of performance. Because detection and alarm activation times are reduced to a minimum, this technique is very useful in determining the time required for the other aspects of the detection/deluge system performance. In addition, since a test using a saturating source is highly repeatable, it can be conveniently used to monitor system performance as part of a routine maintenance and inspection program. Finally, this method easily lends itself to testing individual detection and deluge points in the system, which would not be feasible using actual fire sources.

Figure 9 shows an instrument, manufactured by Detector Electronics Corporation, that is used for measuring the response time of a UV detection system. It consists of a high intensity UV source, two digital timers, and a flow sensor for detection of the presence of water. The first timer is activated when current flows to the UV source and is stopped when the alarm is signalled by the controller. The second timer also starts when the UV source is energized and stops when water flow is detected. Figure 10 shows a similar device manufactured by "Automatic" Sprinkler Corporation. This unit differs in that the second timer is activated by the alarm output from the controller. Thus, the first timer shows the time interval from detector saturation to alarm output, while the second timer shows the interval from alarm output to water deluge. Grinnell Fire Protection Systems Company also manufactures a unit for use with their Primac Systems shown in Figure 11. Their Ultra High Speed Timer is specialized for the timing of deluge system operation. Timing begins when the unit receives the alarm signal from the fire detector. Water flow is detected by its interruption of an optical beam, allowing a non-contact method of determining the point of water deluge.

This measurement of the internal component of the total response time can be misleading as an indicator of the response time that can be expected in an actual fire. This is due to the fact that the level of the UV signal available to the detector from an actual fire, at distances encountered in the field, will likely be much less than saturation. Accordingly, response time that can be expected from an actual fire in a given situation can be many times longer than that measured with a saturating source.

Testing Techniques

As we have seen, fires of munitions materials vary in the level of UV emitted. Also, we have seen how distance, obstructions, or other factors can substantially reduce the UV available to the detector, resulting in delayed alarm indication. Therefore, there is a need to measure the response time of fire detection systems under conditions that duplicate as many of the features of the field installation as possible. The most important of these is a representative radiation source,

preferably actual fire. Also, the spacing of the detectors with respect to the hazard and possible presence of obstructions should be faithfully duplicated. Obviously, this greatly complicates the instrumentation and techniques required to measure the detection system response time. To this end, we have conducted many experiments to test the utility of various response timing methods.

The most rudimentary of these is diagrammed in Figure 12. This system consists of a dual channel digital storage oscilloscope, an electric squib, load resistor, power supply, UV detector, and its controller. With this method, a measured amount of the material in question is placed on a test stand at a distance equal to that in the installation or proposed design. The amount of material is generally small and should be chosen to be equal or less than the quantity of material whose unsuppressed combustion can be tolerated without severe consequence. The electric squib is used to ignite the material and is sized and located so that it does not in itself produce sufficient radiation to trigger the detector.

One channel of the oscilloscope is used to monitor the current flow to the squib by observing the voltage drop across the load resistor. The second channel is used to monitor the detection system alarm output. After power is applied to the squib, current begins to flow, causing the squib to fire. Time elapses as the fire propagates to the material under test. As the fire develops, the level of UV radiation rises until the alarm threshold of the controller is exceeded. This triggers activation of the alarm output. Comparison of the point where current flows to the squib and the point of alarm reveals the system response time.

One drawback to this method is the inclusion of the firing delay of the squib and the flame propagation time in the measured response time. Since many munitions materials are fairly slow burning, this can cause an appreciable error. Use of fast response photosensitive elements to sense the start of the fire may be of some utility to correct for this error. Still, some uncertainty remains as to the state of the fire at the point which is taken to be the beginning of the fire. None-the-less, techniques such as these can be of some value to set approximate bounds on the detection system response time.

Use of high speed photography of either conventional or video types enables actual observation of the events during a fire as they unfold. This permits a more accurate and meaningful establishment of the start of the fire as well as observation of the progression of the fire. A light emitting diode may be connected to the alarm output of the controller and placed in the field of view of the camera to provide a visual indication of alarm. Depending on the timing resolution desired, the number of pictures or frames per second can be selected within a wide range.

Figure 13 shows a high speed video recording system manufactured by Video Logic Corporation, which we have used in some of our experiments. Other systems are also available from other manufacturers. These systems are the video equivalent of conventional high-speed photographic systems, which are also still used for this type of work.

There are few drawbacks to use of high speed photography with respect to accuracy. The investigator is able to observe the progress of the fire and directly identify the point of ignition. Additionally, high speed photographic studies can reveal important details such as the size of the fire at the point of alarm activation. However, cost of the equipment and need for a site where testing with live fire is permitted can be limitations.

The method used to measure response time of a fire detection system must be selected on the basis of the information that is desired. Response time tests using saturating sources of radiation are excellent for determining the minimum response time limits of the system hardware. This method does not, however, necessarily indicate the detection system performance that can be expected during an actual fire. Tests with actual fire are needed to provide the system designer with the information necessary to base decisions about detector placement and coverage density. However, this technique is ill-suited for periodic inspection of the total detection/deluge system performance due to logistic constraints and the inherent variability of fire. Ideally, these two techniques are used together in a complimentary fashion to give a complete range of information that can be used to determine detection/deluge system capability.

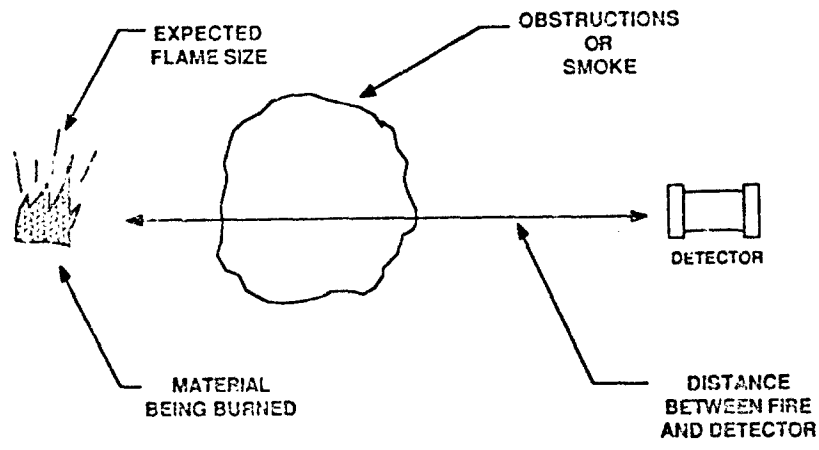

Figure 1 - Factors Affecting Response Time

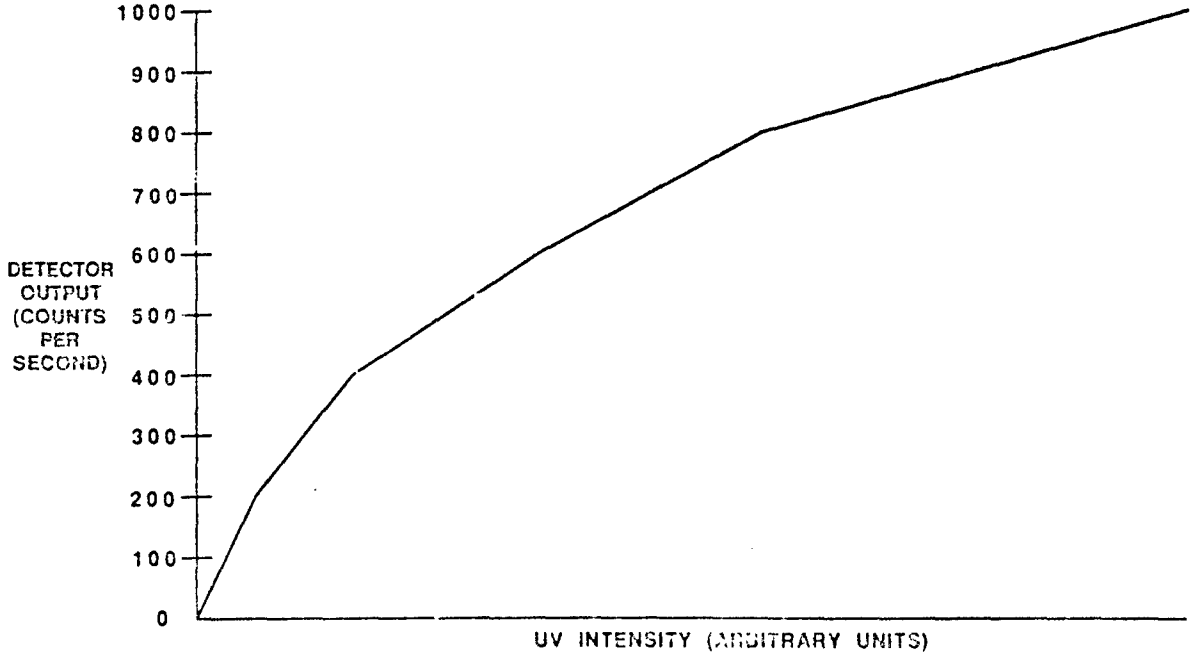

Figure 2 - Detector Output Versus UV Intensity

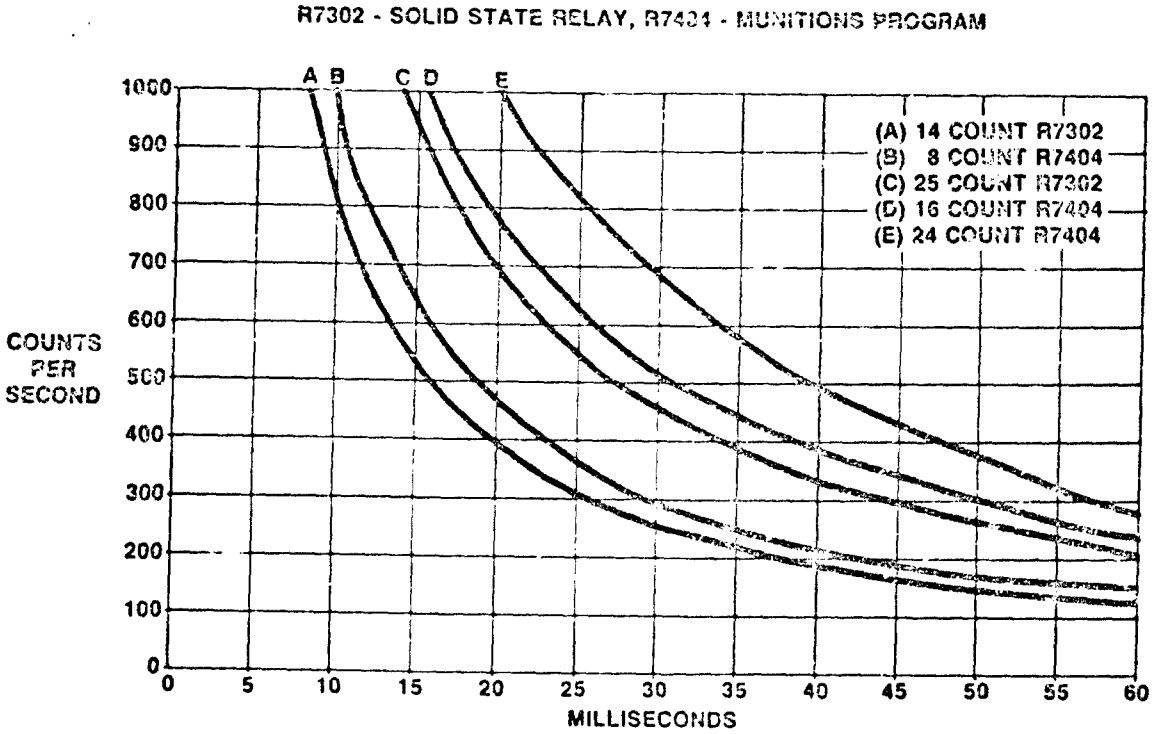

Figure 3 - Response Time Versus Detector Output

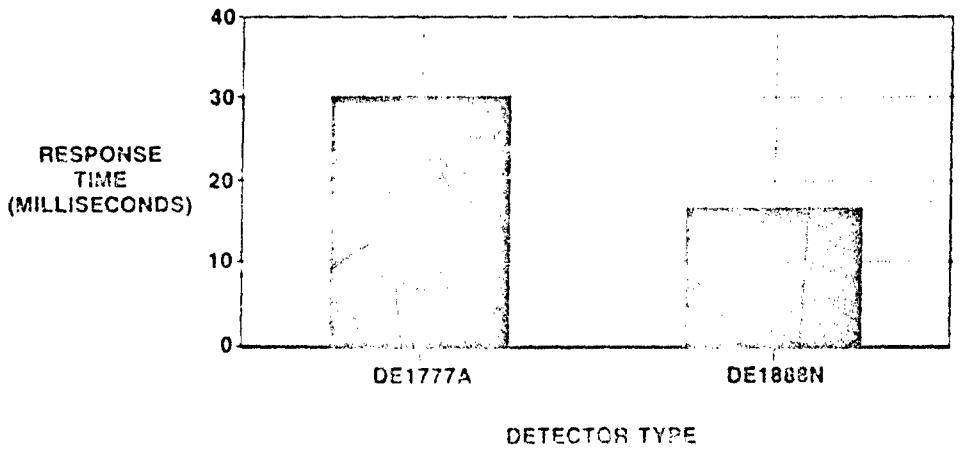

Figure 4 - Response Time with 1.5 Kilograms MP .055

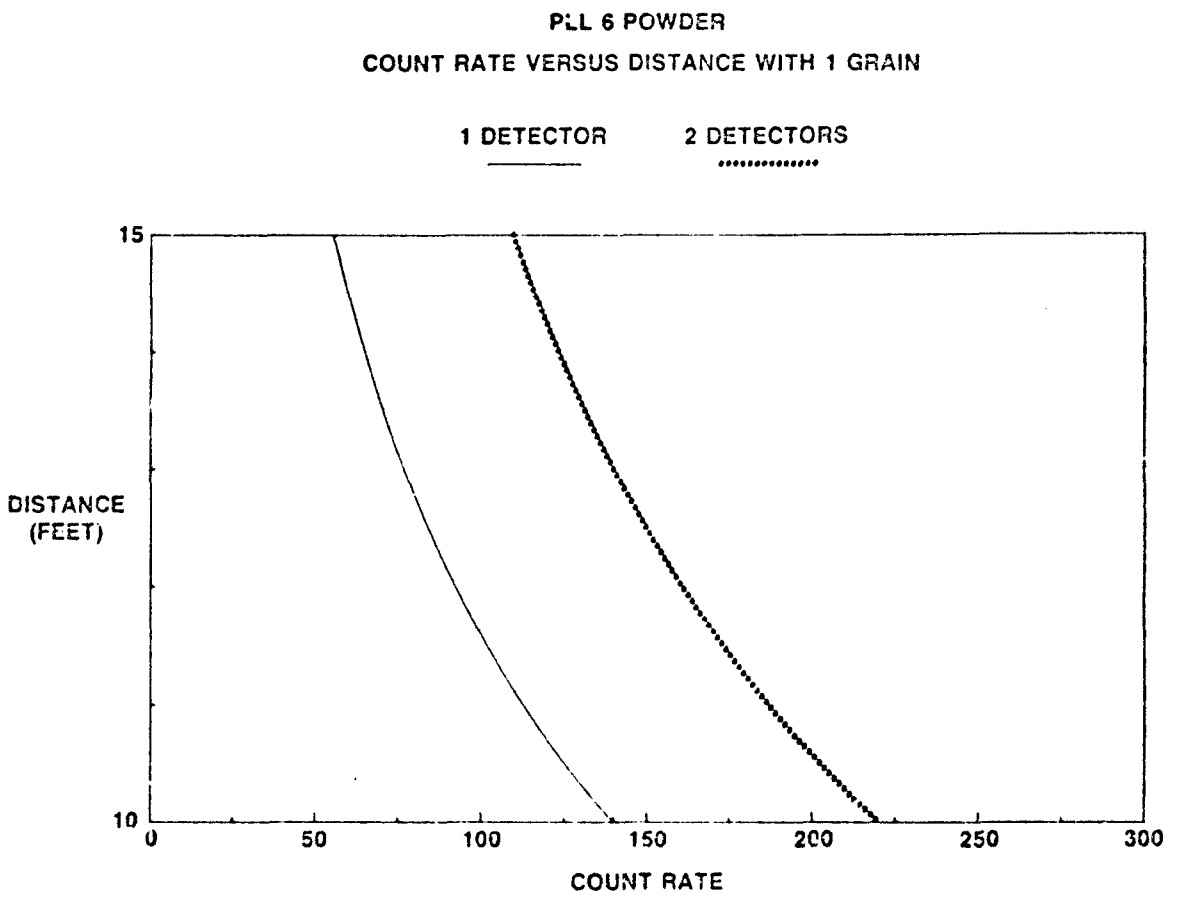

Figure 5 - One versus Two Detectors

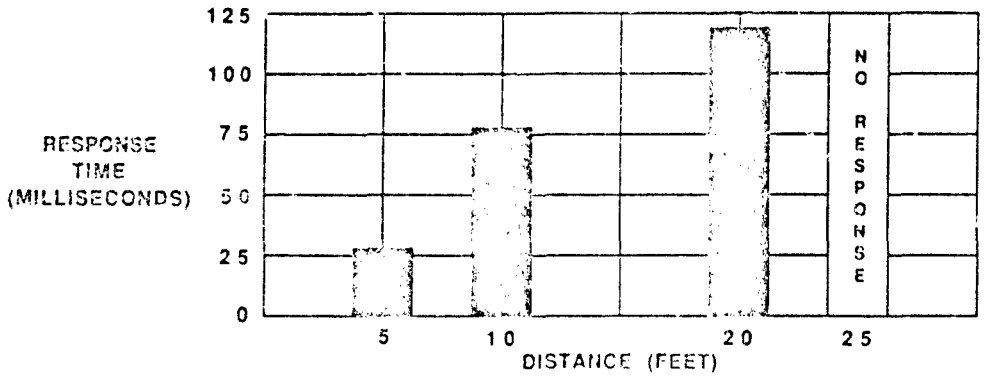

Figure 6 - Response Time Versus Distance

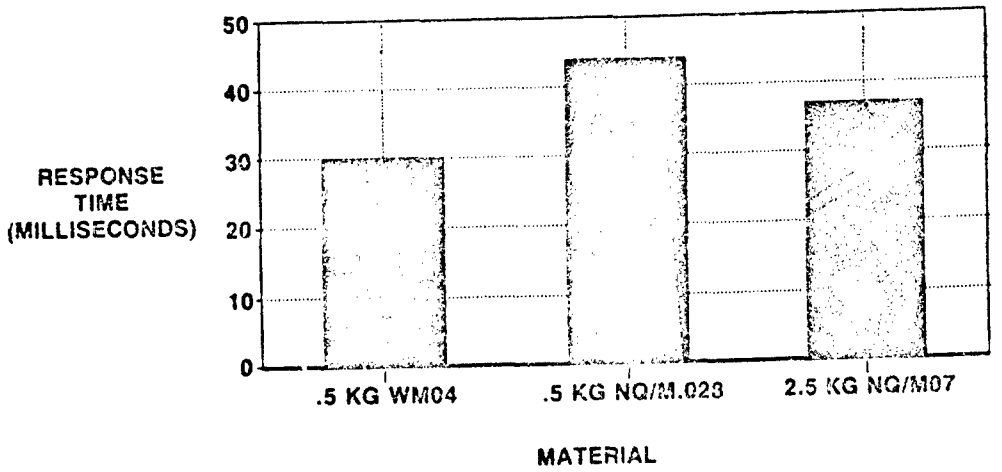

Figure 7 - Response Time with Various Materials at 15 Feet

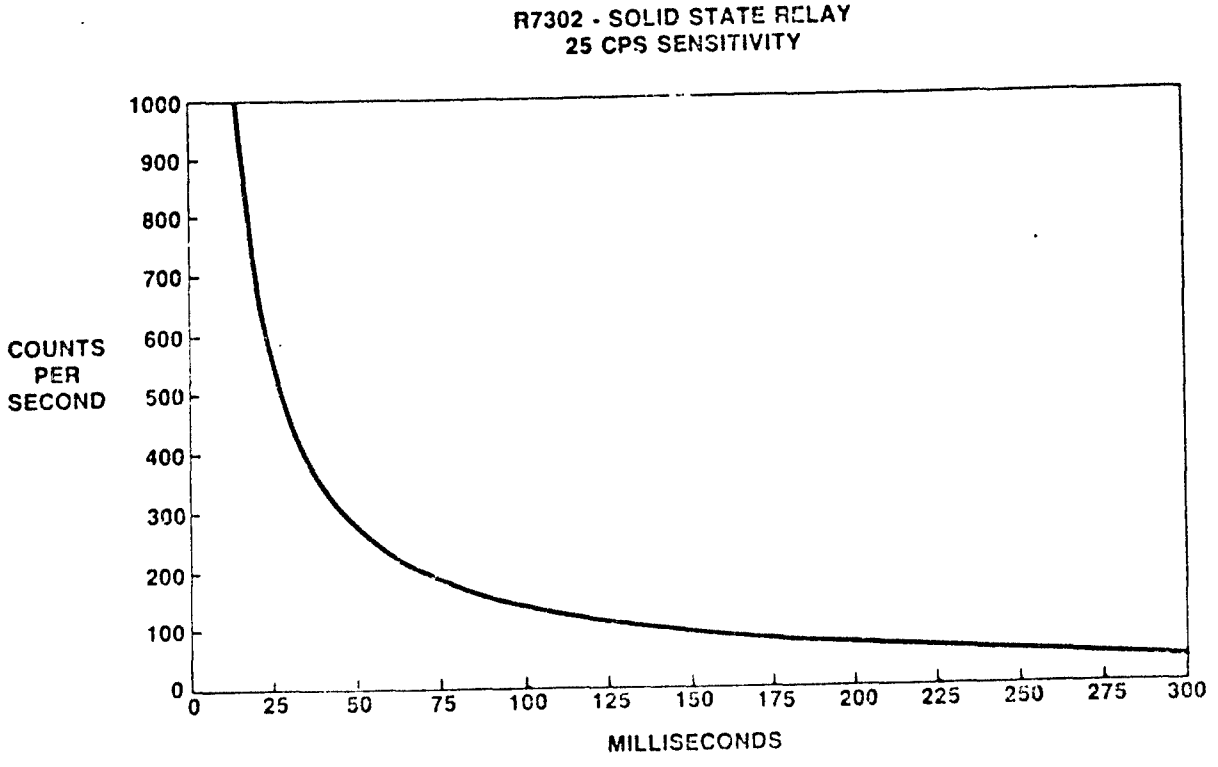

Figure 8 - Response Time Versus Count Rate

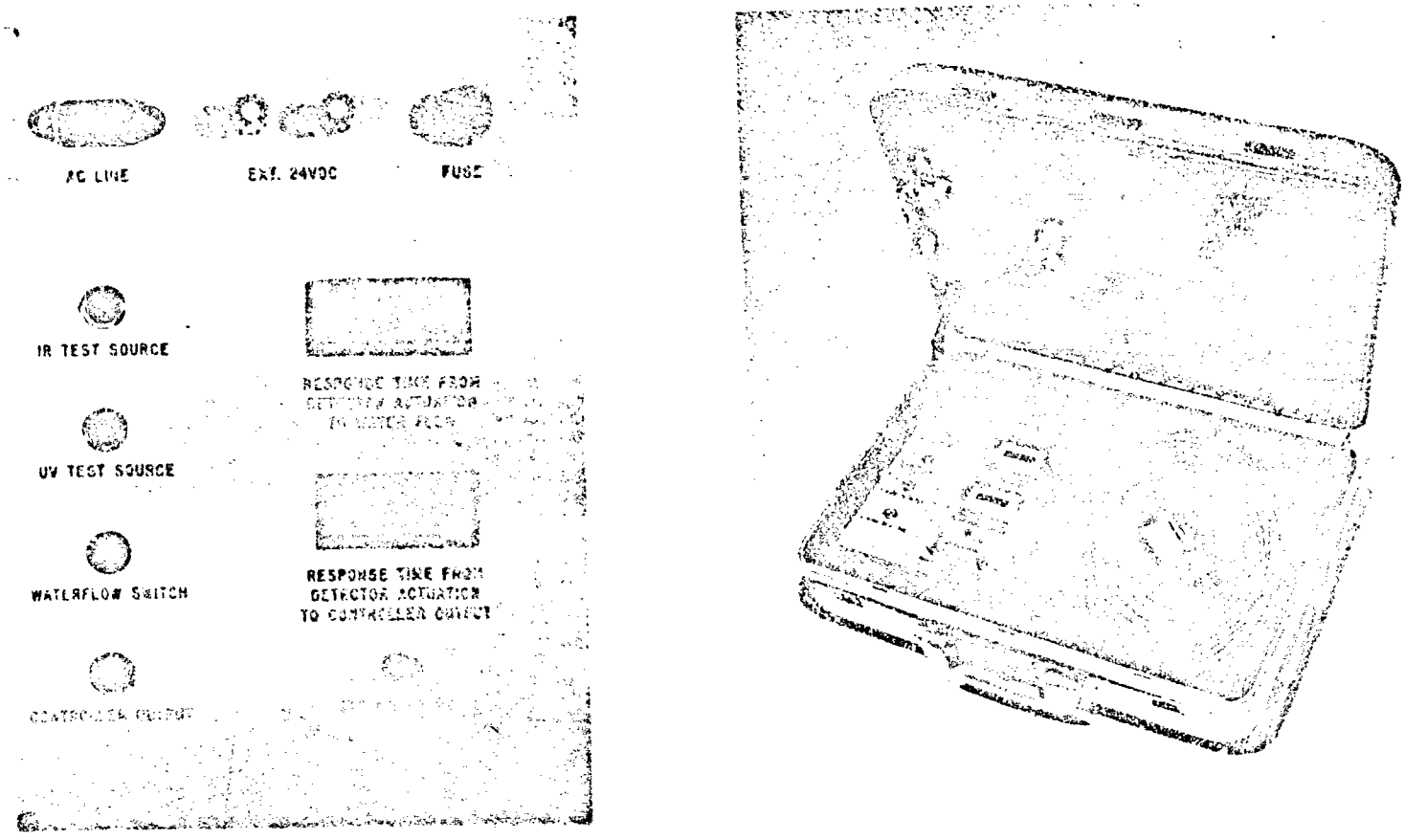

Figure 9 - Detector Electronics Response Timer

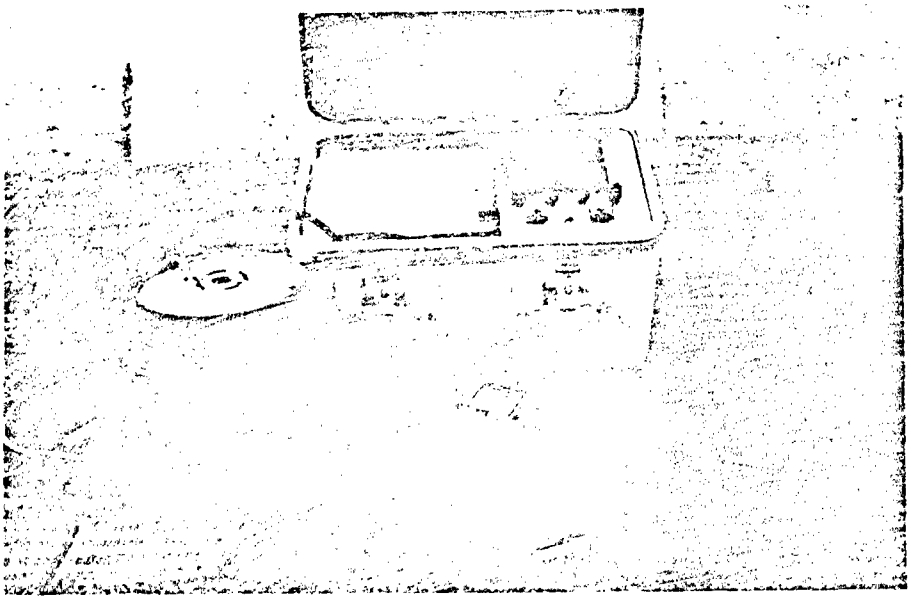

Figure 10 - "Automatic" Sprinkler Corporation Response Timer

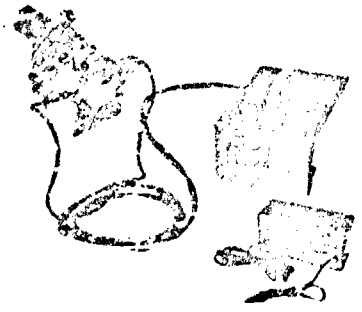

Figure 11 - Grinnell Ultra High Speed Timer

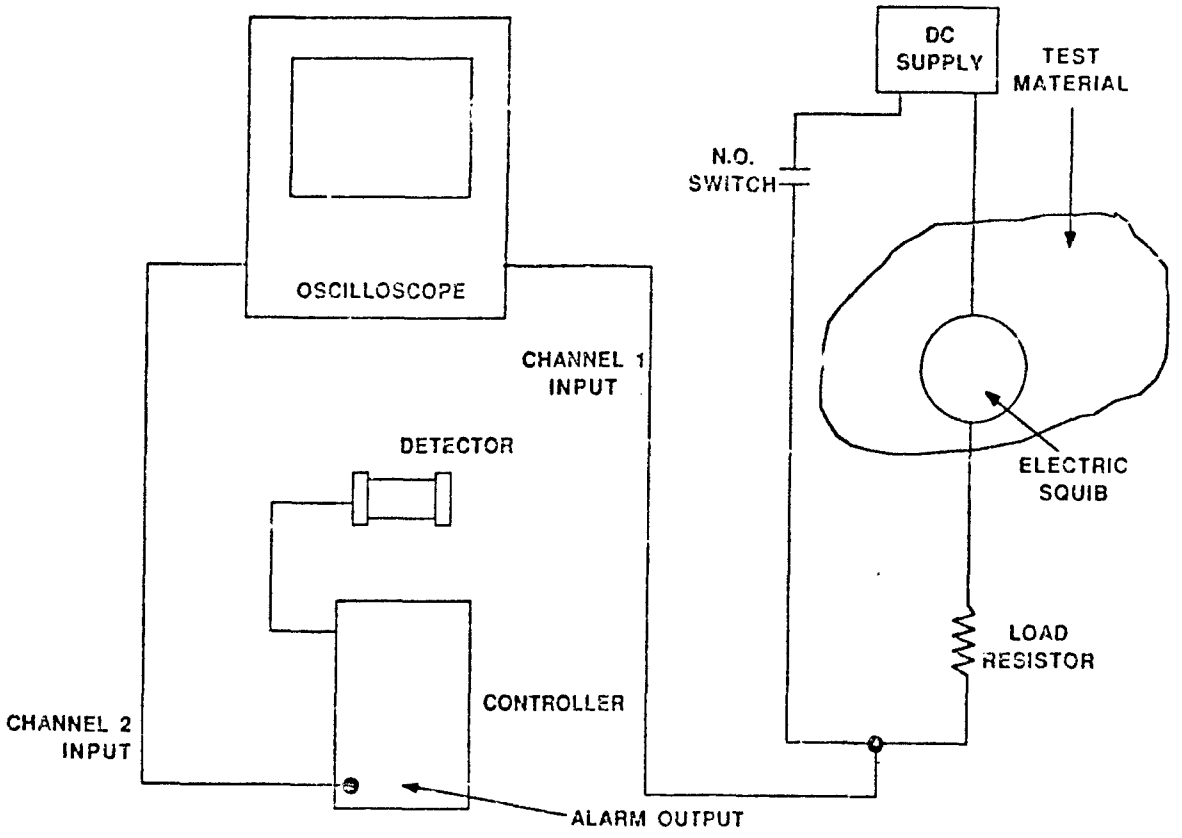

Figure 12 - Test Equipment Configuration

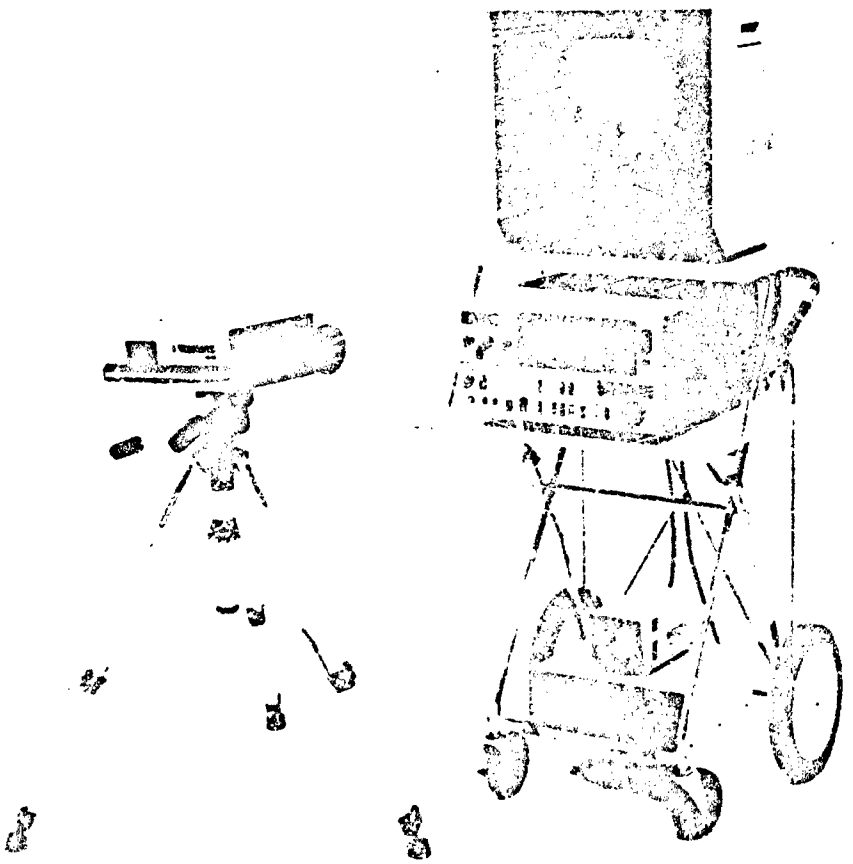

Figure 13 - Video Logic Corporation High Speed Video Photography System

A STUDY ON RESPONSE TIME FOR UV-DETECTION OF FLAMES FROM SINGLE AND DOUBLE BASE PROPELLANT FIRES.

SUMMARY

In order to choose fire-fighting system for powder producing units it is of greatest importance to estimate evere application isolated from each other. This study of varying response times for UV-detectors during propellant fires clearly indicates that

- certain propellants can contribute to remarkably long delay times
- single base propellants contribute to longer delay times compared with double base propellants
- the choice of UV-detector can be decisive for the quickness and efficiency of the sprinkler system
- the transmittance of the quartz glass in the tube front can vary and can be of importance regarding response time.

This study was executed after a fire in a cutting machine for single base propellants. In this case the delay time was approx. 5 seconds, which caused the burning of approx. 200 kg propellant. The cutting room and the equipment were also badly burnt.

Prepared
for
DEPARTMENT OF DEFENSE
TWENTY-THIRD EXPLOSIVES SAFETY SEMINAR
by

Stig E. Dahlberg
Nobel Chemicals AB
S-691 85 Karlskoga, SWEDEN

INTRODUCTION

On August 20, 1986, a fire occured in a cutting machine, for single base propellants, belonging to Nobel Chemicals in Sweden. In order to minimize damage and to protect our staff we use for this type of work a quick sprinkler system with UV-detectors, which, via a control unit, releases the actuators fitted to the sprinkler heads (fig. 1). On this occation the system did not work as it was intended to do. Water was realesed only after approx. 5 seconds and the action was initiated by the bursting of the glass bulbs due to the intense heat. Approx. 200 kg of propellant were burnt during this delay time. The operator, fortunately, suffered only light burns.

In the subsequent investigation we could not find any plausible reason for the delay. We knew from practical experience that delay times for the release of sprinkler systems can vary for different types of propellants and for different compositions. The reason might be that different compositions during a fire emit different spectra or that dust or gas absorbs light within the UV-wave length range. In addition we also knew that the transmittance of the quartz glass of different UV-detectors can vary. With this as a back-ground we decided to investigate the respons time of UV-detectors during a fire for different intermediates used in our powder plants.

TEST DESIGN

Tested intermediates and products are listed in Table 1.

In order to obtain a standardized ignition the method described in Fig. 2 was used.

In the tests, four UV-detector tubes according to Table 2 were used. The main difference betwen the two types of UV-detectors used is deseribed in Fig. 3. The new type has a wider area of sensitivity, extended in the direction of visible light. As a reference detector we used a photo cell, trade name Hemamatsu R 1826.

Test arrangements are described in Fig. 4.

Delay time is defined as the time that elapses between attaining a certain voltage in the photo cell and reaction from the UV-detector. An example is givin in Fig. 5.

We measured the burning rates of the different propellants in order to have an understanding of the various burning properties of the test materials. We used the normal equipment for tests of ignition and burning rate according to Bofors A-standard 7059 with some slight modifications. Each propellant was tested twice. We used 14 g of propellant for each test. An approx. 250 mm long string of propellant was put on top of a fibre board sheet and the sheet was introduced into the test equipment. The sheet inclines 3° against the horizontal plane. A small flame from a gas burner is brought in contact with the upper part of the propellant string. The propellant ignites and is left to burn approx. 80 mm, after which the burning of the next 100 mm is timed by a stop-watch. The test results are the burning rate (r) in mm/s and a visual assessment of the appearence of the flame. The geomitrical form and dimensions of the propellants tested are given in Table 3.

CONCLUSIONS

Delay times in ms for different propellants and UV-detectors are presented in Table 3.

Double base (DB) propellants consistently burn quicker and produce a larger flame compared with single base (SB) propellants. This is mainly due to the fact that SB intermediates contain ethanol and ether and in some cases KNO_3. These three compounds are being removed from the propellant, during subsequent stages of the process.

Analysis of variance

The purpose of the analysis was to find parameters influencing the delay time between photo cell and UV-detectors. For the statistical calculations an existing program for analyses of Vo (muzzle velociy) has been used. The calculations have been made according to the least-square menthod. The analysed results are displayed in Table 3. The following parameters have been analysed:

- Type of propellant according to Table 1
- Type of detector according to Table 2
- SB-propellant compared with DB-propellant

Conclusions of analysis of variance

- Test sample number 9 deviates significantly from the other samples (This propellant was being cut when the fire occured). The powder contributes to a remarkably long delay time.
- The new type of detector is much quicker than the two normal ones. The normal detector with a bad, although approved within specifikations, front glass has a remarkably long delay time compared with the normal detectors.
- SB-propellants contribute to long delay times, while DB-propellants are associated with somewhat shorter delay times.

These conclusions are statistically true with a probability of 95 %.

COMMENTS

The study indicates that the choice of detector is of vital importance to the efficiency of the sprinkler system in a specific application. It is of course also necessary to consider the consequenses of accidental (no fire) release of a very sensitive system when the final choice is made.

The study also indicates that the efficieny of the sprinkler system is affected by the composition of the powders. The efficiency also varies during different stages in the production process due to precense of solvents and salts. It might seem selfevident that IR-detectors are more suitable for certain applications, but this study has been restricted to UV-detectors only.

At last I would like to point out that the tests have been made in the laboratory and in a small scale. The conclusions should therefore not be regarded as the final truth about the efficiency of UV-detectors in various applications. My advice is to make a detailed study for each and every application. There is no standard solution for all problems.

Sprinkler with glass bulb and detonator
BOFORS ACTUATOR

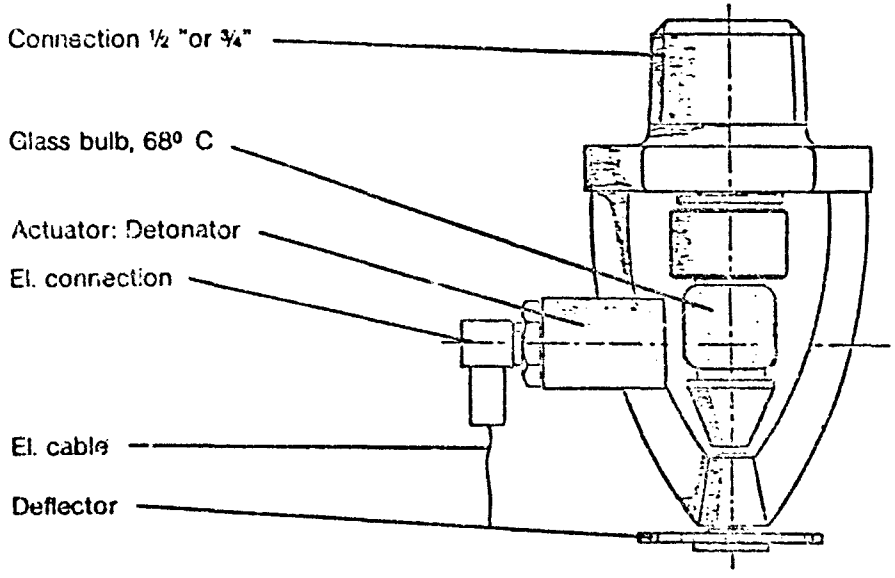

1952

Tested propellents

Powder (nr)	Powder shape	Dimension (mm)	Humidity (%)	Calorific value (cal/g)	Comments
1	Rosett	Grain ~ 5 mm	0.5	800	155 mm Howitzer
2	Tube	4.0x6.2	1	940	Missile Propellant
3	Flake	1.5x10x10	0.5	1240	Intermediates[1]
4	Flake	0.4x10x10	0.5	1230	Finished Dimension
5	Flake	1.5x10x10	0.5	800	Intermediates[1]
6	Flake	0.4x10x10	0.5	1240	Finished Dimension
7	Rosett	Grain ~ 5 mm	3	800	155 mm Howitser
8	Flake	1.5x10x10	1	1230	Intermediates[1]
9	Rod	0.6x0.4	~ 15[2]	980[3]	Salt Powder
10	Flake	0.2x2x2	~ 15[2]	980[3]	Salt Powder
11	Onehole	0.7x1.5x2	~ 15[2]	730[3]	155 mm Howitser
12	Onehole	0.2x1.3x1.2	~ 15[2]	930[3]	Rifle
13	Onehole	0.2x1x1	~ 15[2]	930[3]	Rifle
14	Onehole	0.3x2x5	~ 15[2]	700[3]	40 mm Anti Aircraft

Powders Nos. 1-8 are Double base type

Powders Nos. 9-14 are Singel base type

1) Flakes direct from Differential Rolling Mill

2) Solvents (ethanol, ether, water)

3) Finished Product

Table 1

Sketch showing Ignition of the Test Powder

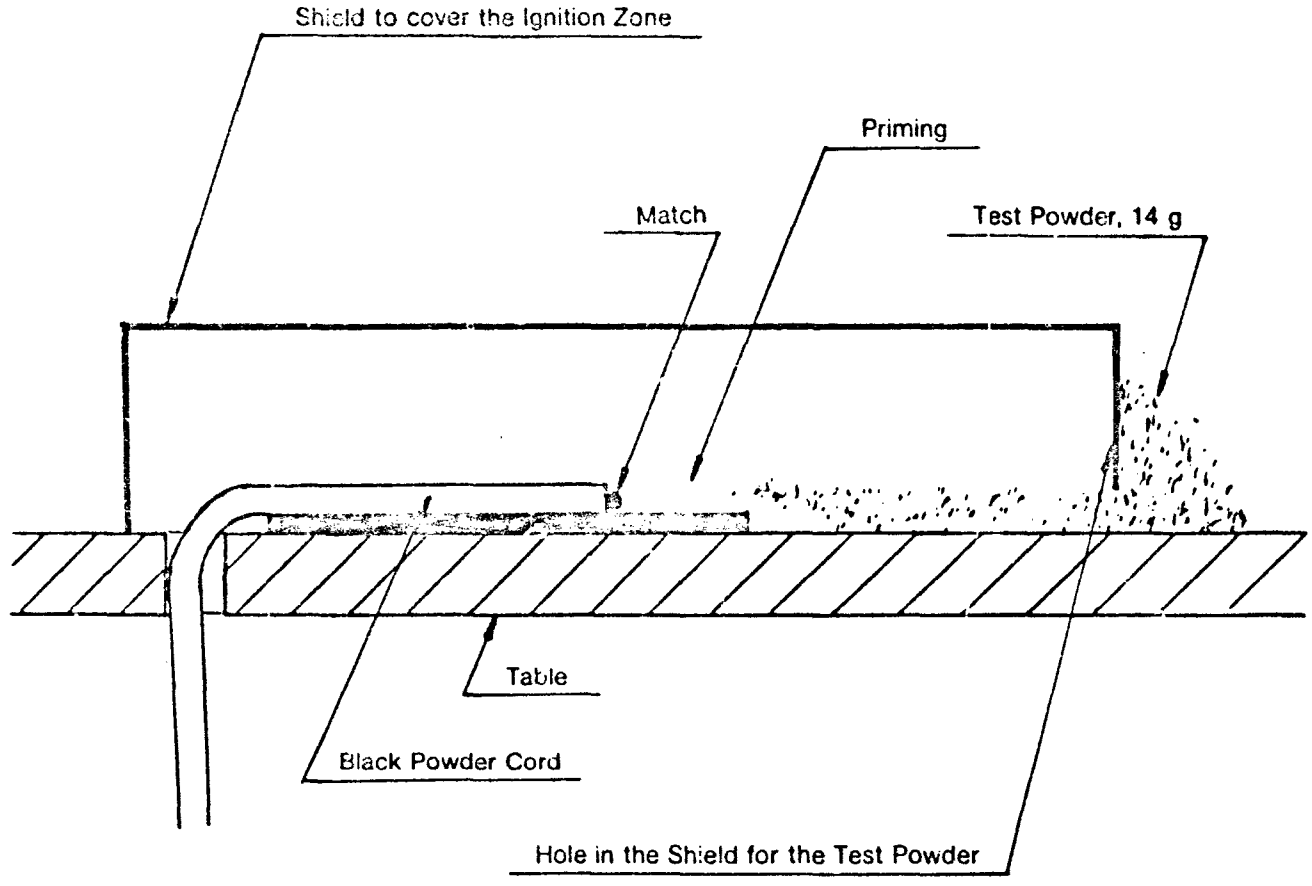

1954

Detector Tubes used at the Tests (manufacturer: Det-Tronics)

Det. (nr)	Symbol	Front glass	Wave length area (nm)
1	DE 1777 A1[1]	Normal	185-245
2	DE 1888 N	Normal	185-265
3	DE 1777 A1[1]	Normal	185-245
4	DE 1777 A1[1]	Bad[2]	185-245

1) This type is normally used in production

2) The transmittance of the quartz glass can vary within accepted limits

The level of sensitivity of the electronic system has been 14 cps (counts per second) during all tests.

UV-detectors Range of Sensitivity

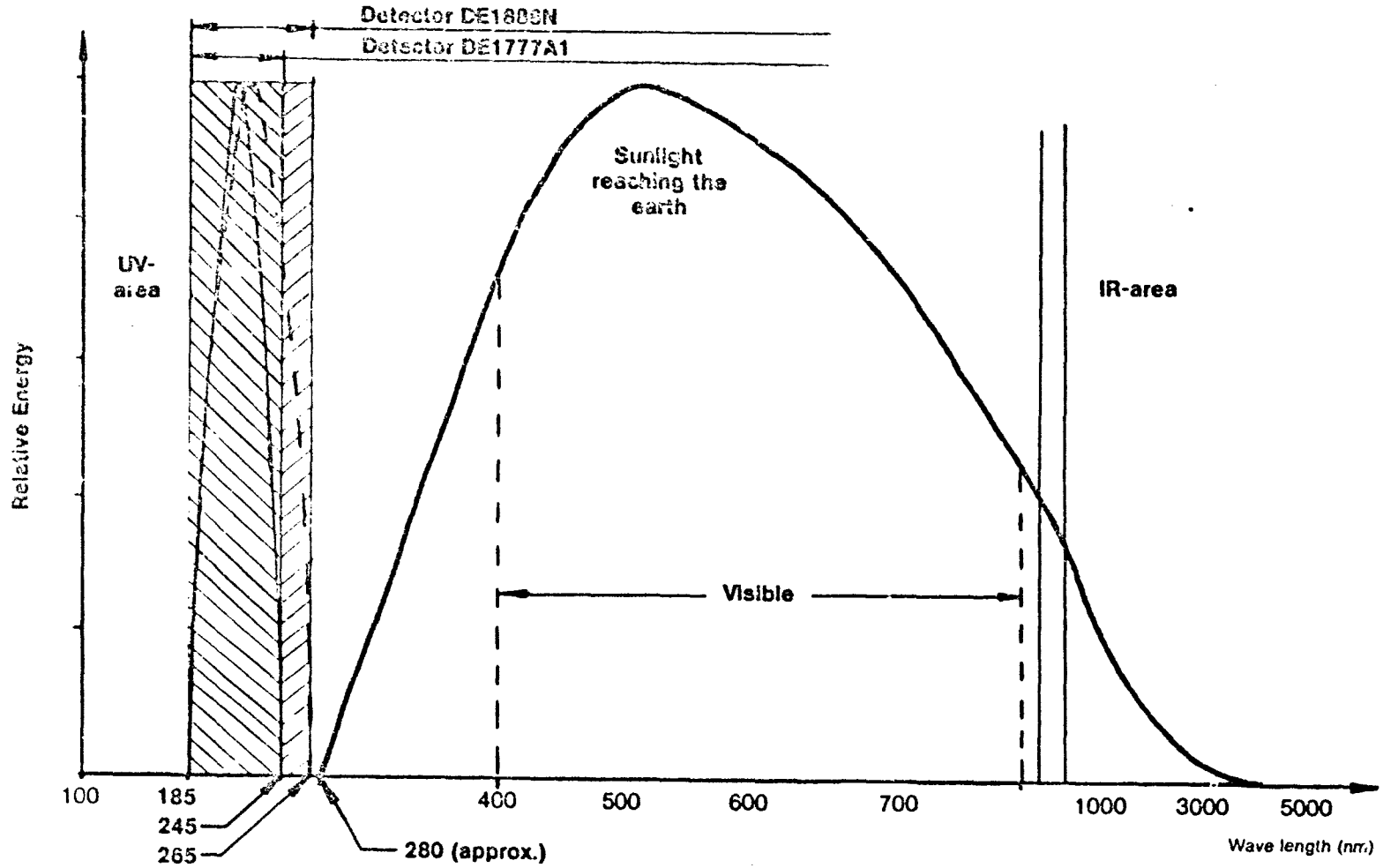

Figure 3

1956

Testarrangement distances in mm

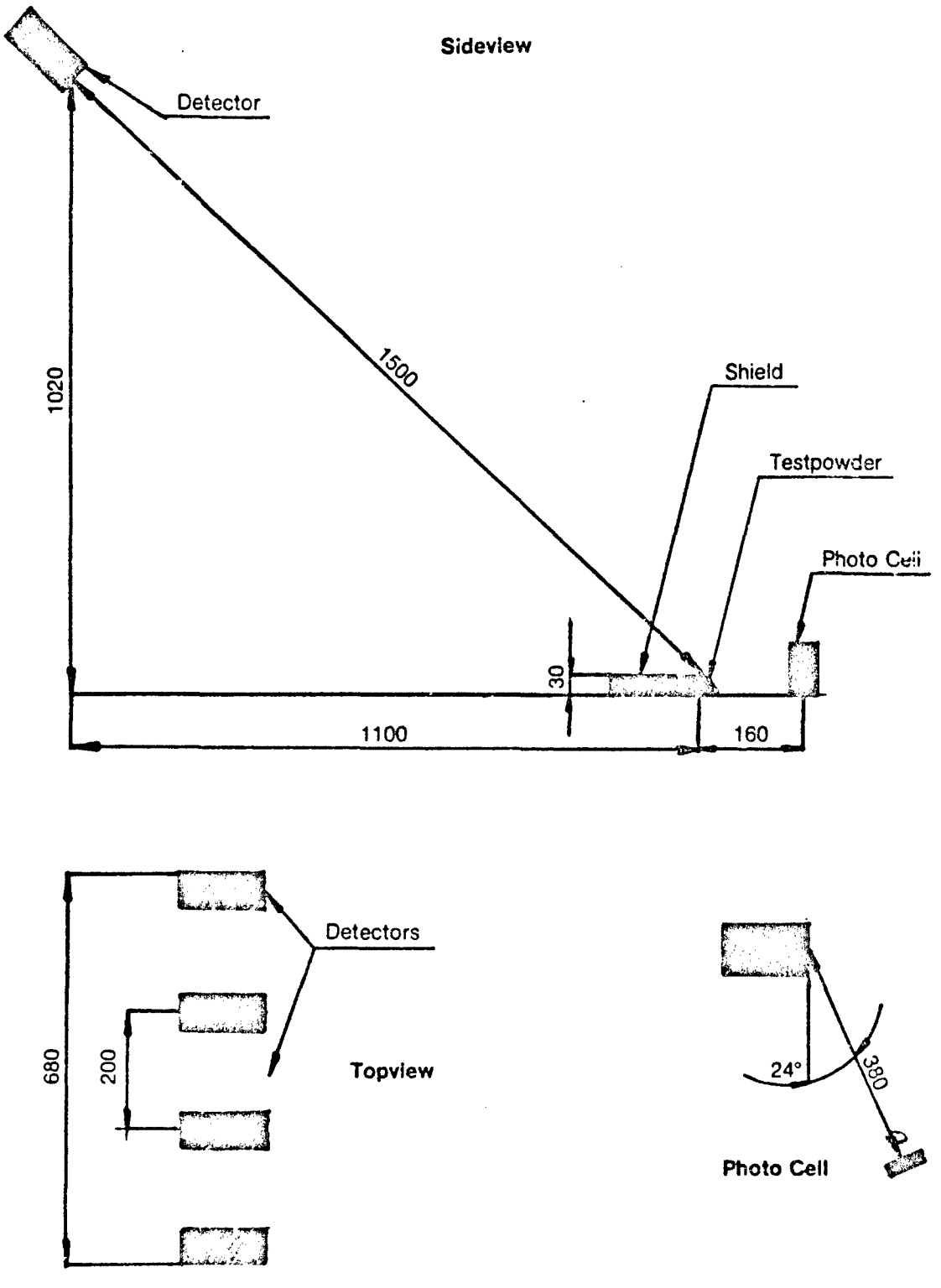

Figure 4

1958

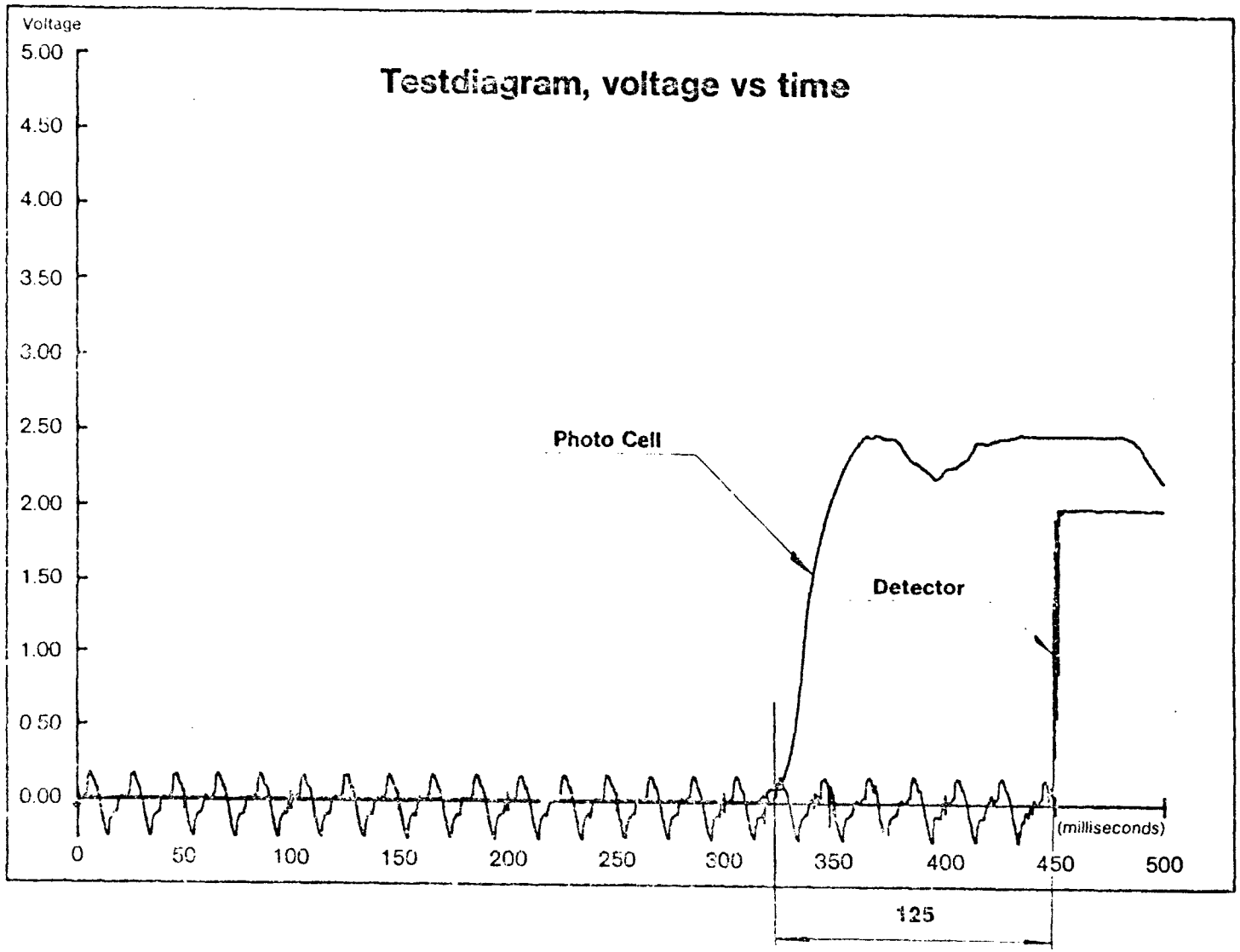
Testdiagram, voltage vs time
Voltage
5.00
4.50
4.00
3.50
3.00
2.50
2.00
1.50
1.00
0.50
0.00
Photo Cell
Detector
(milliseconds)
0
50
100
150
200
250
300
350
400
450
500
125

Testresults, Delay Times and Burning Test

Powder (No.)	Delay Time, (ms)				Stringburning Test		
	Detector (No.)				r (mm/s)		Flame size and colour
	1	2	3	4	Test 1	Test 2	
1	41	21	83	105	10	10	~ 500 mm, whitish
2	170	18	54	329	20	20	400-500 mm, yellowish
3	41	22	24	58	50	33	300-400 mm, yellowish
4	64	18	27	47	50	50	500-600 mm, yellowish
5	40	7	60	27	10	9	~400 mm, whitish
6	84	16	50	50	50	50	~500 mm, yellowish
7	123	19	248	65	10	9	300-400mm, whitish
8	68	21	24	41	50	50	~500 mm, yellowish
9	185	27/ 80*	307	998/ 973*	6	5	200-300 mm, weak violet
10	371/ 492*	33	432	415/ 429*	6	6	200-300 mm, weak violet
11	445/ 18*	4	31	52	7	6	200-300 mm, whitish
12	63	29	57	81/ 117*	4	4	~300 mm, weak violet
13	227	11	30/ 39*	237	4	6	200-400 mm, weak violet pulsating
14	155	28	36	125	2	2	100-200 mm, weak violet pulsating, emitting sparks
$\bar{x}$	141	24	100	244			

* Two tests

The propellants 1-8 are double base

The propellants 9-14 are single base

Table 3

ALUMINIZED EXPLOSIVE HANDLERS SUIT

by

Star Glove and Safety Products
766 Merchant Street
Los Angeles, CA 90021
800-826-2408
213-628-1341

T. Olen Nelson

President

Sales Agent:
Stephen J. Asthalter
P. O. Box 721
Chatham, NJ 07928
201-635-4092

1961

Star's Aluminized Explosive Handlers Suit
Background and Description

Star Glove and Safety Products introduced a three layer aluminized suit consisting of a hood, coat, pants, glove and spats to be worn by pyrotechnic processing handlers to the United States Army Munitions Production Base Modernization Agency (PBM), Dover, New Jersey.

Over the past four years, PBM has tested many suits and materials by exposing them to a "flash off" of a 15 lb pyrotechnic dry granular composition placed in a simulated mixer at an open air site. A requirement of a maximum increase in temperature of 20 degrees Fahrenheit inside a suit was established during a "flash off". The only suit that met that requirement, up to the introduction of the Star suit, was a one piece coverall with an attached hood developed by the Navy Clothing and Textile Research Facility in Natick, Mass. The "Natick" coverall uses an outershell of a (80/20) OPF/PBI 15.5 oz woven fabric, an insulation of Kevlar batt material, and a vapor barrier of a goretex/cotton material.

The Star suit has an outer layer of 10.5 oz aluminized 50/50 PBI/Durvil knit with an insulation of a PBI/Kevlar felt that is also aluminized. The inner layer is an unaluminized 50/50 PBI/Durvil knit. The aluminized outer shell is water repellent. All the materials used in the Star suit are commercially available and are currently being sold by Star and other companies to the firefighting and aerospace industries. Also, the fibers, yarns and fabrics are all made in factories located within the United States. This is in contrast to the Natick suit. The Natick outer fabric is woven with an OPF core yarn that is only made in Japan by a joint venturer of BASF, who has recently succeeded the Celanese Corporation in that joint venture. The core OPF is wrapped with PBI to make the final yarn for this outer shell. This blend was created especially for the Natick suit. A limited amount of the final fabric was woven for the initial suits made for Natick and none has been made since then. This fabric is not being used in any other industry and cannot be considered a commercially available product.

The Star suit has excellent features from the point of view of the wearer.

1. The Star ensemble is 5 pieces. A worker can don the suit independently. During periods when the wearer is in between operations he can remove the hood, jacket and gloves and be relatively comfortable just wearing the spats and pants. The suit comes in six sizes.

2. The use of aluminized knits creates a flexible suit.

3. The weight of the suit is only 14 lbs.

4. The suit has the option of a cooling system that brings cool air into both the hood and the light weight vest. This system has been interfaced with an airline respirator with escape bottle so that the wearer still only needs one air supply hose.

5. The suit's gloves give enough dexterity to be able to use small tools such as pliers and screw drivers.

DEPARTMENT OF DEFENSE EXPLOSIVES SAFETY BOARD
2461 EISENHOWER AVENUE
ALEXANDRIA, VIRGINIA 22331-0600

December 18, 1987

Technical Programs
Division

Mr. Stephen J. Asthalter
P.O. Box 721
Chatham, NJ 07928

Dear Mr. Asthalter,

The Department of Defense Explosives Safety Board (DDESB) expresses their sincere appreciation to you for the informative briefing on your Aluminized Explosive Handlers Suit presented on 17 December 1987. Your development of this clothing provides a milestone improvement in protecting explosives workers from the inherent thermal hazards from ammunition operations in the event of an incident. The use of this clothing and equipment is consistent with DDESB's responsibilities to provide protective clothing and equipment to assure permissible thermal exposure limits are not exceeded.

As discussed yesterday, DDESB extends an invitation to you and your development associates to present papers on this clothing and equipment at the biannual Explosives Safety Seminar to be held in Atlanta, GA 9-11 August 1988.

Thank you again for your excellent briefing.

Sincerely,

Thomas F. Hall, Jr.
Colonel, United States Army
Chairman

Copies Furnished

Jon Bomengen, AMSMC-PBL-A
Mr. T. Olen Nelson

DEPARTMENT OF THE ARMY
HEADQUARTERS US ARMY ARMAMENT, MUNITIONS AND CHEMICAL COMMAND
DOVER, NEW JERSEY 07801-5001

REPLY TO
ATTENTION OF

SMCAR-FSA-P

Mr. Stephen Asthalter
Star Glove and Safety Products, Inc.
766 Merchant St.
Los Angeles, CA 90021

Dear Sir:

The enclosed is a concise statement of the facts concerning the recent history of development of protective clothing as it relates to pyrotechnic operations. It provides, in capsule format, the reason for initiation of the program, together with test procedures and results. A comprehensive final report is being prepared and will be available in the near future.

Encl

J. MATURA
Acting Chief, Munitions Section
AAD, FSAC

1964

PYROTECHNIC SAFETY ENHANCEMENT PROGRAM

PROTECTIVE CLOTHING

As a result of accidents with pyrotechnic mixes, some involving fatalities, a comprehensive program was undertaken to enhance safety in these types of operations. One of the priority investigations was focused on designing protective clothing that would provide the best possbile environment for an operator to survive accidental ignition of in process pyrotechnic mixes.

The initial approach to development of protective clothing was a joint effort of ARDEC and the Navy Clothing and Textile unit at Natick. This involved research into materials and individual testing of candidates utilizing unconsolidated pyrotechnic compositions. From this, we developed a one piece garment that was tested using instrumented mannequins arranged in a blending bay setting with loose pyrotechnic composition in a "mock up" blender. The instrumentation provided a means of measuring the temperature rise inside the garment, on the surface of the mannequin, when the composition was ignited. The temperature of such an ignition was determined to be in the 5000 degree F to 5500 degree F range. Measurement of the temperature rise on the surface of the mannequin was accomplished by the use of skin simulants and thermocouples linked to a computer. The temperature rise was recorded at 30 degree F to 40 degrees F indicating successful protection. The thermocouples were normally located at the head, chest (2 places) abdominal area, one arm and one leg. Subsequent to each of these

test sequences the mannequin was photographed with the garment in place and then as the hood and main garment was removed, photographs were taken at each step to record the condition of clothing and mannequin. In addition, a white cotton undershirt was in place on the mannequin that would provide additional visual evidence of any temperature rise that would cause scorching of the cotton. As a result of the success of these tests, garments were manufactured and distributed to selected plants for their use and commentary.

The feedback data from the plants indicated dissatisfaction in certain areas. Specifically, the complaints centered on the difficulty of getting into and out of the one piece coverall, the difficulty of cleaning the garment (complicated by some shrinkage) abrasion and tearing of the fabric, interference with free movement due to bulk and uncomfortable heat when worn in non-airconditioned areas. It is axiomatic that to provide protection against the type of event encountered, some restriction of movement and level of discomfort will probably be unavoidable. However, we evaluated each criticism and attempted to correct the situation. From this effort, a second generation garment evolved as a result of the cooperative effort of ARDEC and Star Glove and Safety Products of Los Angeles. The new garment is of a two piece design using the same basic protective material except that it is knitted rather than woven (to reduce bulk) and has an aluminized outer layer. The latter not only provides additional thermal protection but also provides for a reduced effort of cleaning. The garment was subjected to the identical test program discussed previously and was equally successful. The

freedom of movement about the workplace has been enhanced by the reduced bulk and the level of effort to get into and out of the garment has been substantially reduced. In addition, we have provided a small, lightweight air conditioning unit that is now part of the breathing apparatus that was developed for the earlier model garment and has been adapted for this latest model.

During the course of the investigation of protective clothing for pyrotechnic operations, it became apparent that work not contemplated in the original scope of work, would be required. Specifically this involved a form of protection for the eyes that would be in addition to the face shield. It was reasoned that, while the shield protected the face and eyes against the apparent affects of the event, the probability of retinal burning due to the amount of light reaching the operator's eyes, was great. As a result a basic literature search and other investigative efforts were undertaken. It now appears probable that we can limit this damaging light by use of a narrow bandpass interference filter. It would involve the use of commercially available interference filters that could block out approximately 98% of the incident light, but would permit normal visual acuity in normal room lighting.

General Purchase Description

ITEM:	Suit, Aluminized, Pyrotechnic Handlers, 5 pieces.
TYPE:	The suit shall consist of fabrics made with PBI, Kevlar and Durvil fibers exclusively. All fabrics and materials used in the suit must be commercially available. The suit shall have passed a test procedure established by the U. S. Army. The test procedure used by the U. S. Army Engineering and Development Center at Picatinny Arsenal, Dover, N. J. is acceptable.
SIZE:	As stated on purchase request.
WEIGHT:	Fourteen Pounds.
FLEXIBILITY:	Shall be of knitted construction to create a flexible suit.
STATIC PROPERTIES:	Fabrics must have same or less electrical resistivity as cotton.
AIR SUPPLY AND COOLING SYSTEM	The suit shall interface with an airline respiratory system with an escape bottle and cooling system. (See separate purchase description.)
DEXTERITY:	The suit's gloves shall give enough dexterity to be able to use small tools such as pliers and screwdrivers.
SHIELD:	The face shield shall be made of .060 polycarbonate and be 8 x 14 inches in size. The outer shell shall have a layer of 99% 24 carat gold vacuum deposit with a silicone coating. This layer will reflect 98% of the radiant heat but will not provide eye protection.

SPECIFICATIONS

ALUMINIZED PYROTECHNIC HANDLERS SUIT

1.0 Fabric Materials
- 1.1 Inner Layer
  - 1.11 Blend: 50/50 Star PBI/Durvil
  - 1.12 Fabric: Knit
  - 1.13 Weight: 10.5 Oz.
- 1.2 Middle Layer
  - 1.21 Blend: 40/60 Star PBI/Kevlar
  - 1.22 Fabric: Aluminized Felt
  - 1.23 Weight: 6 Oz.
- 1.3 Outer Layer
  - 1.31 Blend: 50/50 Star PBI/Durvil
  - 1.32 Fabric: Aluminized Knit
  - 1.33 Weight: 12.5 Oz.
- 1.4 Spat Material
  - 1.41 Tanoak Leather

2.0 Construction
- 2.1 Thread: Size 35/31 Kevlar
- 2.2 Seams: French Construction, double seam, surged
- 2.3 Stitching: 301 Lock Stitch

3.0 Labels
- 3.1 Content Label
- 3.2 Warning Label
- 3.3 Care Label
- 3.4 Manufacturer's label

4.0 Physical Description
- 4.1 Gloves
  - 4.11 Three layers (see materials)
  - 4.12 14 inches long - Gauntlet
  - 4.13 All inseams
  - 4.14 Clute cut
  - 4.15 Universal size
- 4.2 Coat
  - 4.21 Three layers (see materials)
  - 4.22 Front opening with storm flap and velcro closure
  - 4.23 Length - 35 inches
  - 4.24 SCBA pocket on back - optional
  - 4.25 Two inch elastic full hem
  - 4.26 Two piece raglan sleeve
  - 4.27 Kevlar/Durvil thumb cuff #4306
  - 4.28 One inch velcro strips for hood bib with snaps at waist for extension bib

4.3 Pants
- 4.31 Three layers (see materials)
- 4.32 Diagonal fly front with velcro closure
- 4.33 Four belt loops of aluminized leather
- 4.34 Firemans suspenders - heavy duty
- 4.35 Twenty six inch wide pant leg
- 4.36 Re-inforced crotch with outer layer material
- 4.37 Side pocket for escape bottle - optional
- 4.38 Closure strap at cuff

4.4 Hood
- 4.41 Three layer material (see materials)
- 4.42 8x12 Golden polycarbonate anti-fog window with ceramic hardcoat
- 4.43 Twelve inch inner shroud with shoulder flaps
- 4.44 Seven inch outer shroud with shoulder flaps, velcro along hem to attach to coat and elastic underarm straps covered with aluminized material
- 4.45 Fourteen by twenty-one inch bib attached to outer shroud and attached to coat with snaps at waist
- 4.46 Bullard 687-1-ESRT-SL hard hat with Bullard 690-1 air phelem w/vinyl hose, 1/4" industrial interchange and a plastic screw cap option for use with Mine Safety Appliance P/N 487134

4.5 Spats
- 4.51 Aluminized Tanoak shoe cover
- 4.52 Outer layer material only around ankle
- 4.53 Leather instep strap with snap
- 4.54 Velcro closure at back

ELECTRICAL RESISTIVITY IN FABRICS

The test most commonly used to define electrical properties of any fabric is AATCC procedure #76 for electrical resistivity. Results from these tests show the electrical resistivity (and therefore static dissipative properties) of fabrics at the more critical lower humidity levels of 40% RH. Nomex III, a fabric commonly used in the industrial area for coveralls, hoods and glove liners has a resistivity rating much higher than either cotton, FR cotton, PBI/Kevlar and PBI/Durvil blends and may create static.

Below is a graph which displays data from tests of various fabrics. Electrical resistivity is expressed in units of "ohms/cm^2" or "ohm's per square". Since this number is typically very large it is often shown as logorithmic form with units of "logohms". In either case lower numbers mean less resistivity, higher conductance and greater ability to dissipate static. Differences of more than .5 logohms or about 5 ohms per square are significant. The U. S. Air Force, for example, requires less than 3.0×10^{11} ohm/cm^2 or 11.5 logohms at 40% RH for their flight suit fabrics, a specification met by cotton and PBI blends, but not met by untreated Nomex.

ELECTRICAL RESISTIVITY OF FABRICS TESTED

ITEM	LOGOHMS warp x fill
Air Force Requirement	11.5 x 11.5
Nomex III	13.4 x 13.5
100% FR cotton	11.2 x 11.2
40/60 PBI/Kevlar	11.3 x 11.3
50/50 PBI/Durvil Knit	10.6 x 10.7
70/30 Kevlar/Durvil Knit	12.0 x 11.6
PBI/Durvil Knit Glove	10.3 x 10.6
100% Cotton Knit Glove	10.3 x 10.3

All tests performed at 70°F/40% RH in accordance with AATC test #76 using Custom Scientific CS-51 Electrometer.

General Purchase Description

ITEM:	Work Mask, Pressure Demand w/warning light and cooling.
TYPE:	The work mask is a pressure demand airline half mask respirator and self contained breathing apparatus. It enables the user to breathe from a remote air supply source in a hazardous work area. It contains a small cylinder of air rated for 5 minutes escape time which automatically comes on when there is a primary air supply failure. A warning light is provided to alert the user that the escape bottle has been activated and that immediate evacuation of the hazardous area is required. A tee may be fitted in the airline to carry air to the vortex that distributes cool air to a perforated fire retardant P.V.C. vest and a plenum in an air supply hood.
WEIGHT:	Twelve pounds
COMFORT:	The unit shall be back mounted with padded shoulder straps and a cross chest strap for additional weight distribution.
COMPATIBILITY:	The unit shall interface with an aluminized pyrotechnic suit that meets specifications.

MSA Work Mask, Pressure Demand with Warning Light.

BEFORE USE

1. THOROUGHLY CHECK OUT THIS APPARATUS ON RECEIPT PRIOR TO USE.
2. FOR USE ONLY BY QUALIFIED TRAINED PERSONNEL.
3. CAUTION: WEAR IMPERMEABLE PROTECTIVE CLOTHING FOR EXPOSURE TO GASES AND VAPORS WHICH CAN POISON BY SKIN ABSORPTION.

WARNING

1. This device may not provide a satisfactory face seal with certain physical characteristics (such as beards or sprees sideburns), as outlined in ANSI Z88.2-1969, resulting in leakage in connection with the facepiece, which voids or limits the protection. If such a condition exists, the user assumes all risks of death or serious bodily injury which may possibly result.
2. Under no circumstances should this apparatus be used as an underwater device.

INSTRUCTIONS FOR USE AND MAINTENANCE

DESCRIPTION

The MSA Pressure Demand Work Mask is a combination airline respirator and self-contained breathing apparatus. It enables a user to breathe from a remote air-supply source in a hazardous work area. It also contains a small cylinder of air rated for 5 minutes escape time which is used for egress in case of primary air-supply failure. The pressure in the mask is at a slight positive pressure to prevent inward leakage. NOTE: Certain gases such as hydrogen cyanide which poison through the skin or ammonia which irritates the skin may require protective clothing in addition to the apparatus to provide complete protection. This apparatus can be used at temperatures down to -32° F.

PREPARATION FOR USE

The following steps should be followed before putting on the apparatus.

1. Install a new 1.5 volt D size battery in compartment of electronic control box. Turn screw till door swings open, then install battery with button side next to door. Close door and tighten screw.
2. Plug two pronged electrical connector (alongside facepiece breathing tube) into mating receptacle (on belt) and tighten screw. (NOTE: Two prongs are different size and can only be plugged one way).
3. Check cylinder pressure to insure that gauge needle is on or above full mark (2640 psig).
4. Close red and yellow handwheel on regulator.
5. Open the cylinder valve fully.
6. The light in the facepiece should be burning steadily.
7. Hold palm of hand over regulator outlet port and open regulator main line valve (yellow handwheel). Pressure on regulator gauge will rise to same reading as cylinder valve gauge. Close the cylinder valve handwheel.
8. Release the trapped gas at a low rate by a slight movement of the hand away from the regulator outlet and note pressure on gauge. The facepiece light will start flashing at a pressure of 2440 ± 50 psig.
9. Close the regulator main line valve (yellow handwheel), open cylinder valve, place palm of hand over regulator outlet port and open the regulator main line valve (yellow handwheel). Close the cylinder valve and watch the pressure gauge on the regulator. There should be no drop in pressure. If the equipment is leak tight. If there is noticeable deflection of the needle, the equipment should be checked and the leak corrected.
10. Disconnect 2 pronged electrical connector.

DONNING THE APPARATUS

1. Put on the apparatus using the following method:
   - (a) Extend narrow shoulder straps fully.
   - (b) Don the apparatus like a vest.
   - (c) Lean forward and grasp loose ends of adjustable shoulder straps.
   - (d) Pull down till apparatus is in position where waist belt back pads falls across the small of the back.
   - (e) Fasten waist belt securely and snug chest strap if desired.
2. Check both red and yellow handwheels on regulator to insure they are closed.
3. Open cylinder valve handwheel.
4. Attach airline to connector on regulator.
5. The facepiece is put on using the following method:

Pull out the facepiece headband straps so that the ends are at the buckles and grip the straps between thumb and fingers. Insert the chin into lower part of the facepiece and pull headbands back over the head. Adjust headbands as follows:

- (a) See that straps lie flat against the head.
- (b) Tighten lower or neck straps.
- (c) Tighten Side straps (do not adjust forehead or front straps).
- (d) Place both hands on head pad and push in and down towards the neck.
- (e) Repeat operations (b) and (c).
- (f) Tighten forehead or front straps if necessary to position lens for best vision.

Test the mask facepiece for tightness by squeezing the corrugated breathing tube tightly, inhale gently so that the facepiece collapses slightly and hold breath for ten seconds. The facepiece will remain collapsed while breath is held providing the assembly is gas tight. If any leakage is detected around the facial seal readjust the head harness straps. If other than facial seal leakage is detected investigate the condition and correct. The facepiece must be subjected to a tightness test before each use.

6. Plug the two pronged electrical connector (alongside facepiece breathing tube) into mating receptacle (on belt) and tighten screw. (NOTE: Two prongs are different size and can only be plugged one way).
7. Connect facepiece breathing tube to regulator.
8. Open the Main-Line (yellow) valve handwheel fully because the handwheel must be turned as far as possible to insure adequate air flow under varying cylinder pressures.
9. The signal light in the facepiece will be burning steadily.
10. Test line by pass (red) valve by opening it briefly. With the by pass valve open a rush of air should be delivered to the facepiece. If the rush of air is delivered close the by-pass (red) valve. The apparatus is ready for use. If there is no rush of air to the facepiece when the by-pass valve is opened the equipment should be checked and corrected before entering a toxic atmosphere.
11. Breathe normally as the apparatus automatically satisfies any breathing requirement.

SERVICE LIFE

The escape part of this equipment is jointly approved by the National Institute for Occupational Safety and Health, and the Mine Safety and Health Administration as a 10 minute duration unit based on the fact that the equipment when tested by NIOSH on men performing moderate to heavy work and breathing at a rate of 40 liters per minute was found to last 10 minutes.

The user should not expect to obtain exactly 10 minutes service life from this apparatus on each use. The work may be more or less strenuous than in the NIOSH tests. Where work is more strenuous the duration may be shorter, possibly as short as 5 minutes.

The duration of the unit will depend on factors such as:

- (a) the degrees of physical activity of the user
- (b) the physical condition of the user
- (c) the degree of which the user's breathing is increased by excitement, fear or other emotional factors
- (d) the degree of training or experience which the user has had with this or similar equipment
- (e) whether or not the cylinder is fully charged at the start of the work period
- (f) the possible presence in the compressed air of carbon dioxide concentrations greater than the .04% normally found in atmospheric air
- (g) the atmospheric pressure. If used in a pressurized tunnel or caisson at 2 atmospheres (15 psi gauge) the duration will be one-half as long as when used at 1 atmosphere. At 3 atmospheres the duration will be one-third as long.
- (h) the condition of the apparatus

AIR SUPPLY

1. **Air Hose** - Any combination of the following Air Supply Hoses which does not exceed 300 feet may be used.

   See air hose connection instructions Pt. No. 93560? for airline hose and connections. Hose sections vary from 6 in. to 50 ft. lengths.

2. **Pressure** - Air must be supplied to the inlet end of the air hose under a pressure between 75 psig and 90 psig.
3. **Air Source** - The purity of the air supply is the responsibility of the user. The respirator is approved only when the air supplied meets the requirements of Compressed Gas Association Specification G-7.1 for Type 1, Class D Gaseous Air. This requires that the air contain no more than 20 parts per million (ppm) carbon monoxide, not more than 1000 parts per million (ppm) carbon dioxide, and not more than 5 milligrams per cubic meter of oil vapor or oil particulates.

USE IN TOXIC ATMOSPHERE

The apparatus furnishes complete respiratory protection as long as a pressure supply is available to the airline. This pressure must be set at 75-90 psig.

1. Should the airline supply fail the wearer will automatically start breathing air from the apparatus cylinder and the light in the mask will start flashing when the cylinder pressure reaches 1950 ± 50 psig. This signal warns the wearer to immediately leave the toxic area. The apparatus cylinder will supply air for a period of 10 minutes at a use rate of 40 liters per minute. To leave the area the individual should disconnect his airline hose. A check valve automatically checks leakage from the regulator connector.
2. During normal use check the alarm system by pressing the red button on the side of the electronic control box. The facepiece bulb will flash as long as the button is depressed. If the bulb does not flash when the button is held in the depressed position, leave the area immediately and have apparatus checked.
3. During normal use the by-pass (red) handwheel is closed and is used only if the automatic demand regulator becomes inoperative. It provides a continuous flow and should be opened first, then the mainline (yellow) handwheel closed and the by-pass valve adjusted to provide the flow desired.

AFTER USE

1. Unlock the lever on the cylinder valve and close the valve.
2. Release pressure on high pressure hose by opening the by-pass valve slightly.
3. If cylinder pressure is below 2475 psig, replace with full cylinder by following steps:
   - (a) Disconnect pressure switch connector.
   - (b) Disconnect facepiece breathing tube.
   - (c) Disconnect electrical connector (alongside breathing tube).
   - (d) Disconnect the coupling nut at the cylinder valve with wrench.
   - (e) Release the cylinder clamp draw bolt and remove the cylinder.
   - (f) Remove battery from electronic control box and discard.
   - (g) Replace cylinder with a fully charged one and connect the coupling at the cylinder valve with wrench.
   - (h) Connect pressure switch connector.
4. Clean and sanitize the facepiece assembly after removing the communication system, the microphone and signal light. Use MSA Cleaner-Sanitizer (Part No. 34337).
   - (a) Make a solution with the contents of one package added to water, following the instructions on the cleaner-sanitizer carton.
   - (b) Immerse facepiece and tube in the solution and scrub gently until clean.
   - (c) Rinse in clear warm water and shake to air dry.

   CAUTION: Cleaning and sanitizing at the recommended 120° F. temperature will avoid possible shrinkage and distortion of parts of the respirator assembly which would necessitate replacement.
5. Place apparatus in case. Cover assembly face up. Cylinder to rest in the slots provided at the bottom of the case and cylinder valve to rest snugly against the cushion provided at the side of the case. Place the regulator against the side of the case and use the strap to hold in position. Arrange the facepiece assembly along the face side of the case.
6. Store in a cool dry place where possible.

REPAIR

Replacement or repairs shall be done only by qualified persons using parts designed for the breathing apparatus. No attempt should be made to make adjustments or repairs beyond the manufacturer's recommendations. Regulators shall be returned to MSA or to a trained technician for adjustment or repair. Parts shall not be interchanged among devices of different manufacturers.

BATTERY INSTRUCTIONS

For all purpose use use the 1.5 volt D size alkaline manganese type batteries such as:

Eveready - E 95 Burgess - AL2 Mallory - MN 1300

This type of battery will provide service for up to 9.0 hours under conditions of usage.

Manufactured by
MINE SAFETY APPLIANCES COMPANY
PITTSBURGH, PENNSYLVANIA, U.S.A., 15230

MICROCOMPUTER ADAPTATION OF A TECHNICAL MANUAL

David W. Hyde
US Army Engineer Waterways Experiment Station
Vicksburg, Mississippi 39180

ABSTRACT

The Tri-Service Manual "Structures to Resist the Effects of Accidental Explosions", has recently been revised and published. The latest version of this technical manual contains updated information on a variety of explosion effects and structural response. The manual has been adopted for microcomputer usage by the Structural Mechanics Division, Structures Laboratory, US Army Waterways Experiment Station, in the form of a microcomputer program presented by this paper. This program allows the user to display the text of the manual on a microcomputer monitor, search for key words and phrases, display the figures from the manual on a monitor, produce hard copies on a plotter, retrieve data points from curves, and compare test data to the theoretical curves from the manual. At present, it performs a variety of response calculations and will in the future perform all structural response and explosion effects calculations found in the manual.

1975

MICROCOMPUTER ADAPTATION OF A TECHNICAL MANUAL

David W. Hyde
US Army Engineer Waterways Experiment Station
Vicksburg Mississippi 39180

Introduction

The U.S. Army Armament Research, Development and Engineering Center (ARDEC) has recently completed a revision of the Tri-Service Manual "Structures to Resist the Effects of Accidental Explosions". Pending approval of this draft revision as a Tri-Service Manual, the six-volume set has been published as Special Publication ARLCD-SP-84001 by ARDEC (Reference 1). To avoid confusion, this manual will be referred to by its Army designation, TM 5-1300, throughout this text. The latest version of this technical manual contains updated information on a variety of explosion effects and structural response. The manual has been adopted for microcomputer usage by the Structural Mechanics Division, Structures Laboratory, U.S. Army Engineer Waterways Experiment Station (WES), in the form of the computer program presented here -- TMREAD.

TMREAD allows the user to display the text of the manual on a microcomputer monitor and search for key words and phrases. It also allows the user to display the figures from the manual on a monitor, produce hard copies on a plotter, retrieve data points from curves, and compare test data to the theoretical curves from the manual.

Displaying Text

TMREAD is a menu-driven program written for commonly available desktop computers using the Disk Operating System (DOS). From the program's main menu, the user may select to: read or print the table of contents, appendices, or body of any of Volumes 1-6 from TM 5-1300; select a subject from an index; cross-reference a list of tables and figures against a user-selected list of key words; or display the figures of the manual.

While displaying text from TM 5-1300, all of the functions of TMREAD are controlled by the PC's cursor control keys and function keys. The cursor control keys are used to scroll up or down one line or one screen at a time. Scrolling may be repeated rapidly by holding down the cursor control keys. In addition, the function keys enable the user to search either forward or backward through the text for a key word or phrase. The search is not case sensitive. The user may also place a temporary "bookmark" at one place in a passage of text for later return. With the proper hardware, the user may also: change the current screen colors; switch to 43 lines of text per screen (rather than the normal 25); and speed up the keyboard response for faster scrolling.

Displaying Figures

Data for most of the figures from the manual is stored in separate files. The data files for illustrations contain drawing instructions recognized by TMREAD (see Figures 1 and 2), while the files for figures consisting of curves (Figure 3) contain either the data points necessary to recreate the curves, or the coefficients and exponents of polynomial equations used to generate the curves. In the latter case, TMREAD will generate 200 equally spaced data points for each curve in the figure. Figures may be reproduced on most commonly available microcomputer graphics adapter/monitor combinations and on pen plotters supporting the Hewlett-Packard Graphics Language.

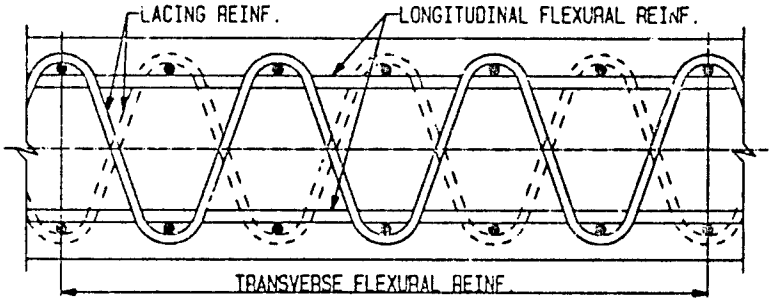

Figure 1. Illustration of lacing reinforcement (Fig. 4-3, Ref. 1)

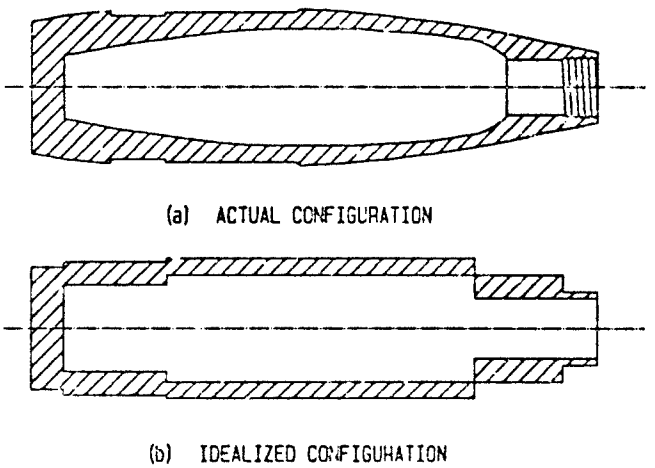

Figure 2. Equivalent cylindrical explosive casings (Fig. 2-242, Ref. 1)

If the selected figure consists of a curve or a set of curves (rather than an illustration), the user has the options of retrieving data points from a curve, zooming in on a portion of a curve, or comparing data from other sources to curves from TM 5-1300. An example of the zoom feature is shown in Figures 3 and 4. The data retrieval function returns a Y value which is interpolated from the data points for each figure. The accuracy of this function is dependent on the spacing between data points, not on the resolution of the display monitor.

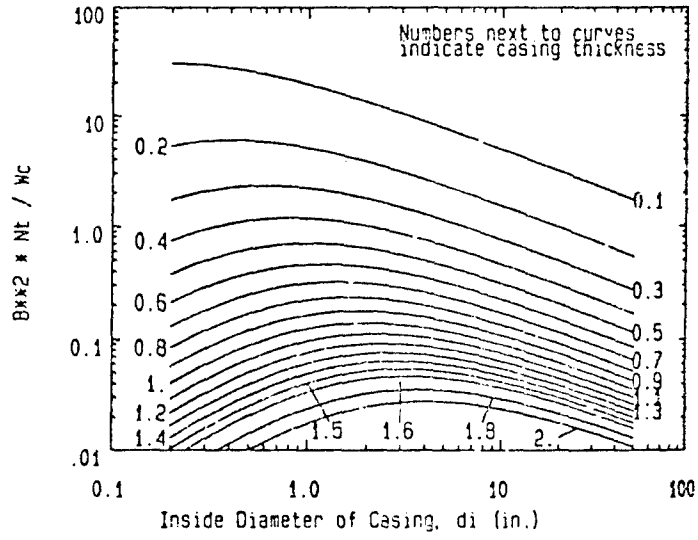

Figure 3. Fragment size parameters (Fig. 2-241, Ref. 1)

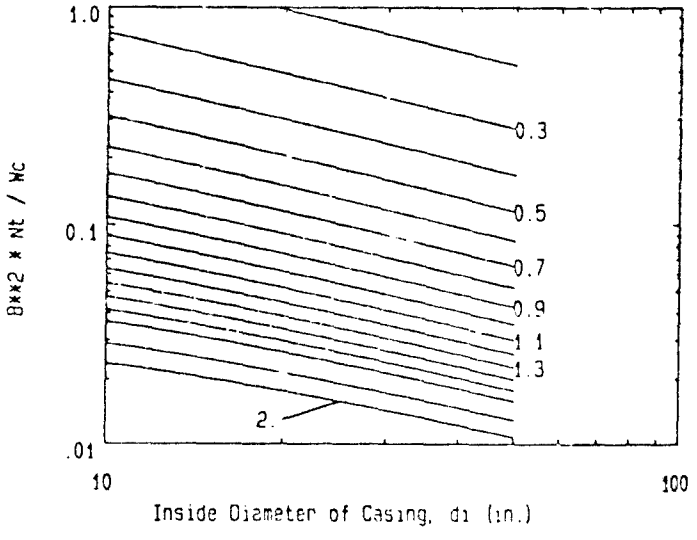

Figure 4. Zoomed Figure 2-241, Ref. 1

While data for most of the curves from the manual are stored in separate files, this was not a practical solution for recreating the response charts found in Volume 3 of the manual. Volume 3 contains over 200 response charts for maximum displacement, time of maximum response, and time of yield for a single-degree-of-freedom system with a bilinear resistance function due to a bilinear loading. Since a closed-form solution for the response of these systems is mathematically awkward, a numerical method is generally used to find the displacement-time history. To adequately reproduce each of these figures with data points would require a large amount of storage space; however, since the numerical solution for the response is fairly straightforward, TMREAD generates the response charts at run-time rather than reading the data from separate files. One advantage to this technique is that the user will not have to interpolate between charts when his loading does not match one of the loadings in the printed manual; all parameters for the loading are specified by the user. An example of a maximum response chart generated by TMREAD is shown in Figure 5.

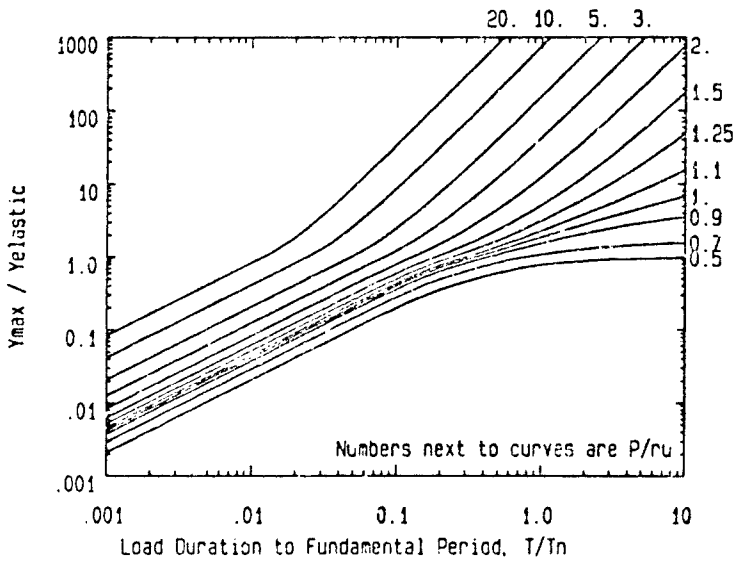

Figure 5. Response chart for bilinear pressure-time loading

Portability

The major routines of TMREAD are written in ANSI standard FORTRAN-77. However, the program makes considerable use of assembly language subroutines to perform graphics operations, scroll menus, and achieve fast screen writing. TMREAD achieves fast screen output by writing directly to display memory, bypassing the slower Basic Input/Output System (BIOS) video functions. Because of extensive use of assembler routines for menu

generation and other video output, it would be difficult at best to move TMREAD to another computer and/or operating system.

Graphics

All of the graphics routines used by TMREAD were developed for microcomputers at WES. TMREAD supports graphics on the following graphics adapter/monitor combinations:

Graphics Card/Monitor	Video Mode	Resolution/Colors
Color Graphics Adapter w/ Color Display	6	640x200x2
Enhanced Graphics Adapter w/ Monochrome Display	15	640x350x4
Enhanced Graphics Adapter w/ Color Display	14	640x200x16
Enhanced Graphics Adapter w/ Enhanced Display, 64 KB video memory installed	14	640x200x16
Enhanced Graphics Adapter w/ Enhanced Display, >64 KB video memory installed	16	640x350x16/64
24 MHz-capable EGA w/ Multisync Monitor	16	640x480x16/64
Video Graphics Array w/ Analog Monitor	19	640x480x16/256K

Plotters that support the Hewlett-Packard Graphics Language are also supported.

Availability

TMREAD is currently in a draft stage and is being reviewed by the sponsors at the Department of Defense Explosive Safety Board (DDESB). When approved for release, the program will be available to government agencies on the WES microcomputer bulletin board, at phone no. (601) 634-3053, or from the DDESB.

REFERENCES

1. U.S. Army Armament Research, Development and Engineering Command, 1987, "Structures to Resist the Effects of Accidental Explosions," Picatinny Arsenal, New Jersey.

HIGH EXPLOSIVE DAMAGE ASSESSMENT USING A MICROCOMPUTER

Julian S. Hamilton, Jr., P.E.[1]

ABSTRACT

Siting of explosive storage and manufacturing facilities is governed by quantity-distance criteria administered by the Department of Defense Explosive Safety Board (DDESB). These criteria are based on personnel exposure risks, as well as acceptable damage to facilities and other assets. This paper discusses a High Explosive Damage Assessment Code (HEXDAM) being developed to operate on a basic microcomputer system that would allow rapid evaluation of blast overpressure effects resulting from changes in explosive quantities or siting relationships. This program is expected to provide a valuable tool for safety offices in monitoring activities and for designers in site layouts. This paper discusses the origin of the code and the status of its development as a damage assessment tool.

CURRENT SITING METHODS

Current methods of explosive safety siting rely on calculated incident overpressures from explosions and established criteria given in publications such as DoD 6055.9-STD (DDESB, 1983). Table 1 gives a summary of these criteria.

Actual application of these criteria to a given ammunition plant or other facility can be time consumming and tedious. The HEXDAM software discussed in this paper could be a significant time-saver for planners and engineers by allowing them to develop facility "models" on a computer and then to use the computer to analyze the models for damage due to explosive events.

DEVELOPMENT OF ENDAM3, PREDECESSOR OF HEXDAM

Background

In 1986, the U.S. Army Strategic Defense Command developed a computer code named ENDAM3 at an approximate cost of $300,000 (Tatom, Spencer, and Roberts, October 1986). The ENDAM3 code (written in FORTRAN 77 and PASCAL programming languages) is the property of the U. S. Government and was planned as a tool for making nuclear blast damage assessments over areas such as cities or military installations.

---

1. Structural Engineer, U.S. Army Corps of Engineers, Huntsville Division, Huntsville, Alabama.

Application

Since the basic airblast equations of the code can also reasonably predict the effects of conventional explosives, it also had potential for damage assessment in support of safety siting evaluations. ENDAM3, with the proper modifications, could allow engineering and planning personnel (at both the installation level and at higher levels) to interactively create computer "models" of an entire installation by entering data on every structure of interest. This data includes the structure location, structure size, structure type, and the quantity of explosives a structure stores or contains (if any).

When used in this way, a properly modified version of ENDAM3 could provide a means of evaluating explosive damage between existing structures as well as between existing and planned structures. Any number of scenarios could rapidly be studied using this tool; therefore, it had obvious potential for siting applications and in the explosive safety approval process.

DEVELOPMENT OF HEXDAM

The Huntsville Division Corps of Engineers (CEHND) decided to modify the ENDAM3 code in phases over a period of several years. This allows evaluation and testing of the code after each phase is complete so that the modifications of subsequent phases can be judiciously selected based on actual code use.

Phase 1 Modifications (FY 87)

ENDAM3 runs only on a Hewlett-Packard 9816 computer, has extensive graphics capabilities and can accept input from a digitizing board as well as from the keyboard. These features require hardware that might not be commonly found in a facility engineering or safety office and were identified as the major limitations for widespread application for explosive safety damage assessment. Specific Phase 1 modifications made to ENDAM3 are given below.

The Office of the Chief of Engineers provided funding to CEHND through the Facility Army System Safety (FASS) program to accomplish Phase 1 modifications to ENDAM3. The modified code was named HEXDAM and was completed in September 1987 at an approximate cost of $25,000.

Software Conversion. Since the IBM-PC has become a standard platform for engineering applications, the ENDAM3 software was modified to run on an IBM-PC/XT/AT (or equivalent) computer.

Reduction of Graphics/Hardware Requirements. To assure the software be usable by installation engineering, planning, and safety offices, the hardware requirements for HEXDAM were kept to a minimum. The required computer is an IBM-PC/XT/AT or compatible with 512 kilobytes of random access memory (RAM), a monochrome graphics card, a monochrome monitor, and a dot matrix printer.

This computer equipment is readily available at an estimated cost of $1500 to $2000. Many installations and safety offices already have such a system or could easily upgrade their existing system.

Weapon Conversion. ENDAM3 simulates airblast damage due to nuclear weapons. Widely accepted overpressure curves are used to predict static and dynamic overpressure at a given distance from a known quantity of explosive. These curves are applicable for both nuclear weapons and conventional weapons. However, the nuclear weapon yield (e.g., 1-kiloton) must be reduced in order to account for the equivalent actual tonnage of TNT that produces the same blast damage. This is because part of the energy of a nuclear weapon yield is released as thermal energy and radiation. This yield-reduction modification was also implemented and consequently, the HEXDAM code properly predicts blast effects from conventional weapons.

Planned Phase 2 Modifications (FY 88)

Several modifications have been identified that would make the code more useful for explosive damage assessment for safety planning. The details on these modifications will be given in another paper presented at this seminar (Tatom, 1988). These modifications are summarized below:

Overpressure/Damage Level/"K-Factor" Entry. The code presently lacks the ability to enter the overpressures and "K-Factors" at which moderate and severe damages occur for each structure (Note: the K-factor is equivalent to a pulse-duration factor that adjusts damages based on the duration of the blast wave as a function of explosive yield). This feature needs to be added so that damage to each structure can be entered based on actual incidents as well as experience, judgement, calculations, research, etc.

Automatic Subdividing of Buildings. If a structure is relatively large (or long and narrow) and the damaging explosion is small to moderate in size and fairly close to the structure, then the parts of the structure closest to the explosion will obviously sustain more damage than those parts that are farther away. However, the code presently can predict a percent damage to the entire structure only. A building in this category can be better modeled by manually subdividing the large building into a group of smaller, adjacent buildings that form the same footprint as the large building. This is very time consuming. Automation of this task would greatly speedup data entry for buildings in this category.

"Zoom" graphics. The ability to zoom-in when viewing the layouts of structures on the computer screen would enhance the usefulness of the code by letting the user view only the structures inside the field of his immediate interest and excluding all others from view.

Later Phase(s)

Pending funding, additional modifications to the software could include further improving the graphics outputs and creating a standard database of

structure damage information that would be acceptable to the safety community for use at installations.

HEXDAM OVERVIEW

A Users Manual has been prepared for HEXDAM giving detailed operating instructions (Tatom and Roberts, 1987); therefore, only a summary of HEXDAM operation is given in this paper.

HEXDAM consists of three separate elements (modules): a preprocessor, HEXDAM1; a processor, HEXDAM2; and a postprocessor, HEXDAM3 (Tatom, 1987). Figure 1 is a functional flow diagram of the code. Each part executes individually from the others. All of the data necessary for HEXDAM is input in the preprocessor, which creates and output file (TPRO) that is fed into the processor. Upon execution of the processor, output files (TPST and TPST2) are created that are fed into the postprocessor, which generates the output data in the form of graphs, displays, and tables.

Capabilities/Limitations

HEXDAM is a flexible, rapid tool for making blast damage assessments resulting from an explosion on a localized area. Specific capabilities include:

1. Prediction of blast damages to 178 different user-selectable structures ranging from administration buildings and ships to ammunition igloos and railroad cars. A complete listing of these structures is given in Table 2 (Tatom and Roberts, 1987).

2. Prediction of shielding effects by each structure (a barricade for example) on nearby structures .

3. Prediction of blast damage resulting from secondary explosion(s) triggered by the initial (i.e., primary) blast.

It should be noted that items 2 and 3 above are significant features of HEXDAM in the realistic modelling of actual plant facilities.

HEXDAM has several limitations, primarily due to the amount of computer memory (RAM) available. The following restrictions apply:

- There can be a maximum of 100 structures.
- Blast effects only are considered.
- No terrain considerations, i.e., the code assumes that all structures are at the same elevation.
- Altitude effects on explosions must be accounted for manually.

Equipment Specification

The execution of HEXDAM requires the hardware equipment, operating system, and memory listed in Table 3 (Tatom and Roberts, 1987). All equipment listed is essential to the correct execution of the program.

HEXDAM OPERATION

Sample Scenario

For purposes of illustrating operation of HEXDAM, a site will be used to provide the necessary input to HEXDAM for program operation. The site selected for this scenario is the proposed Chemical Demilitarization plant at Tooele Army Depot, Tooele, Utah. Upon completion, this plant will demilitarize toxic chemical agent munitions that are stored at the Depot. The final layout of the buildings is still being studied; the layout used for this scenario is dated August 1987 and is shown in Figure 2.

The explosive weight for this scenario is 10,000 pounds of TNT located in the unpack area of building #6 which is the Munitions Demilitarization Building (MDB). (Note: the actual quantity of explosives allowed in the MDB will be limited to 2,500 pounds; however, for illustration purposes, the larger quatitiy of 10,000 pounds has been used.)

Preprocessor (HEXDAM1)

The user keys in "HEXDAM1" to begin execution of the preprocessor. Data required for the execution of HEXDAM are input by keyboard to the preprocessor by the user or else by the use of built-in defaults. The preprocessor is designed to be very user-friendly. The user makes his initial selection from a list of options on the PREPROCESSOR MAIN CONTROL MENU (see Figure 3).

Execution Control Parameters Menu. Option 1 on the control menu allows the display of the EXECUTION CONTROL PARAMETERS MENU. This data menu (which is presented in Figure 4) displays all data set to their default values and allows the user to reset the data to his desired values if he does not wish to use the defaults. The values assigned to the parameters in the EXECUTION CONTROL PARAMETERS MENU, along with the description of structures loaded into the structure data files discussed below, govern the execution of the HEXDAM code for a given case.

Structure Data Files. HEXDAM involves two structure data files: the Master Structure Data File (TSTR) and the Structure Specification Data File (SSDF) which is created by the user.

TSTR contains data for 178 types of structures, including default values for structure characteristics such as length, width, height, angle of rotation, level of damage above which secondary explosion occurs, and yield of secondary explosion. The listing of these pre-programmed structures is given in Table 2.

The user-defined SSDF contains a description of the specific structures to be included in a given scenario. This file is created from the PREPROCESSOR MAIN CONTROL MENU (Figure 3) using Option 3 or else up-dated using Option 4. A sample SSDF is given in Figure 5.

Pressure Data. The only other input data are the incident and dynamic pressure-versus-distance curves which are automatically input in the form of two pre-programmed data files (OP.DAT and DP.DAT).

Preprocessor Output. The primary output from the preprocessor is the TPRO file which is used as an input for the processor without any action on the part of the user. In addition, after preprocessing of data is complete, the "before damage" plan view display is generated. This display, as shown in Figure 6, gives a representation of the location, size and orientation of each structure with respect to the source of explosion. (Note: a two-number structure label is printed directly below each structure; the first number is a sequential identification number and the second number corresponds to the structure type as selected from the Master Structure Specification Data File - see Table 2.)

Processor (HEXDAM2)

The only inputs to the processor are in the form of data files, one of which (TPRO) is created by the preprocessor. TPRO must be accessible to the processor at the time of its execution. Two other files, discussed in the "Pressure Data" paragraph above, are loaded as part of the preprocessor input and must be accessible to the processor when it is executed. No action is required by the user except to key in "HEXDAM2" which begins execution of the processor.

As the processor executes, it outputs diagnostic information and generates data files that are passed to the postprocessor (TPST and TPST2).

Postprocessor (HEXDAM3)

The TPST and TPST2 data files are created by the processor and contain the results of program execution. These files are also the inputs for the postprocessor and must be made available to the postprocessor at the time of its execution. No action is required by the user except to key in "HEXDAM3" which begins execution of the postprocessor.

Output from the postprocessor is in the form of hard-copy tabular data, line graphs and graphics displays that can be sent to the printer. Any of these outputs can be generated when selected from the POSTPROCESSOR MAIN CONTROL MENU (see Figure 7).

Hard-Copy Tabular Data. Damage values are generated for each structure. A portion of this tabular data is given in Table 4. Note that both the resultant incident overpressure and dynamic overpressure are tabulated for each structure. Note also that the occurrence of secondary explosions is flagged.

"After-Damage" Plan View Displays. The after-damage plan view display resembles the "before-damage" display except that the percent damage to each structure is indicated alongside the structure symbol. Figure 8 is an example of this after-damage display; the structures listed in Table 4 are shown in Figure 8.

Graphs. The graphs of damage level versus distance from ground zero graphically depict the damage incurred by the structures in relation to their distances from the burst point. Figure 9 is a plot of one of these graphs.

CONCLUSION

Proper explosive safety siting is a critical issue. As ammunition plants and depots are expanded, the shortage real estate for new facilities sometimes complicates the safety siting process. The HEXDAM computer code, properly developed, can be a useful tool in the site safety planning process.

REFERENCES

1. Department of Defense Explosive Safety Board, DoD 6055.9-STD, Washington, D.C., 25 November 1983.

2. Tatom, Dr. Frank B., Spencer, Bruce L., and Roberts, Mark D., Engineering Analysis, Inc., ENDAM3 Users Manual, Huntsville, Alabama, October 1986.

3. Tatom, Dr. Frank B. and Roberts, Mark D., Engineering Analysis, Inc., High Explosive Damage Assessment Model (HEXDAM) Users Manual, Huntsville, Alabama, September 1987.

4. Tatom, Dr. Frank B. and Roberts, Mark D., Engineering Analysis, Inc., 1988 Department of Defense Explosive Safety Seminar, Refinements to the High Explosive Damage Assessment Model (HEXDAM), Atlanta, Georgia, August 1988.

Table 1 EXPECTED EFFECTS - CLASS/DIVISION 1.1 EXPLOSIVES

DISTANCE DESIGNATION	INCIDENT PRESSURE	SCALED DISTANCE	UNSTRENGHTENED BUILDING DAMAGE	PERSONNEL INJURY	TRANSPORT VEHICLE DAMAGE	SHIP DAMAGE	AIRCRAFT DAMAGE
Barricaded Aboveground Magazine Distance	27 psi	$6W^{0.33}$	100%	DEATH	OVERTURNED & CRUSHED	SEVERE	100%
Barricaded Intraline Distance	12 psi	$9W^{0.33}$	NEARLY 100%	SEVERE OR DEATH	NEARLY 100%	SEVERE	NEARLY 100%
Unbarricaded Aboveground Magazine Distance	8 psi	$11W^{0.33}$	NEARLY 100%	SERIOUS- 20% CHANCE OF EARDRUM RUPTURE	SEVERE	EXTENSIVE	HEAVY
Unbarricaded Intraline Distance	3.5 psi	$18W^{0.33}$	50%	SERIOUS	MODERATE	DOORS & BULK-HEADS BUCKLED	CONSIDERABLE STRUCTURAL
Public Traffic Route Distance (<100,000 lbs HE)	2.3 psi	$24W^{0.33}$	20%	SOME INJURIES DUE TO DEBRIS	LITTLE	MINOR	ONLY MINOR REPAIRS NEEDED
Public Traffic Route Distance	1.7 psi	$30W^{0.33}$	10%	SOME INJURIES DUE TO DEBRIS	NONE	NONE	MINOR DAMAGE- NO REPAIRS NEEDED
Inhabited Building Distance (>250,000 lbs HE)	1.2-0.9 psi	$40W^{0.33}$	5%	SOME INJURIES DUE TO DEBRIS	NONE	NONE	MINOR DAMAGE- NO REPAIRS NEEDED

Table 2 HEXDAM MASTER STRUCTURE SPECIFICATION DATA

STRUCTURE NUMBER	PRESSURE TYPE	STRUCTURE DESCRIPTION	STRUCTURE NUMBER	PRESSURE TYPE	STRUCTURE DESCRIPTION
1	Q	ABRASIVE INDUSTRY/TUNNEL KILN	2	Q	ABRASIVE INDUSTRY/VERTICAL KILN
3	Q	ABRASIVE INDUSTRY/AL. OX./S. CARB.	4	P	ACQUISITION RADARS/TOWER & ANTENNA (MOBILE)
5	Q	ACQUISITION RADARS/VAN (MOBILE)	6	P	ACQUISITION RADARS/ANTENNA (MOBILE)
7	Q	ACQUISITION RADARS/ANTENNA (MOBILE)	8	Q	AIRCRAFT INDUSTRY/MACH. SHOP
9	Q	AIRCRAFT INDUSTRY/ASSY BLDG	10	Q	ALUMINUM INDUSTRY/AUTOCLAVE BLDG
11	Q	ALUMINUM INDUSTRY/ROL.,FAB.,BLDGS	12	P	AMMUNITION DUMPS/ABOVEGROUND BLDG
13	Q	AMMUNITION DUMPS/ABOVEGROUND BLDG	14	P	AMMUNITION DUMPS/R.C. IGLOO
15	P	AMMUNITION DUMPS/COR. STEEL IGLOO	16	P	ANTI-FRICTION BEARING INDUSTRY/MFCT. BLDG
17	Q	ANTI-FRICTION BEARING INDUSTRY/MFCT. BLDG	18	P	BRIDGES/CONCRETE
19	Q	BRIDGES/CONCRETE	20	Q	BRIDGES/TIMBER
21	Q	BRIDGES/STEEL	22	Q	BRIDGES/MAS.SUS.,TR.ARCH
23	Q	BRIDGES/SUS. STEEL	24	Q	BRIDGES/SUS. RE. CNCR.
25	Q	BRIDGES/SUS. WOOD	26	Q	CALCIUM CARBIDE INDUSTRY/ELEC. FURN. BLDG
27	Q	CHEMICAL EQUIPMENT INDUSTRY/MFCT.,ASSY BLDGS	28	Q	CHEMICAL MANUFACTURING INDUSTRY/ELCTLT CELL BLDG
29	Q	CHEMICAL MANUFACTURING INDUSTRY/PROCESS BLDG	30	Q	CHEMICAL MANUFACTURING INDUSTRY/FURNACE BLDG
31	Q	CHEMICAL MANUFACTURING INDUSTRY/SYNTHESIS BLDG	32	Q	CHEMICAL MANUFACTURING INDUSTRY/CNV.,CNCNT. BLDG
33	P	CHEMICAL MANUFACTURING INDUSTRY/STRG TNK,GAS HLD	34	Q	CHEMICAL MANUFACTURING INDUSTRY/ABSORPTION TOWER
35	Q	CHEMICAL MANUFACTURING INDUSTRY/FLTR,FRN.,EV.BL.	36	Q	CHEMICAL MANUFACTURING INDUSTRY/ABS.,CRBD TOWER
37	Q	CHEMICAL MANUFACTURING INDUSTRY/CHMBR,CNVRTR BL.	38	Q	CHEMICAL MANUFACTURING INDUSTRY/FRCTN. TOWER
39	Q	CHEMICAL MANUFACTURING INDUSTRY/PRIN. PROC. AREA	40	Q	CHEMICAL WARFARE AGENT MANUFACTURING/PROCESS BLDG
41	Q	CITY COMPLEX/MISC BLDG	42	Q	CITY COMPLEX/ADMIN BLDG
43	Q	CITY COMPLEX/FACT,MFCT BLDG	44	Q	CITY COMPLEX/PROD,ASSY BLDG
45	Q	ELECTRIC POWER INDUSTRY/MAIN BLDG	46	P	ELECTRIC POWER INDUSTRY/BOILERS,STACKS
47	Q	ELECTRIC POWER INDUSTRY/TURBINE HOUSE	48	Q	ELECTRIC WIRE AND CABLE INDUSTRY/MAJ. PROC. BLDG
49	Q	ELECTRICAL EQUIPMENT INDUSTRY/CST.,FRG.,MCH.,B	50	P	ELECTRICAL EQUIPMENT INDUSTRY/MCH.,ASSY BLDGS
51	Q	ELECTRICAL EQUIPMENT INDUSTRY/MCH.,ASSY BLDGS	52	P	ELECTRONIC EQUIPMENT MANUFACTURING/MAJ. PROD. BLDG
53	Q	ELECTRONIC EQUIPMENT MANUFACTURING/MAJ. PROD. BLG	54	P	EXPLOSIVES LOADING/PR.,LD,FN.,AS.,B
55	Q	EXPLOSIVES LOADING/PR.,LD,FN.,AS.,B	56	Q	FERRO-ALLOYS INDUSTRY/ELECTRIC FURNACE BLDG
57	P	FIRE CONTROL RADARS/ANTENNA (MOBILE)	58	Q	FIRE CONTROL RADARS/VAN (MOBILE)
59	Q	FIRE CONTROL RADARS/ANTENNA (MOBILE)	60	P	FORTS AND CAMPS/ADMIN. BLDG
61	P	FORTS AND CAMPS/ST. HSE,RPR SHOP	62	Q	FORTS AND CAMPS/ST. HSE,RPR SHOP
63	P	GROUND CONTROLLED INTERCEPT RADARS/ANTENNA (FIXED)	64	Q	GROUND CONTROLLED INTERCEPT RADARS/VAN (MOBILE)
65	Q	GROUND CONTROLLED INTERCEPT RADARS/ANTENNA (MOBILE)	66	P	GROUND CONTROLLED INTERCEPT RADARS/ANTENNA (MOBILE)
67	Q	GUIDANCE RADARS/ANTENNA (FIXED)	68	P	GUIDANCE RADARS/CONTROL BLDG

Table 2 HEXDAM MASTER STRUCTURE SPECIFICATION DATA (continued)

STRUCTURE NUMBER	PRESSURE TYPE	STRUCTURE DESCRIPTION	STRUCTURE NUMBER	PRESSURE TYPE	STRUCTURE DESCRIPTION
69	Q	GUIDANCE RADARS/RADAR STRUCTURE	70	Q	GUIDANCE RADARS/VAN (MOBILE)
71	Q	HEAVY MACHINERY INDUSTRY/CST.,FRG.,MCH.,B	72	P	HEIGHT FINDER RADARS/ANTENNA (MOBILE)
73	Q	HEIGHT FINDER RADARS/VAN (MOBILE)	74	Q	HEIGHT FINDER RADARS/ANTENNA (MOBILE)
75	Q	HEIGHT FINDER RADARS/ANTENNA (FIXED)	76	Q	IFF RADARS/ANTENNA (FIXED)
77	P	LOCKS AND DAMS/LOCK PLUS DAM	78	Q	LOCOMOTIVES INDUSTRY/CST.,FRG.,MCH.,B
79	Q	MACHINE TOOLS INDUSTRY/CST.,FRG.,MCH.,B	80	Q	MAGNESIUM INDUSTRY/SEP.,FLT. BLDGS
81	Q	MAGNESIUM INDUSTRY/REFINING FURNACE	82	Q	MAGNESIUM INDUSTRY/RED.,FAB. BLDGS
83	P	MILITARY AIR BASES/ADMIN. BLDG	84	Q	MILITARY AIR BASES/SHOPS,STRG BLDG
85	P	MILITARY AIR BASES/SHOPS,STRG BLDG	86	Q	MILITARY COMMUNICATIONS/LINE POLE
87	Q	MILITARY COMMUNICATIONS/TELEPHONE EQUIP.	88	Q	MILITARY COMMUNICATIONS/MICROWAVE TOWER
89	Q	MILITARY COMMUNICATIONS/RADIO EQUIP.,OUT	90	Q	MILITARY COMMUNICATIONS/RADIO EQUIP.,IN
91	Q	MILITARY HANGARS, AIRCRAFT /STL OR R.C. HNGR	92	P	MILITARY HANGARS, AIRCRAFT /WOOD TR. HANGAR
93	Q	MILITARY HANGARS, AIRCRAFT /MED.,HVY BOMBERS	94	Q	MILITARY HANGARS, AIRCRAFT /LIGHT BOMBER
95	Q	MILITARY HANGARS, AIRCRAFT /DELTA-WING	96	Q	MILITARY HANGARS, AIRCRAFT /RECIP. AIRCRAFT
97	P	MILITARY HANGARS, AIRCRAFT /HELOS	98	Q	MISSILES/EMPTY MISSILE
99	Q	MISSILES/LOADED MISSILE	100	Q	MISSILES/MISSILE VEHICLE
101	Q	MISSILES/OX. TANK TRAILER	102	Q	MISSILES/LIQUID FUEL TR.
103	Q	MISSILES/MIS.CAR,EMPTY M.	104	Q	MISSILES/MIS.CAR,LOED MI.
105	Q	MISSILES/LNCH CONT. CAR	106	Q	MISSILES/LOX CAR
107	Q	MISSILES/LIQUID FUEL CAR	108	Q	MISSILES/AUX. CAR
109	Q	MOTOR VEHICLES INDUSTRY/CST.,FRG.,MCH.,B	110	P	NAVAL INSTALLATIONS/ADMIN.,SUP. BLDG
111	P	NAVAL INSTALLATIONS/AD.,SUP.B.,BRCKS	112	P	NAVAL INSTALLATIONS/SUPPLY BLDG
113	Q	NAVAL INSTALLATIONS/SUPPLY BLDG	114	P	NAVAL INSTALLATIONS/BARRACKS
115	P	NAVAL VESSELS/A/C CARRIERS	116	P	NAVAL VESSELS/SUBMARINES
117	P	NAVAL VESSELS/CRUKS,TRNS.,LSTS	118	P	NAVAL VESSELS/DESTROYERS
119	Q	NON-FERROUS METALS INDUSTRY/ELCTRLTC CELL BL	120	Q	NON-FERROUS METALS INDUSTRY/REFINING BLDG
121	Q	NON-FERROUS METALS INDUSTRY/FURNACE BLDG	122	P	NON-FERROUS METALS INDUSTRY/PROD. BLDG
123	Q	NON-FERROUS METALS INDUSTRY/PRC.,SMLT,FRN.,B	124	Q	NUCLEAR MATERIALS INDUSTRY/RF.,RFCT.,FAB.,B
125	Q	NUCLEAR MATERIALS INDUSTRY/BUBBLE TOWER	126	Q	ORDNANCE INDUSTRY/CST.,FRG.,MCH.,B
127	Q	ORDNANCE INDUSTRY/FND.,FRG.,MCH.,B	128	Q	ORDNANCE INDUSTRY/MCH.,ASSY BLDGS
129	Q	PETROLEUM INDUSTRY/FRCTNTNG TOWER	130	Q	PETROLEUM INDUSTRY/PRIN. PROC. AREA
131	P	PETROLEUM INDUSTRY/STRG TNKS(FULL)	132	P	PETROLEUM INDUSTRY/STRG TNKS(EMPTY)
133	P	PHARMACEUTICALS INDUSTRY/PROD. BLDG	134	Q	PHARMACEUTICALS INDUSTRY/PROD. BLDG
135	Q	PHOTOGRAPHIC FILM INDUSTRY/PROCESS BLDG	136	P	PHOTOGRAPHIC FILM INDUSTRY/PROCESS BLDG

Table 2 HEXDAM MASTER STRUCTURE SPECIFICATION DATA (continued)

STRUCTURE NUMBER	PRESSURE TYPE	STRUCTURE DESCRIPTION	STRUCTURE NUMBER	PRESSURE TYPE	STRUCTURE DESCRIPTION
137	P	PORT FACILITIES/WHARVES,PIERS	138	Q	PORT FACILITIES/HAMMERHD CRANE
139	Q	PORT FACILITIES/PORTAL CRANE	140	Q	PORT FACILITIES/LOCOMOTIVE
141	P	PORT FACILITIES/STORAGE BLDG	142	Q	PORT FACILITIES/STORAGE BLDG
143	P	PROPELLANTS AND COMMERCIAL DYNAMITES IN/MNFCT. BLDG	144	Q	PROPELLANTS AND COMMERCIAL DYNAMITES IN/MNFCT. BLDG
145	Q	RAILROAD YARDS/EMPTY BOX CAR	146	Q	RAILROAD YARDS/LOADED BOX CAR
147	Q	RAILROAD YARDS/EMPTY TANK CAR	148	Q	RAILROAD YARDS/FULL TANK CAR
149	Q	RAILROAD YARDS/LOX CAR	150	Q	RAILROAD YARDS/LOCOMOTIVE
151	Q	RAILROAD YARDS/TOWER	152	Q	RAILROAD YARDS/RND HOUSES,SHOPS
153	P	RAILROAD YARDS/RND HOUSES,SHOPS	154	Q	RUBBER TIRE INDUSTRY/MNFCT. BLDG
155	Q	SHIPBUILDING INDUSTRY/MAJOR SHOPS (SM. VESSELS)	156	Q	SHIPBUILDING INDUSTRY/AS. AREA HVY CR. (SM. VESSELS)
157	Q	SHIPBUILDING INDUSTRY/LIGHT CRANES (SM. VESSELS)	158	Q	SHIPBUILDING INDUSTRY/MAJOR SHOPS (LG. VESSELS)
159	Q	SHIPBUILDING INDUSTRY/AS. AREA HVY CR. (LG. VESSELS)	160	Q	SHIPBUILDING INDUSTRY/LIGHT CRANES (LG. VESSELS)
161	Q	STEEL INDUSTRY/ENTIRE PLANT	162	Q	STEEL INDUSTRY/COKE OVEN
163	Q	STEEL INDUSTRY/COOLER,TOWER	164	Q	STEEL INDUSTRY/BLAST FURNACE
165	Q	STEEL INDUSTRY/FURNACE BLDG	166	Q	STEEL INDUSTRY/MILL BLDG
167	P	STORAGE BATTERIES INDUSTRY/PROD. BLDG	168	Q	STORAGE BATTERIES INDUSTRY/PROD. BLDG
169	P	SURVEILLANCE, E. M. RADARS/ANTENNA (MOBILE)	170	Q	SURVEILLANCE, E. M. RADARS/VAN (MOBILE)
171	P	SURVEILLANCE, E. M. RADARS/TOWER & ANTENNA (FIXED)	172	Q	SURVEILLANCE, E. M. RADARS/ANTENNA (FIXED)
173	Q	SURVEILLANCE, E. M. RADARS/ANTENNA (MOBILE)	174	P	SURVEILLANCE, E. M. RADARS/TOWER & ANTENNA (MOBILE)
175	Q	SYNTHETIC RUBBER INDUSTRY/PROC. BLDG	176	Q	SYNTHETIC RUBBER INDUSTRY/FRCTNTNG TOWER
177	Q	TELECOMMUNICATIONS INSTALLATIONS/HOUSING STRUCT.	178	P	TELECOMMUNICATIONS INSTALLATIONS/HOUSING STRUCT.

Table 3 HEXDAM EQUIPMENT REQUIREMENTS

ITEM	DESCRIPTION
CENTRAL PROCESSING UNIT	IBM PC/XT/AT OR COMPATIBLE
DISK DRIVE	1 FLOPPY DRIVE AND/OR 1 HARD DISK DRIVE
PRINTER*	(WITH GRAPHICS CAPABILITY)
MONITOR*	MONOCHROME OR COLOR
GRAPHICS CARD*	MONOCHROME, CGA, OR EGA
OPERATING SYSTEM	DOS 3.2 OR LATER
RAM	MINIMUM OF 512 KILOBYTES

*NOTE: SELECTION OF THESE ITEMS DEPENDS ON THE AVAILABILTIY OF AN APPROPRIATE DEVICE DRIVER.

Table 4 STRUCTURE DAMAGE TABLE

08/07/88 14:44
STRUCTURE SPECIFICATION DATA FILE: TEAD.DAT
YIELD= 10000.00000 POUNDS
HEIGHT OF BURST= 20.00 FEET

Structure 1-14	
PERCENT DAMAGE	0.00
OVERPRESSURE (PSI)	1.92
DYNAMIC PRESSURE (PSI)	0.00
Structure 2-29	
PERCENT DAMAGE	0.00
OVERPRESSURE (PSI)	1.05
DYNAMIC PRESSURE (PSI)	0.00
Structure 3-83	
PERCENT DAMAGE	0.00
OVERPRESSURE (PSI)	4.12
DYNAMIC PRESSURE (PSI)	0.02
Structure 4-85	
PERCENT DAMAGE	100.00
OVERPRESSURE (PSI)	11.16
DYNAMIC PRESSURE (PSI)	5.99
Structure 5-40	
PERCENT DAMAGE	0.00
OVERPRESSURE (PSI)	11.29
DYNAMIC PRESSURE (PSI)	1.09
Structure 6-40	
PERCENT DAMAGE	99.15
OVERPRESSURE (PSI)	200.00
DYNAMIC PRESSURE (PSI)	200.00
Structure 7-83	
PERCENT DAMAGE	0.00
OVERPRESSURE (PSI)	3.19
DYNAMIC PRESSURE (PSI)	19.86
Structure 8-68	
PERCENT DAMAGE	0.00
OVERPRESSURE (PSI)	62.74
DYNAMIC PRESSURE (PSI)	100.37
Structure 9-38	
PERCENT DAMAGE	0.00
OVERPRESSURE (PSI)	12.47
DYNAMIC PRESSURE (PSI)	2.49
Structure 10-129	
PERCENT DAMAGE	0.00
OVERPRESSURE (PSI)	1.08
DYNAMIC PRESSURE (PSI)	0.02

Structure 11-83	
PERCENT DAMAGE	0.00
OVERPRESSURE (PSI)	5.87
DYNAMIC PRESSURE (PSI)	0.19
Structure 12-129	
PERCENT DAMAGE	0.00
OVERPRESSURE (PSI)	8.79
DYNAMIC PRESSURE (PSI)	1.61
Structure 13-85	
PERCENT DAMAGE	87.16
OVERPRESSURE (PSI)	5.12
DYNAMIC PRESSURE (PSI)	0.01
Structure 14-85	
PERCENT DAMAGE	17.74
OVERPRESSURE (PSI)	2.72
DYNAMIC PRESSURE (PSI)	0.00
Structure 15-149	
PERCENT DAMAGE	0.00
OVERPRESSURE (PSI)	2.04
DYNAMIC PRESSURE (PSI)	0.00
Structure 16-60	
PERCENT DAMAGE	0.00
OVERPRESSURE (PSI)	1.65
DYNAMIC PRESSURE (PSI)	0.00
Structure 17-83	
PERCENT DAMAGE	0.00
OVERPRESSURE (PSI)	1.25
DYNAMIC PRESSURE (PSI)	0.00
Structure 18-83	
PERCENT DAMAGE	0.00
OVERPRESSURE (PSI)	7.15
DYNAMIC PRESSURE (PSI)	1.76
Structure 19-129	
PERCENT DAMAGE	0.00
OVERPRESSURE (PSI)	3.39
DYNAMIC PRESSURE (PSI)	0.00
Structure 20-83	
PERCENT DAMAGE	0.00
OVERPRESSURE (PSI)	5.35
DYNAMIC PRESSURE (PSI)	0.03

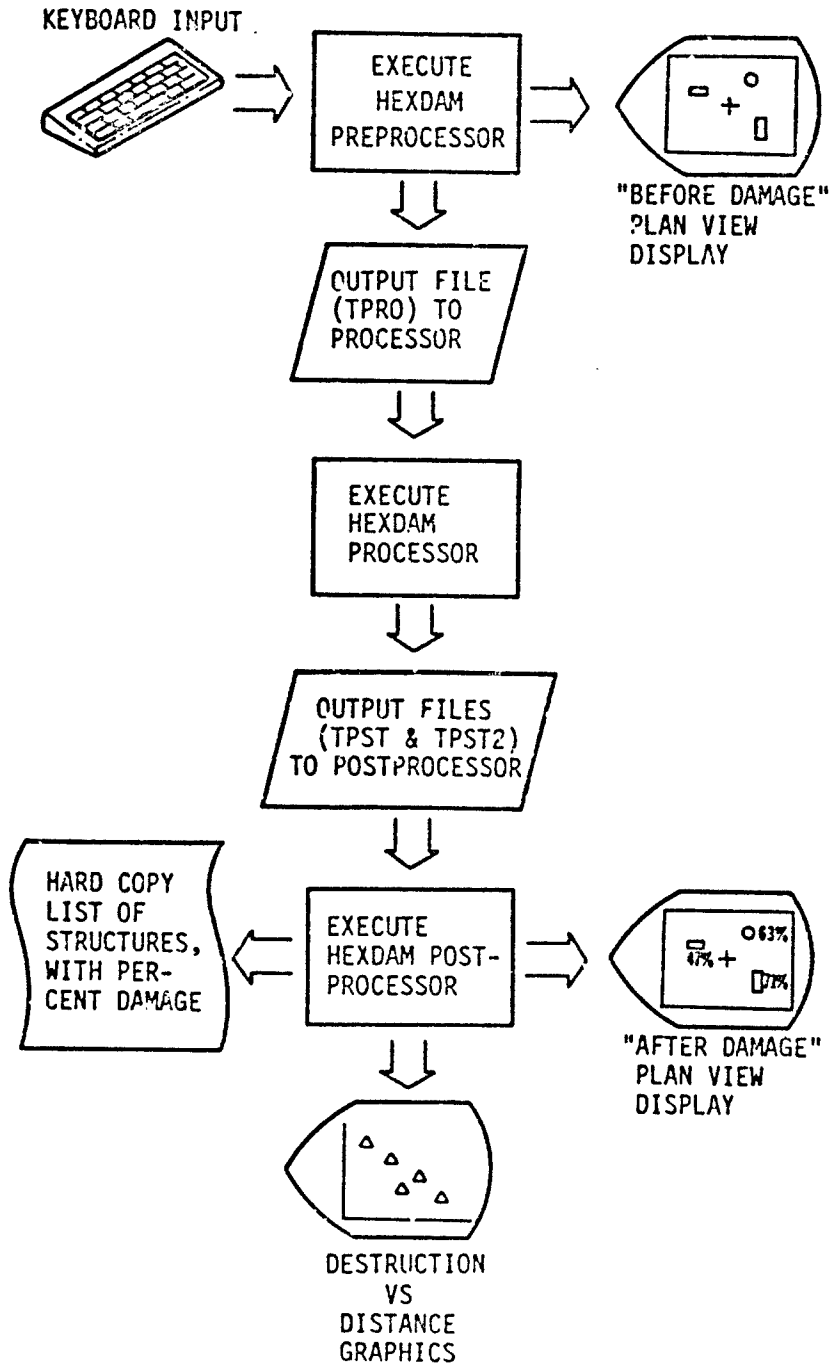

Figure 1 HEXDAM FUNCTIONAL FLOW DIAGRAM (TATOM and ROBERTS, 1987)

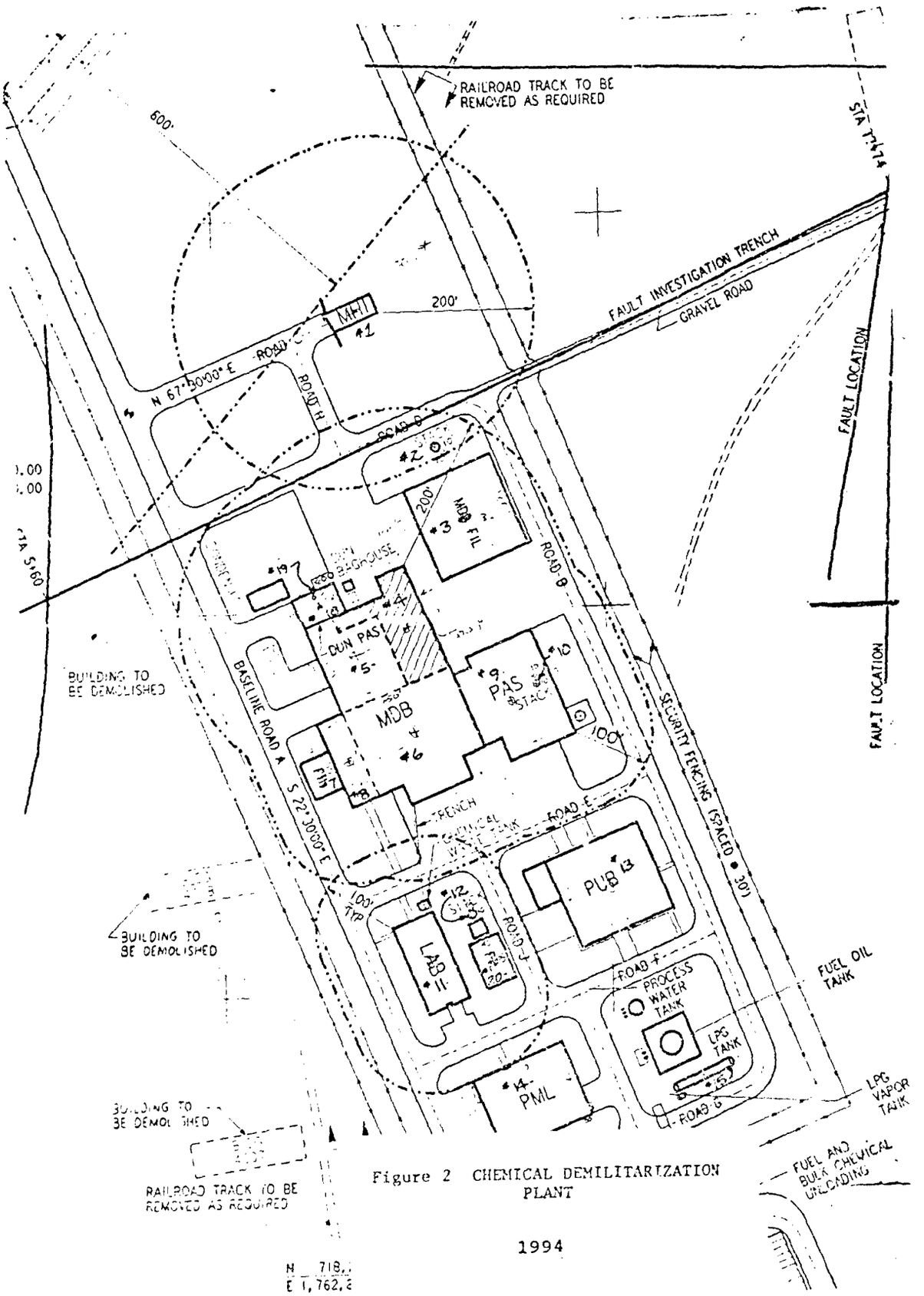

Figure 2 CHEMICAL DEMILITARIZATION PLANT

1994

M A I N C O N T R O L M E N U

H E X D A M P R E P R O C E S S O R

1 - Display EXECUTION CONTROL PARAMETERS MENU
2 - Select STRUCTURE SPECIFICATION DATA FILE
3 - Create STRUCTURE SPECIFICATION DATA FILE
4 - Modify STRUCTURE SPECIFICATION DATA FILE
5 - Print STRUCTURE SPECIFICATION DATA FILE
6 - Preprocess STRUCTURE SPECIFICATION DATA
7 - Print LIST OF STRUCTURE TYPES
8 - Exit HEXDAM PREPROCESSOR

Active structure specification data file: NONE

ENTER THE NUMBER OF THE PREPROCESSOR OPTION DESIRED:

Figure 3 MAIN CONTROL MENU - HEXDAM PREPROCESSOR

E X E C U T I O N C O N T R O L P A R A M E T E R S M E N U

H E X D A M P R E P R O C E S S O R

ITEM	DESCRIPTION(UNITS)	DEFAULT VALUE	CURRENT VALUE
1	SEVERE DAMAGE THRESHOLD (PERCENT)	75.00000	75.00000
2	MODERATE DAMAGE THRESHOLD (PERCENT)	30.00000	30.00000
3	SLIGHT DAMAGE THRESHOLD (PERCENT)	5.00000	5.00000
4	X COORDINATE OF DETONATION POINT	0.00000	1762750.00000
5	Y COORDINATE OF DETONATION POINT	0.00000	718820.00000
6	DETONATION HEIGHT (FEET)	0.00000	20.00000
7	YIELD UNITS (0-POUNDS,1-KILOTONS)	0.00000	0.00000
8	EXPLOSIVE YIELD (POUNDS)	100.00000	10000.00000

To change from default settings:
input item number <ENTER>
input new value <ENTER>

To print menu press "PRINT SCREEN" key.

Press "Q" <ENTER> when all changes are made.

Figure 4 EXECUTION CONTROL PARAMETERS MENU - HEXDAM PREPROCESSOR

08/07/88 14:44

STRUCTURE SPECIFICATION DATA FILE - TEAD.DAT

\HEXDAM\TEAD.DAT

ID									POUNDS
SN	TN	X	Y	L	W	H	AZ	DET.	YIELD
1	14	1762682.00	719380.00	60.00	30.00	15.00	22.50	0.00	0.00000
2	29	1762785.00	719205.00	10.00	10.00	20.00	22.50	0.00	0.00000
3	83	1762820.00	719115.00	120.00	120.00	40.00	22.50	0.00	0.00000
4	85	1762755.00	718980.00	60.00	120.00	30.00	22.50	0.00	0.00000
5	40	1762680.00	718945.00	90.00	120.00	20.00	22.50	0.00	0.00000
6	40	1762755.00	718840.00	150.00	120.00	20.00	22.50	0.00	0.00000
7	83	1762632.00	718786.00	30.00	50.00	40.00	22.50	0.00	0.00000
8	68	1762665.00	718805.00	25.00	120.00	20.00	22.50	0.00	0.00000
9	38	1762875.00	718878.00	100.00	150.00	40.00	22.50	0.00	0.00000
10	129	1762925.00	718900.00	10.00	10.00	100.00	22.50	0.00	0.00000
11	83	1762765.00	718540.00	50.00	120.00	20.00	22.50	0.00	0.00000
12	129	1762820.00	718600.00	10.00	10.00	100.00	22.50	0.00	0.00000
13	85	1763000.00	718635.00	130.00	120.00	30.00	22.50	0.00	0.00000
14	85	1762890.00	718365.00	120.00	100.00	30.00	22.50	0.00	0.00000
15	149	1763120.00	718390.00	90.00	10.00	10.00	22.50	0.00	0.00000
16	60	1762375.00	718165.00	50.00	25.00	10.00	22.50	0.00	0.00000
17	83	1763025.00	718040.00	60.00	100.00	40.00	22.50	0.00	0.00000
18	83	1762630.00	719010.00	60.00	40.00	20.00	22.50	0.00	0.00000
19	129	1762625.00	719035.00	5.00	5.00	100.00	22.50	0.00	0.00000
20	83	1762850.00	718540.00	40.00	60.00	10.00	22.50	0.00	0.00000

Figure 5 STRUCTURE SPECIFICATION DATA FILE

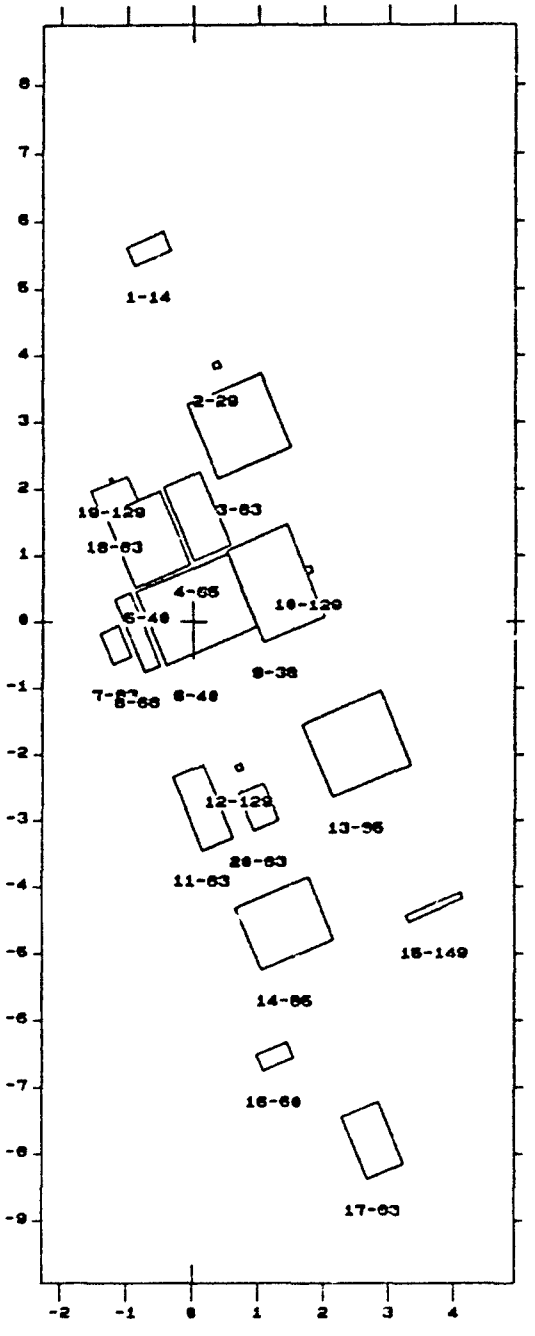

(Distances in 100's of ft)

PLAN VIEW PRIOR TO STRUCTURE DAMAGE (RELATIVE TO DETONATION POINT)

TEAD.DAT 08/07/88 14:44 YIELD= 10300 LB HEIGHT= 20.00 FEET

Figure 6 19"BEFORE DAMAGE" PLAN VIEW

1977

M A I N C O N T R O L M E N U

H E X D A M P O S T P R O C E S S O R

1 - Print DAMAGE TABLE
*2 - Generate PLAN VIEW DISPLAY
*3 - Generate DAMAGE VS DISTANCE GRAPH
4 - Exit PROGRAM

*DENOTES OPTIONS PREVIOUSLY SELECTED

Select on keyboard the option (1-4) desired and then press ENTER:

Figure 7 MAIN CONTROL MENU - HEXDAM POSTPROCESSOR

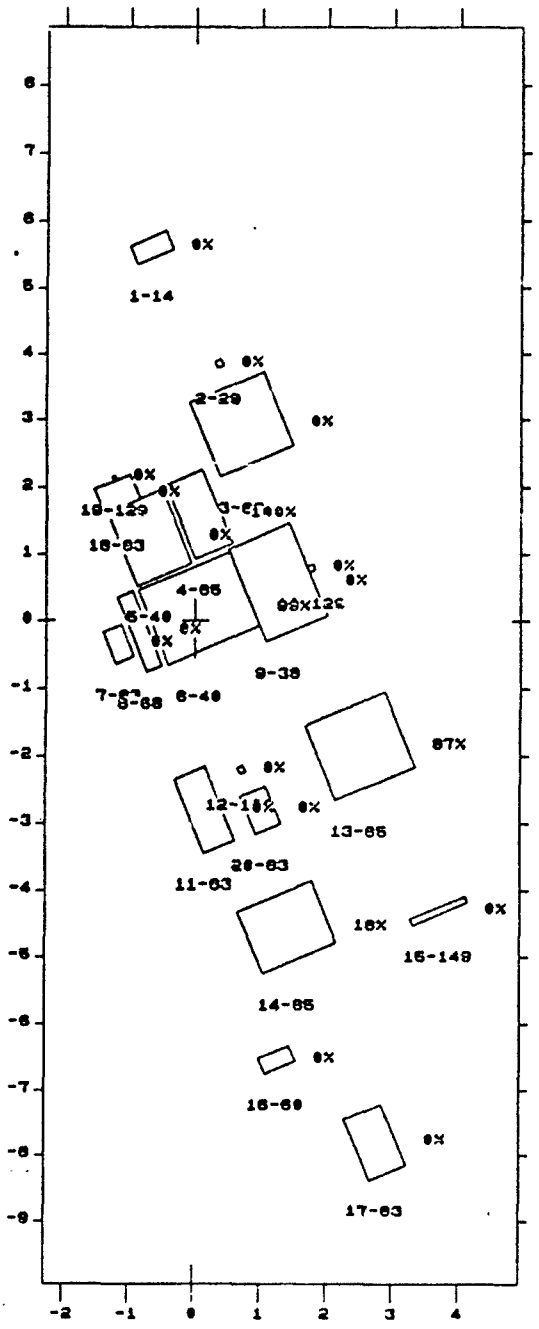

(Distances in 100's of ft - percentages represent mean percent damage)

PLAN VIEW AFTER STRUCTURE DAMAGE (RELATIVE TO DETONATION POINT)

TEAD.DAT 08/27/68 14:44 YIELD= 10000 LB HEIGHT= 20.00 FEET

Figure 8 "AFTER DAMAGE" PLAN VIEW

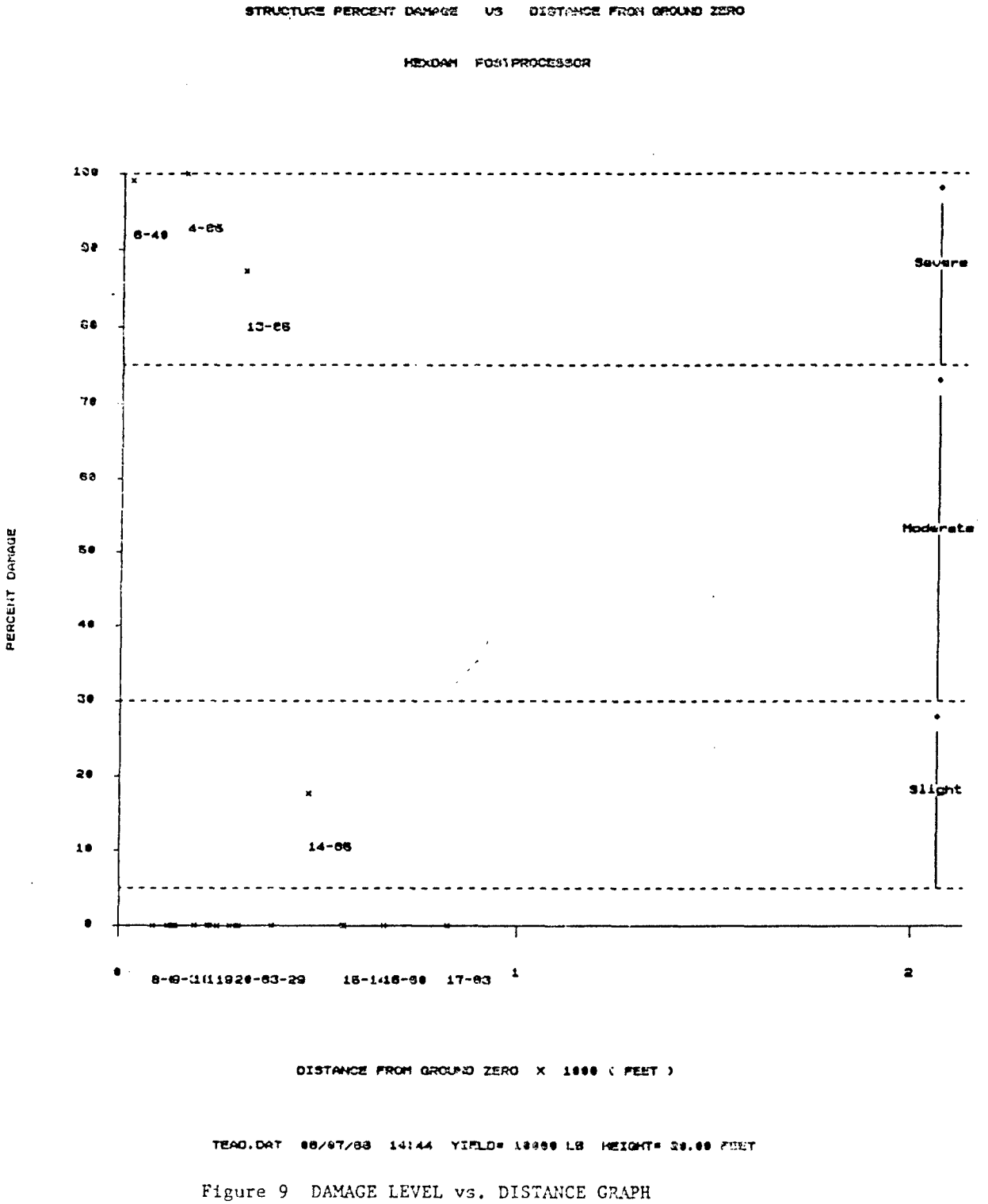

Figure 9 DAMAGE LEVEL vs. DISTANCE GRAPH

REFINEMENTS TO THE HIGH EXPLOSIVE DAMAGE ASSESSMENT MODEL (HEXDAM)

Frank B. Tatom
and
Mark D. Roberts

ENGINEERING ANALYSIS, INC.
Huntsville, Alabama

ABSTRACT

Based on results obtained from the initial evaluation of the High Explosive Damage Assessment Model (HEXDAM) by its users, a number of refinements to the model have been proposed. Such refinements include (1) automatic subdivision of structures, (2) user-specification of damage parameters for individual structures, (3) accounting for the height of tall or elevated structures, and (4) advanced graphics for video display. Certain of these refinements have been incorporated into a new version of the model, identified as HEXDAM-II. Preliminary results from HEXDAM-II demonstrate that such refinements can significantly increase the utility of the HEXDAM concept. Other refinements are scheduled to be incorporated into HEXDAM-III, which should further enhance the utility of the model.

1. INTRODUCTION

The High Explosive Damage Assessment Model (HEXDAM) was originally developed for the Huntsville Division of the U.S. Army Corps of Engineers [1]*, based on the Enhanced Nuclear Damage Assessment Model (ENDAM), which had been previously developed for the U.S. Army Strategic Defense Command [2]. ENDAM, in

*Numbers in brackets correspond to references cited in Section 5.

turn, was derived from the Nuclear Damage Assessment Model originally developed by Engineering Analysis, Inc. as part of a company-funded study [3]. HEXDAM is a useful tool (1) for making blast damage assessments for an explosion in a localized area, and (2) for explosive siting analysis. Based on experience derived from the initial application of HEXDAM [4], certain additional features have been identified which would increase the utility of the program. These features include:

(1) automatic horizontal subdivision of structures located near the point of detonation,

(2) user-specification of damage parameters for individual structures,

(3) accounting for the height of tall or elevated structures, including automatic vertical subdivision, and

(4) advanced graphics, including zoom capability, oblique projections, and contour plotting.

The first and second features, along with the zoom capability of the fourth, have recently been incorporated into HEXDAM-II which, like its predecessor, is designed for use on an IBM PC-XT/AT microcomputer. The third feature, combined with the oblique projection and contour plotting capabilities associated with the fourth feature, will be incorporated into the program in the near future to produce HEXDAM-III, which will also be designed for the IBM PC-XT/AT. Subsequent discussion deals with a detailed description of the existing capabilities of HEXDAM-II, along with the presentation of some preliminary results. A description of the proposed capabilities of HEXDAM-III is also provided.

2. SPECIAL FEATURES OF HEXDAM-II

Consistent with a need to keep equipment requirements as simple as possible, HEXDAM-II is designed for use on an IBM PC-XT/AT microcomputer. As noted previously, the three special features of HEXDAM-II are (1) automatic

horizontal subdivision of structures located near the detonation point, (2) user-specification of damage parameters for individual structures, and (3) zoom graphics capability. In addition, 200 structures can be modeled instead of 100. These features are described in the subsections which follow.

2.1 AUTOMATIC HORIZONTAL SUBDIVISION

In the original HEXDAM the geometric center of the base of a structure was used in calculating the distance from the detonation point, as shown in Figure 1. For situations involving structures whose length and/or width is of the same order of magnitude as the distance from the detonation point, the resulting damage level represents an average value, based on the pressure level computed at the geometric center of the base of the structure. The variation in damage to different portions of the building can be taken into account by subdividing the structure into smaller components, but this is somewhat time-consuming when done by the user using the original HEXDAM.

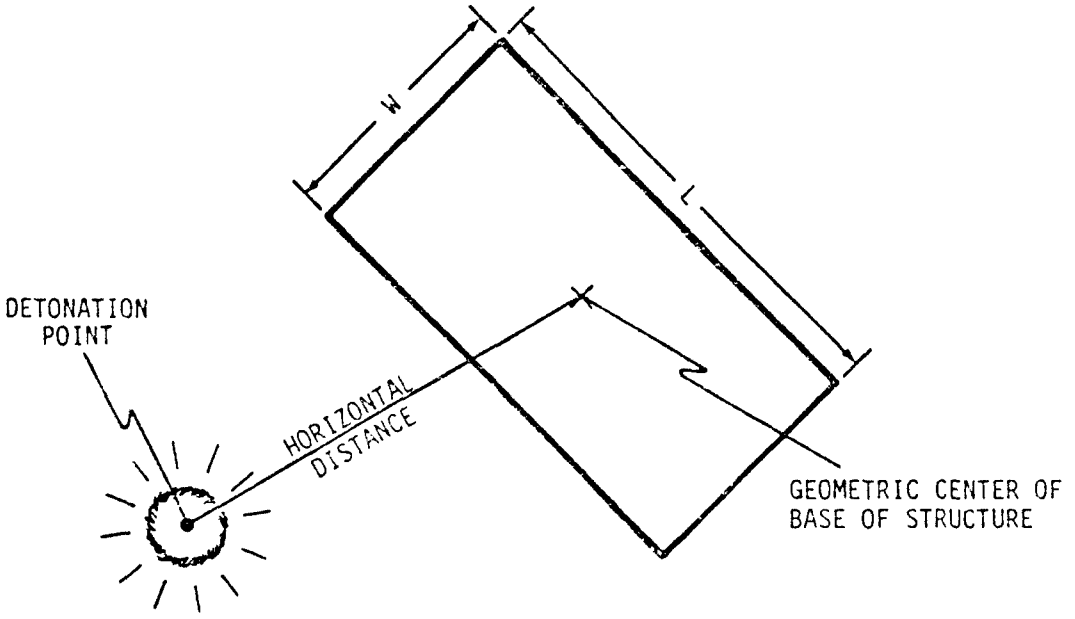

Figure 1. Calculation of Distance Between Detonation Point and Structure

The HEXDAM-II algorithm for the automatic horizontal subdivision of a structure provides for both longitudinal (with respect to length) and lateral (with respect to width) subdivision, as shown in Figure 2. Such subdivision is based on the length and width of the structure as compared with the distance to detonation point, taking into account orientation of the structure relative to the direction of blast propagation. The degree of subdivision is controlled by the horizontal distance fraction, a_h, with a magnitude between 0 and 1, which is user-specified. As the value of the distance fraction decreases, the degree of subdivision increases. In order to make the automatic subdivision feature more practical, the number of structures which can be modeled has been increased from 100 to 200.

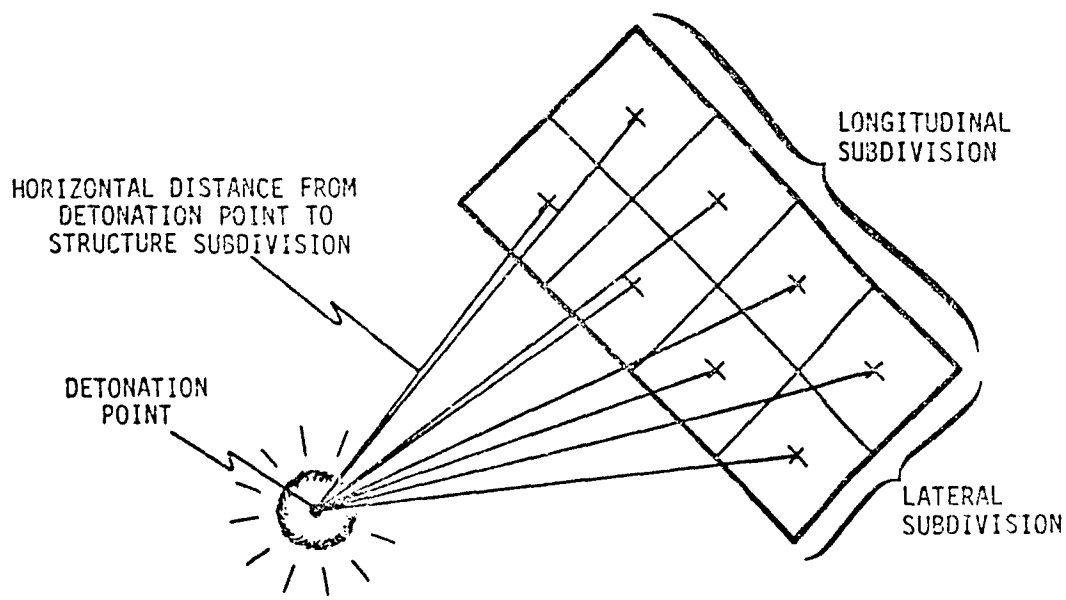

Figure 2. Longitudinal and Lateral Subdivision

An example of longitudinal subdivision (with $a_h = 0.1$) is presented in Figure 3-a. An example of both longitudinal and lateral subdivision (with $a_h = 0.1$) is shown in Figure 3-b. It is important to note that within a given structure all longitudinal subdivisions are uniform, and likewise, all lateral subdivisions.

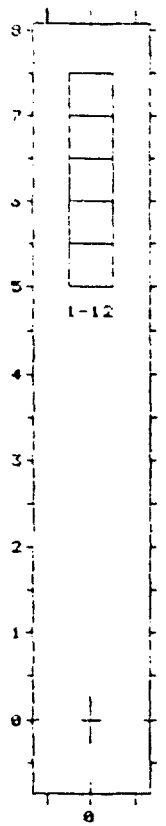

(Distances in 100's of ft)

PLAN VIEW PRIOR TO STRUCTURE DAMAGE (RELATIVE TO DETONATION POINT)

sample.dat 08/03/83 07:56 YIELD= 50000 LB HEIGHT= 0.00 FEET

Figure 3-a. Example of Automatic Longitudinal Subdivision (a_n = 0.1)

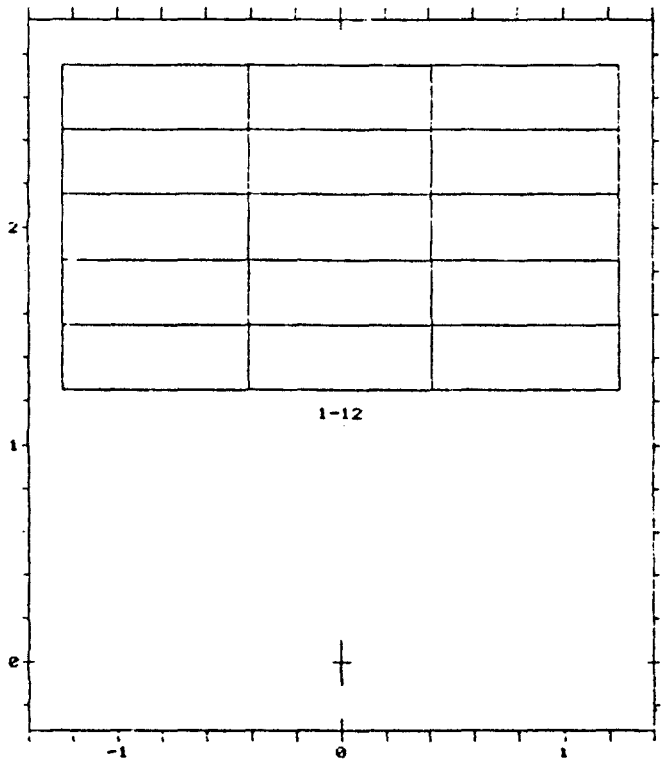

(Distances in 100's of ft)

PLAN VIEW PRIOR TO STRUCTURE DAMAGE (RELATIVE TO DETONATION POINT)

sample.dat 08/03/CS 08:26 YIELD= 2000 LB HEIGHT= 0.00 FEET

Figure 3-b. Example of Automatic Combined Longitudinal and Lateral Subdivision (a_h = 0.1)

The damage level for each subdivision is based on both the distance from detonation point and shielding effects produced by intervening subdivisions. For the case of an explosive yield of 25 tons, the resulting computed damage levels to a typical aboveground building at an ammunition dump, with the same configuration as Figure 3-a, are depicted in Figure 4-a. For the case of an explosive yield of 1 ton, the computed damage levels to a typical aboveground building at an ammunition dump, with the same configuration as Figure 3-b, are presented in Figure 4-b. As expected, those portions of each building which are the most distant from the detonation point, and/or with the most intervening structure subdivisions, experienced the least damage. Correlation of such predicted damage levels with actual observation remains to be accomplished.

2.2 USER-SPECIFICATION OF DAMAGE PARAMETERS

In the original HEXDAM the user could select any structure from a file of 178 different structure types by entering the appropriate structure type number. He could also specify the length, width, height, orientation angle, and location of the structure. In addition, for structures containing explosives, the user could specify the yield of such explosives and the damage threshold level, above which the explosives would detonate. However, the user had no means of specifying structures not contained in the original file, nor could he change the damage parameters associated with any structure in the file.

In HEXDAM-II the user has the option to override the damage parameter values for any structure in the original file by specifying five parameters: (1) the structure classification as sensitive to overpressure, P, or dynamic pressure, Q; (2) the pressure level above which moderate damage occurs; (3) the pressure level above which severe damage occurs; (4) the pulse duration factor* associated with moderate damage; and (5) the pulse duration factor associated with severe damage. An example of the screen display, associated with overriding the damage parameters for an existing structure type, is presented in Figure 5.

*The pulse duration factor is designed to adjust the damage level based on the duration of the blast wave as a function of explosive yield [5].

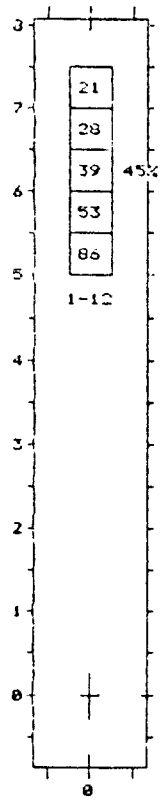

(Distances in 100's of ft - percentages represent mean percent damage)

PLAN VIEW AFTER STRUCTURE DAMAGE (RELATIVE TO DETONATION POINT)

sample.dat 08/03/88 07:56 YIELD= 50000 LB HEIGHT= 0.00 FEET

Figure 4-a. Computed Damage to Structure with Longitudinal Subdivision

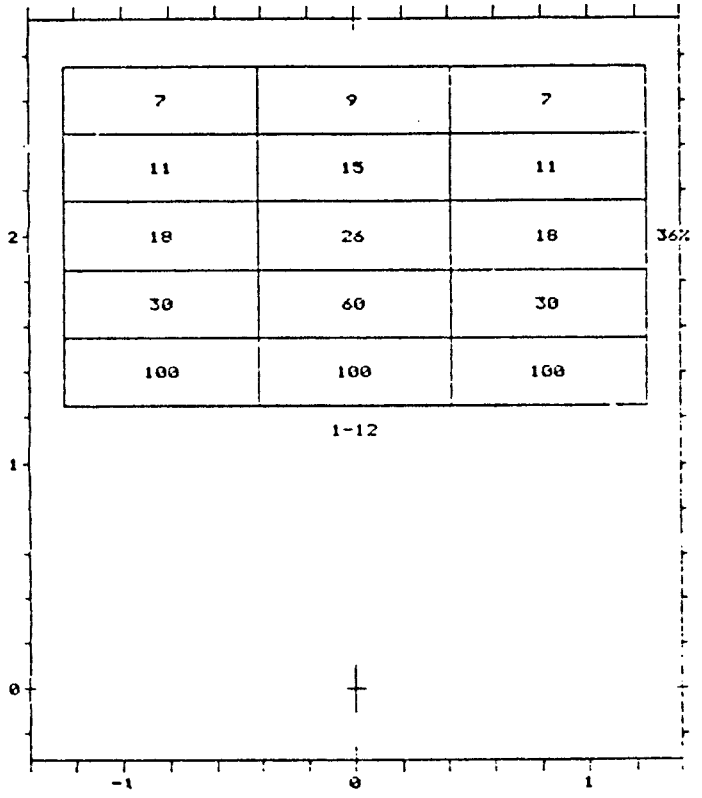

(Distances in 100's of ft - percentages represent mean percent damage)

PLAN VIEW AFTER STRUCTURE DAMAGE (RELATIVE TO DETONATION POINT)

sample.dat 08/03/88 08:26 YIELD= 2000 LB HEIGHT= 0.00 FEET

Figure 4-b. Computed Damage to Structure with Combined Longitudinal and Lateral Subdivision

```
Sequence number   2.

Enter structure type number: 12

Description = AMMUNITION DUMPS/ABOVEGROUND BLDG
Pressure type =   P
Is this the correct structure type? (Y or N): Y
Is the description correct? (Y or N): N
Enter description: AMMUNITION STORAGE FACILITY - BLDG. # 3589

Note: For the following data inputs, pressing 'ENTER'
will accept default value (number in parentheses).

Enter x-coordinate (       0.00 feet): 500
Enter y-coordinate (       0.00 feet): 470
Enter length (     300.00 feet):
Enter width (     150.00 feet): 175
Enter height (      15.00 feet): 20
Enter orientation CCW from x-axis ( 0.00 degrees):
Enter damage level for detonation (  0.00 %): 20
Enter explosive yield (    0.00 pounds): 50000
Do you wish to change damage level parameters (Y or N): Y
Enter pressure type (1=P,2=I): 1
Enter severe damage pulse duration factor (  2):
Enter moderate damage pulse duration factor (  2): 1
Enter severe overpressure level ( 8.00 psi): 8.25
Enter moderate overpressure level ( 4.00 psi): 3.95
Enter yield associated with above pressures (  10000.00000 pounds): 15000

Are the structure data for sequence number   2 correct? (Y or N): Y
```

Figure 5. HEXDAM-II Screen Display for Overriding Damage Parameters

As an alternative to overriding the damage parameters in the original file, with HEXDAM-II the user can create a new structure type by entering "Ø" for the structure type number, and then entering the dimensions, orientation, secondary explosive characteristics, and location of the new structure. He could then specify the five damage parameters previously noted, along with the explosive yield to which such parameters correspond. An example of the screen display for selection process associated with a type "Ø" structure is presented in Figure 6. The characteristics of any new structure, created in this manner, can be stored in a special user-specified structure data file for repeated use.

2.3 ZOOM GRAPHICS CAPABILITY

By means of HEXDAM the user can select and arrange a collection of structures to produce an entire facility. Because of resolution limitations of the video screen, combined with mutual interference of some of the labels identifying

```
Sequence number   3.

Enter structure type number: 0

Structure type = USER DEFINED
Is this correct? (Y or N): Y
Enter description: EXPLOSIVES STORAGE IGLOO

Note: For the following data inputs, pressing <ENTER>
will accept default value (number in parentheses).

Enter x-coordinate (       0.00 feet): 1000
Enter y-coordinate (       0.00 feet): 850
Enter length (       0.00 feet): 50
Enter width (       0.00 feet): 20
Enter height (       0.00 feet): 20
Enter orientation CCW from x-axis ( 0.00 degrees):
Enter damage level for detonation (  0.00 %): 25
Enter explosive yield (     0.00 pounds): 10000
Enter pressure type (1=P,2=Q): 1
Enter severe damage pulse duration factor (  2): 3
Enter moderate damage pulse duration factor (  2):
Enter severe overpressure level ( 8.00 psi): 10.0
Enter moderate overpressure level ( 4.00 psi): 6.25
Enter yield associated with above pressures (  10000.00000 pounds): 5000

Are the structure data for sequence number   3 correct? (Y or N): Y
Save structure in USER DEFINED STRUCTURE DATA FILE? (Y or N): Y

This structure will become structure type 201 in ud.dat
```

Figure 6. HEXDAM-II Screen Display for Creating a New Structure

individual structures, the resulting display of the entire facility may be somewhat cluttered, as depicted in Figure 7. To overcome this problem, the HEXDAM-II software has the capability to enlarge any portion of the display, as specified by the user. This zoom capability, as applied to the region indicated in Figure 7, enlarges the outline of all structures within the region but does not enlarge the print size for labels, as demonstrated in Figure 8. The zoom feature can be used to examine portions of the facility before or after damage assessment is made.

3. SPECIAL FEATURES OF HEXDAM-III

As currently envisioned, HEXDAM-III will be compatible with the IBM PC-XT/AT microcomputer and will have three additional capabilities: (1) accounting for the height of tall or elevated structures, (2) automatic vertical subdivision, and (3) advanced graphics, including oblique projections and contour plotting of pressure and damage levels. A description of these capabilities is provided in the subsections which follow.

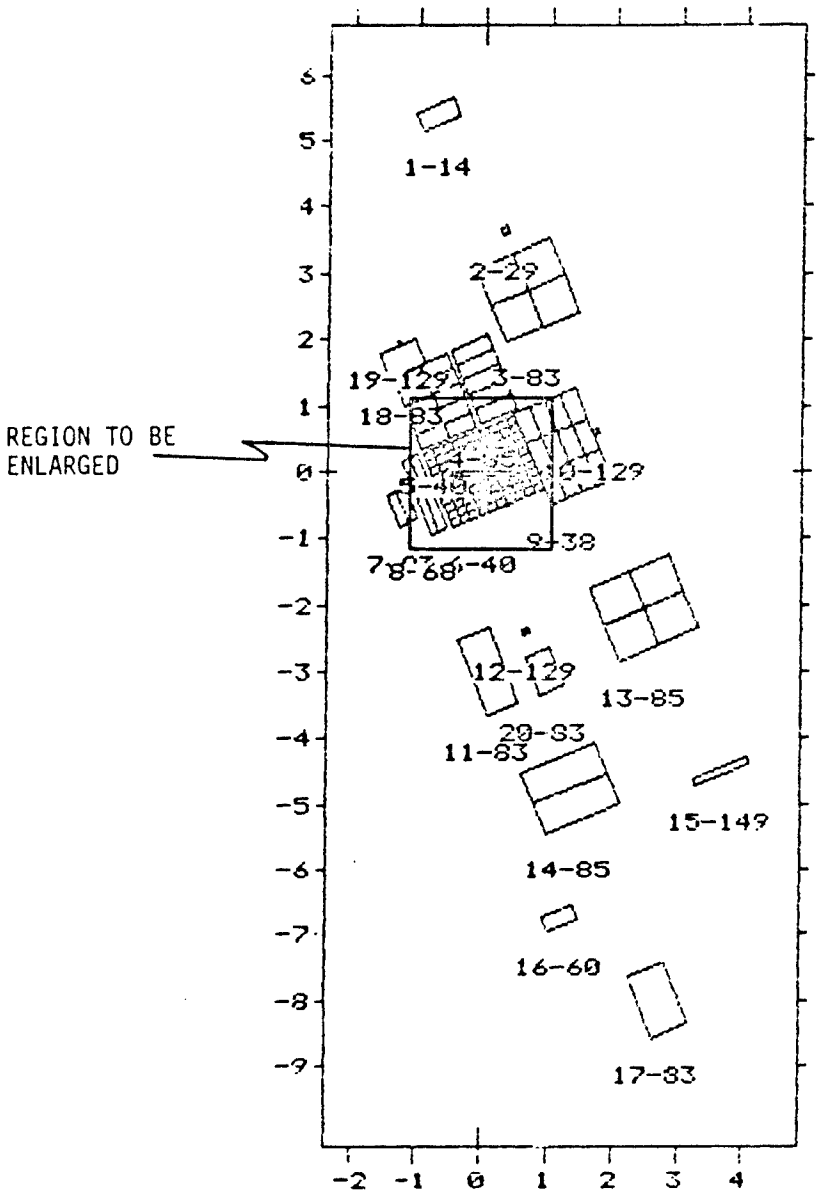

(Distances in 100's of ft)

PLAN VIEW PRIOR TO STRUCTURE DAMAGE (RELATIVE TO DETONATION POINT)

tooele.dat 08/04/88 14:23 YIELD= 2500 LB HEIGHT= 0.00 FEET

Figure 7. HEXDAM-II Facility Display

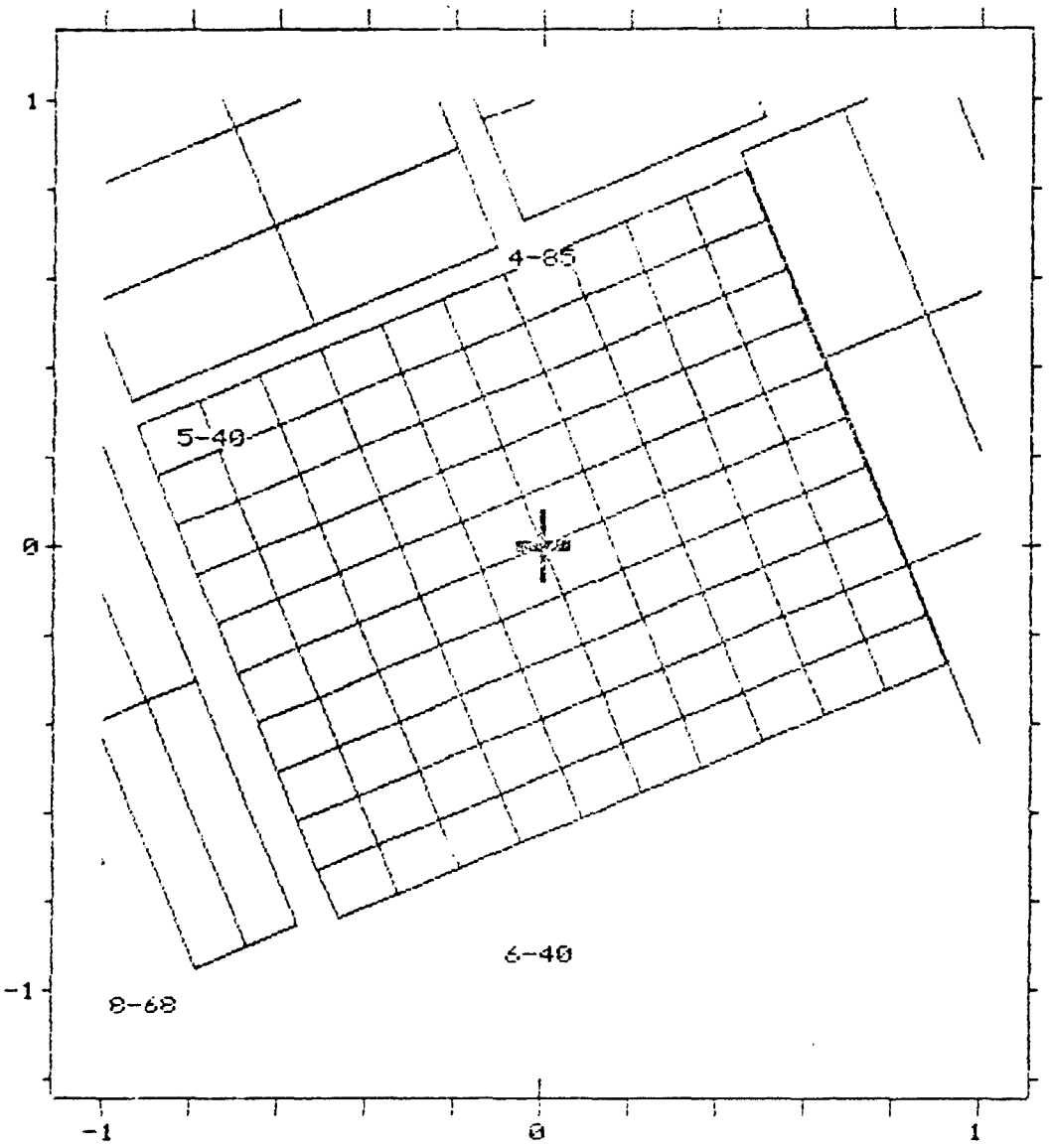

(Distances in 100's of ft)

PLAN VIEW PRIOR TO STRUCTURE DAMAGE (RELATIVE TO DETONATION POINT)

tooele.dat 08/04/88 14:23 YIELD= 2500 LB HEIGHT= 0.00 FEET

Figure 8. HEXDAM-II Zoom Display

3.1 ACCOUNTING FOR STRUCTURE HEIGHT

In both HEXDAM and HEXDAM-II the distance to a structure from the detonation point is taken to be equal to the horizontal distance to the geometric center of the base of the structure. The variation of distance with vertical position is neglected. For tall or elevated structures near the detonation point, the actual distance to different levels may vary significantly. For this reason, for an explosion at ground level, damage to the upper levels of a tall building should be less than damage to the lower levels*, as shown in Figure 9.

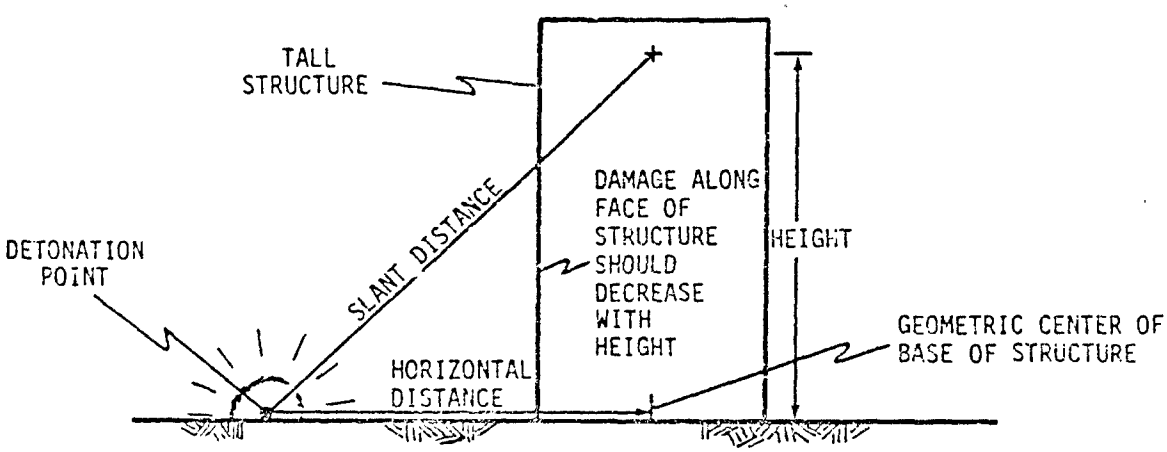

Figure 9. Effect of Structure Height on Damage Level

In HEXDAM-III the distance to a structure will be the slant range to the geometric center of the three-dimensional volume occupied by the structure. In order to compute the variation of damage with height, vertical subdivision of a structure will be required. Such subdivision, as discussed in subsection 3.2, can be performed automatically in a manner similar to that used for horizontal subdivision. For each vertical subdivision, the slant range would be different, and thus a different damage assessment would result, as depicted in Figure 10.

---

*This condition is based on the assumption that the lower level damage is not so severe as to cause the total collapse of the structure.

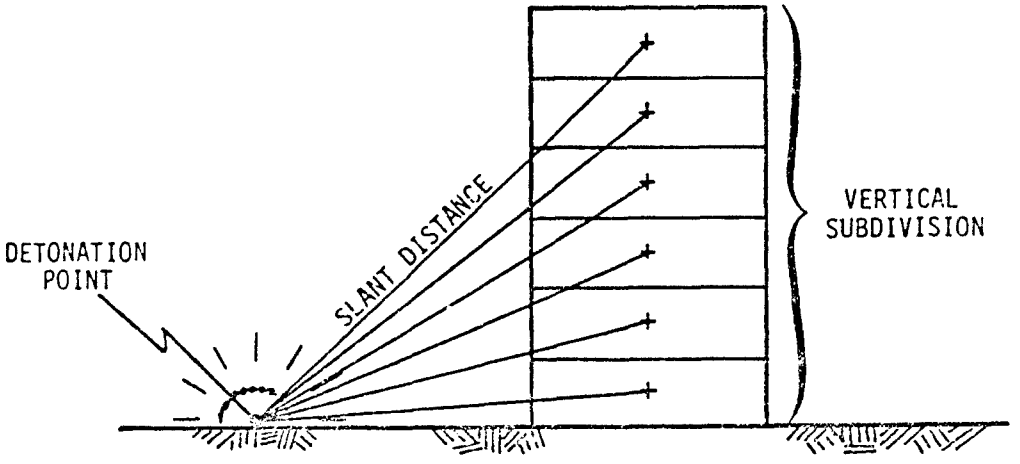

Figure 10. Slant Distance to Vertical Subdivision

3.2 AUTOMATIC VERTICAL SUBDIVIISON

The vertical subdivision algorithm in HEXDAM-III will resemble the horizontal subdivision scheme discussed in subsection 2.1. Such vertical subdivision will be based on the height of the structure as compared to the slant range to the detonation point. The degree of subdivision will be controlled by the vertical distance fraction, a_v, which is user-specified, with a magnitude between Ø and 1, and which may or may not be equal to the horizontal distance fraction, a_h, previously discussed. The degree of vertical subdivision increases as the value of a_v decreases. Notice should be taken that for a given structure, all vertical subdivisions would be equal. As in the case of horizontal subdivision, the damage level would be a function of both the distance from the detonation point and the shielding effect of intervening subdivisions.

3.3 ADVANCED GRAPHICS

As part of HEXDAM-III, two advanced graphics capabilities (oblique projections and contour plotting) would be available as described in the subsections which follow.

3.3.1 Oblique Projections

The addition of height effects in HEXDAM-III produces a need for graphics display with three-dimensional features. The simplest approach to depicting a three-dimensional structure would be to produce plan and elevation views. For greater realism, and ease of interpolation of damage distribution, some type of projection could be used. Based on previous experience with ENDAM [1], the use of oblique projections appears most appropriate. Figure 11 depicts the oblique projection of a tall structure with both horizontal and vertical subdivisions.

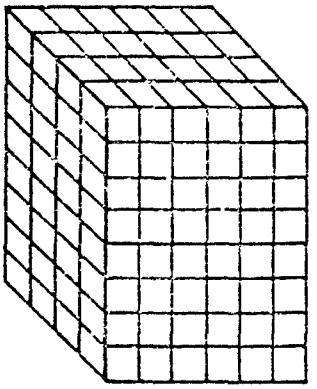

Figure 11. Oblique Projection of Three-Dimensional Structure with Horizontal and Vertical Subdivision

3.3.2 Contour Plotting

To give a more complete picture of the results of an explosion, including both shielding and secondary explosion effects, the use of contour plots would be especially useful. Two types of contours can be envisioned: (1) pressure contours in the horizontal plane covering an entire facility, and (2) damage contours over the face(s) of individual structures.

The pressure contours would provide an overall picture of the distribution of either overpressure or dynamic pressure for an entire facility or any portion

of a facility. The effects of both shielding and secondary explosions would be easily interpreted from such a plot. A typical overpressure plot is depicted in Figure 12.

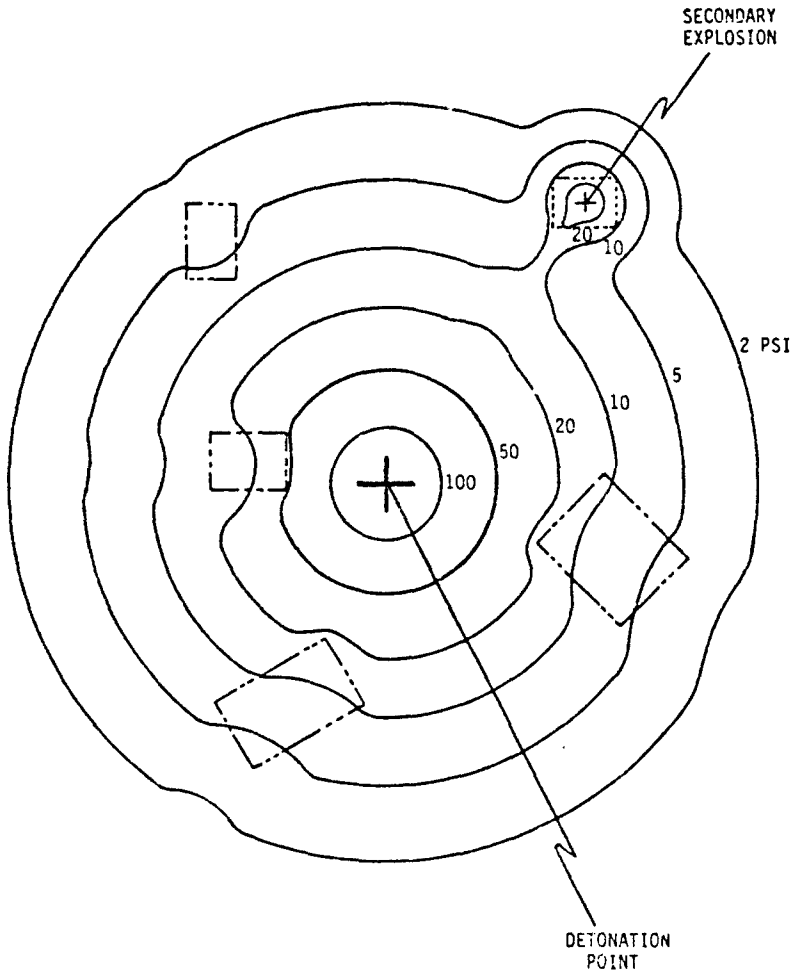

Figure 12. Overpressure Contour Plot for Collection of Structures

Because of three-dimensional considerations, with the oblique projection described in subsection 3.3.1, a need exists to display damage levels in a clear, uncluttered fashion. The use of damage level contours on each face of a structure appears especially suited to this need. An example of such a plot is depicted in Figure 13.

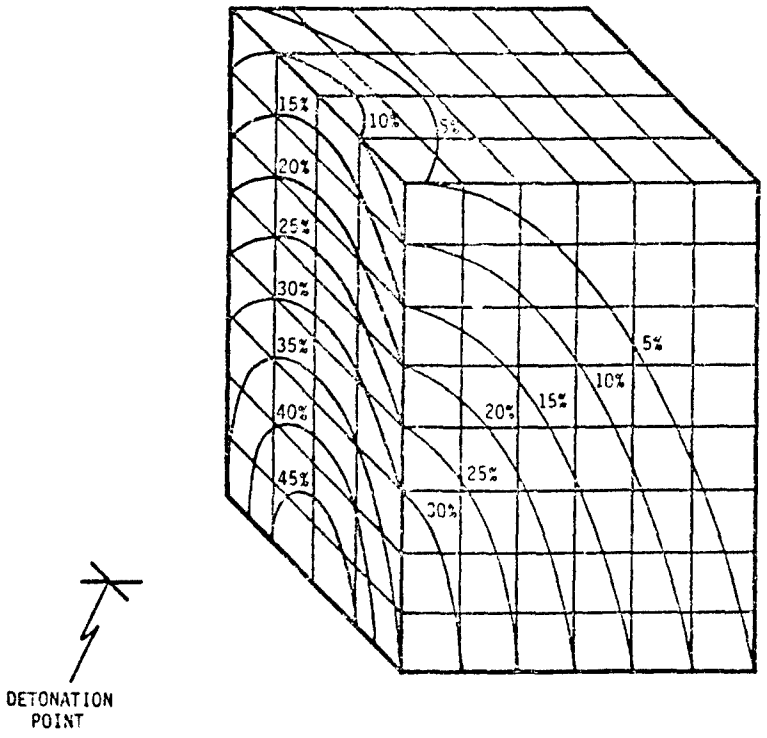

Figure 13. Damage Level Contour Plot for Individual Structure

4. CONCLUSIONS

HEXDAM-II represents a refined version of the original HEXDAM program. Designed for the IBM PC-XT/AT microcomputer, the program possesses certain features which should increase its utility.

The automatic subdivision capability allows the user to readily generate a more detailed picture of the horizontal distribution of damage to structures near the detonation point. Comparison with actual damage levels will be necessary to properly validate and calibrate this feature.

The option which permits the user to specify the damage parameters for an existing structure type, or to add a new structure type, with corresponding damage parameters, greatly extends the application of the program. Calibration of the program with observed damage levels should be significantly facilitated due to this capability.

The zoom feature provides a means for the user to examine in detail the individual structures, or groups of structures which make up a portion of a larger facility. With such a capability available, the analysis of the distribution of damage to structures, especially for cases involving structure subdivision, should be greatly enhanced.

The additional features proposed for HEXDAM-III should further amplify the utility of the model. Taking into account the height of tall or elevated structures permits complete three-dimensional analysis. Such a capability is complemented by the automatic vertical subdivision feature. In similar fashion, because of the three-dimensional considerations, the use of oblique projection graphics should add to the realism and ease of interpretation of the video display. The use of contour plots for pressures and damage levels should also significantly facilitate an overall understanding of the results generated by the model.

HEXDAM-II and HEXDAM-III represent useful, flexible engineering tools for both blast damage assessment and explosive siting analysis. The possibility also exists that the models could be useful in the preliminary design of structures for which anti-terrorist considerations are significant.

5. REFERENCES CITED

1. Tatom, Frank B., and Roberts, Mark D., "High Explosive Damage Assessment Model (HEXDAM) Users Manual", EAI-TR-87-004B, Engineering Analysis, Inc., Huntsville, Alabama, September 22, 1987.

2. Tatom, Frank B., Spencer, Bruce L., and Roberts, Mark D., "ENDAM3 Users Manual, Contract DASG60-84-C-0033, Damage Assessment and Graphics Demonstration", EAI-TR-86-004A, Vol. I and II, Engineering Analysis, Inc., Huntsville, Alabama, October 1986.

3. Smith, S. Ray, "A Simulation Model for Ballistic Missile Defense Damage Assessment", EAI-TM-83-001, Engineering Analysis, Inc., Huntsville, Alabama, May 26, 1983.

4. Hamilton, Julian, S. Jr., and Lahoud, Paul M., "High Explosive Damage Assessment Using a Microcomputer", Twenty-Third DoD Explosives Safety Seminar, Atlanta, Georgia, 9-11 August 1988.

5. Glasstone, Samuel and Dolan, Philip J. (Eds.), The Effects of Nuclear Weapons, U.S. Department of Defense and the Energy Research and Development Administration, Washington, D.C., 1977.

METHODOLOGY ISSUES IN THE APPLICATION OF COMPARATIVE RISK ASSESSMENT TO THE CHEMICAL STOCKPILE DISPOSAL PROGRAM

by

John G. Perry
Robert M. Cutler
William W. Duff
Willard E. Fraize
Brian H. Price
The MITRE Corporation, McLean, Virginia

and

Thomas S. Kartachak
Office of the Program Executive Officer-
Program Manager for Chemical Demilitarization
United States Army
Aberdeen Proving Ground, Maryland

for

Department of Defense
Twenty-third Explosives Safety Seminar
Atlanta, Georgia
9-11 August 1988

ABSTRACT

Probabilistic risk assessment methods were used to analyze the comparative risk of several disposal alternatives for the Chemical Stockpile Disposal Program. The results of that assessment were an important element in the Army's selection of the on-site incineration disposal alternative. This paper summarizes the methods used in the analysis and identifies several methodology issues to be considered in using probabilistic risk analysis for U.S. Army chemical and explosive safety evaluations. These issues include: treatment of non-quantifiable factors; the quality of available hazard data; the application of the D2PC plume dispersion model and census data for the estimation of public risk; the selection of measures of risk and methods to present risk to different audiences; compatibility with established Army hazard analysis practices; the use of a wide range of possible accidents versus the Maximum Credible Event (MCE) approach; interpretation of the results in the light of estimated uncertainty in input data; and the conflict between early risk mitigation and risk assessment of a well-defined system or program.

1.0 Introduction

1.1 Purpose

The purpose of this paper is to summarize and discuss the methods used to conduct a risk assessment in support of the Chemical Stockpile Disposal Program (CSDP). This discussion is intended to assist future risk assessors in the early identification and consideration of methodology issues for their assessments. More rigorous rationale and complete assumptions may be found in the risk assessment itself (*Risk Analysis in Support of the Chemical Stockpile Disposal Program*, U.S. Army, 1987).

1.2 Approach

This paper will present an overview of the essential aspects of the CSDP, followed by a discussion of risk assessment, in general and specific to the CSDP. Several selected methodology issues will be examined and recommendations made concerning the conduct of future risk assessments for chemical operations.

1.3 Other Organizations--Roles and Relationships

The risk analysis of the CSDP involved contributions by many participants. The role of The MITRE Corporation in this effort was to integrate the contributions via the risk assessment methodology described in this paper. The risk assessment participants and their roles are described below with the aid of Figure 1.

1. General Atomics (formerly GA Technologies) was responsible for identifying the accident scenarios and characterizing each in terms of agent release quantity, release mode (spill, detonation, fire, and combinations), agent release time, and the site-specific probability per munition unit; subcontractors supporting General Atomics included H&R Associates, JBF Associates, and Battelle Columbus Division.

2. U.S. Army defined the disposal alternatives and disposal technology, and provided access to the Army-developed agent dispersion computer program, D2PC (Whitacre, et al, 1987).

3. Oak Ridge National Laboratory (ORNL) provided demographic data, meteorological assumptions, and generic fatality estimates (number of potential fatalities for a chemical accident of a given size category); ORNL was also responsible for preparation of the Final Programmatic Environmental Impact Statement (U.S. Army, 1988) and the use of the risk analysis results in the determination of the environmentally-preferred alternative (on-site disposal).

Section 3 will briefly describe how these separate databases and assumptions were combined into an integrated risk assessment model to

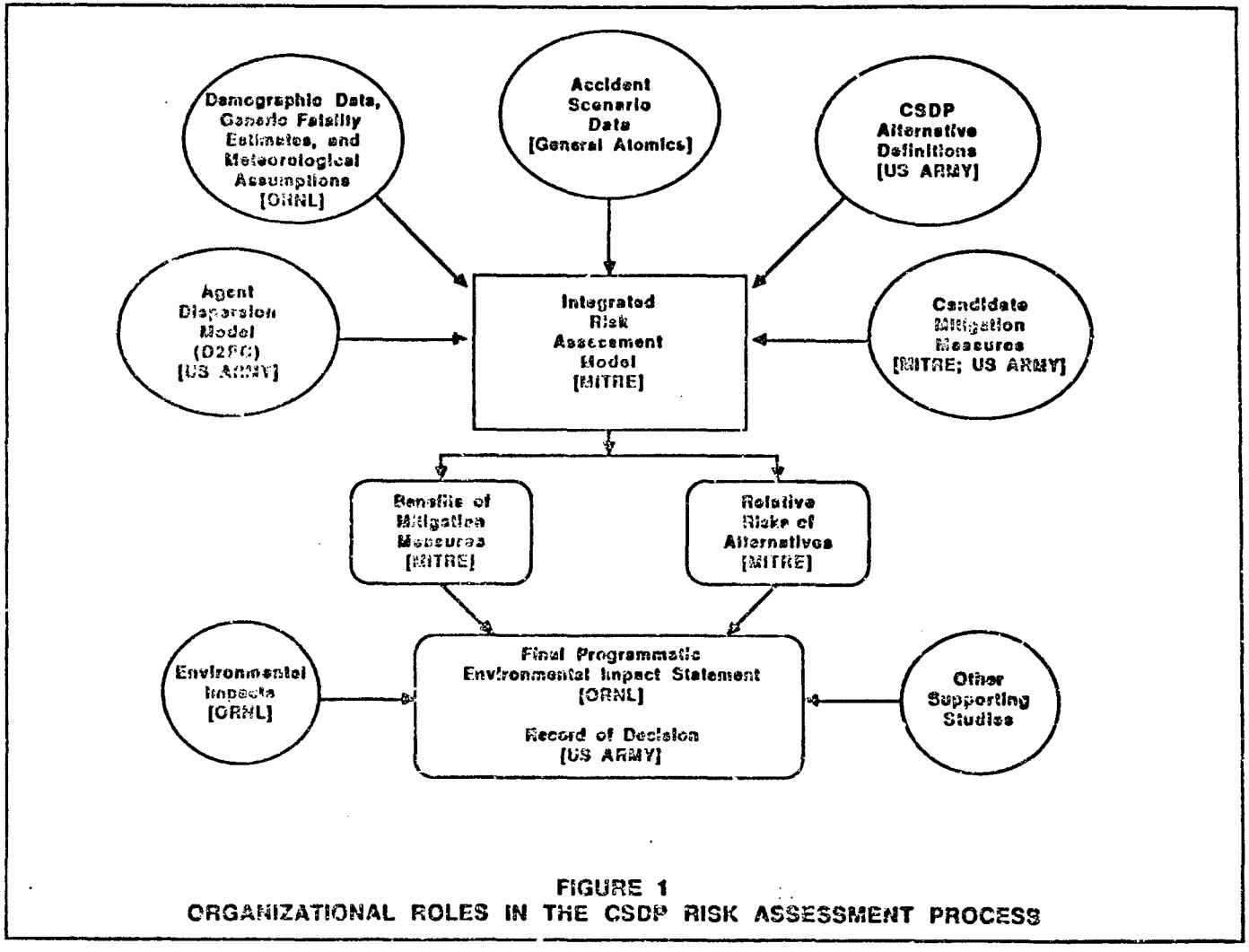

FIGURE 1
ORGANIZATIONAL ROLES IN THE CSDP RISK ASSESSMENT PROCESS

provide useful quantitative estimates of the several selected risk measures in a variety of formats.

2.0 Chemical Stockpile Disposal Program (CSDP)

2.1 Congressional Mandate for Destruction

The U.S. Army was directed by Congress (Public Law 99-145, Title 14, Part B, Section 1412) to destroy the nation's stockpile of lethal, unitary chemical agents and munitions in such a manner as to provide, among other precautions, maximum protection to the general public. In March of 1986 the Army responded with a concept plan for the destruction of the lethal chemical stockpile by 1994 (USATHAMA, 1986), as discussed below.

2.2 Unitary Chemical Munition Stockpile

The chemical stockpile consists of a wide range of munitions and bulk agent storage containers. Three chemical agent types are included: the persistent nerve agent, VX; the non-persistent nerve agent, GB; and the persistent blister agents collectively known as mustards and designated by the symbols H, HT, and HD. Table 1 lists the agents and munitions to be destroyed.

2.2.1 Chemical Agents

The chemical agents involved are, by design, highly lethal. Relatively small exposures via inhalation (measured as the product of atmospheric concentration and exposure time, in units of mg-min/m3) or via skin contact (measured in units of mg/kg of body weight) can be lethal. The nerve agents, GB and VX interfere with the proper functioning of the nervous system (cholinesterase inhibition). Agent GB is highly volatile (a non-persistent agent) and, if spilled, could lead to dispersal by evaporation of agent over a wide area, depending on meteorological conditions. Agent VX is far less volatile (a persistent agent) but is more toxic. A spill would result in less dispersal but its toxic effects would persist in the environment long after release. The mustard agents (represented in the risk assessment by HD) are vesicant agents which lead to chemical burns of mucous membranes, including eyes, or to skin blisters. The mustards are substantially less lethal than nerve agents and are of moderate persistency and volatility (between GB and VX).

For inhalation of atmospherically-dispersed agent, lethality is given by the exposures, expressed in units of [mg-min/m3], listed below:

Agent Type	Exposure for 50% Lethalities in mg-min/m3 (U.S. Army, 1987)
GB	70
VX	30
HD	1500

TABLE 1
MUNITION TYPES TO BE DESTROYED
IN THE CSDP

Munition Type	Chemical Agents Contained	With/without Explosives
Ton Containers	GB, VX, or Mustard	Without
Spray Tanks	VX	Without
Wet-Eye Bombs	GB	Without
Rockets	GB, or VX	With
105 mm Cartridge	GB, or Mustard	With
105 mm Projectile	GB	Without
4.2 inch Mortar	Mustard	With
Land Mines	VX	With
155 mm Projectile	GB, VX, or Mustard	With
8 inch Projectile	GB, or VX	With
500 lb Bomb	GB	Without
750 lb Bomb	GB	Without

2.2.2 Chemical Munitions

The chemical agents are stored in both munitions (with or without explosives or propellants) and bulk storage configurations. Munitions include cartridges, mortars, projectiles, rockets, mines, bombs, and spray tanks. Many are explosively configured to provide for rapid dispersion of the agent and, in the case of rockets, for propulsion toward the target area. The bulk storage containers hold up to 1700 pounds of liquid agent and do not contain explosives. The explosively configured munitions have agent fills in the 1.5 to 15 lb. range.

2.3 Stockpile Locations

The stockpile is currently stored in eight locations throughout the continental U.S. (CONUS): Anniston Army Depot (ANAD), Alabama; Aberdeen

Proving Ground (APG), Maryland; Lexington Blue-Grass Army Depot (LBAD), Kentucky; Newport Army Ammunition Plant (NAAP), Indiana; Pine Bluff Arsenal (PBA), Arkansas; Pueblo Depot Activity (PUDA), Colorado; Tooele Army Depot (TEAD), Utah; and, Umatilla Depot Activity (UMDA), Oregon. These sites are shown in the continued storage alternative of Figure 2. The other alternatives are discussed in Section 2.5.

2.4 Stockpile Disposal Activities Involved

The activities associated with the disposal program alternatives include storage, handling, on-site transport, off-site transport, and plant operations. The risk elements involved in each are highlighted below.

2.4.1 Storage

All chemical munition/agent storage is currently maintained within a chemical exclusion area (security zone) at each installation. All GB-filled munitions plus munitions containing explosives are stored in igloo magazines specifically designed for the storage of ammunition and explosives. The igloos are constructed of reinforced concrete, have steel doors, are covered with earth, and have lightning protection. Most VX-filled munitions and bulk containers are also stored in igloos. The exceptions are VX ton containers at Newport Army Ammunition Depot and VX spray tanks at Tooele Army Depot which are both stored in warehouses. Ton containers of mustard are stored in warehouses at Umatilla Depot Activity; in outdoor storage yards at Aberdeen Proving Ground, Pine Bluff Arsenal, and Tooele Army Depot; and in igloos at Anniston Army Depot.

The munitions are monitored for rust, leakage, or other damage routinely and are periodically repainted or otherwise maintained. Moving or restacking of munitions is involved in these routine inspection and maintenance activities. The total inventory at an installation is handled at a frequency averaging approximately once every five years.

2.4.2 Handling and Transport

Disposal of the chemical stockpile will require the movement of munitions and containers from the storage area to the disposal plant. The handling and transport steps involved in this movement, as assumed for the risk assessment, are as illustrated in Figure 3.

For on-site disposal, pallets of munitions or bulk containers are removed from storage and placed into an on-site transportation package using a forklift. Packing operations occur on or adjacent to the igloo apron or storage area. The shipping package is designed to provide the munitions with protection from collision and fire. The package is loaded on a flat-bed truck and transported in a convoy that includes security, emergency, and decontamination vehicles to a Munitions Holding Igloo (MHI) at the disposal facility. Convoy speed and fuel load are limited by safety

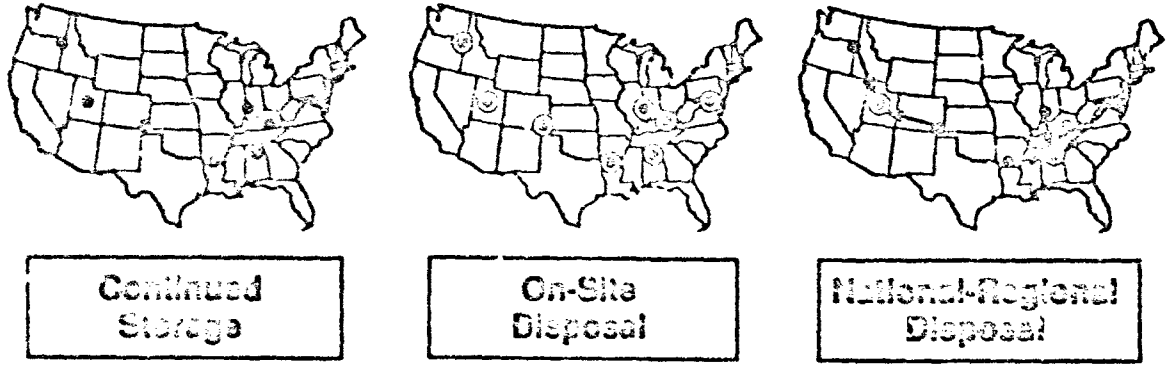

Continued Storage	On-Site Disposal	National-Regional Disposal
Involves:	Involves:	Involves:
• Maintenance Activities	• Handling • On-site Transport • Plant Operations	• Handling • On-site Transport • Short-term Storage • Off-site Transport (rail, air, or water) • Plant Operations

FIGURE 2
CSDP DISPOSAL ALTERNATIVES

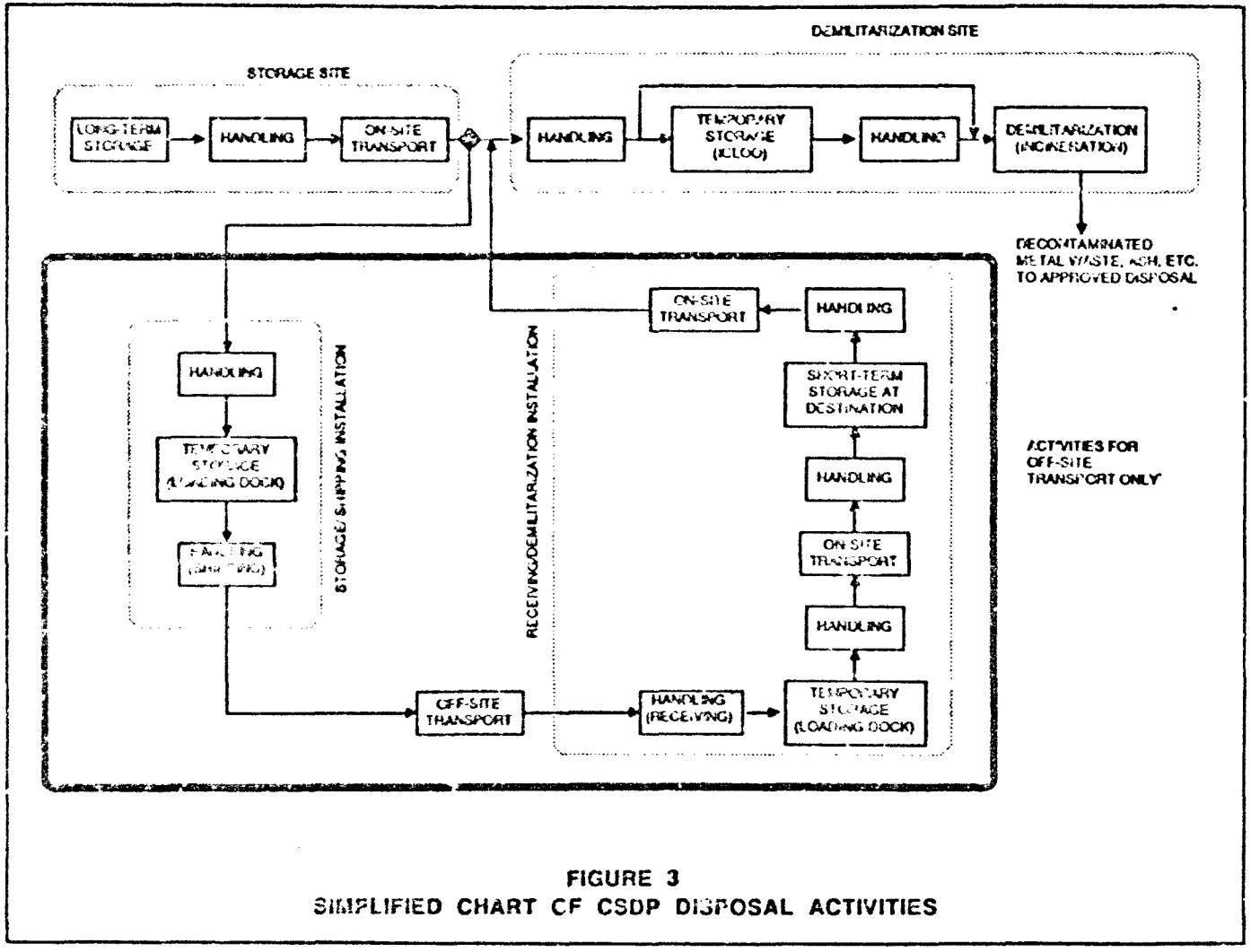

FIGURE 3
SIMPLIFIED CHART OF CSDP DISPOSAL ACTIVITIES

considerations. Upon arrival at the disposal facility the packages are unloaded from the truck and moved into the MHI for temporary storage. Later the package is carried to the Munitions Demilitarization Building (MDB) with a forklift, placed on an elevator, removed from the elevator, and moved to the unpacking area, where the palletized munitions are removed from the transport package.

For regional/national disposal and partial relocation alternatives, off-site transportation package is used. This package is larger, stronger, and more fire-resistant than the on-site package. Palletized munitions or bulk items are loaded into the package at the igloo or storage area. The package is moved by truck to an open holding area and removed form the truck using standard cargo handling equipment. The packages are then loaded on the off-site transporter (rail car or plane) and transported to the destination site. At the receiving site the package is removed from the transporter, placed in an open holding area temporarily and then transported by truck to a storage area. The munitions are removed from the off-site package and placed in a storage facility (e.g., igloo). When the disposal plant is ready to process the munitions, they are removed from storage and placed in an on-site transportation package for movement to the disposal facility. Handling and movement to the MHI and MDB are performed as described above for on-site disposal.

2.4.3 Disposal

The method selected for disposal consists of mechanical disassembly of the munitions, separation into material classes (dunnage, metal parts, energetics, and agent), and incineration. While the Army is proceeding with this mechanical disassembly and separate incineration approach (referred to as the "baseline" technology), it is also evaluating the possible use of "cryofracture" technology wherein whole munitions are cooled to cryogenic temperatures, mechanically fractured into small pieces of mixed material classes, and then fed into a large rotary furnace for final destruction. The risk assessment discussed below is based on the "baseline" demilitarization process. The risk assessment associated with the cryofracture process is discussed in another paper (Cutler, et al, 1988).

The MDB, in which the process takes place, is designed for the confinement of agent. The building is under negative pressure and zoned so that ventilation air flows from areas of no or low contamination to areas of higher contamination. The building ventilation exhaust is treated by charcoal filtration to remove any agent that may be present before release. The stack and building ventilation exhaust, as well as the building work areas, are monitored for agent. The steps involved in the destruction process are described below.

Explosively configured munitions are separated and drained in special explosion containment rooms. Rockets are sheared to separate propellant and explosive components, drained, and fed to a deactivation furnace. Mines are punched and drained; the explosive components are punched out and fed, along with the empty mines, to the deactivation furnace. For the other burstered munitions, the explosives are removed by a machine, sheared, and fed to the deactivation furnace; the munitions are drained and fed to the metal parts furnace. In all cases, the drained agent is fed to a storage tank prior to destruction in a separate, liquid agent incinerator.

Bulk items, which have no explosives, are punched and drained. The agent is fed to a storage tank and the empty bulk container is then conveyed to the metal parts furnace.

Four types of furnace systems are used in the process. The agent drained from the munitions is destroyed in the liquid incinerator. The deactivation furnace is used to destroy explosives and propellants and to decontaminate certain munition hardware. The metal parts furnace burns out agent residues and detoxifies projectile and mortar shells and bulk item containers. The dunnage incinerator treats other combustibles (wooden dunnage, packing material, spent charcoal filters, etc.). The furnace systems and associated feed systems for toxic materials are located in special confinement cubicles and operated remotely. The deactivation furnace is housed in a blast containment room and is equipped with blast gate valves and blast attenuating duct on the exhaust.

Each furnace has its own pollution abatement system to remove acid gases and particulate. Liquid wastes are processed to dry solids and packaged for appropriate disposal. Spent decontamination and suspect liquid wastes are incinerated. There is no liquid effluent from the process. Combustible wastes are incinerated.

2.5 Disposal Alternatives Considered

Of eight programmatic alternatives originally identified for the CSDP, only five were carried through the full scope of the risk assessment. Those five are:

1. The continued storage of the stockpile in its present locations (this is the "no-action" alternative required by the National Environmental Policy Act)

2. On-site disposal of the stockpile at its present storage locations

3. Movement of the CONUS stocks to two regional disposal centers (at ANAD and TEAD)

4. Movement of the CONUS stocks to one national disposal center (at TEAD)

5. Partial relocation of the CONUS stocks (from APG and LBAD) by air to the national disposal site (TEAD) with the remainder of the stockpile destroyed on-site

The other three CSDP alternatives, which will not be discussed in this paper, involve variations on the partial relocation alternative, including an option for water transport of the APG stockpile to Johnston Island in the Pacific Ocean.

For the continued storage alternative, there are risks associated with the storage and storage-related handling activities at the current storage locations.

For on-site disposal, the risks are associated with the (short-term) storage of the stockpile awaiting disposal, from handling and on-site transport activities as the munitions are moved to the disposal facility, and from the plant operations themselves--all occurring at the current eight storage locations.

The risk associated with the regional/national disposal and partial relocation alternatives (collectively called the collocation alternatives) is distributed between the originating sites, the transportation corridors, and the destination/disposal sites. At the originating sites, risk results from handling, on-site transport, and short-term storage activities. The originating sites (APG and LBAD) also bear the risk of take-off aircraft accidents for the partial relocation alternative. The transportation corridors are exposed to the en-route transport risks. The destination sites experience the risks due to handling, on-site transport, and short-term storage of the imported munitions as well as all the risks associated with disposing of the resident and collocated stockpiles.

3.0 Risk assessment

3.1 Purpose of Risk Assessment

Risk assessment is a systematic analysis of an entire group of identified hazards in regard to their potential effect on society or affected individuals. Risk is the name given to the combined measure of both the potential (probability, frequency) and the effect (consequences, damage, injury). As a tool, risk assessment is a useful way to examine risks so that they may be better avoided, reduced, or otherwise controlled. A risk assessment can be used to identify which of a group of hazards contributes the most to overall risk and thus lead to control (mitigation) of that hazard. Or, a risk assessment can be applied to two or more alternatives to aid in the selection of the most desirable. A discussion of the consequences of concurrently using a risk assessment for both purposes is contained in another paper (Price, 1988)

Risk assessment for a system starts with a list of identified hazards. Each hazard can lead to one or more assumed accidents, each with a certain likelihood and consequence. It is these likelihoods and consequences that are ultimately combined as the overall risk for that system. This information is then ranked, combined, or presented in a manner appropriate to the task at hand.

3.2 Specific Role of Risk Assessment for U.S. Army

The primary purpose of the risk assessment for the CSDP was to provide a consistent and quantitative basis for comparing the risks to the public for each of the disposal alternatives. In addition, some higher risk hazards were identified that were subjected to design or procedural changes to reduce their associated risk. This mitigation is discussed in detail in another paper (Perry, et al, 1988).

In this analysis, risk is defined as the expected impact on public safety as a result of the set of possible accidents involving the storage, handling, transporting, and physical destruction of the munitions in the stockpile. Risk is measured by both the probability of a lethal event occurring and the number of public fatalities that might result if the event took place.

The results of the risk analysis were used to support the selection of the environmentally preferred disposal alternative in the Final Programmatic Environmental Impact Statement (U.S. Army, 1988) The results were also used as one of several factors considered by the Army in arriving at its Record of Decision of 23 February 1988 which stated the Army's decision to proceed with the on-site disposal alternative.

The risk assessment methodology is intended to compute the several chosen measures of risk on both a site-specific and total program

(national) level and to display those results in a variety of formats designed to meet the needs of the several intended audiences for the risk analysis.

3.3 Approach to the Risk Assessment in Support of the CSDP

The remainder of section 3 will briefly describe the risk assessment conducted in support of the CSDP. An overview of the risk assessment methodology is shown Figure 4.

3.3.1 Scope of Risk Assessment

Although a vast number of factors could have been considered in the risk assessment, realistic limits on resources required constraint on the scope. For example, only the alternatives described above were included; no consideration was given in this assessment to ocean dumping, nuclear destruction, shipping to OCONUS locations, or other conceivable alternatives. The only effects of accidents included were short-term chemical agent effects to off-post personnel; no consideration was given in this assessment to injuries due to explosion fragments, agent exposure to operating personnel, or non-agent occupational safety and health.

This analysis of risk associated with the CSDP took the following major factors into account:

1. The nature and the severity of the hazards to individuals posed by exposure to chemical agent
2. The munitions and bulk containers in which the agents are contained
3. The activities within the CSDP that could lead to accidental release of agent
4. The accident initiators appropriate for each activity class and munition type
5. The disposal alternatives which specify the activities and the location at which they take place
6. The population groups that could be affected by an accidental agent release

3.3.2 Sources of Data

The organizational responsibility for preparing the several data sources required for the risk analysis has been outlined in section 1.0. In this section, we will present a brief description of the various types of data.

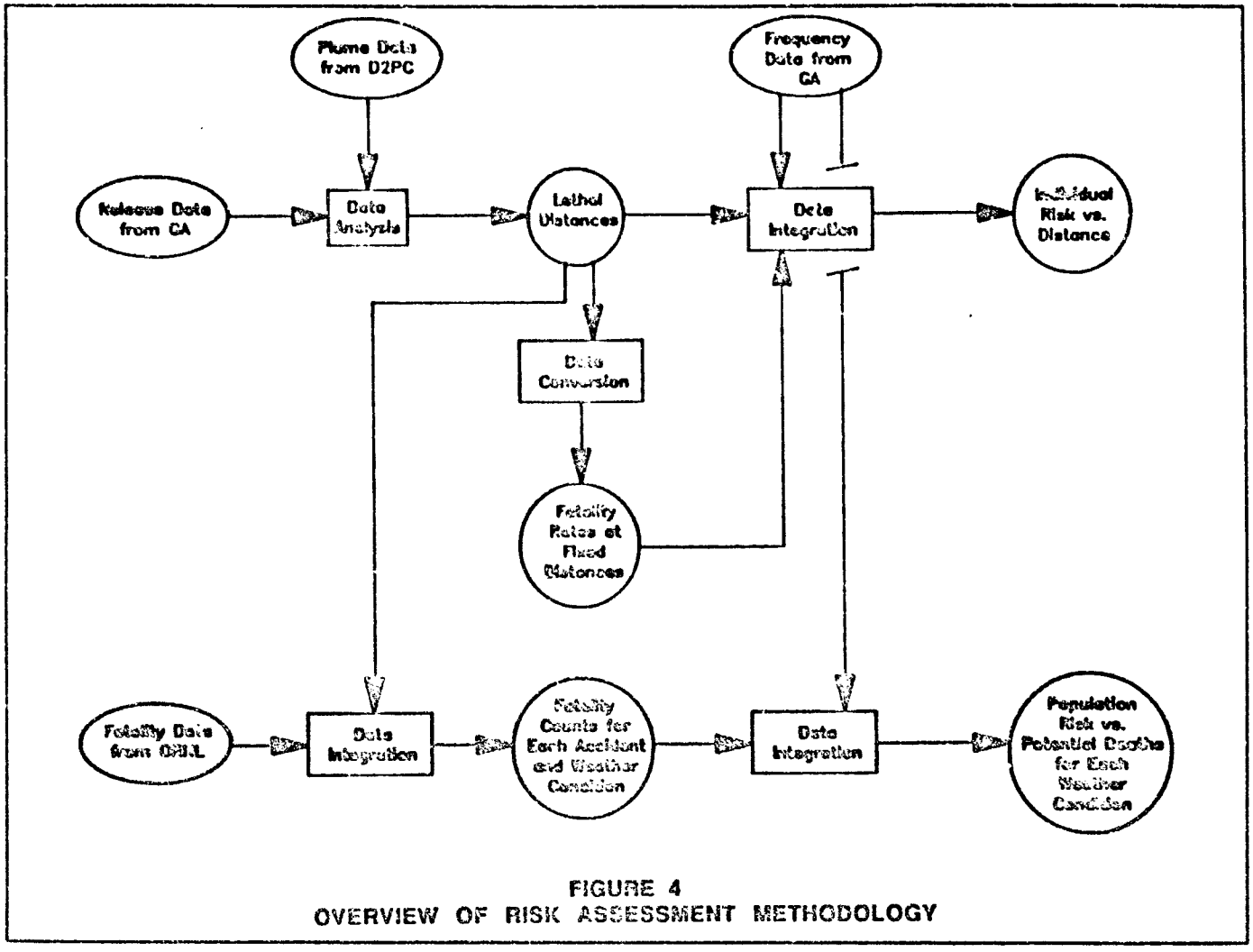

FIGURE 4
OVERVIEW OF RISK ASSESSMENT METHODOLOGY

3.3.2.1 Accident Scenario Data

Accident scenario data was developed by General Atomics, formerly GA Technologies (GA Technologies, 1987a, 1987b, 1987c). The accident scenarios are described by the following:

1. A ten-character identification code which uniquely defines:

   - operational activity (handling, plant operations, etc.)
   - munition type
   - agent type
   - release mode

2. A brief textual description of each scenario, as defined by activity code and scenario number

3. Agent release data, including agent type, mode of release, duration of release, surface type, and location of evaporative releases. This data provides the starting point for calculating the consequences of the accident.

4. Accident probability data. This data provides the starting point for calculating the likelihood of the accident.

This data was provided explicitly in the study by GA Technologies (GA Technologies, 1987a, 1987b, 1987c) or was directly inferable from the accident description. With few exceptions, agent release data is not site-dependent.

3.3.2.2 Census Data

Demographic data was provided by Oak Ridge National Laboratory (ORNL), based on the 1980 census. This data was used to calculate the effect on the public, assuming a given release of chemical agent.

3.3.2.3 Stockpile Data

Some of the accident probability data was given on a "per item" basis. The numbers of items in the stockpile was provided by the Army and used to calculate the overall probability of the accidents associated with each item.

3.3.2.4 Historical Accident Data

Historical data on accidental detonations, leakage, railroad accidents, material handling equipment accidents, and other accidents was used as input to fault trees and event trees to generate the accident probability data included in paragraph 3.3.2.1.

3.3.2.5 Process Data

Demilitarization facility munition destruction rates, transportation capacities, and similar process data was also used to generate accident probability data.

3.3.3 Consequence Estimation

From the information provided in the accident database, the consequences to the public were calculated in four steps: Assume initiation of an accident, determine the amount of agent dispersion, estimate the fatality rate, and estimate potential fatalities.

3.3.3.1 Accident Initiation

The accident initiators considered in the risk assessment are appropriate to the several activity categories described above. Causes of accidental release of agent include catastrophic external events (e.g., tornados, earthquakes, meteor strikes, and airplane crashes), transportation accidents (truck, rail, or aircraft while carrying chemical agent), handling accidents (dropping of a munition or puncturing it with a forklift tine), and accidents associated with plant operations (human error, control system failure, mechanical equipment breakdown, fire). A list of the accident initiators considered, by activity category, is presented in Table 2. When these initiators were applied to different sites, with different munitions and weather conditions, the list of accident scenarios reached many thousands, from which the undesired effects on the public could be calculated.

3.3.3.2 Use of the D2PC Atmospheric Diffusion Program

The Army provided access to a computer program (D2PC) that can calculate various outputs (downwind hazards, evaporation rates, spill areas) from agent accident inputs (amount released, type of release, weather conditions). The accident scenario list provided the necessary information on agent type, release amount, and release mode. Other D2PC input information was either deduced from the scenario (surface type) or assumed (two sets of weather conditions--most likely and worst case). For scenarios involving spills, the amount of expected agent evaporation was first calculated from spill amount, temperature, surface type, and duration of scenario. The amount evaporated or released by detonation was then used to calculate the dispersion of the agent. The amount of agent from each accident scenario assumed to reach different areas (distance and width) was the input for the next calculations. The details of the application of the D2PC program are contained in another paper (Cutler, 1988).

TABLE 2
ACCIDENT INITIATORS

ACTIVITY CATEGORY	ACCIDENT INITIATORS
Storage	Spontaneous munition leak
	Puncture by forklift tine
	Spontaneous rocket motor ignition
	Small or Large aircraft crash into storage area
	Tornado-generated missiles
	Tornado-induced building collapse
	Severe earthquake
	Meteorite strike
	Lightning strike
	Munition(s) dropped during handling
	Fire from internal or external sources
Handling	Munition(s) dropped
	Forklift collision
	Puncture by forklift tine
	Undetected leak
On-site Transport	Munition vehicle collides/overturns
	Aircraft crash onto/near munitions vehicle
	Severe earthquake causing vehicle accident
	Tornado-generated missile
	Tornado-induced vehicle overturn
Rail Transport	Train accident (various severity levels)
	Aircraft crash onto munitions railcar
	Severe earthquake causing rail accident
	Tornado-generated missile
	Tornado-induced rail accident
Air Transport	Aircraft crash on takeoff, while in flight, or on landing
	On-board fire
Plant Operations	Tornado-generated missile
	Meteorite strike
	Aircraft crash (various severity levels)
	Earthquake (various severity levels)
	Excess agent feed to liquid incinerator
	Furnace explosion due to failure of fuel shut-off
	Furnace explosion due to feed of unpunched

3.3.3.3 Estimation of Fatality Rates

The third step in consequence estimation was the determination of the fatality rate (the percentage of exposed individuals expected to die) at specified distances downwind of the agent release point. The D2PC program predicts downwind distances to any specified dosage, expressed as a fatality percentage based on agent toxicity estimates built into the model. For the CSDP risk analysis, downwind distances were computed for three fatality percentages: zero percent, one percent, and 50 percent. To be consistent with procedures adopted by ONWL in their estimation of potential fatalities, fatality rates at fixed downwind distances were estimated by linear interpolation between the zero, one, and 50 percent fatality values. The ten distances selected were 0.1, 0.2, 0.5, 1.0, 2.0, 5.0, 10.0, 20.0, 50.0 and 100.0 kilometers. For each accident scenario and each downwind hazard distance, the potential fatality rate was estimated by piece-wise linear interpolation. A fatality rate of 100 percent was assumed at a downwind hazard distance of zero.

3.3.3.4 Estimation of Potential Fatalities

The final step in consequence estimation was to relate each scenario to the potential number of fatalities that could result, given that the accident occurs. Potential fatalities per event (scenario) is a function of the plume area, the population distribution around each site (from Census data), and the fatality rate estimates obtained in the previous step. The use of the term "potential" refers to the lack of quantification of the preservation of lives that would result from preplanned emergency response measures that would be implemented by the Army and cooperating agencies. For example, no credit was taken for evacuation, or even for the protection afforded by remaining indoors. Thus, actual fatalities are likely to be less than the calculated potential fatalities for worst cases.

Potential fatalities were thus computed as functions of accident location (any of the eight agent storage sites in the continental United States, and locations along the proposed 11 rail routes and two air routes), lethal downwind distance (to the 0 percent fatality, or 'no-deaths' dose), and meteorological conditions.

3.3.4 Probability Estimation

The procedure used to analyze event probability data is illustrated in Figure 5. As part of the preparation of the accident database, General Atomic used generic data (e.g., railway accidents), specific chemical munition related data (e.g., Surveillance leaker reports), and simulant testing (e.g., drop tests) as input to fault trees and event trees, resulting in probability estimates for each scenario. Global data (process rates, stockpile data, transport capacities) and data specific to each site (number of operations required) was combined with the probability estimates (per operation) from the scenario list. The result was the probability for

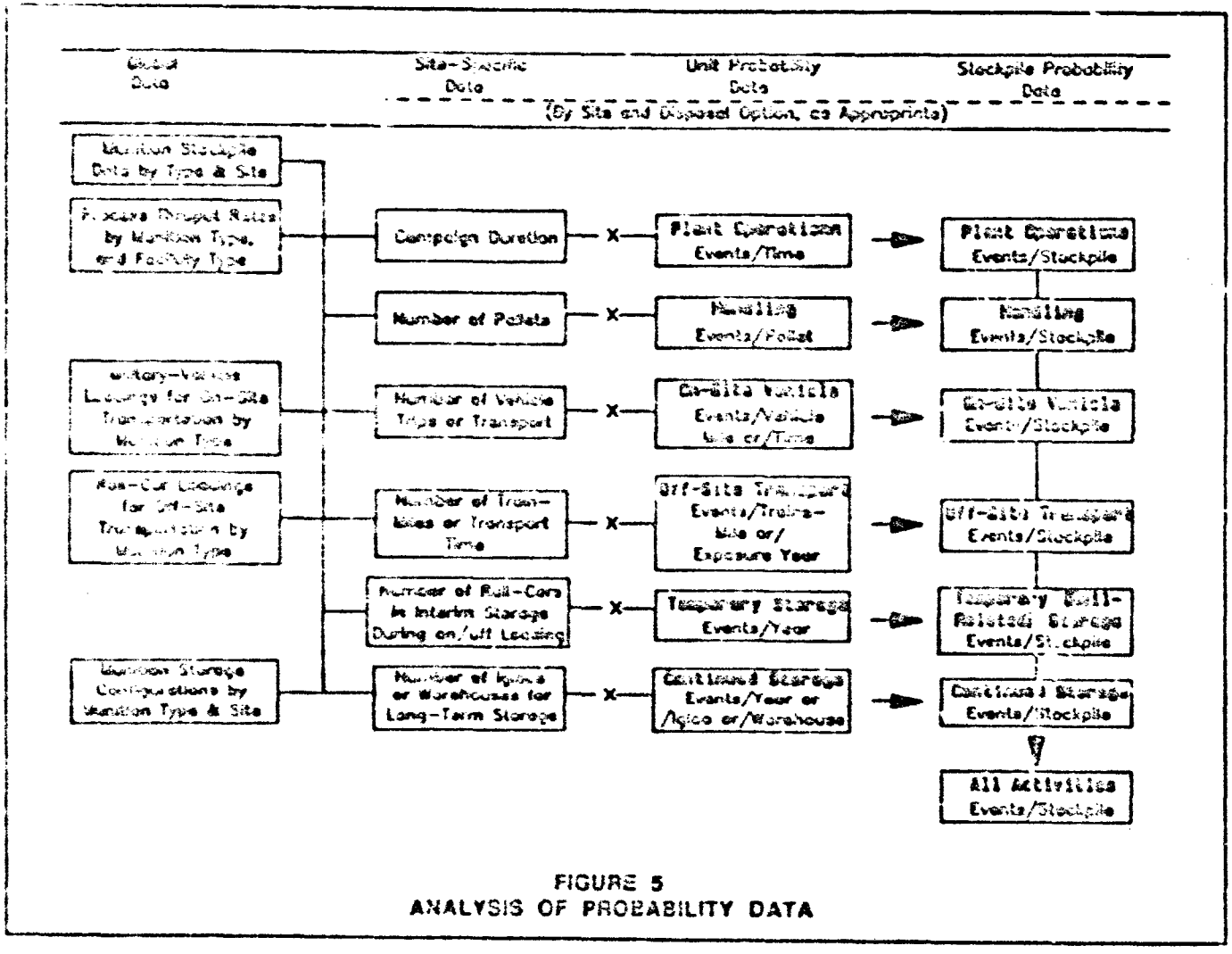

FIGURE 5
ANALYSIS OF PROBABILITY DATA

each accident occurring during the demilitarization of the entire stockpile of one munition type at one site by one alternative. Necessary consideration was given to use of range factors (uncertainty), mean versus median, and probability values for statistically valid results.

3.3.5 Risk Measures

The description of risk as a combination of the probability of an accident and the magnitude of the consequence of that accident can be made in many ways. The most direct is simply the product of the two; in this case, the probability of an accident times the potential number of fatalities should the accident occur. This is referred to as "expected fatalities." Other combinations of probability and consequence are possible and as are other risk-like measures that omit one or the other.

This risk assessment estimated three different measures of risk (expected fatalities, maximum individual risk, and probability of one or more fatalities) and four different risk-like measures, each providing a different perspective on overall program risk. These are described as follows:

1. Expected fatalities, equal to the sum of the risk contribution of all accidents at a site or for the nation, where risk for each accident is the potential number of fatalities (if the accident were to occur) multiplied by the probability of the accident occurring. Note that expected fatalities is proportional to the probability of a fatality-causing event occurring, and will nearly always be a small number--much less than one. For example, an accident with a potential fatality estimate of 12 and a probability of 10-6 (odds of 1 in a million of occurring during the CSDP) would have an expecte fatality value of 12 x 10-6.

2. Maximum individual risk, equal to the probability of a fatal exposure at the site boundary (assumed to be 0.5 km from the on-site disposal/storage operations) or as close as 0.1 km to the centerline of a transportation corridor. It is dependent only on the mix of potential accidents that could happen at the individual's location and, since it applies only to an individual, is independent of population density.

3. Probability of one or more fatalities, equal to the chance that there will be at least one fatality at a given site or for the nation as a whole during the CSDP. This measure is calculated by summing the probabilities of all accidents that could cause one or more fatalities.

4. Maximum lethal distance, equal to the maximum downwind length (given by the 'no-deaths' dose) of the plume from the worst of all identified potential accidents under worst-case weather conditions

at a specific location. Conversely, it is also the minimum distance an individual could be from a given site or transportation corridor and have no risk of lethal exposure during the disposal program.

5. Maximum total time at risk, representing the maximum length of time an individual could be at risk at a fixed location near a site or along a transportation corridor. For those living within the maximum lethal hazard distance, the time at risk is the total time required for stockpile disposal at that site, regardless of where the individual is located. For those individuals along the transportation corridors, the time depends on the distance from the rail line or air corridor. These persons are exposed to a hazard only when a train or aircraft is in the vicinity (defined as the maximum lethal hazard distance in either direction) of them. This time is summed for each agent-bearing train or aircraft that would pass by in each alternative.

6. Maximum number of fatalities, equal to the maximum consequence of all accidents at a site or for the nation. This risk measure is based on worst-case weather conditions, actual population densities (1980 census data, as analyzed by Oak Ridge National Laboratories), and worst possible wind direction (i.e., plume striking the highest number of people without any allowance for preventive/emergency response measures).

7. Person-years-at-risk, equal to the number of people within areas that could experience potentially lethal agent exposure multiplied by the time period during which that worst-case event could take place. This measure does not account for the fact that individuals within the affected population groups who are farther from the potential accident site are at lower risk; all affected individuals are counted if they have any risk at all.

J.3.6 Risk Portrayal Methods

The analysis methodology outlined above provides opportunity to present programmatic risk in many different ways. These ways include:

1. Risk curves, which portray, for the full set of applicable accident scenarios, the probability of exceeding a given number of potential fatalities per event (vertical axis), against the potential fatalities per event (horizontal axis)

2. Risk pictograms, which provide a pictorial indication (the darkness of the shading) of the relative magnitude of each of the measures of risk along with a key to the numerical range represented by each of the shading values

3. Expected fatalities plots, showing mean estimated values of expected fatalities, with uncertainty bands. The expected fatalities value is defined as the sum of the risk (probability times potential fatalities) for all applicable accidents.

Risk curves provide the most detailed information of all display alternatives, and are particularly useful for depicting, by means of their shape, the difference between alternatives dominated by high-probability/low-consequence accidents and those dominated by low probability/high-consequence accidents. Risk pictograms provide a visual impression of the relative magnitude of public risk for all combinations of alternatives and locations. Expected fatalities plots offer the simplicity of a single quantified measure of risk which can be disaggregated into the contributions of individual accidents to the overall risk.

The selection of a preferred risk portrayal method and examples of each are presented in another paper (Fraize, 1988).

3.3.7 Risk Assessment Results

The resultant risk information from the assessment was used both for the comparison of alternatives and the identification of important hazards for mitigation. Detailed information on the each may be found in other papers (Kartachak, 1988 and Perry, 1988, respectively).

4.0 Discussion of Selected Methodology Issues

As may be inferred from the description of the risk assessment, a great many decision points exist in the assessment. In general, when reality was "estimated" by some non-exact process, conservative decisions were made. Some of these decisions were almost insignificant (How many decimal places to retain in the answers?) and had little impact on the assessment. Others were fundamentally crucial for obtaining a meaningful result (What measure of consequence should be used for comparison?). This section will discuss some of the more important methodology issues. The last four issues listed are of sufficient significance that separate papers have been written on them.

4.1 Non-quantifiable Factors

Among the first decisions encountered involved how to deal mathematically with factors which could not be easily quantified. Some factors, like weather stability, could be placed in previously defined categories. Other factors simply could not be quantified or categorized and had to be ignored. Still others would have required a large resource expenditure and were dismissed if all alternatives were affected nearly equally.

4.1.1 Deliberate Acts

Deliberate acts with undesirable effects (e.g., terrorism, sabotage) are essentially unbounded in scope from a prediction standpoint. Any number chosen as the amount of damage done by sabotage can be arguably adjusted up or down. There are very wide ranges of purposes and presumed resources available for such acts. Vulnerability to deliberate acts must be considered subjectively outside the scope of a risk assessment.

4.1.2 Community Response

Community preplanned emergency response capability is, again, a factor that is somewhat unbounded. Facing the demilitarization program, community interest may range from apprehensive to apathetic, with a corresponding effort to establish, augment, equip, or train emergency response activities. Although it is perhaps apparent that community response could be better around fixed sites than along transportation corridors, insufficient information was available to quantify this difference. Thus, the conservative approach was used that no credit was taken for evacuation, or even for the protection afforded by remaining indoors. Thus, actual fatalities are likely to be less than the calculated potential fatalities for most cases.

4.2 Input Data Issues

The quality of the results of the risk assessment is obviously critically dependent on the quality of the input data. Perhaps, less obviously, it is also dependent on the ability to quickly and accurately respond to changes and corrections in data. Complete automated data processing is essential, as is the ability to know what was changed and why (an audit trail). Backups of data were therefore maintained at every step of the assessment. The resulting computer files management effort is substantial, but justified.

4.2.1 Accident Data

A list of all possible hazards and presumed accident scenarios is never complete. Accidents that actually occur are frequently those that were never considered in a hazard analysis. One reason, of course, is that "nobody thought of that" in spite of all the efforts to systematically identify hazards. Another reason is, that once identified, significant hazards are mitigated. Compensating for this lack of completeness is the fact that many of the accident scenarios on the list act as surrogates for other, very similar accident scenarios. For example, a fire due to a small plane crash into a storage warehouse (included) would not be much different from a fire due to large truck crashing into the warehouse (not included). A further discussion on surrogate scenarios and the effect on them by mitigation is contained in another paper (Price, 1988).

4.2.2 Census Data

Any population groups living or working within the maximum hazard distance ("no-deaths" distance for most severe accident) of a potential accident site are at some risk due to the CSDP. Hence, the risk analysis had to consider the risk to the population groups surrounding the eight current stockpile sites plus those along the several transportation corridors. Demographic data defining these population groups was analyzed and supplied to the risk analysis effort by the staff of Oak Ridge National Laboratory using data derived from the 1980 census. About the fixed sites, only persons living beyond the site boundary were accounted for in the estimation of risk to the public. Army and contractor personnel living or working within the site boundaries were not included in the public risk estimation. The accuracy of the demographic data, however, suffers to an unknown degree by virtue of the fact that it represents residences of people, not employment locations, and thus describes the nighttime distribution instead of the daytime distribution of the population.

4.2.3 Stockpile Data

The risk assessment was complicated by the fact that quantity of chemical agent and munitions in the stockpile is classified, requiring special computer procedures and methods of depicting risk. The accident

scenario list gave probabilities on a per item basis, so that it could remain unclassified. After the classified stockpile data was incorporated, the results had the potential for being reverse calculated (under the proper circumstances) to reveal classified information. Since the results had to be presented in an unclassified form, two methods were used to secure the data. The first involved aggregating information into groups so that back calculating is not possible. The second involved presenting data in ranges sufficiently large as to deny meaningful results if back calculated, e.g., pictograms where each shade of gray represents two orders of magnitude of range.

4.3 Comparison with Existing Army Practices

Existing Army requirements for planning a chemical agent operation do not require a risk assessment of the type or scale that was done for the CSDP in support of the Final Programmatic Environmental Impact Statement. Although it is clearly intended primarily for explosives manufacturing operations, DARCOM Regulation 385-3 (1981) requires a hazard analysis for all new DARCOM (now Army Materiel Command) projects that develop facilities. It does specify a criteria for acceptable risk in terms of the probability of not having a catastrophic or critical mishap in 25 years of normal operations. To know if this criteria is met requires the hazard analysis to have some of the properties of a risk assessment (examining a group of hazards for their potential effect and their likelihood of occurrence).

4.4 Use of Multiple Accidents vs. Maximum Credible Event (MCE) Approach

The risk assessment examined a great number of potential accidents and considered frequent contributors of smaller consequences and well as infrequent contributors of larger consequences. The use of the Maximum Credible Event approach, required by DOD 5055.9 and implementing regulations, involves subjectively determining a set of credible accidents within certain guidelines, and selecting from among them the one with the greatest downwind hazard distance. The MCE approach has, based on regulation, a well-defined role for properly locating hazardous operations with respect to the public. If an explosion or spill of chemical agent were to occur, the public effect should be limited because of the distances required by the siting criteria. On the other hand, if two or more alternatives are being compared for "safety," the MCE is clearly not appropriate as the only measure of comparison. It is easy to conceive of a situation where one alternative has a slightly "better" MCE but also has the potential for a much greater number of lesser accidents than the other alternative.

The MCE considers primarily consequence and introduces probability only as a cut-off of "credible" and is thus a less complete measure of risk than, for example, expected fatalities. The risk assessment also was screened for credible accident scenarios, but at a lower level. Thus a

large number of risk contributors was included, not just the maximum contributor. A risk assessment is well suited for comparisons, either of alternatives or of individual hazards for ranking purposes, partially because the effects of inaccurate assumptions are likely to be relatively uniform among the alternatives or hazards. Because of the large number of variables and assumptions, however, it is difficult to regulate a requirement for "satisfactory" risk assessment results.

4.5 Accounting for Uncertainty

Uncertainties in risk estimation arise due to many causes, including the inadequacy of data, inaccuracies in modeling, and the incomplete identification and understanding of accident phenomena. The risk analysis methodology provides for the treatment of uncertainty in the basic hazard data that goes into the analysis. Uncertainty arises in the estimation of both probability and consequences. The uncertainty analysis used in the risk assessment considers probability uncertainty only. The contribution to risk uncertainty of consequence estimation (for example, in estimating potential public fatalities as a result of an agent release) is represented separately (though incompletely) by considering most-likely and worst-case meteorological conditions. The issue of uncertainty is more fully discussed in another paper (Cutler, 1988).

4.6 Risk Measures and Presentation Formats

Selection of the proper risk measure is crucial to a successful risk assessment. It should include both probability and consequence. It should be statistically meaningful and valid when aggregated. The risk measure "expected fatalities" meets these criteria but creates presentation problems when given to audiences that are not used to a probabilistic representation of reality. No one wants to "expect" deaths in a program and just what is a fraction of a death? Other risk-like measures were used to present an indication of the magnitude of the worst accidents or of risk to an individual. This topic is more fully addressed in another paper (Fraize, 1988).

4.7 Tension Between Risk Mitigation and Analysis

Trying to accomplish both functions of a risk assessment (analysis and mitigation) simultaneously creates a tension between the two. If the design is being changed while it is being assessed, it becomes a moving target and opportunities are created for overlooking risk. The design change to mitigate one hazard may introduce another in such a manner as to not be addressed in the risk assessment. A more detail discussion is given in another paper (Price, 1988).

4.8 Application of D2PC

The D2PC atmospheric dispersion model program is too slow and the input/output structure is inappropriate for running the thousands of times required for the risk assessment. Therefore, both the evaporation calculations and the downwind hazard calculations were modeled for the two specific weather conditions used in the risk assessment--most likely and worst case. In all, 12 polynomial formulas for calculating evaporation rates for different agent types, meteorological conditions, and types of surface, were developed using multiple linear regression to determine the polynomial coefficients. The downwind hazard calculations required 60 polynomial formulas for calculating distances to lethal concentrations as functions of agent type, release mode and duration, quantity released to the atmosphere, meteorological conditions, and fatality rate. Details of the application of D2PC to the risk assessment are given in another paper (Cutler, 1988).

5.0 Recommendations

Based on the lessons learned in conducting this risk assessment, the following recommendations are made to other risk assessors for similar programs:

1. Identify methodology issues and appropriate assumptions as early as possible in the risk assessment process. Document the issues and assumptions to reduce miscommunication. A small change in an assumption (e.g., evaporation temperature) can ripple through an enormous number of calculations.

2. Establish quality control and audit trail procedures on incoming data and changes. A small error in the evaporation equation coefficients does a great deal of damage downstream. Changes and error corrections to input data should be well documented so that they can be reversed if necessary.

3. Use as much computer automation as possible. The number of calculations required is substantial. Programmable, relational data bases offer a good way to manipulate a lot of data without writing programs from scratch.

4. Once the risk assessment is complete, extend it into a risk management tool by keeping it updated with design and procedure changes, i.e., resulting from mitigation or improved data.

5. If more than one risk assessment for chemical operations is going to be done within an organization (such as the Army), establish at least some degree of conformity among methodology issues and assumptions. A great deal of energy and resources can be spent resolving these issues. This conformity should exist in three areas:

   a. Methodology--Selection of common measures of risk and screening levels

   b. Assumptions--Meteorological data, spill amounts, degree of specificity

   c. Format--Location of basic assumptions and issues to assist in ready comparability with other risk assessments, standard meanings and terminology

REFERENCES

Cutler, R.M. (August 1988), *The Application of the D2PC Dispersion Model to Large Release of Chemical Agents*, McLean, VA: The MITRE Corporation, presented at the 23rd DoD Explosives Safety Seminar.

Cutler, R.M. and St. Pierre, G. (August 1988), *Hazards and Risks of the Disposal of Chemical Munitions Using a Cryogenic Process*, McLean, VA: The MITRE Corporation, presented at the 23rd DoD Explosives Safety Seminar.

Department of Defense 6055.9, (July 1984), *Ammunition and Explosives Safety Standards*.

Fraize, W.F. (August 1988), *The Presentation of Risk to the Public--Alternative Measures and Formats*, McLean, VA: The MITRE Corporation, presented at the 23rd DoD Explosives Safety Seminar.

GA Technologies Inc. (August 1987a), *Risk Analysis of the Onsite Disposal of Chemical Munitions*, GA-C18562, prepared for the U.S. Army, Office of the Program Executive Officer-Program Manager for Chemical Demilitarization. SAPEO-CDE-IS-87010.

GA Technologies Inc. (August 1987b), *Risk Analysis of the Disposal of Chemical Munitions at National or Regional Sites*, GA-C18563, prepared for the U.S. Army, Office of the Program Executive Officer-Program Manager for Chemical Demilitarization. SAPEO-CDE-IS-87008.

GA Technologies Inc. (August 1987c), *Risk Analysis of the Continued Storage of Chemical Munitions*, GA-C18564, prepared for the U.S. Army, Office of the Program Executive Officer-Program Manager for Chemical Demilitarization. SAPEO-CDE-IS-87009.

Kartachak, T.S. (August 1988), *Significant Hazards and Risks of the Chemical Stockpile Disposal Program*, U.S. Army Program Executive Office-Program Manager for Chemical Demilitarization, presented at the 23rd DoD Explosives Safety Seminar.

Perry, R.B. and Duff, W.W. (August 1988), *Risk Mitigation for the Chemical Stockpile Disposal Program: Identification of Opportunities and Estimation of Potential Benefits*, McLean, VA: The MITRE Corporation, presented at the 23rd DoD Explosives Safety Seminar.

Price, B.H. (August 1988), *The Tension Between Risk Assessment and Risk Mitigation*, McLean, VA: The MITRE Corporation, presented at the 23rd DoD Explosives Safety Seminar.

REFERENCES (Concluded)

U.S. Army Materiel Development and Readiness Command (now Army Materiel Command) Regulation 385-3, (16 November 1981), *Hazard Analysis for Facilities, Equipment and Process Developments*.

U.S. Army Program Executive Office-Program Manager for Chemical Demilitarization (1987), *Risk Analysis in Support of the Chemical Stockpile Disposal Program*, MTR87W00230, The MITRE Corporation, December 1987, SAPEO-CDE-IS-87014.

U.S. Army Program Executive Office-Program Manager for Chemical Demilitarization (January 1988), *Chemical Stockpile Disposal Program, Final Programmatic Environmental Impact Statement*.

U.S. Army Toxic and Hazardous Materials Agency, (15 March 1986), *Chemical Stockpile Disposal Concept Plan*, AMXTH-CD-PR-85047.

Whitacre, C.G. et al. (1987), *Personal Computer Program for Chemical Hazard Prediction*, CRDEC-TR-87021, Aberdeen Proving Ground, MD: Chemical Research, Development & Engineering Center.

THE APPLICATION OF THE D2PC DISPERSION MODEL TO LARGE RELEASES OF CHEMICAL AGENTS

by
Robert M. Cutler
The MITRE Corporation
McLean, Virginia
and
Thomas S. Kartachak
Office of the Program Executive Officer
Program Manager for Chemical Demilitarization
United States Army
Aberdeen Proving Ground, Maryland

for
Department of Defense
Twenty-third Explosives Safety Seminar
Atlanta, Georgia
9-11 August 1988

ABSTRACT

The generalized use of the U.S. Army's D2PC atmospheric dispesion model is described. The inputs to the model included characterizations of hypothetical accident scenarios during the chemical demilitarization program. The accidents were assumed to release agent GB, HD, or VX in a quantity that could be lethal to members of the general public. The model was used to estimate spill evaporation times, lethal distances, fatality rates, plume widths, and public fatality counts. Although no such accidents are expected, this modeling is useful in the comparative assessment and mitigation of the risks of implementing alternative programs at various locations.

I. INTRODUCTION

A. General

The Department of Defense was directed by Congress (Public Law 99-145, Title 14, Part B, Section 1412) to destroy the stockpile of lethal unitary chemical agents and munitions in such a manner as to provide maximum protection to the general public. In order to define and manage the potential for an acute, catastrophic release of chemical agent into the atmosphere, risk analysis and mitigation was undertaken. The background of the destruction program and the details of the risk analysis are described fully in other papers but are only summarized below, in order to orient the reader prior to the presentation of the subject of this paper--the treatment of uncertainty in a comparative risk assessment.

In response to the requirements of Public Law 99-145, by March of 1986 the Army had produced a conceptual plan for the destruction of the lethal chemical stockpile by 1994. The plan for the Chemical Stockpile Disposal Program (CSDP) included three alternatives:

1. On-site destruction of the chemical stocks at their present storage locations.

2. Movement of the chemical stocks by rail to two regional center for chemical destruction.

3. Movement of the chemical stocks by rail to one national center for chemical destruction.

In July of 1986 a Draft Programmatic Environmental Impact Statement (DPEIS) was issued, to be followed in January of 1988 by a Final Environmental Impact Statement (FPEIS). Two additional alternatives were described in the FPEIS:

4. Movement of the chemical stocks by air from two of the present storage sites to a national center, and on-site destruction of the remaining chemical stocks at their present storage locations.

5. Continued storage of the stocks at their present locations for 25 more years.

Each of the five programmatic alternatives was defined as a composite of various activities. The classes of activities included:

1. Storage, both long-term in magazines, warehouses and yards; and short-term in containers awaiting off-site shipment.

2. Handling, for inspection and maintenance during long-term storage; for removal from long-term storage and loading for transport; and for unloading and delivery at destruction plants.

3. On-site transport by truck.

4. Off-site transport by rail.

5. Off-site transport by air

6. Plant operations for destruction of the chemical agents

The risk entailed in each activity was characterized by a representative set of accident scenarios. Each accident scenario is a hypothetical sequence of events beginning with an initiator

(for example, an earthquake), followed by intermediate occurrences (for example, release of the chemical, ignition of the chemical, failure of the fire suppression system, and failure of the containment structure), and ending with a lethal release of chemical agent to the atmosphere.

The Army's D2PC model was applied to each accident scenario in order to estimate lethal downwind distances, fatality rate (as a function of downwind distance), individual risk, and public fatality count. The results depend on the type of chemical agent that is released, the quantity released, the mode of release (for example, detonation of a chemical munition, evaporation of a spill, or incomplete combustion in a fire), and the duration of the release. The results also depend on atmospheric dispersion phenomena, on the toxicological characteristics of the chemical agent, and on the population downwind of the release. Two types of meteorological conditions were considered--"most likely" conditions and "worst-case" conditions. Otherwise, the possible variations and uncertainties of the results were not quantified.

B Agent Releases

The data describing hypothetical releases of lethal chemical agent were limited to a small number of parameters that were considered essential for subsequent dispersion calculations. First, the type of agent, whether GB or HD (used in this analysis to represent all three types of mustard: H, HD, and HT) or VX, was specified because of the importance of both volatility and lethality in the calculations. Next, the quantity released was specified for each of three release modes: spill (requiring the calculation of the amount that would evaporate), detonation, or other (for example, incomplete combustion in a fire, or inadvertent venting from a process). The final release parameter was the duration of the release, which was specified because of the importance of both time available for spill evaporation and human exposure time (which affects lethality). Additional, implicit release specifications included spill environment (since indoor evaporation of spills was pre-calculated and listed as an "other" mode release) and spill surface (since the surface type, whether gravel or non-porous, was deduced from the activity type encoded in the accident scenario description).

C. The D2PC Model

The D2PC model is an analytical Gaussian atmospheric dispersion formulation, modified for mixing layer height and wooded terrain effects, that processes lethal chemical agent release data and meteorological data in order to obtain estimates of downwind lethal distances. In addition to D2PC's Gaussian plume

calculations, the model is used to calculate detonation yield, spill evaporation due to forced or natural convection, vapor depletion on the ground, and the probability of a fatal exposure at any location due to the combined effects of agent inhalation and aerosol deposition on exposed skin. The D2PC model is fully described in its user's manual (Whitacre *et al*, 1987) and is available from the U.S. Army.

D. Prior Applications

The primary use of the D2PC model in the past has been for ensuring the safe siting and scheduling of Army activities involving lethal chemical agents. For this purpose, Maximum Credible Events (MCEs), which represent the largest accidental releases that could reasonably be expected, are postulated and modeled. These MCEs typically involve detonations of one or a few burstered munitions, or spills of the partial or entire contents of one to several bulk (non-burstered) items. Worst-case nighttime meteorological conditions are often assumed to be an atmospheric stability class of F (very stable) and a wind speed of 1 meter per second. For operations that are limited to the daytime, the worst-case stability class is often assumed to be D (neutral). Since detonations of munitions containing VX are taken to release 87 percent aerosol (and 13 percent vapor) in the D2PC model, and since the VX aerosol's transport and skin deposition is assumed to increase with wind speed, a higher wind speed of 8-10 meters per second is often used in such cases. Mixing layer heights are selected within the D2PC model as a function of the site name, the season, and the stability class. The wooded terrain plume parameters (height and width) are often used at the Pine Bluff Arsenal (PBA) site. The model's one percent lethality distance output is compared to the minimum distance from the MCE to the site boundary in order to determine whether the distance is sufficient to protect the public. If necessary to ensure public safety, the activity can be restricted to certain stability classes, wind speeds, or wind directions (corresponding to increased distances to boundary lines).

II. METHODOLOGY

A. Overview

The CSDP risk analysis required that the D2PC model's use be generalized in order to facilitate its application to many hundreds of hypothetical accident scenarios involving many different types of munitions, agents, release modes, and sites. Furthermore, the analysis required that catastrophic accidents with long-distance lethal impacts be considered, with varying fatality rates in the

plumes, and with aerosol evaporation and agent depletion on the ground playing significant roles. On the other hand, in consideration of the inaccuracies inherent in accident scenario release characterizations and in accident frequency estimates (typically having 95-percentile or upper bound estimates of about 10 to 100 times the median or best estimates), accuracy in modeling was considered less important than simplicity of solution and ease of execution. These considerations led to the technical approach described below. Note that, though many of the accident scenarios modeled were site-specific, the dispersion modeling approach described is not site-specific in any way.

B. Meteorological Conditions

Two basic types of meteorological conditions were considered in the analysis, but they should not be confused with the worst-case daytime and worst-case nighttime conditions used in MCE evaluations. In the present analysis, the two conditons are "most-likely" conditions and "worst-case" conditions, defined as follows. Most-likely conditions were chosen to be representative of the effective average of the full range of possible conditions. They could thus be used in combination with the best estimates of accident scenario frequencies in order to obtain best estimates of risk parameters (such as the "expected fatality values," which are based on products of accident frequency estimates and public fatality count estimates). Specifically, the most-likely conditions were chosen as stability class D, wind speed 3 meters per second, and temperature of 20°C.

Worst-case conditions were input to the D2PC model in order to answer questions about the possibility of each accident scenario having a lethal public impact (even if not under most-likely conditions), about the maximum lethal distance that could result from any alternative or activity at any location, and about the maximum public fatality count that could result. Maximum lethal distances and fatality counts proved to be useful for emergency planning purposes. However, results of the worst-case modeling were not factored into the development of expected fatality data and risk curves, since these were based on most-likely conditions assumed to represent an average of all possible conditions. Specifically, the worst-case conditions were chosen as stability class E (moderately stable), wind speed 1 meter per second, and temperature of 30°C.

At all sites and at all times, the height of the mixing layer was chosen to be 750 meters, the Frost exponent of the wind speed power law was taken to be 0.25, and the surface roughness length was taken to be 1 cm.

C. Evaporation of Spills

The modeling process was greatly simplified by separating the treatment of spill evaporation from the treatment of subsequent atmospheric dispersion. Spill evaporation times as functions of spill mass were computed for both meteorological conditions, for all three agent types, and for three combinations of the activity-dependent spill location and surface type (indoor/non-porous, outdoor/non-porous, and outdoor/gravel). The resulting data were curve-fit to polynomial forms for the purpose of further data processing. For any accident which would result in a spill that would evaporate in less time than the accident "duration" (e.g., time for response and clean-up), the duration was reduced to the evaporation time. For any spill that would not evaporate within the "duration," the mass that would evaporate was calculated by multiplying the mass spilled times the "duration" and dividing the result by the time for complete evaporation. Then, the mass evaporated was added to the mass otherwise emitted (if any).

D. Release Modes

Other than the spills described above, two release modes were used in this analysis: detonations and other releases. For detonations of munitions containing HD or VX, exploratory runs of D2PC in its still-air evaporation mode led to the conclusion that aerosols would either evaporate during transport toward off-site population centers, or would be deposited on the ground and subsequently evaporate in a short time. Aerosol evaporation rates are shown in Figure 1. As a result of this situation, all detonations of HD and VX munitions were treated the same as amounts evaporated from spills and amounts otherwise emitted. The quantities were added and treated as a single release by the "semi-continuous" mode, with the duration being two minutes where detonations contribute, or as indicated for the scenario otherwise.

Since all GB releases, whether by detonation or otherwise, are treated as vapors rather than as aerosols within the D2PC model, GB detonations were the only detonations that were evaluated by using D2PC's instantaneous release mode for non-munitions (omitting D2PC's encoded yields for specific munitions--yields which were found to exceed 100 percent at input temperatures representative of munitions in the fires that were assumed to heat the munitions to their detonation temperatures). Combined detonations of GB and other releases of GB were treated as instantaneous releases of the combined mass of the release. Other releases of GB were evaluated using the D2PC model's semi-continuous mode, subject to a minimum duration of two minutes.

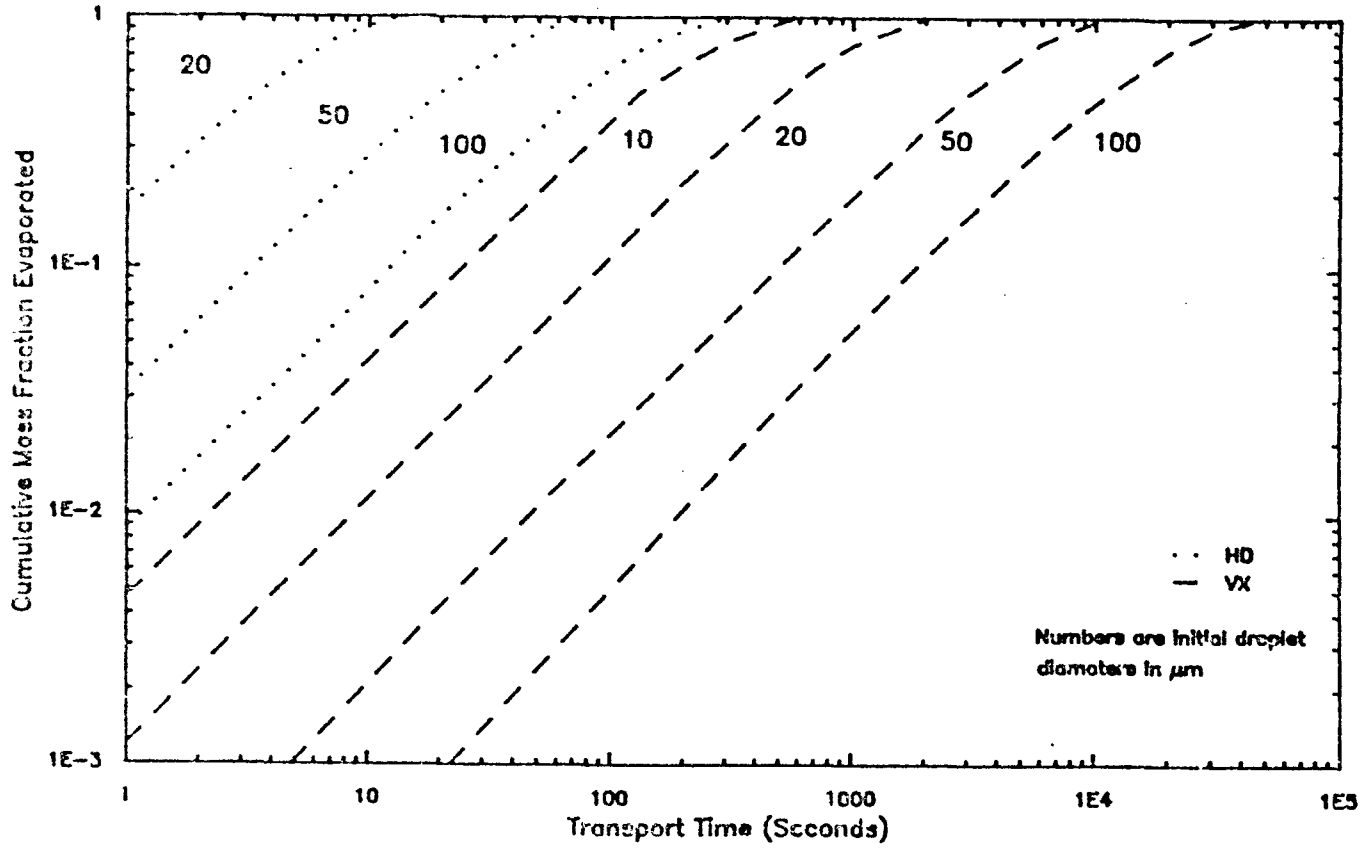

FIGURE 1
AGENT HD & VX AEROSOL EVAPORATION
BASED ON D2PC MODEL

E. Lethal Distances and Areas

In order to facilitate the evaluation of many hundreds of accident scenarios without running the D2PC program for each scenario, we evaluated a limited number of cases using the D2PC model and varying the mass of the release, and we represented the resulting lethal distances as polynomial functions of release quantity. Three fatality rates were considered--zero percent (determined by the "no-deaths" exposures in the D2PC code), one percent (also determined by the D2PC code), and 50 percent (determined by using corresponding exposures as inputs to D2PC--70 mg-min/m^3 for GB, 1500 mg-min/m^3 for HD, or 30 mg-min/m^3 for VX). The only finite release durations considered were 2, 10, 60, and 360 minutes--with the intent that any other durations be decreased to the next lower of these standardized durations. Since agent HD effects are not duration-dependent, the number of polynomial formulae required was 60 (two meteorological conditions times three fatality rates times ten agent-duration combinations--five for GB, one for HD, and four for VX).

Plume widths (lethal area dimensions that are perpendicular to the wind) under most-likely meteorological conditions were required for the estimation of risk at any specified distance from the point of release, and for the estimation of affected areas. Exploratory runs of D2PC led to the conclusion that the width of the plume equivalent to one of constant, maximum exposure could be expressed as $9.13^{\circ}/(\text{Distance in km})^{0.1}$. The results obtained by using this expression are obvious, and are not presented in this paper.

F. Fatality Rates and Counts

In order to estimate risk at specified standard distances (0.1, 0.2, 0.5, 1, 2, 5, 10, 20, 50, and 100 kilometers), we assumed that a 100 percent fatality rate would apply at the point of release, and we linearly interpolated between the 0, 1, and 50 percent fatality rates corresponding to distances obtained by using the polynomial formulae.

In order to estimate public fatality counts, we used the "no-deaths" distances from our polynomial formulae in combination with a fatality count table developed for this purpose by Oak Ridge National Laboratory. We used this table by increasing each non-zero, non-standard "no-deaths" distances to the next higher standard distance. For example, for the purpose of estimating fatalities, an accident with a 3.4 kilometer "no-deaths" distance was treated as a 5 kilometer accident.

III. RESULTS

A. Evaporation Time Curves

The evaporation time curves for the three agents are shown in Figures 2-4. Agent GB evaporates relatively quickly. Agent HD evaporates more slowly. Agent VX evaporation is exceedingly slow.

B. Lethal Distance Curves

The lethal distance curves for all of the agents, release modes, meteorological conditions, and fatality rates considered are shown in Figures 5-20. Agent VX releases result in the greatest lethal distances. For agent GB, distances are somewhat shorter. For agent HD, distances are much shorter. Shorter-duration releases result in greater lethal distances for agents GB and VX; for agent HD, the duration of the release has no effect. As expected, worst-case distances exceed most-likely distances. "No-deaths" distances are somewhat greater than one percent fatality rate distances, which greatly exceed 50 percent fatality rate distances.

C. Fatality Count Tables

Representative fatality count estimates are shown in Tables 1-2. As expected, fatality count estimates increase rapidly with increasing "no-deaths" distance. A less obvious result, not shown on the tables, is that fatality count estimates for most-likely conditions exceed the corresponding counts for worst-case conditions (for identical population distributions, whether average or maximum). This is attributed to the wider plume characteristic of most-likely conditions. Nevertheless, a specified agent release quantity can be seen from the lethal distance figures to result in a much greater lethal distance under worst-case conditions, increasing the worst-case fatality count above the most-likely count for the shorter plume.

Another unexpected result is that, for great "no-deaths" distances, the fatality count estimates for releases at less densely populated locations may exceed the corresponding estimates for releases at more densely populated locations nearby. This can occur at Tooele Army Depot (TEAD) in comparison to Salt Lake City, and at Aberdeen Proving Ground (APG) in comparison to Baltimore. This result is attributed to the plume width's increase with distance. For example, a very massive release in Salt Lake City may result in a narrow, concentrated plume in the city; but the same release at TEAD may result in a much wider plume in Salt Lake City.

IV. CONCLUSIONS AND RECOMMENDATIONS

A generalized approach for the application of the D2PC model to a large number of hypothetical accident scenarios has been developed. In the course of this work, several interesting facts have come to light. Perhaps the most important of these is that the aerosols generated by detonations of HD and VX munitions can be expected to evaporate during atmospheric transport toward areas occupied by the general public. Regarding future applications of D2PC to large numbers of accident scenarios, a generalized approach such as the one described in this paper should be considered if great precision is not required in the results, and if the number of combinations of agent types, release modes, meteorological conditions, fatality rates, etc. is not excessive. The obvious alternative approach to be considered is the modification of the D2PC model so that it can be run efficiently using the accident scenario data base to be evaluated.

REFERENCES

Fraize, W.E. *et al.* (December 17, 1987). *Risk Analysis Supporting the Chemical Stockpile Disposal Program (CSDP)*, MTR-87W00230, McClean, VA: The MITRE Corporation, prepared for the U.S. Army, Office of the Program Executive Officer--Program Manager for Chemical Demilitarization, Aberdeen Proving Ground, MD.

GA Technologies, Inc. (August 1987a). *Risk Analysis of the Continued Storage of Chemical Munitions*, GA-C18564, San Diego, CA.

GA Technologies, Inc. (August 1987b). *Risk Analysis of the Disposal of Chemical Munitions at National or Regional Sites*, GA-C18563, San Diego, CA.

GA Technologies, Inc. (August 1987c). *Risk Analysis of the Onsite Disposal of Chemical Munitions*, GA-C18562, San Diego, CA.

U.S. Army, Program Manager for Chemical Demilitarization (July 1, 1986a). *Chemical Stockpile Disposal Program--Draft Programmatic Environmental Impact Statement*, Aberdeen Proving Ground, MD.

U.S. Army, Program Executive Officer--Program Manager for Chemical Demilitarization (January 1988). *Chemical Stockpile Disposal Program--Final Programmatic Environmental Impact Statement*, Aberdeen Proving Ground, MD.

U.S. Army Toxic and Hazardous Materials Agency (March 15, 1986b). *Chemical Stockpile Disposal Concept Plan*, AMXTH-CD-FR-85047, Aberdeen Proving Ground, MD.

Whitacre, C.G. *et al.* (1987). *Personal Computer Program for Chemical Hazard Prediction*, CRDEC-TR-87021, Aberdeen Proving Ground, MD.

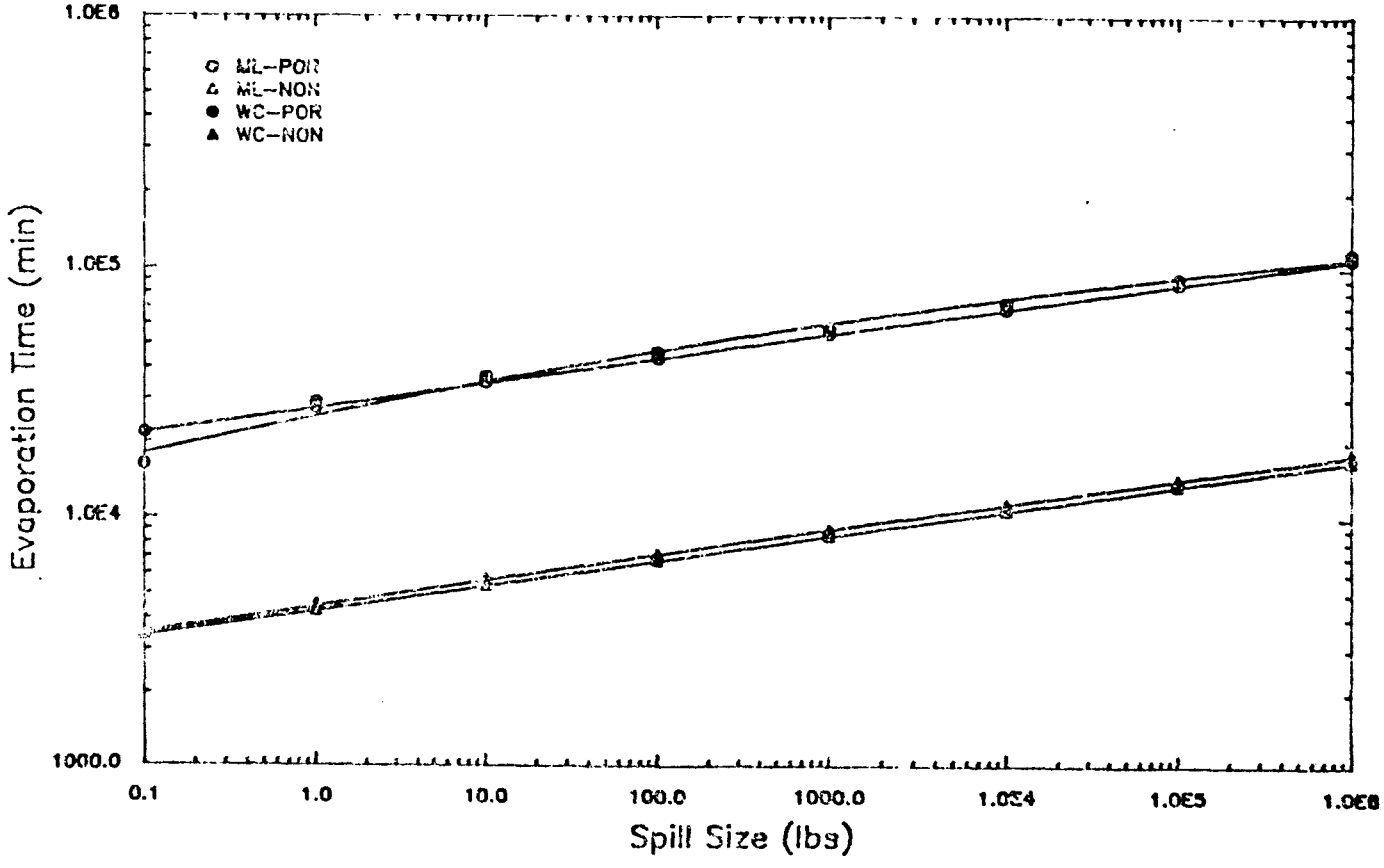

FIGURE 2
EVAPORATION OF HD

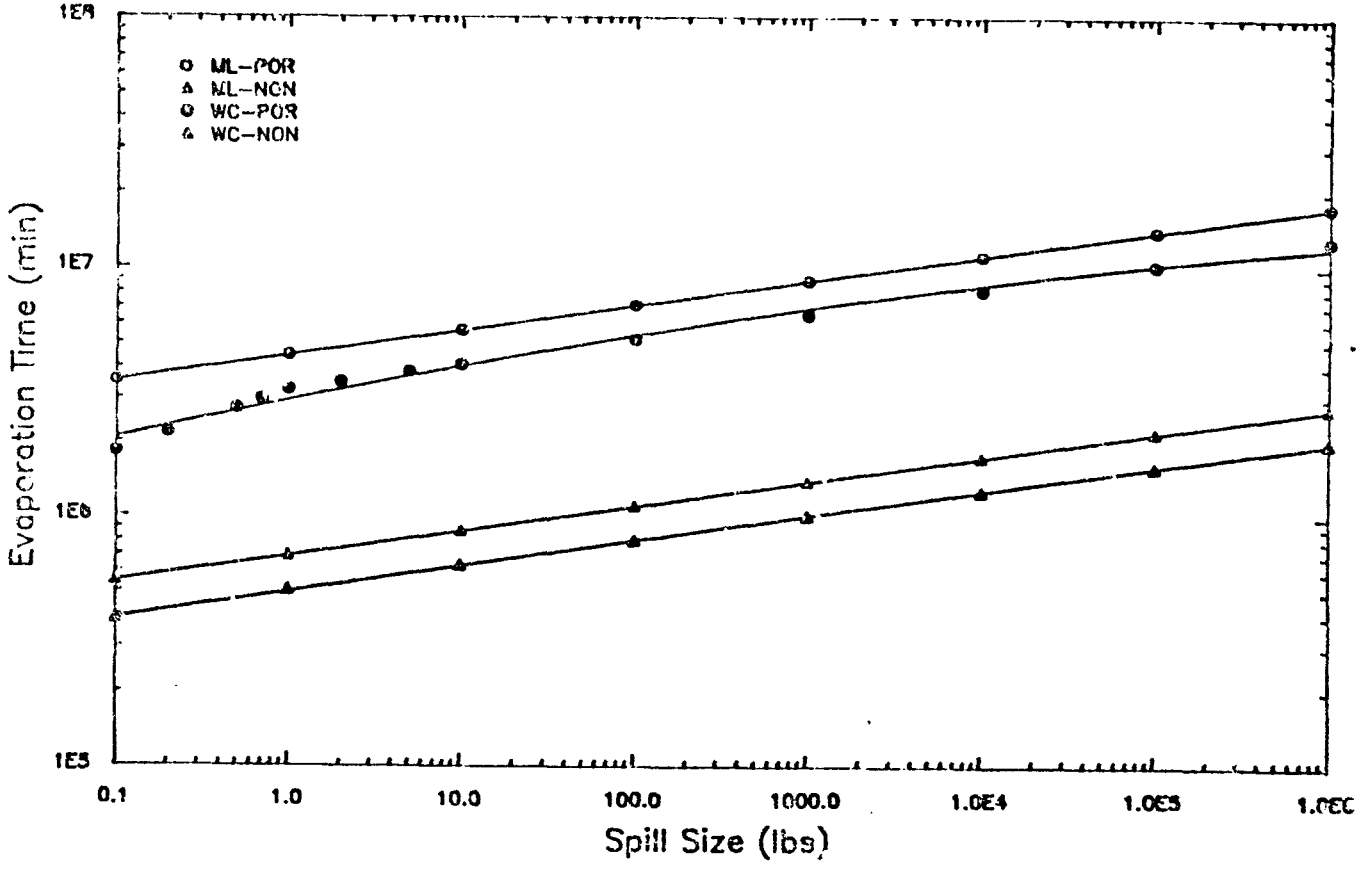

FIGURE 3
EVAPORATION OF VX

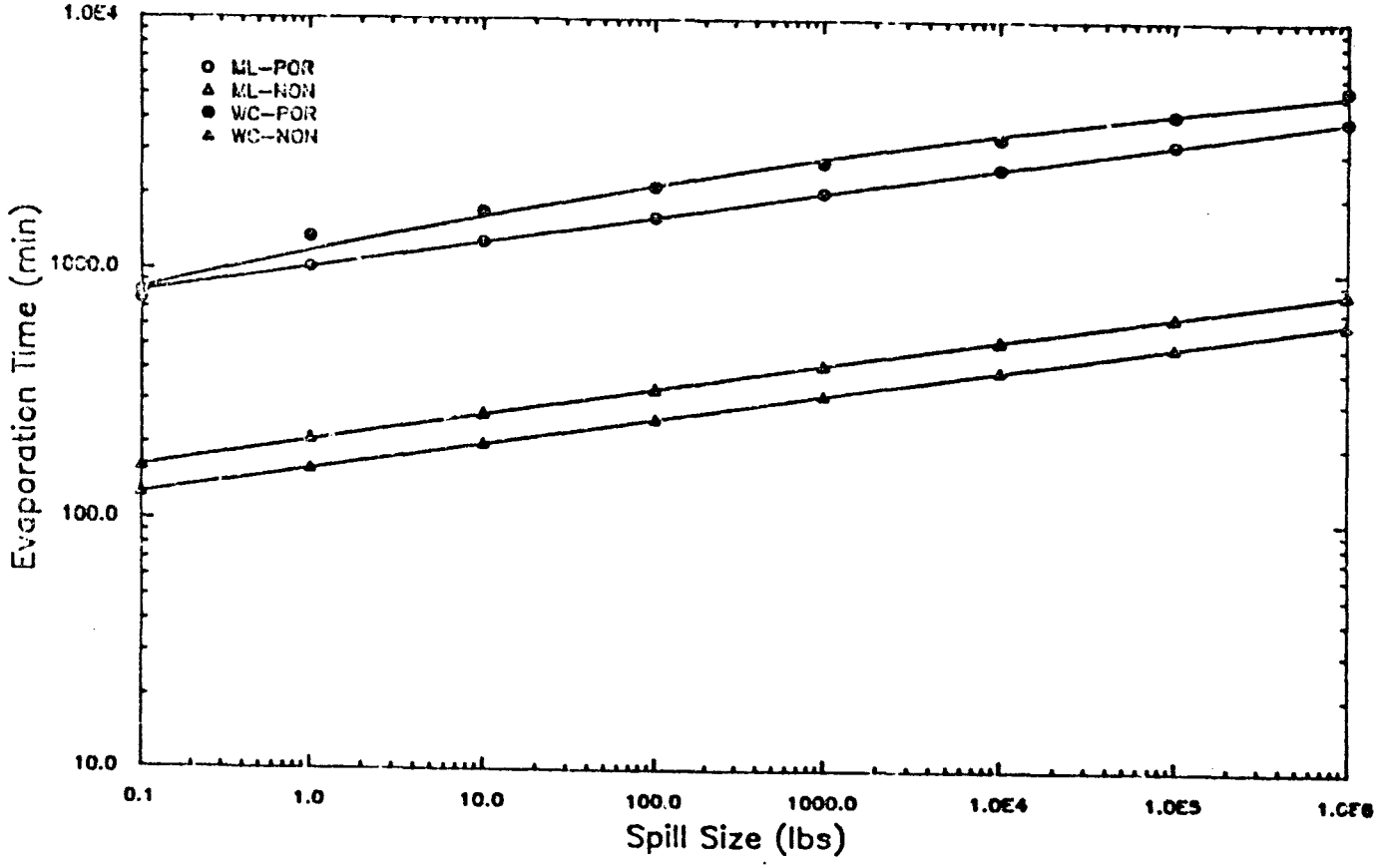

FIGURE 4
EVAPORATION OF GB

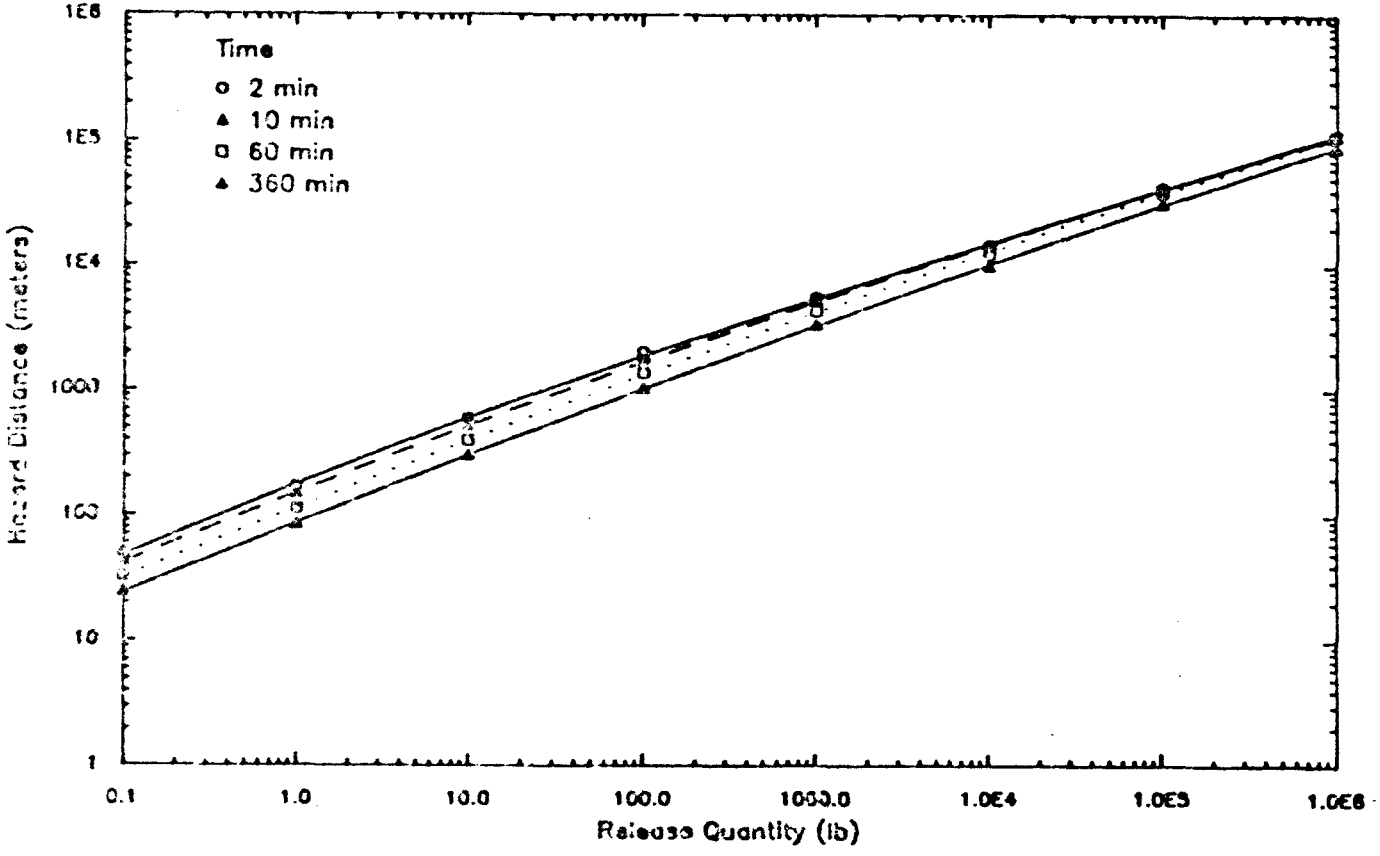

FIGURE 5
HAZARD DISTANCES FOR GB
F/L Weather, 0% Lethality
Semicontinuous Release Mode

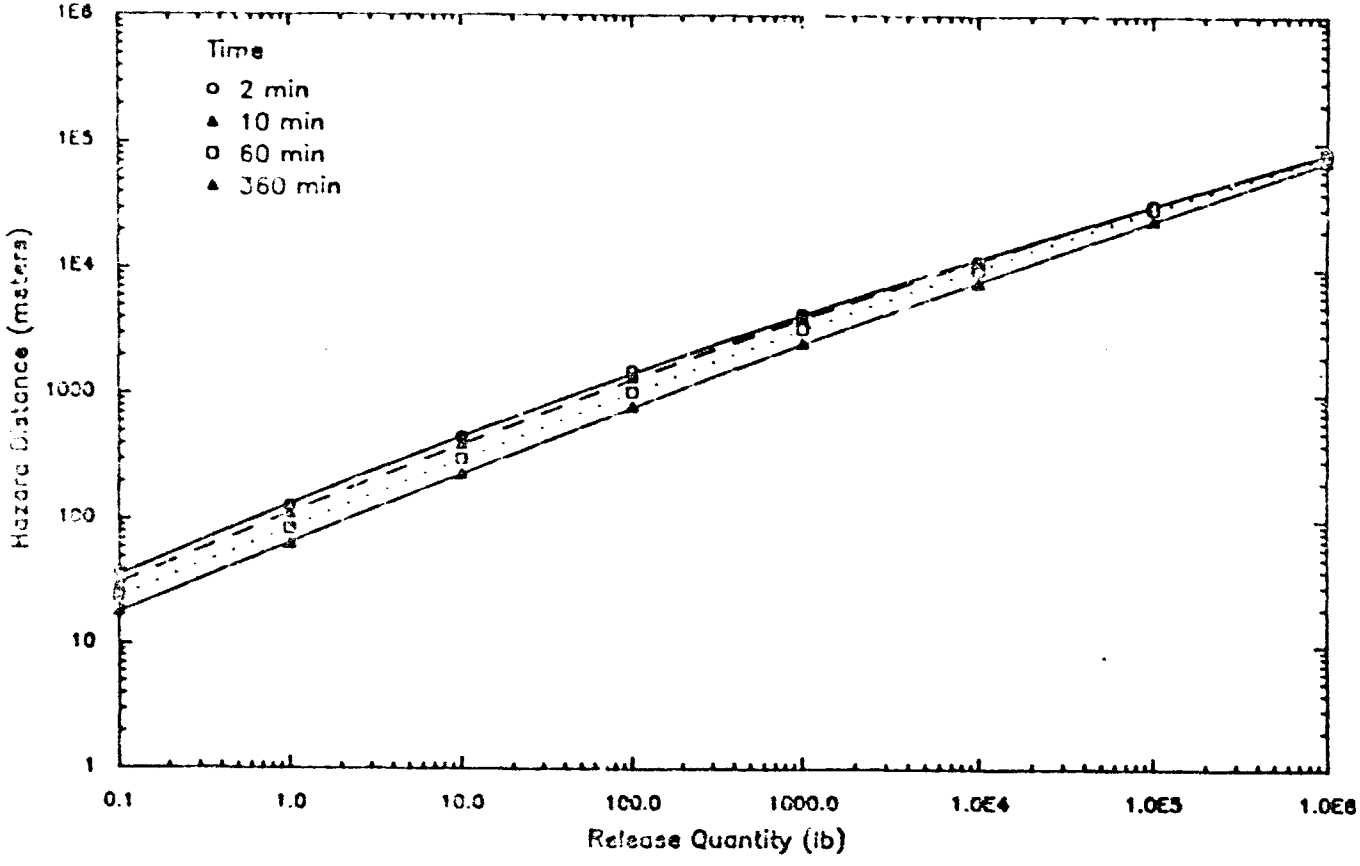

FIGURE 6
HAZARD DISTANCES FOR GB
ML Weather, 1% Lethality
Semicontinuous Release Mode

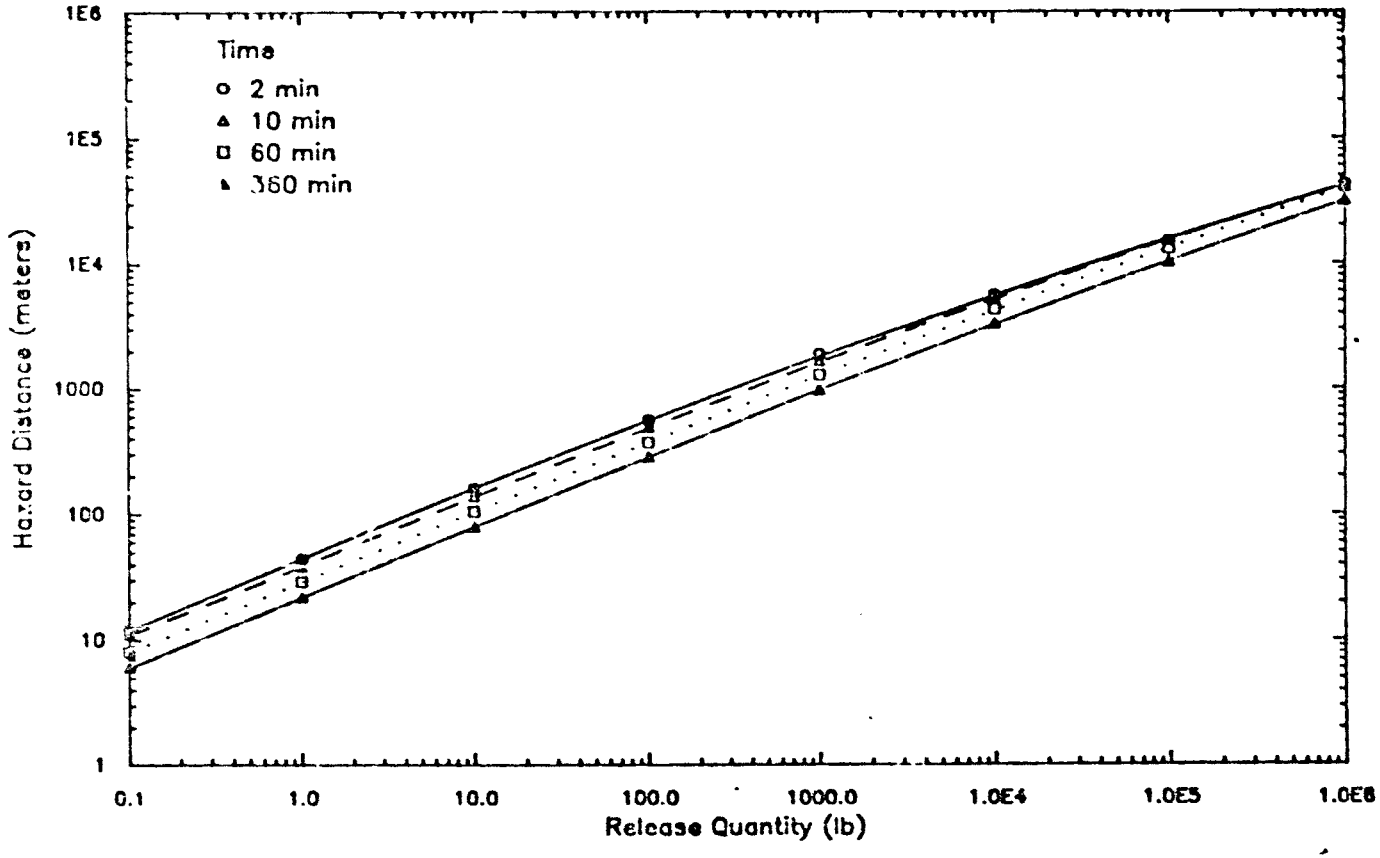

FIGURE 7
HAZARD DISTANCES FOR GB
ML Weather, 50% Lethality
Semicontinous Release Mode

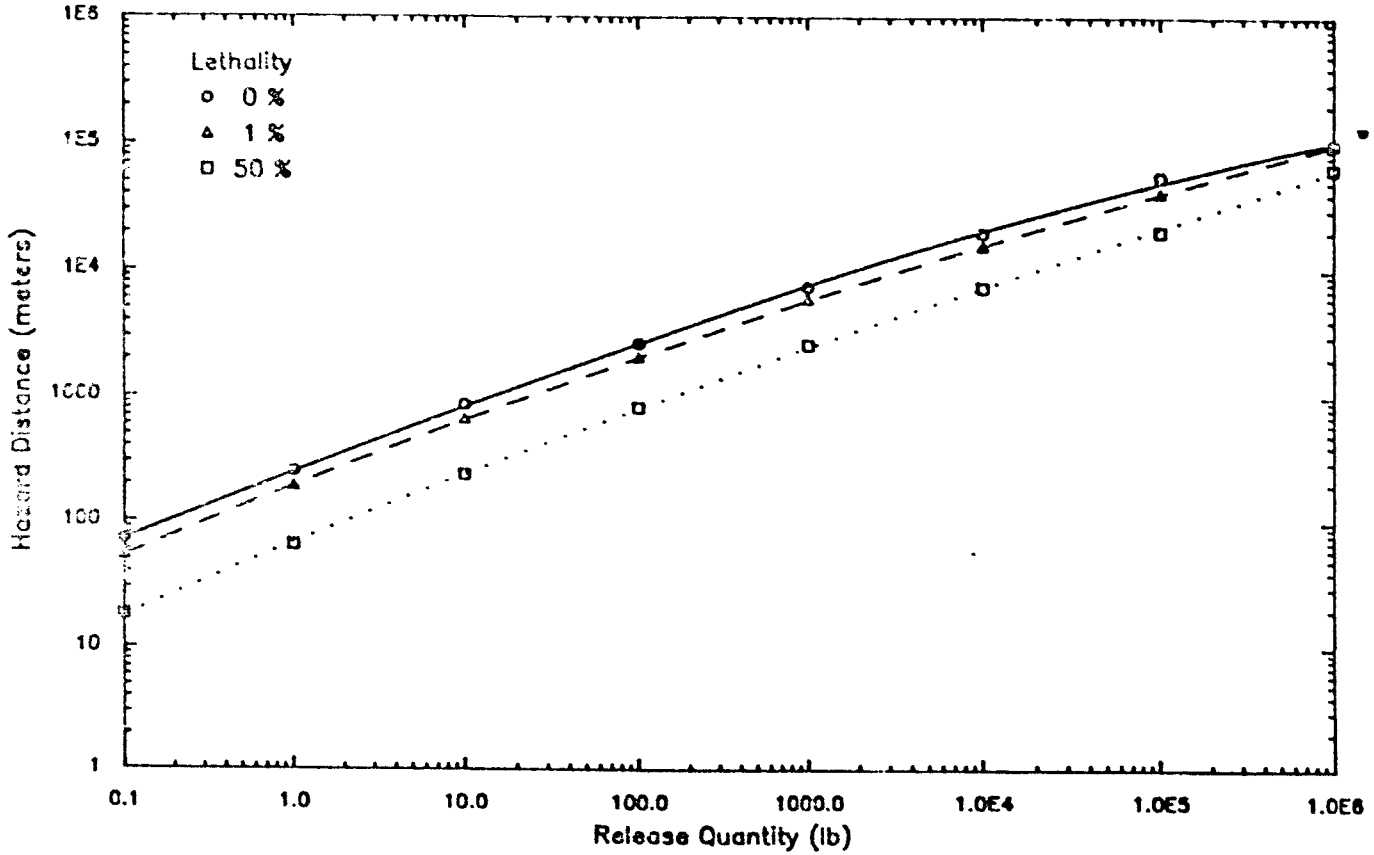

FIGURE 8
HAZARD DISTANCES FOR GB
ML Weather, 0%, 1%, and 50% Lethality
Instantaneous Release Mode

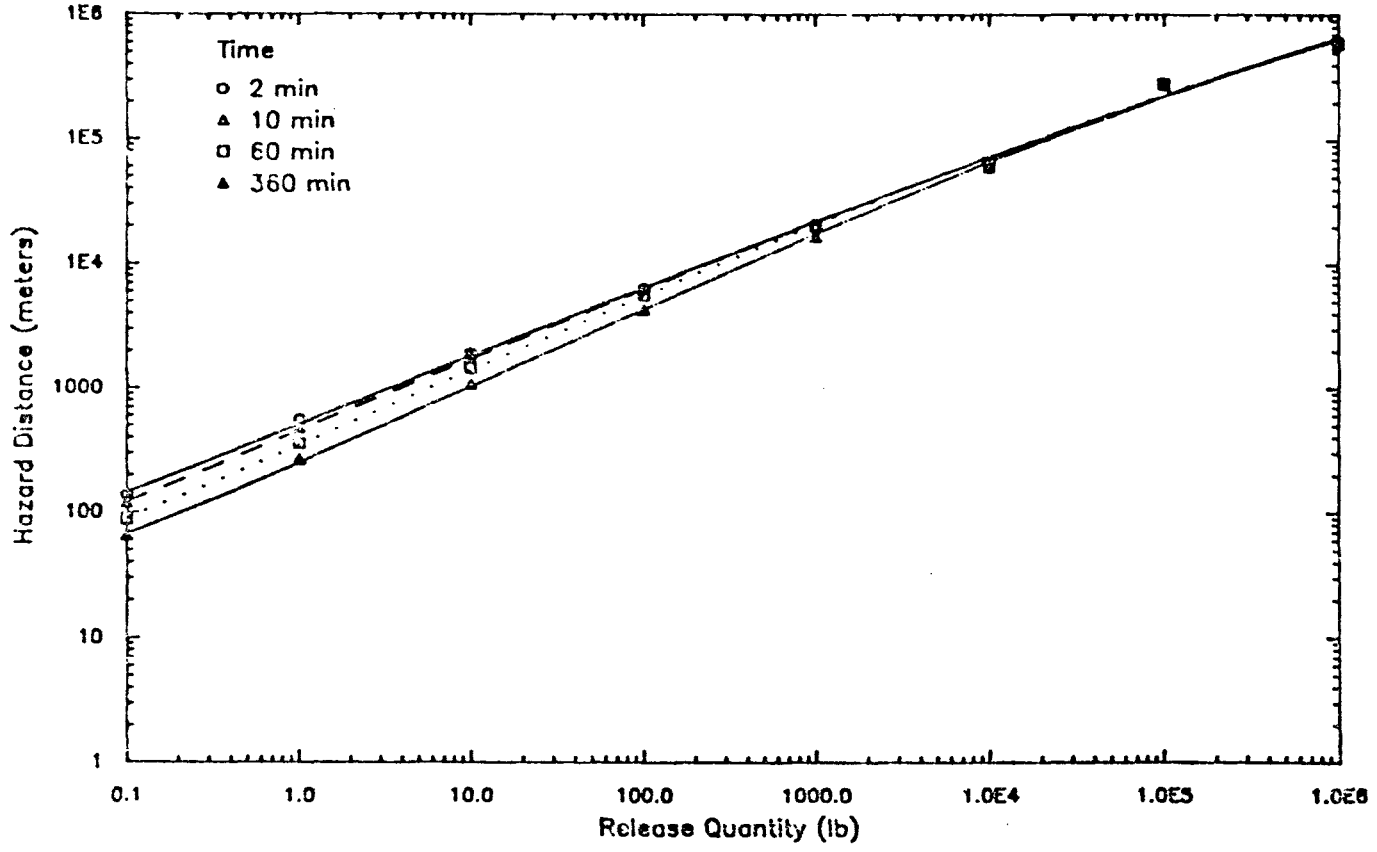

2069

FIGURE 9
HAZARD DISTANCES FOR GB
WC Weather, 0% Lethality
Semicontinuous Release Mode

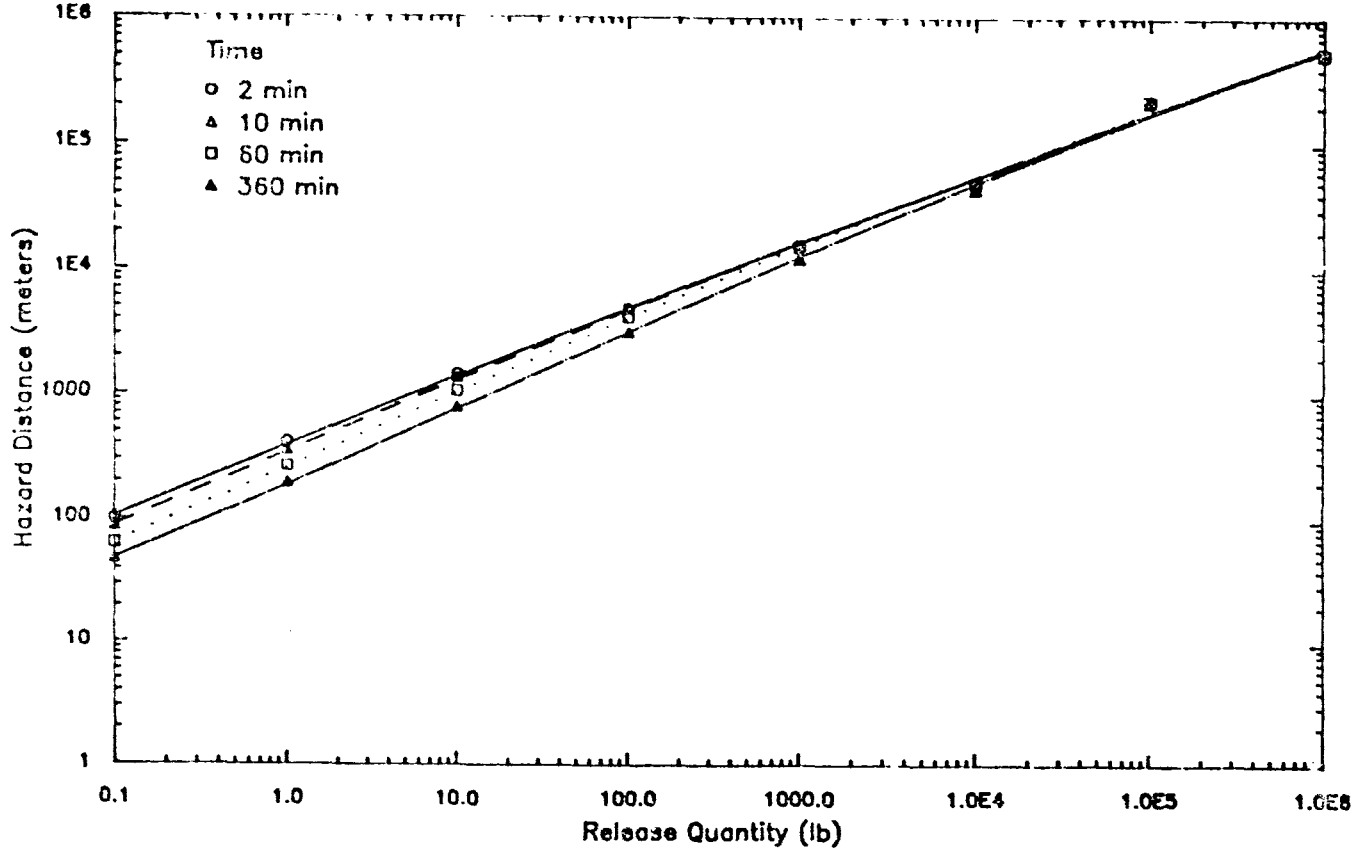

FIGURE 10
HAZARD DISTANCES FOR GB
WC Weather, 1% Lethality
Semicontinuous Release Mode

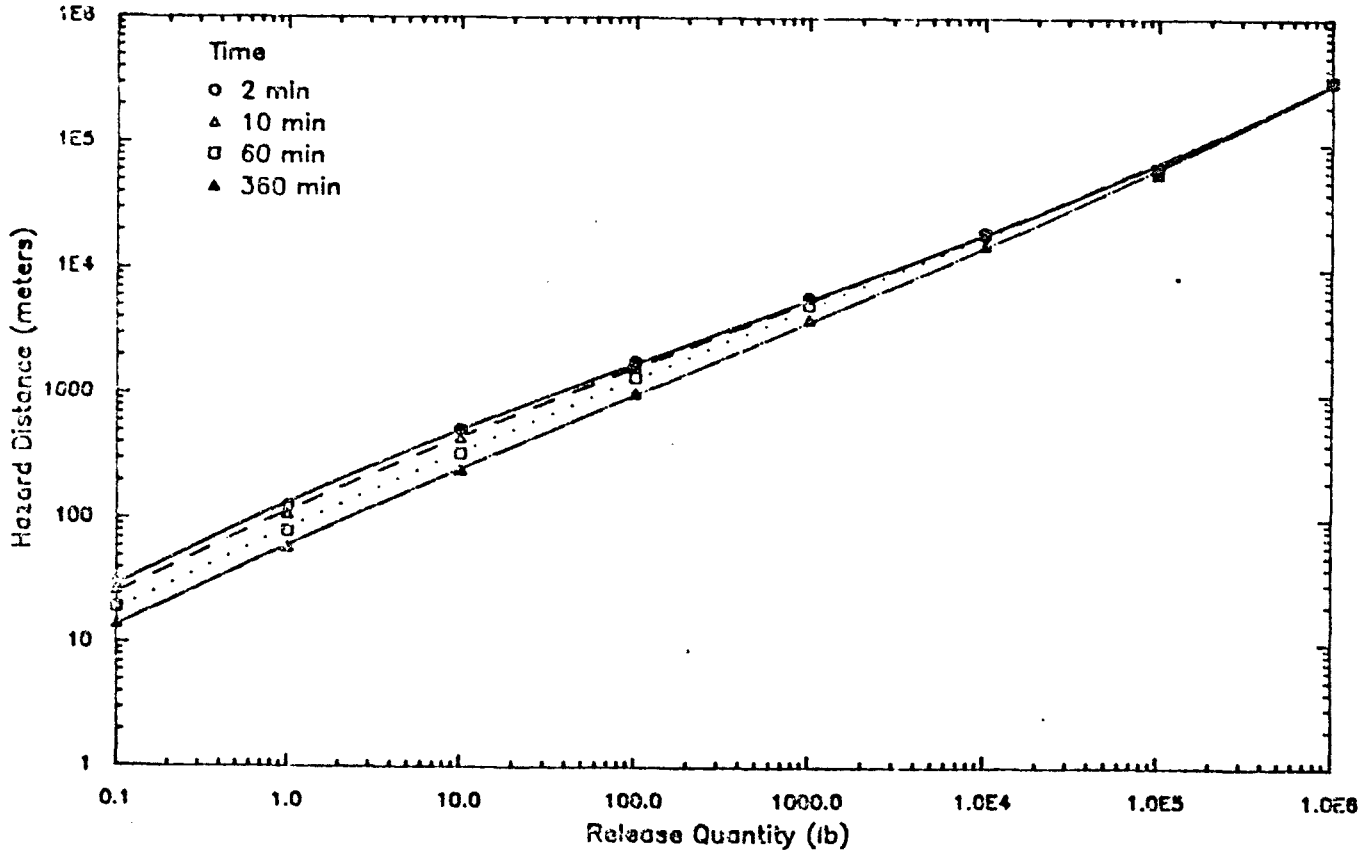

FIGURE 11
HAZARD DISTANCES FOR GB
WC Weather, 50% Lethality
Semicontinuous Release Mode

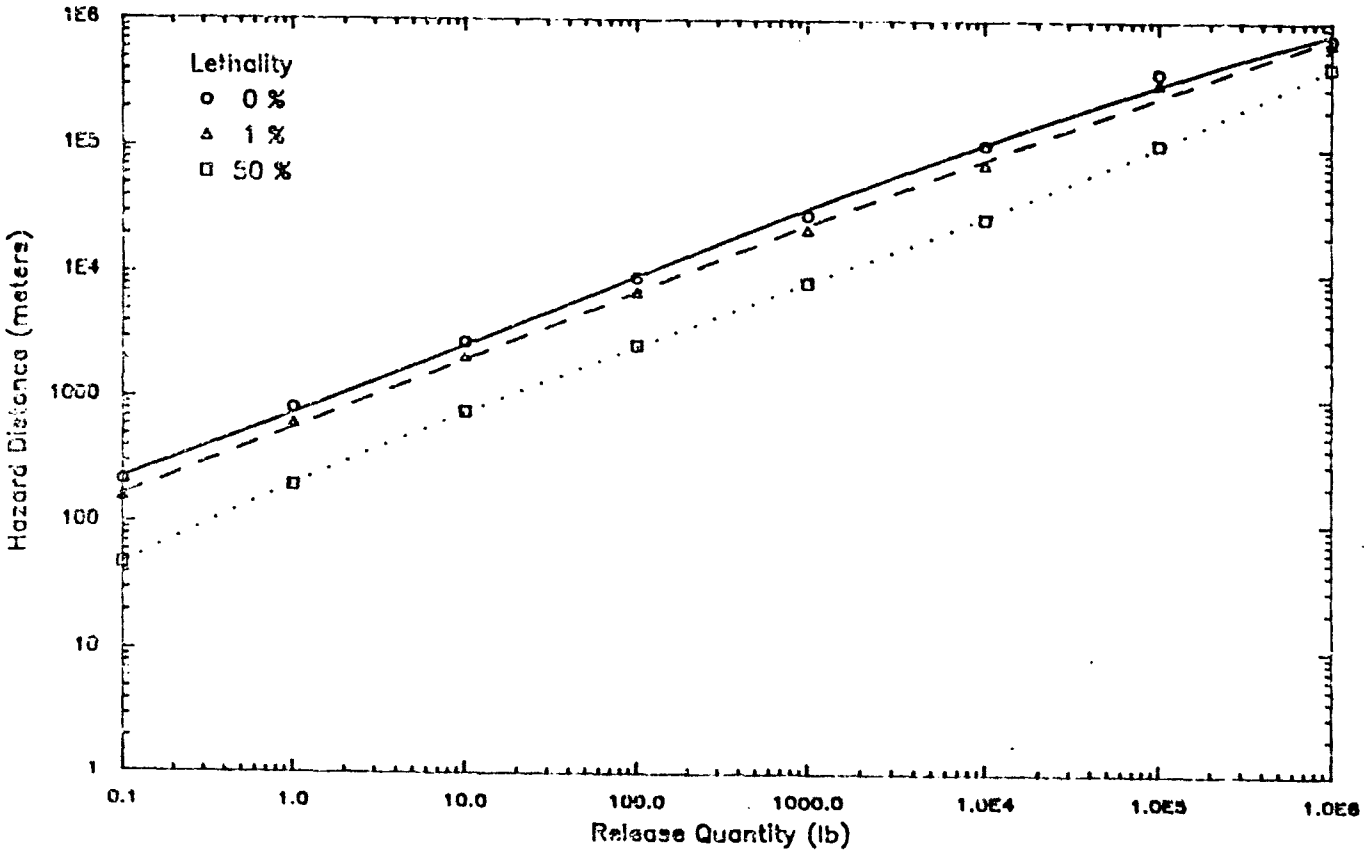

FIGURE 12
HAZARD DISTANCES FOR GB
WC Weather, 0%, 1% and 50% Lethality
Instantaneous Release Mode

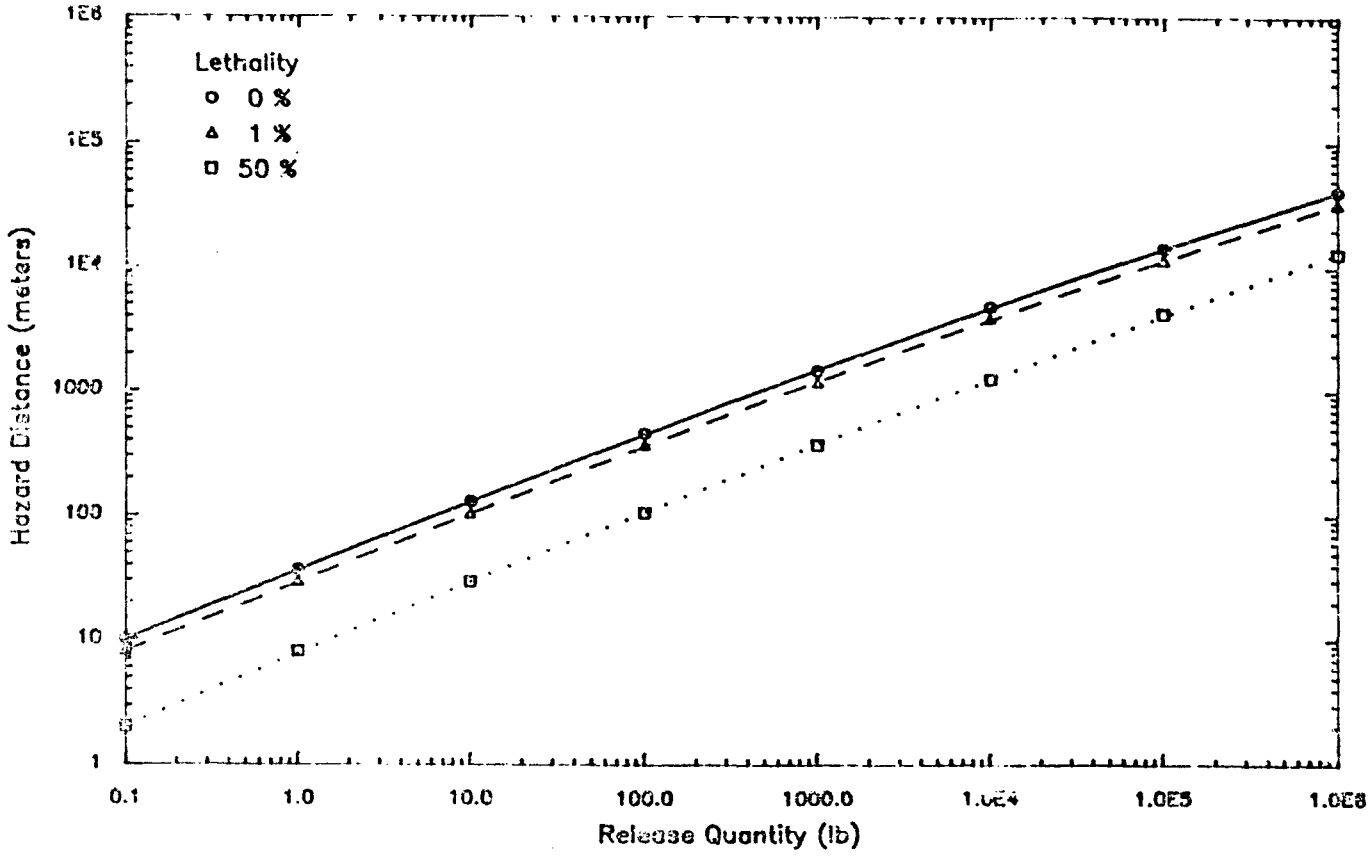

FIGURE 13
HAZARD DISTANCES FOR HD
ML Weather 0%, 1% AND 50% Lethality

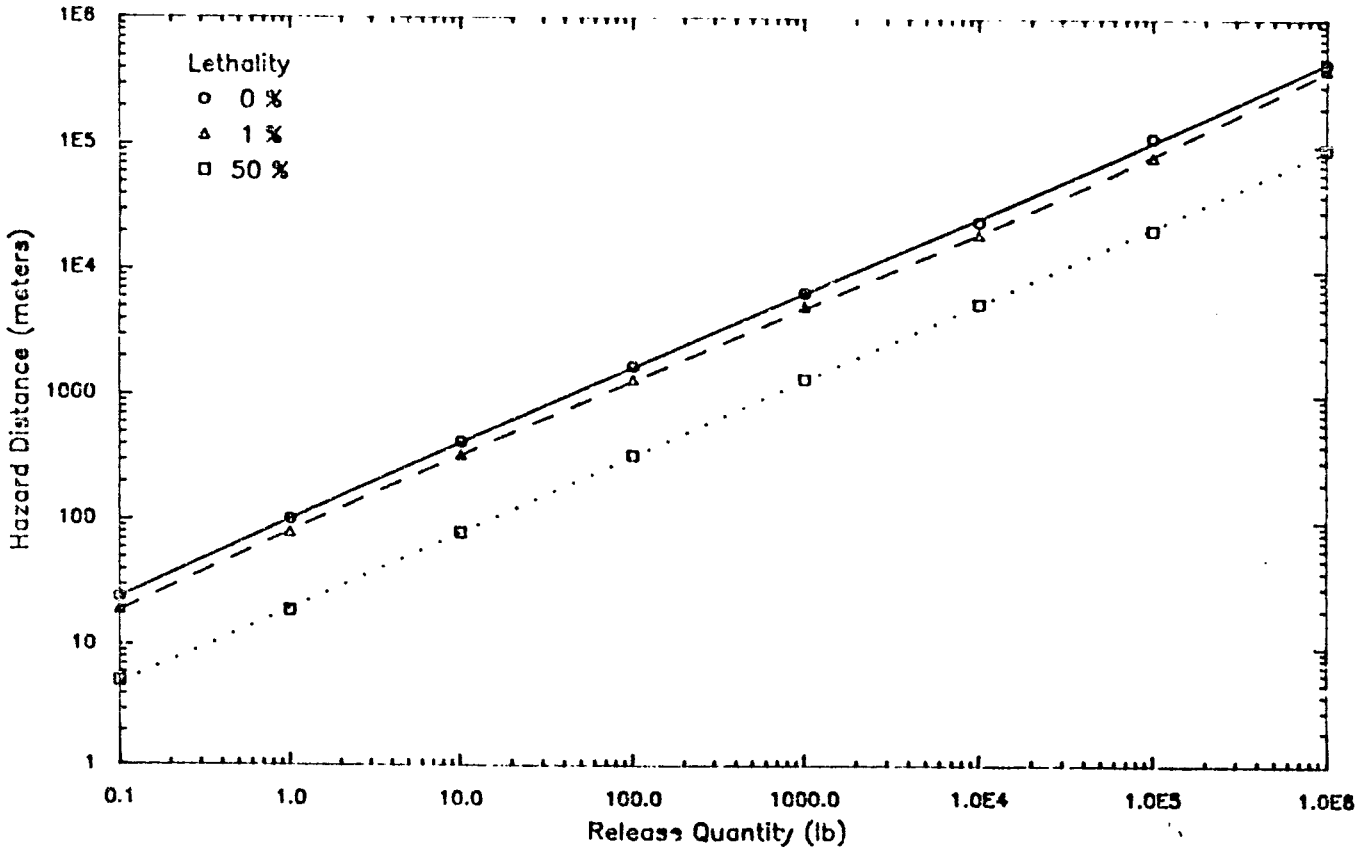

FIGURE 14
HAZARD DISTANCES FOR HD
WC Weather, 0%, 1% and 50% Lethality

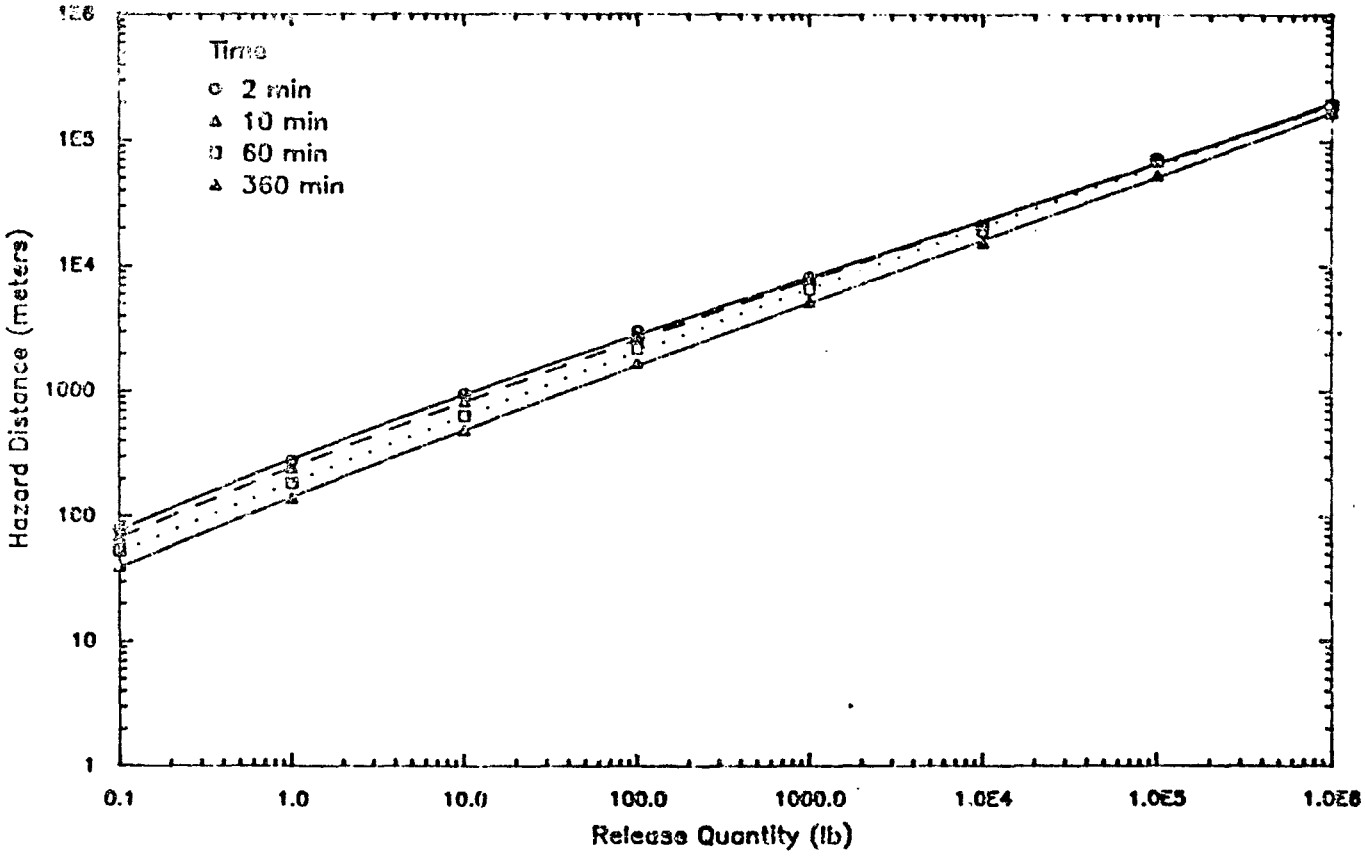

FIGURE 15
HAZARD DISTANCES FOR VX
M1 Weather, 0% Lethality

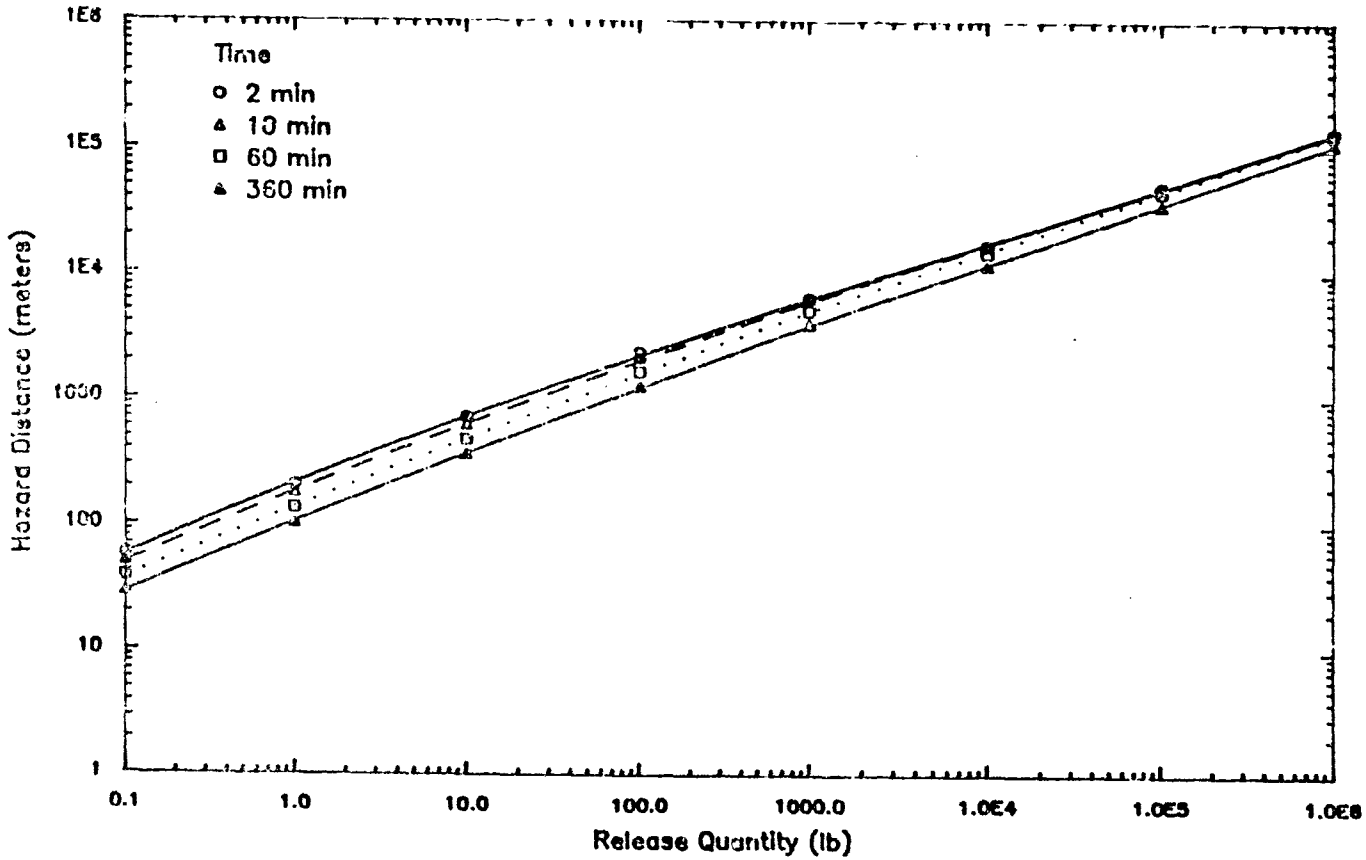

2075

FIGURE 16
HAZARD DISTANCES FOR VX
ML Weather, 1% Lethality

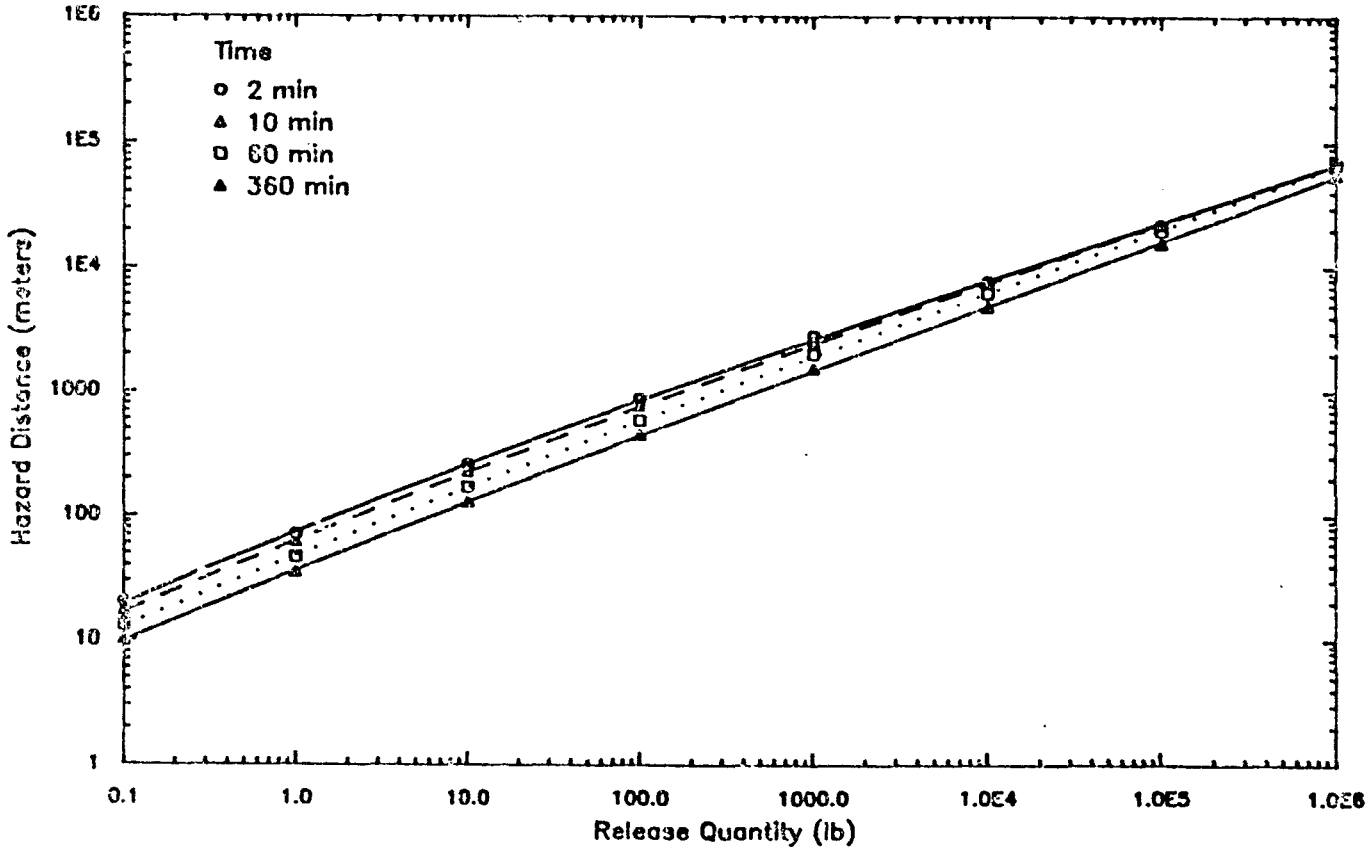

FIGURE 17
HAZARD DISTANCES FOR VX
ML Weather, 50% Lethality

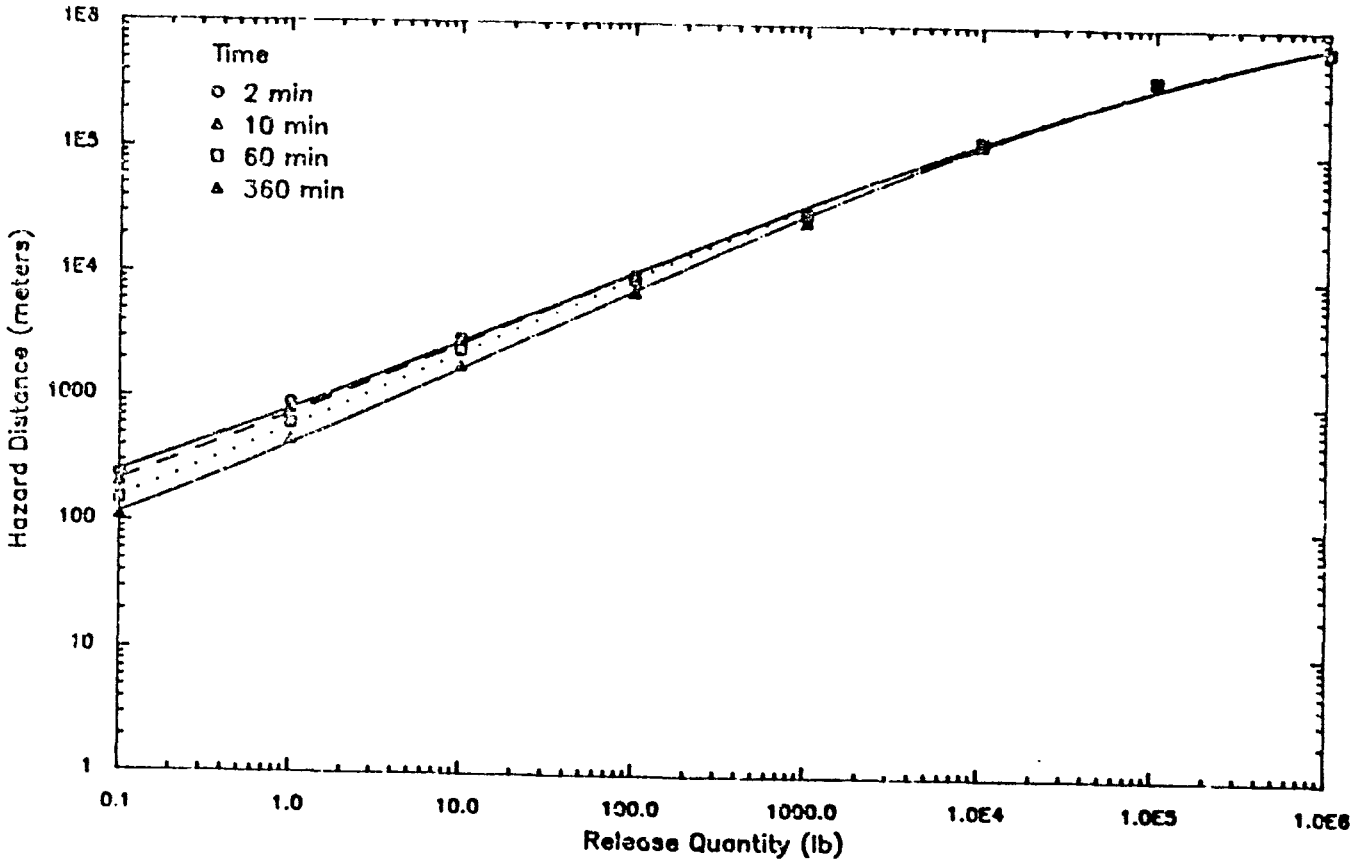

FIGURE 18
HAZARD DISTANCES FOR VX
WC Weather, 0% Lethality

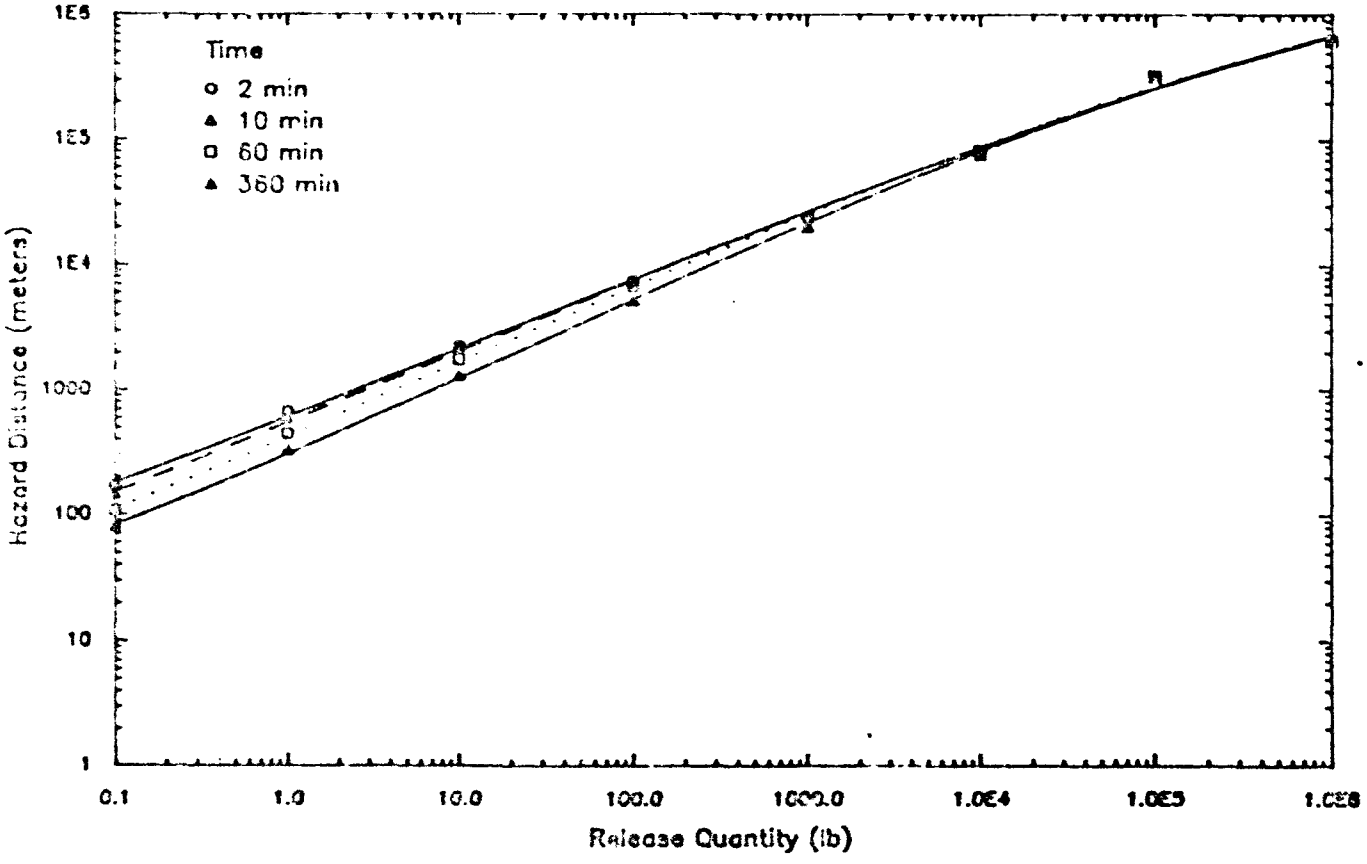

FIGURE 19
HAZARD DISTANCES FOR VX
WC Weather, 1% Lethality

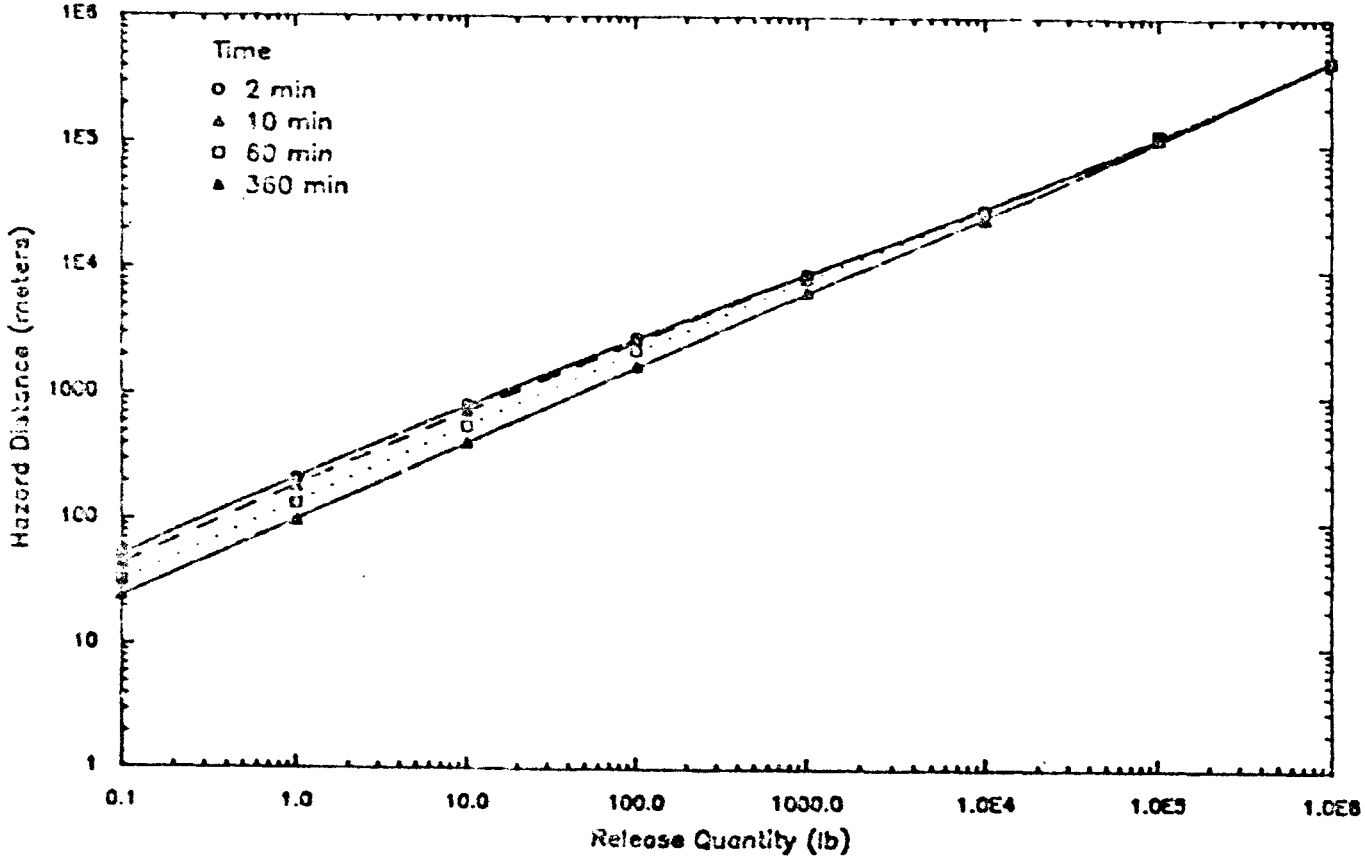

FIGURE 20
HAZARD DISTANCES FOR VX
WC Weather, 50% Lethality

TABLE 1. REPRESENTATIVE PORTION OF POTENTIAL FATALITY DATA

FIXED SITES

WIND DIRECTION & POPULATION DISTRIBUTION (AV=AVG, MX=MAX)	'NO-DEATHS' HAZARD DISTANCE (km)	WEATHER CONDITIONS (ML=MOST LIKELY WC=WORST CASE)	STOCKPILE SITES: ANAD	APG	LBAD	NAAP	PBA	PUDA	TEAD	UMDA
MX	0.1	WC	0.00	0.00	0.00	0.00	0.00	0.00	0.00	0.00
	0.2	WC	0.00	0.00	0.00	0.00	0.00	0.00	0.00	0.00
	0.5	WC	0.00	0.00	0.00	0.00	0.00	0.00	0.00	0.00
	1.0	WC	0.19	43.67	0.16	1.15	1.33	0.07	0.03	0.04
	2.0	WC	0.41	83.25	0.60	2.66	3.16	0.11	0.05	0.26
	5.0	WC	2.85	275.68	18.93	7.41	20.08	0.72	0.17	1.80
	10.0	WC	57.27	834.65	466.74	16.08	38.89	2.85	0.42	18.45
	20.0	WC	1439.30	2294.43	1801.11	141.45	925.70	30.26	1.75	352.17
	50.0	WC	4986.01	42006.78	6570.40	2541.25	5359.40	6301.77	1072.28	2524.63
	100.0	WC	10730.73	120185.14	18640.33	17799.09	15659.83	16472.78	19811.64	9805.66
	200.0	WC	70513.16	343222.33	54119.30	45548.24	40078.22	41630.01	58626.23	23792.57
	500.0	WC	244118.12	793686.56	107246.03	89456.04	106272.32	141613.20	218803.49	49811.72
	1000.0	WC	328832.93	1159756.21	138749.37	96302.03	150350.44	197087.03	311510.94	57108.18
AV	0.1	ML	0.00	0.00	0.00	0.00	0.00	0.00	0.00	0.00
	0.2	ML	0.00	0.00	0.00	0.00	0.00	0.00	0.00	0.00
	0.5	ML	0.00	0.00	0.00	0.00	0.00	0.00	0.00	0.00
	1.0	ML	0.03	2.40	0.01	0.22	0.21	0.01	0.01	0.01
	2.0	ML	0.15	6.26	0.13	0.86	0.66	0.05	0.03	0.05
	5.0	ML	1.72	54.36	6.66	4.94	5.55	0.34	0.16	0.92
	10.0	ML	53.39	218.97	111.73	22.47	31.80	1.61	0.59	15.43
	20.0	ML	508.49	908.85	334.98	82.34	267.51	20.62	2.42	120.30
	50.0	ML	2392.55	10186.39	1960.95	1229.01	1435.40	674.47	116.38	428.01
	100.0	ML	7482.58	35714.69	5349.92	5283.04	4697.39	3671.98	4722.17	1621.43
	200.0	ML	19624.80	91602.05	14634.77	14735.02	13536.42	7993.60	15889.02	5188.97
	500.0	ML	49839.16	219609.11	30159.39	37372.41	26534.84	16294.17	31652.36	10303.52
	1000.0	ML	68544.15	302029.94	41478.41	51398.53	36493.55	22409.48	43531.71	14170.51

TABLE 2. REPRESENTATIVE PORTION OF POTENTIAL FATALITY DATA

POPULATION CENTERS ALONG TRANSPORTATION CORRIDORS

WIND DIRECTION & POPULATION DISTRIBUTION (AV=AVG, MX=MAX)	'NO-DEATHS' HAZARD DISTANCE (mi)	WEATHER CONDITIONS (ML=MOST LIKELY WC=WORST CASE)	POPULATION CENTERS: BEND	BALTIMORE	JACKSON	TERRE HAUTE	SALT LAKE CITY
MX	0.1	WC	0.00	0.00	0.00	117.64	0.00
	0.2	WC	5.05	0.02	0.00	117.64	0.00
	0.5	WC	15.16	83.96	121.36	352.92	27.33
	1.0	WC	20.79	150.34	413.51	497.76	99.76
	2.0	WC	36.32	697.56	431.05	1263.04	211.74
	5.0	WC	176.95	3440.65	708.84	1619.45	893.50
	10.0	WC	436.03	7645.14	893.21	2079.92	2272.02
	20.0	WC	1007.95	19959.93	1695.08	2988.52	6281.94
	50.0	WC	1761.62	48472.42	3736.17	5422.48	23370.27
	100.0	WC	3445.52	116267.38	7780.49	8545.11	73116.38
	200.0	WC	6048.88	273516.83	14967.01	21990.46	120769.73
	500.0	WC	9497.80	746560.90	28002.03	63166.12	228192.46
	1600.0	WC	12401.32	994236.32	36308.94	59594.78	245979.16

THE TENSION BETWEEN RISK ASSESSMENT AND RISK MITIGATION

Brian H. Price
The MITRE Corporation

1.0 INTRODUCTION

Where society must choose among alternative ways to accomplish an inherently hazardous task, comparative risk assessment is becoming the analytical method of choice. Theoretically, at least, comparative risk assessment produces an orderly exposition of each alternative, a complete list of mishaps that could occur, and objective quantification of the constituent and total risks associated with each alternative (Roland, 1988). In the ideal case, all parties to the decision, often including the public, can agree on the results.

The trend toward widespread use of comparative risk assessment is impelled as much by our society's commitment to democratic participation in public decisionmaking as by any demonstrated superiority of the method as an analytical tool. Indeed, the seeming rush to adopt probabilistic methods may be outrunning the development of competent procedures, and of safeguards against inadvertent abuse. It should, therefore, be regarded as a high priority among risk assessment practitioners to identify problems, publicize their existence, and contribute to their resolution.

In support of the Final Programmatic Environmental Impact Statement (FPEIS) on the Chemical Stockpile Disposal Program (CSDP) (U.S. Department of the Army, 1988), alternative concepts for locating the required demilitarization facilities were subjected to a comparative risk assessment (U.S. Department of the Army, 1987a, 1987b, 1987c, 1987d). This study was undertaken in the shadow of a public commitment that the alternative presenting the least risk (to the public and environment) of agent-related accidents would be selected as "environmentally preferred." It is difficult to imagine a situation that could place more emphasis on the completeness, accuracy, and balance of a product of this adolescent assessment technology, since it is in making the effort to compare risks of alternatives that we find so many of our questions and unresolved concerns about methodology.

Many interesting questions did arise during the CSDP risk assessment, and a particular subset of them is identified in this paper. Addressing and resolving these questions would enhance the usefulness of comparative risk assessment in any context. Although many concerns about methodology are raised in this paper, the project team would probably agree that comparative risk assessment was the correct approach to employ, and that, despite such concerns, the outcome of the risk assessment was not distorted fundamentally.

Risk assessment is a group process, involving individuals with different attitudes, organizational roles, and experience bases. Large numbers of technical decisions are made throughout the risk assessment process, normally in the face of major uncertainties, via the well-documented processes of group decisionmaking. Inevitably, therefore, the problems of risk assessment methodology have an organizational or group dynamics component as well as the more neutral technical component. In this paper, both technical and organizational questions are identified and discussed, as both categories can nurture the seeds of failure and mistrust.

In keeping with the view of comparative risk assessment as a process, the discussion of issues is organized around one particularly nettlesome stage of the process: the stage of hazard reduction, referred to as "risk mitigation" throughout CSDP discussions. Risk mitigation is a logical follow-on to the first round of comparative risk assessment. As important contributors to risk are identified by the risk assessors, the design team can make various adjustments to reduce those risks. At no other point in the process do the various concerns raised in the risk assessment come together so concisely, and with such obvious importance for the outcome of the analysis.

Indeed, the risk mitigation stage raises so many pungent issues that could threaten the validity of a risk assessment that risk assessors may sense a real tension between this risk mitigation stage and the other stages of comparative risk assessment. This tension is both technical, and, in cases involving sharply competing interests, personal and organizational. For example, the risk assessor may be distressed to find he is trying to hit a moving target. The process designer may not agree with the "riskmonger's" visions of disaster, but he is generally anxious to find a fix for each specified threat. The outside observer, particularly if he is personally involved in the outcome, may well see this risk assessment-risk mitigation sequence as a "devil's coalition" aimed at prejudicing the comparison of alternatives.

Accordingly, the discussion of issues that follows is organized around this tension between risk assessment and risk mitigation. Resolution of issues here would help throughout the process, and go far toward improving the reliability and acceptability of comparative risk assessment in similar applications.

2.0 THE CSDP RISK ASSESSMENT CONTEXT

Congress has directed the Department of Defense (Public Law 99-145, Title 14, Part B, Section 1412) to destroy the Nation's stockpile of unitary lethal chemical agents and munitions in a manner that minimizes hazards to the public. The Chemical Stockpile Disposal Program (CSDP) has

been devised to accomplish this formidable objective. Responsibility for the CSDP rests with the U.S. Army Program Executive Officer-Program Manager for Chemical Demilitarization (PEO-PM Cml Demil), under whose direction the CSDP risk assessment was performed.

The concept plan for the CSDP (USATHAMA, 1986) included three very general alternatives for siting demilitarization facilities, as follows:

1. On-site destruction of stockpiles at each of the eight continental United States (CONUS) storage locations, with no inter-site transportation of stocks.

2. Movement of all CONUS stockpiles to two "regional" disposal centers, Anniston Army Depot, Alabama, or Tooele Army Depot, Utah.

3. Movement of all CONUS stockpiles to a national disposal center, at Tooele Army Depot.

Since the decision regarding which of these alternatives to pursue met the criteria of "major Federal action" and "significantly affecting the environment" established in the National Environmental Policy Act, the Army proceeded to define and pursue appropriate environmental documentation and to afford affected citizens the opportunity to participate in the environmental assessment process.

A Draft Programmatic Environmental Impact Statement was issued in July 1986, supported by a relatively generalized risk assessment (U.S. Department of the Army, 1986). In keeping with the commitment to consider potential agent hazard to the public as the most important environmental impact, an exhaustive new comparative risk assessment was undertaken in support of the Final Programmatic Environmental Impact Statement (FPEIS) (U.S. Department of the Army, 1987a, 1987b, 1987c and 1987d).

This risk assessment was intended to yield strictly comparable quantitative estimates of total public risk associated with each of the three main program alternatives listed above, and for two variations, as follows:

1. Relocation of the stocks from Aberdeen Proving Ground, Maryland, and Lexington Blue Grass Army Depot, Kentucky, to the regional disposal centers, by means of a military airlift.

2. Continued storage at the present locations, for an indefinite period, representing the "no-action" alternative required by the National Environmental Policy Act.

From the outset, it should be noted, these alternatives were not defined at identical levels of detail. The basic on-site, regional, and

national disposal alternatives were defined by descriptions and decisions reflected to that point by the CSDP concept plan, the Draft Environmental Impact Statement, and by changes and risk mitigation measures adopted as part of, and following, the public hearing process (U.S. Department of the Army, 1987e). As the risk assessment was proceeding, a separate study examined in some detail the possible procedures for movement of agent and munitions on- and off-site (U.S. Department of the Army, 1987f), and a series of analyses, still ongoing, was undertaken to evaluate protective packaging concepts.

The alternatives also were never "frozen" in any stable state for risk assessment purposes. The alternatives evolved throughout the study period, as problems were identified and fixes adopted.

Under the direction of the PEO-PM Cml Demil, a team of contractors undertook to develop the risk assessment, in approximately the following order:

1. Define each alternative in terms of all safety-significant procedures, facilities and equipment.

2. Identify accident-producing sequences of events associated with each element of each alternative.

3. Estimate agent release modes and quantities associated with each such accident.

4. Estimate the frequency of each accident, on some convenient unit basis that could be applied to specific stockpiles.

5. Combine the resulting catalog of accident consequences and frequencies into estimates of risk at each stockpile storage location and transportation corridor, for each program alternative.

6. Summarize, extract and report comparative risks of the alternatives, using varied measures of risk.

7. Identify opportunities to reduce risks associated with "stand-out" accidents, develop appropriate design or procedural fixes, then recalculate total risk for affected alternatives.

8. Report final results, and explain their basis to the public.

It is the seventh of these steps, referred to here as "risk mitigation," which best illuminates the concerns about methodology discussed below.

3.0 TECHNICAL ISSUES

At least four technical issues are raised when risk mitigation is included in a comparative risk assessment. These are labelled as follows:

1. Completeness
2. Maturity of Design Concept
3. Accuracy and Uncertainty in Risk Estimates
4. Comparability of Risks

3.1 Completeness

It is only logical to strive to identify all system hazards that should figure in the comparison of programmatic alternatives. Indeed, the assumption of substantial completeness (that all quantitatively significant risk contributors are included in the summation of risks associated with the alternative) is fundamental to the quantitative comparison of risks. As Roland (1988) points out "...system risk...is evaluated by finding the sum of the present values of the streams of annual expected accidental losses from all system hazards." (emphasis added). To impeach the substantial completeness of a comparative risk assessment is to challenge the credibility of its comparative results.

All of that notwithstanding, it is obvious that we never succeed in identifying and including all possible accident-producing sequences! Certainly, in a study as complex as the CSDP risk assessment, there is no reasonable hope that even the best-motivated, most-experienced and creative assessment team will tumble to every possibility. After all, it is typically the sequence of events that we never dreamed of that actually lead to major system accidents.

How is this paradox resolved in practice? In general, we maintain the credibility of the risk assessment by assuming that accident sequences we have identified are representative of a family of other, unseen sequences, which could lead to the same or similar consequences. Further, we strive to select frequency estimates that, within the error range factors typical of such estimates, might well represent a sum of all such accident sequences within this unseen family of sequences.

An example might be the accident sequences -- an earthquake or direct air crash -- included as initiators of a fire in the agent storage warehouse at the Newport Army Ammunition Plant. A major fire in that warehouse is difficult to imagine, but could have catastrophic consequences. The potential for fires caused by other conditions or operational deviations is

present, we realize, even if we are not able to foresee all the possibilities.

On the other hand, the conditional probability assigned to a fire, given an earthquake, is imprecise, and considered to be conservatively high. The risk assessment team discussed this, among many similar questions, and decided that the earthquake and air crash initiators could be regarded as properly representative of similar, unidentified warehouse fire initiators. This logical process, sometimes explicit and sometimes not, pervades large scale risk assessments, and provides a fair defense against the charge of incompleteness.

However, risk mitigation introduces a new and troublesome threat to the workability of this approach. If the accident sequence "earthquake initiates warehouse fire" represents an unseen family of similar initiators, what is the consequence if we set out to reduce the earthquake hazard by some means that is peculiar to earthquakes, and not applicable to the other initiators?

One risk mitigation measure considered in the CSDP would do just that (U.S. Department of the Army, 1987e). That measure is the installation of a seismically-activated power cutoff switch outside the Newport warehouse, that would interrupt the earthquake accident sequence by eliminating the most likely source of ignition from the warehouse. In consequence, we can reduce the frequency of this accident sequence into virtual insignificance, so that the continued storage alternative at Newport suddenly looks comparatively much better. But, of course, we have lost all measure of those unseen fire accident initiators that the risk assessors believed should be represented. It is possible that the comparability of the risks assigned to the alternatives would be seriously diminished by this well-intentioned effort at risk mitigation.

Contrast this with two other suggested approaches to mitigating the earthquake fire risk: (1) to cut off power to the warehouse at all times except when necessary maintenance activities actually require power; and (2) to install a sprinkler system in the warehouse. The effectiveness of these measures is much less dependent on the exact character of the initiating event. The first measure eliminates the main ignition source most of the time. The second would control or suppress fires of any origin, short of a large jetliner crash on the warehouse.

If we now reduce the estimated frequency of the earthquake-induced warehouse fire, we may feel that we are equally and fairly dealing with the unseen fire initiators that we attributed to the representative earthquake initiator.

There is a second aspect of the completeness issue that came up during the risk mitigation stage of the CSDP risk analysis. This arises from

another methodological convention: the use of a frequency and/or consequence cut-off value. As large and complex as the CSDP accident data base is, it is far smaller than it would be if consideration of hundreds of accident sequences had not been cut short as soon as it became apparent that the agent release or frequency would be negligible. This "screening" activity occurred at each stage of the risk assessment. The written record of screening decisions varies from excellent to non-existent, depending on the stage at which analysts became convinced an accident sequence could be neglected.

However, the basis for eliminating an accident sequence is often specific to a particular design or procedure. Change the assumed design, and an accident that once was "impossible" may become very possible indeed. Now, the process of selecting and adopting risk mitigative measures frequently results in such design or procedural changes -- but we are left with little information and no reliable stimulus to recognize and revive now-forgotten, screened-out accident sequences. We are left to depend on serendipity to identify such potentially serious oversights.

3.2 Maturity of Design

One of the thorniest issues facing risk assessment practitioners is the requisite maturity of designs and procedures to be analyzed. Where one or more alternatives are less mature in their conception, the credibility of comparative risk assessment results is seriously threatened. The introduction of risk mitigation measures complicates the problem further.

In the spirit of constructive teamwork, we want to contribute to safer design decisions throughout the development of a program. On the other hand, the method of choice, quantitative risk assessment, is highly dependent on detailed process information. Accident sequences, with their typical dependence on idiosyncracies of exact designs and exact procedures, are believable only after the design team has specified their intentions in considerable detail.

Faced with a less mature proposal, the risk assessor will predictably develop accident scenarios that are correspondingly general. Not knowing how munitions are to be handled, for example, he might reasonably assume that there is a finite probability of dropping the munitions. The subsequent search for mitigating measures might lead to a general commitment to use conveyors with guards against dropping. If the risk assessor then eliminates from consideration the possibility of a drop -- logical enough in this context -- then we must wonder what may happen at a later stage of the design, when, for example, it is decided that conveyors are inappropriate and forklifts will be used.

In principle, it should be possible to make a record of all such

safety-significant assumptions in the risk analysis, and to require a new analysis when important changes are proposed. Such constant and consistent vigilance is certainly difficult to ensure, however.

Another issue raised by assessing an immature design is whether important accident sequences will escape identification in the first place. The more general a proposal, the more difficult it is to imagine specific event sequences or failures that can produce accidents. As the design matures, however, such possibilities may become clearly evident, whereupon the risk analyst has to play the "bad guy" role, with possibly expensive consequences.

Yet a third issue raised by the necessity to work with immature designs has to do with the assumption of statistical independence of risk mitigation measures. In order to incorporate a presumed reduction of event frequency into the simple mathematics of Risk = Consequence times Frequency, the proposed mitigation measure must be independent of the event sequence we apply it against. For example, an accident initiated by a power failure obviously should not be addressed by a mitigation measure that is dependent of the same power supply. A more subtle example, perhaps, would be an accident causing a direct threat to the operator, countered by a mitigation measure that depends on correct operator reactions. Whenever we are obliged, by the lack of design specificity, to define accident sequences very generally, and we reduce the associated risk by equally indefinite mitigation measures, we are unable to guarantee that this independence requirement is met, or that it will be protected in subsequent design developments.

3.3 Accuracy and Uncertainty in Risk Estimates

Mitigation measures ought to be aimed at the most important contributors to risk, as determined in the risk assessment. If significant errors are made in estimating either the consequence or frequency of accidents, mitigation efforts may be misplaced.

A commonly accepted objective in mitigation analysis is to distribute mitigation efforts in such a way as to achieve the most cost-effective reduction of total risk (Wilson and Crouch, 1988). If a particular source of risk is greatly overestimated, it may receive a disproportionate share of risk mitigation resources. On the other hand, if inaccuracies in the risk assessment result in assigning far too little risk to a potential accident, the result could be worse than a waste of money.

As mentioned earlier, the CSDP risk assessment procedure included several screening steps, in which the data base and analytical workload were pruned back by throwing out accidents that appeared unlikely to contribute significantly to the total risk of an alternative. Screened-out

accidents were, of course, never considered for mitigation. It also happened, however, that accidents originally qualifying for inclusion in the data base were, later, so reduced in risk contribution by applying one or more mitigation measures that they then were screened out. The validity of this screening depends on the accuracy of the information used to perform it. Project priorities, limitations of resources, and the analysts' natural inclination to move on to new problems, practically guarantee that any inaccuracies that led to inappropriate screenings will never be identified. Thus, the risk mitigation step could have the effect of burying a potentially important accident beyond the reach of outside reviewers and of possible resurrection.

Very similar consequences can result when risk mitigation resources are allocated in accordance with the best point estimates of risk, without considering the uncertainty associated with those point estimates. As part of the CSDP risk analysis, estimates of uncertainty were developed for accident frequencies, ranging over two or more orders of magnitude, and differing by as much in some cases. In the CSDP analysis, uncertainty was defined in such a way as to provide a measure of the distribution of the universe of frequencies for a given accident sequence around the "best estimate" frequency used in the risk calculation. (This is not a measure of the accuracy of the estimate. Instead, it reflects the fact that what we call an "accident" is really many possible occurrences of the same sequence of events, at different places and times, and at varying frequencies of recurrence.)

The large ranges of possible frequencies were taken into consideration in the uncertainty analysis, which was performed at the end of the project to quantify the level of confidence that we can ascribe to the ranking of alternatives according to risk differences. However, no such consideration was applied to the selection of accidents to receive risk mitigation attention earlier in the process. Given the large uncertainty ranges assigned to many accident frequencies, it is possible that mitigation resources were misallocated, with implications for the validity of the overall comparative risk assessment.

In defense of the CSDP risk assessment, and the risk assessment community in general, it can be pointed out that similar difficulties arise wherever the existence of uncertainty is acknowledged in the first place. Risk analysts are not better or worse off than other technical analysts, but the problems do represent a serious threat to the usefulness of comparative risk assessment, and efforts to resolve them must be pressed forward.

3.4 Comparability of Risks

A tenet of risk assessment is that "risk is risk" -- that it is valid

to compare two alternatives on the basis of their total estimated risk, without consideration of any differences in the constituents of those risk totals. The same applies to the risk mitigation stage of risk assessment -- reducing risk by a certain amount is equally desirable, however it is accomplished. Being philosophical folks in general, risk analysts are fond of pointing out that the public and politicians often do not view things that way. Instead, they often assign more weight to reducing the risk of very high consequence, very low probability accidents than to very low consequence, relatively frequent accidents. Despite recognizing this seeming disconnect, risk analysts do not modify the mathematics of comparative risk assessment accordingly.

For example, the CSDP risk assessment provides information on the relative contributions to the alternatives of low consequence-high probability and high consequence-low probability accidents, on the assumption that certain audiences might place emphasis on this issue. And, to a degree, this information was preserved in the comparisons presented in the FPEIS: information was included on the maximum fatalities associated with any one accident associated with an alternative, without regard to its frequency of occurrence. However, predominant emphasis was placed on comparing risk measures, such as expected fatalities, that do not preserve such differences in the constituents of risk.

As mentioned above, risk mitigation efforts in the CSDP assessment were generally directed to the higher risk accidents, without regard to whether the risks varied in the relative contributions of consequence and frequency. Excluding the influence of organizational factors, discussed in the following section, two technical questions arise from this. The first relates to the uncertainty concerns raised earlier. As described elsewhere in this seminar (Cutler, 1988), the uncertainty associated with frequencies was often estimated at two or three orders of magnitude, up or down, while the uncertainties associated with agent release consequences were more often in the realm of one order or less. This follows from the fact that the release quantities are usually bounded fairly strictly by the quantity of agent present in any one place, while frequencies are much more free to vary. Should the risk associated with two accidents, one comprising a severe consequence-low probability sequence, the other a low consequence-high probability sequence, receive equal mitigation resources if their net risks are calculated to be equal? Or should mitigation resources be focused on preventing the high consequence accidents, since we are at least pretty sure the consequence is real, whatever the likelihood it will occur? Finally, if these factors affect the alternatives differently, and we apply numerous mitigation measures without regard to them, do we not introduce distortions into the alternatives comparison?

The second concern relating to comparability has to do with the selection of particular mitigation measures. There already exists a

hierarchy of preferences in how we go about mitigating a risk: passive design changes are preferred to active process controls, which are preferred to measures that require human intervention. This preference was reflected not just in the choice of which mitigation measures to incorporate into the CSDP risk assessment, but also, significantly, into the estimates of risk reduction "credit" that should be attributed to each measure. If a problem was, for practical purposes, eliminated by a design modification, much more risk reduction credit was applied than if the problem was addressed by adding a new human checkpoint in the procedure.

But each mitigation approach embraces within it another dimension as well: the degree to which it aims to reduce the frequency component or the consequence component of total risk. If we feel more sure of our estimates of agent release consequences than of our frequency estimates, should we not perhaps favor, and give more credit to, mitigation measures that attack the consequence dimension of a risk? Should we not focus our mitigation resources on those accidents whose risk is dominated by high consequences, rather than high frequency? If these concerns are valid, do we introduce distortions into the comparative risk assessment by performing the risk mitigation step without regard to possible differential impact on the alternatives under consideration?

4.0 ORGANIZATIONAL ISSUES IN RISK ASSESSMENT

Comparative risk assessment takes place within a social context, characterized by a rich interaction of people in both formal and informal groups. Examples of such groups in the case of the CSDP studies included the Army program development staff, EIS team, and the Safety and Surety Division; Oak Ridge National Laboratory, as preparer of the FPEIS; the contractors who participated in the risk assessment; the design contractor; the expert teams established in behalf of the affected communities; Federal officials assigned to assist in the process; and interested citizens at each stockpile location. Each of these groups could, in principle, be characterized in terms of internal role structure, internal influence hierarchies, and group norms, and each could be described in terms of its collective attitudes toward key elements of the CSDP (Fisher, 1974).

While each individual brings unique influences to a group he or she joins, the dynamics of role development and status determination within each group strongly influence the individual's perception of issues the group has chosen to concern itself with (Cantril, 1957). For example, a risk analyst who lives in the vicinity of a proposed CSDP facility site, and who becomes involved in reviewing the CSDP risk assessment in behalf of a group of citizens who would rather see the stockpiles moved to another state, might be more likely to search through risk data on the on-site disposal alternative to find errors of omission and of understated risks. The same individual, six weeks after accepting a job with an Army safety

office, might develop a very different perspective. This is not prejudice, or weakness of character, but rather is the inevitable result of social influence operating within the organizational context.

This is sometimes difficult for engineers and scientists, who have come into the arena of quantitative risk assessment from the rational precincts of mathematics and physical science, to accept in any operational sense. The literature of risk assessment is all about operations research methodologies and the logic of rational decisionmaking under conditions of uncertainty, and not about the dynamics of how risks are perceived and weighted by conflicting interest groups. However, if organizational dynamics can affect how, and indeed, whether, certain sources of risk are perceived and weighted, then the risk assessment community cannot afford to ignore the possible impact on the validity and credibility of its product.

As in the case of the technical issues identified earlier, nowhere are the organizational sources of concern more evident than in the risk mitigation stage of the comparative risk assessment process. We can only scratch the surface of such issues in this context, so this discussion focuses on several issues that have the most potential to impact the validity of a risk assessment. The discussion is intended to avoid any flavor of criticism against any of the Government, public or private groups that participated in the CSDP risk assessment, but instead to identify, based on experiences in the program, the sorts of issues that can arise and which need the dispassionate attention of risk assessment practitioners.

4.1 Comparability Issues

Perception of the immediacy and relative acceptability of risks is highly personal, but is affected strongly by the norms of the groups we associate ourselves with. In the CSDP risk assessment experience, the importance of certain types of risks clearly was seen differently by Army contractor personnel and the expert teams assembled in behalf of the affected communities, and the perceptions of the expert teams varied with the overall predisposition of each community toward each alternative. The preference for allocating risk mitigation resources also differed among these groups.

The allocation of risk mitigation resources among the alternatives is a critical issue in the credibility of the comparative risk assessment. Given an even-handed risk comparison as a starting point, the analyst obviously can introduce conscious or unconscious bias by the simple expedient of identifying many more effective risk mitigation measures for one alternative than for others. This possibility hovers as a deadly threat to credibility.

The logical, and doubtless idealized, defense against this threat is

to allocate risk mitigation resources according to a rational cost-effectiveness rule. For example, we could establish a limit on mitigation expenditures (on some neutral basis), then apply that mitigation budget to each alternative in such a way as to minimize the total risk of the alternative. Ignoring for the moment the considerable technical difficulties of doing this, described earlier, there are powerful forces in organizational dynamics, relating to this issue of risk comparability, that militate against such an approach.

Whatever the supposedly objective information provided by the risk assessment process, equal risks often do not look equal to different participants in a comparative risk assessment. If, for example, you are part of the organization that will be responsible for the safe conduct of the demilitarization operation, you are socially impelled to focus much of your risk mitigation energies on the hazards associated with the plant design and operations, for which your part of the organization is directly responsible, and to devote relatively less energy to mitigation of hazards in, say, continued storage operations or railroad operations. There are very likely to be identified accidents which you feel cannot be tolerated in the accident data base, even if their contribution to total risk would not normally justify special risk reduction efforts, because their very presence in the data base implies the potential for incompetent or irresponsible group function. Both of these responses to the norms of the reference group could lead to serious distortions of the basis for comparing alternatives.

Public perceptions and expressions of concern also can influence the allocation of mitigation resources in "non-rational" ways. In general, the affected public seems to be far more interested in reducing risks that comprise very high consequence-low probability constituents, or which incorporate substantial uncertainties about the degree of impact on human health. In the CSDP case, the Army displayed great sensitivity to the concerns expressed by the public and the expert teams employed in their behalf, and incorporated many mitigation measures accordingly. To the extent that these measures affect alternatives differently, and assuming they would not otherwise have received mitigation attention, the comparative risk assessment is compromised.

4.2 The Creative Environment

Group creativity is essential to the risk assessment process. Risk assessment techniques provide a stimulus and structure for group creativity, but identification of hazards, potential equipment and operator failures, and, especially, complex interactions of subsystems must flow out of the brainstorms of effective work groups.

There is an extensive and expanding literature of small group dynamics

and productivity, and no shortage of helpful information on what factors contribute to, or depress, group creativity. In the risk assessment case, one essential factor is a group norm to the effect that identifying possible accident sequences is highly desirable, and should be rewarded with the appreciation and approval of formal and informal group leaders. As in all brainstorming situations, creativity is stimulated by a group environment that is tolerant of new ideas and hypotheses, and does not immediately subject new thoughts to destructive criticism and censure. In the CSDP risk assessment experience, a strong culture of just this beneficial sort developed among the risk assessment team (as an informal group, drawn from several cooperating organizations).

However, the system design team (also comprising individuals from different formal organizations) was faced with a different sort of job, and developed appropriate norms of orderly process, disciplined thinking and channelled communication. For members of that de facto group, the unconstrained creative processes of the risk assessors may have represented a threat to continued progress, and many of the "far-out" accident sequences identified by the risk assessment team must have seemed silly at best and destructive at worst, and often deserving of sharp criticism.

Such conflict between group norms can increase cohesion among members of both groups, and, in some contexts, can promote the joint productivity of both. This probably was the case in most stages of the CSDP risk assessment, but less positive possibilities are posed by the troublesome risk mitigation stage.

In a situation such as this, where the risk assessment was not performed by a third-party team, but was directed by Army safety personnel answering to the PEO-PM Cml Demil, it is possible that the conflict of norms between the "do-ers" and the "assessors" would tend to suppress of the assessment team's norm of creativity in identifying hazards and pressing their consideration by the design contingent. As members also of the larger group (the CSDP project team as a whole), the assessment group had to deal with the conflict between wanting to share the norms of the larger group, which was also the seat of formal authority, and wanting to defend the activities of the assessment group from any diminution of creative freedom or integrity of its conclusions. One result was perhaps a degree of self-censorship by the risk assessment team; in cases where individuals were less certain of their insights, they were more likely to suspend further consideration of a possible problem rather than to run head-on into the larger team's censure.

It is impossible to assess whether this effect had any important effect on the CSDP risk assessment, since we have no way of knowing whether any significant risks were thereby overlooked. Very possibly, however, it is the accident we never imagined that represents the most serious

unmitigated threat. Any systematic suppression of group creativity is therefore to be avoided through appropriate reporting arrangements and reward systems. Independent third-party risk assessment offers one mechanism to promote these qualities in the context of comparative risk assessments.

5.0 CONCLUSIONS

The technology of quantitative risk assessment is probably the best available means of comparing the integrated total risk of program alternatives such as were considered in the CSDP FPEIS. Nonetheless, theoretical and procedural advances are needed, in order to ensure the validity and credibility of the conclusions of comparative analyses performed with this technology. A number of technical and organizational concerns were raised during the CSDP risk assessment, most of which were highlighted by the risk mitigation stage of the risk assessment. Similar concerns could, and should, be identified in other comparative risk assessments. The risk assessment community should place high priority on identifying, analyzing and resolving such concerns, and should promote a high standard of candor in presenting the strengths and weaknesses of risk assessment methods.

REFERENCES

Cantril, Hadley, 1957. "Perception and Interpersonal Relations", American Journal of Psychiatry 114, pp. 119-126.

Cutler, Robert M., 1988. "The Treatment of Uncertainty in a Comparative Risk Assessment", prepared for presentation at the 23d DoD Explosives Safety Seminar, Atlanta, GA, 9-11 August 1988.

Fisher, B. Aubrey, 1974. Small Group Decision Making: Communication and Group Process. New York: McGraw-Hill Book Company, pp. 49-56.

Roland, H.E., 1988. "The System Safety Domain" Hazard Prevention 24:2, March-April 1988, pp. 24-26.

U.S. Army Toxic and Hazardous Materials Agency, 1986. Chemical Stockpile Disposal Concept Plan. Report AMXTH-CD-FR-85047. Aberdeen Proving Ground, MD.

U.S. Department of the Army, 1986. Draft Programmatic Environmental Impact Statement, Chemical Stockpile Disposal Program. Office of the Program Manager for Chemical Demilitarization, Aberdeen Proving Ground, MD.

U.S. Department of the Army, 1987a. Risk Analysis of the Continued Storage of Chemical Munitions. SAPEO-CDE-IS-87009. Prepared by GA Technologies, Inc. for the Program Executive Officer-Program Manager for Chemical Demilitarization, Aberdeen Proving Ground, MD.

U.S. Department of the Army, 1987b. Risk Analysis of the On Site Disposal of Chemical Munitions. SAPEO-CDE-IS-87010. Prepared by GA Technologies, Inc. for the Program Executive Officer-Program Manager for Chemical Demilitarization, Aberdeen Proving Ground, MD.

U.S. Department of the Army, 1987c. Risk Analysis of the Disposal of Chemical Munitions at Regional or National Sites. SAPEO-CDE-IS-87008. Prepared by GA Technologies, Inc. for the Program Executive Officer-Program Manager for Chemical Demilitarization, Aberdeen Proving Ground, MD.

U.S. Department of the Army, 1987d. Risk Analysis in Support of the Chemical Stockpile Disposal Program. SAPEO-CDE-IS-87014. Prepared by the MITRE Corporation for the Program Executive Officer-Program Manager for Chemical Demilitarization, Aberdeen Proving Ground, MD.

U.S. Department of the Army, 1987e. Mitigation of Public Safety Risks

of the Chemical Stockpile Disposal Program. SAPEO-CDE-IS-87014. Prepared by the MITRE Corporation for the Program Executive Officer-Program Manager for Chemical Demilitarization, Aberdeen Proving Ground, MD.

U.S. Department of the Army, 1987f. Transportation of Chemical Agents and Munitions: A Concept Plan. SAPEO-CDE-IS-87003. Prepared by the MITRE Corporation for the Program Executive Officer-Program Manager for Chemical Demilitarization, Aberdeen Proving Ground, MD.

U.S. Department of the Army, 1988. Final Programmatic Environmental Impact Statement, Chemical Stockpile Disposal Program. Office of the Program Manager for Chemical Demilitarization, Aberdeen Proving Ground, MD.

Wilson, Richard and E.A.C. Crouch. "Risk Assessment and Comparisons: An Introduction", Science 236, April 17, 1987, pp. 267-270.

THE TREATMENT OF UNCERTAINTY IN A COMPARATIVE RISK ASSESSMENT

by
Robert M. Cutler
The MITRE Corporation
McLean, Virginia

for
Department of Defense
Twenty-third Explosives Safety Seminar
Atlanta, Georgia
9-11 August 1988

ABSTRACT

In the assessment of the risk to the public from the Army's Chemical Stockpile Demilitarization Program, uncertainty about the probability of a hypothetical, accidental release of agent was a key factor. Uncertainties in terms of range factors were estimated for initiating events, conditional events, accident scenarios, activity groups, and programmatic alternatives. The significance of the choice of mean frequencies (as opposed to median frequencies) was considered. Also considered were relationships between different frequencies, and duplication between different alternatives. The uncertainties associated with the various alternatives were used to estimate the probability that any specified alternative involves a greater risk than any other alternative. One important finding was that these probabilities of the existence of excess risk cannot be relied upon to produce a single, comparative risk-ordered list of alternatives; comparisons of these probabilities must involve only two alternatives at a time.

I. INTRODUCTION

A. General

The Department of Defense was directed by Congress (Public Law 99-145, Title 14, Part B, Section 1412) to destroy the stockpile of lethal unitary chemical agents and munitions in such a manner as to provide maximum protection to the general public. In order to define and manage the potential for an acute, catastrophic release of chemical agent into the atmosphere, risk analysis and mitigation was undertaken. The background of the destruction program and the details of the risk analysis are described fully in other papers but are only summarized below, in order to orient the reader prior to the presentation of the subject of this paper--the treatment of uncertainty in a comparative risk assessment.

B. Program Alternatives

In response to the requirements of Public Law 99-145, by March of 1986 the Army had produced a conceptual plan for the destruction of the lethal chemical stockpile by 1994. The plan for the Chemical Stockpile Disposal Program (CSDP) included three alternatives:

1. On-site destruction of the chemical stocks at their present storage locations (the "ONS" alternative).

2. Movement of the chemical stocks by rail to two regional center for chemical destruction (the "REG" alternative).

3. Movement of the chemical stocks by rail to one national center for chemical destruction (the "NAT" alternative).

In July of 1986 a Draft Programmatic Environmental Impact Statement (DPEIS) was issued, to be followed in January of 1988 by a Final Environmental Impact Statement (FPEIS). Five additional alternatives (involving partial relocation ["PR"] or continued storage) were described in the supporting documents:

4. Movement of the chemical stocks by C-5 aircraft from two of the present storage sites to a national center for destruction, and on-site destruction of the remaining chemical stocks at their present storage locations (the "PRA" alternative).

5. Movement of the chemical stocks by C-141 aircraft from two of the present storage sites to a national center for destruction, and on-site destruction of the remaining chemical stocks at their present storage locations (the "PRB" alternative).

6. Movement of the chemical stock by water from one of the present storage sites to a destruction plant at Johnson Island (JI) in the Pacific Ocean, and on-site destruction of the remaining chemical stocks at their present storage locations (the "PRW" alternative).

7. Movement of the chemical stock from one present storage site by C-141 aircraft to a national center for destruction, and from another present storage site by water to JI for destruction; and on-site destruction of the remaining chemical stocks at their present storage locations (the "PRC" alternative).

8. Continued storage of the stocks at their present locations for 25 more years (the "STR" alternative).

C. Program Activities

Each of the eight programmatic alternatives was defined as a composite of various activities. The classes of activities included:

1. Storage, both long-term in magazines, warehouses and yards; and short-term in containers awaiting off-site shipment.

2. Handling, for inspection and maintenance during long-term storage; for removal from long-term storage and loading for transport; and for unloading and delivery at destruction plants.

3. On-site transport by truck.

4. Off-site transport by rail.

5. Off-site transport by air.

6. Off-site transport by water.

7. Plant operations for destruction of the chemical agents.

D. Accident Scenarios

The risk entailed in each activity was characterized by a representative set of accident scenarios. Each accident scenario is a hypothetical sequence of events beginning with an initiator (for example, an earthquake), followed by intermediate occurrences (for example, release of the chemical, ignition of the chemical, failure of the fire suppression system, and failure of the containment structure), and ending with a lethal release of chemical agent to the atmosphere.

E. Accident Consequences

Each accident scenario is assigned a representative consequence, in terms of an estimated public fatality count. The consequence depends on the type of chemical agent that is released, the quantity released, the mode of release (for example, detonation of a chemical munition, evaporation of a spill, or incomplete combustion in a fire), and the duration of the release. The consequence also depends on atmospheric dispersion phenomena, on the toxicological characteristics of the chemical agent, and on the population downwind of the release.

Since all of these factors vary in ways that are neither easily nor accurately quantifiable, accident consequence estimates are uncertain. Nevertheless, aggregate accident consequence uncertainties were judged to be equivalent to roughly one order of magnitude or less, while aggregate accident frequency uncertainties (see below) were estimated to be equivalent to roughly two orders of magnitude or more. In order to reduce the uncertainties of consequence estimates, some accident scenarios were subdivided into similar but separate scenarios differing in consequence (and correspondingly differing in frequency). For example, aircrashes onto chemical agent sites were divided into direct and indirect crashes of large or small aircraft. Fires were divided into those suppressed quickly, those suppressed later, and those remaining uncontrolled. Earthquakes were divided into several different categories of strength. Other than by means of such accident subdivisions, no account was taken of consequence uncertainty.

F. Accident Frequencies

Each accident scenario was assigned a frequency, based on an event tree or fault tree calculation, or on a Monte Carlo simulation. The frequency was considered to be a best estimate representing some central tendency of a probability density function of uncertain form. Although the specific type of central tendency and type of distribution were not known, a familiarity with the data and methods used to estimate the frequencies, an inspection of the resulting estimates, and the application of judgment led to a decision that when it became necessary to make assumptions about frequency distributions, they would be assumed to be log-normal.

Further complicating the elaboration of the accident frequency data was the fact that many of the frequencies needed to be treated as classified information because they could be useful to countries unfriendly to the United States by revealing sensitive information about the chemical stockpile. Nevertheless, it can be written here that all of the frequencies of lethal accident scenarios were very low (at least several orders of magnitude less than once per program or once per year). In fact, the frequencies were so much smaller than unity that in informal speech or writing they were often confounded with probabilities (which, unlike frequencies, are limited, *by definition*, to have upper values of unity). Furthermore, the the term probability was used intentionally in a manner that was not strictly correct, because many readers of program documents might tend to associate the strictly correct term, frequency, with an event that has actually occurred, or is actually expected to occur. On the other hand, the term probability was thought to connote better the uncertainty of accident occurrence. Since the actual values on a per year or per

disposal program basis were much less than unity, the numerical difference is inconsequential. The author hopes that he will be excused if he refers to a frequency as a probability (or vice versa) elsewhere in this paper!

G. Accident Uncertainties

Each accident frequency was also assigned an uncertainty. The uncertainty was expressed as the ratio of the frequency's upper limit to its best or median estimate, as described above. This ratio was called the range factor. In some cases, the upper limit used to calculate the range factor was based on mathematical or physical laws that were assumed to be absolute. In other cases, the upper limit was based on judgment. When frequencies could be characterized by probability density functions, 95 percentile values were taken as the upper limits (GA Technologies, 1987a-c). Therefore, when it became necessary to characterize the assumed log-normal distribution of a median frequency, its 95-percentile value was assumed to be equal to the estimated upper limit.

H. Fatality Expectation Values

For each accident scenario, the fatality expectation value or expected fatality value was defined to be the product of the mean frequency and the consequence, in terms of the public fatality count. In a similar manner, the upper limit of the expected fatality value was defined to be the product of the same consequence and the upper limit of the mean frequency. The expected fatality value was selected as the principal unit of measurement of the relative risk entailed in the accident scenario. Thus, references in this paper to numerical values of risk refer to expected fatality values.

II. METHODOLOGY

A. Overview

The central problem is to compare the risks of programmatic alternatives. The risk of each alternative was computed as a best estimate of the expected fatality value. Each alternative's expected fatality value is the sum of the expected fatality values of the constituent activities. Similarly, each activity's expected fatality contribution is the sum of the expected fatality values of the constituent accident scenarios. Unfortunately, the *upper limits* of the expected fatality values cannot be added in this way. The reason is that they are related to varying degrees. The methodology selected for estimating the upper limits of aggregate expected fatality values requires the conversion of

frequencies from medians to means, the combination of related uncertainties, and the combination of unrelated uncertainties. In addition, duplicated accident scenarios needed to be eliminated before comparing programmatic risks. These steps are described below.

B. Medians and Means

Expected values are means by definition. As explained above, the initial best estimate of each accident scenario frequency was taken to be a median, a different measure which therefore needed to be converted to a mean in order to be useful for the estimation of an expected fatality value. For a log-normal distribution (see above):

$$F_{mean} = F_{med} \cdot \exp[(\ln RF_{acc})^2/5.412]$$

where:

F_{mean} = mean accident frequency

F_{med} = median accident frequency

RF_{acc} = range factor of median accident frequency

Typical values of the exponential expression that is multiplied times the median frequency to obtain the mean frequency are listed in Table 1. Note that the exponential term increases more quickly than the range factor, and that it can exceed the range factor itself.

Based on this mean accident frequency, the expected fatality value for any accident is:

$$EF_{acc} = F_{mean} \cdot FC_{acc}$$

where:

EF_{acc} = expected fatality value for accident

FC_{acc} = fatality count for accident

Upper limits of expected fatality values were also calculated.

C. Related Uncertainties

For any single program alternative, and within any one of the seven activity categories (storage, handling, truck transport, rail transport, air transport, water transport, or plant operations),

TABLE 1
MEDIAN TO MEAN CONVERSION FACTORS

Range Factor	Mean/Median
1	1.00
2	1.09
3	1.25
5	1.61
7	2.01
10	2.66
15	3.88
20	5.25
30	8.48
50	16.91
70	28.08
100	50.33
150	103.44
200	178.94
300	408.01
500	1256.70
700	2779.17
1000	6747.34

many of the accident scenarios have much in common with respect to the data and methods used to estimate their frequencies. For example, during handling either an equipment malfunction or an operator error may result in a chemical munition being dropped from a forklift truck, being punctured by a forklift tine, or being involved in a collision of a forklift truck with another object. It is assumed that, if the frequency or risk of any one accident within any specified activity category would be better represented by the upper limit than the mean, then the frequencies or risks of all accidents in the same category were likely to be better represented by their respective upper limits than by their respective means. Therefore, for the purpose of estimating the upper limit of the aggregate expected fatality value for any one activity, the upper limits of the expected fatality values for the individual accidents were obtained by direct summation.

D. Unrelated Uncertainties

Unlike the frequencies of accidents within any *one* of the seven activity categories, the frequencies and risks of accidents drawn from *different* activity categories are not thought to be closely related. Furthermore, the conservatism (overstatement of risk) inherent in the assumption of a close relationship within any single activity may be offset to an undetermined extent by an assumption of no relationship between the frequencies and risks of accidents arising from different activities. Therefore, the risks posed by different activities were combined as independently distributed variables, by summing variances.

E. Duplicate Accidents

The comparison of risks inherent in any two different program alternatives is facilitated by the prior elimination of duplicate accidents. For example, alternative programs A and B may be identical, except that A entails the risk of one additional accident. Though the total risk may be indistinguishable, the elimination of the common accidents shows clearly that the risk of A is greater by the amount of risk inherent in the additonal accident. In another case, alternatives C and D may be identical, with indistinguishable total risks, except that the frequency of one particular accident is greater if alternative C is chosen. The risk of alternative C is greater by an amount equal to the accident frequency difference multiplied by the corresponding fatality count.

Therefore, prior to the comparison of the risks of any two alternatives, and prior to the computations of the limits and uncertainties of the risks of alternatives to be compared,

duplicate accident scenarios having identical frequencies and range factors were eliminated. Where only the frequencies differed, the accident scenario was eliminated only in the case of the program alternative with the lower frequency; the frequency was reduced to the value of the original difference in the case of the alternative with the greater frequency. However, any accident scenario that was part of only one of the two alternatives to be compared was not changed, even though its activity category may have been represented by different accident scenarios within the other alternative.

F. Comparative Risks

All estimated accident frequencies for demilitarization program alternatives were low (several orders of magnitude less than unity), and estimated public risks were low also. Nevertheless, the Army expressed a preference for whatever alternative would present the least risk. As part of the comparison of the risks of the alternatives, a test statistic was defined as a function of the aggregate mean estimate of risk for each alternative being compared, and the estimated uncertainty associated with that risk.

III. RESULTS

A. Risk of Any One Alternative

An example illustration of the risk of each of eight preliminary and unmitigated program alternatives, considered separately, is shown as Figure 1. Since total risk is depicted, accident scenarios common to different alternatives have not been eliminated. For each alternative, the best estimate of the expected fatality value (EF_{alt}) is indicated by the small circle. The upper and lower limits (UEF_{alt} and LEF_{alt}, respectively) are indicated by the bars. The average range of the risk of any one alternative appears to be about three orders of magnitude. The continued storage alternative (STR) appears to be riskier than the other alternatives. However, when one considers the wide average range of uncertainty, the alternatives do not appear to differ greatly otherwise (except that partial relocation by C-5 aircraft ["PRA"] appears to be somewhat riskier than the others). The alternatives that appear to be safest are those whose best estimates of expected fatality values are about 0.01. However, even these alternatives have upper limits approaching one fatality. Only a considerable risk reduction through design changes and other mitigation resulted in the acceptance of one of these alternatives, on-site disposal (ONS)

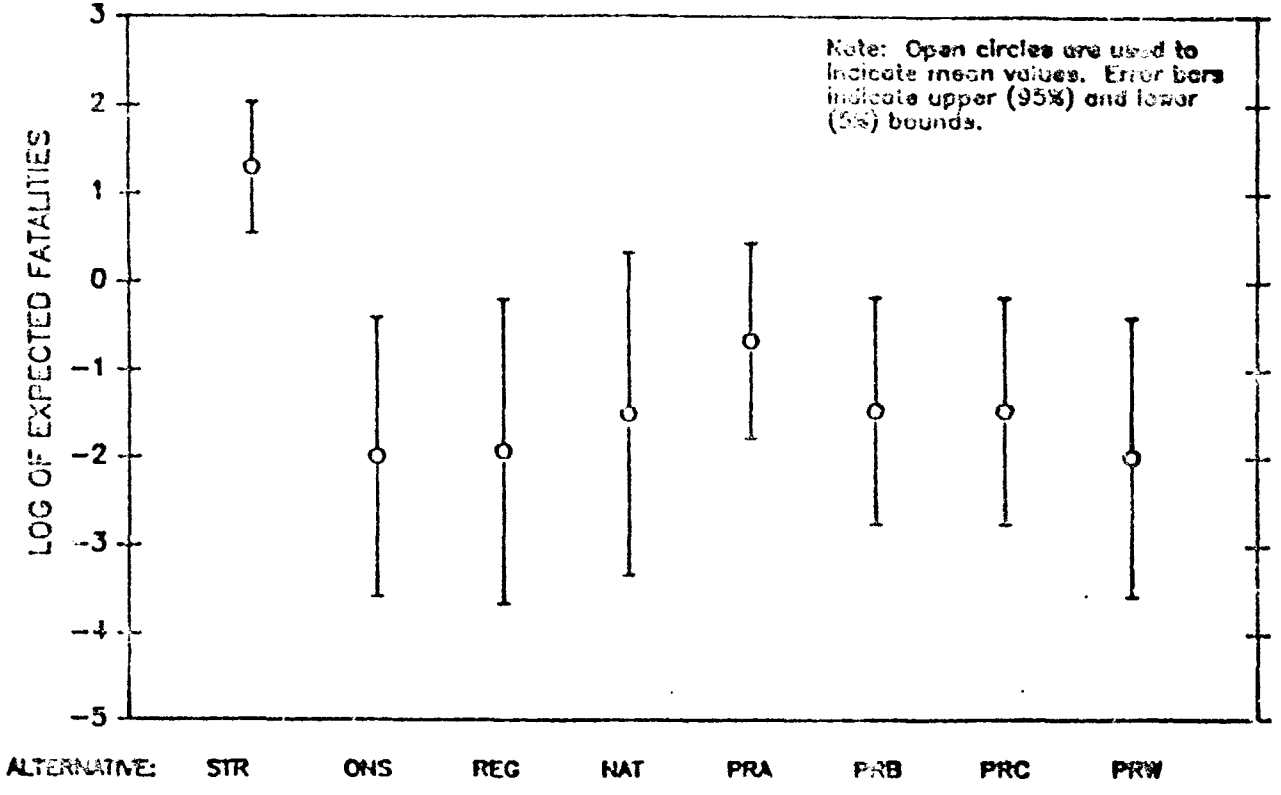

FIGURE 1

SOCIETAL RISK (EXPECTED FATALITIES)
FOR EIGHT PROGRAMMATIC ALTERNATIVES
- UNMITIGATED -

B. Risk Comparison for Any Two Alternatives

An example presentation of probabilities of risk differences is shown as Table 2. For the computation of entries in this table, accidents were eliminated if they were common to each pair of alternatives being compared. As can be seen from the first (top) row of numbers, the probability is 0.99 that continued storage (STR) is riskier than any other alternative. Conversely, as can be seen from the first column of numbers on the left, the probability is 0.01 that any disposal alternative is riskier than continued storage.

More interesting is a comparison of the alternative that appears safest, onsite disposal (ONS), with the alternative that appears to be next-safest, partial relocation by water (PRW). The former alternative is safer with a probability of 0.51. However, "ONS" is safer than partial relocation by air and water (PRC) with a probability of 0.94, while "PRW" is safer than "PRC" with a probability of 0.95! If each of the alternatives "ONS" and "PRW" had been compared to "PRC" only, rather than to each other directly, then "PRW" would have appeared, erroneously, to be safest! How is this possible? One way in which this situation can occur is illustrated schematically in Figure 2. If the "ONS" range factor is relatively large, then the upper limit of the "ONS" risk is likely to exceed the "PRC" risk (while the "PRW" risk is highly unlikely to exceed the "PRC" risk because of their narrower ranges. The situation is further complicated by the elimination of common accident scenarios, which means that any one alternative comprises different sets of accidents, depending on the alternative to which it is being compared. Thus, if "PRW" is more likely to be safer than "PRC" than is "ONS", it does *not* follow that "PRW" is safer than "ONS". There is no such transitive property of risk uncertainty.

IV. CONCLUSIONS AND RECOMMENDATIONS

Risk analyses can be greatly improved by detailed evaluations of associated uncertainties. This is especially so in the case of a program for which the best estimate of risk is low, and in the case of a comparison of alternatives whose risks appear to differ by small amounts. As demonstrated above, alternatives must be compared to each other directly, not to some other option (such as "PRC" above), if the comparison is to be valid. Furthermore, when the best estimates of risk are low for all of the likely alternatives, the ranges of risk uncertainties are critical. The reason for this is that the large uncertainty of the frequency or probability of the undesired event, much more so than the best estimate of frequency or probability, governs its chance of occurrence.

TABLE 2

PROBABILITY OF RISK DIFFERENCES BETWEEN ALTERNATIVES
- Unmitigated Risk -
[Risk measured by Expected Fatalities; probability given in percent]

	STR	ONS	REG	NAT	PRA	PRB	PRC	PRW
STR	--	99	99	99	99	99	99	99
ONS	1	--	48	37	1	6	6	49
REG	1	52	--	37	15	35	35	52
NAT	1	63	63	--	26	49	49	63
PRA	1	99	85	74	--	81	81	99
PRB	1	94	65	51	19	--	69	94
PRC	1	94	65	51	19	31	--	95
PRW	1	51	48	37	1	6	5	--

---

* Example: The probability that PRA (in row 5) is riskier than NAT (in column 4) is 74 percent (value in row 5, column 4). Conversely, the probability that NAT (in row 4) is riskier than PRA (in column 5) is 26 percent. Note that the two results, 74 percent and 26 percent, are complementary and total 100 percent. Thus, the "odds" that PRA is riskier than NAT are 74:26, or about 3:1. These results are based on comparisons of the means and ranges of computed "expected fatalities," after eliminating accident scenario contributions common to the two alternatives being compared (in order to obtain independently distributed data). Note that, since some types of uncertainty have not been considered explicitly, mid-range probabilities (e.g., those between 30 percent and 70 percent) are not believed to substantiate conclusions that risks are different.

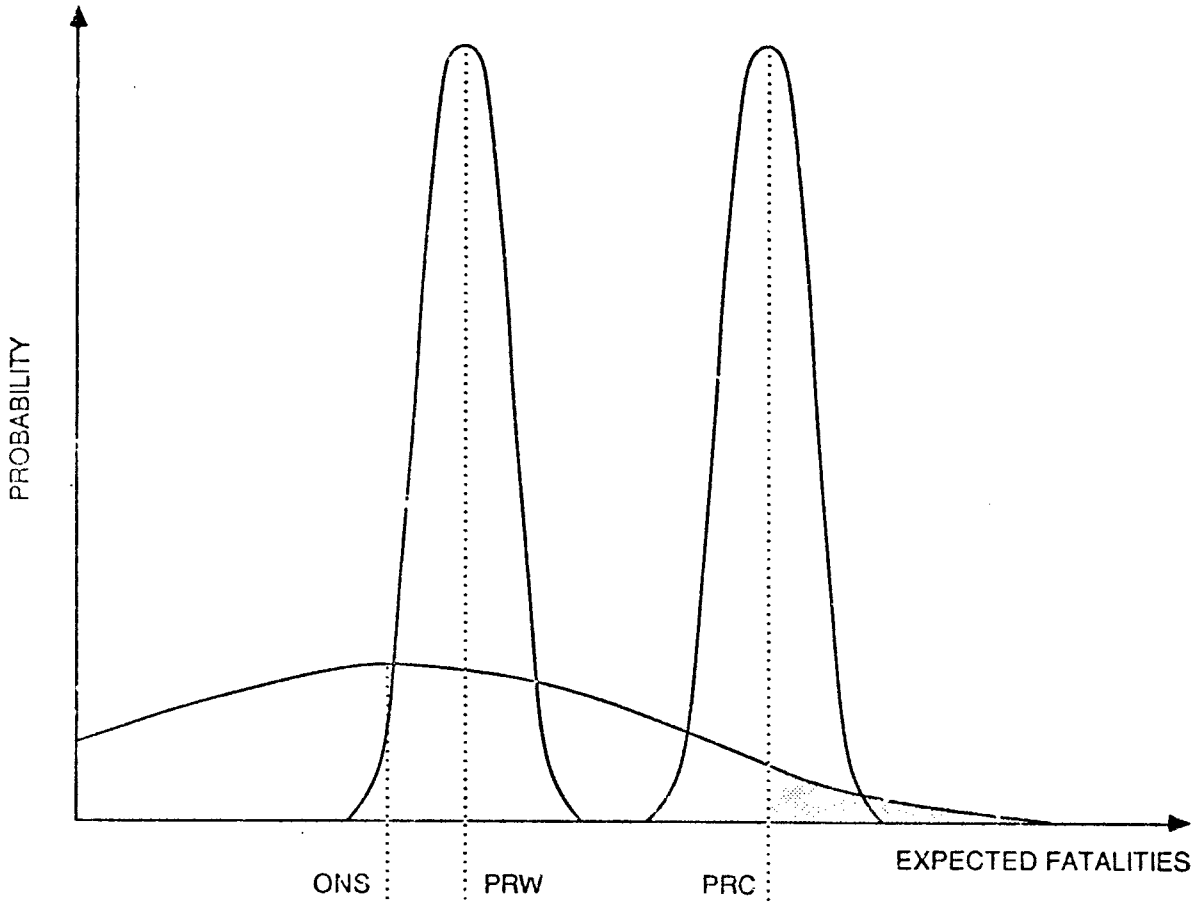

FIGURE 2
COMPARISONS BETWEEN ALTERNATIVES

At the outset of the detailed analysis, a decision is required regarding the extent to which uncertainty will be treated. The analysts must be informed about this decision and they must be given the time and resources to do the work. For the assessment of a program in which uncertainties will be great (because of the nature of the program's risks, or a lack of detailed data and information) or in which the frequencies or probabilities of high-consequence events will be low (in which case uncertainties in the completeness of event identification and in the accuracy of frequency or probability estimation will be important), the resources required for uncertainty analysis may be great, perhaps even greatly in excess of those required to generate best estimates only.

In the generation of best estimates of frequencies or probabilities, care should be taken to be consistent in the use of medians or means. Medians have often been selected instead of means because medians are basic to the formulation of the most commonly used forms of probability density functions, and because they can be estimated with greater precision from a limited sample. Unfortunately, for some of the data required for complex assessments, medians are either unavailable or much less accessible.

For example, suppose that three munitions are observed to detonate, on separate occasions, after exposures to fire that total 133 minutes. The mean time to detonation is about 44 minutes. Additional data would be needed to determine the median time to detonation. To illustrate this point, we can suppose that the individual times to detonation were 1 minute, 11 minutes, and 121 minutes. These times appear to be distributed geometrically about a median of 11 minutes. The four-fold difference between median and mean shows the importance of care in using consistent types of estimates of central tendencies. The additional information, which is often inaccessible or unavailable, needed to estimate the median shows that consistent use of means is often the more practical choice. The reader should also note that, if means are used as input to an analysis, means should also be selected as outputs of any Monte Carlo simulations that are performed. An additional benefit of the choice of means is that a median-to-mean conversion step may be saved and any associated uncertainty will be reduced when expected values are calculated.

Consistency is also necessary in the characterization of uncertainty. The types of uncertainty that are not to be included, if any, should be defined. For example, unidentified errors that may be present in data references, errors in the selection of analytical methodologies, and errors in the risk analysis calculations are often excluded from the quantified uncertainty. In general, it is best to estimate the effect of every source of uncertainty, even though such estimates may be based on judgment alone. This approach can greatly reduce the

systematic understatement of uncertainty inherent in the results of risk analyses.

Furthermore, care should be taken that uncertainties of medians or means are not confused with uncertainties of individual samples or single occurrences of events. Returning to the example of the three detonation times having a median value of 11 minutes, we can see that the uncertainty of a *single* occurrence can be characterized by the factor (which is the geometric standard deviation) of 11 between the median and either of the extreme values (1 or 121). However, since we have a sample size of three results (1, 11, and 121 minutes), and since the standard deviation of the median (as a geometric mean) is proportional to the inverted square root of the sample size, the uncertainty of the *median* is a factor of only $11/\sqrt{3}$ or about 6. If many more observations were available, including 100 each of detonations at about 1 minute, 11 minutes, and 121 minutes, the median time would still be 11 minutes, and the uncertainty of a single observation would still be a factor of 11, but the uncertainty of the median would be only a factor of $11/\sqrt{300}$ or 0.6.

Which should be used, the uncertainty of a single occurrence or the uncertainty of a median or mean? The answer to this question depends on the nature of the program analyzed and on the type of result that is expected (or on the criteria that will be used to evaluate the results). For example, if the subject of the risk analysis is a program that will continue indefinitely with numerous undesirable occurrences, and the goal of the analyst is to quantify the expected (whole) number of occurrences, then the uncertainty of the median or mean should be used. However, if the program is a short-term endeavor that would be abandoned after a single catastrophic occurrence, and the goal of the analyst is to quantify the probability of the unexpected (fractional expected value) occurrence, then the uncertainty of a single occurrence should be used. In any case, uncertainties of medians, means and single occurrences should not be combined indiscriminately.

Risk analyses can be greatly improved by detailed evaluations of associated uncertainties. This is especially so in the case of a program for which the best estimate of risk is low, and in the case of a comparison of alternatives whose risks appear to differ by small amounts. As demonstrated above, alternatives must be compared to each other directly, not to some other option (such as "PRC" above), if the comparison is to be valid. Furthermore, when the best estimates of risk are low for all of the likely alternatives, the ranges of risk uncertainties are critical. The reason for this is that the large uncertainty of the frequency or probability of the undesired event, much more so than the best estimate of frequency or probability, governs its chance of occurrence.

REFERENCES

Dixon, W.J. and F.J. Massey, Jr. (1957). *Introduction to Statistical Analysis*, 2nd edition, McGraw-Hill, New York.

Fraize, W.E. *et al.* (December 17, 1987). *Risk Analysis Supporting the Chemical Stockpile Disposal Program (CSDP)*, MTR-87W00230, McClean, VA: The MITRE Corporation, prepared for the U.S. Army, Office of the Program Executive Officer--Program Manager for Chemical Demilitarization, Aberdeen Proving Ground, MD.

GA Technologies, Inc. (August 1987a). *Risk Analysis of the Continued Storage of Chemical Munitions*, GA-C18564, San Diego, CA.

GA Technologies, Inc. (August 1987b). *Risk Analysis of the Disposal of Chemical Munitions at National or Regional Sites*, GA-C18563, San Diego, CA.

GA Technologies, Inc. (August 1987c). *Risk Analysis of the Onsite Disposal of Chemical Munitions*, GA-C18562, San Diego, CA.

Meyer, Stuart L. (1975). *Data Analysis for Scientists and Engineers*, John Wiley and Sons, New York.

Rohatgi, V.K. (1976). *An Introduction to Probability Theory and Mathematical Statistics*, John Wiley and Sons, New York.

U.S. Army, Program Manager for Chemical Demilitarization (July 1, 1986a). *Chemical Stockpile Disposal Program--Draft Programmatic Environmental Impact Statement*, Aberdeen Proving Ground, MD.

U.S. Army, Program Executive Officer--Program Manager for Chemical Demilitarization (January 1988). *Chemical Stockpile Disposal Program--Final Programmatic Environmental Impact Statement*, Aberdeen Proving Ground, MD.

U.S. Army Toxic and Hazardous Materials Agency (March 15, 1986b). *Chemical Stockpile Disposal Concept Plan*, AMXTH-CD-FR-85047, Aberdeen Proving Ground, MD.

Whitacre, C.G. *et al.* (1987). *Personal Computer Program for Chemical Hazard Prediction*, CRDEC-TR-87021, Aberdeen Proving Ground, MD.

HAZARD CLASSIFICATION OF LIQUID GUN PROPELLANTS

by

William R. Herrera
Southwest Research Institute
San Antonio, Texas

William O. Seals
Army Research Development Engineering Center
Picatinny Arsenal, New Jersey

George Petino, Jr. and Chester Grelecki
Hazard Research Corporation
Rockaway, New Jersey

ABSTRACT

The hazard classification of liquid propellants needs to be addressed because procedures for classification have not been established in the Department of Defense Hazard Classification Bulletin TB 700-2. This bulletin clearly states that it applies to ammunition and explosives other than liquids. However, the bulletin has been used as a guide in the hazard classification of liquid propellants.

Incident reports on explosions or detonations, identify the major modes of ignition as friction, impact, thermal, adiabatic compression, electrostatics, and impingement. In providing an accurate classification, the subject material must be exposed to the same stimuli as experienced in its environmental state. Often small-scale tests do not simulate the actual conditions, and full-scale tests must be performed to account for the critical mass. This paper will address the methodology and tests required to establish the hazard classification of liquid propellants.

INTRODUCTION

The safety community has an interim classification of Class B for liquid gun propellants (LGP). Being designated a liquid propellant, it had been automatically, by definition, classified as an explosive. As such, the DOD Manual TB 700-2 was used in establishing the classification. The manual explicitly states that it applies only to ammunition and explosives other than liquids.[1] Thus, the hazard classification of these liquid gun propellants was based on results of tests that were designed strictly for solid propellants.

The lack of a formal protocol for the hazard classification of liquid propellants within the Department of Defense (DOD) has posed a problem. As a potential remedy for this problem, the NATO AOP-7 706 manual has been evaluated to determine if characterizations and qualification tests were indeed valid for the classification of liquid propellar . The hazard classification scheme of Groups I through IV, as presented in the NATO AOP-7, were considered for

incorporation into this program. This paper will examine the test criterion for liquid propellants under the NATO AOP-7 manual.

BACKGROUND

NATO AOP-7, "Manual of Tests for the Qualification of Explosive Materials for Military Use," cites a scheme for the classification of liquids, qualification tests for determining the hazard classification and the characterization requirements essential for each liquid propellant for acceptance. The scheme for the classification of liquid propellants is shown in Table 1.[2] Qualification tests for the hazard classification of liquid propellants are given in Table 2.[3] The characterization requirements are shown in Table 3.[4]

METHODOLOGY

Small-scale tests can be selected to provide reliable information if the environmental modes of ignition are addressed. The modes of ignition considered critical for evaluating liquid propellants are thermal, compression ignition, impact, card gap, and electrostatic. Critical mass and diameter are parameters that must be obtained by full-scale test methods. As illustrated in Figure 1, once a liquid propellant demonstrates a positive explosive reaction in one of the screening tests, further testing will be continued to determine if the material is a Class A or B explosive (Figure 2). If the liquid propellant does not produce explosive reactions in all the screening tests (Figure 3), then the materials are subjected to the full-scale critical mass and diameter tests.

SCREENING TESTS

The card cap, impact, thermal stability, and electrostatic tests were considered the prime candidates for the screening process. A brief description of each is given below.

Card Gap Test[5]

A typical card gap tester is shown in Figure 4. This test measures the sensitivity of the material to the shock from a detonation. The test apparatus consists of a steel tube (14 cm long x 4.75 cm OD with a 0.55 cm wall thickness), two Pentolite pellets, a C-2 blasting cap, a 15 x 15 x 1 cm mild steel witness plate, cellulose acetate (or equivalent) cards 5 cm diameter by 0.025 cm thick (2 in. diameter x 0.01 in. thick). Detonation is indicated when a clean hole is cut in the witness plate. The test sample and explosive booster should be at 25°C ± 5°C at the time of the test. Should no detonation occur in the first test without cards, it is repeated two times for a total of three tests. If no detonation occurs in the three tests, testing is concluded, and the results are interpreted. If detonation occurs in any one of the first three trials, further testing must be done, where the number of cards used begins with 8, halving or doubling the cards until detonation occurs. This procedures is followed until the point of 50% probability of detonation is obtained. Normally, a maximum of 12 tests is required to determine the 50% value.

Impact Test[6]

A typical sample container of the impact test apparatus is shown in Figure 5. The liquid test sample (0.03 m) is enclosed in a cavity formed by a steel cup, an elastic O-ring, and a steel diaphragm. A piston rests on the diaphragm and carries a vent hole which is blocked by the steel diaphragm. A 2-kg weight is dropped on a steel ball in contact with the piston. A positive result is indicated when the reaction produces enough energy to rupture the diaphragm. Data are reported as the height which yields a 50% probability of initiation.

JANNAF Thermal Stability Study[7]

The JANNAF thermal stability test fixture is a stainless-steel cylinder 0.22 in. in diameter x 1-1/2 in. long, closed at the bottom with a shielded thermocouple and a compression fitting (Figure 6). The fixture is charged with 0.5 cc of sample and closed at the top with a stainless-steel diaphragm, 0.003 in. thick. The assembly is then placed in a bath which is heated at a constant rate of 10°C/min. A second thermocouple and an X-Y recorder are connected with the sample thermocouple so as to yield a plot of differential temperature versus bath temperature. Exothermic reactions appear as positive peaks, endothermic reactions as negative peaks. Results are reported in terms of the temperatures at which significant thermal activity is observed and the temperature at which the burst disk yields.

Electrostatic Test[8]

Electrostatic energy stored in a charged capacitor is discharged to the sample material being tested to determine whether an electrostatic discharge will cause the sample to decompose, flash, burn, etc. The sample is placed on a special holder which assures that the discharge will pass through the sample. The capacitor is charged with a 5000 volt potential; the discharge needle is lowered until a spark is drawn through the sample (the sample being about 20 mg in size). The standard test interval ranges from 0.0001 microfarads and 0.00125 joules (at 5 kV) to 1 microfarad and 12.5 joules (at 5 kV). The test is begun at the 12.5 joule (1 microfarad) level; if results are negative, testing is continued until 20 consecutive negatives are reported at that level. If the result is positive, such as a flash, spark, burn, odor, or noise other than instrument noise, then the next lower test interval is tried, until 20 consecutive negative results are reported. The test is normally conducted at a voltage of 5 kV DC or less. An ambient temperature of 18-32°C (65-90°F) and relative humidity not exceeding 40% are maintained.

RESULTS

The screening tests were conducted on LGP 1846. The results are presented in Table 4.

DISCUSSION OF RESULTS

Card Gap Test

A series of card gap tests were conducted by SwRI on LGP 1846. The results of these tests are presented in Table 4. A series of tests were conducted on LGP 1845 by Hazards Research Corporation in 1981 and have been included in Table 4 for comparison purposes with the results of the tests on the LGP 1846.

The tests conducted by SwRI on the LGP 1846 were conducted in accordance to the test procedure described earlier in this paper with two exceptions. First, a polyethylene liner was used in the LGP 1846 tests to isolate the LGP from the mild steel test tube, thereby precluding any contamination of the LGP. Second, the pentolite disks each weighed approximately 90 grams instead of 60 grams. On the tests conducted on the LGP 1845,[9] there were no "detonations" since the witness plates were dished but not punched with a hole. Similarly, the SwRI tests involving the LGP 1846 resulted in the witness plates being dished but no holes being cut into the plates. The witness plates are severely deformed, but no holes were punched in any of the plates. A test to confirm that the liquid propellant was becoming involved by the detonation of the pentolite and that the damage to the plate was not strictly due to the pentolite charages was conducted. To determine what contribution the LGP was making, the confirmation test was conducted with water instead of liquid propellant. The damage to the witness plate was much less without the LGP. A test was also conducted with a longer mild steel tube (42 cm), the witness plate was less damaged than the plates used for the 14-cm tube tests, indicating that the detonation was not being propagated through the liquid propellant but instead was being attenuated.

Under the classic Department of Defense TB-700-2 manual test procedures, any material designated as a propellant would automatically be classified as an explosive. The criteria for distinguishing between Military Class 7 (DOT Class A) and Military Class 2 (DOT Class B) is the sensitivity value of 70 cards. If the card value for the propellant is 70 or more cards, then the classification is Military Class 7. If the card value is less than 70 or no reaction at 0 cards, the classification is considered Military Class 2. The earlier card gap tests conducted by Hazard Research[7] on LP 1845 were only conducted at the 70-card level. When no reaction occurred at this level then, according to the TB-700-2 classification scheme, LP 1845 was classified as an explosive Military Class 2. This classification protocol does not allow for an accurate hazard assessment for a material when no reaction occurs at zero cards. A material should exhibit an explosive reaction before it is classified as an explosive. To follow the procedure of classification as outlined in the TB-700-2 is inconsistent with the concept of an explosive material.

Impact Tests

The impact value for LGP 1845 and LGP 1846 is 76 cm (30 in.). The impact value reported for nitromethane is 50 cm (20 in.). Nitromethane is shipped by ICC as a flammable liquid. By comparison, the liquid propellants cited are less sensitive than nitromethane yet are classified as a Class B explosive.

Thermal Stability

The thermal stability, under confinement, demonstrates the temperature at which significant thermal activity is observed and the temperature at which a rupture disk yields. The results of the LGP materials indicated that they produce high gas pressures under conditions of confinement. This is consistent with the normal functions of a gun propellant.

Electrostatic Tests

A series of electrostatic tests were conducted by SwRI in accordance with the test protocol outlined earlier in this paper. The sample holder consisted of a 0.0025 cm (0.001 in.) brass shim bonded to a 0.16 cm (0.0625 in.) thick high voltage phenolic dielectric material. The brass metal was connected to the ground lead of the spark generator. A 0.64-cm (0.25-in.) hole was cut into the insulator exposing the metal plate. The sample liquid material was then placed in the small cylindrical cavity created in the insulator. The upper electrode was then lowered near to the bottom electrode (the sample holder) and the charge was then allowed to arc through the liquid sample. Tests were conducted using LGP 1846 and the tests were conducted at energy levels of 180 millijoules (limits of the power supply) with no reaction. Twenty repeat tests were conducted with no reactions.

CONCLUSIONS AND RECOMMENDATIONS

1. The card gap test does not give a fine enough resolution for materials that are relatively insensitive. A more sensitive test procedure is required. The current criteria for a detonation is based upon a damage effect that in some instances can be ambiguous (low order detonation). A more fundamental criteria for a detonation is a measurement of the detonation velocity. It is recommended that the card gap be performed in tubes that are 16 in. or greater and instrumented with detonation probes.

2. The impact test is a measure of sensitivity of a liquid to adiabatic compression of gas bubbles in the vapor phase. Since the results have been obtained with standard ASTM test procedures, it is recommended that this procedure be adopted as a standard screening test for classification of liquid propellants.

3. The results of the thermal stability test under high confinement demonstrates the necessity for developing test procedures which are more representative of the type of containers which are used for normal handling, shipping, and storage.

REFERENCES

1. TB-700-2 Manual Department of Defense, "Explosive Hazard Classification Procedures," p. 1.1

2. NATO AOP-7, "Manual of Tests for the Qualification of Explosive Materials for Military Use," p.

3. NATO AOP-7, "Manual of Tests for the Qualification of Explosive Materials for Military Use," p.

4. NATO AOP-7, "Manual of Tests for the Qualification of Explosive Materials for Military Use," p.

5. TB-700-2 Manual Department of Defense, "Explosive Hazard Classification Procedures," p. 5.3-5.4

6. ASTM Designation D 2540-70, Drop Weight Sensitivity of Liquid Mono Propellants.

7. ASTM Designation 476-73, Thermal Instability of Confined Condensed Phase Systems.

8. NATO AOP-7, "Manual of Tests for the Qualification of Explosive Materials for Military Use," p.

9. Contract Report ARBRL-CR-00454, "Classification of Liquid Gun Propellants and Raw Materials for Transportation and Storage," Hazard Research Corporation, Rockaway, NJ, May 1981 (Table 3, p. 24).

TABLE 1. DOD AND NATO UN HAZARDS GROUPS OF LIQUID PROPELLANTS

Group	Type of Hazard
I	Fire hazard potential (alcohol, hydrocarbon fuel)
II	Flare-type fire (fluorine, LOX)
III	Container rupture or explosion (boranes, methane)
IV	Mass detonation (nitromethane)

Source: DARCOM-R 385-100, Chapter 15.

TABLE 2. NATO QUALIFICATION TESTS FOR HAZARD CLASSIFICATION OF LIQUID PROPELLANTS

Unconfined burning (bonfire)	202.01.002
Impact	201.01.004
Card gap	201.04.002
Minimum pressure for vapor phase ignition	201.08.001
Flash point	201.08.002
Abiabatic compression	202.02.001
Detonation velocity	302.01.001

Optional Tests

Attack by fragment
High velocity impact
Drop test package
Oblique impact
Critical conditions for self-heating

TABLE 3. NATO CHARACTERISTIC QUALIFICATION FOR LIQUID PROPELLANTS

1. General Characteristics
   - 1.1 Composition
   - 1.2 Type/Role
   - 1.3 Related Applications and Compositions
   - 1.4 Fabrications
   - 1.5 Physical Properties
2. Chemical Characteristics
   - 2.1 Stability
   - 2.2 Compatibility
   - 2.3 Toxicity
3. Propellant Characteristics
   - 3.1 Burning Characteristics
   - 3.2 Impulse/Impetus
   - 3.3 Heat of Combustion

TABLE 4. SCREENING TEST RESULTS

CARD GAP TESTS

No. of Tests Conducted	Fluid	Tube Length cm (in.)	No. of Cards	Effects on Plate
3	LGP 1846	14 (5.5)	0	Severely deformed, no hole punched
1	Water	14 (5.5)	0	Slightly deformed, no hole punched
1	LGP 1846	42 (16.5)	0	Severely deformed, no hole punched
2[9]	LGP 1845	14 (5.5)	70	Dished but not punched with a hole

IMPACT TESTS

Sample Identification	Drop Height (in.) 0%	50%	100%
1. LGP 1845	28	30	31
2. LGP 1846	29	30.5	33

JANNAF THERMAL STABILITY

Sample Identification	Temperature of Major Exotherm Onset (°C)	Remarks
1. LGP 1845	135	Very sharp and rapid exotherm, burst disk.
2. LGP 1846	120	

a 42-cm long tube instead of 14 cm tube.

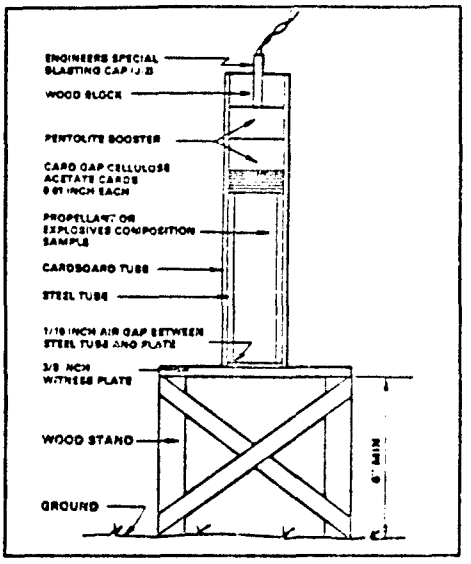

Figure 4. Card Cap Test Configuration

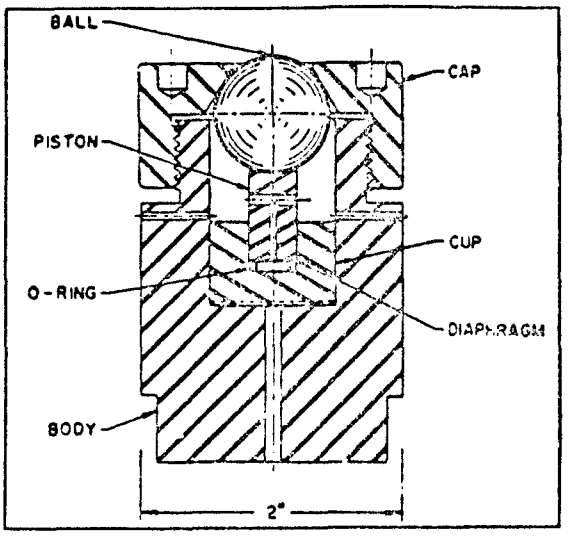

Figure 5. Liquid Sample Holder

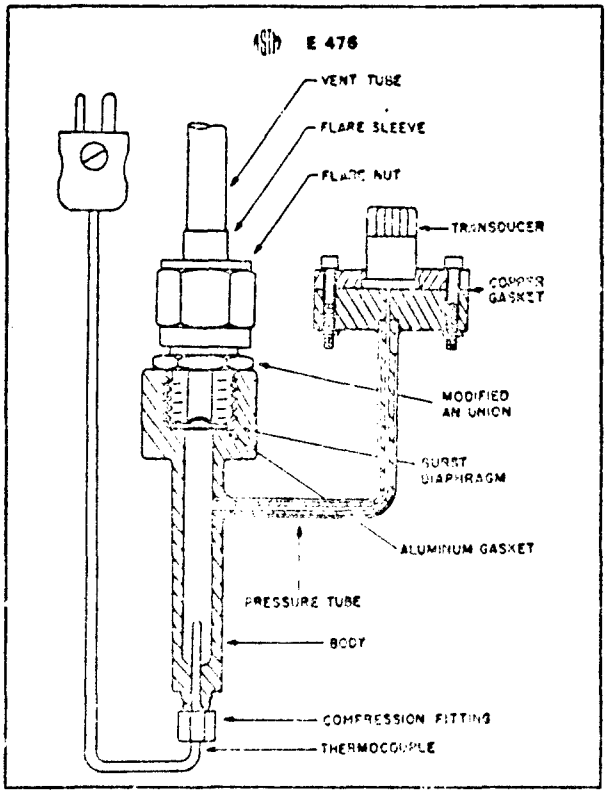

Figure 6. Thermal Stability Bomb Assembly

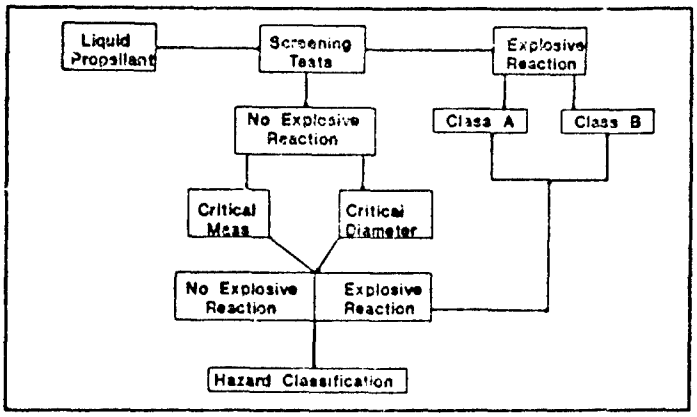

Figure 1. Hazard Classification Methodology

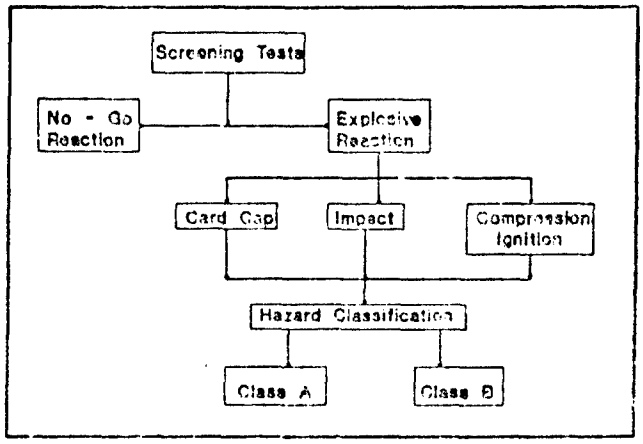

Figure 2. Explosive Reaction Methodology

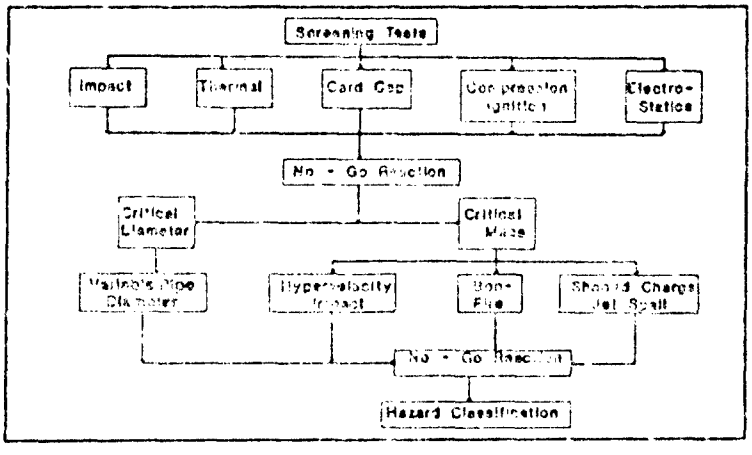

Figure 3. No-Go Reaction Methodology

JOINT HAZARD CLASSIFICATION SYSTEM AUTOMATED DATA BASE

by

Patricia S. Vittitow, USAMC Field Safety Activity

CURRENT PROCEDURES

The U.S. Army Materiel Command Field Safety Activity (FSA), Charlestown, IN manages the Department of Defense (DOD) Joint Hazard Classification System (JHCS). The JHCS contains the hazard classification for approximately 11,000 explosive items. The data fields established in the JHCS are:

a. National Stock Number (NSN).

b. DOD Identification Code (DODIC).

c. Item nomenclature.

d. DOD hazard class/division/storage compatibility group.

e. Fragment/firebrand distances, where appropriate.

f. United Nations serial number (UNS).

g. Department of Transportation (DOT) hazard class.

h. DOT label(s).

i. DOT container marking.

j. Part/drawing numbers.

k. Explosive weights in pounds and kilograms:

(1) Net Explosive Weights (1.1 material) - NEW.

(2) Net Propellant/Pyrotechnic Weights (1.3 material) - NPW.

(3) Explosive Weight for QD Purposes - normally the total weight of NEW and NPW. However, if propellant contribution tests have been conducted, the appropriate value would be entered here.

Currently the JHCS is printed on microfiche and distributed quarterly. FSA is responsible for distributing the microfiche and maintains the master address list for DDESB.

AUTOMATED DATA BASE (ADB) SYSTEM FEATURES

To make the JHCS more accessible by the field and to facilitate easy retrieval of the information available, the JHCS was recently automated. The system is originally intended for DA use, but with the installation of a larger computer system, it is anticipated that the ADB can be extended DOD-wide. Features of the ADB are:

a. Will allow 24-hour computer access worldwide,

b. Can accommodate 10 users simultaneously,

c. Can process up to 600 accesses daily.

The JHCS ADB has six "canned" queries that are menu driven which will enable the user to search for various data elements. The queries contained in the ADB will allow the user to search the JHCS data by:

a. NSN

b. DODIC.

c. Part/drawing number.

d. Nomenclature.

e. Determine magazine storage compatibility for a group of items.

DATA BASE INFORMATION

The data base file is an image of the JHCS Master Data File which is updated monthly. A new data base will be constructed on or shortly after the 15th of each month unless no changes had occurred to the JHCS. The Data Base Management System utilized is INFORMIX combined with SHELL and "C" program interface to effect MENU driven queries. As many as ten users at a time can access the data base file with read only permission (ROP). The ROP will facilitate LOGON procedures and negate the need for password assignment and control.

Computer Host(s)

As an interim solution to Central Systems Design Activity (CSDA) East's hardware/software communications needs, HQAMC will host the ADB until CSDA can procure the required communications hardware/software to support world-wide access. The data will be file transferred from CSDA-East's main frame into HQAMC DDN host computer concurrent with the JHCS file update frequency. It is the intention of CSDA-East to migrate from the HQAMC host onto the data bank main frame or other CSDA computer at which time the communication access is resolved.

Data Base Management System (DBMS) Employed

The DBMS employed is INFORMIX (version 3.0) under the UNIX operating system. INFORMIX is a relational DBMS which allows data to be entered, stored, manipulated, and retrieved. The end user will only be allowed to retrieve data by selection and execution of menu driven queries. Special queries may be developed on an as needed basis.

Data Base Record Layout

The data base record layout consists of 24 data items. See Appendix A for the layout and data item fields and codes.

BEGINNING A QUERY SESSION

It is advisable for any potential user to first seek the professional assistance of their local Directorate of Information Management in establishing the communication link to the HQAMC computer. The link could be through the local area network (LAN) or via the telephone using AUTOVON and 800 toll free dial-up compatibility.

Terminal Type

A terminal configuration should consist of an ANSI keyboard, cathode ray tube (CRT), modem, telephone, and a line printer if hard copy generation is desired. The type of terminal required to communicate with the HQAMC data base host computer is a VT100. Dumb or smart terminals of various manufacturers can be utilized in VT100 mode or emulation thereof. For those users who have no terminal equipment, an IBM compatible PC with communications software such as Crosstalk or Symphony, may be the ideal solution to retrieve JHCS data.

Modem

A 1200 baud modem or acoustic coupler must be configured to the terminal to effect data communication. Two AUTOVON numbers (284-5647 and 284-5311) and one toll free 800 (368-3157) number are available into the HQAMC computer. It should be noted that manual dial-up may be more advantageous over automatic dialing due to the availability of AUTOVON or 800 phone lines at your installation.

LOGON PROCEDURES

The logon procedures that have been developed are extremely easy to use. Due to the menu driven queries no password is required to enter the system. The logon name is "jhcsdb". After logging on the menu is automatically displayed.

Menu Display
The menu that will be displayed follows:

**********JOINT HAZARD CLASSIFICATION SYSTEM**********

1. List of JHCS data by NSN.

2. List of JHCS data by DODIC (DIC).

3. List of JHCS data by PART/DRAWING NR (PD1).

4. List of JHCS data by NOMENCLATURE (ITN).

5. Igloo Storage Compatibility Inquiry.

m. Redisplay this menu.

b. Bye (quit).

Query Retrieval Procedure (Menu Driven)
All queries will be executed from the menu by entering the relative number assigned to a data item name or inquiry job. Inquiry number 5 - Igloo Storage Compatibility, is an inquiry job. Inquiries number 1 through 4 are data item name queries. After entry of each data item query the system will prompt for another query. While another is being keyed, the system is retrieving the previous query entered and stacking the output for display. All query output will be arrayed in 80 character screen width format displaying all the data item in the record(s) selected. If no data appears after the query execution and only the header and "end of last line" are displayed, there are no records in file for the data item(s) entered. To end a session, return to the menu and enter 'b' for bye or quit, LOGOFF will then occur.

Sample Data Retrieval
An example of a data query by NSN and nomenclature is contained in Appendix B.

APPENDIX A

JOINT HAZARD CLASSIFICATION SYSTEM (JHCS)
INFORMIX DATA BASE RECORD LAYOUT

FIELD POS.	DATA ITEM IDENTIFICATION	QUERY MNEMONIC NAME	SIZE	CLASS
* 0	FILE KEY (FIELD POS. 1, 2 & 3)	HCSEQ	15	A/N
* 1	DOD COMPONENT	COM	1	A
* 2	TRI-SERVICE COORDINATION	TSC	1	A
* 3	NATIONAL STOCK NUMBER	NSN	13	N
* 4	ITEM NOMENCLATURE	ITN	48	A/N
* 5	DOD IDENTIFICATION CODE	DIC	4	A/N
* 6	DOD HAZARD CLASS/DIVISION & STORAGE COMPATIBILITY GROUP	IHCSC	6	A/N
6-1	INHABITED BUILDING DISTANCE	IBD	2	N
6-2	DOD HAZARD CLASS/DIVISION	HCD	3	A/N
6-3	STORAGE COMPATIBILITY GROUP	SCG	1	A
7	DEPT OF TRANSPORTATION LABEL (FIRST LABEL)	DL1	1	A/N
8	DEPT OF TRANSPORTATION LABEL (SECOND LABEL)	DL2	1	A/N
9	HAZARD SYMBOL CODE	HSC	2	A
10	DEPT OF TRANSPORTATION LABEL (THIRD LABEL)	DL3	1	A/N
11	UNITED NATIONS ORGANIZATION SERIAL NUMBER	UNS	4	N
12	DOT CLASS/EXEMPTION	DCLCE	2	A
12-1	DEPT OF TRANS. CLASS	DCL	1	A
12-2	DEPT OF TRANS. EXEMPTION	DEX	1	A
13	DEPT OF TRANS. MARKING	DMK	2	A
14	DEPT OF TRANS. EXPANSION	DMX	2	N
*15	DOT EXPLOSIVE REGISTRATION NO.	DER	7	N
16	NET EXPLOSIVE WEIGHT (LBS)	NEW-LBS	7	N OR BLANKS
16.1	NET EXPLOSIVE WEIGHT (KGS)	NEW-KGS	7	N OR BLANKS
17	NET PROPELLANT WEIGHT (LBS)	NPW-LBS	7	N OR BLANKS
17.1	NET PROPELLANT WEIGHT (KGS)	NPW-KGS	7	N OR BLANKS
18	NET EXPLOSIVE QUANTITY DISTANCE WEIGHT (LBS)	NEQ-LBS	7	N OR BLANKS
18.1	NET EXPLOSIVE QUANTITY DISTANCE WEIGHT (KGS)	NEQ-KGS	7	N OR BLANKS
*19	PART OR DRAWING NUMBER (FIRST)	PD1	16	A/N
*20	PART OR DRAWING NUMBER (SECOND)	PD2	16	A/N
*21	PART OR DRAWING NUMBER (THIRD)	PD3	16	A/N

* DATA ITEMS (INDEXED).

APPENDIX B

```
*****   JOINT HAZARD AUTOMATED RETRIEVAL SYSTEM   *****
             *****   QUERY MENU   *****

        1.  List JHCS data by NSN.

        2.  List JHCS data by DODIC (DIC).

        3.  List JHCS data by PART/DRAWING NR (PD1, PD2, or PD3).

        4.  List JHCS data by NOMENCLATURE (ITN).

        5.  Igloo Storage Compatibility Inquiry.

        6.  Ad Hoc Query Form.

        m.  Redisplay this menu.

        b.  Bye (Quit).

Enter selection and carriage return: 1


Enter first NSN:1310000158809
Another NSN ? (Y or N): y
Enter next NSN :1310005420384
Another NSN ? (Y or N): n

Please wait while program runs...
23054
        NSN - 1310000158809
        NSN - 1310005420384

Report is approx.      22 lines long.
Do you wish to print it ? (Y or N): y

Press <Print On> & <Enter> keys to start printing report.
At end of report, press <Print Off> & <Enter> keys.
```

JOINT HAZARD CLASSIFICATION SYSTEM
LIST OF DATA FROM QUERY BY NSN

COM	TSC	-----NSN-----	----------ITEM NOMENCLATURE----------	DIC-
A	N	1310000158809	CARTRIDGE 60 MM HE M49A2	B632

IBD	HCD	SCG	DL1	DL2	HSC	DL3	UNS	DCL	DEX	DMK	DME	DER	NEW-LBS	NEW-KGS	NPW-LBS
08	1.2	E	I				0321	I		AB			0.824	.373763	.015

NPW-KGS	NEQ-LBS	NEQ-KGS	PART-OR-DWG-NO-1	PART-OR-DWG-NO-2	PART-OR-DWG-NO-3
.006803	0.839	.380567			

COM	TSC	-----NSN-----	----------ITEM NOMENCLATURE----------	DIC-
A	N	1310005420384	CARTRIDGE 60 MM HE M49A2	B632

IBD	HCD	SCG	DL1	DL2	HSC	DL3	UNS	DCL	DEX	DMK	DME	DER	NEW-LBS	NEW-KGS	NPW-LBS
08	1.2	E	I				0321	I		AB			0.824	.373763	0.015

NPW-KGS	NEQ-LBS	NEQ-KGS	PART-OR-DWG-NO-1	PART-OR-DWG-NO-2	PART-OR-DWG-NO-3
.006803	0.829	.376031			

END OF LIST

```
Another Query ? (Y or N): n

      *****   JOINT HAZARD AUTOMATED RETRIEVAL SYSTEM   *****
                    *****   QUERY MENU   *****

              1.  List JHCS data by NSN.

              2.  List JHCS data by DODIC (DIC).

              3.  List JHCS data by PART/DRAWING NR (PD1, PD2, or PD3).

              4.  List JHCS data by NOMENCLATURE (ITN).

              5.  Igloo Storage Compatibility Inquiry.

              6.  Ad Hoc Query Form.

              m.  Redisplay this menu.

              b.  Bye (Quit).


      Enter selection and carriage return: 4


      Enter first NOMENCLATURE (in caps):M509

      Another NOMENCLATURE ? (Y or N): n

      This query will take 2-6 minutes per itn.
      Please wait while program runs...
23676
              ITN - 'M509'

      Report is approx.      39 lines long.
      Do you wish to print it ? (Y or N): y

      Press <Print On> & <Enter> keys to start printing report.
      At end of report, press <Print Off> & <Enter> keys.

25109
```

JOINT HAZARD CLASSIFICATION SYSTEM
LIST OF DATA FROM QUERY BY NOMENCLATURE (ITN)

COM	TSC	-----NSN-----	----------ITEM NOMENCLATURE----------	DIC-
A	N	1320009298389	PROJECTILE 8IN HE M509	D651

IBD	HCD	SCG	DL1	DL2	HSC	DL3	UNS	DCL	DEX	DMK	DME	DER	NEW-LBS	NEW-KGS	NPW-LBS
21	1.1	D	I				0168	I		BI					

NPW-KGS	NEQ-LBS	NEQ-KGS	PART-OR-DWG-NO-1	PART-OR-DWG-NO-2	PART-OR-DWG-NO-3

COM	TSC	-----NSN-----	----------ITEM NOMENCLATURE----------	DIC-
A	Y	1320001740760	CHARGE, SPOTTING, FOR PROJECTILES M483A1 + M509	D003

IBD	HCD	SCG	DL1	DL2	HSC	DL3	UNS	DCL	DEX	DMK	DME	DER	NEW-LBS	NEW-KGS	NPW-LBS
	1.1	D	I				0060	I		FF			0.103	.046720	

NPW-KGS	NEQ-LBS	NEQ-KGS	PART-OR-DWG-NO-1	PART-OR-DWG-NO-2	PART-OR-DWG-NO-3
			9272016		

COM	TSC	-----NSN-----	----------ITEM NOMENCLATURE----------	DIC-
A	Y	1320010736010	PROJECTILE 8-INCH M509E1	D651

IBD	HCD	SCG	DL1	DL2	HSC	DL3	UNS	DCL	DEX	DMK	DME	DER	NEW-LBS	NEW-KGS	NPW-LBS
21	1.1	D	I				0168	I		BI					

NPW-KGS	NEQ-LBS	NEQ-KGS	PART-OR-DWG-NO-1	PART-OR-DWG-NO-2	PART-OR-DWG-NO-3
			9362612		

COM	TSC	-----NSN-----	----------ITEM NOMENCLATURE----------	DIC-
N	N	1390002288383	FUZE ASSEMBLY,M509A1/M509B6 PIBD F/CTG DOD C2 NX83	

IBD	HCD	SCG	DL1	DL2	HSC	DL3	UNS	DCL	DEX	DMK	DME	DER	NEW-LBS	NEW-KGS	NPW-LBS
	1.1	D	I				0408	I		AZ					

NPW-KGS	NEQ-LBS	NEQ-KGS	PART-OR-DWG-NO-1	PART-OR-DWG-NO-2	PART-OR-DWG-NO-3

END OF LIST

CATEGORISATION OF DRY NC/NG PROPELLANT PASTE IN DRYING TROLLEYS WITHIN A MODIFIED DRYING BUILDING ENVIRONMENT

N. Cazanis
Explosives Factory Maribyrnong
Department of Defence
MELBOURNE AUSTRALIA

A B S T R A C T

Quantity - Distance problems are encountered with existing propellant paste drying facilities at Explosives Factory Maribyrnong under the present categorisation of 1.1 D for dry NC/NG pastes. If it can be shown that pastes typical of those produced at EFM behave as 1.3C category material at the end of the drying process when distributed and contained in a drying trolley as at EFM, the Quantity - Distance restrictions will be greatly reduced.

A series of large scale trials were conducted with propellant pastes in drying units within a simulated but modified drying building configuration and it was shown that pastes containing only NG and NC with 'N' content of 13% could be regarded as 'mass fire' rather than 'mass explosion' risk when arranged as in the trials.

INTRODUCTION

Propellant paste or powder cake in its dry state is classified under the United Nation Hazard Division of 1.1 D. This classification imposes Quantity - Distance restrictions on the use of the paste drying building at Explosives Factory Maribyrnong.

Trials to investigate the behaviour of dry propellant pastes have been conducted in the past both in Australian and the United Kingdom. Early Australian trials [1,2,3] showed that pastes which consisted of only NG and NC and where the 'N' content of the NC was above 12.6% would burn to detonation under conditions of mild confinement. In later trials [4,5,6] carried out in the United Kingdom, the behaviour of paste was assessed under conditions which would be encountered in the actual drying arrangement. It was again shown that pastes consisting of only NG and NC with 'N' content of less than 12.6% could be considered as 'mass fire' risk under condition of confinement no greater than that obtained when in trays in paste drying units. However, for pastes where the 'N' content of the NC was about 13% contradictory results were obtained in small scale tests, and a detonation did occur when two 25 tray drying units each containing about 110 kg of dry paste were placed side by side.

More recent trials carried out in Australia, at Mulwala Explosives Factory, Yarrawonga, involved a range of dry NC/NG propellant paste compositions including pastes where the 'N' content of the NC was over 13%. These trials were conducted in the open with paste loaded into lightly constructed simulated drying trolleys. No detonations were obtained even in tests where two simulated drying trolleys were placed close to each other. For these trials the paste had been wrapped in calico cloth and then placed on trays for loading into the drying trolleys.

On the basis of the results from these recent trials, there was still insufficient evidence to consider the drying process at EFM within the existing building configuration and environment as a fire hazard only.

A trial which consisted of a series of full-scale tests was carried out with dry paste consisting of only NG and NC with 'N' content of 13%, wrapped in calico cloth and loaded into standard heavily constructed drying trolleys and ignited within simulated drying buildings of modified configuration. The modified drying building arrangement involved the separation of drying trolleys by means of partitioning walls such that each trolley was within a single bay in the simulated drying house building.

EXPERIMENTAL

Site Selection

On initial planning for this series of trials it was considered that up to 500 kg of dry paste may be involved in a single test. For such a quantity of potential 1.1 material a suitably large and remote area was required. The Australian Army was approached and permission was granted for the use of the site and facility at the Proof and Experimental Establishment at Graytown, some 140 km by road from Explosives Factory Maribyrnong. The remote site although suitable for the tests, presented other problems, particularly transporting to the site the quantities of dry paste required.

Paste Drying

Current transport regulations for the transport of dangerous goods prevent the transport of NC/NG pastes, UN Number 0159, if the water content is below 35%. It was therefore necessary to transport the paste wet, and dry the required quantity on site prior to each test.

A number of options for drying the paste were considered but the method selected was by the use of electrically driven axial fan and electric heating elements to blow hot air over the paste which was loaded on trays in a standard paste drying trolley. Although electric heaters would not normally be used within the factory for paste drying, with proper precautions they were considered to provide the required safety at the isolated trials site.

The fan and heater unit were placed about 20 metres from the loaded paste drying trolley and the hot air was ducted through an insulated flexible metal duct. A 62.5 KVA diesel generator to power the heaters was placed a further 100 metres away. The heater elements had a total rating of 38 Kw but depending on ambient conditions only the required number of elements were switched on to give heated air at the entry of the drying trolley of between 45 - 50°C. The elements were also of a design which provided maximum safety in that the conducting wire is enclosed in a finned mild steel tube and should the wire burn out, no sparks would escape into the duct. The generator ducting and drying trucks were earthed to prevent the build up of static electricity.

Paste Composition

NC/NG pastes expected to be produced at EFM are primarily for solvent and semi-solvent propellants. The paste compositions would typically be 49 - 56% NG with the NC having a Nitrogen content of 12.3 - 13.2% For this series of tests, a standard paste composition consisting of 50% NG and 50% NC with a Nitrogen content of 13% was chosen as previous trials at Mulwala Explosives Factory indicated that severity of a fire increased with increasing NC content and increasing Nitrogen content.

Paste Preparation and Loading in Drying Units

The normal paste preparation process at EFM is for paste to be produced in 'sheeted' form, placed on Aluminium perforated trays and stacked into paste drying trolleys. Each tray holds about 4.5 Kg of dry paste and each drying trolley can hold 24 trays in two stacks of 12 trays side by side to give a total load of dry paste of about 110 Kg.

For this series of trials it was also decided that the paste be wrapped in calico cloth as it was taken off the 'sheeting' table and placed on the trays. It was considered that the calico cloth would provide a sufficient barrier to flame propagation to lessen the potential for a mass explosion upon ignition.

The paste drying trolleys used in the trials were standard heavily constructed units which had heavy metal wheels and other metal fittings removed to reduce the fragment hazard should a detonation occur. However structural integrity of the trolleys was not affected and the paste would be burned under the degree of confinement that is imposed by a standard paste drying unit.

Simulated Paste Drying House Building

The drying house at EFM is a timber framed asbestos cement sheet covered building approximately 24 metres wide by 9 metres deep. The interior of the building is open and up to 24 drying trolleys in 8 lines can be connected to overhead air drying ducts. The internal framing of the building divides the area into eight 3 metre wide bays and offers the opportunity to construct light flashproof partitioning walls.

For the trials a representative building design was selected to simulate the configuration of a portion of the actual drying house building. The trial buildings were steel and timber frame structures with galvanised steel roof and wall cladding. Each building was 9 metres wide by 9 metres deep and divided into 3 bays each 3 metres wide and each representative in volume to the 8 bays that would be created if the actual drying house building was partitioned. Although each bay is capable of accommodating 3 drying trolleys, it is proposed that in the modified drying process only one trolley of paste would be placed in each bay for drying and this was the arrangement in these tests.

The partitioning of the trials buildings was achieved by cladding both sides of the internal frame with the same galvanised steel sheet used for covering the external walls. The 'double-skin' partitioning walls should withstand the overpressure better than the single skin external walls and roof to give the necessary protection to the adjoining bays. Also if not providing a complete barrier to the ingress of flame to adjoining bays then at the very least the fireball should have dissipated sufficiently through the external walls and roof to minimise heat input into the paste in the trolley in the adjacent bay to prevent a burn to detonation.

The bays in the trials buildings were also fitted with interconnecting metal ducts to simulate the air-drying ducting of the actual building to assess its risk as a possible flame path.

The actual drying building and the trial simulated drying building layouts are diagrammatically shown on Figure 1.

Instrumentation

For each test in these trials, visual records were obtained by video and high speed photography. In addition blast overpressure recording equipment was installed to obtain a measure of the blast should a detonation occur. Further information was gathered by thermocouples and pressure measuring instrumentation within the individual bays.

Ignition

The ignition of the paste in each test was achieved by the use of igniters consisting of an electric match head and 2 grammes of black powder. Two igniters were placed in the bottom tray in the paste drying trolley to ensure ignition should one igniter fail. In tests where more than one trolley of paste was involved, each trolley was fitted with igniters so that if the receptor trolleys were not ignited by the donor trolley then they could be disposed of by firing as single truck events. This ensured that the firing party did not have to approach a potentially dangerous site and also provides additional confidence that single trolleys of paste will not burn to detonation.

RESULTS

Test No 1 - 19 November 1987

This test was conducted in the open as a preliminary test to observe the behaviour of the burning paste in a standard paste drying trolley prior to undertaking tests within the simulated drying house buildings. The test involved a single trolley of 4.5 Kg dry sheeted paste wrapped in calico cloth on each of 24 trays to give a total load of 110 Kg which is the standard loading adopted for this series of trials.

The paste had been dried over 23.5 hours at 45 - 50°C to a moisture level of 0.2%. The temperature of the paste on firing was estimated at about 30°C.

On ignition the paste burned fiercely without detonation and was nearly all consumed within about 2 seconds. The fireball that developed was directional due to the construction of the drying trolley which has only canvas covers at the front and back for connecting to hot air ducts.

Examination of the trolley after the burn showed that it had suffered relatively little structural damage. The doors on the side through which the paste trays are loaded onto the racks had been blown off and thrown about 4 - 5 metres. Most of the Aluminium paste trays were in place and showed little or no damage.

As there was no detonation no data was collected by the blast overpressure instrumentation which had the pressure probes set 30 metres away from the trolley. The thermocouple which was located about 2 metres from the trolley recorded a maximum temperature of 1150°C. While another thermocouple placed 8 metres away recorded a temperature of 110°C.

Test No 2 - 26 November 1987

In this test one trolley of 110 Kg of dry paste was placed in the end bay of the 3 bay test building. Into each bay interconnecting metal ducting was installed to represent the hot air ducting of the actual drying building. The paste trolley was connected to this overhead duct with a standard canvas connection. This arrangement is shown in Figure 2. Each bay has 3 corrugated steel roof panels replaced by lightly attached fibre glass reinforced plastic panels to represent a venting system of about 6 square metres in area. The side wall to the end bay which did not contain the paste trolley was removed so that the behaviour of the partitioning wall between that bay and the middle ray could be observed. The doors to each bay were closed and secured with a small sliding bolt.

The paste in this test was dried over a period of 23.5 hours to a moisture level of 1.4% and it was estimated that the temperature of the paste on firing was about 32°C.

The paste was ignited in the normal manner and burned fiercely with flames extending out through the roof and the blown open door. Examination of the visual records showed that the doors to the bay with the burning paste and the middle bay blew open very early and almost simultaneously indicating that pressure was leaking into the middle bay as it was developing in the first bay. Also at about the same time the plastic roof panels were blown off ahead of any visible flame and thus behaved as quick operating roof vents.

A side view of the burn showed that the fireball extended about 15 metres in front of the building through the blown open door. A side view into the end bay (Bay 3) which had its external side removed, showed a puff of smoke issuing from the open interconnecting duct.

After firing examination of the site showed that the building had suffered relatively little damage. The sliding bolts which held the doors closed had easily snapped their securing rivets to allow the doors to open early during the initial pressure build up. Apart from the lightly attached plastic roof panels no other roof or wall panels were blown off. Only some of the wall panels at the rear of the bay had been bent back near the roof line. The damage to the partitioning wall was only slight and this had been caused when doors of the paste drying trolley has been blown off and onto the wall. The exposed timber framing of the building only showed surface blacking and charing. Pressure and flame penetration to the adjoining bay had occurred at the partition wall/roof line where no attempt had been made to provide a good seal.

The paste drying trolley itself suffered more damage then the trolley in the previous trial and had been displaced a short distance from its original position but it was still substantially intact.

The blast overpressure instrumentation registered no readings from the probes set 30 metres in front of the building.

The thermocouples placed near the paste trolley gave maximum readings of 1000°C and 925°C. The thermocouple in the adjoining middle bay recorded a maximum of 250°C, possibly because flame that had leaked through the partitioning wall had reached or came very close to the thermocouple. Examination of the middle bay revealed little fire/flame damage and it is considered unlikely that much of this bay had seen temperatures of 250°C for other than very brief periods.

Test No 3 - 10 December 1987

On the basis of the results and observations of the above tests it was decided that for this test an overload arrangement would be used. Two drying trolleys each loaded with 145 Kg of dry paste were placed one in each of the end bays (Bays 1 and 3) of the 3 bay test building as shown in Figure 3. An empty drying trolley was placed in the middle bay (Bay 2). Both loaded trolleys were connected to the overhead interconnecting duct. The higher loading in the paste drying trolleys was achieved by inserting additional trays of 4.5 Kg, wrapped, sheeted paste in between the 24 trays of the standard load.

The paste had been dried to a level of 0.22% moisture and it was estimated that the temperature of the paste on firing was about 36°C.

The trolley of paste in the left hand side bay (Bay 1) was ignited and was burning fiercely for about 2 seconds, when the trolley in Bay 3 ignited and burned with considerable violence but without detonation.

Examination of the site after firing showed that the damage to the building was relatively minor although some wall and roof panels had been blown off the building. The bay, in which the second trolley had burned, suffered the most damage and this second trolley had collapsed. Paste trays had been scattered inside and outside the bay by the violence of the burn.

It was considered that ignition of the second trolley of paste had occurred from the first trolley either by flame or burning debris travelling down the interconnecting duct. It was also possible that flame could have reached into the bay through the partition wall-roof line which was not adequately sealed. A camera placed in the floor of the middle bay, in which the empty paste trolley had been placed, showed considerable flame penetrating at the roof line from the adjoining bays. The temperature recorded by the thermocouple in the middle bay was 415°C.

From the front view it was seen that the fireball from ignition of the trolley in Bay 1 had almost engulfed the entire building and as it was receding the trolley in Bay 3 ignited. A side view showed that the fireball from the burning of the paste in Bay 1 extended about 20 metres in front the the building at its maximum.

No reading was registered by the blast overpressure instrumentation which had probes placed 30 metres in front of the building. A maximum temperature of 935°C was recorded in the bay of the first trolley ignited (Bay 1), while at the other end bay (Bay 3) the thermocouple directly above the paste trolley recorded a temperature of 1330°C.

Test No 4 - 3 May 1988

In this test 3 paste trolleys loaded with 110 Kg of dry paste were placed one in each of the bays of the 3 bay building in the arrangement shown in Figure 4. No plastic roof panels were placed in the roof over any of the bays so as to impose relatively more confinement to the burning paste than in the previous tests.

The overhead ducting from the bay on the left hand side (Bay 1) was carried past the other two bays and had the outlets pointing outward. This was arranged in an attempt to see whether any flame or burning material from the ignition of the paste in the left hand bay entered and travelled down and out the duct. A brass mesh screen was also placed in the duct near the opening over Bay 2 to collect any debris that may enter the duct when the paste in Bay 1 burned. The sealing of bays was improved by using 150mm x 150mm galvinised steel flashing strips over 50mm thick mineral wool insulation blanket around the edges of both sides of the partitioning walls in each bay.

The paste in each trolley was dried to moisture levels of between 0.21% and 0.25%. The temperature of the paste in the trolleys in Bays 1 and 2 on firing was estimated as being between 30°C and 35°C. The paste in the trolley in Bay 3 had completed its drying on the previous evening and the paste had cooled to about 20°C.

The three paste trolleys had been fitted with igniters and the trolley in Bay 1 was ignited first. This burned fiercely. The door was blown open and some external wall panels were also blown off the front and side of Bay 1. There was no propagation of the fire to either the adjoining middle bay or the other end bay. After a period of about 8 minutes the paste trolley in the middle bay was ignited from the firing control station. Again no propagation of the fire to the remaining trolley of paste in the end bay (Bay 3) occurred and this was disposed of after a further wait of about 6 minutes to render the site safe for inspection.

Once again the building suffered only what was considered to be minor structural damage in that the frame was substantially intact. The partitioning walls were still in place and only some external wall panels and doors to Bays 1 and 3 has been dislodged and thrown some distance from the building. The door from Bay 1 was found 15 metres in front of the building while the door from Bay 3 was found about 4 metres in front of Bay 3. The method of sealing around the partitioning walls appear to be effective and it was still in place around both sides of both walls.

Examination of the visual records show that the fire from Bay 1 largely vented out from the front of the building and reached about 18 metres. The ignition of the trolley in Bay 2 resulted in the rear wall of the bay being blown out and the fireball dissipated mainly out the back. For Bay 3 external side wall to the building gave way very early in the burn and the fireball vented out mainly through this side.

In each of these events the paste burned without detonation and no readings were made on the blast overpressure instrumentation. Although a number of roof and wall panels were blown off from each bay the building suffered relatively little structural damage.

As in this test it was arranged to obtain more information on the conditions in the duct during the burn temperature and pressure readings were taken at various points inside the duct. The highest temperature recorded was 460^{o}C just inside the duct from the first bay while further along the duct temperatures of 270^{o}C and 330^{o}C were obtained either side of the screen. Pressure measurements were also made and pressure of 1.72 kPa was recorded in the first but no appreciable pressure could be measured in the duct. The inside of the duct near the opening over Bay 2 where the screen had been placed was examined carefully. No evidence of flame or burned debris arising from the burning of paste trolley in Bay 1 could be found.

Test No 5 - 10 May 1988

The building that was used in test No. 2 was refurbished and modified for this test. A trolley loaded with 110 Kg of dry paste was placed in each of the 3 bays as shown in Figure 5. The partitioning wall between the left hand bay and the middle was lined with 9mm fibre cement board and the partitioning wall between the middle bay and the other bay was lined with 6mm fibre cement board. This was done to obtain some measure of the performance of more suitable building materials that could be used for modifying the actual drying house building.

The trolley of paste in the middle bay would be ignited first and this was connected to the overhead duct which ran into the left hand bay where it was also connected to the trolley in that bay. The duct was carried past the right hand bay and just past the building and left open. A brass screen was placed at this duct opening to again try and collect any debris that may enter the duct from the burning of the trolleys in Bay 1 and Bay 2. The middle bay (Bay 2) was provided with 4.5 square metres of venting area through the roof by removing roof panels. A further 3.6 square metres of venting was provided by removing the door. The left hand bay (Bay 1) had no venting either via the roof or doorway and the right hand bay only had 3.6 square metres of venting via the open doorway.

The sealing around the partitioning had been improved in the same manner as in the building for Test No 4.

The paste in all trolleys was dried to a moisture level of between 0.2% and 0.4% and it was estimated that the temperature of the paste in the trolleys in Bays 1 and 2 was between 30°C and 35°C on firing. The temperature of the paste in the trolley in Bay 3 was estimated at being at about 20°C.

The paste in the trolley in the middle bay was ignited first and burned without the fire propagating to the trolleys in the adjacent bays either via the interconnecting duct (to Bay 1) or the open doorway (Bay 3).

The remaining trolleys which had been fitted with igniters were each disposed of at about 6 minute intervals to render the site safe for inspection. Each trolley of paste burned as a single event and without detonation.

Once again the building was considered to have suffered relatively little structural damage. Some roof and wall panels had been blown off from each bay. The partitioning wall between Bay 1 and Bay 2 had suffered considerable damage about the middle region adjacent to where the paste trolleys were located. Some of the sheets of fibre cement board (Bay 1 side) and galvanised steel wall panels (Bay 2 side) had collapsed. Initial damage had been caused during the burning of the trolley in Bay 2 as visual records show that the closed door to Bay 1 was blown open during the very early stages of the paste burning in Bay 2. As this building had also been used in Test 2 the partitioning wall frame-work may have been weakened sufficiently so as not to be able to withstand a second pressurisation. However any flame that had entered Bay 1 via the partitioning wall did not ignite the paste in the trolley in Bay 1 so only slight damage to the partitioning wall must have occurred during the first burn. More severe damage which resulted in panels been blown off the wall must have occurred during the burning of the trolley in Bay 1 which was ignited for disposal some 6 minutes later.

Although no ignition of the trolley in Bay 1 had occurred via the interconnecting duct from the trolley in Bay 2, close examination of the visual records showed a glow and a puff of smoke issuing from the open end of the duct over the right hand bay. Also a thermocouple placed in the duct inlet in the middle bay recorded a temperature of 470^{o}C.

Small pieces of burned debris were found trapped by the screen at the open end of the duct. These were determined to be burned canvas material from the canvas connection put in place between the trolley and the overhead duct as would be the case during the normal drying process.

Any flame and heat in the duct during the burning of the paste in Bay 2 did not reach or was insufficient to ignite the paste in the trolley in Bay 1. Other thermocouples recorded temperatures of 1230°C in the left hand bay when the trolley in that bay was ignited. Instrumentation for measuring of pressure in the bays recorded a maximum pressure of 2.41 kPa in the middle bay.

No readings were obtained on the blast overpressure measuring equipment during the burning of any of the paste trolleys.

DISCUSSION

A total of ten drying trolleys of paste were burned in these trials. Although some tests involved more than one trolley, each burn can be considered to be a single event. Eight of the trolleys had a standard loading of 110 Kg of dry paste while two trolleys (Test 2) had a 40% increase in the loading to 145 Kg of dry paste. In all tests the paste burned without detonating.

When the separation wall between bays is sealed to prevent the passage of flame and hot gases then paste in a second bay will not be ignited by a fire in the neighbouring bay.

Some transfer of hot gas may occur between bays in the hot air drying ductwork but this does not appear to be sufficient to induce burning in wrapped paste provided burning particulate matter is retained by metal screens. The emission of flame is directional as determined by the location of venting arrangements. Strong winds may influence this to some extent.

Provided the bay separation walls are sealed then fires in more than one bay will occur as individual events.

CONCLUSIONS

This trial has demonstrated that NG/NC paste of a typical composition where the Nitrogen content of the NC is high (13%) will not burn to detonation when wrapped in calico cloth, laid out on drying trays, loaded at the rate of 110 Kg dry paste per drying unit or trolley and each trolley is within its own bay in a drying building. The partitioning walls separating each bay need only be marginally stronger than the roof, end walls or venting systems to withstand the pressurisation in the bay over the short period in which the paste is consumed. Paste prepared in this manner and dried in this arrangement can be classified as 1.3C during the drying process.

ACKNOWLEDGEMENTS

The assistance, co-operation and facilities provided by the Commanding Officer, Proof and Experimental Establishment, Graytown and his staff are gratefully acknowledged.

The author also wishes to express his gratitude to the following organization who have provided much valuable assistance and services during this trial:

- Engineering Development Establishment for blast overpressure measurement instrumentation and visual data gathering and presentation.

- Ordnance Factory Maribyrnong, Instrument Services Section for temperature and pressure measurement and recording.

REFERENCES

1. Coulson, W.H "Categorisation of Propellant Pastes", EC 1452, Summary of Field Trials Held at Compton Vale, EB 1959/25

2. Coulson, W.H "Categorisation of Propellant Pastes", EC 1452, 5th Series of Trials, EB 1960/4

3. Coulson, W.H "Categorisation of Propellant Pastes", EC 1452, 5th Series of Trials, EB 1965/9

4. "The Safety Distance Category Applicable to Propellant Pastes Whilst in Trolleys in Paste Drying Units", Trials (Series 1) - ROF Bishopton, April 1967

5. Berry, A.V "Safety Distance Category of Propellant Pastes in Drying Units", Trials (Series 2) - ROF Bishopton, October 1968

6. Berry, A.V "Safety Distance Category of Propellant Pastes in Drying Units", Trials (Series 3) - ROF Bishopton, April 1969

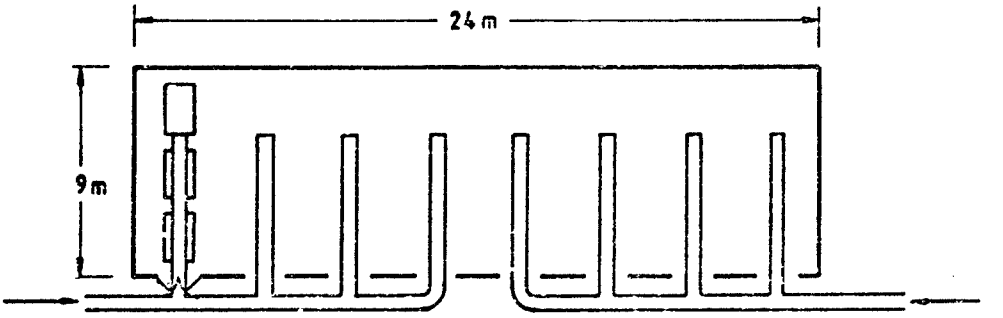

EXISTING DRYING BUILDING ARRANGEMENT AT E.F.M.
8 LINES EACH OF 3 DRYING TROLLEYS

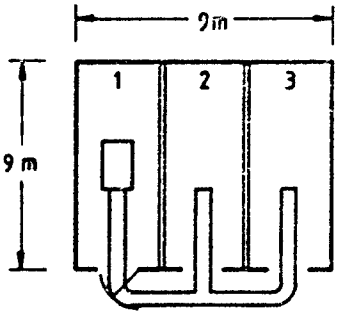

SIMULATED DRYING BUILDING ARRANGEMENT USED IN TRIAL
1 DRYING TROLLEY IN EACH BAY

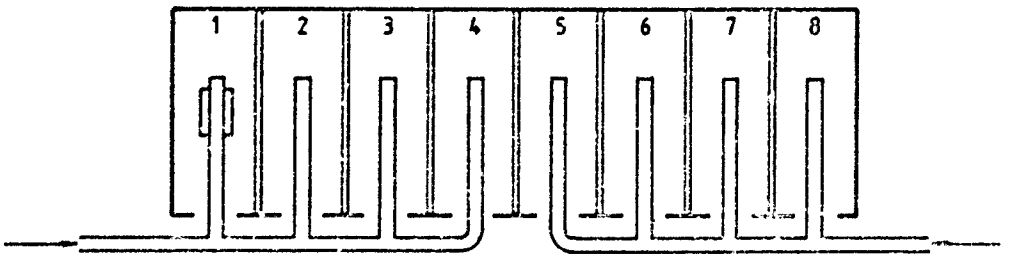

PROPOSED DRYING BUILDING ARRANGEMENT AT E.F.M.
1 DRYING TROLLEY IN EACH OF 8 BAYS

FIGURE 1. DRYING BUILDING ARRANGEMENT

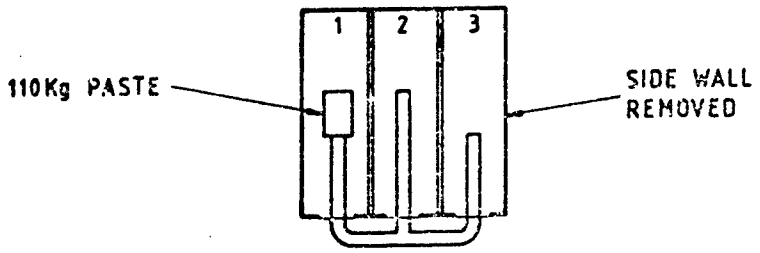

FIGURE 2 ARRANGEMENT FOR TEST 2

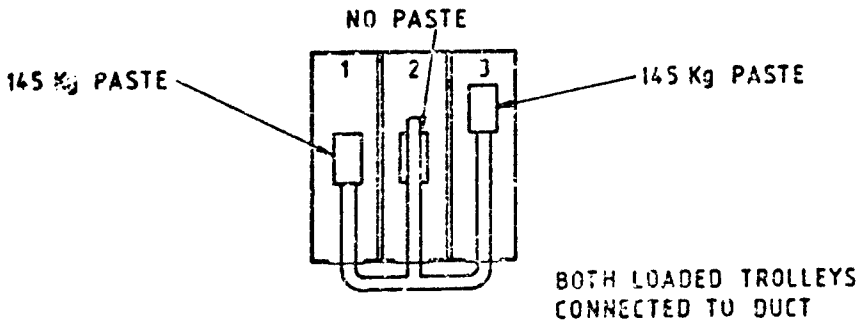

FIGURE 3 ARRANGEMENT FOR TEST 3

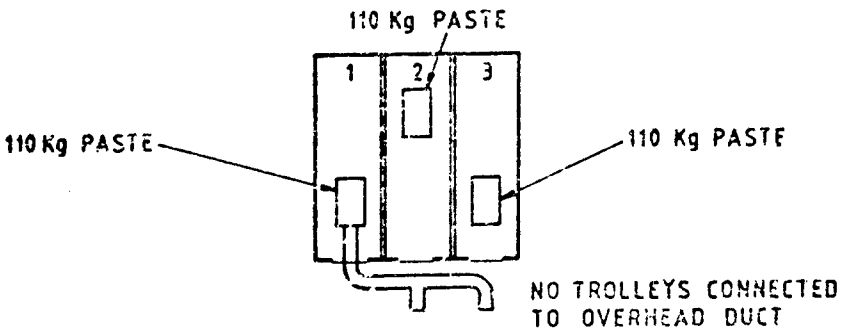

FIGURE 4 ARRANGEMENT FOR TEST 4

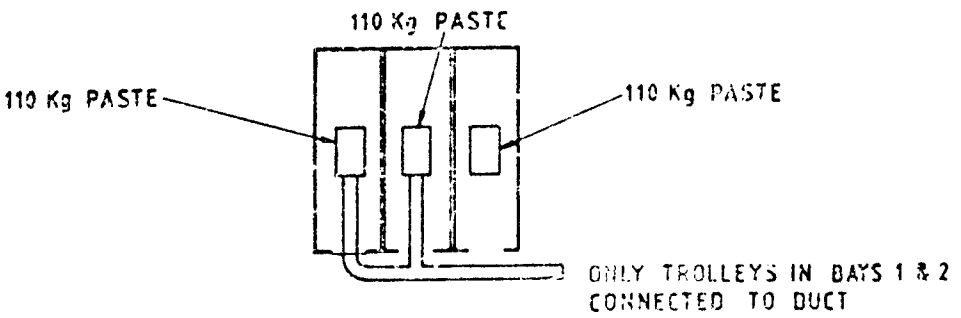

FIGURE 5 ARRANGEMENT FOR TEST 5

FIRE FAST COOK OFF TEST OF EXPLOSIVES AND PROPELLANTS

Yinliang Zhang
Xian Modern Chemistry Research Institute
P.O. Box 18 Xian, China

ABSTRACT

A wood-kerosene fire fast cook off test was suggested. Its flame temperature can reach to 620 °C and the combustion time is about 7 min. It is used to test the cook off behaviour of explosives and propellants which is loaded in a metal case. 12 kints of energetic material, such as TNT, Comp.B, TATB, HQ, DINGU and DH-7 etc., have been tested. Their cook off times were measured and their cook off temperatures were estimated. Finally, their cook off reactions were discussed from fracture scenario of metal case and witness plate. Some pictures of the test are given.

INTRODUCTION

During modern war the effective kill functions of ordnance system depend on detonation performance and vulnerability behaviour of its charges. Because the modern war is very violence the charges loaded in the metal case will be subjected to a number of dangerous stimuli:

1. Fire fast cook off
2. Sympathetic detonation
3. Bullet or fragment impact

4. Shaped charge jet penetration

Therefore, in a condition of practice battle the safety performances of explosives and propellants are very important. In order to prevent ammunitions from accidental explosions it is necessary to load the bombs and warheads with insensitive explosives and propellants.

The high temperature fire is the most dangerous stimulus to ammunitions. Thus we designed an experimental arrangement of wood-kerosene fire fast cook off test to be used to test cook off behaviour of candidate explosives and propellants.

EXPERIMENTAL ARRANGEMENT AND METHOD

The experimental arrangement is shown in Fig.1. It is composed of three parts: fire source, metal case and witness plates. Fire source is a lumber stack which is drenched with kerosene. Its temperature history was measured by means of thermocouple(Fig.2) and the results are shown in Table 1. Metal case is made of steel tube 45# , its i.d. is 40 mm, wall 4mm and length 120 mm. It is sealed with thread lid at two ends (Fig.3). Witness plates are made of Aluminum. They are held in three directions, that is, left, right and rear, of the metal case as to identify the cook off reaction of the materials tested. Measurement of cook off time is performed by means of step-watch. It is defined an interval from initiation to detonation (or explosion) of sample tested. The temperature corresponded to detonation (or explosion) may be estimated accoding to table 1. It is called cook off temperature.

CRITERIA AND METHOD OF ASSESSING COOK OFF REACTION

1. If the witness plates are no deformation and the metal case is no destruction, it is considered that sample did not occur violent reaction.

2. If the witness plates are punched and the lid of metal case is slid away but the cylinder of metal case is not deformed, it is considered that material tested produced combustion.

3. If the witness plates are punched and the metal case is ruptured, it is considered that material tested produced deflagration.

4. If the witness plates are punctured and the metal case is fragmented, it is considered that material tested produced detonation.

RESULTS AND DISCUSSION

Experimental results are shown in Table 2. Number 1 is the propellant DH-7 which contained RDX, its cook off time is 90s ccresponding to temperature 470°C, its cook off reaction is combustion. Numbers 2, 8, 9, 11 and 12 are homogeneous materials. According to their cook off time increasing they can be arranged in order:

$$\text{DINGU} < \text{TATB} < \text{TNT} \leq \text{NQ, GN}$$

In this order the NQ and GN have the best performance to resist the fire fast cook off, their cook off times are longer than 450s and their cook off temperatures are higher than 520°C.They both did not produce any violent reaction (Fig.4). DINGU has a shorter cook off time(105s),

coresponding to cook off temperature 470°C and it produced deflagration (Fig.5).TATB and TNT produced only combustion rather than detonation (Fig.7 and Fig.8). They have a better performance to resist the cook off stimulus. Their cook off times are 210s and 290s, respectively. And their cook off temperatures are 520°C. TNT has a better behaviour to fire fast cook off stimulus, it may be resulted from its endothermic meltting. Number 6 and 7 are mixtures containing RDX, TNT and aluminum or wax. Although they both have longer cook off times (195s and 210s, respectively) and higher cook off temperatures (470°C and 520°C, respectively), they both produced detonation. Thus they have not good vulnerability behaviour to fire fast cook off stimulus. Number 3,4 and 5 are plastic bonded explosives containing RDX and ohter additives. They produced combustion or deflagration rather than detonation to cook off stimulus. Their cook off behaviour is better than Comp.B.

CONCLUTIONS

1. The experimental results showed that the fire fast cook off suggested in this paper can be used to arrange for candidate explosives and propellants.

2. It is well known that the four homogeneous energetic materials, i.e., DINGU, TATB, TNT and NQ, by increasing order of their cook off time, can be arranged in following way:

DINGU -< TATB <= TNT -< NQ

and as subjected to fire fast cook off stimulus DINGU pro-

duced deflagration, TATB and TNT took place combustion, and NQ did not produced any observation reaction.

3. Comp.B produced detonation as subjected to fire fast cook off stimulus.

ACKNOWLEDGEMENTS

The author wish to thank Litian Mi, Jikang Zhang, Yuli Xie, Changguang Wan, Xiuqing Ji, Mingchu Wang, Jiamin Li, Xingwu Wang, Jinqing Li, Zhiyong Ren, Guochao Li, Lin Ying and Minsheng Liu for assistance with the experiments.

REFERENCES

1. M.J.Stosz, Develoment of New Explosives for the U.S. Navy , ICT International Jahrestagung,1982.

2. Lt John D. Corley, Insensitive High Explosives Evalution Techniques , Minutes of the 22nd Explosives safety Seminar, 1986.

3. United Nations, Recommendations on the Transport of Dangerous Goods , Tests and Criteria, First edition, New York,1986.

4. A. Freche, Low Vulnerability Cast Plastic Bonded Explosives , Proceedings of the International Symposium on Pyrotechnies and Explosives October 12-15,1987,Beijing China.

5. Yinliang Zhang, Explosives Vulnerability Test study , BING GONG XUE BAO , part of propellants and Explosives, No.1,1988.

Table 1. Fire Temperature History

time (s)	temp.(°C)	time (s)	temp.(°C)
0	25	270	540
30	280	300	590
45	340	315	620
60	510	330	540
90	470	360	520
120	460	375	550
150	470	390	460
180	440	420	380
210	415	450	320
240	440	480	280

Table 2. Fire Fast Cook Off Test Results

Number	Sample	Cook Off Time(S)	Cook Off Temp.(°C)	Fracture Scenario of Metal Case and Witness Plate	Cock Off Reaction
1	DH-7	90	470	1 lid thrown away case undeformed witness punched	combustion
2	DINGU	105	470	1 lid thrown away case deformed witness punched	deflagration
3	PBXW1	128	470	2 lids thrown away case undeformed witness punched	combustion
4	PBXW2	130	470	2 lids thrown away case ruptured witness punched	deflagration
5	PBXW3	139	470	1 lid thrown away case undeformed witness punched	combustion
6	TNT/RDX/AL	195	470	case fragmented witness punctured	detonation
7	TNT/RDX/WAX (Comp.B)	210	520	case fragmented witness punctured	detonation

(Continuous Table 2.)

8	TATB	210	520	2 lids thrown away case undeformed witness punched	combustion
9	TNT	290	520	2 lids thrown away case undeformed witness punched	combustion
10	TNT/DINGU	360	520	1 lid thrown away case undeformed witness punched	combustion
11	NQ	480	620	no change	no change
12	GN (Guanidine Nitrate)	,80	620	no change	no change

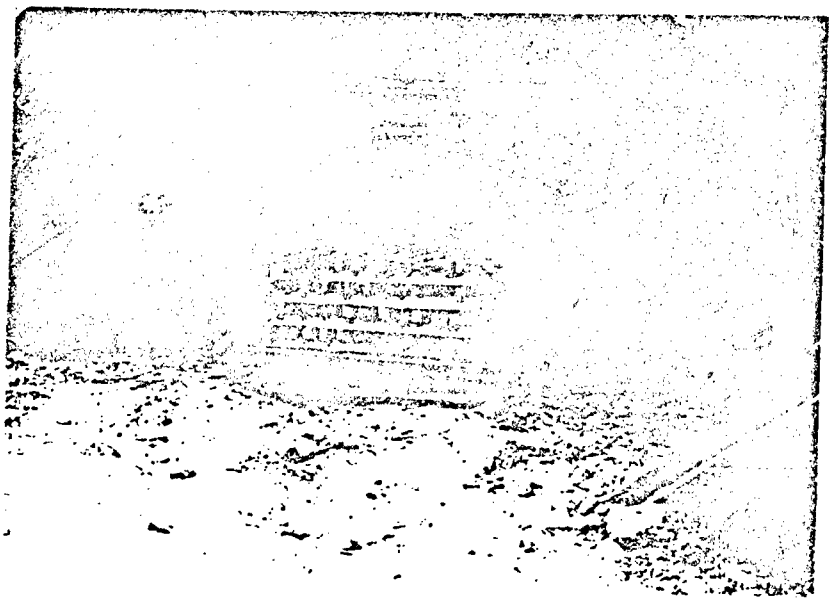

Fig. 1 Experimental Arrangement

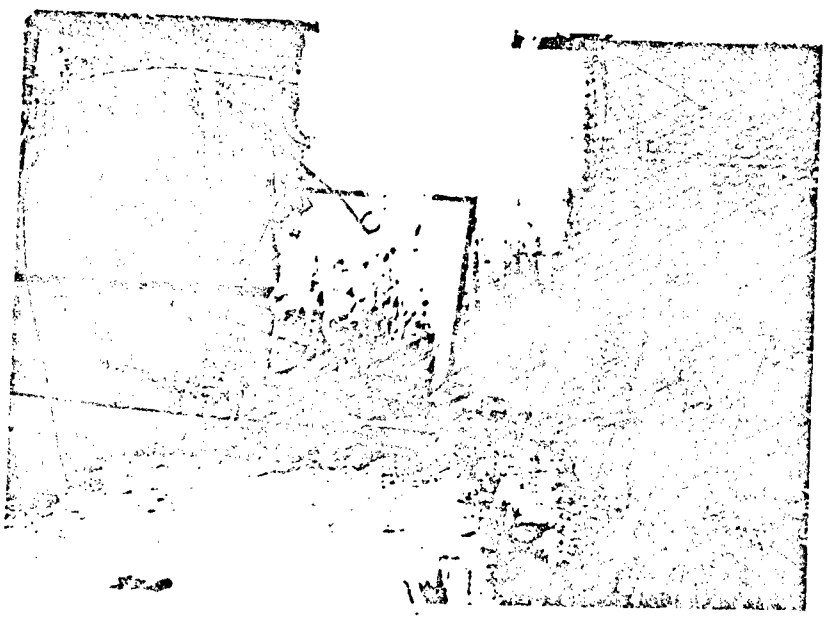

Fig. 2 Fire Temperature Measurement

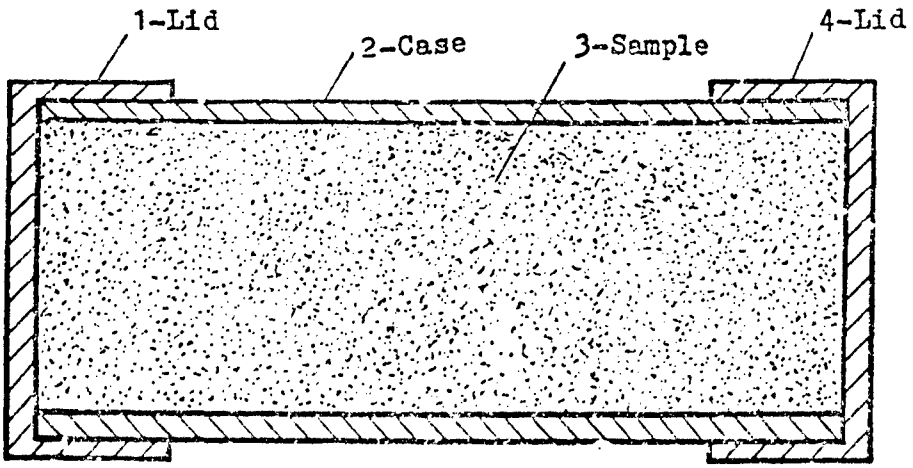

Fig. 3 Metal Case with Sample

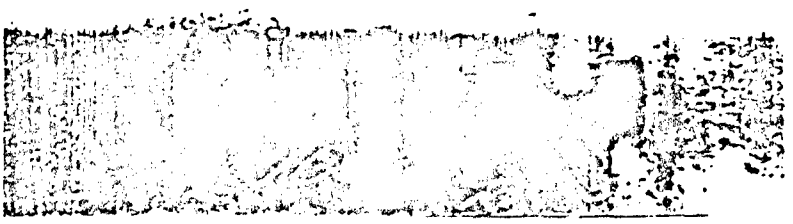

Fig. 4 Cases Recovered for NQ And GN

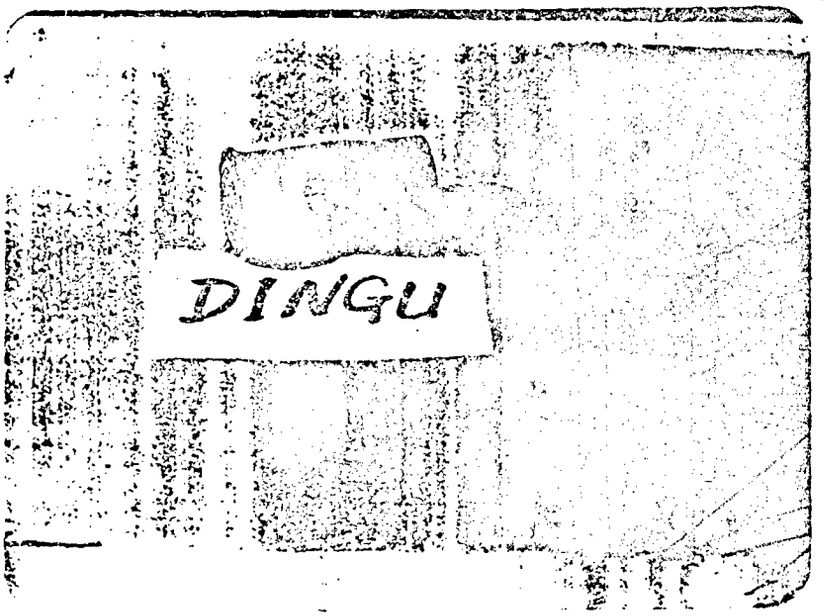

Fig. 5 Case Recovered for DINGU

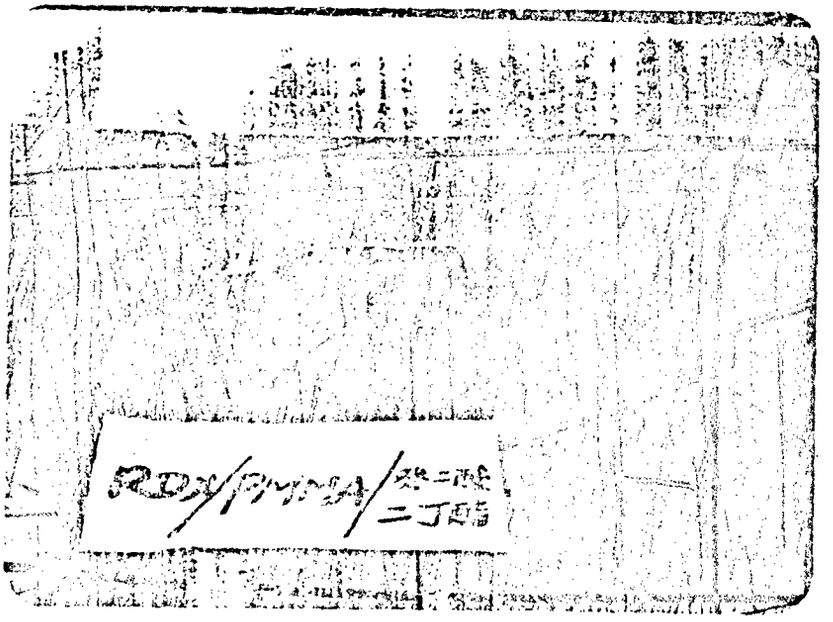

Fig. 6 Case Recovered for PBXN2

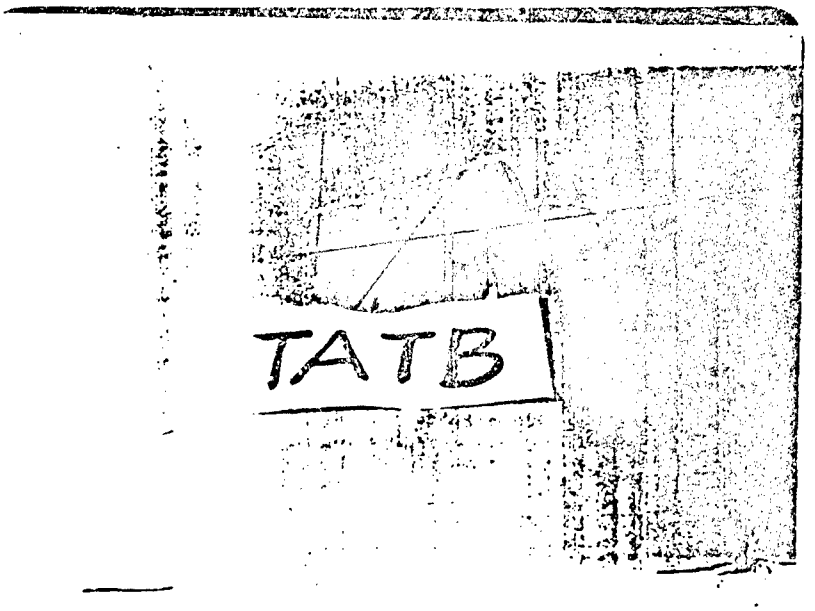

Fig. 7 Case Recovered for TATB

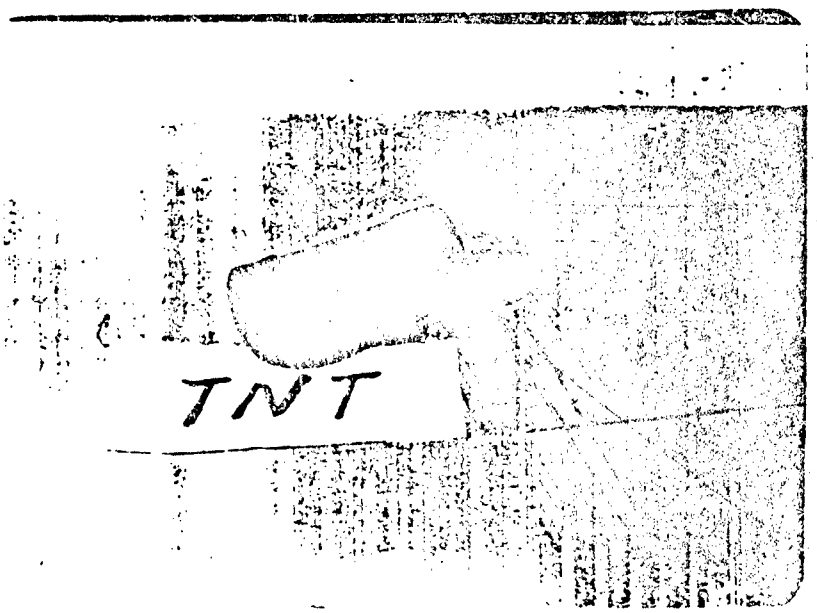

Fig. 8 Case Recovered for TNT

PROBLEMS

IN THE

EXPLOSIVES HAZARD CLASSIFICATION

WORLD?

PREPARED FOR:

DOD EXPLOSIVES SAFETY SEMINAR

BY:

MAJOR ANTHONY R. JOHNSON, USAF

9-11 August 1988

Defense acquisition has played an important and highly visible role in the Air Force for obtaining new or modified weapon systems. There are many facets associated with this process, but perhaps one of the most misunderstood is that of explosives hazard classifications. The purpose of the classification is to accurately characterize the explosive so that in the event of an accident, authorities can effectively respond in an emergency situation. Several problems surfaced as the result of the Peacekeeper acquisition and have continued on to the Small ICBM program. These problems also impact other programs such as the advanced tactical bomber and the advanced tactical fighter.

An explosives hazard classification is an alphanumeric designation that identifies certain characteristics of a component containing explosive material, which in turn, determines shipping, handling and storage requirements. It is usually illegal to ship an explosive component until it has been properly classified by the appropriate authority. The authority rests with the Department of Transportation (DOT), who has delegated authority to the Department of Defense (DOD). However, a distinction should be made between DOT and DOD hazard classifications. DOT classifications are required when contractors ship components containing explosives to a non-DOD installation. It can be requested from the DOT in accordance with procedures and information prescribed in the Code of Federal Regulations (CFR), Title 49-Transportation. Testing required to obtain a DOT classification is not as restrictive as the

procedures used in obtaining a DOD classification.

A DOD explosives hazard classification is required when contractors or DOD personnel ship components containing explosives to a DOD installation. The requirements are outlined in Technical Order (T.O.) 11A-1-47, "Department of Defense Explosives Hazard Classification Procedures" which will be the focus of this dissertation.

DOD explosives hazard classifications are divided into two categories: interim and final. Interim explosives hazard classifications are temporary classifications usually issued in the Air Force by HQ AFSC/IGFW and HQ AD/SES. They are designed for components under development where the design is not fixed. Interim classifications are based on the explosive substances in the component rather than how the explosive is packaged. Interims are issued for no more than one year, but can be renewed if required.

Two complete explosives hazard classification data packages containing the following are required for an interim:

a. A recommended hazard classification, with rationale, from the contractor's safety office.

b. Explosives Hazard Classification Data Record from Data Item Description (DID), DI-L-3311B, to include:

(1) Hazard classification data obtained by testing in accordance with Transport Testing Requirements, T.O. 11A-1-47, Paragraphs 5-2a through j. (For an interim classification only; if the component contains only hazardous materials identified in Title 49 CFR, Section 172.102, Optional Hazard Materials Table,

the T.O. Paragraph 5-2 testing has already been accomplished and need not be reaccomplished); or:

(2) Hazard classification data obtained by comparative analysis, in which case these data must include:

(a) A copy of the final hazard classification for the specific component upon which the analogy was based.

(b) A copy of the test results upon which the final explosives hazard classification was granted.

(c) The type and amount of explosives in the component used for the analogy.

To renew an interim explosives hazard classification, the contractor must submit a request for renewal with copies of the original interim hazard classification and the original Explosives Hazard Classification Data Record, DID DI-E-3311B. Two complete packages must be submitted early enough to allow processing prior to the current interim hazard classification expiration date. (SEE ATCH 1)

Final DOD explosives hazard classifications are appropriate for production components with stable configurations and are based on how the explosive behaves in the component. Finals require approval by the Air Force, Army and Navy. When a request is made for a final hazard classification, an interim will be issued upon request while the final is being processed.

To obtain a final explosives hazard classification, the contractor must submit seven complete data packages containing the following:

a. All components must have the required interim hazard

classification testing accomplished as outlined in one of the methods outlined below.

b. Test results required by T.O. 11A-1-47, Paragraphs 5-3a through g or test results in accordance with an alternate test plan approved by the Department of Defense Explosives Safety Board (DDESB). These tests need not be accomplished if the hazard classification data were obtained by analogy.

c. Items anticipated to be categorized as DOD hazard classification/division/storage compatibility group 1.4S are unique. Paragraph 4-4 of the new draft T.O. 11A-1-47 reads as follows:

> "Compatibility Group S is exceptional in that testing is a prerequisite for assignment to this group. When function testing (at least three repetitions) of an unpackaged article demonstrates that explosive effects are contained within the item itself (as is frequently the case with certain devices such as cable cutters, thermal batteries, and some aircraft escape system components), Division 4, Compatibility Group S may be assigned without further testing."

For items anticipated to be classified 1.4S, the following are required:

a. A recommended 1.4S final hazard classification, with rationale, from the contractor's safety office.

b. Explosives Hazard Classification Data Record, DID DI-E-3311B, Items 1 through 15 and 17.

c. Test results of at least three function tests of the

unpackaged article demonstrating that the explosive effects are contained within the component.

When a part number changes, or a prefix or suffix dash number changes, an explosives hazard classification must be obtained for the newly identified item. The following for either an interim (two data packages) or final (seven data packages) classification are required:

a. A letter from the contractor's safety office with rationale indicating why a change in the number has been made and why a change in classification is not warranted.

b. A copy of the original hazard classification with the original Explosives Hazard Classification Data Record, DID DI-E-3311B. (If the original is a final hazard classification, submit the package for a final hazard classification, and an interim hazard classification will be issued while awaiting final approval.) (SEE ATCH 2)

Finally, each separate shipping configuration of a component requires its own explosives hazard classification. Example: Assembly A contains explosive components. Assembly A requires its hazard classification. Explosive-containing assemblies, if shipped separately from Assembly A, require their own hazard classifications. If Assembly A is shipped as part of a higher assembly, the higher assembly requires its own hazard classification. Because these procedures described above were not strictly adhered to, some minor problems seemingly snowballed.

The symptoms of these problems were always present, but

became readily apparent when a major aerospace contractor submitted explosives hazard classification packages in accordance with DID, DI-E-3311B. The contractor needed to ship various items of a major component for developmental testing for the Small ICBM program. The DID puts T.O. 11A-1-47 on contract and the contractor was required to comply. However, the packages did not even resemble the requirements of the T.O. The packages were subsequently disapproved, as a result. The contractor stated that because of the disapproved explosives hazard classification packages they would not be able to accomplish the testing without impacting cost and schedule for the Small ICBM program. They felt the requirements, although present, were not enforced in the past on the Peacekeeper program. They assumed they would not have to test because they would classify by analogy to Peacekeeper components. Current guidance precluded classification by analogy because the majority of the Peacekeeper components do not have final explosives hazard classifications.

The problem was further compounded because Ogden Air Logistics Center was storing Peacekeeper components at Hill AFB without final explosives hazard classifications. The Peacekeeper weapon system had already been deployed and Ogden wanted the final hazard classifications issued so Systems and Logistics Command could accomplish program management responsibility transfer. The delay in acquiring the final hazard classifications was essentially caused by DOD bureaucratic red tape.

Before the Peacekeeper acquisition, the Air Force had not

undertaken a major missile acquisition since Minuteman. There had been missile modifications but not to the extent experienced in Peacekeeper. As a result the rules for obtaining hazard classifications were different. The requirements were not as well defined as today. If you look at the majority of Minuteman components, you will probably find that they do not have final explosives hazard classifications with the testing required today. When General Electric wanted to classify its reentry vehicle components by analogy to Minuteman for the Small ICBM program, virtually no information was available for the comparison. In December 1986, the DDESB decided the requirements for explosives hazard classification outlined in T.O. 11A-1-47 needed to be strictly enforced. Recent accidents culminating in the Mark 84 incident in Oklahoma convinced the DOD of potential increasing pressure from the DOT. The DOT has delegated the authority to issue hazard classifications to the DOD under a DOT exemption. The exemption can be retracted by the DOT and all classifications would have to be issued by them. So, the DOD had to "clean-up its act" before any backlash from the DOT was felt. This did not prove to be an easy task.

The DDESB felt the issue of properly tested components in accordance with T.O. 11A-1-47 could be rectified within a year. All interims had to be renewed annually and, if the component had not been properly tested, then the renewal would not be reissued until the T.O. requirements were complied with. Finals already granted were not at issue because it was felt the component was accurately classified through the extensive coordination process

in Attachment 2. The example in Attachment 2 shows BMO/AWS as the System Safety Directorate at the Ballistic Missile Office (BMO) at Norton AFB, CA., and focal point for BMO requests for hazard classifications. Their problem was compounded because when a component came up for renewal, the contractor would submit a one page request stating that the component had not changed in explosive quantity or type. It was felt that this was a paperwork exercise and the interim hazard classification would be issued automatically. Unfortunately, a majority of the components were previously issued hazard classifications without the proper T.O. testing accomplished. Under strict enforcement of the requirements, the renewals could not be granted. This caused an uproar in the contractor community. They had not costed testing in their proposals and claimed the testing was out of the scope of their contracts. This was not the case, however, because the DID, DI-L-3311B, included T.O. 11A-1-47 requirements and was on the contract data requirements list. The out of scope issue was dead after conferring with Air Force contracting and legal representatives. The only issue remaining was to insure cost and schedule were not impacted because contractor planning for explosives hazard classifications was based on the old criteria. Numerous workarounds caused the hazard classifications requests to be submitted in a timely manner sometimes with the answer being telefaxed by close of business on the same day with little or no impact to cost or schedule. What subsequently transpired was a huge backlog at the approval authority, Systems Command for the Air Force, for interim hazard classifications.

In an effort to recover from the stricter enforcement of the T.O. requirements, contractors were requested to submit explosives hazard classification test results to insure there were no more close calls as experienced by the first contractor I mentioned. This created a serious backlog at all levels of the Air Force defense acquisition from the project offices to the product divisions to Systems Command itself. It was easy for the project office to put priorities on obtaining explosives hazard classifications because it was only their program in contention for priority. But when the hazard classification requests reached Systems Command, there were a myriad of organizations wanting that same priority attached to their program. There were requests from the Air Force Weapons Laboratory, Aeronautical Systems Division, and the Ballistic Missile Office just to name a few. Compounding the bottleneck, as in the case of the BMO, was with both the Peacekeeper and Small ICBM programs active, prioritizing requests within the project office became a challenging task. For instance, a Peacekeeper component is in the field and Ogden Air Logistics Center wants to insure it has a final hazard classification. Along comes a Small ICBM component requiring an interim hazard classification that must be shipped to Arnold Engineering Development Center in Tennessee for developmental testing in a week. The project office will want the Small ICBM component to be processed first at Systems Command because the Peacekeeper component more than likely has a valid interim. This causes the Peacekeeper component to move lower on the Systems Command stack of hazard classification requests and

the stack will continue to rise as more requests are submitted. Thus, the workload at Systems Command increases while concurrently suffering cutbacks in manpower.

The office of primary responsibility for reviewing and granting explosives hazard classification request for the Air Force is HQ AFSC/IGFW. Previously, there were two individuals who processed hazard classifications. Their duties were numerous and the requests were a small part of their job. Required TDY's sometimes brought hazard classification processing to a standstill until their return. Now with the budget constraints becoming a factor, there is only one person responsible for hazard classifications at Systems Command. The individual has been very responsive to all the BMO requests and, as a result, there have been some close calls but never any impacts to cost and schedule. This is due to the personality of the individual in the position at this point in time and, if this individual elected to leave and be replaced, there is the potential that his replacement may not place the same priority on explosives hazard classifications.

In addition, the manning problem appears to be across the board. Processing final explosives hazard classification requests requires more of a coordination cycle. Once the project office submits the request to Systems Command and Systems Command processes the request, they send an the data package to Ogden Air Logistics Center back to the project office. From there, the requests seem to be in a " black hole" until the approval letter is sent back some months later from Systems Command. It is not

unusual for a request for final to be in the system for six months or more once it is sent from the project office. In my opinion this is an exceptionally long time for processing and may be due to either the organizations not placing the right priority on the request or the same manning problems experienced by Systems Command. Although there have been no major impasses as a result of this slow process, it still puts safety in a bad light to the project office.

Solutions to the problems outlined here need serious consideration. With respect to interim hazard classifications, there needs to be a decentralization of approval authority within the Air Force. The DOT has determined which offices in the Air Force will have approval authority for interims. The DOD should lobby for this decentralization proposal. A DOT sanctioned school that screens prospective students could provide the instruction necessary to accurately classify explosive components. These students could then issue hazard classifications at the product division level. If this proves to be unfeasible, then the DOD should allow product divisions in Systems Command to classify explosive components that have changes in part numbers. The worst-case explosive component could be classified on an interim basis by Systems Command, the current approval authority, and all subsequent configurations of the same component would be classified at the product division level. Systems Command would receive an informational copy of the interim classification for bookkeeping purposes. The post boost vehicle for the Small ICBM has 32 projected part number

changes identified. The actual part number is not known presently because of the volume of changes which may transpire prior to production. The part number changes each time the configuration changes. These ideas could significantly reduce the workload at Systems Command.

In the case of final hazard classifications, some type of traceability for the status of a request throughout the coordination process needs to be maintained. A control data file needs to be created to show where requests have been held for over 30 days to insure bottlenecks are minimized. Several contractors have offered the use of their computer data collection systems. All requests would be tracked by each organization in the coordination process on this system providing easy access to each user on current status. Whether this system is used or something else, a system needs to be put in place to identify potential problems so they can be resolved as quickly as possible.

Realizing manning problems may be here to stay, serious consideration should be given to reorganizing current resources to efficiently use the personnel available. The job of processing explosives hazard classifications cannot be ignored and priorities assessed accordingly. The potential for numerous cost and schedule impacts needs to be addressed and minimized. While everyone has done better than could be expected, the acquisition of some new major weapon systems could essentially "bury" all the coordinating agencies in the process. A lessons learned seminar between all branches of the services should be

contemplated. The seminar could focus on processes that have been successful, identify and resolve problems and make recommendations to the DDESB. Whatever is decided as a result of this discussion, something needs to be done.

INTERIM HAZARD CLASSIFICATION REQUEST ROUTING

INITIAL/RENEWAL/CHANGING PART NUMBERS

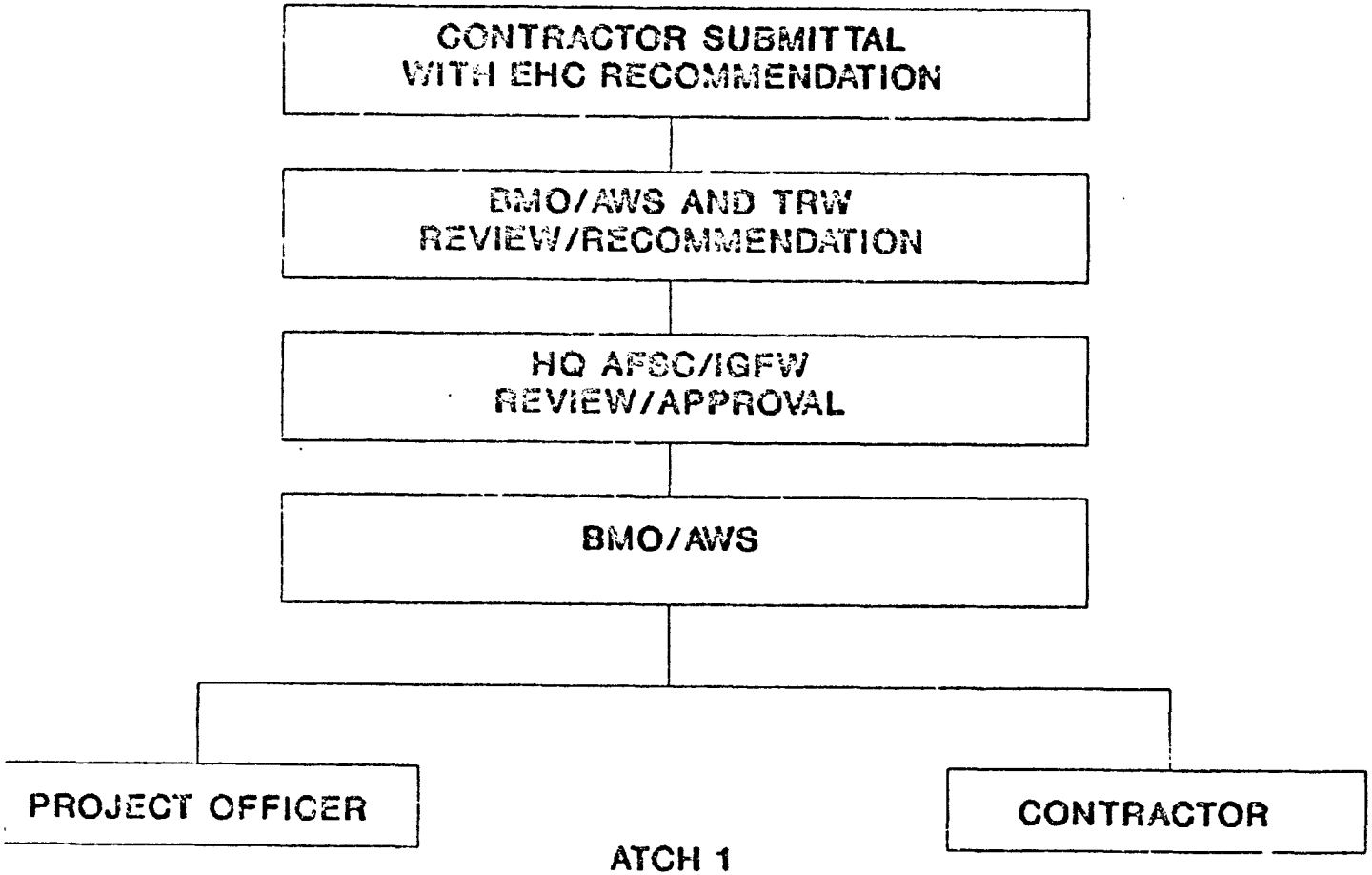

ATCH 1

2185

FINAL HAZARD CLASSIFICATION REQUEST ROUTING

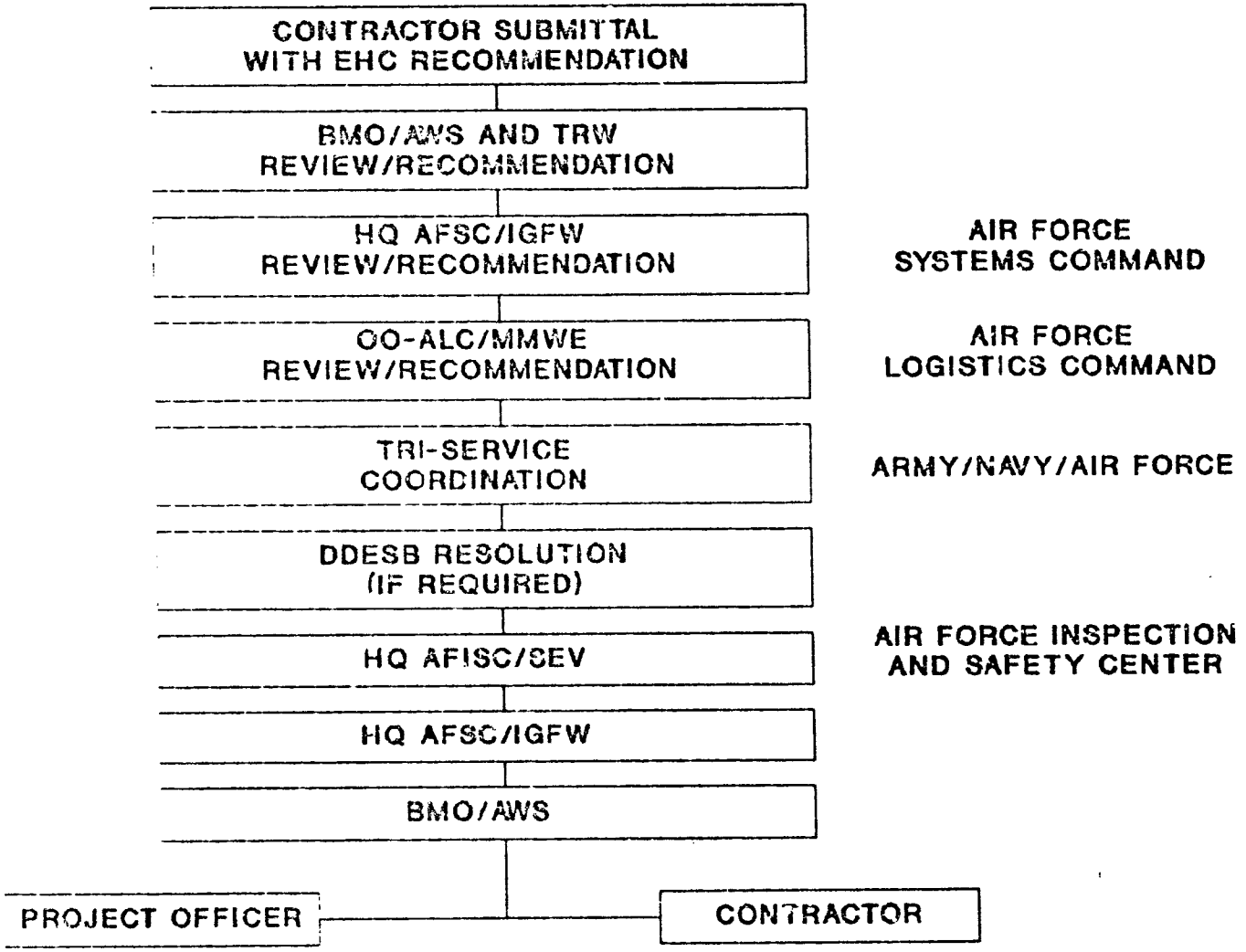

2186

23rd DOD Explosives Safety Seminar
Atlanta, Georgia
9-11 Aug 1988

CONSTRUCTION STANDARD FOR NAVFAC TYPE V MISSILE TEST CELL

Robert N. Murtha
Naval Civil Engineering Laboratory
Port Hueneme, CA

ABSTRACT

Missile Test Cells (MTCs) are a component of a Navy missile maintenance facility used to safely conduct functional tests on All-Up-Round (AUR) missiles to certify their performance reliability before delivery to the Fleet. The Department of Defense Explosives Safety Board (DDESB) has determined that a mishap could occur during the remotely controlled AUR test. This mishap could lead to inadvertent ignition of the rocket motor, inadvertent detonation of the warhead or a combination of both.

The United States Navy is developing construction Standards for a family of MTCs which will meet technical operational requirements, ordnance criteria, and the explosives safety requirements of NAVSEA OP-5. The family will consists of both rectangular and cylinder-shaped reinforced concrete structures designed to safely vent effects from warhead detonation and/or rocket motor ignition away from occupied areas of the adjacent maintenance facility. These Standards will be used to support future military construction (MILCON) projects. The Archect-Engineer firm contracted by the Naval Facilities Engineering Command (NAVFAC) for each MILCON project will use the NAVFAC Standard as the final design for the MTC and simply site adapt the MTC design to the construction site.

This peper describes the NAVFAC Standard for a Type V3 Missile Test Cell which has a rated safe explosives capacity equal to 600 lb TNT.

1.0 INTRODUCTION

A missile test cell (MTC) is a component of an Intermediate Level Maintenance Facility (ILMF) used to safely conduct functional tests on All-Up-Round (AUR) missiles to certify their performance reliability before delivery to the Fleet. An AUR is defined as a complete functional missile, which may or may not include a rocket motor (liquid or solid fuel), booster (solid fuel), conventional warhead, guidance and control section, and safe and arming device. The test simulates the actual flight and intercept capabilities of the AUR missile and is remotely controlled by personnel and equipment located outside the MTC in a test control area of the adjacent Missile Processing Building (MPB). A mishap could occur during an AUR test. This mishap could lead to inadvertent ignition of the rocket motor or inadvertent detonation of the warhead. The MTC must be designed to protect adjacent facilities, personnel, equipment, and missiles from effects of these hazards.

The Naval Civil Engineering Laboratory (NCEL) is developing NAVFAC Standards (Standard Drawings) for the seven types of MTCs described in Table 1-1. Although each Standard will consist of a complete AE design package including architectural, civil, structural, mechanical, electrical, and physical security considerations, this paper will deal primarily with the explosives safety issues of siting and blast resistant design for the hazards of warhead detonation and rocket motor lightoff.

The MTC will be a heavily reinforced concrete structure with a covered passageway leading to the MPB and an unpaved level access area at the opposite end, as shown in Figure 1-1 for the cylinder-shaped NAVFAC Type V MTC. The MTC houses a missile test stand, missile restraint fixture, test missile, and test equipment as shown in Figure 1-2 (typical). An entrance way with a blast resistant door is located in the front wall and a frangible blow-out panel and rocket motor lightoff vents in the rear wall. The reinforced concrete cylinder is cast in the horizontal position using a corrugated metal liner for the inner form. The flat end walls are reinforced concrete circular slabs cast monolithic with the cylinder. The main reinforcement in the cylinder section consists of "hoop" reinforcement. The hoop bars are bent in a circular shape and spliced together with a mechanical butt splice. Stirrups are provided to maintain the integrity of the cross section. Longitudinal and diagonal bars tie the end walls to the cylinder.

The operation of the MTC is such that the blast door is closed and the rocket motor lightoff vents are open when a test is underway. Given detonation of a missile during a test, the resulting shock and gas pressures initially vent only through the lightoff openings. Full venting out the rear wall occurs when the moving blow-out panel is clear of the MTC. The blow-out panel system is designed to limit the gas pressure impulse inside the MTC and leakage pressures on the adjacent unhardened missile processing building. During test setup operations in a cell, its lightoff openings are covered with blast doors to protect its inhabitants and equipment from possible explosions

in other cells where tests are underway. Rocket gases from an inadvertent ignition of a missile rocket motor are safely vented through the lightoff vents. Both exhaust and intake vents are required.

Because the cylinder shape is a new structural concept for MTCs, a full-sized explosives certification test is scheduled prior to approving Navy Standards. This test will be used to validate siting criteria, design loads, and the structural performance. In addition, two rocket motor lightoff tests will be performed to certify the forward and aft restraint systems.

Table 1-1. Description of NAVFAC Standards for Missile Test Cells

NAVFAC Type MTC	Navy Missile	Cell[a] LxWxH (ft)	Door[b] WxH (ft)	Corridor[a] WxH (ft)	Number of Test Stations	Rated Safe Explosives Capacity (lb TNT)
I	STANDARD, WIDE AREA DEFENSE, PHOENIX	40x25x15	6x7	12x8	1	300
II	AMRAAM, SEA SPARROW, HARPOON, PHOENIX, SPARROW, HARM, MAVERICK, SHRIKE, HELLFIRE, SLAM, PENGUIN	40x25x15	6x7	10x8	1,2, or 3	300
III	AMRAAM, SEA SPARROW, RAM, SPARROW, SHRIKE, HELLFIRE	20x15x15	6x7	10x8	1	105
IV	WALLEYE I & II	30x20x8	5x6.5	10x8	1	1,150
V	TOMAHAWK, STANDARD(R&D), SEA LANCE	30x20x8	5x6.5	10x8	1	600
VI	AMMUNITION & EXPLOSIVES	10x10x10	4x7	c	0	40
VII	EXPLOSIVE COMPONENTS	6x6x8	3x7	c	0	10

[a]Clear interior dimensions.

[b]Clear opening.

[c]No corridor required; test cell is designed to fully contain explosion and can be located within a few feet of the Missile Processing Building.

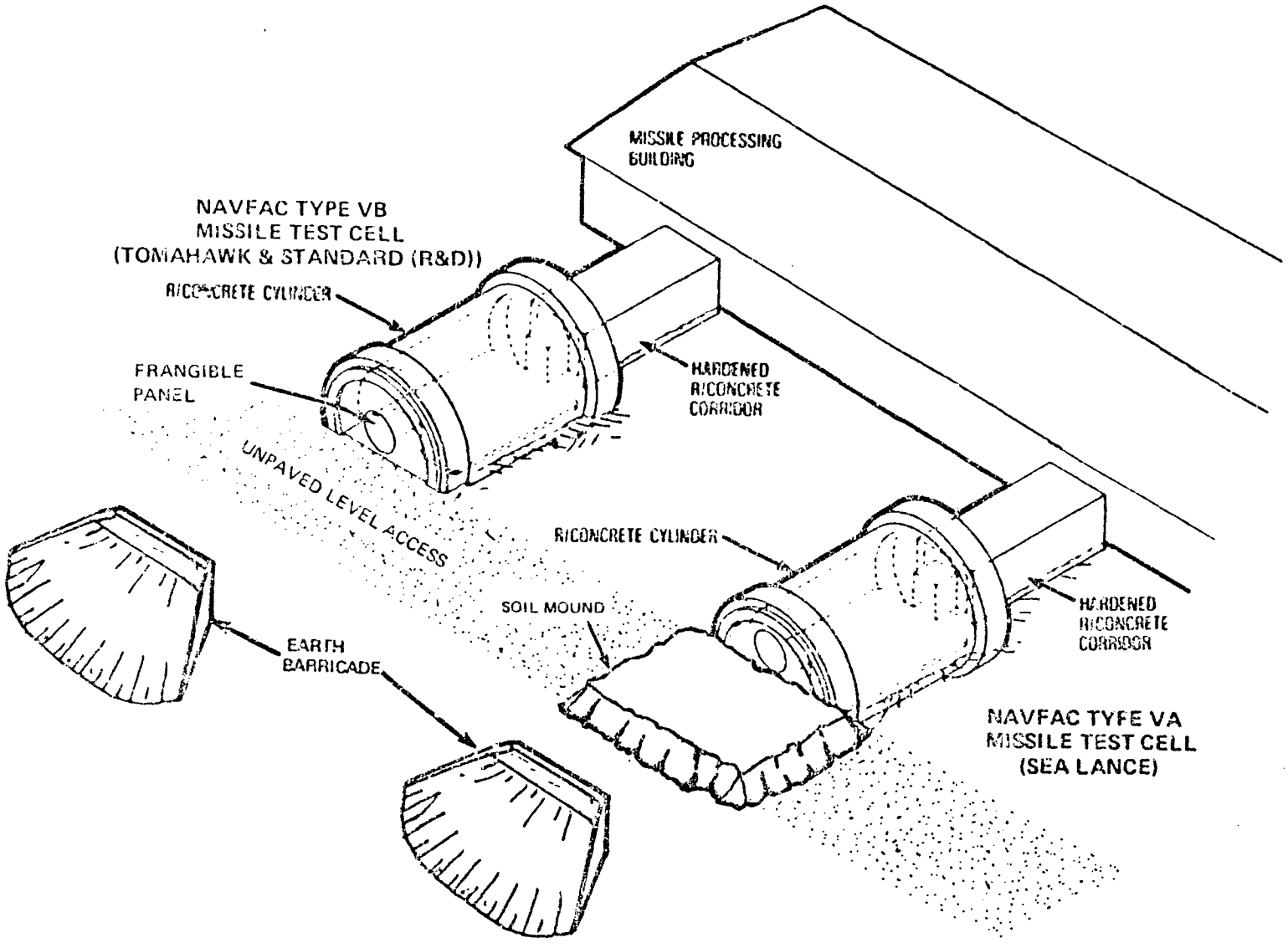

Figure 1-1. NAVFAC Type V missile test cell adjacent to Missile Processing Building.

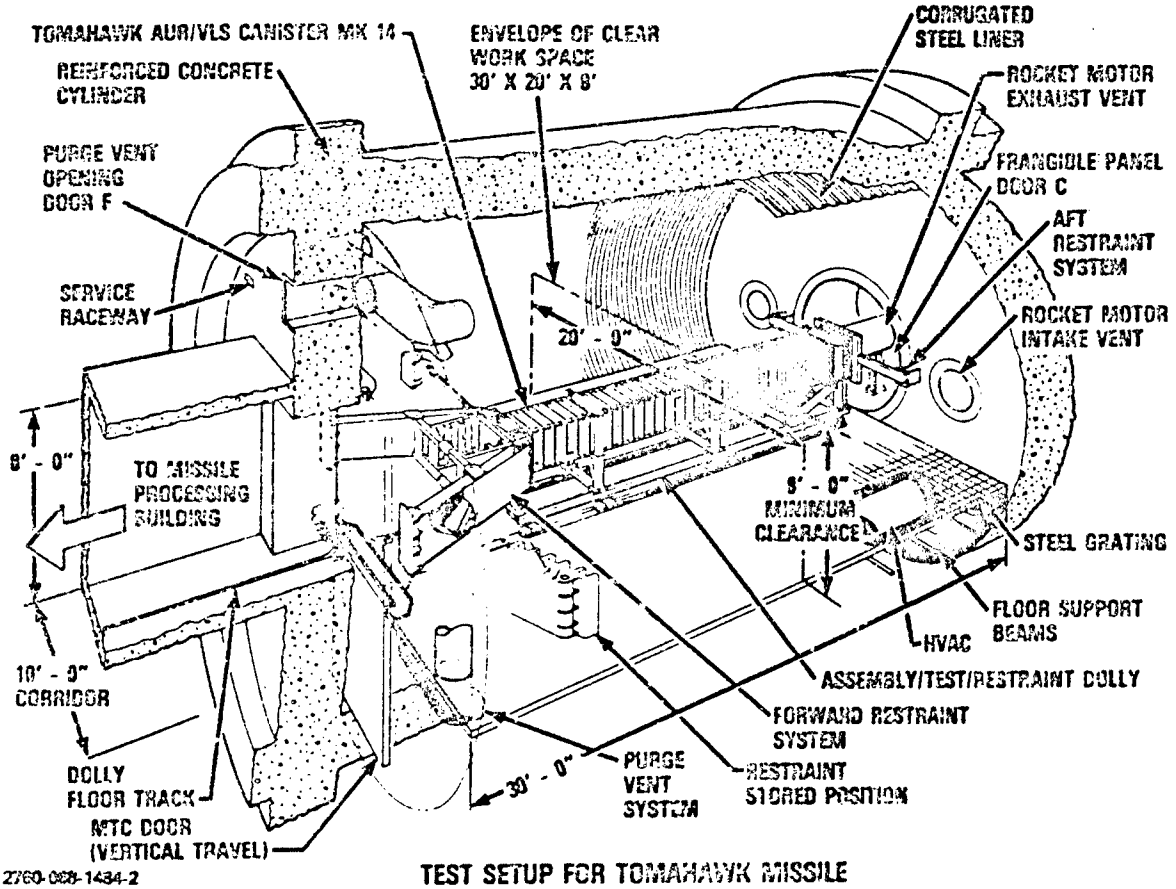

2760-028-1434-2

TEST SETUP FOR TOMAHAWK MISSILE

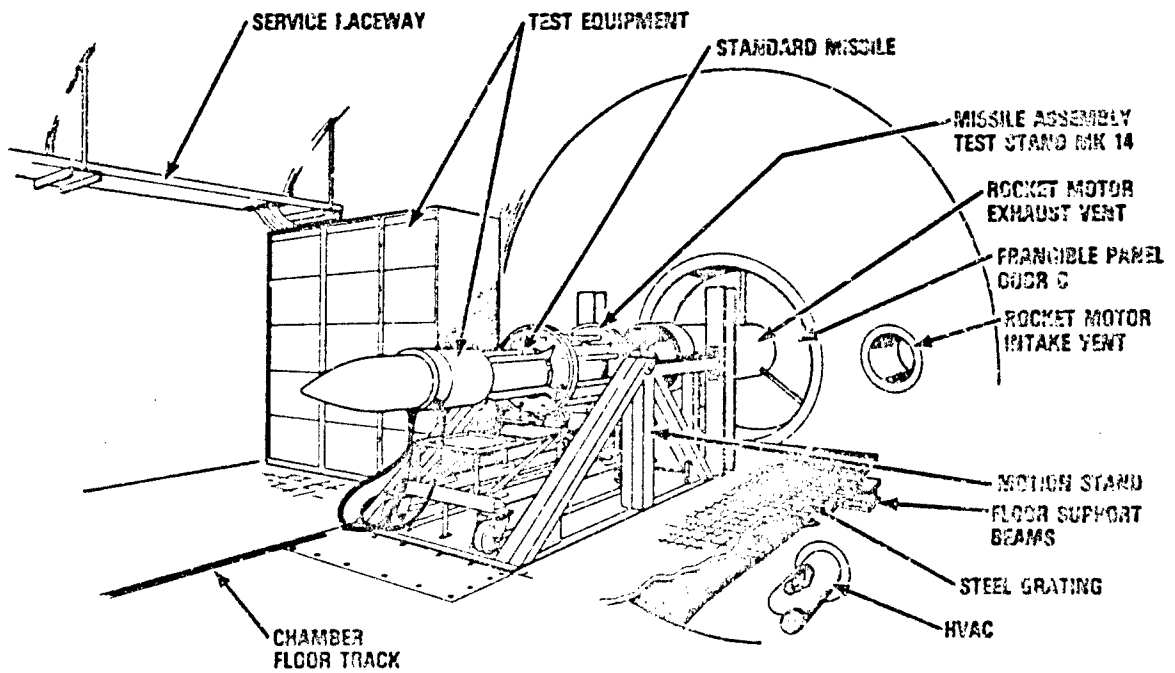

TEST SETUP FOR STANDARD MISSILE

FIGURE 1-2 TEST SETUP FOR NAVFAC TYPE V3 MISSILE TEST CELL

2.0 EXPLOSIVES SAFETY

2.1 MAXIMUM CREDIBLE EVENTS

Siting and design of the Type VB missile test cell shall account for the following maximum credible events (MCEs) during AUR testing of TOMAHAWK and STANDARD(R&D).

2.1.1 Warhead Detonation.

The MCE occurs during an AUR test of the STANDARD(R&D) missile, SM-2, Block IV. A mishap during the AUR test leads to inadvertent detonation of 100 percent of the weight of high explosive in the warhead plus 26 percent of the weight of solid propellant in the rocket motor and booster. The net explosive weight (NEW) of the MCE is:

NEW = 80 lb high explosive in the Mk 125 warhead x 1.08 TNT equivalent factor + 790 lb propellant in the Mk 104 rocket motor x 26% TNT equivalent factor + 1034 lb propellant in the Mk 72 booster x 26% TNT equivalent factor

= 86 + 205 + 269 = 560 lb TNT equivalent

This MCE is based on the results from explosive tests of STANDARD missiles, conducted by the Naval Surface Weapons Center (NSWC), Code R15. NSWC tested missiles with the Mk 115 warhead, and the Mk 56 and Mk 104 rocket motors. Based on analysis of blast overpressures measured in the tests, it was recommended that the NEW for the MCE explosion for STANDARD missile, SM-2, Block II, TACTICAL, be taken equal to 100 percent of the weight of high explosive in the warhead plus 26 percent of the weight of propellant in the rocket motor.

For the purpose of calculating air shock overpressures outside the MTC for siting facilities to meet overpressure limits of NAVSEA OP-5, the design net explosive weight of the design MCE shall be:

NEW = 600 lb TNT equivalent

For the purpose of calculating shock and gas overpressure design loads for structural elements, the design net explosive weight of the design MCE shall be:

NEW = 600 lb TNT equivalent x 1.2 safety factor required by NAVFAC P-397 to account for uncertainities in the structural design process

= 720 lb TNT equivalent

The envelope of possible locations of the design MCE for the Type V MTC shall be as shown in Figure 2-1 and listed below for the actual cylindrical structure:

Surface of Area 101	Minimum Standoff Distance, R_a (ft)
Cylinder Wall (2-3-A, 2-3-D)	9.5
Front Wall (A-D-3)	9.0
Rear Wall (A-D-2)	2.5

2.1.2 Rocket Motor Lightoff

A mishap during an AUR test leads to inadvertent ignition and continuous burning of the rocket motor at maximum thrust. The missile restraint fixture for TOMAHAWK and STANDARD(R&D) safely resists the thrust produced by the rocket motor during its full burn cycle.

2.2 EXPLOSIVES SAFETY OBJECTIVES

Siting and design of the Type VB missile test cell shall meet the following explosives safety objectives as required by the NAVSEA OP-5 safety regulations:

2.2.1 Blast Overpressures

The peak overpressure from warhead detonation shall not exceed 1.2 psi in occupied areas of the MPB. This value is less than the maximum 2.3 psi allowed by NAVSEA OP-5 for remotely controlled operations (paragraph 5-1A.6.3 of NAVSEA OP-5). However, the 1.2 psi criteria precludes the need to evaluate the debris hazard to occupants and contents from possible MPB damage due to the MCE in the MTC.

2.2.2 Hazardous Fragments and Debris

Primary fragments off the AUR and secondary fragments from the MTC and its contents due to the MCE explosion shall result in no more than one fragment per 600 ft^2 with a kinetic energy exceeding 58 ft-lbs in occupied areas of the ILMF. Possible MPB debris resulting from overpressures acting on the MPB need not be considered to be hazardous fragments since these overpressures do not exceed 1.2 psi. The resulting protection afforded occupants and contents of the MPB is equivalent to Protection Category 1, as defined in NAVFAC P-397.

2.2.3 Toxic Gases

No unsafe levels of toxic gases shall penetrate inhabited areas of the ILMF as a result of inadvertent rocket motor lightoff.

2.2.4 Equipment Loss

Test equipment in the MTC has a high replacement cost. Loss of this equipment would severely degrade missile maintenance schedules. Consequently, test equipment in the MTC shall be reusable after rocket motor burnout. This safety objective shall be met by designing a safety vent system that (a) vents the exhaust plume from a Mk 72 rocket booster, (b) limits the pressure and temperature in MTC during the burn phase of the Mk 72 rocket booster to 14.7 psia ± 2 psi and 140°F ± 10°F, and (c) purges air in the MTC of heat, smoke, and contaminants at a minimum rate of one air change every 5 minutes after burnout of the Mk 72 rocket booster.

2.2.5 Damage

The MTC shall be reusable following rocket motor lightoff without major repairs to the structure. The MTC need not be reusable following warhead detonation.

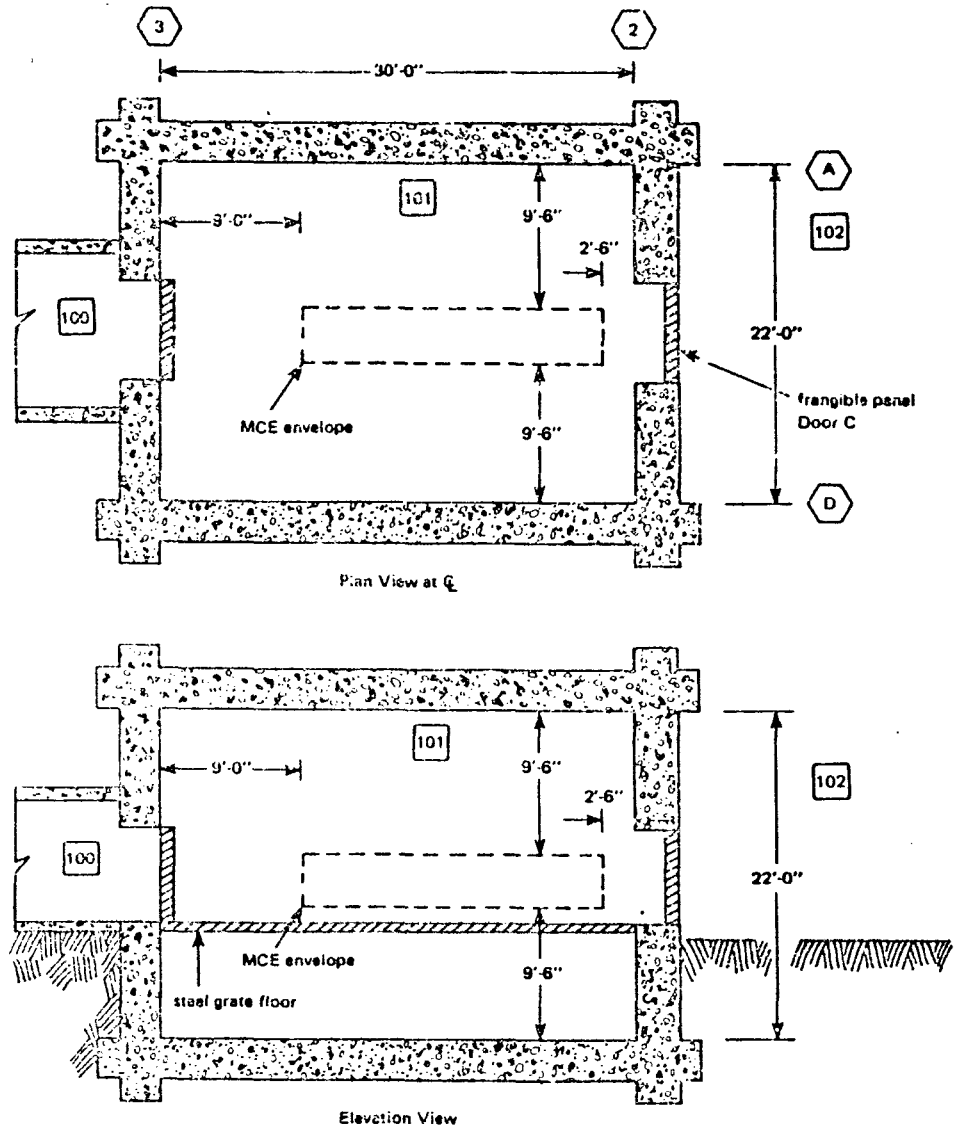

Figure 2-1. Envelope of possible locations of MCE explosion used to calculate the blast design loads (actual cylinder).

3.0 SITING

3.1 GENERAL

The axis of the passageway and MTC shall be perpendicular to the adjacent wall of the MPB, with no bends in the passageway. Groups of MTCs (if required) shall be nested side-by-side as illustrated in Figures 1-1 and 3-1.

3.2 SITING CRITERIA

NCEL conducted explosive tests in 1985 and 1986 at New Mexico Tech in which the blast environment was measured outside MTCs. These results were used to empirically derive criteria for the safe separation distance from a Type VB MTC (with a rated safe explosives capacity of 600 pounds TNT equivalent) to a Missile Processing Building, an adjacent MTC, inhabited buildings, and public highways.

The test structure was a 1:2.6 scale model, reinforced concrete, arch-shaped "horseshoe" structure. Dimensions are shown in Figure 3-2. By volume, the test structure is a 1:2.54 scale model of a rectangular NAVFAC Type I Missile Test Cell. The important constant parameter was the volume, $V = 920\ ft^3$. The values of the fixed parameters in the test structure are as follows:

Parameter	Test Structure
Internal Volume, V (ft^3)	920.00
Floor Width, L_S (ft)	9.72
Floor Length, L_L (ft)	15.42
L_S/L_L	0.63

Variable parameters in the test program included the TNT equivalent net explosive weight, W (pounds), the vent area, A (ft^2), and the vent cover weight, w (psf). The scaled parameters are the scaled distance ($Z = R/W^{1/3}$), charge density (W/V), scaled cover weight ($w/W^{1/3}$), and scaled vent area ($A/V^{2/3}$). The range of parameters in the test program were:

Parameter	Range of Parameter Values for Model Test Structure
Explosive Weight, W (lb TNT)	4.52 to 81.36
Scaled Weight of Vent Cover, $w/W^{1/3}$ ($psf/lb^{1/3}$)	0 to 18.2
Scaled Vent Area, $A/V^{2/3}$	0.13 to 0.34
Scaled Charge Weight, $W/V(lb/ft^3)$	0.005 to 0.088

The incident blast environment outside the test structure was measured at the ground locations shown in Figure 3-3. The test results show that the test structure geometry and vent cover had the following general effects on the external blast environment compared to that from an unconfined hemispherical surface burst (the basis for NAVSEA OP-5 quantity distance relationships):

1. Front Direction - increase in pressure and impulse with no vent cover; pressure and impulse reduced slightly using a vent cover or the smaller vent area, but not below that of an unconfined hemispherical surface burst.

2. Side Direction - significant decrease in pressure and impulse without vent cover; reducing vent area reduces pressure and impulse; with the larger vent area, and a vent cover, pressure and impulse are magnified in the side direction compared to no vent cover. With small vent area and a vent cover, pressure reduced even more, impulse not effected.

3. Back Direction - very significant decrease in pressure and impulse without a vent cover, more significant decrease with a smaller vent area; pressure reduced even more with a small vent area and a vent cover.

As stated earlier, the MTC will be sited such that the peak overpressures shall not exceed 1.2 psi in occupied areas of the MPB. Because of the directional effects of the MTC on the external blast environment, the scaled distance to the back of the MTC where P_{so} is 1.2 psi is significantly reduced from that for a surface burst. "B" direction overpressure data are plotted in Figure 3-4 for tests without vent covers ($w/W^{1/3} = 0$) for one of the three scaled vent areas ($A/V^{2/3} = 0.13$). An average slope of the data was determined from best fit power curves for each W/V. The average slope was then used to derive the upper bound straight-line relationships shown in Figure 3-4. The Z values corresponding to 1.2 psi from these upper bound curves are considered reasonable and safe for developing the siting criteria for points to the back of the MTC within the range of the scaled parameters in this study.

The upper bound Z_R values corresponding to P_{so} = 1.2 psi and no vent cover to the back direction of the MTC are plotted against W/V in Figure 3-5. For the NAVFAC Type V MTC, $W/V = 600/11,404 = 0.053$ lb/ft^3 and $A/V^{2/3} = 38/507 = 0.075$. This $A/V^{2/3}$ value is outside the range of the values tested. Therefore, the following extrapolation procedure was used to determine the safe distance to the rear of the MTC. The safe Z_R values for P_{so} = 1.2 psi to the back of the MTC were obtained from Figure 3-5 and then plotted in Figure 3-6 versus $A/V^{2/3}$. The line was extended and a safe Z_R value of 5.5 ft/lb$^{1/3}$ was obtained for $A/V^{2/3} = 0.075$. With a rated capacity of 600 pounds, the safe distance to the rear is $5.5 \times 600^{1/3} = 46.4$ feet measured from the outside of the vented wall.

The criteria derived above is presented in Figure 3-1 and the table below for a Type VB MTC.

Acceptor	Minimum Safe Distance From Exterior Center of Door C to Acceptor, R (ft)[a]		
	Front, R_F	Side, R_S	Rear, R_R
Adjacent MTC	NA	b	NA
Missile Processing Bldg.[c]	NA	NA	46.4
Inhabited Bldg.[d]	1,250	211[e]	46.4[e]
Public Highway[f]	750	127[e]	27.8[e]

[a] Based on rated safe explosives capacity of MTC equal to 600 lb TNT equivalent and a total frangible vent area of 38 ft^2.

[b] R_s = distance at which Door C meets safety performance requirements under the external design blast loads defined in Section 6.0; in all cases, R_s (minimum) = 17.0 + T_c, where T_c = wall thickness of R/concrete cylinder (ft).

[c] R corresponds to 1.2 psi peak incident blast overpressure.

[d] R_s and R_p correspond to 1.2 psi peak incident blast overpressure; R_f corresponds to safe distance from debris.

[e] This distance will be superceded by the larger safe separation distance required for siting Missile Processing Building.

[f] R equals 60% of the minimum distance allowed for inhabited buildings.

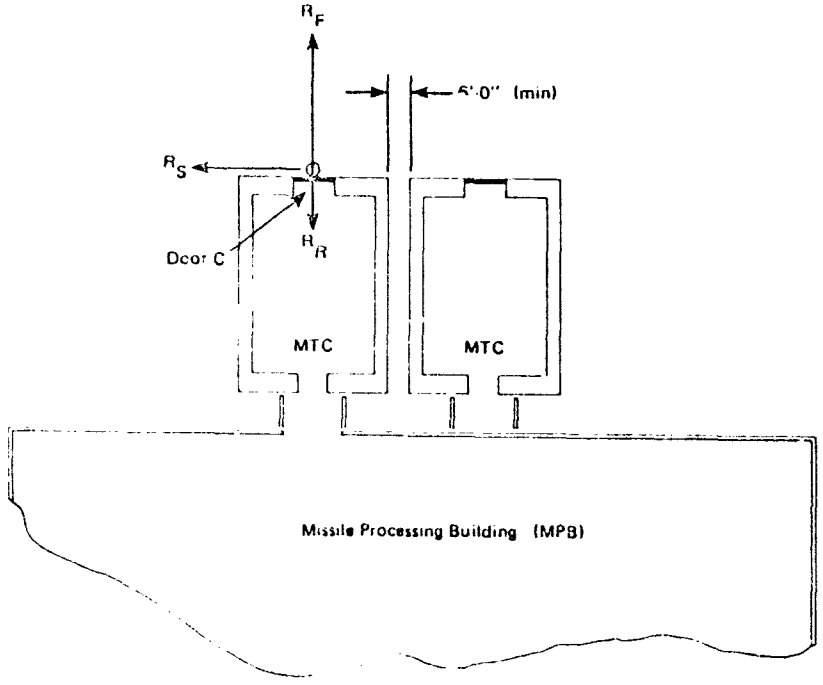

Acceptor	Minimum Safe Distance From Exterior Center of Door C to Acceptor, R (ft)[a]		
	Front, R_F	Side, R_S	Rear, R_R
Adjacent MTC	NA	b	NA
Missile Processing Bldg.[c]	NA	NA	46.4
Inhabited Bldg.[d]	1,250	211[e]	46.4[e]
Public Highway[f]	750	127[e]	27.8[e]

[a] Based on rated safe explosives capacity of MTC equal to 600 lb TNT equivalent and a total frangible area of 38 ft^2.

[b] R_s = distance at which Door C meets safety performance requirements under the external design blast loads defined in Section 6.0; in all cases, R_s (minimum) = 17.0 + T_c, where T_c = wall thickness of R/concrete cylinder (ft).

[c] R_R corresponds to 1.2 psi peak incident blast overpressure.

[d] R_s and R_R correspond to 1.2 psi peak incident blast overpressure; R_f corresponds to safe distance from debris.

[e] This distance will be superceded by the larger safe separation distance required for siting Missile Processing Building.

[f] R equals 60% of the minimum distance allowed for inhabited buildings.

Figure 3-1. Safe separation distances from NAVFAC Type V missile test cell.

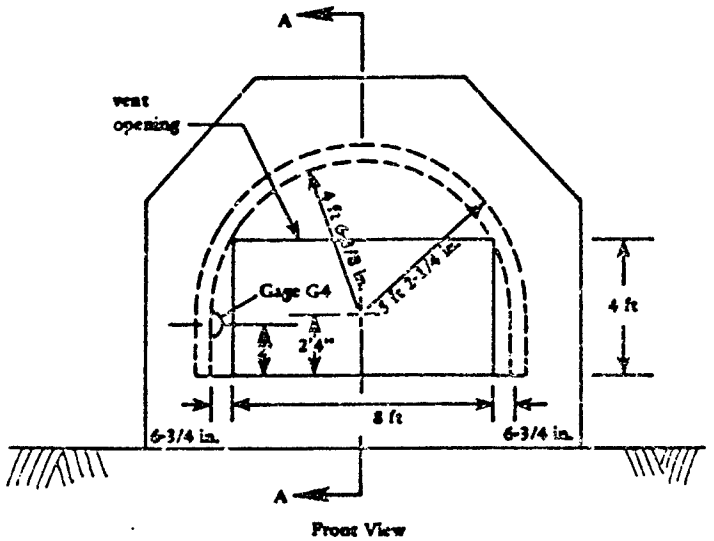

Front View

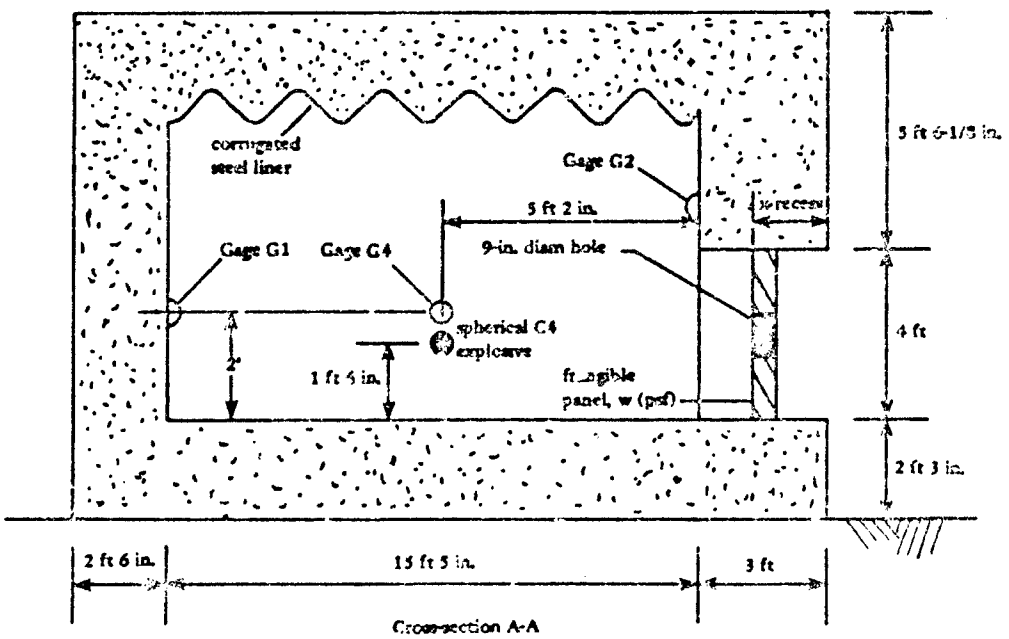

Cross-section A-A

Figure 3-2. Scale model missile test cell.

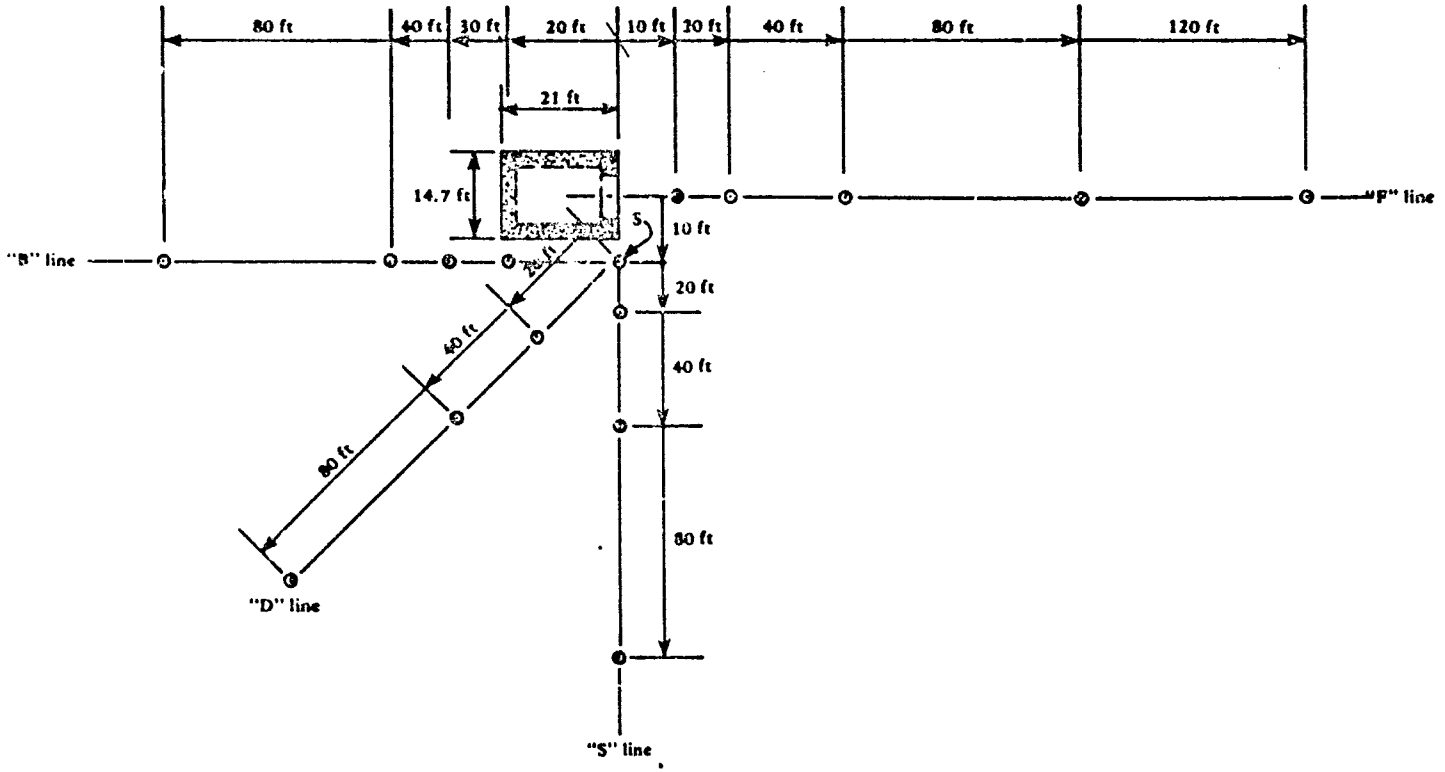

Figure 3-3. External pressure gage locations.

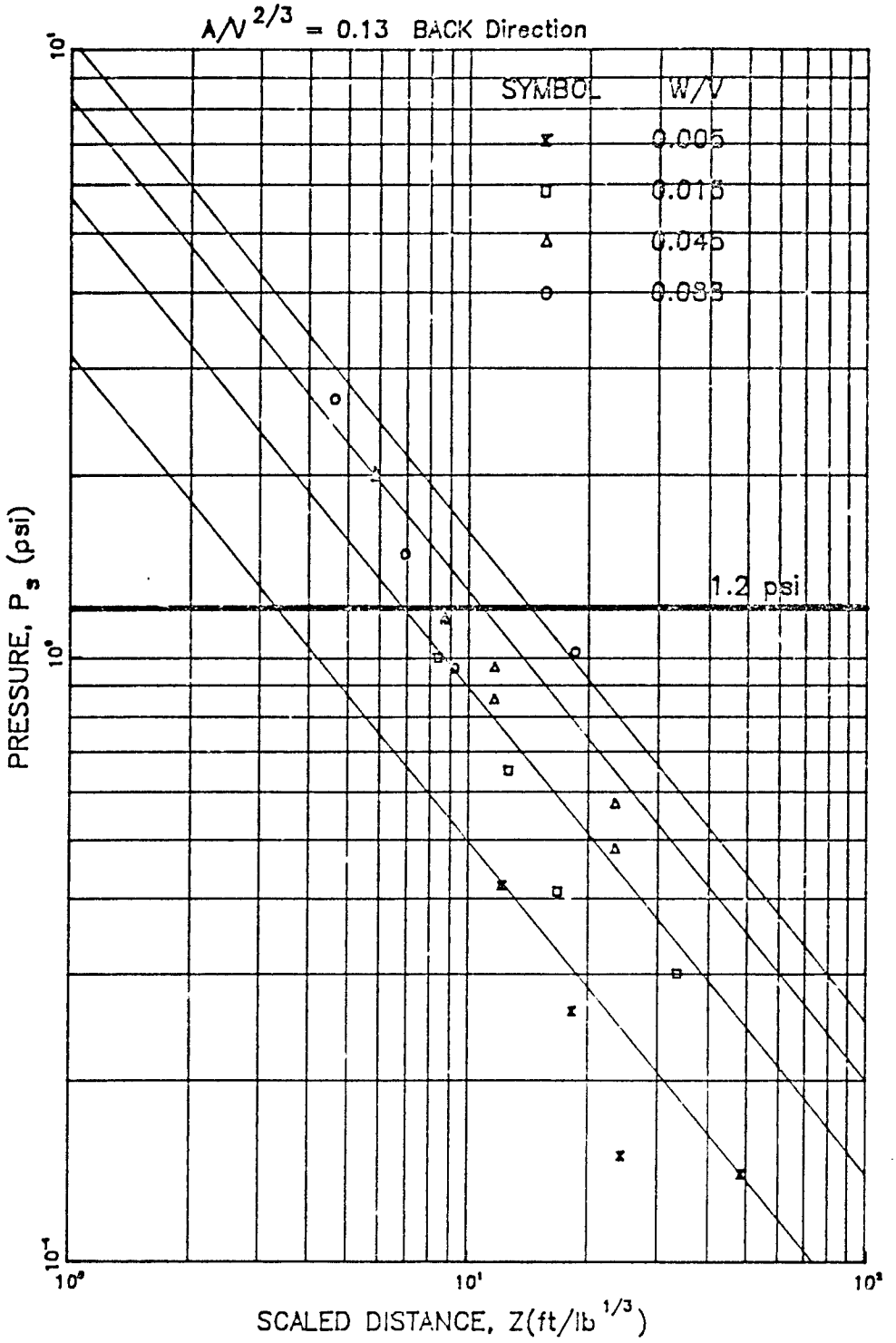

Figure 3-4. P_{so} versus Z to the back ('B') direction of the MTC, $A/V^{2/3} = 0.13$ and $w/W^{1/3} = 0.0$.

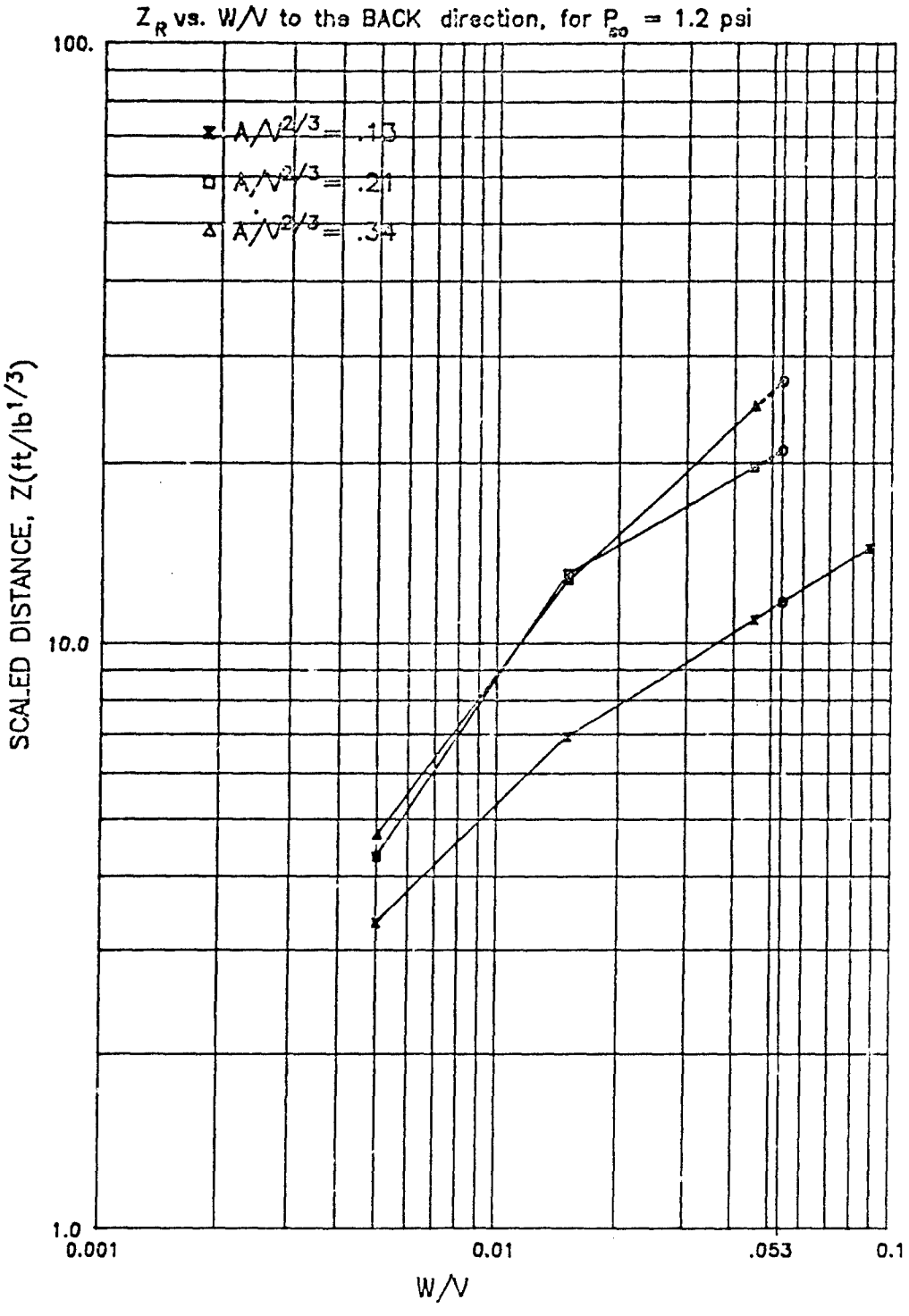

Figure 3-5. Z_R versus W/V for P_{so} = 1.2 psi, to the back of the MTC, $w/W^{1/3}$ = 0.0, no vent cover.

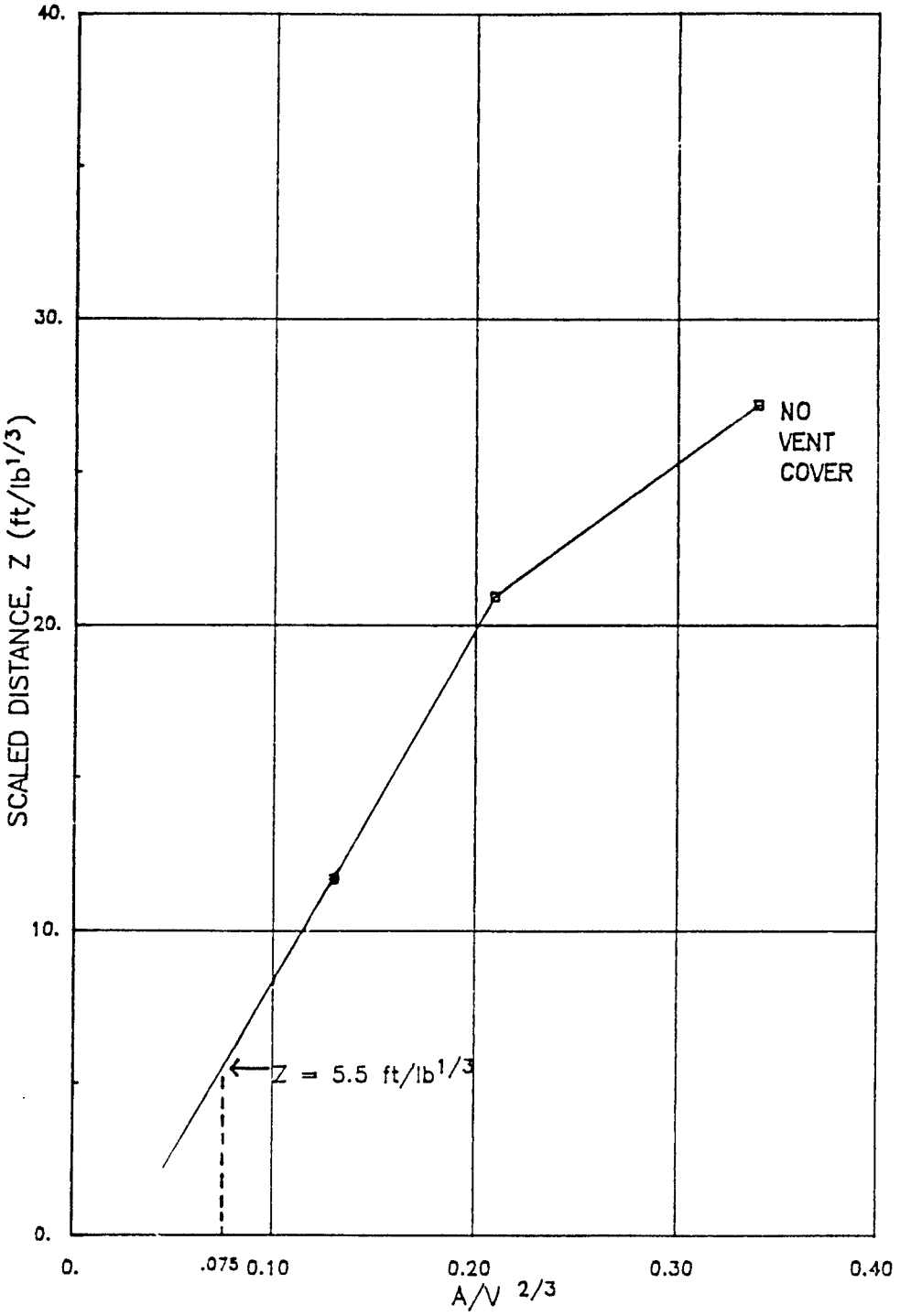

Figure 3-6. Z_R versus $A/V^{2/3}$ for P_{so} = 1.2 psi; W/V = 0.053 lb/ft^3.

4.0 ARCHITECTURAL

4.1 CONCEPTUAL DESIGN

The conceptual design for the NAVFAC Type VB MTC is shown in Figures 4-1 through 4-5. The MTC consists of a covered passageway (Area 100), test cell (Area 101), and unpaved, limited-access area (Area 102).

4.1.1 Covered Passageway (Area 100)

The covered passageway connects Area 101 with the Missile Processing Building (MPB). The structure is designed to protect any personnel or missile in the passageway (during setup operations for an AUR test in Area 101) from the weather and the MCEs in adjacent MTCs where an AUR test could be underway.

4.1.2 Test Cell (Area 101)

The test cell is a cylinder-shaped, reinforced concrete structure where the missile is tested. The structure is designed to vent effects from warhead detonation and rocket motor ignition into Area 102, a safe direction clear of personnel and facilities. Details of the test cell are shown in Figures 4-1 through 4-5.

The reinforced concrete structure will not be reusable following the MCE explosion in Area 101. The blast loads would cause large inelastic deflections of the reinforced concrete elements and doors B and F; blow away doors C, D, and E; and destroy the contents in Area 101. However, the structure will not become a source of debris, and it will have served one of its primary functions which is to vent all explosion effects away from occupied areas.

Door C is the safety vent system for warhead detonation. Door C is either structural steel or reinforced concrete with a mastic weather seal. The force of the MCE explosion in Area 101 will blow out door C and thereby vent explosion products (blast, fire, fragments off the missile, and debris from equipment) into Area 102. Door C is also designed to safely resist the external blast loads and rebound forces resulting from the MCE explosion in adjacent MTCs.

The cutouts covered by doors D, E, and F are part of the safety vent system of the Type VB MTC for rocket motor lightoff. During a test of the STANDARD(R&D) or TOMAHAWK missile, doors A, B, C and F are closed and doors D and E are open. A lightweight, weather-proof membrane covers the door opening. In the event of rocket motor lightoff, differential pressures rupture the membranes in cutouts D and E, and:

- Cutout D vents the rocket motor exhaust into Area 102.
- Cutout E (two identical cutouts) supplies fresh air to limit air temperatures and overpressures in Area 101 during the rocket motor burn phase, thereby protecting test equipment in Area 101.
- Cutout F supplies fresh air to purge Area 101 of heat, smoke, and contaminants released after rocket motor burnout, thereby protecting test equipment in Area 101. During this purge cycle, doors D and E remain open to exhaust air; and door F is opened automatically so that a centrifugal fan will drew fresh air into Area 101 near wall A-D-3.

The reinforced concrete structure, doors, and test equipment are reusable following inadvertent rocket motor lightoff. The weather-proof membranes in cutouts D and E must be replaced. The development of the design concept and criteria for the safety vent system for rocket motor lightoff in the NAVFAC Type VB MTC is contained in Reference 1.

Personnel in Area 101 setting up for an AUR test are protected from the MCEs in adjacent MTCS. Doors A, C, D, E, and F are closed and door B is open when personnel are in Area 101. Doors C, D, E, and F are blast hardened to seal out external blast overpressures and debris from Area 101 due to these MCEs.

4.2 DOORS

Requirements of doors in the Type V MTC are listed below.

Door No.	Clear Opening (ft) Width	Height	Mode: Swing	Slide	Butterfly	No. Leafs: Single	Double	Material: Plastic	Steel	Concrete	Blast Resistant: Nonreusable	Reusable	Hardware: Panic	Lock	Automatic	Notes
A	5.0	6.5						X								a
B	5.0	6.5		X		X			X		X			X	X	b,c,d,e
C	6.00 dia					X			X	X		X				f,g
D	2.5 dia			X		X			X			X		X	X	b,f,h,i
E	2.0 dia			X	X	X			X			X		X	X	b,f,h,i
F	1.25	1.33		X		X			X		X	X		X	X	b,d,i

[a] Optional environmental barrier to control environment in Area 101 when door B is open and Area 101 is occupied. Only required if MPB environment is not consistent with MTC environment.

[b] Door is automatically operated by an electric/hydraulic/pneumatic device and is an element of the safety interlock system.

[c] Manual override.

[d] Door reusable after MCE explosion in adjacent MTC and after MCE rocket motor lightoff in Area 101; door blast hardened but not reusable after MCE explosion in Area 101.

[e] Fire door.

[f] Door reusable after MCE explosion in adjacent MTC and after MCE rocket motor lightoff in Area 101; door not blast hardened for MCE explosion in Area 101.

[g] Diameter of door C is based upon the siting criterion for frangible area: A = 38 ft^2 total. Assumes two 18-inch diameter HVAC openings plus two 24-inch diameter cutout E's.

[h] Light weight, weather-proof membrane covers opening when door is open. Membrane shall rupture at 0.25 psi maximum differential pressure on the membrane.

[i] Manual override required on door; override must be interlocked with adjacent MTCs to prevent opening door when AUR test is underway in adjacent MTCs.

The position of doors (open or closed) is critical to the safety of personnel and equipment in the MTC. The position of doors during various events shall be as follows:

Event	Position	Door					
		A	B	C	D	E	F
During Setup for AUR Test	Open		X				
	Closed	X		X	X	X	X
AUR Test Underway	Open				X	X	
	Closed	X	X	X			X
During Rocket Motor Burn	Open				X	X	
	Closed	X	X	X			X
After Rocket Motor Burnout	Open				X	X	X
	Closed	X	X	X			

4.3 GRATE FLOOR

Area 101 shall have a steel grate floor as shown in Figures 4-1 and 4-2. The following factors should be considered in design of the grate:

- The open area of the grate should be large in order to limit shock wave reflections off the grate and to allow gas overpressures resulting from the MCE explosion to expand into the space below the grate, thereby ensuring that gas and shock overpressure design loads are not exceeded.
- The grate must safely support the dead plus live design loads.
- The open areas in the grate must not be so large that they present a personnel hazard.
- The grate must accommodate a system to guide the test missile on its dolly into the MTC.
- A minimum of two hinged grate doors must be provided for personnel access below the floor.

4.4 EXPLOSIVES SAFETY ENVELOPE

Explosives handling operations must be consistent with assumptions used in the design process. The center of gravity of the NEW for the weapons must not be located any closer to structural surfaces and doors than standoff distances (see Figure 2-1) used to derive the design blast loads. Further, missiles must not be allowed so close to surfaces or doors that in-structure motions from air blast- and crater-induced ground shock will cause sympathetic detonation from an MCE explosion in an adjacent MTC.

The floors of Areas 100 and 101 shall be marked with red lines which designate the explosives safety envelope. All parts of any test missile shall lie within this envelope. These lines are shown in Figure 4-6.

4.5 MISSILE TEST STAND

The test missile is supported in a missile test stand. The test stand for TOMAHAWK and STANDARD (R&D) are shown in Figure 1-2.

4.6 MISSILE RESTRAINT FIXTURE

The Type VB MTC shall have forward and/or rear fixtures to restrain the test missile and resist the thrust from inadvertent lightoff of the rocket motor/booster. The fixture shall be reusable after being subjected to the thrust-time profile from the MCE.

4.7 ROCKET MOTOR EXHAUST TUBE

For the Type VB MTC the rocket motor exhaust tube shall be a 30-inch diameter pipe for cutout D as shown in Figures 4-1 thru 4-3. The tube shall extend into door C (slip joint) and be fastened to the restraint fixture to minimize pipe vibration during the rocket motor burn phase. The tube shall extend to within 6 inches of the AUR rocket motor/booster.

The interior surface of the remanufactured pipe is lined with an ablative coating of HAVEG 41N (manufactured by Haveg Division of Ametek Corp., Wilmington, DE). The HAVEG 41N coating shall be 0.5 inches minimum thickness to protect the pipe from the temperatures produced by burning of the various rocket motors.

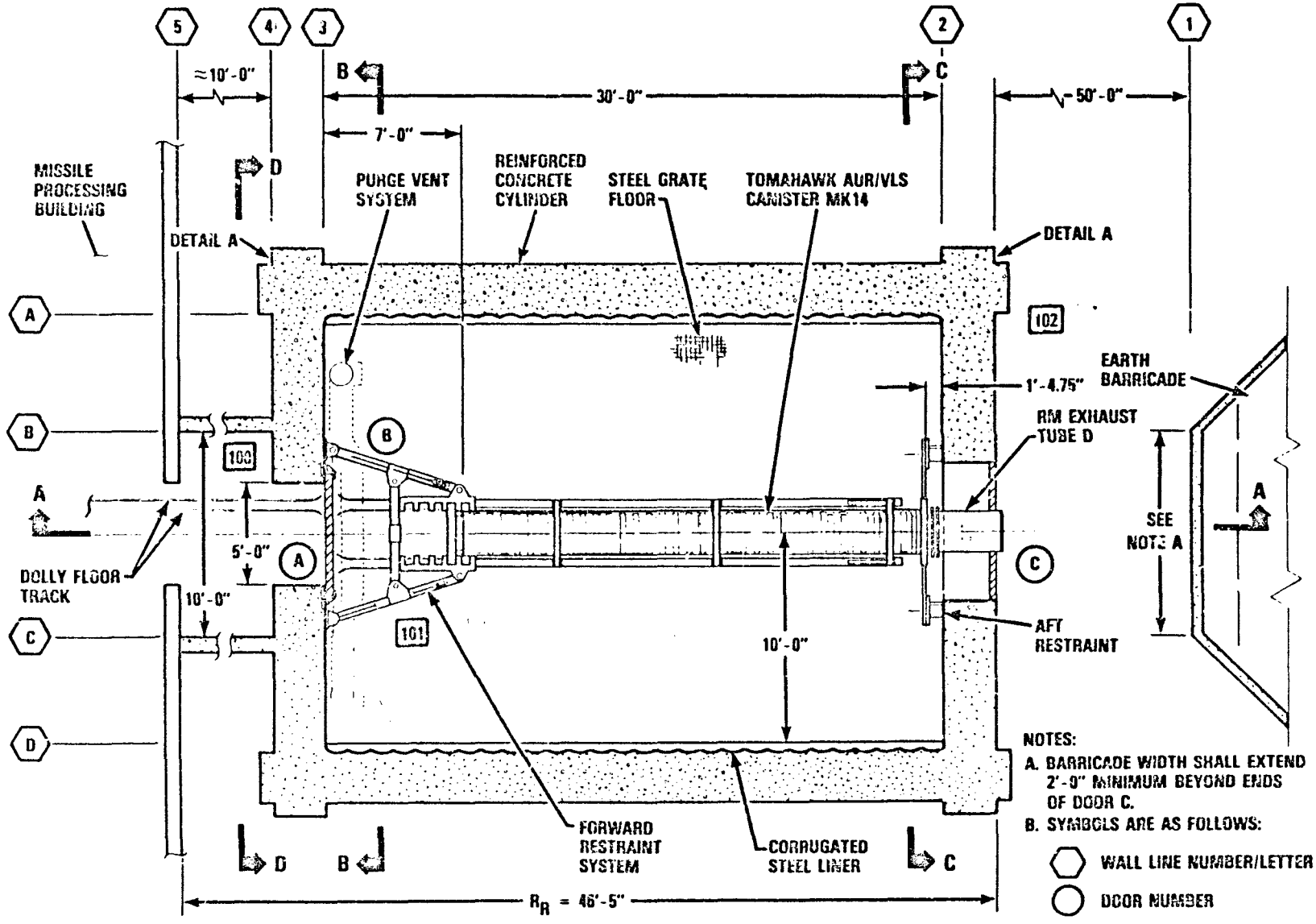

Figure 4-1. Floor plan for NAVFAC Type VB missile test cell.

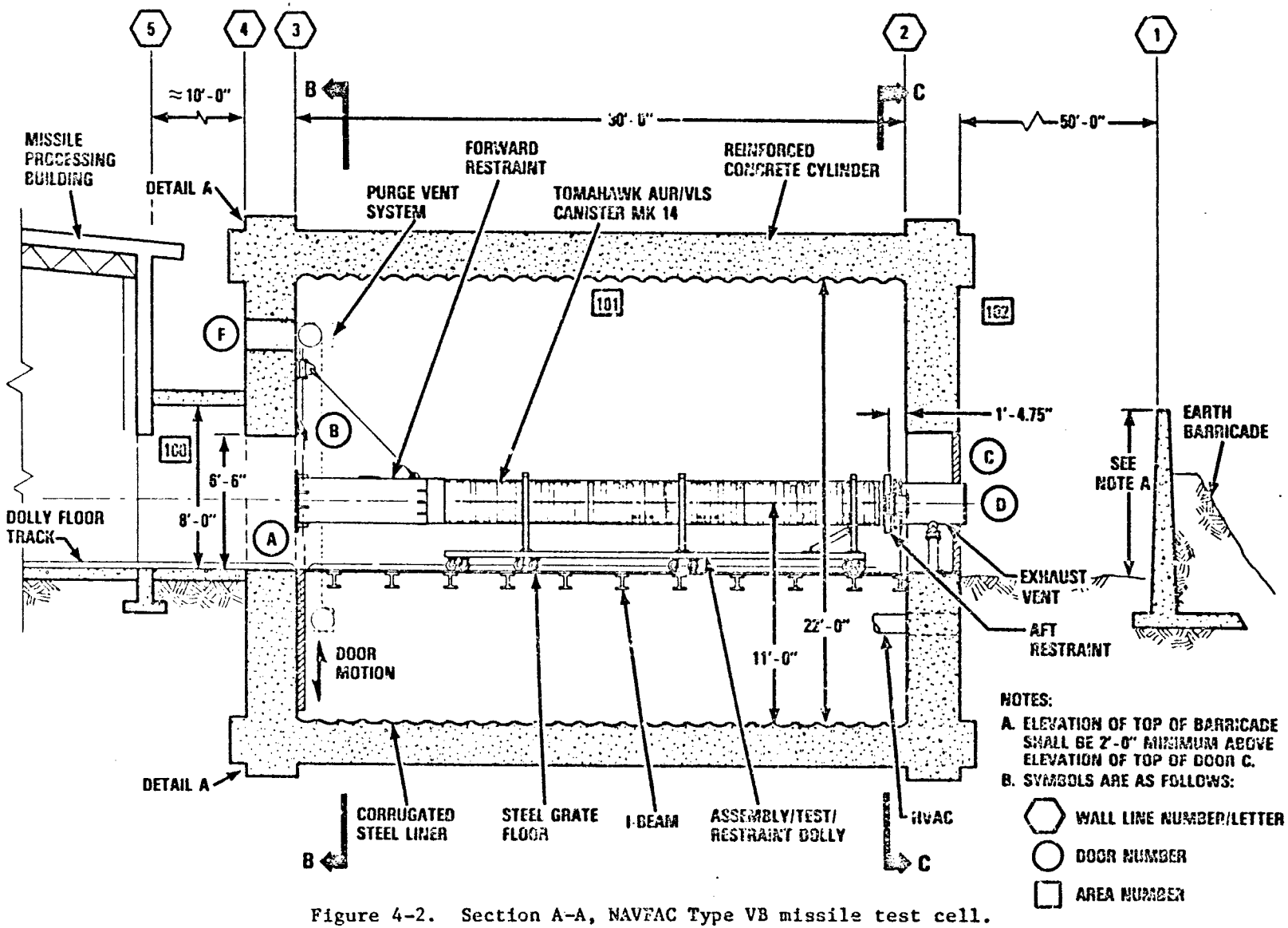

Figure 4-2. Section A-A, NAVFAC Type VB missile test cell.

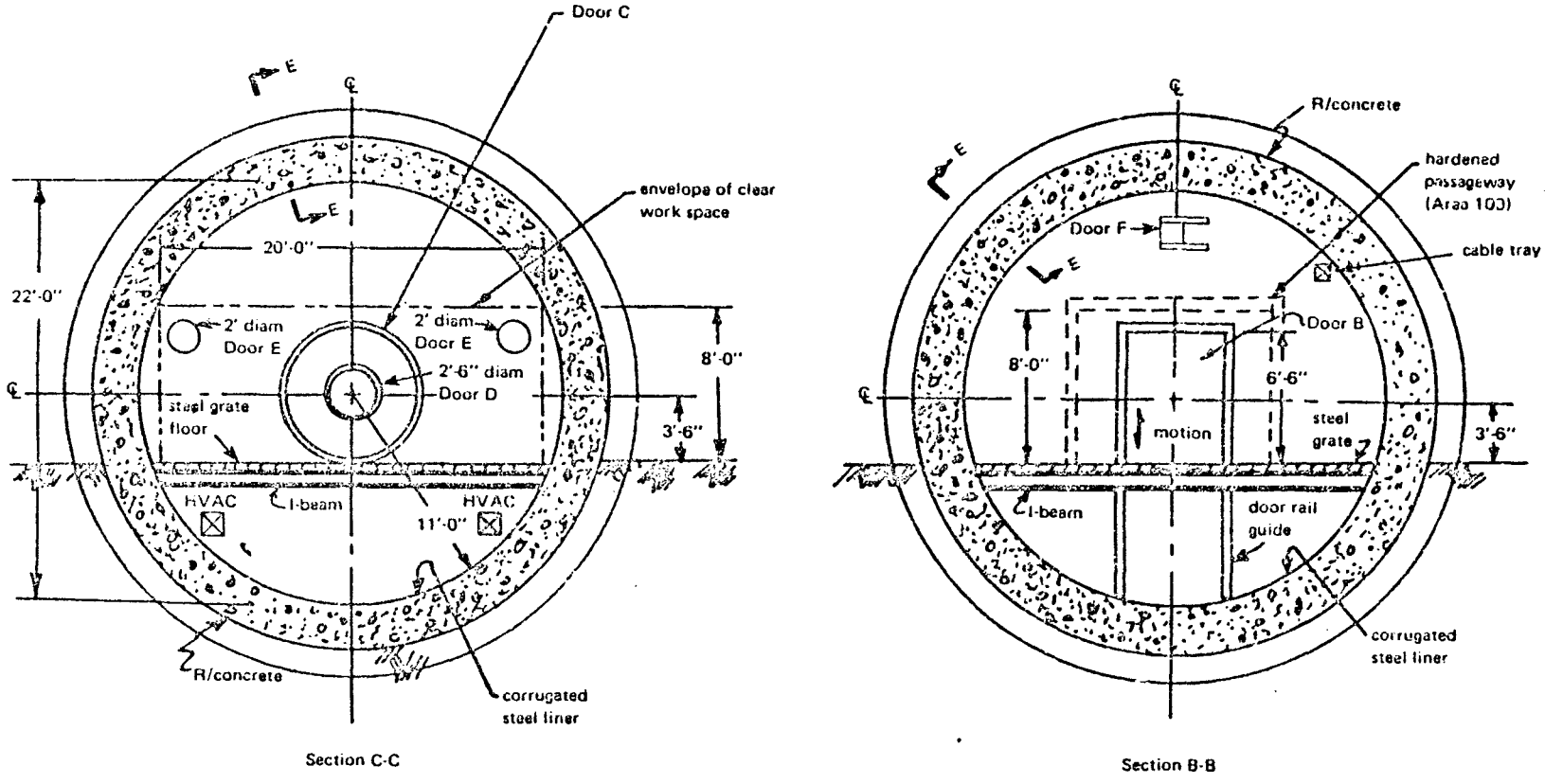

Figure 4-3. Sections B-B and C-C, NAVFAC Type VB missile test cell.

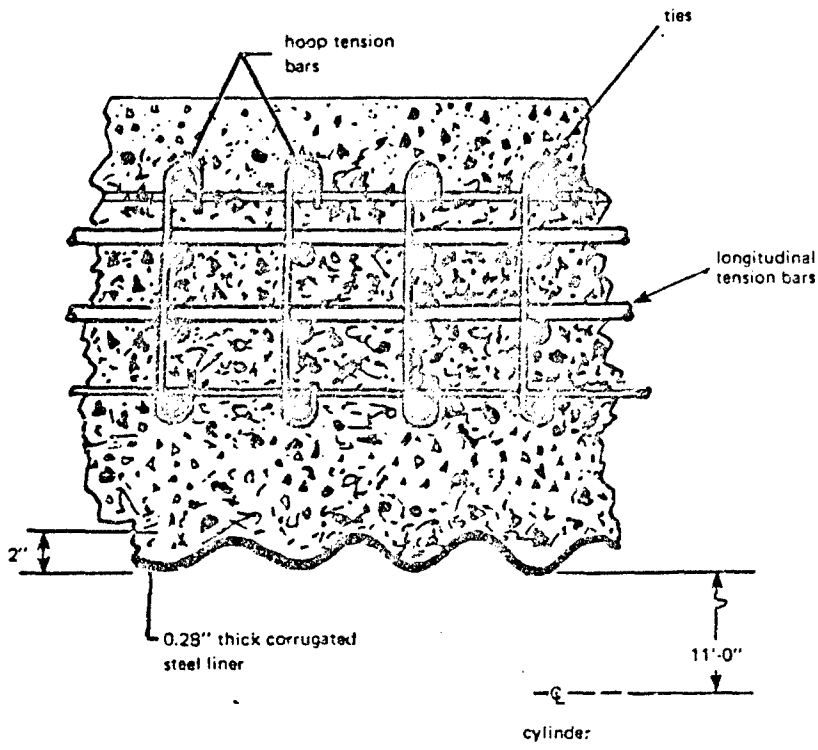

Figure 4-4. Section E-E, NAVFAC Type V missile test cell.

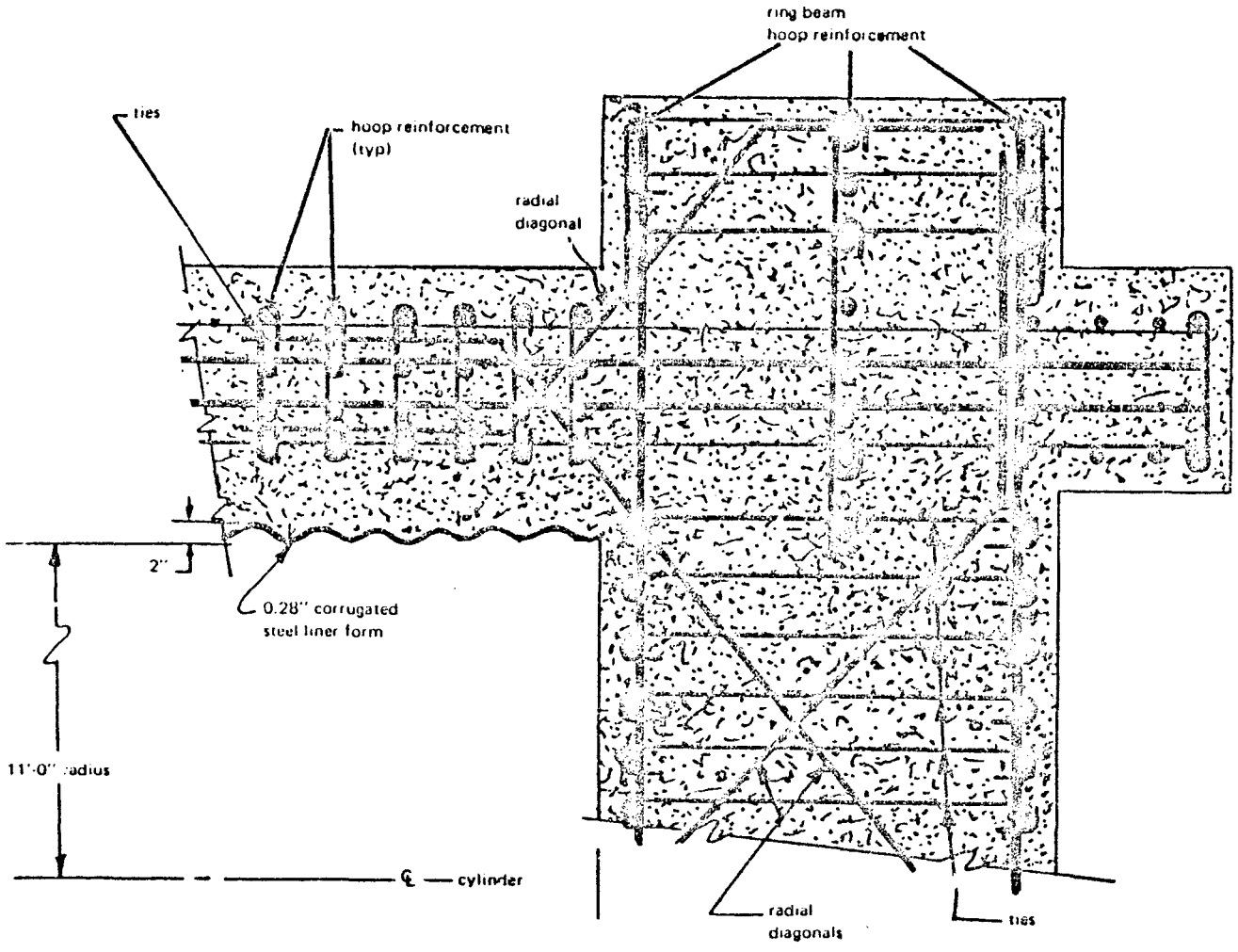

Figure 4-5. Detail A for NAVFAC Type V missile test cell.

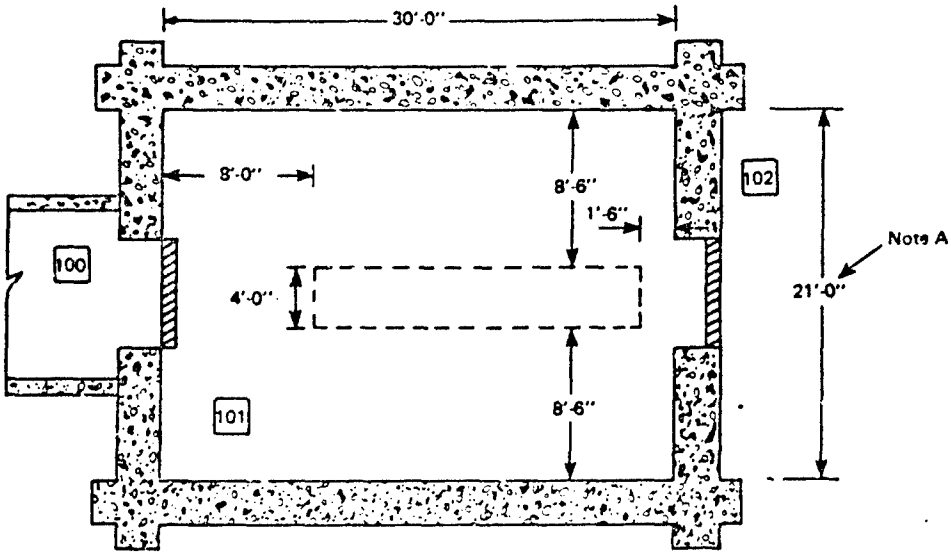

A - Width at floor elevation.

Figure 4-6. Explosives safety envelope for NAVFAC Type V MTC.

5.0 STRUCTURAL

5.1 GENERAL

Structural design of the MTC shall comply with NAVFAC P-397, "Structures to Resist the Effects of Accidental Explosions".

5.2 DESIGN LOADS

5.2.1 Design Blast Loads Inside Test Cell

Design blast loads for interior surfaces of the MTC consist of the initial shock wave loads from the explosive detonation and the long duration gas pressure loads caused by containment of the products of combustion. All surfaces shall be designed to safely resist these design blast loads.

The shock loads were determined with the computer program IMPRESS. IMPRESS, developed by Ammann & Whitney Consulting Engineers, is the basis for the internal shock loads provided in the revised NAVFAC P-397 Design Manual.

The gas loads were determined with the NCEL developed computer program REDIPT (Ref 2). The revised NAVFAC P-397 Design Manual uses data plots from REDIPT as the design internal gas pressure loads for containment structures.

Due to the methods used to measure gas pressures, the shock and gas pressure triangular load-histories should be merged, as shown in Figure 5-1, rather than added. A bilinear load function results with a maximum pressure = B_1 at T = 0 and a duration = T_2.

5.2.2 Design Blast Loads Outside Test Cell

Measured blast loads from the 1986 New Mexico Tech tests were used to derive design blast loads in each direction outside the MTC Figures 5-2 and 5-3 summarize these loads which are conservatively based on worse case results for all tested values of W/V. The covered passageway and rocket motor lightoff vent covers shall be designed to safely resist these design blast loads.

5.2.3 Fragment Design Loads

The reinforced concrete and structural steel surfaces of Area 101, except doors C, D, and E, shall prevent perforation and escape of primary fragments from the MCE explosion in Area 101. The types of missiles to be tested in the Type V MTC are cased weapons, and surfaces of the MTC (except Door C) shall prevent perforation by primary fragments off the missile and secondary debris from test fixtures and equipment.

Minimum required thicknesses of reinforced concrete (f'_c = 4000 psi) and mild steel plate, based on the mass and velocity of fragments measured in tests of the missile systems and penetration theory presented in NAVFAC P-397 were specified.

5.3 REINFORCED CONCRETE

5.3.1 Design Stresses

5.3.1.1. Reinforcing Steel. All reinforcing steel for concrete shall be A615, Grade 60. A statistical analysis of the static yield strength of A615, Grade 60, shows the average yield strength is 10% greater than the minimum value required by the ASTM specifiction. Consequently, the design static yield stress, f_y, shall be:

$$f_y = 1.10 \times 60{,}000 = 66{,}000 \text{ psi}$$

The design static ultimate stress, f_u, for A615, Grade 60, shall be:

$$f_u = 90{,}000 \text{ psi}$$

The dynamic design stress, f_{ds}, shall be:

Element	Type Stress	Dynamic Increase Factor, DIF		Dynamic Design Stress, f_{ds} (psi)
		f_{dy}/f_y	f_{du}/f_u	
Cylinder ($X_u/X_E \leq 6$)	Bending	1.23	1.05	81,200[a]
	Hoop Tension	1.23	1.05	87,800[c]
	Long. Tension	1.23	1.05	81,200[a]
	Diagonal Tension	1.10	1.00	72,600[a]
	Direct Shear	1.10	1.00	72,600[a]
End Wall ($2 \leq \theta_m \leq 4$ deg)	Bending	1.23	1.05	84,500[b]
	Tension	1.23	1.05	81,200[a]
	Diagonal Tension	1.10	1.00	72,600[a]
	Direct Shear	1.10	1.00	77,000[b]

[a] $f_{ds} = f_{dy}$

[b] $f_{ds} = f_{dy} + (f_{du} - f_{dy})/4$

[c] $f_{ds} = (f_{dy} + f_{du})/2$

5.3.1.2 Concrete. The static compressive strength of concrete, f'_c, shall be:

$$3{,}000 \leq f'_c \leq 5{,}000 \text{ psi}$$

The dynamic ultimate strength of concrete shall be:

$$f'_{dc} = DIF\ f'_c$$

where: DIF = 1.25, bending
DIF = 1.00, diagonal tension and bond
DIF = 1.10, direct shear

5.3.1.3 Butt Splices. The strength of all hoop reinforcing steel will be achieved with a mechanical butt splice. This splice shall develop in tension the ASTM specified minimum tensile strength of the reinforcing steel (90,000 psi for Grade 60).

5.3.2 Breaching

All reinforced concrete and steel surfaces of Area 101, except doors C, D, and E, shall prevent breaching of the surface by the MCE explosion in Area 101. This will prevent debris from flying in all directions outside the MTC, except towards Area 102. To meet this performance requirement, the minimum thickness of reinforced concrete in Area 101 shall be based on the following equation (Ref 3):

$$T_c = 4.12\ (R/W^{1/3})^{-0.4}\ W^{1/3}$$

where: R = standoff distance (Figure 2-1)

5.3.3 Allowable Deflections

The maximum allowable deflection, X_u, is defined in terms of either the maximum allowable ductility factor, X_u/X_E, where X_E is the equivalent elastic yield deflection, or the maximum allowable support rotation, θ_u, following formation of the yield line mechanism. The maximum allowable deflections for unlaced reinforced concrete elements shall be as follows:

Area No.	Element	R/Concrete Surface	θ_u (deg)	X_u/X_E
101	Cylinder	2-3-A, 2-3-D	-	6.0
	Rear Wall	A-D-2	4.0	-
	Front Wall	A-D-3	4.0	-

5.4 DOORS

5 4.1 Materials

Doors B, C, D, E, and F shall be constructed from either ASTM A36 or A588 steel.

5.4.2 Design Stresses

The dynamic design stress in bending, f_{ds}, and shear, f_{dv}, shall be as follows:

ASTM Steel	f_y(min) (psi)	f_y[a] (psi)	f_u (psi)	f_{dy}/f_y	f_{du}/f_u	$X_m/X_E \leq 10$ f_{ds}[b] (psi)	$X_m/X_E \leq 10$ f_{dv}[c] (psi)	$X_m/X_E > 10$ f_{ds}[b] (psi)	$X_m/X_E > 10$ f_{dv}[c] (psi)
				High Design Overpressure Range (Doors B and F)					
A36	36,000	39,600	58,000	1.36	1.10	53,900	29,600	56,400	31,000
A588	42,000	46,200	63,000	1.24	1.05	57,300	31,500	59,500	32,700
	46,000	50,600	67,000	1.24	1.05	62,700	34,500	64,600	35,500
	50,000	55,000	70,000	1.24	1.05	68,200	37,500	69,500	38,200
				Low Design Overpressure Range (Doors C, D, E, and F)					
A36	36,000	39,600	58,000	1.29	1.10	51,100	28,100	54,300	29,900
A588	42,000	46,200	63,000	1.19	1.05	55,000	30,300	57,800	31,800
	46,000	50,600	67,000	1.19	1.05	60,200	33,100	62,700	34,500
	50,000	55,000	70,000	1.19	1.05	65,500	36,000	67,500	37,100

[a] Design static yield stress that accounts for an average yield strength which is 10% greater than the minimum value required by the ASTM Specification, $f_y = 1.10\ f_y(\text{min})$.

[b] $f_{ds} = f_{dy}$

[c] $f_{dv} = 0.55\ f_{ds}$

[d] $f_{ds} = f_{dy} + (f_{du} - f_{dy})/4$

5.4.3 Allowable Deflections

The maximum allowable deflection, X_u, is defined in terms of the maximum allowable support rotation, θ_u, following formation of the yield line mechanism. An additional constraint is imposed on the maximum allowable deflection, X_u, by limiting the ductility factor X_u/X_E, where X_E is the equivalent elastic yield deflection. The maximum allowable deflections for the steel doors are:

Door	Type	θ_u (deg)	X_u/X_E
B	Nonreusable	8.0	15
C	Reusable[a]	2.0	5
D, E, F	Reusable[a]	2.0	5
F	Nonreusable	8.0	15

[a]Door will not have to be replaced and occupants of MTC are protected following MCE explosion in adjacent MTC.

A trial door design shall be considered adequate provided the maximum dynamic deflection, X_m, is such that $X_m \leq X_u$ based on the rotational constraint and $X_m/X_E \leq X_u/X_E$ based on the ductility constraint.

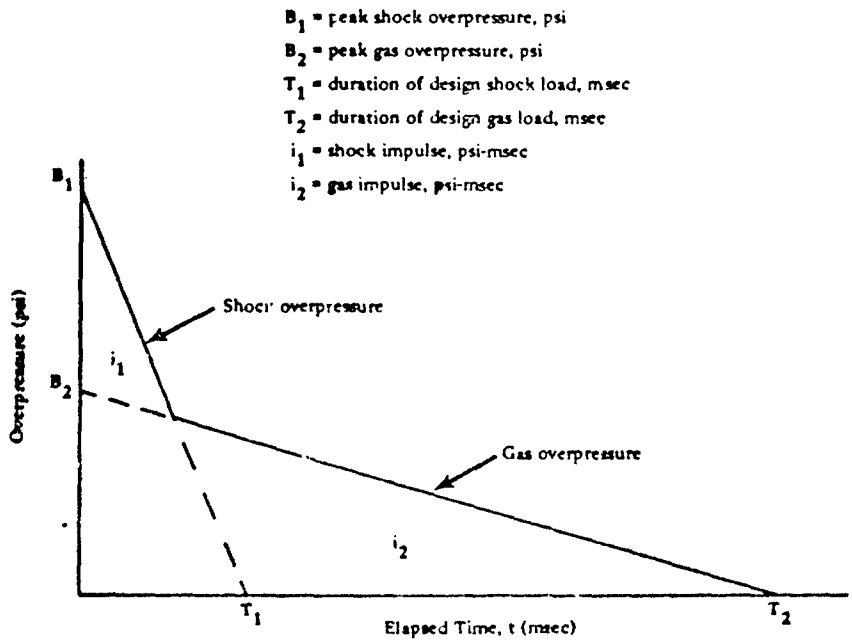

(a) Design blast load inside MTC.

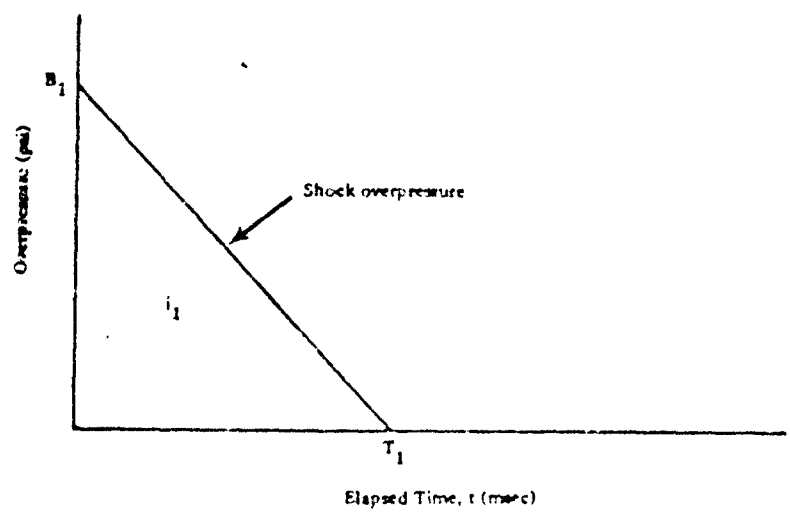

(b) Design blast load outside MTC.

Figure 5-1. Definition of design blast loads for NAVFAC Type V missile test cell.

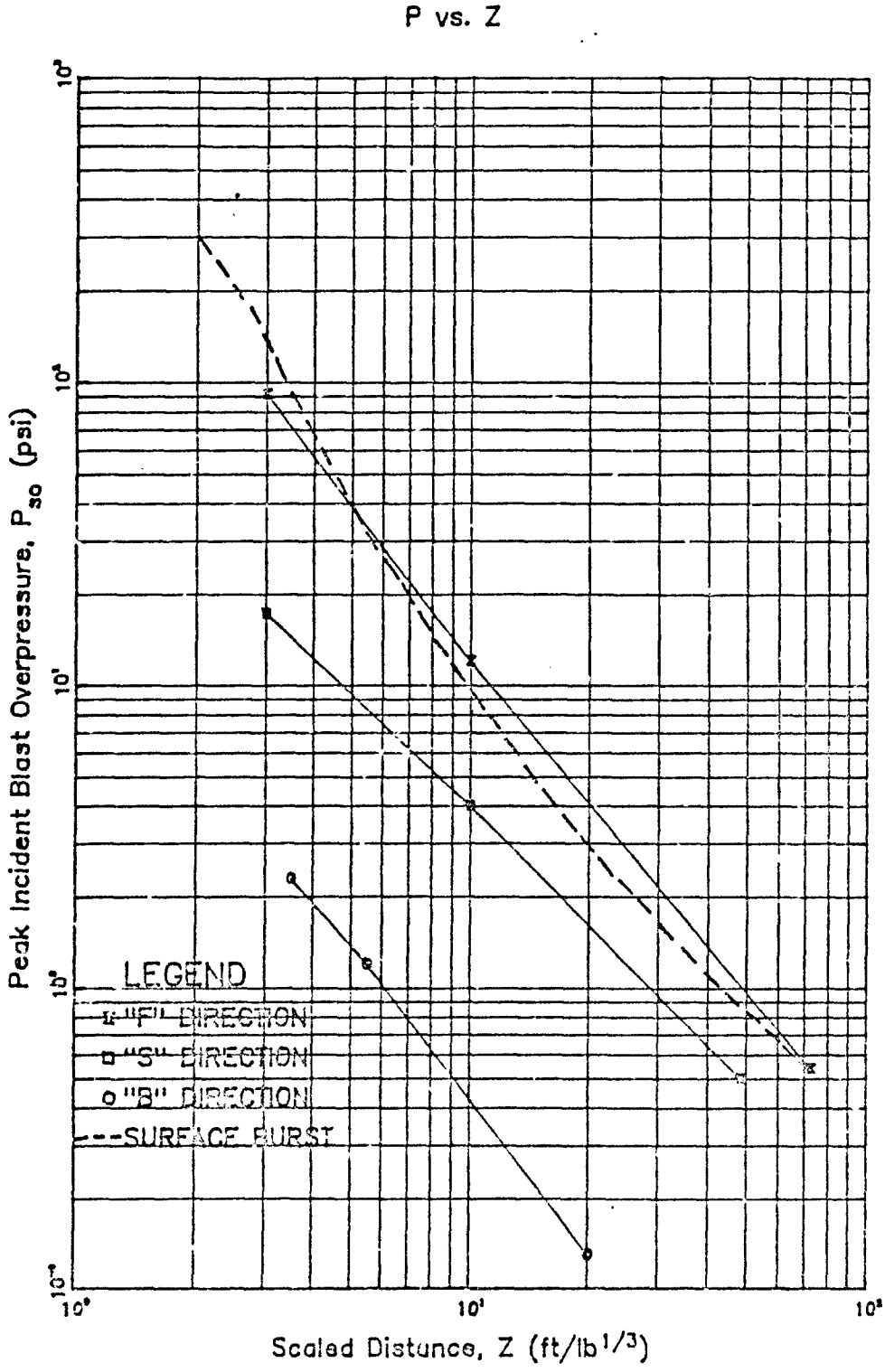

Figure 5-2. Peak incident design pressure outside NAVFAC Type V MTC.

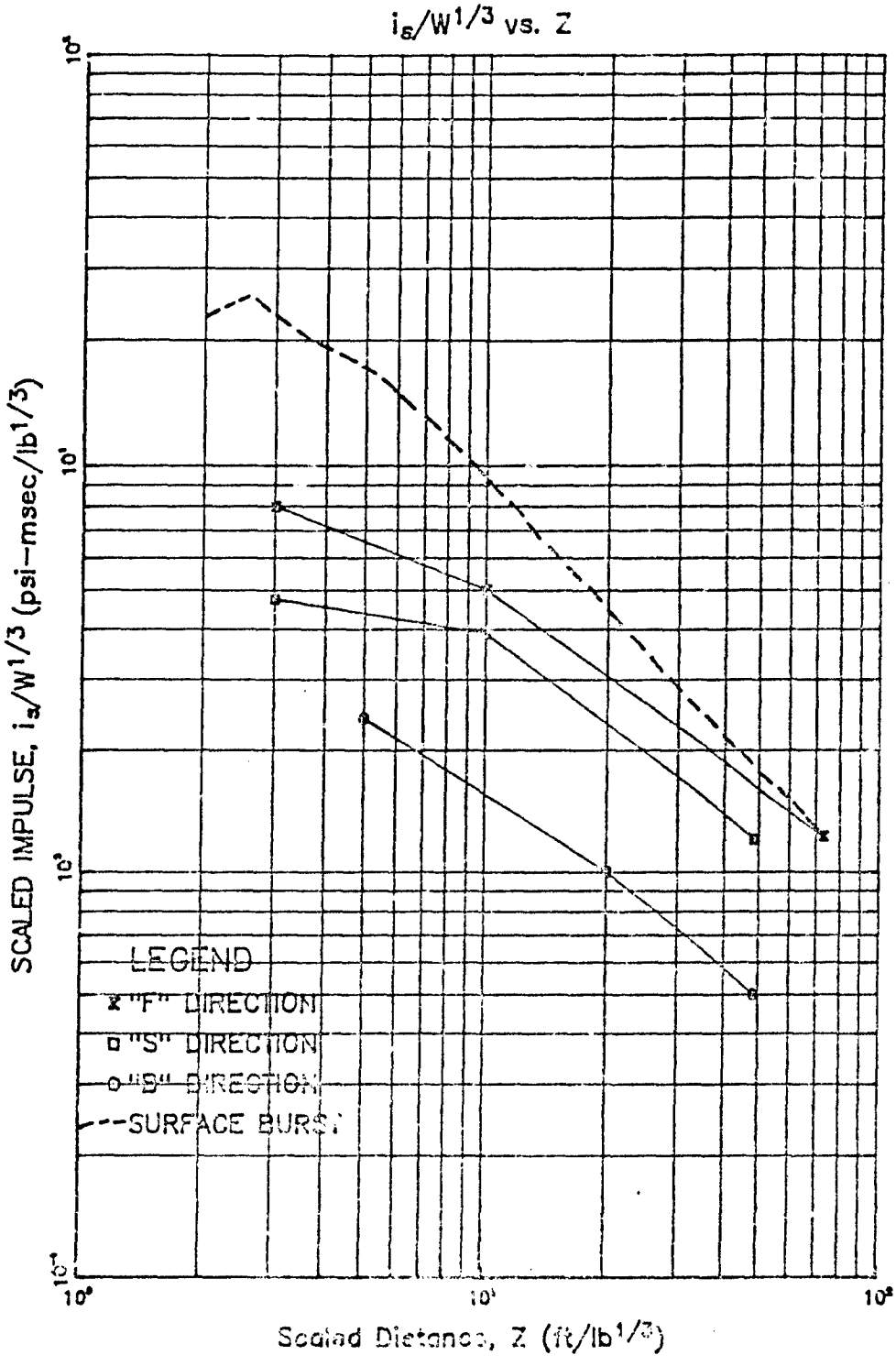

Figure 5-3. Scaled incident design impulse outside NAVFAC Type V MTC.

6.0 CERTIFICATION TEST PROGRAM

6.1 GENERAL

Warhead detonation and rocket motor lightoff tests will be conducted in May/June 1989 at Terminal Effects Research & Analysis Group (TERA), New Mexico Institute of Mining & Technology, Socorro, NM. Tests will be performed on a full-scale model of the Type VB MTC. A final NCEL Test Report should be available by June 1990.

6.2 WARHEAD DETONATION TEST

One explosive test of 720 pounds of TNT will be performed. The test charge will be a cased, divided cylinder. The forward charge (simulating the TOMAHAWK warhead) will contain approximately 520 pounds of explosive; the case will weigh approximately 540 pounds and will be made of steel. The aft charge (simulating the TOMAHAWK rocket motor) will weigh approximately 205 pounds; the case will weigh about 130 pounds and will be made of steel. Separating the two charges will be an inert section representing guidance, batteries, etc. The forward charge is supposed to be similar in its fragmentation performance to that of the BULLPUP warhead found on the TOMAHAWK missile. Test objectives will include the following:

1. Evaluate the constructability, fabrication and inspection procedures, and construction costs of the NAVFAC Standard Type V MTC.

2. Certify the structural safety performance of the Type V MTC under the internal blast, fragment, and debris loads resulting from detonation of the design NEW.

3. Certify the safe siting criteria from detonation of the design NEW.

4. Evaluate design blast loads (external and internal), and fragment and debris hazards resulting from detonation of the design NEW.

6.3 ROCKET MOTOR LIGHTOFF TESTS

Two simulated rocket motor lightoff tests will be performed inside the test structure. Test objectives will include the following:

1. Certify the structural safety performance of the Rear Restraint System using a TOMAHAWK ABL missile with a Mk 106 rocket motor.

2. Certify the structural safety performance of the Forward Restraint System using a STANDARD VLS missile with a Mk 104 rocket motor.

3. Certify the safe internal environmental (temperature and pressure) criteria for the rocket motor vent and purge systems using a STANDARD VLS missile with a Mk 104 rocket motor.

7.0 REFERENCES

1. Naval Civil Engineering Laboratory. Technical Note N-Draft: Basis of Design for NAVFAC Type V Missile Test Cell, by R.N. Murtha and W.A. Keenan. Port Hueneme, CA, May 1988. (Confidential)

2. Minutes of the Twenty-First Explosives Safety Seminar: "Effect of Frangible Panels on Internal Gas Pressures," by J.E. Tancreto and E.S. Helseth, Aug 1984.

3. Effects of Bare and Cased Explosive Charges on Reinforced Concrete Walls, by Hansjorg Hadar, Ernst Basler and Partners, Consulting Engineers, 8029 Zurich, Switzerland. Published in Symposium Proceedings, the Interaction of Non-Nuclear Munitions with Structures, U.S. Air Force Academy, Colo., May 10-13, 1983.

DESIGN, FABRICATION AND PROOF TESTING OF AN ELECTRICAL EXPLOSION CONTAINMENT

Wilfred E. Baker, Wilfred Baker Engineering
San Antonio, Texas, USA

Richard J. Hayes, Center for Electromechanics
University of Texas at Austin
Austin, Texas, USA

ABSTRACT

At the Center for Electromechanics of the University of Texas, a number of pulsed electrical power supplies are being developed. Each power supply generates a tremendous amount of energy which is released in milliseconds. Only explosively-actuated switches can switch the megamp currents in these systems fast enough for proper system function. In normal switching, energies of 0.5 MJ are released in about 1 ms, while in a fault condition, it is possible for 4.5 MJ to be released in about 10 ms. Either energy release is too hazardous for operating personnel in the laboratory containing the equipment.

This paper describes the design, fabrication, and proof testing of safety containments for the explosively-actuated switches. The containments are steel vessels which are constructed so that they can be easily emplaced around the switches, and easily assembled or disassembled. The methods of analysis and design for the containments are discussed, followed by details of fabrication and proof testing using high explosives to simulate the rapid electrical energy releases.

Only minor changes in design were necessary after proof test. Containments fabricated according to the final design have been built, and have proven to be very effective in containing explosion effects in operation in the laboratory.

Introduction

The Center for Electromechanics at the University of Texas (CEM-UT) builds and tests pulsed power supplies utilizing homopolar generators as part of an ongoing research and development effort. These power supplies generate tremendous amounts of energy which are released in milliseconds. At the present time there are no fast-acting opening switches available commercially to handle the large (1.2 megamp) currents and high voltages required in some CEM-UT experiments. To solve this problem, an explosive opening switch has been developed. A sheet of aluminum is used to

connect two copper busbars. Grooves are machined into the aluminum to create a stress concentration factor and allow the insertion of Primacord®. Detonating the Primacord® blows the prescribed aluminum section out of the circuit and opens the switch. The energy released in this explosion is equivalent to 0.5 megajoules and is released in approximately one millisecond. This explosive switch will be used every time the power supply is discharged for an experiment (eventually about once a week).

Another much more severe explosion is also possible if certain elements in the switching circuit should fail. A large (12 ton) copper inductor is used to store and release the energy generated by the homopolar. The inductor stores 4.5 megajoules of electrical energy. In the case of a fault condition all of this energy could be dissipated as an electrical arc at the explosive switch in approximately 10 milliseconds.

While there is only a slight probability that the fault condition will ever occur, the effects of such an explosion in open air could be disastrous. To assure the safety of CEM-UT personnel and equipment, an explosion containment vessel was deemed necessary. There were numerous criteria. One of the more difficult was that the vessel have openings allowing the passage of two 24-inch wide busbars. The busbars must have a gap between them, and the containment vessel openings must allow for electrical insulation. The vessel must also be split at the busbar location so that it can be clamped to the busbar and allow access to the switch without removing the entire vessel. The lower section of the vessel must slip under the lower busbar, which has a maximum height above the base structure of 17 inches. Due to space limitations the width of the vessel could be no greater than 39 inches. To keep the cost and weight of the vessel at a reasonable level it was decided that some plastic deformation in the case of a fault condition would be acceptable. No plastic deformation would be allowed during the standard energy release.

To simulate both the standard and fault condition situations, high explosives would be detonated inside a prototype vessel with an assembled set of busbars in place. Detasheet® was chosen as the explosive because it is readily available in sheets and can be shaped in the same configuration as the actual switch. Detonating Detasheet® results in a rapid (5-10 microsecond) initial energy release and some heating of gases trapped inside the vessel. While the energy release is more rapid than that caused by an electrical arc, it provides for a more severe test of the containment vessel. Using the heat of detonation for Detasheet®, it was determined that 0.244 lbs of the explosive would be equivalent to a 0.5 MJ discharge. To simulate the fault condition of 4.5 MJ, 2.19 lbs of Detasheet®

would be used.

Analysis of Containment

Assuming the quantities of high explosive whose detonation energies matched the normal and fault explosive switch operations, we predicted both internal reflected shock pressures and specific impulses at various locations on the inner surfaces of the containment, and the longer-term quasi-static pressures from heating of air within the containment by the explosions. Methods used are described in Ref. 1.

The dynamic response of the containment to the internal blast loads was analyzed by considering elements from the vessel as relatively simple structures such as rings, beams or plates, and then determining their response as equivalent single-degree-of-freedom (sdof), elastic-plastic structures, using approximation methods from Ref. 2. To aid in these dynamic analyses, a computer program entitled BIGGS, designed to run on an IBM-PC class computer, was used. This program computes the dynamic, elastic-plastic response of simplified structures to any transient loading which can be represented by a series of straight-line segments.

The elements we chose to model the containment vessel for dynamic analysis are shown in Figure 1. This figure also lists the simplifying assumptions made before analyzing element responses.

Under the fault condition explosive loading, the structure was designed so that maximum dynamic deformations of various parts of the containment, computed by the BIGGS program, stayed well below the acceptable limit for a one-time safety structure of $\mu = 15$, where μ is the ratio of dynamic maximum deflection to elastic deflection. Table 1 shows the values for the ductility ratio μ for the final design for the containment. The maximum deformation can be seen to be predicted for the support legs and for the side beams in bending.

Table 1. Maximum Ductility Ratios for Elements of Containment for Explosive Loading Simulating Fault Condition

Element	Ductility Ratio, μ
Cylindrical shell in radial motion	1.39
Side beams	5.24
Flange bolts in tension (20, 1" diameter, high strength bolts)	0.706 (elastic)
Semi-heads, top and bottom	Not analyzed, but less than cylinder response
Support legs	8.13

Design and Fabrication

Following the thorough analysis of the blast loads and response, a vessel was designed which incorporated many standard components. Thirty-six inch O.D. API 5LX-60 line pipe and ASME SA 537 heads were used for the body of the vessel. Bolt-through 100 degree flange sections were welded to the vessel at the busbar openings. Telescoping legs made from standard steel pipe sections were attached to the bottom of the vessel to allow it to slide under the busbar before being raised into position. All fabrication was completed in accordance with ASME Pressure Vessel Code Section VIII, Division I using materials with a minimum yield strength of 50,000 psi. Once completed the entire vessel was stress relieved and then coated with a flexible polyurethane paint. Gaskets of nylon were machined to seal around the busbar opening.

A prototype vessel was built and assembled around a complete busbar and switch assembly. Normally an inductor would be supporting one end of the busbar and two ignitron closing switches would be mounted on the opposite end of the bus. Figure 2 shows a containment vessel in place in the laboratory near the large inductor. In the experiments, support stands were used to support the buswork and pressure transducers at the ignitron and inductor locations monitored the pressure that would be seen in these areas. The equipment was mounted on one of the generator pit covers just as production vessels will be mounted in their final configuration. Using the pit cover as a test bed, the entire experiment was placed on a trailer and transported to the test site. Figure 3 shows a closeup of the test arrangement at the test site. Figure 4 illustrates the experimental configuration and the location of the pressure transducers used to monitor the blast.

Pressure transducer number one (PT#1) was mounted on the bottom head 4 inches from the center toward the inductor end of the busbars. PT#2 was mounted on the side of the vessel at the same height as the busbar. PT#3 was mounted in the top head 4 inches from center and toward the inductor end of the busbar. PT#4 was mounted externally 7 inches from the containment where the glass tubes on the ignitrons would normally be located. PT#5 was located externally at the same height as the vents in the top of the vessel and 4 inches from the O.D. to simulate the location of the inductor. PT#6 was mounted in the top head of the vessel 4 inches from the center toward the pit side of the busbar. This transducer (PT#6) was used to monitor the quasi-static pressure, while PT#1 at approximately the same location monitored the blast or reflected pressure. Two four-channel oscilloscopes, located in a van 100 feet from the blast, were used to

monitor the pressure transducers, and all data were recorded on floppy disks. The scopes were powered by a 2600 Watt portable generator set and protected from any fragmentation by bags of absorbent placed in front of the van. Reduced data from both shots are included in Table 2. Sample traces are shown in Figures 5 and 6.

Table 2. Pressure Readings

Test #1 (0.5 MJ)

PT Location Fig A	PT Type	Peak Pressure (psi)	Duration (milliseconds)	Predicted Peak Pressure (psi)
1	PCB 102 A04	220	3.5	330
2	PCB 102 A03	330	1.0	980
3	PCB 102 A15	(1)	---	42
4	PCB 102 A15	1.9	10.0	1.7
5	PCB 102 A15	5.0	13.4	1.7
6	ENDEVCO 8510B-500	335 (2) 43 - 70	10.4 After 15.0	40.2

Test #2 (4.5 MJ)

PT Location Fig A	PT Type	Peak Pressure (psi)	Duration (milliseconds)	Predicted Peak Pressure (psi)
1	PCB 102 A03	280 (3)	0.75	3,500
2	PCB 102 A03	8,700	3.0	5,800
3	PCB 102 A04	(4)	---	270
4	PCB 102 A15	5	11.5	5.8
5	PCB 102 A15	2.5	9.0	4.8
6	ENDEVCO 8510B-500	(5)	---	227

NOTES:

(1) No data recorded due to bad scope channel, cable, or faulty PT.

(2) This PT was used to measure quasi-static pressure. Peak reading is also given to compensate for reading lost on PT#3.

(3) Still some question as to why this reading is so low compared to Test #1 and predicted pressure.

(4) This channel also failed on Test #1 with a different PT.

(5) Failed immediately.

Shot #1 simulated the energy released with the normal opening of an explosive switch. With all personnel at a safe distance, the explosives were detonated. Before opening the vessel, it was noted that the upper bus bar on the inductor side, which weighs approximately 700 pounds, had shifted about one-half inch. Under normal conditions this bus would be welded to the inductor in addition to the existing clamp. The phenolic insulators between the upper and lower bus on the inductor end had also been blow out about 36 inches by the blast. The nylon busbar gasket has failed at one location and three pieces of nylon weighing 3 to 4 ounces had been through about 10 feet. The damage is apparent in Figure 7. On opening the containment vessel it was noted that one of the 1-inch studs retaining the switch had failed. There was no indication that the nylon gasket had cracked in any location other than where it failed. Furthermore, there was no indication of any damage to the containment vessel. The 1-inch studs were replaced and the shifted insulators and buswork realigned. The failed nylon pieces were taped in place to reduce venting during the second shot. The clamps on the bus bar were also readjusted to better retain the buswork.

Shot #2 simulated a fault condition where both ignitrons would fail and all the energy in an inductor, 4.5 MJ, would be dissipated in the switch. The containment vessel contained the blast of shot #2, but the nylon gasket failed completely. Pieces of the gasket were found up to 150 feet away. Most of the pieces were small, weighing less than half an ounce. The upper busbar moved 30 inches and the phenolic insulators were thrown from the buswork or burned in the vessel. See Figure 8 for an external view of the containment after this shot. Inside the vessel all of the 1-inch studs had failed and the entire commutation piece had raised up at about a 45 degree angle (see Figure 9). The lower busbar was also plastically deformed approximately four inches by the charge going off above it. No evidence of plastic deformation or damage was found on the containment vessel. Several pressure transducer cables were broken by the blast. Even with the considerable damage to the buswork that occurred, the containment vessel still performed its primary function of preventing the endangerment of human life.

Discussion

Initial evaluation of shot #1 indicates that with a few minor adjustments there would have been no damaged or shifted parts. If the only criteria were safety, then shot #2 should also be considered a success. The only fragmentation was relatively light pieces of nylon. However, an inductor or an

ignitron could have been damaged by the moving buswork. In addition to the nylon failure, part of an epoxy coating on some of the buswork came off.

The most critical failure in the system was the fracture of all of the 1-inch studs in the buswork system. These studs have since been replaced with a greater number of shorter, more ductile studs utilizing rolled rather than cut threads to assure adequate strength during future shots. With the studs the buswork and phenolic insulators will not be allowed to move. Testing of the nylon used for the gasket showed that it did not meet the required material specification. Further testing proved that the nylon's ductility could be increased through annealing. While this should be adequate for the low level shots, new materials are being investigated to determine if a new gasket can be developed to withstand the fault condition. The epoxy which cracked due to flexing of the busbar has been replaced with a urethane coating which has excellent ductility.

There were only two modifications to the vessel, and both were to prevent failures of other components. The first was the addition of a support in the bottom half of the vessel to prevent excessive deflection of the lower busbar. This support was constructed of square steel tubing and welded to the bottom half of the vessel at the same location as the containment legs. The second modification was a decrease in the size of the busbar openings. This reduced the total blast force and moment on the nylon gasket by reducing its total surface area by twenty-five percent.

Since the original experiments, six additional containment vessels have been built to be used with CEM-UT's 60 megajoule (six, 10-megajoule homopolars) power supply. By using the aforementioned off-the-shelf components, costs and production time were kept to a minimum. Initial single and multi-generator testing was conducted during the summer of 1987, while full scale tests with four generators discharging simultaneously took place in July 1988. Barring the occurrence of a fault condition, all of the containment vessel and busbar components will be reusable.

References

1. W.E. Baker, J.J. Kulesz, P.S. Westine, P.A. Cox, and J.S. Wilbeck, "A Manual for the Prediction of Blast and Fragment Loading of Structures," DOE/TIC-11268, U.S. Department of Energy, Amarillo, Texas, November 1980.

2. J.M. Biggs, Introduction to Structural Dynamics, McGraw-Hill Book Co., New York, 1964.

SIMPLIFYING ASSUMPTIONS

COMPONENTS ARE NOT CONNECTED SO THEY ARE NOT STRESSED BY OTHER MEMBERS.

SIDE BEAMS ARE OF EQUAL LENGTH.

90° ARC FLANGES (NOT SHOWN) ARE MODELED INDEPENDENTLY OF CYLINDERS USING SHEAR LOADS.

STRESSES ARE ASSUMED TO BE EVENLY DISTRIBUTED (I.E., NO STRESS RISERS)

FLANGE BOLTS ARE MODELED INDEPENDENTLY IN TENSION ONLY.

SUPPORT LEGS ARE MODELED AS SHORT CYLINDERS IN COMPRESSION, FOUR SUPPORTS IN PARALLEL.

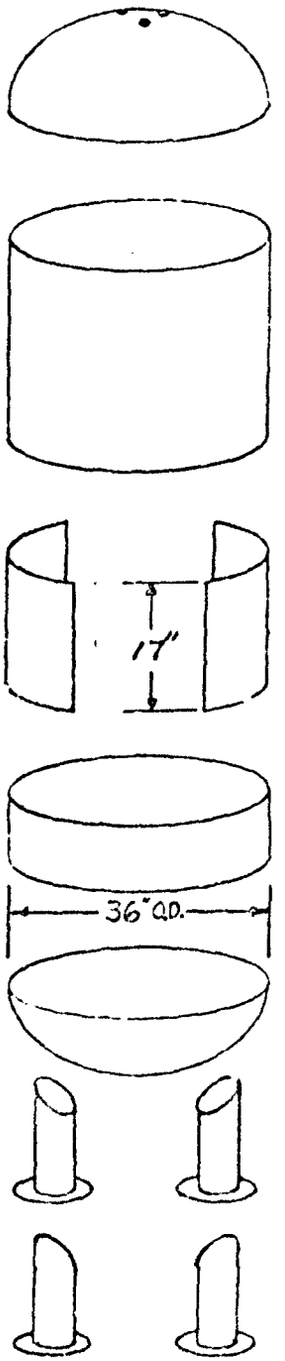

COMPLETE 3/1 HEMI-HEAD (HEAD IS NOT MODELED SINCE IT IS STRONGER THAN CYLINDER.

UPPER CYLINDER UNDER RADIAL PRESSURE BUT WITHOUT AXIAL TENSION AND WITHOUT ADDITIONAL RADIAL FORCES OF SIDE BEAMS.

SIDE BEAMS WITH CLAMPED ENDS AND RADIAL PRESSURE. NO TENSILE LOADING.

LOWER CYLINDER (SAME LOADING AS UPPER.)

LOWER 3/1 HEMI-HEAD (SAME LOADING AS UPPER.)

SUPPORT LEGS.

FIGURE 1

HOW CONTAINMENT IS MODELED IN OUR ANALYSIS

FIGURE 2. CONTAINMENT VESSEL IN PLACE BESIDE AN INDUCTOR IN CEM-UT LABORATORY.

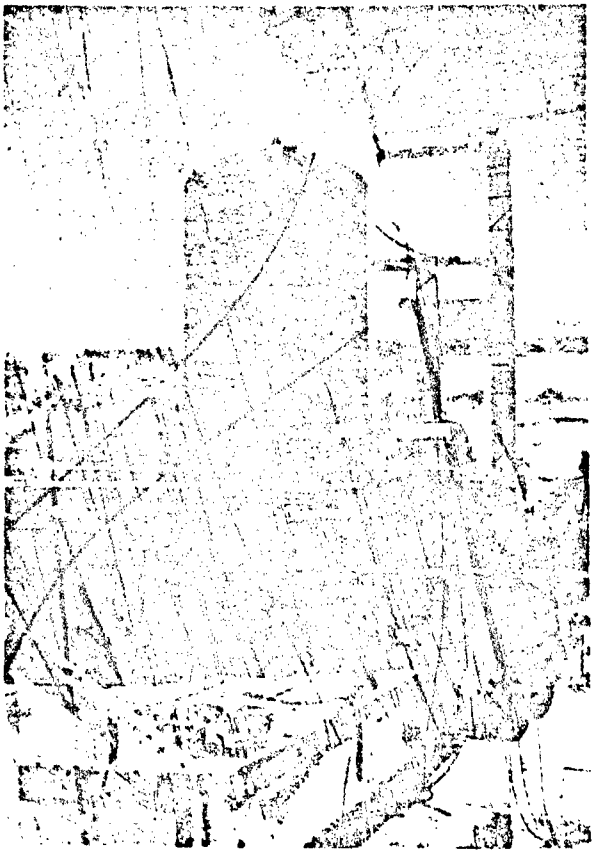

FIGURE 3. CLOSEUP OF CONTAINMENT AND BUSBARS AT TEST SITE.

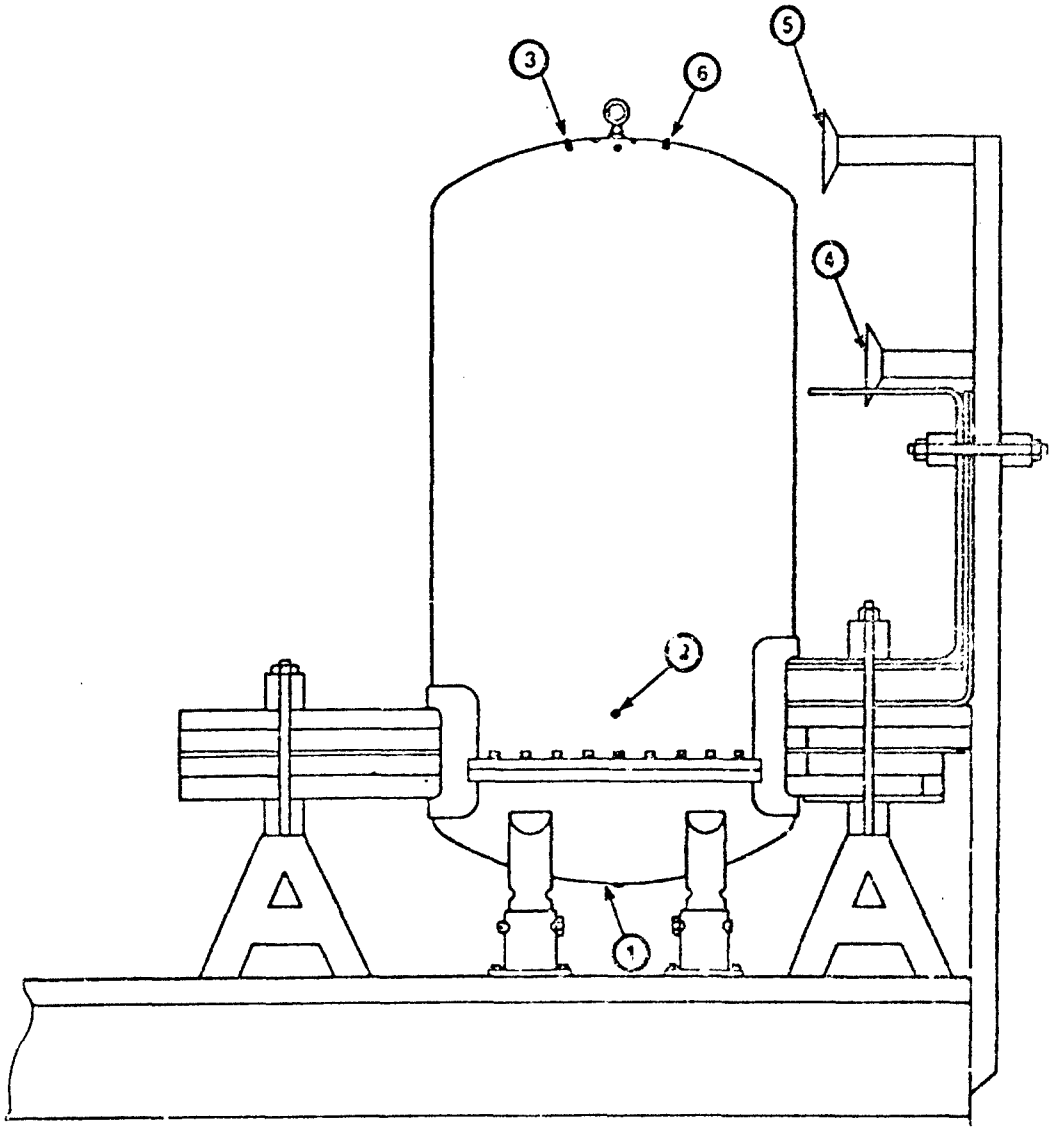

FIGURE 4

TEST SETUP SHOWING PRESSURE TRANSDUCER LOCATIONS.

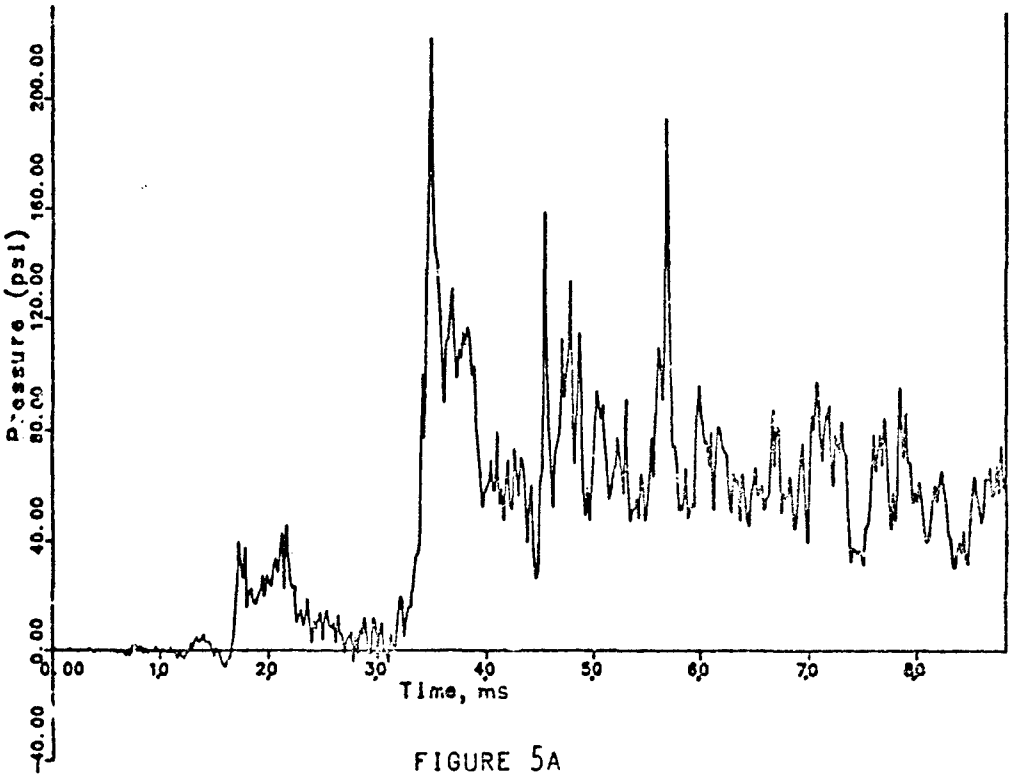

FIGURE 5A

EXPLOSION CONTAINMENT VESSEL, TEST NO. 1
BOTTOM PRESSURE TRANSDUCER

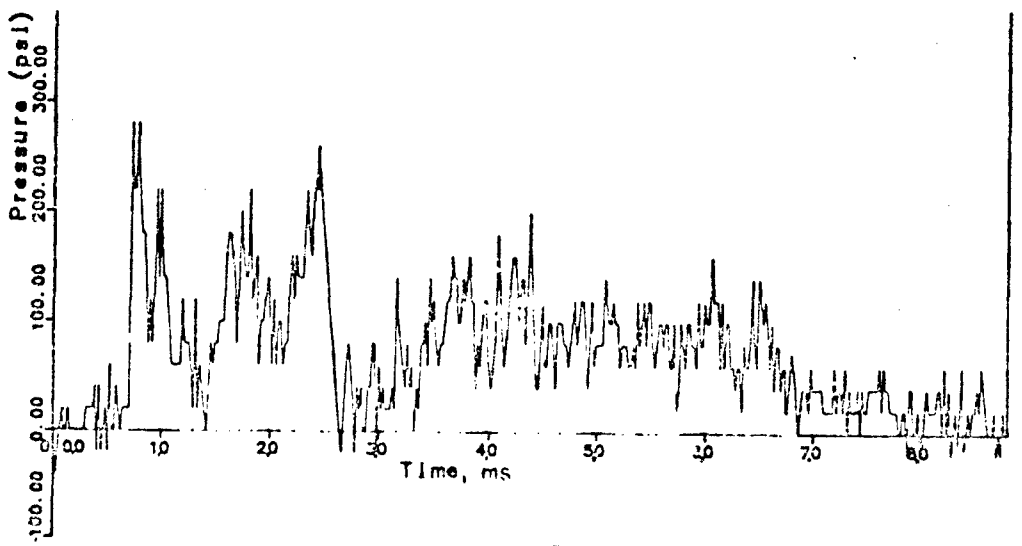

FIGURE 5B

EXPLOSION CONTAINMENT VESSEL, TEST NO. 2
BOTTOM PRESSURE TRANSDUCER

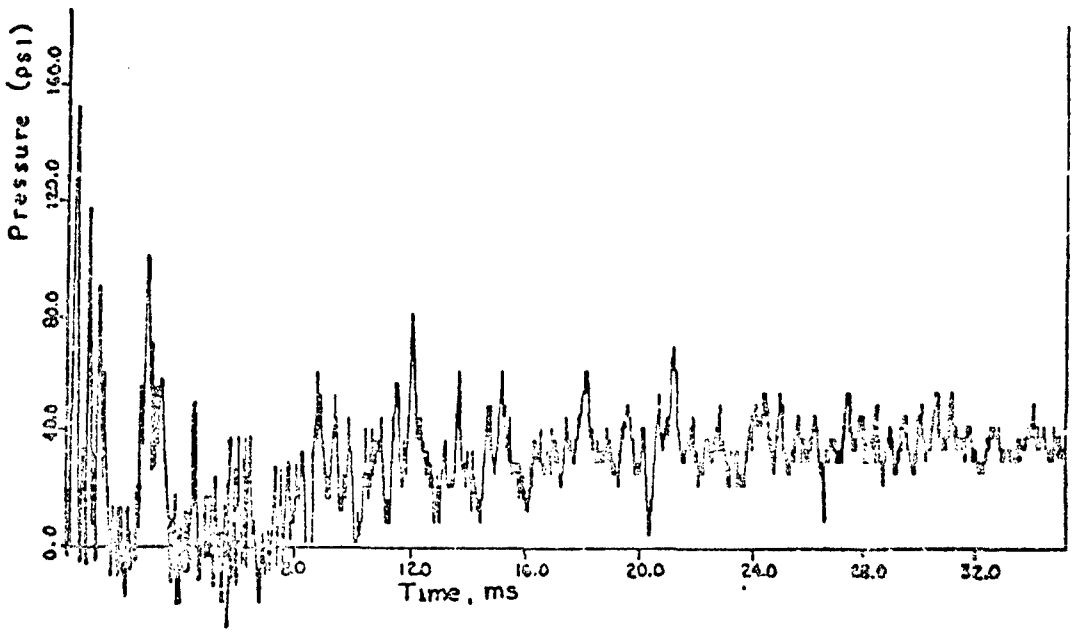

FIGURE 6A

EXPLOSION CONTAINMENT VESSEL, TEST NO. 1
SWITCH HEIGHT PRESSURE TRANSDUCER

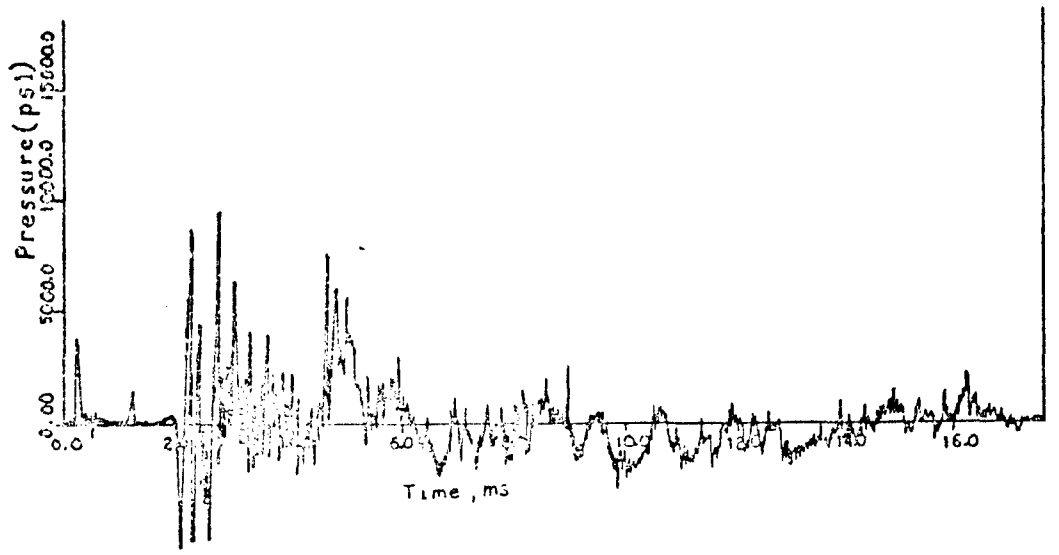

FIGURE 6B

EXPLOSION CONTAINMENT VESSEL, TEST NO. 2
SWITCH HEIGHT PRESSURE TRANSDUCER

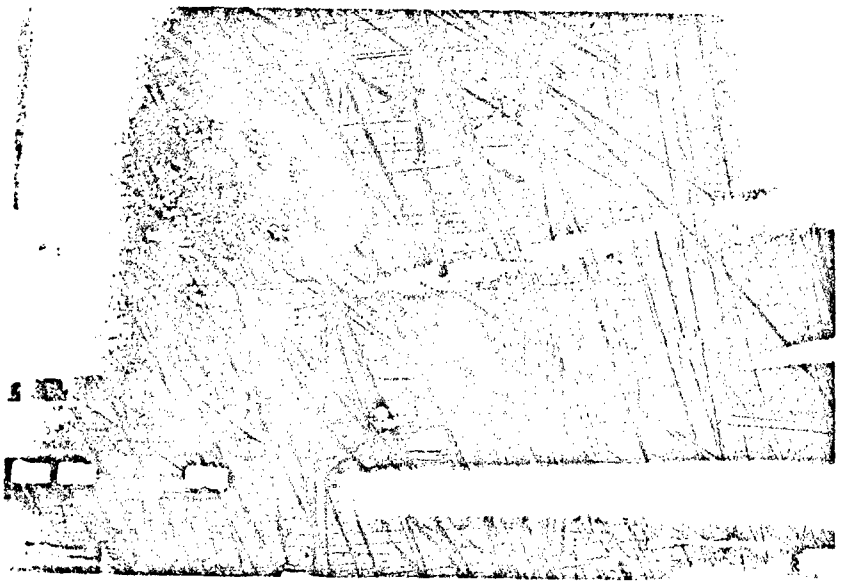

FIGURE 7. DAMAGE TO NYLON GASKET AND DISPLACEMENT OF PHENOLIC INSULATOR FROM SHOT # 1.

FIGURE 8. EXTERNAL VIEW OF DAMAGE FROM SHOT # 2.

FIGURE 9. INTERNAL VIEW OF DAMAGE TO BUSBAR SYSTEM AFTER SHOT #2

Paper Distributed at the:

Twenty-Third DoD Explosives Safety Seminar
Atlanta, Georgia

LITHIUM BATTERY FACILITY BLAST DESIGN ANALYSIS

by

C. James Dahn
Safety Consulting Engineers, Inc.
Rosemont, Illinois 60018

ABSTRACT

This paper describes the preliminary hazards analysis, blast structural analysis and design criteria for the Naval Weapons Support Center (NSWC), in Crane, Indiana

Lithium battery testing, at the Crane Complex, is conducted at a remote outdoor facility. Their analysis showed that this facility is inadequate because the gases liberated during a violent lithium battery explosion are extremely noxious, which results in environmental problems. Also, explosion overpressure and fragments present significant personal and facility hazards. Finally, testing out-of-doors causes testing to be dependent upon proper weather conditions. These factors all significantly impact both the quality and quantity of tests that can be conducted. For all of these reasons, a new in-door, self-contained test facility that can withstand an explosive blast has been designed.

INTRODUCTION

As a result of state-of-art advances in storage battery technology, lithium-based batteries are now used etensively by the U. S. Navy. Extensive testing is required on these newly designed batteries to demonstrate their performance and safety under extreme environments. Also presently designed batteries require extensive quality control and reliability tests to demonstrate their capability for military applications.

The Naval Weapons Support Center (NSWC), Crane, Indiana facility was designated as the testing center for Navy lithium batteries. Over the last eight years, extensive testing of numerous designed batteries was conducted in the following areas.

1. Abusive testing for safety and performance
   - To extreme electrical loads and short circuit testing.
   - To extreme thermal and mechanical loads.
2. Quality control and reliability testing on existing battery designs.
   - Vibration and shock (jolt, jumble, roll)
   - Heat, cold and temperature cycling
   - Routine load performance

Hazardous battery testing was conducted outdoors at a remote location in an open steel bunker which was not adequate to perform repeated tests where explosions could occur. See Figures 1 and 2. The gases liberated during a violent lithium battery explosion are extremely toxic which presented environmental problems. Also, explosion overpressure and fragments from these explosions (during abusive testing) presented significant person-

Figure 1. Present outdoor lithium battery test facility.

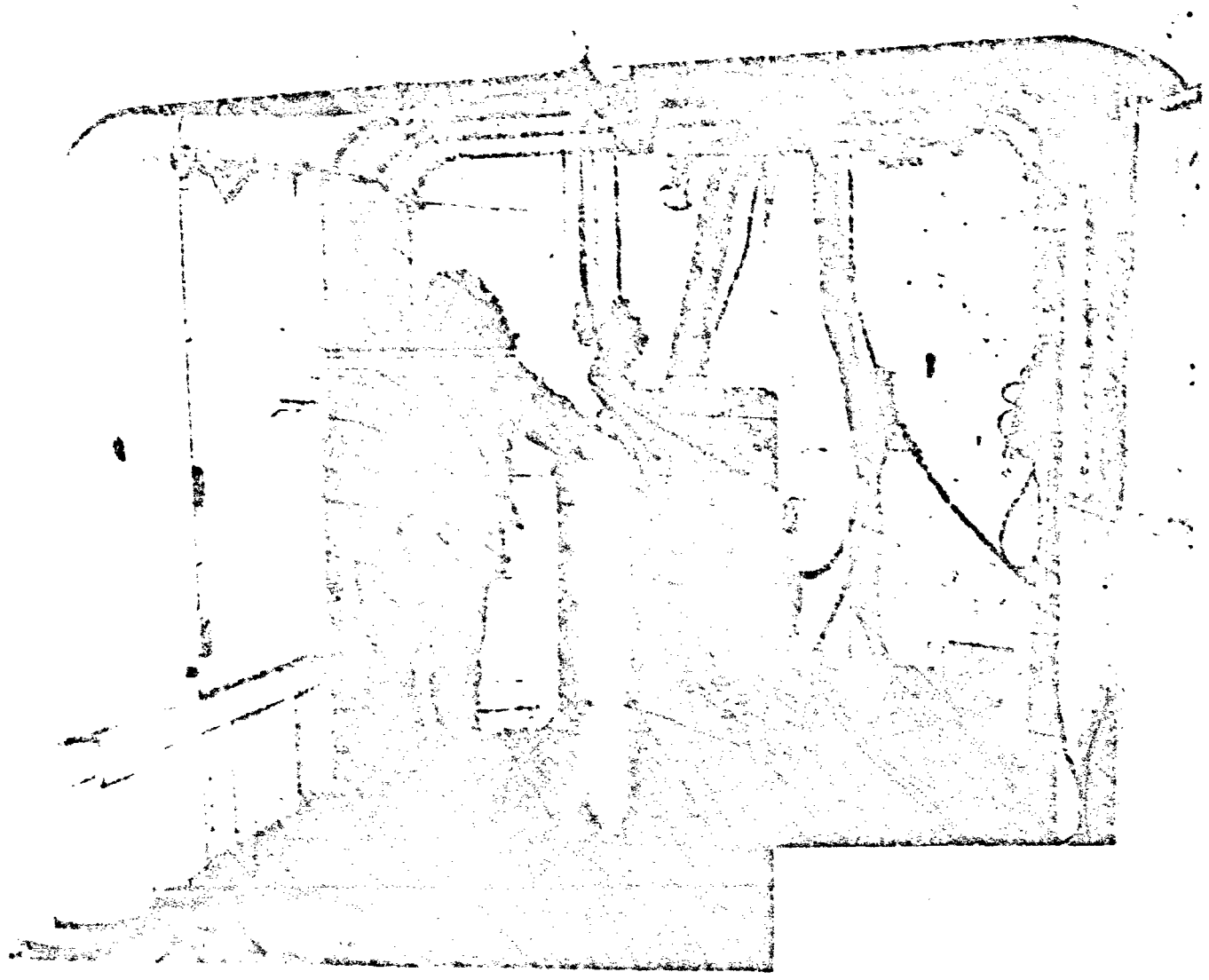

2244

Figure 2. Present typical lithium battery test cell.

nel and facility hazards.

At present, the engineering management staff is located 12 miles away from the test site. The distance from computer data acquisition equipment and the test cells was limited to 100 feet to assure reliability of data acquisition.

In 1987, Northern Division, Naval Facilities Engineering Command, located in Philadelphia, contracted to Lester B. Knight and Associates to design a new self-contained test facility to handle present and future projected lithium battery testing and analysis. This facility would contain all management, engineering, and test support personnel; all equipment and test cells on the one site.

Safety Consulting Engineers, Inc. was contracted by Lester B. Knight to conduct a preliminary hazards analysis of the designed facility prior to and after 35% design completion. In addition, Safety Consulting Engineers, Inc. conducted blast structural analysis and established a design criteria to withstand battery explosions for the test cells. Battery test operations analysis showed that at least 10 test cells should be designed for battery testing. Each of these cells should be designed to completely contain a maximum incident battery explosion and afterward release toxic gases at controlled rates into appropriate gas scrubbers. Additionally two cells should be designed to withstand a worse case, largest battery explosion.

The procedures, methods and resulting design criteria for the test cells and secondary walls to withstand lithium battery explosions are reported in this paper.

HAZARDOUS CONSIDERATIONS

Evaluation

Various hazardous considerations associated with lithium batteries were integrated into the conceptual and detailed planning of the proposed facility.

A runaway reaction of the lithium and the electrolyte can occur under easily predictable conditions (e.g., externally applied heat, shorting, charging, and similar abusive environments), or under unpredictable conditions such as internal failures of a defective or peculiarly damaged cell. Nearly all runaway reactions result only when the lithium anode becomes heated to, or near, its melting point of about 180°C. The possible consequences of such a reaction can be one, or a combination of the following:

a. Slow release of minimal, moderate, or large quantities of highly corrosive and noxious smoke and gases.

b. Rapid venting of the smoke and gases, with potential of pressure build-up if in restricted enclosures.

c. An explosive pressure spike or shock wave, and possible flying projectiles of battery cell parts, and/or associated fixtures.

When batteries are tested abusively, the likelihood of a destructive reaction increases significantly. The design of an enclosed test facility must, therefore, incorporate provisions for accepting both the maximum potential explosive and corrosive vapor release conditions without significant downtime for cleanup after an event.

Unfortunately, the safety provisions normally selected to

control these types of hazards tend to become mutually incompatible when combining them for the same facility. For example, blowout panels are required by code for rooms where explosives are handled to vent blast pressure into a safe area and to minimize blast effects on personnel and sensitive equipment. However the test cells and work rooms, in which noxious gases can be generated, must be completely sealed to prevent noxious gases from entering personnel occupied areas. All noxious gases must exit through suitable gas cleaning devices before being discharged to the environment. Normally such environmental protection devices are not shock resistant.

An initial survey of the lithium battery industry revealed that some facilities have been built to handle moderate-sized cell runaway reactions. These test facilities have generally incorporated both blast resistant and vapor scrubbing provisions.

Based upon an energy comparison, the lithium batteries have approximately 125% TNT weight equivalence. This value is really beyond the worse case battery explosion because in the battery, the chemical reaction is mitigated by internal configuration and reactant contact. Also based on battery explosions damages to date, TNT blast output is very low (10% TNT mass).

Based on Navy lithium battery explosion history, a corrections factor and a conversion factor were both applied to the total battery electrical capacity (watt-hour) to yield a TNT equivalence value. This also translated into a maximum of 60% TNT mass equivalent value of that determined by energy comparison to TNT.

Based on Norwegian Defense Research establishment studies, a 24 amp-hour lithium/SO_2 battery yielded a blast equivalent to 100 grams TNT. Actually, a true TNT equivalent may be much less than this when the impulse may be long and overpressure is low. The test cell blast containment capabilities were set based on this criteria and the maximum battery size expected in inventory permissible. Thus, for the two abusive cells, a 10 lb TNT equivalent was established and all other cells were sized to 5 lb TNT equivalents to accommodate more batteries with much less risk of explosion. Additional testing of worse case battery explosions could yield lower TNT equivalent data permitting testing of larger batteries in the test cells.

Planned activities for the new test facility at Crane include a new battery as the maximum size battery to be tested. This battery should only be tested in the 10lb TNT equivalent test cells because its maximum estimated TNT equivalence is approximately eight pounds.

From a blast standpoint, two of the hazardous test cells (15' x 20' x 10' high) are to be designed to withstand the equivalent detonation of ten pounds of T.N.T.

The rest of the hazardous test cells are to be designed to withstand the equivalent detonation of five pounds of TNT. One cell will be 24 feet high while the others will be 10 feet high. All the cells will be 15 feet x 20 feet.

Control of flying projectiles and overpressure can be accomplished through application of blast resistant construction techniques and through the separation of personnel and high value

items from potential exposure. The control of released corrosive/noxious vapors will be a more challenging problem.

Lithium-Sulfur Dioxide (Li/SO_2) batteries can vent Sulfur Dioxide gas. Lithium-Thionyl Chloride ($Li/SOCl_2$) batteries can vent Thionyl Chloride, which breaks down into SO_2, and HCL with LI_2O particles in the smoke.

The approximate volume of smoke and/or gases which could be generated from battery holding eight liters of electrolyte is felt to be in the order of 262 cubic feet.

A typical procedure for managing these types of vapors is to first pass the smoke through a particle separator to remove the particulate matter, and then pass the gases through a packed type scrubber using alkaline buffered water for removal of the gases.

DESIGN CONSIDERATIONS

Based on results of the Preliminary Hazards Analysis (Energy Trace and Barrier Analysis (ETBA), four test cells for abusive testing would be separated from the six cells for quality performance and reliability tests. See Figure 3. All cell heights would be lower than the room height for both areas. Also, the two high probability explosion cells (10 lb TNT) would be separated from the other two cells.

A second blast barricade would exist between the cell areas and the instrumentation and test setup area. Vapor barriers are required between this area and the personnel occupied areas. Thus, the wall and doors separating the cells from the test setup area are required to withstand blast pressures transmitted through a partially open door from a 10 lb TNT equivalent explo-

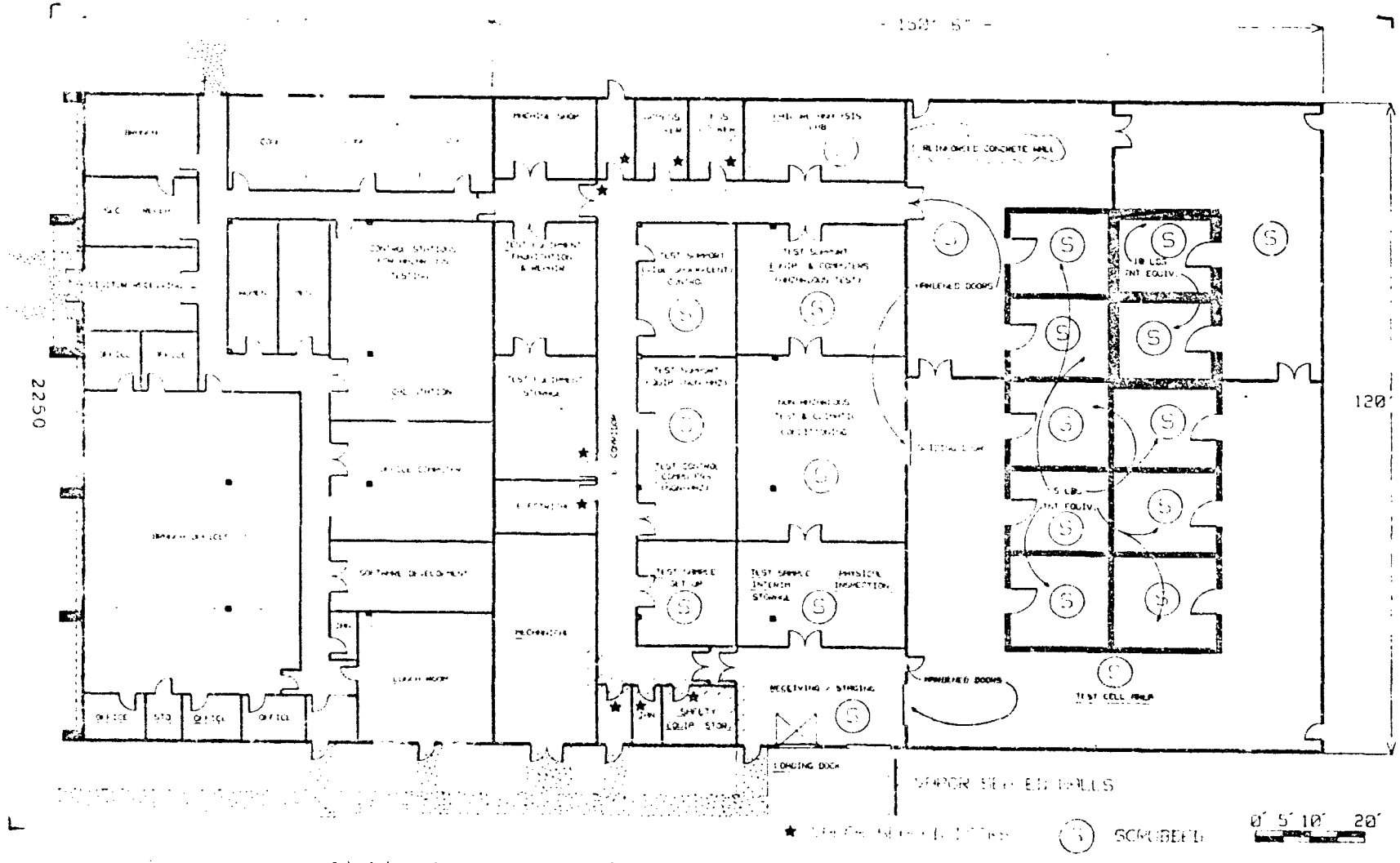

Figure 3. New lithium battery test facility after preliminary hazards analysis.

sion in a test cell with a door open. Also, the separating wall between the three quandrants of test cells would have to withstand comparable explosion pressure from a door accidentally left partly open.

All utilities (e.g., electrical, air, heat, cooling) will be routed into each cell such that blast loads and corrosive gases will not effect them.

Also, each cell will be gas sealed during testing. If an explosion should occur in the cell, all gases will be contained. After stabilization, blast protected vents will be activated, opened slowly to bleed off gas overpressure into a gas scrubbing system outside the building.

BLAST STRUCTURAL ANALYSIS

Test cell sizes and layout were defined based on usage, available area, and equipment expected to be used. Room height was standardized at 10 feet with the exception of one abusive test cell (10 lb TNT equivalent).

Blast structural analysis was conducted utilizing the SCE computer software, BLAST X, which utilizes general energy methods as defined in U. S. Corp of Engineers Report, "HNDM 1110.1-02 "Suppressing Shields". For each test cell the software evaluates contained, vented, and open air structures for structural integrity during and after blast loading. All walls were considered fixed to adjoining walls, floor or roof. Concrete construction with appropriate rebar was considered the most cost effective and utilitarian way to approach the blast containment. Weights of TNT mass equivalence are introduced for a given size

room and concrete thickness as rebar size is calculated to withstand the explosion.

A ductility ratio (maximum/elastic deflection) value of 1.3 was used to provide an additional safety factor in the cell design. Concrete compressive strength of 3000 psi and steel rebar tensile strength of 60,000 psi was utilized in the study. Concrete density of 150 lb/ft^3 was also used.

The blast analysis was conducted using the BLAST X program defined in flow sheet form in Figure 4. A typical blast load on the cell walls is illustrated in Figure 5.

RESULTS OF ANALYSIS

Blast analysis for the two abusive test cells (10 lb TNT equivalence) yielded concrete wall thickness of 24 inches with steel rebar ratios of 0.01. See Table 1 for analysis results on each test cell. The anticipated blast pressure on the nearest walls is 1000 psi. The low yield (5 lb TNT equivalent) test cells walls can be constructed of reinforced concrete 12 inches thick with a rebar ratio of 0.01. The maximum blast pressure on the nearest wall is expected to be 100 psi. Remotely operated blast covers for scrubber vents and hazardous liquid drains, which would be in the failsafe closed condition during testing, were to be designed to withstand the explosion while containing all explosion gases. A backup structure built around the test cells was also designed to withstand blast overpressures if a test cell door should open during an explosion. The walls or this structure were analyzed to require 12 inches of reinforced concrete to withstand the blast load.

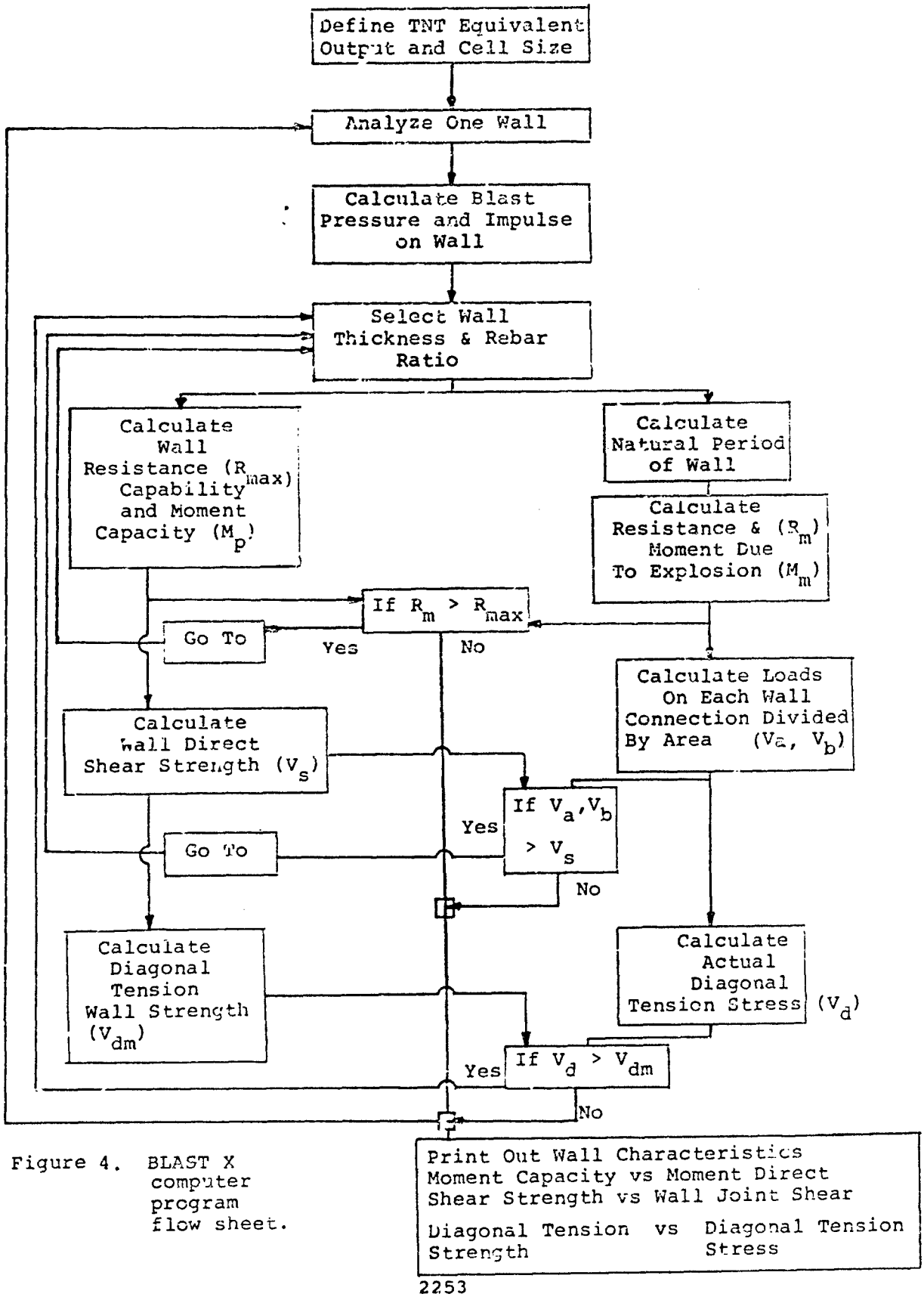

Figure 4. BLAST X computer program flow sheet.

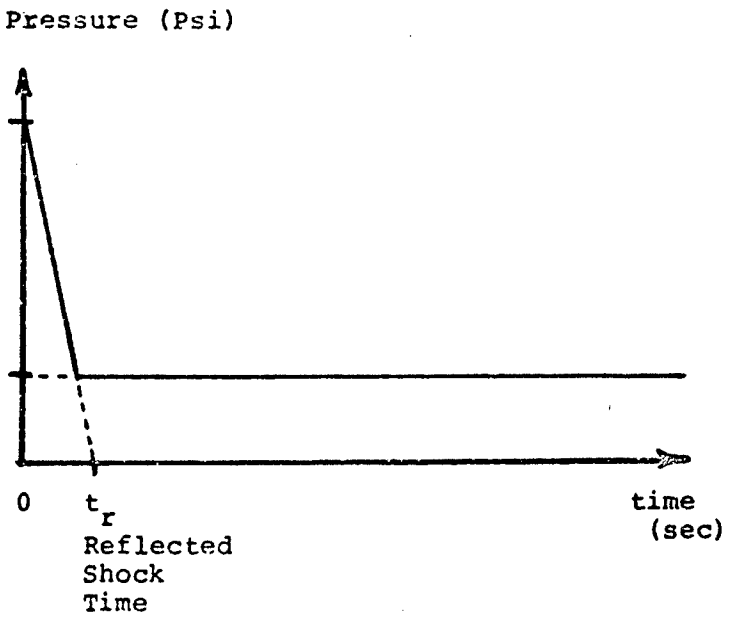

Equation to find maximum resistance for given load

$$\left[\frac{C_1 P_r / r_m}{\frac{T_n}{\pi t_1}\sqrt{2\mu - 1}}\right]^2 + \frac{C_2 P_r / r_m}{1 - \frac{1}{2\mu}} = 0$$

where

P_{sq} - Peak Gas Pressure (Psi)

P_r - Reflected Shock Pressure (Psi)

μ - Ratio of Max to Elastic Deflection

r_m - Max Member Resistance

C_1 - $\frac{P_r - P_{sq}}{P_r}$

C_2 - $\frac{P_{sq}}{P_r}$

T_n - Natural Period of Structure (sec)

T_1 - Reflected Shock Duration (sec)

*Gas Pressure in Contained Cell

Figure 5. Blast pressure load onto test cell wall.

The final design of the test cell and the outer structure is shown in Figure 6.

CONCLUSIONS AND RECOMMENDATIONS

The blast structural analysis study established safe concrete wall thickness and rebar ratio for each of the test cells in the design concept lithium battery test and evaluation facility. Steel rebar ratio had to be increased in the high yield test cells (10 lb TNT) to P = 0.017 to keep concrete wall thicknesses consistent in the test cells. Also, with wall thickness standardized, construct on costs will be reduced and cell interface integrity will be maintained. The walls were designed with excessive safety factor in the elastic range to reduce possible wall cracking which would breech toxic gas containment.

Further tests and analysis are recommended to determine more precise blast pressure profiles from lithium battery explosions. With this information, more exact explosive limits and number on size of lithium batteries permissible for each cell.

The blast analysis study was completed prior to the 35% design completion which greatly aided the facility acquisitions process because changes in test cell configurations were made to provide uniformity in facility construction techniques.

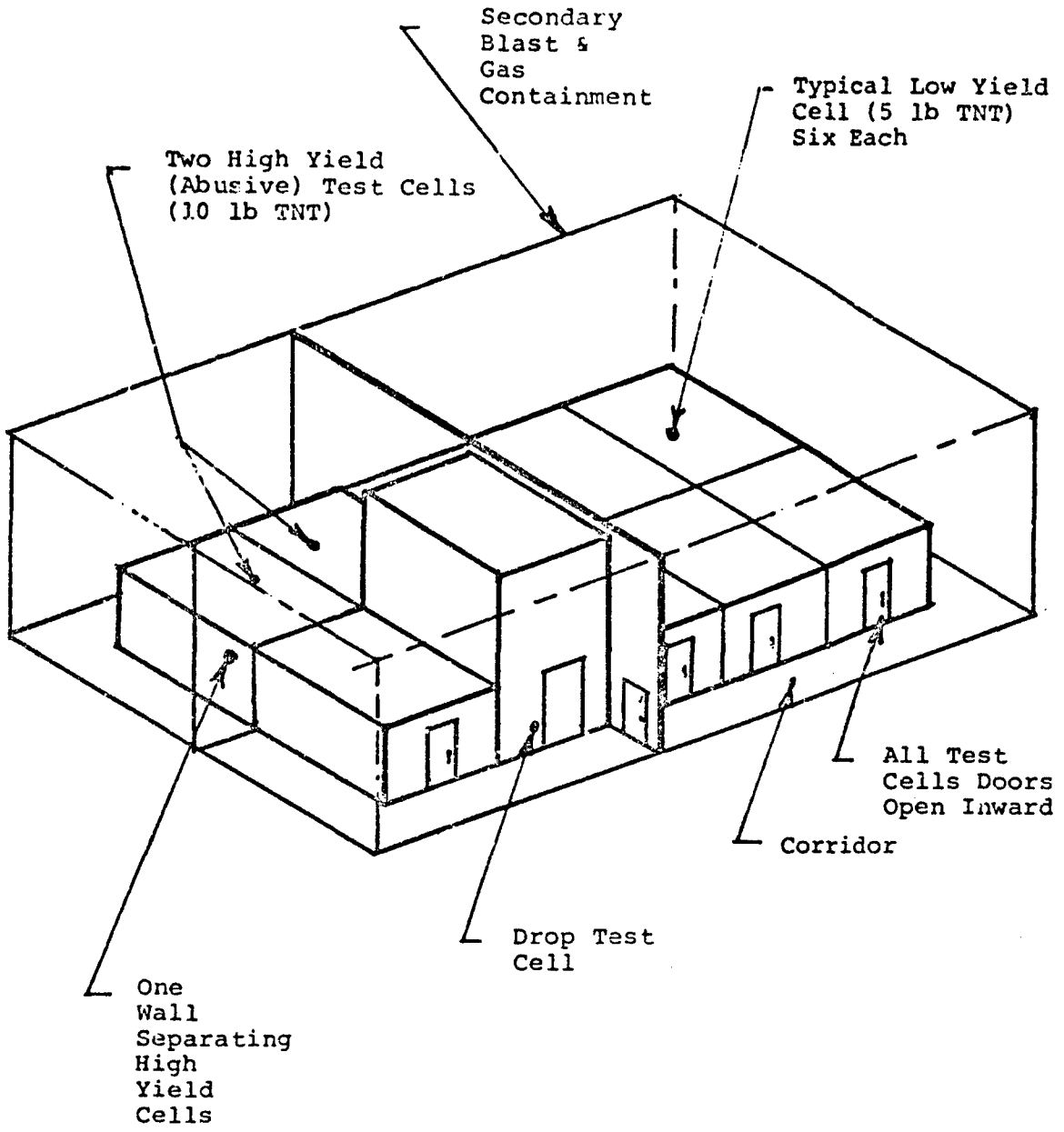

Figure 6. Test cell arrangement for blast containment.

TABLE 1

BLAST ANALYSIS RESULTS FOR LOW AND HIGH YIELD TEST CELLS

(15' X 20' SIZE)

TEST CELL	WALL THICKNESS (inch)	MOMENT CAPACITY OF WALL (in lb/in)	APPLIED MOMENT (in lb/in)	REACTION FORCES ON WALL JUNCTIONS SHORT WALL (lb)	LONG WALL (lb)
1. High Yield (10 lb TNT) 10 ft high	Roof (18")	171,460	144,550	446,830	947,700
	12" @P = 0.017	117,420	114,980	460,290	769,850
	Front wall (18")	171,460	102,040	296,540	890,430
	12" @P = 0.017	117,420	69,620	218,200	645,630
	Side wall (18")	171,460	74,170	253,120	510,900
	12" @ P = 0.017	117,420	52,170	192,860	384,540
2. Low Yield (5 lbs TNT)	Roof 12"	76,205	27,924	115,560	192,500
	Front 12"	76,205	62,130	265,420	374,900
	Side 12"	76,205	34,560	122.080	267,180
3. Low yield (5 lb TNT) 10 ft nigh 1 room	Roof 12"	76,205	64,060	261,690	436,600
	Front 12"	76,205	41,000	129,270	382,070
	Side	76,205	30,160	112,780	224,500

EXPLOSIVE COMPONENT TEST FACILITY

TEST FIRE CELLS

by
Stephen J. Rau
Monsanto Research Corporation
Mound, Miamisburg, Ohio

Prepared for the:
Twenty-third DOD Explosives Saftey Seminar
August 9-11, 1988

ABSTRACT

Monsanto Research Corporation (MRC) in the past year has brought to an operational state, the Explosive Component Test Facility (ECTF). The Explosive Component Test Facility is a Department of Energy (DOE) Facility located at the Mound Plant in Miamisburg, Ohio. The role of the ECTF is to functionally test explosive weapons components produced at Mound for quality assurance purposes as well as for component development purposes.

At the heart of the ECTF are three testing cells or chambers. The three test cells were conceived as cells located indoors with the capability to fully contain the effects of explosions of up to 10 pounds TNT equivalent weight. The ECTF also contains explosive preparation areas, extensive camera rooms for event photography, control rooms for firing, system control, and data retrieval; as well as administrative support areas. In all, the ECTF occupies over 30,000 square feet of space and is a huge advancement in capacity and capability for DOE in the area of testing and diagnostics.

The subject of this paper is the ECTF Test Cells, their design, fabrication, installation, and qualification testing. These efforts have taken place over a time span of five years and have culminated in proof testing in May of 1987.

1. Test Cell Design Criteria

Design criteria were laid out by Mound's operating department for the test cell design. The major criteria are presented with the reasoning for the criteria.

1. The test cell must contain the blast effects from a 10 pound TNT equivalent explosive device.

   Mound, at the time of the project inception, was performing tests in existing chambers of up to 1.5 pounds of TNT with the possibility of 3.0 pound tests in the future. A 10.0 pound limit was chosen as reasonable limit, with extra capability above future projected tests, and within project budget constraints and technical feasibilities.

2. Test Cell useful life must be 30 years or longer.

   Existing chambers at Mound were 30 years old and still being used daily; it was safe to assume that any new chambers may, in fact, be expected to last 30 years. From a practical design standpoint this criteria meant that stresses in the chambers must be totally within the elastic limit of the material.

3. Length of the chambers must be 20 feet long or greater to provide necessary photographic standoff.

4. A large manway for entrance and egress was necessary. Automation of the closing and latching functions was deemed necessary based on the past 30 years experience with heavy mandoors.

5. Multiple viewing windows were mandatory. Existing test cells had single viewports for one axis photography. The new chambers were conceived to have the capability for three axis photography with Rotating Mirror Cameras (RMC).

6. Provisions for up to 150 electrical signal cables entering each test cell must be accomplished with protection of the cables as well as some measure of simplicity and convenience of connections.

7. Multiple ports must be provided to allow heat transfer media to enter and leave the test cell. The heat transfer media is used to thermal condition test specimens prior to firing.

8. The test cell must be provided with a means of venting the detonation gases as well as providing for a high speed air purge. The high speed air purge would allow for relatively rapid re-entry to the chamber after a test.

9. Interior to the test cells, a smooth, stable, and flat working surface was necessary. Testing set-ups are large, complex, and alignment critical; so a sound work surface was to be provided.

10. The ability to extinguish a fire inside the test cells was deemed necessary. Occasionally, expensive equipment is located in the chamber with the explosive device in a barricaded manner. "After" fires could jeopardize this equipment if not quickly extinguished.

11. Illumination of the test cell interior in the secured or sealed up condition was desirable. Hand carrying lights in and out of the test cells was a nuisance under set-up conditions.

2. Test Cell Design

The design of the test cells was accomplished by a team of engineers and designers from Monsanto's Central Engineering Department working in conjunction with Mound engineers and Booker & Associates, the building Architect/Engineering firm. The design developed over a nine to twelve month period which included several interim reviews of work. It should be noted that prior to the start of definitive design, during the conceptual stage, an intensive study of blast and fragment loadings was conducted. The loadings study work was accomplished by Southwest Research Institute (SwRI) under Mound contract.

Basic test cell shell design was accomplished using a Monsanto, in-house computer program called BOSOR. BOSOR is a program that employs finite differences on the governing differential equations of thin shell theory. Transient analysis of the test cell and it's foundation were accomplished with the use of NASTRAN and the creation of a whole vessel model.

Shell geometry and thickness were arrived at using dynamic loading criteria. The basic geometry and thicknesses were then plugged into standard ASME pressure vessel equations and worked in reverse to establish a "Code" pressure rating. The ASME code pressure rating is essentially a static pressure rating and, in this case, the rating is an order of magnitude higher than operating quasi-static detonation loads. Predicted quasi-static loading was 40 psig, ASME code pressure for the test cells is 340 psig.

The most difficult design problem was the non-symmetric loading introduced by charge positions non-coincident with the vessel centerlines on two axes. The non-symmetric loading increased shell thicknesses and dictated a massive foundation to resist the net translational forces and overturning moments. Figure I depicts the vessel geometry and test cell loading scenarios. The test cell to

foundation interface was impossible using standard anchor bolt in concrete treatment. A large steel grillage was embedded in the concrete foundation mass to which the test cell saddle/skid could be directly bolted and welded. Figure II contains test cell basic specifications as a product of the design effort.

Test cell design loads were based on a 12 pound TNT equivalent charge which represents a 20 percent increase over actual working charge limit. Ground rules included imposing a minimum charge stand-off from chamber interior surfaces of three feet.

The calculated overall factor of safety of the design is 1.67 based on uniaxial yield strength of the material. The factor of safety includes the charge factor of safety and some contribution, due to damping of the vessel shell by the internal fragment liner. The dynamic yield strength of the material is not considered in the design or factor of safety calculations because that particular material property is not well known or published. Further conservatism is added to the design by not considering a dynamic material strength, a property which is believed to be considerably higher than published data for this material.

The physical size of the test cells was limited by transportation. On-site construction of the test cells was deemed undesirable from a quality and cost viewpoint. The 14 foot 6 inch diameter of the test cells is the absolute largest diameter vessel of this weight class transportable to Miamisburg, Ohio.

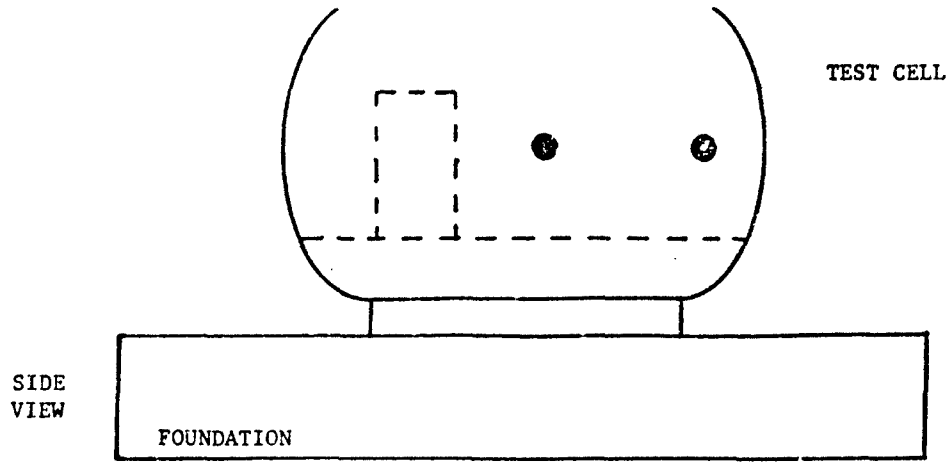

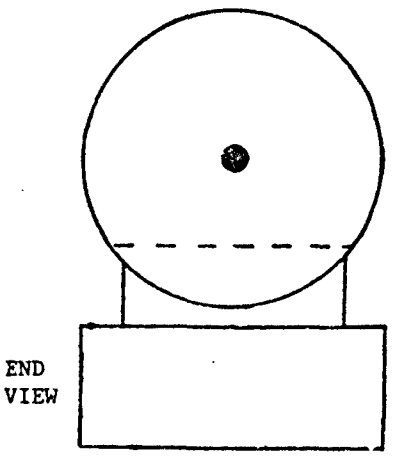

Black dots indicate charge locations for design and testing.

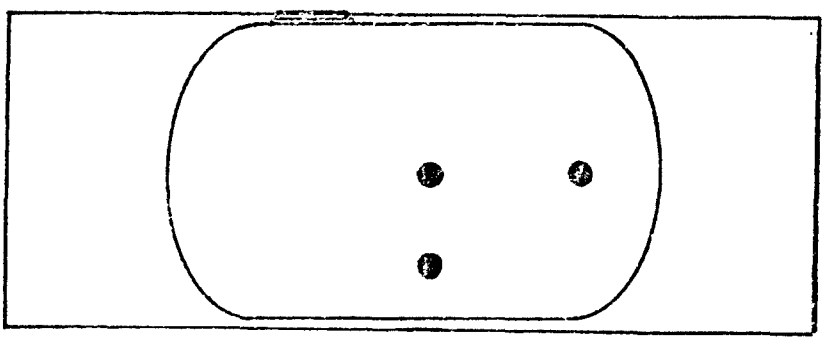

FIGURE I

TEST CELL GEOMETRY

Figure II

Test Cell Specifications

Basic Shape - Horizontal Cylinder with 2:1 Elliptical Heads

Wall Thickness - 1 3/4" Minimum with 5/8" liner.

Dimensions - Diameter, 14 feet, 6 inches
Length, 24 feet
Weight, 100 tons

Material - SA-516 Grade 70 Steel
70,000 psi ultimate, 38,000 psi yield

Viewing Ports - 9 per test cell, 5"w x 10" l x 6" t.

Mandoor - 3 feet, 6 inches x 7 feet

Floor - Poured Reinforced Concrete with 5/8" steel covering.

Foundation Specifications

Concrete Mass 40 feet long, 15 feet wide and 6 feet thick.

Embedded steel grillage to which test cell saddle/skid directly bolts.

The connection is achieved with 32 - 1 1/2" diameter A-490 bolts.

3. Test Cell Fabrication

Fabrication of the three test fire cells was accomplished by VMW Industries of Victoria, Texas, under contract to Monsanto Research Corporation. VMW was chosen as the fabricator because of their extensive experience in fabrication of diving compression and decompression chambers as well as submersible chambers. VMW also had extensive machining capabilities necessary to fabricate the mandoor latching mechanisms. The fabrication process was nine months in duration.

The test cells were fabricated in accordance with American Society of Mechanical Engineers (ASME) Pressure Vessel Code Section VIII, Division I. All of the quality assurance activities required by the ASME Code were performed, including: Material Certifications, Welding Certification, Radiographic Examination of all welds, and Hydrotesting. In addition to the quality assurance built into the ASME Code process, Monsanto arranged for an independent inspector to visit the fabrication plant and report on a weekly basis.

Elliptical head spinning and cylindrical shell rolling were subcontracted by VMW as they did not have the capability of forming the large diameters and thickness required. The spinning capability of head 14 feet 6 inches in diameter exists only two or three places in the United States. Forging of reinforcements were also subcontracted work. Availability of SA 516-70 steel in the specific plate sizes and thickness needed was a problem. The problem was overcome by sourcing the steel from domestic mills as well as European and Japanese mills.

All machining and welding was performed in-house by VMW. Stress relief heat treating was accomplished in a 30 feet x 20 feet x 16 feet furnace. The furnace was modified and made larger for this particular operation. Following the stress relief operation, each test cell was mounted on the bed of a very large milling machine to machine the sealing surface of the mandoor frame. The sealing surface measures 8 feet long and 4 feet wide and is machined to a flatness tolerance of 0.010 inches.

The entire fabrication process took place in the VMW shop except for the attachment of the mounting saddle/skid which would not fit the transportation size envelope.

Each test cell was hydrotested twice to 660 psig. This pressure represents vessel stresses at a level 90 percent of the material yield strength. The first pressurization satisfied the ASME Code requirement. The second pressurization was used to monitor acoustic emission and diagnose welding flaws possibly missed by X-Ray. Acoustic emission testing is used extensively by Monsanto to monitor in-service pressure vessels and in this case the testing was performed by Monsanto in the VMW shop. Acoustic emission testing located no critical flaws and resulted in several expensive attempts to locate predicted flaws. The hydrotesting was uneventful, except that on one test a large gasket failed, which resulted in a very wet fabrication shop.

Mandoor functional testing and painting were the final shop fabrication steps. The test cell project stressed the limit of the VMW shop in many respects, but the final product was of good quality and completed on schedule.

4. Test Cell Transportation and Installation

Transportation of the test cells was a complex process which was completely researched prior to the completion of design and definitized prior to the start of fabrication. The trip from the fabrication shop in Victoria, Texas, to Miamisburg, Ohio, was a five step process involving trucks, barges, and the railroad.

Step 1 of the transportation process used truck transportation for the relatively short 20 mile trip from the fabrication shop to the Victoria barge canal. Moves of this magnitude meet with fairly little regulation in south Texas, so Step 1 was very simple to accomplish.

Step 2 of the transportation process involved a three week barge trip along the intercoastal waterway, Mississippi River, and Ohio River; terminating in Cincinnati, Ohio. Barge transportation is slow, but size and weight limits of the load are seldom of any concern.

Step 3 of the transportation process involved a one mile truck trip from the Ohio River to a rail siding. This step, on the surface, appeared simple; but it was complicated by poor barge off-loading facilities, roads that required a bulldozer to make passible, and hilly terrain. Cincinnati is a fine place to load or unload coal, grain, or chemicals; but unloading large, cumbersome equipment like the test cells proved nearly impossible.

Step 4 of the transportation process required special lowboy rail cars and the assembly of a special train for the 50 mile journey to Miamisburg, Ohio. Soft rail bedding stopped the train within one mile of the start point. After the railbed was repaired, the remainder of the train trip was uneventful. Clearances were very tight and the train traveled at walking speeds near all potential overhead and side impeding structures.

Step 5 of the process required a truck to move the test cells several hundred yards from the Mound rail siding to the ECTF construction site.

Over the road transportation in the state of Ohio was deemed next to impossible due to local and state regulations and bond requirements. Overall, the transportation of the test cells was completely successful with no physical damage sustained to the test cells.

Test cell foundations were complete prior to the arrival of the test cells at the construction site. The attachment of the saddle/skids and actual mounting of the test cells on the foundations proceeded for the two weeks immediately following transportation. Further assembly and fitting of items, such as the large mandoors, was accomplished within one month of the arrival of the test cells on the plant site.

Construction of the ECTF building was scheduled for the 18 months subsequent to the test cell arrival on the construction site. Due to construction activities that were to occur in the upcoming 18 months, the test cells and mechanical parts were secured and weatherproofed as best as possible. Near the end of the ECTF construction, work began anew to bring the test cells to an operational state.

Numerous photographs of the test cells during transportation, installation, and upon completion are included as an Appendix to this paper. Each photo is captioned to briefly explain the content.

5. Test Cell Qualification Testing

Test cell qualification testing is worthy of a very long paper as a subject by itself. The testing objective, methods, and results will be highlighted in this paper with more thorough treatment of the subject matter saved for a future work.

The Qualification Testing Program was undertaken to prove each test cell met or exceeded design performance levels as well as provided operating personnel with a very high level of confidence about operating the new facilities. Additionally, the Qualification Testing Program would provide information about contained detonations of charge sizes nearly ten times larger than previously performed at Mound.

Mound chose to contract with an independent agency to perform actual qualification testing because in-house expertise was not able to be diverted from normal work for the dedicated intensive testing effort. It was also hoped that an independent source would be able to accomplish the work in a shorter period of time due to factors such as reduced learning curve, dedicated work force, and greater experience. Southwest Research Corporation (SwRI) was chosen to perform the testing, and work; and in conjunction with Monsanto, to plan the test program. Data presentation was a SwRI responsibility. Data analysis, for the most part, was to remain Monsanto's task.

A test series of 21 shots was planned, 7 in each test cell, with charge sizes varying from 2.5 pound TNT equivalent to 12.5 pounds. The 2.5 pound shots were designed as shakedown exercises and the 12.5 pound shots represented the 25 percent overtests as required. Charge locations were consistent with design scenarios; that is, center, side, and end located in each test cell. Charge sizes and locations are listed below.

Charge Size	Location
2.5 lb.	center
5.0 lb.	center
7.5 lb.	end
10.0 lb.	center, end, side
12.5 lb.	center

Military explosive C-4 was used to mold the spherical charges. Charge preparation was performed by SwRI personnel at Mound prior to each test shot. Initiation of the charge was achieved by an exploding bridgewire type detonator with booster charge.

The information to be collected from each test shot was extensive and is listed in Figure III with a brief reason for the interest in the particular parameter.

Figure III

Testing Data of Interest

Parameter	Transducer	No	Interest
Blast Pressure	Blast Pressure Transducer	3	Verify charge output and reflections.
Test Cell Motion	Accelerometer	2	Verify overall displacement and rocking motion.
Foundation Motion	Accelerometer	3	" "
Quasi Static Pressure	Pressure Transducer	1	Verify gas pressure and venting time.
Surge Tank Pressure	Pressure Transducer	1	Verify expanded gas pressure and venting times.
System Temperatures	Thermocouples	3	Predict material life based on temperature effects.
Sound Pressure	Microphone	2	Investigate noise hazard.
Ground Motion	Seismometer	2	Access undesirable effects of ground shock.
Strain	Strain Gauges	6	Monitor vessel stress/ strain.

Peak value data is presented in Figure IV corresponding with a 12.5 pound TNT equivalent detonation located at a position in the center of a test cell. Acceleration data is not reported in the table. Actual plots of blast pressure traces are included in the Appendix for added detail.

Charge outputs, in general, agreed well with predicted charge outputs from standard air blast curves. Peak blast pressures as well as specific impulses were within 10 percent of predicted values. Measurement of peak blast pressures at standoff distances less than 4 feet (scaled $Z<2.0$) yielded data with a large amount of scatter and in some cases damaged the transducer.

Pressure wave reflection and resulting amplification effects were much larger than expected. Pressures due to reflections of the initial blast wave were, in some cases, amplified by as much as 4 times over the initial incident pulse. The reflection amplification phenomena was present with side and end mounted transducers.

Quasi-static pressure within the test cell, as measured, was perfectly consistent with predicted values.

Test cell shell response as measured by the numerous strain gauges was well within design constraints. The maximum stress level was attained in the knuckle region of the elliptical head, associated with a 10 pound detonation, end located. The Von Mises stress was determined to be 21,000 psi at this geometric discontinuity. The primary frequency of vessel response was found to be in the range of 350 hertz.

Temperatures recorded during the testing will have no detrimental effects on materials within the test cells or its exhaust system.

The peak sound level in a manned area was 127 dB, which poses no operational restrictions on ECTF operating personnel.

Velocities imparted to the ECTF structure were measured as high as 1.0 inches/second. These velocities, while noticeable, do not threaten the structure, occupants, or equipment. Velocities as high as 5.0 inches/second were recorded associated with the isolated test cell foundations.

Test cell foundation maximum horizontal displacement was found to be no greater than 0.030 inches, which is about half the predicted value.

Data and results reported in this paper, on the qualification testing, are very brief. Volumes of data and analysis exist on the subject which will prove very valuable in future containment vessel design.

FIGURE IV

TEST DATE: 05/13/87 TEST NUMBER: 10 Cell No. 2
TNT EQUIV. CHARGE WT.: 12.5 CHARGE LOCATION: A - Cell Ctr.

SEISMIC/ACOUSTIC:

Peak Sound Pressure Level, dB	119
Peak Vertical Velocity, in/s	0.92
Peak Radial Velocity, in/s	0.29
Peak Transverse Velocity, in/s	0.08
Real-Peak, Vector Sum Velocity, in/s	0.96

BLAST PRESSURE:

Sensor Location	Floor Mount Under Charge
Peak Pressure, psi	7460 @ 4 ft. standoff
Sensor Location	Window Mount, Loc 6, End
Peak Pressure, psi	405 @ 12 ft. standoff
Sensor Location	Window Mount, Loc 7, Side
Peak Pressure, psi	1063 @ 7 ft. standoff

QUASI-STATIC PRESSURE:

Sensor Location	Chamber
Peak Pressure, psi	41.8
Sensor Location	Surge Tank (1 of 3 segments open)
Peak Pressure, psi	3.69

STRAIN:

Sensor Location	Loc 21, Head, Vert.
Peak Strain, micro-in/in	440
Sensor Location	Loc 22, Head, Horiz.
Peak Strain, micro-in/in	432
Sensor Location	Loc 23, Top Ctr., Circum.
Peak Strain, micro-in/in	538
Sensor Location	Loc 24, Top Ctr., Long.
Peak Strain, micro-in/in	233
Sensor Location	Loc 26, Top End, Long.
Peak Strain, micro-in/in	379
Sensor Location	Loc 27, Side Ctr., Circum.
Peak Strain, micro-in/in	341

TEMPERATURE:

Sensor Location	Chamber
Peak Temperature, deg F	212
Sensor Location	Exhaust Pipe
Peak Temperature, deg F	523
Sensor Location	Surge Tank
Peak Temperature, deg F	61.0

Conclusion

This paper serves the purpose of an overview of a five year project. Many papers, or possibly a book, could be compiled on the subject matter. Monsanto considers the ECTF and the Test Cells an unqualified success. It is hoped that this paper and other yet undisclosed information on the subject can be of use to others in the DOD, DOE, and Explosives Technology Community.

Acknowledgments

The success of this project is the combined effort of many contributors whom the author would like to acknowledge:

E. E. Morgenegg, M. W. Ringer, and A. H. Karabininis of the Monsanto Company, St. Louis, Mo. were the principle Design Engineers.

T. C. Wuennenberg of Booker Associates, St. Louis, Mo. was the ECTF Principal Structural Design Engineer.

Southwest Research Institute, San Antonio, Texas, contributed to the initial feasibility study and, finally, to the Qualification Testing Program.

R. E. White and numerous associates performed excellent work on the project.

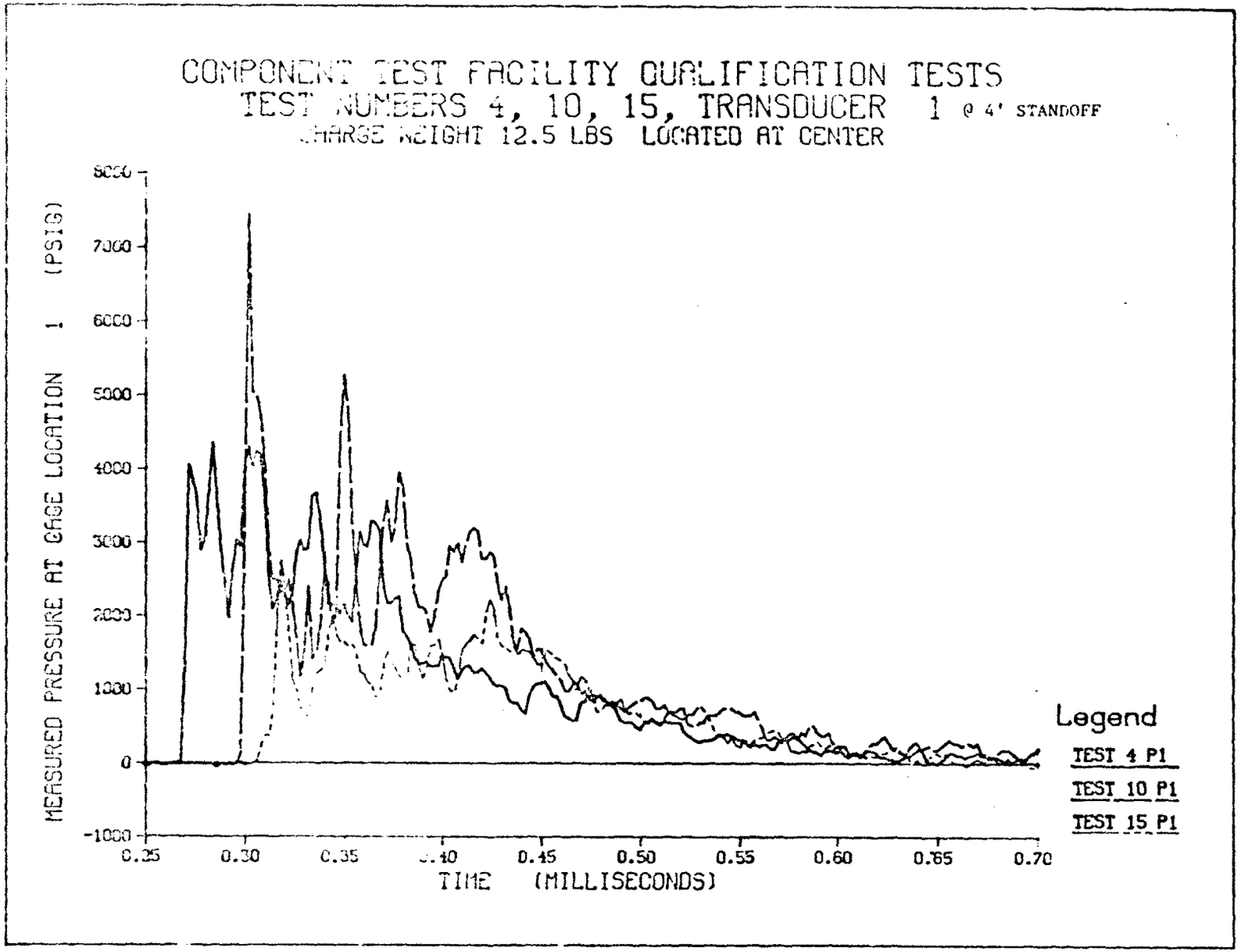

FIGURE 1
2273

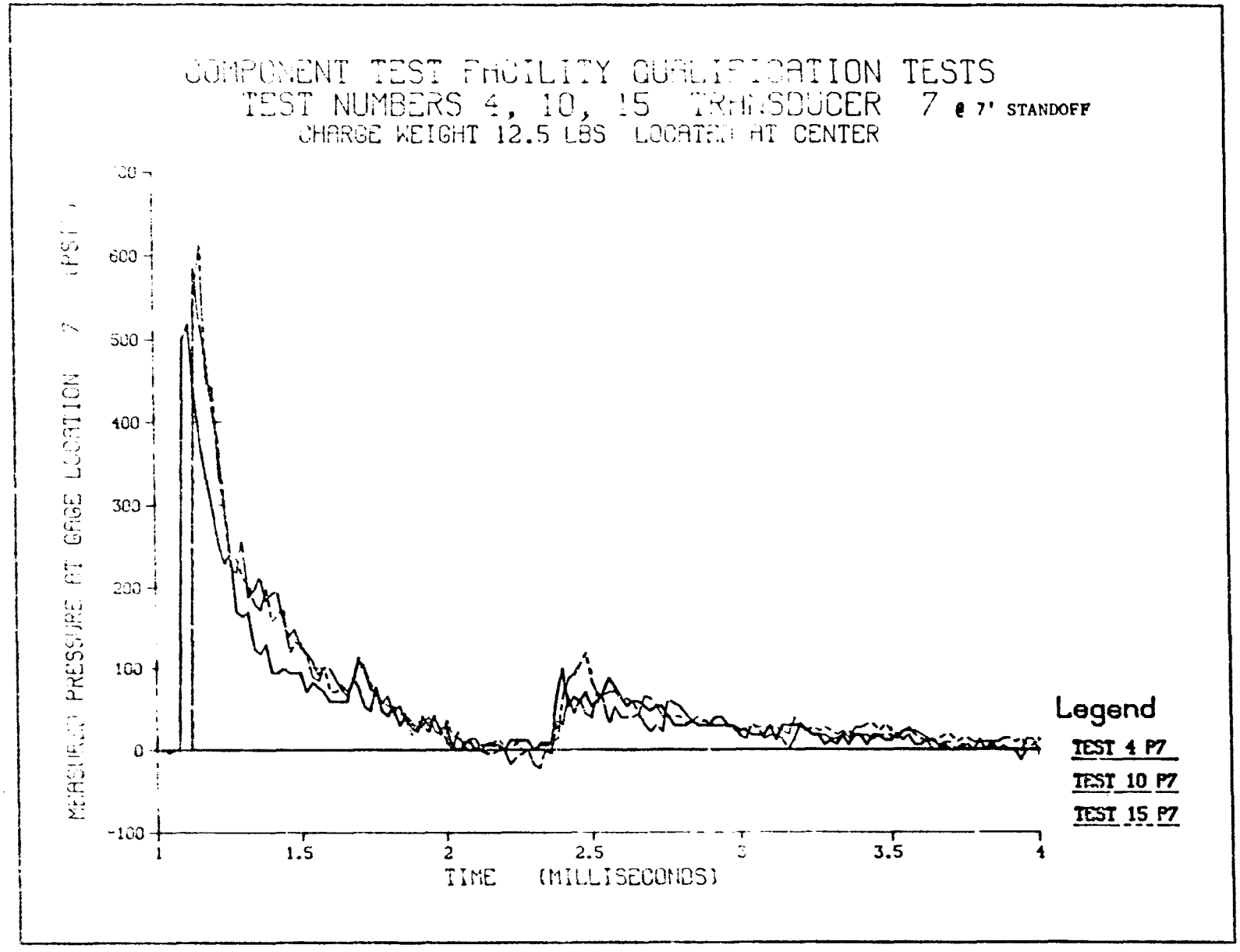
COMPONENT TEST FACILITY QUALIFICATION TESTS
TEST NUMBERS 4, 10, 15 TRANSDUCER 7 @ 7' STANDOFF
CHARGE WEIGHT 12.5 LBS LOCATED AT CENTER
MEASURED PRESSURE AT GAGE LOCATION 7 (PSI)
600
500
400
300
200
100
0
-100
1
1.5
2
2.5
3
3.5
4
TIME (MILLISECONDS)
Legend
TEST 4 P7
TEST 10 P7
TEST 15 P7

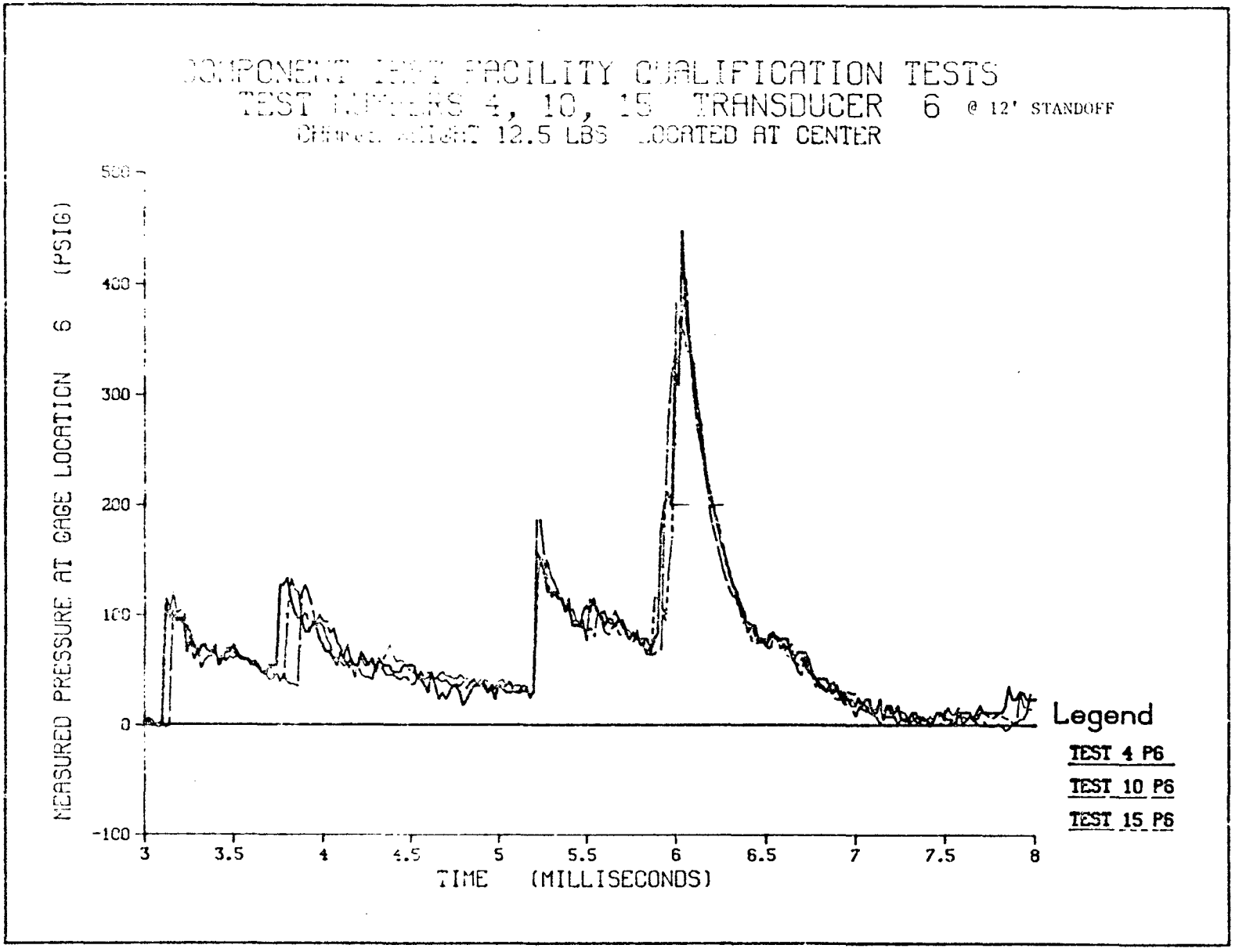

FIGURE 3
2275

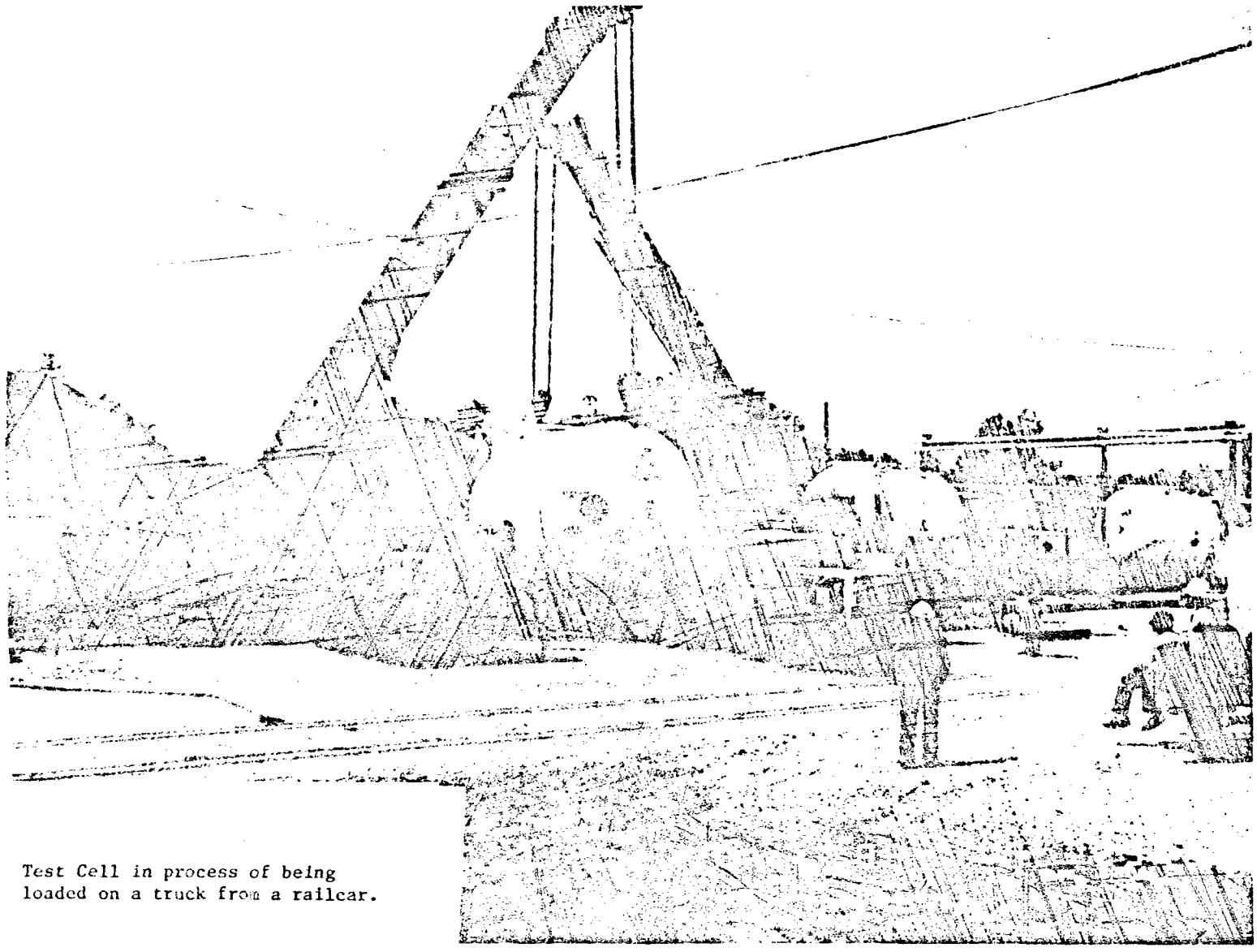

2276

Test Cell in process of being loaded on a truck from a railcar.

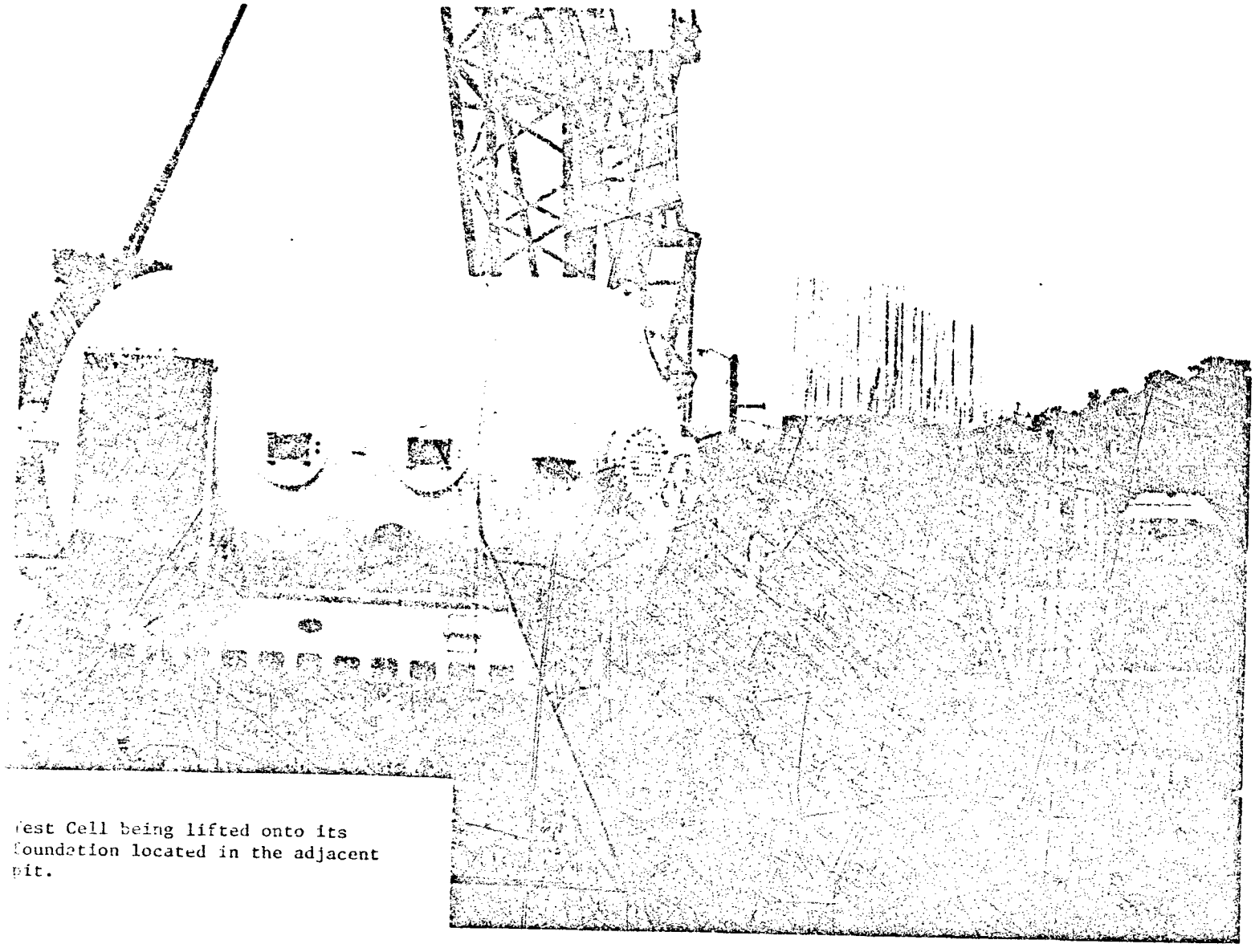

Test Cell being lifted onto its foundation located in the adjacent pit.

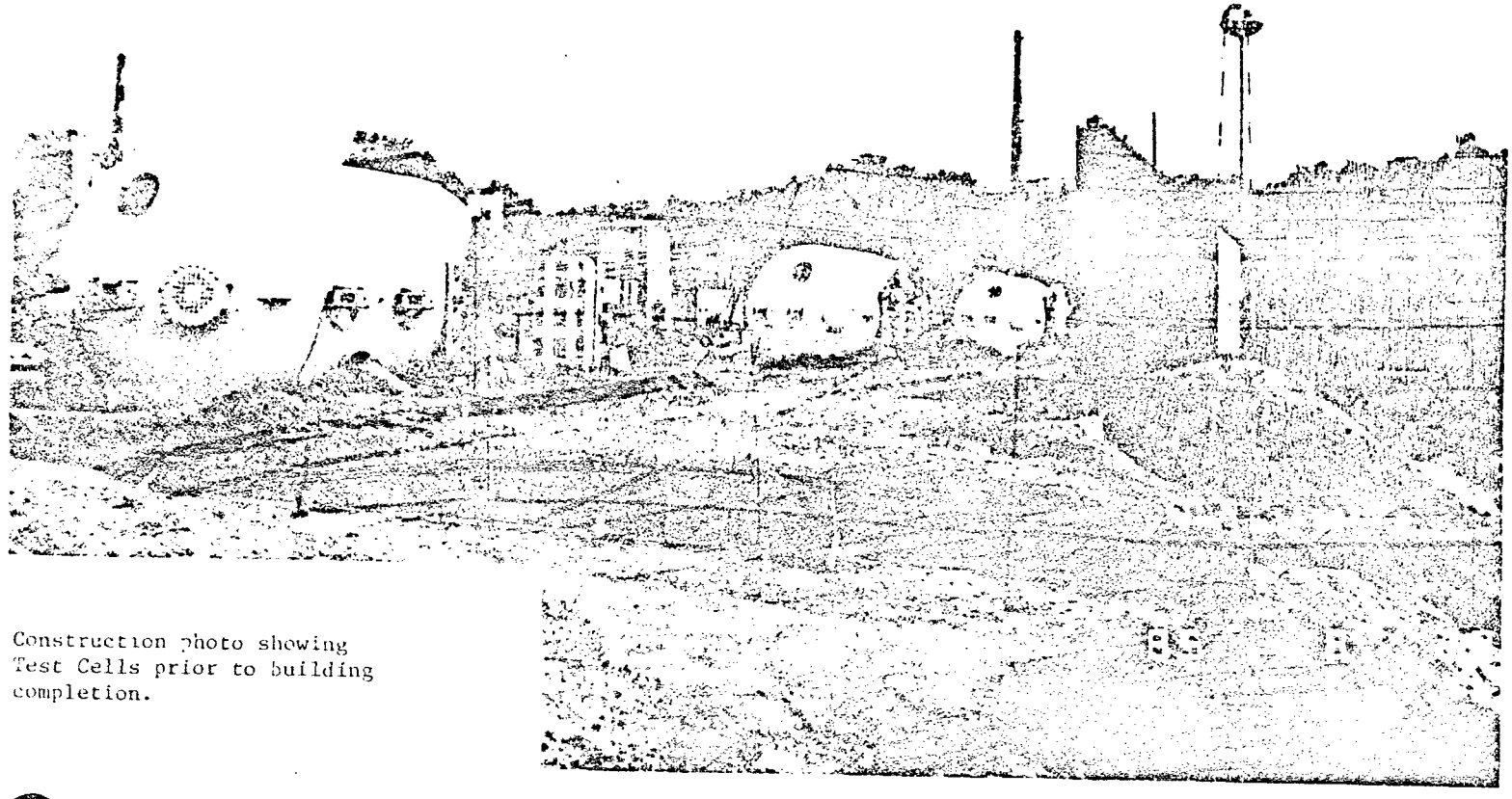

Construction photo showing Test Cells prior to building completion.

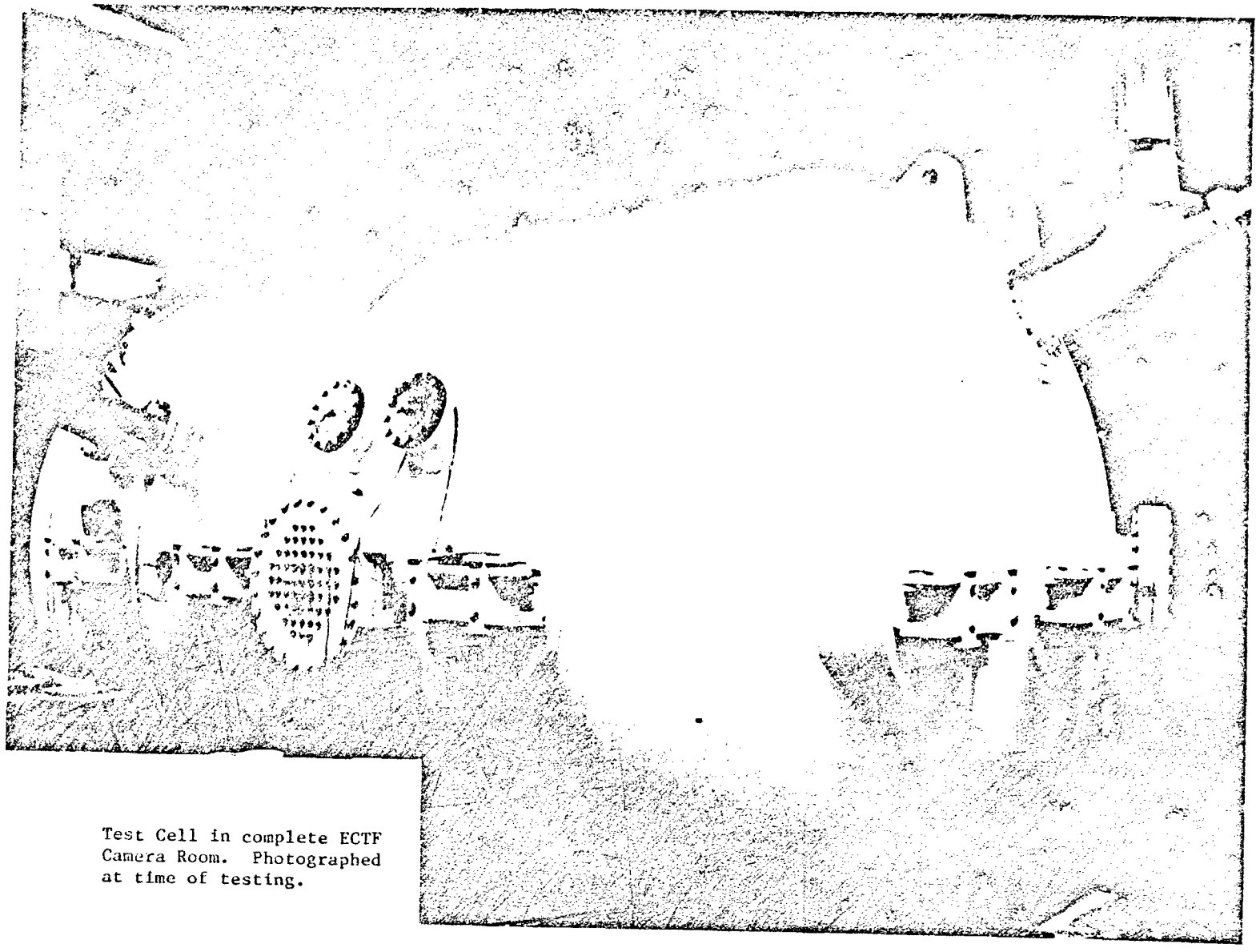

Test Cell in complete ECTF Camera Room. Photographed at time of testing.

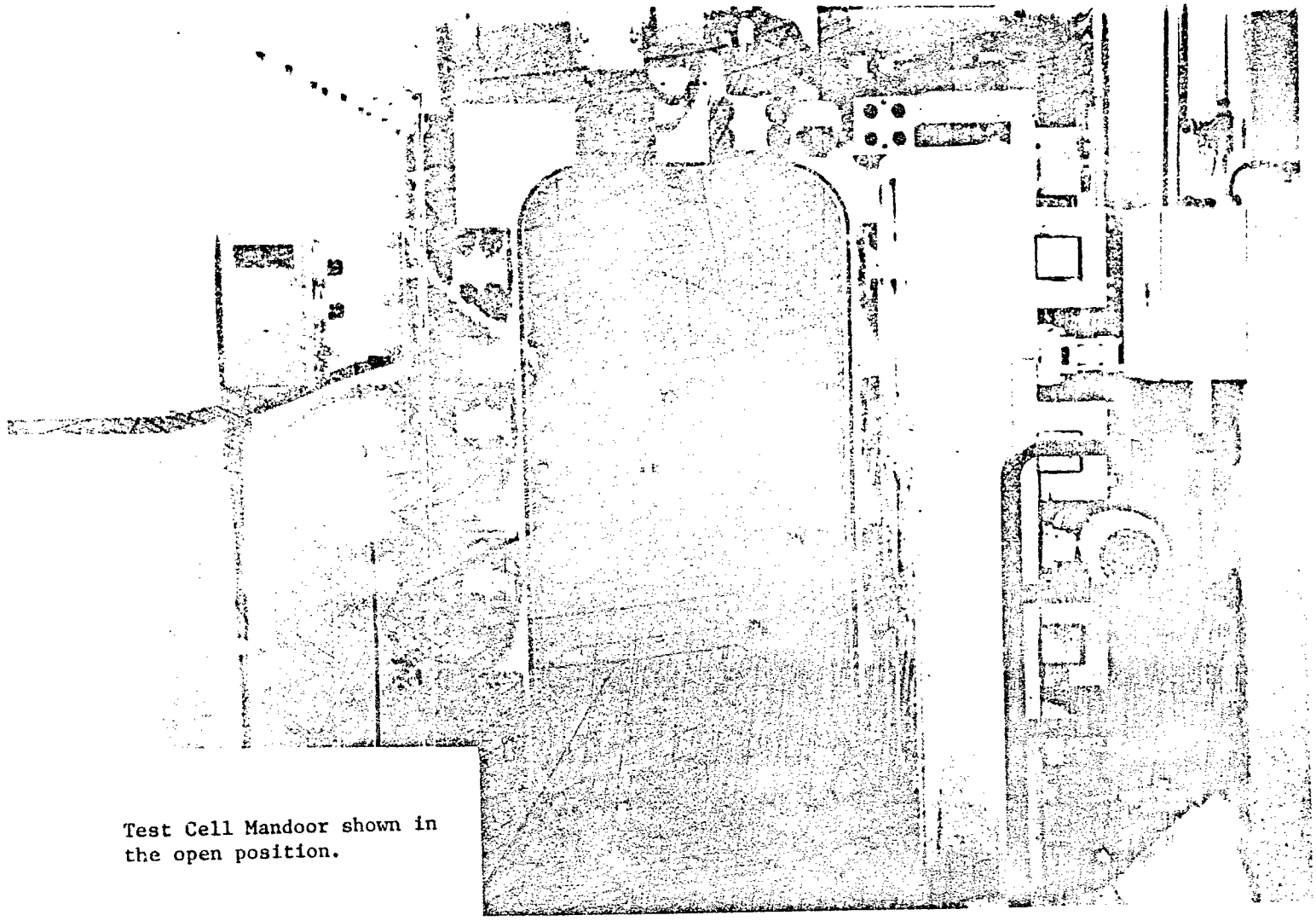

2280

Test Cell Mandoor shown in the open position.

Test Cell Mandoor shown in the closed position.

SWRI-'Blaster' --
Kirt Thistlethwaite
hanging a 12.5 lb. TNT
equivalent charge.

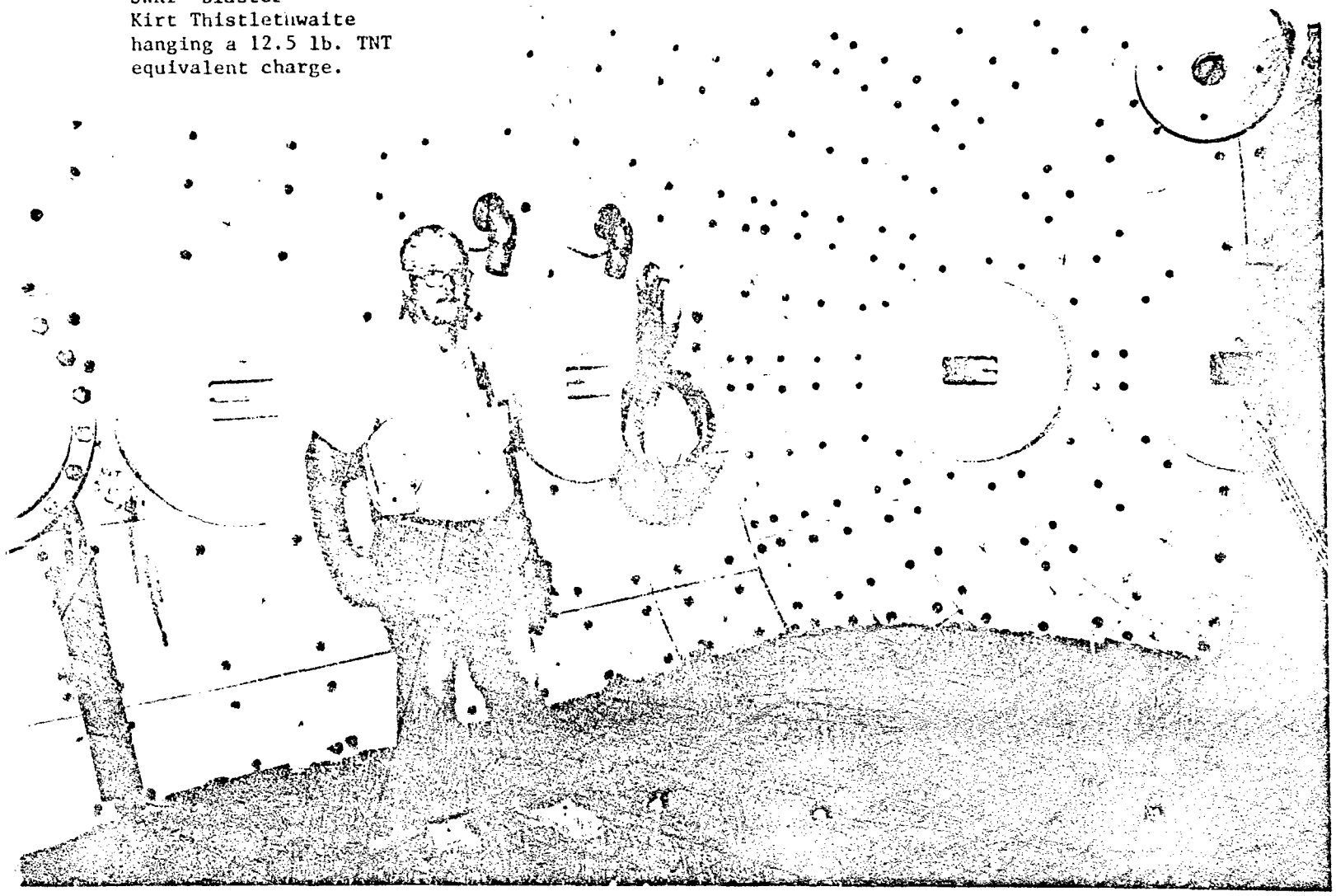

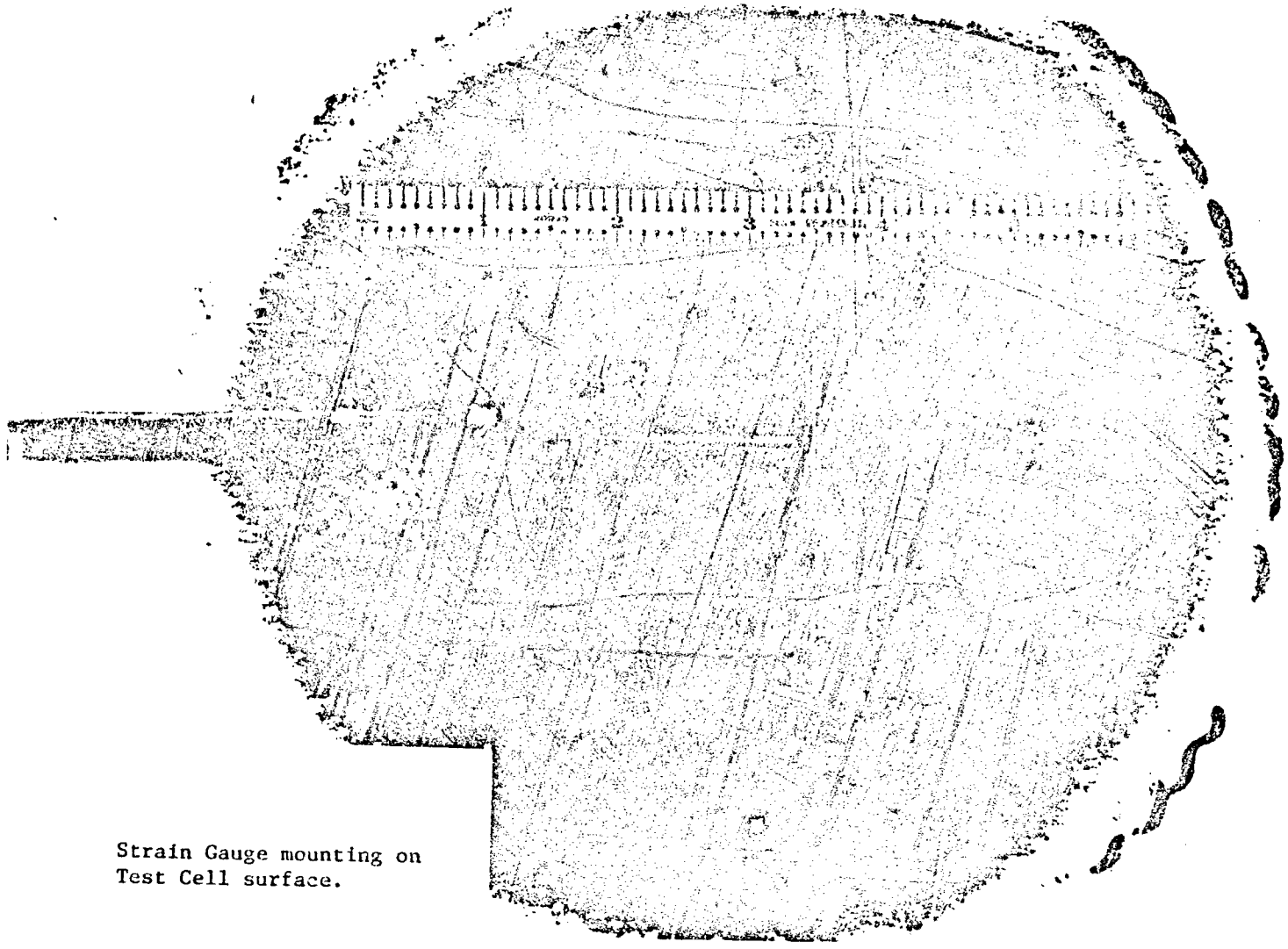

Strain Gauge mounting on
Test Cell surface.

DEVELOPMENT AND PROOF TEST OF AN EXPLOSIVE STORAGE MODULE (ESM)

By

M. Sanai and G. R. Greenfield

SRI International
333 Ravenswood Avenue
Menlo Park, CA 94025

Presented at:

Twenty-Third DoD Explosives Safety Seminar

on

"Test Cell and Explosion Containment Designs"

Atlanta, Georgia
August 9-11, 1988

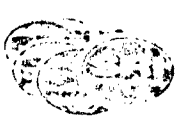

ABSTRACT

We have developed a self-contained, easy-to-use explosive storage module (ESM) and proof-tested three designs using up to 3 lb of Class 1.1 high explosives (HE). The novel design features of the ESM ensure complete containment of the debris produced by a mass detonation of the HE while allowing controlled release of the detonation products without generating a significant airblast. The containment provided by the ESM should allow the user to obtain an exemption from the current quantity/distance (Q/D) requirement for HE storage.

INTRODUCTION AND BACKGROUND

A primary quantity/distance (Q/D) requirement (as published in the March 1986 edition of the Contractor's Safety Manual for Ammunition and Explosives) is that, for 0-100 lb of Class 1.1 HE, a minimum distance of 670 ft must exist between the charge and the closest boundary or inhabited building. An exemption from this requirement may be sought if the HE is stored inside specially designed units that contain the debris, diminish the air shock in case of an accidental mass detonation of HE inside each unit, and prevent sympathetic detonation to adjacent explosive storage modules (ESMs).

We have developed and proof-tested an ESM that should qualify for an exemption from the current Q/D requirement. The novel design features of the ESM ensure complete containment of the debris while allowing controlled release of the detonation products to the outside.

ESM DESIGN

The ESM is designed to function as an independent and self-contained unit. We have developed three designs to store as much as 3 lb of HE inside a single module. As shown in Figure 1, the first design, designated ESM-1, consists of a 0.5-in.-thick, 2-ft-diameter steel cylinder welded at one end to a domed steel cap. The other end is sealed by a domed steel door that pivots on a hinge attached to the cylindrical portion. The door is secured in place by eight quick-lock assemblies spaced 45 degrees apart. The ESM-1 unit is lined with 1-in.-thick plywood to protect against shrapnel impact.

The second design, designated ESM-2, includes a threaded rod-locking mechanism instead of the quick-lock assembly. As shown in Figure 2, the threaded rod coincides with the axis of the cylinder, with

one end attached to the center of the welded dome. The other end of the rod passes through a hole at the center of the door at the opposite end when the door is shut. As shown in Figure 3, a large handwheel on the threaded rod is then turned to secure the door in place. Results of our computer calculations show that the explosion pressure acting on the inside surface of the door extends the rod, thus slowly releasing the detonation products through the circular gap produced between the cylinder and the door.

The strength and diameter of the threaded rod for the ESM-2 are designed to control the gap size and to ensure that the rod does not strain to failure. For example, Figure 4 shows the strain history for a 5-cm-diameter rod made from a high-strength (6.9-kb yield) steel following the detonation of a 1000-g HE charge inside the ESM. The maximum rod strain is 6.8%, which is less than half the 15% failure strain expected for that type of steel.

The third design, designated ESM-3, combines the threaded rod-locking mechanism and the quick-lock assembly. The ESM-3 may also include soft, energy-absorbing washers and several rupture ports to provide better control over the venting of detonation products.

ESM PROOF TESTS

We proof-tested the three ESM designs by securing them to a sturdy steel table and detonating a known amount of HE with the door closed. (Figure 5 shows the ESM-3 unit just before the test.) A combination of Class 1.1 HE was used in these proof tests. For ESM-1, the charge consisted of a combination of mild detonating fuse (MDF) and flexible linear shaped charge (FLSC) or strands of Primacord placed on 9.5-in.-diameter spools. The explosive strands were kept away from the ESM walls by letting the steel rod pass through the clearance hole at the center of each spool. The total explosive weight for the ESM-1 test was 5180 grains (0.74 lb) of PETN. The charge for ESM-2 consisted of 1.5 lb of Detasheet C HE stretched over a low-density foam cylinder that was

supported by the steel rod (see Figure 6). The charge for ESM-3 was similar to that ESM-2 except that it weighed 3 lb.

The videotape and the pressure data from the proof tests clearly showed that all the ESM designs fully contained the explosive debris and allowed a slow release of the detonation products without generating a significant airblast. For example, the postshot view of ESM-3 shown in Figure 7 indicates that the ESM was still integral and the door remained closed following the mass detonation of 3 lb of Detasheet inside the ESM. The blackened areas around the circular gap indicate the expected release paths of the detonation products to the outside.

CONCLUSIONS

The proof tests reported here clearly demonstrated that the three ESM designs are capable of fully containing the shrapnel and debris produced by mass detonation of up to 3 lb of Class 1.1 HE. The videotape and the pressure data from the proof tests showed that the detonation products leaked out of the ESM slowly without producing a significant airblast.

We believe that the storage capacity of the ESM can be increased by using crushable washers and/or fast-acting release ports. However, it may be more cost-efficient to simply procure more ESM units as needed than to modify and proof-test new designs to augment storage capacity.

ACKNOWLEDGMENT

The work reported here was supported mainly by the Westinghouse Corporation of Sunnyvale, California. SRI International holds the patent rights to the ESM designs discussed here. The project supervisor at SRI was Dr. J. D. Colton, Director of Poulter Laboratory. The proof tests were conducted by Mr. T. Gaines and Mr. J. Mattson. The photographic and video documentations of the tests were made by Mr. K. Stapleton.

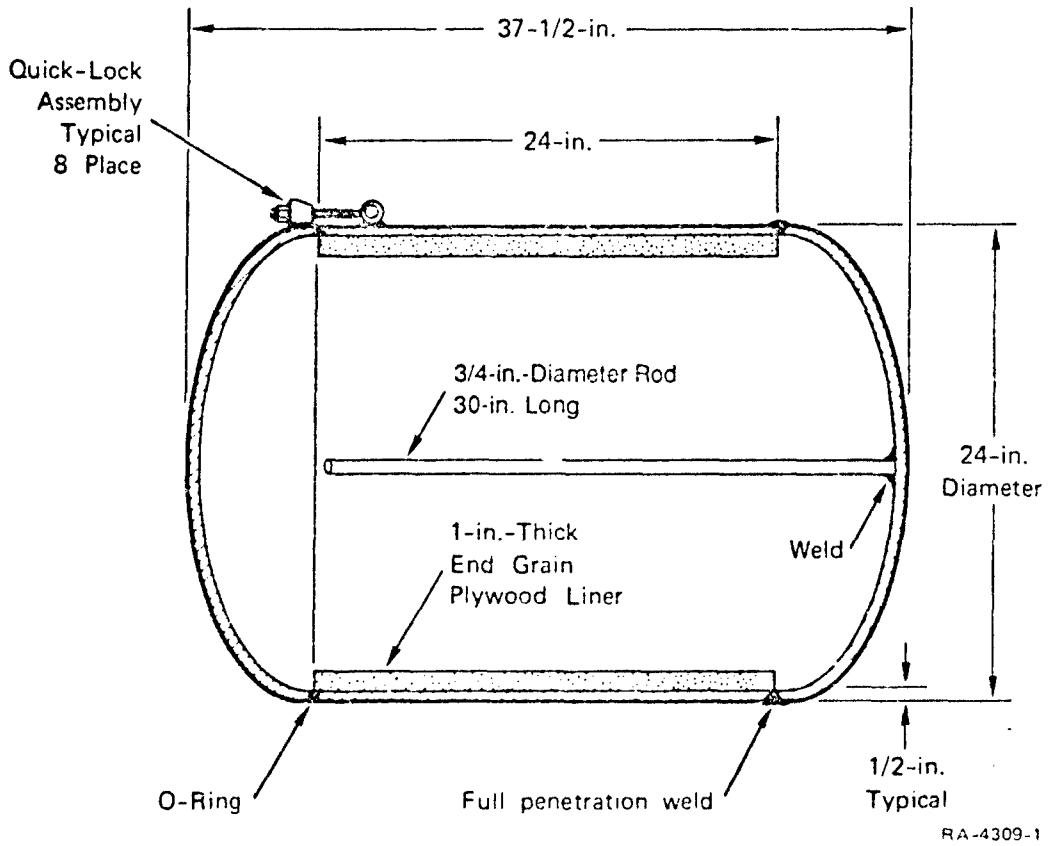

Figure 1. Schematic diagram of ESM-1 design.

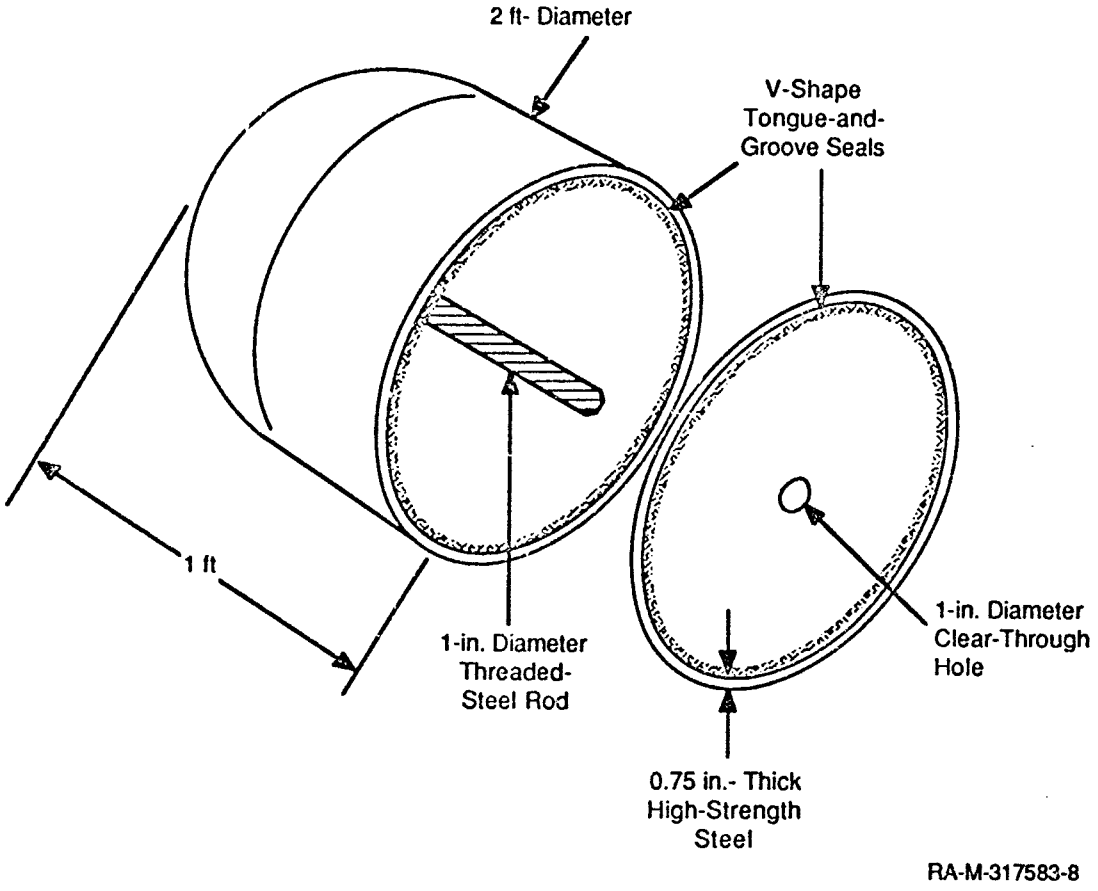

Figure 2. Schematic diagram of ESM-2 design.

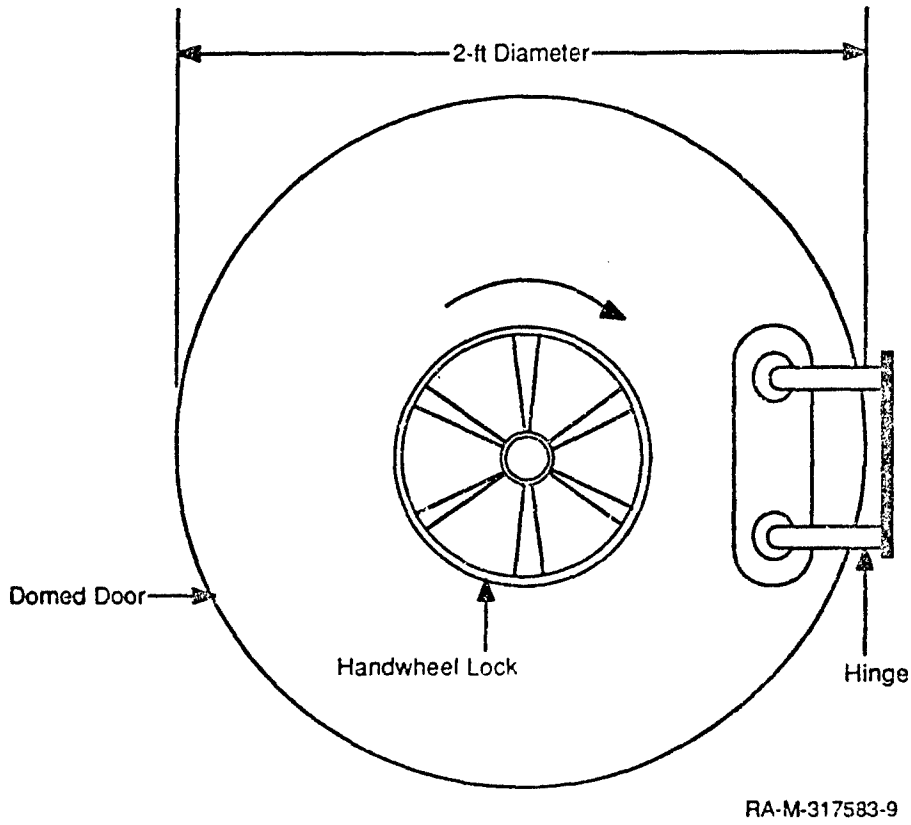

Figure 3. Handwheel lock used in ESM-2 design

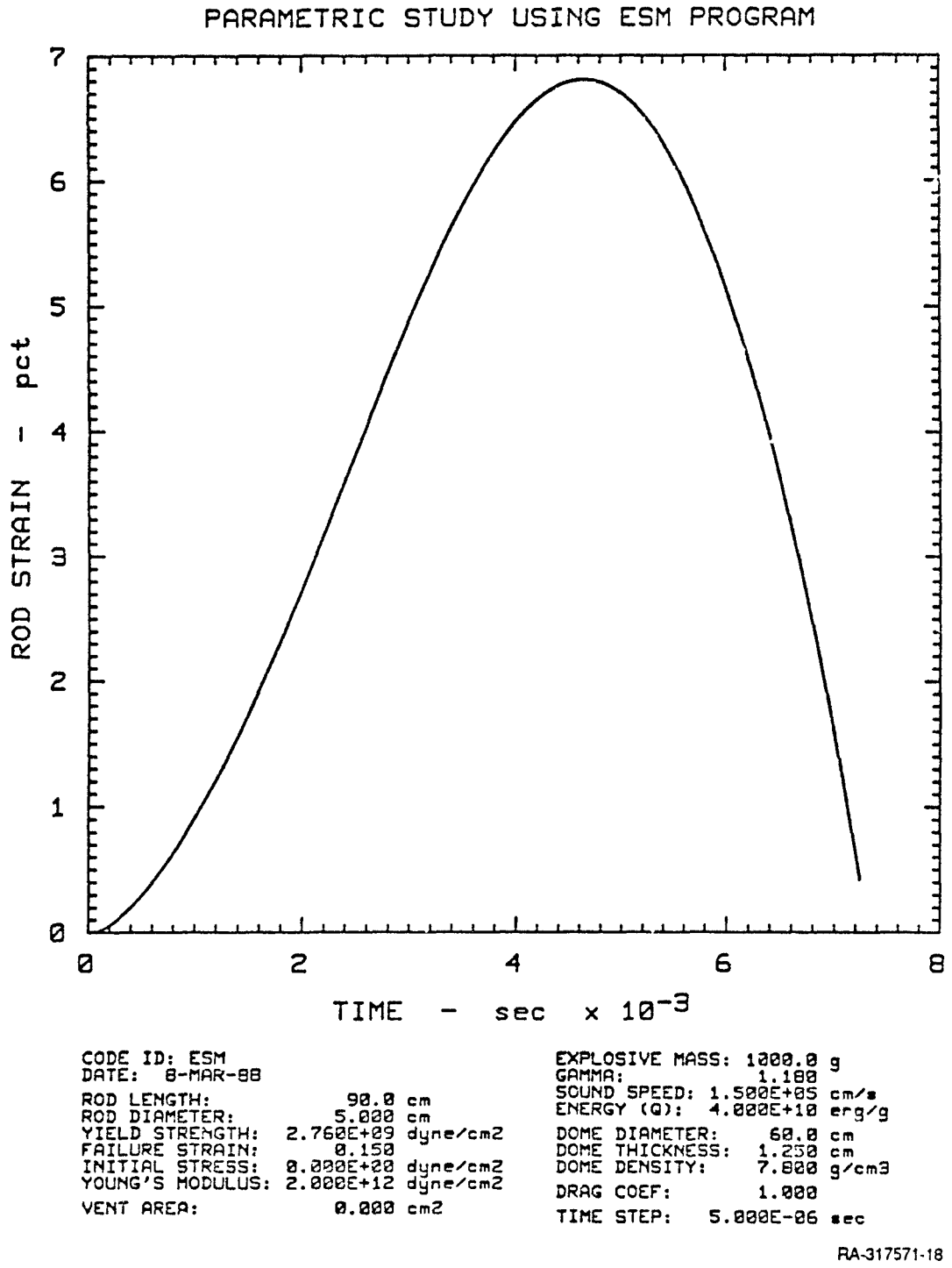

Figure 4. Longitudinal strain of the steel threaded rod used in ESM-2 design.

RP-317571-21

Figure 5. ESM-3 shown before proof test.

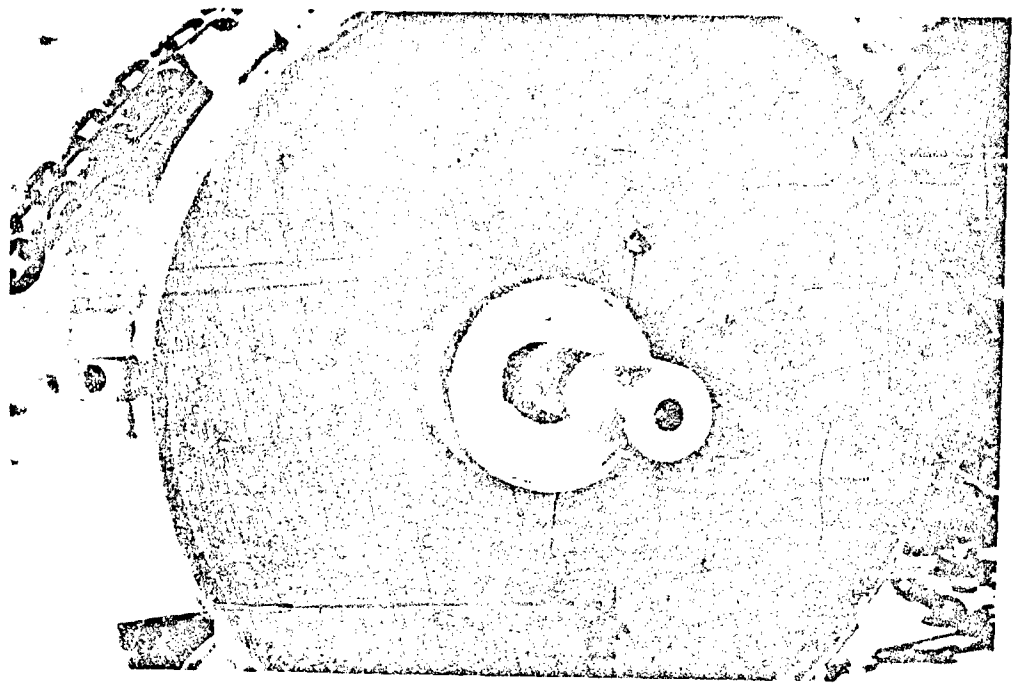

RP-317571-22

Figure 6. Detasheet C charge shown with side ESM-3 unit.

RP-317571-23

Figure 7. ESM-3 unit shown after proof test.

RAAF WALL TRAVERSE TRIALS 1987

(SLIDE 1)

INTRODUCTION

1. DURING THE INTRODUCTION OF THE NATO SAFETY PRINCIPLES FOR THE STORAGE OF EXPLOSIVE ORDNANCE BY THE AUSTRALIAN DEFENCE FORCE, THE ROYAL AUSTRALIAN AIR FORCE INDENTIFIED DEFICIENCIES IN THE TRAVERSE AND WALL DESIGNS USED IN EXPLOSIVE STOREHOUSES, PREPARATION BUILDINGS AND ORDNANCE LOADING APRONS. IN ALL CASES, THE TRAVERSES AND FACILITIES HAD, IN LIGHT OF MODERN THINKING, BEEN CONSTRUCTED WITH INSUFFICIENT CONSIDERATION BEING GIVEN TO EXPLOSIVE EFFECTS. SOME PARTICULAR MASS CONCRETE BUILDINGS WERE SUBJECT TO AN INVESTIGATION BY THE AUSTRALIAN ORDNANCE COUNCIL WHO CONCLUDED THAT, IN ALL PROBABILITY, THE BUILDINGS DESIGN WOULD AGGRAVATE THE EFFECTS OF AN EXPLOSION RATHER THAN REDUCE IT.

2. THE ADOPTION OF THE NATO SAFETY PRINCIPLES ALSO RESULTED IN THE RAAF FORMULATING A PROGRAMME TO UPDATE AND EXTEND EXPLOSIVE STORAGE, PREPARATION AND LOADING FACILITIES AT A NUMBER OF BASES. IT BECAME OBVIOUS TO THE RAAF THAT SOME FORM OF CONTROLLED EVALUATION WAS NEEDED TO TEST THE EFFICIENCY OF EXISTING, INTERIM AND PROPOSED TRAVERSES AND FACILITIES. OUT OF THESE CONSIDERATIONS CAME THE PROJECT TO TEST SCALED MODELS OF THE WALL AND TRAVERSE CONSTRUCTION CURRENTLY USED BY THE RAAF. (SLIDE 2) THE PROJECT WAS TITLED "THE RAAF WALL TRAVERSE TRIAL" AND WAS CONDUCTED AT THE WEAPONS RESEARCH ESTABLISHMENT, WOOMERA, SOUTH AUSTRALIA.

TRIAL AIMS

3. (SLIDE 3) THE AIMS OF THE TRIAL WERE TO :

A. EXAMINE THE EFFECTIVENESS OF SEVERAL TRAVERSE DESIGNS,

B. EVALUATE THE CONSEQUENCES TO MASS CONCRETE WALLS THEN IN USE FOR SOME STORAGE FACILITIES, AND

C. MEASURE THE EXPLOSIVE EFFECTS AT D4 AND D7 DISTANCES AS IN THE QUANTITY DISTANCE TABLES FOR HD 1.1 EO.

TRIAL CONFIGURATION

4. THE TRIAL CONSISTED OF THE SIMULTANEOUS DETONATION OF 36 MK12 1000 LB BOMBS CONTAINING A NET EXPLOSIVE QUANTITY EQUIVALENT TO 8076 KG OF TNT.

5.(SLIDE 4) THE BOMBS WERE DETONATED INSIDE A PENTAGON OF VERTICAL WALL TRAVERSES, TERMED "DONOR" WALLS. THE PENTAGON SHAPED DONOR STRUCTURE CONSISTED OF FIVE TRAVERSE WALLS AS FOLLOWS:

A.(SLIDE 5) ONE WALL OF STANDARD ACROW CONSTRUCTION (METAL EXTERIOR AND EARTH FILLED),

B.(SLIDE 6) TWO WALLS OF TILT SLAB CONSTRUCTION (CONCRETE EXTERIOR AND EARTH FILLED), AND

C.(SLIDE 7) TWO WALLS OF 680MM THICK MASS CONCRETE CONSTRUCTION.

6. LOCATED AT VARYING DISTANCES FROM THE DONOR WALLS WERE A SERIES OF EIGHT "RECEPTOR" WALLS. THESE CONSISTED OF SIX WALL TRAVERSES AND TWO VERTICAL FACE, SINGLE SLOPE TRAVERSES. (SLIDE 8) BEHIND FIVE OF THESE WALLS WERE INERT BOMBS, WITNESS SCREENS AND CANEITE PACKS TO REGISTER THE EFFECTS OF DEBRIS AND FRAGMENTS THAT MIGHT PENETRATE THE "RECEPTOR" WALLS. THE RECEPTOR WALLS WERE CONSTRUCTED AS FOLLOWS:

A. (SLIDE 9) AT 10 METRES: THERE WAS ONE VERTICAL FACE, SINGLE SLOPE TRAVERSE, THE FACE WAS HALF CONCRETE BLOCKS AND HALF METAL, BACKED WITH LAYERED EARTH; (SLIDE 4)

B. AT 16 METRES (D4 DISTANCE): THERE WERE THREE WALLS, ONE TILT SLAB, ONE MASS CONCRETE, ONE VERTICAL FACE SINGLE SLOPE TRAVERSE;

C. AT 48 METRES (D7 DISTANCE): THERE WERE THREE WALLS, ONE ACROW, ONE TILT SLAB AND ONE MASS CONCRETE; AND

D. AT 177 METRES, THERE WAS ONE TILT SLAB WALL.

THE DETONATION

7. THE DETONATION OCCURRED AT 1115 HRS ON 19 AUG 87, AFTER NINE DAYS OF ON-SITE PREPARATIONS. THE RESULTS OF THE DETONATION ARE AS FOLLOWS:

A. (SLIDE 10) AS EXPECTED, ALL DONOR WALLS DISINTEGRATED EXCEPT FOR SOME SHEETS OF THE ACROW WALL WHICH WERE THROWN 200 TO 300 METRES AWAY. A CRATER APPROXIMATELY 19 METRES IN DIAMETER AND 5 METRES DEEP WAS FORMED. THE DONOR WALLS WOULD HAVE EXPERIENCED APPROXIMATELY 3100 ATMOSPHERES OF PEAK REFLECTED PRESSURE;

B.(SLIDE 11) AT 10 METRES. THE VERTICAL FACE, SINGLE SLOPED TRAVERSE WAS THE CLOSEST RECEPTOR WALL TO THE DETONATION. THE FACE OF THE TRAVERSE WOULD HAVE EXPERIENCED APPROXIMATELY 400 ATMOSPHERES OF PRESSURE. THE CONCRETE FACE DISINTERGRATED, THE METAL FACE, ALTHOUGH HEAVILY HOLED WAS STILL INTACT. THE HEIGHT OF THE TRAVERSE WAS REDUCED BY APPROXIMATELY 0.3 METRE AND ABOUT 1/3 OF THE EARTH FILL WAS GONE;

C.(SLIDE 12) AT 16 METRES (D4 DISTANCE). THE FACE OF THE THREE WALLS WOULD HAVE EXPERIENCED APPROXIMATELY 135 ATMOSPHERES OF PRESSURE. THE TILT SLAB WALL WAS TURNED UPSIDEDOWN AND THROWN AGAINST THE CANEITE PACKS 10 METRES BEHIND. ONLY 1/2 THE WALL REMAINED INTACT AND THE EARTH FILL WAS GONE:

THE MASS CONCRETE WALL WAS TOTALLY DESTROYED. TORN FROM ITS BASE THE FAILURE APPEARS TO BE A SHEAR FAILURE DUE TO BOTH IMPACT OF FRAGMENTS FROM THE DONOR WALLS AND BLAST PRESSURE. A NUMBER OF LARGE PIECES OF CONCRETE WERE THROWN 200 TO 300 METRES TO THE REAR AND THE ANALYSIS OF THIS WALL SUGGESTS CATASTROPHIC FAILURE:

THE VERTICAL FACE SINGLE SLOPE TRAVERSE SURVIVED REASONABLY WELL. THE CONCRETE FACE PANELS APPEAR TO HAVE BEEN COMPRESSED INTO THE SOIL FOLLOWED BY FRACTURE INTO RELATIVELY SMALL FRAGMENTS. THE METAL FACE WAS AGAIN HEAVILY HOLED BUT REMAINED INTACT. ABOUT 1/4 OF THE SOIL FROM THE TRAVERSE WAS GONE;

D.(SLIDE 13) AT 48 METRES (D7 DISTANCE). THE FACE OF THE THREE WALLS WOULD HAVE EXPERIENCED APPROXIMATELY 5 ATMOSPHERES. WHILST THE BLAST LOADS WERE REDUCED DRAMATICALLY COMPARED WITH THE D4 DISTANCES, THEY WERE STILL MASSIVE.

THE TILT SLAB AGAIN FAILED BY ROTATING ALLOWING THE SOIL TO ESCAPE. HALF OF THE WALL WAS COMPLETELY DEMOLISHED SUGGESTING THAT IT WAS HIT BY SUBSTANTIAL FRAGMENTS FROM THE DONOR WALLS. THE INTACT PORTION APART FROM TOPPLING SUFFERED ONLY MINOR STRUCTURAL DISTRESS. THE RESULTS SUGGESTED THAT IF THE TILT WALL HAD RETAINED ITS SOIL, IT WOULD HAVE ROTATED ALMOST TO THE POINT OF TOPPLING AND THEN FALLEN BACK:

THE MASS CONCRETE WALL, APART FROM PITTING, REMAINED INTACT: THE ACROW WALL SUFFERED SIGNIFICANT STRUCTURAL DISTRESS. ONE HALF TOPPLED BACKWARDS ONTO THE BOMBS WITH THE REAR FACE OPENING UP. THE OTHER HALF SPLIT IN HALF WITH THE REAR FACE COLLAPSING BACKWARDS AND THE FRONT FACE, AFTER BEING PERFORATED BY FRAGMENTS, COLLAPSING FORWARD.

E.(SLIDE 14) AT 177 METRES, THE TILT SLAB SURVIVED WITH ONLY MINOR PITTING.

BOMB ASSESSMENT

8. THE MK82 AND MK84 BOMBS WHICH WERE POSITIONED AT THE REAR OF SELECTED WALLS, WERE SUBJECTED TO CONSIDERABLE TRANSATION AND ROTATION DURING THE BLAST. IN SOME INSTANCES, THE STEEL PACKING STRAPS HOLDING THE BOMBS WITHIN THEIR PALLETS FAILED AND ALLOWED THE BOMBS TO BE SCATTERED. THE INSPECTION OF THE BOMBS REVEALED THAT ALTHOUGH THERE WAS MUCH DAMAGE TO WALLS AND TRAVERSES, ONLY ONE BOMB SUFFERED ANY DETECTABLE DAMAGE. THE IMPACT DAMAGE TO THE BOMB WAS SHALLOW AND DUCTILE IN NATURE, AND DID NOT CRACK THE CASING. THIS DAMAGE WAS INSUFFICIENT TO CAUSE SHOCK INDUCED DETONATION OF A LIVE BOMB.

SUMMARY

9.(SLIDE 15) TO SUMMARIZE, THE FOLLOWING OBSERVATIONS WERE MADE:

A. BOTH VERTICAL FACE, SINGLE SLOPE TRAVERSES, ALTHOUGH EXTENSIVELY DAMAGED, STOPPED ALL LOW ANGLE HIGH VELOCITY FRAGMENTS;

B. THE TILT SLAB AND MASS CONCRETE WALLS AT 16 METRES (D4 DISTANCE) WOULD HAVE BEEN THROWN GREATER DISTANCES EXCEPT FOR THE EARTH BACKED CANEITE PACKS LOCATED BEHIND THEM. HOWEVER, DEBRIS FROM THE WALLS WAS STILL THROWN UP TO 300 METRES AWAY. CONCRETE TYPE WALLS SHOULD BE AVOIDED AT THE D4 DISTANCES, SINCE THE DEMOLITION OF SUCH TYPE WALLS PROVIDE MASSIVE, AND POTENTIALLY DESTRUCTIVE FRAGMENTS, AS WAS EVIDENT BY THE DAMAGE INFLICTED ON THE CANEITE PACKS;

C.(SLIDE 16) THE TILT SLAB AND ACROW WALLS AT 48 METRES (D7 DISTANCE) EXHIBITED LITTLE INHERENT STABILITY AND WOULD BE OVERTURNED UNDER A MUCH LESS SEVERE BLAST ENVIRONMENT THAN WAS GENERATED IN THIS TRIAL. IN CASES WHERE THE OVERTURNING OF A WALL IS OF SIGNIFICANCE SUCH TRAVERSES SHOULD BE AVOIDED;

D. THE MASS CONCRETE WALL AT 48 METRES (D7 DISTANCE) WITHSTOOD THE DETONATION. THE MAJOR DISCREPANCY WAS A CALCULATED INELASTIC DEFLECTION OF APPROXIMATELY 650MM YET THE WALL EXHIBITED NO VISIBLE SIGNS OF DISTRESS. THIS TYPE OF WALL WOULD BE GOOD AS A RECEPTOR TRAVERSE FOR THE PROTECTION OF PROCESS BUILDINGS CONTAINING SMALL QUANTITIES OF EXPLOSIVES OR TO PROTECT NON EXPLOSIVE BUILDINGS CONTAINING PERSONNEL; AND

E. DESPITE THE EXTERNAL STRUCTURAL DAMAGE TO MOST WALLS, IF LIVE BOMBS HAD BEEN IN PLACE BEHIND THE WALLS, SYMPATHETIC DETONATION WOULD NOT HAVE OCCURRED.

FILM

11. I WOULD NOW LIKE TO SHOW YOU A COMPOSITE TAPE OF THE EVENT, AND WILL BE PLEASED TO ANSWER QUESTIONS AT ITS CONCLUSION.

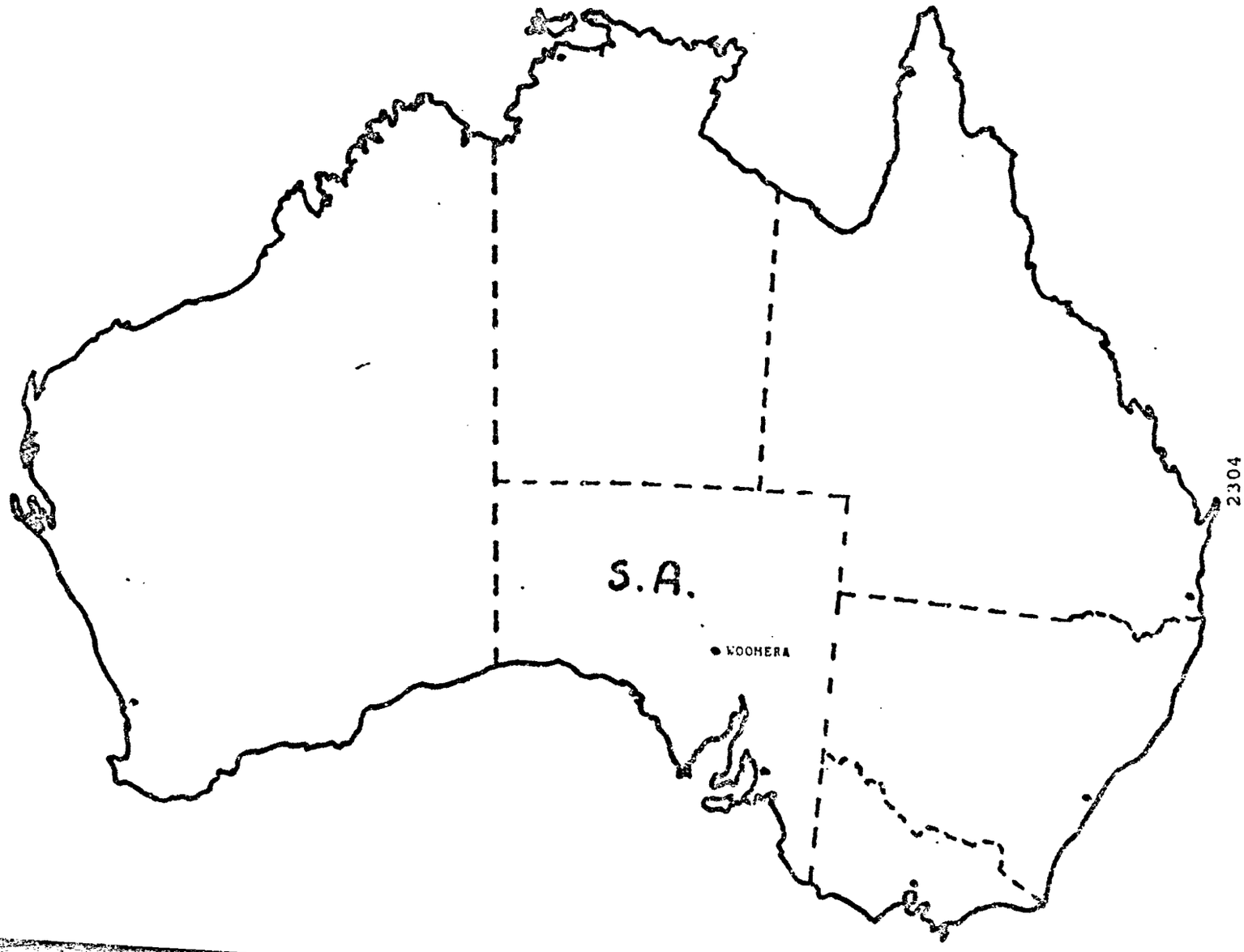
S.A.
WOOMERA
2304

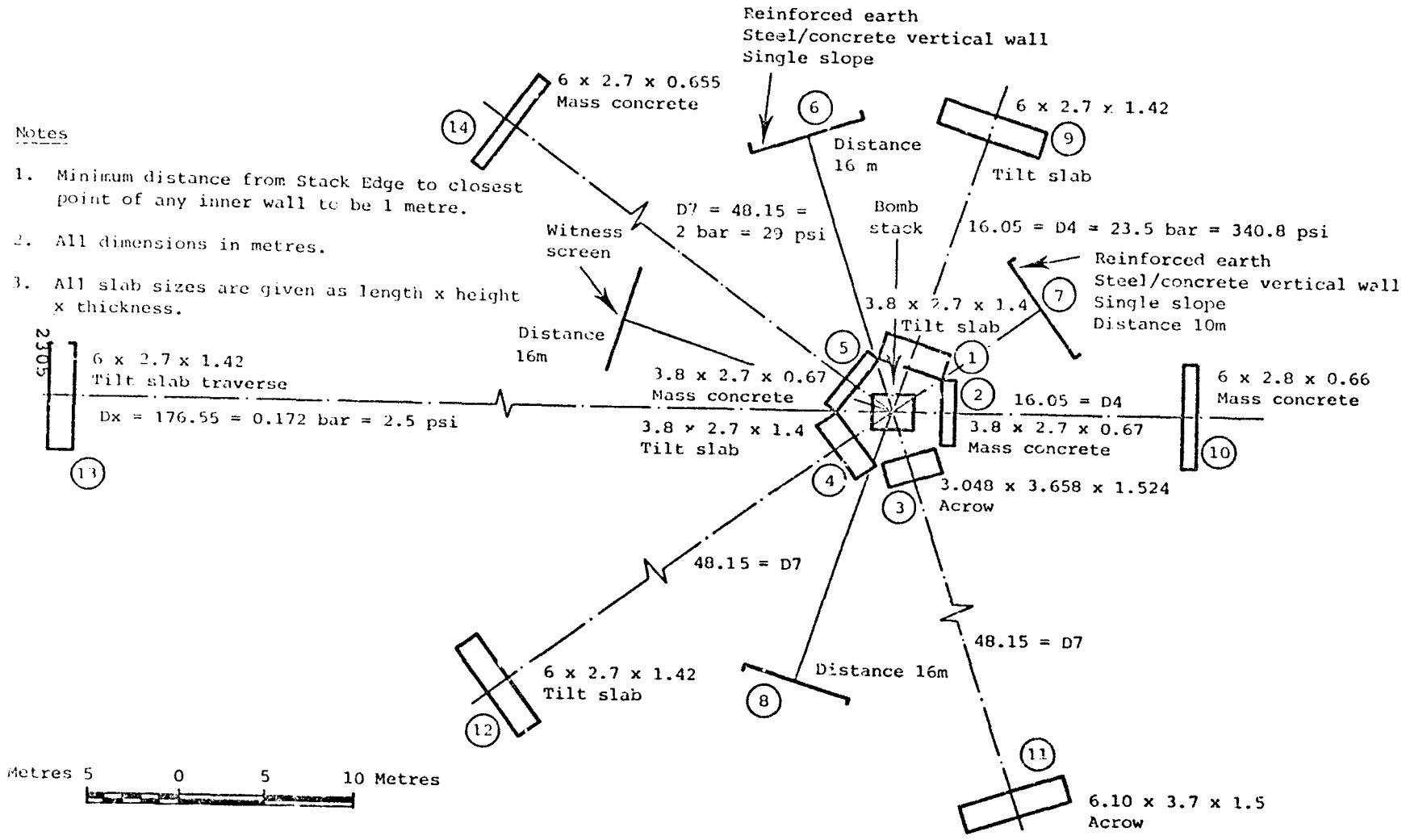
Notes
1. Minimum distance from Stack Edge to closest point of any inner wall to be 1 metre.
2. All dimensions in metres.
3. All slab sizes are given as length x height x thickness.
Reinforced earth
Steel/concrete vertical wall
Single slope
6 x 2.7 x 0.655
Mass concrete
Distance
16 m
6 x 2.7 x 1.42
Tilt slab
D7 = 48.15 =
2 bar = 29 psi
Bomb
stack
16.05 = D4 = 23.5 bar = 340.8 psi
Witness
screen
Distance
16m
3.8 x 2.7 x 1.4
Tilt slab
Reinforced earth
Steel/concrete vertical wall
Single slope
Distance 10m
2.705
6 x 2.7 x 1.42
Tilt slab traverse
Dx = 176.55 = 0.172 bar = 2.5 psi
3.8 x 2.7 x 0.67
Mass concrete
16.05 = D4
6 x 2.8 x 0.66
Mass concrete
3.8 x 2.7 x 1.4
Tilt slab
3.8 x 2.7 x 0.67
Mass concrete
3.048 x 3.658 x 1.524
Acrow
48.15 = D7
48.15 = D7
6 x 2.7 x 1.42
Tilt slab
Distance 16m
6.10 x 3.7 x 1.5
Acrow
Metres 5 0 5 10 Metres

ACROW METAL WALL

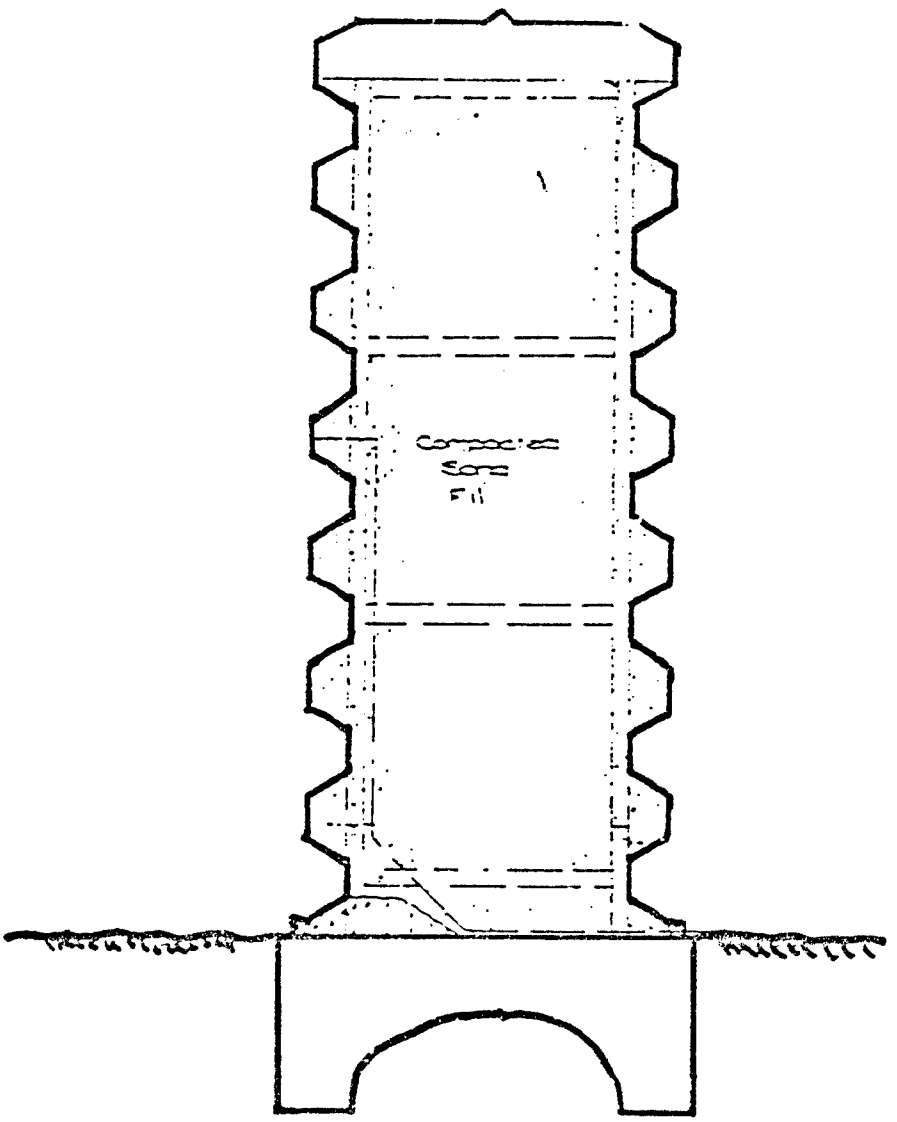

MASS CONCRETE WALL

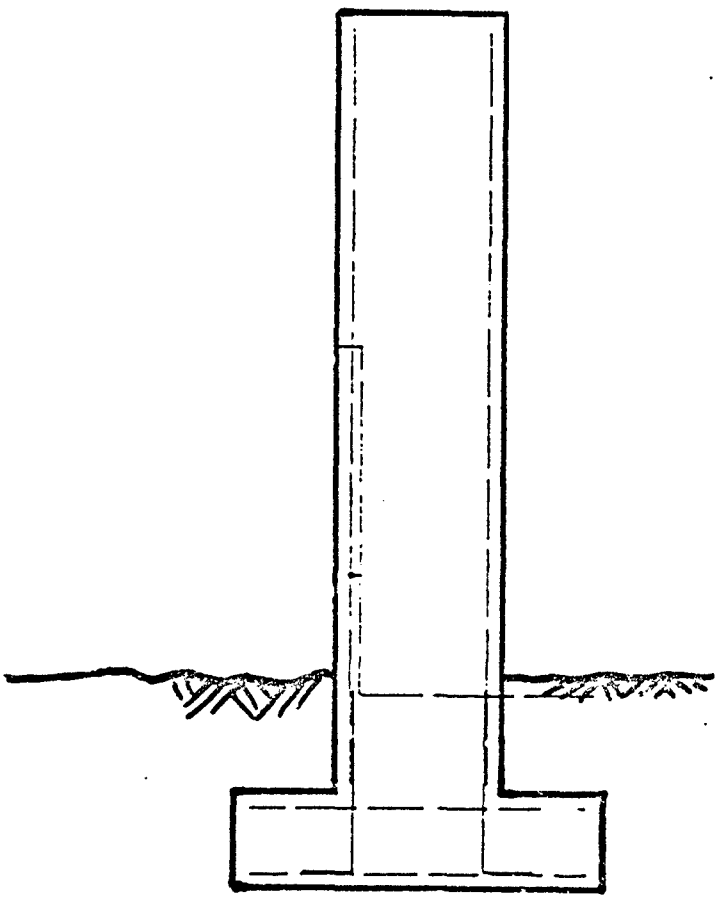

VERTICAL FACE SINGLE SLOPE

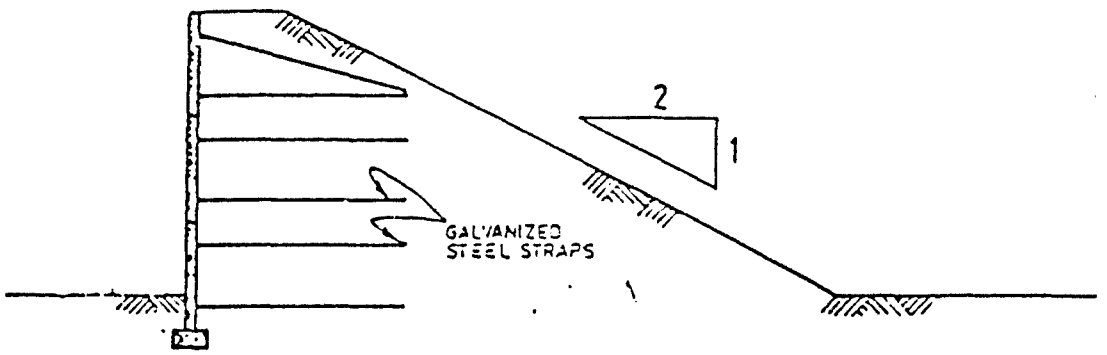

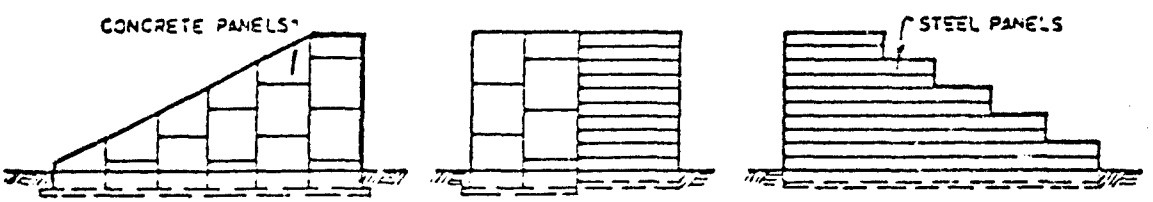

SIDE FRONT SIDE

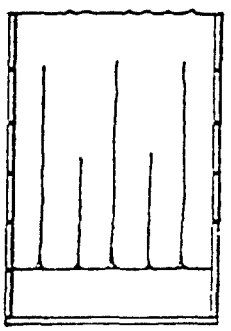

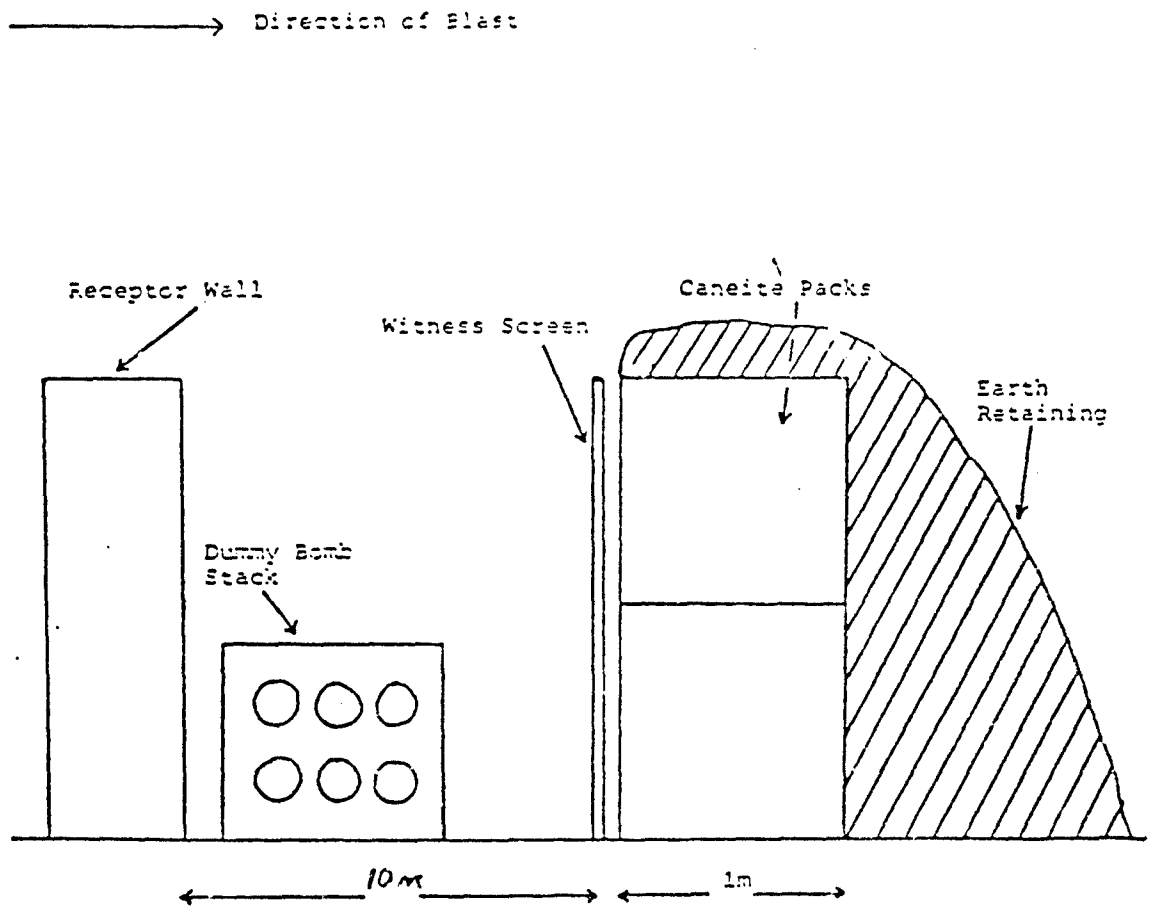
Direction of Blast
Receptor Wall
Witness Screen
Caneite Packs
Earth Retaining
Dummy Bomb Stack
10m
1m

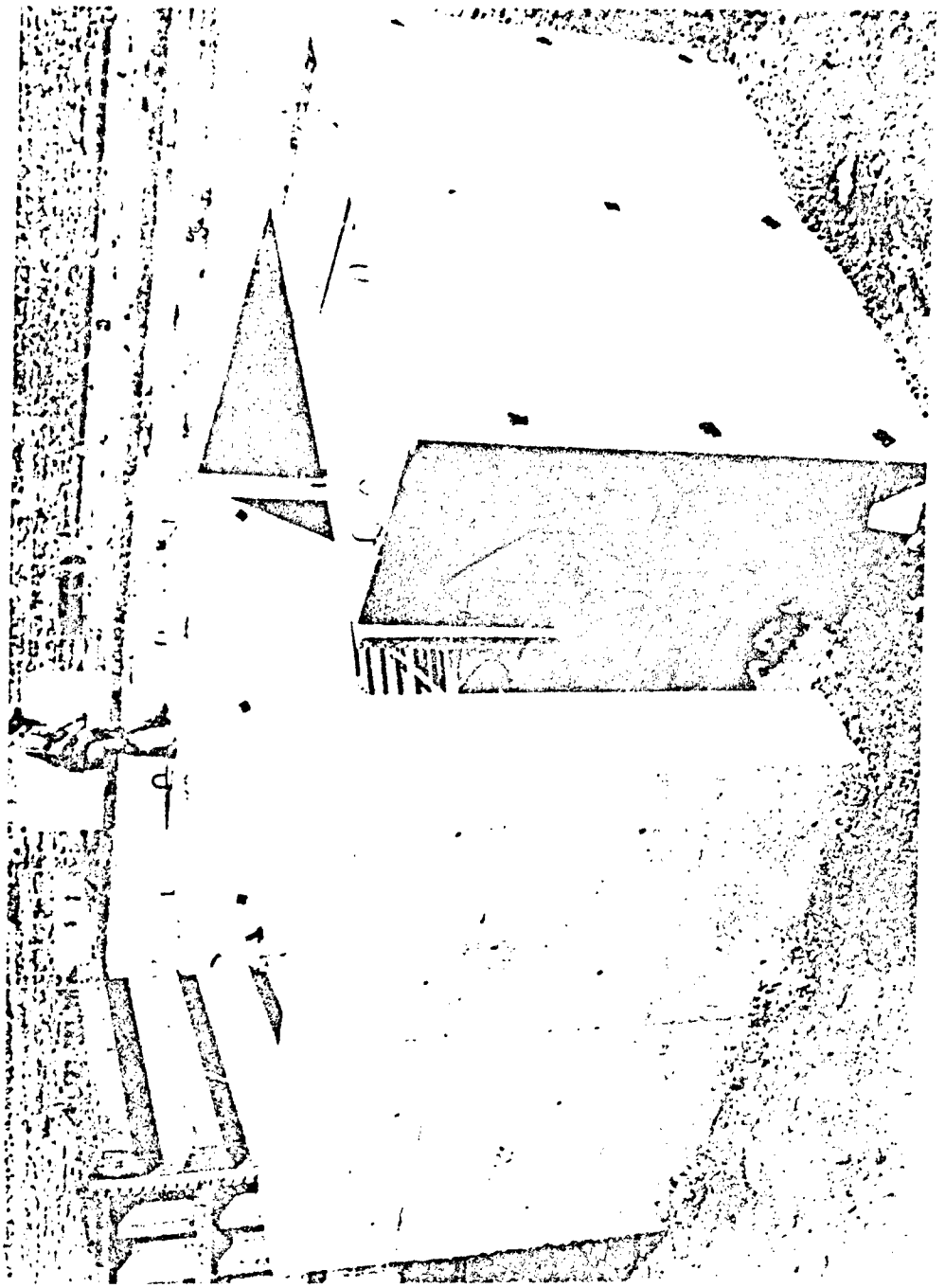

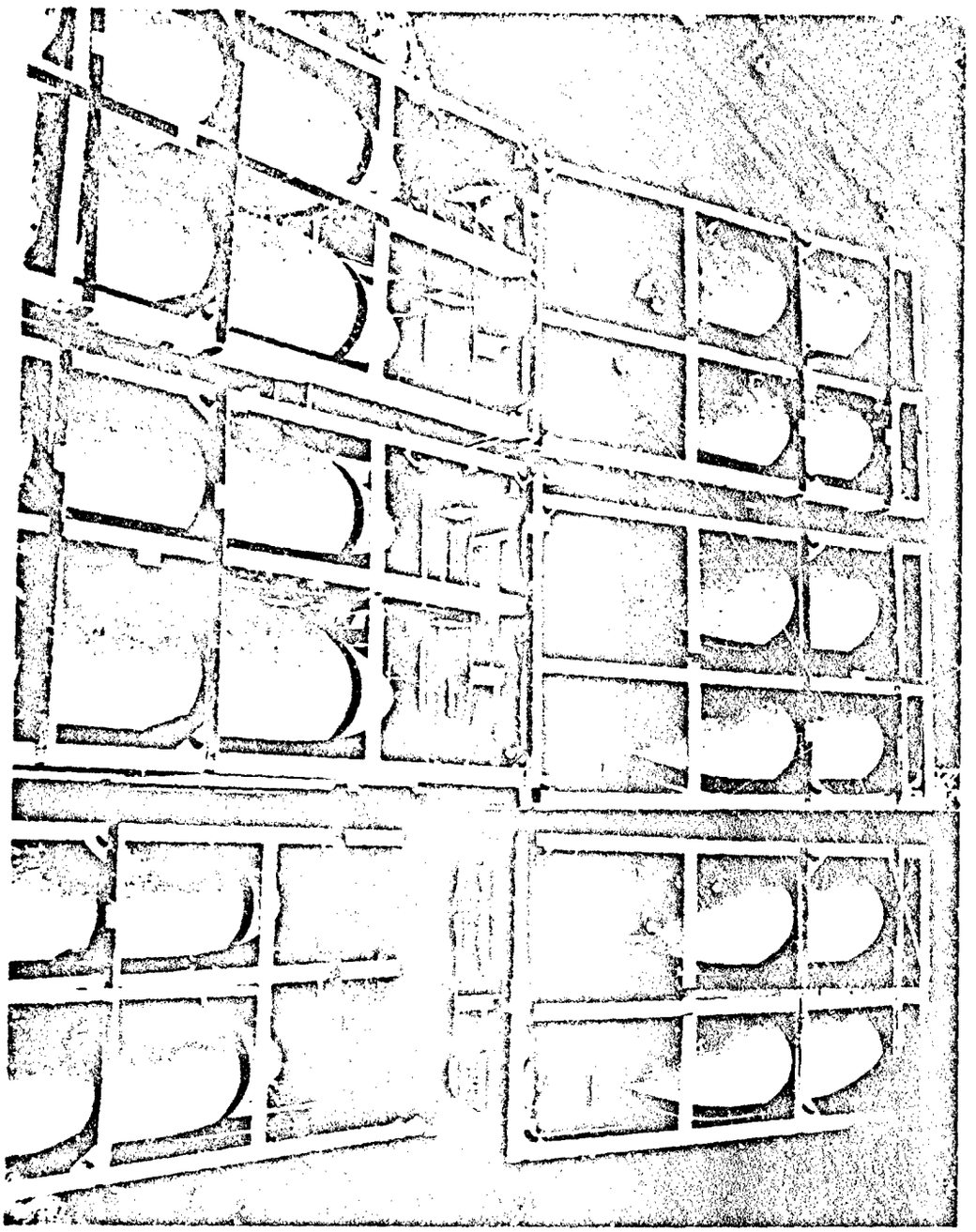

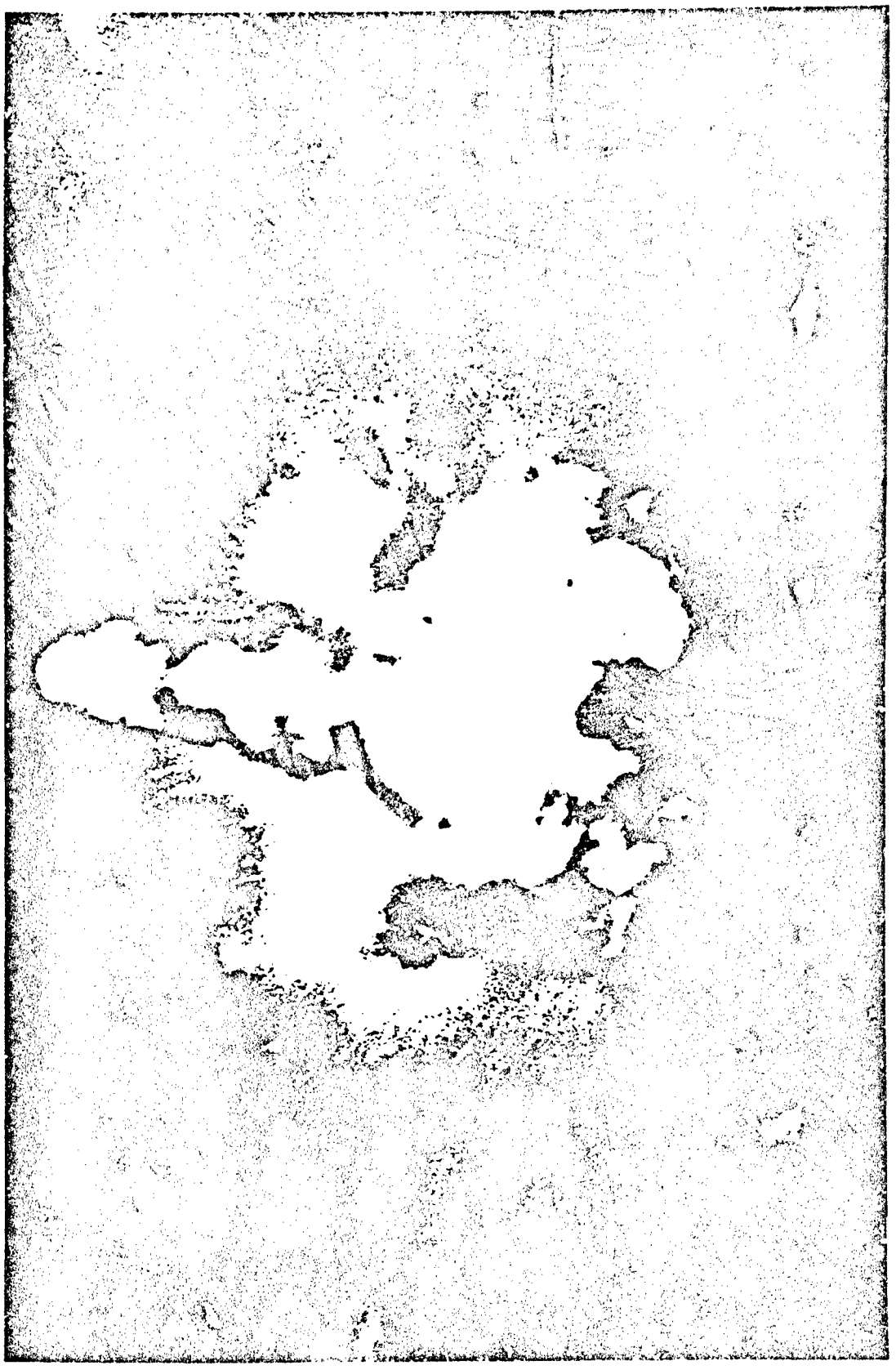

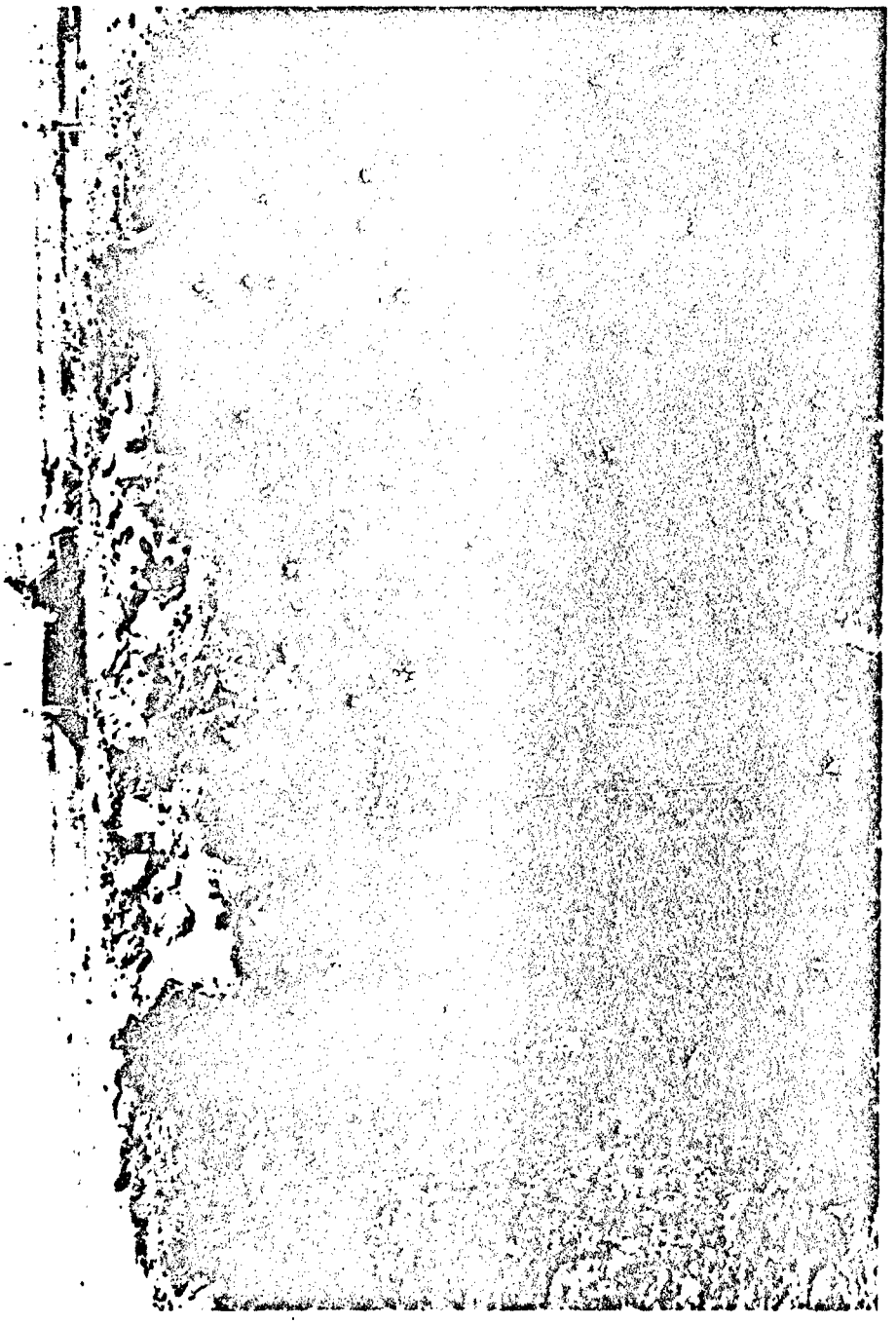

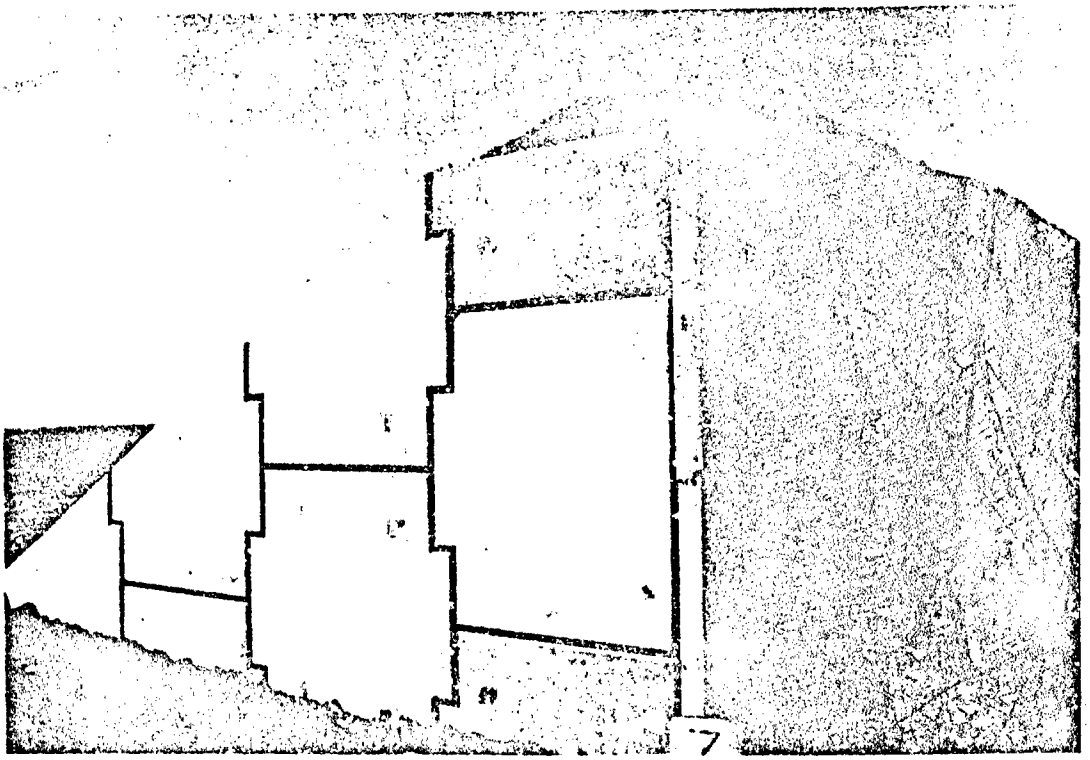

Front

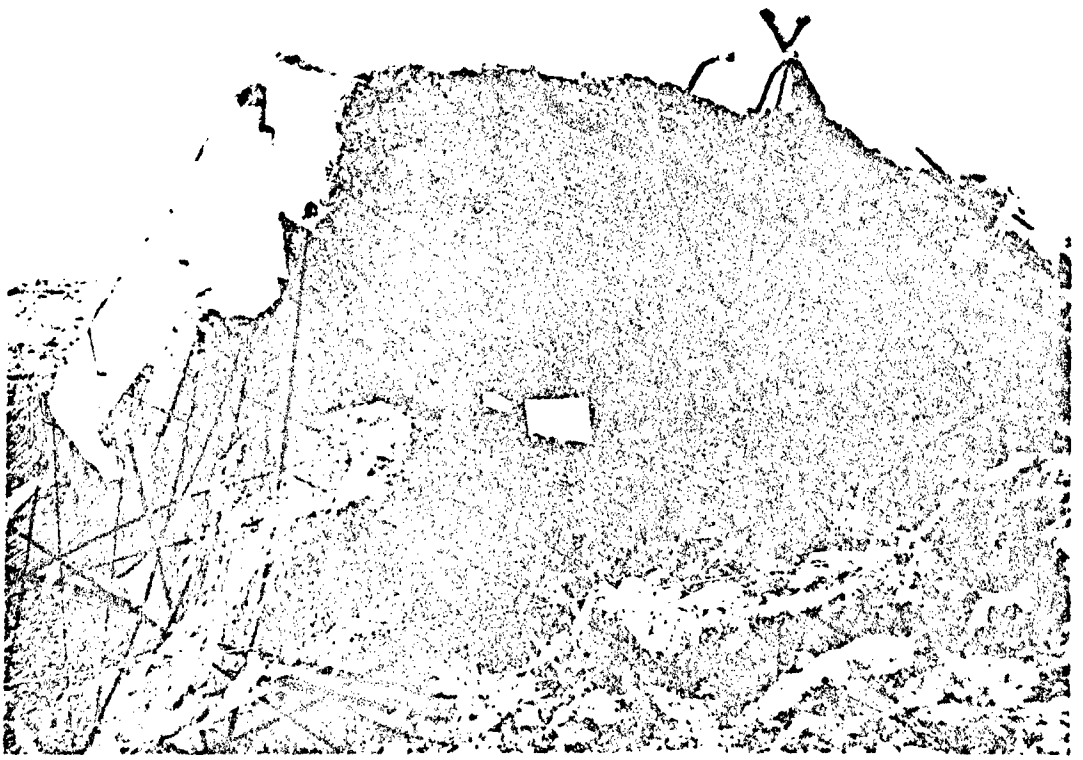

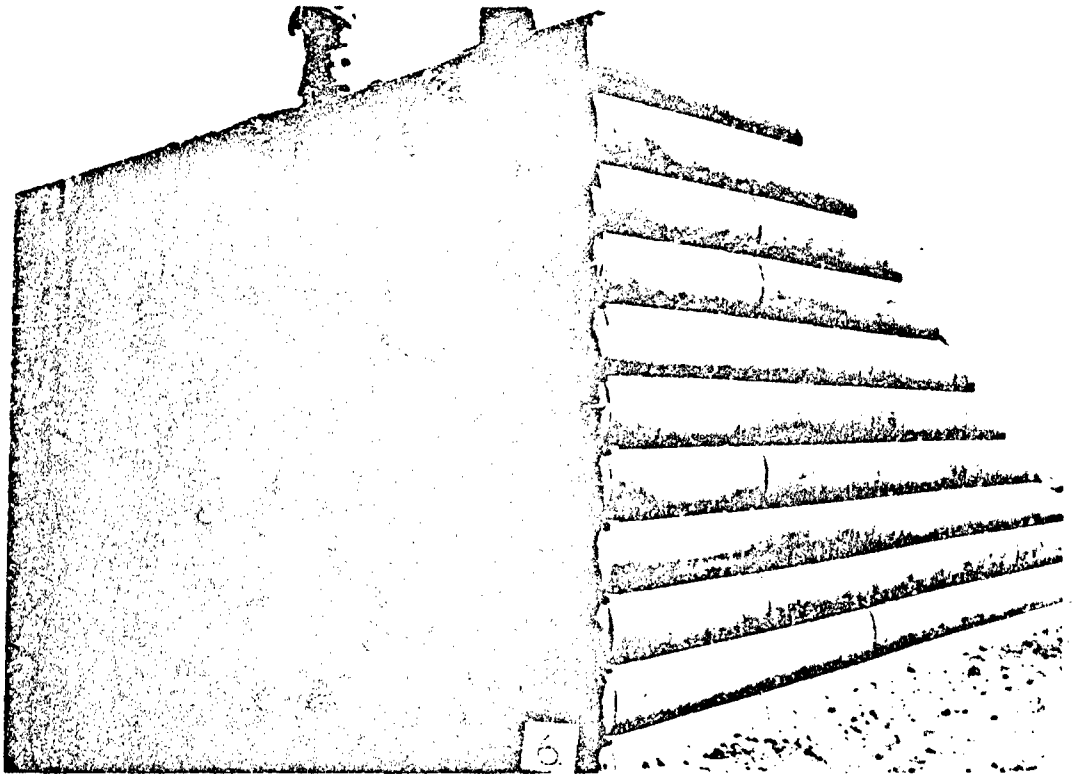

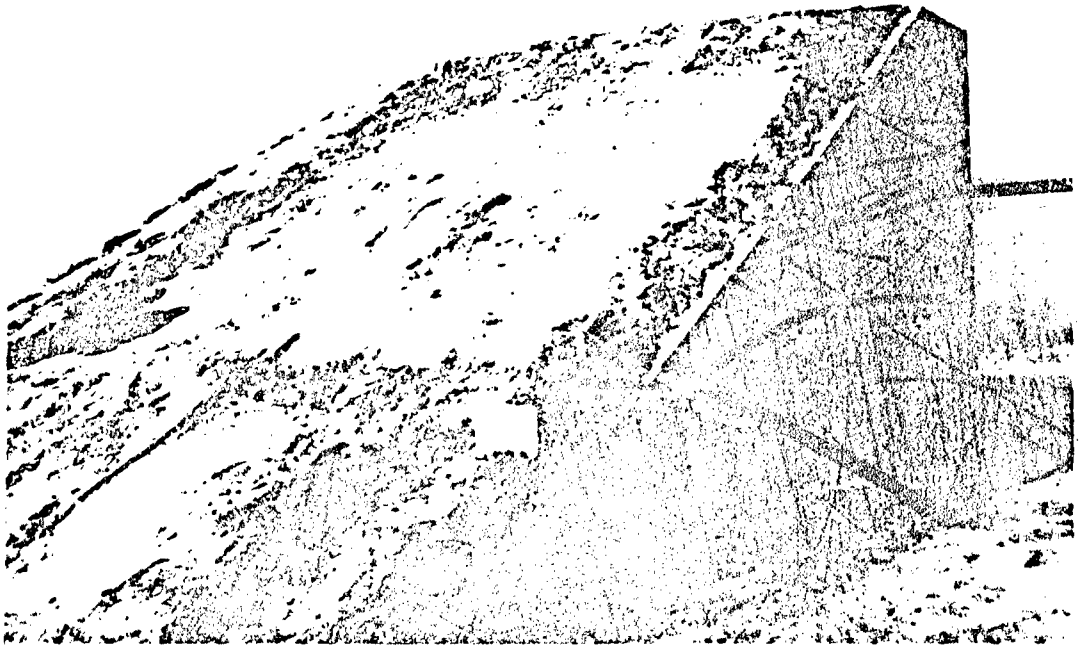

Front

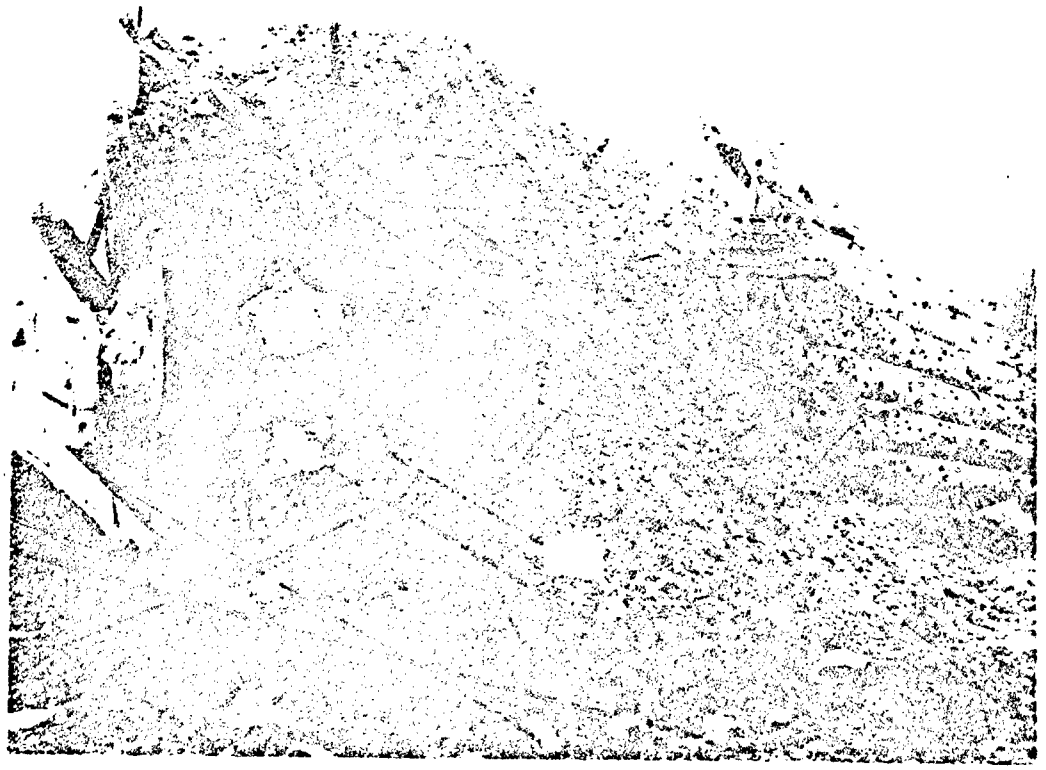

Rear


Side
Bottom
Top


Front

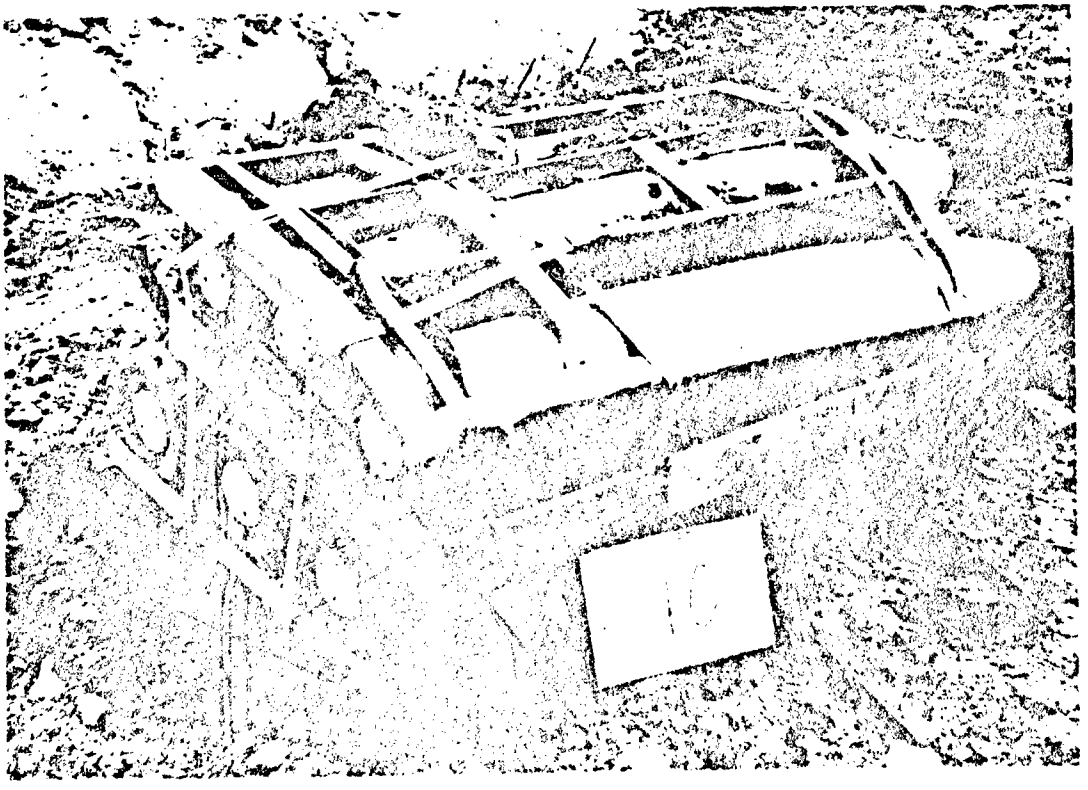

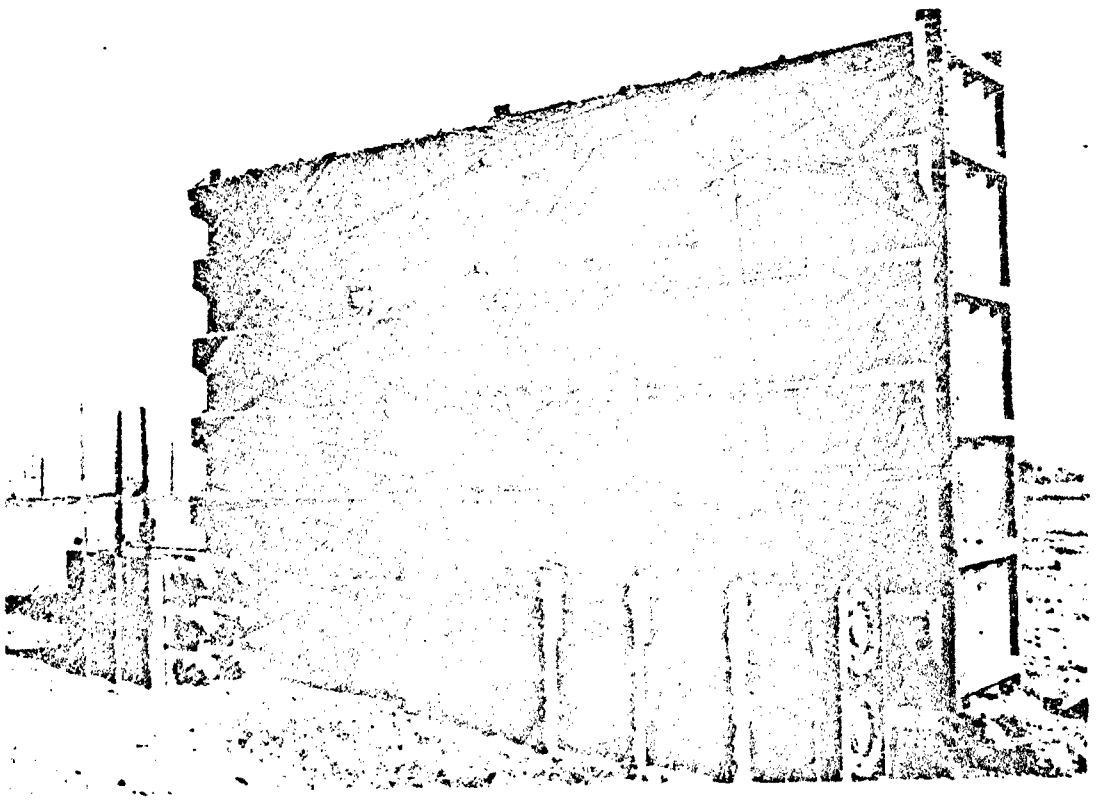

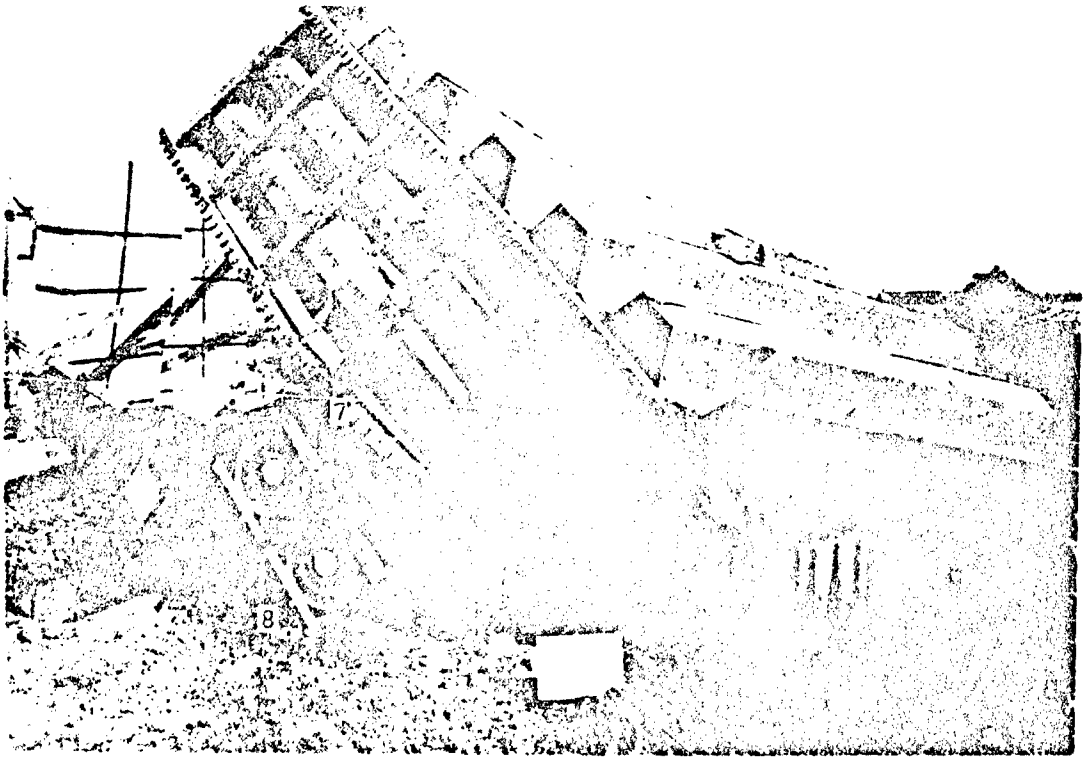

Front

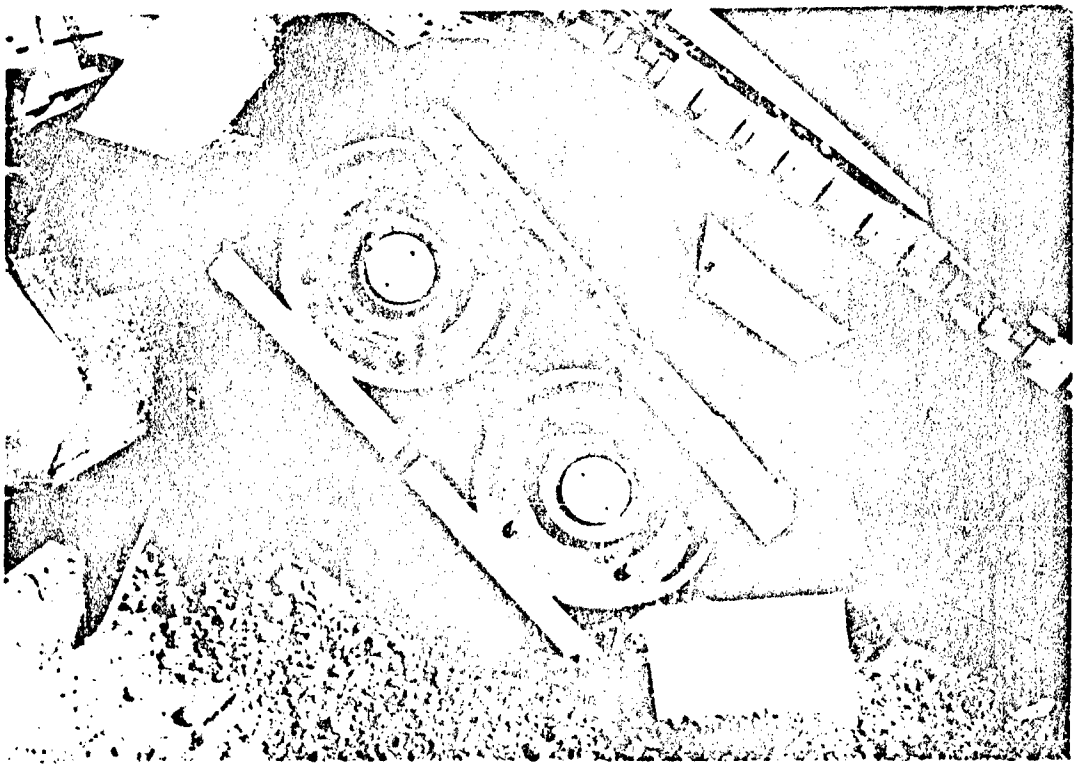

Front

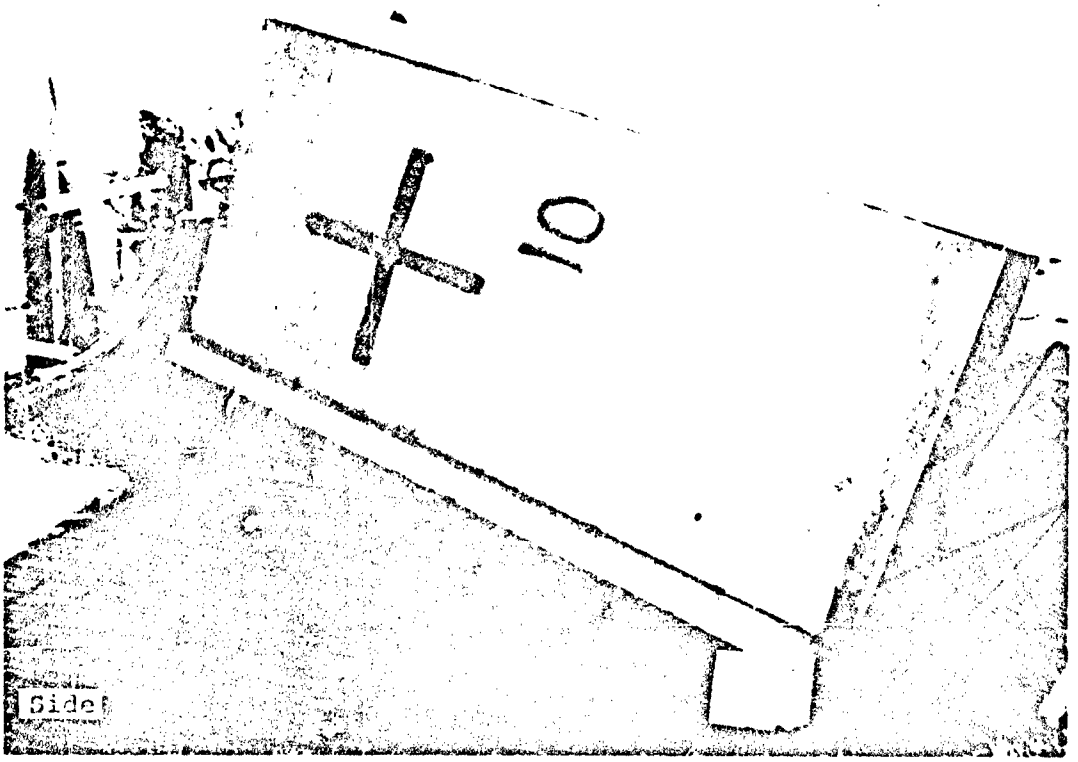

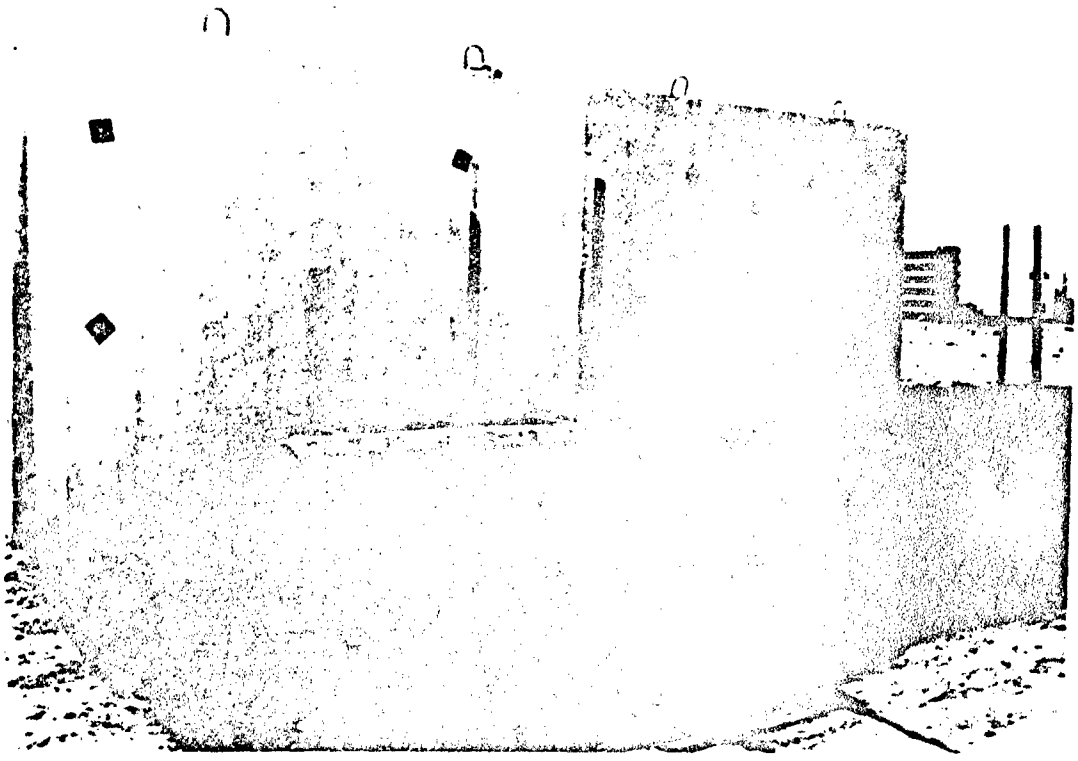

BARRICADES

by
Adib R. Farsoun
Structural Engineer

U.S. Army Engineer Division, Huntsville
Huntsville, Alabama

ABSTRACT

This paper identifies new barricade types which can be used to protect buildings, installation access points, explosive handling facilities, and high-value equipment storage areas. The concepts presented herein have been extracted from Definitive (Conceptual) Drawings under development by the U.S. Army Engineer Division, Huntsville.

1.0 INTRODUCTION

1.1 Background

The traditional barricades used at Army facilities have, for the most part, been limited to earth mounds, timber, and cast-in-place revetted retaining wall structures. These traditional systems are fast becoming obsolete due to newer cost effective retaining wall systems. In part, this was recognized in May 1978 when Corps of Engineers staff elements recommended and received approval from Department of Defense Explosive Safety Board (DDESB) to use the reinforced earth system as an alternate to conventional systems. Since its approval, this reinforced earth system has been used on several Army projects with demonstrated effectiveness as a protective structure. The performance of this system, coupled with the number of alternatives now available for retaining the earth, identified a need for updating criteria and barricade types. At the direction of Headquarters, U.S. Army Corps of Engineers (HQUSACE), the Huntsville Division prepared a set of Definitive Drawings (DEF 149-30-01) delineating barricade types suitable in shielding assets against fragment hazard and blast attenuation in the near range. The concepts presented promulgate criteria found in AMC-R-385-100, DOD 6055.9STD, and AR 385-64.

1.2 Use of Barricades

Barricades, for the most part, have been used as intervening structures between explosive handling facilities. Recent studies have found barricades to be a highly cost effective means of providing blast and fragment protection to existing construction. The Naval Facilities Engineering Command identified the reinforced earth berm suitable for upgrading survivability of existing buildings. Also, in recent months there have been an awareness and a special need for protecting government assets in CONUS and OCONUS from terrorist threats and attacks. This, therefore, placed increased emphasis on identifying unobtrusive barricade structures suitable for reducing vulnerabilities to assets. The newer systems appear to fit these requirements.

1.3 Selection of Barricade Type

Selection of which barricade to use is no simple task. Considerations must be given to:

- Boundary constraints
- Geotechnical conditions
- Availability of materials
- Availability of special contractors
- Aesthetic requirements
- Necessary service life
- Barricade heights
- Relocation requirements
- Cost

1.4 Definitive Drawings Procurement Procedures

Army installations may request copies of Definitive Drawing (DEF 149-30-01) from the Huntsville Division. Inquiries should be directed to:

Commander
U.S. Army Engineer Division, Huntsville
ATTN: CEHND-ED-ES (Service Section)
PO Box 1600
Huntsville, AL 35807-4301
205-895-5560 or AUTOVON 742-5560

Technical inquiries should be directed to Mr. Adib Farsoun, commercial 205-895-5410 or AUTOVON 742-5410.

2.0 CRITERIA

2.1 General

Barricading in the traditional sense has been used between adjoining buildings/structures to:

a. Allow buildings to be separated by barricaded intraline distance ($9w^{1/3}$ft., $3.60\ Q^{1/3}$m),

b. Protect ammunitions, explosives, structures, operations, or personnel by limiting the effect of an explosion and

c. Eliminate the necessity for totaling net explosive weight (NEW) by restricting explosive communication.

2.2 Means of Barricading

The three means of barricading frequently used in achieving the above objectives are (1) effective dividing walls, (2) effective earth barricades, and (3) structural burial.

2.3 Function and Limitation

Barricades are intervening structures located between the donor (source) and the acceptor (receiver). Their primary function is to reduce further explosion communication and fragment damage. They do provide protection against high velocity, low-angle fragments although the barricades may be destroyed in the process. Barricades do provide limited protection against blast overpressures in the near range (a distance of 2 to 10 times the barricade height). However, they are ineffective in reducing blast pressures in the far range (inhabited building or public traffic route distance).

2.4 Location of Barricades

The location of a barricade(s) is a compromise. The closer a barricade is to the stack of ammunition or explosives or buildings the less the height and length of the barricade required to secure proper geometry for intercepting projections. However, barricades located near the donor structure will not modify the blast wave overpressure at the downstream acceptor structure. On the other hand, by locating barricades near the target structure (acceptor) the effects of the reflected pressure are reduced. The Naval Facilities Engineering Command has studied the effects of aerodynamic obstructions on overpressure effects. Tests conducted found when long obstructions are placed within one height of the structure, blast pressures approached side on levels.

2.5 Types of Barricades

While the current practice in barricade construction has been limited somewhat to earth mounds, single revetted, earth steel bins and reinforced earth systems, the number of alternatives to retain earth has been significantly increased especially precast concrete systems. Since these newer systems are essentially modern equivalents of earlier systems, it is fair to surmise that they are just as effective as the conventional barricades presently in use. These newer systems are less costly, quicker to build, and will tolerate more significant settlement than the traditional cast-in-place retaining wall system.

3.0 BARRICADES

3.1 General

With the exception of the earth mound type, barricades can be classified as retaining wall structures located between an explosive source and a protected facility or building. They can be single revetted or double revetted. In most cases, project constraints dictate which type should be considered/ selected, and due to the different types now available, the engineer's choice is difficult at best. As previously discussed, the cast-in-place (CIP) retaining wall type has been significantly used as a barricade structure. Even with the newer systems now available, the CIP wall system continues to be economical at small wall heights (up to 15 feet). However, above 15 feet the trend is in the direction of precast wall systems. These systems can be constructed for 30 to 50 percent less than conventional walls. Representative 1988 cost and installation rates for high walls are as follows:

	Conventional CIP	Precast Systems
Cost (per sq. ft. of wall face)	$60 to $70	$30 to $40
Installation Rate (sq. ft. per shift)	$200 (10 man crew)	$1000 (5 man crew)

3.2 Earth Mound (B1), Figure 1

The earth mound type barricade with slopes not steeper than 2 to 1 and crest 3 feet wide is the traditional system used in the vicinity of ammunition or explosive storage facilities. The barricade is easily constructed with local fill materials using unskilled labor. Because of requirement for flat slopes, they are unsuitable near site boundaries and near obstructions. They are most suited as intervening structures between adjoining facilities. To minimize slope erosion, seeding or chemical treatment shall be provided. The former method is widely used.

3.3 Reinforced Earth Mounds (B2 and B3), Figures 2 and 3

These barricades use soil reinforcements embedded in the soil to form a reinforced soil composite system that has high internal stability, thus allowing slopes steeper than the soil's natural angle of repose. The result is reduced fill when compared to the conventional unreinforced earth mound (B1). These barricades provide economic solutions to conditions where right-of-way is limited and when fill is scarce or expensive. Soil reinforcements are generally polymer type materials with varied grid configurations. Design of these reinforced slopes will involve determining desired slope geometry, number and type of reinforcements, embedded lengths and vertical spacing. Technical services are usually available from product manufacturers and/or technical literature. With slopes steeper than 50 degrees, the wrap around technique (B3) is recommended to simplify construction. Erosion protection may be provided over the finished sloped faces as required.

3.4 Timber W/Tieback (B4 and B5), Figures 4 and 5

The timber tieback walls B4 and B5 are earth-retention systems frequently used at Army facilities to stop fragments. They differ from other retaining wall systems only because earth pressures acting on the facing elements are resisted by tiebacks. Walls under 10 feet generally are economically constructed without tiebacks. Consideration must be given to corrosion protection of tiebacks when installed in aggressive environments. The method of protection shall give consideration to groundwater PH, when applicable, and soluble sulfate contents. These barricade types are constructed with unskilled labor.

3.5 Sand Bag - Single Revetted (B6), Figure 6

This barricade type is constructed of sand bags filled with sand and stacked atop one another to form a gravity-type wall. Sand bag single revetted are very flexible, easy to erect, and relatively inexpensive. They are most suited in remote areas. Aesthetically, they are not pleasing, and the sand bags may become a source of secondary fragments.

3.6 Concrete Gravity Wall - Single Revetted (B7), Figure 7

Commonly constructed of non-reinforced concrete. They resist earth pressure by virtue of their weight or mass, which provides stability against overturning and sliding. They are relatively simple structures and can be build with unskilled labor. Gravity walls are commonly constructed with battered front face with either vertical or stepped backs. They are suitable for most types of backfill with the exception of very soft clay, organic silt or silt clay because of large lateral or overturning pressures. When used to resist fragments only, the backfill may be deleted. With special finishes at the front face it is possible to achieve desired aesthetics (exposed aggregate, colored concrete, etc.).

3.7 Timber - Double Revetted (B8), Figure 8

This barricade is similar to the single revetted types B4 and B5. The double revetted timber barricade is suited for construction near site boundaries or near obstructions. Consideration shall be given to overturning when siting near buildings to be protected.

3.8 Reinforced Soil - Single Revetted (B9), Figure 9

a. When thinking of reinforced soil, we naturally think of the retaining wall system introduced under the proprietary name "The Reinforced Earth Company." As mentioned in Section 1.0 above, this system has been used on several Army projects as an effective means of barricading structures, operating lines, etc. Since its introduction, several modern equivalents of this system are now on the market. In brief, the concept of soil retention is reinforcement of the backfill to create a self-supporting block of soil.

b. This barricade concept consists of approved fill (free-draining) reinforced with successive layers of reinforcing strips which in turn are connected to facing elements. These facing elements can either be metal or concrete panels stacked atop one another. Typically, the length of reinforcements range from 0.70 to 1.0 times the wall height. This embedment requirement is typical of most "stabilized earth" systems, and is necessary to prevent reinforcement pullout. Vertical spacing between reinforcements varies from 1 to 3 feet and horizontal spacing from 2 to 5 feet. Metal strips, when used, are galvanized to protect against corrosion. This reinforced earth barricade system offers several advantages in terms of flexibility, ease and speed of construction, product quality, and appearance. Manufacturers of similar systems are identified.

3.9 Reinforced Soil - Double Revetted (B10), Figure 10

This barricade type is similar to type B9, but uses the double revetted concept in lieu of the single revetted. This is most suited where right-of-way is limited an in close proximity of buildings. Unlike type B9, the design must give consideration to overturning when significant overpressures are anticipated.

3.10 Wrap Around Retaining Wall (B11), Figure 11

This barricade concept is similar to type B3 discussed above. The concept utilizes the wrap around technique which allow vertical wall face construction. The polymer reinforcements provide a corrosion-free system, while providing substantial savings over conventional retaining wall system (cast-in-place, gravity, etc.). The non-load bearing facing element is optional and can be either timber, steel or concrete. It provides desired architectural finish. The concept utilizes drain rock at the front face for reducing hydrostatic earth pressure build-up.

3.11 Waffle Crete Retaining Wall (B12), Figure 12

This wall is a joint venture between Tensar and Van Doren Industries also known as Geowall system. This retaining wall system uses waffle crete panels for the facing and tensar geogrid as soil reinforcements. Walls as high as 16 feet are possible with this system. As most reinforced earth systems, the length of reinforcement is approximately 0.70 times the wall height. The system's benefits are similar to other reinforced earth structures. The system offers a maintenance free structure with a wide variety of architectural finishes.

3.12 Cantilever Retaining Wall (B13), Figure 13

Several Army facilities have used this traditional system as an effective means for protecting facilities and in particular ammunition storage magazines. This traditional cast-in-place concrete system is fast becoming obsolete due to the high cost when compared to the newer retaining wall systems. Counterfort walls are normally used for heights greater than 20 feet. Both types (cantilever and counterfort) require careful design and significant formwork. Due to their rigidity, they are susceptible to cracking due to settlement. In locations of poor soil condition, they require large bases to satisfy allowable soil bearing pressures.

3.13 Precast Double Tees (B14), Figure 14

This retaining wall system consists of a precast double tee wall panel and anchored to a cast-in-place concrete footing. The system utilizes post-tensioning bars threaded into anchors embedded in the footing to resist soil earth pressures. This innovative retaining system was recently used on I-70 in Colorado for Colorado Division of Highways. Structural Engineer and General Contractor were Deleuw Cather and Flatiron Structures Company, respectively. This retaining wall concept is suitable for constructing barricades. The system is aesthetically pleasing and can be efficiently used when high barricades are required.

3.14 Concrete Blast Wall (B15), Figure 15

This is the traditional effective dividing wall composed of laced reinforced concrete and designed in conformance with TM 5-1300 [Ref. 3]. Its effectiveness to protect personnel and facilities has been demonstrated by the unfortunate occurrences of accidental explosions of munitions and explosives. This concept is most suited for resisting blast pressure loadings, and usually used to resist the explosive output of close-in detonations. Although the construction of this laced reinforced concrete system is similar to conventional wall systems, some changes in the fabrication and construction procedures are required.

3.15 Composite Wall System (B16), Figure 16

A newcomer to protective design is this composite structural system marketed under the registered trademark (ASP Walling System). This ASP system (Agan Steel Panels) provides an alternate to type B15 discussed above. The composite walling system of steel and concrete provides protection against weapons effects to include blast fragment resistance. The system consists of formed steel sheets that are interlocked to constitute the formwork prior to concrete placement. The system, according to manufacturer's literature, can be designed to cater to an extensive range of conventional military weapons.

3.16 Steel Bin (B17), Figure 17

The steel bin barricade has been widely used on Army projects. This barricade type consists of lightweight pre-engineered steel members assembled in place to form a box-like structure. The bins are filled with soil or rock to form the retaining wall system. The bins are occasionally tilted backward for greater stability. The structural elements, comprising the walls, are easily transported and assembled without the need of heavy equipment. Site preparation is minimal. Walls up to 40 feet in height are possible, and the system can be disassembled, transported, and reinstalled when necessary. The system's unique design allows flexing against minor unforeseen ground movements (settlement). As most retaining structures, the backfill shall be well-graded pervious materials for proper drainage. The cross-section shown may be constructed without the exterior berm when fragments are the controlling design condition.

3.17 Concrete Cribbing (B18), Figure 18

Concrete crib walls provide effective protection of facilities at a reasonable cost. Built like log cabins, the precast element creates a box-like structure which when filled with granular soil provides stability against overturning. Crib walls, when used as a barricade, provide a relative cheap barricade. The system is flexible enough to tolerate some differential settlement. The cross section is shown without the earth berm behind the crib. This configuration is most suited for fragment resistance. Stability of the retaining wall system against blast pressures requires the inclusion of an earth berm to resist the overturning.

3.18 Precast Concrete Bin (B19), Figure 19

Precast concrete for retaining walls has become a popular system for retaining the soil (holding back the earth). One advantage of this system is rapidity of construction, quality and tolerance to settlement. Interlocking precast bins are stacked atop one another and filled with granular soil. No mechanical or grouted connections are required. Precast units arrive on the job site ready for installation. Installation rates to 2,000 sq. ft. a day are possible with a crew of four (three laborers and one foreman). Some advantages are: reduced on-site labor, easily erected, reduced costs, erected regardless of temperature, and aesthetically pleasing.

3.19 Precast T-Wall (B20), Figure 20

T-Wall is a precast concrete retaining wall system that is engineered for economy. This system incorporates the advantages of precast concrete, namely quality control, improved construction scheduling and long life. T-Wall is available through local precasters. As with most systems, select backfill is required with subgrade compaction to 95 percent standard density. Battered wall section is possible. The obvious advantages are simplicity, ease of construction and flexibility to meet project geometry with standard components.

3.20 Timber Crib (B21), Figure 21

Components of a timber crib are similar to concrete crib walls. Present state-of-the-art is to interlock the structural members using mechanical connectors, as opposed to earlier methods of connections using lapped (notched) joints. Timber crib walls are moderately flexible and, therefore, can tolerate differential settlement. Using various combinations of base width, timber crib walls are suitable for heights of approximately 30 feet. It is generally accepted that battered crib sections offer several advantages:

a. Less structure is required than for a vertical wall the same height.

b. Crib fill is likely to ravel out the front face of the structure.

c. Vegetation is more easily planted and established.

One drawback of timber cribbing is the necessity for timber treatment with preservative or pressure-treatment.

3.21 Earth-Filled Concrete Wall (B22), Figure 22

This system uses a double cast-in-place retaining wall system. The box-like structure is filled with granular fill. As all cast-in-place structures, extensive forming is required and system is susceptible to cracking due to settlement. This system is effective near boundaries and obstructions.

4.0 CONCLUSIONS AND RECOMMENDATIONS

4.1 Conclusions

a. Retaining wall systems used as barricades at Army facilities have been limited. Earth mounds, timber-revetted and cast-in-place concrete have been the traditional systems used. These systems have occasionally been replaced by steel bins and the patented reinforced earth systems.

b. Barricades meeting the required criteria can be built from newer retaining wall systems. The newer systems are less costly and quicker to build.

c. The U.S. Army Engineer Division, Huntsville has identified a wide range of retaining wall systems suitable for adaptation to barricade construction for protecting structures, operations, etc. As stated in sections of this report, the barricades have limited effectiveness against blast overpressures. They are most effective against high velocity, low angle fragments. Since it is recognized that the barricade may be destroyed when subjected to blast load overpressure, the designer must give consideration to barricade overturning when barricades are sited in close proximity of protected facilities.

d. DoD 6055.9-STD eludes to the necessity for testing unproven intervening barriers (paragraph 5.c.2.). Since many of the barricade types identified in this study are modern equivalents of earlier tested systems (i.e. The Reinforced Earth Company), they are as effective as the traditional systems presently used.

e. Selection of a suitable system entails a wide variety of choices. Consideration must be given to site constraints, aesthetics, material availability, limitations and cost. Some systems have height limitations, others require special backfill.

f. The survey of retaining wall systems revealed a trend toward precast systems due to higher quality and tolerance to settlement.

4.2 Recommendations

a. Designers should be allowed to select a barricade that meets not only functional criteria, but also aesthetics.

b. Require designers to obtain cost data from system manufacturers based on specific design requirements and features.

c. Require designers to provide complete contract plans for all competitive alternates suited for the particular site.

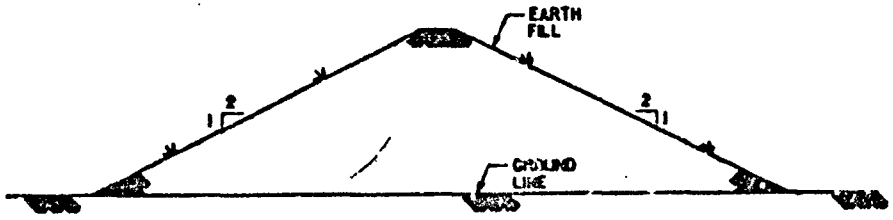

BI - EARTH MOUND

REMARKS:

1. CAN BE RAPIDLY CONSTRUCTED WITH UNSKILLED LABOR.
2. NO HEIGHT OR LENGTH LIMITATIONS.
3. UNSUITABLE WHERE SPACE IS LIMITED.
4. REQUIRES SOIL STABILIZATION (SEEDING, ETC.)
5. REQUIRES REPEATED MAINTENANCE.

2335

FIGURE 1

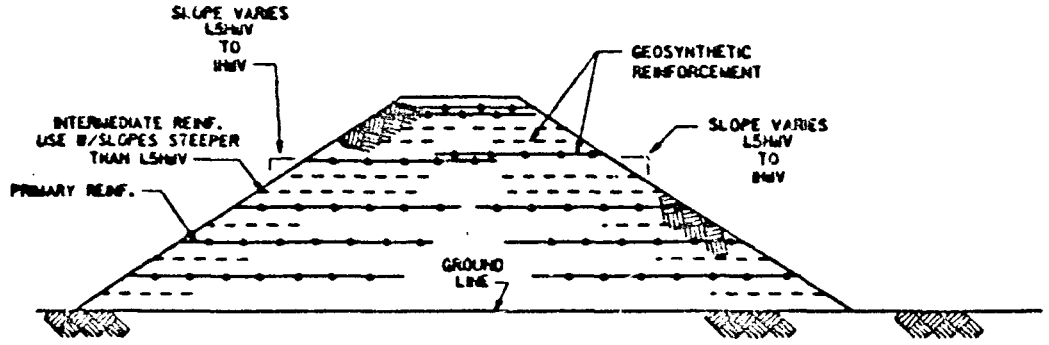

B2 - REINFORCED EARTH MOUND

REMARKS:

1. REDUCED FILL REQUIREMENT OVER UNREINFORCED EARTH MOUND.
2. EFFICIENT CONSTRUCTION AND USE OF LAND.
3. CAN BE RAPIDLY CONSTRUCTED WITH UNSKILLED LABOR.
4. ALLOWS CONSTRUCTION OF STEEPER SLOPES THAN THE SOIL'S NATURAL ANGLE OF REPOSE.
5. NO HEIGHT OR LENGTH LIMITATIONS.
6. REINFORCEMENT IS LIGHTWEIGHT AND EASILY CUT ON SITE.
7. REQUIRES SOIL STABILIZATION. GRASS COVER, IF USED, IS DIFFICULT TO MAINTAIN.
8. GEOSYNTHETIC REINFORCEMENT IS PLASTIC MESH MADE OF HIGH-DENSITY POLYMERS.
   SOURCE: THE TENSAR CORP.
   P.O.BOX 986
   MORROW, GA. 80260
   (404) 968-3255

2336

FIGURE 2

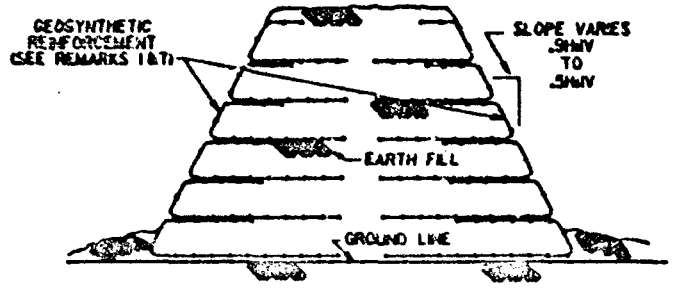

B3 - WRAP-AROUND REINFORCED EARTH MOUND

REMARKS:

1. A FINE MESH POLYMER NET REQUIRED FOR EROSION CONTROL.
2. REQUIRES LESS FILL THAN B1 OR B2.
3. CAN BE LOCATED CLOSE TO SITE BOUNDARIES OR OBSTRUCTIONS.
4. CAN BE RAPIDLY CONSTRUCTED WITH UNSKILLED LABOR.
5. REINFORCEMENT IS LIGHTWEIGHT AND EASILY CUT ON SITE.
6. TEMPORARY SUPPORTS REQUIRED AT FACES DURING CONSTRUCTION.
7. GEOSYNTHETIC REINFORCEMENT IS PLASTIC MESH MADE OF HIGH-DENSITY POLYMERS.

SOURCE: THE TENSAR CORP.
P.O.BOX 986
MORROW, GA. 80260
(404) 968-3255

2337

FIGURE 3

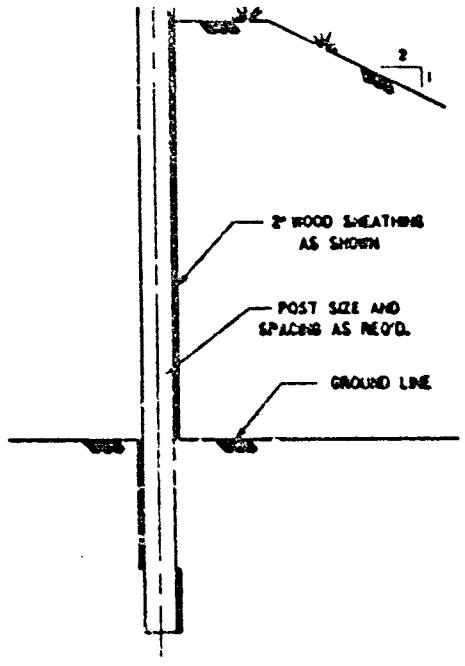

TYPE A - WALL HEIGHT
10 FEET OR LESS

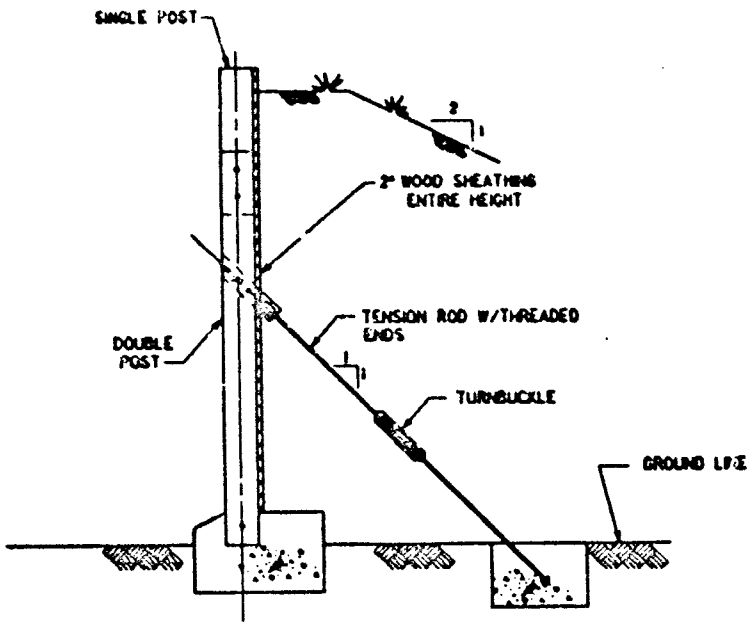

TYPE B - WALL HEIGHT
GREATER THAN 10 FEET

B4 - TIMBER - SINGLE REVETTED

REMARKS:

1. ALL LUMBER SHALL BE PRESSURE TREATED WITH PRESERVATIVES.
2. CAN BE RAPIDLY CONSTRUCTED WITH UNSKILLED LABOR.
3. REQUIRES SOIL STABILIZATION (SEEDING, ETC.)
4. AESTHETICALLY NOT PLEASING.
5. REQUIRES REPEATED MAINTENANCE.

FIGURE 4

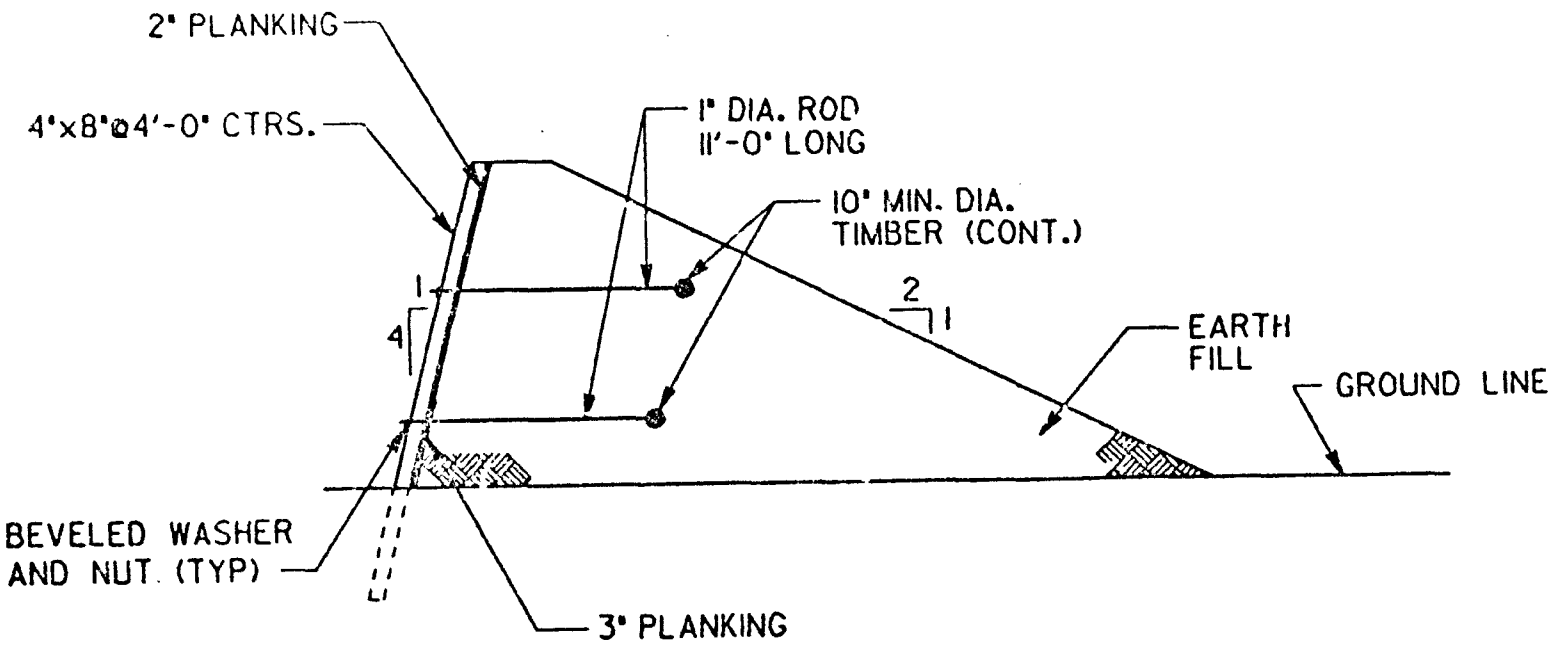

2339

B5 - TIMBER - SINGLE REVETTED

REMARKS:

1. ALL LUMBER SHALL BE PRESSURE TREATED WITH PRESERVATIVES.
2. CAN BE RAPIDLY CONSTRUCTED WITH UNSKILLED LABOR.
3. REQUIRES SOIL STABILIZATION (SEEDING, ETC.)
4. AESTHETICALLY NOT PLEASING.
5. REQUIRES REPEATED MAINTENANCE.

FIGURE 5

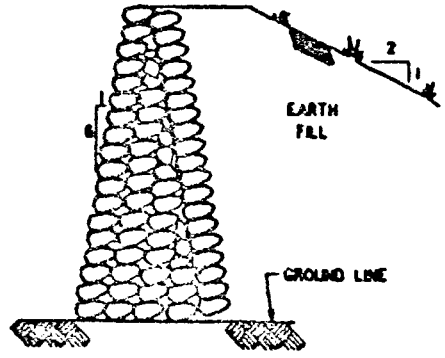

B6 - SAND BAG - SINGLE REVETTED

REMARKS:

1. SANDBAGS MAY BECOME SECONDARY FRAGMENTS AS A RESULT OF HIGH OVERPRESSURES.
2. AESTHETICALLY NOT PLEASING.
3. SIMPLE TO CONSTRUCT WITH UNSKILLED LABOR.
4. SUITABLE FOR REMOTE LOCATIONS.
5. SANDBAGS WILL DETERIORATE WITH TIME.
6. REQUIRES SLOPE STABILIZATION IF CONSTRUCTED FOR OTHER THAN TEMPORARY USE.

FIGURE 6

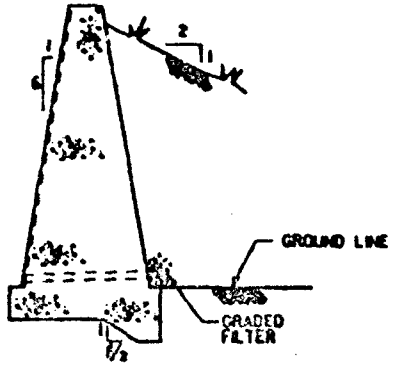

B7 - CONCRETE GRAVITY WALL - SINGLE REVETTED

REMARKS:

1. CAN BE BUILT WITH UNSKILLED LABOR AND LOCALLY AVAILABLE MATERIALS.
2. EXPOSED AGGREGATE FINISH POSSIBLE.
3. DELETE IF ONLY FRAGMENT RESISTANCE REQUIRED.
4. IF EARTH FILL IS PLACED BEHIND WALL, STABILITY OF WALL MUST BE CHECKED ON A CASE-BY-CASE BASIS.

2341

FIGURE 7

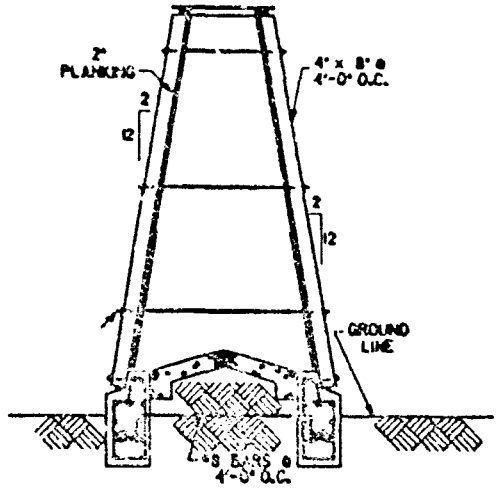

B8 - TIMBER - DOUBLE REVETTED

REMARKS:

1. ALL LUMBER SHALL BE PRESSURE TREATED WITH PRESERVATIVES.
2. CAN BE RAPIDLY CONSTRUCTED WITH UNSKILLED LABOR.
3. CAN BE LOCATED CLOSE TO SITE BOUNDARIES OR RESTRICTIONS.
4. CAN TOLERATE SIGNIFICANT AMOUNT OF SETTLEMENT.
5. AESTHETICALLY NOT PLEASING.
6. REQUIRES REPEATED MAINTENANCE.

FIGURE 8

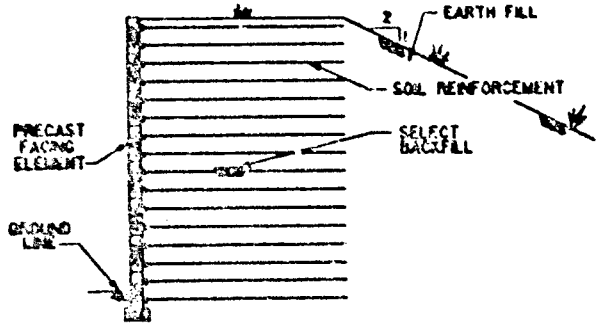

B9 - REINFORCED SOIL - SINGLE REVETTED

REMARKS:

1. CAN BE ECONOMICALLY AND RAPIDLY CONSTRUCTED.
2. REQUIRES SHALLOW FOUNDATION.
3. VARIETY OF ARCHITECTURAL FACING ELEMENTS AND FINISHES AVAILABLE (CRUCIFORM, HEXAGONAL, RIBBED, ETC.)
4. NO HEIGHT OR LENGTH LIMITATIONS.
5. FACING ELEMENTS ARE REUSABLE.
6. WALLS CAN BE LOCATED CLOSE TO SITE BOUNDARIES OR OBSTRUCTIONS.
7. SYSTEM ADAPTABLE TO SLOPING WALL CONFIGURATIONS AND TO TIERS.
8. SYSTEM CAN TOLERATE SIGNIFICANT AMOUNT OF SETTLEMENT.
9. REPAIR CAN BE ACCOMPLISHED ON INDIVIDUAL FACING ELEMENTS.
10. GALVANIZED STRIPS, STEEL WIRE MESH, GEOSYNTHETIC, ETC. ARE USED FOR SOIL REINFORCEMENT.
11. GRANULAR MATERIALS ARE GENERALLY USED TO PROVIDE PROPER DRAINAGE. SELECTION OF BACKFILL SHALL BE AS RECOMMENDED BY THE SYSTEMS MANUFACTURER.
12. REQUIRES SLOPE STABILIZATION (SEEDING, ETC.).
13. PATENTED SYSTEMS:
    a. REINFORCED EARTH CO.
    1911 TWENTY SECOND ST. N.W.
    WASH., D.C. 20037
    (202) 223-3434

    b. VSL CORPORATION
    101 ALBRIGHT WAY
    LOS GATOS, CA. 95030
    (408) 866-5000

    c. NILFISK WALLS
    P.O. BOX 2012
    EUREKA, CA. 95502
    (707) 443-5093

2343

FIGURE 9

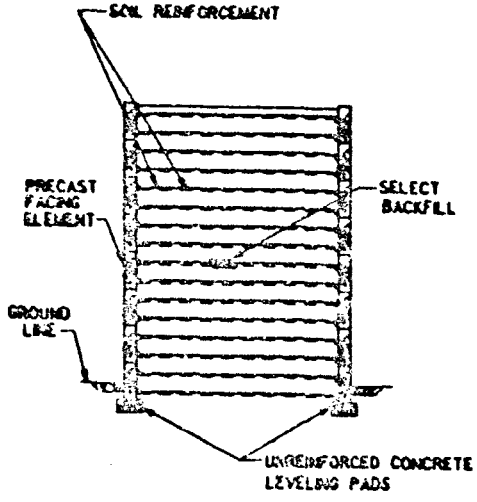

B10 - REINFORCED SOIL - DOUBLE REVETTED

2344

FIGURE 10

REMARKS:

1. CAN BE ECONOMICALLY AND RAPIDLY CONSTRUCTED.
2. REQUIRES SHALLOW FOUNDATION.
3. VARIETY OF ARCHITECTURAL FACING ELEMENTS AND FINISHES AVAILABLE (CRUCIFORM, HEXAGONAL, RIBBED, ETC.)
4. NO HEIGHT OR LENGTH LIMITATIONS.
5. FACING ELEMENTS ARE REUSABLE.
6. WALLS CAN BE LOCATED CLOSE TO SITE BOUNDARIES OR OBSTRUCTIONS.
7. SYSTEM ADAPTABLE TO SLOPING WALL CONFIGURATIONS AND TO TIERS.
8. SYSTEM CAN TOLERATE SIGNIFICANT AMOUNT OF SETTLEMENT.
9. REPAIR CAN BE ACCOMPLISHED ON INDIVIDUAL FACING ELEMENTS.
10. GALVANIZED STRIPS, STEEL WIRE MESH, GEOSYNTHETIC, ETC. ARE USED FOR SOIL REINFORCEMENT.
11. GRANULAR MATERIALS ARE GENERALLY USED TO PROVIDE PROPER DRAINAGE. SELECTION OF BACKFILL SHALL BE AS RECOMMENDED BY THE SYSTEMS MANUFACTURER.
12. REQUIRES SLOPE STABILIZATION (SEEDING, ETC.).
13. PATENTED SYSTEMS:
    a. REINFORCED EARTH CO.
       1414 TWENTY SECOND ST. N.W.
       WASH., D.C. 20037
       (202) 223-3434
    b. VSL CORPORATION
       101 ALBRIGHT WAY
       LOS GATOS, CA. 95030
       (408) 356-5200
    c. HILFIKER WALLS
       P.O. BOX 2012
       EUREKA, CA. 95502
       (707) 443-5093

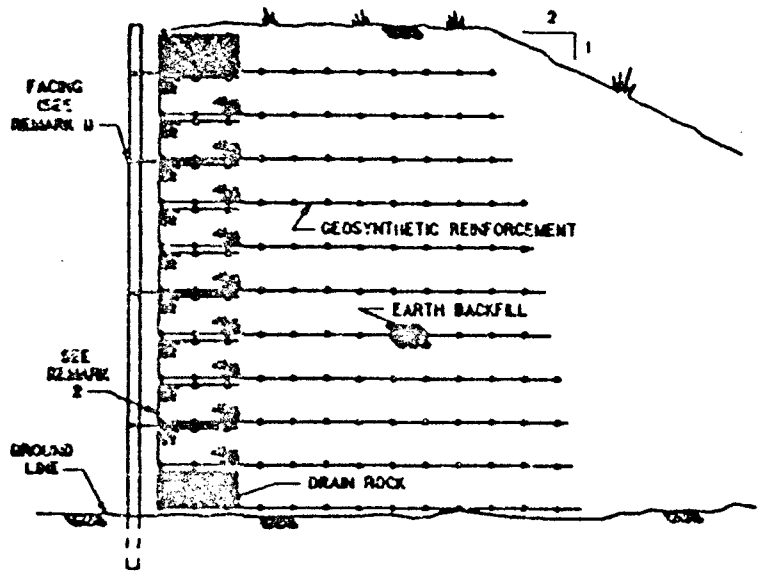

B11 - WRAPAROUND RETAINING WALL

REMARKS:

1. FACING CAN BE SELECTED TO ACHIEVE DESIRED ARCHITECTURAL FINISH. EXAMPLE: SOLDIER PILE AND LAGGING FACING, PRECAST CONCRETE, ETC.
2. GEOSYNTHETIC FINE MESH IS USED TO CONTAIN SOIL OR SAND FILL.
3. CAN BE ECONOMICALLY AND RAPIDLY CONSTRUCTED.
4. REQUIRES SHALLOW FOUNDATION.
5. SYSTEM CAN TOLERATE SIGNIFICANT AMOUNT OF SETTLEMENT.
6. REQUIRES SLOPE STABILIZATION (SEEDING, ETC.).
7. GEOSYNTHETIC REINFORCEMENT IS PLASTIC MESH MADE OF HIGH DENSITY POLYMER.
8. SUPPLIER:

   TENSAR CORPORATION
   P.O. BOX 49526
   ATLANTA, GA. 30359
   (404) 325-0814

2345

FIGURE 11

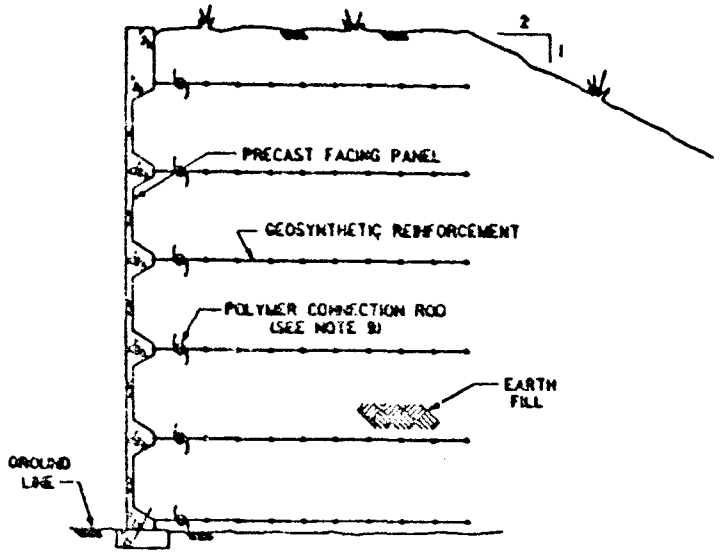

2346

B12 - WAFFLE-CRETE RETAINING WALL

REMARKS:

1. PRECAST FACING PANELS ARE LIGHTWEIGHT.
2. PANELS MUST BE EXTERNALLY BRACED DURING CONSTRUCTION.
3. WALL REQUIRES BATTER OF 1/8" PER FOOT.
4. VARIETY OF DIFFERENT PRECAST FACING PANELS ARE AVAILABLE, WITH WIDE VARIETY OF FINISHES.
5. LIMITED TO 20 FEET IN HEIGHT.
6. PROPRIETARY WAFFLE-CRETE PANELS SHOWN. OTHER FACING SYSTEMS MAY BE SUBSTITUTED.
7. REQUIRES SLOPE STABILIZATION (SEEDING, ETC.).
8. GEOSYNTHETIC REINFORCEMENT IS PLASTIC MESH MADE OF HIGH DENSITY POLYMER.
9. POLYMER CONNECTION ROD IS USED TO CONNECT THE PRECAST FACING PANEL TABS TO THE GEOSYNTHETIC REINFORCEMENTS.
7. SUPPLIER:
   TENSAR CORPORATION
   P.O. BOX 49526
   ATLANTA, GA. 30359
   (404) 325-0814

FIGURE 12

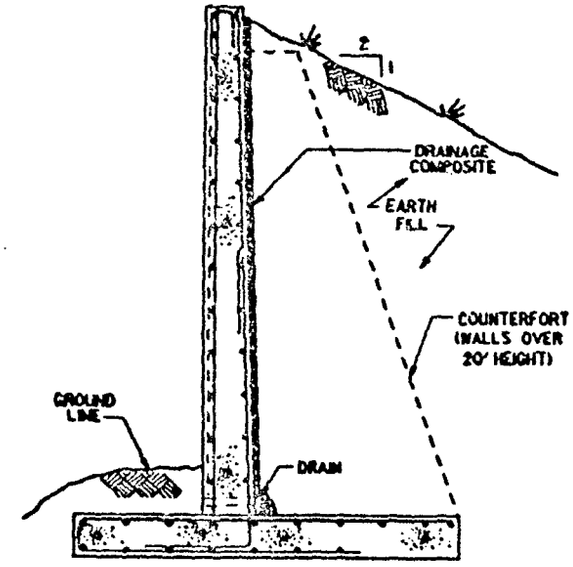

B13 - CANTILEVER RETAINING WALL

REMARKS:

1. REQUIRES EXTENSIVE FORMING AND CONSTRUCTION TIME.
2. NOT COST EFFECTIVE FOR HIGH WALLS.
3. CONCRETE THICKNESS, REINFORCING STEEL, AND TOE LENGTH MUST BE DESIGNED ON A CASE-BY-CASE BASIS.

2347

FIGURE 13

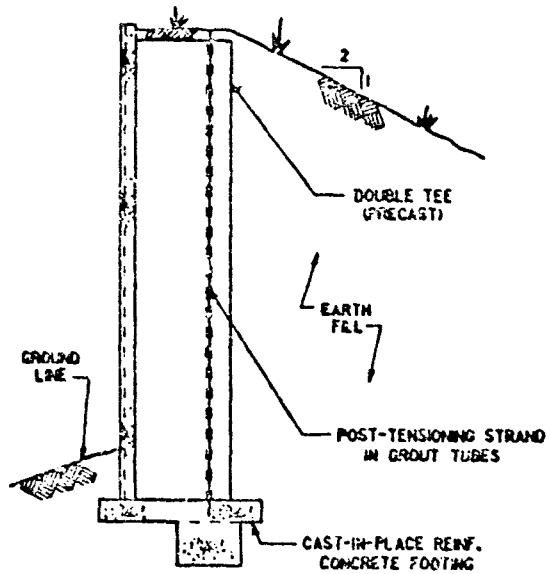

B14 - PRECAST DOUBLE TEES

REMARKS:

1. REQUIRES NO COSTLY FORMWORK.
2. VARIETY OF ARCHITECTURAL FINISHES POSSIBLE.
3. WITHOUT PRESTRESSING, THICK STEMS AND MORE THAN NORMAL REINFORCEMENTS REQUIRED.
4. CRANE EQUIPMENT REQUIRED FOR HANDLING AND ERECTION.
5. SHIMS FOR LEVELING AND NON-SHRINK, NON-METALLIC GROUT REQUIRED PRIOR TO POST-TENSIONING.
6. FOOTINGS REQUIRE ANCHORS FOR POST-TENSIONING.
7. AN INNOVATIVE RETAINING SYSTEM USED BY COLORADO DIVISION OF HIGHWAYS.

FIGURE 14

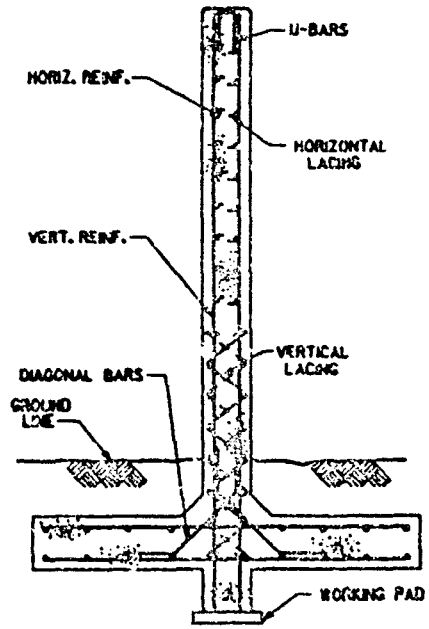

B15 - CONCRETE BLAST WALL

REMARKS:

1. WALL MUST BE DESIGNED IN ACCORDANCE WITH THE REQUIREMENTS OF TM 5-1300 (SEE REFERENCES, SHEET 1).

2. USUALLY USED TO RESIST THE EXPLOSIVE OUTPUT OF CLOSE-IN-DETONATIONS (HIGH INTENSITY PRESSURE WITH SHORT DURATIONS)

3. REQUIRES SPECIAL FABRICATION AND CONSTRUCTION PROCEDURES.

4. DESCRIPTIONS OF OTHER BLAST WALL CONFIGURATIONS CAN BE FOUND IN TM 5-1300.

5. FOR PROPERLY DESIGNED WALL, EARTH FILL BEHIND IS NOT REQUIRED.

FIGURE 15

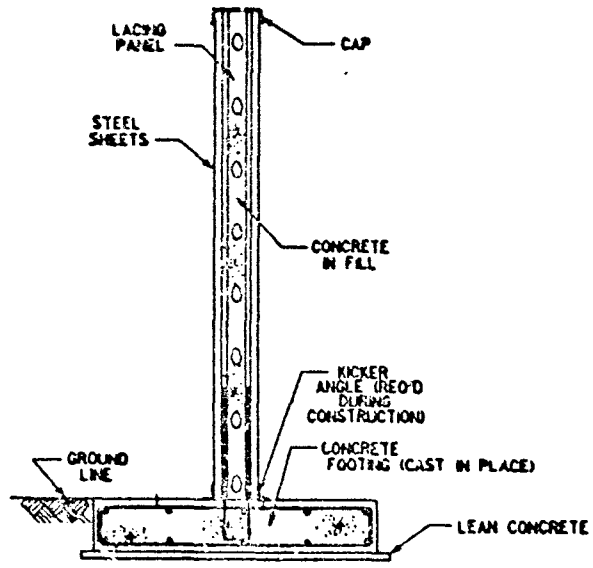

B16 - COMPOSITE WALL SYSTEM

REMARKS:

1. AESTHETICALLY PLEASING.
2. CAN BE ECONOMICALLY AND RAPIDLY CONSTRUCTED WITH UNSKILLED LABOR.
3. AVAILABLE IN DIFFERENT THICKNESSES.
4. PROVIDES HIGH RESISTANCE TO FRAGMENT PENETRATION.
5. FOR PROPERLY DESIGNED WALL, EARTH FILL BEHIND WALL IS NOT REQUIRED.
6. PATENTED:
   INNOVATIVE MILITARY TECHNOLOGY
   60 EAST 42ND ST. SUITE 2580
   NEW YORK, N.Y. 10165
   (212) 599-2030

2350

FIGURE 16

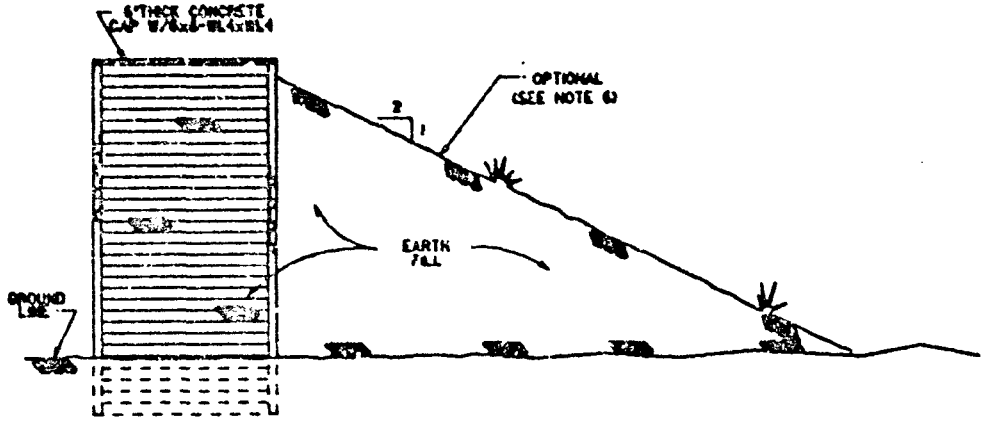

B17 - STEEL BIN

REMARKS:

1. STEEL BINS ARE PRE-ENGINEERED STRUCTURES EASILY TRANSPORTED TO REMOTE AREAS.
2. MINIMUM SITE PREPARATION REQUIRED.
3. EASILY ASSEMBLED WITH LIGHT WEIGHT EQUIPMENT.
4. AVAILABLE IN WALL HEIGHTS TO 40 FEET.
5. CAN BE DISASSEMBLED AND REINSTALLED WHEN NECESSARY.
6. DELETE IF ONLY FRAGMENT RESISTANCE REQUIRED.
7. SUPPLIERS:
   a. ARMCO CONSTRUCTION PRODUCTS
      DEPT. LCP-2584
      BOX 800
      MIDDLETON, OHIO 45042
   b. REPUBLIC STEEL, TERRA-WALL
      4416 LOUISVILLE RD. N.E.
      CANTON, OHIO 4470-
      (216)438-5984

2351

FIGURE 17

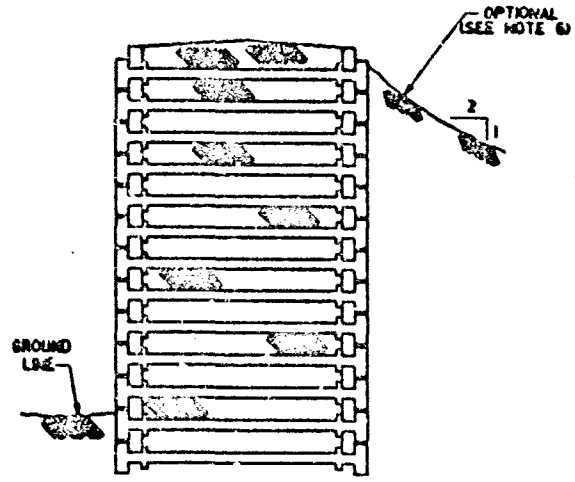

2352

B18 - CONCRETE CRIBBING

REMARKS:

1. CRIB PRECAST STRUCTURAL MEMBERS (HEADERS AND STRETCHERS) EASILY TRANSPORTED AND ERECTED.
2. MINIMUM SITE PREPARATION REQUIRED.
3. IMPROVED STABILITY CAN BE ACHIEVED WITH 1:6 WALL BATTER (NOT SHOWN).
4. CRIB WALLS CAN BE CONSTRUCTED TO HEIGHTS OVER 45 FEET. HEIGHTS OVER 15 FEET NORMALLY REQUIRE TWIN-CELL CONSTRUCTION AT BASE OF WALL.
5. CAN BE DISASSEMBLED AND REINSTALLED WHEN NECESSARY.
6. DELETE IF ONLY FRAGMENT RESISTANCE REQUIRED.
7. SUPPLIERS:

CRIBLOCK RETAINING WALLS OF AMERICA, INC.
6760 JIMMY CARTER BLVD.
SUITE 140
NORCROSS, GA. 30071
(404) 242-1918

EVERGREEN SYSTEMS, INC.
KINGS PARK, N.Y.
(213) 762-7967

CONCRIB - HILFIKER RETAINING WALLS
3900 BROADWAY
EUREKA, CA. 95501

DEPENDABLE CONCRETE PRODUCTS CO.
P.O. BOX 296
CARY, ILL. 60013
(312) 639-2303

FIGURE 18

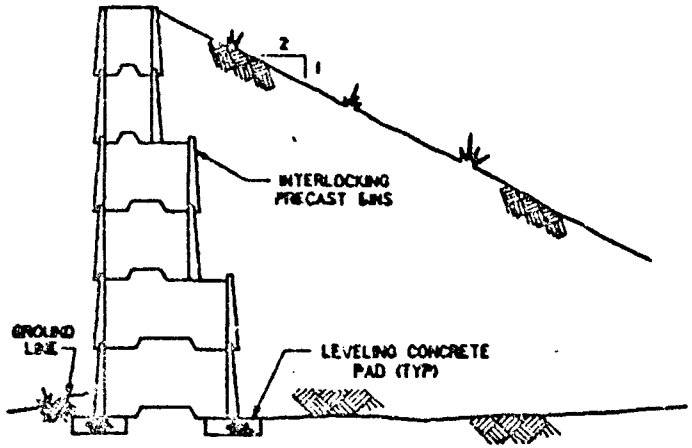

B19 - PRECAST CONCRETE BIN

REMARKS:

1. CAN BE ECONOMICALLY AND RAPIDLY CONSTRUCTED.
2. ERECTION UNAFFECTED BY CLIMATIC CONDITIONS.
3. ON-SITE LABOR AND FORM COSTS ARE SMALL.
4. AESTHETICALLY PLEASING. SELECTED SURFACE FINISHES POSSIBLE.
5. CAN TOLERATE DIFFERENTIAL SETTLEMENT.
6. CAN BE DISMANTLED AND RELOCATED.
7. TRADEMARK:
   1. DOUBLEWAL CORPORATION
      59 EAST MAIN STREET
      PLAINVILLE,CT. 06062
      TEL: (203)793-0295
   2. MODUWALL PRECAST CONCRETE
      ADDRESS: NOT AVAILABLE
   3. TINDALL CONCRETE PRODUCTS
      P.O. BOX 1778
      SPARTANBURG, S.C. 29304
      TEL: (803)576-3230

FIGURE 19

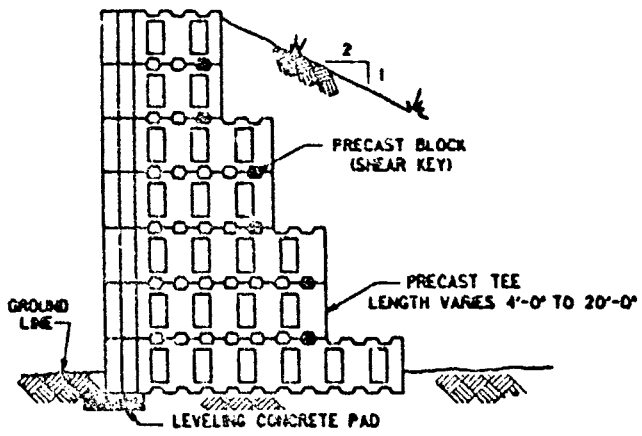

B20 - PRECAST T-WALL

REMARKS:

1. CAN BE RAPIDLY ERECTED BY A SMALL CREW.
2. HEIGHT LIMITATION 27'-0"
3. STORAGE AND ERECTION SIMPLIFIED DUE TO RIB SYMMETRY.
4. PRECAST ELEMENTS ARE MANUFACTURED BY LOCAL PRECASTERS.
5. WALL MAY BE BATTERED.
6. PATENTED:

THE NEEL COMPANY
6520 DEEPFORD STREET
SPRINGFIELD, VA. 22150
TEL: (703)922-6778

7. PRECASTER:

TINDALL CONCRETE PRODUCTS
P.O. BOX 1778
SPARTANBURG, S.C. 29304
TEL: (803)576-3230

FIGURE 20

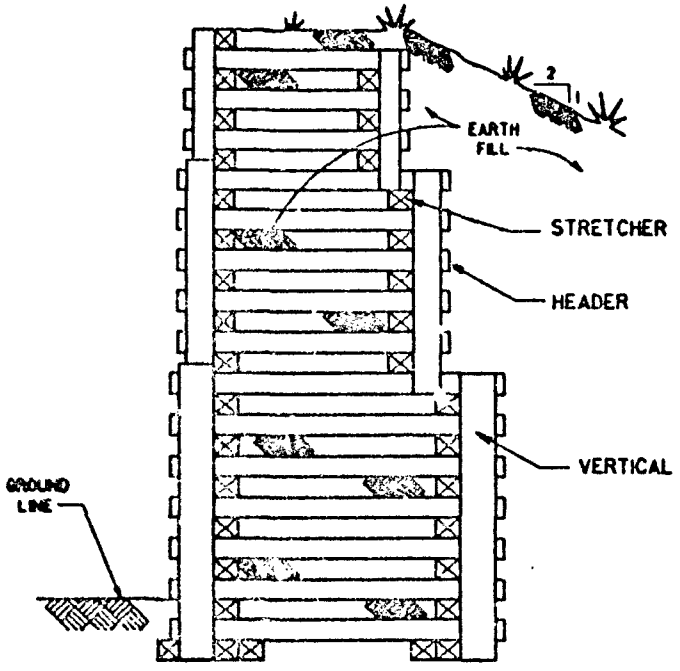

B21 - TIMBER CRIB

REMARKS:

1. ALL TIMBER SHALL BE PRESSURE TREATED.
2. ALL STRETCHERS SHALL BE LAID HORIZONTALLY.
3. FILL, IN AND BEHIND CRIB, SHALL BE FREE DRAINING.
4. HEIGHT LIMITATION APPROXIMATELY 30 FEET.

2355

FIGURE 21

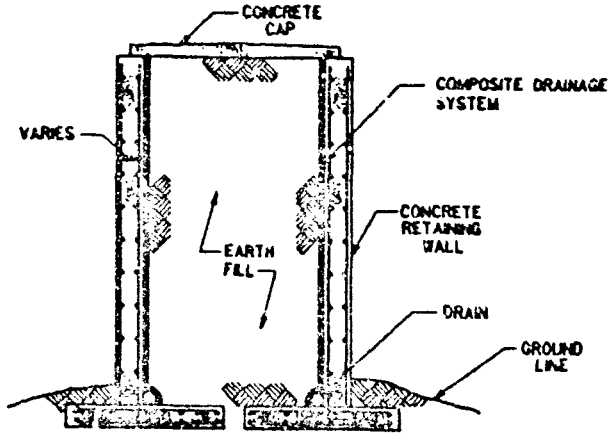

B22 - EARTH FILLED CONCRETE WALL

REMARKS:

1. REQUIRES EXTENSIVE FORMING.
2. GREATER HEIGHTS WILL CAUSE HIGH SOIL BEARING PRESSURE.
3. CANNOT TOLERATE SETTLEMENT.
4. CAN BE LOCATED NEAR BOUNDARIES OR OBSTRUCTIONS.
5. SEE "B13-CANTILEVER RETAINING WALL" FOR ADDITIONAL INFORMATION.

2356

FIGURE 22

DESIGN AND TEST
OF A
SMALL CYLINDRICAL SHIELD

BY

Phineas A. Cox
Patrick H. Zabel
Southwest Research Institute
San Antonio, Texas

AND

Martha C. Artiles
FMC Corporation
San Jose, California

ABSTRACT

A design study was conducted to develop a small cylindrical shield to mitigate the blast effects of a scaled munition with an effective weight of 1.7 lb of Composition C-4 explosive. The goal was to protect from extensive damage an adjacent structure

which lay parallel to the axis of the cylinder. Three references were found which provided test data for similar configurations and blast loading. The data were analyzed and correlated to a simple one-dimensional analytical model. The model included plastic behavior, with provisions for varying the shield and charge parameters. The analytical procedure, correlated to data from the literature, led to the design of a cylindrical shield of annealed stainless steel. Results of six tests confirmed that a satisfactory design had been achieved.

INTRODUCTION

During war-time battle conditions it is often necessary to store munitions adjacent to manned structures. Unless precautions are taken, accidental detonation of these munitions can severely damage the structure. Additionally, if the structure fails, injury to U.S. troops or even death can occur. The shield presented in this paper was designed and tested to mitigate damage from such explosions. To avoid classification, actual munitions are not identified in the paper. The procedure is generic and can be applied to different munitions.

A design procedure was developed from first principals and correlated with published data. A shield was then designed according to the procedure, built, and tested for adequacy. Field tests confirmed that design requirements had been met.

DESIGN REQUIREMENTS

A shield was required to mitigate the explosive and fragment effects from a munition with an effective weight of 1.7 lb of Composition C-4 explosive. Feasibility and proof of principle were sought, not an optimized shield. No geometry was prescribed other than the length, which was to be about 24 inches, long enough to surround completely the munition. Rupture of the shield was permissible so long as an adjacent structure, to which the shield was mounted, was not breached or rendered inoperable. As additional objectives, low weight and a small cross-sectional area were deemed desirable attributes of the shield.

DESIGN APPROACH

Two basic design options were considered:

(1) allow the structure to which it is attached to form an integral part of the shield boundary, or

(2) design a totally independent shield which is lightly attached to the structure.

Option one was discarded for one primary reason. While the structure to which the shield was attached could safely absorb some energy, the amount was unknown. Further, to predict reliably the amount would be difficult and was beyond the intended scope of the program. Without such information, design of a shield would be a "hit or miss" proposition.

Option two was chosen because it could be designed without detailed knowledge of the strength and tolerance of the adjacent structure. Further, it offered the possibility for complete lateral containment, which would eliminate all loads on the structure except possibly a small disturbance through the mount.

A configuration was chosen under option two which provided less than full containment, but adequate protection. It was a cylinder with its ends capped, but not strengthened against the internal explosion. Thus, explosive products were allowed to escape through the ends of the cylinder, after some attenuation, but not through the cylindrical part of the shield. Complete sealing of the shield was possible, but not necessary to meet the design objectives. Adequate protection was provided by this approach as demonstrated by the field testing described later in the paper.

With the configuration set, it was necessary to develop details of the design. Extensive plastic straining of the shield material was sought to maximize energy absorption. A small cross-sectional area was desirable, but loads on the shield increase in inverse proportion to the area of the cross section. Thus, methods to describe the loading on the shield as well as its response to the loading were required.

INTERNAL BLAST LOADING

Close to a high explosive, the blast loading is characterized by very high pressures and short durations. Because of this, loading on the structure usually can be described by the impulse in the blast, i.e., the area under the

p(t) curve. The use of impulse to describe the loading suggests that the loading is completed while displacements of the structure are small, much less than the final displacements. This condition holds for the loading on the shield. In addition to the impulsive loading associated with the close-in effects from the blast, a quasi-static pressure will be produced in the shield by the heating of the air and the release of the detonation products. Even though the ends are not permanently sealed, the confinement will be sufficient to cause build-up of a high quasi-static pressure.

Impulse

For field testing the charge geometry of Figure 1 was developed to simulate the munition. It consists of two separate charges, each with an equivalent weight of Composition C-4. The equivalent weight accounts for the fact that the munition charges were lightly cased in metal. A non-metal tubing surrounds the two spaced charges to hold them in position. It also simulates, approximately, the actual munition casing. Because of their separation, impulsive loads from the two charges were not additive; however, both charges contribute to the quasi-static pressure within the shield.

Because of the requirement to keep the cross-sectional area small, the shield wall was within one charge radii of the charge surface. In this regime, Baker, et. al., [1] gives an approximation for the reflected impulse from a cased spherical charge as:

$$i_r = \frac{\sqrt{2M_T E}}{4\pi R^2} \qquad (1)$$

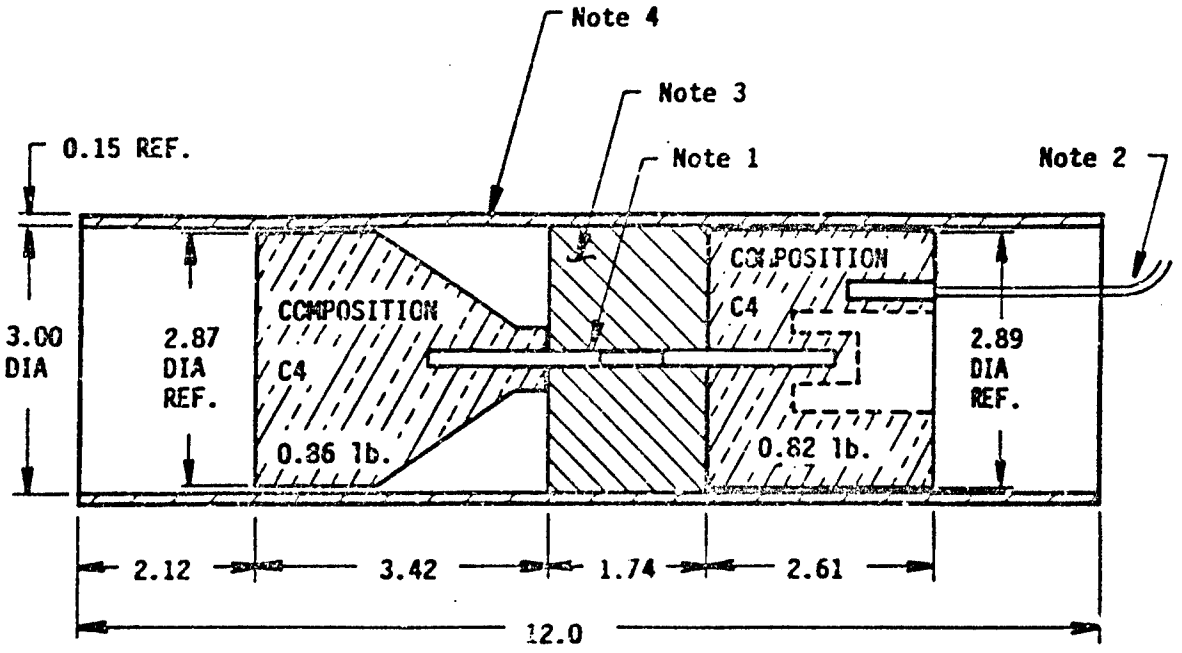

Notes:

1. Approx. 3-1/2 in. of 50 grain/ft. Primacord with No. 6 Non-electric Blasting Cap on each end.
2. RP 83 Exploding Bridge Wire Initiator.
3. Polyurethane Foam
4. Fiberglass-Epoxy Pipe 3 in. ID x 0.15 in. Wall.

Figure 1. Charge Assembly

In Equation (1)

R = distance from the charge center to the loaded surface

M_T = total mass (explosive, casing, air, etc.) between the charge center and the loaded surface

E = total energy in the explosive

Although the charge geometry in Figure 1 was not spherical, and, in fact, was somewhat difficult to describe, Equation (1) was considered adequate for the peak reflected impulse. Also, because the charge shape is somewhat cylindrical, the impulse was assumed to be constant along the length of each charge, a length of about one cylinder diameter. Thus, the loading is taken as being more severe than would be produced by a spherical charge of the same mass and energy, all other factors being equal.

Quasi-Static Pressure

Quasi-static pressure will build rapidly in the shield and will reach nearly the same value that would be achieved in a closed chamber. This occurs because the ends are initially plugged and venting is delayed. The pressure will then decay faster than it would in a sealed volume, but the decay will be long relative to the structural response time. Thus, the shield will be treated as closed for purposes of predicting the peak value of the quasi-static pressure and the decay of the pressure will be neglected over the response time of the shield.

Baker, et. al., [2] gives an equation for the peak quasi-static pressure as a function of charge weight, W (lb of TNT), and the internal volume, V, as:

$$P_{qs} = 2049\ (W/V)^{.9393} \quad \text{for } W/V \geq 0.7\ lb_{TNT}/FT^3 \qquad (2)$$

This is the high W/V regime, and Equation (2) is a fit to data for $0.7 \leq W/V \leq 5$. Within this range the 1-σ variation was given as 30%. For $W/V > 5$, Equation (2) was assumed to provide a suitable extrapolation for the pressure.

ANALYSIS METHOD

A simple analysis method was needed which would permit estimates of the wall thickness, or maximum strain for a given wall thickness, for different combinations of charge mass and geometry, charge specific energy, casing thickness, shield diameter and material of construction. This generality would permit analysis of the desired shield as well as similar configurations for which test data were available in the open literature. It was considered necessary to correlate the analysis method with actual test results to assure a realistic design for testing.

Procedure

The analysis procedure followed the work by Cox, et al [3]. It is based on an energy balance in which the strain energy absorbed by the cylindrical shield is equated to the sum of the initial kinetic energy imparted to the cylinder by the impulse and the work of the quasi-static pressure. For a uniformly loaded cylinder (Figure 2), in which plane stress conditions are assumed to exist, the relationship is

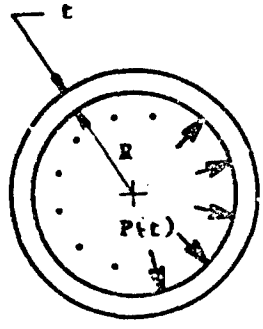

Figure 2. Cross-Section of the Shield

$$\frac{i_r^2}{\rho t^2 \sigma_y} + \frac{\sigma_y}{E} = 2\frac{\Delta R}{R}\left(1 - \frac{P_{qs} R}{t\sigma_y}\right) \qquad (3)$$

In addition to the geometry of Figure 2 and the loading parameters already defined, terms in Equation (3) are:

σ_y = effective yield stress

E = elastic modulous

ρ = material density

ΔR = maximum radial expansion of the cylinder

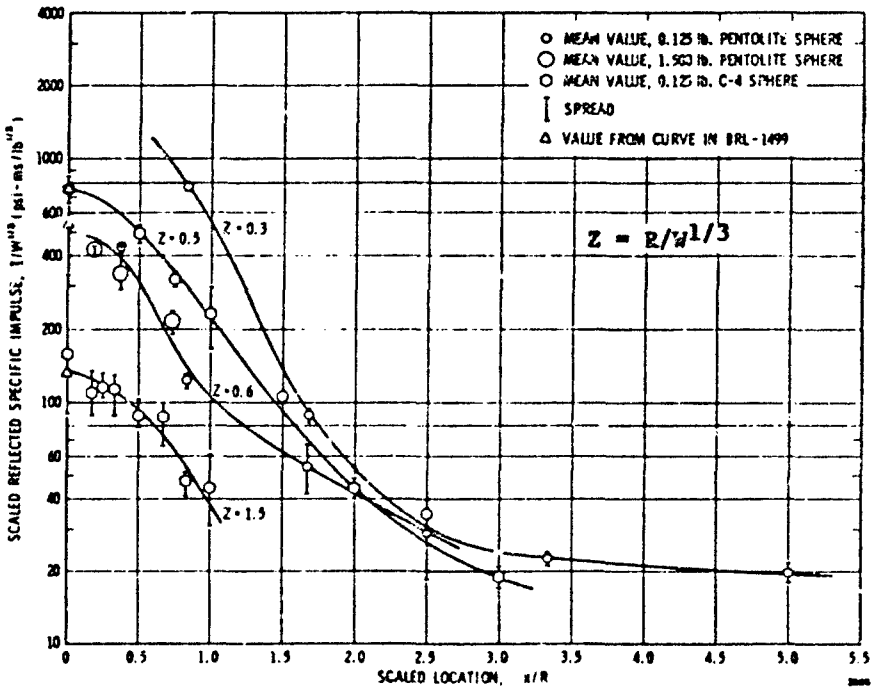

Figure 3. Reflected Impulses for Spherical Charges in Air [4]

Equation (3) accounts for the elastic and plastic strain energy, conservatively assumes a zero rise time for the quasi-static pressure, and treats strain rate effects and strain hardening through appropriate selection of the effective yield stress. The thickness is readily found from Equation (3) using the quadratic formula.

The P_{qs} term in Equation (3) is predicted by Equation (2) for closed or initially capped cylinders; otherwise it is zero. Equation (1) gives i_r. An adjustment to i_r is made for spherical charge geometry as discussed next.

Axial strains were ignored in the derivation Equation (3). To account approximately for their effect, an average reflected impulse over a length of one cylinder diameter is used in place of the peak impulse. As noted in the discussion of the internal loading, the charge geometry of Figure 1 is assumed to yield a nearly constant impulse over a length of one cylinder diameter. Furthermore, this average impulse is taken as that predicted by Equation (1). Thus, for a spherical charge, the peak reflected impulse given by Equation (1) is reduced to yield the average pressure. The reduction can be made with the help of Figure 3, which gives reflected impulse for close-in spherical charges as a function of X/R, the scaled distance along the reflecting surface. As a first approximation, one finds for Z = 0.5 that the ratio of average to peak impulse from $0 \leq X/R \leq 0.5$ is 0.78. This reduction factor was used when analyzing published results for tests with spherical charges.

Correlation with Published Data

Three sources were located in the literature which gave test data on cylinders subjected to internal explosions. Test configurations were similar to the desired shield, and four data sets were extracted from the references for correlation with predictions made by Equation (3).

Data Set 1

Reference 5 gives the maximum amount of explosive which can be contained by 6061-T6 aluminum cylinders of various sizes. Test strains were not given, but failure strains were cited as approximately 10%. Additionally, the ratio of cylinder length to internal diameter was only specified as being bounded by $5 \leq L/D \leq 6$. Test charges were centrally placed and closure was achieved by setting a 500 lb weight on one end of vertically oriented cylinders.

Two data points were analyzed for cylinders with a 1 inch wall thickness:

	Internal diameter, d	Maximum Contained C-4 Charge
Case 1(a)	5 in.	0.639 lb
Case 1(b)	10 in.	2.403 lb

The 10 in. diameter data point required a slight extrapolation to the test data.

To compare with these data points, the cylinder thickness was calculated from Equation (3), with i_r and P_{qs} given by Equations (1) and (2), respectively. Equation (1) was multiplied by 0.78 to give an average pressure for a spherical charge over a length along the cylinder of one diameter. An iteration was performed by varying the effective yield stress, σ_y, to match the 1 inch thickness determined by test for a total strain of 10%. The results were:

case 1(a) σ_y = 140,000 psi

case 1(b) σ_y = 120,000 psi

By comparison, static properties for 6061-T6 are:

Yield Strength: F_{ty} = 35,000 psi

Ultimate Strength: F_{tv} = 38,000 psi

Further, the material is not regarded as being strain rate sensitive. Thus, the comparisons with Data Set 1 suggested that the analytical procedure is quite conservative.

Data Set 2

Test results for a closed cylinder of 6061-T6 aluminum were also given in Reference 5. For this case the maximum radial expansion was measured, and the spherical charge was encased in aluminum of thickness 0.025 in. Data for the cylinder are:

d = 6 inches

t = 1 inch

L/d = 4.43

Charge = 0.353 lb Comp B

ΔR = 0.1 inches (measured)

The specific energy, E, for Comp B explosive [1] is 2.15 x 10^6 ft-lb/lb.

For this case, Equation (3) was solved for the radial expansion, ΔR. In evaluating the reflected impulse, Equation (1) was again multiplied by the 0.78 factor to give an average value for a spherical charge and the mass of the casing was included in M_T. As for Data Set 1, the effective yield stress was varied to give agreement with the experiment. The value calculated was

σ_y = 68,000 psi

which is less than twice the static yield stress. This result gave better correlation between experiment and the analysis procedure than found for Data Set 1, perhaps because the strain was better defined. Still, the comparision indicated that the procedure is conservative.

Data Set 3

Reference 6 gives data for cylinders of 304 stainless steel, tested according to the same procedures described for Data Set 1. Experimental results were given graphically as a function of the cylinder diameter and

thickness and the maximum contained weight of spherical C-4 charges. Unfortunately, no measured strains or failure strains were given. Two data points were selected from a fit to the data:

	Internal Diameter, d	Explosive Weight	Wall Thickness
Case 3(a)	5 inches	1.76 lb	0.778 inches
Case 3(b)	10 inches	9.92 lb	1.303 inches

Because a failure strain was not given, Equation (3) was used to predict the strain produced in the tests. For this approach the effective yield stress must be chosen in advance. For annealed 304 stainless steel static values are:

Yield strength: F_{ty} = 40,000 psi

Ultimate strength: F_{tv} = 80,000 psi

Elastic Modulous: E = 28 x 10^6 psi

Further, 304 stainless steel is rate sensitive. Peak strain rates can be estimated as $V/\Delta R$, where V is the velocity of the cylinder wall imparted by the impulse. Using this approach, peak strain rates are expected to be in the range of 2000 in/in/sec to 3000 in/in/sec, which will increase the dynamic yield strength to 1.5 to 2.0 times the static yield strength. Thus, an effective dynamic yield stress, accounting for both strain hardening and strain rate effects of the material, was selected as

$$\sigma_y = 70{,}000 \times 1.8 = 126{,}000 \text{ psi}$$

Following the procedures described previously, but solving for the maximum strain, $\Delta R/R$, Equation (3) gave for Cases 3(a) and 3(b):

	$\Delta R/R$
Case 3(a)	.6
Case 3(b)	.4

Uniaxial failure strains as high as 0.55 is given for annealed stainless steel, but this value is believed to be too high for a biaxial state of stress as found in the cylinder. The agreement between the analysis procedure and results for the stainless steel cylinders in this data set appeared to be better than that obtained for the aluminum cylinders in Data Sets 1 and 2; however, some degree of conservatism in the procedure was still indicated.

Date Set 4

Reference 7 gives results for tests in Germany on ST37 steel cylinders with bare cylindrical charges and no end closure. Three data points were chosen for evaluation. Data analyzed were:

	Cylinder			TNT Charge		Measured Maximum
	I.D.	L	t	weight	L/D	Strain
Case 4(a)	5.906 in.	5.906 in.	0.177 in.	0.11 lb	1.55	7.5%
Case 4(b)	5.906 in.	23.62 in.	0.177 in.	0.22 lb	3.10	>25% (ruptured)
Case 4(c)	5.906 in.	5.906 in.	0.394 in.	0.11 lb	1.55	1%

Equation (3) again was used to find the effective dynamic yield stress required to match the measured strain. No adjustments were made to Equation (1) when computing reflected impulse for the cylindrical charges, and the quasi-static pressure was zero. The results, including the calculated strains, were:

	σ_y	Calculated Strain
Case 4(a)	35,000 psi	7.6%
Case 4(b)	35,000 psi	30.2%
Case 4(c)	50,000 psi	1.1%

By comparison, properties for the ST37 steel are:

Yield strength: F_{TY} = 34,000 psi

Ultimate strength: F_{TV} = 52,000-64,000 psi

Elastic modulous: E = 30 x 10^6 psi

These results suggest that the procedure is somewhat unconservative or that the steel is not strain rate sensitive. One factor in the procedure that could cause the strain to be underestimated is that the impulse given by Equation (1) may be low for a true cylindrical charge.

Conclusions from the Experimental/Analytical Comparisons

The experimental/analytical comparisons have shown that:

- The procedure is very conservative for the aluminum cylinders in Data Sets 1 and 2, requiring an effective yield stress that was much higher than can be expected for a material with low strain hardening and low strain rate sensitivity.

- The procedure gives reasonable, but slightly conservative results for 304 stainless steel cylinders. Predicted maximum strains are believed to be too high for biaxial states of stress.

- Results for the German steel cylinders is good, but somewhat unconservative. The method for predicting impulsive loads on the cylinder may be unconservative for true cylindrical charges.

The correlation with 304 stainless steel gave confidence in the analytical procedure for the design of a shield with this material. Further, the 304 stainless steel appears to exhibit high ductility without rupture in the configuration required and exhibits strain hardening and strain rate sensitivity, both of which are desirable for this application. Thus, the design of a stainless steel shield was undertaken, using Equations (1) through (3) to compute loads and wall thickness, for the charge geometry of Figure 1.

SHIELD DESIGN

A five inch internal diameter was chosen to contain the 3.30 inch diameter charge configuration. This diameter permitted clearance for other parts of the munition, which extend beyond the charge diameter, and also

allowed for shock absorbing material between the munition and the wall if such material should be required.

As noted in the Design Requirements, the shield must be 24 inches long to completely contain the munition; however, the severe loading is limited to a 12 inch segment which spans the charge. Thus, two cylinders were used; a 24 inch cylinder to contain the quasi-static pressure and provide protection to the munition from external threats, and a 12 inch cylinder to reinforce the longer cylinder over the charge.

The shield wall thickness was computed using the analysis method already described. The effective dynamic yield stress (the same as used for Data Set 3) was σ_y = 126,000 psi, which accounted for strain hardening and strain rate effects in the 304 stainless steel. The design strain, $\Delta R/R$, was set at 25%, approximately half of that required to match experimental results in Data Set 3. The required wall thicknesses were found to be:

For $i_r + P_{qs}$: 0.94 inches

For P_{qs} only: 0.407 inches

The design was implemented with seamless 304 tubing of the following sizes:

(1) 6 inch O.D. x 0.5 inch wall x 24 inches long

(2) 7 inch O.D. x 0.5 inch wall x 12 inches long

Light machining was required to assemble the cylinders with a light press fit. A second assembly was made with a 0.25 inch wall for the outer cylinder to test for conservatism in the standard design. End caps, 0.25 inch thick, were provided for closures on some tests.

DESIGN VERIFICATION

The simulated explosive for the munition (Figure 1) was used for field testing the shield. Each explosive charge provided its contribution in the correct relative geometric location and magnitude. The charges were connected with Primacord to assure that both would detonate. One charge had an exploding bridge wire initiator installed.

Test Set-Up

The shield was tested in the fixture of Figure 4, which assured that, in the event the shield failed, no fragments would leave the test site. Baffles were emplaced to stop the end caps on some tests. The shield was suspended in the large cylinder with two loops of wire (Figure 5).

Results

Test 1 (Figure 5) was conducted with the alternate shield design, which had a 0.25 inch thick outer cylinder over the charge. This shield failed but revealed a very ductile mode of failure with few fragments. Figure 6 shows the standard shield still suspended in the fixture after Test 2. This test was conducted without any mitigating material around the charge. Scabbing is

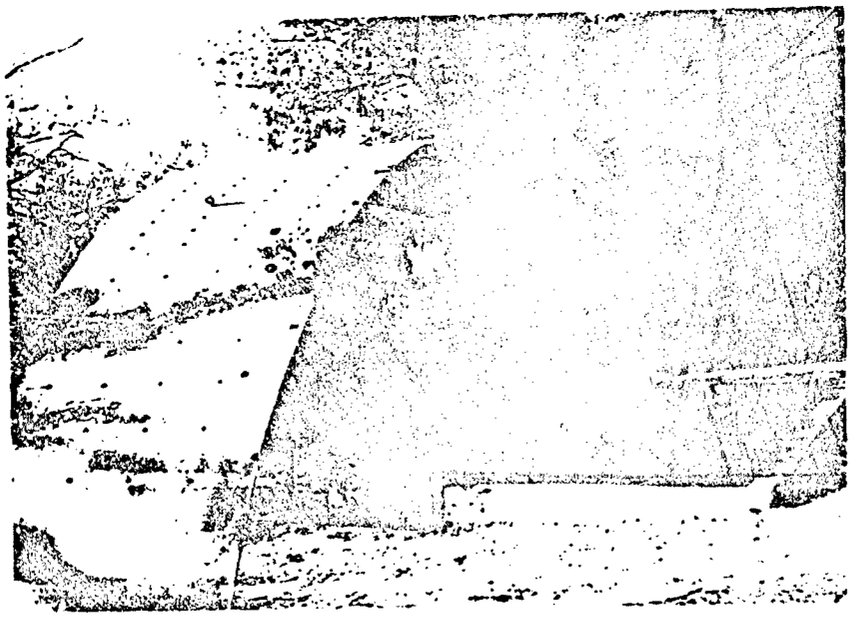

Figure 4. Component Test Set-up, Test 1

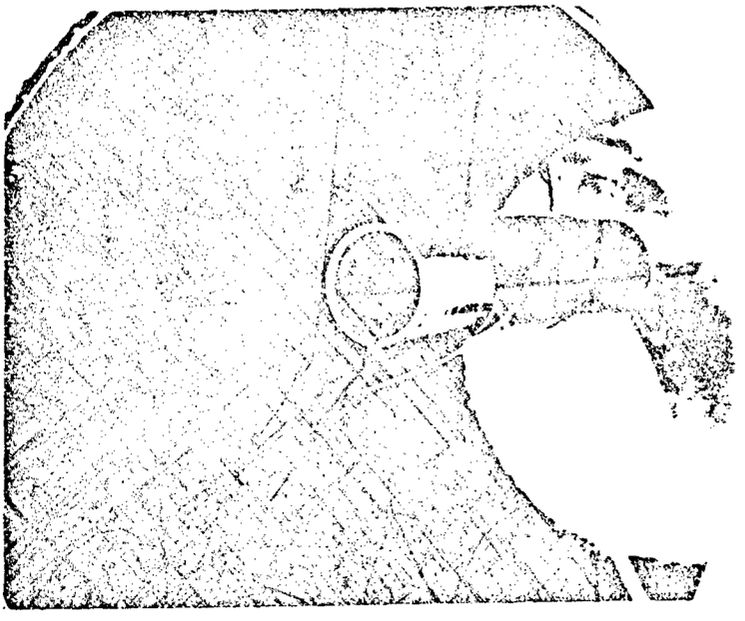

Figure 5. Component before Test 1

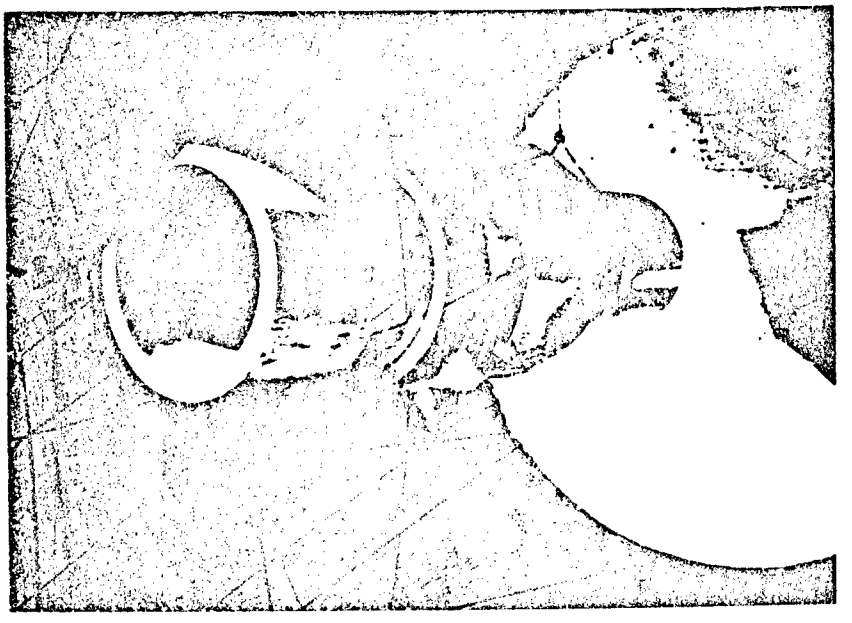

Figure 6. Test Specimen After Test 2

evident on the outside of the shield but no longitudinal cracks occurred. Since the shield remained basically intact, in the wire loops, lateral loads on the shield evidently were small.

Figures 7 and 8 show post test results for Test 3. It was identical to Test 2 except that 1 inch of lightweight cement was placed between the charge and the wall and end caps were tacked to the ends of the cylinder. Splitting of the outer tube occurred (Figure 8) but the scabbing was eliminated.

Distortion measurements for Tests 2 and 3 are given in Figures 9 and 10, respectively. They show that greater distortions occurred in Test 3, produced by the additional confinement afforded by the end caps, by the addition of the buffering material, or both. The additional expansion explains the

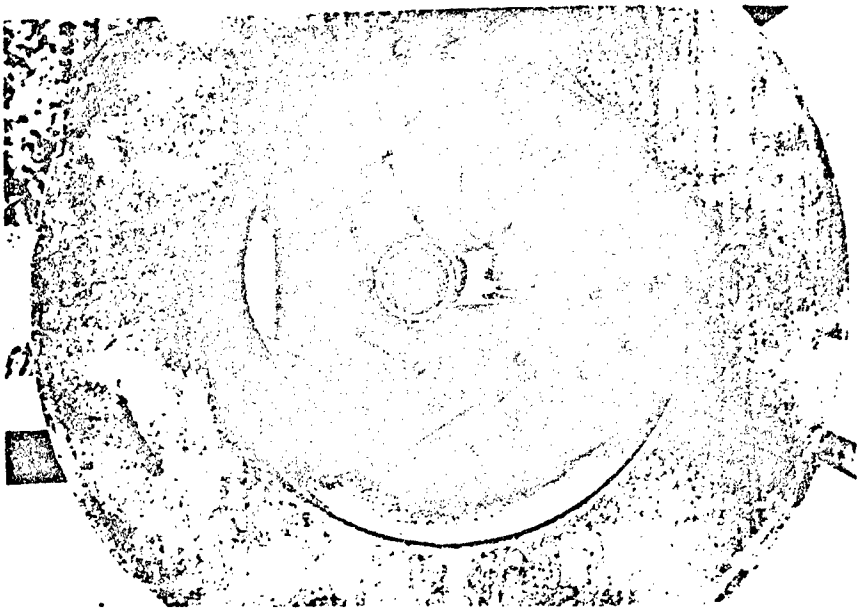

Figure 7. Containment Cylinder after Test 3

Figure 8. Damage to Containment Cylinder, Test 3

Note: Diameters shown are the means of four measurements.

Mitigating material: 1 in. air
No end discs.

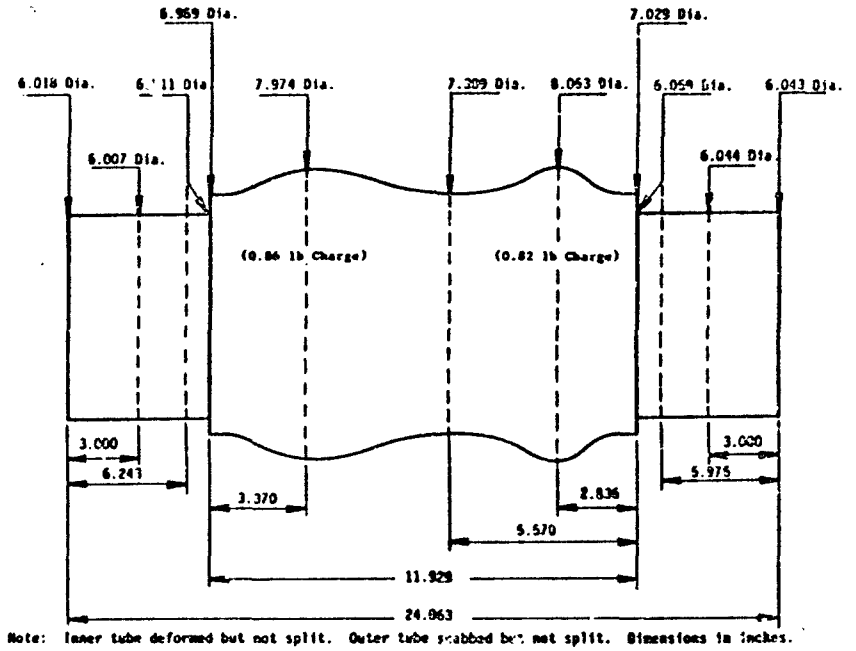

Note: Inner tube deformed but not split. Outer tube scabbed but not split. Dimensions in inches.

Figure 9. Cylinder Profile, Test 2

Note: Diameters shown are means of four measurements.

Mitigating material, 1 in., light-weight cement. End discs installed.

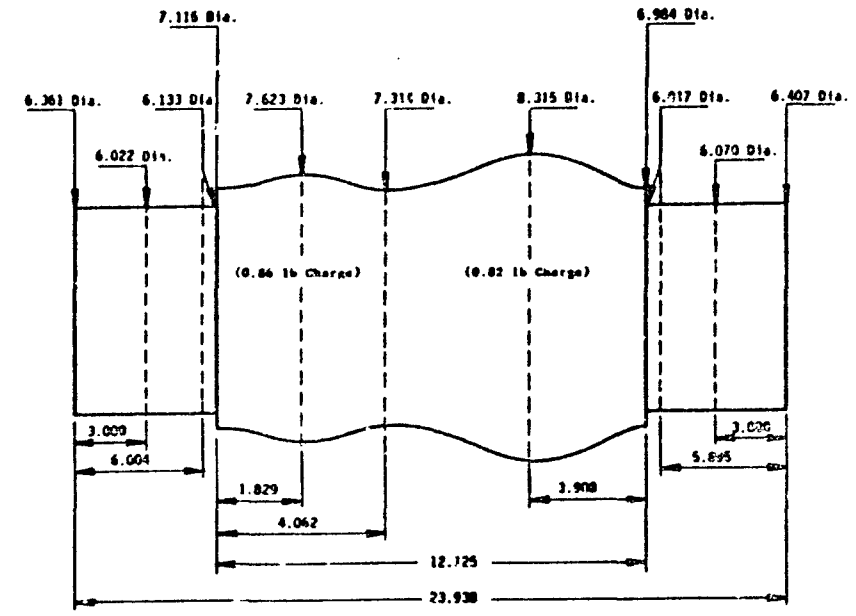

Note: Outer tube split at two places. Inner tube deformed but not split. Dimensions in inches.

Figure 10. Cylinder Profile, Test 3

longitudinal cracking in Test 3 which was not evident in Test 2. Both tests were successful in that the adjacent structure would be protected. Note that the ends of the inner cylinder in Test 3 were slightly flared after the test. This was caused by blast wave reflections from the end caps, producing higher local pressures.

Similar test results were obtained in four more tests made with the same basic shield configuration. There were no catastrophic ruptures. In all these tests, end caps were used, and, in all cases, the ends of the inner cylinder flared slightly. In the last four tests, the shields were mounted on a scaled structure with a thin metal clamp near each end. The only time this mount failed was when the flare resulting from the end cap was within the mount. In that instance, one end of the cylinder came free but the mount at the other end held. In none of the tests was the structure damaged.

In the tests with buffering material, the outer tube usually split but the split was not aligned with splits in the inner tube. There was no scabbing of the outer surface. Where there was an air gap and no buffering layer between charge and inner tube, the exterior surface of the outer tube again scabbed. In short all of the results of Tests 2 and 3 were repeated. Residual strains in all six tests are given in Table 1.

Table 1. Residual Strain in Containment Cylinders

Test	Mitigating Materials	% Strain at Larger Explosive Portion		% Strain at Smaller Explosive Portion		Outer Surface Scabbed
		Inner Surface	Outer Surface	Inner Surface	Outer Surface	
2*	1 in. air	21%	15%	19%	14%	yes
3	1 in. lt.wt. cement	27%	19%	12%	9%	no
5	1/2 in. Isodamp + 1/2 in. air	35%	25%	17%	12%	no
6	1 in. lightweight cement	21%	15%	18%	13%	no
7	1/4 in. Isodamp + 3/4 in. lt.wt. cem.	33%	23%	16%	11%	no
8	1 in. air	22%	16%	16%	11%	yes

* no end caps.

CONCLUSIONS AND RECOMMENDATIONS

Conclusions

The shield concept developed and tested in this work was proven to be very successful for containing the designated munition and protecting an adjacent structure. Adding materials between the charge and the wall controlled scabbing in the shield but increased overall distortions slightly. Because scabbing was not detrimental to adjacent structure, mitigating materials are not necessary.

A reduction in weight of the shield for single munitions can also be achieved by more precise matching of the shield to the load and by other choices of material, such as by the use of composites. Following similar procedures, shields can be designed to house two munitions. Such a shield should weigh less than two individual shields but the overall cross section may be increased.

Recommendations

Additional work is recommended to optimize the single shield concept through improved matching of shield to load and the use of more efficient materials. In addition, it is recommended that a design be investigated for a shield which houses two or more munitions to see if more efficient storage of multiple munitions can be achieved than that afforded by the use of multiple individual shields.

REFERENCES

1. W. E. Baker, P. S. Westine, J. J. Kulesz, J. S. Wilbeck and P. A. Cox, "A Manual for the Prediction of Blast and Fragment Loadings on Structures," DOE/TIC-11268, Prepared by Southwest Research Institute for U.S. Department of Energy, Albuquerque Operations Office, Amarillo Area Office, Pantex Plant, Amarillo, TX, November 1980.

2. W. E. Baker, C. E. Anderson, B. L. Morris and D. K. Wauters, "Quasi-Static Pressure, Duration and Impulse for Explosions in Structures," SwRI.

3. P. A. Cox, P. S. Westine, J. J. Kulesz, and E. D. Esparza, "Analysis and Evaluation of Suppressive Shields," Edgewood Arsenal Contractor Report ARCEL-CR-77028, Jan. 1978.

4. A. B. Wenzel and E. D. Esparza, "Measurements of Pressure and Impulses at Close Distances from Explosive Charges Buried and in Air," Final Report prepared by Southwest Research Institute for U.S. Army Mobility Equipment Research and Development Center, Fort Belvoir, VA 22060, Contract No. DAAK02-71-C-0393, August 1972.

5. L. Avrami, E. Dalrymple and F. Schwartz, "A Large Containment Capsule for Nuclear Reactor Irradiation of Explosive Materials," Picatinny Arsenal T. R. #3673, April 1968 (AD668674).

6. A. McKenzie and E. Dalrymple, "The Dependence of Dynamic Strength of Cylindrical Pressure Vessels on Geometric Parameters," Picatinny Arsenal T.M. #1026, May 1963 (AD 406622).

7. H. Hommel, "Explosive Testing of Steel Pipe," Report No. 4170, Institute for the Chemistry of Propellant and Explosive Materials, 31 December 1970. Translated by Dr. William Wei, SwRI, October 1987.

Lightning Proof Environment for Explosives

Roy B. Carpenter

Background

Lightning and the related secondary effects present a significant hazard to those who handle flammables, explosives, nuclear products and their storage facilities. History has proven that the conventional techniques in use today are not 100% effective. Explosive storage bunkers have exploded due to lightning and handling facilities have been set on fire by lightning strikes, and by its secondary effects created by nearby strikes. Most of these situations were either "protected" by NFPA 78 criteria, or by general industry standards.

From the days when explosives were developed, up to this present hour, lightning has proven to be an adversary that has often circumvented our protection attempts. Not always, but with distressing frequency, and at unexpected times and locations.

In dealing with this problem, the tendency has been to explain away the problem by implying that the protection was not quite up to standards. This position may suppress public reaction; however, it does not provide a long term solution. A study of the lightning strike mechanism and the related phenomena provide a key to the loss mechanism and facilitate the derivation of a safe protective system that can be made 100 percent effective.

The Cause Mechanism Premise

To understand the cause, it is necessary to understand the lightning mechanism and its related secondary effects. To that end, a review of the fundamentals is necessary.

A charged cloud develops a very strong electrostatic potential through some internal mechanism. Scientists have estimated this potential to be in the order of ten to the eighth volts. As a result, the electrostatic field beneath that cloud, reaches values of between 10 to 30 thousand volts per meter of elevation above earth, during a mature storm. This field induces a charge on the earth, beneath that cloud, of equal but opposite potential. It may be considered an electrical shadow as illustrated by Figure 1.

As the cloud moves, so does that electrical shadow. As it enters the area of concern, it charges everything within its sphere of influence, <u>including the explosives stroage facilities and its contents</u>.

When the charge within the cloud reaches the critical level, the resulting potential causes the air beneath that cloud to ionize, forming downward moving streamers called "step leaders." As they move toward earth, they bring that cell potential with them, as illustrated by Figure 2. As the leader approaches earth, streamers are formed,from earth bound facilities moving upward

toward the leaders. The first streamer to make contact with a leader, closes the circuit and "Charge Neutralization" begins. This mechanism may be thought of as the equivellent of a wire being lowered from the cloud to earth; the first structure it terminates on becomes part of the circuit - conductor or not.

The Charged Cloud Impact

Figure 1

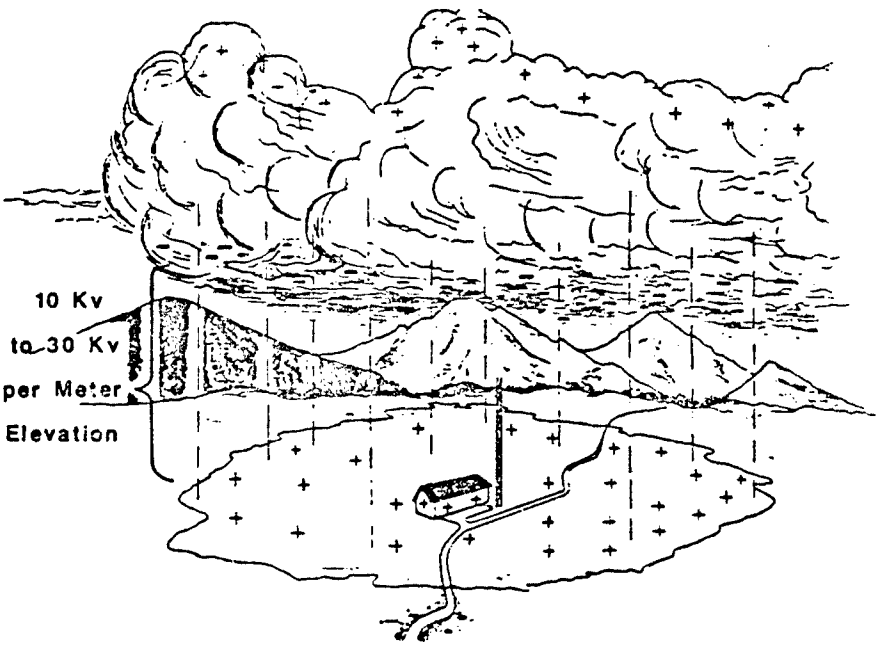

The Strike Discharge Process

Figure 2

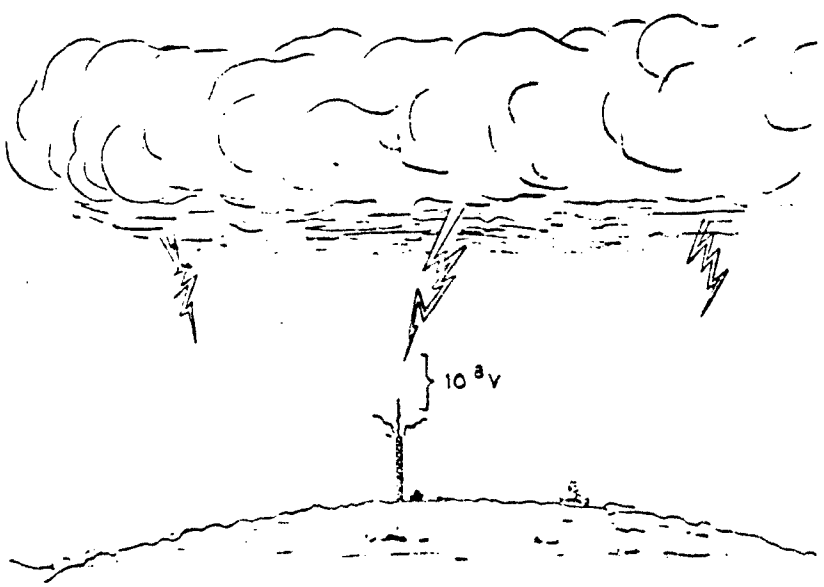

Charge Neutralization is the process of transferring electrons from a body with a surplus (the cloud) to one with a deficiency (earth under the cloud); as illustrated by Figure 3. This action takes an average of 20 microseconds. However, there are often many surges of current in the lightning channel (called a flash) as the various earth bound charge centers move to the stroke channel and are neutralized; there are between one and 26 of these individual current surges

Figure 3

THE CHARGE NEUTRALIZATION MECHANISM

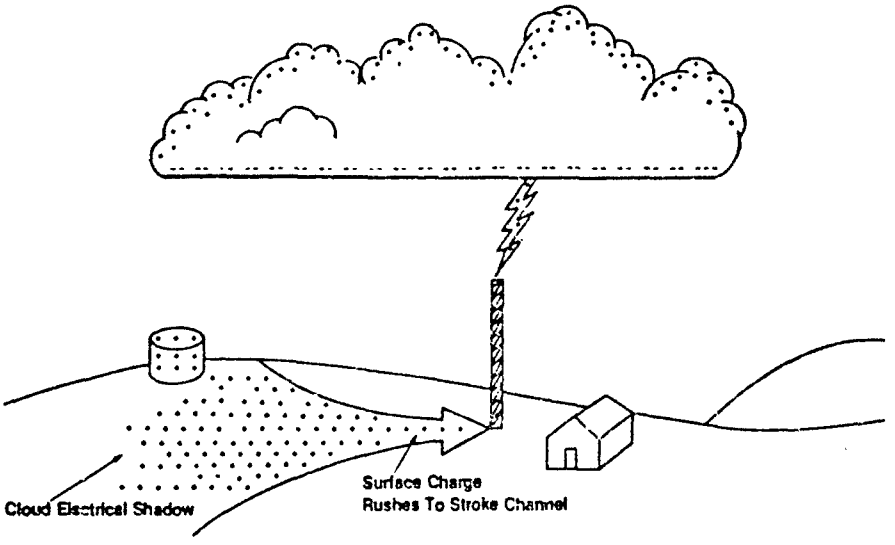

If there are at least semi-conductive paths between all of the area charged and the terminus of the stroke, then the area is totally neutralized. However, if there are electrically isolated pockets of charge, there can be "secondary effects" with severe consequences. One of these effects is the so called "Bound Charge," described by the American Petroleum Institute in their Bulletin 300 2A on lightning and static electricity.

The Bound Charge hazard as illustrated by Figure 4, is believed to be the cause of most lightning related explosions in explosives and flammables handling facilities. This cause is quite similar to that related to static electricity except that the "static" was induced by the storm as opposed to other charging mechanisms. When the charge neutralization process was terminated and the stroke channel de-ionized, this bound charge will be left on any body isolated from direct electrical contact with earth.

Since oil, dry wood, dry concrete and many other materials are essentially insulators, they cannot transfer the charge in the usual 20 microsecond interval available for neutralization. The induced charge is therefore "bound" by the insulative qualities of the material itself, or its interface with local earth.

Figure 4

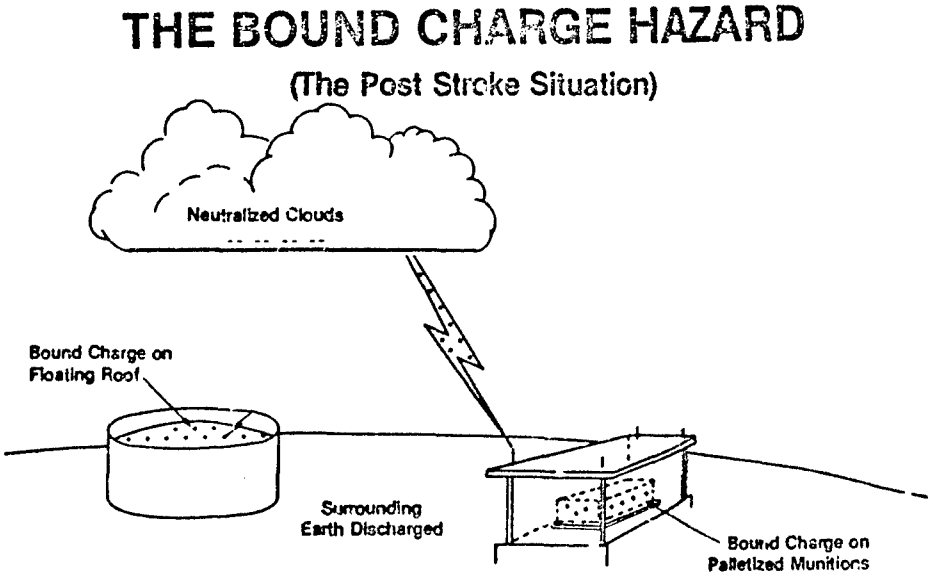

Bound Charges Cause Secondary Arcs

This Bound Charge is usually at a very high potential, perhaps equal to that of the cloud; but now, at a difference with respect to its surrounding; that is, the surrounding discharged earth or its container. The potential is usually high enough to create an arc between it and the closest conductive body that was discharged by the stroke. If the conditions are "right" an explosion or a fire is initiated.

This phenomena is known to be the common cause of petroleum storage tank fires; and most likely bunker explosives. In petroleum tanks, arcs have been observed to form between the floating roof and the tank wall, igniting the vapors around the seal - also illustrated by Figure 4. The obvious conclusion is that the primary cause of bunker explosions, are the secondary effects (bound charge), not the strike itself. The strike itself seldom comes in direct contact with explosives in a bunker.

The charge motion itself can also create a significant hazard as it moves from where it was induced to the terminus of the stroke. With the lightning strike, a large volume of charge is being transferred from a wide area in a few micro- seconds. This charge will take the path of least resistance; discontinuities in that path are conducive to arking. In the wrong place these arcs can and will ignite, explode or damage inter-face materials between conductive and non-conductive elements in the path of the moving charges.

Another factor related to nearby strikes is the Electromagnetic Pulse (EMP) of Figure 5. The EMP is the direct result of a nearby lightning stroke and the related severe magnetic field. di/dt's in the order of 100,000 amperes per microsecond are not uncommon in a lightning channel. And, as with any fast moving electrical current, there is a related, very strong magnetic field. Any form of conductor emersed within that field will be

the recipiant of an induced charge which is usually additive with the others forms of secondary effects.

Figure 5

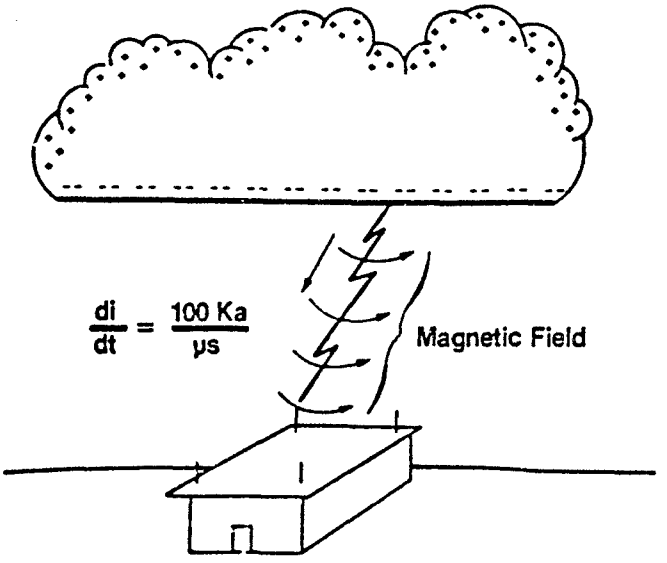

The Character of Positive Protection

Positive protection must provide a safe environment under any circumstance; and not be subject to failures. That is, the potential for system compromise must be insignificant. In dealing with the phenomena, lightning, this means that the following functions must be accomplished:

1. Eliminate the potential for direct strikes to the critical site. This will also eliminate the EMP.

2. Eliminate the possibility of earth current transients, caused by the passage of the charge through the site of concern.

3. Eliminate the potential for bound charges within the area of concern.

These objectives rule out the use of any system based on collection and diversion technologies. To demonstrate, a review of these contemporary technologies is mandated.

Conventional Protective Concepts

Lightning Rod (Air Terminal) systems are designed to provide a "preferred path" for the lightning current, by capturing the stroke and diverting the resulting current flow around the protected area. See Figure 6. In addition to their questionable reliability in that function, they often encourage the stroke;

and thereby encourage the secondary effects because the stroke energy is brought within or near to the area of concern.

Improvements in air terminal concepts such as the Radioactive Air Terminal, the Laser Terminal, the french "Helita", etc. do not solve the basic problem. That is, the stroke is brought to within the area of concern. As a result the better they work, as an attractor, the higher the risk to the protected explosives.

Divert The Strike

Figure 6

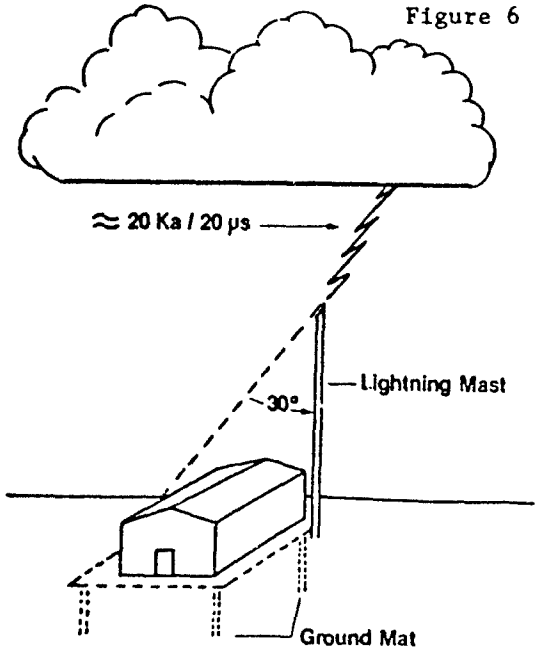

Faraday Cage

Figure 7

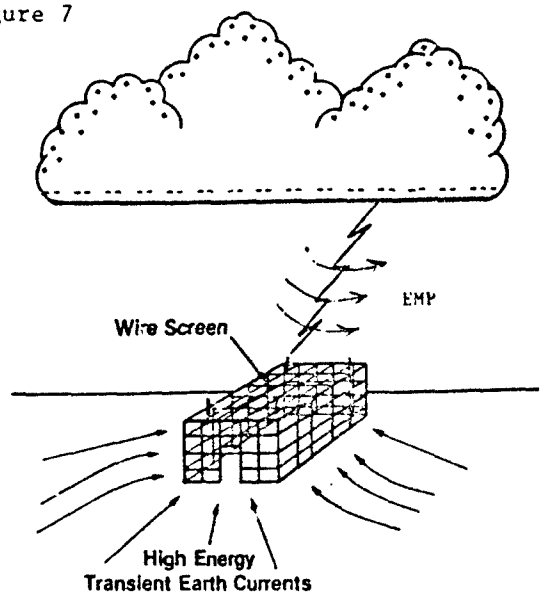

The Faraday Cage of Figure 7, does solve some of the foregoing problems, but not all. As a result, it does reduce the risk. The system surrounds the protected area with an electrostatic shield, including all sides, top and bottom. The shielding effect eliminates any electrostatic induced phenomena. However, it has no effect on the Electromagnetic Pulse (EMP). Further, the impact on the charging effect of the storm cell field is of dubious value. There is no concrete data available as to Faraday cage impact on static charge during storm conditions. However, the cost to implement a satisfactory system will be very high and, the design impractical for some facilities.

Charge Dissipation, Positive Protection

An obvious premise,for positive protection, simply stated is: "No strike, no fires or explosion". What also appears to be true, but less obvious is: "No bound charge, no fire or explosion." Therefore, any system that can be shown to prevent the direct strike and/or eliminate the potential for a bound charge, will provide positive protection for explosives and flammables. The Dissipation Array™ has been proven to be just such a system. It constantly drains the charge from a protected area, as a result the protected site is virtually without a significant charge, even in the midst of intense storm.

Based on a well known electrostatic phenomena called: "Point Discharge", the Dissipation Array System (DAS™) as its name implies, dissipates the charge slowly and constantly throughout the life of the storm. It is based on a principle known as Point Discharge which provides the media for passing the charge from the site into the surrounding atmosphere. Point discharge is a phenomena that occurs when a sharp point is exposed to a strong electrostatic field. That point takes an electron from the adjacent air molecule, leaving it a free ion. The storms electrostatic field draws that ion away from the point and the process is repeated as long as the electrostatic field creates a high enough potential to continue the ionization process. The ion flow increases exponentially with an increase in the field strength and linearly with wind or air motion. When large amounts of ions are produced, it creates a related phenomena called corona or " St. Elmo's Fire". The DAS™ does just that, it creates massive ionization during a mature storm. Discharge currents of up to 1/2 ampere, have been measured from a single system.

A form of the DAS is illustrated by Figure 8 which illustrates the three basic components and its functional impact on the protected site. They function as follows:

1. The Ground Current Collector (GCC) collects the induced charge as it enters the area to be protected, providing a ready conductor to collect that charge, providing a preferred path for the charge.

2. The Service Wires (SW) provide a preferred path from the GCC to the ionizer. Since there is a continuous flow of charge, the GCC - SW provides the preferred path for the flow of storm related charge. Therefore, little charge is admitted to the protected site.

3. The Ionizer provides the interface between the site and the storm system, passing the induced charge on to the air molecules via thousands of properly deployed points. These then constantly carry the charge away from the site.

The more intense the storm, the higher the ionization current. Visivble Corona has often been observed around an Ionizer during active storms at night. As illustrated by Figure 9, the protected area is left virtually free of charge, thereby eliminating the cause of the bound charge.

Customer history has proven that the residual charge is so low that no secondary arcs would form, where prior to the DAS, secondary arcs would frequently ignite light hydrocarbons and hydrogen. A prior Lightning Eliminators and Consultants, (LEC) Inc. paper provides the results of a 15 year study involving over 650 systems and 4000 system-years of data which prove the reliability of the DAS concept. The DAS installations at PPG Chemical of Lake Charles, Louisiana, and Phillips Petroleum of Freeport, Texas provide excellent examples of the capability of

the DAS to deal with the unwanted charge; and to eliminate fires and explosives even in the most sensitive areas.

Figure 8

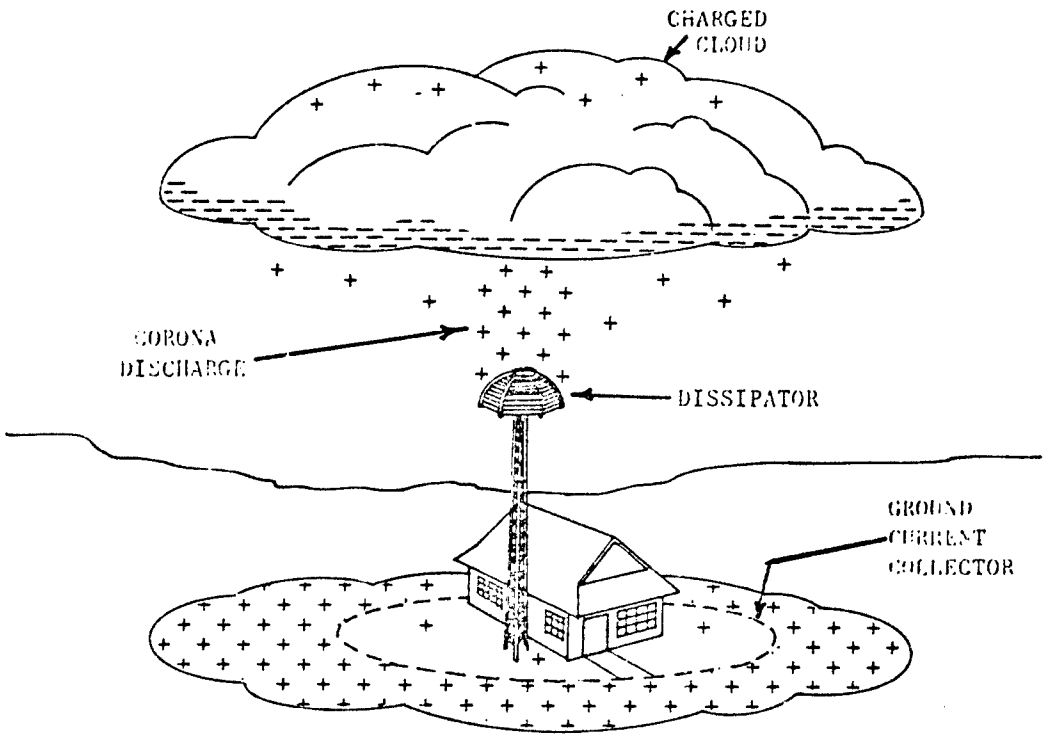

Figure 9

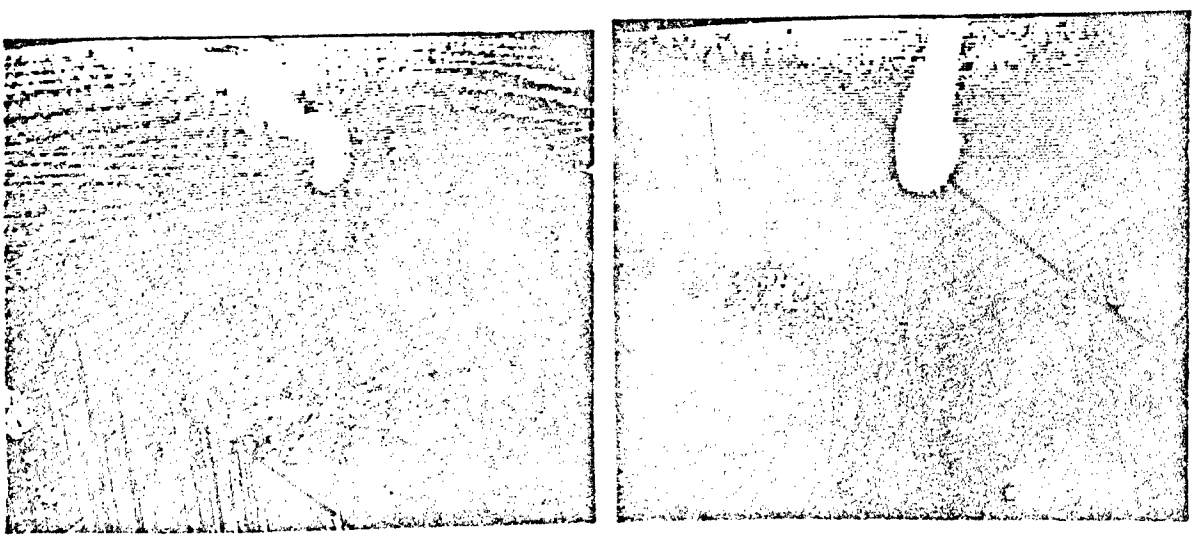

Implementing a DAS™ System

Since the DAS is composed of three subsystems, these must each be designed to perform the required function for the given application. Figure 10 illustrates a potential deployment concept for two applications, an oil storage tank, and an explosives storage bunker.

Figure 10

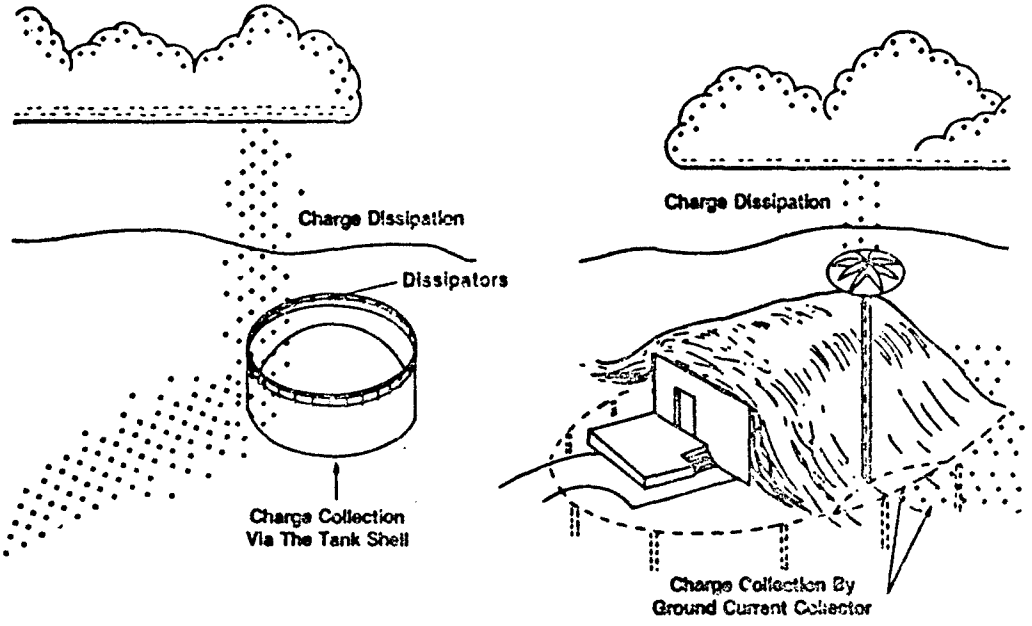

The Floating Roof Tank is protected through use of a circumferential Ionizer mounted to the tank rim. The tank will provide the Service Wire function; and the tank bottom plates provide the Ground Current Collector function.

LEC has protected several hundred tanks this way, some of which have been in service for up to 15 years. In contrast to prior history, none of these tanks have been struck, and none have experienced a "seal fire" since the installations were complete.

The Bunker is protected through use of an Ionizer mounted on a tower beside the bunker. Redundant service wires connect the Ionizer to the circumferential Ground Current Collector. The collector keeps the charge out of the bunker area; and will bypass any charge or earth current around the site, preventing it from passing through the site. As a result, all potential secondary effects are eliminated.

This concept has been implemented in Thailand for the Royal Thai Navy, protecting a large concentration of explosives in a seacoast area with a very high Isokeraunic number (ie. about 170 lightning days per year).

Figure 11 illustrates the installation of a DAS on a hydrogen

off-gas stack. Prior to this installation, any mature lightning storm in the plant area would cause the stacks to ignite, due to the secondary effects - not a direct strike. In the subsequent 8 year history, there has never been a hydrogen stack ignition. PPG Chemical Company of Lake Charles, Louisiana, has subsequently ordered similar protection for other sites.

Figure 11, typical H_2 Stack Protection

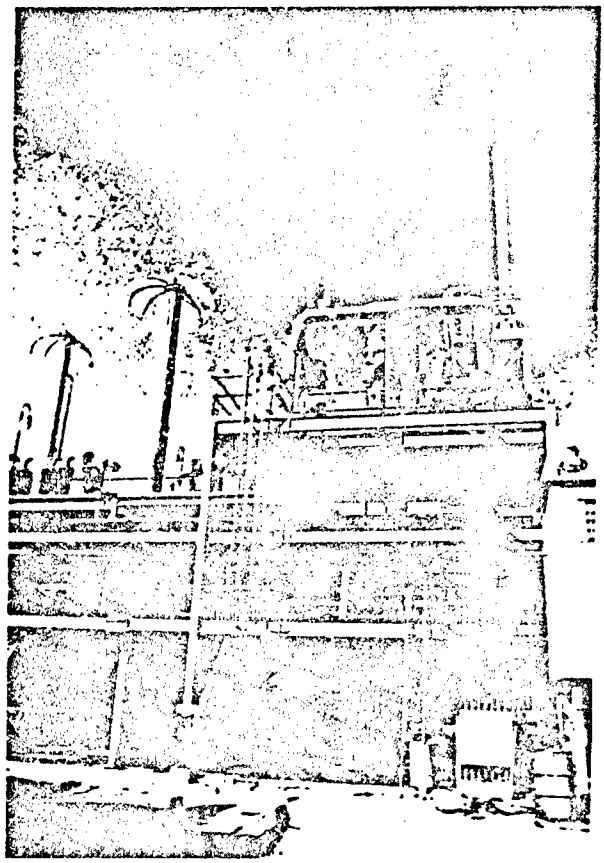

WARNING EXPLOSIVES HANDLERS OF IMPENDING LIGHTNING

By Lon D. Santis[1]

ABSTRACT

This paper gives an overview of the methods that can provide warning of impending lightning to explosives handlers. The methods discussed range from the simplest, most inexpensive to the state-of-the-art. Warning that lightning will enter a sensitive area can be accomplished by visual or public techniques and instrumented techniques. Visual or public techniques include climatology, weather forecasts, and weather observations. Instrumented techniques include AM radio methods or spheric detectors, electric field measurements, wave differentiation or interferometry, and network systems. Evacuation procedures and criteria are mentioned.

INTRODUCTION

If lightning strikes an explosive or explosive device, detonation is very probable, regardless of the precautions taken. Even a near miss could cause a detonation. Many studies have shown that a lightning strike can initiate electroexplosive devices several miles away (1-6).[2] Only a direct strike is of concern when no electroexplosive devices are involved.

A number of industrial activities are sensitive to an unexpected lightning discharge. Munitions operations, fueling activities, and any other endeavors that involve explosive materials are particularly vulnerable. Because of the volatility of the materials, devastating financial or personnel losses could occur in the event of a lightning strike. A system that provides warning of the approach of a thunderstorm is essential to the safety and efficiency of such operations. In the past, lightning warning techniques offered only moderate improvements in safety and efficiency. Recently, however, the ability to warn if lightning will enter a particular area has improved.

Lightning is a threat to any surface or underground operation using volatile materials. Although surface operations are more vulnerable, electric systems and spark-sensitive materials underground at any depth are susceptible to lightning. If lightning strikes conductors leading underground, the energy imparted into the grounding system is too much to handle. The current travels (possibly miles) underground, bleeding itself off and arcing along the way (7). Even if lightning strikes the ground above, dangerous currents can travel nearly 3,000 feet deep in mountainous terrain and over 500 feet in flat terrain (8).

---

[1]Mining Engineer, Pittsburgh Research Center, Bureau of Mines, U.S. Department of the Interior, Pittsburgh, PA.

[2]Underlined numbers in parentheses refer to items in the list of references at the end of this report.

There are two ways to reduce the hazard. The first is the implementation of a lightning warning system (LWS), and the second is the hardening of the operation or the initiating system to initiation by lightning. The discussion in this paper is limited to lightning warning methods and procedures.

Thunderstorms develop in two ways. The first is the frontal type storm caused by a cold air mass overtaking a warm air mass. The second is the convective-type storm caused by the solar heating of the Earth's surface or the right combination of wind direction and topographical features (9,10). In both cases, the cloud becomes electrified by the movement of water particles carried by the rising warm air.

It is relatively easy to predict where an active thunderstorm will travel during its lifetime. The problem of lightning warning, however, is a very difficult one because of the random behavior of lightning and site-dependent variables such as weather patterns, degree of vulnerability, warning time requirements, and schedule flexibility. Hence, it is much more difficult to predict when and where the first strike will occur. The first strike is the very first discharge from a thundercloud.

The methods that can provide warning of a lightning discharge are visual or public methods, and instrumented techniques. Of the instrumented techniques, both single-station (spheric detection, electric field, and wave differentiation or interferometry) and network (magnetic direction finding, time of arrival, and satellite) systems will be discussed.

VISUAL OR PUBLIC TECHNIQUES

Visual or public methods are those that involve simply making casual observations or using information generated for the public.

Climatology: On a global scale, lightning behaves haphazardly, but on a local scale, it tends to move into an area in a habitual fashion. It is very important to understand the tendencies of lightning in your location. Determination of the yearly local weather patterns may be obtained by analyzing the following--

1) Number of discharges per square kilometer per year (see figure 1 (11)). Operations in areas of high flash densities should incorporate the best LWS, whereas operations in areas of low flash densities may opt for a less expensive LWS.

2) Prevailing storm direction.

3) Type of storm, frontal or convective, that predominates.

4) Seasonal variations in lightning activity. Although lightning can occur at any time of year, summer months are the worst (see figures 2-4 (12)).

5) Time of day variations in lightning activity. Usually the hours of noon to 5:00 p.m. are the worst (13).

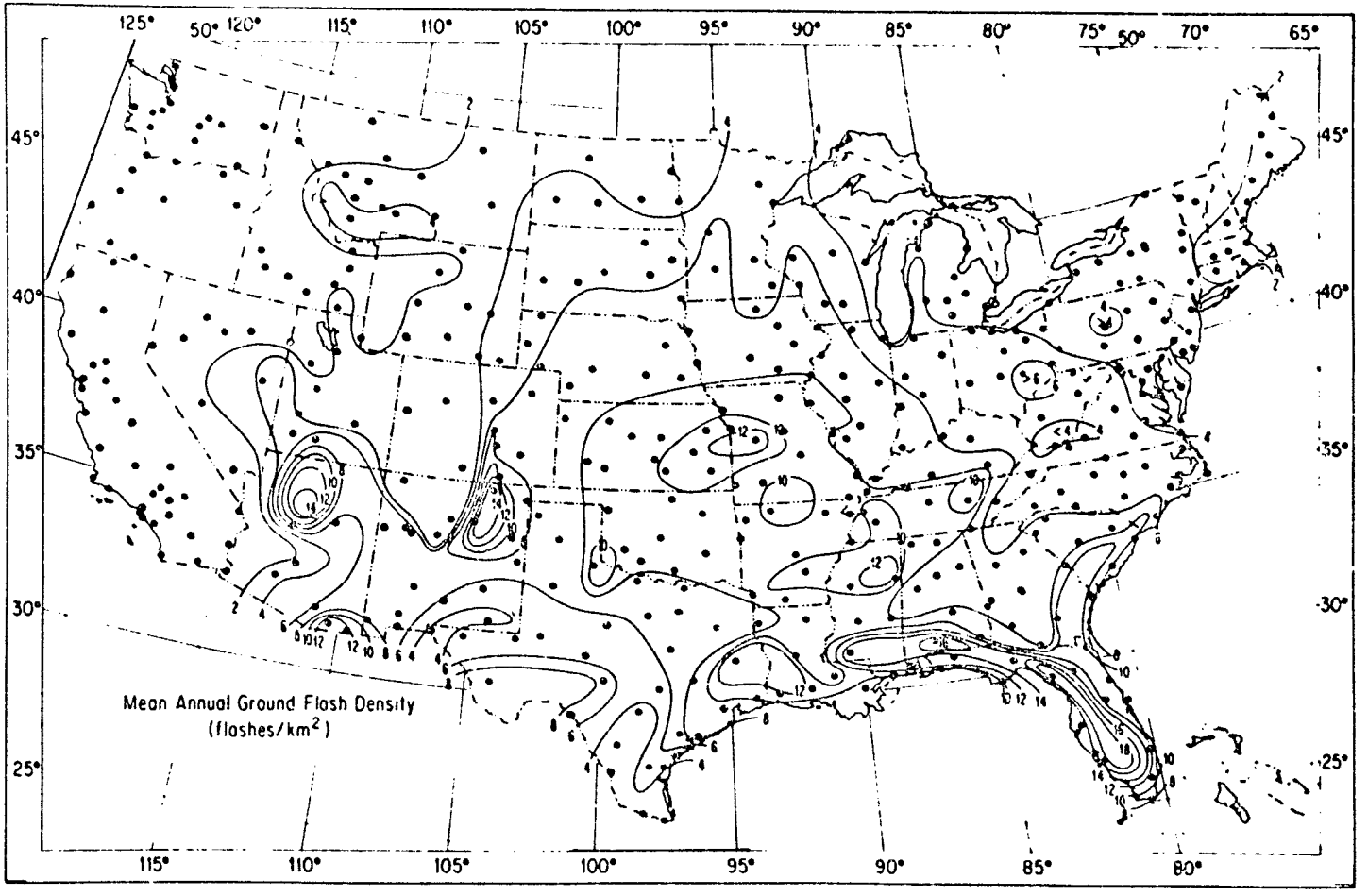

Figure 1. Contour map of mean annual lightning strike density.

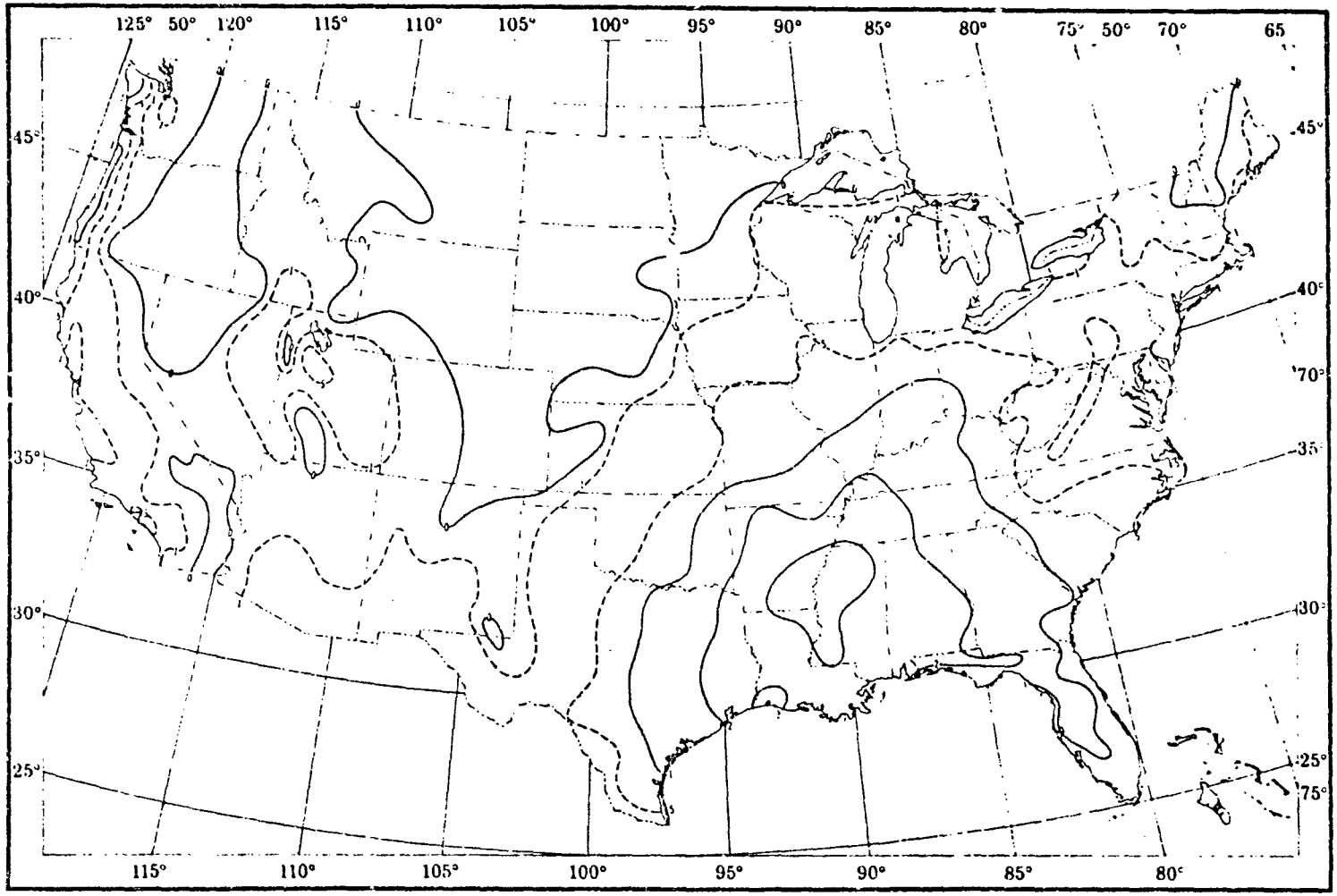

FIG. 2 MEAN NUMBER OF THUNDERSTORMS - JANUARY.

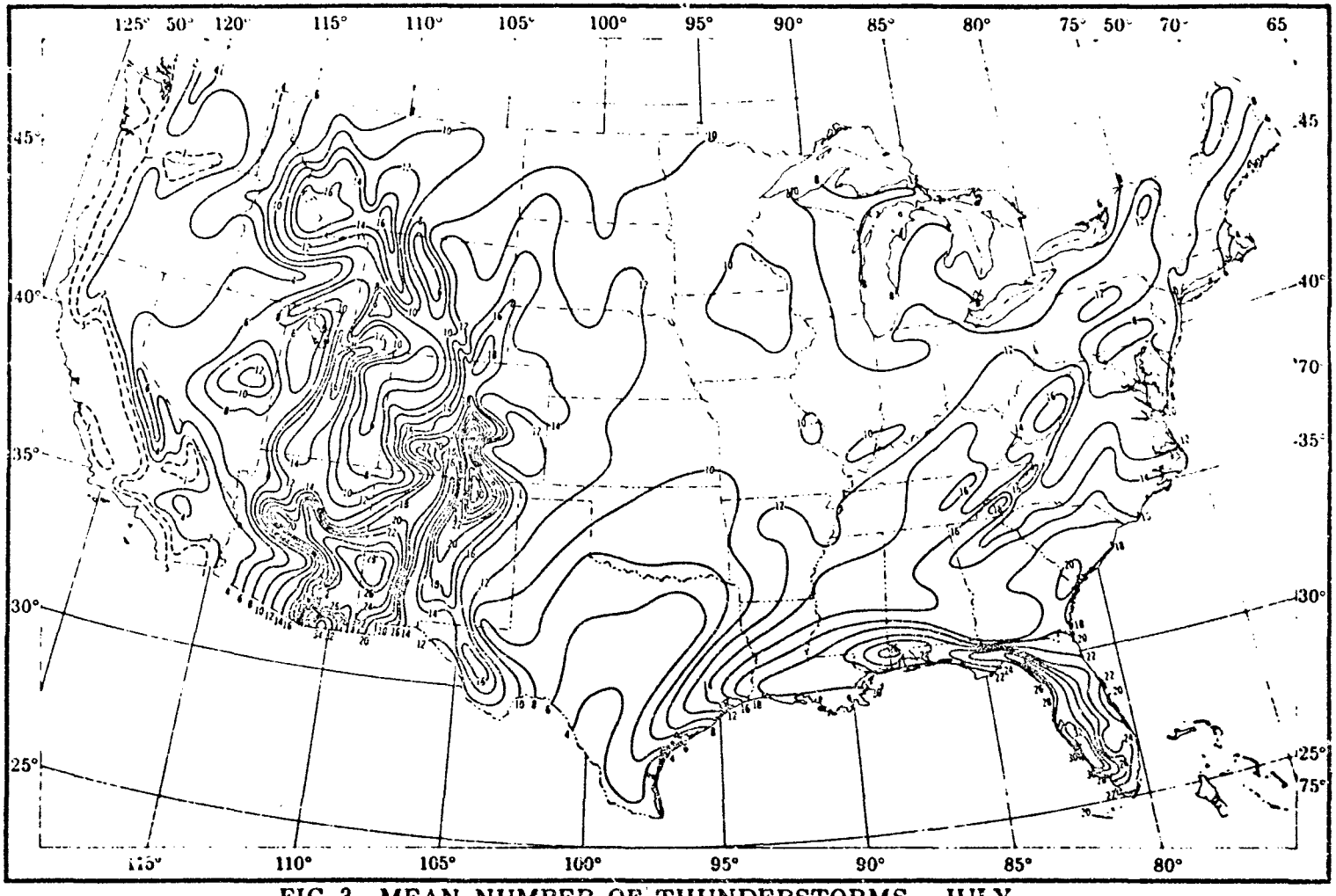

FIG. 3 MEAN NUMBER OF THUNDERSTORMS - JULY.

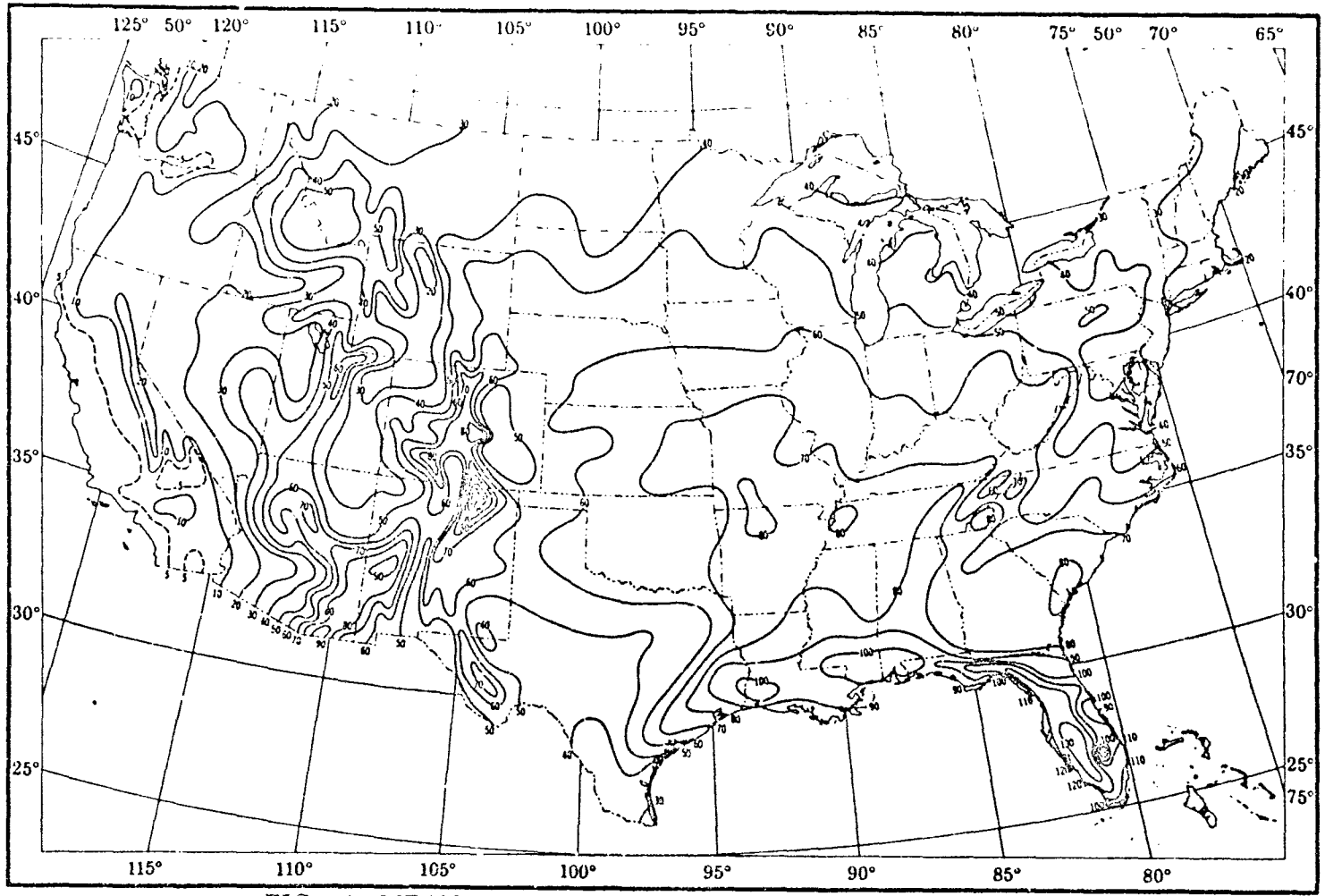

FIG. 4 MEAN NUMBER OF THUNDERSTORMS - ANNUAL.

If possible, sensitive activities should be scheduled at times of low lightning activity. Mine Safety and Health Administration (MSHA) records show that only 7% of lightning-caused premature initiations of explosives in mining operations occurred during the morning hours.

To supplement this information and gain a more individualized perspective, routinely record observations on days that lightning occurs, and look for patterns. Record such information as the date and time, the kind of storm, the direction it came from, how long it lasted, the weather conditions, how the warning (if any) was received, and if any strikes occurred nearby.

Weather Forecasts: Weather forecasts alone are not reliable as a lightning warning technique. Like the variables mentioned above, they only indicate when trouble can be expected. A person charged with sensitive activities should actually become an amateur meteorologist. Learn how to read a weather map and look for a cold front pushing a warm front (frontal-type storms). Convective-type storms are much more difficult to predict but occur almost every day in some areas (Florida and mountainous areas) during certain times of the year.

If possible, subscribe to the Weather Channel or a local radar station through either cable, satellite, or closed circuit broadcasts to obtain up-to-the-minute visual information on storm activity. Level 3 or above on a radar plan position indicator usually means electrical activity is in progress or imminent. If neither of these broadcasts is received, call the local National Weather Service (NWS) weather information service to receive updated information before sensitive activities begin. The local NWS also broadcasts 24-hour weather reports on a frequency between 162.400 and 162.550 MHz. Some radios can pick up this frequency but it can also be picked up with a special radio which costs about $15.

Observations: By making routine observations, one will have a better idea of what to expect, and will learn to recognize when sensitive activities should stop. Prediction of thunderstorms for an area does not always mean that they will arrive. Even if thunderstorms do arrive, it is possible that the vulnerable area is situated such that the storm activity will skirt around it. Conversely, thunderstorms may occur when they were not predicted.

Monitor the sky in the direction where storms usually develop or where they were predicted and look for cumulonimbus cloud formations, particularly anvil-type clouds, and darkening of the sky. Lightning begins to form when the cloud tops of summer convective storms reach about 23,000 feet (14). Winter thunderstorm tops develop at much lower altitudes and are harder to predict.

Keep alert for indicators that can give warning that a lightning discharge may occur nearby, like--

1) Illumination of distant clouds caused by lightning discharges.

2) Thunder. Thunder can be heard up to 8 miles from the source (15). The distance to the strike in miles is equal to the time between visual observation and thunder arrival in seconds divided by five.

3) Rain or hail. A cloud giving as little as 3 mm/hour precipitation can produce lightning (16).

4) Relative humidity and temperature. Moist air aids in the development of thunderstorms, and it is unlikely that lightning would form below certain limits (17) (see figure 5).

5) A sudden drop in barometric pressure or temperature, or a change in wind direction, especially a 180° change. These changes often indicate the approach of a cold front.

6) Luminescence around high or pointed objects (St. Elmo's fire).

Using the above-mentioned tactics with AM radio methods will provide a very inexpensive way to warn of potential lightning hazards. However, this approach has substantial drawbacks, such as

1) The warning criteria are subjective.

2) Possible insufficient warning time to evacuate sensitive area.

3) A nearby lightning discharge may occur without any of the previously mentioned indicators.

INSTRUMENTED TECHNIQUES

AM Radio: The use of an ordinary AM radio is one of the simplest methods of detecting lightning. Most people are familiar with lightning's distinctive static crackling noises that disturb reception during thunderstorms. Every lightning discharge creates strong atmospherics (radio waves) throughout the AM radio band. By tuning the receiver to an unused or clear frequency in the lower end of the band, and listening for these static bursts, one can determine if lightning is occurring within 20 to 100 miles, depending on the sensitivity of the receiver.

Lightning comes from an electrically active cell within a thundercloud. As a cell builds in intensity, lightning occurs more regularly. As the cell decays, so do the spheric bursts. Through the life of a cell, usually 1/2 to 1 hour, lightning flashes two to three times per minute. This rate varies greatly but usually peaks at about 10 discharges per minute (18). By listening to the radio and counting the number of bursts in 1 minute, every 5 to 10 minutes, one can get a feel for whether a storm is building or decaying. This approach is subject to large errors because two or more cells may be active at one time within listening range and there is no way to distinguish among them.

The loudness of the bursts give some idea of how close the activity is. If the static on an AM radio gets increasingly louder, the storm is probably moving closer. Again, this is subject to large errors owing to the overlap of other cells and the variability of lightning itself. The strength of the spheric bursts is a function of the distance to and the strength of the discharge. The current in a cloud-to-ground lightning bolt could peak anywhere between 1 and 200 kiloamperes; thus, a very intense strike far away would sound the same as a very close weak strike.

Figure 5. Temperature vs. Relative Humidity Threshold for Lightning Formation.

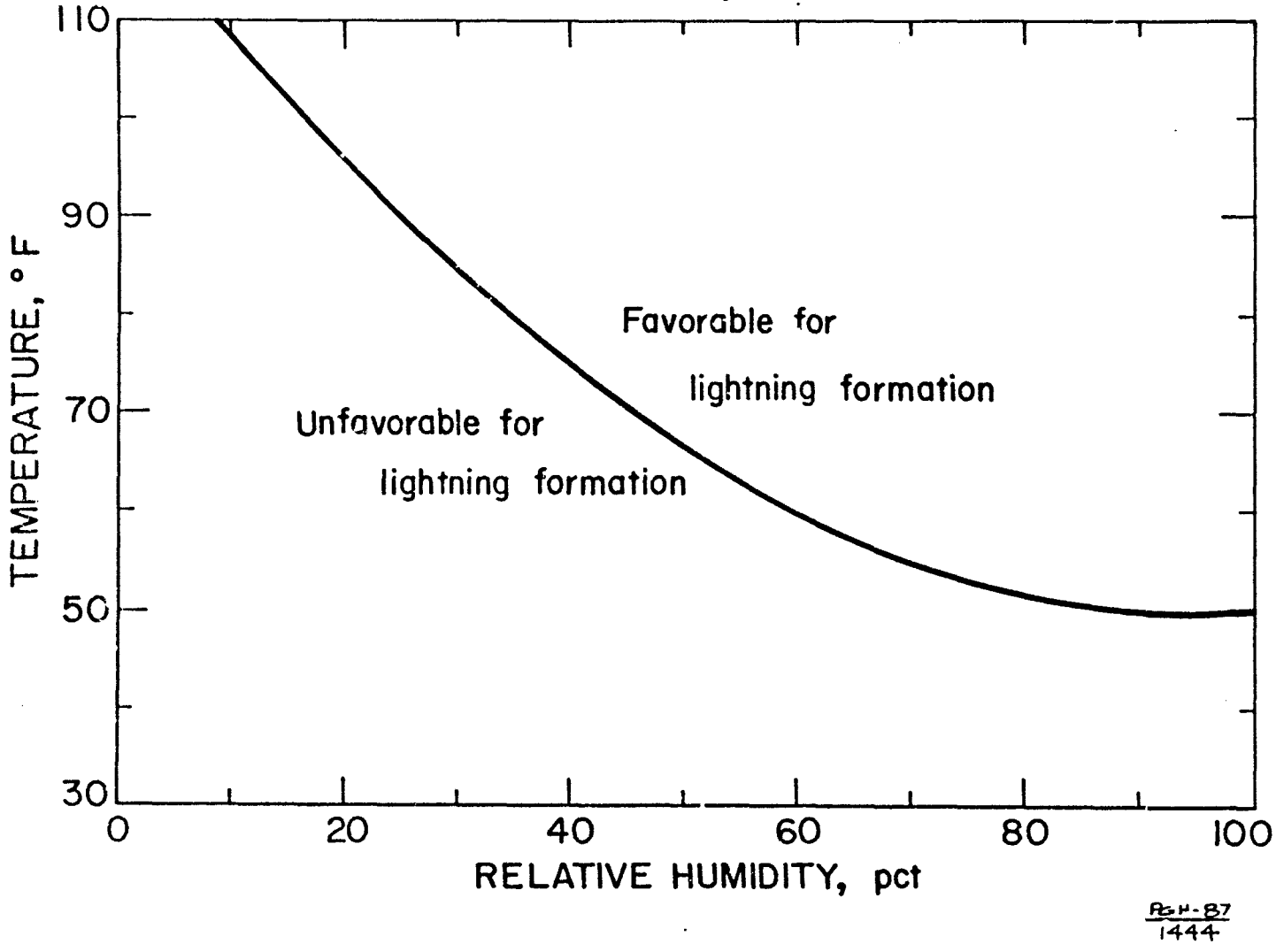

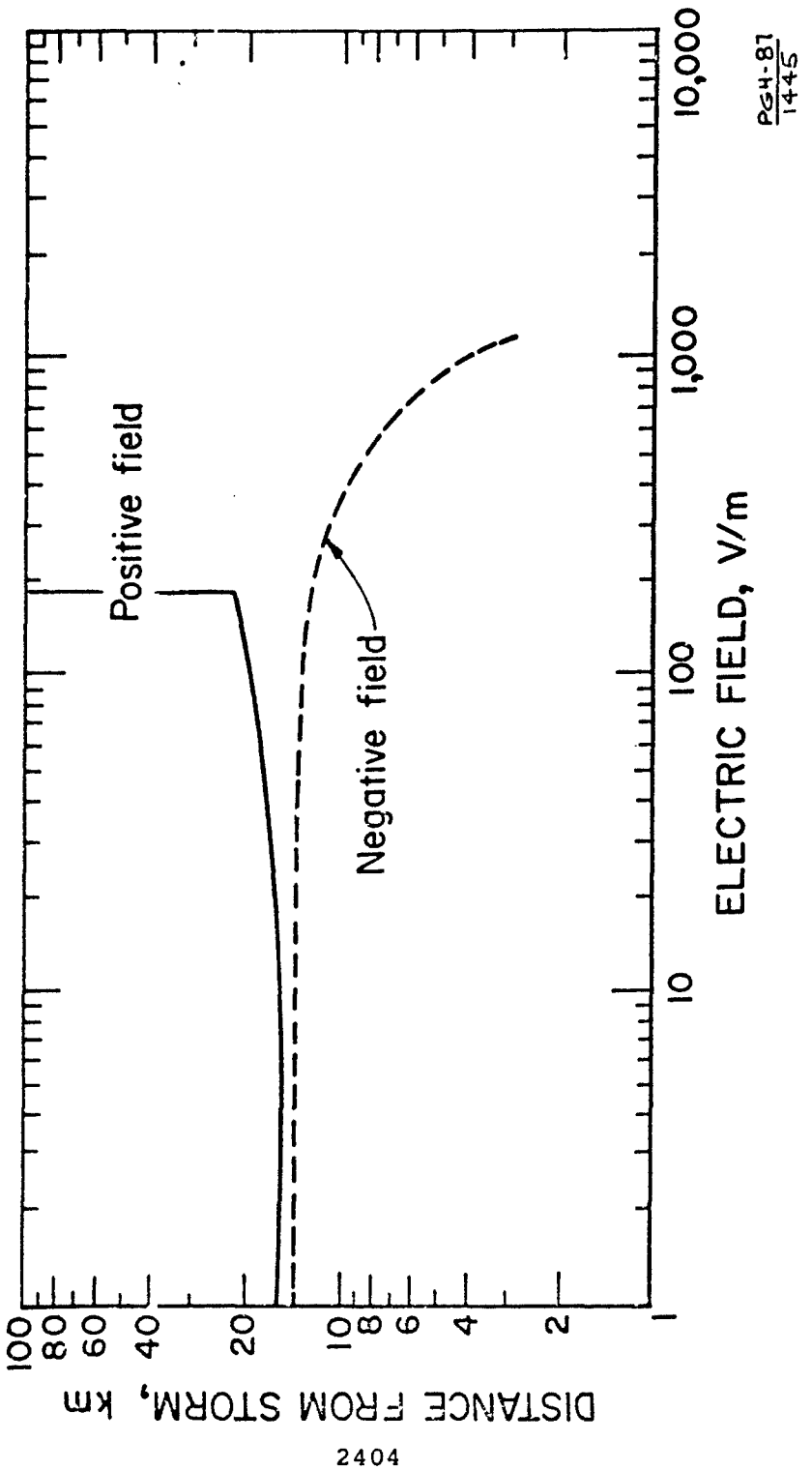

Figure 7. Typical Surface Electric Field Around a Thundercloud.

The advantages of using the AM radio method of lightning warning are--

1) It is inexpensive.

2) No training is required.

3) No special equipment is needed (most operations have an AM radio on site already).

There are significant disadvantages since the method--

1) Gives no indication of storm direction (see figure 6).

2) Gives poor indication of storm distance.

3) Has very subjective warning criteria.

4) Cannot filter out static that may sound like lightning but actually could be caused by electrical equipment, powerlines, dust storms, corona discharge, a faulty radio, or other sources (19).

5) Cannot operate automatically.

6) Exhibits overall poor efficiency.

The main problem with the use of an AM radio as a lightning warning device is that it is very subjective. As with any subjective method, the operator must decide if conditions warrant a stoppage of operations. Underestimation leads to safety concessions; overestimation leads to unnecessary downtime. However, it is better than nothing, and when used with visual or public methods, it offers a cautious operator greatly improved safety.

Spheric Detectors: Spheric detectors also monitor radio waves to detect a discharge. These devices are merely AM radios with added circuitry to eliminate the human factor and unwanted signals. Some of the newer detectors are reasonably reliable as they use statistical analysis methods to monitor the growth and decay of a thunderstorm (20-22). Most devices have range settings and predetermined criteria for alarm. They work well in areas where only frontal-type storms develop (23).

Wave Differentiation or Interferometry: This method involves the differentiation of the radio wave spectrum emitted from a thunderstorm. Various activities in a thunderstorm produce different frequencies. By monitoring, differentiating, and relating these signals, the devices determine the approximate distance to and the direction of the thunderstorm. One system incorporates radar precipitation images to determine if a cloud formation is electrically active (24). The French developed a system, SAFIR, that actually maps discharges in three dimensions using three remote stations (25). These devices are very useful but are also very expensive.

Atmospheric Electrostatic Field: This method monitors the electric (E) field between the cloud and the ground. The thundercloud environment is essentially a huge capacitor. The cloud acts as one plate, the earth acts as

Figure 6.
DEFICIENCIES IN NONDIRECTIONAL SPHERIC DETECTION

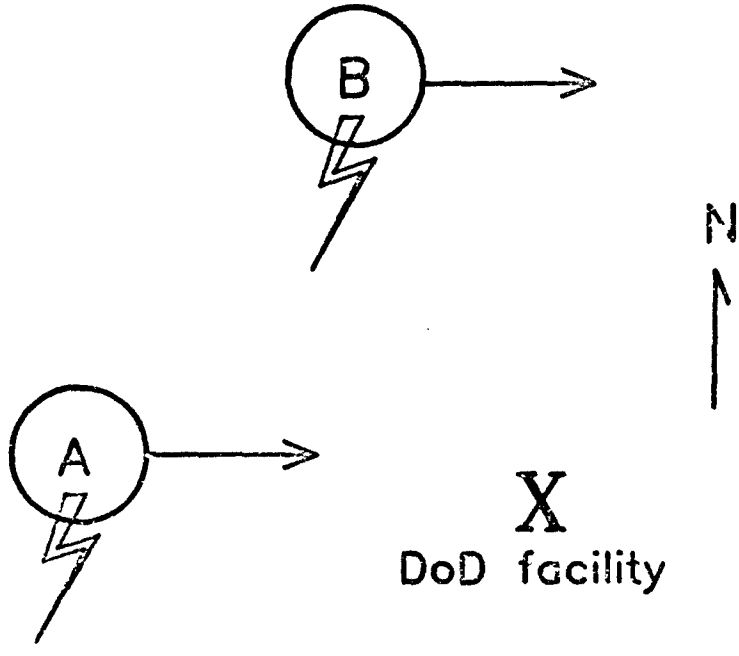

Both cells would sound the same, but with easterly movement, only cell A would pass over the facility.

the oppositely charged other plate, and the lightning bolt acts as the discharge path. See figure 7 for a representation of the surface electric field around a typical thundercloud (26). Notice how the field reverses polarity at a distance of 15 kilometers (10 miles) and builds appreciably inside of 10 kilometers (6 miles).

By monitoring the electric field at the ground surface, a probability that a discharge will occur in the vicinity can be reached. Generally, fair weather fields are around +100 volts per meter, and lightning will form when the field reaches -2 to -5 kilovolts per meter. This method provides the only verified ground-based way to warn of the first strike of a thundercloud building overhead. This quality is especially important in areas where convective-type storms develop. However, operations should not rely upon electric field measurements as the sole method of warning because of the influence of space charges; also they may only allow minutes or even seconds to take any action.

When an electrically active cloud moves in, corona from grounded objects cause a masking or screening layer of space charge near the ground surface. This influences the magnitude of the E-field measured at ground level. This can give erroneous information on the location and magnitude of the charged area aloft. Even under fair weather conditions, there are many processes that introduce space charge into the atmosphere, including blowing snow or dust, splashing water, engine exhausts, industrial emissions, and high-voltage powerlines. Wind can transport these space charges many miles (27,28).

Regardless, a particular site could arrive at criteria to stop sensitive operations and evacuate personnel when--

1) The E-field reverses polarity and/or steadily builds.

2) The E-field crosses the site-dependent threshold.
   a) Start with 2 kilovolts per meter.
   b) Through experience, determine if this value is suitable.
   c) Adjust threshold accordingly.

Networks: The development of lightning detection networks (see figure 8) has made the biggest breakthrough in the area of lightning warning. Networks provide the best real-time, real-location detection of individual lightning strokes (29). Presently two methods are used: magnetic direction finding (MDF), and time of arrival (TOA) location finding.

The MDF network employs an array of two crossed loop antennas to determine an azimuth to the discharge (30). A central computer then triangulates between two or more remote stations to determine the location of the discharge. The network records and stores almost every (70%-90%) flash within the network's range. A lightning display system (LDS) can receive real-time or stored information on lightning activity. The network covers the contiguous United States, although detection efficiency is poor in the northern Midwest. The network determines the location (within a few miles), polarity, multiplicity, and peak current of a particular strike. It computes flash rates and flash densities for a particular area. Flashes can be color coded chronologically. This allows easy determination of the direction the storm is moving and its velocity (31-34). Figure 9 is a typical display from

Figure 8. Lightning Detection Networks.

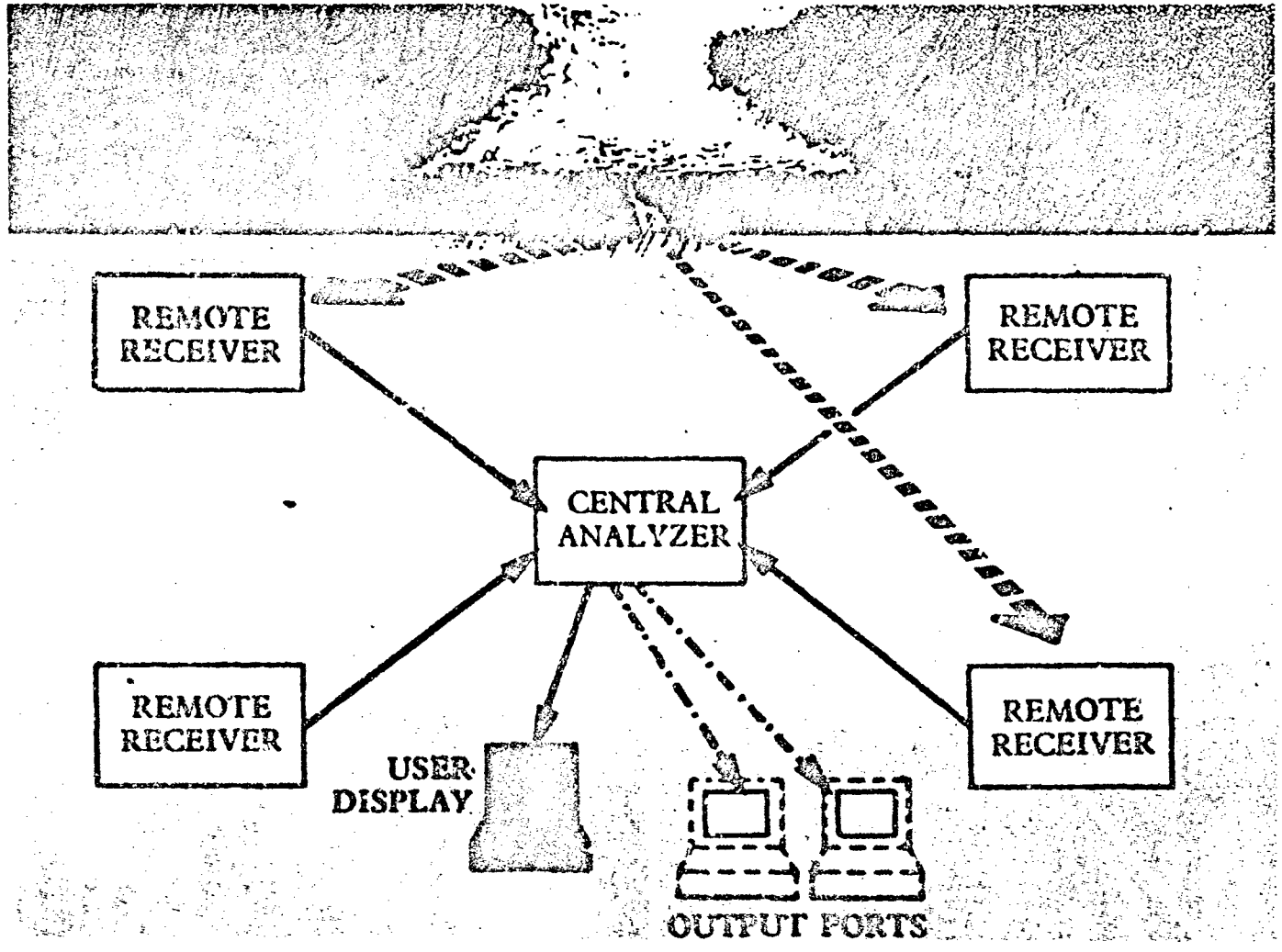

Figure 9. MDF Network Display.

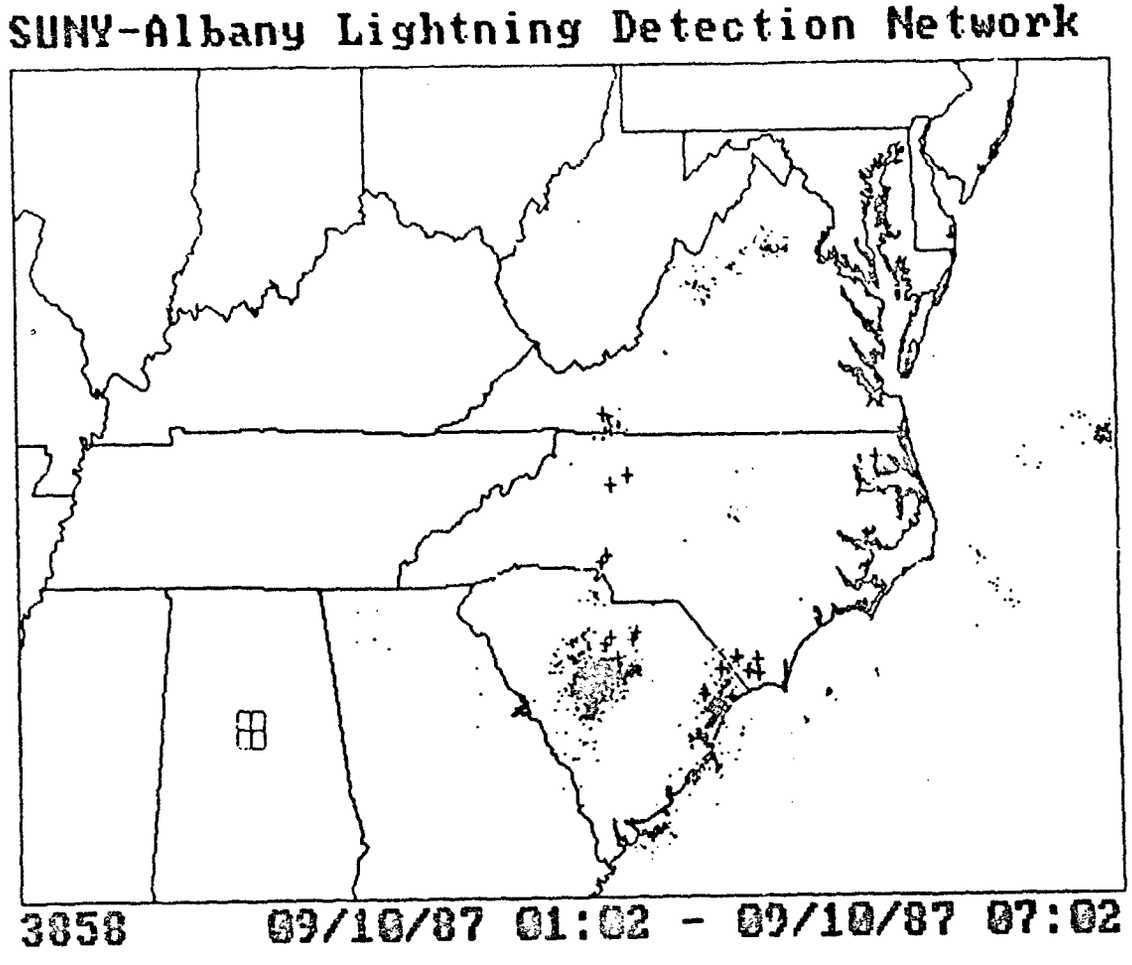

the network. Dots are negative discharges, and plus signs are positive discharges. Six color codes in 1-hour increments provide a chronological record of each event.

The other network, TOA, uses an array of simple whip antennas to record the real-time (within microseconds) that the very low frequency (VLF) wave peak from a discharge arrives. Again, a central computer triangulates between two or more remote stations to find the location of the flash. Output from the TOA network is similar to that of the MDF network (35).

The TOA network offers a service called the Weather Sentinel Service (WSS). For a moderate monthly fee, the network will monitor a user-defined area within the network's range for lightning flashes. As soon as it senses a discharge in the defined area, the WSS computer notifies the subscriber via numeric or digital display, or microprinter. Pager systems and audible alarms notify the user of new messages. Perhaps the best definition of the warning area is a bullseye-like set of range circles at 10, 25, and 50 miles radius. This would tell if a storm is moving closer to or away from the sensitive area.

The WSS also provides general weather information that could be useful, such as--

1) Predicted high and low temperatures.

2) Relative humidities and dew points.

3) Maximum possible rainfall.

4) % chance of precipitation.

5) % chance of severe weather.

6) % of possible sunshine.

7) Atmospheric inversion.

8) Many other parameters (36,37).

See figure 10 for the network's coverage area.

A third network has been proposed. NASA is investigating the possibility of using satellites to detect the illumination of cloud tops caused by lightning (38). This project is still in the development stages. It does not appear to offer any significant advantages over the existing networks other than detecting intercloud discharges. These discharges occur up to 6 minutes before the first cloud-to-ground strike. This could give very short warning of the first strike.

See Table 1 for a summary of available commercial lightning warning devices.

Figure 10. TOA Network Coverage Area.

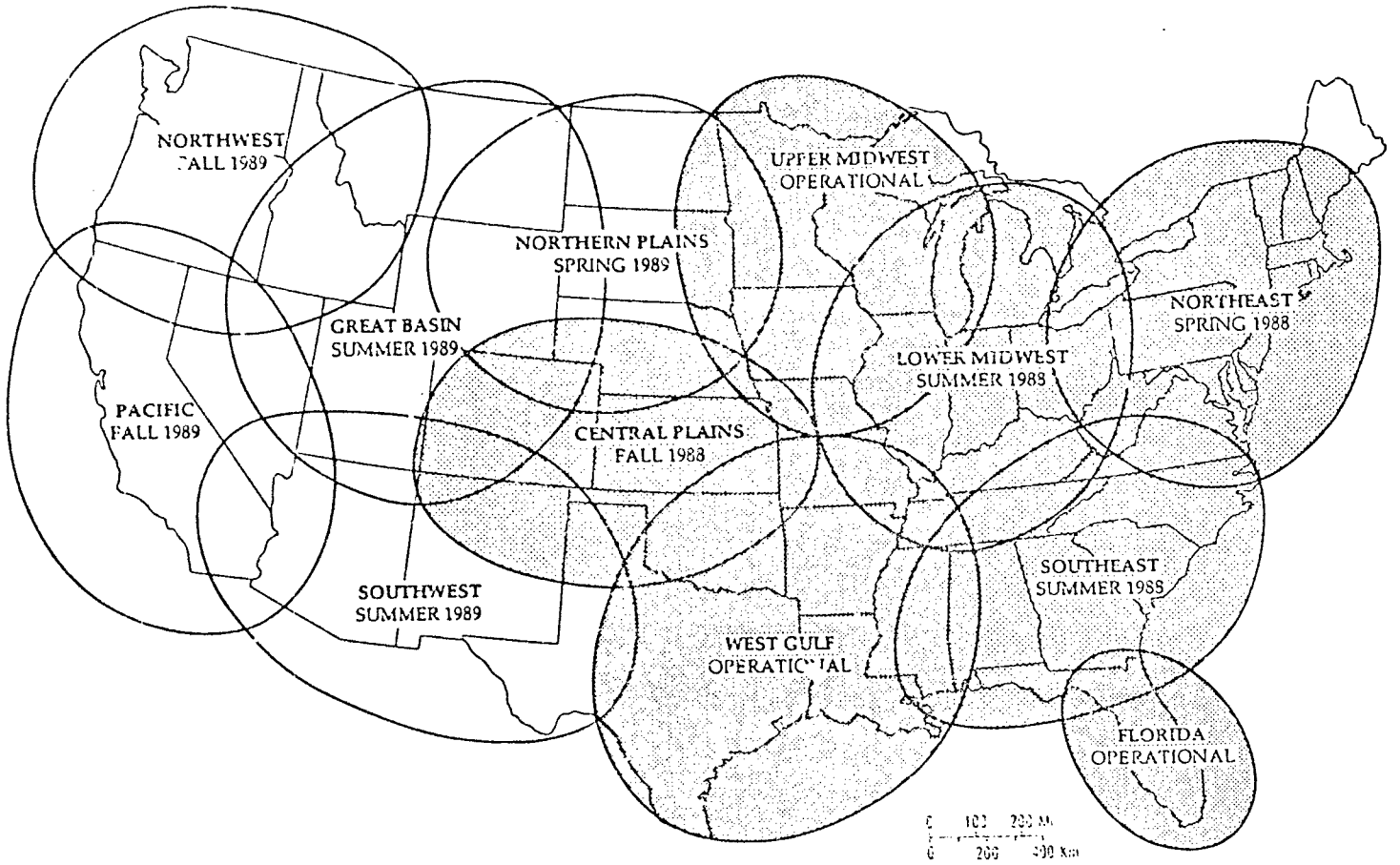

Table 1. Commercial Lightning Warning Systems

Method	Cost	Reliability[1]	Efficiency[2]
Electric field measurement	$790 to $11,000	90%-65%	Good to very good
Spheric detectors	$60 to $16,000	95%-60%	Poor to very good
Wave Differentiation	$4,000 to $30,000	N/A[3]	Good to excellent
MDF network	$19,000/yr plus LDS ($9,000)	90%-70%	Excellent
TOA network	$10,000 plus options	90%-70%	Excellent
Weather Sentinel Service	$100 to $150 per month	90%-70%	Very good

[1]Percentage of strikes detected.

[2]Ability of system to give warning without false alarms.

[3]Not applicable, devices detect electrically active regions.

EVACUATION PROCEDURES AND CRITERIA

Under certain conditions, lightning could set off electroexplosive devices many miles away. From the existing literature on thunderstorm development (39), where D is equal to the range sensitivity of the operation to lightning in miles, the following recommendations can be made for safe distances from known electrical activity. When E-field measurements are available, the safe distance is D plus 5 miles. When E-field measurements are not available, the safe distance is D plus 25 miles. For operations where no electric initiators are used, D is 0 because a direct strike is necessary. For operations where standard electric initiators are used, D is 20 miles in mountainous terrain and 5 miles in flat terrain (40). Mountainous terrain is more hazardous because the strata typically have high resistivity values, allowing dangerous currents to travel farther. Other facilities such as underground or nuclear operations or those using special initiators need to determine their own unique D.

As soon as a hazard is present, immediately remove personnel from the vulnerable area. Employ an alarm system to notify the workers as soon as possible. Do not try to pick up explosives already unloaded. Resume operations only if 30 minutes has passed and there was no indication of lightning activity.

CONCLUSIONS

Because of the unpredictable behavior of lightning, a lightning warning system that provides valid warning 100% of the time has not been and probably will not be developed. However, an operation can obtain substantial improvements in safety and efficiency by using some form of LWS. The following conclusions can be drawn:

1) Base the decision as to what type of lightning warning system to install on the following criteria.
   a) Degree of protection desired.
   b) Warning time necessary.
   c) Type of storms (frontal or convective) that predominate.
   d) Affordable cost. In general, the effectiveness of a lightning warning system is proportional to its cost.

2) Any effective LWS will be a combination of--
   a) Short-to-medium range forecasting to avoid times of high lightning probability, and
   b) Immediate hazard detection and prompt evacuation of the sensitive area.

3) The most effective instrumentation seems to be a combination of devices based on spheric detection and electric field measurement (41).

4) Network systems provide the most reliable spheric detection method.

5) Cost reductions could be made by using other spheric methods instead of networks at the expense of effectiveness.

6) E-field measurements provide the only verified way to warn of the first strike. This quality is especially important in areas where convective storms develop.

7) E-field measurements alone are not recommended as a LWS. Accompany them with a spheric method.

8) Always use visual and/or public methods.

APPENDIX. LIGHTNING WARNING LIST OF MANUFACTURERS[3]

Spheric detectors

Atmospheric Research Systems, Inc.
2350 Commerce Park Drive, N.E.
Suite 3
Palm Bay, FL 32905
(303) 725-8001

Nuclear Instruments Corp.
2345 W. Mill Road
Milwaukee, WI 53209
(414) 228-8800

Safety Devices, Inc.
7910-A Hill Park Ct.
Lorton, VA 22079
(703) 550-9899 or
(703) 339-6650

Signal Design, Inc.
3 Autry
Irvine, CA 92718
(714) 581-2870

E-Field

3M/Static and EMC
P.O. Box 2963
Bld. 590
Austin, TX 78769-2963
(512) 834-1800

Atmospheric Research Systems, Inc.
2350 Commerce Park Drive, N.E.
Suite 3
Palm Bay, FL 32905
(303) 725-8001

Electroforces, Inc.
P.O. Box 523772
Miami, FL 33152
(305) 594-0304

---

[3]This list of manufacturers does not claim to be complete nor is it an endorsement of a particular company or product.

Electronique 2000
8, rue Rere Champhine
38600 Fontaine, France
(76) 26 53 27

Environmental Sensing Technology
1054 Hawthorne Ave., East
St. Paul, MN 55106
(612) 776-9668

Interstate Electrostatics Corp.
8627 Guthrie Rd.
Box 216
Calhan, CO 80808
(719) 683-2419

Lightning Eliminators Consultants, Inc.
13007 Lakeland Rd.
Santa Fe Springs, CA 90670
(213) 946-6886

Monroe Electronics, Inc.
100 Housel Ave.
Lyndonville, NY 14098
(716) 765-2254

Qualimetrics, Inc.
P.O. Box 41039
Sacramento, CA 95841
(916) 923-0055

MDF Network

Bureau of Land Management
3905 Vista Ave.
Boise, ID 83705
(208) 334-9880

State University of New York at Albany
Dept. of Atmospheric Science, ES216
1400 Washington, Ave.
Albany, NY 12222
(518) 442-4555

TOA Network and Weather Sentinel Service

Atmospheric Research Systems, Inc.
2350 Commerce Park Drive, N.E.
Suite 3
Palm Bay, FL 32905
(303) 725-8001

R*Scan Corp.
Minnesota Supercomputer Center
1220 Washington Ave. South, Suite 2170
Minneapolis, MN 55415-1258
(612) 333-1424

Wave Differentiation or Interferrometry

Aviation Safety Systems/3M
6530 Singletree Dr.
Columbus, OH 43229
(614) 885-3310

Lightning Location and Protection, Inc.
1001 South Euclid Ave.
Tucson, AZ 85719
(602) 624-9967

ONERA
29 Avenue D'La Division Le'Clerk
92320 Chatillion, France

Sperry Aerospace Group
P.O. Box 21111
Phoenix, AZ 85036-1111
(602) 867-2311

REFERENCES

1. Fedoroff, B. T., and O. E. Sheffield. Electricity, Extraneous and Hazards Associated with it. Definition in Encyclopedia of Explosives and Related Items, V. 5, Picatinny Arsenal, Dover, NJ, 1972, pp. E35-E38.
2. Davey, C. T. and W. J. Dunning. A Study of Packaging and Shipping Procedures for Small Electroexplosive Devises (NASA contract report No. F-C1853), Franklin Institute Research Laboratories, May 1966 - Aug. 1967, 77 pp.
3. Berger, K. Protection of Underground Blasting Operations. Ch. in Lightning, ed. by R. H. Golde. Academic Press, v. 2, 1977, pp. 633-657.
4. North, H. S. Initiation of Electroexplosive Devises by Lightning. Paper in Proc. of the 6th Symp. on Electroexplosive Devices, San Francisco, CA, July 8-10, 1969, pp.3-8.
5. Johnson, R. L., W. M. Sherrill, J. D. Moore, and D. E. Janota. Evaluation and Improvement of Electrical Storm Warning Systems (BuMines contract J0387207, Southwest Research Institute). Nov. 1979, 98 pp.
6. Golde, R. H. Mining and Blasting. Section in Lightning Protection, Chemical Publishing Co., 1973, pp. 133-138.
7. Explosives Today. Safety in Electric Detonators. Series 2, No. 42, June 1986, AECI Explosives and Chemicals Ltd., 4 pp.
8. Work cited in reference 3.
9. Cianos, N. and E. T. Pierce. Methods for Lightning Warning and Avoidance (McDonnell Douglas Astronautics Company contract 6-73-300H, Stanford Research Institute). May 1974, 80 pp.
10. Banta, R. M., and C. B. Schaaf. Thunderstorm Genisis Zones in the Colorado Rocky Mountains as Determined by Traceback of Geosynchronous Satellite Images. Monthly Weather Review, V. 115, No. 2, Feb., 1987, pp. 463-476.
11. MacGorman, D. R., M. W. Maier, and W. D. Rust. Lightning Strike Density for the Contiguous United States from Thunderstorm Duration Records (U. S. Nuclear Regulatory Commission contract NRC-01-79-007, National Oceanic and Atmospheric Administration). NUREG/CR-3759, May 1984, 43 pp.
12. Changery, M. J. National Thunderstorm Frequencies for the Contiguous United States (U. S. Nuclear Regulatory Commission contract FIN B1056, National Oceanic and Atmospheric Administration). NUREG/CR-2252, Nov. 1981, 22 pp.
13. Work cited in reference 9.
14. Moore, C. B., M. Brook, and E. P. Krider. A Study of Lightning Protection Systems. New Mexico Institute of Technology, Socorro, NM. October 1981, 101 pp.
15. Pierce, E. T. Lightning Warning and Avoidance. Ch. in Lightning, ed. by R. H. Golde, Academic Press, v. 2, 1977, pp. 497-518.
16. Moore, C. B., and B. Vonnegut. The Thundercloud. Ch. in Lightning, ed. by R. H. Golde, Academic Press, v. 1, 1977, pp. 51-92.
17. Work cited in reference 15.
18. Work cited in reference 14.
19. Work cited in reference 14.
20. Atmospheric Research Systems, Inc. Data sheets on the Flash Warning System (FWS-4A). 2350 Commerce Park Drive, N. E., Suite 3, Palm Bay, FL 32905.
21. Signal Design, Inc. Data sheets on the Spescom 20-5 Lightning Warning System. 3 Autry, Ervine, CA 92718.

22. Eriksson, A. J., Kuhn P. C., and H. J. Geldenhuys. An Improved Lightning Warning System. S.A.I.E.E. Symposium on Electronics in Mining, 1984, pp. 5E1 to EE12.
23. Work cited in reference 5.
24. 3M. Pamphlet on the Stormscope. 3M Center, St. Paul, MN 55144-1000.
25. Richard, P., A. Soulage, P. Laroche, and J. Appel. The SAFIR Lightning Monitoring and Warning System, Applications to the Aerospace Activities. Paper in Proceedings of the 1988 Int. Aerospace and Ground Conf. on Lightning and Static Electricity, NOAA, Apr. 19-22, 1988, Oklahoma City, OK, pp. 383-390.
26. Work cited in reference 14.
27. Work cited in reference 9.
28. Markson, M., and B. Anderson. New Electric Field Instrumentation and the Effects of Space Charge at the Kennedy Space Center. Airborne Research Associates, Weston, MA, Spring, 1983, 8 pp.
29. Work cited in reference 5.
30. Krider, E. P., R. C. Nogle, and M. A. Uman. A Gated Wideband Magnetic Direction Finder for Lightning Return Strokes. J. of Applied Meteorology, v. 15, March 1976, pp. 301-305.
31. Orville, R. E. Nowcasting Using Lightning Location Techniques. Paper in 2nd Int. Symp. on Nowcasting, Norrkoping, Sweden, Sept. 3-7, 1984, pp. 523-524.
32. Orville, R. E., R. B. Pyle, and R. W. Henderson. Reliability and Availability of Data for Utility Companies from the East Coast SUNYA Lightning Detection Network. Paper in Proceedings of the 12th Inter-Ram Conference for the Electric Power Industry, Baltimore, MD, Apr. 9-12, 1985, pp. 50-54.
33. Orville, R. E. Private Communication, Sept., 1987.
34. Vance, D. L. The Geographical Distribution of Lightning, Forestry and Range Requirements and Interests. Paper in Proceedings of the Workshop on the Need for Lightning Observation from Space, Feb. 13-15, 1979, pp. 110-114.24. 35. Atmospheric Research Systems, Inc. Data sheets on the Lightning Position and Tracking System (LPATS). 2350 Commerce Park Drive, N. E., Suite 3, Palm Bay, FL 32905.
36. R*Scan Corp. Pamphlets on the Weather Sentinel Service. Minnesota Supercomputer Center, 1200 Washington Ave. South, Suite 2170, Minneapolis, MN 55415-1258.
37. Bauer, K. G. (R*Scan Corp.). Private communication, Sept., 1987.
38. Christian, H. J., W. W. Vaughn, and J. C. Dodge. The Detection and Location of Lightning from Space. A.I.A.A. Technical Information Service, NY, 1985.
39. Work cited in reference 9.
40. Work cited in reference 5.
41. Guthrie, M. A. Lightning Warning Systems for Explosive Operations/ Facilities. U. S. Nav. Surf. Weapons Cent., Dahlgren, VA, ADP000462, Aug., 1982, 20 pp.

ELIMINATION OF STATIC CHARGE USING RADIO-ACTIVE ISOTOPES

Static Electricity has been recognised as a potential hazard that could cause serious accidents in several types of industries, i.e. synthetic textiles, powder handling, solvent handling, explosives etc. It is, therefore, a matter of prime importance that ways and means have to be devised to successfully combat this threat and eliminate the charges developed by static electricity from hazard-prone environments. In this paper an attempt has been made to present the subject of elimination of static charges using radio-active isotopes with special reference to the explosive industry. It would be relevant to highlight some basic aspects relating to static electricity, its mode of generation, methods of its suppression etc before going over to the discussions on the suppression method adopting use of radio-isotopes.

2. STATIC ELECTRICITY AND ITS MODE OF GENERATION

Static Electricity is definable as the accumulated immobile electric charges present in various materials. It is essentially a surface phenomenon. It is generated when two different materials come into contact and are separated or when friction is induced between them as by rubbing. Though the name tribo-electricity has been employed as an alternative, it is not always necessary to have friction for generation of static charges. Some of the typical industrial situations wherein static electricity is generated concerns operations like fluid flow, grinding, sieving, pouring, moving, stirring etc. As the charge builds up, there exists the potential danger of its exceeding a threshold limit, i.e. resistance of the air gap between the charged material and another object, earthed or otherwise. If this happens, the charge gets discharged through a spark. The electrical energy of a conducting object carrying a charge is given by

$$E = 10^{-3} \frac{CV^2}{2}$$

Where

E = Energy is micro-joules (10^{-6} joules)

C = Capacity of the object, picofarads (10^{-12} farads)

V = Potential. Kilo Volts (10^{3} Volts)

2.1 E.g - A Metal plate could have a capacitance of 10 pf. Thus a metal plate is charged to a potential of 20 kv has an energy of about 2 mj.

The capacitance of an insulated human body could be 400pf. Assuming that a potential of 10,000 Volts is generated in a process involving manual operations, the energy associated with such a system would be

$$E = 1/2 \times 400 \times 10^{-12} \times 10,000 \times 10,000 = 0.02 \text{ Joules.}$$

2.2 It has been seen that some of the primary explosives like lead azide, lead styphnate, mercury fulminate etc could be ignited at energies lower than 0.02 Joules.

3. SOME TYPICAL ACCIDENTS CAUSED BY STATIC ELECTRICITY IN THE FIELD OF EXPLOSIVES MANUFACTURE

3.1 Example -1 : In 1955 in UK, while lead styphnate was being weighed, ignition occured. The enquiry revealed that the most likely cause of the accident was release of static electricity from the Operator's body.

3.2 Example - 2 : In India, while cut waste propellant was being poured from a Container on to a concrete platform for destruction purposes, ignition took place. The reason was attributed to static electricity.

3.2.3 There could be a host of similar accidents in various parts of the world. While there might be several causes that could lead to a fire or accident, static electricity stands out as one of the prime culprits.

4. METHODS OF ELIMINATION OF STATIC ELECTRICITY

Broadly speaking, there are two basic methods of elimination of static charges. These are

4.1 Prevention of static generation

4.2 Accelerating the rate of dissipation

4.3 Prevention of static generation could be achieved by reduction of friction, changing the potential of the contact elements, blending of different fibres (in textile industry) etc.

4.4 Acceleration of the rate of decay of the charge is feasible by adoption of measures like earthing and bonding of equipments, humidification, avoidance of non-conductors and ionisation. All these methods are in use in various countries. There are merits and demerits attributable to each system. E.g. in a process building manufacturing pyrotechnic compositions, it would be unwise to operate at high relative humidity conditions. The excess humidity will render the composition inactive, erratic in behaviour and unreliable. While humidification, earthing, bonding etc. are essential features one might still prefer to operate under a lower margin of ambient humidity to overcome the aforesaid problems. In such situations, it is considered worthwhile to adopt a charge dissipation system based on ionisation of air through the use of radioactive isotopes.

5. CHARGE ELIMINATION BY RADIOACTIVE ISOTOPES

Radio isotopes continue to emit α , β or γ radiations selectively throughout the period of their half life. Such radiations possess the property of ionising the air through which these pass. The liberated ions are free to react with the accumulated charges and neutralise their polarity.

5.1 Fig - 1 · Overleaf illustrates the schematic arrangement for elimination of static charges using radio isotopes.

5.2 The radioactive source is a weak β emitter in the form of TL-204 isotope. This isotope has a half life of nearly 3 1/2 years. The isotope is itself housed in a shielded holder which could be metallic or of plastic construction. A plastic cover is desirable as there would be less chance of secondary emmisions. The holder is provided with a removable cover which could be opened or closed by remote control.

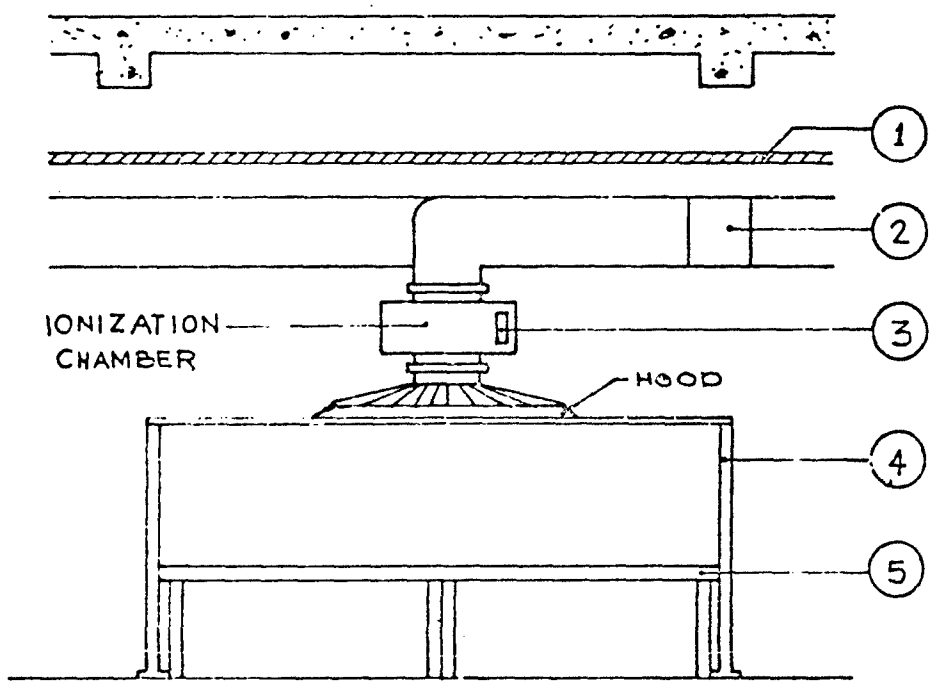

FIG. 1

SCHEMATIC ARRANGEMENT FOR ELIMINATION OF STATIC CHARGES USING RADIOISOTOPES

1) FALSE CEILING
2) G.I DUCT
3) RADIO ACTIVE SOURCE (β-EMITTER)
4) SUPPORT
5) WORK TABLE

The holder itself is housed in a hooded enclosure which provides proper geometric cover to the personnel engaged so that they are not exposed to harmful radiations. A stream of conditioned air is allowed to flow through the isotope when the former gets ionised. The ionised air thereafter flows over the work area where static hazard-prone explosives are handled. Thus effective neutralisation of the static charges takes place even under reduced relative humidity in the environment. There is no gainsaying the fact that other essential measures like wearing conducting footwear and cotton clothing by the personnel and use of conductive or anti-static flooring are indispensable to ensure safety.

6. PERSONNEL SAFETY

The very mention of radio isotopes conjures up visions of hazards to personnel from deleterious nuclear radiations. It is for this reason that a weak β emmitter like TL-204 has been chosen duly ensuring adequate shielding from harmful radiations. The personnel are never exposed to direct radiations and only ionised air is permitted to permeate the working area.

7. SUMMARY

Static Electricity is a major factor causing diverse accidents in the explosive industry. While it is necessary to check the generation of a statically charged environment, elimination of such charges assumes greater importance. It is possible to use a radio isotopic source like TL-204 in a compact form, the radiation emanating from which is made to ionise an air stream passing over the work area. Thus a safe working environment is achieved, simultaneously obviating processing problems arising from high humidity conditions.

V PADMANABHAN
GENERAL MANAGER
ORDNANCE FACTORY
DEHU ROAD,PUNE-412 113
(INDIA)

Chairman's Closing Remarks

On behalf of the Secretary of Defense, I would like to thank each of you for your attendance and participation in this Seminar. It is through international interchanges of this type that we learn from each other and increase our overall knowledge of explosives safety, as well as cement friendships with individuals from the nations involved. Special thanks are due the Honorable Grant Green, Assistant Secretary of Defense for Force Management and Personnel, for his Keynote address; Mr. Lewis Walker, Deputy Assistant Secretary of the Army (Environment, Safety and Occupational Health); and Brigadier General David Nydam, Program Executive Officer - Program Manager for Chemical Demilitarization, for their presentations to the assembly. I would also like to thank each of you who presented papers. Without you there would be no Seminar.

I would ask that each of you take time when you arrive at home to write what you did or did not like about the Seminar with suggestions you may have for improvement. These comments are very important to us.

May each of you have a safe trip home. If there are no further comments to be presented, I hereby declare these proceedings closed.

23d DDESB EXPLOSIVES SAFETY SEMINAR
Attendance List

ABRISZ, Gary W.	USA Def Ammo Ctr & Sch, Savanna, IL 61074-9639
ABROL, Satish C.	USAF/LEEES, Washington, DC 20332
ADAMS, Richard T.	Naval Sea Systems Cmd, Washington, DC 20362-5101
ALKER, Keith	ARE Southwell, England
ALLAIN, Jean-Pierre	French Government, France
ALLEN, John E.	HQ, Ballistic Msl Office, Norton AFB, CA 92409-6468
ALLES, John W.B., Cdr	Royal Netherlands Navy, Holland
ALVAREZ, Roman, Jr.	Weapons Safety Div, Hill AFB, UT 84056-5990
AMIABLE, Ingenieur General	Svc Technique des Poud. et Explo, Paris, France
ANDREWS, Sidney B.	Naval Sur Warfare Ctr, Dahlgren, VA 22448
ANKESHEILN, Wade F.	Weapons Safety Div, Hill AFB, UT 84056-5990
ANSELL, Ed G.	USA Defense Ammo Ctr & School, Savanna, IL 61074
ANSPACH, Earl E.	Sverdrup Technology, Inc., Arnold AFB, TN 37389
ARCHER, John W.	Douglas Aircraft Co., Long Beach, CA 90846
ARMSTRONG, Lawrence H.	Ministry of Defence (Navy), Bath, Avon, England
ASH, Richard W.	AMC FSA, Charlestown, IN 47111-9669
ATHALTER, Stephen J.	Star Glove and Safety Products, Chatham, NJ 07928
ATHERTON, John	Burgoynes, Inc., Marietta, GA 30062
AUST, James M., MSgt	TAC/SEW, Langley AFB, VA 23665-5563
AUYERS, Joseph L.	Wyle Laboratories, Huntsville, AL 35807
BAHL, David K.	DCASMA Van Neys, CA 91401-2713
BAILEY, Floyd D.	Bur of Alcohol, Tobacco & Firearms, Atlanta, GA 30301
BAJPAYEE, T.S.	Bureau of Mines, Pittsburgh, PA 15236
BAKER, Charles F.	University of California, Livermore, CA 94550
BAKER, Jon P.	The Boeing Co., Seattle, WA 98124-2499
BAKER, Quentin A.	Wilfred Baker Engineering, San Antonio, TX 78209
BAKER, Wilfred E.	Wilfred Baker Engineering, San Antonio, TX 78209
BALADI, George, Dr.	AF Weapons Lab, Kirtland AFB, NM 87117-6008
BALLARD, Carl S.	USA Engr District, Norfolk, Norfolk, VA 23510-1096
BAPTISTA, Clifford, Capt	TAC Langley AFB, VA 23665-5001
BARCLAY, Don E.	Lone Star AAP, Texarkana, TX 75505-9101
BARKER, Darrell D.	Mason & Hanger-Silas Mason Co., Amarillo, TX 79117
BARKER, Donna C.	DDESB Secretariat, Alex., VA 22331-0600
BARNES, Floyd M., MSgt	HQ AF Space Cmd, Peterson AFB, CO 80914-5000
BARR, Michael J.	Los Alamos Nat'l Lab, Los Alamos, NM 87545
BARTIS, J.J.	103IFG/SE, East Granby, CT 06026-5000
BAYS, M.	Naval Wpns Supt Ctr, Crane, IN 47522-5000
BEATTIE, Anthony	Dept. of Environment, UK
BECHT, Cord, Maj	German Army Material Ofc, Bad Neuenahr, Germany
BENNETT, George T.	1776 AFW, Andrews AFB, DC 20331-5000
BENTZ, George	3M Company, St. Paul, MN 55133-3131
BEQUETTE, Gary W.	Los Alamos Nat'l Lab, Los Alamos, NM 87545
BERGBAUER, Daniel M.	Naval Ord Station, Indian Head, MD 20640-5000
BERGER, Henri J., Dr.	S.N.P.E., Center-de-Recherches-du-Bouchet, France
BERNECKER, Richard, R., Dr.	Naval Surface Warfare Center, Silver Spring, MD 20903
BERNIER, Carroll, LCDR	Indian Island Det, Hadlock, WA 98339-5307
BERTOLI, Donald J.	302 TAW(AFRES) Peterson AFB, CO 80914
BESSON, Jacques, I.C.A.	Delegation Generale pour l'Armement,Saint-Cloud, France
BIENZ, Andreas F.	Ernst Basler & Partners LTD, Switzerland
BISHOP, Albert L.	Boeing Company, Seattle, WA 98124

BISHOP, Nancy G.	Exp Saf Req , Hill AFB, UT 84056-5609
BITTNER, G. Scott	Morton Thiokol, Inc., Brigham City, UT 84302-0689
BLAU, Sullivan E.	Morton-Thiokol, Inc., Brigham City, UT 84302-0689
BLINDE, David R.	Honeywell, New Brighton, MN 55112
BLOSE, Thomas L.	Naval Weapons Center, China Lake, CA 93555-6001
BLOWERS, Dennis	Beech Aircraft Corp., Wichita, KS 67201
BOERO, Rick R., TSgt	TFWC/SEW, Nellis AFB, NV 89191-5000
BOESE, Doyle H.	Field Safety Activity, Charlestown, IN 47001-9669
BOIMEL, Arie	Israel Military Industries, NY 10022
BOISSEAU, Francois-Xavier	S.N.P.E., Center-de-Recherches-du-Bouchet, France
BOLGER, John M.	Explosives Technologies International, Canada
BONNER, Clark D.	Ireco Inc., West Jordan, UT 84088
BONOMO, Mark S.	United Engineers & Contractors, Denver, CO 80217
BONZON, Lloyd L.	Sandia Nat'l Lab, Albuquerque, NM 87185
BOOM, Jan G.	Department of Defense, Holland
BORG, George, Dr.	Embassy of Australia, Washington, DC 20036
BOTTJER, Gary	US Army Safety Center (HQDA), Ft. Rucker, AL 36362
BOWEN, David S.	USA Engr District, Mobile, AL 36628-0001
BOWEN, E.R.	Travis AFB, CA
BOWLES, Patricia K.	Southwest Research Institute, San Antonio, TX 78284
BREEN, Clarence F.	NASA, Hampton, VA 23665
BRIGMANIS, Edmund	American Co., Stanford 06904-0060
BRINKMAN, Erma E.	Olin Corporation, East Alton, IL 62024
BROOKS, Alfred	Federal Railroad Assoc., Wash., DC 20590
BROWN, Warren R.	Olin Corporation, Badger AAP, Baraboo, WI 53913
BRUNING, Steven F.	Newcomb & Boyd, Atlanta, GA 30318-7761
BRUNO, Fred A.	DCASMA Orlando, Orlando, FL 32803
BRYANT, James R., MSgt	102 Fighter Interceptor Wing, Otis ANGB, MA 02542-5001
BUCHER, Michael A.	Naval Weapon Station, Concord, CA 94520-5000
BUCHHOLTZ, Walter C.	AF Engr & Svcs Ctr, Tyndall AFB, FL 32403-6001
BULLARD, David	Teledyne McCormick Selph, Hollister, CA 95024-0006
BULLOCK, Jim	Motorola Inc., Scottsdale, AZ 85252
BULMASH, Gerald	Ballistic Research Lab., Aberdeen Proving Gd., MD 21005
BULTMANN, E.H., Dr.	University of New Mexico, Albuquerque, NM 87131
BURNIEWICZ, Henry	Boston-FOXTRACT, Boston, MA 02210
BURRELL, Samuel	AF Astronautics Laboratory, Edwards AFB, CA 93523-5000
BYRD, John L., Jr.	Dir, USA Def Ammo Ctr & School, Savanna, IL 61074-9639
CAESAR, Donald E.	Magnavox Electronic Systems Co., Fort Wayne, IN 46808
CAIN, Bruce S.	NAVFACENGCOM, Alexandria, VA 22332-2300
CAMPBELL, Clarance J.	AMC Field Safety Activity, Charlestown, IN 47111-9669
CANADA, Chester, Dr.	DDESB, Alex., VA 22331-0600
CANNON, James A.	USA Chemical B, D & E Center, Aberdeen Proving Gd, MD
CANNON, Paul C.	Olin Corp.-Def Systems Group, Marion, IL 62959-9801
CAREW, Donald L.	HQs, First Air Force, Langley AFB, VA 23665-5009
CARL, Stephen P.	DCASR Atl, 805 Walker St., Marietta, GA 30060-2789
CASHIN, Richard H.	USA South, SOFR-SA, Ft Clayton, Miami, FL 34004--5000
CATES, Charles	DDESB, Alex., VA 22331-0600
CAUTHEN, Carroll E.	Weapons Quality Engr Ctr., NWS, Concord, CA 94520-5000
CESSARIO, Thomas	Morton Thiokol, Elkton, MD 21921
CHAKRABARTY, P.N., Dr.	Ordnance Factory Board, Calcutta, India

CHAMPION, Matthew M.	ETI Explosives Tech Int., Wilmington, DE 19809-2867
CHANDLER, Albert N.	Applied Ordnance Technology, Arlington, VA 22202
CHANG, Wei Shing	Bureau of Explosives, Short Hills, NJ 07078
CHANPONG, J.	Bernard Johnson, Inc., Houston, TX 77056
CHASE, Robert E.	Materials Technology Lab., Watertown, MA 02172-0001
CHIZALLET, Maurice	Societe MATRA, Cedex, France
CHOI, Rack J.	Korea Explosives Co., Ltd., Chung-Ku, Seoul, Korea
CHOONG, Seon	Agency for Defense Dev, Daejeon, Korea
CHURILLO, Charles J.	AD/XRS, Eglin AFB, FL 32542-5000
CICHOCKI, Anthony	103TFG/SE, East Granby, CT 06026-5000
CIHUNKA, Colleen K.	Twin Cities AAP, New Brighton, MN 55112-5000
CLAPP, Roger C.	Martin Marietta Missile Systems, Orlando, FL 32855
CLARK, Eugene	DDESB, Alex., VA 22331-0600
CLARK, Thomas L.	Sverdrup Technology, Inc., Arnold AFB, TN 37389-5000
CLARY, Val	Space Division, Los Angeles, CA 90009-2960
CLEAVELAND, Leroy	Day & Zimmermann, Inc., Kansas AAP, Parson, KS 67357
CLIME, Robert, CAPT	DDESB, Alex., VA 22331-0600
CLINTON, Steve	Hayes, Seay, Mattern, Inc., Roanoke, VA 24034
CLOONAN, James T.	SM-ALC/DPCT, McClellan AFB, CA 95652-5990
COAD, Roger D.	Los Alamos Nat'l Lab, Los Alamos, NM 87545
COLEMAN, Daniel H.	US Treasury, Alcohol, Tobacco & Firearms, Dallas, TX
COLLINS, Jon D.	ICTA Inc., Torrance, CA 90505-6557
COLLINS, William E.	Armament Div, Eglin AFB, FL 32542-5000
COLLIS, Dave	New Mexico Inst. of Mining & Technology, Socorro, NM
CONLEY, John H.	USA Combat Sys Test Activity, APG, MD 21005-5059
COPELAND, William	Aerojet Solid Prop Co., Sacramento, CA 95852-1699
COULSON, John R.	Coulson Consulting Corp., Wilmington, DE 19809
COULTER, George A.	Ballistic Research Lab., APG, MD 21005-5066
COURTRIGHT, Clarence W.	Los Alamos Nat'l Lab, Los Alamos, NM 87545-0050
COVELL, Robert	Teledyne McCormick Selph, Hollister, CA 95024-0006
COWAN, George H.	IRECO, Inc., Bettendorf, Iowa 52722
COX, Phineas A.	Southwest Research Inst., San Antonio, TX 78284
CRATEN, Joseph D.	USA Toxic & Haz Materials Agency, APG, MD 21010
CROCK, Mitchell R.	Hercules Inc., McGregor, TX 76657-1999
CROSLEY, William	Detector Eletronics
CROSSETTE, John S.	Hq, V Corps, USAREUR, APO NY 09079
CROWLEY, Daniel E.	Bureau of Alcohol, Tobacco & Firearms, Wash., DC 20226
CROZE, Gilbert	Matra Aerospace Inc., Arlington, VA 2202
CROZIER, Charles O.	Def Contract Admin Svc Region, Marietta, GA 30060
CRUZ, Ignacio	DDESB, Alex., VA 22331-0600
CURRY, Ronald K., CDR	Naval Safety Ctr for Expl Sys Safety, Norfolk, VA 23511
CUTLER, Robert M.	The Mitre Corporation, McLean, VA 22102
DAHLBERG, Stig E.	Nobel Chemicals AB, Sweden
DAHN, Carl J.	Safety Consulting Engrs, Inc., Rosemont, IL 60018
DALTON, Bruce	Naval Ord Station, Indian Head, MD 20640-5000
DANIELSEN, Anna J.	Weapons Quality Engr Ctr., NWS, Concord, CA 94520-5000
DAVIDSON, Edward	USARJ, Camp Zama, Japan 96343-00565
DAVIDSON, Robert H.	Reliability & Maint Dept, Patuxent River, MD 20670-5304
DAVIS, Barry	Centers for Disease Control, Atlanta, GA 30333
DAVIS, Jo O.	Sandia National Lab, Albuquerque, NM 87185-5800

DAVIS, Johnny S.	ASD/SEV, Wright-Patterson AFB, OH 45433-6503
DAVIS, Landon K.	USA WES,Vicksburg, MS 39180-0631
DAVIS, Leland E.	Morton Thiokol, Inc., Brigham City, UT 84302-0524
DAY, Douglas M.	Radford Army Ammo Plant, Radford, VA 24141-0299
DAYE, James O.	Naval Sea Supt Ctr, Atlantic, Portsmouth, VA 23702-5098
DAYWALT, Raymond A.	Naval Weapons Supt Ctr, Crane, IN 47522-5000
DEDMAN, Oneal	Pine Bluff Arsenal, AR 71603-9500
DENISON, Thomas S.	Honeywell Inc., Def Sys Gp, Minnetonka, MN 55343
DERETA, Nicholas	LDS Church Security, Salt Lake City, UT 84010
DERICKSON, Jon	Karios Company, Mountain View, CA 94043
DERR, Ronald, Dr.	Nav Wpns Ctr, Code 38, China Lake, CA 93555-6001
DICKERSON, H. Boyd	Hayes, Seay, Mattern, Inc., Roanoke, VA 24034
DILTS, Charles D.	McDonnell Douglas Astronautics Co, Titusville, FL 32780
DITTMAN, Harry A.	Defense Contracts Admin, Cleveland, OH 44135-2063
DOBBS, Norval	Ammann & Whitney, NY, NY 10014
DODGEN, James E.	Dodgen Engr. Company, Colorado Springs 80934
DOTTS, J.E.	Sandia National Lab., Albuquerque, NM 87185
DOUTHAT, C. David	USA Engr Div-Huntsville, AL 35807-4301
DOW, G. Scott	DLA Quality Assur Mgmt Supt Ofc, Marietta, GA 30060
DOW, Robert	NAVEODTECH CENTER, Indian Head, MD 20640
DRAKE, James	DDESB, Alex., VA 22331-0600
DRILLEAU, M.	Societe National des POUDRES, France
DROUX, Rolland	C.E.A. - Centre D'Etudes De Vaujours, France
DRURY, Alton G.	Federal Cartridge Company, Anoka, MN 55303
DUFF, William W.	The Mitre Corporation, McLean, VA 22102
DUNCAN, Kendal M.	Safety Office, ARDEC Picatinny AR, NJ 07806-5000
DUNHAM, Allen, Capt	174TFW New York Air Nat'l Guard, Syracuse, NY
DUNHAM, C. Allen	DCASMA Syracuse, NY 13021
DUNSETH, Clifford A.	USA Safety Center, Ft. Rucker, AL 36362-5363
DUPUIS, Gardy J.	62 MSSQ/DPCT, McChord AFB, WA 98438-5000
DURBIN, William F.	Naval Weapons Center, Ridgecrest, CA 93555-6001
DeMILLE, Curtis	Trojan Corp., P.O. Box 310, Spanish Fork, UT 84660
DeMILLE, Curtis L.	Trojan Corporation, Spanish Fork, UT 84660
EDDY, John	Defense Nuclear Agency, Alexandria, VA 22310
EDMONDSON, John N.	UK Atomic Energy Authority, Warrington, England
EINERTH, Bengt	National Inspectorate of Explo & Flammables, Sweden
EISAMAN, J.V.	Boeing Aerospace, P.O. Box 3707, Seattle, WA 98124
ELLENBURG, John R.	Martin Marietta, Orlando, FL 32855-5837
ELLIOTT, Sid M.	Northrop, Perry, GA 31069
ELLIS, B.J., Wing Cdr	Royal Australian AF, Aust Embassy, Wash., DC 20036
ENDICOTT, David W.	Morton Thiokol, Inc., Brigham City, UT 84302-0689
ENGELBRETSON, Alfred	Department of National Defense, Ottawa, Canada
EPSTEIN, Alex	Israel Military Industries, New York, NY 10022
ESPARZA, Edward D.	Southwest Research Inst., San Antonio, TX 78284
ETHRIDGE, Noel H.	Aberdeen Pesearch Ctr., MD 21001-0548
EVANS, Michael D.	Arnold Engr & Dev Ctr, Arnold AFB, TN 37129
EYTAN, Reuben	Eytan Building Design Ltd., Israel
FACCINI, Ernest	NM Institute of Mining & Tech, Socorro, NM
FADORSEN, Gary A.	Automotive Sprinkler Corp., Cleveland, OH

FALLEN, Gary J.	Space Ordnance Systems, Canyon Country, CA 91351
FANNIN, Gerald F.	Tinker AFB, Oklahoma City, OK 73145-5990
FARSOUN, Adib R.	Corps of Engrs, Huntsville Div, AL 35805-1957
FASIG, H.C.	Schneider Services International
FATZ, Ray	US Army Safety Office, Wash., DC 20310
FAUX, Neal D.	Weapons Safety Div, Hill AFB, UT 84056-5990
FELICE, Joe F.	Whittaker Ordnace. Hollister, CA 95023
FELLER, Shaul, Dr.	Rafael, Haifa, P.O. Box 2250, Israel
FENG, Kuo K.	Canadian Explo Research Lab, Ontario, Canada K1A-0G1
FENNELL, James S.	Olin Corporation, St. Marks, FL 32355
FERRARO, Carlo	Ofc of the Chief of Naval Operations, Wash, DC 20350
FINLEY, Dennis K.	MOT-Sunny Point, Southport, NC 28461-5000
FLOOD, Matthew, 1Lt	2701 EODS, Hill AFB, UT 84056
FLORY, Robert A.	Washington Research Center, Alexandria, VA 22310-0395
FLOYD, James Q.	Robins AFB, Robins, GA 31098
FOGLIETTA, Jim P.	Wyle Laboratories, Norco, CA 91760
FOULK, David W.	USA Central Ammo Mgmt Cmd, Fort Shafter, HI 96858-5465
FRAIZE, Willard E.	The Mitre Corporation, McLean, VA 22102
FRAZIER, Wayne R.	NASA Safety Div, Wash., DC 20546
FREEMAN, Anthony L.	Micronics International, Enterprise, CA 92621
FRENCH, Stephen H., COL	USA Central Ammo Mgmt Ofc (PAC), Ft Shafter, HI 96858
FRITTS, Art B.	21AF, McGuire AFB, NJ 08641-5002
FUGELSO, L. Erik	Los Alamos Nat'l Lab, Los Alamos, NM 87545
GALLAGHER, Richard N.	43 BMW, Andersen AFB, Guam 96334-5000
GANDHI, S.J.	FMC Corporation, Santa Clara, CA 95052
GEIGER, Gordon	Bristol Aerospace Limited, Winnipeg, Canada
GERTH, Eberhard W.	LUWA Ltd., Bethesda, MD 20814
GIBBS, Roderick, Capt	1STRAD, Vandenberg AFB, CA 93437-5000
GIPBS, Ross A.	Dept of Nat'l Defense, Manitoba, Canada R3J0T0
GIBSON, Jerry L., MSgt	12th AF, Bergstrom AFB, TX 78743-5002
GION, Edmund J.	USA Ballistic Research Lab., AFG, MD 21005-5066
GODDARD, Glen E.	Mason & Hanger-Newport AAP, IN 47966-0458
GOH, Yong Kiat, CAPT	Ministry of Defence, Singapore
GOLD, Ted	Teledyne McCormick Selph, Hollister, CA 95024-0006
GOLDIE, Roger H.	Los Alamos Nat'l Lab, Los Alamos, NM 87545
GOLDRING, Peter N.	ICI Americas, Wilmington, DE 19897
GOLDSTEIN, Selma	Los Alamos National Lab, NM 87545
GOLIGER, Jean	S.N.P.E., Center-de-Recherches-du-Bouchet, France
GOLLER, Carolyn A.	Aerojet Solid Prop Company, Sacramento, CA 95852-1699
GOOLD, J.J.	Secretary, Exp Storage & Transport Cmte, Australia
GORDON, David L.	IRECO Incorporated, West Jordan, UT 84088-9699
GRACE, P.J.	Aerojet Solid Prop Co., Sacramento, CA 95853-1699
GRAEF, Warren D.	LTV Aerospace & Defense, Camden, AR 71701
GRAHAM, Kenneth J.	Atlantic Research Corp., Gainesville, VA 22065-1699
GREEN, Grant S., Jr.	Asst Secy of Defense, Force Mgmt & Pers, Wash, DC 20310
GREEN, Gregg C.	Martin Marietta Astro. Group, Denver, CO 80201
GREENFIELD, Gary	SRI International
GREENWADE, Edward	Pan Am World Svcs, Inc., Patrick AFB, FL 32925
GREIGER, Gord	Bristol Aerospace Ltd., Winnipeg, Canada
GREMILLION, Edward C.	Mason Chamberlain Inc., NSTL Base, MS 39529-7099

GROCE, Thomas A.	Hercules Incorp., Rocket Ctr, WV 26726
GRUBBS, Curtis T, MSgt	7th Air Force, Osan AB, Korea
GUARIENTI, Richard	Lawrence Livermore Nat'l Lab, Livermore, CA 94550
GUTHRIE, Mitchell	Kilkeary, Scott and Assoc., Arlington, VA 22202
HAGERUR, Jack E., LCDR	Damocles Haztrcl, Inc., Great Falls, VA 22066
HAINES, Robert O.	Iowa AAP, Middletown, IA 52638-5000
HALL, C.	Holston Defense Corporation, Kingsport, TN 37660
HALL, Paul H.	Polaris Msl Fac Atlantic, Charleston, SC 24908-5700
HALL, Thomas F., COL	DDESB, Alex., VA 22331-0600
HALLAS, William E.	Universal Prop Co., Box 1140, Phoenix, AZ 85029
HALLUN, Leslie H.	McDonnell Douglas Astro. Co., Titusville, FL 32775
HALTOM, Phillip T.	Day & Zimmermann, Lone Star AAP, Texarkana, TX 75501
HAMILTON, Del	HQ MAC/ICF, Scott AFB, IL 62225-5101
HAMILTON, Glen D.	Olin Defense Systems, Independence, MO 64050
HAMILTON, Julian S.	USA Corps of Engrs-Huntsville Div, AL 35807
HAMMEL-MUELLER, Juergen	HQs, USAF Europe, APO NY 09094
HAMMER, William R.	AFSC Andrews AFB, MD 20334-5000
HANTEL, Lawrence W.	Los Alamos National Lab, NM 87545
HARRIS, Alma	Rocky Mount Arsenal, Commerce City, CO 80022-2180
HARRIS, Alma T.	Rocky Mountain Arsenal, Commerce City, CO 80022-2180
HARRIS, Roy W.	TRW, San Bernardino, CA 92402-1310
HART, Francis E.	USA Missile Command, Redstone Arsenal, AL 35898-5103
HAYDON, Douglas S.,Lt.Col.	63d Military Airlift Wing, Norton AFB, CA 92409-5174
HAYES, John R.	USA Constr Engr Research Lab, Champaign, IL 61820-1305
HAYES, Pascal K.	Patel Engineers, Huntsville, AL 35810
HE, Cheng-Zhi	Engr Design & Research Institute, P.R.C.
HEFELFINGER, Richard	McDonnell Douglas Astro Co., Titusville, FL 32780
HEILMAIN, Volker	Amt Fuer Studten Und Uebungen, Germany
HEINZE, Lynn F.	Weapons Safety Div, Hill AFB, UT 84056-5990
HELLE, Charles J.	CBC, Sao Paulo, Brazil
HENDERSON, Jon	Safety Svcs Organ, Kent, UK
HENRY, Robert E.	Lawrence Livermore Nat'l Lab, Livermore, CA 94550
HERCHBERGER, Chester K.	DCASR Los Angeles, El Segundo, CA 90245
HERRERA, Wm. R.	SWRI, San Antonio, TX 78232
HERRON, Roger A.	USA Ballistic Research Lab, Aberdeen PG, MD 21005
HERRREACH, Allen M.	1606 AEW, Kirtland AFB, NM 87117-5000
HESSLER, George R.	McDonnell Douglas Astronautics Co, St. Charles, MO
HEWITT, Owen L.	Nav Fac Engr Cmd, Norfolk, VA 23511
HICKMAN, Jeannie H.	USA South, SOPP-SA, Ft Clayton, Miami, FL 34004-5000
HICKMAN, John C.	Computer Sciences Corp., Wallops Is., VA 23337
HIGHLANDS, William H.	Atmospheric Research Systems, Inc., Palm Bay, FL 32905
HILL, Donald J.	DCASMA-Twin Cities, St. Paul, MN 55116-1893
HILL, Donald J.	DCASR, St. Louis, MO 63101-1193
HILLS, Dan J.	7th Inf Div, Fort Ord, CA 93941
HITES, Walter	Pope AFB, NC 28308
HOAG, Robert W., CAPT	Naval Undersea Warfare Engr Sta, Keyport, FL 98345-0580
HOFFMAN, Norman H.	Technical Ordnance, Inc., Waconia, MN 55387
HOLMES, Fred	Martin Marietta, Vandenberg AFB, CA 93437
HOLYFIELD, Robert L.	Atlantic Research Corp., Camden AR 71701
HOUSE, Joel W.	SVERDRUP Inc., Eglin AFB, FL 32542

HOWELL, Edward	DDESB, Alex., VA 22331-0600
HUDSON, Fred, Dr.	ARC, 5945 Wellington Road, Gainsville, VA 22065
HUDSON, Melvin C.	Naval Ord Station, Indian Head, MD 20640-5000
HUEHN, Wilfried, Maj	Materialamt der Bundeswehr, Germany
HUFFAKER, James	Martin Marietta Energy Sys, Inc., Oak Ridge, TN 37831
HULTENGREN, Larry C.	US State Dept., Washington, DC 20520
HUNT, Eddie T.	USA Strategic Def Cmd, Huntsville, AL 35807-3801
HUNTER, Dennis	New Mexico Inst. of Mining & Technology, Socorro, NM
HUTCHINGS, William D.	WR-ALC/SEW, Robins AFB, GA 31098-5990
HUTTON, Albert, COL	DDESB, Alex., VA 22331-0600
HWANG, Man-Kee	Poongsan Metal Corporation, Seoul, Korea
ITIAK, Richard	DCASR PHIL-QS, Philadelphia, PA 19101
JACKSON, Lawrence H.	Naval Surface Warfare Ctr, Dahlgren, VA 22448
JACKSON, Ronnie L.	Texas Instruments Inc., Dallas, TX 75265
JACKSON, William D.	Goex, Inc., West Cleburne, TX 76031
JACOBS, Raymond L.	Tinker AFB, Oklahoma City, OK 73145-5990
JARRETT, C.L.	Hercules Aerospace Co., DeSota, KS 66018
JEFFERSON, Joseph E.	Sooner Defense of Florida, Lakeland, FL 33807
JENSSEN, Arnfinn	Norwegian Defence Constr Svc, Oslo, Norway
JENUS, Joseph	AD/XRS, Eglin AFB, FL 32542-5000
JEONG KOOK, Kim	Agency for Defense Dev, Daejeon, Korea
JOACHIM, Charles E.	USAE Waterways Experiment Station, Vicksburg, MS 39180
JOHNSON, Jim	Atlantic Research Corp., Camden, AR 71701
JOHNSON, Nicholas F.	Dept. of Environment, UK
JOHNSON, William J.	Paul Rizzo Assocs., Inc., Pittsburgh, PA 15235
JONES, Earl F.	NUWES, Keyport, WA 98345-0580
JONES, Forest M.	Aerojet Solid Prop. Co., Sacramento, CA 95852
JOSEPHSON, Carl H.	Ensign Bickford Aerospace Co., Simsbury, CT 06070
JOSEPHSON, Larry H.	Naval Weapons Center, China Lake, CA 93555-6001
JOYNER, Taylor	New Mexico Inst. of Mining & Technology, Socorro, NM
JUNGERS, Niholas	Lockheed Msl & Space Co., Sunnyvale, CA 94088-3504
KAH LENG, Yap, Ms	Ministry of Defence, Singapore
KARTACHAK, Thomas S.	Aberdeen Proving Ground, MD 21010-5401
KATICH, Michael S.	Stresau Laboratory, Inc.
KATTAU, Charles P.	DCASR Atlanta, GA 30060-2789
KAUFMAN, Susan, Maj	Secretary of the AF, Pentagon, Wash., DC 20310
KEENAN, William A.	Naval Civil Engr Lab., Port Hueneme, CA 93043-5003
KELLER, Bill H.	Naval Ord Test Unit, Cape Canaveral, FL 32920
KELLEY, R.	CEMRO-EDS, 215 No. 17th St., Omaha, NE 68102-4978
KELLEY, Robert W.	Corps of Engrs, Omaha District, Omaha, NE 68102-4978
KELLY, Martha, Maj	Tactical Air Command, Langley AFB, VA 23665-5563
KELLY, Phillip G.	Mason & Hanger-Silas Mason Co., Amarillo, TX 79177
KENNEDY, L.O.	Weapons Sta., Charleston, S.C.
KENNEDY, Lynn W., Dr.	S-Cubed Div of Maxwell Labs, Albuquerque, NM 87106
KERKER, Daniel L., MSgt	AFISC/SEW, Norton AFB, CA 92409
KERNEN, Patrick	Service Tech Poudres Et Explo, Paris, France
KERNS, Avery J.	Dr. Ing. Mario Biazzi Soc. An., McDonough, NY 13801
KHALID, Abed	Nathan Hale Group, 10306 Eaton Pl., Fairfax, VA 22030
KIGER, Sam A.	Waterways Exp. Sta., Vicksburg, MS 39180-3696
KINCH, Judson M.	Northrop Corporation (Ventura), Newbury Park, CA 91320

KING, Cecile D.	DCASR Dallas, TX 75202-4399
KINGERY, Charles N.	USA Ballistic Research Lab, Aberdeen PG, MD 21005
KIVITY, Y.	Rafael, Israel
KLAPMEIER, Kenneth M.	Detector Electronics Corp., Mpls., MN 55438
KLEPONIS, Francis A.	TECOM, MD
KNOX, Joseph	USA Test & Eval Command, APG, MD 21005-5055
KNUTSSON, Leif B.	AB Bofors, Sweden
KO, Byung S.	Korea Explosives Co., Ltd., Chung-Ku, Seoul, Korea
KOCH, David L.	Morton-Thiokol Inc., Brigham City, UT 84302-0524
KONGEHL, Helmut F., Lt.Col.	Federal Ministry of Defence, Germany
KOSSOVER, David	Ammann & Whitney, NY, NY 10014
KOSTERMANS, G.S.M.	Mil Cmte on Dangerous Goods, The Hague, Netherlands
KRACH, Fred G.	Monsanto Research Corp., Miamisburg, OH 45342
KRATOVIL, Edward W.	NAVSEASYSCOM, Washington, DC 20362-5101
KRAUSE, Wm. C.	Boeing Military Airplanes, Wichita, KS 67277-7730
KRAUSHAAR, Gary M.	Aerojet System Safety, Sacramento, CA 95852-1699
KREPS, Raymond E.	Eastern Space & Msl Ctr, Patrick AFB, FL 32925-5172
KRESGE, Richard L.	ADWC/SEWE, Tyndall AFB, FL 32403-5000
KRESS, Jack A.	Naval Weapons Supt Ctr, Crane, IN 47522-5000
KRISTOFF, Frank T.	Hercules Inc., Radford, VA 24121-0299
KRONICK, Richard A.	Lockheed Missile & Space Co., Charleston, SC 29411
KRUPA, Mike	Texas Instruments, Lewisville, TX 75067
KUMER, Peter O.	Ernst Basler & Partners LT, Switzerland
KWIEDOROWICZ, Laurie	Aberdeen Proving Ground, MD 21010-5423
LAATSCH, Edward	Cad-Con Facilities Design, Inc., Fairfax, VA 22031
LAI, Leonard, COL	HQ Department of the Army, Wash., DC 20310
LAIDLAW, Bryan G.	Defence Research Est. Suffield, Alberta, Canada
LAINE, Pekka	Tech Research Centre of Finland, ESPOO, Finland
LAMPE,	HQ AMC, 5001 Eisenhower Ave., Alex., VA 22333-0001
LANE, John C., CMSgt	10th Air Force, Bergstrom AFB, TX 78743-6002
LANGA, Robert R.	McDonnell Douglas Corp., St. Louis, MO 63166-0516
LARSON, Arnold E.	Picatinny Arsenal, NJ 07806-5000
LASELL, Richard B.	Naval Weapons Center, China Lake, CA 93555-6001
LAWRENCE, Mark B.	WRALC/QL, Robbins AFB, GA 31098
LAWRENCE, William	BRL, Aberdeen Proving Ground, MD 21005-5066
LEE, Robert A.	Morton Thiokol, Inc., Shreveport, LA 71130
LEGARDE, Jerry M.	Honeywell, Inc., Twin City AAP, New Brighton, MN 55112
LEGARE, Jake	Aviation Applied Tech, Fort Eustis, VA 23604-5577
LEMCOOL, Richard J.	Mason Chamberlain Inc., NSTL Base, MS 39529-7099
LEMLEY, Jerrell T., CMSgt	HQ, SAC, Offutt AFB, NE 68113-5001
LEWIS, Larry M.	Martin Marietta Strategic Sys, Vandenberg AFB, CA 93437
LIBERSKY, Larry	NM Institute of Mining & Tech, Socorro, NM 87801
LIGHTHISER, Thomas P.	USADACS, ATTN: SMCAC-AV, Savanna, IL 61074
LIM, Chee Hong	Ministry of Defence, Singapore
LINDSEY, Patrick D.	Corps of Engrs, Omaha District, Omaha, NE 68102-4978
LIPP, Curtis	Aerojet General Corp., Sacramento, CA
LOFTON, Layne B.	Rt. 4, Box 515, Marshall, TX 75670
LONG, Alvin H.	Tracor Aerospace, East Camden, AR 71701
LONGO, Vito	SPF Incorporated, Baileys Crossroads, VA 22041
LOPES, Peter	Cullinet Software, Westwood, MA

LORENZ, Richard A.	Boeing Military Airplanes, Wichita, KS 67277-7730
LOVVORN, Charles J.	Mason Chamberlain Inc., NSTL Base, MS 39529-7099
LOWE, William F.	AF Armament Lab, Eglin AFB, FL 32542-5434
LOYD, Robert A.	USA Armament, Mun & Chem Cmd, Rock Is., IL 61299
LUCHT, Roy A.	Los Alamos National Lab, Los Alamos, NM 87545
LUTTRELL, David L.	437MAW, USAF, Charleston AFB, SC 29404-5174
LaHOUS, Paul M.	USA Engr Div, CEHND-ED-CS, Huntsville, AL 35807-4301
MADSEN, Niels K.	Demex Consulting Engineers, Frederiksberg, Denmark
MAHONEY, Patricia L.	Los Alamos National Lab, NM 87545
MANNSCHRECK, Wm. A.	Naval Safety Ctr, Norfolk, VA 23511
MARCHAND, Kirk A.	SRI, San Antonio, TX 78284
MARDON, Joseph P.	Canoga Park, CA 91303
MARS, Larry	Sverdrup Technology Inc., MS 39529
MARSHALL, John W.	AF Astronautics Lab, Edwards AFB, CA 93523-5000
MARTHA, Robert N.	Nav Civil Engr Laboratory, Port Hueneme, CA 93043
MARTIN, John	Motorola Inc., Scottsdale, AZ 85252
MARTINEZ, Rick	Stafford, VA 22554
MASON, Jim	Aerojet Tech Systems, Sacrameto, CA 95813
MATHEWS, Jack S., Col	DDESB, Alex., VA 22331-0600
MATULA, Melvin G.	Lockheed Msl & Space Co., Inc., St. Marys, GA 31558
MCDANIEL, Edward G.	MCCDC, Quntico, VA 22134
MEIERAN, Sigmund	Command Safety Office, Point Mugu, CA 93042-5000
MERRILL, Claude	AF Astronautics Lab., Edwards AFB, CA 93523-5000
MEYERS, Gerald E.	US Department of State, Rockville, MD 20854
MIKEL, John W.	Weapons Quality Engr Ctr., NWS, Concord, CA 94520-5000
MILLER, Craig A.	Kresky Signs, Inc., Petaluma, CA 94953
MILLER, Henry R.	Uniroyal Chemical Co., Joliet AAP, Joliet, IL 60434
MILLER, Jerry R.	Toole Army Depot, Toole, UT 84074-5004
MILLER, Parker D.	Naval Weapons Center, China Lake, CA 93555-6001
MILLIS, D.A.	COMARCO, Inc., Ridgecrest, CA 93555
MILLS, Clifton E.	Warner-Robins AFB, GA 31098-5990
MISTER, Charles A.	Ammo Surveillance, Fort Bliss, TX 79916-6025
MIVEL, John W.	Code 354, Bldg. IA-10, Concord, CA 94520
MONTA, Robert M.	Martin Marietta, Orlando, FL 32855
MONTROSS, J.E.	Morton Thiokol, Inc., Brigham City, UT 84502-0689
MOODY, DeWitt H.	Consultant, Orlando, FL 32809-6845
MOORE, C.J.	Air Force Military Training Ctr, 78236-5000
MOORE, Kenneth J.	Rockwell International Corp., KSC, FL 32815
MOORE, Michael W.	Martin Marietta Manned Space Sys, New Orleans, LA 70189
MOORE, Verence D.	NSWC/WO, Silver Spring, MD 20903-5000
MORAN, Edward	DDESB, Alex., VA 22331-0600
MORCOS, Michael	Pacific Missile Test Ctr, Point Mugu, CA 93042
MOREAU, M.	Societe National des POUDRES, France
MORGAN, Charles E.	NUWES Keyport, Keyport, WA 98345-0580
MORGAN, Larry E.	USAMC Field Safety Cmd, Chrlestown, IN 47111-9669
MORING, Michael L.	Fraioli-Blum-Yesselman Assoc., Inc., Norfolk, VA 23502
MORLAN, Henri	AEROSTATIALU, Les Mureaux, France
MORRISON, George, E.	Tactical Air Cmd, Langley AFB, VA 23665-5001
MORRISON, William C.	Ofc of Surf Mining Reclam & Enf, Pittsburgh, PA 15220
MORRISON, William C., Col	AFISC/SEW, Norton AFB, CA 92409-5001

MORVAN, Pascal, Dr.	5 BP 41, 56998 Lorient-Naval, France
MOXLEY, Robert C.	SA-ALC (AFLC), Kelly AFB, TX 78241-5000
MSGT KUNKLE, Ron	HQ AFOTE/SE, Kirtland AFB, NM 87117
MUELLER, Daniel R.	USA Corps of Engrs - Mobile, Mobile, AL 36628-0001
MUILU, Matti E.	Finnish Defence Forces Research Center, Finland
MUMMA, George B.	Martin Marietta Aerospace, Lakewood, CO 80235
MURAT, E., MSgt	131TFW, Safety, Florissart, MO 63031
MURBY, Edwin	Explosives Factory Maribyrnong, DoD, Australia 3032
MURFEE, J.A., Jr.	USAMICOM, Redstone Arsenal, AL 35898-5249
MURPHY, David J.	Lockheed Missiles & Space Co., Santa Cruz, CA 95060
MURPHY, Louis G.	Defense Logistics Ageny, NY, NY 10014-4811C
McALLISTER, Donald H.	Naval Weapons Station, Seal Beach, CA 90740-5000
McCANDIE, Ian R., CAPT	National Defense Hqs., Ontario, Canada
McCLELLAN, Timothy R.	Morton Thiokol, Longhorn Div, Marshall, TX 75670
McCLESKEY, Francis R.	Kilkerry, Scott,, & Assoc., King George, VA 22485
McCORKLE, Larry G.	Austin Powder Co., McArthur, OH 45651
McCORMICK, Bill G.	Los Alamos National Lab, NM 87545
McDONALD, Jack L.	DCASMA San Antonio, TX 78294-1040
McGILLICUDDI, Hugh	W.R. Grace Company, NW Wash., DC 20006
McHALE, James M.	Honeywell Inc., Joliet, IL 60435
McKENZIE, Allen K.	Morton Thiokol, Brigham City, UT 84302
McLAIN, J.P.	New Mexico Inst. of Mining & Technology, Socorro, NM
McMAHON, G.W.	USA Waterways Exper Station, Vicksburg, MS 39180
McMILLAN, Erik G.	Tac Fighter Weapons Ctr, Nellis AFB, NV 89191-5000
McNAIL, Earl M.	Martin Marietta Manned Space Sys, New Orleans, LA 70189
McWILLIAMS, Dusty A.	Douglas Helicopter Co., Mesa, AZ 85205
NAPADENSKY, Hyla	Napadensky Energetics, Inc., Evanston, IL 60201
NASH, John T.	Dept of the Army, Washington, DC 20310-0103
NASH, Keith A., TSgt	AEDC, Arnold AFB, TN 37389-5000
NEE, Larry M.	General Defense Corp., St. Petersburg, FL 33742
NEFF, Ronald A.	Milan AAP, Milan, TN 38358-5000
NELSON, Donald H.	USA Corps of Engrs, Vicksburg, MS 39180-0631
NETT, Dal M.	USA Combat Systems Test Activity, APG, MD 21009-5059
NEWEERN, Robert	DDESB, Alex., VA 22331-0600
NEYRINCK, Ronny G.	Belgian Army, Belgium
NICKERSON, Howard D.	Naval Facilities Engr Cmd, Alexandria, VA 22332-2300
NIEDERHAEUSER, Franz R.	Switzerland
NIERGARTH, Charles C.	Aerojet Ordnance Co., Chino, CA 91709
NIGHTENGALE, James H.	Martin Marietta Manned Space Sys, New Orleans, LA 70189
NORBERG, Donald W.	United Engineers & Contractors, Denver, CO 80217
NORVAN, Pascal	Direction Des Constructions, Navales, France
NYDAM, David A., BG	Chemical Demil, Aberdeen Proving Gd., MD 21010-5401
O'BRIEN, Richard B.	Aerojet General, La Jolla, CA 92037
OH, Chong Seon	Agency for Defense Dev, Dae Jeon, Korea
OLIVER, Howard	KDI Precision Products Inc., Cincinnati, OH 45245
OLSON, Allen W.	Honeywell Proving Ground, Elk River, MN 55330
OLSON, Dave	Kresky Signs, Inc., Petaluma, CA 94953
OLSON, Doug	Center for Explo Tech Research, Socorro, NM 87801
OLSON, Fric T.	AMC FSA, Charlestown, IN 47111-9669
ONG, Ju Heng, CAPT	Ministry of Defence, Singapore

OPEL, Merv C.	ICI America, Inc., Charlestown, IN 47111
OPSCHOOR, Gerald	Prins Maurits Laboratory TNO, The Netherlands
OVERBAY, Larry W.	USA Aberdeen Proving Ground, MD 21005-5059
OWENS, Lonnie	NASA Safety Div, Washington, DC 20546
PACQING, Leonard C.	DCASR Los Angeles, El Segundo, CA 90245
PADMANABHAN, Shari V.	Ordnance Factory, Dehu Road, Maharashtra, India
PAGE, Art	ETI Explosives Tech Int., Wilmington, DE 19809-2867
PAKULAK, Jack M., Jr.	Cmdr, China Lake, CA 93555-6001
PAKULAK, Mary S.	Naval Weapons Center, China Lake, CA 93555--6001
PAL, Shri K.D.	Ordnance Factory, Itarsi, India
PALFREEMAN, Brian D.	CIL Inc., Quebec, Canada
PAPAS, Bill P.	Martin Marietta Astronautics Gp, Denver, CO 80123
PAPP, Attila G.	Mason & Hanger-Silas Mason Co., Amarillo, TX 79177
PAPPAS, Robert A.	Naval Air Engr. Ctr., Lakehurst, NJ 08733
PARK, Cindy	Lake City AAP, Independence, MO 64050
PARKES, David A.	Black & Veatch, Kansas City, MO 64114
PARR, Michael J.	Martin Marietta Manned Space Sys, New Orleans, LA 70189
PARSONS, Gary H.	AF Armament Lab, Eglin AFB, FL 32542-5434
PATIGALIA, Edward N.	Department of Energy, Washington, DC 20545
PATRICK, Gwyn C.	CDR Test & Eval Cmd, APG, MD 21005-5005
PATTERSON, Joe	Reliability & Maintenance, Patuxent River, MD
PATTESON, M.G.	NSWC/DL, Dahlgren, VA 22448-3000
PENA, Steven P., TSgt	USAFSO, APO Miami 34001-5000
PERRY, John G.	The Mitre Corporation, McLean, VA 22102
PERRY, Robert B.	Mgr for Chem Demil, Aberdeen Proving Gd, MD 21010-5401
PERSSON, P.A., Dr.	CETR, New Mexico Tech, Socorro, NM 87801
PETEREIN, Brent	Olin Corporation, E. Alton, IL 62024
PETERS, Charles R.	Cdr, USA ARDEC, Picatinny Arsenal, NJ 07806-5000
PETTIT, Patricia A.	AF Wright Aeronics Lab, Wright-Patterson AFB, OH 45433
PICARD, Jean-Louis	SNC Defence Products Ltd., Montreal, Canada
PIERCE, Cathy	Boston-FOXTRACT, Boston, MA 02210
PINSON, Kirk S.	Reliability & Maint Dept, Patuxent River, MD 20670-5304
POLAND, J.A.	103TFG/SE, East Granby, CT 06026-5000
POLCYN, Michael A.	Southwest Research Inst., San Antonio, TX 78284
POLINS, Stan	LTV Msls & Electronics Group, Horizon City, TX 79927
POPE, Alvin	Mason & Hanger Engr, Lexington, KY 40511
POTTERTON, Terry M.	NASA GSFC/Wallops Is., VA 23337-5099
POWELL, Milton T.	Wyle Laboratories, Huntsville, AL 35807
PRENDERGAST, Joseph, Capt	USAF, Albuquerque, NM 87120
PRESTON, Joe	SWFPAC
PREVATT, Gary E.	6510 ABG, Edwards AFB, CA 93523-5000
PRICE, Brian H.	The Mitre corporation, McLean, VA 22102
PRICE, Paul D.	AFISC/SEW, Norton AFB, CA 92409
PRYDE, Keith W.,SSgt	TFWC/SEW, Nellis AFB, NV 89191-5000
PUNTURERI, Carl, Capt	HQ SAC, Offutt AFB, NE 68113-5001
PURCELL, Michael	Applied Research Assoc., Inc., Tnydall AFB, FL 32403
QUINN, K.M.	Schneider Services International
RAFALSKI, Paul H.	USDOI Nat'l Park Service, Wash., DC 20013-7127
RAGAN, Elmer W.	2750th ABW/SE, Wright-Patterson AFB, OH 45433-5000
RAMBAUT, Michael L.	Commissariat A L'Energie Atomique, Paris, France

RAMSDELL, Paul A.	ETI Explosives Tech Int., Wilmington, DE 19809-2867
RANDOLPH, Tommy J.	McDonnell Douglas Astro Co., Titusville, FL 32780
RANKINS, James T.	USAF Wright Aeronautical Lab, Wright-Patterson AFB, OH
RAU, Stephen J.	Monsanto Research Corp., Miamisburg, OH 45432-0032
RAWLS, J. Richard	NASA Langley Research Ctr, Hampton, VA 23665-5225
REAMS, Christopher S.	NEDED, Code 50A, NWS, Yorktown, VA 23691-5000
REED, Jack W.	Sandia Nat'l Labs, Albuquerque, NM 87185
REES, Norman J.	Dir, Ministry of Defence, Kent, Great Britain
REEVES, Charles T.	Lockheed Missiles & Space Co., Sunnyvale, CA 94088-3504
REEVES, Harry	New Mexico Inst. of Mining & Technology, Socorro, NM
REEVES, John A.	Naval Weapons Station, Concord, CA 94520-5000
REEVES, Tom	10151 Amelia Ct., Cupertino, CA 95014
REINHARD, E. Daniel	Dep Dir for Health & Safety, USN, Wash., DC 20360-5000
RHEA, Richard L.	Olin Corporation, St. Marks, FL 32355
RHOADES, Eric	NASA - Kennedy Space Ctr, FL 32899
RICHARDSON, David E.	Hercules, Inc., Magna, UT 84044-0098
RICHARDSON, Devaughn	Martin Marietta Ord. Systems, Milan AAP, TN 38358
RICHMOND, Donald R.	EG&G Mason Research Inst., Albuquerque, NM 87119-9024
RIVERS, Doug	3M Company, St. Paul, MN 55144
ROBB, Dave	Robins AFB, GA 31098-6001
ROBERTS, Brian J.	Royal Australian AF, Canberra, Australia
ROBERTSON, Thomas R.	Energy, Mines & Resources, Ontario, Canada KIA0E4
ROBINSON, Ralph D.	Field Cmd Def Nuclear Agency, Kirtland AFB, NM 87115
RODLAND, Harold M.	HQ ATC/IGFG, Randolph AFB, TX 78150-5001
RODRIGUEZ, John	HQ AMC, 5001 Eisenhower Ave., Alex., VA 22333-0001
ROLLINS, Charles H.	AFISC/SEW, Norton AFB, CA 92409
ROOT, George L.	P.O. Box 458, Edwards, CA 93523
ROSENBERG, Alt	Nobel Ind-Sweden AB, Karlshoga, Sweden
ROSENDORFER, Theo	Messerschmitt-Bolkow-Blohm GmbH, Hagenauer Forst
ROSS, Boyce L.	USA Engr Div-Huntsville, AL 35807-4301
ROVELL, Charles A.	LTV Aerospace & Defense, Dallas, TX 75265-5907
ROZINKA, M.J.	Morton Thiokol, Inc., Brigham City, UT 84502-0689
RUTISHAUSER, Paul W.	Ammo Surveillance Div, Tooele AD, Tooele, UT 84074-5010
RYLANDER, Jon L.	Northrop, Perry, GA 31069
SABLAN, Fredericks W.	2750 AEW/DPCT, Wright-Patterson AFB, OH 45324
SALLY, John	Comarco, Inc., Ridgecrest, CA 93555
SANAI, Mosen, Dr.	SRI International
SANCHEZ, Felipe B.	Naval Surface Warfare Ctr, Dahlgren, VA 22448-5000
SAND, Larry	USA Corps of Engrs, Omaha, NE 68102
SANDROCK, Stephen E.	The Nathan Hale Group, Fairfax, VA 22030
SANTIS, Lon D.	Bureau of Mines, Pittsburgh, PA 15236
SAUNDERS, Duane E.	Magnavox Electronic Systems Co., Fort Wayne, IN 46808
SAWYER, F. Ronald	Nat'l Aero & Space Admin, Wallops Is., VA
SAWYER, Ray	DDESB, Alex., VA 22331-0600
SAYLORS, James A.	Bernard Johnson Inc., Houston, TX 77056
SCARBOROUGH, Duane S.	Picatinny Arsenal, NJ 07806-5000
SCARDINO, Philip J.	AF Contract Mgmt Div/SE, Kirtland AFB, NM 87118-5000
SCHAEFER, S.	Test Ctr, Postfach 1280, 4470 Meppen, France
SCHAICH, Eberhard, Maj	Materialamt der Bundeswehr, Germany
SCHMIDT, Bernd A., 1Lt	TFWC/SER, Nellis AFB, NV 89191-5000

SCHNEIDER, B.	University of New Mexico, Albuquerque, NM 87131
SCHNEIDER, James P.	McEntire ANGB, Eastover, SC 29044-9690
SCHREINER, James R.	NDANG, Fargo ND
SCHUM, Robert R.	DCASMA Twin Cities, St. Paul, MN 55116-1893
SCOTT, James F.	6545 Test Gp/SE, Hill AFB, UT 84056-5000
SCOTT, Richard J.	Allied Signal Aerospace Co., Tempe, AZ 85284
SCOTT, Warren W.	Lockwood, Andrews & Newnan, Inc., Houston, TX 77042
SEALS, Bill	ARDEC, Picatinny Arsenal, Dover, NJ 07081-5000
SEOW, Kee Yee	Chartered Chemical Industries, Singapore
SERRANO, John O.	DELCO Systems, Goleta, CA 93117
SEXSTONE, Peter A.	Secretary ESTC, London, England
SEYMOUR, Richard B.	Martin Marietta Astro Group, Denver, CO 80201
SHACKELFORD, Mark	BEI Defense Systems, Camden, Arkansas 71701
SHANNAN, Joe E.	Mason & Hanger-Silas Mason Co., Iowa AAP, Mdltown, IA
SHARLAND, John F., Brig.	Dir, Land Services Ammo, Oxfordshire, England
SHARPLESS, Don J.	Los Alamos National Lab, NM 87545
SHAW, Harry B.	Ministry of Defence, Navy Dept., Bath, England
SHEFFY, Michael	4 Hotmer St., Rishonle Zion, Israel 75201
SHESSI, Michael, MAJ	IDS, Washington, DC 20008
SHEU, Poon Tien	CDC-Construction & Dev PTE Ltd, Singapore
SHIRLEY, Agnes J.	USAMC Field Safety Act, Charlestown, IN 47111-9669
SHIRLEY, Clinton G.	Sandia National Lab, Albuquerque, NM 87185
SHOOP, Marion C.	Program Exec Off-Ammo, Alexandria, VA 22333-0001
SHOPHER, Kenneth R.	Integrated Systems Analysts, Yucaipa, CA 92399
SHORE, James S.	USE Waterways Exper Sta., Vicksburg, MS 39180-0631
SHULTS, Richard H.	Atlantic Research Corp., Gainsville, VA 22065
SHURTLEFF, Edgar M.	Jet Propulsion Lab, Pasadena, CA 91109
SIDMAN, Sumner	Raython Company, Orlando, FL 32861-6927
SILER, Kenneth	DLA, Marietta, GA 30068
SIMON, E.D.	Martin Marietta
SINGH, A.K.	CRS Sirrine, Inc., Greenville, SC 29606
SKEEN, Larry L.	Mason & Hanger-Silas Mason Co., Amarillo, TX 79177
SMITH, Alan J.	United Kingdom Ministry of Defence, St. Louis, MO 63166
SMITH, C. Richard	General Dynamics Pomona Div, Pomona, CA 91769
SMITH, Dale W.	Ford Aerospace Corp., Newport Beach, CA 92658-9983
SMITH, Dennis R.	Martin-Marietta Aerospace, Orlando, FL 32855
SMITH, Earle L.	AFISC/SEW, Norton AFB, CA 92409
SMITH, Lawrence E.	USA Armament Munitions & Chem Cmd, Rock Is., IL 61299
SMITH, Matthew J.	DCASMA Twin Cities, St. Paul, MN 55116-1893
SMITH, Michael W.	Morton Thiokol, Brigham City, UT 84302
SMITH, Roger W., LCDR	Defense Nuclear Agency, Kirtland AFB, NM 87115-5000
SMITH, Ronald A.	Nalval Undersea Warfare Engr, Keyport, WA 98345
SMITH, Wayne E.	US Naval Wpns Sta., China Lake, CA 93555-6001
SMITH, Willard J., Capt	USAF ADWC, Tyndall AFB, FL 32403-5000
SMITH, William D.	Advanced Tech, Inc., Arlington, VA 22202
SMUDA, James F., CDR	Defense Nuclear Agency, Kirtland AFB, NM 87115-5000
SNIDER, Donald D.	DCASR Chicago, IL 60666-0475
SNYER, William H.	Denver Research Institute, Denver, CO 80208
SOLEAU, Edward W.	LTV Missiles & Elec Group, Gp Msl Div, Dallas, TX 75265
SPERLING, Mike	Aerojet Ordnance Co., Downey, CA 90241

SPIVEY, Kathy A.	Wilfred Baker Engineering, San Antonio, TX 78209
SPOTZ, Robert H.	CO, Naval Ordnance Station, Indian Head, MD 20640-5000
STANCKIEWITZ, Charles	USAMC FSA, ATTN: AMXOS-PE, Charlestown, IN 47111-9669
STENSLAND, Per	Royal Norwegian Navy Materiel Command, Norway
STEVENSON, Randy N.	Northrop, Perry, GA 31069
STILES, Wayne E., Capt	HQ Alaskan Air Cmd, IGFW, Elmendorf AFB, AK 99506-5001
STILLIONS, C.A.	Sverdrup/ETG, Arlington, VA 22209-2454
STUDEBAKER, William R.	AF Wright Aeronics Lab, Wright-Patterson AFB, OH 45433
STUFFLE, G.	Crane, IN
SUEKER, Wayne R.	Honeywell Inc., Joliet, IL 60435
SUGARMAN, Samuel H.	Bulova Systems & Instr Corp., Valley Stream, NY 11582
SUMNER, Sidmon	Raytheon Co., 113 Foxridge Run, Longwood, FL 32750
SUMRALL, T.S.	Morton Thiokol, Inc., Huntsville, AL 35807-7501
SUTHERLAND, Sarah Z.	DDESB Secretariat, Alex., VA 22331-0600
SWISDAK, Michael	NSWC, Silver Springs, VA 20903-5000
SYMONDS, Peter C.	Weapon Engineering (RAF), London, England
TANCRETO, James E.	Naval Civil Engr Lab, Port Hueneme, CA 93043-5003
TARAS, Darwin N.	HQ, USA Materiel Cmd, Alex., VA 22333-0001
TATOM, Frank B.	Engineering Analysis, Inc., Huntsville, AL 35801-5909
TAYLOR, Truman	USA Safety Ctr, Fort Rucker, AL 36362-5363
TENBRINK, Wayne A.	Naval Weapon Station, Concord, CA 94520-5001
THIBEDEAU, Richard N.	TRW, San Bernardino, CA 92402-1310
THOMAS, Chester A.	Hughs Aircraft Company, Tucson, AZ 85734
THOMAS, Joseph L.	Kansas AAP, Parsons, KS 67357-9107
THOMPSON, Frank K.	US Coast Guard Hqs., Washington, DC 20593-0001
THOMPSON, Gary B.	Hercules Aerospace Co., Salt Lake City, UT 84130-0181
THOMPSON, John R.	HQ USA Arm, Mun & Chem Cmd, Rock Is., IL 61299
THOMPSON, Richard	Tracor Aerospace, Inc., Austin, TX 78725
THORNTON, J. N.	Morton Thiokol, Inc., Brigham City, UT 84302
TILSON, David L.	USA Corps of Engrs, Vicksburg, MS 39180-0631
TINKLER, William	Ministry of Defense, Kent, England
TOENJES, Kurt A., Capt	Federal Ministry of Defence, Germany
TOLLINGER, John	Naval Weapons Station, Colts Neck, NJ 07722
TOMPKINS, David R.	Wyle Laboratories, Norco, CA 91760
TOW, Peng Soon, CAPT	Ministry of Defence, Singapore
TRAKIMAS, Richard	W.R. Grace Company, Lexington, MA 02173
TRIMBLE, Craig N.	Bernard Johnson, Inc., Dallas, TX 75228
TSUCHIYA, Jim H.	Hercules Inc., McGregor, TX 76657-1999
TUOKKO, Seppo S.	Ministry of Defense, Finland
TUTTLE, Peter G.	DCASR-QS, Boston, MA 02210
TUTTY, Malcom G.	Eglin AFB, FL 32542-5000
UNDERHILL, Thomas P., MAJ	Department of National Defense, Ottawa, Canada
VAIDYANATHON, H.	Dept of Nat'l Defence, Canada
VALDEZ, DENISE I.	Sunflower AAP, DeSota, KS 66018-0640
VAUSHER, Abraham L.	McDonnell Douglas Astronautics, CA 92647
VAZQUEZ, Pedro	CAD-CON Facilities Design, Inc.
VERNON, Gary L.	Fort McClellan, AL 36205-5000
VETTER, Eric S.	Rockwell International, Downey, CA 90241
VICK, C.V.	Aerojet Solid Prop Co., Sacramento, CA 95853-1699

VICKERS, Marvin E.	Naval Sea Supt Ctr, Pacific, San Diego, CA 92138-5548
VITTITOW, Pat	USAMC Field Safety Activity, Charlestown, IN
VRETBLAD, Bengt E.	Fort F (Royal Swedish Fortification Admin, Sweden
WAGER, Phil	Naval Civil Engr Lab
WAGMAN, James	AF Weapons Lab, Kirtland AFB, NM 87117-6008
WALKER, David W.	British Navy Staff, Wash., DC 20008
WALKER, Lewis D.	Ofc, Secretary of the Army, Wash., DC 20310
WALSH, James	NAVORDMISTESTSTA, WSMR, NM
WALTERS, James C.	USA Nuclear & Chemical Agency, Springfield, VA 22150
WALTERS, Jeffrey L.	Black & Veatch Engrs-Arch., Overland Park, KS 66211
WANG, Zhong-Qian	China Academy of Railway Sci, Beiging, China 100081
WARD, Jerry	DDESB, Alex., VA 22331-0600
WARWICK, W.	United Tech, PO Box 49028, San Jose, CA 95161-9028
WATSON, Jerry L.	USA BRL, Aberdeen PG, MD 21005
WATTS, Howard D.	NSWC, Silver Spring, MD 20903-5000
WEBSTER, Edward A.	McDonnell Douglas Astr. Co., Huntington Beach, CA 92647
WEBSTER, Larry D.	Naval Surface Warfare Center, Dahlgren, VA 22405
WERNSMAN, Robert L., CAPT	Ofc of the Chief of Naval Operations, Wash, DC 20350
WEST, Buddy	AF Armament Div, Eglin AFB, FL 32542-5000
WESTENBURG, Tom	USA Corps of Engrs., Omaha, NE
WHEELER, R.H.	Schneider Svcs International, Arnold AFB, TN 37389
WHITE, Charles A.	23AF/SEV, Hurlburt Fld, FL 32544-5000
WHITE, Greg, LTC	Australian Ordnance Council, Australia
WHITE, Jim	KSA, Inc., Arlington, VA 22201
WHITE, John J.	Battelle, Colombus Div, Columbus, OH 43201
WHITE, Lawrence G.	Bureau of Alcohol, Tobacco & Firearms, Wash., DC 20226
WHITFIELD, Lorenzo	436 Mil Airlift Wing, Dover AFB, Dover, DE 19902-5174
WHITNEY, Mark C.	Southwest Research Inst., San Antonio, TX 78284
WILBOURNE, Joseph C.	Naval Ord Station, Indian Head, MD 20640-5000
WILCOSKI, James	no address given
WILKIE, Barbara	McDonnell Douglas, Titusville, FL 32780
WILLIAMS, Doyle G.	AMCCOM, Louisiana AAP, Shreveport, LA
WILLIAMS, Marvin B.	USACAW, APO SF 96305
WILLIAMSON, A. Edward	Health & Safety Executive, Merseyside, England
WILLIAMSON, Ken, MSgt	Shaw AFB, SC 29152-5000
WILLIAMSON, Ted	Det 9, Boeing, Seattle, WA
WILSON, Jack R.	Air National Guard
WILSON, Robert L.	Propellex Corp., Edwardswille, IL 62025-0387
WINGATE, Mark A.	Olin Defense Systems, Independence, MO 64050
WINKELER, Karl-H	German AF Supt Cmd, West Germany
WOLFE, Larry K.	HQ, Military Airlift Cmd, Scott AFB, IL 62225-5101
WOLFE, Vernon E.	Hercules Incorporated, Wilmington, DE 19894
WOLFGANG, L. Gary	Ravenna Arsenal, Inc., Ravenna, OH 44266-9297
WOOD, John L., Capt	AFLMC/LGM, Gunter AFB, AL 36114-6693
WOODY, Sam, LTC	DCASR, St. Louis, MO 63101-1194
WOOTEN, Larry, Capt	AF Weapons Lab, Kirtland AFB, NM 87117-6008
WORSHAM, Wm. K.	Martin Marietta Msl Systems
WRIGHT, Terry P.	Naval Ship Weapon Systems Engr Sta, Port Hueneme, CA
WRIGHT, Tony P., Brig.	UK Ordnance Board, London, England
YAMAMOTO, Akihiko	Nippon Oil & Fats Co., LTD, NY, NY 10166

YANCEY, William A.	Hi-Test Laboratories, Inc., Buckingham, VA 23921-0226
YUTMEYER, William P.	AMC Field Safety Activity, Charlestown, IN 47111-9669
ZAKRZEWSKI, Peter H.	Def Contract Admin Svcs Region, St. Louis, MO 63101
ZAUGG, Mark	Toole Army Depot, Toole, UT 84074-5004
ZEMAN, Sam	Morton Thiokol, Inc., Huntsville, AL 35807-8107
ZHENG, Li	Engr. Design & Research Inst., Beijing, China 100081
ZREBIEC, Donald L.	Naval Air Engr Center, Lakehurst, NJ 08733--5000
ZUCKERWISE, Jeffrey H.	DCASMA Springfield, NJ 07081